

**THIRTY-FIFTH
INTERNATIONAL
SYMPOSIUM ON COMBUSTION**

PROGRAM

THE COMBUSTION INSTITUTE

OFFICERS / EXECUTIVE COMMITTEE

Katharina Kohse-Höinghaus, President
James F. Driscoll, Vice President/President Elect
Marcus Aldén, Vice President/Section Affairs

Derek Dunn-Rankin, Treasurer
Reginald E. Mitchell, Secretary
Hideaki Kobayashi, Secretary Section Affairs

BOARD OF DIRECTORS

Marcus Aldén
Jacqueline H. Chen
Meredith Colket
Philippe Dagaut
Philip de Goeij
James F. Driscoll
Derek Dunn-Rankin
Peter Glarborg
Iskender Gökalp
Brian Haynes*
In-Seuck Jeung
Hideaki Kobayashi
Katharina Kohse-Höinghaus
Michikata Kono
Chung King Law*
Peter Lindstedt
Reginald E. Mitchell
Peter Nelson
Stephen B. Pope
Fei Qi
Raffaele Ragucci
Robert Sawyer*
Christof Schulz
Daniel J. Seery*
Gregory Smallwood
Nickolai Smirnov
Mitchell D. Smooke
Charles K. Westbrook*
Phillip R. Westmoreland
Margaret S. Wooldridge
Qiang Yao

Lund Institute of Technology, Sweden
Sandia National Laboratories, USA
United Technologies Research Center, USA
Centre National de la Recherche Scientifique, France
Eindhoven University of Technology, Netherlands
University of Michigan, USA
University of California, USA
Technical University of Denmark, Denmark
Centre National de la Recherche Scientifique, France
University of Sydney, Australia
Seoul National University, Korea
Tohoku University, Japan
Bielefeld University, Germany
University of Tokyo, Japan
Princeton University, USA
Imperial College, United Kingdom
Stanford University, USA
Macquarie University, Australia
Cornell University, USA
University of Science and Technology of China, China
Istituto di Ricerche sulla Combustione, Italy
University of California – Berkeley, USA
IVG, University of Duisburg-Essen, Germany
Retired, USA
National Research Council Canada, Canada
Moscow State University, Russian Federation
Yale University, USA
Lawrence Livermore National Laboratory, USA
University of Massachusetts, USA
University of Michigan, USA
Tsinghua University, China

* Honorary

THE COMBUSTION INSTITUTE COMMITTEE

Marcus Aldén, Chair, Lund Institute of Technology, Sweden
Hideaki Kobayashi, Vice Chair/Sec, Tohoku University, Japan
Amer Amer, Saudi Aramco Research and Development, Saudi Arabia
Shigeru Azuhata, Hitachi Ltd., Japan
Rob Bastiaans, Eindhoven University of Technology, Netherlands
Henning Bockhorn, Karlsruhe Institute of Technology, Germany
Amelle Cessou, CORIA-CNRS, France
Andrea D'Anna, Università degli Studi di Napoli Federico II, Italy
Amir de Oliveira, Campus Universitário-Trindade, Brazil
Neven Duic, University of Zagreb, Adria
Edgar Fernandes, University of Lisbon, Portugal
Nick Glumac, University of Illinois at Urbana-Champaign, USA (Central)
Daniel Haworth, The Pennsylvania State University, USA (Eastern)
William Jones, Imperial College, London, UK
David Katoshevski, Ben-Gurion University, Israel
Larry Kostiuik, University of Alberta, Canada
Chang Eon Lee, Inha University, Korea
Ta-Hui Lin, National Cheng Kung University, Taiwan

Amable Liñán, University of Madrid, Spain
Ola Lish, FOI, Sweden
Terese Løvås, Norwegian University of Science and Technology, Norway
Mohy S. Mansour, Cairo University, Egypt
Assaad Masri, University of Sydney, Australia
Kiumars Mazaheri, Tarbiat Modares University, Iran
Bart Merci, Ghent University, Belgium
Pradip Kumar Pandey, Infotech Enterprises LTD., India
Kalyanasundaram Seshadri, Univ. of California, San Diego, USA (Western)
John Simmie, National University of Ireland, Galway, Ireland
George Skevis, CPERI, Greece
Nickolai Smirnov, Moscow State University, Russian Federation
Hakan Serhad Soyhan, Sakarya Üniversitesi, Turkey
Andrzej Teodorczyk, Warsaw University of Technology, Poland
Cesar Trevino, National Autonomous University of Mexico, Mexico
Tamás Turányi, Institute of chemistry, Eötvös University, Hungary
Qiang Yao, Tsinghua University, China
S.A. Zhdanok, The National Academy of Sciences of Belarus, Belarus

FINANCE COMMITTEE

Don Lucas, Chair, Lawrence Berkeley National Laboratory, USA
Ken Brezinsky, University of Illinois, USA

Derek Dunn-Rankin, Treasurer, University of California, Irvine, USA
Peter Lindstedt, Imperial College, UK

NOMINATION COMMITTEE FOR DIRECTORS

Philippe Dagaut, Chair, CNRS, France
Marcos Chaos, FM Global Research Division, USA
Andrea D'Anna, Università degli Studi di Napoli Federico II, Italy
Philip de Goeij, Eindhoven University of Technology, Netherlands

In-Seuck Jeung, Seoul National University, Korea
Terese Løvås, Norwegian University of Science and Technology, Norway
Stephen B. Pope, Cornell University, USA
Bin Yang, Tsinghua University, China

BOARD OF DIRECTOR ELECTION TELLER COMMITTEE

Simone Hochgreb, Chair, University of Cambridge, UK
S. Scott Goldsborough, Argonne National Laboratory, USA
Mark Linne, Chalmers University of Technology, Sweden

Reginald E. Mitchell, Stanford University, USA
Zhuyin Ren, Tsinghua University, China
Barbara Waronek, The Combustion Institute, USA

SITE COMMITTEE

Uwe Riedel, Chair, Institut für Verbrennungstechnik, Germany
Jeffrey Berghthorson, McGill University, Canada
Nabiha Chaumeix, CNRS, France

Derek Dunn-Rankin, University of California, Irvine, USA
Shengyang (Steven) Shy, National Central University, Taiwan
Qiang Yao, Tsinghua University, China

THIRTY-FIFTH SYMPOSIUM COMMITTEES

TECHNICAL PROGRAM COMMITTEE

PROGRAM CO-CHAIRS

Suk Ho Chung, University of King Abdullah Science & Technology, Saudi Arabia

Thierry Poinsot, Institut de Mécanique des Fluides de Toulouse, CNRS, France

COLLOQUIUM CO-CHAIRS

Reaction Kinetics

Henry J. Curran, NUI Galway, Ireland
Tiziano Faravelli, Politecnico di Milano, Italy
Pierre-Alexandre Glaude, CNRS, France
Tiangfeng Lu, University of Connecticut, USA
Matthias Olzmann, Karlsruher Institut für Technologie, Germany

Soot, PAH & Other Large Molecules

Meredith B. Colket, United Technologies Research Center, USA
Pascale Desgroux, University of Lille 1/CNRS, France
Markus Kraft, University of Cambridge, UK
Murray Thomson, University of Toronto, Canada

Diagnostics

Frank Beyrau, Imperial College London, UK
Mark Linne, Chalmers University of Technology, Sweden
Bruno Renou, CORIA, France

Laminar Flames

Suresh K. Aggarwal, University of Illinois at Chicago, USA
Charles McEnally, Yale University, USA
Sergey Minaev, Far-Eastern Federal University, Russia
William Roberts, KAUST, Saudi Arabia
Kalyansundaram Seshadri, University of California, USA
Chih-Jen Sung, University of Connecticut, USA

Turbulent Flames

Jonathan Frank, Sandia National Laboratories, USA
Ömer Gülder, University of Toronto, Canada
Terese Løvås, Norwegian University of Science & Technology, Norway
Wolfgang Meier, DLR, Germany
Mamoru Tanahashi, Tokyo Institute of Technology, Japan
Denis Veynante, CNRS-Ecole Centrale Paris, France

Heterogeneous Combustion & Material Synthesis

Yei-Chin Chao, National Cheng Kung University, Taiwan
Christopher R. Shaddix, Sandia National Laboratories, USA
Minghou Xu, Huazhong University of Science and Technology, China
Richard A. Yetter, Pennsylvania State University, USA
Xiaolin Zheng, Stanford University, USA

Spray and Droplet

Alessandro Gomez, Yale University, USA
Rainer Koch, Karlsruhe Institute of Technology, Germany
Masato Mikami, Yamaguchi University, Japan

Detonations, Explosion and Supersonic Combustion

Nabiha Chaumeix, ICARE-CNRS, Orléans, France
Jeong-Yeol Choi, Pusan National University, Korea
Matei Radulescu, University of Ottawa, Canada
Joseph Shepherd, California Institute of Technology, USA

Fire Research

Bogdan Dlugogorski, The University of Newcastle, Australia
Ritsu Dobashi, The University of Tokyo, Japan
Naian Liu, University of Science and Technology of China, China
Guillermo Rein, Imperial College London, UK

Stationary Combustion Systems and Environmental Impact

Bassam Dally, The University of Adelaide, Australia
JoAnn Lighty, University of Utah, USA
Qiang Yao, Tsinghua University, China

IC Engine and Gas Turbine Combustion

André Boehman, University of Michigan, USA
Michael J. Brear, University of Melbourne, Australia
Daniel C. Haworth, Pennsylvania State University, USA
Christian Oliver Paschereit, Technische Universität Berlin, Germany
Wolfgang Polifke, Technische Universität München, Germany
Eiji Tomita, Okayama University, Japan

New Technology Concepts, Reacting Flows and Fuel Technology

Mário Costa, Instituto Superior Técnico, Portugal
Mara de Joannon, IRC-CNR, Italy
Nam Il Kim, Chung-Ang University, Korea
Tonghun Lee, University of Illinois at Urbana-Champaign, USA

REVIEW COMMITTEE

Tahir Abbas, Cinar Ltd.
John Abraham, Purdue University
Suresh K. Aggarwal, University of Illinois-Chicago
Ajay K. Agrawal, University of Alabama
Jeongmin Ahn, Syracuse University
Tetsuya Aizawa, Meiji University
Fumiteru Akamatsu, Osaka University
V'yacheslav Akkerman, West Virginia University
Michela Alfè, IRC-CNR
Robert A. Altenkirch, University of Alabama-Huntsville
Zeyad Alwahabi, University of Adelaide
Maria Alzueta, University of Zaragoza
Mats Andersson, Chalmers University of Technology
Christian Angelberger, IFP Energies Nouvelles
Barbara Apicella, Institute of Research on Combustion, (IRC-CNR)
Sourabh V. Apte, Oregon State University
Octavio Armas, Mecánica Aplicada e Ingeniería de Proyectos
Katsuo Asato, Gifu University
Peter Ashman, University of Adelaide
Burak Atakan, Universität Duisburg-Essen
Arvind Atreya, University of Michigan
Laurent Audouin, IRSN, Institut de Radioprotection ed de
C. Thomas Avedisian, Cornell University
Richard Axelbaum, Washington University in St. Louis
Akihiko Azetsu, Tokai University

Joao Toste Azevedo, Instituto Superior Tecnico
Valeri Babushok, NIST
William D. Bachalo, Artium Technologies Inc
Xue-Song Bai, Lund University
Francoise Baillot, CORIA UMR Université de Rouen
Nicolas Bal, CERIB
Ramanarayanan Balachandran, University College London
Javier Ballester, University of Zaragoza
Rosario Ballesteros, UCLM
Robert Barlow, Sandia National Laboratories
R.J.M. Bastiaans, Eindhoven University of Technology
Saptarshi Basu, Indian Institute of Science
Frédérique Battin-Leclerc, CNRS
C. Regis Bauwens, FM Global
Luc Bauwens, University of Calgary
Christian Beck, Siemens
Frank Behrendt, Technische Universität Berlin
Tarek Beji, Ghent University
John Bell, LBNL
Josette Bellan, Jet Propulsion Laboratory
Marc Bellenoue, ENSMA
Per-Erik Bengtsson, Lund University
Beth Anne Bennett, Yale University
Ahmed Bentaib, IRSN
Jeff Berghthorson, McGill University

Michael Beyer, Physikalisch-Technische Bundesanstalt
 Craig Beyler, Research Commercialization and SBIR Center
 David Bhatt, Indian Institute of Technology
 Subrata Bhattacharjee, San Diego State University
 Sankar Bhattacharya, Monash University
 Fabrizio Bisetti, KAUST
 John Black, University of Manchester
 Henrik Bladh, Lund University
 Guillaume Blanquart, California Institute of Technology
 Henning Bockhorn, KIT
 Benjamin Boehm, TU Darmstadt, EKT
 Andre Boehman, University of Michigan
 Stani Bohac, University of Michigan
 Heidi Böhm, University of Duisburg
 Matthieu Boileau, CNRS, EM2C Laboratory
 Giulio Borghesi, NASA-JPL
 Roda Bounaceur, University de Lorraine
 Gilles Bourque, Rolls-Royce Canada
 Tom Bowman, Stanford University
 Isaac Boxx, DLR
 Malte Braack, Kiel University
 Christian Brackmann, Lund University
 Derek Bradley, University of Leeds
 Kyle Brady, University of Connecticut
 Marina Braun-Unkhoff, German Aerospace Center
 Michael Brear, University of Melbourne
 Günter Brenn, Graz University of Technology
 Ken Brezinsky, University of Illinois-Chicago
 Pascal Bruel, CNRS
 Claudio Bruno, United Technologies Research Center
 Morgan Bruns, University of Texas at Austin
 Valery Bunev, Russian Academy of Science
 Michael Burke, Argonne National Laboratory
 Iain Burns, University of Strathclyde
 Kendal Bushe, University of British Columbia
 Kathryn Butler, NIST
 Vitaly Bychkov, Umeå University
 Viatcheslav Bykov, Karlsruhe Institute of Technology
 Sébastien Caillat, École des Mines de Douai
 Giovanni Campa, Ansaldo Energia S.P.A.
 Sébastien Candel, Ecole Centrale Paris
 Robert Cant, University of Cambridge
 Campbell Carter, US Air Force Research Laboratory
 Marco Castaldi, City College of New York
 Guillaume Castanet, LEMTA, Université de Lorraine, CNRS
 Laurent Catoire, ENSTA Paris Tech
 Antonia Cavaliere, University Federico II Naples
 Carlo Cavallotti, Politecnico Di Milans
 Armelle Cessou, CNRS
 Min Suk Cha, KAUST
 Nilanjan Chakraborty, Newcastle University
 Satyanarayanan R. Chakravarthy, Indian Institute of Technology Madras
 Qing Nian Chan, University of New South Wales
 Beei-Huan Chao, University of Hawaii at Manoa
 Jenny Chao, FM Global
 Xing Chao, Oxigraf Inc.
 Yei-Chin Chao, Institute of Aeronautics & Astronautics
 Marcos Chaos, FM Global
 Alexandros Charogiannis, Imperial College London
 Prateep Chatterjee, FM Global
 Swetaprovo Chaudhuri, Indian Institute of Science
 Nabih Chaumeix, ICARE-CNRS Orleans
 Harsha Chelliah, University of Virginia
 Haixiang Chen, State Key Laboratory of Fire Science
 Jacqueline Chen, Sandia National Laboratories
 Jyh-Yuan Chen, University of California-Berkeley
 Lei Chen, Massachusetts Institute of Technology
 Wei-Hsin Chen, National Cheng Kung University
 Zheng Chen, Peking University
 C.-L. Chiang, National Tsing-Hua University
 Ashwin Chinnayya, ISAE-ENSMA
 Gyungmin Choi, Pusan National University
 Jeong-Yeol Choi, Pusan National University
 Wanki Chow, Hong Kong Polytechnic University
 Mouldi Chrigui, Technical University of Darmstadt
 Farid Christo, University of Adelaide
 Suk Ho Chung, KAUST
 Anna Ciajolo, IRC-CNRS
 Gaby Ciccarelli, Queen's University
 Matthew Cleary, University of Sydney
 Noel Clemens, University of Texas-Austin
 Pedro Coelho, Instituto Superior Tecnico
 Jerald Cole, Hydrogen Ventures, LLC.
 Olivier Colin, IFPEN
 Meredith Colket, United Technologies Research Center
 Jean-Louis Consalvi, Polytech'Marseille
 Gaetano Continillo, Università del Sannio
 Francesco Contino, Urije Universiteit Brussel
 Alexis Coppalle, INSA of Rouen
 Bruno Coriton, Sandia National Laboratories
 Mário Costa, Instituto Superior Técnico
 Francesco Creta, University of Rome La Sapienza
 Brian Crosland, Carleton University
 Benedicte Cuenot, CERFACS
 Alberto Cuoci, Politecnico di Milano
 Henry J. Curran, National University of Ireland
 Scott Curran, Oak Ridge National Laboratory
 Philippe Dagaut, CNRS-INSIS
 Rainer Dahms, Sandia National Laboratories
 Bassam Dally, University of Adelaide
 Nico Dam, Technical University of Eindhoven
 Yves D'Angelo, CORIA
 Andrea D'Anna, University of Naples Federico II
 Apurba K. Das, Alstom Power Inc.
 S. Dasappa, ASTRA / CGPL
 Amitava Datta, Jadavpur University
 David F. Davidson, Stanford University
 Kevin Davis, Reaction Engineering International
 James R. Dawson, Norwegian University of Science and Technology
 Marc Day, Lawrence Berkeley National Laboratory
 Guillaume Dayma, University of Orleans
 Ashoke De, Indian Institute of Technology Kanpur
 L.P.H. de Goey, TU Eindhoven
 Silvana De Iuliis, CNR IENI
 Jaap de Vries, FM Global
 Anthony M. Dean, Colorado School of Mines
 Steven Dean, Pennsylvania State University
 John E. Dec, Sandia National Laboratories
 Ralf Deiterding, German Aerospace Center (DLR)
 Michael A. Delichatsios, University of Ulster
 Adam Dempsey, Oak Ridge National Laboratory
 Ingemar Debratt, Chalmers University of Technology
 Pascale Desgroux, CNRS/Université Lille1
 Paul DesJardin, University of Buffalo
 Olaf Deutschmann, Karlsruhe Institute of Technology
 Cécile Devaud, University of Waterloo
 Francesca di Mare, German Aerospace Center
 S. di Stasio, Italian National Research Council (CNR-IM)
 Daniel L. Dietrich, NASA Glenn Research Center
 Pascal Diévert, Princeton University
 Friedrich Dinkelacker, Universität Hannover
 Benjamin Ditch, FM Global
 Hyungrok Do, University of Notre Dame
 Ritsu Dobashi, University of Tokyo
 Sándor Dobé, MTA TTK
 Pascale Domingo, CNRS-CORIA
 Stephen Dooley, University of Limerick
 Sergey Dorofeev, FM Global
 Michael Drake, General Motors R&D
 Thomas Dreier, University Duisburg-Essen
 Edward L. Dreizin, NJ Institute of Technology
 Andreas Dreizler, TU Darmstadt
 James Driscoll, University of Michigan
 Frederick L. Dryer, Princeton University
 Dougal D. Drysdale, Edinburgh University
 Florent Duchaine, CERFACS
 Sébastien Ducruix, CNRS-EM2C
 Anthony Dufour, Université de Lorraine
 Matthew Dunn, University of Sydney
 Derek Dunn-Rankin, University of California, Irvine
 Daniel Durox, Laboratoire EM2C
 Christophe Duwig, Lund Institute of Technology
 Ariel Dvorkin, Israel Institute of Technology
 Seth Dworkin, Ryerson University
 Tarek Echehki, North Carolina State University
 Eric Eddings, University of Utah
 Jack Edwards, North Carolina State University
 Fokion Egolfopoulos, University of Southern California
 Christian Eigenbrod, Universität Bremen
 Abderrahman el Bakali, Université Lille 1

Hossam El-Asrag, Ansys, Inc.
 Janet Ellzey, University of Texas-Austin
 Alexander Emelianov, JIHT RAS
 Takuma Endo, Hiroshima University
 Alexander Eremin, Russian Academy of Science
 Jonathan Essel, Naval Air Warfare Center
 Paul Ewart, Oxford University
 Alessandro Faccinnetto, Université Lille 1
 Michael Fairweather, University of Leeds
 Mengxiang Fang, Zhejiang University
 Tiziano Faravelli, Politecnico di Milano
 Aamir Farooq, KAUST
 Paul Ferkul, NCSER
 Ravi Fernandes, RWTH Aachen/PTB
 Carlos Fernandez-Pello, University of California-Berkeley
 Daniel Ferry, CINAM UMR-CNRS 7325
 Benoit Fiorina, Ecole Centrale Paris, Laboratoire EM2C
 Brain T. Fisher, University of Alabama
 Christa Fittschen, University of Lille / CNRS
 Thomas Fletcher, Brigham Young University
 Jason Floyd, Research Commercialization and SBIR Center
 Stefano Fontanesi, UNIMORE
 Catalin Fotache, UTRC
 Fabrice Foucher, University Orleans
 Rene Fournet, Université de Lorraine
 Fleming Frandsen, Technical University of Denmark
 Jonathan Frank, Sandia National Laboratories
 Benedetta Franzelli, EM2C Laboratory-CNRS
 Alessio Frassoldati, Politecnico di Milano
 Michael Frenklach, UC Berkeley
 Gernot Friedrichs, University of Kiel
 Sergey Frolov, Semenov Institute of Chemical Physics
 David Frost, McGill University
 Andres Fuentes, Universidad Técnica Federico Santa María
 Frederik Fuest, Ohio State University
 Hajime Fujimoto, Doshisha University
 Osamu Fujita, Hokkaido University
 Naoya Fukushima, Tokyo Institute of Technology
 Christer Fureby, Swedish Defence Research Agency FOI
 Roman Fursenko, Institute of Theoretical and Applied Mechanics, SB RAS
 Sergey Futko, Chemical Physics Laboratory
 Takayuki Fuyuto, Toyota Central R&D Labs
 Chiara Galletti, University of Pisa
 Maria Reyes Garcia, University of Castilla-La Mancha
 Pedro L. Garcia-Ybarra, UNED
 Laurent Gasnot, University of Lille
 Manolis Gavaises, City University of London
 Hai-Wen Ge, Chrysler Group LLC
 Klaus Peter Geigle, German Aerospace Center (DLR)
 Thomas Gerber, Paul Scherrer Institut
 Dirk Geyer, Darmstadt University
 Ahmed Ghoniem, MIT
 Eugenio Giacomazzi, ENEA
 Alexis Giauque, ONERA
 Laurent Gicquel, CERFACS
 Olivier Gicquel, CNRS-EM2C
 Paola Giudicianni, IRC-CNR
 Peter Glarborg, Technical University of Denmark
 Pierre-Alexandre Glaude, CNRS
 Nick Glumac, University of Illinois
 Iskender Gökalp, CNRS-ICARE
 Ponnuthurai Gokulakrishnan, CSE
 S. Scott Goldsborough, Argonne National Laboratory
 Claude Goldsmith, Brown University
 Michael Gollner, University of Maryland-College Park
 Alessandro Gomez, Yale University
 Candido Gomez, Universidad de Jaén
 Elke Goos, DLR
 Robert Gordon, Rolls-Royce Canada
 Sam Goroshin, McGill University
 Hiroshi Gotoda, Ritsumeikan University
 Dimitris Goussis, National Technical University
 William Green, Massachusetts Institute of Technology
 J. Barry Greenberg, Israel Institute of Technology
 Frederic Grisch, CORIA
 Clinton Groth, University of Toronto
 Ray Grout, NREL
 Andrea Gruber, SINTEF Energy Research
 Vladimir Gubernov, P.N. Lebedev Physical Institute
 Felix Guethe, Alstom
 Eric Guillaume, LNE
 Ömer Gülder, University of Toronto
 Hongsheng Guo, National Research Council
 Ankur Gupta, Rolls-Royce Corporation
 Ashwani K. Gupta, University of Maryland
 Rajender Gupta, University of Alberta
 Sreenath Gupta, Argonne National Laboratory
 Eva Gutheil, Heidelberg University
 Rory Hadden, University of Edinburgh
 Bob Hall, UTRC
 Matt Hall, University of Texas, Austin
 Fabien Halter, University of Orléans
 Steve Hammack, University of Illinois-Urbana-Champaign
 Nils Hansen, Sandia National Laboratories
 Ronald K. Hanson, Stanford University
 Yannis Hardalupas, Imperial College London
 Lawrence B. Harding, Argonne National Laboratory
 Nozomu Hashimoto, CRIEPI
 Christian Hasse, TU Freiberg
 Nils Erland L. Haugen, SINTEF Energy Research
 Evatt Hawkes, University of New South Wales
 Daniel C. Haworth, Pennsylvania State University
 Hiroshi Hayasaka, Hokkaido University
 Naoki Hayashi, Nagoya University
 Brian S. Haynes, University of Sydney
 Yaping He, University of Western Sydney
 Ethan Hecht, Sandia National Laboratories
 Ansgar Heilig, Bertrandt AG
 Santosh Hemchandra, Indian Institute of Science
 Olivier Herbinet, CNRS-LRGP
 Juan Hernandez, Universidad de Castilla-La Mancha
 Jose Herreros-Arellano, University of Birmingham
 John Hewson, Sandia National Laboratories
 Andrew Higgins, McGill University
 Taro Hirasawa, Chubu University
 Simone Hochgreb, University of Cambridge
 Bing Hu, Cummins Inc
 Erjiang Hu, Xi'an Jiaotong University
 Longhua Hu, University of Science and Technology of China
 Zhiqian Hu, Huazhong University of Science and Technology
 Xinyan Huang, Imperial College London
 Kevin Hughes, University of Leeds
 Kang Huh, Pohang University of Science and Technology
 Xin Hui, University of Connecticut
 Johan Hult, MAN Diesel & Turbo
 Mohmoud Idir, CNRS
 Matthias Ihme, Stanford University
 Yuji Ikeda, Imagineering, Inc.
 Hong Im, KAUST
 Osamu Imamura, Nihon University
 Antonella Ingenito, University of Rome La Sapienza
 Atsushi Ishihara, Saitama Institute of Technology
 Kazuhiro Ishii, Yokohama National University
 Hiroyuki Ito, Kanagawa University
 Scott Jackson, Los Alamos National Laboratory
 Thomas L. Jackson, University of Illinois
 Helga Jander, GWDG
 Johannes Janicka, TU-Darmstadt
 Peter Jansohn, Paul Scherrer Institute
 Marcis Jansons, Wayne State University
 Ahren Jasper, Sandia National Labs
 Jay B. Jeffries, Stanford University
 Anker Jensen, Technical University of Denmark
 In-Seuck Jeung, Seoul National University
 Chunsheng Ji, Sandia National Laboratories
 J. Ji, State Key Laboratory of Fire Science
 Carmen Jiménez, CIEMAT
 Santiago Jiménez, LIFTEC (CSIC)
 Craig Johansen, University of Calgary
 Robert Johansson, Chalmers University of Technology
 Jaclyn Johnson, Michigan Technological University
 Grunde Jomaas, Technical University of Denmark
 Paul Joseph, University of Ulster
 Yiguang Ju, Princeton University
 Fang Jun, State Key Laboratory of Fire Science
 Matthew Juniper, University of Cambridge
 Leonid Kagan, Tel Aviv University
 Sebastian Kaiser, University of Duisburg-Essen
 Gautam Kalghatgi, Aramco
 Frank Kameier, Fachhochschule Dusseldorf University

A. Murty Kanury, Oregon State University
 Ashwani Kapila, Rensselaer Polytechnic Institute
 Dheeraj S.K. Kapilavai, GE Global Research
 Ann Karagozian, University of California
 Adonios Karpets, Texas A&M University
 Jiro Kasahara, Nagoya University
 Aslan Kasimov, KAUST
 Tina Kasper, University of Duisburg-Essen, IVG
 Viswanath Katta, Innovative Scientific Solutions Inc.
 R. Kaushik, Gurukul Kangri University
 Nobuyuki Kawahara, Okayama University
 Hiroshi Kawanabe, Kyoto University
 Sean Kearney, Sandia National Lab
 Martin Keller, Chalmers University of Technology
 Andreas Kempf, Universität Duisburg Essen
 David Kessler, Naval Research Laboratory
 Imad Khalek, Southwest Research Institute
 Boris Khasainov, Institute PPRIME-CNRS
 Renza Khatami, Northeastern University
 Johannes Kiefer, University of Aberdeen
 Masao Kikuchi, JAXA
 Pia Kilpinen, Åbo Akademi University
 Daejoong Kim, Sogang University
 Nam Il Kim, Chung-Ang University
 Wookyoung Kim, United Technologies Research Center
 Yongmo Kim, Hanyang University
 Kuniyuki Kitagawa, Nagoya University
 Toshiaki Kitagawa, Kyushu University
 Alexey Kiverin, Joint Institute for High Temperatures of RAS
 Charles B. Kiyanda, Los Alamos National Lab, Concordia University
 Lars Kjåldam, VTT Technical Research Centre of Finland
 Michael Klassen, Combustion Science and Engineering
 Rudolph Klemmens, Warsaw University of Technology
 Alexander Kliimenco, University of QLD
 Konstantin V. Klinkov, University of Bremen
 Stephen Klippenstein, Argonne National Laboratory
 Reinhold Kneer, RWTH Aachen University
 Omar Knio, Duke University
 Edward Knudsen, Bosch Research & Technology Center
 Vadim Knyazev, Catholic University of America
 Denis Knyazkov, Novosibirsk State University
 Hideaki Kobayashi, Tohoku University
 Markus Köhler, German Aerospace Center (DLR)
 Katharina Kohse-Höinghaus, Bielefeld University
 Jim Kok, IIAV
 Sage Kokjohn, University of Wisconsin-Madison
 Hemanth Kolla, Sandia National Laboratories
 Shigeo Kondo, AIST
 Song-Chang Kong, Iowa State University
 Alexander Konnov, Lund University
 Heeseok Koo, Seoul National University
 Sanghoon Kook, University of New South Wales
 Larry Kostuk, University of Alberta
 Umit Koçlu, Missouri University of Science and Technology
 Markus Kraft, University of Cambridge
 J.C. Kramlich, University of Washington
 Werner Krebs, Siemens AG
 Sundar Rajan Krishnan, Mississippi State University
 Andreas Kronenburg, University of Stuttgart
 Sergey Kudriakov, CEA/Saclay
 Waruna Kulatilaka, Spectral Energies, LLC
 Rohit Kulkarni, Alstom
 Kamal Kumar, University of Connecticut
 Sudarshan Kumar, IIT Bombay
 Kenneth K. Kuo, Pennsylvania State University
 Vadim Kurdyumov, CIEMAT
 Ryoichi Kurose, Kyoto University
 Kazunori Kuwana, Yamagata University
 Mike Kuznetsov, Karlsruhe Institute of Technology
 Oh Chae Kwon, Sungkyunkwan University
 Philip Kwong, University of Adelaide
 Dimitrios Kyritsis, University of Illinois-Urbana-Champaign
 Guilhem Lacaze, Sandia National Laboratories
 Deanna Lacoste, Ecole Centrale Paris
 K.N. Lakshmisha, Indian Institute of Science
 Cecilia Lam, Natural Resources
 Nathalie Lamoureux, Université Lille1, CNRS
 Magin Lapuerta, University of Castilla-La Mancha
 Chris Lautenberger, Reax Engineering Inc.
 Chung K. Law, Princeton University
 Malcolm Lawes, University of Leeds
 Chris Lawn, Queen Mary University
 Patrick Leclercq, DLR- German Aerospace Center
 Vivien Lecoustre, University of Maryland
 Bok Jik Lee, University of Cambridge
 Chang Sik Lee, Hanyang University
 Chia-Fon Lee, University of Illinois at Urbana-Champaign
 Jeremiah Lee, United Technologies Research Center – UTC
 John H.S. Lee, McGill University
 Kyeong Lee, Argonne National Laboratory
 Seong-Young Lee, Michigan Technological University
 Tonghun Lee, University of Illinois at Urbana-Champaign
 Uendo Lee, Korea Institute of Industrial Technology
 Guillaume Legros, University Pierre-et-Marie Curie
 Jiao Lei, University of Science and Technology of China
 Alfred Leipertz, Universität Erlangen-Nürnberg
 Fabrice Lemoine, Université de Lorraine
 Walter R. Lempert, Ohio State University
 Gyoergy Lendvay, Hungarian Academy of Sciences
 Bertrand Leroux, Air Liquide
 Yiannis Levendis, Northeastern University
 Howard Levinsky, University of Groningen
 Yeshayahou Levy, Israel Institute of Technology
 Juan Li, Nanjing Normal University
 Qinghai Li, Tsinghua University
 Shuiqing Li, Tsinghua University
 Suhui Li, GE Global Research
 Wenjun Li, Exxon Mobil Research and Engineering Company
 Yuyang Li, University of Science and Technology of China
 Zhengqi Li, Harbin Institute of Technology
 Zhenshan Li, Tsinghua University
 Mikhail Liberman, KTH Royal Institute of Technology
 Tim Lieuwen, Georgia Institute of Technology
 Assa Lifshitz, Hebrew University of Jerusalem
 JoAnn S. Lighty, University of Utah
 David Lignell, Brigham Young University
 Gregory Lilik, Sandia National Laboratories
 William P. Linak, United States EPA
 R.P. Lindstedt, Imperial College
 Mark Linne, Chalmers University
 Gregory Linteris, NIST
 Andrei Lipatnikov, Chalmers University
 Fengshan Liu, National Research Council
 Kai Liu, Cummins Combustion Research
 Naian Liu, University of Science and Technology
 Slawo Lomnicki, Louisiana State University
 Marshall B. Long, Yale University
 Terese Løvås, Norwegian University of Science and Technology
 Tianfeng Lu, University of Connecticut
 Kun Luo, Zhejiang University
 Bin Ma, Yale University
 Lin Ma, University of Leeds
 Tingguang Ma, Oklahoma State University
 Ulrich Maas, Karlsruhe Institute for Technology
 John C. Mackie, University of Sydney
 Gaetano Magnotti, Sandia National Laboratories
 Shankar Mahalingam, University of Alabama
 Yasser Mahmoudi, Delft University of Technology
 Julien Manin, Sandia National Laboratories
 John Mantzaras, Paul Scherrer Institute
 Samuel Manzello, NIST
 Anthony J. Marchese, Colorado State University
 Amir Mardani, AE Sharif
 Stephen Margolis, Sandia National Laboratories
 Sathesh Mariappan, Indian Institute of Technology Kanpur
 Matti Maricq, Ford Motor Company
 Andrew J. Marquis, Imperial College London
 Francesco Marra, Istituto di Ricerca sulla Combustione
 Michele Marrocco, ENEA
 André Marshall, University of Maryland
 Paul Marshall, University of North Texas
 J.B. Martz, University of Michigan
 Kaoru Maruta, Tohoku University
 Assaad Masri, University of Sydney
 Patrizio Massoli, Istituto Motori- CNR
 Marc Massot, Ecole Centrale Paris
 Epaminondas Mastorakos, University of Cambridge
 Moshe Matalon, University of Illinois-Urbana-Champaign
 Olivier Mathieu, Texas A&M University
 Akiko Matsuo, Keio University

Fabian Mauss, BTU Cottbus
 Sara McAllister, USDA Forest Service
 Randall McDermott, National Institute of Standards and Technology
 Charles McEnally, Yale University
 Kevin McGrattan, National Institute of Standards and Technology
 Keith McManus, GE Global Research Center
 Chris Mealy, United States Navy
 Alexander Mebel, Florida International University
 Paul Medwell, University of Adelaide
 Marco Mehl, Lawrence Livermore National Laboratory
 Ranjan S. Mehta, CFD Research Corporation
 Wolfgang Meier, DLR Stuttgart
 M. Pinar Menguc, Özyeğin University
 Shyam Menon, University of Southern California
 Suresh Menon, Georgia Institute of Technology
 Wilson Merchan-Merchan, University of Oklahoma
 Bart Merci, Ghent University
 Xavier Mercier, CNRS-PC2A
 Rémy Mével, California Institute of Technology
 Jean-Baptiste Michel, IFPEN
 Paul Miles, Sandia National Laboratory
 Fletcher Miller, San Diego State University
 J. Houston Miller, George Washington University
 James Miller, Argonne National Laboratory
 Joseph Miller, Air Force Research Laboratory
 Richard Miller, Clemson University
 Sergey Minaev, Engineering School FEPU
 Manickam Minakshi, Murdoch University
 Yuki Minamoto, St. John's College
 Patrizia Minutolo, CNR
 Reginald E. Mitchell, Stanford University
 Constandinos Mitsingas, University of Illinois-Urbana Champaign
 Gaurav Mittal, University of Akron
 Akira Miyoshi, University of Tokyo
 Yasuhiro Mizobuchi, Japan Aerospace Exploration Agency
 Jonas P. Moeck, Technische Universität Berlin
 Alejandro Molina, National University of Colombia
 Penelope Monkhouse, Heidelberg University
 Aimee Morgans, Imperial College London
 Osamu Moriue, Kyushu University
 Sebastian Mosbach, University of Cambridge
 Jean-Michel Most, CNRS-ENSMA
 Vincent Moureau, CORIA-CNRS
 Charles J. Mueller, Sandia National Laboratories
 Michael Mueller, Princeton University
 Alexander Mukasyan, University of Notre Dame
 Achintya Mukhopadhyay, Jadavpur University
 Ramakanth Munipalli, HyPerComp Inc.
 Eiichi Murase, Kyushu University
 T. M. Muruganandam, IIT Madras
 Mark Musculus, Sandia National Laboratories
 Lawrence Muzio, FERCO
 Chitralkumar Naik, Reaction Design Inc.
 Sameer Naik, Purdue University
 Masaya Nakahara, Ehime University
 Hisashi Nakamura, Tohoku University
 Yuji Nakamura, Hokkaido University
 Shinji Nakaya, University of Tokyo
 Ichiro Naruse, EcoTopia Science Institute
 Graham Nathan, University of Adelaide
 Salvador Navarro-Martinez, Imperial College
 Vedha Nayagam, NASA Glenn Research Center
 Iliyana Naydenova, Technical University of Sofia
 Sergio Negro, University of Toronto
 Peter F. Nelson, Macquarie University
 Serguei Nester, Cabot Corporation
 Hoi Dick Ng, Concordia University
 André Nicolle, IFPEN
 Franck Nicoud, University of Montpellier
 Ulrich Niemann, University of California, San Diego
 Kyle Niemeyer, Oregon State University
 Stephen Niksa, Niksa Energy Associates LLC
 Shinnosuke Nishiki, Kagoshima University
 Makihito Nishioka, University of Tsukuba
 Nicolas Noiray, Alstom
 Berthold Noll, DLR Stuttgart
 Hiroshi Nomura, Nihon University
 William Northrop, University of Minnesota
 Vasily Novozhilov, University of Ulster
 Jacqueline O'Connor, Penn State University

Joseph Oefelein, Sandia National Laboratories
 Matthew Oehlschlaeger, RPI
 Yasuhiro Ogami, Akita Prefectural University
 Chang Bo Oh, Pukyong National University
 Hideo Ohtani, Yokohama National University
 Yasushi Oka, Yokohama National University
 Keiichi Okai, University of Tokyo
 Sandra Olson, NASA
 Timothy Ombrello, US Air Force Research Laboratory
 Elaine Oran, University of Maryland
 Patrick Obwald, German Aerospace Center
 Francois-Xavier Ouf, IRSN
 Bedii Özdemir, Istanbul Technical University
 Samuel Paolucci, University of Notre Dame
 Roussos Papagiannakis, Hellenic Air Force Academy
 Miltiadis Papalezandris, University Louvain
 Alessandro Parente, ULB
 Jeong Park, Pukyong National University
 Suhan Park, Hanyang University
 Andrzej Pekalski, Shell
 Perrine Pepiot, Cornell University
 Cécile Pera, IFP Energies Nouvelles
 Peter Perez-Diaz, GE Global Research
 Federico Perini, University of Wisconsin-Madison
 Oren Petel, Carleton University
 Bernhard Peters, University of Luxembourg
 Eric L. Petersen, Texas A&M University
 Brian Peterson, Technische Universität Darmstadt
 Sebastian Pfadler, Siemens AG
 Michael Pfitzner, Bundeswehr University Munich
 Lyle Pickett, Sandia National Laboratories
 Laurent Pillier, CNRS-PC2A
 Michael Pilling, University of Leeds
 Thomas Pino, Université Paris-Sud
 Sarma Pisupati, Penn State University
 Heinz Pitsch, RWTH Aachen University
 Robert Pitz, Vanderbilt University
 William J. Pitz, Lawrence Livermore National Laboratory
 Igor Plaksin, University of Coimbra
 Thierry Poinot, CNRS
 Alexei Poludnenko, Naval Research Laboratory
 Stephen B. Pope, Cornell University
 Jacobo Porteiro, University of Vigo
 Jason Porter, Colorado School of Mines
 Mohamed Pourkashanian, University of Leeds
 Joseph Powers, University of Notre Dame
 Hugues Pretrel, IRSN
 Fei Qi, University of Science and Technology of China
 Li Qiao, Purdue University
 Yu Qiao, Huazhong University of Science and Technology
 James G. Quinieri, University of Maryland
 Vasudevan Raghavan, IIT Madras
 Raffaele Ragucci, IRC CNR
 Abhijeet Raj, Petroleum Institute
 Mandhapati Raju, Convergent Science Inc
 Venkat Raman, University of Texas at Austin
 A. Ramesh, IIT Madras
 Juan Ramos, Universidad de Malaga
 Ali S. Rangwala, Worcester Polytechnic Institute
 Brent Rankin, Innovative Scientific Solutions, Inc
 Eliseo Ranzi, Politecnico di Milano
 Pratap Rao, Worcester Polytechnic Institute
 Xing Rao, Michigan State University
 Artur Ratkiewicz, University of Bialystok
 Albert Ratner, University of Iowa
 R. V. Ravikrishna, IISc
 Larry Redekopp, University of Southern California
 Robert Reeves, Sandia National Laboratories
 Jonathan Regele, Iowa State University
 Rolf Reitz, University of Wisconsin-Madison
 Ning Ren, FM Global
 Zhuyin Ren, Tsinghua University
 Michael Renfro, University of Connecticut
 Bruno Renou, CORIA
 Pedro Reszka, Universidad Tecnica Federico Santa Maria
 Julien Réveillon, CORIA
 Eleonore Riber, CERFACS
 Guillaume Ribert, CNRS
 Edward Richardson, University of Southampton
 Henning Richter, Nano-C Inc

Uwe Riedel, Institut für Verbrennungstechnik
Daniel Roberts, CSIRO
William Roberts, King Abdullah University of Science and Technology
Vincent Robin, Institut Supérieur de l'Aéronautique et de l'Espace
Jose Rodrigues-Fernandez, UCLM-Universidad de Castilla-La Mancha
Dirk Roekaerts, Delft University of Technology
Paul Ronney, University of Southern California
Brandon Rotavera, Sandia National Laboratories
David Rothamer, University of Wisconsin-Madison
Fernando Rubiera, INCAR-CSIC
Adam Ruggles, Sandia National Labs
Anthony Ruiz, Sandia National Labs
Francisco Ruiz, Illinois Institute of Technology
Jaakko Saastamoinen, VTT Technical Research Center of Finland
Pino Sabia, Institute of Research on Combustion
Justin Sabourin, Physical Sciences, Inc.
Amsini Sadiki, EKT – Darmstadt University of Technology
Abhishek Saha, Princeton University
Kozo Saito, University of Kentucky
Antonio Sanchez, Universidad Carlos III de Madrid
Rodrigo Sanchez-Gonzalez, Dept. of Chemistry at Texas A&M University
Alexander Santamaria, University of Antioquia
Paul-Antoine Santoni, Università di Corsica Pasquale Paoli
Robert Santoro, Pennsylvania State University
Josep Sanz-Argent, Universidad Castilla-La Mancha
Mani Sarathy, KAUST
Richard Saurel, PolyTech Marseille
Alexei Saveliev, NCSU
Robert Sawyer, University of California at Berkeley
Priyank Saxena, Solar Turbines
Sergei Sazhin, University of Brighton
Fabrizio Scala, CNR
Heiko Schmidt, Brandenburg University of Technology
Thomas Schmitt, CNRS
Ingmar Schoegi, Louisiana State University
Thierry Schuller, CNRS
Christof Schulz, University of Duisburg-Essen
Douglas Schwer, Naval Research Laboratory
David Sedarsky, Chalmers University of Technology
Thomas Seeger, Universität Siegen
Daisuke Segawa, Osaka Prefecture University
Reinhard Seiser, University of California at San Diego
Laurent Selle, Institute of Fluid Mechanics of Toulouse
Baris A. Sen, Pratt & Whitney-United Technologies
Joseph Senecal, Kiddie-Fenwal
Osvalda Senneca, C.N.R.
Zeynep Serinyel, CNRS Orleans
Kalyansundaram Seshadri, University of California at San Diego
Tom Settersten, Sandia National Labs
Seyed-A Seyed-Reihani, University of Illinois – Urbana-Champaign
Christopher R. Shaddix, Sandia National Labs
Evgeny Shafirovich, The University of Texas at El Paso
Tariq Shamim, Masdar Institute of Science and Technology
Jaishree Sharma, PSU & Siemens Energy Inc
Benjamin D. Shaw, University of California
Alexander K. Shchekin, St. Petersburg State University
David Sheen, National Institute of Standards and Technology
Changdong Sheng, Southeast University
Joseph E. Shepherd, California Institute of Technology
Daisuke Shimokuri, Hiroshima University
Masayasu Shimura, Tokyo Institute of Technology
Junji Shinjo, Japan Aerospace Exploration Agency, Brunel University
Andrey Shmakov, Voevodsky Institute of Chemical Kinetics & Combustion
Mark Short, Los Alamos National Lab
Vladimir Shvartsberg, Institute of Chemical Kinetics & Combustion
Shengyang Shy, National Central University
Volker Sick, University of Michigan
Geoff Silcox, University of Utah-Dept. of Chemical Engineering
Camilo Silva, Technische Universität München
Joel Silver, Southwest Sciences, Inc.
Albert Simeoni, University of Edinburgh
John Simmie, National University of Ireland
Satbir Singh, Carnegie Mellon University
William A. Sirignano, University of California at Irvine
Baptiste Sirjean, University of Lorraine
Raghu Sivaramakrishnan, Argonne National Laboratory
Magnus Sjöberg, Sandia National Labs
Scott Skeen, Sandia National Laboratory
Trygve Skjold, GexCon AS
Nadezda Slavinskaya, Institute of Combustion Technology, DLR
Gregory Smith, SRI International
Mitchell Smooke, Yale University
Alexander Snegirev, St. Petersburg State Polytechnic University
Andrzej Sobiesiak, University of Windsor
Roberto Solimene, National Research Council
Sankar K. Som, Indian Institute of Technology
Steven F. Son, Purdue University
Giancarlo Sorrentino, CNR-Institute of Research on Combustion
Akira Sou, Kobe University
Michael Spearpoint, University of Canterbury
Ezio Spessa, Politecnico di Torino
S. Sreedhara, Indian Institute of Technology
Kalyan Kumar Srinivasan, Mississippi State University
Adam Steinberg, University of Toronto
Daniel Steinhurst, Nova Research Inc
Björn Stelzner, Technische Universität Bergakademie Freiberg
Mark Stewart, Pacific Northwest National Laboratory
Michael Stöhr, German Aerospace Center (DLR)
Stanislav Staliarov, University of Maryland
Vladimir Strezov, Macquarie University
Andrea Strzelec, Texas A&M University
Etienne Studer, CEA
Priya Subramanian, Max Planck Institute for Dynamics
Hyun Kyu Suh, Kongju National University
R.I. Sujith, Indian Institute of Technology Madras
Hongyan Sun, Air Force Research Laboratory
Jinhua Sun, University of Science & Technology of China
Wenting Sun, Georgia Institute of Technology
Peter Sunderland, University of Maryland
Chih-Jen Sung, University of Connecticut
James Sutherland, University of Utah
Jeffrey Sutton, Ohio State University
Masataro Suzuki, Nagaoka University Technology
Sayaka Suzuki, National Institute of Standards & Technology
Yuji Suzuki, The University of Tokyo
Nedunchezian Swaminathan, Cambridge University
Milan Szori, Szegedi Tudományegyetem
James Szybist, Oak Ridge National Laboratory
Craig Taatjes, Sandia National Laboratories
Fumiaki Takahashi, Case Western Reserve University
Shuhei Takahashi, Gifu University
Franco Tamanini, FM Global
Mitsuaki Tanabe, Nihon University
Mamoru Tanahashi, Tokyo Institute of Technology
Farouk Tanvir, University of South Carolina
Alex M.K.P. Taylor, Imperial College London
Brian Taylor, U.S. Naval Research Laboratory
Luis Tay-Wo-Chong, Alstom Switzerland
Andrzej Teodorczyk, Warsaw University of Technology
Dominique Thevenin, Otto-Von-Guericke-Universität Magdeburg
Murray Thomason, University of Toronto
Stefan Thynell, Penn State University
Zhao Feng Tian, University of Adelaide
Zhen-Yu Tian, Chinese Academy of Sciences
James S. T'ien, Case Western Reserve University
Alison S. Tomlin, University of Leeds
Matteo Tommasini, Politecnico di Milano
Kenichi Tonokura, University of Tokyo
Jose L. Torero, University of Queensland, Australia
Hiroyuki Torikai, Hiroshima University
Luca Tosatto, MIT
Pal Toth, Institute for Clean and Secure Energy
Janos Toth, Budapest University of Technology and Economics
Elisa Toulson, Michigan State University
Robert Tranter, Argonne National Laboratory
Dale Tree, Brigham Young University
Antonio Tregossi, CNR Institute of Research in Combustion
Jürgen Troe, GWDG
Arnaud Trounev, University of Maryland
Karine Truffin, IFP Energies
Wing Tsang, NIST
Stephen Tse, Rutgers University
Kazuya Tsuboi, Okayama University
Nobuyuki Tsuboi, Kyushu Institute of Technology
Mitsuhiro Tsue, University of Tokyo
Takashi Tsuruda, Akita Prefectural University
Mark J. Tummers, TU Delft University of Technology
Toshihisa Ueda, IJ4U
Kentaro Umeki, Lulea University of Technology
Akira Umemura, Nagoya University

Javier Urzay, Stanford University
 Knut Vagsther, Telemark University College
 Mauro Valorani, Università di Roma La Sapienza
 Philip van Eyk, The University of Adelaide
 Kevin Van Geem, Universiteit Gent
 Jeroen van Oijen, Eindhoven University of Technology
 Randy Vander Wal, Penn State University
 Guillaume Vanhove, University of Lille
 Anatoly Vasiliev, Lavrentyev Institute of Hydrodynamics SB RAS
 Prabhakar Venkateswaran, Iowa State University
 Steven Verstockt, Ghent University
 Luc Vervisch, CORIA
 Denis Veynante, Ecole Centrale Paris-CNRS
 Bernard Veyssiere, ENSMA National School of Aeronautics & Mechanical
 Ronan Vicquelin, Ecole Centrale Paris
 Pierre Vidal, ENSMA National School of Aeronautics & Mechanical
 Xavier Viegas, Universidad de Coimbra
 Kornio Viktor, Eindhoven University of Technology
 Angela Violi, University of Michigan
 Florent Virot, ENSMA National School of Aeronautics & Mechanical
 Stefan Voss, TU Bergakademie Freiberg
 Steven Wagner, Technische Universität Darmstadt
 Guanghua Wang, GE Global Research Center
 Hai Wang, Stanford University
 Haifeng Wang, Purdue University
 Jianping Wang, Peking University
 Peiyong Wang, Xiamen University
 Qingsong Wang, University of Science and Technology of China
 Yi Wang, FM Global
 Hiroaki Watanabe, CRIEPI
 Hirotatsu Watanabe, Tokyo Institute of Technology
 Bryan Weber, University of Connecticut
 Roman Weber, Institute of Energy Process Engineering and Fuel Technology
 Joseph A. Wehrmeyer, Arnold Air Force Base
 Oliver Welz, Sandia National Laboratories
 Jennifer Wen, University of Warwick
 Michael Wensing, Friedrich-Alexander University, Erlangen
 Richard West, Northeastern University
 Charles K. Westbrook, Lawrence Livermore National Laboratory
 Phillip R. Westmoreland, North Carolina State University
 Kevin Whitty, The University of Utah
 Indrek Wichman, Michigan State University
 Stefan Will, Universität Erlangen-Nürnberg
 Alan Williams, University of Leeds
 Benjamin Williams, University of Oxford
 Forman Williams, University of California at San Diego
 Franz Winter, Vienna University of Technology
 Irenaeus Wloka, University of Duisburg-Essen
 Piotr Wolanski, Warsaw University of Technology
 Sang Hee Won, Princeton University
 Margaret S. Wooldridge, University of Michigan
 Mary J. Wornat, Louisiana State University
 Hongwei Wu, Curtin University
 Ming-Hsun Wu, National Cheng Kung University
 Jun Xia, Brunel University
 Jack Xin, University of California, Irvine
 Yuxuan Xin, Princeton University
 Minghou Xu, Huazhong University of Science and Technology
 Hiroshi Yamasaki, Nihon University
 Yong Yan, University of Kent
 Bin Yang, Tsinghua University
 Haiping Yang, Huazhong University of Science and Technology
 Hong Yao, Huazhong University of Science and Technology
 Qiang Yao, Tsinghua University
 Loo Yap, Flame Tech
 Kenji Yasunaga, National Defense Academy of Japan
 C.L. Yeh, Feng Chia University
 Richard A. Yetter, Penn State University
 Chun-Yang Yin, Murdoch University
 Jack Yoh, Seoul National University
 Takeshi Yokomori, Keio University
 Jerome Yon, CNRS, Université et INSA de Rouen
 Chun Sang Yoo, Ulsan National Institute of Science and Technology
 Ji Hyung Yoo, University at Buffalo
 Akira Yoshida, Tokyo Denki University
 Ryo Yoshiie, Nagoya University
 Xiaoqing You, Tsinghua University
 Gregory Young, U.S. Navy
 Dunxi Yu, State Key Laboratory of Coal Combustion
 Hong-Zeng Yu, FM Global
 Kenneth Yu, University of Maryland
 Yun Yu, Curtin University
 Lili Yuliaty, Brawijaya University
 Shaye Yungster, NASA Glenn Research Center
 Michael Zachariah, University of Maryland
 Judit Zádor, Sandia National Laboratories
 Nikolaos Zarzalis, Karlsruhe Institute of Technology
 Yuri Zeigarnik, Russian Academy of Science
 Wei Zeng, Sandia National Laboratories
 Stephen Zeppieri, United Technologies Research Center
 Dongke Zhang, The University of Western Australia
 Feng Zhang, University of Science and Technology of China
 Hai Zhang, Tsinghua University
 Jingwei Zhang, Conoco Phillips
 Lian Zhang, Monash University
 Lidong Zhang, University of Science and Technology of China
 Mingchuan Zhang, Shanghai Jiao Tong University
 Yu Zhang, Navistar Inc
 YuYin Zhang, Institute of Automotive Engineering
 Dan Zhao, Nanyang Technological University Singapore
 Haibo Zhao, Huazhong University of Science and Technology
 Xiaolin Zheng, Stanford University
 Chongwen Zhou, National University of Ireland in Galway
 Hao Zhou, Institute for Thermal Power Engineering
 Huaichun Zhou, Tsinghua University
 Yuegui Zhou, Shanghai Jiao Tong University
 Huayang Zhu, Colorado School of Mines
 Min Zhu, Tsinghua University
 Lars Zigan, Institute of Engineering Thermodynamics
 Laurent Zimmer, Ecole Centrale Paris
 Ratiba Zitoun, National School of Aeronautics and Mechanical
 Nico Zobel, Fraunhofer Institute for Factory Operation and Automation IFF.

WORK-IN-PROGRESS POSTERS

Matthias Ihme, Stanford University, USA Ahren Jasper, Sandia National Laboratories, USA Judit Zádor, Sandia National Laboratories, USA

HOST COMMITTEE

Chris Shaddix, Chair - Sandia National Laboratories
 Melissa Betz - Sandia National Laboratories
 Marc Day - Lawrence Berkeley National Lab
 Matthias Ihme - Stanford University
 Jackie Chen, Co-Chair - Sandia National Laboratories
 Don Lucas - Univ. of California, Berkeley/Lawrence Berkeley National Lab
 Reggie Mitchell - Stanford University

PROGRAM ADVISORY COMMITTEE

Suk Ho Chung, Program Co-Chair, KAUST, Saudi Arabia
 Thierry Poinsot, Program Co-Chair, CNRS, France
 Robert Barlow, Sandia National Laboratories, USA
 Frédérique Battin-Leclerc, CNRS, France
 Jacqueline H. Chen, Sandia National Laboratories, USA
 Philip de Goeij, Eindhoven University, Netherlands
 Philippe Dagaut, CNRS, France
 James Driscoll, University of Michigan, USA
 Fokion Egolfopoulos, University of Southern California, USA
 Katharina Kohse-Höinghaus, University of Bielefeld, Germany
 Kaoru Maruta, Tohoku University, Japan
 Epaminondas Mastorakos, University of Cambridge, UK
 Paul Ronney, University of California, USA
 Volker Sick, University of Michigan, USA
 Jose Torero, University of Edinburgh, UK
 Charles Westbrook, Lawrence Livermore National Laboratory (USA)

Qiang Yao, Tsinghua University, China

EDITORIAL BOARD

EDITORS

Volker Sick, University of Michigan, USA

Alison S. Tomlin, University of Leeds, UK

ASSOCIATE EDITORS

Maria Alzueta, Universidad de Zaragoza, Spain
Frank Behrendt, Berlin Institute of Technology, Germany
Jacqueline H. Chen, Sandia National Laboratories, USA
Mario Costa, Instituto Superior Técnico, Portugal
Henry J. Curran, NUI Galway, Ireland
Pascale Desgroux, Lille University of Science and Technology, France
Olaf Deutschmann, Karlsruhe Institut für Technologie, Germany
Sergey Dorofeev, FM Global, USA
Andreas Dreizler, Technische Universität Darmstadt, Germany
Tiziano Faravelli, Politecnico di Milano, Italy
Carlos Fernandez-Pello, University of California, Berkeley, USA
Jonathan Frank, Sandia National Laboratories, USA
Olivier Gicquel, Ecole Centrale Paris, France
Nils Hansen, Sandia National Laboratories, USA
Daniel Haworth, Pennsylvania State University, USA
Andrew J. Higgins, McGill University, Canada
Satoru Ishizuka, University of Hiroshima, Japan
In-Seuck Jeung, Seoul National University, Korea
Jenny Jones, University of Leeds, UK
Yiguang Ju, Princeton University, USA
Andreas Kempf, Universität Duisburg-Essen
Steve Klippenstein, Argonne National Laboratory, USA
Dimitrios Kyritsis, University of Illinois, USA
Alexander Konnov, Lund University, Sweden
Mitsuo Koshi, University of Tokyo, Japan

K.N. Lakshmisha, Indian Institute of Science, India
Howard Levinsky, University of Groningen, Netherlands
Tim Lieuwen, Georgia Institute of Technology, USA
Greg Linteris, NIST, USA
Terese Løvås, Norwegian University of Science and Technology, Norway
Atsushi Makino, Japan Aerospace Exploration Agency, Japan
John Mantzaras, Paul Scherrer Institute, Switzerland
Assaad Masri, University of Sydney, Australia
Keith McManus, GE Corporate Research and Development, USA
Masato Mikami, Yamaguchi University, Japan
Alejandro Molina, National University of Colombia, Columbia
Joseph Oefelein, Sandia National Laboratories, USA
Matthias Olzmann, Karlsruhe Institut für Technologie, Germany
Fei Qi, University of Science and Technology of China, China
Guillermo Rein, Imperial College London, UK
David Reuss, University of Michigan, USA
Mani Sarathy, KAUST, Saudi Arabia
Christof Schulz, Universität Duisburg-Essen, Germany
Kal Seshadri, University of California, San Diego, USA
Leonardo Tognotti, University of Pisa, Italy
Arnaud Trounev, University of Maryland, USA
Tamas Turanyi, Eötvös University, Hungary
Denis Veynante, École Centrale Paris, France
Hai Wang, Stanford University, USA
Min Xu, Shanghai Jiao Tong University, China

BERNARD LEWIS FELLOWSHIP COMMITTEE

Matthew Oehlschlaeger, Chair, Rensselaer Polytechnic Institute, USA
Alessio Frassoldati, Politecnico di Milano, Italy
Xin He, Tsinghua University, China

Olivier Herbinet, LRGP, CNRS, France
Angela Violi, University of Michigan, USA
Xiaolin Zheng, Stanford University, USA

GOLD MEDAL AWARD NOMINATIONS COMMITTEE

Mara de Joannon, Chair, IRC-CNR, Italy
Pascale Desgroux, University of Lille 1/CNRS, France
Osamu Fujita, Hokkaido University, Japan
John Mantzaras, Paul Scherrer Institute, Switzerland

Graham Nathan, University of Adelaide, Australia
Elaine Oran, University of Maryland, USA
Ishwar Puri, McMaster University, Canada

GOLD MEDAL AWARD SELECTION COMMITTEE

Sébastien Candel, Chair, CNRS, Ecole Centrale Paris, France
Andreas Dreizler, Technische Universität Darmstadt
Brian S. Haynes, The University of Sydney, Australia
Simone Hochgreb, University of Cambridge, UK

Hideaki Kobayashi, Tohoku University, Japan
Phillip R. Westmoreland, North Carolina State University, USA
Forman Williams, University of California, USA
Margaret S. Wooldridge, University of Michigan, USA

SILVER MEDAL AWARDS COMMITTEE

Rob Barlow, Co-Chair, Sandia National Laboratories, USA
Frédérique Battin-Leclerc, Co-Chair, CNRS, France
Kaoru Maruta, Co-Chair, Tohoku University, Japan
Nabiha Chaumeix, CNRS-Orleans, France
John Dold, University of Manchester, UK
Andreas Dreizler, Darmstadt University of Technology, Germany
Derek Dunn-Rankin, University of California, Irvine, USA
Tiziano Faravelli, Politecnico di Milano, Italy

Hong Im, KAUST, Saudi Arabia
Ann Karagozian, University of California, Los Angeles, USA
Markus Kraft, Cambridge University, UK
Assaad Masri, University of Sydney, Australia
Ichiro Naruse, Nagoya University, Japan
Murray Thomson, University of Toronto, Canada
Jose Torero, University of Queensland, Australia

INDUSTRY RELATIONS COMMITTEE

Christof Schulz, Chair, University of Duisburg-Essen, Germany
Meredith Colket, United Technologies Research Center, USA

Gautam Kalghati, Saudi Aramco, Saudi Arabia
Min Xu, Shanghai Jiao Tong University, China

MEDIA AND OUTREACH COMMITTEE

Margaret S. Wooldridge, Chair, University of Michigan, USA
Hong Im, King Abdullah University of Science & Technology, Saudi Arabia
Timothy Jacobs, Texas A&M University, USA
Sebastian Kaiser, Universität Duisburg Essen, Germany

Larry Kostiuk, University of Alberta, Canada
Xiaoqing You, Tsinghua University, China
Judit Zádor, Sandia National Laboratories, USA
Johan Zetterberg, Lund University, Sweden

ICISS COMMITTEE

Marcus Aldén, Lund University, Sweden

Henry J. Curran, National University of Ireland, Ireland

Hideaki Kobayashi, Tohoku University, Japan
Xiaolin Zheng, Stanford University, USA

*BERNARD LEWIS FELLOWSHIP
AWARDEES*

CONGRATULATIONS TO:

Casey Allen, Marquette University, USA

Benedetta Franzelli, Stanford University, USA

Carmela Russo, Istituto di Ricerche sulla
Combustione, Italy

Zhandong Wang, University of Science &
Technology of China, China

Fujia Wu, Princeton University, USA

The Bernard Lewis Fellowship was established to encourage high quality research in combustion by young scientists and engineers. These Fellowships are to be awarded at each International Combustion Symposium. Recipients must be either students or combustion scientists who have received their last educational degree within three years, an author on a paper accepted at the Thirty-Fifth Symposium, the presenter of that paper, and a member of The Combustion Institute.

35th INTERNATIONAL SYMPOSIUM ON COMBUSTION
San Francisco, California USA
Monday 4 August 2014

WELCOME – 8:00 am

BREAK

Room	Ballroom A	Ballroom B	Ballroom C	Bayview A	Seacliff A & B	Seacliff C & D	Pacific L & M	Pacific N & O
	Turbulent Premixed and Edge Flames	Laminar Flame Speed I	Oxygenated Fuels	Engine DNS Simulation	CARS, Endoscopes and Tracers	Biomass and Municipal Waste	Flame Spread I	Biomass and Coal Combustion
11:30	Break (15 min)							
Room	Ballroom A	Ballroom B	Ballroom C	Bayview A	Seacliff A & B	Seacliff C & D	Pacific L & M	Pacific N & O
	Turbulent Premixed and Edge Flames	Laminar Flame Speed II	Oxygenated Fuels	Engine DNS Simulation	CARS, Endoscopes and Tracers	Biomass and Municipal Waste	Flame Spread II	Biomass and Coal Combustion
13:00 LUNCH								
Room	Ballroom A	Ballroom B	Ballroom C	Bayview A	Seacliff A & B	Seacliff C & D	Pacific L & M	Pacific N & O
	Topical Review	Turbulent Combustion Models and Validation	Novel Fuels	Ignition and Autoignition in all Conditions	Diagnostics Advanced Techniques	Coal and Oxyfuel Combustion	Fire Research	CLC & Fluidized
15:55	BREAK (30 min)							
Room	Ballroom A	Ballroom B	Ballroom C	Bayview A	Seacliff A & B	Seacliff C & D	Pacific L & M	Pacific N & O
	Unsteady and Turbulent Flames	Laminar Flame Speed IV	Rates Coefficients/ Theory	Ignition and Autoignition in All Conditions	PIV/PLIF	Coal and Oxyfuel Combustion	Fire Research	

TUESDAY, 5 AUGUST 2012								
WELCOME – 8:00 am								
BREAK WiC Coffee Break								
Room	Ballroom A	Ballroom B	Ballroom C	Bayview A	Seacliff A & B	Seacliff C & D	Pacific L & M	Pacific N & O
	Turbulent Premixed Flame Structure	Laminar Premixed and Diffusion Flames	Small Esters and Aldehydes	Acoustically Forced Flames	PAH and Soot Formation	Coal Combustion	Microgravity and Smouldering Combustion	Supersonic Combustion and Ignition
11:20	BREAK (15 mins)							
Room	Ballroom A	Ballroom B	Ballroom C	Bayview A	Seacliff A & B	Seacliff C & D	Pacific L & M	Pacific N & O
	Turbulent Premixed Flame Structure	Laminar Premixed and Diffusion Flames	Small Esters and Aldehydes	Flame Dynamics	PAH and Soot Formation	Catalytic Combustion	Microgravity and Smouldering Combustion	Supersonic Combustion and Ignition
12:50	LUNCH (85 mins)							
Room	Ballroom A	Ballroom B	Ballroom C	Bayview A	Seacliff A & B	Seacliff C & D	Pacific L & M	Pacific N & O
	Topical Review	Laminar Extinction and Edge Flame	Alkenes/Alkanes	Thermoacoustics of Annular Combustor	Diffusion/Soot	Combustion Synthesis and Catalytic Processes	Fire Suppressant	Explosions
15:55	BREAK (20 mins)							
Room	Ballroom A	Ballroom B	Ballroom C	Bayview A	Seacliff A & B	Seacliff C & D	Pacific L & M	Pacific N & O
	Spray and Turbulent Flames	Laminar Extinction and Edge Flame	Branched Aromatics	Flame Dynamics	Soot Engines	Combustion Synthesis and Catalytic Processes		Explosions

WEDNESDAY, 6 August 2012								
WELCOME – 8:00 am								
	BREAK							
Room	Ballroom A	Ballroom B	Ballroom C	Bayview A	Seacliff A & B	Seacliff C & D	Pacific L & M	Pacific N & O
	Turbulent Flame Structure	Laminar Flames and Alcohols	Low Temperature Kinetics	Swirled Combustion	Soot Kinetics and Diagnostics	Spray Flames	Electric Field and Plasma Assisted Combustion	
11:20	BREAK (15 min)							
Room	Ballroom A	Ballroom B	Ballroom C	Bayview A	Seacliff A & B	Seacliff C & D	Pacific L & M	Pacific N & O
	Turbulent Flame Structure	Laminar Flames and Alcohols	Low Temperature Kinetics, Ignition	Swirled Combustion	Soot Kinetics and Diagnostics	Spray Flames	Electric Field and Plasma Assisted Combustion	
12:50	LUNCH (85 min)							
Room	Ballroom A	Ballroom B	Ballroom C	Bayview A	Seacliff A & B	Seacliff C & D	Pacific L & M	Pacific N & O
	Topical Review	Flames in Narrow Channels	Ether and Alcohol Kinetics	Swirl Combustion and Piston Engines	Effects of PAH and Soot Formation	Mild Combustion	Plasma Assisted Combustion I	
15:30	BREAK (20 min)							
Room	Ballroom A	Ballroom B	Ballroom C	Bayview A	Seacliff A & B	Seacliff C & D	Pacific L & M	Pacific N&O
	Turbulent Flames Structure	Laminar Flames Structure	Ether and Alcohol Kinetics	Swirl Combustion and Piston Engines		Mild Combustion	Plasma Assisted Combustion II	

THURSDAY, 7 August 2012

WELCOME – 8:00 am

BREAK

Room	Ballroom A	Ballroom B	Ballroom C	Bayview A	Seacliff A & B	Seacliff C & D	Pacific L & M	Pacific N & O
	Turbulent Flames	Instability and Thermoacoustics	Hydrocarbon Fuels	Droplet and Microgravity Combustion	Soot and Nonparticle Diagnostics	Pool Fire and Fire Modeling	Micro Reactor and Micro-Channel Combustion	Detonation
11:20	BREAK (15 min)							
Room	Ballroom A	Ballroom B	Ballroom C	Bayview A	Seacliff A & B	Seacliff C & D	Pacific L & M	Pacific N & O
	Turbulent Flames	Instability and Thermoacoustics	Hydrocarbon Fuels	Droplet and Microgravity Combustion	Soot and Nonparticle Diagnostics	Pool Fire and Fire Modeling	Micro Reactor and Micro-Channel Combustion	Detonation
12:50	LUNCH (85 min)							
Room	Ballroom A	Ballroom B	Ballroom C	Bayview A	Seacliff A & B	Seacliff C & D	Pacific L & M	Pacific N & O
	Turbulent Flame Structure Analysis	Instabilities in Swirled Flames	Ignition Delay and Flame Speeds for Larger Fuels	LES of Spray Flames	Liquid Propellant	Fire Modeling II	Micro-Channel Combustion	Detonation

FRIDAY, 8 AUGUST 2012								
WELCOME – 8:00 am								
	BREAK (35 min for room conversion)							
Room	Ballroom A	Ballroom B	Ballroom C	Bayview A	Seacliff A & B	Seacliff C & D	Pacific L & M	Pacific N & O
	Flame Dynamics and Critical Phenomenon	Unsteady Flame and Ignition/Extinction	Species Sensing	Piston Engines: Emissions and Diagnostics	Clusters, Particle Inception and Growth	New Approaches and Propellants	Microscale Combustion	Supersonic Combustion
11:20	BREAK (15 min)							
Room	Ballroom A	Ballroom B	Ballroom C	Bayview A	Seacliff A & B	Seacliff C & D	Pacific L & M	Pacific N & O
	Flame Dynamics and Critical Phenomenon	Unsteady Flame and Ignition/Extinction	Species Sensing	Piston Engines: Emissions and Diagnostics	Clusters, Particle Inception and Growth	New Approaches and Propellants	Oxy Fuel Combustion	Supersonic Combustion
12:50	LUNCH (85 min)							
Room	Ballroom A	Ballroom B	Ballroom C	Bayview A	Seacliff A & B	Seacliff C & D	Pacific L & M	Pacific N & O
	Topical Review	Laminar Flame Speed III	Mechanisms and Uncertainty Analysis	Piston Engine Modeling and Emission	Turbulence and Soot	Aluminum Combustion Synthesis	Coal and Biomass	Solid Waste and Emission
15:55	BREAK (20 mins)							
Room	Ballroom A	Ballroom B	Ballroom C	Bayview A	Seacliff A & B	Seacliff C & D	Pacific L & M	Pacific N & O
	Partially Premixed Turbulent Flames		Small Hydrocarbons	Piston Engine Modeling and Emission	Turbulence and Soot			Solid Waste and Emission

35th INTERNATIONAL SYMPOSIUM ON COMBUSTION
San Francisco, California USA
Monday 4 August 2014

WELCOME – 8:00 am
HOTTEL LECTURE–8:30 am

Understanding explosions: From catastrophic accidents to the creation of the universe *Elaine Oran*

Session Chairs: T. Poinso and S.-H. Chung
(Ballrooms on Street Level)

BREAK

Room	Ballroom A	Ballroom B	Ballroom C	Bayview A	Seacliff A & B	Seacliff C & D	Pacific L & M	Pacific N & O
	Turbulent Premixed and Edge Flames <i>Chairs:</i> <i>R.W. Dibble</i> <i>L. Vervisch</i>	Laminar Flame Speed I <i>Chairs:</i> <i>F. Egolfopoulos</i> <i>V. Giovangigli</i>	Oxygenated Fuels <i>Chairs:</i> <i>D.F. Davidson</i> <i>P. Glarborg</i>	Engine DNS Simulation <i>Chairs:</i> <i>O. Colin</i> <i>D.C. Haworth</i>	CARS, Endoscopes and Tracers <i>Chairs:</i> <i>M. Colket</i> <i>S. Kaiser</i>	Biomass and Municipal Waste <i>Chairs:</i> <i>A. Jasper</i> <i>P. Pepiot</i>	Flame Spread I <i>Chairs:</i> <i>C. Fernandez-Pello</i> <i>S.L. Olson</i>	Biomass and Coal Combustion <i>Chairs:</i> <i>M. Costa</i> <i>D. Zhang</i>
10:15	1A01: Investigation of pressure effects on the small scale wrinkling of turbulent premixed bunsen flames <i>R. Fragner, F. Halter, N. Mazellier, C. Chauveau, I. Gökalp</i>	1B01: Uncertainty in stretch extrapolation of laminar flame speed from expanding spherical flames <i>F. Wu, W. Liang, Z. Chen, Y. Ju, C.K. Law</i>	1C01: Some aspects of combustion chemistry of C1-C2 oxygenated fuels in low pressure premixed flames <i>G. Vourliotakis, G. Skevis, M.A. Founti</i>	1D01: Direct numerical simulation of the effect of compression on the flow, temperature and composition under realistic engine conditions <i>M. Schmitt, C.E. Frouzakis, A.G. Tomboulides, Y.M. Wright, K. Boulouchos</i>	1E01: Femtosecond coherent anti-stokes raman scattering thermometry at 5 kHz in a gas turbine model combustor <i>C.N. Dennis, C. Slabaugh, I.G. Boxx, W. Meier, R.P. Lucht</i>	1F01: LIBS measurements and numerical studies of potassium release during biomass gasification <i>H. Fatehi, Y. He, Z. Wang, Z.S. Li, X.-S. Bai, M. Aldén, K.F. Cen</i>	1G01: Experimental validation of a correlation capturing the boundary layer effect on spread rate in the kinetic regime of opposed-flow flame spread <i>S. Bhattacharjee, W. Tran, M. Laue, C. Paolini, Y. Nakamura</i>	1H01: Release of chlorine from the slow pyrolysis of NaCl-loaded cellulose at low temperatures <i>M.U. Rahim, X. Gao, H. Wu</i>
10:35	1A02: LES of turbulent combustion: On the consistency between flame and flow filter scales <i>R. Mercier, V. Moureau, D. Veynante, B. Fiorina</i>	1B02: Laminar burning velocities of premixed nitromethane / air flames: An experimental and kinetic modeling study <i>C. Mounaim-Rousselle, F. Halter, G. Dayma, P. Dagaut, P. Brequigny, T. Dubois</i>	1C02: Unimolecular decomposition of formic and acetic acids: A shock tube / laser absorption study <i>A.E. Elwardany, E.F. Nasir, E. Es-sebbar, A. Farooq</i>	1D02: Ignition in compositionally and thermally stratified <i>n</i> -heptane/air mixtures: A direct numerical simulation study <i>M. Talei, E.R. Hawkes</i>	1E02: Development of temperature evaluation of pure Rotational Coherent Anti-Stokes Raman Scattering (RCARS) spectra influenced by spatial averaging effects <i>Y. Gao, T. Seeger, A. Leipertz</i>	1F02: Experimental study on the coexistent dual slagging in biomass-fired furnaces: Alkali-induced slagging and silicate melt-induced slagging <i>Y. Niu, Y. Zhu, H. Tan, X. Wang, S. Hui, W. Du</i>	1G02: Thermal structure of flame spread in partially premixed atmospheres and effects of fuel Lewis number <i>K. Yamamoto, S. Seo, K. Mori</i>	1H02: Radiative intensity, NO emissions, and burnout for oxygen enriched biomass combustion <i>J. Thornock, D. Tovar, D.R. Tree, Y. Xue, R. Tsiava</i>

Room	Ballroom A	Ballroom B	Ballroom C	Bayview A	Seacliff A & B	Seacliff C & D	Pacific L & M	Pacific N & O
10:55	1A03: Local volumetric dilatation rate and scalar geometries in a premixed methane-air turbulent jet flame <i>L. Cifuentes, C. Dopazo, J. Martín, P. Domingo, L. Vervisch</i>	1B03: On the accurate determination of burning velocities from spherically expanding flames experimental and numerical study of H ₂ /air flames <i>E. Varea, J. Beeckmann, H. Pitsch, Z. Chen, B. Renou</i>	1C03: Ab initio and kinetic modeling studies of formic acid oxidation <i>P. Marshall, P. Glarborg</i>	1D03: Direct numerical simulation of PRF70/air partially premixed combustion under IC engine conditions <i>F. Zhang, R. Yu, X.-S. Bai</i>	1E03: Development of two-beam femtosecond / picosecond one-dimensional Rotational Coherent Anti-Stokes Raman Spectroscopy: Time-resolved probing of flame wall interactions <i>A. Bohlin, M. Mann, B.D. Patterson, A. Dreizler, C.J. Klierer</i>	1F03: Mechanism of chromium oxidation by alkali and alkaline earth metals during municipal solid waste incineration <i>H. Hu, Z. Xu, H. Liu, D. Chen, K. Li, A. Li, H. Yao</i>	1G03: Temperature and CO ₂ fields of a downward spreading flame over thin cellulose: A comparison of experimental and computational results <i>W. Tran, C. Paolini, J.R. Villaraza, S. Bhattacharjee, S. Takahashi</i>	1H03: Combustion of biomass in jet flames <i>R. Weber, Y. Poyraz, A.M. Beckmann, S. Brinker</i>
BREAK								
	Turbulent Premixed and Edge Flames <i>Chairs:</i> <i>R.W. Dibble</i> <i>L. Vervisch</i>	Laminar Flame Speed II <i>Chairs:</i> <i>F. Egolfopoulos</i> <i>V. Giovangigli</i>	Oxygenated Fuels <i>Chairs:</i> <i>D.F. Davidson</i> <i>P. Glarborg</i>	Engine DNS Simulation <i>Chairs:</i> <i>O. Colin</i> <i>D.C. Haworth</i>	CARS, Endoscopes and Tracers <i>Chairs:</i> <i>M. Colket</i> <i>S. Kaiser</i>	Biomass and Municipal Waste <i>Chairs:</i> <i>A. Jasper</i> <i>P. Pepiot</i>	Flame Spread II <i>Chairs:</i> <i>C. Fernandez-Pello</i> <i>S.L. Olson</i>	Biomass and Coal Combustion <i>Chairs:</i> <i>M. Costa</i> <i>D. Zhang</i>
11:45	1A04: Leading edge statistics of turbulent, lean, H ₂ -air flames <i>A. Amato, M.S. Day, R.K. Cheng, J.B. Bell, T.C. Lieuwen</i>	1B04: The curvature Markstein length and the definition of flame displacement speed for stationary spherical flames <i>G.K. Giannakopoulos, M. Matalon, C.E. Frouzakis, A.G. Tomboulides</i>	1C04: Experimental study of the kinetics of ethanol pyrolysis and oxidation behind reflected shock waves and in laminar flames <i>M. Bozkurt, D. Nativel, M. Aghsaee, M. Fikri, N. Chaumeix, C. Schulz</i>	1D04: Modes of reaction front propagation in <i>n</i> -heptane/air mixture with temperature gradient <i>P. Dai, Z. Chen, S. Chen, Y. Ju</i>	1E04: Application of the tracer combination TEA/acetone for multi-parameter laser-induced fluorescence measurements in IC engines with exhaust gas recirculation <i>S. Lind, J. Trost, L. Zigan, A. Leipertz, S. Will</i>	1F04: Effect of MgCl ₂ loading on the evolution of reaction intermediates during cellulose fast pyrolysis at 325 °C <i>D. Liu, Y. Yu, Y. Long, H. Wu</i>	1G04: Flame spread over electric wire with high thermal conductivity metal core at different inclinations <i>L. Hu, Y. Zhang, K. Yoshioka, H. Izumo, O. Fujita</i>	1H04: Fluidized bed gasification of lignite char with CO ₂ and H ₂ O: A kinetic study <i>F. Scala</i>
12:10	1A05: Edge flame structure in a turbulent lifted flame: A direct numerical simulation study <i>S. Karami, M. Talei, E.R. Hawkes, H. Yu</i>	1B05: Experimental and modeling study of the effect of elevated pressure on lean high-hydrogen syngas flames <i>M. Goswami, J.G.H. van Griensven, R.J.M Bastiaans, A.A. Konnov, L.P.H. de Goey</i>	1C05: A shock tube study of CH ₃ OH + OH → products using OH laser absorption <i>L.T. Zaczek, K.-Y. Lam, D.F. Davidson, R.K. Hanson</i>	1D05: A LES methodology based on reduced schemes to compute knocking in internal combustion engines <i>A. Misdariis, O. Vermorel, T. Poinsot</i>	1E05: Three-dimensional flame measurements using fiber-based endoscopes <i>M.W. Kang, X. Li, L. Ma</i>	1F05: Carbonate formation during lignin pyrolysis under CO ₂ and its effect on char gasification <i>H. Watanabe, K. Shimomura, K. Okazaki</i>	1G05: Upward flame spread in large enclosures: Flame growth and pressure rise <i>S.L. Olson, S.A. Gokoglu, D.L. Urban, G.A. Ruff, P.V. Ferkul</i>	1H05: Measurement of particulate matter and trace elements from a coal-fired power plant with a novel electrostatic precipitator <i>C. Wang, X. Liu, D. Li, J. Si, B. Zhao, M. Xu</i>

Room	Ballroom A	Ballroom B	Ballroom C	Bayview A	Seacliff A & B	Seacliff C & D	Pacific L & M	Pacific N & O
12:35	1A06: Heat release imaging in turbulent premixed methane-air flames close to blow-off <i>J. Kariuki, A. Dowlut, R. Yuan, R. Balachandran, E. Mastorakos</i>	1B06: Effect of dilution gas on burning velocity of hydrogen-premixed meso-scale spherical laminar flames <i>M. Nakahara, F. Abe, K. Tokunaga, A. Ishihara</i>	1C06: Adventures on the C ₃ H ₅ O potential energy surface: OH + propyne, OH + allene and related reactions <i>J. Zádor, J.A. Miller</i>	1D06: Combustion regime classification of HCCI/PCCI combustion using Lagrangian fluid particle tracking <i>N. Fukushima, M. Katayama, Y. Naka, T. Oobayashi, M. Shimura, Y. Nada, M. Tanahashi, T. Miyauchi</i>	1E06: Endoscopic temperature imaging in a four-cylinder IC engine via two-color toluene fluorescence <i>C. Gessenhardt, C. Schulz, S.A. Kaiser</i>	1F06: Study on one-dimensional steady combustion of highly densified biomass briquette (Bio-coke) in air flow <i>T. Nakahara, Y. Hui, H. Ito, O. Fujita</i>	1G06: Upslope fire spread through porous forest fuel beds: The role of convection cooling <i>N. Liu, J. Wu, L. Zhang, Z. Deng, K. Sato</i>	1H06: LES of swirl-stabilised pulverised coal combustion in IFRF furnace No.1 <i>G. Olenik, O.T. Stein, A. Kronenburg</i>
LUNCH								
	Invited Topical Review <i>Chairs:</i> <i>S.B. Pope</i> <i>M. Smooke</i>	Turbulent Combustion Models and Validation <i>Chairs:</i> <i>J.A. Sutton</i> <i>D. Veynante</i>	Novel Fuels <i>Chairs:</i> <i>M. Olzmann</i> <i>X. You</i>	Ignition and Autoignition in all Conditions <i>Chairs:</i> <i>H.G. Im</i> <i>M. Musculus</i>	Diagnostics Advanced Techniques <i>Chairs:</i> <i>R.P. Lucht</i> <i>M.W. Renfro</i>	Coal and Oxyfuel Combustion <i>Chairs:</i> <i>B.S. Haynes</i> <i>R.E. Mitchell</i>	Fire Research <i>Chairs:</i> <i>N. Liu</i> <i>G. Rein</i>	CLC & Fluidized <i>Chairs:</i> <i>D. Che</i> <i>B.B. Dally</i>
14:15	1A07/08: Multicomponent transport in laminar flames <i>Vincent Giovangigli</i>	1B07: Large Eddy Simulation of premixed turbulent combustion using approximate deconvolution and explicit flame filtering <i>P. Domingo, L. Vervisch</i>	1C07: Unimolecular decomposition of tetrahydrofuran: Carbene vs. Diradical pathways <i>M. Verdicchio, B. Sirjean, L.S. Tran, P.-A. Glaude, F. Battin-Leclerc</i>	1D07: Ignition delay time measurements behind reflected shock-waves for a representative coal-derived syngas with and without NH ₃ and H ₂ S impurities <i>O. Mathieu, J.W. Hargis, A. Camou, C. Mulvihill, E.L. Petersen</i>	1E07: Simultaneous planar and volume cross-LIF imaging to identify out-of-plane motion <i>S. Meares, V.N. Prasad, M. Juddoo, K.H. Luo, A.R. Masri</i>	1F07: A sophisticated model to predict ash inhibition during combustion of pulverized char particles <i>Y. Niu, C.R. Shaddix</i>	1G07: A study on burning of crude oil in ice cavities <i>H.F. Farahani, X. Shi, A. Simeoni, A.S. Rangwala</i>	1H07: Magnetite loaded carbon fine particles as low-cost CO ₂ adsorbent in a sound assisted fluidized bed <i>M. Alfé, P. Ammendola, V. Gargiulo, F. Raganati, R. Chirone</i>
14:40		1B08: Filtered density function simulation of a realistic swirled combustor <i>N. Ansari, P.A. Strakey, G.M. Goldin, P. Givi</i>	1C08: Effect of furans on particle formation in diffusion flames: An experimental and modelling study <i>M. Sirignano, M. Conturso, A. D'Anna</i>	1D08: A shock tube study of the autoignition characteristics of RP-3 jet fuel <i>C. Zhang, B. Li, F. Rao, P. Li, X. Li</i>	1E08: Interference free spontaneous Raman spectroscopy for measurements in rich hydrocarbon flames <i>G. Magnotti, D. Geyer, R.S. Barlow</i>	1F08: Flamelet model for pulverized coal combustion <i>J. Watanabe, K. Yamamoto</i>	1G08: Chemical characterization of particle emissions from controlled burns of biomass fuels using a high resolution time-of-flight aerosol mass spectrometer <i>L. Qi, D. Cocker III, S. Hosseini, H. Jung, W. Miller, D. Weise, Y. Huang, Z. Zhou</i>	1H08: Modelling rates of gasification of a char particle in chemical looping combustion <i>M.A. Saucedo, J.S. Dennis, S.A. Scott</i>

Room	Ballroom A	Ballroom B	Ballroom C	Bayview A	Seacliff A & B	Seacliff C & D	Pacific L & M	Pacific N & O
	Unsteady and Turbulent Flames <i>Chairs:</i> <i>S.B. Pope</i> <i>M. Smooke</i>	Laminar Flame Speed IV <i>Chairs:</i> <i>L.P.H. de Goey</i> <i>H. Kobayashi</i>	Rates Coefficients/ Theory <i>Chairs:</i> <i>O. Welz</i> <i>J.A. Miller</i>	Ignition and Autoignition in All Conditions <i>Chairs:</i> <i>H.G. Im</i> <i>M. Musculus</i>	PIV/PLIF <i>Chairs:</i> <i>F. Beyrau</i> <i>J. Frank</i>	Coal and Oxyfuel Combustion <i>Chairs:</i> <i>B.S. Haynes</i> <i>R.E. Mitchell</i>	Fire Research <i>Chairs:</i> <i>N. Liu</i> <i>G. Rein</i>	
16:25	1A11: Experimental investigation of Darrieus-Landau instability effects on turbulent premixed flames <i>G. Troiani, F. Creta, M. Matalon</i>	1B11: Experimental and kinetic studies of acetylene flames at elevated pressures <i>X. Shen, X. Yang, J. Santner, J. Sun, Y. Ju</i>	1C11: Kinetic studies of the reaction of atomic sulfur with acetylene <i>S. Ayling, Y. Gao, P. Marshall</i>	1D11: Autoignition behavior of synthetic alternative jet fuels: An examination of chemical composition effects on ignition delays at low to intermediate temperatures <i>D.J. Valco, G. Gentz, C. Allen, M. Colket, T. Edwards, S. Gowdagiri, M.A. Oehlschlaeger, E. Toulson, T. Lee</i>	1E11: Investigation of flame propagation in a partially premixed jet by high-speed-stereo-PIV and acetone-PLIF <i>J. Weinkauff, P. Trunk, J.H. Frank, M.J. Dunn, A. Dreizler, B. Böhm</i>	1F11: Accuracy of the single-film model in the prediction of coal char conversion rates under oxy-fuel and conventional combustion conditions <i>C. Gonzalo-Tirado, S. Jiménez</i>	1G11: An investigation of the detailed flame shape and flame length under the ceiling of channel <i>Z. Gao, J. Ji, H. Wan, J. Sun</i>	
16:50	1A12: Performance of conditional source-term estimation model for LES of turbulent premixed flames in thin reaction zones regime <i>N. Shahbazian, M.M. Salehi, C.P.T. Groth, Ö.L. Gülder, W.K. Bushe</i>	1B12: Influence of the reactant temperature on particle entrained laminar methane – air premixed flames <i>M. Lee, S. Ranganathan, A.S. Rangwala</i>	1C12: Pressure-dependent branching in the reaction of $^1\text{CH}_2$ with C_2H_4 and other reactions on the C_3H_6 potential energy surface <i>L. Ye, Y. Georgievskii, S.J. Klippenstein</i>	1D12: The autoignition of Liquefied Petroleum Gas (LPG) in spark-ignition engines <i>K.J. Morganti, M.J. Brear, G. da Silva, Y. Yang, F.L. Dryer</i>	1E12: 3kHz PIV / OH-PLIF measurements in a gas turbine combustor at elevated pressure <i>I.G. Boxx, C. Slabaugh, P. Kutne, R.P. Lucht, W. Meier</i>	1F12: Effect of minerals on surface morphologies and competitive reactions during char gasification in mixtures of O_2 and CO_2 <i>H. Watanabe, K. Okazaki</i>	1G12: Merging behavior of facade flames ejected from two windows of an under-ventilated compartment fire <i>K. Liu, L. Hu, M.A. Delichatsios, F. Tang, Z. Qiu, L. He</i>	
17:15	1A13: Conditional moment closure modelling for HCCI with temperature inhomogeneities <i>F. Salehia, M. Talei, E.R. Hawkes, C. S. Yoo, T. Lucchini, G. D'Errico, S. Kook</i>	1B13: Experimental and modeling studies of the acetone addition in $\text{H}_2/\text{O}_2/\text{Ar}$ flames at low pressure <i>V. Dias, J. Vandooren, H. Jeanmart</i>	1C13: “Third-body” collision efficiencies for combustion modeling: Hydrocarbons in atomic and diatomic baths <i>A.W. Jasper, C.M. Oana, J.A. Miller</i>	1D13: Development of a skeletal oxidation mechanism for biodiesel surrogate <i>Y. Chang, M. Jia, Y. Li, Y. Zhang, M. Xie, H. Wang, R.D. Reitz</i>	1E13: Investigation on rapid consumption of fine scale unburned mixture islands in turbulent flame via 10 kHz simultaneous CH-OH PLIF and SPIV <i>A. Johchi, Y. Naka, M. Shimura, M. Tanahashi, T. Miyauchi</i>	1F13: Study on N_2O reduction with synthetic coal char and high concentration CO during oxy-fuel combustion <i>C. Wang, Y. Du, D. Che</i>	1G13: Experimental study on behavior of sidewall fires at varying height in a corridor <i>J. Ji, Y. Fu, K. Li, J. Sun</i>	
	17:45: MEMBERS MEETING in Ballroom B				18:00: Young Researcher Mixer at Jillian’s Sport Bar			

TUESDAY, 5 AUGUST 2014

PLENARY LECTURE–8:30 am

Advanced laser diagnostics for an improved understanding of flame wall interactions *Andreas Dreizler and B. Böhm*

Session Chairs: M. Aldén and S.-H. Chung
(Ballrooms on Street Level)

BREAK

WiC Coffee Break –Location will be announced

Room	Ballroom A	Ballroom B	Ballroom C	Bayview A	Seacliff A & B	Seacliff C & D	Pacific L & M	Pacific N & O
	Turbulent Premixed Flame Structure <i>Chairs:</i> <i>B.R. Coriton</i> <i>Ö.L. Gülder</i>	Laminar Premixed and Diffusion Flames <i>Chairs:</i> <i>M.B. Long</i> <i>M.J. Thomson</i>	Small Esters and Aldehydes <i>Chairs:</i> <i>H.J. Curran</i> <i>A. Farooq</i>	Acoustically Forced Flames <i>Chairs:</i> <i>R.W. Pitz</i> <i>T. Schuller</i>	PAH and Soot Formation <i>Chairs:</i> <i>N. Hansen</i> <i>M.J. Wornat</i>	Coal Combustion <i>Chairs:</i> <i>S. Niksa</i> <i>Q. Yao</i>	Microgravity and Smouldering Combustion <i>Chairs:</i> <i>S. Bhattacharjee</i> <i>O. Fujita</i>	Supersonic Combustion and Ignition <i>Chairs:</i> <i>U. Maas</i> <i>M.I. Radulescu</i>
10:05	2A01: Life of flame particles embedded in premixed flames interacting with near isotropic turbulence <i>S. Chaudhuri</i>	2B01: Dominant chemical source and reaction modes in lean H ₂ /air flames <i>M. Ayoobi, I. Schoegl</i>	2C01: The role of prompt reactions in ethanol and methylformate low-pressure flames <i>N.J. Labbe, R. Sivaramakrishnan, S.J. Klippenstein</i>	2D01: Nonlinear dynamics of a self-excited thermoacoustic system subjected to acoustic forcing <i>S. Balusamy, L.K.B. Li, Z. Han, M.P. Juniper, S. Hochgreb</i>	2E01: PAH formation and soot morphology in flames of C ₄ fuels <i>M. Schenk, N. Hansen, H. Vieker, A. Beyer, A. Götzhäuser, K. Kohse-Höinghaus</i>	2F01: Comprehensive numerical modeling of ignition of coal dust layers in different configurations <i>A.K. Sahu, K.A. Joshi, V. Raghavan, A.S. Rangwala</i>	2G01: Phenomenological model of soot production inside a non-buoyant laminar diffusion flame <i>G. Legros, J.L. Torero</i>	2H01: Numerical estimation of thrust performance on rotational detonation engine in a hydrogen-oxygen mixture <i>N. Tsuboi, Y. Watanabe, T. Kojima, A.K. Hayashi</i>
10:30	2A02: On the alignment of principal fluid-dynamic strain-rates with the 3D flamelet-normal in a premixed turbulent V-flame <i>T. Sponfeldner, F. Beyrau, I.G. Boxx, Y. Hardalupas, W. Meier, A.M.K.P. Taylor</i>	2B02: Chemical interactions between 1,2,4-trimethylbenzene and <i>n</i> -decane in doped counterflow gaseous diffusion flames <i>F. Carbone, A. Gomez</i>	2C02: A theoretical kinetics study of the reactions of methylbutanoate with hydrogen and hydroxyl radicals <i>L. Zhang, Q. Chen, P. Zhang</i>	2D02: Wall-temperature effects on flame response to acoustic oscillations <i>D. Mejia, L. Selle, R. Bazile, T. Poinso</i>	2E02: Flame structure of a low-pressure, laminar premixed and lightly sooting acetylene flame and the effect of ethanol addition <i>T. Bierkandt, T. Kasper, E. Akyildiz, A. Lucassen, P. Oßwald, M. Köhler, P. Hemberger</i>	2F02: Interpreting coal conversion under elevated H ₂ pressures with FLASHCHAIN and CBK <i>S. Niksa</i>	2G02: Simplified model to predict the difference between flammability limits of a thin material in normal gravity and in microgravity environment <i>S. Takahashi, T. Ebisawa, S. Bhattacharjee, T. Ihara</i>	2H02: Cavity ignition in supersonic flow by spark discharge and pulse detonation <i>T.M. Ombrello, C.D. Carter, C.-J. Tam, K.-Y. Hsu</i>

Room	Ballroom A	Ballroom B	Ballroom C	Bayview A	Seacliff A & B	Seacliff C & D	Pacific L & M	Pacific N & O
10:55	2A03: Influence of combustion on principal strain-rate transport in turbulent premixed flames <i>A.M. Steinberg, B.R. Coriton, J.H. Frank</i>	2B03: Experimental and kinetic modeling investigation on laminar premixed benzene flames with various equivalence ratios <i>J. Yang, L. Zhao, W. Yuan, F. Qi, Y. Li</i>	2C03: Kinetic studies of methyl acetate pyrolysis and oxidation in a flow reactor and a low-pressure flat flame using molecular-beam mass spectrometry <i>X. Yang, D. Felsmann, N. Kurimoto, J. Krieger, T. Wada, T. Tan, E.A. Carter, K. Kohse-Höinghaus, Y. Ju</i>	2D03: Thermal versus acoustic response of velocity sensitive premixed flames <i>S. Bomberg, T. Emmert, W. Polifke</i>	2E03: Dehydrogenation and growth of soot in premixed flames <i>C. Russo, A. Tregrossi, A. Ciajolo</i>	2F03: Dynamic behavior of sodium release from pulverized coal combustion by phase-selective laser-induced breakdown spectroscopy <i>Y. Yuan, S. Li, Q. Yao</i>	2G03: Microgravity flammability limits of ETFE insulated wires exposed to external radiation <i>A.F. Osorio, K. Mizutani, O. Fujita, C. Fernandez-Pello</i>	2H03: Mixing-related low frequency oscillation of combustion in an ethylene-fueled supersonic combustor <i>Z.-G. Wang, M.-B. Sun, H.-B. Wang, J.-F. Yu, J.-H. Liang, F.-C. Zhuang</i>
BREAK								
	Turbulent Premixed Flame Structure <i>Chairs:</i> <i>B.R. Coriton</i> <i>Ö.L. Gülder</i>	Laminar Premixed and Diffusion Flames <i>Chairs:</i> <i>M.B. Long</i> <i>M.J. Thomson</i>	Small Esters and Aldehydes <i>Chairs:</i> <i>H.J. Curran</i> <i>A. Farooq</i>	Flame Dynamics <i>Chairs:</i> <i>M.P. Juniper</i> <i>L. Selle</i>	PAH and Soot Formation <i>Chairs:</i> <i>N. Hansen</i> <i>M.J. Wornat</i>	Catalytic Combustion <i>Chairs:</i> <i>J. Ellzey</i> <i>Z.-Y. Tian</i>	Microgravity and Smouldering Combustion <i>Chairs:</i> <i>S. Bhattacharjee</i> <i>O. Fujita</i>	Supersonic Combustion and Ignition <i>Chairs:</i> <i>U. Maas</i> <i>M.I. Radulescu</i>
11:35	2A04: Simultaneous multi-species and temperature visualization of premixed flames in the distributed reaction zone regime <i>B. Zhou, C. Brackmann, Z.S. Li, M. Aldén, X.-S. Bai</i>	2B04: Experimental and kinetic modeling study of laminar coflow diffusion methane flames doped with 2-butanol <i>H. Jin, W. Yuan, Y. Wang, Y. Li, F. Qi, A. Cuoci, A. Frassoldati, T. Faravelli</i>	2C04: Kinetics of premixed acetaldehyde + air flames <i>M. Christensen, M.T. Abebe, E.J.K. Nilsson, A.A. Konnov</i>	2D04: The response of stratified swirling flames to acoustic forcing: Performance and limits to G-equation models <i>Z. Han, S. Hochgreb</i>	2E04: Novel aspects in the pyrolysis and oxidation of 2,5-dimethylfuran <i>K. Alexandrino, Á. Millera, R. Bilbao, M.U. Alzueta</i>	2F04: Direct synthesis of supported palladium catalysts for methane combustion by stagnation swirl flame <i>Y. Zong, S. Li, F. Niu, Q. Yao</i>	2G04: Parametric study on the smoldering combustion of a thin solid in a narrow space <i>Y. Uchida, K. Kuwana, G. Kushida</i>	2H04: Weak and strong ignition of hydrogen/oxygen mixtures in shock tube systems <i>K.P. Grogan, M. Ihme</i>
12:00	2A05: Turbulence-chemistry interaction in lean premixed hydrogen combustion <i>A.J. Aspden, M.S. Day, J.B. Bell</i>	2B05: Fuel density effect on near nozzle flow field in small laminar coflow diffusion flames <i>Y. Xiong, M.S. Cha, S.-H. Chung</i>	2C05: High temperature measurements for the rate constants of C ₁ -C ₄ aldehydes with OH in a shock tube <i>S. Wang, D.F. Davidson, R.K. Hanson</i>	2D05: Large Eddy Simulations of multiple transcritical coaxial flames submitted to a high-frequency transverse acoustic modulation <i>L. Hakim, A. Ruiz, T. Schmitt, M. Boileau, G. Staffelbach, S. Ducruix, B. Cuenot, S. Candel</i>	2E05: Influence of substituted furans on the formation of polycyclic aromatic hydrocarbons in flames <i>L.S. Tran, B. Sirjean, P.-A. Glaude, K. Kohse-Höinghaus, F. Battin-Leclerc</i>	2F05: Hetero-homogeneous combustion of syngas mixtures over platinum at fuel-rich stoichiometries and pressures up to 14 bar <i>M. Schultze, J. Mantzaras, F. Grygier, R. Bombach</i>	2G05: Computational smouldering combustion: Predicting the roles of moisture and inert contents in peat wildfires <i>X. Huang, G. Rein, H. Chen</i>	2H05: Ignition by transient hot turbulent jets: An investigation of ignition mechanisms by means of a PDF/REDIM method <i>A. Ghorbani, G. Steinhilber, D. Markus, U. Maas</i>

Room	Ballroom A	Ballroom B	Ballroom C	Bayview A	Seacliff A & B	Seacliff C & D	Pacific L & M	Pacific N & O
12:25	2A06: Structure of a high Karlovitz n -C ₇ H ₁₆ premixed turbulent flame <i>B. Savard, B.D. Bobbitt, G. Blanquart</i>	2B06: A computational and experimental study of coflow laminar methane/air diffusion flames: Effects of fuel dilution, inlet velocity, and gravity <i>S. Cao, B. Ma, B.A.V. Bennett, D. Giassi, D.P. Stocker, F. Takahashi, M.B. Long, M.D. Smooke</i>	2C06: Kinetics of oxidation of cyclohexanone in a jet-stirred reactor: Experimental and modeling <i>Z. Serinyel, C. Togbé, A. Zaras, G. Dayma, P. Dagaut</i>	2D06: A reduced-order model for the onset of combustion instability: Physical mechanisms for intermittency and precursors <i>V. Nair, R. Sujith</i>	2E06: Experimental and kinetic modeling study of premixed o -xylene flames <i>L. Zhao, Z. Cheng, L. Ye, F. Zhang, L. Zhang, F. Qi, Y. Li</i>	2F06: Characterization of the NO-soot combustion process over the La _{0.8} Ce _{0.2} Mn _{0.7} Bi _{0.3} O ₃ catalyst <i>F. Bin, C. Song, G. Lv, X. Li, X. Cao, J. Song, S. Wu</i>	2G06: Experimental study on merged flame characteristics from multifire sources with wood cribs <i>W. Weng, D. Kamikawa, Y. Hasemi</i>	2H06: Numerical study on the spontaneous-ignition features of high-pressure hydrogen released through a tube with burst conditions <i>H.J. Lee, S.D. Kim, S.H. Kim, J.H. Park, I.-S. Jeung</i>
LUNCH								
	Invited Topical Review <i>Chairs:</i> <i>M. Linne</i> <i>J. Shinjo</i>	Laminar Extinction and Edge Flame <i>Chairs:</i> <i>M. Matalon</i> <i>I. Schoegl</i>	Alkenes/Alkanes <i>Chairs:</i> <i>F. Mauß</i> <i>C. Westbrook</i>	Thermoacoustics of Annular Combustor <i>Chairs:</i> <i>J. Driscoll</i> <i>L. Selle</i>	Diffusion/Soot <i>Chairs:</i> <i>A. D'Anna</i> <i>S. Dworkin</i>	Combustion Synthesis and Catalytic Processes <i>Chairs:</i> <i>M. Mansour</i> <i>J. Mantzaras</i>	Fire Suppressant <i>Chairs:</i> <i>E.L. Petersen</i> <i>F. Takahashi</i>	Explosions <i>Chairs:</i> <i>A.R. Kasimov</i> <i>I.-S. Jeung</i>
14:15	2A07/08: The role of separation of scales in the description of spray combustion <i>Antonio Sanchez</i> <i>J. Urzay,</i> <i>A. Liñán</i>	2B07: Experimental investigations of the influence of pressure on critical extinction conditions of laminar nonpremixed flames burning condensed hydrocarbon fuels, jet fuels, and surrogates <i>R. Gehmlich, A. Kuo, K. Seshadri</i>	2C07: Constrained reaction volume shock tube study of n -heptane oxidation: Ignition delay times and time-histories of multiple species and temperature <i>M.F. Campbell, S. Wang, C.S. Goldenstein, R.M. Spearrin, A.M. Tulgestke, L.T. Zaczek, D.F. Davidson, R.K. Hanson</i>	2D07: Sensitivity of LES-based flame transfer functions for turbulent swirled flames and impact on the stability of azimuthal modes <i>M. Bauerheim, G. Staffelbach, N.A. Worth, J.R. Dawson, L.Y.M. Gicquel, T. Poinsot</i>	2E07: Modulation of sooting tendency by magnetic effects <i>A. Jocher, H. Pitsch, T. Gomez, G. Legros</i>	2F07: Doping mechanism of vanadia/titania nanoparticles in flame synthesis by a novel optical spectroscopy technique <i>Y. Ren, Y. Zhang, S. Li, C.K. Law</i>	2G07: Experimental study of the effect of CF ₃ I addition on the ignition delay time and laminar flame speed of methane, ethylene, and propane <i>O. Mathieu, J. Goulier, F. Gournel, M.S. Mannan, N. Chaumeix, E.L. Petersen</i>	2H07: Experimental study of spherical-flame acceleration mechanisms in large-scale propane-air flames <i>C.R. Bauwens, J.M. Berghthorson, S.B. Dorofeev</i>

Room	Ballroom A	Ballroom B	Ballroom C	Bayview A	Seacliff A & B	Seacliff C & D	Pacific L & M	Pacific N & O
14:40	Spray and Turbulent Flames <i>Chairs:</i> M. Linne J. Shinjo	2B08: Structure and extinction of water-laden methane/air nonpremixed flames <i>R.E. Padilla,</i> <i>V. Ricchiutti,</i> <i>S. Karnani,</i> <i>D. Dunn-Rankin,</i> <i>T. Pham</i>	2C08: Shock tube measurements of the rate constants for seven large alkanes + OH <i>J. Badra,</i> <i>A.E. Elwardany,</i> <i>A. Farooq</i>	2D08: The effect of baffles on self-excited azimuthal modes in an annular combustor <i>N.A. Worth,</i> <i>J.R. Dawson</i>	2E08: An experimental and computational study on soot formation in a coflow jet flame under microgravity and normal gravity <i>B. Ma, S. Cao,</i> <i>D. Giassi,</i> <i>D.P. Stocker,</i> <i>F. Takahashi,</i> <i>B.A.V. Bennett,</i> <i>M.D. Smooke,</i> <i>M.B. Long</i>	2F08: Curved wall-jet burner for synthesizing titania and silica nanoparticles <i>M.A. Ismail,</i> <i>N.K. Memon,</i> <i>M.S. Mansour,</i> <i>D.H. Anjum,</i> <i>S.-H. Chung</i>	2G08: Combustion inhibition and enhancement of cup-burner flames by CF ₃ Br, C ₂ H ₂ F ₃ , and C ₃ H ₂ F ₃ Br <i>F. Takahashi,</i> <i>V.R. Katta,</i> <i>G.T. Linteris,</i> <i>V.I. Babushok</i>	2H08: Numerical simulation of dilute and dense layered coal-dust explosions <i>R. Houim, E.S. Oran</i>
15:05	2A09: LES of a methanol spray flame with a stochastic sub-grid model <i>W.P. Jones,</i> <i>A.J. Marquis,</i> <i>D. Noh</i>	2B09: Extinction limits and flame structures of 1-butanol and diethyl ether non-premixed flames <i>J. Hashimoto,</i> <i>K. Tanoue, N. Taide,</i> <i>Y. Nouno</i>	2C09: Influence of the double bond position on the oxidation of decene isomers at high pressures and temperatures <i>A. Fridlyand,</i> <i>S.S. Goldsborough,</i> <i>K. Brezinsky,</i> <i>S.S. Merchant,</i> <i>W.H. Green</i>	2D09: A new pattern of instability observed in an annular combustor: The slanted mode <i>J.-F. Bourgouin,</i> <i>D. Durox, J.P. Moeck,</i> <i>T. Schuller, S. Candel</i>	2E09: Challenges and artifacts of probing high-pressure counterflow laminar diffusion flames <i>L. Figura, F. Carbone,</i> <i>A. Gomez</i>	2F09: Volumetric flame synthesis of one-dimensional molybdenum oxide nanostructures <i>S. Srivastava,</i> <i>W. Merchan-Merchan,</i> <i>M. Desai, A.V. Saveliev</i>	2G09: Effects of water sprays on the flame propagation in hydrogen / air / steam mixtures <i>H. Cheikhravat,</i> <i>J. Goulhier, A. Bentaib,</i> <i>N. Meynet, N. Chaumeix,</i> <i>C.-E. Paillard</i>	2H09: Self-similar propagation of expanding spherical flames in large scale gas explosions <i>W.K. Kim, T. Mogi,</i> <i>K. Kuwana, R. Dobashi</i>
15:30	2A10: Influence of spray/combustion interactions on auto-ignition of methanol spray flames <i>C. Heye, V. Raman,</i> <i>A.R. Masri</i>	2B10: Extinction studies of non-premixed iso-Cetane and Decalin flames <i>B. Li, Y. Zhang,</i> <i>H. Zhang,</i> <i>F.N. Egolfopoulos</i>	2C10: Ignition of alkane-rich FACE gasoline fuels and their surrogate mixtures <i>S.M. Sarathy,</i> <i>G. Kukkadapu,</i> <i>M. Mehl, W. Wang,</i> <i>T. Javed, S. Park,</i> <i>M.A. Oehlschlaeger,</i> <i>A. Farooq, W.J. Pitz,</i> <i>C.-J. Sung</i>	2D10: A theoretical study of mean azimuthal flow and asymmetry effects on thermo-acoustic modes in annular combustors <i>M. Bauerheim,</i> <i>M. Cazalsens,</i> <i>T. Poinsot</i>	2E10: Numerical study of the effects of pressure on soot formation in laminar coflow n-heptane/air diffusion flames between 1 to 10 atm <i>J.-L. Consalvi,</i> <i>F. Liu</i>	2F10: Mechanically activated combustion synthesis of molybdenum silicides and borosilicides for ultrahigh-temperature structural applications <i>M.S. Alam,</i> <i>E. Shafirovich</i>	2G10: Characterization of interactions between hot air plumes and water sprays for sprinkler protection <i>X. Zhou</i>	2H10: Time-resolved temperature measurements for inert and reactive particles in explosive atmospheres <i>F. Beyrau,</i> <i>M.A. Hadjipanayis,</i> <i>R.P. Lindstedt</i>
BREAK								

[illegible]

WEDNESDAY, 6 August 2014

PLENARY LECTURE–8:30 am

Combustion noise *Ann P. Dowling and Y. Mahmoudi*

Session Chairs: W. Polifke and T. Poinso

(Ballrooms on Street Level)

BREAK

Room	Ballroom A	Ballroom B	Ballroom C	Bayview A	Seacliff A & B	Seacliff C & D	Pacific L & M	Pacific N & O
	Turbulent Flame Structure <i>Chairs:</i> <i>F. Bisetti</i> <i>A.R. Masri</i>	Laminar Flames and Alcohols <i>Chairs:</i> <i>T. Kasper</i> <i>R.P. Lindstedt</i>	Low Temperature Kinetics <i>Chairs:</i> <i>F. Battin-Leclerc</i> <i>J. Zádor</i>	Swirled Combustion <i>Chairs:</i> <i>C. Berat</i> <i>M. Stöhr</i>	Soot Kinetics and Diagnostics <i>Chairs:</i> <i>H.A. Michelsen</i> <i>P.E. Bengtsson</i>	Spray Flames <i>Chairs:</i> <i>R. Balachandran</i> <i>B. Cuenot</i>	Electric Field and Plasma Assisted Combustion <i>Chairs:</i> <i>D. Dunn-Rankin</i> <i>S.H. Won</i>	
10:05	3A01: Spatio-temporal characteristics of temperature fluctuations in turbulent non-premixed jet flames <i>T.A. McManus,</i> <i>M.J. Papageorge,</i> <i>F. Fuest, J.A. Sutton</i>	3B01: Combustion chemistry of alcohols: Experimental and modeled structure of a premixed 2-methylbutanol flame <i>A. Lucassen,</i> <i>S. Park, N. Hansen,</i> <i>S.M. Sarathy</i>	3C01: Towards a quantitative understanding of the role of non-Boltzmann reactant distributions in low-temperature oxidation <i>M.P. Burke,</i> <i>C.F. Goldsmith,</i> <i>Y. Georgievskii,</i> <i>S.J. Klippenstein</i>	3D01: Key parameters governing the precessing vortex core in reacting flows: An experimental and analytical study <i>C.O. Paschereit,</i> <i>K. Oberleithner,</i> <i>S. Terhaar</i>	3E01: Kinetics of nascent soot oxidation by molecular oxygen in a flow reactor <i>J. Camacho,</i> <i>H. Wang</i>	3F01: On the dynamics of spray flames in turbulent flows <i>Y. Dagan, E. Arad,</i> <i>Y. Tambour</i>	3G01: Effect of an external electric field on the propagation velocity of premixed flames <i>M. Sanchez-Sanz,</i> <i>D.C. Murphy,</i> <i>C. Fernandez-Pello</i>	
10:30	3A02: First and second order Lagrangian conditional moment closure method in turbulent nonpremixed flames <i>K. Han, K.Y. Huh</i>	3B02: Understanding the reaction pathways in premixed flames fueled by blends of 1, 3-Butadiene and <i>n</i> -Butanol <i>N. Hansen,</i> <i>M. Braun-Unkhoff,</i> <i>T. Kathrotia,</i> <i>A. Lucassen, B. Yang</i>	3C02: Probing the low-temperature chain-branching mechanism for <i>n</i> -butane autoignition chemistry via time-resolved measurements of ketohydroperoxide formation in photolytically initiated <i>n</i> -C ₄ H ₁₀ oxidation <i>A.J. Eskola, O. Welz,</i> <i>J. Zádor, I.O. Antonov,</i> <i>L. Sheps, J.D. Savee,</i> <i>D.L. Osborn,</i> <i>C.A. Taatjes</i>	3D02: Transient effects of fuel-air mixing in a partially-premixed turbulent swirl flame <i>M. Stöhr, C.M. Arndt,</i> <i>W. Meier</i>	3E02: Detailed modelling of soot oxidation by O ₂ and OH in laminar diffusion flames <i>A. Khosousi,</i> <i>S.B. Dworkin</i>	3F02: Reaction zone visualisation in swirling spray <i>n</i> -heptane flames <i>R. Yuan, J. Kariuki,</i> <i>A. Dowlut,</i> <i>R. Balachandran,</i> <i>E. Mastorakos</i>	3G02: Electromagnetically induced vortex in laminar coflow diffusion flames by applying AC electric field <i>Y. Xiong, M.S. Cha,</i> <i>S.-H. Chung</i>	

Room	Ballroom A	Ballroom B	Ballroom C	Bayview A	Seacliff A & B	Seacliff C & D	Pacific L & M	Pacific N & O
10:55	3A03: A tabulated chemistry CMC model applied to a lifted methane-air jet flame <i>O. Colin, J.-B. Michel</i>	3B03: A comparative study of <i>n</i> -propanol, propanal, acetone, and propane in laminar flames <i>J. Gong, S. Zhang, Y. Cheng, Z. Huang</i>	3C03: Quantitative measurements of HO ₂ / H ₂ O ₂ and intermediate species in low and intermediate temperature oxidation of dimethyl ether <i>N. Kurimoto, B. Brumfield, X. Yang, T. Wada, P. Diévar, G. Wysocki, Y. Ju</i>	3D03: Reacting flow in an industrial gas turbine combustor: LES and experimental analysis <i>G. Bulat, E. Fedina, C. Fureby, W. Meier, U. Stopper</i>	3E03: Rate coefficients and product branching ratios for the oxidation of phenyl and naphthyl radicals: A theoretical RRKM-ME study <i>V.V. Kislov, R.I. Singh, D.E. Edwards, A.M. Mebel, M. Frenklach</i>	3F03: Analysis of segregation and bifurcation in turbulent spray flames: a 3D counterflow configuration <i>A. Vié, B. Franzelli, Y. Gao, T. Lu, H. Wang, M. Ihme</i>	3G03: Influence of electric fields on premixed laminar flames: Visualization of perturbations and potential for suppression of thermoacoustic oscillations <i>J. Kuhl, G. Jovicic, L. Zigan, S. Will, A. Leipertz</i>	
<p style="text-align: center;">BREAK</p> <p style="text-align: center;">Remember to visit our sponsors and thank them for their support</p> <p style="text-align: center;">US National Science Foundation (NSF)</p> <p style="text-align: center;">GOLD SPONSOR: LaVision</p> <p style="text-align: center;">SILVER SPONSORS: Elsevier; Santa Clara University; CD-adapco; TSI; Dantec Dynamics; FM Global; KAUST; Cambridge Press; Photon; Princeton Instruments; Quantel Lasers; Taylor & Francis</p>								
	Turbulent Flame Structure <i>Chairs: F. Bisetti A.R. Masri</i>	Laminar Flames and Alcohols <i>Chairs: T. Kasper R.P. Lindstedt</i>	Low Temperature Kinetics, Ignition <i>Chairs: F. Battin-Leclerc J. Zádor</i>	Swirled Combustion <i>Chairs: C. Berat M. Stöhr</i>	Soot Kinetics and Diagnostics <i>Chairs: H.A. Michelsen P.E. Bengtsson</i>	Spray Flames <i>Chairs: R. Balachandran B. Cuenot</i>	Electric Field and Plasma Assisted Combustion <i>Chairs: D. Dunn-Rankin S. H. Won</i>	
11:35	3A04: Large eddy simulation / conditional moment closure modeling of swirl-stabilized non-premixed flames with local extinction <i>H. Zhang, A. Garmory, D.E. Cavaliere, E. Mastorakos</i>	3B04: A DNS study of self-accelerating cylindrical hydrogen-air flames with detailed chemistry <i>Y.X. Xin, C.S. Yoo, J.H. Chen, C.K. Law</i>	3C04: Effect of non-thermal product energy distributions on ketohydroperoxide decomposition kinetics <i>C.F. Goldsmith, M.P. Burke, Y. Georgievskii, S.J. Klippenstein</i>	3D04: Detection and prevention of blowout in a lean premixed gas-turbine model combustor using dynamical system theory <i>S. Domen, H. Gotoda, T. Kuriyama, Y. Okuno, S. Tachibana</i>	3E04: Soot nanostructure evolution in premixed flames by High Resolution Electron Transmission Microscopy (HRTEM) <i>B. Apicella, P. Pré, M. Alfé, A. Ciajolo, V. Gargiulo, C. Russo, A. Tregrossi, D. Deldique, J.-N. Rouzaud</i>	3F04: Droplet/ligament modulation of local small-scale turbulence and scalar mixing in a dense fuel spray <i>J. Shinjo, J. Xia, A. Umemura</i>	3G04: Partial oxidation of methane in a temperature-controlled dielectric barrier discharge reactor <i>X. Zhang, M.S. Cha</i>	

Room	Ballroom A	Ballroom B	Ballroom C	Bayview A	Seacliff A & B	Seacliff C & D	Pacific L & M	Pacific N & O
12:00	3A05: Filtered tabulated chemistry for non-premixed flames <i>A. Coussement, T. Schmitt, B. Fiorina</i>	3B05: Differential diffusion effects inclusion with flamelet generated manifolds for the modeling of stratified premixed cooled flames <i>A. Donini, R.J.M. Bastiaans, J.A. van Oijen, L.P.H. de Goey</i>	3C05: An analytical approximation for low- and high-temperature autoignition for dimethyl ether-air mixtures <i>J. Beeckmann, L. Cai, A. Berens, N. Peters, H. Pitsch</i>	3D05: Flame shape transition in a swirl stabilised liquid fueled burner <i>A. Renaud, S. Ducruix, P. Scoufflaire, L. Zimmer</i>	3E05: Morphology of nascent soot in ethylene flames <i>M. Schenk, S. Lieb, H. Vieker, A. Beyer, A. Götzhäuser, H. Wang, K. Kohse-Höinghaus</i>	3F05: Evidence for supercritical mixing layers in the ECN spray A <i>Z. Falgout, M. Rahm, Z. Wang, M. Linne</i>	3G05: An experimental investigation of oil gasification process by microwave induced non-equilibrium plasma combustion <i>T. Yamamoto, T. Tsuboi, Y. Iwama, R. Tanaka</i>	
12:25	3A06: Numerical and experimental investigation of turbulent DME jet flames <i>A. Bhagatwala, T. Lu, H. Shen, J.A. Sutton, J.H. Chen</i>	3B06: Direct numerical simulations of probe effects in low-pressure flame sampling <i>V. Gururajan, F.N. Egolfopoulos, K. Kohse-Höinghaus</i>	3C06: Ignition delay times of diethyl ether measured in a high-pressure shock tube and a rapid compression machine <i>M. Werler, L.R. Cancino, R. Schiessl, U. Maas, C. Schulz, M. Fikri</i>	3D06: Short- and long-term dynamic modes of turbulent swirling premixed flame in a cuboid combustor <i>K. Aokia, M. Shimura, S. Ogawa, N. Fukushima, Y. Naka, Y. Nada, M. Tanahashi, T. Miyauchi</i>	3E06: Probing the smallest soot particles in low-sooting premixed flames using laser-induced incandescence <i>H. Bladh, N.-E. Olofsson, T. Mouton, J. Simonsson, X. Mercier, A. Faccinetto, P.-E. Bengtsson, P. Desgroux</i>	3F06: Non-equilibrium gas-liquid interface dynamics in high-pressure liquid injection systems <i>R.N. Dahms, J.C. Oefelein</i>	3G06: Plasma assisted combustor dynamics control <i>W.K. Kim, J. Snyder, J. Cohen</i>	
LUNCH								
	Invited Topical Review <i>Chairs:</i> <i>J. Torero</i> <i>A. Trouvé</i>	Flames in Narrow Channels <i>Chairs:</i> <i>P.D. Ronney</i> <i>T. Yokomori</i>	Ether and Alcohol Kinetics <i>Chairs:</i> <i>A. Frassoldati</i> <i>S.M. Sarathy</i>	Swirl Combustion and Piston Engines <i>Chairs:</i> <i>J. Oefelein</i> <i>S. Richard</i>	Effects of PAH and Soot Formation <i>Chairs:</i> <i>M. Alzueta</i> <i>M. Frenklach</i>	Mild Combustion <i>Chairs:</i> <i>C. Devaud</i> <i>M. de Joannon</i>	Plasma Assisted Combustion I <i>Chairs:</i> <i>M.S. Cha</i> <i>T. Ombrello</i>	
14:15	3A07/08: Solid combustion research in microgravity as a base of fire safety in space <i>Osamu Fujita</i>	3B07: Effect of thermal expansion on flame propagation in channels with nonslip walls <i>B. Demircok, D.M. Valiev, V. Akkerman</i>	3C07: A computational study on the kinetics of unimolecular reactions of ethoxyethylperoxy radicals employing CTST and VTST <i>Y. Sakai, H. Ando, H.K. Chakravarty, H. Pitsch, R.X. Fernandes</i>	3D07: Modeling heat loss effects in the large eddy simulation of a model gas turbine combustor with premixed flamelet generated manifolds <i>F. Proch, A.M. Kempf</i>	3E07: Further experimental and modelling evidences of soot fragmentation in flames <i>M. Sirignano, A. D'Anna</i>	3F07: Visualization of MILD combustion from jets in cross-flow <i>J. Sidey, E. Mastorakos</i>	3G07: <i>In-situ</i> species diagnostics and kinetic study of plasma activated ethylene pyrolysis and oxidation in a low temperature flow reactor <i>J.K. Lefkowitz, M. Uddi, B.C. Windom, G. Lou, Y. Ju</i>	

Room	Ballroom A	Ballroom B	Ballroom C	Bayview A	Seacliff A & B	Seacliff C & D	Pacific L & M	Pacific N & O
14:40	Turbulent Flames Structure <i>Chairs: J. Torero A. Trouvé</i>	3B08: An asymptotic study of the transition from slow to fast burning in narrow channels <i>L. Kagan, P. Gordon, G. Sivashinsky</i>	3C08: Chlorine atom-initiated low-temperature oxidation of prenil and isoprenol: The effect of C=C double bonds on the peroxy radical chemistry in alcohol oxidation <i>O. Welz, J.D. Savee, D.L. Osborn, C.A. Taatjes</i>	3D08: Large-eddy simulations of the ignition sequence of an annular multiple-injector combustor <i>M. Philip, M. Boileau, R. Vicquelin, E. Riber, T. Schmitt, B. Cuenot, D. Durox, S. Candel</i>	3E08: Experimental study of soot size decrease with pyrolysis temperature rise <i>A. Emelianov, A. Eremin, E. Gurentsov, E. Mikheyeva, M. Yurischev</i>	3F08: Subgrid scale modelling for MILD combustion <i>Y. Minamoto, N. Swaminathan</i>	3G08: Time-resolved radical species and temperature distributions in an Ar-O ₂ -H ₂ mixture excited by a nanosecond pulse discharge <i>Z. Yin, Z. Eckert, I.V. Adamovich, W.R. Lempert</i>	
15:05	3A09: Stabilization of piloted turbulent flames with inhomogeneous inlets <i>S. Meares, V.N. Prasad, G. Magnotti, R.S. Barlow, A.R. Masri</i>	3B09: Self-accelerating flames in long narrow channels <i>V.N. Kurdyumov, M. Matalon</i>	3C09: Kinetics of the high-temperature combustion reactions of dibutylether using composite computational methods <i>M.J.A. Rashidi, A.C. Davis, S.M. Sarathy</i>	3D09: Ignition probability of a partially premixed burner using LES <i>L. Esclapeza, E. Riber, B. Cuenot</i>	3E09: Influence of sulphur addition on emissions of polycyclic aromatic hydrocarbons during biomass combustion <i>T. Streibel, F. Mühlberger, R. Geißler, M. Saraji-Bozorgzad, T. Adam, R. Zimmermann</i>	3F09: Scaling for high intensity swirl based ultra-low emission flameless combustor operating with liquid fuels <i>V.M. Reddy, A. Katoch, W.L. Roberts, S. Kumar</i>	3G09: Nanosecond plasma enhanced H ₂ /O ₂ /N ₂ premixed flat flames <i>S. Nagaraja, T. Li, J.A. Sutton, I.V. Adamovich, V. Yang</i>	
BREAK								
	Turbulent Flames Structure <i>Chairs: J. Torero A. Trouvé</i>	Laminar Flames Structure <i>Chairs: W. Kim C.K. Law</i>	Ether and Alcohol Kinetics <i>Chairs: S.M. Sarathy A. Frassoldati</i>	Swirl Combustion and Piston Engines <i>Chairs: J. Oefelein S. Richard</i>		Mild Combustion <i>Chairs: C. Devaud M. de Joannon</i>	Plasma Assisted Combustion II <i>Chairs: M.S. Cha T. Ombrello</i>	
15:50	3A10: Numerical simulation of oxy-fuel jet flames using unstructured LES-CMC <i>A. Garmory, E. Mastorakos</i>	3B10: Electron ionization, photoionization and photoelectron/photoion coincidence spectroscopy in mass-spectrometric investigations of a low-pressure ethylene/oxygen flame <i>D. Felsmann, K. Moshhammer, J. Krüger, A. Lackner, A. Brockhinke, T. Kasper, T. Bierkandt, E. Akyildiz, N. Hansen, A. Lucassen, P. Oßwald, M. Köhler, G.A. Garcia, L. Nahon, P. Hemberger, A. Bodi, T. Gerber, K. Kohse-Höinghaus</i>	3C10: Pyrolysis of ethanol: A shock-tube/TOF-MS and modeling study <i>J. Kiecherer, C. Bänisch, T. Bentz, M. Olzmann</i>	3D10: The effect of spark timing and negative valve overlap on spark assisted compression ignition combustion heat release rate <i>R.J. Middleton, J.B. Martz, L.K. Manofskv Olesky, G.A. Lavoie, M.S. Wooldridge, D.N. Assanis</i>		3F10: Effect of hydrogen addition on the flame structure of natural-gas jet-in-hot-coflow flames <i>L.D. Arteaga Mendez, E.H. van Veen, M.J. Tummers, D.J.E.M. Roekaerts</i>	3G10: Effect of non-equilibrium plasma on two-stage ignition of <i>n</i> -heptane <i>S. Nagaraja, W. Sun, V. Yang</i>	

[illegible]

THURSDAY, 7 August 2014

PLENARY LECTURE—8:30 am

Developments in internal combustion engines and implications for combustion science and future transport fuels *Gautam T. Kalghatgi*

Session Chairs: V. Sick and T. Poinso
(Ballrooms on Street Level)

BREAK

Room	Ballroom A	Ballroom B	Ballroom C	Bayview A	Seacliff A & B	Seacliff C & D	Pacific L & M	Pacific N & O
	Turbulent Flames <i>Chairs:</i> <i>R.S. Cant</i> <i>P. Domingo</i>	Instability and Thermoacoustics <i>Chairs:</i> <i>L. Gicquel</i> <i>C.H. Sohn</i>	Hydrocarbon Fuels <i>Chairs:</i> <i>M. Braun-Unkoff</i> <i>R. Tranter</i>	Droplet and Microgravity Combustion <i>Chairs:</i> <i>E. Gutheil</i> <i>E. Mastorakos</i>	Soot and Nanoparticle Diagnostics <i>Chairs:</i> <i>P. Desgroux</i> <i>C. Schulz</i>	Pool Fire and Fire Modeling <i>Chairs:</i> <i>M.A. Delichatsios</i> <i>A. Simeoni</i>	Micro Reactor and Micro-Channel Combustion <i>Chairs:</i> <i>D. Kyritsis</i> <i>R. Yetter</i>	Detonation <i>Chairs:</i> <i>C.R. Bauwens</i> <i>S. Navarro-Martinez</i>
10:05	4A01: Impact of heat loss on V to M shape transition of confined swirling flames <i>T.F. Guiberti, D. Durox, P. Scoufflaire, T. Schuller</i>	4B01: Numerical study of unstable hydrogen/air flames: shape and propagation speed <i>C.E. Frouzakis, N. Foglia, A.G. Tomboulides, C. Altantzis, M. Matalon</i>	4C01: Laminar flame speeds, counterflow ignition, and kinetic modeling of the butene isomers <i>P. Zhao, W. Yuan, H. Sun, Y. Li, A.P. Kelley, X. Zheng, C.K. Law</i>	4D01: A detailed numerical simulation of spherically symmetric <i>n</i> -butanol droplet combustion and comparisons with experimental data <i>E.A Fahd, Y.C. Liu, C.T. Avedisian, F.L. Dryer, T.I. Farouk</i>	4E01: Species measurements in a nitrogen-diluted, ethylene air diffusion flame using direct sampling mass spectrometry and tunable diode laser absorption spectroscopy <i>H.R. Melroy, E.M. Adkins, M.J. Pause, J.H. Miller</i>	4F01: Effect of gravity on puffing phenomenon of liquid pool fires <i>H. Abe, A. Ito, H. Torikai</i>	4G01: Sooting limits and PAH formation of <i>n</i> -hexadecane and 2,2,4,4,6,8,8-heptamethylnonane in a micro flow reactor with a controlled temperature profile <i>H. Nakamura, S. Suzuki, T. Tezuka, S. Hasegawa, K. Maruta</i>	4H01: Propagation mechanisms of supersonic combustion waves <i>M.D. Kellenberger, G. Ciccarelli</i>
10:30	4A02: Unburned mixture fingers in premixed turbulent flames <i>A.N. Lipatnikov, V.A. Sabelnikov, S. Nishiki, T. Hasegawa</i>	4B02: Pulsating instability in H ₂ –air partially premixed flames <i>F. Yang, W. Kong</i>	4C02: High temperature rate constants for H/D + <i>n</i> -C ₄ H ₁₀ and I-C ₄ H ₁₀ <i>S.L. Peukert, R. Sivaramakrishnan, J.V. Michael</i>	4D02: Autoignition behavior of a spherical cluster consisted of a center fine droplet and surrounding twelve fine droplets <i>H. Kataoka, H. Yamashita, J. Tada, Y. Oka, Y. Morinaga, M. Itai, D. Segawa, T. Kadota</i>	4E02: Local gas heating in sooting flames by heat transfer from laser-heated particles investigated using rotational CARS and LII <i>E. Nordström, N.-E. Olofsson, J. Simonsson, J. Johnsson, H. Bladh, P.-E. Bengtsson</i>	4F02: Evolution of heat feedback in medium pool fires with cross air flow and scaling of mass burning flux by a stagnant layer theory solution <i>L. Hu, J. Hu, S. Liu, W. Tang, X. Zhang</i>	4G02: Effect of radical quenching on CH ₄ /air flames in a micro flow reactor with a controlled temperature profile <i>Y. Kizakii, H. Nakamura, T. Tezuka, S. Hasegawa, K. Maruta</i>	4H02: The effect of transverse shock propagation on the shock-to-detonation transition process for an insensitive explosive <i>E.K. Anderson, T.D. Aslam, S.I. Jackson</i>

Room	Ballroom A	Ballroom B	Ballroom C	Bayview A	Seacliff A & B	Seacliff C & D	Pacific L & M	Pacific N & O
10:55	4A03: Modelling of mean flame shape during premixed flame flashback in turbulent boundary layers <i>A. Gruber, A.R. Kerstein, D. Valiev, C.K. Law, H. Kolla, J.H. Chen</i>	4B03: Minor-species structure of premixed cellular tubular flames <i>C.A. Hall, W.D. Kulatilaka, N. Jiang, J.R. Gord, R.W. Pitz</i>	4C03: Experimental and kinetic modeling study of trans-2-butene oxidation in a jet-stirred reactor and a combustion bomb <i>Y. Fenard, P. Dagaut, G. Dayma, F. Halter, F. Foucher</i>	4D03: Ferrofluid droplet vaporization under very large magnetic power: Effects of pressure and effective thermal conductivity of liquid <i>C.F.C. Cristaldo, M.M. Vargas, F.F. Fachini</i>	4E03: Single-shot, time-resolved planar laser-induced incandescence (TR-LII) for soot primary particle sizing in flames <i>Z.W. Sun, D.H. Gu, G.J. Nathan, Z.T. Alwahabi, B.B. Dally</i>	4F03: Buoyant pool fires under imposed circulations before the formation of fire whirls <i>J. Lei, N. Liu, K. Satoh</i>	4G03: Characteristics of <i>n</i> -butane weak flames at elevated pressures in a micro flow reactor with a controlled temperature profile <i>S. Kikui, T. Kamada, H. Nakamura, T. Tezuka, S. Hasegawa, K. Maruta</i>	4H03: An experimental study on the onset processes of detonation waves downstream of a perforated plate <i>H. Qin, J.H.S. Lee, Z. Wang, F.-C. Zhuang</i>
BREAK								
	Turbulent Flames <i>Chairs:</i> <i>R.S. Cant</i> <i>P. Domingo</i>	Instability and Thermoacoustics <i>Chairs:</i> <i>L. Gicquel</i> <i>C.H. Sohn</i>	Hydrocarbon Fuels <i>Chairs:</i> <i>M. Braun-Unkoff</i> <i>R. Tranter</i>	Droplet and Microgravity Combustion <i>Chairs:</i> <i>E. Gutheil</i> <i>E. Mastorakos</i>	Soot and Nanoparticle Diagnostics <i>Chairs:</i> <i>P. Desgroux</i> <i>C. Schulz</i>	Pool Fire and Fire Modeling <i>Chairs:</i> <i>M.A. Delichatsios</i> <i>A. Simeoni</i>	Micro Reactor and Micro-Channel Combustion <i>Chairs:</i> <i>D. Kyritsis</i> <i>R. Yetter</i>	Detonation <i>Chairs:</i> <i>C.R. Bauwens</i> <i>S. Navarro-Martinez</i>
11:35	4A04: Impact of fuel composition on the recirculation zone structure and its role in lean premixed flame anchoring <i>S.H. Hong, S.J. Shanbhogue, A.F. Ghoniem</i>	4B04: Flames in context of thermo-acoustic stability bounds <i>M. Hoeijmakers, V. Kornilov, I. Lopez, L.P.H. de Goeij, H. Nijmeijer</i>	4C04: Experimental and modelling study of speciation and benzene formation pathways in premixed 1-hexene flames <i>A. Nawdiyal, N. Hansen, T. Zeuch, L. Seidel, F. Mauß</i>	4D04: The role of micro-convection induced by support fiber in droplet combustion processes <i>Y.C. Liu, Y. Xu, M.C. Hicks, C.T. Avedisian</i>	4E04: A new diagnostic for volume fraction measurement of metal-oxide nanoparticles in flames using phase-selective laser-induced breakdown spectroscopy <i>Y. Zhang, S. Li, Y. Ren, Q. Yao, S.D. Tse</i>	4F04: Treatment of local extinction in CFD fire modeling <i>A.Y. Snegirev, A.S. Tsoy</i>	4G04: Direct numerical simulation of micro combustion in a narrow circular channel with a detailed kinetic mechanism <i>E. Miyata, N. Fukushima, Y. Naka, M. Shimura, M. Tanahashi, T. Miyauchi</i>	4H04: Detonation limits in rough-walled tubes <i>A. Starr, J.H.S. Lee, H.D. Ng</i>
12:00	4A05: Fuel effects on leading point curvature statistics of high hydrogen content fuels <i>A. Marshall, J. Lundrigan, P. Venkateswaran, J. Seitzman, T.C. Lieuwen</i>	4B05: Time-domain analysis of thermo-acoustic instabilities in a ducted flame <i>T. Sayadi, V. le Chenadec, P. Schmid, F. Richecoeur, M. Massot</i>	4C05: Dissociation of ortho-benzynes radicals in the high temperature fall-off regime <i>P.T. Lynch, C.J. Annesley, R.S. Tranter</i>	4D05: Multistage oscillatory “cool flame” behavior for isolated alkane droplet combustion in elevated pressure microgravity condition <i>T.I. Farouk, M.C. Hicks, F.L. Dryer</i>	4E05: Laser-based <i>in-situ</i> measurement and simulation of gas-phase temperature and iron atom concentration in a pilot-plant nanoparticle synthesis reactor <i>O.M. Feroughi, S. Hardt, I. Wlokas, T. Hülser, H. Wiggers, T. Dreier, C. Schulz</i>	4F05: Numerical simulation of under-ventilated liquid-fueled compartment fires with flame extinction and thermally-driven fuel evaporation <i>S. Vilfayeau, N. Ren, Y. Wang, A. Trouvé</i>	4G05: Characteristics of opposed flow partially premixed flames in mesoscale channels at low strain rates <i>M.J. Lee, M.S. Cho, N.I. Kim</i>	4H05: Effect of spatial heterogeneity on near-limit propagation of a stable detonation <i>J. Li, X. Mi, A.J. Higgins</i>

Room	Ballroom A	Ballroom B	Ballroom C	Bayview A	Seacliff A & B	Seacliff C & D	Pacific L & M	Pacific N & O
12:25	4A06: Turbulence-flame interaction and fractal characteristics of H ₂ -air premixed flame under pressure rising condition <i>B. Yenerdag, N. Fukushima, M. Shimura, M. Tanahashi, T. Miyauchi</i>	4B06: The response of a harmonically forced premixed flame stabilized on a heatconducting bluff-body <i>K.S. Kedia, A.F. Ghoniem</i>	4C06: Production of major reaction products in the initial steps of the thermal decomposition of naphthalene. Experimental shock-tube results and computer simulation <i>A. Laskin, C. Tamburu, F. Dubnikov, A. Lifshitz</i>	4D06: Numerical modeling of auto-ignition of isolated fuel droplets in microgravity <i>A. Cuoci, A. Frassoldati, T. Faravelli, E. Ranzi</i>	4E06: Numerical and experimental investigation of the process steps in a spray flame reactor for nanoparticle synthesis <i>C. Weise, J. Menser, S.A. Kaiser, A.M. Kempf, I. Wlokas</i>	4F06: Application of a subgrid soot-radiation model in the numerical simulation of a heptane pool fire <i>P. Chatterjee, Y. Wang, K.V. Meredith, S.B. Dorofeev</i>	4G06: Experimental and numerical investigations on premixed CH ₄ /air combustion in a mesoscale channel with cavities <i>J. Wan, A. Fan, Y. Liu, H. Yao, W. Liu</i>	4H06: Effects of porous walled tubes on detonation transmission into unconfined space <i>N. Mehrjoo, Y. Gao, C.B. Kiyanda, H.D. Ng, J.H.S. Lee</i>
LUNCH								
	Turbulent Flame Structure Analysis <i>Chairs:</i> <i>A. Dreizler</i> <i>K.Y. Huh</i>	Instabilities in Swirled Flames <i>Chairs:</i> <i>I. Boxx</i> <i>T.C. Lieuwen</i>	Ignition Delay and Flame Speeds for Larger Fuels <i>Chairs:</i> <i>N. Chaumeix</i> <i>T. Zeuch</i>	LES of Spray Flames <i>Chairs:</i> <i>G. Lacaze</i> <i>M. Ihme</i>	Liquid Propellant <i>Chairs:</i> <i>B.D. Shaw</i> <i>F. Williams</i>	Fire Modeling II <i>Chairs:</i> <i>R. Dobashi</i> <i>L.W. Kostiuk</i>	Micro-Channel Combustion <i>Chairs:</i> <i>Y. Nakamura</i> <i>M. Tanahashi</i>	Detonation <i>Chairs:</i> <i>A.J. Higgins</i> <i>H.D. Ng</i>
14:15	4A07: Three-dimensional topology of turbulent premixed flame interaction <i>H. Kolla, J.H. Chen, R. Griffiths, S.R. Cant, W. Kollmann</i>	4B07: Thermo-acoustic instabilities in lean premixed swirl-stabilized combustion and their link to acoustically coupled and decoupled flame macrostructures <i>S. Taamallah, Z.A. LaBry, S.J. Shanbhogue, A.F. Ghoniem</i>	4C07: Experimental and modeling study of fuel interactions with an alkyl nitrate cetane enhancer, 2-ethyl-hexyl nitrate <i>S.S. Goldsborough, M.V. Johnson, C. Banyon, W.J. Pitz, M. McNenly</i>	4D07: Analysis of high-pressure diesel fuel injection processes using LES with real-fluid thermodynamics and transport <i>G. Lacaze, A. Misdariis, A. Ruiz, J.C. Oefelein</i>	4E07: Thermal and electrolytic decomposition and ignition of HAN-water solutions <i>P. Khare, V. Yang, G.A. Risha, R.A. Yetter</i>	4F07: Estimation of local mass burning rates for steady laminar boundary layer diffusion flames <i>A.V. Singh, M.J. Gollner</i>	4G07: An experimental and numerical investigation of premixed syngas combustion dynamics in mesoscale channels with controlled wall temperature profiles <i>A. Brambilla, M. Schultze, C.E. Frouzakis, J. Mantzaras, R. Bombach, K. Boulouchos</i>	4H07: Qualitative modeling of the dynamics of detonation with losses <i>L.M. Faria, A.R. Kasimov</i>
14:40	4A08: Flame structure analysis for categorization of lean premixed CH ₄ /air and H ₂ /air flames at high Karlovitz numbers: Direct numerical simulation studies <i>H. Carlsson, R. Yu, X.-S. Bai</i>	4B08: Stability analysis of a swirled spray combustor based on flame describing function <i>C. Mirat, D. Durox, T. Schuller</i>	4C08: Ignition delay times of conventional and alternative fuels behind reflected shock waves <i>Y. Zhu, S. Li, D.F. Davidson, R.K. Hanson</i>	4D08: Large eddy simulation of dilute acetone spray flames using CMC coupled with tabulated chemistry <i>S. Ukai, A. Kronenburg, O.T. Stein</i>	4E08: Hypergolic ignition and flame structures of hydrazine/nitrogen tetroxide co-flowing plane jets <i>H. Tani, H. Terashima, M. Koshi, Y. Daimon</i>	4F08: Numerical modeling of melting and dripping process of polymeric material subjected to moving heat flux: Prediction of drop time <i>Y. Kim, A. Hossain, Y. Nakamura</i>	4G08: Analysis of the flame structure for lean methane-air combustion in porous inert media by resolving the hydroxyl radical <i>B. Stelzner, C. Keramiotis, S. Voss, M.A. Founti, D. Trimis</i>	4H08: Modelling of deflagration to detonation transition using flame thickening <i>S. Yu, S. Navarro-Martinez</i>

[illegible]

FRIDAY, 8 AUGUST 2014

PLENARY LECTURE—8:30 am

Combustion kinetic and fuel property effects of transportation fuels *Fred Dryer*

Session Chairs: S.-H. Chung and K. Kohse-Höinghaus
(Ballrooms on Street Level)

BREAK

Room	Ballroom A	Ballroom B	Ballroom C	Bayview A	Seacliff A & B	Seacliff C & D	Pacific L & M	Pacific N & O
	Flame Dynamics and Turbulent Flames <i>Chairs:</i> S. Ducruix H.Najm	Unsteady Flame and Ignition/Extinction <i>Chairs:</i> J. Park A.L. Sanchez	Species Sensing <i>Chairs:</i> B. Böhm J.B. Jeffries	Piston Engines: Emissions and Diagnostics <i>Chairs:</i> J.-Y. Chen D. Reuss	Clusters, Particle Inception and Growth <i>Chairs:</i> P. Minutolo H. Wang	New Approaches and Propellants <i>Chairs:</i> A. Cessou S.R. Chakravarthy	Microscale Combustion <i>Chairs:</i> N.I. Kim K. Maruta	Supersonic Combustion <i>Chairs:</i> J.P. Boris V. Raman
10:05	5A01: Prediction of NO _x in premixed high-pressure lean methane flames with a MMC-partially stirred reactor <i>B. Sundaram, A.Y. Klimenko, M.J. Cleary, U. Maas</i>	5B01: Flame dynamics of equivalence ratio oscillation in a stagnating laminar lean methane/air premixed flame <i>H. Tomita, R.A.M. Rosdzimin, S. Miyamae, T. Yokomori, T. Ueda</i>	5C01: Measurements and modelling of HCN and CN species profiles in laminar CH ₄ /O ₂ /N ₂ low pressure flames using LIF/CRDS techniques <i>N. Lamoureux, H.E. Merhubi, L. Gasnot, C. Schoemaecker, P. Desgroux</i>	5D01: Improving ion current of sparkplug ion sensors in HCCI combustion using sodium, potassium, and cesium acetates: experimental and numerical modeling <i>R.H. Butt, Y. Chen, J.H. Mack, S. Saxena, R.W. Dibble, J.-Y. Chen</i>	5E01: Surface reactivity of homogenous polycyclic aromatic hydrocarbon nano-clusters <i>D. Chen, J. Akroyd, S. Mosbach, M. Kraft</i>	5F01: Rate-ratio asymptotic analysis of the structure and mechanisms of extinction of nonpremixed CH ₄ /N ₂ -O ₂ /N ₂ O/N ₂ flames <i>K. Seshadri, X.-S. Bai, F. Williams</i>	5G01: Radical quenching on metal surface in a methane-air premixed flame <i>Y. Saiki, Y. Suzuki</i>	5H01: Influence of hydrodynamic instabilities on the propagation mechanism of fast flames <i>L. Maley, R. Bhattacharjee, S.-M. Lau-Chapdelaine, M.I. Radulescu</i>
10:30	5A02: Impacts of turbulence-chemistry interaction and low temperature ignition on premixed <i>n</i> -heptane/air flames <i>B.C. Windom, S.H. Won, B. Jiang, Y. Ju, S.D. Hammack, T.M. Ombrello, C.D. Carter</i>	5B02: Impact of chemistry models on flame-vortex interaction <i>S. Lapointe, B.D. Bobbitt, G. Blanquart</i>	5C02: Towards simultaneous calibration-free and ultra-fast sensing of temperature and species in the intrapulse mode <i>R.S.M. Chrystie, A. Farooq</i>	5D02: Investigation of <i>iso</i> -octane combustion in a homogeneous charge compression ignition engine seeded by ozone, nitric oxide and nitrogen dioxide <i>J-B. Masurier, F. Foucher, G. Dayma, P. Dagaut</i>	5E02: Towards a predictive model for polycyclic aromatic hydrocarbon dimerization propensity <i>J.S. Lowe, J.Y.W. Lai, P. Elvati, A. Violi</i>	5F02: Supercritical pyrolysis of <i>n</i> -dodecane with colloidal platinum-decorated graphene sheets <i>H.S. Sim, R.A. Yetter, D.M. Dabbs, I.A. Aksay</i>	5G02: Thermal and chemical structures formed in the micro burner of miniaturized hydrogen-air jet flames <i>A. Hossain, Y. Nakamura</i>	5H02: Ignition and supersonic combustion behavior of liquid ethanol in a scramjet model combustor with cavity flame holder <i>S. Nakaya, Y. Hikichi, Y. Nakazawa, K. Sakaki, M. Choi, M. Tsue, M. Kono, S. Tomioka</i>

Room	Ballroom A	Ballroom B	Ballroom C	Bayview A	Seacliff A & B	Seacliff C & D	Pacific L & M	Pacific N & O
10:55	5A03: Turbulent transport in premixed flames approaching extinction <i>K.H.H. Goh, P. Geipel, R.P. Lindstedt</i>	5B03: Structure and stability of premixed flames stabilized behind the trailing edge of a cylindrical rod at low Lewis numbers <i>V.N. Kurdyumov, Y. Shoshin, L.P.H. de Goey</i>	5C03: High-temperature <i>iso</i> -butene absorption diagnostic for shock tube kinetics using a pulsed quantum cascade laser near 11.3 μm <i>R.M. Spearrin, S. Li, D.F. Davidson, J.B. Jeffries, R.K. Hanson</i>	5D03: In-cylinder soot precursor growth in a low-temperature combustion diesel engine: Laser-induced fluorescence of polycyclic aromatic hydrocarbons <i>C.A.J. Leermakers, M.P.B. Musculus</i>	5E03: Reaction pathways for the growth of polycyclic aromatic hydrocarbons during the supercritical pyrolysis of <i>n</i> -decane, as determined from doping experiments with 1- and 2-methylnaphthalene <i>S.V. Kalpathy, N.B. Poddar, S.P. Bagley, M.J. Wornat</i>	5F03: A detailed kinetic study of the thermal decomposition of tetraethoxysilane <i>D. Nurkowski, P. Buerger, J. Akroyd, M. Kraft</i>	5G03: Experimental and theoretical study on the interaction between two identical micro-slot diffusion flames: Burner pitch effects <i>A. Kosugi, N. Sato, K. Kuwana, T. Hirasawa, Y. Nakamura</i>	5H03: Simultaneous gas density and fuel concentration measurements in a supersonic combustor using laser induced breakdown <i>H. Do, C.D. Carter, Q. Liu, T.M. Ombrello, S.D. Hammack, T. Lee, K.-Y. Hsu</i>
<p style="text-align: center;">BREAK</p> <p style="text-align: center;">Farewell Reception begins at 17:30 at Justin Herman Plaza, outside Hyatt Regency</p>								
	Flame Dynamics and Turbulent Flames <i>Chairs:</i> <i>S. Ducruix</i> <i>H. Najm</i>	Unsteady Flame and Ignition/Extinction <i>Chairs:</i> <i>A.L. Sanchez</i> <i>J. Park</i>	Species Sensing <i>Chairs:</i> <i>B. Böhm</i> <i>J.B. Jeffries</i>	Piston Engines: Emissions and Diagnostics <i>Chairs:</i> <i>J.-Y. Chen</i> <i>D. Reuss</i>	Clusters, Particle Inception and Growth <i>Chairs:</i> <i>P. Minutolo</i> <i>H. Wang</i>	New Approaches and Propellants <i>Chairs:</i> <i>K. Brezinsky</i> <i>S.R. Chakravarthy</i>	Oxy Fuel Combustion <i>Chairs:</i> <i>B. Dlugogorski</i> <i>D. Trimis</i>	Supersonic Combustion <i>Chairs:</i> <i>J.P. Boris</i> <i>V. Raman</i>
11:35	5A04: Propagation, dissipation, and dispersion of disturbances on harmonically forced, non-premixed flames <i>N.A. Magina, V. Acharya, T. Sun, T.C. Lieuwen</i>	5B04: The influence of carbon monoxide and hydrogen on the structure and extinction of nonpremixed and premixed methane flames <i>V. Amin, G. Katzlinger, P. Saxena, K. Seshadri, E. Pucher</i>	5C04: Early flame propagation in a spark-ignition engine measured with quasi 4D-diagnostics <i>B. Peterson, E. Baum, B. Böhm, A. Dreizler</i>	5D04: Two-tracer LIF imaging of preferential evaporation of multi-component gasoline fuel sprays under engine conditions <i>L.M. Itani, G. Bruneaux, A. di Lella, C. Schulz</i>	5E04: The importance of reversibility in modeling soot nucleation and condensation processes <i>N.A. Eaves, M.J. Thomson, S.B. Dworkin</i>	5F04: Simulations of heterogeneous propellant combustion: Effect of particle orientation and shape <i>M. Plaud, S. Gallier, M. Morel</i>	5G04: Fundamental investigation on the fuel-NO _x emission of the oxy-fuel combustion using a tubular flame burner <i>D. Shimokuri, S. Fukuba, S. Ishizuka</i>	5H04: A computational study of supersonic combustion in strut injector and hypermixer flow fields <i>C. Fureby, K. Nordin-Bates, K. Petterson, A. Bresson, V.A. Sabelnikov</i>

Room	Ballroom A	Ballroom B	Ballroom C	Bayview A	Seacliff A & B	Seacliff C & D	Pacific L & M	Pacific N & O
12:00	5A05: Irreversible entropy production rate in high-pressure turbulent reactive flows <i>G. Borghesi, J. Bellan</i>	5B05: Fundamental physics of flame development in an autoigniting dual fuel mixture <i>Z. Wang, J. Abraham</i>	5C05: Calibration-free, high-speed, in-cylinder laser absorption sensor for cycle-resolved, absolute H ₂ O measurements in a production IC engine <i>O. Witzel, A. Klein, C. Meffert, C. Schulz, S.A. Kaiser, V. Ebert</i>	5D05: Determination of soot onset and background particulate levels in a spark-ignition engine <i>M.D. Hageman, S.S. Sakai, D.A. Rothamer</i>	5E05: Damköhler number effects on soot formation and growth in turbulent nonpremixed flames <i>A. Attili, F. Bisetti, M.E. Mueller, H. Pitsch</i>	5F05: Experimental investigation of cellular instability in Ammonium Perchlorate (AP) and fine AP-binder mixtures <i>N. Gurram S.R. Chakravarthy</i>	5G05: The chemical role of CO ₂ in pyrite thermal decomposition <i>W. Lv, D. Yu, J. Wu, L. Zhang, M. Xu</i>	5H05: Direct numerical simulation of supersonic combustion with thermal nonequilibrium <i>H. Koo, V. Raman, P.L. Varghese</i>
12:25	5A06: Sound generation by premixed flame annihilation with full and simple chemistry <i>C. Jiménez, A. Haghir, M.J. Brear, M. Talei, E.R. Hawkes</i>	5B06: Multi-scale modeling of dynamics and ignition to flame transitions of high pressure stratified <i>n</i> -heptane/toluene mixtures <i>W. Sun, S.H. Won, X. Gou, Y. Ju</i>	5C06: Infrared laser absorption sensors for multiple performance parameters in a detonation combustor <i>C.S. Goldenstein, R.M. Spearrin, J.B. Jeffries, R.K. Hanson</i>	5D06: Study on the phase relation between ion current signal and combustion phase in a HCCI combustion engine <i>G. Dong, Y. Chen, Z. Wu, L. Li, R. Dibble</i>	5E06: Soot precursor formation and limitations of the stabilomer grid <i>K.O. Johansson, J.Y.W. Lai, S.A. Skeen, D.M. Popolan-Vaida, K.R. Wilson, N. Hansen, A. Violi, H.A. Michelsen</i>	5F06: Flame structure and particle combustion regimes in premixed methane-iron-air suspensions <i>P. Julien, S. Whiteley, S. Goroshin, M.J. Soo, D.L. Frost, J.M. Bergthorson</i>	5G06: Experimental investigation of structure and stabilization of spray oxyfuel flames diluted by carbon dioxide <i>G. Cléon, D. Honoré, C. Lacour, A. Cessou</i>	5H06: Large Eddy Simulations of the HIFiRE scramjet using a compressible flamelet/progress variable approach <i>A. Saghafian, D.A. Philips, L. Shunn, F. Ham</i>
LUNCH								
	Invited Topical Review <i>Chairs:</i> <i>S. Hochgreb H. Pitsch</i>	Laminar Flame Speed III <i>Chairs:</i> <i>G. Blanquart C.-J. Sung</i>	Mechanisms and Uncertainty Analysis <i>Chairs:</i> <i>T. Faravelli A. Tomlin</i>	Piston Engine Modeling and Emission <i>Chairs:</i> <i>G. Bruneaux G. Kalghatgi</i>	Turbulence and Soot <i>Chairs:</i> <i>M. Kraft G. Smallwood</i>	Aluminum Combustion Synthesis <i>Chairs:</i> <i>J.M. Bergthorson S. Li</i>	Coal and Biomass <i>Chairs:</i> <i>J.S. Lighty R. Weber</i>	Solid Waste and Emission <i>Chairs:</i> <i>X. Guo H. Yao</i>
14:15	5A07/08: Partial premixing and stratification in turbulent flames <i>Assaad R. Masri</i>	5B07: High temperature oxidation of formaldehyde and formyl radical: A study of 1,3,5-trioxane laminar burning velocities <i>J. Santner, F.M. Haas, F.L. Dryer, Y. Ju</i>	5C07: Fast solvers for large kinetic mechanisms using adaptive preconditioners <i>M.J. McNenly, R.A. Whitesides, D.L. Flowers</i>	5D07: Turbulence-chemistry interactions in a heavy-duty compression-ignition engine <i>V.R. Raj Mohan, D.C. Haworth</i>	5E07: Investigation of soot formation in pressurized swirl flames by laser measurements of temperature, flame structures and soot concentrations <i>K.P. Geigle, M. Köhler, W. O'Loughlin, W. Meier</i>	5F07: Computer modelling of nano-aluminium agglomeration during the combustion of composite solid propellants <i>K. Balbudhe, A. Roy, S.R. Chakravarthy</i>	5G07: Large eddy simulation of coal combustion in a large-scale laboratory furnace <i>M. Rabaçal, B.M. Franchetti, F.C. Marincola, F. Proch, M. Costa, C. Hasse, A.M. Kempf</i>	5H07: The experimental and mechanism study of novel heterogeneous Fenton-like reactions using Fe _{3-x} Ti _x O ₄ catalysts for Hg ₀ absorption <i>C. Zhou, L. Sun, J. Xiang, S. Hu, S. Su, A. Zhang</i>

Room	Ballroom A	Ballroom B	Ballroom C	Bayview A	Seacliff A & B	Seacliff C & D	Pacific L & M	Pacific N & O
14:40	<p>Partially Premixed Turbulent Flames</p> <p><i>Chairs:</i> <i>S. Hochgreb</i> <i>H. Pitsch</i></p>	5B08: A study of propagation of spherically expanding and counterflow laminar flames using direct measurements and numerical simulations <i>J. Jayachadran, A. Lefebvre, R. Zhao, F. Halter, E. Varea, B. Renou, F.N. Egolfopoulos</i>	5C08: Validating and exploiting predictive models by incorporating an instrumental model <i>D.R. Yeates, W. Li, P.R. Westmoreland, W. Speight, T. Russi, A. Packard, M. Frenklach,</i>	5D08: LES prediction and analysis of knocking combustion in a spark ignition engine <i>A. Robert, S. Richard, O. Colin, L. Martinez, L. de Franqueville</i>	5E08: Simultaneous planar measurements of temperature and soot volume fraction in a turbulent non-premixed jet flame <i>S.M. Mahmoud, G.J. Nathan, P.R. Medwell, B.B. Dally, Z.T. Alwahabi</i>	5F08: Gas-surface thermochemistry and kinetics for aluminum particle combustion <i>J. Glorian, L. Catoire, S. Gallier, N. Cesco</i>	5G08: Use of synthetic oxygen carriers for chemical looping combustion of Victorian brown coal <i>S. Rajendran, S. Zhang, R. Xiao, S. Bhattacharya</i>	5H08: Hg oxidation reaction mechanism on Fe ₂ O ₃ with H ₂ S: Comparison between theory and experiments <i>L. Xue, T. Liu, X. Guo, C. Zheng</i>
15:05	5A09: Imaging measurements and LES-CMC modeling of a partially-premixed turbulent dimethyl ether/air jet flame <i>B.R. Coriton, M. Zendejdel, S. Ukai, A. Kronenburg, O.T. Stein, S.-K. Im, M. Gamba, J.H. Frank</i>	5B09: Comparative study on the laminar flame speed enhancement of methane with ethane and ethylene addition <i>S. Ravi, T.G. Sikes, A. Morones, C.L. Keesee, E.L. Petersen</i>	5C09: Determining predictive uncertainties and global sensitivities for large parameter systems: A case study for n-butane oxidation <i>É. Hébrard, A.S. Tomlin, R. Bounaceur, F. Battin-Leclerc</i>	5D09: Combined effects of flow/spray interactions and EGR on combustion variability for a stratified DISI engine <i>W. Zeng, M. Sjöberg, D. Reuss</i>	5E09: Simultaneous instantaneous measurements of soot volume fraction, primary particle diameter, and aggregate size in turbulent buoyant diffusion flames <i>B.M. Crosland, K.A. Thomson, M.R. Johnson</i>	5F09: Quenching distance of flames in hybrid methane-aluminum mixtures <i>J. Palecka, P. Julien, S. Goroshin, J. M. Berghthorson, D.L. Frost, A.J. Higgins</i>	5G09: Combustion kinetics and particle fragmentation of raw and torrefied biomass in a drop tube furnace <i>F.F. Costa, G. Wang, M. Costa</i>	5H09: Analysis of mercury species over CuO-MnO ₂ -Fe ₂ O ₃ /γ-Al ₂ O ₃ catalysts by thermal desorption <i>P. Wang, S. Hu, J. Xiang, S. Su, L. Sun, F. Cao, X. Xiao, A. Zhang</i>
15:30	5A10: The influence of combustion SGS sub-models on the resolved flame propagation. Application to the LES of the cambridge stratified flames <i>R. Mercier, T. Schmitt, D. Veynante, B. Fiorina</i>	5B10: Laminar flame speeds of n-decane, n-butylbenzene, and n-propylcyclohexane mixtures <i>A. Comandini, T. Dubois, N. Chaumeix</i>	5C10: Uncertainty analysis of the kinetic model prediction for high-pressure H ₂ /CO combustion <i>X. Li, X. You, F. Wu, C.K. Law</i>	5D10: Influence of flow and ignition fluctuations on cycle-to-cycle variations in early flame kernel growth <i>C. Pera, V. Knop, J. Reveillon</i>	5E10: Comparison of one-dimensional turbulence and direct numerical simulations of soot formation and transport in a nonpremixed ethylene jet flame <i>D.O. Lignell, G.C. Fredline, A.D. Lewis</i>	5F10: Combustion characteristics of monodispersed aluminum nanoparticle streams in post flame environment <i>C. Kong, Q. Yao, D. Yu, S. Li</i>	5G10: Ignition behaviors of pulverized coal particles in O ₂ /N ₂ and O ₂ /H ₂ O mixtures in a drop tube furnace using flame monitoring techniques <i>C. Zou, L. Cai, D. Wu, Y. Liu, S. Liu, C. Zheng</i>	5H10: Insights into the mechanism of heterogeneous mercury oxidation by HCl over VOx/TiO ₂ catalyst: Periodic density functional theory study <i>B. Zhang, J. Liu, G. Dai, M. Chang, C. Zheng</i>

[illegible]

ORAL PRESENTATION AUTHORS

<i>Author.....Paper #</i>	<i>Author.....Paper #</i>	<i>Author.....Paper #</i>	<i>Author.....Paper #</i>
Abe, F.1B06	Arteaga Mendez, L.D.3F10	Bergthorson, J.M.2H07,	Brear, M.J.1D12, 5A06
Abe, H.4F01	Aslam, T.D.4H025F06, 5F09	Brequigny, P.1B02
Abebe, M.T.2C04	Aspden, A.J.2A05	Beyer, A.2E01, 2F12, 3E05	Bresson, A.5H04
Abraham, J.5B05	Assanis, D.N.3D10, 3D12	Beyrau, F.2A02, 2H10	Brezinsky, K.2C09
Acharya, V.5A04	Attili, A.5E05	Bhagatwala, A.2B12, 3A06	Brinker, S.1H03
Adam, T.3E09	Avedisian, C.T.4D01, 4D04	Bhattacharjee, R.5H01	Brockhinke, A.3B10
Adamovich, I.V.3G08, 3G09	Ayling, S.1C11	Bhattacharjee, S.1G01,	Brumfield, B.3C03
Adkins, E.M.4E01	Ayoobi, M.2B011G03, 2G02	Bruneaux, G.5D04
Aghsaee, M.1C04	Babushok, V.I.2G08	Bhattacharya, S.5G08	Bruno, A.5E12
Akkerman, V.3B07	Badra, J.2C08	Bian, H.2C12	Buerger, P.5F03
Akroyd, J.5E01, 5F03	Bagley, S.P.5E03	Bierkandt, T.2E02, 3B10	Bulat, G.3D03
Aksay, I.A.5F02	Bai, X.-S.1B10, 1D03	Bilbao, R.2E04	Burke, M.P.3C01, 3C04
Akyildiz, E.2E02, 3B101F01, 2A04, 4A08, 5F01	Bin, F.2F06	Bushe, W.K.1A12
Alam, M.S.2F10	Balachandran, R.1A06, 3F02	Biseti, F.2B13, 5E05	Butt, R.H.5D01
Aldén, M.1E10, 1F01,	Balbudhe, K.5F07	Biswas, P.1F09	Cai, L.1D09, 3C05,
.....2A04, 3G11	Balusamy, S.1B09, 2D01	Bladh, H.3E06, 4E023C12, 5G10
Alexandrino, K.2E04	Bänsch, C.3C10	Blanquart, G.2A06,	Camacho, J.3E01
Alfé, M.1H07, 3E04	Banyon, C.4C075B02, 5E13	Camou, A.1D07
Allen, C.1D11	Barlow, R.S.1E08,	Bobbitt, B.D.2A06, 5B02	Campbell, M.F.2C07
Allison, P.M.2D123A09, 5A13	Bodi, A.3B10	Cancino, L.R.3C06
Altantzis, C.4B01	Bastiaans, R.J.M.1B05, 3B05	Bohlin, A.1E03	Candel, S.2D05, 2D09,
Alwahabi, Z.T.4E03, 5E08	Battin-Leclerc, F.1C07, 2C11,	Böhm, B.1E11, Tue Plenary3D08, 5E11
Alzueta, M.U.2E042E05, 4C09, 5C095C04, 5D12	Cant, R.S.4A07
Amato, A.1A04	Bauerheim, M.2D07, 2D10	Boileau, M.2D05, 3D08	Cao, F.5H09
Amin, V.5B04	Baum, E.5C04, 5D12	Bombach, R.2F05, 4G07	Cao, S.2B06, 2E08
Ammendola, P.1H07	Bauwens, C.R.2H07	Bomberg, S.2D03	Cao, X.2F06
Anderson, E.K.4H02	Bazile, R.2D02	Bood, J.1E10	Carbone, F.2B02, 2E09
Anderson, S.L.2F11	Beckmann, A.M.1H03	Borghesi, G.5A05	Carlsson, H.4A08
Ando, H.3C07	Beeckmann, J.1A10,	Boulouchos, K.1D01, 4G07	Carnell Jr., W.F.1E09
Anjum, D.H.2F081B03, 3C05	Bounaceur, R.2C11,	Carstensen, H.-H.1C10
Annesley, C.J.4C05	Bell, J.B.1A04, 2A054C09, 5C09	Carter, C.D.2H02,
Ansari, N.1B08	Bellan, J.5A05	Bourgouin, J.-F.2D095A02, 5H03
Antonov, I.O.3C02	Bengtsson, P.-E.3E06, 4E02	Boxx, I.G.1E01, 1E12, 2A02	Carter, E.A.2C03
Aokia, K.3D06	Bennett, B.A.V.2B06, 2E08	Bozkurt, M.1C04	Catoire, L.5F08
Apicella, B.3E04	Bentaib, A.2G09	Brackmann, C.2A04	Cavaliere, D.E.3A04
Arad, E.3F01	Bentz, T.3C10	Brambilla, A.4G07	Cazalens, M.2D10
Arndt, C.M.3D02	Berens, A.3C05	Braun-Unkhoff, M.3B02	Cen, K.F.1F01

<i>Author</i>	<i>Paper #</i>
Cesco, N.	5F08
Cessou, A.	5G06
Cha, M.S.	2B05, 3G02, 3G04
Chakravarthy, S.R.	5F05, 5F07
Chakravarty, H.K.	3C07
Chang, M.	5H10
Chang, Y.	1D13
Chatterjee, P.	4F06
Chaudhuri, S.	2A01,2A12, 2A13
Chaumeix, N.	1C04, 2G07,2G09, 5B10
Chauveau, C.	1A01
Che, D.	1F13
Cheikhavat, H.	2G09
Chen, D.	1F03, 5E01
Chen, H.	2G05
Chen, J.H.	2B12, 3A06,3B04, 4A03, 4A07
Chen, J.-Y.	1D10, 5D01
Chen, J.	5H13
Chen, L.L.	2A11
Chen, Q.	2C02
Chen, S.	1D04
Chen, Y.	2D12,5D01, 5D06
Chen, Z.	1B01, 1B03, 1D04
Cheng, R.K.	1A04
Cheng, Y.	3B03
Cheng, Z.	2E06, 3C11
Chirone, R.	1H07
Cho, M.S.	4G05
Choi, M.	5H02
Christensen, J.M.	5C12
Christensen, M.	2C04
Chrystie, R.S.M.	5C02
Chung, S.-H.	2B05,2B13, 2F08, 3G02
Ciajolo, A.	2E03, 3E04
Ciccarelli, G.	4H01
Cifuentes, L.	1A03
Cleary, M.J.	5A01
Cléon, G.	5G06
Cocker III, D.	1G08
Cohen, J.	3G06
Colin, O.	3A03, 5D08
Colket, M.	1D11

<i>Author</i>	<i>Paper #</i>
Comandini, A.	5B10
Commodo, M.	5E12
Consalvi, J.-L.	2E10
Conturso, M.	1C08
Coriton, B.R.	2A03,5A09, 5A12
Costa, F.F.	5G09
Costa, M.	5G07, 5G09
Cotter, E.	1F09
Coussement, A.	3A05
Cracknell, R.F.	3D11
Creta, F.	1A11
Cristaldo, C.F.C.	4D03
Crosland, B.M.	5E09
Cserháti, M.	5C11
Cuenot, B.	2D05,3D08, 3D09
Cung, K.D.	5D13
Cuoci, A.	2B04, 4D06
Curran, H.J.	5C11
Dabbs, D.M.	5F02
Dagan, Y.	3F01
Dagaut, P.	1B02, 2C06,3C12, 4C03, 5D02
Dahms, R.N.	3F06
Dai, G.	5H10
Dai, P.	1D04
Daimon, Y.	4E08
Dally, B.B.	4E03, 5E08
D'Anna, A.	1C08, 3E07, 5E12
Davidson, D.F.	1C05, 2C05,2C07, 4C08, 5C03
Davies, T.J.	3D11
Davis, A.C.	3C09
Dawson, J.R.	2D07, 2D08
Day, M.S.	1A04, 2A05
Dayma, G.	1B02, 2C06,4C03, 5D02
de Bruycker, R.	1C10
de Falco, G.	5E12
de Francqueville, L.	5D08
de Goey, L.P.H.	1B05,3B05, 3B11, 4B04, 5B03
de Silva, G.	1D12
Deldique, D.	3E04
Delichatsios, M.A.	1G12
Demirgok, B.	3B07

<i>Author</i>	<i>Paper #</i>
Deng, Z.	1G06
Dennis, C.N.	1E01
Dennis, J.S.	1H08
D'Errico, G.	1A13
Desai, M.	2F09
Desgroux, P.	3E06, 5C01
Devaud, C.B.	3F11
Diamantis, D.J.	5C13
Dias, V.	1B13
Dibble, R.W.	5D01, 5D06
Diévert, P.	3C03, 3G12
di Lella, A.	5D04
Dirrenberger, P.	4C09
Do, H.	5H03
Dobashi, R.	2H09
Domen, S.	3D04
Domingo, P.	1A03, 1B07
Dong, G.	5D06
Donini, A.	3B05
Dopazo, C.	1A03
Dorofeev, S.B.	2H07, 4F06
Dovizio, D.	3F11
Dowling, A.P.	Wed Plenary
Dowlut, A.	1A06, 3F02
Dreier, T.	4E05
Dreizler, A.	1E03, 1E11,Tue Plenary, 5C04, 5D12
Driscoll, J.F.	2D12
Dryer, F.L.	1D09, 1D12, 4D01,4D05, Fri Plenary, 5B07
Du, W.	1F02
Du, Y.	1F13
Dubnikov, F.	4C06
Dubois, T.	1B02, 5B10
Ducruix, S.	2D05, 3D05
Dunn, M.J.	1E11
Dunn-Rankin, D.	2B08
Durox, D.	2D09, 3D08,4A01, 4B08
Dworkin, S.B.	3E02, 5E04
Eaves, N.A.	5E04
Ebert, V.	5C05
Ebisawa, T.	2G02
Eckert, Z.	3G08
Edwards, D.E.	3E03
Edwards, T.	1D11

<i>Author</i>	<i>Paper #</i>
Egolfopoulos, F.N.	2B10,3B06, 5B08
Ehn, A.	1E10, 3G11
Elvati, P.	5E02
Elwardany, A.E.	1C02, 2C08
Emelianov, A.	3E08
Emmert, T.	2D03
Eremin, A.	3E08
Esclapez, L.	3D09
Eskola, A.J.	3C02
Es-sebbar, E.	1C02
Faccinetto, A.	3E06
Fachini, F.F.	4D03
Fahd, E.A.	4D01
Falgout, Z.	3F05
Fan, A.	4G06
Fang, J.	1F09
Farahani, H.F.	1G07
Faravelli, T.	2B04, 4D06
Faria, L.M.	4H07
Farooq, A.	1C02, 2C08,2C10, 5C02
Farouk, T.I.	4D01, 4D05
Fatehi, H.	1F01
Fedina, E.	3D03
Felsmann, D.	2C03, 3B10
Fenard, Y.	4C03
Ferkul, P.V.	1G05
Fernandes, R.X.	3C07
Fernandez-Pello, C.	1G09,2G03, 3G01
Feroughi, O.M.	4E05
Figura, L.	2E09
Fikri, M.	1C04, 3C06
Fiorina, B.	1A02,3A05, 5A10
Flowers, D.L.	5C07
Foglia, N.	4B01
Foucher, F.	4C03, 5D02
Founti, M.A.	1C01, 4G08
Fragner, R.	1A01
Francheti, B.M.	5G07
Frank, J.H.	1E11, 2A03,5A09, 5A12
Franzelli, B.	3F03, 5E11
Frassoldati, A.	2B04, 4D06
Fredline, G.C.	5E10

<i>Author</i>	<i>Paper #</i>
Frenklach, M.	3E03, 5C08
Fridlyand, A.2C09
Frost, D.L.	5F06, 5F09
Frouzakis, C.E.	1D01, 1B04,4B01, 4G07
Fry, A.1F10
Fu, Y.1G13
Fuest, F.3A01, 5A13
Fujita, O.1G04, 1F06,2G03, Wed Topical
Fukuba, S.5G04
Fukushima, N.1D06,3D06, 4A06, 4G06
Fureby, C.3D03,3G11, 5H04,
Gallier, S.5F04, 5F08
Gamba, M.5A09
Gao, X.1H01
Gao, Y.1C11,1E02, 3F03, 4H06
Gao, Z.1G11
Garcia, G.A.3B10
Gargiulo, V.1H07, 3E04
Garmory, A.3A04, 3A10
Gasnot, L.5C01
Gehmlich, R.2B07
Geigle, K.P.5E07
Geipel, P.5A03
Geißler R.3E09
Gentz, G.1D11
Georgievskii, Y.1G12,3C01, 3C04
Gerber, T.3B10
Gersen, S.5C12
Gessenhardt, C.1E06
Geyer, D.1E08
Ghoniem, A.F.4A04,4B06, 4B07
Ghorbani, A.2H05
Giannakopoulos, G.K.1B04
Giassi, D.2B06, 2E08
Gicquel, L.Y.M.2D07
Giovangigli, V.Mon Topical
Givi, P.1B08
Glarborg, P.1C03, 5C12
Glaude, P.-A.1C07, 2C11,2E05, 4C09

<i>Author</i>	<i>Paper #</i>
Glorian, J.5F08
Goh, K.H.H.5A03
Gökalp, I.1A01
Gokoglu, S.A.1G05
Goldenstein, C.S.2C07, 5C06
Goldin, G.M.1B08
Goldsborough, S.S.2C09, 4C07
Goldsmith, C.F.3C01, 3C04
Gollner, M.J.4F07
Gölzhäuser, A.2E01,2F12, 3E05
Gomez, A.2B02, 2E09
Gomez, T.2E07
Gong, J.3B03
Gonzalo-Tirado, C.1F11
Gord, J.R.4B03
Gordon, P.3B08
Gore, J.P.1G10
Goroshin, S.5F06, 5F09
Goshayeshi, B.1H10
Gosselin, K.R.1E09
Goswami, M.1B05
Goto, T.3B12
Gotoda, H.3D04
Gou, X.5B06
Goulier, J.2G07, 2G09
Gourmel, F.2G07
Goussis, D.A.5C13
Gowdagiri, S.1D11
Green, W.H.2C09
Griffiths, R.4A07
Grogan, K.P.2H04
Groth, C.P.T.1A12
Gruber, A.4A03
Grygier, F.2F05
Gu, D.H.4E03
Gui, B.5H11
Guiberti, T.F.4A01
Gülde, Ö.L.1A12
Guo, X.5H08
Gurentsov, E.3E08
Gurram, N.5F05
Gururajan, V.3B06
Haas, F.M.1D09, 5B07
Hadjipanayis, M.A.2H10
Hageman, M.D.5D05
Haghir, A.5A06

<i>Author</i>	<i>Paper #</i>
Hakim, L.2D05
Hall, C.A.4B03
Halter, F.1A01, 1B02,4C03, 5B08
Ham, F.5H06
Hammack, S.D.5A02, 5H03
Han, K.3A02
Han, Z.2D01, 2D04
Hansen, N.2E01, 3B01,3B02, 3B10, 4C04, 5E06
Hanson, R.K.1C05, 2C05,2C07, 4C08, 5C03, 5C06
Hardalupas, Y.2A02
Hardt, S.4E05
Hargis, J.W.1D07
Hasegawa, S.4G01,4G02, 4G03
Hasegawa, T.4A02
Hasemi, Y.2G06
Hashemi, H.5C12
Hashimoto, J.2B09
Hasse, C.5G07
Hawkes, E.R.1A05, 1A13,1D02, 2B12, 5A06
Haworth, D.C.5D07
Hayakawa, A.3B12
Hayashi, A.K.2H01
Haynes, B.S.2F13
He, L.1G12
He, Y.1F01
Hébrard, É.5C09
Hemberger, P.2E02, 3B10
Herbinet, O.2C11, 4C09
Heye, C.2A10
Heyne, J.1D09
Hicks, M.C.4D04, 4D05
Higgins, A.J.4H05, 5F09
Hikichi, Y.5H02
Hill, L.G.2H11
Hirasawa, T.5G03
Hochgreb, S.1B09,2D01, 2D04
Hoeijmakers, M.4B04
Honeré, D.5G06
Hong, S.H.4A04
Hossain, A.4F08, 5G02
Hosseini, S.1G08

<i>Author</i>	<i>Paper #</i>
Houim, R.2H08
Hsu, K.-Y.2H02, 5H03
Hu, H.1F03, 5H12, 5H13
Hu, J.4F02
Hu, L.1G04, 1G12, 4F02
Hu, S.5H07, 5H09
Hu, X.5H12
Huang, H.W.1C09, 2D11
Huang, X.2G05
Huang, Y.1G08
Huang, Z.3B03
Huh, K.Y.3A02
Hui, S.1F02
Hui, Y.1F06
Hülser, T.4E05
Hurtig, T.3G11
Husson, B.2C11
Hwang, J.2D13
Ihara, T.2G02
Ihme, M.2D12, 2H04,2H13, 3F03, 5A11
Im, S.-K.5A09
Ishihara, A.1B06
Ishizuka, S.5G04
Ismail, M.A.2F08
Itai, M.4D02
Itani, L.M.5D04
Ito, A.4F01
Ito, H.1F06
Iwama, Y.3G05
Iyer, K.N.1F09
Izumo, H.1G04
Jackson, S.I.2H12, 4H02
Jasper, A.W.1C13
Javed, T.2C10
Jayachandran, J.5B08
Jeanmart, H.1B13
Jeffries, J.B.5C03, 5C06
Jeung, I.-S.2H06
Ji, J.1G11, 1G13
Jia, M.1D13
Jiang, B.3G12, 5A02
Jiang, N.4B03
Jiménez, C.5A06
Jiménez, S.1F11
Jin, H.2B04
Jocher, A.2E07

<i>Author</i>	<i>Paper #</i>
Johansson, K.O.	5E06
Johchi, A.	1E13
Johnson, J.	5D13
Johnson, M.R.	5E09
Johnson, M.V.	4C07
Johnsson, J.	4E02
Jones, W.P.	2A09
Joo, S.	2D13
Joshi, K.A.	2F01
Jovicic, G.	3G03
Ju, Y.	1B01, 1B11, 1D04, 2C03, 3C03, 3G07, 3G12, 5A02, 5B06, 5B07
Juddoo, M.	1E07
Julien, P.	5F06, 5F09
Jung, H.	1G08
Juniper, M.P.	2D01
Kadota, T.	4D02
Kagan, L.	3B08
Kaiser, S.A.	1E06, 4E06, 5C05
Kalghatgi, G.I.	Thur Plenary
Kalpathy, S.V.	5E03
Kamada, T.	4G03
Kamal, M.M.	1B09
Kamikaw, D.	2G06
Kanai, K.	4B09
Kang, M.W.	1E05
Karami, S.	1A05
Kariuki, J.	1A06, 3F02
Karnani, S.	2B08
Kasimov, A.R.	4H07
Kasmi, A.E.	2F12
Kasper, T.	2E02, 3B10
Kataoka, H.	4D02
Katayama, M.	1D06
Kathrotia, T.	3B02
Katoch, A.	3F09
Katta, V.R.	2G08
Katzlinger, G.	5B04
Kedia, K.S.	4B06
Keel, S.I.	1A09
Keesee, C.L.	5B09
Kellenberger, M.D.	4H01
Kelley, A.P.	4C01
Kempf, A.M.	3D07, 4E06, 5G07

<i>Author</i>	<i>Paper #</i>
Keramiotis, C.	4G08
Kerstein, A.R.	4A03
Khalil, M.	3A11
Khare, P.	4E07
Kholgy, M.	2E11
Khosousi, A.	3E02
Kiecherer, J.	3C10
Kiefer, M.	3B11
Kikui, S.	4G03
Kim, J.	2D13
Kim, K.	3A12
Kim, N.I.	4G05
Kim, S.D.	2H06
Kim, S.H.	2H06
Kim, W.K.	2H09, 3G06
Kim, Y.	4F08
Kislov, V.V.	3E03
Kiyanda, C.B.	4H06
Kizakii, Y.	4G02
Klein, A.	5C05
Kliwer, C.J.	1E03
Klimenko, A.Y.	5A01
Klippenstein, S.J.	1C12, 2C01, 3C01, 3C04
Knop, V.	5D10
Kobayashi, H.	3B12
Kodavasal, J.	3D12
Köhler, M.	2E02, 3B10, 5E07
Kohse-Höinghaus, K.	2C03, 2E01, 2E05, 2F12, 3B06, 3B10, 3E05
Kojima, T.	2H01
Kolla, H.	4A03, 4A07
Kollmann, W.	4A07
Kong, C.	5F10
Kong, W.	4B02
Konnov, A.A.	1B05, 2C04
Kono, M.	5H02
Koo, H.	5H05
Kook, S.	1A13
Kornilov, V.	4B04
Koshi, M.	4E08
Kosugi, A.	5G03
Kouotou, P.M.	2F12
Kraft, M.	2C13, 5E01, 5F03

<i>Author</i>	<i>Paper #</i>
Krisman, A.	2B12
Kristensson, E.	1E10
Kronenburg, A.	1H06, 4D08, 5A09
Krüger, J.	2C03, 3B10
Kudo, T.	3B12
Kuhl, J.	3G03
Kukkadapu, G.	2C10
Kulatilaka, W.D.	4B03
Kumar, S.	3F09
Kuo, A.	2B07
Kurdyumov, V.N.	3B09, 5B03
Kurimoto, N.	2C03, 3C03
Kuriyama, T.	3D04
Kushida, G.	2G04
Kutne, P.	1E12
Kuwana, K.	2G04, 2H09, 5G03
Kweon, C.-B.	5D13
Kwon, O.B.	1A09
Kyritsis, D.	5C13
Labahn, J.W.	3F11
Labbe, N.J.	2C01
LaBry, Z.A.	4B07
Lacaze, G.	3A11, 4D07
Lackner, A.	3B10
Lacour, C.	5G06
Lai, J.Y.W.	5E02, 5E06
Lalit, H.U.	1G10
Lam, K.-Y.	1C05
Lamoureux, N.	5C01
Lapointe, S.	5B02
Larfeldt, J.	3G11
Larsson, A.	3G11
Laskin, A.	4C06
Lau-Chapdelaine, S.-M.	5H01
Laue, M.	1G01
Lavoie, G.A.	3D10, 3D12
Law, C.K.	1B01, 2A12, 2A13, 2F07, 2F11, 3B04, 4A03, 4C01, 5C10
le Chenadec, V.	4B05
Lee, H.J.	2H06
Lee, J.H.S.	4H03, 4H04, 4H06
Lee, M.	1B12
Lee, M.C.	2D13
Lee, M.J.	4G05

<i>Author</i>	<i>Paper #</i>
Lee, S.-Y.	5D13
Lee, T.	1D11, 5H03
Lee, W.J.	1A09
Leermakers, C.A.J.	5D03
Lefebvre, A.	5B08
Lefkowitz, J.K.	3G07
Legros, G.	2E07, 2G01
Lei, J.	4F03
Leipertz, A.	1E02, 1E04, 3G03
Lempert, W.R.	3G08
Lewis, A.D.	5E10
Li, A.	1F03, 5H12, 5H13
Li, B.	1D08
Li, B.	2B10
Li, D.	1H05
Li, J.	4H05
Li, K.	1F03, 1G13
Li, L.	5D06
Li, L.K.B.	2D01
Li, P.	1D08
Li, S.	2F03, 2F04, 2F07, 4E04, 5F10
Li, S.	4C08, 5C03
Li, T.	3G09
Li, W.	5G08
Li, X.	1D08
Li, X.	1E05
Li, X.	2F06
Li, X.	5C10
Li, Y.	1D13
Li, Y.	2B03, 2B04, 2C12, 2E06, 3C11, 4C01
Li, Z.S.	1F01, 2A04, 3G11
Liang, J.-H.	2H03
Liang, W.	1B01
Liao, K.-P.	2B11
Lieb, S.	3E05
Lieuwen, T.C.	1A04, 4A05, 5A04
Lifshitz, A.	4C06
Lignell, D.O.	5E10
Lin, J.Y.	2A11
Liñán, A.	Tue Topical
Lind, S.	1E04
Lindstedt, R.P.	2H10, 5A03
Linne, M.	3F05
Linteris, G.T.	2G08

<i>Author.....Paper #</i>	<i>Author.....Paper #</i>	<i>Author.....Paper #</i>	<i>Author.....Paper #</i>
Lipatnikov, A.N.1B10,2A11, 4A02	Manin, J.5D11	Mercier, X.3E06	Nahon, L.3B10
Liu, C.C.2A11	Mann, M.1E03	Meredith, K.V.4F06	Nair, V.2D06
Liu, D.1F04	Mannan, M.S.2G07	Merhubi, H.E.5C01	Najm, H.N.3A11
Liu, F.2E10	Manofskv Olesky, L.K.3D10	Meynet, N.2G09	Naka, Y.1D06,1E13, 3D06, 4G04
Liu, H.1F03, 5H12, 5H13	Mansour, M.S.2F08	Mi, X.4H05	Nakahara, M.1B06
Liu, J.5H10	Mantzaras, J.2F05, 4G07	Michael, J.V.4C02	Nakahara, T.1F06
Liu, N.1G06, 4F03	Marin, G.B.1C10	Michel, J.-B.3A03	Nakamura, H.4G01,4G02, 4G03
Liu, P.5H12	Marincola, F.C.5G07	Michelsen, H.A.5E06	Nakamura, Y.1G01,4F08, 5G02, 5G03
Liu, Q.5H03	Markus, D.2H05, 3B11	Middleton, R.J.3D10	Nakaya, S.5H02
Liu, S.4F02, 5H11	Marquis, A.J.2A09	Mikheyeva, E.3E08	Nakazawa, Y.5H02
Liu, S.5G10	Marshall, A.4A05	Miller, J.H.4E01	Nasir, E.F.1C02
Liu, T.5H08	Marshall, P.1C03, 1C11	Miller, J.A.1C06, 1C13	Nathan, G.J.4E03, 5E08
Liu, W.4G06	Martin, J.1A03	Miller, W.1G08	Nativel, D.1C04
Liu, X.1H05	Martinez, L.5D08	Millera, Á.2E04	Navarro-Martinez, S.4H08
Liu, Y.4G06, 5G10	Martz, J.B.3D10, 3D12	Mimoto, R.3B12	Nawdiyal, A.4C04
Liu, Y.C.4D01, 4D04	Maruta, K.4G01,4G02, 4G03	Minamoto, Y.3F08	Newale, A.S.1G10
Long, M.B.2B06, 2E08	Masri, A.R.1E07, 2A10,3A09, Fri Topical	Minutolo, P.5E12	Ng, H.D.4H04, 4H06
Long, Y.1F04	Massot, M.4B05	Mirat, C.4B08	Ngamou, P.H.T.2F12
Lopez, I.4B04	Mastorakos, E.1A06, 3A04,3A10, 3F02, 3F07	Misdariis, A.1D05, 4D07	Nijmeijer, H.4B04
Lou, G.3G07	Masurier, J.-B.5D02	Miyamae, S.5B01	Niksa, S.2F02
Low, F.5H13	Matalon, M.1A11, 1B04,2B11, 3B09, 4B01	Miyata, E.4G04	Nilsson, E.J.K.2C04
Lowe, J.S.5E02	Mathieu, O.1D07, 2G07	Miyauchi, T.1D06, 1E13,3D06, 4A06, 4G06	Nishiki, S.4A02
Lu, K.1G12	Mauß, F.4C04	Mizutani, K.2G03	Niu, F.2F04
Lu, T.3A06, 3F03	Mazellier, N.1A01	Moeck, J.P.2D09	Niu, Y.1F02, 1F07
Lucassen, A.2E02, 3B01,3B02, 3B10	McDermott, R.J.1G10	Mog, T.2H09	Noh, D.2A09
Lucchini, T.1A13	McDougall, A.P.3D11	Moiz, A.5D13	Nordin-Bates, K.5H04
Lucht, R.P.1E01, 1E12	McManus, T.A.3A01	Montanaro, A.5D13	Nordström, E.4E02
Lundrigan, J.4A05	McNenly, M.J.4C07, 5C07	Morel, M.5F04	Nouno, Y.2B09
Luo, K.H.1E07	Meares, S.1E07, 3A09	Morganti, K.J.1D12	Nurkowski, D.5F03
Lv, G.2E12, 2F06	Mebel, A.M.3E03	Mori, K.1G02	Oana, C.M.1C13
Lv, W.5G05	Medwell, P.R.5E08	Morinaga, Y.4D02	Oberleithner, K.3D01
Lv, Y.2H13	Meffert, C.5C05	Morones, A.5B09	Oefelein, J.C.3A11, 3F06, 4D07
Lynch, P.T.4C05	Mehl, M.2C10, 4C09	Mosbach, S.2C13, 5E01	Oehlschlaeger, M.A.1D11, 2C10
Ma, B.2B06, 2E08	Mehrjoo, N.4H06	Moshhammer, K.3B10	Ogawa, S.3D06
Ma, L.1E05	Meier, W.1E01, 1E12,2A02, 3D02, 3D03, 5E07	Mossa, F.M.S.2D11	Oka, Y.4D02
Ma, Y.2E13	Mejia, D.2D02	Mounaim-Rousselle, C.1B02	Okazaki, K.1F05, 1F12
Maas, U.2H05, 3B11,3C06, 5A01	Melroy, H.R.4E01	Moureau, V.1A02	Okuno, Y.3D04
Mack, J.H.5D01	Memon, N.K.2F08	Mouton, T.3E06	Olenik, G.1H06
Magina, N.A.5A04	Menser, J.4E06	Mueller, M.E.5E05	Olivier, H.3C12
Magnotti, G.1E08,3A09, 5A13	Merchan-Merchan, W.2F09	Mühlberger, F.3E09	Olm, C.5C11
Mahmoud, S.M.5E08	Merchant, S.S.2C09	Mulvihill, C.1D07	Olofsson, N.-E.3E06, 4E02
Mahmoudi, Y.Wed Plenary	Mercier, R.1A02, 5A10	Murphy, D.3G01	O'Loughlin, W.5E07
Maley, L.5H01		Musculus, M.P.B.5D03	Olson, S.L.1G05
		Nada, Y.1D06, 3D06	Olzmann, M.3C10
		Nagaraja, S.3G09, 3G10	
		Nagy, T.5C11	

<i>Author</i>	<i>Paper #</i>
Ombrello, T.M.	2H02,
.....	5A02, 5H03
Oobayashi, T.	1D06
Oran, E.	Hottel, 2H08
Osborn, D.L.	1D09,
.....	3C02, 3C08
Osorio, A.F.	2G03
Oßwald, P.	2E02, 3B10
Packard, A.	5C08
Padilla, R.E.	2B08
Paillard, C.-E.	2G09
Palecka, J.	5F09
Pálvölgyi, R.	5C11
Pang, H.	2E12
Pantano, C.	2B11
Paolini, C.	1G01, 1G03
Papageorge, M.J.	3A01
Park, J.	1A09
Park, J.H.	2H06
Park, S.	2C10, 3B01
Paschereit, C.O.	3D01
Patterson, B.D.	1E03
Pause, M.J.	4E01
Pera, C.	5D10
Peters, N.	1A10, 3C05
Petersen, E.L.	1D07,
.....	2G07, 5B09
Peterson, B.	5C04, 5D12
Petersson, P.	3G11
Petterson, K.	5H04
Peukert, S.L.	4C02
Pham, T.	2B08
Philip, M.	3D08
Philips, D.A.	5H06
Pickett, L.M.	5D11
Pitsch, H.	1B03, 1D09, 2E07,
.....	3C05, 3C07, 3C12, 5E05
Pitz, R.W.	4B03
Pitz, W.J.	2C10,
.....	4C07, 4C09
Plaud, M.	5F04
Poddar, N.B.	5E03
Poinsot, T.	1D05, 2D02,
.....	2D07, 2D10
Polifke, W.	2D03
Popolan-Vaida, D.M.	5E06
Poyraz, Y.	1H03

<i>Author</i>	<i>Paper #</i>
Prasad, V.N.	1E07, 3A09
Pré, P.	3E04
Proch, F.	3D07, 5G07
Pucher, E.	5B04
Qi, F.	2B03, 2B04,
.....	2C12, 2E06, 3C11
Qi, L.	1G08
Qiao, Y.	5H11
Qin, H.	4H03
Qiu, Z.	1G12
Rabaçal, M.	5G07
Rabl, S.	3D11
Radulescu, M.I.	5H01
Raganati, F.	1H07
Raghavan, V.	2F01
Rahim, M.U.	1H01
Rahm, M.	3F05
Raj Mohan, V.R.	5D07
Rajendran, S.	5G08
Raman, V.	2A10, 5H05
Ranganathan, S.	1B12
Rangwala, A.S.	1B12, 1G07,
.....	2F01
Rankin, B.A.	1G10
Ranzi, E.	4D06
Rao, F.	1D08
Rashidi, M.J.A.	3C09
Ravi, S.	5B09
Reddy, V.M.	3F09
Rein, G.	2G05
Reitz, R.D.	1D13
Ren, N.	4F05
Ren, Y.	2F07, 4E04
Renaud, A.	3D05
Renfro, M.W.	1E09
Renou, B.	1B03, 5B08
Reuss, D.	5D09
Reveillon, J.	5D10
Riber, E.	3D08, 3D09
Ricchiutti, V.	2B08
Richard, S.	5D08
Richecoeur, F.	4B05
Risha, G.A.	4E07
Robert, A.	5D08
Roberts, W.L.	3F09
Roekaerts, D.J.E.M.	3F10
Rosdzimin, R.A.M.	5B01

<i>Author</i>	<i>Paper #</i>
Rotavera, B.	1C09
Rothamer, D.A.	5D05
Rouzaud, J.-N.	3E04
Roy, A.	5F07
Ruff, G.A.	1G05
Ruiz, A.	2D05, 4D07
Russi, T.	5C08
Russo, C.	2E03, 3E04
Sabelnikov, V.A.	4A02, 5H04
Saghafian, A.	5H06
Saha, A.	2A12, 2A13
Sahu, A.K.	2F01
Saiki, Y.	5G01
Sakai, S.S.	5D05
Sakai, Y.	3C07
Sakaki, K.	5H02
Salehi, M.M.	1A12
Salehia, F.	1A13
Sanchez, A.	Tue Topical
Sanchez-Sanz, M.	3G01
Santner, J.	1B11, 5B07
Saraji-Bozorgzad, M.	3E09
Sarathy, S.M.	2B13, 2C10,
.....	3B01, 3C09, 3C12
Sato, N.	5G03
Sato, T.	4B09
Satoh, K.	1G06, 4F03
Saucedo, M.A.	1H08
Savard, B.	2A06
Savee, J.D.	3C02, 3C08
Saveliev, A.	2F09
Saxena, P.	5B04
Saxena, S.	5D01
Sayadi, T.	4B05
Scala, F.	1H04
Scheer, A.M.	1C09
Schenk, M.	2E01, 3E05
Schiessl, R.	3C06
Schmid, P.	4B05
Schmitt, M.	1D01
Schmitt, T.	2D05, 3A05,
.....	3D08, 5A10
Schoegl, I.	2B01
Schoemaecker, C.	5C01
Schuller, T.	2D09, 4A01, 4B08
Schultze, M.	2F05, 4G07

<i>Author</i>	<i>Paper #</i>
Schulz, C.	1C04, 1E06,
.....	3C06, 4E05, 5C05, 5D04,
Scott, S.A.	1H08
Scouflaire, P.	3D05,
.....	4A01, 5E11
See, Y.C.	5A11
Seeger, T.	1E02
Segawa, D.	4D02
Seidel, L.	4C04
Seitzman, J.	4A05
Selle, L.	2D02
Seo, S.	1G02
Serinyel, Z.	2C06
Seshadri, K.	2B07,
.....	5B04, 5F01
Shaddix, C.R.	1F07
Shafirovich, E.	2F10
Shahbazian, N.	1A12
Shanbhogue, S.J.	4A04, 4B07
Shen, H.	3A06
Shen, X.	1B11
Sheps, L.	3C02
Shi, X.	1G07
Shimokuri, D.	5G04
Shimomura, K.	1F05
Shimura, M.	1D06, 1E13,
.....	3D06, 4A06, 4G06
Shinjo, J.	3F04
Shoshin, Y.	5B03
Shunn, L.	5H06
Shy, S.S.	2A11
Si, J.	1H05
Sick, V.	5D12
Sidey, J.	3F07
Sikes, T.G.	5B09
Sim, H.S.	5F02
Simeoni, A.	1G07
Simmie, J.M.	1C10
Simonsson, J.	3E06, 4E02
Singh, A.V.	4F07
Singh, R.I.	3E03
Sirignano, M.	1C08, 3E07
Sirjean, B.	1C07, 2E05
Sivaramakrishnan, R.	2C01,
.....	4C02
Sivashinsky, G.	3B08
Sjöberg, M.	5D09

<i>Author.....Paper #</i>	<i>Author.....Paper #</i>	<i>Author.....Paper #</i>	<i>Author.....Paper #</i>
Skeen, S.A.5D11, 5E06	Swaminathan, N.3F08	Tranter, R.S.4C05	Villaraza, J.R.1G03
Skevis, G.1C01	Taamallah, S.4B07	Tree, D.R.1H02	Vincze, G.5C11
Slabaugh, C.1E01, 1E12	Taatjes, C.A.1C09,	Tregrossi, A.2E03, 3E04	Violi, A.5E02, 5E06
Smooke, M.D.2B06, 2E083C02, 3C08	Trimis, D.4G08	Voss, S.4G08
Snegirev, A.Y.4F04	Tachibana, S.3D04, 4B09	Troiani, G.1A11	Vourliotakis, G.1C01
Snyder, J.3G06	Tada, J.4D02	Trost, J.1E04	Wada, T.2C03, 3C03
Sohn, C.H.3G12	Taide, N.2B09	Trouvé, A.4F05	Wan, H.1G11
Song, C.2E12, 2F12	Takahashi, F.2B06,	Trunk, P.1E11	Wan, J.4G06
Song, J.2E12, 2F122E08, 2G08	Tse, S.D.4E04	Wang, C.1F13, 1H05
Soo, M.J.5F06	Takahashi, S.1G03, 2G02	Tsiava, R.1H02	Wang, G.5G09
Spearrin, R.M.2C07,	Talei, M.1A05, 1A13,	Tsoy, A.S.4F04	Wang, H.2F11, 3E01,
.....5C03, 5C061D02, 2B12, 5A06	Tsuboi, N.2H013E05, 3F03
Speelman, N.3B11	Tam, C.-J.2H02	Tsuboi, T.3G05	Wang, H.1D13
Speight, W.5C08	Tambour, Y.3F01	Tsue, M.5H02	Wang, H.3A12
Sponfeldner, T.2A02	Tamburu, C.4C06	Tulgestke, A.M.2C07	Wang, H.-B.2H03
Srivastava, S.2F09	Tan, H.1F02	Tummers, M.J.3F10	Wang, K.1H09
Staffelbach, G.2D05, 2D07	Tan, T.2C03	Turányi, T.5C11	Wang, L.2E12
Starr, A.4H04	Tanahashi, M.1D06, 1E13,	Uchida, Y.2G04	Wang, P.5H09
Stein, O.T.1H06, 4D08, 5A093D06, 4A06, 4G06	Uddi, M.3G07	Wang, Q.2D11
Steinberg, A.M.2A03	Tanaka, R.3G05	Ueda, T.5B01	Wang, S.2C05, 2C07
Steinhilber, G.2H05	Tang, F.1G12	Ukai, S.4D08, 5A09	Wang, W.2C10
Stelzner, B.4G08	Tang, W.4F02	Umemura, A.3F04	Wang, X.1F02, 1F09
Stocker, D.P.2B06, 2E08	Tani, H.4E08	Urban, D.L.1G05	Wang, Y.2B04
Stoehr, K.-D.1A10	Tanoue, K.2B09	Urban, J.L.1G09	Wang, Y.2C12
Stöhr, M.3D02	Taylor, A.M.K.P.2A02	Urzay, J.Tue Topical	Wang, Y.4F05, 4F06
Stopper, U.3D03	Terashima, H.4E08	Uygun, Y.3C12	Wang, Z.1F01
Strakey, P.A.1B08	Terhaar, S.3D01	Valco, D.J.1D11	Wang, Z.2C12
Streibel, T.3E09	Tessitore, G.5E12	Valiev, D.M.3B07, 4A03	Wang, Z.3F05
Su, S.5H07, 5H09	Tezuka, T.4G01, 4G02, 4G03	Valkó, É.5C11	Wang, Z.4H03
Sudholt, A.1D09	Thomson, K.A.5E09	van Geem, K.M.1C10	Wang, Z.5B05
Sujith, R.2D06	Thomson, M.J.2E11, 5E04	van Griensven, J.G.H.1B05	Wang, Z.-G.2H03
Sun, H.4C01	Thornock, J.1H02	van Oijen, J.A.3B05, 3B11	Warner, M.2F13
Sun, J.1B11,	Tian, Z.-Y.2F12	van Veen, E.H.3F10	Warth, V.2C11
.....1G11, 1G13	Togbé, C.2C06, 3C12	Vandooren, J.1B13	Watanabe, H.1F05, 1F12
Sun, L.5H07, 5H09	Tokunaga, K.1B06	Varea, E.1B03, 5B08	Watanabe, J.1F08
Sun, M.-B.2H03	Toma, M.2B13	Varga, T.5C11	Watanabe, Y.2H01
Sun, T.5A04	Tomboulides, A.G.1B04,	Vargas, M.M.4D03	Weber, R.1H03
Sun, W.3G10, 5B061D01, 4B01	Varghese, P.L.5H05	Wei, J.2E12
Sun, Z.W.4E03	Tomiooka, S.5H02	Venkateswaran, P.4A05	Wei, M.5H11
Sundaram, B.5A01	Tomita, H.5B01	Verdicchio, M.1C07	Weingarten, J.2E11
Sung, C.-J.2C10	Tomlin, A.S.5C09	Vermorel, O.1D05	Weinkauff, J.1E11
Sutherland, J.C.1H10	Torero, J.L.2G01	Vervisch, L.1A03, 1B07	Weise, C.4E06
Sutton, J.A.3A01,	Torikai, H.4F01	Veynante, D.1A02, 5A10	Weise, D.1G08
.....3A06, 3G09, 5A13	Toulson, E.1D11	Vicquelin, R.3D08	Welz, O.3C02, 3C08
Suzuki, K.4B09	Tovar, D.1H02	Vié, A.3F03	Wendt, J.O.L.1F10
Suzuki, S.4G01	Tran, L.S.1C07, 2E05	Vieker, H.2E01, 2F12, 3E05	Weng, W.2G06
Suzuki, Y.5G01	Tran, W.1G01, 1G03	Vilfayeau, S.4F05	Werler, M.3C06

<i>Author.....</i>	<i>Paper #</i>
Westmoreland, P.R.	5C08
Whiteley, S.	5F06
Whitesides, R.A.	5C07
Wiggers, H.	4E05
Will, S.	1E04, 3G03
Williams, B.J.	1F09
Williams, F.	5E01
Wilson, K.R.	5E06
Windom, B.C.	3G07, 5A02
Witzel, O.	5C05
Wlokas, I.	4E05, 4E06
Wolk, B.M.	1D10
Won, S.H.	3G12, 5A02, 5B06
Wooldridge, M.S.	3D10
Woolley, R.	2D11
Wornat, M.J.	5E03
Worth, N.A.	2D07, 2D08
Wright, Y.M.	1D01
Wu, D.	5G10
Wu, F.	1B01, 2A12, 5C10
Wu, H.	1H01, 1F04
Wu, J.	1G06, 5G05
Wu, S.	2F06
Wu, Z.	5D06
Wysocki, G.	3C03
Xia, J.	3F04
Xiang, J.	5H07, 5H09
Xiao, R.	5G08
Xiao, X.	5H09
Xie, M.	1D13
Xin, Y.X.	2F11, 3B04
Xiong, Y.	2B05, 3G02
Xu, M.	1H05, 5G05, 5H11
Xu, Y.	4D04
Xu, Z.	1F03
Xuan, Y.	5E13
Xue, L.	5H08
Xue, Y.	1H02
Yamamoto, K.	1F08, 1G02
Yamamoto, T.	3G05
Yamashita, H.	4D02
Yang, B.	2F11, 3B02, 3C11
Yang, F.	4B02
Yang, J.	2B03
Yang, J.	2D11
Yang, S.I.	2A11

<i>Author.....</i>	<i>Paper #</i>
Yang, V.	3G09, 3G10, 4E07
Yang, W.	1H09
Yang, X.	1B11, 2C03, 3C03
Yang, Y.	1D12
Yang, Z.	5H11
Yao, H.	1F03, 4G06, 5H12, 5H13
Yao, Q.	2F03, 2F04, 4E04, 5F10
Ye, L.	1C12, 2E06
Yeates, D.R.	5C08
Yenerdag, B.	4A06
Yetter, R.A.	4E07, 5F02
Yin, Z.	3G08
Yokomori, T.	5B01
Yoo, C.S.	1A13, 3B04
Yoon, J.H.	1A09, 2D13
Yoon, Y.	2D13
Yoshida, S.	4B09
Yoshioka, K.	1G04
You, X.	5C10
Yu, D.	5F10
Yu, D.	5G05
Yu, H.	1A05
Yu, J.-F.	2H03
Yu, R.	1B10, 1D03, 4A08
Yu, S.	4H08
Yu, Y.	1F04, 5H11
Yuan, R.	1A06, 3F02
Yuan, W.	2B03, 2B04, 3C11, 4C01
Yuan, Y.	2F03
Yuristchev, M.	3E08
Zaczek, L.T.	1C05, 2C07
Zádor, J.	1C06, 3C02
Zak, C.D.	1G09
Zaras, A.	2C06
Zendejdel, M.	5A09
Zeng, W.	5D09
Zettervall, N.	3G11
Zeuch, T.	4C04
Zhan, Z.	1F10
Zhang, A.	5H07, 5H09
Zhang, B.	5H10
Zhang, C.	1D08
Zhang, D.	2E13
Zhang, F.	1D03

<i>Author.....</i>	<i>Paper #</i>
Zhang, F.	2C12, 2E06
Zhang, H.	2B10
Zhang, H.	3A04
Zhang, L.	1G06
Zhang, L.	2C02, 2E06, 2C12, 3C11
Zhang, L.	5G05, 5H13
Zhang, P.	2C02
Zhang, Q.	5H12
Zhang, S.	3B03
Zhang, S.	5G08
Zhang, X.	3C11
Zhang, X.	3G04
Zhang, X.	4F02
Zhang, Y.	1D13
Zhang, Y.	1F10
Zhang, Y.	1G04
Zhang, Y.	2B10, 2D11
Zhang, Y.	2F07, 4E04
Zhang, Z.	2E13
Zhao, B.	1H05
Zhao, H.	1H09
Zhao, L.	2B03, 2E06
Zhao, P.	4C01
Zhao, R.	5B08
Zheng, C.	1H09, 5G10, 5H08, 5H10
Zheng, X.	4C01
Zhou, B.	2A04
Zhou, C.	5H07
Zhou, R.	1B09
Zhou, X.	2G10
Zhou, Z.	1G08
Zhu, J.	3G11
Zhu, M.	2E13
Zhu, Y.	1F02, 4C08
Zhuang, F.-C.	2H03, 4H03
Zigan, L.	1E04, 3G03
Zimmer, L.	3D05
Zimmermann, R.	3E09
Zong, Y.	2F04
Zou, C.	5G10
Zsély, I.G.	5C11

HOTTEL LECTURE: UNDERSTANDING EXPLOSIONS - FROM CATASTROPHIC ACCIDENTS TO CREATION OF THE UNIVERSE

Elaine S. Oran, University of Maryland, College Park, United States

This paper focuses on two extremes of explosions: the general class of Type Ia supernova (SNIa), which are surprisingly uniform thermonuclear explosions of white dwarf stars, and a specific gasoline vapor-cloud explosion that occurred at the Buncefield fuel depot in 2005. In both cases, recurring questions are whether an initial spark or small, local ignition could result in a detonation, and if so, how could this happen? The broader question is: What is the origin of the Deagration-to-Detonation Transition (DDT) in confined, partially confined, and unconfined systems? The importance of DDT to SNIa is based on the use of these objects as cosmological "standard candles" that are used for measuring distances and curvature in the universe. The importance of DDT to Buncefield is related to design and operational safety of industrial plants and storage facilities. Combinations of observations, specific laboratory experiments, and selected numerical simulations have given us information and some understanding of the DDT process and its likelihood. Numerical simulation both of large- and small-scale phenomena in these reactive flows were important ingredients in the studies. The invention and discovery of numerical algorithms, including (but not limited to) monotone methods, implicit large-eddy simulation, and adaptive mesh refinement, enabled these simulations certainly as much as the increase in computer speed and memory. Unresolved issues that arose in these studies are the nonequilibrium, non-Kolmogorov properties of the turbulence and turbulent fluctuations in these flows, and how these prepare the system for transitions, and how to represent the chemical reactions and energy release in the high temperatures and pressures that are near and might signal a transition.

elaine.oran@gmail.com

1A01 INVESTIGATION OF PRESSURE EFFECTS ON THE SMALL SCALE WRINKLING OF TURBULENT PREMIXED BUNSEN FLAMES

Romain Fragner¹, Fabien Halter^{1,2}, Nicolas Mazellier², Christian Chauveau¹, Iskender Gökalp¹

¹Centre National de la Recherche Scientifique Institut de Combustion, France ²Université d'Orléans, France

High pressure turbulent premixed flames have been significantly studied in the past decade. The eloquent flame images obtained under high pressure conditions attest the large changes in flame front wrinkling enhanced by the pressure increase. Among the explanation attempts, pressure was assumed to promote Darrieus-Landau (DL) instabilities. More recently the role of the laminar flame thickness was also identified as a key parameter for the flame/turbulence interactions. The objective of the current study is to contribute to this debate by isolating the effects of the suspected parameters. To do so, turbulent methane/air flames are investigated in a high pressure combustion test facility. A multigrid turbulence promoter system has been developed and implemented to obtain a more intense, isotropic and homogeneous turbulence at the burner exit. The pressure range is 0.1–0.4MPa, and the mixture composition is varied between ER=0.7 and ER=1.0. Instantaneous flame images have been collected using Mie scattering tomography and exploited to analyze flame–turbulence interactions under controlled conditions. Flame and turbulence parameters have been independently varied under DL instability free conditions to isolate the effect of the laminar flame thickness and that of the small scale turbulence eddies. The stretching of the turbulence energy spectrum towards smaller turbulent length scales is identified as the main reason for the enhanced flame front wrinkling under high pressure flame conditions, together with the reduction of the laminar flame thickness. The Taylor micro-scale appears to be the regulating turbulence scale for flame–turbulence interactions.

fabien.halter@univ-orleans.fr

1A02 LES OF TURBULENT COMBUSTION: ON THE CONSISTENCY BETWEEN FLAME AND FLOW FILTER SCALES

R. Mercier^{1,2}, V. Moureau³, D. Veynante^{1,2}, B. Fiorina^{1,2}

¹Ecole Centrale Paris, France ²CNRS, France ³CORIA - CNRS, France

A recurrent issue in premixed combustion LES is that the flame thickness is smaller than the grid size. Broadening of the reactive layer is then mandatory to ensure a proper propagation of the filter flame front. The reactive flow governing equations exhibit then two filter operators of different sizes dedicated to the flow field and the flame front, respectively. The consistency issues between flame and flow filter sizes in LES of turbulent premixed flames are discussed in the present article. A general mathematical formalism considering two different filter sizes is proposed. A new closure of the resulting LES balance equations system is derived in the framework of the Filtered TABulated Chemistry for LES (F-TACLES) formalism. The new model, called F2-TACLES, is first validated by computing 1-D premixed filtered flames. Then an LES of the complex turbulent premixed PRECCINSTA swirl burner is successfully performed. In particular, the new model formulation improves the prediction of resolved flame/turbulence interactions.

renaud.mercier@graduates.centraiens.net

1A03 LOCAL VOLUMETRIC DILATATION RATE AND SCALAR GEOMETRIES IN A PREMIXED METHANE-AIR TURBULENT JET FLAME

Luis Cifuentes¹, César Dopazo¹, Jesús Martín¹, Pascale Domingo², Luc Vervisch²

¹LIFTEC, Spain ²CORIA - CNRS, France

The local volumetric dilatation rate, namely, the rate of change of an infinitesimal fluid volume per unit volume, $\nabla \cdot \mathbf{u}$, is an important variable particularly in flows with heat release. Its tangential and normal strain rate components, a_T and a_N , respectively, account for stretching and partially for separation of *iso*-scalar surfaces. A three-dimensional Direct Numerical Simulation (DNS) of a turbulent premixed methane-air flame in a piloted Bunsen burner configuration has been performed by solving the full conservation equations for mass, momentum, energy and chemical species. Results for the volumetric dilatation rate as a function of the *iso*-scalar surface geometry, characterized by the mean and gauss curvatures, k_m and k_g , are obtained in several zones (reactants, preheat, reacting and products) of the computational domain. Flat *iso*-scalar surfaces are the most likely geometries in agreement with previous DNS. The relationship between density and reaction progress variable, under the constant-pressure flow assumption [Combust. Flame 61:87-102 (1985)], leads to an expression for $\nabla \cdot \mathbf{u}$ with contributions from reaction and molecular diffusion, with a significant contribution from the latter; this approximate expression for the volumetric dilatation rate is in good agreement with DNS results. The joint pdf of a_N and a_T confirms that the line $a_T + a_N = 0$ separates mostly expansive flow regions from compressive zones.

lcifuentes@unizar.es

1A04 LEADING EDGE STATISTICS OF TURBULENT, LEAN, H₂-AIR FLAMES

A. Amato¹, M.S. Day², R.K. Cheng², J. Bell², T. Lieuwen¹

¹Georgia Institute of Technology, United States ²Lawrence Berkley National Laboratory, United States

Several studies have utilized leading points concepts to explain the sensitivity of turbulent burning rates to fuel/oxidizer composition, especially in negative Markstein length mixtures. Leading point theories suggest that the premixed turbulent flame speed is controlled by the flame front characteristics at the flame brush leading edge, or, in other words, by the flamelets that advance farthest into the unburned mixture (the so-called leading points). Furthermore, several authors have postulated that these leading edge flamelets have an inner structure similar to a critically perturbed laminar flame, i.e., the local stretch rate approaches the extinction value at which the maximum possible laminar burning velocity is reached.

In order to investigate these hypotheses for leading points burning rates, this paper analyzes the flame front structure at the leading edge of turbulent, lean ($\phi = 0.31$) premixed H₂/air flames, utilizing a database of Direct Numerical Simulations (DNS) previously reported by Aspden *et al.* We calculate local flame front curvature, thickness, and burning velocity and compare these values to reference quantities obtained from stretched laminar flames computed numerically in different geometrical configurations (a counterflow twin flame, a tubular counterflow flame and an expanding cylindrical flame). These comparisons show that curvatures and burning velocities approach those of “critically” stretched laminar flames for the highest turbulent intensity case, but not for the lower turbulence intensity cases. In all cases, however, the structure of the flame front at the leading edge seems to closely mirror laminar flame calculations.

alberto.amato@gatech.edu

1A05 EDGE FLAME STRUCTURE IN A TURBULENT LIFTED FLAME: A DIRECT NUMERICAL SIMULATION STUDY

Shahram Karami¹, Mohsen Talei², Evatt R. Hawkes^{1,2}, Hongfeng Yu³

¹University of New South Wales, Australia ²University of New South Wales, Australia ³University of Nebraska-Lincoln, United States

A turbulent lifted slot-jet flame is studied using Direct Numerical Simulation (DNS). A single step chemistry model was employed with a mixture-fraction dependent activation energy which can reproduce qualitatively the dependence of laminar burning rate on equivalence ratio that is typical of hydrocarbon fuels. The basic structure of the flame base is first examined by considering the time evolution of fields of temperature, reaction rate, scalar dissipation rate and velocity, with findings as follows. The leading flame edges exhibit a single branch close to the stoichiometric contour, rather than tribrachial structure. There is no evidence of a rich inner premixed flame or detached diffusion flame islands, in contrast with previous DNS of hydrogen flames. There are two kinds of flame holes which occur. The first is caused by turbulent structures that push the flame towards the oxidiser causing high dissipation rates and extinction. The second is caused by local downstream motion of the flame edge followed by flame healing at an upstream position. Hook-like structures are observed to result from large turbulent eddies and entrainment. The averaged structure is then examined. The entrainment flow is shown to be diverted around the flame base causing locally upstream streamwise velocities. A budget of terms in the transport equation for product mass fraction is used to reveal a complex, twodimensional stabilisation mechanism involving upstream transport of products on the lean side balanced by entrainment into richer conditions, and on the rich side, upstream turbulent transport and entrainment from leaner conditions balancing streamwise convection.

s.karami@unsw.edu.au

1A06 HEAT RELEASE IMAGING IN TURBULENT PREMIXED METHANE-AIR FLAMES CLOSE TO BLOW-OFF

J. Kariuki¹, A. Dowult², R. Yuan¹, R. Balachandran², E. Mastorakos¹

¹University of Cambridge, United Kingdom ²University College London, United Kingdom

Estimates of the Heat Release (HR) of unconfined lean premixed methane-air flames stabilized on an axisymmetric bluff body have been measured for conditions increasingly closer to blowoff. Simultaneous imaging of OH- and CH₂O-PLIF was performed, and HR measurements obtained using the pixel-by-pixel multiplication of the OH- and CH₂O-PLIF images. Blow-off was approached by slowly reducing the fuel flow rate. At conditions far from blow-off, HR occurred along the shear layer, whereas at conditions near blow-off, HR was also observed inside the Recirculation Zone (RZ). Localised extinctions along the flame front were seen at conditions away from blow-off, and increased in frequency and size as blow-off was approached. At conditions near blow-off, HR was detected on the boundary of flame pockets inside the RZ which had detached from the fragmented flame at the attachment point. Regions void of OH in the RZ near blow-off were often seen to be filled with CH₂O. Regions void of both OH and CH₂O were also observed, but less often, indicating the presence of both preheated gases and fresh reactants inside the RZ. Such images do not show a connection with the annular air jet, implying the cold reactants entered the RZ from the top. No significant correlation between HR and flame front curvature was obtained for the near unity Lewis number flames investigated. The measurements reported here are useful for model validation and for exploring the changes in turbulent premixed flame structure as extinction is approached.

jmk62@cam.ac.uk

1A07/08 TOPICAL REVIEW: MULTICOMPONENT TRANSPORT IN LAMINAR FLAMES

Vincent Giovangigli, CMAP-Ecole Polytechnique, France

The transport fluxes and transport coefficients derived from the kinetic theory of polyatomic gas mixtures are discussed. The mathematical structure of transport linear systems and numerical algorithms for fast evaluation of accurate transport coefficients are presented. The impact of thermal diffusion and volume viscosity on flame structures and of thermodynamic nonidealities on cold mixing layers are investigated.

giovangi@cmaph.polytechnique.fr

1A09 HEAT-LOSS-INDUCED SELF-EXCITATION IN LAMINAR LIFTED COFLOW-JET FLAMES

Won June Lee¹, Jeong Park¹, Oh Boong Kwon¹, Jin Han Yoon², Sang In Keel²

¹Pukyong National University, Korea ²Korea Institute of Machinery and Materials, Korea

Laminar lifted propane coflow-jet flame diluted with nitrogen was experimentally investigated to clarify the effect of coflow air. Flame stability maps with the functional dependencies of fuel jet velocity and fuel mole fraction were examined at various coflow air velocities. Those are very sensitive to coflow air velocity and the liftoff height varied more sensitively to coflow air velocity than fuel jet velocity. Four regimes were identified by coflow air velocity: (I) a Heat-Loss-Induced Self-Excitation (HLISE) in $0 \leq V_{co} \leq 2.5$, (II) a stationary lifted flame in $2.5 < V_{co} \leq 10$, (III) an intermittent HLISE in $10 < V_{co} < 40$, and (IV) a stationary lifted flame in $V_{co} \geq 40$. There existed a critical lift-off height over which an intermittent HLISE was restored. Such regimes and the intermittent HLISE were shown to appear because the tribrachial flame speed was influenced by several competition factors: fuel concentration gradient (flame curvature), conductive heat loss from premixed wings to trailing diffusion flame, and preheated, partially premixed reactant influx into tribrachial flame due to introducing coflow air. The mechanisms of such regimes and the intermittent HLISE were discussed. The characterizations of liftoff height in such regimes, the intermittent HLISE, and the critical liftoff height were described by the functional dependencies upon related physical parameters.

jeongpark@pknu.ac.kr

1A10 LOW TEMPERATURE OSCILLATIONS OF DME COMBUSTION IN A JET-STIRRED REACTOR

Klaus-Dieter Stoehr, Joachim Beeckmann, Norbert Peters, Institut fuer Technische Verbrennung, Germany

The low temperature oxidation behavior of DME in a jet-stirred reactor is investigated. There have been numerous investigations on the low temperature reaction kinetics of DME. In this work, the focus is set on the instabilities that arise at very low temperatures (in the order of 580K) in a jet-stirred reactor and a numerical analysis of the source of these oscillations is performed. A stability map was created where the parameters at which the oscillations were observed are displayed. The temperature oscillations at higher temperatures (around 1000K) have been shown to be caused by ignition-extinction phenomena, whereas the oscillations observed at low temperatures are believed to be of thermokinetic origin, with the build-up of a semi-stable species Hydroperoxide-Methylformate (HPMF), its dissociation at increasing temperatures with the subsequent formation of large quantities of formaldehyde that increase the temperature giving rise to the first-stage ignition observed and at the same time act as inhibitor to the reaction. The continuous flow through the reactor brings the system back to its original state, and the process begins anew.

K.D.Stoehr@itv.rwth-aachen.de

1A11 EXPERIMENTAL INVESTIGATION OF DARRIEUS-LANDAU INSTABILITY EFFECTS ON TURBULENT PREMIXED FLAMES.

Guido Troiani¹, Francesco Creta², Moshe Matalon³

¹ENEA C.R. Casaccia, Italy ²University of Rome, Italy ³University of Illinois at Urbana-Champaign, United States

The turbulent propagation speed of a premixed flame can be significantly enhanced by the onset of Darrieus-Landau (DL) instability within the wrinkled and corrugated flamelet regimes of turbulent combustion. Previous studies have revealed the existence of clearly distinct regimes of turbulent propagation, depending on the presence of DL instabilities or lack thereof, named here as super- and subcritical respectively, characterized by different scaling laws for the turbulent flame speed.

In this study we present experimental turbulent flame speed measurements for propane/air mixtures at atmospheric pressure, variable equivalence ratio at Lewis numbers greater than one obtained within a Bunsen geometry with particle image velocimetry diagnostics. By varying the equivalence ratio we act on the cut-off wavelength and can thus control DL instability. The classification of observed flames into sub/supercritical regimes is achieved through the characterization of their morphology in terms of flame curvature statistics. Numerical low-Mach number simulations of weakly turbulent two-dimensional methane/air slot Bunsen flames are also performed both in the presence or absence of DL instability and are observed to exhibit similar morphological properties.

We show that experimental normalized turbulent propane flame speeds S_T/S_L are indeed subject to two distinct scaling laws, as a function of the normalized turbulence intensity U_{rms}/S_L , depending on the sub/supercritical nature of the propagation regime. We also conjecture, based on the experimental results, that at higher values of turbulence intensity a transition occurs whereby the effects of DL instability become shadowed by the dominant effect of turbulence.

francesco.creta@uniroma1.it

1A12 PERFORMANCE OF CONDITIONAL SOURCE-TERM ESTIMATION MODEL FOR LES OF TURBULENT PREMIXED FLAMES IN THIN REACTION ZONES REGIME

Nasim Shahbazian¹, M. Mahdi Salehi², Clinton P.T. Groth¹, Ömer L. Gülder¹, W. Kendal Bushe²

¹University of Toronto, Canada ²University of British Columbia, Canada

Conditional Source-term Estimation (CSE) is a Subfilter-Scale (SFS) model for representing turbulence chemistry interactions in turbulent reactive flows. In the present study, the CSE model is coupled with a two-dimensional Flame-Generated Manifold (FGM) chemistry reduction technique and modified laminarflame-based Probability Density Function (PDF) and applied to Large Eddy Simulation (LES) of laboratoryscale turbulent premixed flames. CSE estimates conditional moments by solving an inverse problem and uses a conditional moment closure to determine the influence of the unresolved turbulence on the reaction rates. While the CSE model has been used extensively in simulating turbulent non-premixed flames, the study represents a first application of the combustion model to LES of premixed flames. Two axisymmetric Bunsen-type premixed turbulent methane-air flames are examined corresponding to lean and stoichiometric conditions with both lying within the thin reaction zones regime. The LES predictions are compared to available experimental data for the two flames. The predictions of the CSE model are also compared to those of a more traditional flamelet-based approach: the Presumed Conditional Moment (PCM) with Flame Prolongation of Intrinsic low-dimensional manifolds (FPI) tabulated chemistry, or so-called PCMFPI model. The comparisons of the CSE and PCM-FPI models allow the relative importance of deviations from the standard flamelet assumption to be assessed for flames lying outside the flamelet premixed combustion regime. The performance of CSE for LES of turbulent premixed combustion is evaluated. The CSE combustion model is found to be stable and converges to physically meaningful values. It also yields LES results that agree very well with experiment, both qualitatively and quantitatively, and would seem able to incorporate correctly the influence of turbulent strain on conditionally-filtered quantities and hence burning rate as flame behaviour deviates from that of a flamelet in the thin reaction zones regime.

shahbazian@utias.utoronto.ca

1A13 CONDITIONAL MOMENT CLOSURE MODELLING FOR HCCI WITH TEMPERATURE INHOMOGENEITIES

Fatemeh Salehi¹, Mohsen Talei¹, E.R. Hawkes¹, Chun Sang Yoo², Tommaso Lucchini³, Gianluca D'Errico³, Sanghoon Kook¹

¹University of New South Wales, Sydney, Australia ²Ulsan National Institute of Science and Technology, Republic of Korea

³Politecnico di Milano, Italy

This paper presents an approach for modelling combustion in Homogeneous Charge Compression Ignition (HCCI) conditions based on the first order Conditional Moment Closure (CMC) method. The model is implemented into the open source C++ Computational Fluid Dynamic (CFD) code known as OpenFOAM. Direct Numerical Simulations (DNSs) are used to evaluate the performance of the CFD-CMC solver. In the DNS cases, ignition of a lean *n*-heptane/air mixture with thermal inhomogeneities is simulated for nine cases, with two different mean temperatures and several different levels of thermal stratification. Results from the CFD-CMC solver are in excellent agreement with the DNS for cases which exhibit a spontaneous sequential ignition mode of combustion whereas for the case in which a mixed mode of deflagration and spontaneous ignition exists, the CMC underpredicts the ignition delay. Further investigation using the

DNS data demonstrates that this discrepancy is primarily attributed to the first order closure assumption. Conditional fluctuations are found to be more significant in the case with deflagrations. Further analysis of the DNS shows that scalar dissipation fluctuations are the cause of conditional fluctuations.

f.salehi@unsw.edu.au

1B01 UNCERTAINTY IN STRETCH EXTRAPOLATION OF LAMINAR FLAME SPEED FROM EXPANDING SPHERICAL FLAMES

Fujia Wu¹, Wenkai Liang¹, Zheng Chen², Yiguang Ju¹, Chung K. Law^{1,3}

¹Princeton University, United States ²Peking University, China ³Tsinghua University, China

The present work investigated the uncertainties associated with the extrapolation of stretched flames to zero stretch in flame speed measurements using expanding spherical flames. Direct numerical simulations of time evolution of expanding spherical flames from a small ignition kernel to a propagating front with sufficiently large radius provide the relations between stretched flame speed and stretch rate that can be used to assess the uncertainty of extrapolation models. It is found that the uncertainties of flame extrapolation largely depend on the mixture Lewis numbers. While the uncertainty is minimized for stoichiometric H₂/air and *n*-heptane/air flames, the uncertainty can be as high as 60% for lean H₂/air mixtures, and 10% for lean and rich *n*-heptane/air mixtures. The present findings show that the weakly stretched flame assumption fails for lean hydrogen mixtures, and give a good explanation to the discrepancies between experiments and model predictions for H₂/air as well as the discrepancies between measurements of *n*-heptane/air using spherical and counterflow flames. A relation between extrapolation uncertainties and the product of Markstein number and Karlovitz number is provided, which can be useful for uncertainty quantification of future and existing measurements.

fujiauwu@princeton.edu

1B02 LAMINAR BURNING VELOCITIES OF PREMIXED NITROMETHANE/AIR FLAMES: AN EXPERIMENTAL AND KINETIC MODELING STUDY

P. Brequigny¹, G. Dayma², F. Halter¹, C. Mounaïm-Rousselle¹, T. Dubois³, P. Dagaut²

¹University of Orléans, France ²CNRS-INSIS, France ³Centre de Recherche de Solaize, France

Due to its high lubricity, nitromethane is a fuel regularly used in model engine or more generally in race engine. The objective of this study is to improve our knowledge and understanding of the combustion of nitromethane for better evaluating its potential as fuel for automotive spark-ignition engines. To achieve this goal, unstretched laminar burning velocities of nitromethane-air mixtures were measured by using spherical propagation methodology at 423 K over a pressure range from 0.5 to 3 bar and equivalence ratios from 0.5 to 1.1. The data indicated a typical adverse effect of pressure on laminar burning velocities. Based on the work done by Zhang, a new detailed kinetic model including 88 species and 700 reactions was developed. Comparisons between experimental and simulated un-stretched laminar flame speed were made and showed good agreement. The proposed kinetic model was also used to successfully simulate published experiments and rationalize the unusual occurrence of maximum flame speed in the fuel-lean region.

guillaume.dayma@cnrs-orleans.fr

1B03 ON THE ACCURATE DETERMINATION OF BURNING VELOCITIES FROM SPHERICALLY EXPANDING FLAMES EXPERIMENTAL AND NUMERICAL STUDY OF H₂/AIR FLAMES

Emilien Varea¹, Joachim Beeckmann¹, Heinz Pitsch¹, Zheng Chen², Bruno Renou³

¹RWTH Aachen University, Germany ²Peking University, China ³CORIA, France

Laminar burning velocities of hydrogen/air mixtures can show discrepancies up to 30%, making chemical mechanism validation and improvement difficult. The source of uncertainties may come from different factors influencing at each processing and post-processing steps the final value. Considering a spherically expanding flame configuration, reflection on the accuracy of the formulations, used to derive the desired quantity, is proposed. Starting from the exact definition of the laminar burning velocity, two formulations – direct and indirect flame speeds – are derived for spherical flames. Each single source of uncertainty involved in the formulations is pointed out. The emphasis is focused on a specific mixture at an equivalence ratio of 0.50, atmospheric pressure, and an initial temperature of 300 K. This point represents the best tradeoff between low ratio of flame velocity and recording sampling rate and the occurrence of cellular flames (*Le* < 1). An extensive experimental and numerical study (1D spherically expanding flames) of this mixture is carried out. As a result, the experimental laminar burning velocities determined by using the direct flame speed or the indirect flame speed formulae depict different values. However, when numerically determined, both formulae yield the same value. This paves the way to understand and identify the experimental error sources. Stretch and Lewis numbers effects (super-adiabatic temperatures) as well as radiation processes (burned gas motion) are studied. Nonetheless, they do not show to be the main source of uncertainty. The extrapolation procedure (linear or non-linear) according to the limited number of experimental points (rapid apparition of cellular structure) appears as the main factor influencing the discrepancy in laminar burning velocities.

emilien.varea@itv.rwth-aachen.de

1B04 THE CURVATURE MARKSTEIN LENGTH AND THE DEFINITION OF FLAME DISPLACEMENT SPEED FOR STATIONARY SPHERICAL FLAMES

G.K. Giannakopoulos¹, M. Matalon², C.E. Frouzakis³, A.G. Tomboulides¹

¹University of Western Macedonia, Greece ²University of Illinois, Urbana-Champaign, United States

³Aerothermochemistry and Combustion Systems Laboratory, Switzerland

The separate effects of flame stretch and flame curvature are investigated in the present study considering a stationary spherical flame configuration that experiences no stretch but has a finite curvature. A theoretical expression for the flame displacement speed, derived from asymptotic analysis, is compared with numerical simulations exhibiting very good agreement between the two. The notion of the *curvature Markstein length* is introduced, a coefficient which is independent from diffusion and chemical reaction effects, in contrast to the Markstein length associated with total flame stretch. It is shown that its value depends strongly on the isosurface chosen to define the flame, exhibiting large variations in the preheat zone and more insensitive behavior close to the burned side.

atompoulidis@uowm.gr

1B05 EXPERIMENTAL AND MODELING STUDY OF THE EFFECT OF ELEVATED PRESSURE ON LEAN HIGH-HYDROGEN SYNGAS FLAMES

M. Goswami¹, J.G.H. van Griensven¹, R.J.M Bastiaans¹, A.A. Konnov², L.P.H. de Goey¹

¹Eindhoven University of Technology, Netherlands ²Lund University, Sweden

New laminar burning velocity measurements of 85:15% (by volume) H₂-CO and H₂-N₂ mixtures with O₂-He oxidizer are reported at lean conditions and elevated pressures (1 atm to 10 atm). Experiments are conducted using the heat flux method at initial temperature of 298 K. In this technique a near adiabatic flame is stabilized by balancing the heat loss from the flame to the burner with heat gain to the unburnt gas mixture such that no net heat loss to the burner is observed. A new facility was designed for such high pressure burner stabilized flame experiments. The results obtained are compared with five chemical kinetic schemes from literature for syngas mixtures at elevated pressures. Large differences are observed between the kinetic schemes and the experiments which can be attributed to certain key chemical reactions. A study of the kinetics is performed through reaction rate and sensitivity analysis which indicate that a high uncertainty still remains in important reactions that drive the production and consumption of species such as H, HO₂ and OH. For lean mixtures the reaction H+O₂(+M)=HO₂(+M) contributes significantly to the deviation of models from the experiments. The present analysis in the lean mixture regime suggests the need for further studies in assessment and modification of rate constants for this reaction.

m.goswami@tue.nl

1B06 EFFECT OF DILUTION GAS ON BURNING VELOCITY OF HYDROGEN-PREMIKED MESO-SCALE SPHERICAL LAMINAR FLAMES

Masaya Nakahara¹, Fumiaki Abe¹, Kenichi Tokunaga¹, Atsushi Ishihara²

¹Ehime University, Japan ²Saitama Institute of Technology, Japan

Aiming to make clear a method for improving combustion of micro/meso-scale flames, effects of dilution gas and characteristic chemical reaction time τ_c on the burning velocity of meso-scale flames were studied experimentally using H₂-O₂-Dilution gas mixtures. The meso-scale outwardly propagating spherical laminar flames, in a flame radius r_f range of approximately from 1 to 5 mm, were observed by using sequential schlieren images recorded under appropriate ignition condition. The mixtures at each equivalence ratio $\phi = 0.5 \sim 1.0$ were diluted with Ar, CO₂ or N₂ to set different laminar burning velocities ($S_{L0} = 15 \sim 90 \text{ cm/s}$) at so-called unstretched flames, because τ_c can vary depending on S_{L0} . The radius r_f and the burning velocity S_{Ll} of micro-scale flames were estimated from obtained images. Macro-scale laminar flames with $r_f > 7 \text{ mm}$ were also examined for comparison. It was found that the burning velocities of meso-scale flames for the mixtures diluted with CO₂ at $\phi = 0.5 \sim 1.0$ have a tendency to decrease with increasing r_f , and approach those of macro-scale flames, whereas such a trend cannot be seen for the mixtures diluted with Ar as well as N₂ at $\phi = 0.7 \sim 1.0$. This shows flame size and Karlovitz number to have optimum values to improve burning velocity. The S_{Ll} at the same r_f ; however, tended to meaningfully decrease with the Lewis number Le and the Markstein number Ma , in respective of the dilution gas types in addition to ϕ . It also becomes clear that the observed optimal values of each dilution gas are little dependent on τ_c .

mnakahara@eng.ehime-u.ac.jp

1B07 LARGE EDDY SIMULATION OF PREMIKED TURBULENT COMBUSTION USING APPROXIMATE DECONVOLUTION AND EXPLICIT FLAME FILTERING

Pascale Domingo, Luc Vervisch, CORIA, France

Approximate deconvolution and explicit filtering of scalar fields are used to construct a new approach to sub-grid scale modeling in Large Eddy Simulation (LES) of premixed turbulent flames. This modeling is designed to handle any form of chemical description, Arrhenius or tabulated. The closure of the unresolved terms relies on the explicit filtering of their exact expressions computed after an approximate deconvolution of the resolved scalars. A specific numerical

treatment is needed to capture the deconvoluted peak burning rate over the coarse LES mesh. The method is first tested in the canonical laminar filtered flame context with two strategies for the unresolved fluxes, which are based either on a full approximate deconvolution, or, on the introduction of a corrective factor applied to the resolved diffusive flux. This factor is dynamically determined from the deconvoluted/filtered burning rates to preserve basic filtered flame front properties (propagation speed and thickness). Then, a three-dimensional turbulent Bunsen flame studied experimentally by Chen et al. [Combust. Flame 107 (1996) 223:244] is simulated.

domingo@coria.fr

1B08 FILTERED DENSITY FUNCTION SIMULATION OF A REALISTIC SWIRLED COMBUSTOR

N. Ansari¹, P.A. Strakey², G.M. Goldin³, P. Givi¹

¹University of Pittsburgh, United States ²National Energy Technology Laboratory, United States ³ANSYS Inc., United States

The Scalar Filtered Mass Density Function (SFMDf) methodology is employed for Large Eddy Simulation (LES) of the PRECCINSTA burner from DLR. This burner involves a swirling flow configuration and provides a good model of the combustor in gas turbines. In SFMDf, the effects of unresolved scalar fluctuations are taken into account by considering the probability density function of subgrid scale scalar quantities. The modeled SFMDf transport equation is solved numerically via a Lagrangian Monte Carlo scheme coupled with a finite volume flow solver on unstructured grids. The simulated results are assessed via comparison with experimental data and show reasonable agreements. This demonstrates the capability of SFMDf for LES of complex flows, and warrants future applications of the methodology for LES of practical combustor configurations. This work represents the first attempt in implementing FDF for LES of a practical gas turbine combustor.

naa56@pitt.edu

1B09 FAVRE- AND REYNOLDS-AVERAGED VELOCITY MEASUREMENTS: INTERPRETING PIV AND LDA MEASUREMENTS IN COMBUSTION

M. Mustafa Kamal, Ruigang Zhou, Saravanan Balusamy, Simone Hochgreb, University of Cambridge, United Kingdom

Previous studies using Particle Image Velocimetry (PIV) and Laser Doppler Anemometry (LDA) have raised the question of how these measurements should be compared. This study reports on the difference between the Favre-averaged and the Reynolds-averaged velocity statistics for a turbulent burner using PIV and LDA for unconditional and conditional velocity measurements. The experimental characterization of flow fields of premixed and stratified methane/air flames is carried out under globally turbulent lean conditions (global equivalence ratio at 0.75), over a range of stratifications and swirl numbers. Unconditioned velocity data was acquired using aluminium oxide to seed the flow field. Conditioned measurements were performed using vegetable oil aerosol as seed, which burns through the flame front, thus allowing only the non-reacting flow velocities to be obtained. A critical comparison of unconditioned velocity profiles measured using both PIV and LDA, including axial, radial, and tangential components is made against conditioned and reconstructed mean velocities at different cross-sections of the flame. The comparison reveals how the differences between the Favre-averaged (unconditioned) and the Reynolds-averaged (conditioned) velocity measurements in the flame brush region can be accounted for using the mean progress of reaction, and highlights the limits of the accuracy and agreement between PIV and LDA measurements.

mmk44@cam.ac.uk

1B10 THREE-DIMENSIONAL DIRECT NUMERICAL SIMULATION STUDY OF CONDITIONED MOMENTS IN TURBULENT REACTING FLOWS

R. Yu¹, A.N. Lipatnikov², X.S. Bai¹

¹Lund University, Sweden ²Chalmers University of Technology, Sweden

In order to gain further insight into (i) the use of conditioned quantities for characterizing turbulence within a premixed flame brush and (ii) the influence of chemical reactions on turbulent scalar transport, a 3D DNS study of a statistically planar, one-dimensional reaction front that self-propagates in statistically stationary, homogeneous, isotropic, forced turbulence was performed by numerically integrating Navier-Stokes and level set equations. The density was assumed to be constant in order (i) to avoid the influence of combustion on the flow and, therefore, to know the true turbulence characteristics as reference quantities for assessment of conditioned moments and (ii) to separate the influence of chemical reactions on turbulent transport from the influence of pressure gradient induced by heat release. Numerical simulations were performed for two turbulence Reynolds numbers (50 and 100) and four ratios of the front speed to the rms turbulent velocity (0.1, 0.2, 0.5, and 1). Obtained results show that, first, the mean flame brush thickness is decreased when a ratio of the front speed to the rms velocity is increased. Second, although the gradient diffusion closure yields the right direction of turbulent scalar flux obtained in the DNS, the diffusion coefficient D_t determined using the DNS data depends on the mean combustion progress variable. Moreover, D_t is decreased when the front speed is increased, thus, indicating that chemical reaction affects turbulent scalar transport even in a constant-density case. Third, conditioned moments of the velocity field differ from counterpart mean moments, thus, disputing the use of conditioned velocity

moments for characterizing turbulence within a premixed flame brush. Fourth, computed conditioned enstrophies are close to the mean enstrophy in all studied cases, thus, suggesting the use of conditioned enstrophy for characterizing turbulence within a premixed flame brush.

Rixin.yu@energy.lth.se

1B11 EXPERIMENTAL AND KINETIC STUDIES OF ACETYLENE FLAMES AT ELEVATED PRESSURES

Xiaobo Shen^{1,2}, Xueliang Yang¹, Jeffrey Santner¹, Jinhua Sun², Yiguang Ju¹

¹Princeton University, United States ²University of Science and Technology of China, China

The kinetic effects of CO₂ and H₂O dilution on the laminar flame speed of acetylene at elevated pressure has been investigated experimentally using outwardly propagating spherical flames from 1 to 20 atm. A high pressure kinetic model is assembled by including pressure dependent elementary reaction rates determined by recent theoretical calculations and experimental measurements. It is found that, unlike other hydrocarbons, the kinetic inhibition caused by CO₂ dilution on acetylene flame speeds via CO₂+H=CO+OH is reduced at both fuel rich and lean conditions due to the existence of direct CO₂ formation pathways (HCCO+O₂ and CH₂+O₂) in acetylene oxidation. On the other hand, the inhibiting kinetic effects of water dilution on acetylene flame speed are promoted because the shifting equilibrium of the H₂O+O=OH+OH reaction inhibits production of O radicals needed for the O+C₂H₂=HCCO+H chain propagation reaction. Detailed analysis on the combustion chemistry of acetylene reveals that C₂H₂+O, HCCO+O₂, HCO+O₂, CH₃+HO₂, H+C₂H₃, CO+OH, CH₂(S)+C₂H₂, and HCO decomposition are among the most important reactions for predicting the laminar flame speed, especially at high pressures. The results show that the new High Pressure model (HP-Mech) improved prediction of flame speeds of acetylene with CO₂ and H₂O dilution.

xueliang@Princeton.edu

1B12 INFLUENCE OF THE REACTANT TEMPERATURE ON PARTICLE ENTRAINED LAMINAR METHANE – AIR PREMIXED FLAMES

Minkyu Lee, Sreenivasan Ranganathan, Ali S. Rangwala, Worcester Polytechnic Institute, United States

This study investigates the laminar burning velocity of premixed methane-air mixtures, entrained with micron-sized (75-90 μm) coal dust particles over a range of gas phase equivalence ratios (0.9-1.2), dust concentrations (0-250 g/m³) and reactant temperatures (297, 350, 400 K) using a novel Bunsen-burner type experimental design. The experimental results show that, the laminar burning velocity is enhanced by the increase in the reactant temperature, irrespective of the equivalence ratio of the mixture. Addition of coal particles in fuel lean ($\phi < 1$) mixtures increases the laminar burning velocity initially, but after a certain concentration of dust addition this trend is altered. The dust concentration value, where this variation is observed, increases with increase in reactant temperature. In other words, the reactant temperature plays a significant role in the trend of increase in laminar burning velocity with dust addition. For $\phi > 1$, at a given reactant temperature, a linear decay of burning velocity with dust addition is observed. When a combustible dust particle interacts with the flame zone, it extracts energy from the flame and releases volatiles, thereby changing the equivalence ratio. This local increase in the equivalence ratio and the heat sink effect, are found to be influenced by the reactant temperature. A mathematical model including these effects is developed and the model predictions are compared with the experimental results. The results are in a good agreement for fuel lean and stoichiometric mixtures; whereas the model is found to under predict results for fuel rich cases.

mlee@wpi.edu

1B13 EXPERIMENTAL AND MODELING STUDIES OF THE ACETONE ADDITION IN H₂/O₂/AR FLAMES AT LOW PRESSURE

Véronique Dias, Jacques Vandooren, Hervé Jeanmart, Université Catholique de Louvain, Belgium

The addition of acetone to stoichiometric and rich hydrogen/oxygen/argon flames has been investigated by measuring the intermediate species concentration. Two premixed acetone/hydrogen/oxygen/argon flames were stabilized at low pressure (27 mbar) on a Spalding-Botha type burner at two equivalence ratios, $\phi = 1.1$ and 1.72. Identification and monitoring of signal intensity profiles of species within the flames were carried out using molecular beam mass spectrometry. The detected species throughout the flame thickness are CH₃COCH₃ (acetone), H₂, O₂, Ar, H, OH, CO, CO₂, H₂O, HO₂, CH₃, CH₄, CH₂O (formaldehyde), CH₃CO (acetyl radical), C₂H₂ (acetylene) and C₂H₄ (ethylene). The UCL mechanism has been extended to acetone kinetics, and has been assessed for these flames with a particular attention to the effect of the equivalence ratio on the intermediate species concentrations. Using this model, we established the main acetone degradation pathway in both flames at low pressure: CH₃COCH₃ → CH₃COCH₂ → CH₂CO → CH₃ → CH₂O → HCO → CO → CO₂.

veronique.dias@uclouvain.be

1C01 SOME ASPECTS OF COMBUSTION CHEMISTRY OF C1-C2 OXYGENATED FUELS IN LOW PRESSURE PREMIXED FLAMES

George Vourliotakis, George Skevis, Maria A. Founti, National Technical University of Athens, Greece

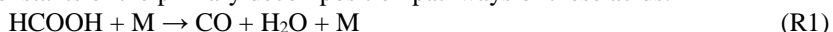
The increasing utilization of renewable fuels in the transportation and industrial sectors has sparked an interest in understanding the combustion of relevant major fuel components. Among them, smaller, oxygenated compounds are of particular importance, both as neat fuels and as potential blending agents in engines operating on practical fuels. Additionally, oxygenated exhaust species, e.g. small aldehydes, are harmful and are expected to be regulated by future emission standards. The assessment of the effect of specific fuel components on overall engine efficiency and performance, as well as on pollutants formation, needs to be tackled through a detailed kinetics approach that inherently allows such a correlation. In the present work, a single, in-house developed, detailed chemical kinetic mechanism is utilized in order to model and analyze 5 stoichiometric or near stoichiometric low-pressure laminar premixed flames of C1-C2 oxygenated fuels; flames of the two smallest aldehydes (formaldehyde and acetaldehyde) and the two smallest alcohols (methanol and ethanol) are considered. The mechanism is shown to satisfactorily reproduce fuel decay as well as major and intermediate species profiles. Reaction path analysis is extensively utilized in order to scrutinize the controlling elementary steps. Parts of the mechanism are identified for further model improvement, based on critical evaluation of available specific rate constants. Early branching ratios and reactions between the major carbonyl or alkoxy products with oxygen carriers appear to be pivotal for the overall oxidation process.

gvou@central.ntua.gr

1C02 UNIMOLECULAR DECOMPOSITION OF FORMIC AND ACETIC ACIDS: A SHOCK TUBE / LASER ABSORPTION STUDY

A. Elwardany, E.F. Nasir, Et. Es-sebbar, A. Farooq, King Abdullah University of Science and Technology, Saudi Arabia

The thermal decomposition of formic acid (HCOOH) and acetic acid (CH₃COOH), two carboxylic acids which play an important role in oxygenate combustion chemistry, were investigated behind reflected shock waves using laser absorption. The rate constants of the primary decomposition pathways of these acids:



were measured using simultaneous infrared laser absorption of CO, CO₂ and H₂O at wavelengths of 4.56, 4.18 and 2.93 microns, respectively. Reaction test conditions covered temperatures from 1230 to 1821 K and pressures from 1.0 to 6.0 atm for dilute mixtures of acids (0.25 – 1.0%) in argon. The rate constants of dehydration (R1) and decarboxylation (R2) reactions of formic acid were calculated by fitting exponential functions to the measured CO, CO₂ and H₂O time-history profiles. These two decomposition channels were found to be in the low-pressure limit and have a branching ratio, k_1/k_2 , of approximately 20. The best-fit Arrhenius expressions for R1 and (R2) were found to be:

$$k_1 = 1.94 \times 10^{17} \exp(-29872/T) \text{ cm}^3 \text{ mole}^{-1} \text{ s}^{-1} (\pm 17\%)$$

$$k_2 = 8.873 \times 10^{13} \exp(-23108/T) \text{ cm}^3 \text{ mole}^{-1} \text{ s}^{-1} (\pm 21\%)$$

The rate constants for acetic acid decomposition were obtained by fitting simulated profiles, using an acetic acid pyrolysis mechanism, to the measured species time-histories. The branching ratio, k_3/k_4 , was found to be approximately 2. The decarboxylation reaction of acetic acid appears to be in the falloff region over the tested pressure range:

$$k_3 \text{ 1 atm} = 1.77 \times 10^{11} \times \exp(-28679/T) \text{ s}^{-1} (\pm 10\%)$$

$$k_4 \text{ 6 atm} = 1.95 \times 10^{12} \times \exp(-31330/T) \text{ s}^{-1} (\pm 10\%)$$

The acetic acid dehydration reaction is in the low-pressure limit over 1 – 6 atm, and was best-fit with the following Arrhenius expression:

$$k_4 = 1.057 \times 10^{12} \times \exp(-29867/T) \text{ s}^{-1} (\pm 12\%)$$

aamir.farooq@kaust.edu.sa

1C03 AB INITIO AND KINETIC MODELING STUDIES OF FORMIC ACID OXIDATION

Paul Marshall¹, Peter Glarborg²

¹University of North Texas, United States ²Technical University of Denmark, Denmark

A detailed chemical kinetic model for oxidation of HOCHO in flames has been developed, based on theoretical work and data from literature. Ab initio calculations were used to obtain rate coefficients for reactions of HOCHO with H, O, and HO₂. Modeling predictions with the mechanism have been compared to the experimental results of de Wilde and van Tiggelen who measured the laminar burning velocities for HOCHO flames over a range of stoichiometries and dilution ratios. The modeling predictions are generally satisfactory. The governing reaction mechanisms are outlined based on calculations with the kinetic model. Formic acid is consumed mainly by reaction with OH, yielding OCHO, which dissociates rapidly to CO₂ + H, and HOCO, which may dissociate to CO + OH or react with OH or O₂ to form more stable products. The branching fraction of the HOCHO + OH reaction, as well as the fate of HOCO, determines the oxidation rate

of formic acid. At lower temperatures HO_2 , formed from $\text{HOCO} + \text{O}_2$, becomes an important chain carrier and modeling predictions become sensitive to the $\text{HOCHO} + \text{HO}_2$ reaction.

pgl@kt.dtu.dk

1C04 EXPERIMENTAL STUDY OF THE KINETICS OF ETHANOL PYROLYSIS AND OXIDATION BEHIND REFLECTED SHOCK WAVES AND IN LAMINAR FLAMES

M. Bozkurt¹, D. Nativel², M. Aghsaei¹, M. Fikri¹, N. Chaumeix², C. Schulz¹

¹University of Duisburg-Essen, Germany ²ICARE, CNRS-INSIS, France

The pyrolysis and oxidation of ethanol mixtures at high temperature is studied in a shock tube in the 1047 to 2518 K range at initial pressures of 1.06 and 2.07 bar. Pyrolysis and oxidation intermediates were investigated with high-repetition-rate Time-Of-Flight Mass Spectrometry (TOF-MS). Ignition delay times were determined from chemiluminescence measurements and the OH concentration was determined with high time resolution from ring dye laser absorption measurements. Laminar flame speeds of ethanol in air were measured in a spherical bomb for initial temperatures between 318 and 473 K at 1, 2, and 5 bar and for equivalence ratios from 0.7 to 1.5. The measurements were compared to simulations based on various mechanisms from the literature. This comparison showed that the model developed by Ranzi et al. provides the best agreement with the measured data for ethanol oxidation at high temperature.

mustapha.fikri@uni-due.de

1C05 A SHOCK TUBE STUDY OF $\text{CH}_3\text{OH} + \text{OH} \rightarrow \text{PRODUCTS}$ USING OH LASER ABSORPTION

Luke T. Zaczek, King-Yiu Lam, David F. Davidson, Ronald K. Hanson, Stanford University, United States

The rate coefficient for the reaction of methanol (CH_3OH) with the hydroxyl (OH) radical was determined in reflected shock wave experiments at temperatures of 961-1231 K and pressures of 1.18-1.48 atm. Pseudo-first order reaction conditions were achieved with mixtures of CH_3OH and *Tert*-Butyl Hydroperoxide (TBHP) diluted in argon. Rapid thermal decomposition of TBHP at high temperatures was used as a fast OH radical source, and OH time-histories were measured using laser absorption of OH radicals near 306.7 nm. The rate coefficient of the title reaction was found from best-fit comparison of simulated OH profiles with measured data, using simulations from the Wang et al. USC-Mech II reaction mechanism (2009). The results of the current study can be expressed in Arrhenius form by $k_1 = 2.86 \times 10^{13} \exp(-1510/T[\text{K}]) \text{ cm}^3\text{mol}^{-1}\text{s}^{-1}$ over the experimental temperature range. A detailed uncertainty analysis was performed, with estimated uncertainties of $\pm 11\%$ and $\pm 12\%$ at 961 K and 1231 K, respectively. The current results agree well with the results of Hess and Tully (1989), Vandooren and Van Tiggelen (1981), and Xu and Lin (2007).

zaczek1@stanford.edu

1C06 ADVENTURES ON THE $\text{C}_3\text{H}_5\text{O}$ POTENTIAL ENERGY SURFACE: OH + PROPYNE, OH + ALLENE AND RELATED REACTIONS

Judit Zádor¹, James A. Miller²

¹Sandia National Laboratories, United States ²Argonne National Laboratory, United States

We mapped out the stationary points and the corresponding conformational space on the $\text{C}_3\text{H}_5\text{O}$ potential energy surface relevant for the OH + allene and OH + propyne reactions systematically and automatically using the KinBot software at the UCCSD(T)-F12b/cc-pVQZ-F12//M06-2X/6-311++G(d,p) level of theory. We used RRKM-based 1-D master equations to calculate pressure- and temperature-dependent, channelspecific phenomenological rate coefficients for the bimolecular reactions propyne + OH and allene + OH, and for the unimolecular decomposition of the CH_3CCHOH , $\text{CH}_3\text{C(OH)CH}$, $\text{CH}_2\text{CCH}_2\text{OH}$, $\text{CH}_2\text{C(OH)CH}_2$ primary adducts, and also for the related acetonyl, propionyl, 2-methylvinoxy, and 3-oxo-1-propyl radicals. The major channel of the bimolecular reactions at high temperatures is the formation propargyl + H_2O , which makes the title reactions important players in soot formation at high temperatures. However, below ~ 1000 K the chemistry is more complex, involving the competition of stabilization, isomerization and dissociation processes. We found that the OH addition to the central carbon of allene has a particularly interesting and complex pressure dependence, caused by the low-lying exit channel to form ketene + CH_3 bimolecular products. We compared our results to a wide range of experimental data and assessed possible uncertainties arising from certain aspects of the theoretical framework.

jzador@sandia.gov

1C07 UNIMOLECULAR DECOMPOSITION OF TETRAHYDROFURAN: CARBENE VS. DIRADICAL PATHWAYS

Marco Verdicchio, Baptiste Sirjean, Luc Sy Tran, Pierre-Alexandre Glaude, Frédérique Battin-Leclerc, Université de Lorraine, France

The unimolecular decomposition of Tetrahydrofuran (THF), a building block of possible secondgeneration biofuels, was studied at the CBS-QB3 level of theory. As its initial initiation routes remain unknown, a large number of pathways were explored involving three types of fundamental elementary mechanisms: diradicalar, carbenic and pericyclic. Based on the computed potential energy surfaces, thermochemical data and high-pressure limit rate constants were

determined and included in a detailed chemical kinetic mechanism for THF pyrolysis. Simulations were performed and compared to pyrolysis products of the literature, measured behind reflected shock waves. The kinetic analyses showed that THF unimolecular decomposition is initiated by reactions involving diradicals and carbenes. A pericyclic rearrangement was also shown to be crucial in its thermal decomposition. Acyclic isomers of

THF are major products of its unimolecular initiation and are predominantly formed from diradical intermediates isomerization and from the pericyclic reaction. The major pathway in the decomposition of carbenes ultimately yields two molecular products (CH_2O and propene). Initial C-C and C-O bond fissions in the acyclic THF isomers lead to the formation of the initial radicals: ethyl, allyl and vinyloxy ($\bullet\text{CH}_2\text{CHO}$). This study brings a new understanding on the nature of initial radicals and molecules formed in the unimolecular initiation of the THF ring.

baptiste.sirjean@univ-lorraine.fr

1C08 EFFECT OF FURANS ON PARTICLE FORMATION IN DIFFUSION FLAMES: AN EXPERIMENTAL AND MODELLING STUDY

Mariano Sirignano, Marielena Conturso, Andrea D'Anna, Università degli Studi di Napoli Federico II, Italy

Furans have recently raised as possible transportation fuels which can be produced from biological sources and biotechnological methods. Their role on combustion-generated particle formation results quite unexplored. Few studies showed that DMF among the other furanic hydrocarbons seems to have a great tendency to form soot precursors. This unexpected trend should be kept in mind before a further usage of furans, especially DMF, as transportation fuels.

The effect of furans as substituent to traditional fuels has been investigated both experimentally and numerically in a counter-flow diffusion flame. Furan, 2-methylfuran and 2,5-dimethylfuran have been chosen as standards for furanic fuels. Optical techniques, previously validated, namely laser induced fluorescence and incandescence, have been adopted to detect small nanoparticles and soot aggregates, respectively. On the modelling part, a MultiSectional approach has been used to confirm the sooting tendency experimentally found for the investigated fuels. Gas phase kinetic scheme available in literature for oxidation and decomposition of furans has been integrated in an existent detailed kinetic mechanism.

Experimental findings confirmed by modelling results show that furans increase the particle production. Furan has the lowest impact on the particle production whereas 2,5-dimethylfuran and 2-methylfuran show a remarkable increase of detected signals. In particular, 2-methylfuran has a greater tendency to produce particles than 2,5-dimethylfuran.

Modelling analysis showed that in the 2-methylfuran large amount of C₄-species and thus benzene and PAHs are produced. In 2,5-dimethylfuran decomposition one of the main products is phenol, that leads to cyclopentadiene and thus naphthalene formation, although the overall PAHs and first particle production result less strong than in 2-methylfuran. However, different combustion conditions can change the effectiveness of these channels and might invert the particle production tendency of 2-methylfuran and 2,5-dimethylfuran.

marianosirignano@yahoo.it

1C09 INFLUENCE OF TEMPERATURE AND RESONANCE STABILIZATION ON THE *ORTHO*- EFFECT IN CYMENE OXIDATION

B. Rotavera, A.M. Scheer, H. Huang, D.L. Osborn, C.A. Taatjes, Sandia National Laboratories, United States

Cymenes are monoterpenes composed of a benzene ring with *iso*-propyl and methyl substituents, and the proximity of the two alkyl groups enables relevant analysis into the *ortho*- effect of polysubstituted aromatics, in which low-temperature ignition is more facile for *ortho*-substitution. The initial steps of RO₂-related reactions from Cl-initiated oxidation of *ortho*-, *meta* and *para*-cymene were studied at low pressure (8 torr) over the temperature range 450 K – 750 K using Multiplexed Photoionization Mass Spectrometry (MPIMS). Ratios of cyclic ether formation (related to chain-propagation and OH formation) relative to HO₂-loss (related to chain-termination) were measured as a function of temperature to characterize the *ortho*- effect. The main results are two-fold:

- (i) Cyclic ether yields indicate significant chain propagation below 700 K only in *o*-cymene oxidation; above 700 K the yields of the three cymenes converge.
- (ii) The competition between chain-propagation channels stemming from resonance- and non-resonance-stabilized initial cymene radicals changes significantly with temperature.

Cyclic ether yields in *m*- and *p*-cymene oxidation are negligible below 650 K, indicating minimal chain-propagation. In contrast, *o*-cymene exhibits significant cyclic ether formation, attributed to the facile 6- and 7-membered-ring transition states in the formation of hydroperoxyalkyl (QOOH) intermediates from alkylperoxy radicals (ROO). The cyclic ether/HO₂-loss ratio in *o*-cymene oxidation is defined as unity at 450 K and decreases to ~ 0.10 at 700 K. The ratio for the three cymenes converges at 700 K, indicating an upper limit of temperature for the *ortho*- effect. The cyclic ether yields from *o*-cymene oxidation indicate a competition between resonance- and nonresonance- stabilized initial radicals at lower temperature. At higher temperature cyclic ethers arise solely from non-resonance-stabilized initial radicals because of the back-dissociation of weakly bound ROO from resonance-stabilized R + O₂ reactants.

cataatj@sandia.gov

1C10 EXPERIMENTAL AND COMPUTATIONAL STUDY OF THE INITIAL DECOMPOSITION OF GAMMA-VALEROLACTONE

Ruben De Bruycker¹, Hans-Heinrich Carstensen¹, John M. Simmie², Kevin M. Van Geem¹, Guy B. Marin¹

¹Ghent University, Belgium ²National University of Ireland, Ireland

The thermal decomposition of Gamma-Valerolactone (GVL) diluted 1:10 mol/mol in nitrogen was studied experimentally in a tubular flow reactor. Variation of the temperature from 873 K to 1073 K for a residence time of approximately 400 ms at 0.17 MPa covered the complete GVL conversion range from 1% to 98 %. Comprehensive 2D MS analysis of the effluent revealed that the main products observed at temperatures below 1000 K are CO, CO₂, C₄-olefins and 4-pentenoic acid. Initially, GVL is consumed predominantly through isomerization to 4-pentenoic acid, although minor contributions of bimolecular decomposition channels cannot be ruled out. CBS-QB3 level characterization of the C₅H₈O₂ potential energy surface reveals the existence of a low energy barrier for ring-opening to 4-pentenoic acid. The weak C-C bond between C₂ and C₃ in 4-pentenoic acid allows formation of radicals that further convert gamma-valerolactone or 4-pentenoic acid. The 4-pentenoic acid yield increases steadily with rising temperature before a sharp decrease around 1010 K. The latter can be explained by radical chemistry taking over at high temperatures.

kevin.vangeem@ugent.be

1C11 KINETIC STUDIES OF THE REACTION OF ATOMIC SULFUR WITH ACETYLENE

Sean Ayling, Yide Gao, Paul Marshall, University of North Texas, United States

Laser flash photolysis of CS₂ precursor was employed to generate ground-state S(³P) atoms, which were monitored with time-resolved resonance fluorescence as they reacted with C₂H₂ in a large excess of Ar bath gas. Temperatures from 295-1015 and pressures from 10-500 mbar were investigated. A pressure-dependence was observed at all temperatures, revealing that adduct formation is the dominant reaction channel. The necessary stability suggests H₂CCS or possibly HCCSH are the products at high temperatures, so that the reaction is spin-forbidden. The fall-off curves may be represented with a broadening factor $F_{\text{cent}} = 0.6$, and low and high-pressure limiting rate constants of $k_0 = 1.3 \times 10^{-17} (\text{T/K})^{-4.0} \exp(-2040 \text{ K/T}) \text{ cm}^6 \text{ molecule}^{-2} \text{ s}^{-1}$ and $k_{\infty} = 1.26 \times 10^{-11} \exp(-10.3 \text{ kJ mol}^{-1}/\text{RT}) \text{ cm}^3 \text{ molecule}^{-1} \text{ s}^{-1}$, respectively. An entrance barrier to recombination of about 10 kJ mol⁻¹ is proposed to arise where the singlet and triplet potential energy curves cross.

marshall@unt.edu

1C12 PRESSURE-DEPENDENT BRANCHING IN THE REACTION OF ¹CH₂ WITH C₂H₄ AND OTHER REACTIONS ON THE C₃H₆ POTENTIAL ENERGY SURFACE

Lili Ye^{1,2}, Yuri Georgievskii¹, Stephen J. Klippenstein¹

¹Argonne National Laboratory, United States ²University of Science and Technology of China, China

A number of reactions on the C₃H₆ Potential Energy Surface (PES) are of central importance to various combustion environments. High level theoretical methods were used to predict the temperature and pressure dependent kinetics for these reactions. The rovibrational properties of the key stationary points in the systems were determined with the CCSD(T)/cc-pVTZ method. High accuracy energies for these stationary points were obtained via the consideration of basis set, higher-order correlation, core-valence, anharmonic vibrational, relativistic, and diagonal Born-Oppenheimer corrections. Variable Reaction Coordinate Transition State Theory (VRC-TST) was employed to treat the barrierless channels on the PES, while for channels possessing a distinct barrier, rate coefficients were instead obtained with conventional transition state theory employing rigid-rotor harmonic oscillator assumptions. For the VRC-TST calculations, the interaction energies required for the evaluation of the reactive flux were evaluated with the CASPT2/cc-pVTZ approach for the orientational sampling, coupled with one-dimensional corrections based on higher accuracy evaluations along the minimum energy path. A priori predictions for the temperature and pressure-dependent rate coefficients were obtained through master-equation calculations incorporating these TST predictions for the microcanonical rate coefficients coupled with a simple model for the collisional energy transfer rates. These theoretical predictions compare favorably with the limited experimental data. The analysis yields modified Arrhenius rate expressions for the ¹CH₂ + C₂H₄, C₂H₃ + CH₃, CH₂CHCH₂ + H, CH₃CCH₂ + H, and CH₃CHCH + H recombination reactions as well as for the dissociations and isomerizations of propene and cyclopropane.

sjk@anl.gov

1C13 "THIRD-BODY" COLLISION EFFICIENCIES FOR COMBUSTION MODELING: HYDROCARBONS IN ATOMIC AND DIATOMIC BATHS

Ahren W. Jasper¹, C. Melania Oana¹, James A. Miller²

¹Sandia National Laboratories, United States ²Argonne National Laboratory, United States

The collisional energy transfer dynamics relevant to the unimolecular kinetics of linear, branched, and cyclic hydrocarbons, including both radicals and saturated and unsaturated molecules, in atomic and diatomic baths is studied via

classical trajectories. A set of full-dimensional Potential Energy Surfaces (PESs) suitable for efficient trajectory simulations involving large hydrocarbons (C_xH_y) colliding with any of seven baths ($M = \text{He, Ne, Ar, Kr, H}_2, \text{N}_2, \text{O}_2$) is validated against direct dynamics calculations for two small systems. The PESs are then used to calculate Lennard-Jones collision parameters, and a general rule for calculating these parameters based only on the number of carbon atoms and the bath gas is obtained. Next, the PESs are used to calculate low-order moments of the collisional energy transfer function relevant to low-pressure-limit unimolecular kinetics for a total of 266 systems (38 unimolecular reactants in 7 baths), with a focus on the average angular momentum and total energy transferred in deactivating collisions. These moments are used to quantify the relative rotational and total collision efficiencies of the 7 baths for the various hydrocarbon reactants. Trends in the collision efficiencies with respect to the chemical structures of the hydrocarbon reactants are discussed.

ajasper@sandia.gov

1D01 DIRECT NUMERICAL SIMULATION OF THE EFFECT OF COMPRESSION ON THE FLOW, TEMPERATURE AND COMPOSITION UNDER REALISTIC ENGINE CONDITIONS

M. Schmitt¹, Christos E. Frouzakis¹, A.G. Tomboulides², Y.M. Wright¹, K. Boulouchos¹

¹Swiss Federal Institute of Technology, Switzerland ²University of Western Macedonia, Greece

The Homogeneous-Charge Compression Ignition (HCCI) process has been shown to depend strongly on thermal and mixture stratification. To connect this knowledge to engine conditions a better understanding of the evolution of the flow, temperature and species concentrations during the compression stroke is needed. In this work, the effect of compression on the flow, temperature and composition is investigated using Direct Numerical Simulation (DNS). The initial conditions are obtained by a separate DNS of the intake stroke in an open valve setup including thermal and species mixing. The results showed significant changes of the turbulence and temperature fields during compression: The increasing pressure lowers the kinematic viscosity, which result in smaller turbulent length scales and strongly increased dissipation rates. The temperature fluctuations away from the walls decrease slightly in the first half and increase strongly in the second half of the compression stroke. The strongly increasing fluctuations towards Top Dead Center (TDC) are due heat transfer to the walls and turbulent transport. At TDC the turbulent flow field is anisotropic, and the axial rms velocity is approximately 30% smaller compared to the rms velocity in the radial and azimuthal directions. The integral length scale of the temperature is approximately 25% higher than the integral length scale of the turbulent kinetic energy. The stratification of the species concentration is found to be practically negligible.

frouzakis@lav.mavt.ethz.ch

1D02 IGNITION IN COMPOSITIONALLY AND THERMALLY STRATIFIED *N*-HEPTANE/AIR MIXTURES: A DIRECT NUMERICAL SIMULATION STUDY

Mohsen Talei, E.R. Hawkes, University of New South Wales, Australia

This paper presents a Direct Numerical Simulation (DNS) study of ignition characteristics in compositionally and thermally stratified *n*-heptane/air mixtures, relevant to Homogeneous Charge Compression Ignition (HCCI) engines. Nine two-dimensional cases with three mean temperatures within the NTC region are considered. It is shown that as the level of stratification increases, the heat release rate has a lower peak in the first stage for the mean temperature of 850K. An opposite behaviour is observed for the mean temperature of 950K. Inspection of the homogeneous ignition delay for the cases with the mean temperature of 850K suggests that distribution of ignition delay time at the initial conditions leads to the observed behaviour. However, for the mean temperature of 950K, increasing the level of stratification causes mixture fractions which exhibit a larger amount of low temperature heat release to be introduced into the domain, which causes an overall increase in the peak heat release rate in the first stage. In the second stage of ignition, stratification reduces the peak heat release rate relative to a homogeneous case for all three mean temperatures. However, a non-monotonic behaviour for the peak heat release rate in the second stage is observed. This behavior for cases with the mean temperatures of 950 and 1000K can be attributed to the mixture-fraction dependence of ignition delay times, which shows a local minimum at mixtures which are rich of the mean mixture fraction. Due to this effect, increased levels of stratification results in the introduction of a larger range of mixture fractions having similar ignition delay times. However, for cases with the mean temperature of 850K, the distribution of homogeneous ignition delay time does not explain the non-monotonic behaviour suggesting that molecular mixing plays an important role for these cases.

m.talei@unsw.edu.au

1D03 DIRECT NUMERICAL SIMULATION OF PRF70/AIR PARTIALLY PREMIXED COMBUSTION UNDER IC ENGINE CONDITIONS

F. Zhang, R. Yu, X.S. Bai, Lund University, Sweden

Three-dimensional Direct Numerical Simulations (DNS) are performed to study the ignition and combustion process of a Primary Reference Fuel (PRF) under conditions relevant to Partially Premixed Combustion (PPC) engines. Detailed transport properties together with a skeletal PRF chemical kinetic mechanism are employed in the simulations. The initial partially premixed charge is prescribed according to a two-injection of fuel strategy with 50% Exhaust Gas

Recirculation (EGR). The motion of the piston, hence, the effect of compression of the charge due to piston motion is considered. The simulations are performed on a fine mesh with a spatial resolution of 1.2 micrometers in a cubic domain of 614 micrometers on each side. The results show that there are three distinctive combustion regions in a domain under PPC conditions, a lean homogeneous mixture region, a fuel-rich region, and in between a region with stoichiometric mixture. Auto-ignition occurs first in the lean and stoichiometric mixture regions, followed by a partially premixed flame in the fuel-rich region and at last a CO oxidation phase in the fuel-rich region. In the lean mixture region, the fuel and combustion intermediates such as CO are consumed almost completely due to relatively fast combustion and abundant oxygen. CO formed in the regions with stoichiometric and fuel-rich mixtures is consumed in a mixing controlled mode, which requires high level turbulence mixing or sufficiently long residence time. NO is formed mainly due to premixed combustion in the region with stoichiometric mixture.

Xue-Song.Bai@energy.lth.se

1D04 MODES OF REACTION FRONT PROPAGATION IN *N*-HEPTANE/AIR MIXTURE WITH TEMPERATURE GRADIENT

Peng Dai¹, Zheng Chen¹, Shiyi Chen¹, Yiguang Ju²

¹Peking University, China ²Princeton University, United States

Usually different autoignition modes can be generated by a hot spot in which ignition occurs earlier than that in the surrounding mixture. However, for large hydrocarbon fuels with Negative Temperature Coefficient (NTC) behavior, ignition happens earlier at lower temperature than that at higher temperature when the temperature is within the NTC regime. Consequently, a cool spot may also result in different autoignition modes. In this study, the modes of reaction front propagation caused by temperature gradient are investigated numerically for *n*-heptane/air mixture at initial temperature within and below the NTC regime. For the first time, different autoignition modes caused by a cool spot with positive temperature gradient are identified. It is found that the initial temperature gradient has a dramatic impact on autoignition modes. With the increase of the positive temperature gradient of the cool spot, supersonic deflagration, detonation, shock-induced detonation, and shock-induced supersonic deflagration are sequentially observed. It is found that shock compression of the mixture between the deflagration wave and leading shock wave produces an additional ignition kernel, which determines the autoignition modes. Furthermore, the cool spot is compared with the hot spot with temperature below the NTC regime. Similar autoignition modes are observed for the hot and cool spots. A regime map in terms of the normalized temperature gradient and acoustic-to-excitation time scale ratio is drawn for different autoignition modes. It is shown that the transition between different autoignition modes is not greatly affected by the NTC behavior. Therefore, like hot spot, the cool spot may also generate knock in engines when fuels with NTC behavior is used and the temperature is within the NTC regime.

cz@pku.edu.cn

1D05 A LES METHODOLOGY BASED ON REDUCED SCHEMES TO COMPUTE KNOCKING IN INTERNAL COMBUSTION ENGINES

Antony Misdariis^{1,2}, Olivier Vermorel², Thierry Poinsot³

¹Renault SAS, France ²CERFACS, France ³Institut de Mécanique des Fluides de Toulouse, France

The prediction of Autoignition (AI) delay is an essential prerequisite to account for abnormal combustions (e.g. knock or super knock) that can appear in Internal Combustion (IC) engines. In this paper, a simple model called Ignition to Propagation Reduced Scheme (IPRS) is proposed to add AI predictions in reduced chemical schemes, which are classically used to compute in-cylinder combustion in the context of Large Eddy Simulations (LES). The IPRS principle is to use a single two-reaction reduced scheme and adapt the pre-exponential factor of the fuel oxidation reaction as a function of the temperature: one value is used at low temperatures to correctly predict AI delays and another one can be used at higher temperatures, where heat release occurs, to keep the flame propagation properties of the chemical scheme. After a first section that introduces the model, Perfectly Stirred Reactors and 1D flames simulations are used to verify that: (1) the modification of the pre-exponential constant of the Arrhenius law at low temperature does not alter the propagation properties of the reduced scheme and (2) this modification is sufficient to accurately predict AI delays. In a following section this model is implemented in a 3D LES solver to compute AI in a simplified IC engine for which results with complex chemistries are available and may be used as a reference for comparison. In the last section this model is applied to a highly downsized engine to illustrate its ability to predict AI in real engine configurations.

misdariis@cerfacs.fr

1D06 COMBUSTION REGIME CLASSIFICATION OF HCCI/PCCI COMBUSTION USING LAGRANGIAN FLUID PARTICLE TRACKING

Naoya Fukushima¹, Makito Katayama¹, Yoshitsugu Naka¹, Tsutomu Oobayashi¹, Masayasu Shimura¹, Yuzuru Nada²,

Mamoru Tanahashi¹, Toshio Miyauchi³

¹Tokyo Institute of Technology, Japan ²The University of Tokushima, Japan ³Meiji University, Japan

A new combustion regime classification method is proposed for HCCI/PCCI combustion based on Lagrangian fluid particle tracking. The performance of the present method is demonstrated with the time trace of net heat conduction to

local mixture which is one of the quantities best representing the phenomena. Local combustion regimes are classified based on magnitudes of the maximum and minimum heat conduction on each fluid particle throughout the combustion process into autoignition, flame propagation and flame enclosing. Direct Numerical Simulations (DNS) of turbulent HCCI/PCCI combustion are conducted with different initial temperature fluctuations. A detailed kinetic mechanism including 53 species and 325 elementary reactions is used for methane–air reaction and a reduced kinetic mechanism including 37 species and 61 reactions is adopted for *n*-heptane–air reaction. The present DNS results show that the combustion process is highly sensitive to initial temperature fluctuations. The proposed method is applied to DNS results and the characteristics of fluid element classified into each combustion regime are investigated. By adopting appropriate threshold for the maximum and minimum heat conduction to local mixture, the contributions of three combustion regimes to whole fuel consumption can be discussed. The autoignition regime is dominant for lower temperature fluctuation case. However, the flame propagation and flame enclosing regimes turn to be significant for higher temperature fluctuation case where the autoignition regime is less than 20 % and only triggers combustion start. Such qualitative tendency is confirmed in two fuel species. However, quantitatively, the transition of dominant combustion regime from autoignition to flame propagation/flame enclosing takes place at lower temperature fluctuation for the *n*-heptane–air mixture case. This classification method can be extended for any physical or chemical quantities, for example, reaction paths of each fluid element. Therefore, the proposed classification method effectively characterizes the turbulent combustion process in HCCI/PCCI engines.

nfukushim@navier.mes.titech.ac.jp

1D07 IGNITION DELAY TIME MEASUREMENTS BEHIND REFLECTED SHOCK-WAVES FOR A REPRESENTATIVE COAL-DERIVED SYNGAS WITH AND WITHOUT NH₃ AND H₂S IMPURITIES

O. Mathieu, J. Hargis, A. Camou, C. Mulvihill, E.L. Petersen, Texas A&M University, United States

The composition of a representative coal-derived syngas was determined by averaging 40 practical coal syngas compositions from the literature and corresponds to a departure from many recent studies which only focus on syngas blends containing just CO and H₂. Ignition delay times have been measured behind reflected shock waves for this averaged mixture with an equivalence ratio of 0.5 (0.4554% CO/0.3297% H₂/0.1032% CO₂/0.0172% CH₄/0.2407% H₂O/0.8538% O₂ in 98% Ar (mol. %)) at around 1.7, 13, and 32 atm. The same mixture was also investigated with impurities (200 ppm of NH₃ and 50 ppm of H₂S). Care was taken when working with the blends containing H₂O and NH₃ to avoid errors in the shock-tube composition; direct measurement of the water vapor mole fractions were performed using a tunable diode laser absorption diagnostic near 1.38 μ m. The effect of the various constituents on the ignition delay time was also investigated by comparing to results from a baseline mixture (H₂/CO/O₂/Ar) and results with this baseline mixture with only one of the other constituents of the syngas (*i.e.* CO₂, CH₄, H₂S). Experimental data were compared with recent detailed kinetics mechanisms from the literature. Results showed that, under the conditions of this study, extending the mixture composition to include realistic concentrations of species beyond just the CO and H₂ does not have a very large effect on the ignition delay time for a coal-derived syngas. However, a comparison of this coal-derived syngas with a syngas derived from biomass, tested in an earlier study by the authors, exhibited large differences due to the larger CH₄ concentration in the bio-derived syngas. Two chemical kinetic models from the literature were found suitable to reproduce these data over most of the range of mixtures, temperatures, and pressures investigated, namely the mechanisms associated with Galway and with Princeton.

olivier.mathieu@tamu.edu

1D08 A SHOCK TUBE STUDY OF THE AUTOIGNITION CHARACTERISTICS OF RP-3 JET FUEL

Changhua Zhang, Bin Li, Fan Rao, Ping Li, Xiangyuan Li, Sichuan University, China

Autoignition delay time measurements were performed for gas-phase RP-3/air mixtures behind reflected shock waves at temperatures of 650-1500 K, pressures of 1-20 atm, and equivalence ratios of 0.2, 1.0, and 2.0. Ignition delay times were determined using electronically excited CH* and/or OH* emissions and reflected shock pressure monitored through the shock tube sidewall. The dependence of the ignition delay times upon temperature, pressure and equivalence ratio has been investigated at high temperatures. Correlation expressions for the ignition delay under different equivalence ratios and pressures have been deduced separately. The global activation energy for RP-3/air varies significantly as the ignition pressure changes. A Negative Temperature Coefficient (NTC) effect for RP-3 at 10 atm was observed in the temperature range of 750-850 K. Current results were compared with available Jet-A ignition data, showing good agreement with previous results of Jet-A. Based on the composition identification of RP-3, a mixture of 88.7% *n*-decane and 11.3% 1,2,4-trimethylbenzene by mole has been proposed as a surrogate for RP-3. Surrogate mechanism simulations were performed by using the mechanism proposed by Peters. The simulations show good agreement with the experimental data over wide ignition conditions. Sensitivity analyses were carried out to identify the important reactions in the ignition process and to explain the experimental phenomena. Current work provides a fundamental database for the development and validation of surrogate kinetic models for RP-3 jet fuel.

lpscun@scu.edu.cn

1D09 IGNITION CHARACTERISTICS OF A BIO-DERIVED CLASS OF SATURATED AND UNSATURATED FURANS FOR ENGINE APPLICATIONS

Alena Sudholt^{1,2}, Liming Cai¹, Joshua Heyne², Francis M. Haas², Heinz Pitsch¹, Frederick L. Dryer²

¹RWTH Aachen University, Germany ²Princeton University, United States

The ignition characteristics in form of Derived Cetane Numbers (DCN) of the class of saturated and unsaturated furans are investigated experimentally in an ignition quality tester. Further, quantum chemistry calculations at CBS-QB3 level of theory are applied to determine Bond Dissociation Energies (BDEs) and thereby the initial reactions of the ignition process for all fuels. Using the calculated BDEs, it is found that the ignition characteristics are similar within the groups of furans and tetrahydrofurans, but strongly differ among one another. It is shown that the ignition behavior of unsaturated furans is determined by the ring structure, which correlates with a negligible side chain influence. Hence, furan fuel structures can be chosen with respect to available production pathways and ease of applicability in engines. For tetrahydrofurans, on the contrary, the side chain length defines the area of application. Tetrahydrofurans with short side chains are potential candidates for SI application, whereas 2-butyltetrahydrofuran is shown to be a candidate for diesel application. The influence of the number and location of double bonds in the ring are illustrated with the DCN and BDE study of dihydrofurans and the influence of further functional groups is evaluated for (tetrahydro) furfuryl alcohols.

To investigate possible fuel application scenarios, in a second part of this study furans and tetrahydrofurans are investigated in blends with *n*-heptane and diesel. A DCN mixing rule is found to be approximately linear and for blends with up to 20 mol% furans, the side chain structure (alkyl, alcohol) has no influence on the blend DCN.

a.sudholt@itv.rwth-aachen.de

1D10 COMPUTATIONAL STUDY OF THE PRESSURE DEPENDENCE OF SEQUENTIAL AUTO-IGNITION FOR PARTIAL FUEL STRATIFICATION WITH GASOLINE

Benjamin Wolk, Jyh-Yuan Chen, University of California-Berkeley, United States

Fuel stratification is a potential strategy for reducing the maximum pressure rise rate in HCCI engines. Simulations of Partial Fuel Stratification (PFS) have been performed using CONVERGE with a 96-species reduced mechanism for a 4-component gasoline surrogate. Comparison is made to experimental data from the Sandia HCCI engine at a compression ratio 14:1 at intake pressures of 1 bar and 2 bar. Analysis of the heat release and temperature in the different equivalence ratio (ϕ) regions reveals that sequential auto-ignition of the stratified charge occurs in order of increasing ϕ for 1 bar intake pressure but in order of decreasing ϕ for 2 bar intake pressure. Increased low- and intermediate temperature heat release at 2 bar intake pressure compensates for decreased temperatures in higher- ϕ regions due to evaporative cooling from the liquid fuel spray and decreased compression heating from lower values of the ratio of specific heats. At 1 bar intake pressure, the premixed portion of the charge auto-ignites before the highest- ϕ regions and the sequential auto-ignition occurs too fast for useful reduction of the maximum pressure rise rate compared to HCCI. Conversely, at 2 bar intake pressure, the premixed portion of the charge auto-ignites last, after the higher- ϕ regions. More importantly, the sequential auto-ignition occurs over a longer time period than at 1 bar intake pressure such that a sizable reduction in the maximum pressure rise rate compared to HCCI can be achieved.

bmwolk@berkeley.edu

1D11 AUTOIGNITION BEHAVIOR OF SYNTHETIC ALTERNATIVE JET FUELS: AN EXAMINATION OF CHEMICAL COMPOSITION EFFECTS ON IGNITION DELAYS AT LOW TO INTERMEDIATE TEMPERATURES

Daniel Valco¹, Gerald Gentz², Casey Allen³, Meredith Colket⁴, Tim Edwards⁵, Sandeep Gowdagiri⁶, Matthew A. Oehlschlaeger⁶, Elisa Toulson², Tonghun Lee⁷

¹University of Illinois, Urbana-Champaign, United States ²Michigan State University, East Lansing, United States

³Marquette University, Milwaukee, United States ⁴United Technologies Research Center, United States

⁵Wright-Patterson Air Force Base, United States ⁶Rensselaer Polytechnic Institute, United States

⁷University of Illinois, United States

The autoignition characteristics of military aviation fuels (JP-5 and JP-8), proposed camelina-derived hydroprocessed renewable jet fuel replacements (HRJ-8 and HRJ-5), Fischer-Tropsch fuels (Shell and Sasol), three Sasol isoparaffinic solvents, as well as 50/50 volumetric blends of the alternative fuels with the conventional fuels are examined. Experiments were conducted in a rapid compression machine and shock tube at compressed temperatures of $625\text{K} \leq T_c \leq 1000\text{K}$, a compressed pressure of 20 bar, and under stoichiometric and lean conditions. Several implicit properties of alternative fuels related to their physical and chemical properties prompted a study of the influence of chemical composition on autoignition, including the influence of isoparaffinic, cycloparaffinic, and aromatic structures. In addition, interesting combustion phenomena at low-temperature conditions are investigated under lean conditions, specifically concerning jet fuel blend reactivity, where a convergence in blend reactivity to the reactivity of either a conventional or alternative fuel is observed.

tonghun@illinois.edu

1D12 THE AUTOIGNITION OF LIQUEFIED PETROLEUM GAS (LPG) IN SPARK-IGNITION ENGINES*Kai J. Morganti¹, Michael J. Brear¹, Gabriel da Silva¹, Yi Yang¹, Frederick L. Dryer²**¹The University of Melbourne, Australia ²Princeton University, United States*

This paper presents an experimental and numerical study of the autoignition of C₃ and C₄ hydrocarbon mixtures in a CFR octane rating engine. The four species examined — propane, propylene (propene), *n*-butane and *iso*-butane — are the primary constituents of Liquefied Petroleum Gas (LPG), and are also important intermediates in the oxidation of larger hydrocarbons. In-cylinder pressure data was acquired for both autoigniting and non- autoigniting operation at the same engine test conditions. The non-autoigniting traces were used to calibrate and validate a two-zone engine model in a prior work by the group, thus enabling the inclusion of the unburned charge chemical kinetics for further examination in this paper. The autoignition of the various fuel mixtures is examined using the C₀-C₄ kinetic model of Healy, which is coupled with the C₁-C₂-NO_x kinetic model of Dagaut and Dayma. Variations in the residual gas concentrations of both Carbon Monoxide (CO) and the unreacted/partially reacted hydrocarbons do not appear to have a significant effect on autoignition. However, physically reasonable concentrations of Nitric Oxide (NO) are found to be a strong promoter of autoignition in almost all cases, in keeping with several, more fundamental studies. The inclusion of the latter is also required in order to obtain good agreement between the measured and modelled autoignition timing. This in turn suggests that kinetic interaction between hydrocarbon fuels and NO plays an important role in octane rating, and its inclusion is important when modelling the autoignition of hydrocarbons in spark-ignition engines.

mjbrear@unimelb.edu.au

1D13 DEVELOPMENT OF A SKELETAL OXIDATION MECHANISM FOR BIODIESEL SURROGATE*Yachao Chang¹, Ming Jia¹, Yaopeng Li¹, Yanzhi Zhang¹, Maozhao Xie¹, Hu Wang², Rolf D. Reitz²**¹Dalian University of Technology, China ²University of Wisconsin–Madison, United States*

A new biodiesel surrogate model is proposed which includes normal alkane, saturated methyl ester and unsaturated methyl ester components. In the surrogate model, Methyl Decanoate (MD) and Methyl 5-Decenoate (MD5D) were chosen to respectively represent the saturated methyl ester and unsaturated methyl ester in biodiesel, and *n*-decane was included to match the energy content and C/H/O ratio of actual biodiesel fuel. Based on a decoupling methodology, an oxidation mechanism for the biodiesel surrogate was constructed by integrating the skeletal C₄-C_n sub-mechanisms for *n*-decane, MD and MD5D, a reduced C₂-C₃ mechanism, and a detailed H₂/CO/C₁ mechanism. The final mechanism for the biodiesel surrogate is composed of 60 species and 169 reactions. The mechanism was validated against experimental data, including ignition delay times in shock tubes and major species concentrations in jet-stirred reactors over wide operating conditions. Moreover, the mechanism was employed to simulate the combustion and emission characteristics of an engine operated in a low temperature combustion mode with SME as fuel. The overall agreement between the predictions and measurements is satisfactory.

jjaming@dlut.edu.cn

1E01 FEMTOSECOND COHERENT ANTI-STOKES RAMAN SCATTERING THERMOMETRY AT 5 kHz IN A GAS TURBINE MODEL COMBUSTOR*Claresta N. Dennis¹, Carson Slabaugh¹, Isaac G. Boxx², Wolfgang Meier², Robert P. Lucht¹**¹Purdue University, United States ²German Aerospace Center DLR, Germany*

Single-laser-shot temperature measurements at 5 kHz were performed in the DLR Gas Turbine Model Combustor (GTMC) using femtosecond (fs) Coherent Anti-Stokes Raman Scattering (CARS). Measurements were performed at various heights and radial locations within the flame in order to resolve the spatial flame structure and compare to previously published studies. The combustor was operated at a global equivalence ratio of 0.65 and 10 kW thermal power. Single laser shot temperature measurements are reported in the GTMC flame between 400 and 2300 K with less than 3.0% error. Power spectral density analysis of the temperature measurements yielded the characteristic thermo-acoustic pulsation frequency previously reported at 308 Hz. These results demonstrate the usefulness of fs-CARS for the investigation of highly turbulent combustion phenomena.

cfineman@purdue.edu

1E02 DEVELOPMENT OF TEMPERATURE EVALUATION OF PURE ROTATIONAL COHERENT ANTI-STOKES RAMAN SCATTERING (RCARS) SPECTRA INFLUENCED BY SPATIAL AVERAGING EFFECTS*Yi Gao¹, Thomas Seeger^{1,2}, Alfred Leipertz¹**¹University of Erlangen-Nuremberg, Erlangen, Germany ²University of Siegen, Germany*

The issue of spatial averaging effect arises in CARS temperature measurements when the probe volume consists of temperature gradients, a situation frequently encountered in turbulent reacting flows where flow patterns are irregular and temperature gradients are typically steep. In present work, the spatial averaging effect is specially manifested from the rotational CARS measurements performed on a premixed flame of a Wolfhard-Parker slot burner. To deal with the spatial averaging effect, a new dual-temperature fitting model is developed and then applied to evaluate the measured rotational

CARS spectra. Comparing with the traditional single-temperature fitting model, an improved spectral fitting and therefore, temperature and concentration evaluation by using the dual-temperature fitting model that accounts for the spatial averaging effects, is demonstrated. Finally, the feasibility of the dual-temperature model is shown in turbulent spray flames. In addition, a polarization approach to suppress the non-resonant part of the CARS signal was applied for all measurements.

thomas.seeger@uni-siegen.de

1E03 DEVELOPMENT OF TWO-BEAM FEMTOSECOND/PICOSECOND ONE-DIMENSIONAL ROTATIONAL COHERENT ANTI-STOKES RAMAN SPECTROSCOPY: TIME-RESOLVED PROBING OF FLAME WALL INTERACTIONS

Alexis Bohlin¹, Markus Mann², Brian D. Patterson¹, Andreas Dreizler², Christopher J. Klier¹

¹Sandia National Laboratories, United States ²FG Reaktive Strömungen und Messtechnik, Germany

Hybrid femtosecond / picosecond rotational Coherent Anti-Stokes Raman Spectroscopy (CARS) is developed utilizing a two-beam phase-matching approach for one-dimensional (1D) measurements demonstrated in an impinging jet burner to probe time-resolved Head On Quenching (HOQ) of a methane/air premixed flame at $\Phi=1.0$ and Reynolds number = 5000. Single laser-shot 1D temperature profiles are obtained over a distance of 4 mm by fitting the pure-rotational N₂ CARS spectra to a spectral library calculated from a time-domain CARS code. An imaging resolution of ~61 μm is obtained in the 1D-CARS measurements. The acquisition of single-shot 1D-CARS measurements, as opposed to traditional point-wise CARS techniques, enables new spatially correlated conditional statistics to be determined, such as the position, magnitude, and fluctuations of the instantaneous temperature gradient. The temperature gradient increases as the flame approaches the metal surface, and decreases during quenching. The standard deviation of the temperature gradient follows the same trend, increasing as the flame front approaches the surface, and decreasing after quenching.

cjklier@sandia.gov

1E04 APPLICATION OF THE TRACER COMBINATION TEA/ACETONE FOR MULTI-PARAMETER LASER-INDUCED FLUORESCENCE MEASUREMENTS IN IC ENGINES WITH EXHAUST GAS RECIRCULATION

S. Lind, J. Trost, L. Zigan, A. Leipertz, S. Will, Universität Erlangen-Nürnberg, Germany

The present study introduces an advanced measurement technique for multi-parameter imaging in optically accessible IC engines which is based on two Planar Laser-Induced Fluorescence (PLIF) techniques. A LIF tracer mixture consisting of TriEthylAmine (TEA) and acetone is used for the simultaneous determination of air/fuel-ratio, temperature and exhaust gas/air concentration in a Direct-Injection Spark-Ignition (DISI) engine with Exhaust Gas Recirculation (EGR). This investigation describes the suitability of the tracer mixture for a temperature and air concentration measurement applying a two-wavelength excitation scheme of the tracer acetone. The simultaneous measurement of the air/fuel-ratio is possible by applying a one-wavelength LIF technique using the effect of oxygen quenching of the TEA fluorescence signal intensity. At first the spectral properties of the tracer mixture are studied to show the separability of the fluorescence signals of both tracers and to identify possible tracer interactions. Fluorescence calibration at IC engine conditions is conducted with pure acetone and with an acetone/TEA mixture to visualize possible interactions. The tracer mixture is then applied in an optically accessible IC engine for temperature determination, which is compared to results of the commonly used successive application of the two individual techniques. The results confirm the suitability of this measurement technique for the simultaneous determination of air/fuel-ratio, air concentration and temperature in combustion devices like IC engines, which helps in the optimization of mixture formation and the subsequent processes such as ignition and pollutant formation.

lars.zigan@cbl.uni-erlangen.de

1E05 THREE-DIMENSIONAL FLAME MEASUREMENTS USING FIBER-BASED ENDOSCOPES

MinWook Kang, Xuesong Li, Lin Ma, Virginia Tech, United States

This work describes instantaneous three-dimensional (3D) flame measurements using Fiber-Based Endoscopes (FBEs). The measurement technique used FBEs to gather projections of the target flame from various orientations simultaneously, based on which a 3D tomographic reconstruction was then performed to obtain 3D flame measurements. Both experimental and numerical results are reported to illustrate the capabilities of the measurement technique, and study its limitations. These results demonstrate the feasibility of obtaining instantaneous 3D measurements with sub-mm spatial resolution at kHz using FBEs, and also the practical advantages of FBEs for overcoming optical access and reducing equipment cost.

LinMa@vt.edu

1E06 ENDOSCOPIC TEMPERATURE IMAGING IN A FOUR-CYLINDER IC ENGINE VIA TWO-COLOR TOLUENE FLUORESCENCE

C. Gessenhardt, C. Schulz, S.A. Kaiser, University of Duisburg-Essen, Germany

Building on the development of a large-aperture, UV-transparent endoscope designed specifically for use in IC engines, the gas-phase temperature in a fired, multi-cylinder engine was imaged based on Laser-Induced Fluorescence

(LIF) of a fuel tracer. Laser light at 266 nm was formed into a light sheet via a laser-input endoscope and excited fluorescence of toluene, port-fuel injected in a mixture with the base fuel *iso*-octane. The resulting UV-LIF signal was collected by an endoscope head in the combustion chamber, split into two wavelength-channels by a dichroic beam splitter, and detected on two separate cameras. Exploiting the temperature-dependence of the LIF spectrum, quantitative images of temperature were derived from the pixelwise ratio between the two images. We describe the procedures for cross-registration of the two images and calibration of the LIF-temperature conversion, which are more challenging compared to fully optically accessible engines. To assess the systematic error we performed a quasi-dimensional simulation matched in detail to engine data. Between intake-valve closure and mid-compression, the temperatures derived from the model and that from LIF agreed within 5 K, while the difference increased to 50 K at 28°CA before compression top-dead center. In addition to such quantitative imaging in the compression stroke, residual unburnt fuel was detected evaporating from the piston top. This feature unexpectedly enabled qualitative imaging even after combustion. Predicted by the simulation, the initial back-flow of exhaust gas into the intake during gas exchange could be visualized on a single-shot basis.

sebastian.kaiser@uni-due.de

1E07 SIMULTANEOUS PLANAR AND VOLUME CROSS-LIF IMAGING TO IDENTIFY OUT-OF-PLANE MOTION

S. Meares¹, V.N. Prasad¹, M. Juddoo¹, K.H. Luo^{2,3}, A.R. Masri¹

¹The University of Sydney, Australia ²University College London, United Kingdom ³Tsinghua University, China

A novel approach is introduced to identify the presence of out-of-plane motion that has historically plagued planar measurements of reactive structures evolving in turbulent flames. The technique combines Planar (P) and Volume (V) cross imaging (V orthogonal to P) of Laser-Induced Fluorescence from the hydroxyl radical (P-V-XLIF-OH). Two high-speed Nd: YAG-pumped dye lasers with a pulsing rate of 10kHz, are tuned to a transition of OH at 283.01nm. One beam is formed into a laser sheet, less than 120µm thick while the other beam is formed into a volume that is 3.4mm thick. The thin laser sheet (P) traverses the middle of the jet, while the thick Volume (V) is oriented at 90 degrees to the thin laser sheet and aligned to cover the outer edges of the flame. Sequences of planar and volume cross-LIF images of OH are collected in a range of flames approaching blow-off using two separate intensified CMOS cameras operating at a repetition rate of 10kHz. The plane-volume overlap is marked on the respective joint images to enable the identification of whether the changes in OH structures are due to out-of-plane motion. Using turbulent piloted non-premixed flames of Compressible Natural Gas (CNG) as a test-bed, it is shown that while out-of-plane motion impacts an average of around 12% of the sampled images, the rate of change of “breakages” and “closures” of OH structures was found to be unaffected. The same flames measured here were computed using Large Eddy Simulations with detailed chemistry. Two techniques mimicking both the experimental set-up and also using the local azimuthal velocity to identify out-of-plane motion were found to support the conclusions of the measurements.

shaun.meares@sydney.edu.au

1E08 INTERFERENCE FREE SPONTANEOUS RAMAN SPECTROSCOPY FOR MEASUREMENTS IN RICH HYDROCARBON FLAMES

G. Magnotti¹, D. Geyer², R.S. Barlow¹

¹Sandia National Laboratories, United States ²FB Maschinenbau- und Kunststofftechnik, Germany

The capability to simultaneously acquire two orthogonal component of a Raman spectrum has been added to the Sandia Raman\Rayleigh\CO-LIF instrument for combustion measurements. This addition allows removing unpolarized fluorescence interference signal from Raman spectra extending the applicability of the instrument to rich hydrocarbon flames. The optical set-up and the data analysis approach are described. The instrument is tested in challenging rich laminar and turbulent methane/air flames, deemed inaccessible with the previous instrument. Experimental results show good agreement with laminar calculations performed with Chemkin. The approach also avoids the cumbersome calibration procedures required for data collected with the previous version of the instrument in presence of mild fluorescence interference. The drawback is a drop in the instrument precision, in particular for CO₂ and O₂ concentrations.

gmagnot@sandia.gov

1E09 FORMALDEHYDE FLUORESCENCE AS A MARKER FOR SCALAR DISSIPATION THROUGH LOCAL EXTINCTION

Kathryn R. Gosselin, William F. Carnell, Jr., Michael W. Renfro, University of Connecticut, United States

A co-annular, counterflow diffusion burner was used to stabilize a local extinction point off centerline. The extinction point was measured using Planar Laser-Induced Fluorescence (PLIF) of Hydroxyl (OH) and formaldehyde (CH₂O). The PLIF measurements through the local extinction point were compared to results from a two-dimensional numerical simulation with a comprehensive chemical kinetics model, and good qualitative agreement is shown. In flames with local extinction, local scalar dissipation rate is a key parameter governing the extinction process but measurements of this rate are complicated. Previous work has suggested that the formaldehyde fluorescence profile width may be a useful marker for local scalar dissipation rate since formaldehyde persists outside the flame sheet and its width is dominated by

global mixing rates. This relationship is further tested in this work for conditions prior to, during, and after local extinction. Prior to the extinction point, the formaldehyde fluorescence exhibits self-similar behavior with respect to mixture fraction, as in a standard counterflow flame. However, close to the extinction region, the formaldehyde signal departs from self-similar behavior as hot products induce secondary production of formaldehyde. Formaldehyde width is found to be a useful marker for local scalar dissipation within a vigorously burning flame; however, it cannot be used as a direct marker in the presence of local extinction. Since the formaldehyde fluorescence signal increases significantly following local extinction, a combination of formaldehyde fluorescence width and intensity can still help identify local extinction points and scalar dissipation rates just prior to extinction.

kathryn@engr.uconn.edu

1E10 ADVANCEMENTS IN RAYLEIGH SCATTERING THERMOMETRY BY MEANS OF STRUCTURED ILLUMINATION

Elias Kristensson, Andreas Ehn, Joakim Bood, Marcus Aldén, Lund University, Sweden

Laser-induced Rayleigh scattering is commonly employed for two-dimensional temperature measurements and offers benefits such as high accuracy, easily interpreted data and low experimental complexity. Yet the approach suffers from an interference often referred to as stray light, an umbrella term used for all spurious light being detected. As Rayleigh scattering is an elastic scattering phenomenon, distinguishing between stray light and the signal of interest is not straightforward. In high-temperature environments, Rayleigh signals are weak due to low molecular densities, which make stray light interferences particularly cumbersome, impairing both the reliability and accuracy of Rayleigh thermometry, especially when applied in harsh combustion environments. In this paper we present an experimental solution to greatly mitigate this issue. The method, Structured Laser Illumination Planar Imaging (SLIPI), employs an intensity modulated laser sheet to add a recognizable signature to the signal photons. This unique signature allows utilization of a post-processing algorithm that isolates and extracts the desired Rayleigh signal, thereby minimizes measurement uncertainties caused by stray light. The fidelity of the proposed method is first verified by comparing with conventional Rayleigh thermometry under ideal, i.e. stray light-free, measurement conditions. The technique is then employed under more realistic measurement conditions, where the results conclusively illustrate that the current operating range for Rayleigh thermometry can be increased significantly by means of SLIPI.

joakim.bood@forbrf.lth.se

1E11 INVESTIGATION OF FLAME PROPAGATION IN A PARTIALLY PREMIXED JET BY HIGH-SPEED-STEREO-PIV AND ACETONE-PLIF

J. Weinkauff¹, P. Trunk¹, J. Frank², M.J. Dunn³, A. Dreizler¹, B. Böhm¹

¹Technische Universität Darmstadt, Germany ²Sandia National Laboratories, United States ³The University of Sydney, Australia

This paper presents an experimental study of flame propagation through a partially-premixed flow following ignition. A combination of simultaneous high-speed acetone Planar Laser Induced Fluorescence (PLIF) and stereoscopic Particle Image Velocimetry (PIV) was utilized for time-resolved measurements of mixture fraction, flow field and flame position. This provides access to the major quantities needed to characterize non-premixed flames. High quality mixture fraction measurements with signal-to-noise ratios up to 120 for unity mixture fraction were made feasible using a combination of a conventional high-speed laser at 10 kHz for LIF excitation and a wavelet based de-noising algorithm to reject camera noise. It was observed that flame propagation in the far-field of a partially-premixed jet takes place in a premixed mode, with the flame propagating through highly stratified mixtures until it approaches locations containing mixtures outside the flammability limits. In these areas the flame recedes and further propagation is controlled by mixing processes of air and fuel. Even though flame propagation is then mixing-controlled, the flame is not observed to switch into a non-premixed mode. Instead, mixing ahead of the flame takes place until locally premixed flammable mixtures are recovered for subsequent flame propagation.

bboehm@ekt.tu-darmstadt.de

1E12 3kHz PIV / OH-PLIF MEASUREMENTS IN A GAS TURBINE COMBUSTOR AT ELEVATED PRESSURE

I. Boxx¹, C. Slabaugh², P. Kutne¹, R.P. Lucht², W. Meier¹

¹Institut für Verbrennungstechnik, Germany ²Purdue University, United States

This study was designed to test the feasibility of acquiring simultaneous PIV/OH-PLIF measurements at multi-kHz rates in a turbulent swirl flame at pressures relevant to modern industrial gas turbine combustors. To accomplish this, Particle Image Velocimetry (PIV) and Planar Laser-Induced Fluorescence of the hydroxyl radical (OH-PLIF) were applied simultaneously at 3 kHz to study the dynamics of a lean partially-premixed turbulent swirl-stabilized flame of natural gas in an optically accessible, high-pressure combustion test rig at 5 bars. With 0.25mJ/pulse at 283nm for the OH-PLIF measurements, a Signal-to-Noise Ratio (SNR) of 4.1 was achieved over a region measuring 20×80mm. Absorption of the excitation laser proved to be the greatest challenge in this study, resulting in a significant variation in SNR from one side of the OH-PLIF images to the other. A procedure based on modelling the absorption according to the mean OH-distribution

was used to semi-quantitatively correct for this effect. A gradient-based edge-detection algorithm was used to identify reaction zone locations in the resulting images. These were used to compute mean distributions of flame surface density. With 2.5mJ/pulse at 532nm for the PIV system, velocity fields measuring 20×80mm were measured at a resolution of 1.25mm. Consistent with prior measurements in the burner, the flame shows strong thermo-acoustic pulsation, with a peak frequency of 388Hz. Phase-averages of the PIV and OH* data indicate these pulsations are driven by the same resonant feedback mechanism responsible for thermo-acoustic pulsation in the burner at atmospheric pressure. No evidence of a precessing vortex core, known to dominate the flow-field of the burner at atmospheric-pressure conditions, was observed.

isaac.boxx@dlr.de

1E13 INVESTIGATION ON RAPID CONSUMPTION OF FINE SCALE UNBURNED MIXTURE ISLANDS IN TURBULENT FLAME VIA 10 KHZ SIMULTANEOUS CH-OH PLIF AND SPIV

Ayane Johchi¹, Yoshitsugu Naka¹, Masayasu Shimura¹, Mamoru Tanahashi¹, Toshio Miyauchi²

¹Tokyo Institute of Technology, Japan ²Meiji University, Japan

High repetition rate simultaneous CH-OH Planar Laser Induced Fluorescence (PLIF) and Stereoscopic Particle Image Velocimetry (SPIV) measurement has been developed. The high speed simultaneous measurement system has 10 kHz acquisition rate and over 1.0 second measurement duration time. The developed system is applied to methane-air turbulent jet premixed flame in order to investigate flame and flow dynamics of turbulent combustion field. The obtained simultaneous CH and OH PLIF images well represent dynamics of turbulent flame in shear flow. In high intensity turbulence, the number of flame wrinklins increases and flame front shows a very complicated geometry. Since large scale vortical structures developed due to Kelvin-Helmholtz instability, large scale unburned mixture islands are often created and ejected into the downstream. Around the flame tip in high Reynolds number condition ($U_0 = 20$ m/s, $Re_\lambda = 257$), the formation of fine scale unburned mixture islands are observed. The dominant flame structure is investigated using Proper Orthogonal Decomposition (POD) analysis. It is shown that the formation of small scale unburned mixture islands and its rapid consumption are statistically meaningful around the tip of the high Reynolds number jet premixed flame. Their statistical values such as size and consumption rate are estimated. The mean consumption rate is around 1.2 m/s, which is about three times faster than the laminar burning velocity (0.39 m/s). In this study, the importance of CH acquisition with high repetition rate as flame marker is also discussed.

ajohchi@navier.mes.titech.ac.jp

1F01 LIBS MEASUREMENTS AND NUMERICAL STUDIES OF POTASSIUM RELEASE DURING BIOMASS GASIFICATION

H. Fatehi¹, Y. He^{1,2}, Z. Wang², Z.S. Li¹, X.S. Bai¹, M. Aldén¹, K.F. Cen²

¹Lund University, Sweden ²Zhejiang University, China

This paper reports on a joint numerical and experimental investigation of the release of potassium from biomass during gasification process. In this work, Laser-Induced Breakdown Spectroscopy (LIBS) was adopted to measure quantitatively the concentration of potassium from gasifying biomass. The effect of temperature on the potassium release is investigated in hot gas mixture of CO₂, H₂O with different concentration of O₂. A biomass thermochemical conversion model is employed to study the physical and chemical processes inside the particle. A sub-model is developed to simulate the various stages of potassium release during biomass conversion and to improve the chemical kinetic mechanism and chemical kinetic constants of the release rate. Two stages of the potassium release associated to devolatilization and char reaction and ash-cooking stages are proposed. The rate of release of potassium during char reaction and ash-cooking stages follows a first order Arrhenius expression as $2.5 \times 10^{5 \pm 0.2} \exp(-266 \times 10^3/RT)$. The kinetics rate constants along with the reaction path appear to be able to predict the potassium release with an acceptable accuracy.

Hesameddin.fatehi@energy.lth.se

1F02 EXPERIMENTAL STUDY ON THE COEXISTENT DUAL SLAGGING IN BIOMASS-FIRED FURNACES: ALKALI-INDUCED SLAGGING AND SILICATE MELT-INDUCED SLAGGING

Yanqing Niu, Yiming Zhu, Houzhang Tan, Xuebin Wang, Shi'en Hui, Wenzhi Du, Xi'an Jiaotong University, China

Aiming to the coexistence of serious alkali-induced and silicate melt-induced slagging during biomass combustion, the effects of Si, Al and K on the dual slagging are studied by addition of aluminosilicate compounds and thirty biomasses. For alkali-induced slagging mainly caused by alkali metal aerosols, addition of aluminosilicate compounds, such as kaolin and SiO₂, can remove about 80% of gaseous-K at 1273K, and 40%-60% at 1088K. Although SiO₂ shows higher effect on gaseous-K removal, especially at 1088K (62.5%), it needs further consideration because that it also exacerbates silicate melt-induced slagging by reaction with KCl and formation of low melting silicates. For silicate melt-induced slagging, IDT (Initial deformation temperature) can be as the evaluation index. The higher the IDT is, the lower the silicate melt-induced slagging potential is. IDT increases with increase in Al₂O₃ and SiO₂/K₂O, and decreases with increase in K₂O, SiO₂, SiO₂/Al₂O₃, and (SiO₂+K₂O)/Al₂O₃, and the significances are ordered as: Al₂O₃ > K₂O > SiO₂ > SiO₂/K₂O > SiO₂/Al₂O₃ > (SiO₂+K₂O)/Al₂O₃. Moreover, a set of evaluation criterion on silicate melt-induced slagging

potential is proposed, and as the true reflection of the potential of silicate melt-induced slagging, the $K_2O-SiO_2-Al_2O_3$ ternary phase diagram is constructed on basis of the ash properties of the thirty biomasses at the same time. It indicates that the $K_2O-SiO_2-Al_2O_3$ ternary diagram constructed on basis of pure K_2O , SiO_2 and Al_2O_3 underestimates the IDT of pure biomass. All those provide useful guideline for biomass selection and slagging reduction.

yqniu85@mail.xjtu.edu.cn

1F03 MECHANISM OF CHROMIUM OXIDATION BY ALKALI AND ALKALINE EARTH METALS DURING MUNICIPAL SOLID WASTE INCINERATION

Hongyun Hu, Zhang Xu, Huan Liu, Dunkui Chen, Kaidi Li, Aijun Li, Hong Yao

Huazhong University of Science and Technology, China

The influence of alkali and alkaline earth metals on Cr(VI) formation during Municipal Solid Waste (MSW) incineration has drawn much attention due to the high toxicity of Cr(VI). In the present work, the distribution of Cr(VI) in MSW incineration ash residues sampled from various plants were measured. The results show that the oxidation of chromium in combustion process is determined by the content of free CaO (f-CaO) in the MSW and is facilitated by alkali metals such as potassium in the flue gas cooling process. Considering that the content of f-CaO is low in MSW, the oxidation of Cr_2O_3 in the case of low mole ratio of Ca and Cr was investigated. The mixture of CaO and Cr_2O_3 was heated at temperatures ranged from 973 to 1373 K and the oxidation of Cr_2O_3 was measured by determining the oxygen consumption using an online mass spectrometer. According to the results, more chromium is oxidized in the thermal treated mixture at 1173 K than at higher temperatures. Part of chromium is oxidized to form $CaCrO_4$ and the unoxidized chromium remains in the form of Cr_2O_3 at 1173 K. In contrast, Cr_2O_3 is prior to form $Ca_3(CrO_4)_2$ at temperatures higher than 1173 K and the unoxidized chromium is mostly transformed into $CaCr_2O_4$. The formation of $CaCr_2O_4$ is temperature dependent which took place at temperatures higher than 1173 K in both oxidative and oxygen-lean atmosphere. Compared with Cr_2O_3 , $CaCr_2O_4$ is more easily oxidized affected by CaO or K_2CO_3 , indicating that more chromium would be oxidized during MSW incineration when chromium is transformed into $CaCr_2O_4$. Measures should be taken to suppress the formation of $CaCr_2O_4$ such as the control of the operating temperature and CaO addition.

hyao@mail.hust.edu.cn

1F04 EFFECT OF $MgCl_2$ LOADING ON THE EVOLUTION OF REACTION INTERMEDIATES DURING CELLULOSE FAST PYROLYSIS AT 325 °C

Dawei Liu, Yun Yu, Yu Long, Hongwei Wu, Curtin University, Australia

This study reports the effect of $MgCl_2$ loading on the evolution of reaction intermediates during the fast pyrolysis of cellulose (as a biomass model compound) at 325 °C. The loading of $MgCl_2$ significantly changes the reaction pathways of cellulose pyrolysis and enhances the cross-linking of hydroxyl groups to release water even during the heating-up stage, as a result of the weakened hydrogen bonding networks during both the wet impregnation and the heating processes. Such a highly cross-linked cellulose strongly affects the evolution of reaction intermediates during the subsequent isothermal pyrolysis at 325°C, i.e., producing the water-soluble intermediates rich in cross-linked structures. The loading of $MgCl_2$ may catalyse the interactions between the watersoluble and water-insoluble portions in pyrolysing cellulose, depending on the Mg distribution. Our results indicate that the water-insoluble Mg has a little effect on the pyrolysis of sugar structures in the water-insoluble portion, which still proceeds in a similar way as that of raw cellulose, i.e., dominantly via depolymerization. Whereas the water-insoluble Mg has a strong catalytic effect on the pyrolysis of non-sugar structures in the water-insoluble portion into more condensed structures, leading to a high char yield from the pyrolysis of the $MgCl_2$ -loaded cellulose.

Yun.Yu@curtin.edu.au

1F05 CARBONATE FORMATION DURING LIGNIN PYROLYSIS UNDER CO_2 AND ITS EFFECT ON CHAR GASIFICATION

Hirotsu Watanabe, Kiyomi Shimomura, Ken Okazaki, Tokyo Institute of Technology, Japan

This work aims to study the transition of the chemical form of the alkali minerals during pyrolysis under a CO_2 atmosphere, and its effect on gasification. Lignin containing a high concentration of Na was heated under a CO_2 or Ar atmosphere, and the chemical form of Na in both chars was characterized using water extraction and capillary electrophoresis. These chars were then gasified in air at various temperatures. As a result, capillary electrophoresis analysis showed that the organic-Na component of raw lignin was changed to carbonate during pyrolysis under CO_2 . Almost all the Na in char prepared under CO_2 was water-soluble carbonate, while water-insoluble Na was found only in char prepared under Ar. Water-insoluble Na was expected to be R-COONa or -CNa in which Na is strongly bonded with the char-matrix, leading to resistance to water extraction. It was clearly shown that the chemical form of Na in lignin char strongly depended on the presence of CO_2 during pyrolysis. Considering these experimental findings, a mechanism for transition of the chemical form of Na during pyrolysis under CO_2 was proposed. In addition, significant differences between these chars appeared during gasification. The lowest temperature at which char gasification advances for char prepared under CO_2 was

1073 K, while that for char prepared under Ar was 923 K. Raman spectroscopy indicated that no significant differences between the carbon structures of these chars were apparent. Therefore, the observed increase in gasification temperature was caused by transition of the chemical form of Na under CO₂. In fact, -CNa, which is the most important catalyst in char gasification, was not formed; although carbonate was formed during lignin pyrolysis under CO₂. This has an important implication for combustion or gasification of not only lignin but also Na ion-exchanged coal.

watanabe.h.ak@m.titech.ac.jp.

1F06 STUDY ON ONE-DIMENSIONAL STEADY COMBUSTION OF HIGHLY DESIFIED BIOMASS BRIQUETTE (BIO-COKE) IN AIR FLOW

Takero Nakahara, Yan Hui, Hiroyuki Ito, Osamu Fujita, Hokkaido University, Japan

Combustion experiments of cylindrical Bio-Coke (BIC), a highly densified biomass briquette, have been conducted to investigate whether quasi-one-dimensional steady combustion is attained in room temperature air flow. In the experiments, air flow velocity is selected as a main test parameter. Fuel consumption rate when only the bottom face of BIC sample burns is determined as the regression rate of combustion zone at the bottom face. In addition, one-dimensional calculation based on an energy equation at the combustion zone has been conducted to understand the mechanism to determine the criteria of steady combustion and also to predict the effect of water and volatile matter contents in BIC on extinction limit. The results show that steady combustion of the BIC sample is attained in air flow velocity of 4.67 m/s or larger, in contrast, extinction is observed in 3.82 m/s or lower. The criteria for steady combustion is explained by temperature decrease of combustion zone according to the calculation of energy balance at the reaction face. Though the dominant mechanism for extinction as a result of temperature decrease of reaction face is radiation heat loss, the latent heat necessary for water and volatile matter had also non-negligible effect on the criteria of steady combustion.

ofujita@eng.hokudai.ac.jp

1F07 A SOPHISTICATED MODEL TO PREDICT ASH INHIBITION DURING COMBUSTION OF PULVERIZED CHAR PARTICLES

Yanqing Niu¹, Christopher R. Shaddix²

¹Xi'an Jiaotong University, China ²Sandia National Laboratories, United States

Final burnout of char particles from practical fuels such as coal and biomass occurs in the presence of a large ash component. Also, newly utilized coal resources, such as those from India, often contain much larger ash fractions than have traditionally been utilized. In the past, the inhibitory influence of ash on pulverized coal particle combustion has been most frequently modeled using an ash film model, though such films are rarely found when examining partially combusted particles. Conversely, some measurements have suggested that mineral components exposed on the surface of burning pulverized coal (pc) particles may diffuse back into the char matrix, the effect of which can be modeled as an ash dilution effect. To explore the implications of these different ash inhibition models on the temporal evolution of char combustion during burnout, we have developed a new computational model that considers the possibility of an ash film effect, an ash dilution effect, or some arbitrary combination of the two effects acting in tandem, which is the most realistic scenario. This new model predicts that restricted diffusion through the ash film has a significant impact on the char burnout rate throughout its lifetime, whereas char dilution only inhibits combustion significantly when most of the char has been consumed and the combustion mode shifts from predominantly external diffusion control to mixed diffusion control, with sensitivity to both external and internal diffusion resistance. The comparison of the model predictions with experimental results also confirms the previously suggested need to include gasification reaction steps when modeling coal char combustion.

yqniu85@mail.xjtu.edu.cn

1F08 FLAMELET MODEL FOR PULVERIZED COAL COMBUSTION

Junya Watanabe, Kenji Yamamoto, Hitachi Research Laboratory, Japan

A new flamelet model has been developed that is applicable to the pulverized coal combustion simulation. First, a modeling approach was adopted that considered the coupling with both the devolatilization and the char combustion. The validity of the developed flamelet model was examined in a simple two-dimensional pulverized coal jet field ignited by burnt co-flows. The accuracy of the model was evaluated by comparing its instantaneous distributions of temperature, CO₂ mass fraction, and OH mass fraction with those of a detailed chemistry model. Good agreement was obtained in terms of the overall features of turbulent structures and combustion state, although the flamelet model showed slightly quicker ignition due to the transitional state in the ignition process being insufficiently reproducible.

junya.watanabe.yu@hitachi.com

1F09 RELATIONSHIP BETWEEN PYROLYSIS AND ORGANIC AEROSOL EMISSION DURING COAL COMBUSTION

Xiaofei Wang¹, Emma Cotter¹, Kannan N. Iyer², Jiayi Fang¹, Brent J. Williams¹, Pratim Biswas¹

¹Washington University in St. Louis, United States ²Indian Institute of Technology, India

Coal combustion is one of the major emission source of atmospheric organic aerosols, especially in developing countries. However, the formation mechanisms of organic aerosols during coal combustion have not been adequately

studied. This study presents a detailed comparison of the chemical compositions between organic aerosol emissions from coal combustion and organic tars from coal pyrolysis, which is an early stage of coal combustion. Two coals, PRB coal and ILL#6 coal, were combusted in a laboratory drop-tube furnace coal combustor; and pyrolyzed in a flat-flame system, which is used as a fast pyrolysis device. The compositions of organic constituents of the combustion aerosols and pyrolysis products were measured by an Aerosol Mass Spectrometer (AMS) and a Thermal desorption Aerosol Gas chromatography–mass spectrometer (TAG). The chemical composition of major species for both combustion organic aerosols and pyrolysis products are hydrocarbons, carboxylic acids and aromatic compounds. A list of specific organic compounds has been identified. The similarities of the chemical compositions strongly suggest that the coal pyrolysis products are the precursors of the organic aerosols. In addition, more carboxylic acids/oxygenated organic compounds were found in the combustion aerosols, indicating that many pyrolysis products are oxidized before final emissions of organic aerosols. Thermal Gravimetric Analysis (TGA) was also conducted to study the pyrolysis process of the two coals. The activation energy distributions were calculated from their TGA results using a Distributed Activation Energy Model (DAEM).

pbiswas@wustl.edu

1F10 ASH AEROSOL FORMATION FROM OXY-COAL COMBUSTION AND ITS RELATION TO ASH DEPOSIT CHEMISTRY

Zhonghua Zhan¹, Andrew Fry¹, Yanwei Zhang^{1,2}, Jost O.L. Wendt¹

¹University of Utah, United States ²Zhejiang University, China

To investigate ash aerosol and ash deposition formation in oxy-coal combustion, experiments on air combustion and oxy-coal combustion with 50% inlet oxygen with CO₂ (referred to as OXY50) were conducted on a 100 kW rated pilot-scale self-sustained oxy-fuel combustor with Powder River Basin coal. A Berner Low Pressure Impactor (BLPI), a Scanning Mobility Particle Sizer (SMPS), and an Aerodynamic Particle Sizer (APS) were used for ash aerosol sampling and Particle Size Distribution (PSD) analysis. A novel temperature-controlled ash deposition probe system was used for ash deposition collection. The ash aerosol PSDs given by BLPI and SMPS/APS were extremely consistent, indicating high-quality data. The data suggested that OXY50 did not change the ash aerosol formation mechanisms, but increased the formation of central mode particles due to higher combustion temperature. The inside deposits with sizes less than 4.6 μm showed higher Si and lower Na and S in OXY50 than in air combustion. To ascertain the relationship between ash aerosol and ash deposition, ash aerosol with sizes less than 2.36 μm was related to inside deposits in chemistry, where sodium showed straightforward relationship between ash aerosol and inside deposits, namely, higher Na in ash aerosol resulted in higher Na in inside deposits. Their absolute values were also comparable. The contribution of S and Si to inside deposits showed particle size selectivity. That is, S in ultrafine and fine modes and Si in ultrafine mode contributed significantly to the inside deposits. The results indicated that the prediction of initial layer deposit chemistry was possible by knowing the chemistry of the ash aerosol.

Jost.Wendt@Utah.Edu

1F11 ACCURACY OF THE SINGLE-FILM MODEL IN THE PREDICTION OF COAL CHAR CONVERSION RATES UNDER OXY-FUEL AND CONVENTIONAL COMBUSTION CONDITIONS

Cristina Gonzalo-Tirado, Santiago Jiménez, LIFTEC, Spain

The accuracy of the single-film model in the calculation of char burning rates and particle temperatures in conventional and oxy-fuel combustion conditions has been investigated taking as a reference the results obtained with a model with detailed gas-phase kinetics. Both models have been applied to subbituminous coal and anthracite char particles in different sizes (60-1000 μm), in N₂ and CO₂-rich atmospheres with a low and a high oxygen concentration. For 120 μm char particles, the models' predictions have been also compared over an ample range of ambient gas temperatures (1373-1823 K) and oxygen concentrations (4-50%). High particle diameters, bulk gas temperatures and oxygen concentrations result in CO-flames closer to the particle surface; however, the specific effects of the flame strongly depend on the coal rank and combustion conditions. In general, the single-film model accuracy is quite high in terms of burning rate predictions, except for fine anthracite particles burning at moderate bulk gas temperatures and high O₂ concentrations; greater deviations have been found regarding particle temperatures, even in cases where the corresponding combustion rates are very similar. The oxy-combustion of the reactive coal is found to be faster than its conventional combustion, except for the finest particles; although qualitatively similar, the difference in rates is overestimated if the single-film model is considered.

yago@litec.csic.es

1F12 EFFECT OF MINERALS ON SURFACE MORPHOLOGIES AND COMPETITIVE REACTIONS DURING CHAR GASIFICATION IN MIXTURES OF O₂ AND CO₂

Hirotsu Watanabe, Ken Okazaki, Tokyo Institute of Technology, Japan

This study aims to investigate the effect of minerals on surface morphologies and competitive reactions during char gasification in mixtures of O₂ and CO₂. Char gasification experiments were performed in O₂/Ar, Ar/CO₂, and O₂/CO₂ environments to study char structure evolution utilizing different gases and competitive reactions between char-O₂ and -

CO₂ gasification. Chars gasified under Ar/CO₂ or O₂/CO₂ were observed to have large pores on their surface, while chars gasified under O₂/Ar did not have them. The reaction between catalyst/carbon interfaces was key in explaining the difference in surface morphologies of chars gasified under O₂ and CO₂. High specific surface area and large pores produced by gasification in CO₂ increased char gasification rates in diffusion-controlled regime. Then, two coals of different ash composition (including high Alkali and Alkaline Earth Metallic (AAEM) and low AAEM species) were used to study competitive reactions between O₂ and CO₂ on the active sites. When chars prepared from coals including a low AAEM species were used, the char gasification rate in O₂/CO₂ environments was almost 60 % of the sum of those in O₂/Ar and Ar/CO₂ environments, regardless of specific surface area. This indicated that char-O₂ and -CO₂ reactions were competitive. However, when chars prepared from coals including a high AAEM species were used, higher Ca and Na concentrations were detected on the char surface, and the char gasification rate in O₂/CO₂ environments was almost the same as the sum of gasification rates in O₂/Ar and Ar/CO₂ environments, implying that Ca and Na played an important role as active sites. Unlike air environments, all surrounding gases were reactive in the O₂/CO₂ environments. Therefore, a sufficient active site, mainly consisting of catalyst in this study, was important not only to enhance char gasification reactions but also to prevent competitive reactions between char-O₂ and CO₂ gasification.

watanabe.h.ak@m.titech.ac.jp.

1F13 STUDY ON N₂O REDUCTION WITH SYNTHETIC COAL CHAR AND HIGH CONCENTRATION CO DURING OXY-FUEL COMBUSTION

Chang'an Wang, Yongbo Du, Defu Che, Xi'an Jiaotong University, China

Oxy-fuel combustion can realize large-scale CO₂ capture and low nitric oxides emission from coal-fired power plants, which has lately received growing attention. The present study aims at the N₂O reduction mechanism with high concentration CO in oxy-fuel combustion. One self-made synthetic coal was employed to investigate the promotion of high level CO on N₂O reduction. Both experimental and kinetic studies of N₂O reduction in the presence of high level CO have been conducted. Experimental results indicate that CO plays a significant role in enhancing N₂O reduction on char surface. More N₂O, compared with NO, is decomposed in low temperature zone. With the increase of temperature, a noticeable increase in N₂O reduction ratio can be observed regardless of CO. Fe₂O₃ exhibit the most obvious promotion on the N₂O reduction among the major metal oxides in coal ash. The contribution of fixed carbon to N₂O reduction is superior to that of metal oxides. Kinetics analysis shows that the apparent activation energy of the N₂O reduction with char can be reduced by high level CO, which is quite valuable for further reducing N₂O emission in oxy-fuel combustion.

dfche@mail.xjtu.edu.cn

1G01 EXPERIMENTAL VALIDATION OF A CORRELATION CAPTURING THE BOUNDARY LAYER EFFECT ON SPREAD RATE IN THE KINETIC REGIME OF OPPOSED-FLOW FLAME SPREAD

Subrata Bhattacharjee¹, Wynn Tran¹, Matthew Laue¹, Christopher Paolini¹, Yuji Nakamura²

¹San Diego State University, United States ²Hokkaido University, Japan

In opposed-flow flame spread over solid fuels, an increase in flow velocity eventually leads to flame extinguishment. While the chemical time is independent of the flow velocity, the residence time of the oxidizer at the flame leading edge is inversely proportional to the flow velocity. A competition between the two leads to a situation where finite-rate kinetics dominates the flame spread behavior, leading to blow-off extinguishment. The ratio of the two competing, the Damkohler number, captures this finite-rate effect and has been used to correlate the nondimensional spread rate with opposing flow velocity and ambient oxygen level. Although qualitatively successful, these correlations show considerable spread in the data despite the use of several variations of the definition of the Damkohler number. One possible reason could be the neglect of the developing boundary layer in front of the flame by the experimentalists. In this work we present new flame spread data over ashless filter paper acquired in an eight meter tall vertical steel chamber in which a sample is moved at desired velocities to create a relative opposing flow. The developing boundary layer over the fuel sample is shown to have a significant effect on the measured spread rate and flame shape that do not correlate with opposing flow velocity if an Oseen flow approximation is used. Once the data is adjusted for the developing boundary layer using an effective flow velocity formula obtained from scaling arguments and refined through computational results, the correlation improves drastically, establishing the importance of the boundary layer in the kinetic regime. Much of the spread rate data available in literature do not mention the development length and must be cautiously used.

prof.bhattacharjee@gmail.com

1G02 THERMAL STRUCTURE OF FLAME SPREAD IN PARTIALLY PREMIXED ATMOSPHERES AND EFFECTS OF FUEL LEWIS NUMBER

Kazuhiro Yamamoto¹, Satoshi Seo², Koichi Mori²

¹Nagoya University, Japan ²Toyohashi University of Technology, Japan

The experimental study on the flame spread in partially premixed atmospheres was presented. Two samples of different filter thickness and density were used. Fuels of hydrogen, methane, and propane were added in the opposed air,

focusing on the fuel Lewis number (Le). In the partially premixed atmospheres, the pyrolysis zone and the region of high temperature are expanded. Since the flame temperature is increased, the heat transfer rate to the preheat zone of the filter is promoted, which is confirmed by the de Ris's formula of the thermally thin model. The heat transfer due to the heat conduction from the flame is 65 to 70 % of total heat transfer. By comparing the results of the preheated air, the corresponding temperature rise caused by fuel addition is evaluated. For all fuels, the linear increase of temperature rise with the fuel concentration (C_f) is confirmed. However, at the fixed fuel concentration, the temperature rise depends on the fuel type. Generally, there are two factors directly related with thermal structure of combustion field such as the flame temperature. One is the heat of combustion (H), and the other is the fuel Lewis number, because the opposed flow is the lean mixture. Since Le is proportional to the inverse of the fuel diffusivity, the temperature rise could be corrected by $1/Le$. Resultantly, for all fuels, the same dependence of the temperature rise on ($C_f \cdot H/Le$) is observed. Thus, the Lewis number is a very important and useful parameter to discuss the thermal structure and the flame spread rate in partially premixed atmospheres.

kazuhiro@mech.nagoya-u.ac.jp

1G03 TEMPERATURE AND CO₂ FIELDS OF A DOWNWARD SPREADING FLAME OVER THIN CELLULOSE: A COMPARISON OF EXPERIMENTAL AND COMPUTATIONAL RESULTS

Wynn Tran¹, Jeanie Ray Villaraza¹, Christopher Paolini¹, Subrata Bhattacharjee¹, Shuhei Takahashi²

¹San Diego State University, United States ²Gifu University, Japan

Flame structure of a downward flame spreading over thermally thin cellulose in a normal gravity quiescent environment is investigated in this work. A novel experimental set up called the flame stabilizer is used to arrest the motion of the flame by moving the fuel sample. The frozen flame is then probed by a K-type fine-wire thermocouples and a Non-Dispersive Infrared Radiation (NDIR) sensor with force induction to produce the experimental temperature and CO₂ concentration fields. A previously used two dimensional, steady computational model is used to generate the computational fields which are compared to the experimental measurements. The measured peak value of CO₂ compares quite well with the computational prediction, but the peak temperature measured is significantly lower than the computational peak temperature. The overall measure and computed fields are similar in shape and size. The flame spread rates also agree reasonably well. Although a downward moving flame over thin solid fuel is often considered a laminar flame, the fluctuation data from the probes indicates that there is considerable presence of turbulence along the outer edge of the flame.

prof.bhattacharjee@gmail.com

1G04 FLAME SPREAD OVER ELECTRIC WIRE WITH HIGH THERMAL CONDUCTIVITY METAL CORE AT DIFFERENT INCLINATIONS

Longhua Hu^{1,2}, Yangshu Zhang¹, Kosuke Yoshioka², Hirokazu Izumo², Osamu Fujita²

¹University of Science and Technology of China, China ²Hokkaido University, Japan

This paper reveals experimentally the Flame Spread Rate (FSR) [both upward (concurrently) and downward (opposed)] over electric wire with high thermal conductivity metal core at different inclination angles, which is new in view of that previous works about such inclination effect are mainly focusing on the material (wood, PMMA.....) where the conductivity through media itself is not so important. Polyethylene (PE) insulated copper (Cu) wires with inner core diameter (d_c) of 0.30 mm, 0.50 mm 0.80 mm and insulation thickness (δ_p) of 0.15 mm, 0.30 mm are studied with inclination angles ranged from -90° to +90°. Their behaviors are examined in both naturally normal (Hefei city with altitude of 50 m; 100 kPa) and a reduced (Lhasa city with altitude of 3650 m; 64 kPa) ambient pressure atmosphere. Results show that with increase in inclination angles from -90° to 90°, the FSR first decreases and then increases ("U" trend) with its value being lowest at nearly horizontal condition (0°) in both pressures, which is quite different from what we normally know for other materials with low thermal conductivity. Two characteristic lengths, the flame base width (W_f) and the pyrolysis zone length (L_p), are found to account for this special variation behavior with their variation trend with inclination angle consistent with that of FSR. A simplified heat balance analysis concerning core thermal conduction effect is performed to calculate the FSR in relation to these two characteristic lengths, thermal conductivity of the metal core as well as the effective convection heating of the wire by the flame base. The calculated FSR are shown to be in fairly good agreement with the measured values at different inclination angles for different inner core (wire) diameters in both ambient pressures.

ofujita@eng.hokudai.ac.jp

1G05 UPWARD FLAME SPREAD IN LARGE ENCLOSURES: FLAME GROWTH AND PRESSURE RISE

Sandra L. Olson¹, Suleyman A. Gokoglu¹, David L. Urban¹, Gary A. Ruff¹, Paul V. Ferkul²

¹NASA Glenn Research Center, United States ²National Center for Space Exploration Research, United States

Upward flame spread tests were conducted on thin fuels in a sealed chamber capable of accommodating large-scale samples (1 m length). The primary objective of these tests was to measure flame spread and pressure rise in a large sealed chamber during and after flame spread and to characterize that data as a function of sample material, initial pressure,

and sample size. The flame spread rate as a function of initial pressure has been measured for a given fuel and found to vary as $\sim P^2$ in agreement with Grashof number scaling. The burning rate per unit area for a fixed pressure has been shown to be a constant independent of fuel area density or quantity of fuel burned. A steady upward flame spread was observed only at low pressure. The pressure rise in a sealed chamber has been shown to scale with the quantity of fuel burned, and the peak pressure has been shown to scale inversely with initial pressure, in agreement with the pressure dependence of the characteristic time associated with a simple analytical solution of an energy balance. The pressure rise per mass of fuel burned exhibits an exponential decay with burn-time, also in agreement with the analytical solution.

sandra.olson@nasa.gov

1G06 UPSLOPE FIRE SPREAD THROUGH POROUS FOREST FUEL BEDS: THE ROLE OF CONVECTION COOLING

Naian Liu, Jinmo Wu, Linhe Zhang, Zhihua Deng, Kohyu Satoh, University of Science and Technology of China, China

This paper presents a systematical analysis on the role of convection cooling in upslope line fire spread (with linear flame fronts) over pine needle fuel bed. The slope angles were varied within $0 \sim 30^\circ$ in experiments. The experimental data of heat flux, gas temperature and gas velocity are used to justify the significant effect of convection cooling in line fire spread. Especially the respective contributions by natural convection and forced convection to fuel pre-heating are investigated by experimental data and computations. The results indicate that besides radiation heating which is always dominant in fuel pre-heating, both natural convection and forced convection exert impacts on fuel pre-heating of line fire spread, but with different spatial influence ranges. Natural convection takes effect in a region from far field to near field (close to the flame), while forced convection (induced by the air entrainment of the flame) plays an important role within the region close to the flame. With increasing slope angles, the convection cooling is dominated by natural convection under lower slope angles, with comparable intensity as compared to radiation loss, and is jointly dominated by natural and forced convections under higher slope angles. The fire line contour has marked impact on the convection heating, and compared to convex flame front, a linear flame front involves a much shorter spatial influence range of convection heating ahead of the flame front.

liunai@ustc.edu.cn.

1G07 A STUDY ON BURNING OF CRUDE OIL IN ICE CAVITIES

Hamed Farmahini Farahani¹, Xiachuan Shi¹, Albert Simeoni², Ali S. Rangwala¹

¹Worcester Polytechnic Institute, United States ²University of Edinburgh, United Kingdom

In-Situ Burning (ISB) is a practical means of oil spill cleanup in icy conditions. This study considers one example of oil spill scenario: burning oil in an ice cavity. A new set of parameters to the classical problem of confined pool fires in vessels arises under these unique conditions. The icy walls of the cavity create a significant heat sink causing considerable lateral heat losses, especially for the small cavity sizes (5-10 cm). The melting of ice due to the heat from the flame causes the cavity geometry to change. Specifically, the diameter of the pool fire increases as the burning proceeds. This widening causes the fuel to stretch laterally thereby reducing its thickness at a faster rate. The melted ice water causes the oil layer to rise up, which causes the ullage height ratio to decrease. The reduction in ullage and increase in diameter counter-act the reduction in thickness due to the widening. This results in a strong coupling between the mass loss rate (\dot{m}) and the geometry change of the pool and cavity. To systematically explore this process, experiments were performed in circular ice cavities of varying diameters. It was found that due to the cavity expansion the average \dot{m} of crude oil in the ice cavity is greater than the \dot{m} in a pan. For example, while efficiency of 10 cm pan is close to 100%, its \dot{m} found to be 50% less than the \dot{m} in an ice cavity with similar initial diameter. A mathematical model was developed to predict mass loss rates and efficiencies which are in reasonable agreement with the experimental results. Extension of the model to larger sizes, comparable to realistic situation in the Arctic is discussed.

ffarahani.hamed@gmail.com

1G08 CHEMICAL CHARACTERIZATION OF PARTICLE EMISSIONS FROM CONTROLLED BURNS OF BIOMASS FUELS USING A HIGH RESOLUTION TIME-OF-FLIGHT AEROSOL MASS SPECTROMETER

Li Qi^{1,2}, David Cocker III¹, SeyedEhsan Hosseini¹, Heejung Jung¹, Wayne Miller¹, David Weise³, Yeru Huang², Zhiguang Zhou²

¹University of California, Riverside, United States

²National Research Center for Environmental Analysis and Measurements, China ³Foreset Fire Laboratory, United States

A total of forty-nine burns were conducted at the Missoula Fire Sciences Lab consisting of nine fuel types; i.e., chamise scrub oak, ceanothus, maritime chaparral, coastal sage scrub, California sage brush, Manzanita, oak savanna, oak woodland and masticated mesquite. This paper focuses on the bulk chemical characterization of particles produced during flaming, mixed and smoldering phases using a HR ToF-AMS. The evolution of OM/OC, H/C, O/C and N/C from fire ignition to extinction was measured to capture the transient and integrated chemical composition of the non-refractory portion of the particles. Real time elemental ratios and empirical formulas derived with respect to Modified Combustion Efficiency (MCE) are reported. For each fuel, the hydrogen fragment ions dominate the Unit Mass Resolution (UMR) mass

spectra with no specific fragment ions attributable to an individual ecological combination. An interference ion in the UMR m/z 73, a fragment normally attributed to levoglucosan, is noted. Therefore, the results imply that $C_2H_4O_2^+$ (m/z 60.021) plus $C_3H_5O_2^+$ (m/z 73.029) are more sufficient to estimate the contribution of levoglucosan with the overall average contribution fraction ranging from 0.74% for coastal sage to 1.93% for chamise.

luciaqi@gmail.com

1G09 IGNITION OF CELLULOSE FUEL BEDS BY HOT METAL PARTICLES

James L. Urban, Casey D. Zak, C. Fernandez-Pello, The University of California-Berkeley, United States

The ignition of natural combustible material by hot metal particles is an important fire ignition pathway by which wildland and urban spot fires are started. There are numerous cases reported of wild fires started by clashing power-lines, or from sparks generated by machines or engines. Similarly there are many cases reported of industrial fires caused by grinding and welding sparks. In this work, the effect of metal type on the ability of hot metal particles to cause flaming ignition of powdered cellulose fuel beds is studied experimentally. The materials studied are stainless steel, aluminum, brass and copper. These metals are representative of clashing conductors (aluminum and copper) and those involved in machine friction and hot work such as welding (stainless steel and brass). Particles of various sizes from 2 to 12 mm in diameter are heated to various temperatures between 575 - 1100°C before impacting the fuel bed. The results show a hyperbolic relationship between particle size and temperature, with the larger particles requiring lower temperature to ignite the cellulose than the smaller particles. For large particles all the metals show similar ignition boundary is not very sensitive to particle diameter. Although these trends indicate that particle energy is important in the capability of the particle to ignite the fuel, both energy and temperature are important factors of the particle ignition capabilities, but they alone are not enough to determine ignition. The thermal properties of the metal play a lesser role with exception for the energy of melting if it occurs. It also appears that the controlling ignition mechanisms by large particles are different than those from the small particles. The former appears to be determined primarily by the particle surface temperature while the later by the particle energy.

JLUrban@berkeley.edu

1G10 QUANTITATIVE INFRARED IMAGING OF IMPINGING TURBULENT BUOYANT DIFFUSION FLAMES

Ashish S. Newale^{1,2}, Brent A. Rankin^{1,3}, Harshad U. Lalit¹, Jay P. Gore¹, Randall J. McDermott⁴

¹Purdue University, United States ²CD-adapco, United States ³Innovative Scientific Solutions Inc., United States

⁴National Institute of Standards and Technology, United States

A buoyant fire impinging on a horizontal ceiling at a certain distance from the fuel source occurs in many practical fire scenarios. Motivated by this application, infrared radiation from buoyant diffusion flames with and without impingement on a flat plate is studied using a quantitative comparison of measured and simulated images. The measured quantitative images of the radiation intensity are acquired using a calibrated high speed camera. Simulated radiation intensities are rendered in the form of images and compared quantitatively with the measured images. The simulated radiation intensities are obtained using the radiative transfer equation with local absorption coefficients evaluated using a narrowband radiation model. The instantaneous local species concentrations, soot volume fractions, and temperatures necessary for these simulations are calculated using the Fire Dynamics Simulator (FDS) version 6. The measured images reveal that the characteristic necking and bulging ($7\text{Hz} \pm 1\text{Hz}$) of the free buoyant flame is suppressed to a large extent by impingement on the plate. The roll-up vortices in the impinging flame are much smaller than those in the free flame. The stagnation point boundary layer inferred from the computed images is thicker at some instances than that inferred from the measurements. Qualitative and quantitative comparisons between the measured and computed infrared images for both the free and the impinging fires reveal many similarities as well as differences potentially useful for model improvements.

ashish.newale@gmail.com

1G11 AN INVESTIGATION OF THE DETAILED FLAME SHAPE AND FLAME LENGTH UNDER THE CEILING OF CHANNEL

Zihe Gao, Jie Ji, Huaxian Wan, Jinhua Sun, University of Science and Technology of China, China

An experimental investigation of the flame shape and flame length under the ceiling of a channel is presented, which is a very important but not fully understood issue in previous studies. Altogether 48 experiments of four series fire environments were performed, with fire in the open, flush with a wall without ceiling, at the longitudinal centerline of a channel and flush with the sidewall of channel. The shape of flame extending under the ceiling is basically a circular for fire located at the longitudinal centerline of channel, whereas for fire placed flush with sidewall, it is a half of an ellipse. Analysis shows that the long axes of the ellipse changes from perpendicular to the intersecting line of ceiling and sidewall to parallel to it with increasing Heat Release Rate (HRR). The changing behavior arises from the competition between air entrainment enhancement of generated large-scale eddies and air entrainment restriction of the corner structure above fire source. With regard to longitudinal flame extension of fire flush with sidewall, special large-scale eddies are generated right below the ceiling. When flame extension is short under small HRR, with aid of these large-scale eddies the effect of

air entrainment enhancement is more significant, leading to shorter longitudinal flame extension than the transverse one. With increasing of HRR, the incremental entrained air is insufficient and the confinement effect of the intersecting ceiling and sidewall becomes more dominant, thus the transverse flame extension only restricted by ceiling is longer. Based on the experimental data and dimensional analysis, simple correlations are proposed for total flame extensions in longitudinal and transverse directions, respectively. And the critical dimensionless heat release rate $Q^*_{critical}$ can be calculated at 0.60, under which the longitudinal and transverse flame lengths are equal to each other.

jijie232@ustc.edu.cn.

1G12 MERGING BEHAVIOR OF FACADE FLAMES EJECTED FROM TWO WINDOWS OF AN UNDER-VENTILATED COMPARTMENT FIRE

Kaihua Lu^{1,2}, Longhua Hu¹, Michael Delichatsios², Fei Tang¹, Zengwei Qiu¹, Linghui He¹

¹University of Science and Technology of China, China ²University of Ulster, United Kingdom

This paper investigates the merging behavior of flames ejected from two parallel windows of an under-ventilated compartment fire using a LPG gas burner. A reduced-scale model (about 1:4) of a compartment fire with a facade wall has been constructed where the window dimensions and the separation distance between them varied during the experiments. The flames ejected from the windows were recorded by a CCD camera. The excess heat release of the fuel burning outside the windows was high enough to produce flames controlled by three-dimensional entrainment. Temperatures inside the compartment, the flame merging probability, the distance from neutral plane to flame lowest merging point, and the height of the facade flames before and during merging were measured. The temperature measurements inside the under-ventilated compartment fires do not change with total heat release rate or the window separation distance, thus indicating that the same heat is produced inside the compartments. The flame merging probability and the flame merging point distance are normalized and well correlated using the facade flame height for completely non-merging flames and the separation distance between the windows. Finally, the facade flame height normalized by the facade flame height for completely non-merging flames is well correlated with the ratio of surface of the air entrained between the windows as the separation distance changes divided by the total surface area from all sides available for entrainment. For the present case this ratio is a function of the ratio of the flame merging point distance over the facade flame height for completely non-merging flames which is finally used for the correlation of merging flame heights.

m.delichatsios@ulster.ac.uk

1G13 EXPERIMENTAL STUDY ON BEHAVIOR OF SIDEWALL FIRES AT VARYING HEIGHT IN A CORRIDOR

Jie Ji, Yanyun Fu, Kaiyuan Li, Jinhua Sun, University of Science and Technology of China, China

A set of small-scale experiments on sidewall fires was conducted in a model corridor. The mass loss rate, the ceiling jet flame length and the maximum ceiling temperature were investigated by correlating with the distance of the fire source and ceiling. The results show that as the effective ceiling height decreases, the mass loss rates increase due to the enhanced heat feedbacks from the ceiling and ceiling jet to fuel. The mass loss rates are greater for fuel pans with long edge attaching sidewall compared to those with short edge attaching sidewall, due to the enhanced confinement effect. A simplified equation predicting the mass loss rate per unit area is developed involving the dimensionless effective ceiling height and the length ratio of pan edges attached and perpendicular to the sidewall. Besides, a correlation is established between the dimensionless longitudinal length of ceiling jet flame and the dimensionless heat release rate, with taking into account the effects of heat release rate, effective ceiling height, pan size and layout. The maximum ceiling temperature rise for flame intermittently hitting the ceiling can be expressed using the similar form as McCaffrey's model. A modified correlation for the maximum ceiling temperature by taking into account the effect of pan layout and the aspect ratio of pan edges is proposed.

kyli@ustc.edu.cn

1H01 RELEASE OF CHLORINE FROM THE SLOW PYROLYSIS OF NaCl-LOADED CELLULOSE AT LOW TEMPERATURES

Muhammad Usman Rahim, Xiangpeng Gao, Hongwei Wu, Curtin University, Australia

This study reports the release of Cl from the slow pyrolysis of NaCl-loaded cellulose at 150–400 °C, providing new data to better understand the low-temperature release of Cl during biomass pyrolysis. The results show that the form and amount of the Cl released during the slow pyrolysis of the NaCl-loaded cellulose strongly depends on temperature. At temperatures below 300 °C, Cl is released mainly as HCl(g), while the release of tar-Cl is clearly evidenced at 350 °C or higher. The release of both HCl (g) and total Cl (including gaseous HCl and tar Cl) begins at 200 °C, reaches the corresponding maximum values (~53% for HCl and ~71% for total Cl) at 350 °C, and then levels off with further increasing temperature to 400 °C. The amount of organically bound Cl in solid residues after pyrolysis also increases from ~6% at 150 °C to ~36% at 300 °C, expressed as % of Cl in solid residues. Further increasing temperature to 350–400 °C

leads to the depletion of organically-bound Cl in the solid residues. Our data clearly demonstrate that interactions between Cl and cellulose organic structure are responsible for the release of HCl (g) and tar-Cl during biomass pyrolysis.

h.wu@curtin.edu.au

1H02 RADIATIVE INTENSITY, NO EMISSIONS, AND BURNOUT FOR OXYGEN ENRICHED BIOMASS COMBUSTION

Josh Thornock¹, Daniel Tovar¹, Dale R. Tree¹, Yuan Xue², Remi Tsiava³

¹Brigham Young University, United States ²Air Liquide, United States ³Air Liquide, France

As concern over global climate change continues, the use of biomass as a substitute for coal is one method of reducing CO₂ emissions. One of the primary problems with utilizing biomass in boilers originally designed to burn coal is burnout. Biomass particles cannot be economically ground to the fine particle size typical of coal particles, creating a problem for particle burnout. The impact of oxygen injection in a swirl-stabilized burner on particle burnout and NO emissions was investigated by measuring NO and LOI, as well as flame characteristics, including flame imaging, flame intensity, and flame temperature. The results showed that when a low momentum flow of pure (> 99%) oxygen is introduced into the center of a swirl stabilized biomass flame, an inverted diffusion flame is produced with oxygen in the center and volatiles on the outside of the flame. This high intensity center flame is surrounded by a lower intensity turbulent air/volatiles flame. This high temperature inner flame can heat incoming particles more rapidly than a conventional air flame improving burnout and flame stabilization without increasing effluent NO as long as the center flame does not extend into and disturb the fuel rich recirculation zone. Oxygen injection can therefore be used to improve burnout without increasing NO formation.

treed@byu.edu

1H03 COMBUSTION OF BIOMASS IN JET FLAMES

Roman Weber, Yunus Poyraz, An Marcel Beckmann, Stefan Brinker, Clausthal University of Technology, Germany

Flames of mixed wood, sawdust, fermentation-process residues and grain residues have been fired at 15kW thermal input to determine flame ignition, temperature levels, NO_x emissions, combustibles burnout as well as fly ash slagging propensity. South African Middleburg coal has been combusted under similar conditions. Near the burner, the in-flame temperatures of the coal flame are around 100°C higher than in the biomass flames and the fastest ignition has been observed for the coal flame. Combustibles burnout is good, exceeding 99.2% for all the fuels. For mixed wood and saw dust, around 50-60% of the fuel nitrogen has been converted to NO whilst for the fermentation and grain residues as well as for the coal, the nitrogen conversion rates are in the 14-17% range.

Ash deposition experiments have been carried out in the 950-1200°C temperature range. Around three times more deposit (when normalized to the fuel ash content) is formed for biomass fuels than for the coal. For biomass fuels, a good correlation between deposition rate and particles temperature has been obtained. Sticking efficiency of the impacting particles has been estimated to be 0.01-0.08 at 970°C and 0.36 at 1170°C.

roman.weber@ievb.tu-clausthal.de

1H04 FLUIDIZED BED GASIFICATION OF LIGNITE CHAR WITH CO₂ AND H₂O: A KINETIC STUDY

Fabrizio Scala, Istituto di Ricerche sulla Combustione, Italy

Gasification of a lignite char with either CO₂ or H₂O at atmospheric pressure was studied in a lab-scale fluidized bed apparatus at different bed temperatures (750-900°C) and gas concentrations. CO₂ concentrations in the range 20-100% and H₂O concentrations in the range 10-70% were used in the batch experiments. The carbon conversion rate was measured by following the outlet CO and CO₂ concentrations with time. A predictive kinetic model for both CO₂ and H₂O gasification of the lignite char was developed from the experimental results, that was able to correctly predict the evolution of carbon conversion versus time. Both gasification reactions kinetics followed a Langmuir-Hinshelwood (L-H)-type equation. The activation energy of the CO₂ gasification reaction was larger than that of steam gasification, indicating a larger reactivity of the lignite char towards H₂O in the investigated temperature range, as expected. Interestingly, the structural parameters of the kinetic expressions of the two gasification reactions were the same, suggesting that CO₂ and H₂O are likely to attack the same carbon surface sites on this char.

scala@irc.cnr.it

1H05 MEASUREMENT OF PARTICULATE MATTER AND TRACE ELEMENTS FROM A COAL-FIRED POWER PLANT WITH A NOVEL ELECTROSTATIC PRECIPITATOR

Chao Wang, Xiaowei Liu, Dong Li, Junping Si, Bo Zhao, Minghou Xu, Huazhong University of Science and Technology, China

The particulate matter and trace elements from a 660 MW coal-fired power plant boiler which equipped with a novel electrostatic precipitator were sampled and analyzed. To promote the thermal efficiency of power plant, a low

temperature economizer was installed at the inlet of electrostatic precipitator to collect the heat of flue gas. The low temperature economizer can reduce flue gas temperature, and then affect the operation of electrostatic precipitator. Therefore, this experiment was carried out to investigate the collection characteristics of this novel electrostatic precipitator on particulate matter. What's more, the distribution of trace elements in solid combustion residues was also studied. The results indicated that the low temperature economizer markedly decreased the amount of particulate matter at the outlet of electrostatic precipitator. The collection efficiency of electrostatic precipitator on particulate matter was improved significantly by the low temperature economizer, whereby the collection efficiencies of PM_{2.5} and PM_{1.0} could reach 99.7 % and 99.2 % respectively. Most of trace elements remained in the fly ash collected by the electrostatic precipitator, and less than 10 % remained in the bottom ash, but very rare emitted from the electrostatic precipitator. The low temperature economizer not only reduced the emission of particulate matter, but also diminished the emissions of trace elements in flue gas. The enrichment characteristics of trace elements in submicron particles were also studied.

xwliu@hust.edu.cn

1H06 LES OF SWIRL-STABILISED PULVERISED COAL COMBUSTION IN IFRF FURNACE NO.1

G. Olenik, O.T. Stein, A. Kronenburg, Universität Stuttgart, Germany

Swirl-stabilised turbulent flow and pulverised coal combustion in the semi-industrial (2:5MW) IFRF furnace No. 1 are for the first time simulated by means of large eddy simulation and compared to results from the experimental campaign and RANS predictions by (Weber et al. 1992). The large eddy simulation uses the Euler-Lagrange framework for two-phase flows and relatively simple sub-models for the particle heat-up, devolatilisation, char combustion and radiation governing the pulverised coal combustion process are employed. The simulations yield improved predictions of the velocity statistics, the temperature distribution in the swirl region and result in a favourable agreement of the mean species profiles along the burner centerline compared with the measurements. Furthermore, the transient Euler-Lagrange approach allows for a cross-comparison of the velocity and scalar statistics between the two phases and the comparison of the mean axial velocity and temperature shows the two phases to be near thermal and kinetic equilibrium along the burner axis. Individual particle time histories, which are crucial for the coal combustion sub-processes and overall flame stabilisation, are analysed. It is found that there is a lack of oxygen in the inner swirl region leading to a decreased volatile burning rate, which could however, be related to the simplified EBU turbulence-chemistry interaction model.

o.stein@itv.uni-stuttgart.de

1H07 MAGNETITE LOADED CARBON FINE PARTICLES AS LOW-COST CO₂ ADSORBENT IN A SOUND ASSISTED FLUIDIZED BED

M. Alfe¹, P. Ammendola¹, V. Gargiulo¹, F. Raganati², R. Chirone¹

¹Istituto di Ricerche sulla Combustione - CNR, Italy, ²Università degli Studi Federico II, Italy

CO₂ adsorption with solid sorbents is one of the most promising options for post-combustion CO₂ capture strategies. Typical post-combustion flue-gas conditions are CO₂ 1–15% vol. and atmospheric pressure and the performances of solid sorbents under typical flue gas conditions have been poorly investigated. In that condition the CO₂ uptake capacity is influenced primarily by material functionality effects rather than material pore metrics so materials with a distinctive surface chemistry (presence of activated surface atoms or sites) could find applications in adsorption technologies. The sorbent selection so became a key point because the materials should be convenient from the economic point of view but versatile in post-combustion conditions. Recent studies of CO₂ adsorption on low-cost iron metal oxide surfaces strongly encourage the possible use of metal oxide as sorbents, but the tendency of magnetite particles to agglomerate causes a lowering of CO₂ uptake capacity. The dispersion of magnetite nanoparticles on carbonaceous matrix appears to be a promising strategy to overcome this shortcoming. This work investigates the adsorption behavior of CO₂ on composite materials prepared coating a low-cost commercial Carbon Black (CB) with magnetite fine particles. The CO₂ capture capacity of composites produced at different CB load was evaluated on the basis of the breakthrough times measured at atmospheric pressure and room temperature in a lab-scale fixed bed micro-reactor. A CB-FM composite has been selected to verify the possibility of carrying out a two-stage operation and the thermochemical stability in a sound assisted fluidized bed. To this aim the reactor has been firstly operated for CO₂ adsorption and then for regeneration. The effect of multiple cycles of adsorption and desorption steps has been also quantified.

paola.ammendola@irc.cnr.it

1H08 MODELLING RATES OF GASIFICATION OF A CHAR PARTICLE IN CHEMICAL LOOPING COMBUSTION

Marco A. Saucedo, John S. Dennis, Stuart A. Scott, University of Cambridge, United Kingdom

Rates of gasification of lignite char were compared when gasification with CO₂ was undertaken in a fluidised bed of either (i) an active Fe-based oxygen carrier used for chemical looping or (ii) inert sand. The kinetics of the gasification were found to be significantly faster in the presence of the oxygen carrier, especially at temperatures above 1123 K. An analytical solution assuming pseudo-binary diffusion of species was developed to account for external and internal mass transfer and for the effect of the looping agent. The model also included the effects of the evolution of the pore structure at

different conversions. The results are compared with a full numerical model using the Stefan-Maxwell equations. Excellent agreement was observed between the rates predicted by the two models and those observed experimentally at $T \leq 1123$ K. At 1173 K, the pseudo-binary model predicted slightly higher rates than the full numerical solution. It was found that a significant share of the error of the predicted rates with the analytical solution was caused by an underestimation of intraparticle diffusional resistance rather than by assuming a pseudo-binary system external to the particle. Both models suggested that the presence of Fe_2O_3 led to an increase in the rate of gasification because of the rapid oxidation of CO by the oxygen carrier to CO_2 . This resulted in the removal of CO and maintained a higher mole fraction of CO_2 in the mixture of gas around the particle of char, *i.e.* within the mass transfer boundary layer surrounding the particle. This effect was most prominent at ~20% conversion when (i) the surface area for reaction was a maximum and (ii) because of the accompanying increase in porosity, intraparticle resistance to gas mass transfer within the particle of char had fallen, compared with that in the initial particle.

mas225@cam.ac.uk

1H09 SYNERGETIC EFFECTS OF A MIXTURE OF IRON ORE AND COPPER ORE AS OXYGEN CARRIERS IN CHEMICAL-LOOPING COMBUSTION

Weijin Yang, Haibo Zhao, Kun Wang, Chuguang Zheng, Huazhong University of Science and Technology, China

Iron ore is a cheap and nontoxic Oxygen Carrier (OC) in Chemical Looping Combustion (CLC) system. However, it performs good recyclability while low reactivity in the CLC of solid fuels. Copper ore exhibits very high reactivity and oxygen uncoupling behavior, while suffers from tendency towards sintering and agglomeration during consecutive redox cycles at a higher temperature (e.g., 900~1000 °C). In this work, a mixture of hematite and copper ore was used as oxygen carrier for CLC of syngas and coal. Through the isothermal redox experiments at 950 °C in a thermogravimetric analyzer, it is found that there are synergetic effects between iron ore and copper ore, and copper ore could be more efficiently utilized when the mixing ratio of copper ore is maintained 10-20wt%. As the mixing ratio of copper ore is 20wt%, the reduction reaction of the mixer OC is no longer endothermic, which is beneficial to the controllability of the fuel reactor temperature. The fluidized bed experiments were carried out to verify the reactivity of the mixing ore OCs at the same reaction temperature. It is observed that the mixing ore OC with 20wt% copper ore has a better reactivity with the gasification products (especially H_2) of low-volatile anthracite than the pure hematite, and leads to a higher fuel conversion rate and CO_2 yield. The mixture of iron ore and copper ore is expected to address simultaneously reactivity, recyclability, cost and environmental concerns of OCs.

klinsmannzhhb@163.com

1H10 PREDICTION OF OXY-COAL FLAME STAND-OFF USING HIGH-FIDELITY THERMOCHEMICAL MODELS AND THE ONE-DIMENSIONAL TURBULENCE MODEL

Babak Goshayesi, James C. Sutherland, The University of Utah, United States

An Eulerian One-Dimensional Turbulence (ODT) model is applied to simulate oxy-coal combustion, with specific aim at predicting flame stand-off distances. Detailed gas-phase chemical kinetics based on GRI3.0 are utilized and the gas-phase equations are fully coupled to models in the particle phase. A high-fidelity model for devolatilization is considered that predicts evolution of several light gas species as well as char as products of devolatilization. The mass, momentum and energy governing equations are fully coupled between the particle and the gas phase. Likewise, char oxidation and gasification are both considered. Results indicate that char oxidation and gasification are both significant during the later stages of devolatilization. The impact of wall temperature and mixing rate on oxy-coal flame is simulated and discussed where flame stand-off is used as a metric to compare the simulation prediction with experimental data. The data show evidence that there is kinetic limitation to the flame standoff distance. Finally, results show that ODT can provide quantitative agreement with experimental data in predicting flame standoff in oxy-coal jet flames.

James.Sutherland@utah.edu

TUESDAY PLENARY LECTURE: ADVANCED LASER DIAGNOSTICS FOR AN IMPROVED UNDERSTANDING OF PREMIXED FLAME-WALL INTERACTIONS

A. Dreizler, B. Böhm, Technische Universität Darmstadt, Germany

This review discusses the role of laser diagnostics in combustion science and technology. In its first part, it may guide understanding of advanced diagnostic methods, and is particularly helpful for non-specialized experimentalists. Various challenges for future developments and applications of optical combustion diagnostics are highlighted. In the second part of this review, flame-wall interactions are selected for a more in-depth discussion. Flame-wall interactions are scientifically interesting and are of great importance to any enclosed practical combustion process. Following a description of current understanding, the focus is on using optical diagnostics to probe thermal, fluidic and chemical properties of head-on and sidewall quenching. The review ends with a discussion of issues and implications for future experimental research and specific diagnostic needs.

dreizler@csi.tu-darmstadt.de

2A01 LIFE OF FLAME PARTICLES EMBEDDED IN PREMIXED FLAMES INTERACTING WITH NEAR ISOTROPIC TURBULENCE

Swetaprovo Chaudhuri, Indian Institute of Science, India

Flame particles are surface points that always remain embedded on, by comoving with a given *iso*-scalar surface within a flame. Tracking flame particles allow us to study the fate of propagating surface locations uniquely identified throughout their evolution with time. In this work, using Direct Numerical Simulations we study the finite lifetime of such flame particles residing on *iso*-temperature surfaces of statistically planar H₂-air flames interacting with near-isotropic turbulence. We find that individual flame particles as well as their ensemble, experience progressively increasing tangential straining rate (K_t) and increasing negative curvature (k) near the end of their lifetime to finally get annihilated. By studying two different turbulent flow conditions, flame particle tracking shows that such tendency of local flame surfaces to be strained and cusped towards pinch-off from the main surface is a rather generic feature, independent of initial conditions, locations and ambient turbulence intensity levels. The evolution of the alignments between the flame surface normals and the principal components of the local straining rates are also tracked. We find that the surface normals initially aligned with the most extensive principal strain rate components, rotate near the end of flame particles' lifetime to enable preferential alignment between the surface tangent and the most extensive principal strain rate component. This could explain the persistently increasing tangential strain rate, sharp negative curvature formation and eventual detachment.

schaudhuri@aero.iisc.ernet.in

2A02 ON THE ALIGNMENT OF FLUID-DYNAMIC PRINCIPAL STRAIN-RATES WITH THE 3D FLAMELET-NORMAL IN A PREMIXED TURBULENT V-FLAME

T. Sponfeldner¹, F. Beyrau¹, I. Boxx², Y. Hardalupas¹, W. Meier², A.M.K.P. Taylor¹

¹Imperial College London, United Kingdom ²Deutsches Zentrum für Luft- und Raumfahrt, Germany

Statistics of the alignment of fluid-dynamic principal strain-rates and the local flamelet-normal in a premixed turbulent V-flame (methane-air, $Re_t = 450$, $\phi = 0.8$) were measured experimentally using simultaneous Stereoscopic Particle Image Velocimetry (SPIV) and Planar Laser-Induced Fluorescence of OH (OH-PLIF). The use of a second OH-PLIF sheet, oriented in a crossed-plane imaging configuration enabled conditioning of the statistics with respect to through-plane flame orientation. The statistics show the geometric alignment changes significantly with the distance between the flame and the location where the strain-rate field is evaluated. It was observed that approximately one Taylor microscale upstream of the flame, the fluid-dynamic principal strain-rates show no preferential alignment with the flamelet. With increasing proximity to the flame, the most extensive principal strain-rate is observed to align preferentially perpendicular to the local flamelet-normal. In the immediate vicinity of the flame, where local fluid-dynamics are dominated by dilatation, the principal extensive strain-rate is observed to align preferentially parallel to the local flamelet-normal. The realignment of the principal strain-rates in the immediate vicinity of the flame is clearly the result of local flow acceleration caused by heat-release at the reaction zone. As the most extensive principal strain-rate tends to align preferentially perpendicular to the local flamelet-normal outside the region of heat-release, the data indicate that high scalar gradients observed ahead of the flamelet are produced by the local turbulent flow-field, rather than destroyed by it.

isaac.boxx@dlr.de

2A03 INFLUENCE OF COMBUSTION ON PRINCIPAL STRAIN-RATE TRANSPORT IN TURBULENT PREMIXED FLAMES

A.M. Steinberg¹, B.R. Coriton², J.H. Frank²

¹University of Toronto, Canada ²Sandia National Laboratories, United States

The transport of principal strain-rates (s_i) was experimentally investigated using high-repetition-rate (10 kHz) Tomographic Particle Image Velocimetry (T-PIV) and OH Planar Laser Induced Fluorescence (PLIF) in a $Re_j = 13,000$ turbulent premixed flame. These measurements allowed calculation of the source terms in the s_i transport equation associated with the strain-rate and vorticity fields. Furthermore, the Lagrangian derivatives of s_i could be calculated by tracking fluid elements through space and time using the T-PIV data. These Lagrangian derivatives and the resolved source terms allowed the combined effects of the unresolved source terms to be inferred, namely the pressure Hessian, viscous dissipation, density gradients, and viscosity gradients. Statistics conditioned on the location of Lagrangian fluid elements relative to the flame showed slight reductions in the strain-rate and vorticity source-terms within the flame, indicating that these aspects of the turbulence were attenuated by the flame. Comparing the difference between the inferred source-terms in the vicinity of the flame to the non-reacting flow showed that attenuation of s_i arose due to density and viscosity gradients within the flame. The effects of flame-induced dilatation were small relative to the turbulent strain-rate and no change was found in the relative alignment of vorticity and strain-rate through the flame.

steinberg@utias.utoroto.ca

2A04 SIMULTANEOUS MULTI-SPECIES AND TEMPERATURE VISUALIZATION OF PREMIXED FLAMES IN THE DISTRIBUTED REACTION ZONE REGIME

Bo Zhou, Christian Brackmann, Zhongshan Li, Marcus Aldén, Xue-Song Bai, Lund University, Sweden

Structures of turbulent premixed flames, operating in the thin and distributed reaction zone regimes, were investigated for stoichiometric premixed methane/air jet flames with jet Reynolds number up to 36000 and corresponding Karlovitz number up to 400. Multi-species planar laser-induced fluorescence with high spatial resolution was applied to simultaneously image combinations of CH/OH/CH₂O and HCO/OH/CH₂O. In addition, OH/CH₂O imaging was performed in combination with simultaneous Rayleigh scattering thermometry. The CH and HCO layers showed progressive broadening along the axial distance for flames with Reynolds number above 19000. At Reynolds number 36000, a mean CH layer thickness more than 10 times larger than that under laminar condition was observed, providing a clear experimental evidence of distributed reaction zone flowing to turbulence/flame interaction. Additionally, spatial correlations between species show that OH and CH₂O locate at mutually exclusive regions. In contrast, both CH and HCO can overlap substantially with CH₂O. The regions of strong CH/HCO signals correspond to regions with weak CH₂O signals. Moreover, CH and HCO are shown to be able to penetrate deeper into the OH layer than CH₂O. Regions where CH and HCO appear distributed show a rather homogeneous temperature distribution with reduced maximum temperature compared with non-distributed conditions.

Zhongshan.li@forbrf.lth.se

2A05 TURBULENCE-CHEMISTRY INTERACTION IN LEAN PREMIXED HYDROGEN COMBUSTION

A.J. Aspden¹, M.S. Day², J.B. Bell²

¹Cranfield University, Bedfordshire, United Kingdom ²Lawrence Berkeley National Laboratory, United States

This paper presents three-dimensional direct numerical simulation of lean premixed hydrogen flames at an equivalence ratio of $\ell = 0.4$ over a range of turbulence levels from $Ka = 1$ to 36. The simulations form part of a larger effort to construct a DNS database that can be used by the community for model construction and validation. We have focussed on producing well-resolved simulations with conditions representative of atmospheric laboratory-scale flames. After an overview of phenomenological trends with increasing Karlovitz number, we examine the factors that lead to an observed decorrelation between fuel consumption and heat release in the flame at $Ka = 36$. We show that in this flame the fuel consumption is greatly enhanced in regions of positive curvature, which corresponds to an elevation of the radical pool throughout the entire flame. In particular, we identify three reactions that, driven by high molar concentrations of radicals at low temperatures, are responsible for high levels of heat release away from regions of fuel consumption, thereby accounting for the observed decorrelation between fuel consumption and heat release.

a.j.aspden@cranfield.ac.uk

2A06 STRUCTURE OF A HIGH KARLOVITZ n-C₇H₁₆ PREMIXED TURBULENT FLAME

Bruno Savard, Brock Bobbitt, Guillaume Blanquart, California Institute of Technology, United States

Results from a series of Direct Numerical Simulations (DNS) of a high Karlovitz, slightly lean ($\phi = 0.9$), n-C₇H₁₆/air premixed turbulent flame are presented. The flame is statistically flat and is subjected to an inflow of homogeneous isotropic turbulence. A 35-species and 217-reaction mechanism [Bisetti et al. Combust. Flame 159 (2012) 317-335] is used to represent the chemistry. Two simulations have been performed: one with unity Lewis number to assess the effects of turbulence on chemistry, and the other with non-unity Lewis numbers to analyze how turbulence affects differential diffusion. The Karlovitz numbers are 280 and 220 respectively. The first simulation reveals that the turbulent flame brush is strongly affected by turbulence as enhanced mixing largely thickens the preheat zone. However, the turbulent flame structure (i.e. the correlation between species and temperature) is similar to that of a one-dimensional flat flame, suggesting that turbulence has limited effect on chemistry. In the second simulation, the flame structure is affected by turbulence, as differential diffusion effects are weakened. It is suggested that this result is attributed to the fact that turbulence drives the effective species Lewis numbers towards unity through an increase in effective species and thermal diffusivities. Finally, the reaction zones of both the unity and the non-unity Lewis number turbulent flames remain thin, and are locally broken (only to some extent for the unity Lewis number flame, and more strongly for non-unity).

bsavard@caltech.edu

2A07 / 2A08 TOPICAL REVIEW: THE ROLE OF SEPARATION OF SCALES IN THE DESCRIPTION OF SPRAY COMBUSTION

Antonio Sanchez, Javier Urzay, Amable Liñán, Universidad Carlos III de Madrid, Spain

The present paper deals with the description of the interacting multiscale processes governing spray vaporization and combustion downstream from the near-injector atomization region in liquid-fueled burners. One of the main objectives is to emphasize the progress made in the mathematical description and understanding of reactive spray flows by incorporation of rationally derived simplifications based on the disparity of length and time scales present in the problem.

In particular, we aim to show how the disparity of the scales that correspond –with increasing values of their orders of magnitude– to the droplet size, interdroplet spacing, and width of the spray jets, ensures the validity of their homogenized description. The two-way coupling associated with exchanges of mass, momentum, and energy between the gas and the liquid phases is dominated by the homogenized exchanges with the gas provided collectively by the droplets, and not by the direct interaction between neighboring droplets. The formulation is used as a basis to address nonpremixed spray diffusion flames in the Burke-Schumann limit of infinitely fast chemical reactions, with the conservation equations written in terms of chemistry-free coupling functions that allow for general nonunity Lewis numbers of the fuel vapor. Laminar canonical problems that have been used in the past to shed light on different aspects of spray-combustion phenomena are also discussed, including spherical spray clouds and structures of counterflow spray flames in mixing layers. The presentation ends with a brief account of some open problems and modeling challenges.

asanchez@ing.uc3m.es

2A09 LES OF A METHANOL SPRAY FLAME WITH A STOCHASTIC SUB-GRID MODEL

W.P. Jones, A.J. Marquis, D. Noh, Imperial College London, United Kingdom

This paper describes the Large Eddy Simulation (LES) of a methanol/air turbulent nonpremixed spray flame. An Eulerian stochastic field method is employed for the turbulence-chemistry interaction of the gas phase while a Lagrangian formulation is used for the liquid phase. A reduced reaction mechanism (18 species and 14 reactions) is adopted and stochastic models are used to account for the influence of sub-grid scale (sgs) motions on droplet dispersion and evaporation. Comparisons of the predicted gas phase and droplet statistics with measurements show a good agreement confirming that the droplet dispersion and evaporation models used in this work are adequate. The general features of the spray flame such as the occurrence of external group combustion and its development into separate combusting islands are well captured.

dongwon.noh10@imperial.ac.uk

2A10 INFLUENCE OF SPRAY/COMBUSTION INTERACTIONS ON AUTO-IGNITION OF METHANOL SPRAY FLAMES

Colin Heye¹, Venkat Raman¹, Assaad R. Masri²

¹The University of Texas at Austin, United States ²The University of Sydney, Australia

Auto-ignition of sprays plays a key role in diesel engines, high-altitude relight of aircraft engines, and augmenters. The ignition process occurs exclusively at the small scales and represents the interaction of evaporation, turbulent mixing, and combustion. Here, a Large Eddy Simulation (LES) methodology combined with a Probability Density Function (PDF) approach is used to simulate a series of methanol spray flames. To account for the small-scale interaction between spray droplets and the gas-phase combustion process, a stochastic model is proposed. Detailed chemical kinetics is used along with *In-Situ* Adaptive Tabulation (ISAT) to accelerate the computations. The simulations produce very good agreement with experimental data. From the LES computations, it is postulated that the ignition process happens through two different mechanisms: an entrainment process that traps droplets in high-temperature oxidizer pockets, and a stratified premixed process. It is shown that without the explicit model for the spray/combustion coupling, a more premixed propagation is observed due to the artificial mixing induced by the algorithm. Finally, it is shown that increased subfilter mixing leads to a reduction in peak temperatures, where ignition kernels are dissipated quickly.

cheye@utexas.edu

2A11 CORRELATIONS OF HIGH-PRESSURE LEAN METHANE AND SYNGAS TURBULENT BURNING VELOCITIES: EFFECTS OF TURBULENT REYNOLDS, DAMKÖHLER, AND KARLOVITZ NUMBERS

S.S. Shy¹, C.C. Liu¹, J.Y. Lin¹, L.L. Chen¹, A.N. Lipatnikov², S.I. Yang³

¹National Central University, Taiwan ²Chalmers University of Technology, Sweden ³National Formosa University, Taiwan

This paper investigates correlations of high-pressure turbulent burning velocities (S_T) using our recent S_T measurements of lean methane and syngas spherical flames at constant elevated pressures (p) and constant turbulent Reynolds numbers ($Re_T = u' L_i / \nu$), where u' , L_i , and ν are the r.m.s. turbulent fluctuation velocity, the integral length scale of turbulence, and the kinematic viscosity of reactants, respectively. Such constant constraints are achieved by applying a very large high-pressure, dual-chamber explosion facility that is capable of controlling the product of $u' L_i$ in proportion to the decreasing ν due to the increase of p . We have found that, contrary to popular scenario for S_T enhancement with increasing p at any fixed u' , S_T actually decreases similarly as laminar burning velocities (S_L) with increasing p in minus exponential manners when values of Re_T are kept constant. Moreover, S_T increases noticeably with increasing Re_T varying from 6,700 to 14,200 at any constant p ranging from 0.1 MPa to 1.0 MPa. It is found that a better correlation for the normalization of S_T is a power-law relation of $S_T/u' = a Da^b$, where $Da = (L_i/u') (S_L/\delta_F)$ is the turbulent Damköhler number, $\delta_F \approx \alpha/S_L$ is the laminar flame thickness, and α is the thermal diffusivity of unburned mixture. Thus, the very scattering S_T data for each of lean methane and syngas mixtures can be merged on their S_T/u' vs. Da curves with very small data fluctuations. For lean methane flames with the Lewis number (Le) ≈ 1 , $S_T/u' \approx 0.12 Da^{0.5}$ supporting a distributed reacton

zone model anticipated by Ronney (1995), while for lean syngas flames with $Le \approx 0.76 \ll 1$, $ST/u' \approx 0.52Da^{0.25}$ supporting a theory predicted by Zimont (1979). A simple physical mechanism is proposed in attempt to explain what causes the aforesaid discrepancy on the power-law constants.

sshhy@ncu.edu.tw

2A12 PROPAGATION SPEEDS OF EXPANDING TURBULENT FLAMES OF C₄ TO C₈ *N*-ALKANES AT ELEVATED PRESSURES: EXPERIMENTAL DETERMINATION, FUEL SIMILARITY, AND STRETCH-AFFECTED LOCAL EXTINCTION

Fujia Wu¹, Abhishek Saha¹, Swetaprovo Chaudhuri¹, Chung K. Law^{1,2}

¹Princeton University, United States ²Tsinghua University, China

In this study we experimentally investigated the propagation and the associated propagation speeds of expanding C₄ to C₈ *n*-alkane flames in near-isotropic turbulence, at atmospheric and elevated pressures, using a *constant-pressure*, dual-chamber, fan-stirred vessel. The motivation of the work is to explore whether the previously observed fuel similarity for C₄-C₈ *n*-alkanes for laminar flames also holds for turbulent flames, and to investigate the possible influence of mixture nonequidiffusion on the stretchaffected flame structure especially the occurrence of local extinction. Extensive results show that within the present parametric range of investigation, relevant for the flamelet and thin-reaction zones in the conventional turbulent combustion regime diagram, the turbulent flame speeds of stoichiometric and rich mixtures of these fuels, whose Lewis numbers (Le) are close to or smaller than unity, indeed assume similar values at various pressures, equivalence ratios and turbulence intensities. However, the corresponding lean flames, whose Le is greater than unity, exhibit strong propensity of local extinction, ostensibly caused by local stretch through the $Le > 1$ mixture nonequidiffusion.

fujiauwu@princeton.edu

2A13 ON FLAME-TURBULENCE INTERACTION IN CONSTANT-PRESSURE EXPANDING FLAMES

Swetaprovo Chaudhuri^{1,2}, Abhishek Saha¹, Chung K. Law^{1,3}

¹Princeton University, United States ²Indian Institute of Science, India ³Tsinghua University, China

In this paper we present one of the first high-speed Particle Image Velocimetry measurements to quantify flame-turbulence interaction in centrally-ignited constant-pressure premixed flames expanding in near-isotropic turbulence. Measurements of mean flow velocity and *rms* of fluctuating flow velocity are provided over a range of conditions both in the presence and absence of the flame. The distributions of stretch rate contributions from different terms such as tangential straining, normal straining and curvature are also provided. It is found that the normal straining displays non-Gaussian *pdf* tails whereas the tangential straining shows near Gaussian behavior. We have further tracked the motion of the edge points that reside and co-move with the edge of the flame kernel during its evolution in time, and found that within the measurement conditions, on average the persistence time scales of stretch due to pure curvature exceed that due to tangential straining by at least a factor of two.

asaha@princeton.edu

2B01 DOMINANT CHEMICAL SOURCE AND REACTION MODES IN LEAN H₂/AIR FLAMES

Mohsen Ayoobi, Ingmar Schoegl, Louisiana State University, United States

Chemical Explosive Mode Analysis (CEMA) is used to illustrate how source terms and reactions associated with state variables drive the combustion process across a large database of lean, premixed H₂/air flames with detailed chemistry. Using an eigenanalysis of chemical sources terms, chemical source modes and associated reaction modes are distinguished. A mode motion is defined to indicate whether source terms within the flame structure are promoting or counteracting the dominant chemical source mode. Mode sources are then defined from source terms to further differentiate dominant sources (i.e. species or temperature) that promote or counteract a chemical source mode. Similarly, mode participation distinguishes promoting reactions from counteracting ones. Based on mode sources and mode participation, transition temperatures are introduced to track dominant species and reactions within the flame structure. Concepts are detailed for one reference case ($\phi = 0.99$ and $T_{in} = 302K$), which is then applied to a large database of simulated test cases with distributed inlet temperature (300-800 K) and equivalence ratio (0.1-1). In all cases, transitions are correlated to the adiabatic flame temperature for a simulation. Results show a perfect collapse of temperatures associated with the definition of the flame sheet in the context of CEMA. Furthermore, transitions within the flame structure show trends that clearly illustrate that flames with similar adiabatic temperatures have a comparable chemical structure.

ischoegl@lsu.edu

2B02 CHEMICAL INTERACTIONS BETWEEN 1,2,4-TRIMETHYLBENZENE AND *N*-DECANE IN DOPED COUNTERFLOW GASEOUS DIFFUSION FLAMES

Francesco Carbone, Alessandro Gomez, Yale University, United States

The chemical interaction of the two-components of a jet fuel surrogate, *n*-decane and 1,2,4-Trimethylbenzene (TMB), was studied by adding several hundreds ppm of each chemical to two counteflow diffusion flames, one using

methane and the other ethylene as baseline fuels. The objective was to look into evidence of synergistic effects due to the interaction of these reference fuels, that are representative of alkenes and aromatics that make up the bulk of practical fuels. The dopants were added in the same proportions as the Aachen surrogate of jet fuel. The flames presented two distinct environments: the permanently blue methane flame and the incipiently sooting ethylene flame provide well defined temperature-time histories and chemical environments, with the one based on ethylene being relatively more oxygen-deficient. Profiles of critical pyrolysis products and of some stable soot precursors were determined from GC/MS analysis of gas samples extracted from the flames and compared with results from the OPPDIFF model using a lumped chemical mechanism. The production rate of aromatics in both flames, the overproduction of methane in the ethylene flame and the decrease in the concentration of acetylene in the methane flame, when adding the two components simultaneously, were the principal evidence of some synergistic effects that the model for the most part fails to capture. Most other species reveal no synergy, their concentration being the sum of the contributions of the each component used individually, partly because of the doping approach with the addition of small amounts of the reactants in question.

Francesco.carbone@yale.edu

2B03 EXPERIMENTAL AND KINETIC MODELING INVESTIGATION ON LAMINAR PREMIXED BENZENE FLAMES WITH VARIOUS EQUIVALENCE RATIOS

Jiuzhong Yang, Long Zhao, Wenhao Yuan, Fei Qi, Yuyang Li, *University of Science and Technology of China, China*

Chemical structures of six laminar premixed benzene/oxygen/argon flames with equivalence ratios from 0.75 to 2.0 were investigated at 30 Torr. Dozens of flame species, especially radicals and large aromatics, were qualitatively identified and quantitatively measured using Synchrotron Vacuum UltraViolet PhotoIonization Mass Spectrometry (SVUV-PIMS). A kinetic model was developed from our previous models of aromatic fuels to simulate the decomposition of benzene and formation of large aromatics, and was validated against the measured mole fraction profiles of flame species. Based on the rate of production analysis in the leanest and richest flames, the decomposition processes of benzene and the fate of C₆ and smaller products were discussed in detail. Benzene, phenyl radical and cyclopentadienyl radical are concluded as key precursors of large aromatics, and the inhibited formation of PAHs in rich benzene flames compared with rich alkylbenzene flames mainly derives from the low production of benzyl radical, which consisted with the observed trends of the sooting tendencies of benzene and alkylbenzenes in previous studies.

yuygli@ustc.edu.cn

2B04 EXPERIMENTAL AND KINETIC MODELING STUDY OF LAMINAR COFLOW DIFFUSION METHANE FLAMES DOPED WITH 2-BUTANOL

Hanfeng Jin¹, Wenhao Yuan¹, Yizun Wang¹, Yuyang Li¹, Fei Qi¹, Alberto Cuoci², Alessio Frassoldati², Tiziano Faravelli²
¹University of Science and Technology of China, China ²Politecnico di Milano, Italy

In order to understand the interactions between 2-butanol and hydrocarbon fuels in combustion chemistry, experimental and kinetic modeling investigations were performed to study laminar coflow diffusion methane flames doped with two inlet mole fractions of 2-butanol (1.95% and 3.90%) in this work. Mole fractions of flame species along the flame centerline, particularly unsaturated C₂-C₅ hydrocarbons, C₆-C₁₆ aromatics and some free radicals, were measured using Synchrotron Vacuum UltraViolet PhotoIonization Mass Spectrometry (SVUV-PIMS). A detailed kinetic model was developed to simulate the fuel decomposition and the formation of benzene and PAHs in the investigated flames. The simulated results can reproduce the observed effects of 2-butanol addition. The reaction pathway analysis reveals that resonantly stabilized radicals, such as propargyl, cyclopentadienyl, phenyl, and benzyl radicals, are major precursors of indene and naphthalene. With the increasing inlet mole fraction of 2-butanol, the formation of these resonantly stabilized radicals increase significantly. PAHs with more carbon atoms, including acenaphthylene, phenanthrene, pyrene, and fluoranthene, dominantly derive from indenyl and naphthyl radicals.

fqi@ustc.edu.cn

2B05 FUEL DENSITY EFFECT ON NEAR NOZZLE FLOW FIELD IN SMALL LAMINAR COFLOW DIFFUSION FLAMES

Yuan Xiong, Min Suk Cha, Suk Ho Chung, *King Abdullah University of Science and Technology, Saudi Arabia*

Flow characteristics in small coflow diffusion flames were investigated, focusing particularly on a near nozzle region, and considering the buoyancy force exerted on fuel with densities lighter and heavier than air (methane, ethylene, propane, and *n*-butane). The flow fields were visualized through the trajectories of seed particles. The particle image velocimetry technique was also adopted for quantitative velocity field measurements. The results showed that the buoyancy force exerted on fuel as well as on burnt gas significantly distorted near nozzle flow fields. For fuels with densities heavier than air, recirculation zones were formed very close to the nozzle, emphasizing the importance of the relative density of fuel to air on the flow field. Nozzle heating influenced the near nozzle flow field particularly for lighter fuels (methane and ethylene). Numerical simulations were also conducted, focusing specifically on the effect of specifying inlet boundary conditions for fuel. The results showed that the fuel inlet boundary with fully developed velocity profile should be

specified inside the fuel tube to permit satisfactory prediction of flow field. The calculated temperature fields also indicated the importance of the selection of the location of inlet boundary, especially in testing various combustion models that include soot through small coflow diffusion flames.

min.cha@kaust.edu.sa

2B06 A COMPUTATIONAL AND EXPERIMENTAL STUDY OF COFLOW LAMINAR METHANE/AIR DIFFUSION FLAMES: EFFECTS OF FUEL DILUTION, INLET VELOCITY, AND GRAVITY

S. Cao¹, B. Ma¹, B.A.V. Bennett¹, D. Giassi¹, D.P. Stocker², F. Takahashi², M.B. Long¹, M.D. Smooke¹

¹Yale University, United States ²NASA Glenn Research Center, United States

The influences of fuel dilution, inlet velocity, and gravity on the shape and structure of laminar coflow CH₄-air diffusion flames were investigated computationally and experimentally. A series of nitrogen-diluted flames measured in the Structure and Liftoff in Combustion Experiment (SLICE) on board the International Space Station was assessed numerically under microgravity (μ g) and normal gravity (1 g) conditions with CH₄ mole fraction ranging from 0.4 to 1.0 and average inlet velocity ranging from 23 to 90 cm/s. Computationally, the MC-Smooth vorticity-velocity formulation was employed to describe the reactive gaseous mixture, and soot evolution was modeled by sectional aerosol equations. The governing equations and boundary conditions were discretized on a two-dimensional computational domain by finite differences, and the resulting set of fully coupled, strongly nonlinear equations was solved simultaneously at all points using a damped, modified Newton's method. Experimentally, flame shape and soot temperature were determined by flame emission images recorded by a digital color camera. Very good agreement between computation and measurement was obtained, and the conclusions were as follows. (1) Buoyant and nonbuoyant luminous flame lengths are proportional to the mass flow rate of the fuel mixture; computed and measured nonbuoyant flames are 22% and 28% longer, on average, than their 1 g counterparts; the effect of fuel dilution on flame length is negligible when the length is normalized by the methane flow rate. (2) Buoyancy-induced reduction of the flame radius through radially inward convection near the flame front is demonstrated. (3) Buoyant and nonbuoyant flame structure is mainly controlled by the fuel mass flow rate, where there are minor effects from fuel dilution and inlet velocity.

su.cao@yale.edu

2B07 EXPERIMENTAL INVESTIGATIONS OF THE INFLUENCE OF PRESSURE ON CRITICAL EXTINCTION CONDITIONS OF LAMINAR NONPREMIXED FLAMES BURNING CONDENSED HYDROCARBON FUELS, JET FUELS, AND SURROGATES

R. Gnehmlich, A. Kuo, K. Seshadri, University of California at San Diego, United States

Critical conditions of extinction are measured for high molecular weight hydrocarbon fuels, jet fuels and surrogates at pressures up to 0.4 MPa. The hydrocarbon fuels tested are *n*-heptane, cyclohexane, *n*-octane, *iso*-octane, and *n*-decane. Jet fuels tested include JP-8 and Jet-A. The surrogates tested are the Aachen surrogate, consisting of 80% *n*-decane and 20% 1,3,5-trimethylbenzene by mass, and the 2nd generation POSF 4658 Princeton surrogate consisting of 49.6% *n*-dodecane, 24.3% *iso*-octane, 19.8% *n*-propylbenzene, and 6.3% 1,3,5-trimethylbenzene by mass. The counterflow, condensed-fuel configuration is employed. Air diluted with nitrogen at 298 K is injected onto the surface of a pool of heptane. The mass fraction of oxygen in the oxidizer stream is represented by $Y_{O_2}/2$. A flame is stabilized in the stagnation point boundary layer that is established above the liquid-gas interface. At a selected value of pressure p , and at a selected value of $Y_{O_2}/2$, the flow velocity of the oxidizer stream is increased until extinction takes place. The strain rate at extinction is calculated. The experiment is repeated for a range of pressures. The general ordering of extinction strain rates of hydrocarbon fuels was observed and found to be in general agreement with the predictions of kinetic models and experiments conducted at atmospheric pressure in earlier experiments and computations. An initial linear increase of extinction strain rate with pressure is observed at pressures up to 0.175 MPa, followed by a general flattening of the curves up to 0.35 MPa. At pressures above 0.35 MPa, extinction strain rates of some fuels begin to decrease with increased pressures. These general trends are consistent with results previously measured for *n*-heptane, *n*-hexane, and *n*-decane flames in a similar configuration.

rgnehmlich@ucsd.edu

2B08 STRUCTURE AND EXTINCTION OF WATER-LADEN METHANE/AIR NONPREMIXED FLAMES

R.E. Padilla¹, V. Ricchiutti², S. Karnani¹, D. Dunn Rankin¹, T. Pham³

¹University of California-Irvine, United States ²Politecnico Di Milano, Italy ³California State University of Los Angeles, United States

An experimental and computational study investigates the influence of water vapor addition into the methane stream of a nonpremixed flame using a counterflow configuration. Adding water into the fuel stream simulates combustion systems that naturally contain water, such as in methane hydrates. Experimental results in the literature indicate that methane hydrate flames contain approximately 1 mole of water per mole of methane entering the reaction zone. Similarly, the current experiments show that in the counterflow configuration the fuel stream can contain just over one mole of water per mole of methane before flame extinguishment occurs. The results indicate that water has relatively little effect on peak

temperature, but the location of the peak moves toward the air nozzle with increasing water addition. Computationally, CANTERA, an open source program is used to perform chemical kinetic calculations introducing water vapor into the fuel stream. GRI MECH 3.0 and GRI 2.1 (reduced model) kinetics mechanisms were used to determine the critical conditions of water carrying capacity in flames and flame temperatures at extinction. The results indicate that water promotes fuel side endothermic reactions which are responsible for limiting chain initiating, propagating, and branching reactions, ultimately leading to flame extinguishment.

padilla.re@gmail.com

2B09 EXTINCTION LIMITS AND FLAME STRUCTURES OF 1-BUTANOL AND DIETHYL ETHER NON-PREMIXED FLAMES

Jun Hashimoto, Kimitoshi Tanoue, Norihiro Taide, Yoshito Nouno, Oita University, Japan

Extinction limits measurements on non-premixed flames were carried out by using a counterflow burner, for 1-butanol flames and Diethyl Ether (DEE) flames. Studies were carried out by injecting a fuel stream made up of fuel and nitrogen from one duct and an oxidizer stream made up of oxygen and nitrogen from the other duct. The flame structure was also measured. Concentrations of stable species were measured by removing gas samples from the reaction zone using a quartz microprobe and analyzing them in a gas chromatograph. The temperature profile was measured by using a thermocouple. Numerical calculations were also performed by using detailed chemistry at conditions corresponding to those used in the experiments to validate chemical kinetics. Experimental results showed that DEE flames have almost the same value of the extinction limits as 1-butanol flames, at same stoichiometric mixture fraction, Z_{st} , and equilibrium temperature. Extinction limits of 1-butanol flames increased monotonically with increasing Z_{st} , suggesting that flames become stronger and more difficult to extinguish, monotonically. On the other hand, extinction limits of DEE flames decreased once with increase in Z_{st} at low Z_{st} range. After that, they started to increase. Measured profiles of the temperature and major species showed a similar structure for both fuels. Calculated profiles agreed well with experimental data. By contrast, profiles of minor species showed differences between fuels. Furthermore, calculated results for minor species did not match with experimental results. The reproducibility of chemical kinetic computations and variations in extinction limits for Z_{st} was discussed.

hashimoto-jun@oita-u.ac.jp

2B10 EXTINCTION STUDIES OF NON-PREMIXED *ISO*-CETANE AND DECALIN FLAMES

Bo Li^{1,2}, Yang Zhang², Hai Zhang², Fokion N. Egolfopoulos¹

¹University of Southern California, United States ²Tsinghua University, China

The extinction characteristics of non-premixed *iso*-cetane and decalin flames were investigated in the counterflow configuration at atmospheric pressure and a fuel-carrying stream temperature of 443 K. The flow velocities were measured using particle image velocimetry and the locally determined preflame strain rate was determined at extinction. Two recently developed kinetic models were used to model the data for flames of *iso*-cetane and decalin as well as previously determined data for *n*-tetradecane and *n*-hexadecane flames for comparison reasons. The effect of uncertainty of Lennard-Jones potential parameters on the prediction of extinction limits of non-premixed heavy *n*-alkanes flames was assessed as well. Results revealed that the computed extinction strain rates of non-premixed *iso*-cetane flames are lower than the experimental ones. It was found that due to the higher production of relative stable species, *iso*-cetane is less reactive compared to *n*-hexadecane as expected. The computed extinction strain rates of non-premixed decalin flames were found to over-predict the experimental data. At near-extinction conditions, analysis showed that the kinetics of oxidation of decalin are controlled by reactions involving small hydrocarbon fragments and that fuel related intermediates are consumed upstream of the main reaction zone.

egolfopo@usc.edu

2B11 A FLOW PATTERN THAT SUSTAINS AN EDGE FLAME IN A STRAINING MIXING LAYER WITH FINITE THERMAL EXPANSION

K.-P. Liao, M. Matalon, C. Pantano, University of Illinois at Urbana-Champaign, United States

The role of thermal expansion in diffusion edge flames is investigated numerically in the strained mixing layer configuration. We are able to access both the positive as well as the negative edge flame speed regime when density variation, and therefore full hydrodynamic coupling, is present. The computational approach employs a homotopy method to gradually map the solutions from the computationally simpler constant-density flow to the more challenging variable-density case. Particular attention is paid to the role of boundary conditions and how they, in turn, can induce an undesirable streamwise pressure gradient in the trailing diffusion flame that affects the edge flame speed. A new approach is designed to eliminate this adverse pressure gradient. Previous studies observe that the ratio of the edge flame speed to the premixed stoichiometric laminar flame velocity scales approximately as the square root of the ratio of the cold stream density to the stoichiometric density (which is lower). At least for the small set of parameters investigated here, it is found that the speedup of the normalized edge flame velocity might be superlinear on the density ratio, a fact we attribute to the lack of

pressure gradient behind the edge flame. This result is new and complements previous results, for different boundary conditions, which strongly suggest that the edge flame speed is a strong function of the particular hydrodynamic boundary conditions employed in the simulations.

kliao2@illinois.edu

2B12 TRIBRACHIAL, TETRABRACHIAL AND PENTABRACHIAL STRUCTURES IN DIMETHYL ETHER EDGE-FLAMES AT NTC CONDITIONS

Alex Krisman¹, Evatt R. Hawkes¹, Mohsen Talei¹, Ankit Bhagatwala², Jaqueline H. Chen²

¹The University of New South Wales, Australia ²Sandia National Laboratories, United States

The structure and stabilisation mechanism of partially premixed, laminar, Dimethyl Ether (DME) flames are investigated using two-dimensional Direct Numerical Simulation (DNS). The simulations are performed at a pressure of 40 atmospheres and at oxidiser temperatures above the ignition temperature of 700, 900, 1100, 1300, and 1500 K, while keeping the lift-off length approximately fixed by varying the inlet velocity. DME exhibits two stage ignition below approximately 1100 K and a Negative Temperature Coefficient (NTC) regime from approximately 800 to 1100 K. The DNS results are investigated by considering the thermochemical structure of the flames and by applying a transport budget analysis to key chemical species. The results show a transition from a lifted flame stabilised by propagation to a flame stabilized by autoignition with increasing temperature. At 700 K, the flame has a classical tribrachial structure similar to freely propagating edge flames at non-autoignitive conditions. The intermediate temperature cases reveal a complex transition involving multiple heat release pathways *upstream* of the stabilization point. At 900 K, the flame consists of a main-tribrachial structure and an additional upstream branch due to low temperature chemistry: this is termed a tetrabrachial flame. At 1100 and 1300 K, two upstream branches are observed in addition to the main tribrachial structure, one due to low temperature chemistry and the other due to high temperature chemistry, which initiates autoignition and stabilises the flame: these are termed pentabrachial flames. At 1500 K, the low temperature upstream branch is suppressed, so there is only one upstream branch due to high temperature chemistry which proceeds to autoignition, this flame has a tetrabrachial structure, but one which is different from that observed in the 900 K case.

a.krisman@unsw.edu.au

2B13 STABILIZATION AND STRUCTURE OF *N*-HEPTANE TRIBRACHIAL FLAMES IN AXISYMMETRIC LAMINAR JETS

F. Bisetti, S.M. Sarathy, M. Toma, S.H. Chung, King Abdullah University of Science and Technology, Saudi Arabia

A set of tribrachial flames of *n*-heptane/air is simulated with finite rate chemistry and detailed transport in a realistic laminar jet configuration for which experimental data are available. The flames differ by the temperature of the unburnt mixture and stabilization height, which controls the mixture fraction gradient ahead of the flame front. The simulations reproduce the lift-off heights in the experiments, showing that the flame stabilizes further downstream as the unburnt temperature decreases. For the lowest unburnt temperature, resulting in a weak mixture fraction gradient at the tribrachial point, positive stretch along the rich premixed wing leads to an increase in the rate of chemical reaction in the whole flame. The tribrachial flame burning velocity exceeds that in the unstretched, one-dimensional flame. For the highest temperature, the flame stabilizes closest to the nozzle. Large flame tilt, large mixture fraction gradient, and small radius of curvature lead to a reduction in the heat release rate and the flame propagates slower than its one-dimensional counterpart. The observed behavior is explained with a detailed analysis of the flame geometry, differential diffusion effects, flame stretch, and transport of heat and mass from the burnt gases to the flame front.

fabrizio.bisetti@kaust.edu.sa

2C01 THE ROLE OF PROMPT REACTIONS IN ETHANOL AND METHYLFORMATE LOW-PRESSURE FLAMES

N.J. Labbe, R. Sivaramakrishnan, S.J. Klippenstein, Argonne National Laboratory, United States

Simulations for low-pressure flames of ethanol and methylformate have been performed using a detailed kinetics model. In particular, H and CH₃ + Fuel radical prompt reactions have been characterized theoretically in this work and these are shown to make a pronounced impact in predicting intermediates formation. Theoretical calculations for H + CH₃CHOH and CH₃ + CH₃CHOH predict that at low pressures recombinations are minor processes and prompt reactions (addition-eliminations) dominate the reaction flux. Direct abstraction was also considered in H + CH₃CHOH and theory suggests that abstraction at the CH₃-site forming CH₂CHOH is the only important channel. This is counter-intuitive to an assumption that CH₃CHO would be the dominant abstracted product based on analogies. Low pressure ethanol flame simulations indicate that prompt reactions from H + CH₃CHOH and CH₃ + CH₃CHOH are a major source for C₂H₄ and C₃H₆ respectively. Similar results are observed in simulations of low pressure methylformate flame. Prompt reactions from H + CH₂OCHO and CH₃ + CH₂OCHO have a significant impact on CH₃OH and C₂H₄ predictions respectively. The present results suggest that the prompt reactions of relatively stable fuel radicals with ubiquitous flame radicals such as H, O, OH and CH₃ should be considered in combustion models.

raghu@anl.gov

2C02 A THEORETICAL KINETICS STUDY OF THE REACTIONS OF METHYLBUTANOATE WITH HYDROGEN AND HYDROXYL RADICALS

Lidong Zhang, Qinxue Chen, Peng Zhang, The Hong Kong Polytechnic University, China

The chemical kinetics for the reactions of Methylbutanoate (MB) with hydrogen and hydroxyl radicals were studied theoretically with the *ab initio* transition state theory. In addition to the hydrogen abstraction reactions of MB by the radicals, the potential energy surfaces of MB+H and MB+OH were further investigated to search for additional significant hydrogen addition channels, which are followed by β -scission reactions to produce non-hydrogen and non-water products, respectively. Stationary points on the potential energy surfaces were calculated at the QCISD(T)/CBS//B3LYP/6-311++G(d,p) level. Phenomenological rate coefficients for temperature and pressure-dependent reactions were calculated over broad ranges of temperature (200-2500 K) and pressure (1.3×10^{-3} - 10^2 atm) by solving the time-dependent multiple-well master equation. The theoretical rate coefficients were compared with the available experimental and theoretical data and observed discrepancies were analyzed. The predicted rate coefficients are represented in the forms that may readily be used in combustion modeling of MB.

pengzhang.zhang@polyu.edu.hk

2C03 KINETIC STUDIES OF METHYL ACETATE PYROLYSIS AND OXIDATION IN A FLOW REACTOR AND A LOW-PRESSURE FLAT FLAME USING MOLECULAR-BEAM MASS SPECTROMETRY

Xueliang Yang¹, Daniel Felsmann², Naoki Kurimoto¹, Julia Krüger², Tomoya Wada¹, Ting Tan¹, Emily A. Carter¹, Katharina Kohse-Höinghaus², Yiguang Ju¹

¹Princeton University, United States ²Bielefeld University, Germany

The combustion kinetic of Methyl Acetate (MA) pyrolysis and oxidation was studied experimentally in an atmospheric flow reactor and a low-pressure flat flame using Molecular-Beam Mass Spectrometry (MBMS). Rate constants such as for MA radical decomposition as well as H-abstraction of MA by O, H, OH, CH₃, and HO₂ radicals were computed by high-level *ab initio*-RRKM master equation calculations. A new methyl acetate kinetic model was developed and compared with existing models. Two-dimensional direct numerical simulations were conducted and the results were used to validate the zero-dimensional prediction in a flow reactor. The MA pyrolysis and oxidation results in the flow-reactor experiments showed that MA decomposition to CH₃+CH₃+CO₂ and CH₃OH+CH₂CO is the dominant pathways, which is consistent with the theoretical prediction of the new model. In addition, a two-stage MA oxidation was observed between 800 K and 1050 K, suggesting the possible existence of low-temperature chemistry for MA oxidation. The low-pressure flame experiment at a rich condition suggested that MA has unique reaction pathways to form aldehydes, ketones, and acids. Comparison with previous kinetic models showed that the present model considerably improved the predictability of species-temperature histories in the flow reactor and successfully identifies the main reaction pathway of ketene and acetic acid in a low pressure flame for the first time.

yju@princeton.edu

2C04 KINETICS OF PREMIXED ACETALDEHYDE + AIR FLAMES

Moah Christensen, Mengistu T. Abebe, Elna J.K. Nilsson, Alexander A. Konnov, Lund University, Sweden

Non-stretched laminar burning velocities of acetaldehyde + air mixtures at initial gas mixture temperatures of 298, 318, 338, 348 and 358 K are reported for the first time. The flames were stabilized on a perforated plate burner at 1 atm using the heat flux method at conditions where the net heat loss from the flame to the burner is zero. Uncertainties of the measurements were analyzed and assessed experimentally. The overall accuracy of the burning velocities was estimated to be typically better than ± 1 cm/s. Experimental results were compared with predictions of several kinetic models from the literature. Recent model of Leplat developed for acetaldehyde and ethanol oxidation showed the closest agreement with the measurements. The effects of initial temperature on the adiabatic laminar burning velocities of acetaldehyde were interpreted using the correlation $S_L = S_{L0} (T/T_0)^\alpha$. Particular attention was paid to the variation of the power exponent α with equivalence ratio. The existence of a minimum in α in the slightly rich mixtures is demonstrated experimentally and confirmed computationally. The model of Leplat et al. was further analyzed using sensitivity analysis and it was concluded that the deviation of the modelled results when comparing with experiments is not a result of the fuel specific reactions.

Moah.Christensen@forbrf.lth.se

2C05 HIGH TEMPERATURE MEASUREMENTS FOR THE RATE CONSTANTS OF C₁-C₄ ALDEHYDES WITH OH IN A SHOCK TUBE

Shengkai Wang, David F. Davidson, Ronald K. Hanson, Stanford University, United States

The overall rate constants for the reactions of hydroxyl radicals (OH) with a series of aldehydes, formaldehyde (CH₂O), acetaldehyde (CH₃CHO), propionaldehyde (C₂H₅CHO) and *n*-butyraldehyde (n-C₃H₇CHO), were studied behind reflected shock waves at temperatures of 950 - 1400 K and pressures of 1 - 2 atm. OH radicals were produced by rapid thermal decomposition of Tert-Butyl Hydroperoxide (TBHP), and OH time-histories were monitored by narrow-linewidth

UV laser absorption of the well-characterized $R_1(5)$ line in the OH A-X (0, 0) band near 306.69 nm. The overall rate constants were inferred by fitting simulated OH profiles to the measured OH time histories using detailed mechanisms of Veloo et al. (2013), USC Mech-II (2007) and GRI Mech 3.0. The measured high-temperature aldehydes + OH rate constants can be expressed in Arrhenius form, in units of $\text{cm}^3\text{mol}^{-1}\text{s}^{-1}$ and K, as

$$\begin{aligned}k_{\text{CH}_2\text{O}} &= 1.02 \times 10^7 T^{1.92} \exp(779/T) \pm 13\% \\k_{\text{CH}_3\text{CHO}} &= 4.32 \times 10^6 T^{2.02} \exp(716K/T) \pm 22\% \\k_{\text{C}_2\text{H}_5\text{CHO}} &= 5.94 \times 10^6 T^{1.98} \exp(823K/T) \pm 17\% \\k_{\text{nC}_3\text{H}_7\text{CHO}} &= 5.36 \times 10^6 T^{2.06} \exp(658K/T) \pm 15\%\end{aligned}$$

No pressure dependence was observed in these measurements. The measured rate constant for the formaldehyde + OH reaction is consistent with previous experimental studies from Peeters et al. (1991) and Vasudevan et al. (2004) within $\pm 20\%$. For $\text{C}_2\text{-C}_4$ aldehydes + OH, this study provides the first direct rate constant measurement at high temperatures. More general rate constant expressions covering a much wider temperature range (200 - 1600 K) were also determined by combining current measurements with existing low temperature data in the literature. These wide-range expressions were seen to be in excellent agreement with most existing experimental data.

sk.wang@stanford.edu

2C06 KINETICS OF OXIDATION OF CYCLOHEXANONE IN A JET-STIRRED REACTOR: EXPERIMENTAL AND MODELING

Z. Serinyel^{1,2}, C. Togbé², A. Zaras², G. Dayma^{1,2}, P. Dagaut²

¹Université d'Orléans, France ²CNRS-INSIS, France

The kinetics of oxidation of cyclohexanone (CAS 108-94-1) was studied experimentally in a fused silica Jet Stirred Reactor (JSR) for the first time. The experiments were performed in the temperature range 530–1220 K, at an operating pressure of 10 atm, for equivalence ratios ranging from 0.5 to 4, and with an initial fuel concentration of 1000 ppm ($\phi = 0.5$; 1.0 and 2.0) and 1500 ppm ($\phi = 4.0$). Concentration profiles of reactants, stable intermediates and products were measured at fixed residence time and variable temperature by Gas Chromatography (GC) and Fourier Transform Infrared spectrometry (FTIR) after sonic probe sampling. Cyclic intermediates experimentally observed include, 2-cyclohexen-1-one, cyclopentene, cyclopentadiene and aromatics such as benzene and toluene, the latter in trace amounts only for rich mixtures. The experimental data were used to validate a detailed kinetic reaction mechanism. A reasonable agreement between the present experimental results and the computations was observed. Kinetic analyses (sensitivity and reaction paths) were used to interpret the results.

zeynep.serinyel@cnrs-orleans.fr

2C07 CONSTRAINED REACTION VOLUME SHOCK TUBE STUDY OF *N*-HEPTANE OXIDATION: IGNITION DELAY TIMES AND TIME-HISTORIES OF MULTIPLE SPECIES AND TEMPERATURE

M.F. Campbell, S. Wang, C.S. Goldenstein, R.M. Spearrin, A.M. Tulgestke, L.T. Zaczek, D.F. Davidson, R.K. Hanson
Stanford University, United States

Ignition delay times of normal heptane have been measured at temperatures ranging from 651 to 823 K and at pressures between 6.1 and 7.4 atm at an equivalence ratio of 0.75 in 15% O_2 /5% CO_2 /Ar and in 15% O_2 /Ar mixtures behind reflected shock waves in a shock tube. Time-history measurements of fuel, OH, aldehydes (mostly CH_2O), CO_2 , H_2O , and temperature were also measured under these conditions. These time-histories provide critically needed kinetic targets to test and refine large reaction mechanisms. Measurements were acquired using a novel constrained reaction volume approach, wherein a sliding gate valve confined the reactant mixture to a region near the endwall of the shock tube. A staged driver-gas filling strategy, combined with driver section extensions, driver inserts, and driver gas tailoring, was used to obtain constant-pressure test times of up to 55 milliseconds, allowing observations of the chemistry in the Negative Temperature Coefficient (NTC) region. Experiments with conventional shock tube filling were also performed, showing similar overall Ignition behavior. Comparisons between current data and simulations using the Mehl et al. *n*-heptane mechanism (2011) are provided, revealing that the mechanism generally under-predicts first-stage ignition delay times in the NTC region, and that at low temperatures it over-predicts the extent of fuel decomposition during first stage ignition.

matthew.campbell@stanford.edu

2C08 SHOCK TUBE MEASUREMENTS OF THE RATE CONSTANTS FOR SEVEN LARGE ALKANES + OH

Jihad Badra, Ahmed Elwardany, Aamir Farooq, King Abdullah University of Science and Technology, Saudi Arabia

Reaction rate constants for seven large alkanes + hydroxyl (OH) radicals were measured behind reflected shock waves using OH laser absorption. The alkanes, *n*-hexane, 2-methyl-pentane, 3-methylpentane, 2,2-dimethyl-butane, 2,3-dimethyl-butane, 2-methyl-heptane, and 4-methyl-heptane, were selected to investigate the rates of site-specific H-abstraction by OH at secondary and tertiary carbons. Hydroxyl radicals were monitored using narrow-line-width ring-dye laser absorption of the $R_1(5)$ transition of the OH spectrum near 306.7 nm. The high sensitivity of the diagnostic enabled

the use of low reactant concentrations and pseudo-first-order kinetics. Rate constants were measured at temperatures ranging from 880 K to 1440 K and pressures near 1.5 atm. High-temperature measurements of the rate constants for OH + *n*-hexane and OH + 2,2-dimethyl-butane are in agreement with earlier studies, and the rate constants of the five other alkanes with OH, we believe, are the first direct measurements at combustion temperatures. Using these measurements and the site-specific Habstraction measurements of Sivaramakrishnan and Michael (2009) [1, 2], general expressions for three secondary and two tertiary abstraction rates were determined as follows (the subscripts indicate the number of carbon atoms bonded to the next-nearest-neighbor carbon):

$$\begin{aligned} S_{20} &= 1.58 \times 10^{-11} \exp(-1550 \text{ K}/T) \text{ cm}^2 \text{ molecule}^{-1} \text{ s}^{-1} (887 - 1327 \text{ K}) \\ S_{30} &= 2.37 \times 10^{-11} \exp(-1850 \text{ K}/T) \text{ cm}^2 \text{ molecule}^{-1} \text{ s}^{-1} (887 - 1327 \text{ K}) \\ S_{21} &= 4.5 \times 10^{-12} \exp(-793.7 \text{ K}/T) \text{ cm}^2 \text{ molecule}^{-1} \text{ s}^{-1} (833 - 1440 \text{ K}) \\ T_{100} &= 2.85 \times 10^{-11} \exp(-1138.3 \text{ K}/T) \text{ cm}^2 \text{ molecule}^{-1} \text{ s}^{-1} (878 - 1375 \text{ K}) \\ T_{101} &= 7.16 \times 10^{-12} \exp(-993 \text{ K}/T) \text{ cm}^2 \text{ molecule}^{-1} \text{ s}^{-1} (883 - 1362 \text{ K}) \end{aligned}$$

aamir.farooq@kaust.edu.sa

2C09 INFLUENCE OF THE DOUBLE BOND POSITION ON THE OXIDATION OF DECENE ISOMERS AT HIGH PRESSURES AND TEMPERATURES

Aleksandr Fridlyand¹, S. Scott Goldsborough^{1,2}, Kenneth Brezinsky¹, Shamel S. Merchant³, William H. Green³

¹University of Illinois at Chicago, United States ²Argonne National Laboratory, United States

³Massachusetts Institute of Technology, United States

High pressure, single pulse shock tube oxidation experiments were conducted in order to probe the chemical kinetic effects of the double bond position in long alkenes. All oxidation experiments were carried out with approximately 100 ppm of 1-decene, cis-2-decene, cis-5-decene, and trans-5decene, in argon, at stoichiometric conditions. The experimental conditions covered the pressure range of 40-66 bar and temperature range of 850 – 1500 K, with an average reaction time of 2 ms. Gas chromatographic measurements of the stable intermediates indicated an increased reactivity for the isomers with more centrally located double bonds, and no influence on the results from the cis-trans configuration was observed at these conditions. Significantly different yields in most of the intermediate species measured were observed. Chemical kinetic models were assembled with the aid of the Reaction Mechanism Generator where these are able to adequately predict the major product species of all isomers investigated. Simulation of the experiments indicates significantly different reaction pathways that each decene isomers undergoes, controlled entirely by the position of the double bond. The implication for fuels with such molecular structure being that reactivity as well as pollutant formation characteristics can be significantly different depending on the position of the double bond in very similar molecules.

afridly2@uic.edu

2C10 IGNITION OF ALKANE-RICH FACE GASOLINE FUELS AND THEIR SURROGATE MIXTURES

S. Mani Sarathy¹, Goutham Kukkadapu², Marco Mehl³, Weijing Wang⁴, Tamour Javed¹, Sungwoo Park¹,

M.A. Oehlschlaeger⁴, Aamir Farooq¹, William J. Pitz³, Chih-Jen Sung²

¹King Abdullah University of Science and Technology, Saudi Arabia ²University of Connecticut, United States

³Lawrence Livermore National Laboratory, United States ⁴Rensselaer Polytechnic Institute, United States

Petroleum derived gasoline is the most widely-used transportation fuel for light-duty vehicles. In order to aid in developing chemical kinetic models for gasoline, this study focuses on the ignition propensity of two alkane-rich FACE gasoline test fuels and their corresponding Primary Reference Fuel (PRF) blend utilizing fundamental combustion experiments. Shock tube ignition delay times are measured in two separate facilities at pressures of 10, 20, and 40 bar, temperatures from 715 to 1500 K, and two equivalence ratios. Rapid compression machine ignition delay times are measured for fuel/air mixtures at pressures of 20 and 40 bar, temperatures from 632 to 745 K, and two equivalence ratios. Detailed hydrocarbon analysis is also performed on the FACE gasoline fuels, and the results are used to formulate multicomponent gasoline surrogate mixtures. Furthermore, detailed chemical kinetic modeling results are presented to provide insights into the relevance of utilizing PRF and multicomponent surrogate mixtures to reproduce the ignition behavior of the alkane-rich FACE gasoline fuels. The two FACE gasoline fuels and their corresponding PRF mixture display similar ignition behavior at intermediate and high temperatures, but differences are observed at low temperatures. These trends were mimicked by corresponding surrogate mixture models, except for the amount of heat release in the first stage of a two-stage ignition events, when observed.

mani.sarathy@kaust.edu.sa

2C11 THE OXIDATION OF LARGE ALKYL BENZENES: AN EXPERIMENTAL AND MODELING STUDY

Frédérique Battin-Leclerc, Valérie Warth, Roda Bounaceur, Benoit Husson, Olivier Herbinet, Pierre-Alexandre Glaude

CNRS - Université de Lorraine, France

This paper describes the first development of detailed kinetic models for the alkylbenzenes actually present in diesel fuels. Thanks to a new version of the software EXGAS dedicated to alkylbenzenes, the first detailed models for the oxidation of alkylbenzenes with an alkyl chain containing more than 4 atoms of carbon have been automatically generated.

These models are based on an aromatic reaction base consisting of a recent ethylbenzene detailed kinetic model. They involve a new type of primary reaction, ipso-addition, and new generic rules for the estimation of kinetic parameters involved in primary and secondary mechanisms. The existing experimental data on the oxidation of *n*-propylbenzene and *n*-butylbenzene, as well as new results on the oxidation of *n*-hexylbenzene obtained in a jet-stirred reactor from 500 to 1100 K under 1 bar, have been successfully modeled. Simulations well reproduce the more important low temperature reactivity which is observed for *n*-hexylbenzene compared to *n*-butylbenzene. This new tool has been also used to generate models for alkylbenzenes from *n*-propylbenzene up to *n*-decylbenzene. Simulations using this model show an important enhancement of low-temperature reactivity when the alkyl chain in the compounds increases. Flow rate analyses show that this significant increase is due to an influence of resonance stabilized benzylic radicals obtained from the reactant by H-abstractions on the carbon atom neighboring the ring.

Frederique.Battin-Leclerc@univ-lorraine.fr

2C12 INVESTIGATION ON PRIMARY DECOMPOSITION OF ETHYLCYCLOHEXANE AT ATMOSPHERIC PYROLYSIS

Zhandong Wang, Huiting Bian, Yu Wang, Lidong Zhang, Yuyang Li, Feng Zhang, Fei Qi,
University of Science and Technology of China, China

To get a better understanding of the combustion chemistry of cycloalkanes with long side chain, the pyrolysis of ethylcyclohexane (ECH) was studied in a flow reactor at atmospheric pressure. The pyrolysis species were analyzed by two methods, synchrotron Vacuum Ultraviolet (VUV) photoionization mass spectrometry and gas chromatography. Dozens of species were identified and quantified, including lots of isomers. The emphasis of this study is to investigate the primary decomposition of ECH, including its initial decomposition, isomerization, and further reactions of the cyclic C_8H_{15} radicals formed from the H-abstraction of ECH. The observation of C_8H_{16} alkene indicates the existence of ring-opening isomerization of ECH. The ring-opening isomerization of cyclic C_8H_{15} radicals produces alkenyl radicals, whose further decomposition constitutes the various chain and branched intermediates in ECH pyrolysis. The formation of isoprene and vinylcyclopentane is discussed, which highlights reactions of radical addition on the double bond of alkenyl radicals, such as oct-6-en-1-yl and oct-5-en-1-yl radicals. The theoretical calculation on the reaction pathways of oct-6-en-1-yl and oct-5-en-1-yl radicals also shows the internal H-migration pathways via eight- or nine-membered rings might be competitive to those via five- or six-membered rings. On the other hand, the decomposition of cyclic C_8H_{15} radicals causes the formation of cyclic intermediates, i.e. C_8H_{14} alkenes, methylenecyclohexane and cyclohexene, which are potential aromatic precursors.

zld@ustc.edu.cn

2C13 INFLUENCE OF EXPERIMENTAL OBSERVATIONS ON *N*-PROPYLBENZENE KINETIC PARAMETER ESTIMATES

Sebastian Mosbach, Markus Kraft, University of Cambridge, United Kingdom

We calculate the derivatives of best estimates of kinetic parameters of an *n*-propylbenzene shock tube oxidation model, as determined by a weighted least-squares optimisation, with respect to experimental observations and compare these derivatives to some influence diagnostics based on omission of data points which are widely used in linear regression analysis. The considered data set comprises of 2378 measured concentrations of 37 stable species at various temperatures, pressures, and equivalence ratios. The methods studied are computationally affordable, as they require only a single optimisation and do not require the use of surrogates. We find that the diagnostics offer many insights into how individual observations influence parameter estimates, such as which observations determine which parameters to what extent. Additionally, the significance of non-linearities is investigated. While we observe that they can be of substantial importance to the derivatives, and improve the numerical conditioning of the involved matrix inversion, we find that results obtained from the linear omission-based diagnostics frequently agree, at least qualitatively, with those obtained from the derivatives.

mk306@cam.ac.uk

2D01 NONLINEAR DYNAMICS OF A SELF-EXCITED THERMOACOUSTIC SYSTEM SUBJECTED TO ACOUSTIC FORCING

Saravanan Balusamy, Larry K.B. Li, Zhiyi Han, Matthew P. Juniper, Simone Hochgreb, University of Cambridge, United Kingdom

We experimentally study the nonlinear dynamics of a self-excited thermoacoustic system subjected to acoustic forcing. Our aim is to relate these dynamics to the behavior of universal model oscillators subjected to external forcing. The self-excited system under study consists of a swirl-stabilized turbulent premixed flame (equivalence ratio of 0.8 and thermal power of 13.6 kW) enclosed in a quartz tube with an open-ended exit. We acoustically force this system at different amplitudes and frequencies, and measure its response with pressure transducers and OH* chemiluminescence from the flame. By analyzing the data with the power spectral density and the Poincaré map, we find a range of nonlinear dynamics, including (i) a shifting of the self-excited frequency towards or away from the forcing frequency as the forcing

amplitude increases; (ii) an accompanying transition from periodicity to two-frequency quasiperiodicity; and (iii) an eventual suppression of the self-excited amplitude, indicating synchronization of the self-excited mode with the forced mode. By further analyzing the data with the Hilbert transform, we find evidence of phase trapping, a partially synchronous state characterized by frequency locking without phase locking.

All of these dynamics can be found in universal model oscillators subjected to external forcing. This suggests that such oscillators can be used to accurately represent thermoacoustically self-excited combustors subjected to similar forcing. It also suggests that the analytical solutions to such oscillators can be used to guide the reduction and analysis of experimental or numerical data obtained from real thermoacoustic systems, and to identify effective methods for open-loop control of their dynamics.

l.li@gatescambridge.org

2D02 WALL-TEMPERATURE EFFECTS ON FLAME RESPONSE TO ACOUSTIC OSCILLATIONS

D. Mejia¹, L. Selle^{1,2}, R. Bazile¹, T. Poinso^{1,2}

¹Université de Toulouse, France ²CNRS - IMFT, France

This paper presents an experimental investigation of combustion instabilities for a laminar premixed flame stabilized on a slot burner. For certain operating conditions, the system exhibits an unstable mode locked on the Helmholtz mode of the burner. It is shown that the instability can be controlled and even suppressed by changing solely the temperature of the burner rim. A theoretical model accounting for this parameter in the flame transfer function is devised and the physical mechanisms for the temperature dependence of the flame response are investigated.

laurent.selle@imft.fr

2D03 THERMAL VERSUS ACOUSTIC RESPONSE OF VELOCITY SENSITIVE PREMIXED FLAMES

S. Bomberg, T. Emmert, W. Polifke, Technische Universität München, Germany

Premixed flames respond to velocity perturbations by fluctuations in heat release rate ("thermal response"), which in turn generate acoustic perturbations ("acoustic response"). The latter may subsequently influence the velocity field such that self-excited thermoacoustic instability occurs. The present paper investigates interrelations between the thermal and the acoustic response of premix flames. An analysis of the system dynamics that properly represents the underlying causality of acoustics-flow-flame-acoustics interactions reveals a flame-inherent feedback loop, which is independent of the acoustic environment of the flame, i.e. the acoustic impedances of plenum and combustor. The eigenmodes of this flame-inherent feedback loop coincide with poles of the acoustic scattering matrix of the flame. The corresponding frequencies, where the acoustic response is maximum, are in general quite different from frequencies where the thermal response is strong (excess gain" of the flame transfer function). Even more remarkable, the inherent flame modes may develop thermoacoustic instability independently from the acoustic modes of the combustor. Experimental results from two combustor test rigs with laminar conical as well as turbulent swirl flames are scrutinized. Unstable modes are identified that are strongly related to flame-inherent eigenmodes, but do not necessarily match the acoustic modes of the combustor.

polifke@tum.de

2D04 THE RESPONSE OF STRATIFIED SWIRLING FLAMES TO ACOUSTIC FORCING: PERFORMANCE AND LIMITS TO G-EQUATION MODELS

Zhiyi Han, Simone Hochgreb, University of Cambridge, United Kingdom

The gradient of local equivalence ratio in reacting mixtures significantly affects the flame structure and their corresponding response to acoustic velocity perturbations. We study the effect of acoustic velocity fluctuations on flames created by two co-annular, swirling streams with different equivalence ratios to simulate the effects of pilot-main split. The flames are stabilized both by a bluff body and by swirl. The flame responses were measured via chemiluminescence in the linear perturbation range, as a function of frequency. A linearized version of the G-equation model is employed to describe the flame dynamics, combined with effects of axial and azimuthal velocity perturbations downstream of the swirlers. The model accounts for the phase shift between the main acoustic and swirler vortical perturbations, which propagate at different speeds. The very different flame structures generated by different fuel splits lead to different flame responses. The model is shown to capture many of the features of the premixed flame as well as the flame with fuel enrichment on the outside, but fails in the case of the globally richer and inner enriched flames.

zh253@cam.ac.uk

2D05 LARGE EDDY SIMULATIONS OF MULTIPLE TRANSCRITICAL COAXIAL FLAMES SUBMITTED TO HIGH-FREQUENCY A TRANSVERSE ACOUSTIC MODULATION

L. Hakim^{1,2}, A. Ruiz³, T. Schmitt^{1,2}, M. Boileau^{1,2}, G. Staffelbach³, S. Ducruix^{1,2}, B. Cuenot³, S. Candel^{1,2}

¹CNRS, France ²Ecole Centrale Paris, France ³CERFACS, France

This article describes a numerical investigation that explores the dynamics of multiple cryogenic jet flames interacting with high frequency transverse acoustic modes. This research is motivated by the numerous issues associated with high-frequency instabilities in liquid rocket engines. Large Eddy Simulations are carried out in a complex flow configuration which is turbulent, reactive, transcritical and in the absence or presence of a large amplitude acoustic motion.

The geometry is that of a model scale experimental configuration. Results obtained by exploiting high end computational resources demonstrate the feasibility of such calculations, provide insight in the coupling process, exhibit features which are found in experiments and complement the experimental data. Depending on the acoustic environment (dominated by velocity or pressure oscillations), selective responses of the cryogenic jets and flames can be observed and analyzed. It is found that the flames are more compact when they are made to interact with the transverse acoustic motion and that the dense core length is notably reduced. In the span-wise direction, the flames and dense cores are flattened, a feature which is also found in experiments. The unsteady motion observed experimentally is well retrieved numerically. The simulations highlight the mechanisms that can feed energy in the transverse mode and suggest possible descriptions of the instability driving process. The light methane jet is shaken by the acoustic motion and impacts the dense oxygen stream alternatively on its top and bottom sides. The unsteady heat release rate and the corresponding acoustic Rayleigh term produced by the flames prove to be different according to the flame position regarding the acoustic environment.

layal.hakim@gmail.com

2D06 A REDUCED-ORDER MODEL FOR THE ONSET OF COMBUSTION INSTABILITY: PHYSICAL MECHANISMS FOR INTERMITTENCY AND PRECURSORS

Vineeth Nair, Raman Sujith, Indian Institute of Technology Madras, India

In combustors, the transition from low-amplitude, aperiodic fluctuations termed combustion noise to large-amplitude, periodic oscillations termed combustion instability is presaged by an intermediate regime in flow conditions characterized by bursts of intermittent, high-amplitude, periodic oscillations that appear in a near-random fashion amidst aperiodic fluctuations. In this study, we show that, a reduced-order model from first principles that incorporates the hydrodynamic-acoustic coupling can reproduce these intermittent burst oscillations, and the subsequent flow-acoustic lock-on observed in combustors. The physical mechanism that leads to intermittency in pressure fluctuations is described using the model. The paper concludes by illustrating ideas that use intermittency in the signal as an early warning signal—a precursor—to an impending combustion instability.

v.vineeth.nair@gmail.com

2D07 SENSITIVITY OF LES-BASED FLAME TRANSFER FUNCTIONS FOR TURBULENT SWIRLED FLAMES AND IMPACT ON THE STABILITY OF AZIMUTHAL MODES

M. Bauerheim^{1,2}, G. Staffelbach¹, N.A. Worth³, J.R. Dawson³, L.Y.M. Gicquel¹, T. Poinso⁴

¹CERFACS, France ²Société Nationale d'Etude et de Construction de Moteurs d'Aviation, France

³NTNU, Norway ⁴IMFT Toulouse, France

This paper describes a numerical study of azimuthal unstable modes in the annular combustor of Cambridge. LES is used to compute Flame Transfer Functions (FTF) and a Helmholtz solver to predict the overall stability of the combustor. FTF quantify the interaction between acoustics and the turbulent swirled flames. They must be known with precision because instabilities are very sensitive to subtle changes. The effects of azimuthal confinement (corresponding to the annular combustor equipped with 12 or 18 burners), thermal boundary conditions and fuel type (methane or ethylene) on FTFs are simulated here using LES of a single 20 degree ($N = 18$) or 30 degree ($N = 12$) sector. A double-sector LES is also computed to investigate flame / flame interactions. These LES-based FTFs are then used as inputs for a Helmholtz solver and results show that 1) subgrid-scale LES models lead to marginal effects on FTF while 2) azimuthal confinement, thermal conditions and fuel type strongly affect the flame response to acoustics and therefore control the stability of the azimuthal mode. Computations show that the annular experiment performed with methane should be stable while ethylene should lead to azimuthal unstable modes as observed experimentally.

bauerheim@cerfacs.fr

2D08 THE EFFECT OF BAFFLES ON SELF-EXCITED AZIMUTHAL MODES IN AN ANNULAR COMBUSTOR

Nicholas A. Worth¹, James R. Dawson²

¹University of Cambridge, United Kingdom ²Norwegian University of Science and Technology, Norway

In this paper the effect of inserting baffles on the self-excited azimuthal modes and unsteady heat release rate in an annular combustor are investigated experimentally. Particular attention is given to their effect on the time-varying behaviour of azimuthal modes observed in recent experiments and Large Eddy Simulations (LES) in azimuthally symmetric annular chambers. This time-varying behaviour causes the azimuthal modes to switch back and forth between spinning and standing wave modes. With the addition of a single baffle, the azimuthal symmetry of the chamber was broken leading to a coupling between the Clockwise (CW) and Anticlockwise (ACW) azimuthal acoustic waves. This eliminated the time-varying behaviour and promoted standing wave modes. It was found that 3 or more baffles were required to achieve significant damping of the modes. Since almost perfect standing wave modes occurred with the addition of a single baffle, high-speed chemiluminescence measurements were obtained to characterise the unsteady heat release rate at the pressure node and anti-node. Previous studies have shown that maximum and minimum heat release rate is produced at the anti-nodes and nodes respectively. It was found that peak fluctuations at the anti-nodes result from

axisymmetric fluctuations in heat release rate caused by pressure fluctuations driving axial mass flow fluctuations at the burner inlet. At the pressure nodes, an anti-symmetric transverse structure was observed producing negligible heat release rate via the mechanism of cancellation. This latter result suggests that transverse velocity fluctuations play an important mechanistic role in azimuthal modes.

james.r.dawson@ntnu.no

2D09 A NEW PATTERN OF INSTABILITY OBSERVED IN AN ANNULAR COMBUSTOR: THE SLANTED MODE

J.F. Bourgouin^{1,2}, D. Durox^{1,2}, J.P. Moeck³, T. Schuller^{1,2}, S. Candel^{1,2}

¹CNRS, France ²Ecole Centrale Paris, France ³TU Berlin, Germany

In annular combustion chambers of aero-engines and gas turbines, acoustic coupling may arise from azimuthal modes. Such a coupling raises many scientific issues which are considered in a small number of fundamental experiments. The present investigation focuses on this problem and provides experimental data on a special type of combustion instability in which the thermo-acoustic resonant coupling involves a combination of modes. This produces an unusual pattern of flame responses in which the distribution of heat release rate is slanted. Data are provided in the form of free radical light intensity patterns (interpreted as heat release rate distributions) and microphone signals detected in the plenum and chamber. It is shown that the slanted pattern is the signature of a combination of two modes with coinciding frequencies, the first being a standing azimuthal mode while the second is an axial mode. Measurements of the flame describing function on a single matrix burner at the fundamental frequency are used to explain the observed phase shift and amplitude in the flame responses of the different injectors in the annular combustor.

daniel.durox@ecp.fr

2D10 A THEORETICAL STUDY OF MEAN AZIMUTHAL FLOW AND ASYMMETRY EFFECTS ON THERMO-ACOUSTIC MODES IN ANNULAR COMBUSTORS

M. Bauerheim¹, M. Cazalens², T. Poinsot³

¹CERFACS, France ²Société Nationale d'Etude et de Construction de Moteurs d'Aviation, France

³Institut de Mécanique des Fluides de Toulouse, France

The objective of this paper is to develop an analytical model to capture two symmetry breaking effects controlling the frequency and nature (spinning, standing or mixed) of azimuthal modes appearing in annular chambers: 1) Using two different burner types distributed along the chamber 2) Considering the mean azimuthal flow due to the swirlers or to effusion cooling. The ATACAMAC (Analytical Tool to Analyze and Control Azimuthal Modes in Annular Chambers) methodology is applied using the linearized acoustic equations with a steady and uniform azimuthal mean flow. It provides an analytical implicit dispersion relation which can be solved numerically. A fully analytical resolution is possible when the annular chamber is weakly coupled to the burners. Results show that symmetry breaking, either by mixing burners types or with a mean azimuthal flow, splits the azimuthal modes into two waves with different frequencies and structures. Breaking symmetry promotes standing modes but adding even a low azimuthal mean flow fosters spinning modes so that the azimuthal mean flow must be taken into account to study azimuthal modes.

bauerheim@cerfacs.fr

2D11 OSCILLATING FLAMES IN OPEN TUBES

J. Yang¹, F.M.S. Mossa¹, W.H. Huang¹, Q. Wang², R. Woolley¹, Y. Zhang¹

¹The University of Sheffield, United Kingdom ²Shanghai Jiao Tong University, China

When a flame passes down a tube that is open at both ends a self induced fluctuating pressure/flow field is created which the flame has to traverse. Here fuel rich ($1.1 < \Phi < 1.4$) propane-air flames have been filmed travelling down a 20 mm internal diameter quartz tube. Fluctuations in the flame's progression were observed to increase as the flame propagated down tube, achieving maximum oscillation amplitude of ± 10 mm at 220 Hz that decayed as the flame progressed further towards the end of the tube. The impact of the periodic pressure gradients on the flame shape could be discerned with tongues of unburned reactants pushed into the products as well as the corresponding rapid acceleration of the flame into the unburned mixture. The impact of the pressure fluctuations on flame chemistry was monitored by capturing the CH* and C₂* chemiluminescence using a high speed colour camera. The CH*/C₂* was observed to decrease as the flame was pulled back towards the burned mixture; and increased when the pressure oscillations in the tube pushed the flame forwards. This was consistent throughout the flame progress even when small oscillations in the flame position were measured. This could be a significant feature of flames in this environment.

Rob.Woolley@sheffield.ac.uk

2D12 COUPLING OF FLAME GEOMETRY AND COMBUSTION INSTABILITIES BASED ON KILOHERTZ FORMALDEHYDE PLIF MEASUREMENTS

Patton M. Allison, Yuntao Chen, Matthias Ihme, James F. Driscoll, University of Michigan, United States

Flame geometry was found to play an important role in determining when strong pressure fluctuations associated with a combustion instability occur in a gas turbine model combustor. The goals of this study were to use flame surface area as a more accurate way to quantify the flame shape and the heat release rate, in lieu of chemiluminescence; to

accurately resolve both the spatial structure and the time history of the heat release fluctuations, and to show that kilohertz PLIF diagnostics provide a new way to achieve these goals. The dual-swirl burner, developed at DLR Stuttgart by W. Meier et al., was operated using Dimethyl Ether (DME) to study flame surface area, flame brush, flame length, and heat release rate. To understand the instability, accurate measurements are needed of the correlation between heat release rate fluctuations and pressure fluctuations. Thus heat release rate must be recorded as a function of time and space. However conventional chemiluminescence offers only a line-of-sight measurement. High-speed formaldehyde planar laser-induced fluorescence was applied to study the motion of flame surfaces in response to the pressure oscillations of the instability. The flame surface density and surface area fluctuated at the acoustic frequency and displayed motions correlated with the Precessing Vortex Core (PVC) rotation. In non-resonating flames, the behavior of the formaldehyde structure and marked flame surfaces were dominated by the PVC motion, but the degree of surface area fluctuations was reduced compared to unstable flames. Results show that the frequency of the combustion instability varies with several operational conditions, including gas velocity, equivalence ratio, and convective time delays.

patton.allison@gmail.com

2D13 INVESTIGATION INTO THE CAUSE OF HIGH MULTI-MODE COMBUSTION INSTABILITY OF H₂/CO/CH₄ SYNGAS IN A PARTIALLY-PREMIxed GAS TURBINE MODEL COMBUSTOR

Min Chul Lee^{1,2}, Jisu Yoon¹, Sungpeel Joo¹, Jeongjin Kim¹, Jeongjae Hwang¹, Youngbin Yoon¹

¹Seoul National University, Korea ²KEPCO Research Institute, Korea

In this paper, the fuel composition effects of H₂/CO/CH₄ syngas (0~100% for each component gas) on the self-excited high multi-mode (mainly the 3rd and 4th with their harmonics) Combustion Instability (CI) characteristics have been studied in a partially-premixed swirl-stabilized gas turbine model combustor by investigating phase-resolved high-speed OH* Planar Laser Induced Fluorescence (OH-PLIF) and OH* chemiluminescence at a rate of 12.5 kHz and analyzing the Proper Orthogonal Decomposition (POD), spatiotemporal Rayleigh Index (RI), and time-lag. Phase-synchronized OH-PLIF images suggested critical clues of CI driving mechanisms, including the periodic alternation of flame attachment/detachment and vortex coupling with everlasting flames at the outer recirculation zone due to high hydrogen fuels' high reactivity. These PLIF results also demonstrated that the relatively short mixing length and highly fuel-dependent flame length are the root causes of a high instability-mode and sensible mode-shift. Thus, PLIF images were used to calculate the flame length by obtaining the intensity-weighted centroid for the more precise Time-Lag Analysis (TLA). The spatiotemporal RI results indicated that the fuel composition affects the location and intensity of CI driving/damping, RI frequency, and instability mode and frequency. POD analysis from high-speed OH* images showed that the distinct coherent structures and large roll-up of flames are responsible for generating flame oscillations for each mode. High cross-correlation between the POD modes showed the convection of these coherent structures and axially-alternative swirl-like flame motions. At some particular compositions of H₂/CH₄/CO, high multi-mode CI was observed (e.g., the 3rd, 4th, and 6th modes appear simultaneously) and the original TLA could not be applicable, since the acoustic pressure wave is not simply sinusoidal but largely distorted. Thus, a new time-lag model using skewness time (T_{skew}) was proposed to reflect the distortion from multi-mode CI and the accuracy of this model's accuracy was verified using the experimental data.

ybyoon@snu.ac.kr

2E01 PAH FORMATION AND SOOT MORPHOLOGY IN FLAMES OF C4 FUELS

M. Schenk¹, N. Hansen², H. Vieker¹, A. Beyer¹, A. Götzhäuser¹, K. Kohse-Höinghaus¹

¹Bielefeld University, Germany ²Sandia National Laboratories, United States

In this work, we describe experimental studies on the formation of Polycyclic Aromatic Hydrocarbons (PAH's) in opposed-flow atmospheric-pressure flames of *n*-butane, *i*-butane, *isobutene*, and *i*-butanol and on the morphology of nascent soot particles sampled from premixed atmospheric-pressure flames of the same fuels. To identify the major contributors to the molecular growth mechanism in the opposed-flow flames, we employed flame-sampling molecular-beam mass spectrometry with Electron Ionization (EI) and *in-situ* Gas-Chromatography (GC) with mass spectrometric detection. The EI- and GC-EI mass spectra indicate that several pathways with different building blocks can contribute to molecular growth. Besides the commonly accepted hydrogen-abstraction-C₂H₂-addition steps, we found reactions of the methyl radical to be important steps. This observation is also supported by the complexity of the mass spectra which indicates that at least one of the building blocks is rather small. The importance of phenyl radicals as building blocks seems to be limited. We also used helium-ion microscopy to unravel the influence of the fuel structure on the morphology of nascent soot particles and we found that the observed differences in shape and size of the sampled soot particles are a likely due to a combined effect of temperature, residence time, and chemical nature of the fuel.

nhansen@sandia.gov

2E02 FLAME STRUCTURE OF A LOW-PRESSURE, LAMINAR PREMIXED AND LIGHTLY SOOTING ACETYLENE FLAME AND THE EFFECT OF ETHANOL ADDITION

T. Bierkandt¹, T. Kasper¹, E. Akyildiz¹, A. Lucassen², P. Oßwald³, M. Köhler³, P. Hemberger⁴

¹University of Duisburg-Essen, Germany ²Sandia National Laboratories, United States ³German Aerospace Center - DLR, Germany

⁴Paul Scherrer Institut, Switzerland

The flame structure of a fuel-rich ($\phi = 2.4$), laminar premixed, and lightly sooting acetylene flame at 40 mbar and the influence of ethanol addition on the species pool was investigated. Special emphasis was put on the analysis of important soot precursors like propargyl, benzene, and the polyynes. The mole fractions of more than 50 stable and radical species up to $m/z=170$ are obtained experimentally in the flames by molecular-beam mass spectrometry (MBMS) in combination with Single-Photon Ionization (SPI) by Vacuum Ultraviolet (VUV) radiation from the Advanced Light Source (ALS) in Berkeley, CA, USA. For the neat acetylene flame, successful measurements were performed with a combination of MBMS and imaging photoelectron photoion coincidence spectrometry (iPEPICO) at the VUV beamline at the Swiss Light Source (SLS) in Villigen, Switzerland and add additional species information to the data set. Some interesting isomers (C_3H_2 , C_4H_5 , C_4H_2O) can be clearly identified by comparison of measured Photoionization Efficiency (PIE) curves or Threshold Photoelectron (TPE) spectra with Franck-Condon simulations or literature spectra, respectively. Because of apparatus improvements, the chemical resolution in this study goes beyond prior work and provides a high-quality data set for the development of reaction mechanisms at fuel-rich, low-pressure conditions.

tina.kasper@uni-due.de

2E03 DEHYDROGENATION AND GROWTH OF SOOT IN PREMIXED FLAMES

C. Russo, A. Tregrossi, A. Cialjolo, IRC - CNR, Italy

Dehydrogenation of soot occurring in premixed sooting flames burning methane and ethylene was studied in detail by quantitative FT-IR analysis of the aromatic and aliphatic hydrogen tethered to soot. Soot dehydrogenation and the steep increase of the light absorption coefficient were observed to be particularly evident in the ethylene flame in respect to the methane flame.

The measurement of the hydrogen quality of soot along the flame axis appeared to give useful insights in the dehydrogenation and growth processes occurring during soot formation. The discrimination between aliphatic and aromatic hydrogen showed that the aliphatic hydrogen of ethylene soot, mainly due to methylene groups, is early and preferentially removed from soot. Thus, ethylene soot formation rate reduction after the aliphatic hydrogen consumption could be due to the decrease of radical sites formation and the consequent loss of reactivity toward further carbon addition. Coagulation and thermal annealing of the particles accompanied by a negligible dehydrogenation become the predominant phenomena. In this last phase of soot formation the steep rise of the absorption coefficient is a signature of the increase of interconnected aromatic structures and marks the end of soot formation and growth process. In the methane flame the decrease of aliphatic hydrogen was found to be delayed in respect to the maximum soot formation rate probably because of the lower presence of hydrogen atoms in the soot formation region necessary for radical site activation. The coagulation and internal structural rearrangements of carbon, occurring in the last phase of soot formation, was particularly favored in the ethylene flame causing the steep rise of the absorption coefficient.

carmela.russo@irc.cnr.it

2E04 NOVEL ASPECTS IN THE PYROLYSIS AND OXIDATION OF 2,5-DIMETHYLFURAN

Katiuska Alexandrino, Ángela Millera, Rafael Bilbao, María U. Alzueta, University of Zaragoza, Spain

In order to contribute to the study of the behavior of 2,5-Dimethylfuran (2,5-DMF), a promising biofuel to be used as fuel or additive in automotive applications, an experimental and kinetic modeling study of the pyrolysis and oxidation of 2,5-DMF has been carried out using a well controlled flow reactor installation. The influence of temperature, stoichiometry, 2,5-DMF concentration, and pressure has been analyzed. A detailed chemical kinetic mechanism built from different literature sources was used to describe the pyrolysis and oxidation of 2,5-DMF under the experimental conditions studied. Results attained extend the existing experimental database on 2,5-DMF and, for the first time, its tendency to form soot is analyzed. Additionally, the effect of pressure, which would be of interest for the use of this compound as a part of diesel fuels, has been evaluated.

uxue@unizar.es

2E05 INFLUENCE OF SUBSTITUTED FURANS ON THE FORMATION OF POLYCYCLIC AROMATIC HYDROCARBONS IN FLAMES

Luc Sy Tran¹, Baptiste Sirjean¹, Pierre-Alexandre Glaude¹, Katharina Kohse-Höinghaus², Frédérique Battin-Leclerc¹

¹Université de Lorraine, France ²Bielefeld University, Germany

The structure of low-pressure (40 kPa) rich laminar premixed flames of two potential new biofuels, 2,5-DimethylFuran (DMF) and 2-MethylFuran (MF), has been investigated using gas chromatography after sampling by a

sonic probe. This work follows a study of the same flames made using Electron-Ionization Molecular-Beam Mass Spectrometry (EI-MBMS). Temperature profiles have been measured using a thermocouple with and without the probe and compared with those obtained during EI-MBMS experiments, showing the important influence of the probe geometry. The mole fraction profiles above the burner of numerous products and intermediates (31 for MF, 40 for DMF) have been quantified, including all the isomers which were globalized during EI-MBMS experiments, as well as some heavier aromatic products such as ethylbenzene and styrene. The profiles of these aromatics confirmed their significantly enhanced formation in the case of DMF compared to MF, which was already shown in the previous study. The model of the oxidation of these two substituted furans have been up-dated to include new reactions for the formation of C8 aromatics, as well as reactions proposed in literature for large Polycyclic Aromatic Hydrocarbons (PAH) formation. Simulations shows a significant enhancement effect on the formation of PAH, such as pyrene or phenanthrene: their maximum mole fractions are increased by a factor of more than 400 in the DMF flame compared to that of MF, while it is only a factor 3 in the case of benzene. Simulations show that PAH mole fractions are also slightly larger in the DMF flame than in a flame of a gasoline surrogate containing toluene as an octane improver under the same conditions. However the PAH mole fractions in the DMF flame are significantly lower than in a flame of pure toluene, showing that this biofuel could be an interesting octane improver in replacement of aromatics.

Frederique.Battin-Leclerc@univ-lorraine.fr.

2E06 EXPERIMENTAL AND KINETIC MODELING STUDY OF PREMIXED *O*-XYLENE FLAMES

Long Zhao, Zhanjun Cheng, Lili Ye, Feng Zhang, Lidong Zhang, Fei Qi, Yuyang Li
University of Science and Technology of China, China

Three premixed *o*-xylene/O₂/Ar flames with various equivalence ratios (0.75, 1.00 and 1.79) have been carried out at low pressure (4.0 kPa). Synchrotron Vacuum Ultraviolet Photoionization Mass Spectrometry (SVUV-PIMS) was used for the identification of flame species and the measurement of their mole fractions. A detailed kinetic model consisting of 236 species and 1331 reactions was developed and validated against the measured mole fraction profiles of flame species. According to the rate of production analysis, *o*-xylene mainly decomposes via radical attack reactions, including the H-abstraction and ipso-addition reactions. *o*-Xylyl radical is yielded from the H-abstraction of *o*-xylene, and is a key intermediate leading to the formation of smaller species. In the formation of Polycyclic Aromatic Hydrocarbons (PAHs), the structure of adjacent methyl groups facilitates the formation of bicyclic aromatic species such as indane and 1,4-dihydronaphthalene, and leads to several fuel-specific pathways for the formation of indene and naphthalene in *o*-xylene combustion. Consequently, relatively high concentration levels of PAHs are produced while phenyl and benzyl radicals cannot be sufficiently produced, which explains the comparable sooting tendency of *o*-xylene to those of toluene and ethylbenzene.

yuygli@ustc.edu.cn

2E07 MODULATION OF SOOTING TENDENCY BY MAGNETIC EFFECTS

A. Jocher^{1,2}, H. Pitsch², T. Gomez¹, G. Legros¹
¹Institut Jean le Rond d'Alembert, France ²RWTH Aachen University, Germany

Experimental investigations assess for the first time the influence of the gradient of the square of the magnetic flux density (B^2 gradient) on the soot production into a laminar axisymmetric non-premixed flame. The steady nonsmoking ethylene flame is established into a coflowing mixture, composed of oxygen and nitrogen, over a Santoro type burner. This burner is located in an electromagnet. The flame experiences different magnitudes of upward B^2 gradients, ranging from 0 to 5.9 T²/m, as well as different oxygen contents of the coflow, ranging from 21 % to 50 % in volume. Soot volume fraction is mapped into the flame by the Laser Extinction Measurement technique. Increasing the magnitude of the B^2 gradient allows the modulation of soot production in the flame. This modulation is enhanced by increasing oxygen content, as oxygen exhibits a relatively high paramagnetic susceptibility. Furthermore, the aforementioned modulation is shown to enable the shift among similar soot concentration profiles into the flame, just as the variation of oxygen content can do. Consequently, modulation of the inner flame structure by magnetic effects could contribute to the control of oxyfuel combustion. That clearly represents the original outcome of the present paper.

guillaume.legros@upmc.fr

2E08 AN EXPERIMENTAL AND COMPUTATIONAL STUDY ON SOOT FORMATION IN A COFLOW JET FLAME UNDER MICROGRAVITY AND NORMAL GRAVITY

Bin Ma¹, Su Cao¹, Davide Giassi¹, Dennis P. Stocker², Fumiaki Takahashi², Beth Anne V. Bennett¹, Mitchell D. Smooke¹, Marshall B. Long¹
¹Yale University, United States ²NASA Glenn Research Center, United States

Upon the completion of the Structure and Liftoff in Combustion Experiment (SLICE) in March 2012, a comprehensive and unique set of microgravity coflow diffusion flame data was obtained. This data covers a range of conditions from weak flames near extinction to strong, highly sooting flames, and enabled the study of gravitational effects

on phenomena such as liftoff, blowout and soot formation. The microgravity experiment was carried out in the Microgravity Science Glovebox (MSG) on board the International Space Station (ISS), while the normal gravity experiment was performed at Yale utilizing a copy of the flight hardware. Computational simulations of microgravity and normal gravity flames were also carried out to facilitate understanding of the experimental observations. This paper focuses on the different sooting behaviors of CH₄ coflow jet flames in microgravity and normal gravity. The unique set of data serves as an excellent test case for developing more accurate computational models. Experimentally, the flame shape and size, lift-off height, and soot temperature were determined from line-of-sight flame emission images taken with a color digital camera. Soot volume fraction was determined by performing an absolute light calibration using the incandescence from a flame-heated thermocouple. Computationally, the MC-Smooth vorticity-velocity formulation was employed to describe the chemically reacting flow, and the soot evolution was modeled by the sectional aerosol equations. The governing equations and boundary conditions were discretized on an axisymmetric computational domain by finite differences, and the resulting system of fully coupled, highly nonlinear equations was solved by a damped, modified Newton's method. The microgravity sooting flames were found to have lower soot temperatures and higher volume fraction than their normal gravity counterparts. The soot distribution tends to shift from the centerline of the flame to the wings from normal gravity to microgravity.

bin.ma@yale.edu

2E09 CHALLENGES AND ARTIFACTS OF PROBING HIGH-PRESSURE COUNTERFLOW LAMINAR DIFFUSION FLAMES

Lorenzo Figura, Francesco Carbone, Alessandro Gomez, Yale University, United States

An experimental study was conducted on two C₂H₄/O₂/N₂ laminar diffusion flames with identical compositions and strain rate, but operated at 0.292 MPa and 2.5 MPa, respectively, to assess pressure effects on the onset of soot formation. The low-pressure flame was permanently blue, whereas the highpressure one was under conditions of incipient sooting. Both flames had nominally identical temperature-time history. Using gas sampling through quartz microprobes followed by GC/MS analysis and addressing potential artifacts associated with the diagnostic intrusiveness and probe-induced chemistry, we demonstrated that the flame structure was resolved even at the highest pressures, as shown by the good agreement with respect to major species between the experimental results and a onedimensional computational model of the flame with detailed chemistry and transport. The increase in soot propensity correlates with an increase in the concentration of soot precursors like the aromatics and acetylene. Comparison with model predictions shows that the concentration of aromatics is systematically overpredicted. An ancillary computational study to estimate the sensitivity to changes in the velocity boundary conditions showed that minor species like the aromatics may be sensitive to these details under certain conditions, because of changes in the temperature-time history that affects predominantly the slow chemistry.

alessandro.gomez@yale.edu

2E10 NUMERICAL STUDY OF THE EFFECTS OF PRESSURE ON SOOT FORMATION IN LAMINAR COFLOW *N*-HEPTANE/AIR DIFFUSION FLAMES BETWEEN 1 TO 10 ATM

Jean-Louis Consalvi¹, Fengshan Liu²

¹Aix-Marseille Université, France ²National Research Council of Canada, Canada

Laminar nitrogen-diluted *n*-heptane diffusion flames burning in coflow air were numerically simulated at pressures from 1 to 10 atm. Numerical simulations were performed by using a detailed reaction mechanism containing 175 species and 1086 reactions and a sectional soot model. The soot model consists of inception as a result of the collision of two pyrene molecules, heterogeneous surface growth and oxidation following the hydrogen abstraction acetylene addition (HACA) mechanism, soot particle coagulation and PAH surface condensation. Comparisons with available experimental data indicate that the numerical model reproduces successfully the influence of pressure on the flame structure and soot production. All the soot formation processes are enhanced with increasing pressure and HACA dominates the soot mass growth over the pressure range considered. PAH condensation is the most sensitive process to pressure whereas the inception and HACA processes exhibit similar pressure dependency. These trends are directly related to the pressure dependence of the molar concentrations of the species involved in soot formation. The increase in the molar concentrations of benzene and pyrene with pressure results from both physical and chemical effects. Propargyl recombination and interconversion of phenyl to benzene dominate the formation of benzene low in the flame over the pressure range considered, though the contributions of the addition of acetylene to *n*-butadienyl radical increases significantly with pressure in the flame centerline region.

Fengshan.liu@nrc-cnrc.gc.ca

2E11 A STUDY OF THE EFFECTS OF THE ESTER MOIETY ON SOOT FORMATION AND SPECIES CONCENTRATIONS IN A LAMINAR COFLOW DIFFUSION FLAME OF A SURROGATE FOR B100 BIODIESEL

Mohammadreza Kholghy, Jason Weingarten, Murray John Thomson, University of Toronto, Canada

To better understand the effect of ester functional group on soot formation and further expand the applicability of detailed soot models to more complex fuels, a numerical and experimental study is performed to investigate soot formation

for a Biodiesel B100 surrogate in an atmospheric laminar coflow diffusion flame. The surrogate is a mixture of 50% *n*-decane and 50% methyl octanoate. The combustion chemistry and soot formation are solved using a detailed chemical kinetic mechanism with 288 species and 2073 reactions and a detailed sectional soot model. The mechanism is obtained by combining the detailed fuel oxidation mechanism with a subsection of a C1-C2 fuel oxidation mechanism with an enhanced PAH formation scheme to predict PAH formation/growth up to benzopyrene. Soot volume fraction and temperature profiles are compared to experimentally measured values. In addition, the effect of ester functional group on soot formation is studied by numerically comparing the biodiesel flame with a pure *n*-decane flame. The model could successfully predict the temperature profiles in the biodiesel flame. The maximum value of soot volume fraction is also reproduced with a factor of two in the flame. However the model needs further improvements to predict the correct profiles for soot volume fraction for the entire flame. The biodiesel flame has significantly less soot concentrations than *n*-decane. This is despite the fact that the concentration of soot precursors and soot oxidation rates are higher in the *n*-decane flame. It is concluded that the reduced soot concentrations in the biodiesel flame are not caused by direct oxidation of soot particles with oxygen atoms from the ester functional group.

murray.thomson@utoronto.ca

2E12 A COMPARATIVE STUDY OF THE PHYSICAL PROPERTIES OF IN-CYLINDER SOOT GENERATED FROM THE COMBUSTION OF *N*-HEPTANE AND TOLUENE/*N*-HEPTANE IN A DIESEL ENGINE

Jiangjun Wei, Chonglin Song, Gang Lv, Jinou Song, Lin Wang, Huating Pang, Tianjin University, China

In this study, we examined the similarities and dissimilarities in the physical properties of the in-cylinder soot obtained during combustion of *n*-heptane and a toluene/*n*-heptane mixture (TRF20, 20% toluene by volume) in a heavy-duty diesel engine. A total cylinder sampling system was used to sample the in-cylinder soot during different combustion phases, and the morphology, size, fractal dimension and nanostructure of the soot particles were examined by high-resolution transmission electron microscopy and Raman scattering spectrometry. The oxidation reactivity of soot particles was also evaluated in terms of apparent activation energy using thermogravimetric analysis. The results showed that throughout the combustion process, soot aggregates from the combustion of TRF20 generally exhibited more primary particles and larger-sized clusters as compared with the *n*-heptane soot aggregates. Despite the different fuel formulations, both *n*-heptane and TRF20 showed similar trends during the combustion process in terms of changes in fractal dimension of soot aggregates, mean primary particle size and nanostructure (characterized by fringe length, separation distance and tortuosity). The presence of toluene, however, led to a decrease in the fractal dimensions of the aggregates and a concurrent increase in the mean size of primary particles. Moreover, in the same combustion stages, the mean fringe length for the TRF20 soot was smaller than that for the *n*-heptane soot, while the mean separation distance and tortuosity for the TRF20 soot were both larger than those for the *n*-heptane soot. Relative to the *n*-heptane soot, the TRF20 soot had less graphitic organization and lower resistance to oxidation.

songchonglin@tju.edu.cn

2E13 EFFECT OF A HOMOGENEOUS COMBUSTION CATALYST ON THE NANOSTRUCTURE AND OXIDATIVE PROPERTIES OF SOOT FROM BIODIESEL COMBUSTION IN A COMPRESSION IGNITION ENGINE

Yu Ma, Mingming Zhu, Zhezi Zhang, Dongke Zhang, The University of Western Australia, Australia

The effect of a ferrous picrate based homogeneous combustion catalyst on the properties of soot from the combustion of a biodiesel in a compression ignition engine was systematically studied. Soot samples from the combustion of a Reference petroleum Diesel (RD) and the Biodiesel (BD), with and without the catalyst treatment, were collected when the engine was maintained under a constant condition of 2800rpm speed and 5.5Nm load, and subsequently analysed using Transmission Electron Microscopy (TEM) for their nanostructures and Thermogravimetric Analyser (TGA) for the oxidative reactivity. The results showed that compared to the soot from BD, the sizes of both primary soot and aggregates from the catalyst treated biodiesel were consistently smaller; while the nanostructure and fractal dimension remained similar, indicating that there were no dramatic changes in the mechanisms of the soot nucleation and agglomeration. Furthermore, soot from the catalyst treated biodiesel possessed higher oxidative reactivity as indicated by the lower ignition temperature and faster oxidation rate than those of soot from BD. In addition, the primary soot and aggregates from BD were smaller and the soot had a higher order in its nanostructure with greater oxidative reactivity, in comparison to those from RD. A mechanism of the working of the catalyst was proposed in that the catalyst promotes the biodiesel combustion process leaving fewer soot precursors and also accelerates the oxidation of soot particles, resulting in smaller sizes of the primary soot and soot aggregates and the reduced overall soot emissions.

dongke.zhang@uwa.edu.au

2F01 COMPREHENSIVE NUMERICAL MODELING OF IGNITION OF COAL DUST LAYERS IN DIFFERENT CONFIGURATIONS

Akhilesh Kumar Sahu¹, Kulbhushan A. Joshi², Vasudevan Raghavan¹, Ali S. Rangwala²

¹Indian Institute of Technology Madras, India ²Worcester Polytechnic Institute, United States

Ignition of coal dusts deposited over sufficiently hot surfaces represents a common industrial hazard. If these surfaces are above a minimum threshold temperature, then the heat transfer from them and the associated chemical heat release can cause spontaneous ignition. This ignition front can be an ignition site for nearby combustibles as well, which depends on the location of ignition and the corresponding surface temperature attained by the coal dust. A comprehensive numerical study of ignition process of coal dust layers in different configurations, by solving the coupled Navier-Stokes and energy equations, provides a clear insight of the thermal field in the coal layer as well as the flow field over the coal surface. Such study will also provide quantitative information about the convective heat transfer coefficient, which varies for different cases. In this study, ignition phenomena of coal dusts deposited over a flat plate, wedges of different angles and a 3D corner, have been analyzed using a comprehensive numerical model. The governing equations are solved using Ansys FLUENT and user defined functions. The model has been validated using experimental results and is used to study the effect of wedge angles and the direction of gravity vector on the ignition process.

raghavan@iitm.ac.in

2F02 INTERPRETING COAL CONVERSION UNDER ELEVATED H₂ PRESSURES WITH FLASHCHAIN[®] AND CBK

Stephen Niksa, Niksa Energy Associates LLC, United States

Rapid devolatilization at heating rates faster than 10³°C/s does not provide enough time for appreciable bridge hydrogenation so tar yields are not appreciably enhanced under the H₂ pressures associated with entrained coal gasification technology. Conversely, tar yields under slow heating conditions are strongly enhanced. The mechanisms proposed for bridge hydrogenation and its associated impact on fragment recombination in FLASHCHAIN[®] depict these tendencies within the measurement uncertainties for H₂ pressures to 15 MPa. Whereas tar yields from rapid devolatilization diminish for progressively higher pressures, total weight loss passes through a minimum at some H₂ pressure around 1 MPa, because char hydrogasification counteracts the lower weight loss associated with lower tar yields. A single, nth-order methanation reaction within the CBK framework gave results within the measurement uncertainties through 15 MPa H₂, and accurately interpreted a database representing 32 coals of rank from lignite to anthracite; pressures to 21 MPa; heating rates from 1 to 10³°C/s; temperatures from 550 to 1100°C; reaction times to 180 s; and particle diameters to 1 mm. The assigned hydrogasification reactivities are far less variable than those for conventional char gasification, and show no consistent trend with rank.

neasteve@gmail.com

2F03 DYNAMIC BEHAVIOR OF SODIUM RELEASE FROM PULVERIZED COAL COMBUSTION BY PHASE-SELECTIVE LASER-INDUCED BREAKDOWN SPECTROSCOPY

Ye Yuan, Shuiqing Li, Qiang Yao, Tsinghua University, China

In this paper, we examine the *dynamic* behavior of sodium (Na) release during the pulverized coal combustion of Zhundong lignite using a laminar, Hencken flat-flame burner technique. By subtly utilizing the gap between the excitation energies of the gas and particle phases, a new low-intensity Laser-Induced Breakdown Spectroscopy (LIBS) is developed to distinguish the sodium existences in the particle or gas phases along the combustion process. Within the coal flame domain, the Na atomic spectra in the particle phase are clearly detected that consistently agree with NIST database. For the first time, the *in situ* verification of the Na releases accompanying with coal devolatilization is fulfilled when the ambience temperature is high enough. The residence time, indicating Na release from particle to gas phases, is determined from the signal. By using a theoretical analysis, the Na release time approximately coincides with the characteristic pyrolysis time of lignite, further approving the observation above. The effects of ambience temperature, coal rank and oxygen concentration are further discussed. This work may initiate the possibility for exploring the formation of fine particulate during the coal combustion.

lishuiqing@mail. tsinghua.edu.cn

2F04 DIRECT SYNTHESIS OF SUPPORTED PALLADIUM CATALYSTS FOR METHANE COMBUSTION BY STAGNATION SWIRL FLAME

Yichen Zong, Shuiqing Li, Fang Niu, Qiang Yao, Tsinghua University, China

The titania supported palladium nano catalysts (Pd@TiO₂) are synthesized in one-step using a premixed Stagnation Swirl Flame (SSF) with ultra-fine spray system. This novel SSF method, with features of short residence time and fast quenching, produces nanosized (< 2.5 nm) palladium particles being well dispersed on the 7-8 nm TiO₂ particle surface, with an overall specific surface area of 210-220 m²/g. The X-ray photoelectron spectroscopy (XPS) results indicate that the collected palladium particles are a mixture of both Pd and PdO, whereas the TiO₂ support is mainly in anatase

phase by X-Ray Diffraction (XRD). A revised Population Balance Model (PBM) by incorporating coagulation, sintering and scavenging of the binary system (Pd and TiO₂) is developed to explain the *in-situ* doping mechanism of Pd@TiO₂ composites in the flame domain. Then, we use the synthesized nano catalyst to conduct the catalytic combustion of methane under 5-15% Pd loadings. It exhibits more excellent activity than those in the literature under identical temperatures. The T₂₀, as 20% methane conversion temperature, can reduce to as low as 293 °C at 15% Pd loading. It is because that the Pd@TiO₂ catalysts made from the stagnation flame show a good dispersion of size-controlled palladium on TiO₂ which may not be accessible by wet-chemistry and even other flame synthesis routes.

lishuiqing@mail.tsinghua.edu.cn

2F05 HETERO-/HOMOGENEOUS COMBUSTION OF SYNGAS MIXTURES OVER PLATINUM AT FUEL-RICH STOICHIOMETRIES AND PRESSURES UP TO 14 BAR

Marco Schultze, John Mantzaras, Felix Grygier, Rolf Bombach, Paul Scherrer Institute, Switzerland

The catalytic and gas-phase combustion of H₂/CO/O₂/N₂ mixtures was investigated in a platinum-coated channel-flow reactor at fuel-rich equivalence ratios 2 to 7, H₂:CO volumetric ratios 1:2 to 5:1, pressures 1 to 14 bar, and wall temperatures 750 to 1250 K. In situ, 1-D Raman measurements of major gas-phase species concentrations over the catalyst boundary layer assessed the catalytic processes. Gas-phase combustion was monitored by planar Laser-Induced Fluorescence (LIF) of the OH radical at pressures $p \leq 5$ bar and of hot O₂ at $p > 5$ bar, wherein OH-LIF was not applicable due to strong quenching. Simulations were performed with an elliptic 2-D model that included detailed heterogeneous and homogeneous chemical reaction mechanisms. The capacity of O₂-LIF to assess the flame front positions at elevated pressures and rich stoichiometries has been demonstrated. The employed reaction schemes reproduced the measured H₂, CO and O₂ catalytic conversions as well as the flame positions and shapes over the entire investigated parameter range. Even though the catalytic conversion of the limiting O₂ reactant was nearly transport-limited, the competition between H₂ and CO for O₂ consumption allowed for evaluation of the catalytic kinetics. Under rich stoichiometries, the oxidation of CO(s) via the HCOO(s) reaction pathway was significant. The sensitivity of gaseous combustion on catalytic reactions was strong, exemplifying the need of accurate surface chemistry description in modeling syngas hetero-/homogeneous combustion. In particular, adsorption of the H radical considerably inhibited gaseous combustion, especially at the lowest H₂:CO ratios. For a given stoichiometry, the sensitivity of homogeneous ignition on the inlet concentration of CO was modest, as the preferential catalytic oxidation of CO increased the H₂:CO ratio over the gaseous induction zone.

ioannis.mantzaras@psi.ch

2F06 CHARACTERIZATION OF THE NO-SOOT COMBUSTION PROCESS OVER THE La_{0.8}Ce_{0.2}Mn_{0.7}Bi_{0.3}O₃ CATALYST

Feng Bin^{1,2}, Chonglin Song¹, Gang Lv¹, Xiaodong Li¹, Xiaofeng Cao¹, Jinou Song¹, Shaohua Wu¹

¹Tianjin University, China ²Chinese Academy of Science, China

The combustion of diesel soot in NO+O₂/He atmospheres was investigated by temperature-programmed oxidation (TPO), X-ray Photoelectron Spectroscopy (XPS), and in-situ Diffuse Reflectance Fourier Transform (DRIFT) technology, with the aim to demonstrate the participation of nitric oxide species and surface carbon-oxygenated complexes in the process. According to the TPO results, two main adsorption periods for nitric oxide species were observed: one was from 50 to about 180 °C and the other occurred in the temperature range of 180–400 °C. The DRIFT results indicated that the first adsorption period was mainly associated with weakly adsorbed NO, bidentate nitrite and unidentate nitrate, monodentate nitrate, chelating nitrate and bridging nitrate, while the second uptake was related to nitrite and free nitrate species. Based on the XPS and DRIFT results, possible reaction processes for the NO_x-soot combustion are proposed based on the Langmuir–Hinshelwood mechanism. First, the carbon-oxygenated groups, including carboxyls, lactones, and anhydrides were formed at free carbon sites by the oxidation 1 of dissociative nitrates. Such moieties were so stable that they could not be further oxidized, even at 400 °C, without the presence of a catalyst. Second, the adsorption of NO+O₂ resulted in the formation of nitrates on the MnO_x surface of the catalyst. Then, the surface-activated nitrates, with activity decreasing in the order: chelating nitrates > bridging nitrates > monodentate nitrates > free ionic nitrates, further oxidized these carbon-oxygenated complexes with subsequent release of CO₂, NO, and N₂.

songchonglin@tju.edu.cn

2F07 DOPING MECHANISM OF VANADIA/TITANIA NANOPARTICLES IN FLAME SYNTHESIS BY A NOVEL OPTICAL SPECTROSCOPY TECHNIQUE

Yihua Ren¹, Yiyang Zhang¹, Shuiqing Li¹, Chung K Law^{1,2}

¹Tsinghua University, China ²Princeton University, United States

Flame synthesis of V-doping TiO₂ is studied by in-situ diagnostic of phase selective Laser-Induced Breakdown Spectroscopy (LIBS). We apply this novel optical spectroscopy to tracing the gas-to-particle phase transition of V and Ti species, as low-intensity laser only excites V and Ti present in the particle phase but not in the gas phase. Both V and Ti atomic signals appear early at the burner exit and plateau downstream after a distance about 14 mm. Compared with signals

in pure Ti synthesis, the signal of Ti in the doping synthesis is significantly strengthened due to the lower band gap of V-doped TiO₂. The doping mechanism is then inferred from the observations. It is deduced that the substantial collision and mixing of the nucleated V and Ti oxides occur even at burner rim and persist through the entire process. The signal intensities of both V and Ti increase with laser power and tend to the saturation value at about 20 mJ/pulse. In the saturation region, the ratio of V and Ti signal intensities is almost proportional to the doping ratio of V and Ti in the particle phase, showing feasibility of utilizing the optical method to measure the doping ratio.

zhangyiyang@tsinghua.edu.cn

2F08 CURVED WALL-JET BURNER FOR SYNTHESIZING TITANIA AND SILICA NANOPARTICLES

Mohamed A. Ismail, Nasir K. Memon, Morkous S. Mansour, Dalaver H. Anjum, Suk Ho Chung
King Abdullah University of Science and Technology, Saudi Arabia

A novel Curved Wall-Jet (CWJ) burner was designed for flame synthesis, by injecting precursors through a center tube and by supplying fuel/air mixtures as an annular-inward jet for rapid mixing of the precursors in the reaction zone. Titanium dioxide (TiO₂) and Silicon Dioxide (SiO₂) nanoparticles were produced in ethylene (C₂H₄)/air premixed flames using Titanium TetraIsoPropoxide (TTIP) and HexaMethylDiSilOxane (HMDSO) as the precursors, respectively. Particle image velocimetry measurements confirmed that the precursors can be injected into the flames without appreciably affecting flow structure. The nanoparticles were characterized using X-ray diffraction, Raman spectroscopy, the Brunauer–Emmett–Teller (BET) method, and high-resolution transmission electron microscopy. In the case of TiO₂, the phase of nanoparticles could be controlled by adjusting the equivalence ratio, while the particle size was dependent on the precursor loading rate and the flame temperature. The synthesized TiO₂ nanoparticles exhibited high crystallinity and the anatase phase was dominant at high equivalence ratios ($\phi > 1.3$). In the case of SiO₂, the particle size could be controlled from 11 to 18 nm by adjusting the precursor loading rate.

nasir.memon@kaust.edu.sa

2F09 VOLUMETRIC FLAME SYNTHESIS OF ONE-DIMENSIONAL MOLYBDENUM OXIDE NANOSTRUCTURES

S. Srivastava¹, W. Merchan-Merchan², M. Desai², A.V. Saveliev¹
¹North Carolina State University, United States ²University of Oklahoma, United States

An opposed laminar flow flame formed with methane/acetylene and oxygen enriched-air was used for controlled synthesis of 1-D molybdenum oxide nanostructures directly in the gas phase. Raw material was introduced into oxidizer side of the flame in the form of solid molybdenum wires with ~99% purity. Molybdenum oxide vapors formed in the gas phase were transported in the flame environment possessing strong thermal and chemical gradients. The generated nanostructures were collected thermophoretically from the flame volume. Essential morphological variations of generated nanomaterials were observed depending on flame position and probe parameters. The mechanism behind the synthesis of the spherical and 1-D nanoforms is analyzed and modeled numerically. The nanorods growth model involves monomer formation, nucleation and growth. The monomer formation is through the oxidation and vaporization of the probe material. The nucleation model is based on the Classical Nucleation Theory. It calculates the number of nuclei present, their surface energy and the critical size of the nuclei. The model calculates the trajectory of the particles as they are transported in the flame volume. The growth model considers the contribution of the monomers diffusing onto the nanoparticle surface as well as the effect of the atoms impinging directly onto the growth sites. The ends of the cylindrical 1-D nanorods grow by the phenomenon of rough growth while the lateral sides exhibit layered growth.

asaveliev@ncsu.edu

2F10 MECHANICALLY ACTIVATED COMBUSTION SYNTHESIS OF MOLYBDENUM SILICIDES AND BOROSILICIDES FOR ULTRAHIGH-TEMPERATURE STRUCTURAL APPLICATIONS

Mohammad S. Alam, Evgeny Shafirovich, The University of Texas at El Paso, United States

Molybdenum silicides and borosilicides are promising structural materials for gas-turbine power plants. A major challenge, however, is to simultaneously achieve high oxidation resistance and acceptable mechanical properties at high temperatures. For example, molybdenum disilicide (MoSi₂) has excellent oxidation resistance and poor mechanical properties, while Mo-rich silicides such as Mo₅Si₃ (called T₁) have much better mechanical properties but poor oxidation resistance. One approach is based on the fabrication of MoSi₂–T₁ composites that combine high oxidation resistance of MoSi₂ and good mechanical properties of T₁. Another approach involves the addition of boron to Mo-rich silicides for improving their oxidation resistance through the formation of a borosilicate surface layer. In particular, Mo₅SiB₂ (called T₂) phase is considered as an attractive material. In the present paper, MoSi₂–T₁ composites and materials based on T₂ phase are obtained by mechanically activated SHS. Use of SHS compaction (quasi-isostatic pressing) significantly improves oxidation resistance of the obtained MoSi₂–T₁ composites. Combustion of Mo–Si–B mixtures for the formation of T₂ phase becomes possible if the composition is designed for the addition of more exothermic reactions leading to the

formation of molybdenum boride. These mixtures exhibit spin combustion, the characteristics of which are in good agreement with the spin combustion theory. Oxidation resistance of the obtained Mo–Si–B materials is independent on the concentration of Mo phase in the products so that the materials with a higher Mo content are preferable because of better mechanical properties.

eshafirovich2@utep.edu

2F11 KINETICS OF CATALYTIC OXIDATION OF ETHYLENE OVER PALLADIUM OXIDE

Y.X. Xin¹, B. Yang², H. Wang³, S.L. Anderson⁴, C.K. Law^{1,2}

¹Princeton University, United States ²Tsinghua University, China ³Stanford University, United States

⁴University of Utah, United States

Catalytic oxidation of ethylene was experimentally studied by wire microcalorimetry and mass spectrometry over the temperature range of 400 to 800 K at atmospheric pressure. The catalyst is a Palladium Oxide (PdO) surface on a polycrystalline palladium wire. For mixtures containing 0.3-0.6% C₂H₄ and 3.75 % O₂ in N₂, the heat release rate as well as the mole fractions of gas-phase species were identified. Experimental observation revealed the temperature-dependent channels for the C₂H₄ oxidation, with mixed H₂ release and H₂O production below 580 K and complete oxidation to CO₂ and H₂O above 600 K. Analysis of the global reaction kinetics shows that for 620 ≤ T ≤ 740 K the surface catalytic reaction rate is the first order in ethylene concentration and has an activation energy of 48.2 ± 1.4 kJ/mol. A surface chemistry model is proposed and the dissociative adsorption rate constant of C₂H₄ on PdO surface was determined by fitting the experimental data.

yxin@princeton.edu

2F12 LOW-TEMPERATURE DEEP OXIDATION OF OLEFINS AND DME OVER COBALT FERRITE

Zhen-Yu Tian^{1,2}, Patrick Mountapmbeme Kouotou¹, Achraf El Kasmi¹, Patrick Hervé Tchou Ngamou¹,

Katharina Kohse-Höinghaus¹, Henning Vieker¹, André Beyer¹, Armin Götzhäuser¹

¹Bielefeld University, Germany ²Chinese Academy of Sciences, China

This work reports the facile synthesis of cobalt ferrite catalysts by Pulsed Spray Evaporation Chemical Vapor Deposition (PSE-CVD) for low-temperature oxidation of dimethyl ether and olefin exhaust emission. To better understand the structure-performance relationship, the prepared thin films were comprehensively characterized in terms of phases, surfaces and redox properties. A well-crystallized inverse spinel structure was revealed by both XRD and Raman analyses. Helium Ion Microscopy (HIM) images show that the obtained films have cauliflower structure with apparent open porosity. The catalytic performance of the as-prepared cobalt ferrite was evaluated with a fixed bed quartz reactor-FTIR system. The results indicate that the cobalt ferrites were very active for the total oxidation of propene, *n*-butene and DME at low temperature and no CO was observed during the oxidation processes. The attractive performance of cobalt ferrite catalysts are attributed to a redox mechanism which involves the synergistic effect of the morphology, reducibility and lattice oxygen mobility.

tianzhenyu@iet.cn

2F13 FORMATION OF N₂ AND N₂O IN INDUSTRIAL COMBUSTION OF AMMONIA OVER PLATINUM

Maximilian Warner, Brian S. Haynes, The University of Sydney, Australia

The catalytic combustion of ammonia over a 95%Pt/5%Rh gauze has been investigated in an oxygen/steam environment using a flow reactor. Direct measurements of byproduct N₂ and N₂O selectivities have been made over a wide range of process conditions: temperature 450-815°C; pressure 1-3 bar; mass flux 0.12 to 1.12 kg m⁻² s⁻¹; ammonia mole fraction 7-13%; and inlet oxygen-ammonia feed ratio 1.4 to 3. The results show that, while both N₂ and N₂O selectivities decrease with increasing temperature, the influence of other process variables is important. The formation of N₂O is significantly reduced at higher values of the oxygen-ammonia feed ratio so attempts to increase burner throughput by reducing this ratio may lead to increased N₂O formation in the burner.

A model for product sensitivities based on mass-transfer-limited combustion and detailed microkinetic description of the surface N₂- and N₂O-forming steps is developed. Explicit expressions incorporating all the process and gauze parameters in the system are obtained for the individual product sensitivities. The model is found to provide excellent descriptions of the entire data set, both for oxygen and temperature dependence. The model also describes available literature data even for data obtained under very different conditions from ours (gauze dimensions, combustion in air, temperatures up to 1000°C and mass fluxes up to 50 times those studied in this work).

Fundamental relations between the activation energies for the reactions of surface nitrogen atoms that lead to NO and byproduct formation are extracted from the data. These values provide a target for fundamental studies. The approach developed here is applicable to a wide range of catalyzed mass-transfer-limited reactions such as combustion and partial oxidation.

brian.haynes@sydney.edu.au

2G01 PHENOMENOLOGICAL MODEL OF SOOT PRODUCTION INSIDE A NON-BUOYANT LAMINAR DIFFUSION FLAME

G. Legros¹, J.L. Torero²

¹University of Paris - CNRS, France ²The University of Queensland, Australia

An original phenomenological model for soot production inside a laminar, at plate boundary layer diffusion flame is presented. The model is compared with experimental measurements conducted in microgravity. For the experiments, the fuel, ethylene, is injected through a flat porous burner into an oxidizer stream flowing parallel to the burner surface. The oxidizer is a mixture of 35% oxygen and 65% nitrogen. The fuel and oxidizer velocities are systematically varied. The analysis of the data shows that the streamwise location of the maximum flame height can be considered an unambiguous characteristic length of the flame as opposed to the maximum visible flame length. Analysis of the streamwise location of the maximum flame height enables to establish the transition between "open-tip" and "closed-tip" behavior as well as scaling laws for the soot volume fraction. A scaled soot volume fraction is found to follow a linear relationship with the streamwise coordinate normalized by the burner length. This correlation appears to be valid for all conditions studied.

guillaume.legros@upmc.fr

2G02 SIMPLIFIED MODEL TO PREDICT THE DIFFERENCE BETWEEN FLAMMABILITY LIMITS OF A THIN MATERIAL IN NORMAL GRAVITY AND IN MICROGRAVITY ENVIRONMENT

Shuhei Takahashi¹, Tomoya Ebisawa¹, Subrata Bhattacharjee², Tadayoshi Ihara¹

¹Gifu University, Japan ²San Diego State University, United States

Most flammability tests for a material to be used for manned space activity are conducted on ground although there are many reports that the flammability limit in microgravity is different from that in normal gravity. Hence, it is important to predict the gap between the limits in normal gravity and microgravity. We set up the simplified scale model to describe the flame spread over a thin material, and derived the expression for Damköhler number, Da , and the non-dimensional radiative loss factor, R_{rad} for the flame spread over a thermally thin PMMA sheet. The empirical constants for the non-dimensional numbers were evaluated by fitting with the experimental results in N_2 balance. The experimental blow-off limits were obtained by the downward spread tests in normal gravity with varying the balance gas as N_2 , Ar and CO_2 . We compared the predicted blow-off limits with the experimental results for each balance condition, and the predicted limits well agreed with the experimental results quantitatively. With Da and R_{rad} , we obtained flammability map for a thin PMMA sheet, which predicted the flammable region under the Limiting Oxygen Index (LOI). The LOIs in normal gravity were 17.2%, 12.1% and 24.5% for N_2 , Ar, CO_2 balance condition whereas the estimated Minimum Oxygen Concentrations (MOCs) in microgravity were 11%, 8% and 12%, respectively. The gap between the LOI and MOC was 12.5% for CO_2 balance. As predicted, robust flame was observed in microgravity condition at 21% oxygen level, which is 3.5% lower than the LOI. The simplified model also predicted the flow velocity where the flame became most robust. The predicted results well explained the behavior of the flame spread obtained in microgravity condition where the oxygen concentration was below LOI.

shuhei@gifu-u.ac.jp

2G03 MICROGRAVITY FLAMMABILITY LIMITS OF ETFE INSULATED WIRES EXPOSED TO EXTERNAL RADIATION

Andres F. Osorio¹, Ken Mizutani², Carlos Fernandez-Pello¹, Osamu Fujita²

¹University of California-Berkeley, United States ²Hokkaido University, Japan

In the present work the normal gravity (1g) and microgravity (μg) flammability limits ETFE insulated copper wires exposed to an external radiant flux were studied. Experiments with sample wires of a 0.50mm copper core and 0.15mm ETFE insulation thickness are conducted in oxygen concentrations ranging from 20% to 32% and external radiant fluxes from 0 to 25kW/m². Results show that the combination of μg conditions and addition of an external radiant flux are able to extend the range of oxygen concentrations over which ETFE insulated wires are flammable. In the experiments, μg conditions resulted in a 6% decrease in the LOC, while at the maximum value, external radiant fluxed resulted in an additional 6%. Microgravity limits flame heat losses, making possible to reduce flame temperature and maintain the necessary heat transfer to achieve a critical solid decomposition rate. External radiation is able to further compensate for reductions in flame temperature, resulting in lower LOC in 1g and μg . The results obtained with ETFE are also compared to available results with Polyethylene (PE) and show that μg conditions have a larger impact in ETFE than PE highlighting the importance of studying fire behavior of materials used in space applications.

ofujita@eng.hokudai.ac.jp

2G04 PARAMETRIC STUDY ON THE SMOLDERING COMBUSTION OF A THIN SOLID IN A NARROW SPACE

Yosuke Uchida¹, Kazunori Kuwana¹, Genichiro Kushida²

¹Yamagata University, Japan ²Aichi Institute of Technology, Japan

This paper studies the smoldering propagation along a thin solid in a narrow space. It particularly focuses on the formation of a fingering pattern caused by an instability mechanism—an important phenomenon from a fire safety point of view because the formation of such a pattern increases the smoldering velocity. Two hypotheses are made by reviewing previous

studies. The first hypothesis proposes the Lewis number as a key parameter, and a fingering pattern including the local extinction and the split of fingers is formed when the Lewis number is well below unity. The second hypothesis proposes that such a fingering pattern can be formed without convection effects. The results of numerical simulations and experiments presented herein confirm both hypotheses.

kuwana@yz.yamagata-u.ac.jp

2G05 COMPUTATIONAL SMOULDERING COMBUSTION: PREDICTING THE ROLES OF MOISTURE AND INERT CONTENTS IN PEAT WILDFIRES

Xinyan Huang¹, Guillermo Reina¹, Haixiang Chen²

¹Imperial College London, United Kingdom ²University of Science and Technology of China, China

Smouldering combustion is the slow, low-temperature, flameless burning of porous fuels and is the most persistent type of combustion phenomena. It is the driving phenomenon of wildfires in peatlands, like those causing haze episodes in Southeast Asia and Northeast Europe, but poorly understood. In this work, we develop a multi-physics 1-D model of a reactive porous media with an open-source code Gpyro to investigate the phenomenon with an emphasis on the role of the moisture and inert contents. This model solves the species, momentum, and energy conservation equations and heterogeneous chemical reactions. A previously developed 5-step reaction scheme for peat, including evaporation of water, is adopted to describe the drying and thermal and oxidative degradation during smouldering combustion. The model predicts the transient temperature, species, and reaction profiles during ignition, spread, and extinction. The predicted smouldering thresholds related to the critical moisture and inorganic contents show a good agreement with the experimental results in literature for a wide range of peat types and organic soils. The influences of the kinetic parameters, physical properties, and ignition protocols are investigated. This is the first time that a physics-based model of smouldering peat fires is developed, thus helping to understand this important natural and widespread phenomenon.

x.huang12@imperial.ac.uk

2G06 EXPERIMENTAL STUDY ON MERGED FLAME CHARACTERISTICS FROM MULTIFIRE SOURCES WITH WOOD CRIBS

Wenguo Weng¹, Daisuke Kamikawa², Yuji Hasemi³

¹Tsinghua University, China ²Forestry and Forest Product Research Institute, Japan ³Waseda University, Japan

This paper describes a series of experiments that were carried out to study merged flame characteristics. A specially designed wood crib burner were operated with the square burner configurations of 2 by 2 and 3 by 3, and various separation distances of 0, 1.5, 3 and 5 cm. The heat release rate, the mass loss rate, the heat feedback from the flame to the fuel surface, and the radiative heat flux were measured. The corresponding combustion efficiency and pyrolysis efficiency are calculated. The experimental data of the radiative heat flux from the merged flame are compared with the computed values of an empirical model from a single fire. Experimental data show that bigger separation distance and more burners advance the combustion efficiency due to more entrained ambient air; however have no obvious effects on the pyrolysis progress. The overall trend of the computed radiative heat flux is similar to that of the experimental data for the merged flame; only the times of the computed peak radiative heat fluxes are always lower than those of the experimental data.

wgweng@tsinghua.edu.cn

2G07 EXPERIMENTAL STUDY OF THE EFFECT OF CF₃I ADDITION ON THE IGNITION DELAY TIME AND LAMINAR FLAME SPEED OF METHANE, ETHYLENE, AND PROPANE

O. Mathieu¹, J. Goulier², F. Gourmel², M. S. Mannan¹, N. Chaumeix², E. L. Petersen¹

¹Texas A&M University, United States ²CNRS - INSIS, France

Since no suitable replacement has been found for halon 1301 (CF₃Br), the approach for the next generation of fire suppressants has been to identify diverse agents or blends of agents for specific applications. Halon 13001 (CF₃I) is a possible candidate for unoccupied areas. However, there are very few fundamental data to help in validating its detailed kinetics mechanism. In this study, ignition delay time and laminar flame speed measurements of the effects of CF₃I on CH₄, C₂H₄, and C₃H₈ have been investigated for the first time. The ignition delay times were obtained in a shock tube with mixtures of fuel/O₂/CF₃I highly diluted in 98% argon (vol.), and the flame speeds were measured using an expanding, spherical flame. Results from the new experiments show a significant decrease in the laminar flame speed for small additions of suppressant. The effects on the ignition delay time are strongly dependent on the hydrocarbon: the ignition delay time of CH₄ is significantly decreased by CF₃I addition, while a significant increase in the ignition delay time was observed for the lowest temperatures investigated with C₂H₄. Ignition delay times for C₃H₈ were mostly unchanged, except for the lowest temperatures (below 1400 K) where a small decrease in the reactivity was observed. Compared to recent results obtained with CF₃Br, CF₃I showed a smaller suppressant effect under the conditions investigated. A detailed kinetics mechanism assembled from a C1-C3 mechanism from NUI Galway and a CF₃I sub-mechanism from NIST predicts well the results obtained in the shock tube with CH₄ and C₃H₈. The C₂H₄ data with CF₃I are however poorly predicted, pointing at some deficiencies in the model for C₂H₄/CF₃I interactions.

olivier.mathieu@tamu.edu

2G08 COMBUSTION INHIBITION AND ENHANCEMENT OF CUP-BURNER FLAMES BY CF_3Br , C_2HF_5 , $\text{C}_2\text{HF}_3\text{Cl}_2$, AND $\text{C}_3\text{H}_2\text{F}_3\text{Br}$

Fumiaki Takahashi¹, Viswanath R. Katta², Gregory T. Linteris³, Valeri I. Babushok³

¹Case Western Reserve University, United States ²Innovative Scientific Solutions, Inc., United States

³National Institute of Standards and Technology, United States

Numerical simulations have been performed to study the combustion inhibition and unwanted enhancement processes by fire-extinguishing agents: CF_3Br (Halon 1301) and replacements (C_2HF_5 , $\text{C}_2\text{HF}_3\text{Cl}_2$, and $\text{C}_3\text{H}_2\text{F}_3\text{Br}$), in cup-burner flames in normal Earth gravity. A propane-ethanol-water fuel mixture, prescribed for a Federal Aviation Administration (FAA) aerosol can explosion simulator test, was used as the fuel. The time-dependent, two-dimensional numerical code, which includes a detailed kinetic model (up to 241 species and 3918 reactions), diffusive transport, and a gray-gas radiation model, revealed unique *two-zone* flame structure and predicted the minimum extinguishing concentration of agent when added to the air stream. The general trend was similar to the microgravity flames studied previously but more evident. The peak reactivity spot (i.e., reaction kernel) at the flame base stabilized a trailing flame in a buoyancy-induced entrainment flow. As the mole fraction of agent in the coflow (X_a) was increased gradually: (1) the *premixed*-like reaction kernel weakened (i.e., lower heat release rate) (but nonetheless formed at higher temperature and velocity); (2) the flame base detached from the burner rim and stabilized increasingly inwardly and higher above the burner rim until finally blowoff-type extinguishment occurred; (3) the calculated maximum flame temperature remained at nearly constant (≈ 1800 K) or mildly increased; and (4) the total heat release of the entire flame decreased (inhibited) for CF_3Br but increased (enhanced) for the halon replacements. In the trailing flame with the halon replacements, *two-zone* flame structure (with double heat-release-rate peaks) developed: H_2O (a hydrocarbon- O_2 combustion product, in the inner zone, and the fuel component) was converted further to HF and CF_2O through exothermic reactions in the outer zone; CO_2 was formed in-between. As a result, the unusual (non-chain branching) reactions and the combustion enhancement (increased total heat release) due to the halon-replacement addition occurred primarily in the trailing *diffusion* flame.

fxt13@case.edu

2G09 EFFECTS OF WATER SPRAYS ON THE FLAME PROPAGATION IN HYDROGEN/AIR/STEAM MIXTURES

H. Cheikhraoui, J. Goulier, A. Bentaib, N. Meynet, N. Chaumeix, C.-E. Paillard, CNRS-INSIS, France

Flammability limits of H_2 /air/steam mixtures, as well as lean flammability limits of H_2 /air/water mist at 358, 373 and 383 K for the first and 298 K for the second, for 100 kPa, were experimentally determined. The mixtures were not flammable for H_2 mol% ≥ 55 . The droplets interaction with flame was experimentally investigated. The effect of large droplets (SMD = 200-250 μm) on laminar H_2 /air flames was found to be marginal especially as the flame speed is rapid compared to the droplet one. Coupling between combustion front and droplet vaporization zone is possible if the flame speed and the droplet velocity are of the same order of magnitude and in the same direction then, the combustion is strongly accelerated. Non-flammable H_2 /air/steam mixtures at 85°C and 110°C were made explosive by aspersion with cold water spray. The mixture is generally ignited near the limit, but the pressure increase is limited due to the slow flame motion compared to the droplet one. The burned gas bubble is rapidly dragged downward. The water mist effect on the deflagration of H_2 /air mixtures were studied for various equivalence ratios. With droplets diameter < 10 μm , the maximum combustion pressures, with or without aspersion, were similar when the turbulence in the vessel is approximately comparable. However, the pressure rise is slowed in presence of mist and the decrease of K_G can reach 25%.

chaumeix@cnrs-orleans.fr

2G10 CHARACTERIZATION OF INTERACTIONS BETWEEN HOT AIR PLUMES AND WATER SPRAYS FOR SPRINKLER PROTECTION

Xiangyang Zhou, FM Global, United States

One important aspect of the complex sprinkler protection process is the interaction between the water spray and the fire plume. In order to provide suitable data for the development and validation of a LES-based fire protection models, such as FireFOAM, a series of small-scale experiments were conducted to examine the interaction of hot air plumes and water sprays through combined gas-liquid velocity and droplet size measurements. Laser-based Particle Image Velocimetry (PIV) was used to acquire the spatially-resolved velocity data; and a Shadow Imaging System (SIS) was used to measure the water droplet size and volume flux. Hot air plumes with three convective heat release rates (1.6, 2.1 and 2.6 kW) were selected to interact with a water spray at a discharge rate of 0.084 Lpm. The velocity field of the hot air plume and ceiling flow with/without water spray, the droplet size and volume flux of water spray with/without hot air plume were measured. The interaction between the hot air plume and water spray was characterized by the location of the interaction boundary with the momentum ratio of the hot air to that of the spray. The results showed that the momentum ratio and the evaporation effect due to hot air on the water droplets played a significant role to change the interaction structure and the ceiling layer pattern.

xiangyang.zhou@fmglobal.com

2H01 NUMERICAL ESTIMATION OF THRUST PERFORMANCE ON ROTATIONAL DETONATION ENGINE IN A HYDROGEN-OXYGEN MIXTURE

Nobuyuki Tsuboi¹, Yusuke Watanabe¹, Takayuki Kojima², A. Koichi Hayashi³

¹Kyushu Institute of Technology, Japan ²JAXA, Japan ³Aoyama Gakuin University, Japan

The numerical simulations of 2D and 3D rotating detonation engines in a hydrogen-oxygen mixture are carried out by using the detailed chemistry model. The comparison of 2D/3D flowfield for the same injection conditions shows that the overall flow structure coincides and both rotating velocities are approximately 90% of CJ value. However, I_{sp} for 2D RDE is approximately 10 sec. larger than I_{sp} for 3D RDE. The effects of chamber depth for 3D RDE are small on I_{sp} . The grid resolution study shows that the higher grid resolution produces detonation cellular structure, however, its effects on I_{sp} are approximately a few second. Though I_{sp} in the smallest scale for higher mass flow is approximately 10 s larger than the other large scales, I_{sp} for low mass flow is not affected by the scale. Though I_{sp} and thrust are governed by the stagnation pressure and micro nozzle area ratio, mass flow rate from the injector also depends on these parameters. I_{sp} and thrust for RDE are found to be correlated by the mass flow rate as well as the conventional rocket engine. This means that two important parameters such as A^*/A and p_0 can be replaced to one parameter as the mass flow rate.

tsuboi@mech.kyutech.ac.jp

2H02 CAVITY IGNITION IN SUPERSONIC FLOW BY SPARK DISCHARGE AND PULSE DETONATION

Timothy M. Ombrello¹, Campbell D. Carter¹, Chung-Jen Tam², Kuang-Yu Hsu³

¹U.S. Air Force Research Laboratory, United States ²Taitech, United States ³Innovative Scientific Solutions, United States

Ignition of an ethylene fueled cavity in a supersonic flow was achieved through the application of two energy deposition techniques: a spark discharge and Pulse Detonator (PD). High-frequency shadowgraph and chemiluminescence imaging showed that the spark discharge ignition was passive with the ignition kernel and ensuing flame propagation following the cavity flowfield. The PD produced a high-pressure and temperature exhaust that allowed for ignition at lower tunnel temperatures and pressures than the spark discharge, but also caused significant disruption to the cavity flowfield dynamics. Under certain cavity fueling conditions a multiple regime ignition process occurred with the PD that led to decreased cavity burning and at times cavity extinction. Simulations were performed of the PD ignition process, capturing the decreased cavity burning observed in the experiments. The PD exhaust initially ignited and burned the fuel within the cavity rapidly. Simultaneously, the momentary elevated pressure from the detonation caused a blockage of the cavity fuel, starving the cavity until the PD completely exhausted and the flowfield could recover. With sufficiently high cavity fueling, the decrease in burning during the PD ignition process could be mitigated. Cavity fuel injection and entrainment of fuel through the shear layer from upstream injection allowed for the spark discharge ignition process to exhibit similar behavior with peaks and valleys of heat release (but to a lesser extent). The results of using the two energy deposition techniques emphasized the importance of cavity fueling and flowfield dynamics for successful ignition.

timothy.ombrello.1@us.af.mil

2H03 MIXING-RELATED LOW FREQUENCY OSCILLATION OF COMBUSTION IN AN ETHYLENE-FUELED SUPERSONIC COMBUSTOR

Zhen-guo Wang¹, Ming-bo Sun¹, Hong-bo Wang¹, Jiang-fei Yu¹, Jian-han Liang¹, Fengchen Zhuang²

¹Science and Technology on Scramjet Laboratory, China ²Academy of Equipment, China

The present work investigated combustion instabilities inside an ethylene-fueled scramjet combustor mounted on a Mach 2.1 direct-connected test facility with an inflow stagnation temperature of 846K. Effects of fueling schemes on the combustion stability characteristics were examined. The experimental results suggest that the oscillation modes correlate with mixing status closely. For the cases with a thermal throat or stable shock trains, flame fluctuation exists in a mode of thermoacoustic type oscillation with a broad frequency range. While for the cases without a thermal throat, if a fuel/air premixed region from the injection to the cavity flameholder exists, cavity pilot flame could reignite the fuel/air mixture and acquire a Deflagration-Detonation Transition (DDT) procedure. This process couples with the flame quenching upstream the injection location and a DDT-type low frequency oscillation can be formed.

wind_flowcfd@163.com

2H04 WEAK AND STRONG IGNITION OF HYDROGEN/OXYGEN MIXTURES IN SHOCK TUBE SYSTEMS

Kevin P. Grogan, Matthias Ihme, Stanford University, United States

Detailed simulations of hydrogen/oxygen mixtures are performed to study the weak and strong ignition regimes in a shock tube system. An Adaptive Mesh-Refinement (AMR) algorithm in conjunction with a detailed chemistry representation is used to resolve physically relevant features such as the viscous boundary layer, the shock bifurcation region, and the ignition kernels. The simulations employ a second-order accurate, Navier-Stokes solver that is modified to include a finite-rate kinetic mechanism, wall heat transfer, and detailed mass, thermal, and viscous diffusion transport

properties. The operating conditions considered in this study span the thermodynamic state-space in the weak and strong ignition regime. The treatment of wall heat transfer was found to significantly alter the characteristics of ignition. The computations show that the mixing of the thermally stratified fluid, which carries different momentum and enthalpy, introduces inhomogeneities in the core-region behind the reflected shock. These inhomogeneities act as localized ignition kernels. During the induction period, these kernels slowly expand and eventually transition to a detonation wave that rapidly consumes the unburned mixture. A detailed analysis was performed to show that the transition from ignition kernel to detonation is well-described by the SWACER mechanism.

kgrogan@stanford.edu

2H05 IGNITION BY TRANSIENT HOT TURBULENT JETS: AN INVESTIGATION OF IGNITION MECHANISMS BY MEANS OF A PDF/REDIM METHOD

A. Ghorbani¹, G. Steinhilber², D. Markus¹, U. Maas²

¹Physikalisch-Technische Bundesanstalt, Germany ²Karlsruhe Institute of Technology, Germany

Understanding ignition of combustible mixtures by hot jets of burnt gases plays an important role in explosion protection. In this work a PDF method in conjunction with a Reaction-Diffusion Manifold (REDIM) is used to investigate the ignition of a hydrogen/air mixture by a hot turbulent jet. In accordance with experimental results it is observed in numerical investigations that after an ignition delay time the ignition is typically initiated at the jet head vortex. The scope of the current work is to investigate the mechanisms leading to ignition and explain the processes governing the ignition delay time as well as the ignition location. It is shown that macro- as well as micromixing and the chemical kinetics have a profound influence on the ignition process and that a realistic model for the ignition process has to account for all these processes in combination with a transient description of the jet penetration.

asghar.ghorbani@ptb.de

2H06 NUMERICAL STUDY ON THE SPONTANEOUS-IGNITION FEATURES OF HIGH-PRESSURE HYDROGEN RELEASED THROUGH A TUBE WITH BURST CONDITIONS

Hyoung Jin Lee¹, Sung Don Kim², Sei Hwan Kim², Ji Hyun Park², In-Seuck Jeung²

¹PGM R&D Laboratory, Korea ²Seoul National University, Korea

High-pressure hydrogen can undergo a spontaneous ignition when it is released into the air abruptly. However, the ignition mechanism remains imperfect because it can be varied easily with flow development affected by the burst conditions. Numerical simulations are conducted for the cylindrical tube with various burst conditions and some results are validated from the previous experimental data. Burst pressure of maximum 40 MPa are simulated for two pressure boundaries which are classified by spherical and flat shape. The results show that the ignition features can be different with burst conditions. Basically, the shock interactions which can be induced by a spherical pressure boundary can play a role for the ignition as making separated two mixing and reaction regions in the core and boundary layer of the tube. Also, the reaction in the core region can assist to form a complete flame when the burst pressure is relatively low, but it is possible to initiate the ignition by only reaction region near the boundary layer without the reaction in a core region when the burst pressure is high. The numerical results can explain a plausible reason why the previous experimental ignition feature is different from the reported ignition mechanism as showing that the ignition is initiated by only reaction region developed from the boundary layer.

enjjs@snu.ac.kr

2H07 EXPERIMENTAL STUDY OF SPHERICAL-FLAME ACCELERATION MECHANISMS IN LARGE-SCALE PROPANE-AIR FLAMES

C. Regis Bauwens^{1,2}, Jeffrey M. Berghthorson², Sergey B. Dorofeev¹

¹FM Global, United States ²McGill University, Canada

Large-scale experiments examining spherical-flame propagation of propane-air flames up to a diameter of 1.2 m were performed. Throughout these experiments, the growth of the Darrieus- Landau instability was directly observed and detailed measurements show that the increase of flame velocity follows a pattern of self-similar oscillatory growth that has not been previously reported. These oscillations are found to be the result of periodic growth and saturation of a narrow range of length scales that follows each generation of cell formation. Based on these observations, a new method to estimate the fractal-acceleration exponent is proposed based on the amplitude and frequency of these oscillations. Comparisons between the fractal exponents derived by this method and a direct power law fit show reasonable agreement with one another, as well as with values reported by previous studies.

carl.bauwens@fmglobal.com

2H08 NUMERICAL SIMULATION OF DILUTE AND DENSE LAYERED COAL-DUST EXPLOSIONS

Ryan W. Houim, Elaine S. Oran, University of Maryland, United States

Multidimensional time-dependent simulations were performed to study the interaction of a stoichiometric natural-gas detonation with layers of coal dust. The simulations used a high-order compressible numerical method for fluid dynamics and included an Eulerian kinetic theory-based granular multiphase model applicable to dense and dilute particle

volume fractions. Two cases were considered: a loose dust layer with an initial volume fraction of 1%, and a dense dust layer with an initial volume fraction of 47%. For both cases, the final result is a coupled complex consisting of an accelerating shock leading a coal-dust flame. Initially, a shock is produced from remnants of a gaseous detonation. This shock decays due to mechanical and thermal losses from lifting and entraining the coal dust. The lifted dust subsequently ignites in the shock-heated air and produces a structure similar to a mixing-limited nonpremixed flame. The flame is ignited by a wave of burning coal dust that follows the shock. The distance between the shock and ignition point is determined by the induction length of carbon char, which is ~ 170 cm and ~ 15 cm for the 47% and 1% cases, respectively. The burning of coal particles is predominantly from heterogeneous reactions with carbon char, and methane combustion is a secondary effect. Mixing of air and particles is induced by relative velocity between the gas and solid phases. Burning coal particles produces pressure waves that accelerate the shock from Mach 2.2 to 2.6 for the dilute layer and from Mach 1.7 to 1.8 in the dense layer.

ryan.houim@gmail.com

2H09 SELF-SIMILAR PROPAGATION OF EXPANDING SPHERICAL FLAMES IN LARGE SCALE GAS EXPLOSIONS

Woo Kyung Kim¹, Toshio Mogi¹, Kazunori Kuwana², Ritsu Dobashi¹

¹The University of Tokyo, Japan ²Yamagata University, Japan

In the present study, the onset of self-acceleration and self-similarity during a large-scale gas explosion has been investigated experimentally. The critical Peclet number (dimensionless flame radius), $Pe_c = r/\delta$, the experimental acceleration exponent, α , and the fractal excess, d , are evaluated from the results of field experiments of hydrogen/air, methane/air, and propane/air mixtures at various concentrations. Experimental results show that Pe_c for the onset of self-acceleration correlates with Markstein number, Ma , of the mixture, which expresses the intensity of diffusional-thermal instability. This result demonstrated that the onset of self-acceleration depends on the hydrodynamic instability as well as intensity of diffusional-thermal instability. The value of power law exponent of flame radius, α , increased with an increase in $Pe - Pe_c$, and then it reached a limiting value from which the fractal dimension was calculated. In particular, it was verified the self-acceleration ($\alpha > 1$) and the self-similarity ($\alpha = \text{constant}$) of expanding spherical flame are definitely existed, through the experimental data of large-scale field tests. In addition, the practical fractal dimensions for the accidental gas explosions are evaluated. The experimental three-dimensional fractal dimension for real flames exist in range of $D_3 \approx 2.2$ -2.35 in the present study. It was confirmed that the fractal dimension of the expanding spherical flame in an accidental gas explosion is affected by the instabilities. It is expected that the present results help improve the accuracy of the risk assessment of explosion hazards.

youwoo2@gmail.com

2H10 TIME-RESOLVED TEMPERATURE MEASUREMENTS FOR INERT AND REACTIVE PARTICLES IN EXPLOSIVE ATMOSPHERES

F. Beyrau, M.A. Hadjipanayis, R.P. Lindstedt, Imperial College, United Kingdom

The current study extends the understanding of the dynamics of the ignition process of fuel-air mixtures caused by laser-irradiated particles via the quantification of the particle heating process. Temperature measurements have been conducted under different irradiance in order to investigate the relationship between the absorption-emission properties of inert and reactive particles using emission spectroscopy. Temporal temperature information has been obtained at different boundary conditions for a range of carbon based powders including carbon blacks and graphites, as well as silicon carbide powders of different sizes. The particle size was found to have a significant impact on the heating process. Specifically, finer particles led to enhanced heating rates due to the reduced mass and thermal capacity, and the rate increase with irradiance for both inert and reactive particles was also quantified. The particle surface temperatures necessary to cause ignition of a surrounding charge were obtained and two different ignition regimes were observed. For non-reactive particles, the surface temperature plays the major role and for silicon carbide particles the ignition temperature was found to be 1200 ± 200 K. By contrast, results obtained with reactive powders that feature similar times to ignition suggest that the temperature is not the only ignition criterion.

p.lindstedt@imperial.ac.uk

2H11 IS THE DETONATION "DEAD ZONE" REALLY DEAD?

L.G. Hill, Los Alamos National Laboratory, United States

This paper examines the phenomenon of detonation *Dead Zones* (DZs), whereby weak regions of a detonation shock fail to trigger prompt reaction, thus leaving behind pockets of substantially unburned explosive. That DZs are distinctly identifiable structures is a consequence of the fact that HE reaction rates are highly sensitive to the local thermodynamic state. A key unanswered question is the extent to which DZs react on a delayed timescale, and whether they contribute a significant amount of useful energy to their surroundings. I begin by addressing DZs in general, categorizing them according to the multiple contexts in which they arise. Next, I discuss what is known and/or believed about DZ reactivity. The majority of the paper is devoted to exploring DZs that occur in a particular scenario called

Transverse Initiation. Specifically, I present a *Cylinder Expansion* (CYLEX) test experiment in which a faster HE core (PBX 9501, 95 wt% HMX) is surrounded slower HE annulus (PBX 9502, 95 wt% TATB). The fast component "pulls" the detonation in the slow component faster than it would naturally travel, but leaves a DZ in the slow layer adjacent to the fast layer. By combining the usual CYLEX diagnostics with detonation front curvature measurements and by introducing a novel analysis, I am able to quantify-evidently for the first time for any class of DZ-the amount and timescale of energy released. The analysis predicts that a $\sim 0.2 \mu s$ induction time exists during which essentially no material burns, after which the contributed energy rises to half its ultimate value in $\sim 1.6 \mu s$. The reaction approaches its ultimate value asymptotically, ultimately liberating $\sim 80\%$ of the energy released by a PBX 9502 detonation.

lgh@lanl.gov

2H12 AN ANALYTIC METHOD FOR TWO-DIMENSIONAL WALL MOTION AND PRODUCT ISENTROPE FROM THE DETONATION CYLINDER TEST

Scott I. Jackson, Los Alamos National Laboratory, United States

The cylinder test provides a measurement of detonation product's ability to perform work on adjacent material. Historically, direct numerical simulation has been required to derive the product energy content and isentrope from experiments of cylinder expansion driven by detonation products. One-dimensional analytic methods have not been able to accurately recover these parameters when the cylinder motion is compressible, exhibiting shocks. For incompressible cylinder motion, analytic one-dimensional approximations more accurately recover the isentrope, but still only approximate the two-dimensional cylinder motion and energy. This work provides a fully two-dimensional model that recovers the exact outer cylinder shape from experimental measurements. The inner cylinder shape and product isentrope are also exactly recovered in the limit of incompressible case motion. An alternate methodology also approximates the inner case shape and isentrope for compressible case motion, effectively allowing accurate isentrope determination for any cylinder test. The isentrope derived from a PBX 9502 cylinder test with compressible motion is shown to agree well with a reference isentrope. The errors associated with the one-dimensional flow assumption are also quantified. The incompressible case model can be used to estimate case shape and velocity from a given isentrope, providing a maximum fragment velocity.

sjackson@lanl.gov

2H13 COMPUTATIONAL ANALYSIS OF RE-IGNITION AND RE-INITIATION MECHANISMS OF QUENCHED DETONATION WAVES BEHIND A BACKWARD FACING STEP

Yu Lv, Matthias Ihme, Stanford University, United States

Re-ignition and re-initiation mechanisms of quenched detonation waves passing over a backward facing step are investigated by a high-resolution discontinuous Galerkin method, in which the reaction chemistry is described using a detailed chemical model. A stoichiometric Hydrogen/Oxygen mixture with different diluents (Argon and Nitrogen) is considered to assess effects of the mixture-composition and reactivity on the initiation process. It is found that the mixture reactivity and the spatio-temporal evolution of the diffracted detonation wave are critical in controlling formation and growth of the ignition kernels, and the possible transition to detonation. Due to curvature effects and the increasing shock angle, the incident shock-wave transitions from a regular reflection to a Mach reflection. Through parametric studies, it is shown that for more reactive Argon-diluted mixtures, ignition first appears behind the regular shock reflection, which is followed by spontaneous re-initiation through the SWACER-mechanism. By replacing Argon with Nitrogen, the reactivity reduces and re-ignition through Mach-reflection is observed. The subsequent re-initiation is primarily controlled by flame-acoustic and wave-wave interactions. Hot-spot re-initiation behind the Mach stem is not found due to the short ignition window that exists over the limited range of shock angles. A theoretical model is developed to confirm these findings and to quantify the coupling between incident shock-angle, thermodynamic state of the shock-compressed mixture, reactivity, and residence time. Effects of viscous-diffusive transport are assessed, and it is shown that viscous-dissipation at the wall promotes ignition and extends the detonation limit.

ylv@stanford.edu

WEDNESDAY PLENARY LECTURE: COMBUSTION NOISE

Ann P. Dowling, Yasser Mahmoudi, University of Cambridge, Cambridge, United Kingdom

Combustion noise is becoming increasingly important as a major noise source in aeroengines and ground based gas turbines. This is partially because advances in design have reduced the other noise sources, and partially because next generation combustion modes burn more unsteadily, resulting in increased external noise from the combustion. This review reports recent progress made in understanding combustion noise by theoretical, numerical and experimental investigations. We first discuss the fundamentals of the sound emission from a combustion region. Then the noise of open turbulent flames is summarized. We subsequently address the effects of confinement on combustion noise. In this case not only is the sound generated by the combustion influenced by its transmission through the boundaries of the combustion chamber, there is also the possibility of a significant additional source, the so-called 'indirect' combustion noise. This involves hot spots (entropy

fluctuations) or vorticity perturbations produced by temporal variations in combustion, which generate pressure waves (sound) as they accelerate through any restriction at the exit of the combustor. We describe the general characteristics of direct and indirect noise. To gain further insight into the physical phenomena of direct and indirect sound, we investigate a simple configuration consisting of a cylindrical or annular combustor with a low Mach number flow in which a flame zone burns unsteadily. Using a low Mach number approximation, algebraic exact solutions are developed so that the parameters controlling the generation of acoustic, entropic and vortical waves can be investigated. The validity of the low Mach number approximation is then verified by solving the linearized Euler equations numerically for a wide range of inlet Mach numbers, stagnation temperature ratios, frequency and mode number of heat release fluctuations. The effects of these parameters on the magnitude of the waves produced by the unsteady combustion are investigated. Finally, the magnitude of the indirect and direct noise generated in a model combustor with a choked outlet is analyzed for a wide range of frequencies, inlet Mach numbers and stagnation temperature ratios.

apd1@cam.ac.uk

3A01 SPATIO-TEMPORAL CHARACTERISTICS OF TEMPERATURE FLUCTUATIONS IN TURBULENT NON-PREMIXED JET FLAMES

Thomas A. McManus, Michael J. Papageorge, Frederik Fuest, Jeffrey A. Sutton, The Ohio State University, United States

We report new results from high-repetition-rate (10 kHz) 2D temperature imaging to characterize the temporally-fluctuating nature of the well-known DLR series of turbulent non-premixed jet flames. Specifically, we present temporally-based statistics of temperature fluctuations at multiple simultaneous spatial positions with a specific focus on characterizing the effects of Reynolds number. DLR B ($Re = 22,800$) was found to exhibit a much higher probability of large temporal gradients as compared to DLR A ($Re = 15,200$). While the higher Reynolds number should promote higher fluctuations, the levels were commensurate with an increased effect due to high levels of local flame extinction and re-ignition in DLR B as compared to DLR A. The joint probability density function between the temperature fluctuation and the natural logarithm of the square of the temporal gradient was examined as a function of axial position. For axial positions near the nozzle, both flames exhibited negative correlation between T' and the natural logarithm of the square of the temporal gradient. With increasing axial distance, DLR A exhibited statistical independence, while DLR B continued to exhibit a negative correlation between the two quantities. These results suggest a Reynolds number-dependence on the spatial development of statistical independence. Integral time scales also are reported for both flames as a function of axial and radial position. The integral time scales are seen to increase with increasing axial and radial position and decrease with increasing Reynolds number as expected from theory.

sutton.235@osu.edu

3A02 FIRST AND SECOND ORDER LAGRANGIAN CONDITIONAL MOMENT CLOSURE METHOD IN TURBULENT NONPREMIXED FLAMES

Karam Han, Kang Y. Huh, Pohang University of Science and Technology, Korea

The Lagrangian CMC method is developed by conditionally averaging the quantities associated with Lagrangian particles originating from the nozzle exit. It involves multiple flame groups of sequentially injected fuel, each of which shares the same conditional flame structure under the same residence time. The probability, p_k , to find the k^{th} group is assumed proportional to the partial mean mixture fraction, ξ^k , to obtain local flame structure as a weighted average by p_k . The Lagrangian CMC method allows flexibility of flamelet based methods and requires less computational load than Eulerian CMC. It is implemented in OpenFOAM and applied with first and second order closure to the piloted jet diffusion flames near extinction, Sandia Flame D and E. Results show good agreement for all conditional profiles and noticeable improvement by second order correction of four rate limiting steps in the GRI 3.0 mechanism. Good agreement is achieved for conditional variances and covariances among temperature and species involved in the rate limiting reaction steps.

huh@postech.ac.kr

3A03 A TABULATED CHEMISTRY CMC MODEL APPLIED TO A LIFTED METHANE-AIR JET FLAME

Olivier Colina, Jean-Baptiste Michela, IFP Energies Nouvelles, France

This paper explores the possibility to close the conditional reaction rate in the Conditional Moment Closure (CMC) turbulent combustion model using tabulated chemistry. This combination, called TCMC (Tabulated CMC), is based on the resolution of transport equations for the conditional mean and variance of the progress variable mass fraction $Y_c = Y_{CO} + Y_{CO_2}$ in which chemical source terms are taken from a look-up table built with homogeneous reactors calculations. First and second order TCMC closures (respectively TCMCI and TCMCII) are proposed and are compared on the lifted methane-air flame experiment of Cabra. In this configuration, it is shown that the first order model is unable to predict a lifted flame, whereas TCMCII gives correct results in terms of mean composition and temperature. These results are found comparable to those obtained by Michel with the ADF-PCM (Approximated Diffusion Flame Presumed Conditional Moment) flamelet model based on the same progress variable and tabulated kinetics. On the contrary, conditional flame profiles are different in the liftoff zone, and liftoff height predictions are improved with TCMCII.

Finally, the CPU time of TCMCII is found less than ten times that of ADF-PCM, using a unique mesh for all transport equations, which makes TCMC a realistic alternative to tabulated flamelet models.

olivier.colin@ifpen.fr

3A04 LARGE EDDY SIMULATION/CONDITIONAL MOMENT CLOSURE MODELING OF SWIRL-STABILIZED NON-PREMIXED FLAMES WITH LOCAL EXTINCTION

Huangwei Zhang¹, Andrew Garmory², Davide E. Cavaliere¹, Epaminondas Mastorakos¹

¹University of Cambridge, United Kingdom ²Loughborough University, United Kingdom

The Large Eddy Simulation (LES)/three-dimensional Conditional Moment Closure (3D-CMC) model with detailed chemistry and finite-volume formulation is employed to simulate a swirl-stabilized nonpremixed flame with local extinction. The results demonstrate generally good agreement with the measurements concerning velocity, flame shape, and statistics of flame lift-off, but the penetration of fuel jet into the recirculation zone is under-predicted possibly due to the over-predicted swirl velocities in the chamber. Localised extinctions are seen in the LES, in agreement with experiment. The local extinction event is shown by very low heat release rate and hydroxyl mass fraction and reduced temperature, and is accompanied by relatively high scalar dissipation. In mixture fraction space, CMC cells with strong turbulence-chemistry interaction and local extinction show relatively large fluctuations between fully burning and intermediate distributions. The probability density functions of conditional reactedness, which shows how far the conditionally-filtered scalars are from reference fully burning profiles, indicate that for CMC cells with local extinction, some reactive scalars demonstrate pronounced bimodality while for those cells with strong reactivity the PDFs are very narrow.

hz283@cam.ac.uk

3A05 FILTERED TABULATED CHEMISTRY FOR NON-PREMIXED FLAMES

A. Coussement, T. Schmitt, B. Fiorina, CNRS, France

The objective of the present study is to design a modeling strategy for LES of laminar diffusion flame regimes, i.e. without SGS wrinkling. A nonpremixed model dedicated to capture unresolved laminar flame structure is then proposed. For that purpose, the Filtered Tabulated Chemistry for Large Eddy Simulation is adapted to diffusion flames. A filtered look-up table computed from a collection of strained 1-D counterflow flames is generated. The filtered flame structure and thickness is captured with three controlling variables which are the filtered mixture fraction, the filtered progress variable and the filter size. This approach is successfully applied to 1-D and 2-D unresolved counter-flow flame simulations. The filter size governs the minimal thickness of the filtered thermal layer.

thomas.schmitt@ecp.fr

3A06 NUMERICAL AND EXPERIMENTAL INVESTIGATION OF TURBULENT DME JET FLAMES

Ankit Bhagatwala¹, Tianfeng Lu², Han Shen³, Jeffrey A. Sutton³, Jacqueline H. Chen¹

¹Sandia National Laboratories, United States ²University of Connecticut, United States ³The Ohio State University, United States

Results are presented here from direct numerical simulation of a temporally-evolving planar slot jet flame and an experimental measurements within spatially-evolving axisymmetric jet flame operating with DME (Dimethyl Ether, CH_3OCH_3) as the fuel. Both simulation and experiment are conducted at a Reynolds number of 13050. The Damköhler number, stoichiometric mixture fraction and fuel and oxidizer compositions also are matched between simulation and experiment. Simultaneous OH/CH_2O PLIF imaging is performed experimentally to characterize the spatial structure of the turbulent DME flames. The simulation shows a fully burning flame initially, which undergoes partial extinction and subsequently, reignition. The scalar dissipation rate (χ) increases to a value much greater than the laminar extinction value causing the extinction. As the turbulence decays, χ relaxes and the flame reignites. The reignition process is seen to be strongly dependent on the local χ value. Statistics of OH and CH_2O (formaldehyde) are compared between simulation and experiment and found to agree. The applicability of OH/CH_2O product imaging as a surrogate for peak heat release rate is investigated. The concentration product is found to predict peak heat release rate extremely well in the simulation data. When this product imaging is applied to the experimental data, a similar extinction/reignition pattern also is observed in the experiments as a function of axial position. A new 30-species reduced chemical mechanism for DME was also developed as part of this work.

abhagat@sandia.gov

3A07/ 3A08 TOPICAL REVIEW: SOLID COMBUSTION RESEARCH IN MICROGRAVITY AS A BASE OF FIRE SAFETY IN SPACE

Osamu Fujita, Hokkaido University, Japan

This paper introduces fire safety standards for flammability evaluation of solid material intended for use in a spacecraft habitat. Two types of existing standards include material evaluation by pass/fail criteria corresponding to Test 1

of NASA STD 6001B and evaluation by a flammability index such as maximum oxygen concentration (MOC) corresponding to the improved Test 1. The advantage of the latter is the wide applicability of the MOC index to different atmospheres in spacecraft. Additionally, the limiting oxygen index (LOI) method is introduced as a potential alternative index for the evaluation using the improved Test 1 method. When criteria based on an index such as MOC or LOI are applied for material screening, the discrepancy of the index to the actual flammability limit in microgravity such as minimum limiting oxygen concentration (MLOC) is essential information for guaranteeing fire safety in space because material flammability can be higher in microgravity. In this paper, the existing research on the effects of significant parameters on material flammability in microgravity are introduced, and the difference between the limiting value in microgravity and the indices given by the standard test methods on the ground is discussed. Finally, on-going efforts to develop estimation methods of material flammability in microgravity according to normal gravity tests are summarized.

ofujtia@eng.hokudai.ac.jp

3A09 STABILIZATION OF PILOTED TURBULENT FLAMES WITH INHOMOGENEOUS INLETS

S. Meares¹, V.N. Prasad¹, G. Magnotti², R.S. Barlow², A.R. Masri¹

¹The University of Sydney, Australia ²Sandia National Laboratories, United States

This paper investigates the stabilization mechanism of turbulent jet flames with highly inhomogeneous inlet conditions. A modification of the standard piloted burner is employed here with the addition of a central tube (inner) carrying fuel that can slide within the existing (outer) tube carrying air. Both tubes are located within the pilot annulus and inhomogeneity is varied by translating the inner tube upstream of the jet exit plane. Two flames with identical air/fuel ratios, bulk jet velocities and pilot conditions but different levels of homogeneity in the fuel/air mixture are selected for detailed investigations. Measurements are performed using Sandia's Raman-Rayleigh-LIF line facility, and Large Eddy Simulation (LES) using the stochastic fields approach are also conducted for the same flames. Results reported here focus on the early stabilization region. The flame with inhomogeneous inlet conditions is more stable being at 57% of blow-off compared to the homogeneous counterpart, which is at 78% of blow-off. It is found that, very close to the jet exit plane, premixed combustion dominates the flame with an inhomogeneous profile. This is in contrast to the homogeneous case, which behaves like a diffusion flame. Further downstream, but still within the pilot region, partial mixing starts to occur between richer samples and hot combustion products. A comparison of the relative conditional scalar dissipation rates, χ_r , shows that in the upstream region, and within the reactive limits, the homogeneous case has higher values of χ_r . Premixed combustion with higher rates of heat release and lower scalar dissipation rates in the near field are therefore key reasons for the improved stability of the flames with inhomogeneous inlets. These findings are corroborated by results from LES.

shaun.meares@sydney.edu.au

3A10 NUMERICAL SIMULATION OF OXY-FUEL JET FLAMES USING UNSTRUCTURED LES-CMC

A. Garmory¹, E. Mastorakos²

¹Loughborough University, United Kingdom ²University of Cambridge, United Kingdom

A finite volume Conditional Moment Closure (CMC) formulation has been developed as an LES sub-grid combustion model. This allows unstructured meshes to be used for both LES and CMC grids making the method more applicable to complex geometry. The method has been applied to an oxy-fuel jet flame. This flame offers new challenges to combustion modelling due to a high CO₂ content in the oxidiser stream and significant H₂ content in the fuel stream. The density ratio of the two streams is of the order 5 and the viscosity of the two streams will also differ. All the flames simulated showed localised extinction in the region around 3-5 jet diameters downstream of the nozzle, which is in very good agreement with the experiment. Trends for conditional and unconditional statistics with changing levels of H₂ in the fuel are correctly captured by the LES-CMC method, although different levels of agreement are observed for different species and temperature. This maybe due to the effect of differential diffusion not being included in the current formulation. The degree of extinction is also correctly predicted to increase as the H₂ content of the jet is reduced, showing the ability of the CMC method to predict complex turbulence-chemistry interaction phenomenon in the presence of changing fuel composition.

a.garmory@lboro.ac.uk

3A11 UNCERTAINTY QUANTIFICATION IN LES OF A TURBULENT BLUFF-BODY STABILIZED FLAME

Mohammad Khalil, Guilhem Lacaze, Joseph C. Oefelein, Habib N. Najm, Sandia National Laboratories, United States

We address the forward uncertainty quantification problem in Large-Eddy Simulation of a turbulent nonpremixed hydrocarbon flame, focusing on parametric uncertainty. More specifically, we examine the effect of uncertainty in the Smagorinsky constant and turbulent Prandtl and Schmidt numbers on specific quantities of interest. To conduct this analysis 25 LES simulations are performed, from which a surrogate model is build, based on polynomial chaos expansion, for the quantities of interest. This enables global sensitivity analysis and forward propagation of uncertainty, providing marginal and joint distributions on the outputs of interest. A non-intrusive polynomial chaos method is used to construct the surrogate models, avoiding the need to modify the deterministic LES forward solver. The accuracy of the surrogates is

examined using global error measures. The results provide insights on the underlying structure of the LES simulation, the impact of different parameters on specific observables, and correlations among different quantities of interest.

mkhalil@sandia.gov

3A12 EFFECT OF MOLECULAR TRANSPORT ON PDF MODELING OF TURBULENT FLAMES

Haifeng Wang, Kukjin Kim, Purdue University, United States

Comprehensive studies are performed to evaluate the effect of molecular transport on the Probability Density Function (PDF) modeling of turbulent flames. The widely used Sandia piloted jet flame E is chosen as the validation test case. Three configuration cases are considered: neglecting the molecular transport (Case-A), considering the molecular transport (Case-B), and considering both the molecular transport and its effect on mixing (Case-C). Extensive testing is done to assess the effect of molecular transport on the performance of the different mixing models and on the prediction of the flame extinction limit. It is found that the molecular transport has quite a significant effect on the prediction of the upstream mixing layer between the pilot stream and the coflow, where the turbulence level is weak or it is laminar and hence the molecular transport dominates the turbulent transport. Accounting for the molecular transport increases the models' resistance (for the IEM model and the modified Curl model) to flame extinction and yields a burning flame with a lower mixing rate that can cause global extinction without molecular transport. A modification to the mixing frequency is introduced to account for the effect of the molecular diffusion on mixing. With such a modification, the modeled flame sustainability is further enhanced and a lower mixing rate can be used, which enhances the ability of the IEM model and the modified Curl model which were previously found to yield a burning flame solution only at a highly increased rate of mixing.

haifeng@purdue.edu

3B01 COMBUSTION CHEMISTRY OF ALCOHOLS: EXPERIMENTAL AND MODELED STRUCTURE OF A PREMIXED 2-METHYLBUTANOL FLAME

A. Lucassen¹, S. Park², N. Hansen¹, S.M. Sarathy²

¹Sandia National Laboratories, United States ²King Abdullah University of Science and Technology, Saudi Arabia

This paper presents a detailed investigation of 2-methylbutanol combustion chemistry in lowpressure premixed flames. This compound is particularly interesting because it is a lignocellulosicbased, next-generation biofuel. The detailed chemical structure of a stoichiometric low-pressure (25 Torr) flame was determined using flame-sampling molecular-beam mass spectrometry. A total of 55 species were identified and subsequently quantitative mole fraction profiles as function of distance from the burner surface were determined. In an independent effort, a detailed flame chemistry model for 2-methylbutanol was assembled based on recent knowledge gained from combustion chemistry studies for butanol isomers and isopentanol (3-methylbutanol). Experimentally determined and predicted mole fraction profiles were compared to demonstrate the model's predictive capabilities, and to suggest areas where improvement is needed. Examples of individual mole fraction profiles are discussed together with the most significant fuel consumption pathways to highlight the combustion chemistry of 2-methylbutanol.

arnas.lucassen@gmail.com

3B02 UNDERSTANDING THE REACTION PATHWAYS IN PREMIXED FLAMES FUELED BY BLENDS OF 1,3-BUTADIENE AND N-BUTANOL

N. Hansen¹, M. Braun-Unkhoff², T. Kathrotia², A. Lucassen¹, B. Yang³

¹Sandia National Laboratories, United States ²German Aerospace Center –DLR, Germany ³Tsinghua University, China

The oxidation of 1,3-butadiene/*n*-butanol flames was studied in a combined experimental and modeling work. The goal is to provide a detailed combustion chemistry model that allows for identification of the important pathways for butadiene and butanol oxidation as well as the formation of soot precursors and aromates. Therefore, the chemical composition has been investigated for three low-pressure (20-30 torr) premixed flames, with different shares of butanol ranging between 25% to 75% compared to butadiene in 50% argon. Mole fraction profiles of reactants, products, and intermediates including C₃H_x and C₄H_x radicals as well as monoaromates such as benzyl radicals, were measured quantitatively as a function of height above burner surface employing flame-sampled Molecular-Beam Mass Spectrometry (MB-MS) utilizing photoionization with tunable vacuum-ultraviolet synchrotron radiation. The comparison of measured species profiles with modeling results provides a comprehensive view of the reaction model's quality and predictive capability, with respect to the combustion chemistry of the fuels considered. In general, a good agreement was found between experimental and modeled results. Reaction flux and sensitivity analysis were used to get more insight into the combustion of the fuel.

marina.braun-unkhoff@dlr.de

3B03 A COMPARATIVE STUDY OF N-PROPANOL, PROPANAL, ACETONE, AND PROPANE IN LAMINAR FLAMES

Jing Gong, Shuang Zhang, Yu Cheng, Zuohua Huang, Xi'an Jiaotong University, China

The laminar flame speeds of C₃ oxygenated fuels (*n*-propanol, propanal and acetone) and hydrocarbon (propane) were measured in a combustion bomb to compare the different combustion characteristics between alcohol, aldehyde,

ketone, and alkane. Propanal shows the highest flame speeds while acetone flame speeds give the lowest one. The experimental observations are further interpreted with chemical kinetic models. The effects of distinctive molecular structures on the fuel consumption pathways are clarified. Propanal can easily generate large H atom pool that enhances the oxidation, leading to the high flame speeds. However, acetone forms methyl radical (CH_3) and has lower flame speeds as the consequence. The subsequent maximum concentrations of H, OH and CH_3 confirm the analyses. It is found that propanal yields the highest H and OH concentrations while acetone produces the lowest H and OH concentrations among all tested fuels. Moreover, acetone presents higher CH_3 concentration, especially in fuel rich side. *n*-Propanol and propane show comparable flame speeds for the similarity of their intermediate species pool generated from the oxidation of fuels, especially H and OH. The different kinetics among the hydrocarbon series with the same carbon numbers can provide a horizontal view in the hierarchical hydrocarbon chemistry.

zhhuang@mail.xjtu.edu.cn

3B04 A DNS STUDY OF SELF-ACCELERATING CYLINDRICAL HYDROGEN-AIR FLAMES WITH DETAILED CHEMISTRY

Y.X. Xin¹, C.S. Yoo^{2,4}, J.H. Chen², C.K. Law^{1,3}

¹Princeton University, United States ²Sandia National Laboratories, United States ³Tsinghua University, China

⁴Ulsan National Institute of Science and Technology, Korea

The self-accelerating expanding cylindrical stoichiometric hydrogen-air flames at eight atmospheres were studied via two-dimensional Direct Numerical Simulation (DNS) of the full compressible Navier-Stokes equations with detailed chemistry. The flame morphology and propagation were finely resolved by the application of a time step of 2.5 ns and a grid size of 4 microns. Temporally, the intermittent, pulsating propagation of the flame front is captured through examining its propagation velocity. Spatially, the flame front is found to be comprised of segments exhibiting similar propagation properties, *i.e.* the intermittent instantaneous propagation of the flame front is attributed to the development of cellular structures induced by hydrodynamic instability. The long-term average propagation velocity of the flame front is described by a power law, with a self-acceleration exponent of 1.22 for the flame radius with respect to time. The increase in the global flame velocity is shown to be primarily a consequence of increased flame surface area, with the *local* front propagation velocity remaining largely at the constant laminar flame speed for the near-unity Lewis number mixture studied herein.

yxin@princeton.edu

3B05 DIFFERENTIAL DIFFUSION EFFECTS INCLUSION WITH FLAMELET GENERATED MANIFOLDS FOR THE MODELING OF STRATIFIED PREMIXED COOLED FLAMES

A. Donini, R.J.M. Bastiaans, J.A. van Oijen, L.P.H. de Goey, Eindhoven University of Technology, Netherlands

CFD predictions of flame position, stability and emissions are essential in order to obtain optimized combustor designs in a cost efficient way. However, the numerical modeling of practical combustion systems is a very challenging task. As a matter of fact, the use of detailed reaction mechanisms is necessary for reliable predictions, especially for highly diffusive fuels. Unfortunately, the modeling of the full detail of practical combustion equipment is currently prohibited by the limitations in computing power, given the large number of species and reactions involved. The Flamelet Generated Manifold (FGM) method reduces these computational costs by several orders of magnitude without losing too much accuracy. Hereby, FGM enables the application of reliable chemistry mechanisms in CFD simulations of combustion processes. In the FGM technique the progress of the flame is generally described by a few control variables. For each control variable a transport equation is solved during run-time. The flamelet system is computed in a pre-processing stage, and a manifold with all the information about combustion is stored in a tabulated form. In the present paper, the FGM model is implemented for the analysis of partially premixed non-adiabatic flames, including the effects of differential diffusion. Subsequently, a computational analysis of partially premixed non-adiabatic flames is presented. In this scope, a series of test simulations is performed using FGM for a two dimensional geometry, characterized by a distinctive stratified methane/air inlet, and compared with detailed chemistry simulations. The results indicate that detailed simulations are well reproduced with the FGM technique.

A.Donini@tue.nl

3B06 DIRECT NUMERICAL SIMULATIONS OF PROBE EFFECTS IN LOW-PRESSURE FLAME SAMPLING

Vyaas Gururajan¹, Fokion N. Egolfopoulos¹, Katharina Kohse-Höinghaus²

¹University of Southern California, United States ²Bielefeld University, Germany

Speciation studies of low-pressure flames using intrusive sampling and molecular beam mass spectrometry analysis are essential towards developing and validating combustion models. In order to assess potential probe-induced effects, direct numerical simulations of a realistic experimental configuration were carried out using a finite-volume fully compressible code as well as detailed descriptions of chemical kinetics and molecular transport. A 50 mbar rich propene/oxygen/argon flame was modeled for which experimental data are available. The effects of the probe and

supporting flange, non-adiabaticity, sampling location, and compressibility when there is suction through the sampling orifice were assessed. Results showed that even under adiabatic conditions, the presence of the probe-flange assembly affects the flow field two-dimensionally. Furthermore, the effects of heat loss and compressibility were found to be significant at the sampling location. Important radicals for fuel oxidation such as OH and HCO, and for soot formation such as C_3H_3 are affected by the sampling procedure and their concentrations at the sampling location can differ notably compared to unperturbed one-dimensional flames.

gururaja@usc.edu

3B07 EFFECT OF THERMAL EXPANSION ON FLAME PROPAGATION IN CHANNELS WITH NONSLIP WALLS

Berk Demirgok¹, Damir Valiev², Vyacheslav Akkerman¹

¹West Virginia University, United States ²Sandia National Laboratories, United States

Propagation of premixed flames in narrow channels is investigated by means of extensive direct numerical simulations of the complete system of combustion and hydrodynamic equations, incorporating transport properties (thermal conduction, diffusion and viscosity) and Arrhenius chemical kinetics. The system includes the continuity and Navier-Stokes equations as well as those for the energy and species balances. A flame propagates from the closed end of a channel to the open one. An initially planar flame front gets corrugated due to wall friction and thereby accelerates. The main characteristics of the flame acceleration such as the flame shape, propagation speed and acceleration rate are scrutinized. It is demonstrated that the acceleration promotes with the thermal expansion coefficient, Θ , but weakens with the Reynolds number related to the flame propagation, Re . The present computational results support the theoretical prediction of Bychkov in a wide range of Θ and Re . While very good quantitative and qualitative agreement between computational and analytical results is found for realistically large thermal expansion, $8 \leq \Theta \leq 12$, it deteriorates with the decrease in Θ . Specifically, the theory and modeling do not agree, quantitatively, for $6 \leq \Theta \leq 8$, but they demonstrate a qualitative resemblance (the exponential state of acceleration) if Re is small enough. Finally, the exponential acceleration has never been observed for $\Theta < 6$, hence the theory completely breaks in that case. On the other hand, the latter result fits other works in this field and thereby allows reconciling various formulations on the flame acceleration.

Vyacheslav.Akkerman@mail.wvu.edu

3B08 AN ASYMPTOTIC STUDY OF THE TRANSITION FROM SLOW TO FAST BURNING IN NARROW CHANNELS

L. Kagan¹, P. Gordon², G. Sivashinsky¹

¹Tel Aviv University, Israel ²The University of Akron, United States

Motivated by recent theoretical developments in the dynamics of slow isobaric flames evolving in narrow channels (thick flames), the present study is concerned with non-isobaric flames. A reduced Darcy-like one-dimensional model capable of capturing an abrupt transition from slow conduction-driven to fast compression-driven burning is derived through an appropriate asymptotic procedure. Specifically, the adopted approach is based on the distinguished limit where the scaled width of the channel is deemed comparable to the system's Mach number, used as a parameter of expansion. The transition is caused by the friction-induced gradual pile up of the pressure and formation of an extended preheat zone adjacent to the advancing front. Upon some induction period this development leads to a localized thermal explosion triggering the transition.

kaganleo@post.tau.ac.il

3B09 SELF-ACCELERATING FLAMES IN LONG NARROW CHANNELS

Vadim N. Kurdyumov¹, Moshe Matalon²

¹CIEMAT, Spain ²University of Illinois at Urbana-Champaign, United States

In this work we extend our earlier asymptotic one-dimensional results of flame propagation in long narrow channels open at both ends to two-dimensional flames. The analysis follows two tracks; a multi-scale asymptotic study that assumes that the channel height is much smaller than its length, in which case the flame propagates quasi-steadily throughout the channel, and a full numerical study of the unsteady propagation. During the early stages of propagation the flame accelerates at a nearly constant rate, independent of the channel height. In sufficiently narrow channels, the flame retains a constant acceleration until it reaches the end of the channel, consistent with our earlier work. In wider channels, however, the flame begins to accelerate at an increasingly faster rate when it reaches a certain, reaching exceedingly large speeds at the end of the channel. We show that the self-acceleration of the flame is due to the combined effects of gas expansion and lateral flame confinement. The gas expansion that results from the heat released by the chemical reactions produces a continuous flow of burned gas directed towards the ignition end and sets a pressure gradient that drives the fresh unburned gas towards the other end of the channel. Thriving for fuel, the flame extends towards the fresh mixture and propagates faster and, because of the lateral confinement, the gas expansion induces large straining on the elongated flame surface that further increases its propagation speed. The asymptotic approximation properly predicts the initial propagation stage, the location within the channel where the sudden acceleration begins and the early stages of the self-accelerating process. When the propagation speed becomes sufficiently large, the quasi-steady approximation fails. The full numerical

study confirms and extends the asymptotic results, showing that in long but finite channels premixed flames could self-accelerate reaching velocities that are ten-to-twenty times larger than the laminar flame speed.

vadim.k@ciemat.es

3B10 ELECTRON IONIZATION, PHOTOIONIZATION AND PHOTOELECTRON/PHOTOION COINCIDENCE SPECTROSCOPY IN MASS-SPECTROMETRIC INVESTIGATIONS OF A LOW-PRESSURE ETHYLENE/OXYGEN FLAME

Daniel Felsmann¹, Kai Moshhammer¹, Julia Kruger¹, Alexander Lackner¹, Andreas Brockhinke¹, Tina Kasper², Thomas Bierkandt², Erdal Akyildiz², Nils Hansen³, Arnas Lucassen³, Patrick Oßwald⁴, Markus Kohler⁴, Gustavo A. Garcia⁵, Laurent Nahon⁵, Patrick Hemberger⁶, Andras Bodí⁶, Thomas Gerber⁶, Katharina Kohse-Höinghaus¹

¹Bielefeld University, Germany ²University of Duisburg-Essen, Germany ³Sandia National Laboratories, United States

⁴German Aerospace Center, Germany ⁵Synchrotron SOLEIL, France ⁶Swiss Light Source, Switzerland

Quantitative species data for the development and critical examination of combustion mechanisms are in high demand regarding the need for predictive combustion models that may assess the emission potential of current and emerging fuels. Mass spectrometric investigation is one of the often-used techniques to provide mole fractions of stable and reactive intermediates including radicals from specifically designed laboratory experiments. Molecular-Beam Mass Spectrometry (MBMS) has been coupled with Electron Ionization (EI) and Photoionization (PI) to determine the species compositions, and combinations of these techniques have been successful in the investigation of the combustion pathways in flames of numerous hydrocarbon, oxygenated and nitrogenated fuels. As a novel diagnostics to be combined with flame-sampling mass spectrometry, Photoelectron/Photoion Coincidence spectroscopy (PEPICO) has recently emerged, and its potential as a complement of existing techniques is just about being explored. In a multi-laboratory investigation, the present study has thus combined four different MBMS spectrometers (in Bielefeld, Germany, the Advanced Light Source in Berkeley, USA, the Swiss Light Source in Villigen, Switzerland and the SOLEIL synchrotron in St. Aubin, France) to study a rich premixed argon-diluted lowpressure (40 mbar) ethylene-oxygen flame under comparable conditions. This was done with the aim of illustrating the respective properties and capabilities of the methods under these conditions, with an emphasis on the power offered by the synchrotron-based techniques, including PEPICO, for combustion chemistry studies. Examples include comparisons of selected species quantification as well as PEPICO spectra measured at different instruments.

kmoshhammer@uni-bielefeld.de

3B11 VALIDATION OF A NOVEL NUMERICAL MODEL FOR THE ELECTRIC CURRENTS IN BURNER-STABILIZED METHANE-AIR FLAMES

N. Speelman¹, M. Kiefer², D. Markus³, U. Maas⁴, L.P.H. de Goey¹, J.A. van Oijen¹

¹Eindhoven University of Technology, The Netherlands ²Bosch Thermotechnik GmbH, Germany

³Physikalisch-Technische Bundesanstalt, Germany ⁴Karlsruhe Institute of Technology, Germany

This study presents measurements of electrical currents in flat flames, induced by externally applied electrical potentials. In addition to these measurements, a theoretical and numerical model for ionized methane-air flames was developed to predict the electric currents based on the charged particle distribution in the flame. Our model comprises Poisson's equation and a multi-component diffusion model in order to incorporate an electric field in the existing CHEM1D combustion software. A comparison of the numerical simulations and experimental data showed a good agreement in the observed current-voltage characteristic for different electrode distances. The model also predicts the dependence of the saturation current on the equivalence ratio well for lean mixtures. Deviations were found in the rich regime, which are largely attributed to shortcomings in the chemical mechanism. For strong applied electric fields the electric current is independent of the applied field strength. This saturation effect is caused by the depletion of electrons from the flame plasma and a domination of the electric forces over Fick diffusion for the cations. According to the simulations, the diodic effect is mostly defined by the distance that the heavier and less mobile ions have to travel to reach the negatively charged electrode.

n.speelman@tue.nl

3B12 NO FORMATION/REDUCTION MECHANISMS OF AMMONIA/AIR PREMIXED LAMINAR FLAMES AT VARIOUS EQUIVALENCE RATIOS AND AMBIENT PRESSURES

Akihiro Hayakawa, Takashi Goto, Rentaro Mimoto, Taku Kudo, Hideaki Kobayashi, Tohoku University, Japan

Ammonia is one of a carbon-free fuels and its application to internal combustion engines are expected. However, few studies of ammonia flame, especially at high pressure, were carried out because ammonia had not been supposed to use as a fuel due to its lower combustion characteristics. The most of NO_x which is formed from ammonia flame is considered to be a fuel NO_x. The objectives of this study were to investigate experimentally the fundamental characteristics, such as NO emission and chemiluminescence, of ammonia/air flame not only at atmospheric pressure but also under high pressure and to explore NO formation/reduction mechanism using numerical simulation. Experiments were

carried out using a nozzle-type burner. The NH_2 ammonia alpha band spectra were observed and it found that it decided the color of ammonia flame. A burned gas was sampled from the burner stabilized ammonia flame. The mole fraction of NO decreased with the increase in equivalence ratio at atmospheric pressure. Reaction path analysis was performed and it was clarified that the decrease in mole fraction of NO for rich mixtures was caused by the reduction of by NH_i ($i = 2, 1, 0$). A high pressure experiments were performed using a high pressure combustion facility for stoichiometric ammonia flame. As a results, the decrease in the mole fraction of NO was experimentally observed and its tendency was qualitatively agreed with the results of numerical simulation. It was clarified that the third body reaction $\text{OH} + \text{H} + \text{M} = \text{H}_2\text{O} + \text{M}$ played an important role in the reduction of mole fraction of NO at high pressure.

hayakawa@flame.ifs.tohoku.ac.jp

3C01 TOWARDS A QUANTITATIVE UNDERSTANDING OF THE ROLE OF NON-BOLTZMANN REACTANT DISTRIBUTIONS IN LOW-TEMPERATURE OXIDATION

Michael P. Burke, C. Franklin Goldsmith, Yuri Georgievskii, Stephen J. Klippenstein, Argonne National Laboratory, United States

An essentially universal assumption of chemical kinetics is that bimolecular reactions only occur between reactants of rovibrational energy described by a Boltzmann (thermal) distribution. Given that the O_2 mole fraction is roughly 20% under nearly all relevant low-temperature combustion situations, there is significant potential for molecules to undergo reactive collisions with O_2 on the same time scale as the energy-transferring collisions necessary to achieving a Boltzmann distribution. Within the context of low-temperature combustion, this phenomenon conceivably gives rise to an entirely non-Boltzmann sequence involving multiple reactions of fuel-derived radicals with O_2 to produce multiple OH radicals. Given the complex interplay among simultaneous internal isomerizations, energy-transferring collisions, dissociations and reactive collisions across multiple reaction surfaces, estimating the extent of deviations from conventional thermal assumptions is not straightforward. A novel methodology is presented for quantifying the role on non-Boltzmann reactant distributions in order to establish a better understanding of the nature of these effects and their magnitude. As a case study, we implement the methodology to explore the effect of non-Boltzmann reactants on product branching fractions of the $\text{QOOH}^* + \text{O}_2$ reaction from *n*-propyl oxidation as well as its associated dependence with O_2 mole fraction, temperature, and pressure. While we do not anticipate that non-Boltzmann reaction sequences will substantially alter ignition predictions at higher pressures (at least for propane), it appears that consideration of non-Boltzmann reaction sequences may be required for interpretations of experimental measurements commonly used to investigate the $\text{R} + \text{O}_2$ and $\text{QOOH} + \text{O}_2$ reactions central to engine-relevant ignition behavior. With regard to observable signatures of these effects in experiments, the presence of a stronger-than-usual O_2 mole fraction dependence may be a likely indicator of non-Boltzmann $\text{QOOH}^* + \text{O}_2$ behavior.

mpburke@anl.gov

3C02 PROBING THE LOW-TEMPERATURE CHAIN-BRANCHING MECHANISM FOR *N*-BUTANE AUTOIGNITION CHEMISTRY VIA TIME-RESOLVED MEASUREMENTS OF KETOHYDROPEROXIDE FORMATION IN PHOTOLYTICALLY INITIATED *N*- C_4H_{10} OXIDATION

A.J. Eskola, O. Welz, J. Zádor, I.O. Antonov, L. Sheps, J.D. Savee, D.L. Osborn, C.A. Taatjes Sandia National Laboratories, United States

Ketohydroperoxide formation in Cl-atom initiated low-temperature (550 K – 700 K) oxidation of *n*-butane was investigated using a time-of-flight *m/z* spectrometer and either tunable synchrotron radiation or ~ 10.2 eV fixed energy for ionization. Experiments were performed at 1 – 2 atm pressure using a new high-pressure reactor and also at ~ 5 Torr pressure for comparison. Direct kinetic observations of ketohydroperoxide formation qualitatively agree with previous atmospheric pressure jetstirred reactor studies of Battin-Leclerc where the maximum ketohydroperoxide signal was observed near 600 K. Oxidation of partially deuterated *n*-butanes provided additional information on QOOH radical intermediates involved in ketohydroperoxide formation. The photoionization spectrum of the observed ketohydroperoxide signal is independent of pressure and is the same when using different deuterium substituted *n*-butanes, suggesting that one isomer is essentially prevalent in *n*-butane oxidation. It is concluded that 4-hydroperoxy-2-butyl + O_2 is the main reaction leading to ketohydroperoxide and 3-hydroperoxybutanal is the dominant ketohydroperoxide that is observed.

cataatj@sandia.gov

3C03 QUANTITATIVE MEASUREMENTS OF HO_2 / H_2O_2 AND INTERMEDIATE SPECIES IN LOW AND INTERMEDIATE TEMPERATURE OXIDATION OF DIMETHYL ETHER

Naoki Kurimoto, Brian Brumfield, Xueliang Yang, Tomoya Wada, Pascal Diévert, Gerard Wysocki, Yiguang Ju Princeton University, United States

As two of the most important species that characterize hydrocarbon low temperature ignition, HO_2 and H_2O_2 formation during Dimethyl Ether (DME) oxidation was quantified using the same experimental conditions, for the first time, in an atmospheric flow reactor at low and intermediate temperature range. Dual-Modulation Faraday Rotation Spectroscopy (DM-FRS) and Molecular Beam Mass Spectrometry (MBMS) were used to measure HO_2 and H_2O_2

respectively. DME and other important intermediate species such as CH_2O and CO are also measured by MBMS between 500 and 1150 K at different fuel concentrations. Species profiles in the reactor were calculated by using both zero- and two-dimensional computations with different detailed kinetics for cross-validation and comparison with experimental results. The models predict adequately the low and intermediate oxidation temperature windows near 600 K and 1000 K, respectively. However, both models overpredicted the DME consumption as well as CO , HO_2 and H_2O_2 formations at the low temperature oxidation window by more than a factor of four. Moreover, although the model predicted reasonably well the formation of CH_2O and CO/CO_2 at the intermediate temperature oxidation window, the concentration of H_2O_2 was also over-predicted, suggesting the large uncertainties existing in the DME low temperature chemistry and in HO_2 chemistry at intermediate temperature. Furthermore, to analyze the uncertainty of the low temperature chemistry, a QOOH branching ratio using measured CH_2O to CO concentrations was derived. The comparison between modeled and measured QOOH branching ratio suggests that the branching ratio of QOOH decomposition to CH_2O is too low in the current DME models.

kurimoto@princeton.edu

3C04 EFFECT OF NON-THERMAL PRODUCT ENERGY DISTRIBUTIONS ON KETOHYDROPEROXIDE DECOMPOSITION KINETICS

C. Franklin Goldsmith, Michael P. Burke, Yuri Georgievskii, Stephen J. Klippenstein, Argonne National Laboratory, United States

The decomposition of ketohydroperoxides (OQ'OOH) to two radicals is commonly predicted to be the key chain branching step in low-temperature combustion. The possibility of a direct decomposition of the OQ'OOH from its initially produced energy distribution is studied with a combination of Master Equation (ME) and direct trajectory simulations. The temperature and pressure dependent rate constants for the thermal decomposition of a ketohydroperoxide, $\text{HOCH}_2\text{CH}_2\text{CHO}$, to four product channels were computed using RRKM/ME methods. Direct dynamics calculations were initiated from a transition state in the $\text{O}_2 + \text{QOOH}$ reaction network to understand the fraction of energy in that transition state that is converted into the internal energy of the OQ'OOH . A novel approach to solving the master equation is used to determine the probability that a vibrationally hot OQ'OOH either will be stabilized to a thermal distribution or will react to form new products. Under most conditions, the majority of vibrationally excited OQ'OOH will be quenched into a thermal distribution. At higher internal energies and lower pressures, however, a significant fraction of the hot OQ'OOH will decompose rather than thermalize. Proper interpretation of low-pressure experiments may require inclusion of vibrationally hot intermediates, particularly if a chemical kinetic mechanism is optimized against the low-pressure data.

sjk@anl.gov

3C05 AN ANALYTICAL APPROXIMATION FOR LOW- AND HIGH-TEMPERATURE AUTOIGNITION FOR DIMETHYL ETHER - AIR MIXTURES

J. Beeckmann, L. Cai, A. Berens, N. Peters, H. Pitsch, RWTH Aachen University, Germany

Dimethyl ether has proven to be one of the most attractive alternatives to traditional fossil oil derived fuels for compression ignition engines. In this study, a skeletal mechanism consisting of 32 species and 49 elementary reactions, based on the detailed mechanism proposed by Fischer, is further reduced to a short 36-step mechanism describing first and second stage ignition as well as the rapid transition to final products. A global 4-step mechanism is derived by introducing steady state assumptions of intermediate species. An analytical solution for the ignition delay times of the first stage of ignition in the low temperature regime and the beginning of its transition to the intermediate temperature regime is presented. The important competition of the β -scission and the reaction with molecular oxygen of the hydroperoxy-methoxymethyl radical ($\text{C}_2\text{OCH}_2\text{O}_2\text{H}$) is quantified by the introduction of a parameter β , related to the competition of chain-branching and chain-propagation. The calculated values agree very well with those of the 36-step mechanism. Also for the high temperature regime, an analytical solution is presented, which agrees well with the experiments and the values calculated with the 36-step mechanism.

jbeeckmann@itv.rwth-aachen.de

3C06 IGNITION DELAY TIMES OF DIETHYL ETHER MEASURED IN A HIGH-PRESSURE SHOCK TUBE AND A RAPID COMPRESSION MACHINE

M. Werler¹, L.R. Cancino², R. Schiessl¹, U. Maas¹, C. Schulz², M. Fikri²

¹Karlsruhe Institute of Technology, Karlsruhe, Germany ²University of Duisburg-Essen, Germany

Ignition delay times of Diethyl Ether (DEE)/air/argon mixtures were studied in a shock tube at various equivalence ratios in the temperature range from 900 to 1250 K at pressures of 10, 20, and 40 bar and in a rapid compression machine (RCM) between 500 and 1060 K at pressures between 2.5 and 13 bar. The RCM results show that ignition delay times of DEE exhibit a pronounced region (between 590 and 800 K) where ignition delay times are weakly temperature dependent only while above 833 K and below 590 K, the ignition delay times are strongly temperature dependent. Two-stage ignition was observed in the temperature range from 500 to 665 K in the RCM measurements. At the conditions of the shock tube a strong pressure and temperature dependence was observed, but no NTC behavior was found

within the investigated temperature range. A modified mechanism based on the original model from (Yasunaga et al. 2010) well describes the measurements.

mustapha.fikri@uni-due.de

3C07 A COMPUTATIONAL STUDY ON THE KINETICS OF UNIMOLECULAR REACTIONS OF ETHOXYETHYLPEROXY RADICALS EMPLOYING CTST AND VTST

Yasuyuki Sakai¹, Hiromitsu Ando¹, Harish Kumar Chakravarty², Heinz Pitsch², Ravi X. Fernandes³

¹University of Fukui, Japan ²RWTH Aachen University, Germany ³Physikalisch-Technische Bundesanstalt, Germany

Diethyl Ether (DEE) has favorable properties as a diesel fuel component, including its outstanding cetane number. To utilize this promising fuel, more and more knowledge on the chemical kinetics of DEE oxidation will be required. For the present article, the rate constants of unimolecular reactions of ethoxyethylperoxy radicals, which are main intermediates in the oxidation of DEE under the engine relevant conditions, have been computationally investigated and compared with those of alkanes. Geometries, vibrational frequencies, and energies of reactants, products, and transition states were calculated according to the procedure of the CBS-QB3 method. The high-pressure limiting rate constants were estimated in the temperature range of 500 – 2000 K by using a conventional transition state theory and variational transition state theory with hindered rotor approximation for low frequency torsional modes for both reactants and transition states. Intrinsic reaction coordinate calculations have been performed in order to verify the connectivity between transition states and local minima. It was found, in comparison with alkanes, that some low-temperature oxidation reactions are influenced by the oxygen atom in the ether group. For instance, the rate constant of intramolecular 1,5-hydrogen shift reactions for 1-ethoxyethylperoxy radical is 5.6 times larger than that of alkyl peroxy radicals at 700 K. The subsequent β -fission reaction of this hydrogen shift product is 150 times faster than that of alkyl hydroperoxy radicals. These characteristic rate constants are given in three-parameter modified Arrhenius form for the refinement of predictive chemical kinetic models being developed.

y_sakai@u-fukui.ac.jp

3C08 CHLORINE ATOM-INITIATED LOW-TEMPERATURE OXIDATION OF PRENOL AND ISOPRENOL: THE EFFECT OF C=C DOUBLE BONDS ON THE PEROXY RADICAL CHEMISTRY IN ALCOHOL OXIDATION

Oliver Welz, John D. Savee, David L. Osborn, Craig A. Taatjes

Sandia National Laboratories, United States

The chlorine atom-initiated oxidation of two unsaturated primary C₅ alcohols, prenol (3-methyl-2-buten-1-ol, (CH₃)₂CCHCH₂OH) and isoprenol (3-methyl-3-buten-1-ol, CH₂C(CH₃)CH₂CH₂OH), is studied at 550 K and low pressure (8 Torr). The time- and isomer-resolved formation of products is probed with multiplexed photoionization mass spectrometry (MPIMS) using tunable vacuum ultraviolet ionizing synchrotron radiation. The peroxy radical chemistry of the unsaturated alcohols appears much less rich than that of saturated C₄ and C₅ alcohols. The main products observed are the corresponding unsaturated aldehydes – prenal (3-methyl-2-butenal) from prenol oxidation and isoprenal (3-methyl-3-butenal) from isoprenol oxidation. No significant products arising from QOOH chemistry are observed. These results can be qualitatively explained by the formation of resonance stabilized allylic radicals via H-abstraction in the Cl + prenol and Cl + isoprenol initiation reactions. The loss of resonance stabilization upon O₂ addition causes the energies of the intermediate wells, saddle points, and products to increase relative to the energy of the initial radicals and O₂. These energetic shifts make most product channels observed in the peroxy radical chemistry of saturated alcohols inaccessible for these unsaturated alcohols. The experimental findings are underpinned by quantum-chemical calculations for stationary points on the potential energy surfaces for the reactions of the initial radicals with O₂. Under our conditions, the dominant channels in prenol and isoprenol oxidation are the chain-terminating HO₂-forming channels arising from radicals, in which the unpaired electron and the OH group are on the same carbon atom, with stable prenal and isoprenal co-products, respectively. These findings suggest that the presence of C=C double bonds in alcohols will reduce low-temperature reactivity during autoignition.

onwelz@sandia.gov

3C09 KINETICS OF THE HIGH-TEMPERATURE COMBUSTION REACTIONS OF DIBUTYLETHER USING COMPOSITE COMPUTATIONAL METHODS

Mariam J. Al Rashidi¹, Alexander C. Davis², S. Mani Sarathy¹

¹King Abdullah University of Science and Technology, Saudi Arabia ²National Institute of Standards and Technology, United States

This paper investigates the high-temperature combustion kinetics of Dibutyl Ether (DBE), including unimolecular decomposition, H-abstractions by H, H-migrations, and C-C/C-O β - scission reactions of the DBE radicals. The energetics of H-abstraction by OH radicals is also studied. All rates are determined computationally using the CBS-QB3 and G4 composite methods in conjunction with conventional transition state theory. The B3LYP/6- 311++G(2df,2pd) method is used to optimize the geometries and calculate the frequencies of all reactive species and transition states for use in ChemRate. Some of the rates calculated in this study vary markedly from those obtained for similar reactions of alcohols or

alkanes, particularly those pertaining to unimolecular decomposition and β -scission at the α - β C-C bond. These variations show that analogies to alkanes and alcohols are, in some cases, inappropriate means of estimating the reaction rates of ethers. This emphasizes the need to establish valid rates through computation or experimentation. Such studies are especially important given that ethers exhibit promising biofuel and fuel additive characteristics.

mariam.elrachidi@kaust.edu.sa

3C10 PYROLYSIS OF ETHANOL: A SHOCK-TUBE/TOF-MS AND MODELING STUDY

Johannes Kiecherer, Cornelia Bansch, Tobias Bentz, Matthias Olzmann, Karlsruher Institut für Technologie, Germany

The pyrolysis of ethanol was studied in a shock tube behind reflected shock waves in the temperature range 1300-1510 K at pressures of about 1.1 bar by using time-of-flight mass spectrometry for detection. For the first time, concentration-time profiles of $\text{C}_2\text{H}_5\text{OH}$, $\text{C}_2\text{H}_4\text{O}$, $(\text{C}_2\text{H}_2 + \text{C}_2\text{H}_4 + \text{C}_2\text{H}_6)$, H_2O , and CH_4 were simultaneously recorded. It could be shown that under our experimental conditions the major products are H_2O and C_2H_4 which are mainly formed in the reaction $\text{C}_2\text{H}_5\text{OH} \rightarrow \text{C}_2\text{H}_4 + \text{H}_2\text{O}$ (R1). From the measured concentration-time profiles of H_2O , the rate coefficient of reaction (R1) could be directly determined. The results can be expressed by the Arrhenius equation $k_1(T, P \sim 1.1 \text{ bar}) = (2.5 \pm 1.0) \cdot 10^{10} \exp(-23320 \text{ K}/T) \text{ s}^{-1}$ with an estimated uncertainty of $\pm 40\%$. The experimental concentration-time profiles were modeled with a mechanism from Marinov, and a very good agreement was found. Moreover, rate coefficients for the most important decomposition steps of ethanol were calculated from statistical rate theory by solving a thermal multichannel master equation. In addition to (R1) the barrierless bond fission channels $\text{C}_2\text{H}_5\text{OH} \rightarrow \text{CH}_3 + \text{CH}_2\text{OH}$ (R2) and $\text{C}_2\text{H}_5\text{OH} \rightarrow \text{C}_2\text{H}_5 + \text{OH}$ (R3) were taken into account. The specific rate coefficients were obtained from RRKM theory (R1) and the Statistical Adiabatic Channel Model (R2 and R3) with molecular and transition state data from quantum chemical calculations at CCSD(T)-F12/def2-QZVPP//MP2/ccpVQZ level of theory. The results were fitted to recently published experimental values of k_1 , k_2 , and k_3 . The calculated rate coefficients give a similar good representation of the concentration-time profiles if inserted in the Marinov mechanism.

matthias.olzmann@kit.edu

3C11 PYROLYSIS OF 2-METHYL-1-BUTANOL AT LOW AND ATMOSPHERIC PRESSURES: MASS SPECTROMETRY AND MODELING STUDIES

Xiaoyuan Zhang¹, BinYang², Wenhao Yuan¹, Zhanjun Cheng¹, Lidong Zhang¹, Yuyang Li¹, Fei Qi¹

¹University of Science and Technology of China, China ²Tsinghua University, China

In order to better understand the high temperature chemistry of large alcohol containing 5 carbon atoms, the pyrolysis of 2-methyl-1-butanol from 750 to 1400 K was investigated in a flow reactor at the pressures of 30 and 760 Torr. About 25 pyrolysis species including some radicals and reactive intermediates were identified and quantified using synchrotron vacuum ultraviolet photoionization mass spectrometry. A kinetic model with 177 species and 994 reactions was developed and tested by the measured molefraction profiles of pyrolysis species. Rate Of Production (ROP) and sensitivity analysis were used to reveal the decomposition characters of 2-methyl-1-butanol and the effect of pressure. Compared with butanol isomers, the contributions of unimolecular reactions in 2-methyl-1-butanol are much lower than H abstraction reactions, which show a similar decomposition rule of *i*-butanol rather than 1-butanol.

byang@tsinghua.edu.cn

3C12 AN EXPERIMENTAL AND MODELING STUDY OF *N*-OCTANOL COMBUSTION

Liming Cai¹, Yasar Uygur¹, Casimir Togbé², Heinz Pitsch¹, Herbert Olivier¹, Philippe Dagaut², S. Mani Sarathy³

¹RWTH Aachen University, Germany ²CNRS-INSIS, France ³King Abdullah University of Science and Technology, Saudi Arabia

This study presents the first investigation on the combustion chemistry of *n*-octanol, a long chain alcohol. Ignition delay times were determined experimentally in a high-pressure shock tube, and stable species concentration profiles were obtained in a jet stirred reactor for a range of initial conditions. A detailed kinetic model was developed to describe the oxidation of *n*-octanol at both low and high temperatures, and the model shows good agreement with the present dataset. The fuel's combustion characteristics are compared to those of *n*-alkanes and to short chain alcohols to illustrate the effects of the hydroxyl moiety and the carbon chain length on important combustion properties. Finally, the results are discussed in detail.

lcai@itv.rwth-aachen.de

3D01 KEY PARAMETERS GOVERNING THE PRECESSING VORTEX CORE IN REACTING FLOWS: AN EXPERIMENTAL AND ANALYTICAL STUDY

S. Terhaar¹, K. Oberleithner², C.O. Paschereit¹

¹Technische Universität Berlin, Germany ²Monash University, Australia

This report deals with an experimental and analytical study of the occurrence of self-excited hydrodynamic instabilities in swirling combustor flows. Different flow field types are measured for varying combustor operating

conditions using stereoscopic particle image velocimetry. The properties of the flow field are connected to the flame shapes encountered. It is shown that the appearance of a helical flow instability, featuring a precessing vortex core, is strongly dependent on the flame shape. Flames attached to the burner exit may suppress the precessing vortex core if the flame features a sufficient length, while suppression is not observed for very short attached and all detached flames. Linear hydrodynamic stability analysis is carried out on the time-averaged flow, yielding an excellent prediction of the instability frequency and the wavemaker location and proving that the self-excited oscillations are driven by a hydrodynamic instability. A parametric model study investigating the role of the backflow velocity, the swirl intensity, and the density distribution is carried out, revealing that the backflow on the jet axis and the density gradient in the shear layer are essentially the parameters that determine the suppression or excitation of the instability.

steffen.terhaar@tu-berlin.de

3D02 TRANSIENT EFFECTS OF FUEL-AIR MIXING IN A PARTIALLY-PREMIKED TURBULENT SWIRL FLAME

M. Stöhr, C.M. Arndt, W. Meier, German Aerospace Center, Germany

Unsteady interactions of flow, fuel-air mixing and reaction in a lean partially-premixed turbulent swirl flame are investigated using simultaneous PIV, OHPLIF and acetone-PLIF with a repetition rate of 10 kHz. The flame is operated with methane and air in a gas turbine model combustor at ambient temperature and pressure. Transport and mixing of fuel is visualized by fluorescence of acetone, which was added with 9% by volume to the methane and was verified to have no major effects on the flame characteristics. The dominant unsteady flow structures are a Precessing Vortex Core (PVC) in the shear layer of the inner recirculation zone and the Lower Stagnation Point (LSP) at the flame root. The measurements show that fuel and air entering the combustion chamber are at first largely unmixed. The PVC, however, periodically passes through the unmixed gas and causes strong mixing. A well-mixed zone of unburned fuel and air is formed around the vortex, and then ignited by recirculating burned gas. Subsequently, the PVC causes a roll-up of the reaction zone, which in turn leads to a strong local heat release. At the flame root, the PVC induces periodic changes in the composition of the unburned gas, which varies between pure air and well-mixed fuel and air. Reaction is locally quenched at the LSP during phases where fresh air without fuel is present. Subsequently, fuel and air are entrained and mixed by the PVC and ignited at the boundary of recirculating burned gas. Reaction at the flame root then reappears until the next local quenching event. Generally, the results show that the strong enhancement of fuel-air mixing induced by the PVC contributes significantly to the stabilization of the flame, and that the flame dynamics can only be properly understood when an analysis of transient mixing mechanisms is included.

michael.stoehr@dlr.de

3D03 REACTING FLOW IN AN INDUSTRIAL GAS TURBINE COMBUSTOR: LES AND EXPERIMENTAL ANALYSIS

G. Bulat¹, E. Fedina², C. Fureby², W. Meier³, U. Stopper³

¹Siemens Industrial Turbomachinery Ltd., United Kingdom ²The Swedish Defence Research Agency – FOI, Sweden

³Deutsches Zentrum für Luft- und Raumfahrt – DLR, Germany

In this investigation the physics of the reacting swirling flow of a commercial industrial gas turbine burner (SGT-100) was researched using combustion Large Eddy Simulation (LES) and experiments. In the experimental studies the flow field, temperature and major species concentrations were measured using Particle Image Velocimetry (PIV), OH Planar Laser-Induced Fluorescence (OH-PLIF), one-dimensional laser Raman scattering and OH chemiluminescence imaging. For the finite-rate chemistry LES, two global and two skeletal reaction mechanisms were utilized to evaluate the accuracy and tradeoffs of global and skeletal reaction mechanisms. This type of assessments has previously been carried out for simple flames but not for industrial flames at laboratory conditions with detailed measurement data. The LES predictions generally show very good agreement with the experimental data for the flow field, temperature and major species. Different reaction mechanisms do not affect the flow field as much as the temperature and species profiles, which show clear imprints of the selected reaction mechanism. The results further indicate that the industrially flame is best captured with the skeletal reaction mechanisms, whilst the global mechanisms predict too compact flames. The results from the skeletal reaction mechanisms are then used in conjunction with the experimental data to assess the flame characteristics which best can be described as interacting flamelets embedded in an environment of distributed reaction zones.

fureby@foi.se

3D04 DETECTION AND PREVENTION OF BLOWOUT IN A LEAN PREMIKED GAS-TURBINE MODEL COMBUSTOR USING DYNAMICAL SYSTEM THEORY

Shohei Domen¹, Hiroshi Gotoda¹, Taku Kuriyama¹, Yuta Okuno¹, Shigeru Tachibana²

¹Ritsumeikan University, Japan ²Japan Aerospace Exploration Agency, Japan

We propose a novel online method of detecting Lean Blowout (LBO) in a laboratory-scale premixed-type gas-turbine model combustor from the viewpoint of dynamical system theory that enables us to quantify the complexity in combustion instability. The multiscale entropy method and nonlinear forecasting method, which have not been previously adopted for the analysis of combustion instability, demonstrate that combustion instability close to LBO exhibits much

more complicated stochastic dynamics than fractional Brownian motion. The permutation entropy, which can be estimated by quantifying the rank order pattern of components in phase space vectors constructed from the short time-series data of pressure fluctuations, is used as a control variable to prevent LBO. The online method proposed in this work has the potential to control the complex combustion state close to LBO.

gotoda@se.ritsumei.ac.jp

3D05 FLAME SHAPE TRANSITION IN A SWIRL STABILISED LIQUID FUELED BURNER

Antoine Renaud^{1,2}, Sébastien Ducruix^{1,2}, Philippe Scoufflaire^{1,2}, Laurent Zimmer^{1,2}

¹CNRS, France ²Ecole Centrale Paris, France

A laboratory-scale two-stage swirling burner fueled with dodecane is studied experimentally with the help of high speed imaging. For a lean operating point at 73 kW, fuel staging is changed and a hysteresis cycle is highlighted. The flame is first lifted from the injector plane and exhibits a strong thermo-acoustic instability. The transition to a more stable state is studied by changing the staging parameter while keeping the power constant. Thanks to a well-controlled environment, several runs are performed to ensure that the phenomena observed during these transitions are reproducible. In less than 10 ms, flashback happens in the inner recirculation zone and the flame attaches itself to the injector in a tulip-like shape. The spray then presents a wider angle. Thermo-acoustic instabilities are barely detected and the flame exhibits a strong response to the precessing vortex core. The flame finally widens into a more common V-shaped flame, either in less than 50 ms (for half of the experiments) or after more than 500 ms.

antoine.renaud@ecp.fr

3D06 SHORT- AND LONG-TERM DYNAMIC MODES OF TURBULENT SWIRLING PREMIXED FLAME IN A CUBOID COMBUSTOR

Kozo Aoki¹, Masayasu Shimura¹, Shinichi Ogawa¹, Naoya Fukushima¹, Yoshitsugu Naka¹, Yuruzu Nada², Mamoru Tanahashi¹, Toshio Miyauchi³

¹Tokyo Institute of Technology, Japan ²The University of Tokushima, Japan ³Meiji University, Japan

Direct Numerical Simulation of hydrogen–air turbulent swirling premixed flame in a cuboid combustor is conducted to investigate thermoacoustic instability and dynamic modes of turbulent swirling premixed flame in combustors. A detailed kinetic mechanism and temperature dependency of physical properties are considered in DNS. Two swirl number cases of 0.6 and 1.2 are investigated. Large-scale helical vortical structures are generated near the inlet of combustion chamber, and a lot of fine-scale vortices emerge downstream. Flame structure is engulfed by the vortical structures and depends largely on the swirl number. Spectral analysis of pressure oscillation on walls shows that quarter-wave mode of longitudinal acoustics has the largest energy, and that characteristic oscillations are found at higher frequencies. To investigate oscillation modes of pressure and heat release rate fields, Dynamic Mode Decomposition (DMD) is applied to DNS results. It is shown that there is differences between dominant frequencies in spectral analysis of time-series pressure data at one point of walls and DMD of time-series pressure field data. DMD of pressure field reveals that the quarter-wave mode in longitudinal acoustics has the largest energy for the case of $S=0.6$. Furthermore, it is clarified that the transverse acoustic plane waves and pressure oscillations induced by large-scale vortical motions play important roles for the pressure oscillations in combustors. DMD of heat release rate field reveals that the DMD modes of pressure with high amplitude do not necessarily have coupling with fluctuations of heat release rate. Interactions between dynamic modes of pressure and heat release rate is also discussed.

mshimura@navier.mes.titech.ac.jp

3D07 MODELING HEAT LOSS EFFECTS IN THE LARGE EDDY SIMULATION OF A MODEL GAS TURBINE COMBUSTOR WITH PREMIXED FLAMELET GENERATED MANIFOLDS

F. Proch, A. M. Kempf, University of Duisburg-Essen, Germany

Large eddy simulation results are presented for a model gas turbine combustion chamber, which is operated with a premixed and preheated methane / air mixture. The off-center position of the high axial momentum confined jet burner causes a strong outer recirculation, which stabilizes the flame. Turbulent combustion is modeled by the Flamelet Generated Manifolds (FGM) technique, which is combined with the Artificial Thickened Flame (ATF) approach. The influence of different heat loss modeling strategies on flame propagation and structure is investigated. Besides the established method of using burner-stabilized flames as basis for the non-adiabatic tabulation, an alternative approach based on freely propagating flames with heat loss inclusion by scaling of the energy equation source term is presented. Different grid resolutions are applied to study the impact of cell size and filter width on the results, the effect of subfilter modeling is also examined. The simulation setup and the modeling approach are validated by comparison of computed statistics against measurements, a good overall agreement between simulation and experiment is observed. However, the length of the flame was slightly under-predicted; it is shown that a simple method for consideration of strain effects on the flame has the potential to improve the predictions here. The effect of heat loss on the combustion process is then characterized further based on probability density functions obtained from the simulation results.

fabian.proch@uni-duisburg.de

3D08 LARGE-EDDY SIMULATIONS OF THE IGNITION SEQUENCE OF AN ANNULAR MULTIPLE-INJECTOR COMBUSTOR

M. Philip^{1,2}, M. Boileau^{1,2}, R. Vicquelin^{1,2}, E. Riber³, T. Schmitt^{1,2}, B. Cuenot³, D. Durox^{1,2}, S. Candel^{1,2}
¹CNRS, France ²Ecole Centrale Paris, France ³CERFACS, France

The ignition transient is a critical fundamental phase in combustion systems that has strong practical implications. While this phenomenon has been extensively studied on single injector configurations, the burner-to-burner propagation of a full annular combustor is rarely investigated, due to the size and complexity of the geometry involved. For this purpose, an annular experimental setup has been developed at EM2C, featuring sixteen swirl injectors and quartz tubes providing a direct optical access to the flame. Ignition has been investigated systematically on this device, thus providing a large experimental database. In this work, this experiment is computed in the Large Eddy Simulation (LES) framework by carrying out massively parallel computations. The ability of turbulent combustion models to properly retrieve the flame structure and propagation at the largest scales is not yet fully assessed and is investigated in this paper by comparing two conceptually different combustion modeling approaches, namely the Filtered TABulated Chemistry (F-TACLES) and the flame thickening with reduced chemistry (TFLES). Qualitative and quantitative comparisons between both simulations and experiment show an overall excellent agreement.

maxime.philip@ecp.fr

3D09 IGNITION PROBABILITY OF A PARTIALLY PREMIXED BURNER USING LES

L. Esclapez^{1,2}, E. Riber¹, B. Cuenot¹
¹CERFACS, France ²SNECMA Villaroche, France

To comply with stringent pollutant emission regulation, low-emission aeronautical gas turbines rely on lean premixed combustion. Such technology raises the issue of ensuring a reliable ignition since the combustor operates closer to blow-off. Ignition is however known as a stochastic phenomenon, associated to various sources of system variability. These variabilities and their impact on the success or failure of ignition are still not fully understood. In this paper, Large Eddy Simulation (LES) of laser ignition sequences in an academic swirled turbulent partially premixed burner are performed to obtain statistical information at three selected ignition locations representative of the various ignition scenarios observed. The velocity and mixing fields are first validated against measurements to eliminate uncertainty associated with the non-reacting flow. LES is then shown to recover the ignition statistical behavior and probability for the selected ignition locations. Moreover, LES analysis allows to identify the various mechanisms that drive ignition failure or success. Statistics of flame displacement speed are used to demonstrate the effect of curvature and stretch in regions of intense turbulence and the impact of partial premixing on the ignition process.

esclapez@cerfacs.fr

3D10 THE EFFECT OF SPARK TIMING AND NEGATIVE VALVE OVERLAP ON SPARK ASSISTED COMPRESSION IGNITION COMBUSTION HEAT RELEASE RATE

Robert J. Middleton¹, Jason B. Martz¹, Laura K. Manofsky Olesky¹, George A. Lavoie¹, Margaret S. Wooldridge¹, Dennis N. Assanis²
¹University of Michigan, United States ²Stony Brook University, United States

Spark Assisted Compression Ignition (SACI) combustion is capable of partially decoupling combustion phasing from peak heat release rate, overcoming one of the major challenges associated with low temperature combustion. Experimental SACI studies have shown that for a given combustion phasing, peak heat release rate can be modulated by trading the fraction of the fresh charge consumed by flame propagation with the fraction consumed by auto-ignition. The chemical and physical mechanisms controlling the changes in heat release rate are not well known. The current work uses computational simulation to explore these modes through the combined control of spark timing and charge temperature via changes in negative valve overlap. Open cycle CFD simulation results are compared with experimental data to validate a newly developed SACI model, and used to gain insight into the processes governing combustion behavior. The simulations predict a 43% reduction in the peak rate of heat release with increasing spark advance, while at the same time the unburned charge mass at the time of auto-ignition decreases by only 23%. Detailed analysis of the end-gas thermodynamic state prior to auto-ignition shows as spark is advanced, the end-gas thermal and compositional distributions vary with the fraction of the charge consumed by the flame. The reduction in the rate of peak rate of heat release during the auto-ignition process is therefore a function of both the mass of the end-gas and the end-gas reactivity.

rjmidd@umich.edu

3D11 UNDERSTANDING THE RELATIONSHIP BETWEEN IGNITION DELAY AND BURN DURATION IN A CONSTANT VOLUME VESSEL AT DIESEL ENGINE CONDITIONS

S. Rabl¹, T.J Davies², A.P. McDougall², R.F. Cracknell²
¹Shell Global Solutions, Germany ²Shell Global Solutions, United Kingdom

Experiments were performed in a constant volume vessel, with fuel sprays injected into the vessel at various different pressure and temperature conditions chosen to represent diesel engine operation at various loads.

A range of diesel primary reference fuels (i.e. mixtures of cetane and heptamethylnonane) of varying Cetane Number (CN) were tested, and as expected lower CN fuels have longer ignition delays. Burn period was plotted against ignition delay and two distinct trends can be seen: “mainly diffusion” diesel combustion in which burn period decreases with ignition delay and “mainly pre-mixed” diesel combustion in which burn period increases with ignition delay. There is typically a minimum in plots of burn period versus ignition delay which represents the transition between the two types of combustion mode. Higher CN, higher engine load and higher boost pressure favour “mainly diffusion” combustion whilst lower CN, lower loads and non-boosted conditions favour “mainly pre-mixed” combustion.

Cracknell@shell.com

3D12 THE EFFECT OF DILUENT COMPOSITION ON HOMOGENEOUS CHARGE COMPRESSION IGNITION AUTO-IGNITION AND COMBUSTION DURATION

Janardhan Kodavasal¹, George A. Lavoie¹, Dennis N. Assanis², Jason B. Martz¹

¹University of Michigan, United States ²Stony Brook University, United States

In this work, the effect of diluent composition is studied on the ignition timing and combustion duration of Homogeneous Charge Compression Ignition (HCCI) combustion. Full-cycle 3D Computational Fluid Dynamics (CFD) simulations were performed using two different dilution schemes, one which employs air dilution and the other which employs external Exhaust Gas Recirculation (eEGR) dilution. Both cases used a fixed breathing strategy, and had the same fueling rate and engine speed typical of automotive applications. A premixed fuel-air mixture was used in the intake charge to avoid the fuel stratification effects associated with direct injection, while the valve events were selected to minimize the internal residual and its associated thermal and compositional stratification. With ignition timing held constant near Top Dead Center (TDC) for both methods, there is a 10% increase in the combustion duration going from air to eEGR dilution. While the thermal stratification prior to ignition is similar for both methods, the eEGR-dilute case has an overall higher temperature throughout the charge. A reactivity stratification analysis, based on the distribution of ignition delays within the charge prior to ignition, showed nearly identical initial reactivity for the two methods, with the higher temperatures of the eEGR case compensating for this method's lower oxygen content. A quasidimensional multi-zone model was subsequently used to decouple the chemical kinetic and thermodynamic effects of eEGR on the combustion process. This analysis showed that the primary factor contributing to the longer combustion duration for the eEGR-dilute case is the lower ratio of specific heats (γ) in the unburned charge post-ignition which is thought to lower the rate of compression-induced heating of the unburned charge by the ignited and burning regions, leading to slower sequential auto-ignition.

jkodavasal@anl.gov

3E01 KINETICS OF NASCENT SOOT OXIDATION BY MOLECULAR OXYGEN IN A FLOW REACTOR

Joaquin Camacho, Hai Wang, Stanford University, United States

Oxidation kinetics of soot is typically measured with well aged soot as substrates. Recent studies show that nascent soot can have structures and surface composition drastically different from mature, graphitized soot. In the present study, the kinetics of nascent soot oxidation by molecular oxygen was observed at temperatures of 950, 1000 and 1050 K for molecular oxygen concentrations ranging from 1000 to 7800 ppm at ambient pressure in a coupled burner-stabilized stagnation flame burner and laminar aerosol flow reactor. The reactant particles, 10-20 nm in diameter, were freshly synthesized from premixed flames of ethylene, *n*-heptane, and toluene and introduced into the flow reactor continuously. The kinetics of particle oxidation was measured through electric mobility measurement of particle size distributions before and after oxidation. It was found that the specific oxidation rate is an order of magnitude larger than that predicted by the classical Nagle Strickland-Constable (NSC) correlation. The result suggests that the surface of nascent soot is considerably more reactive towards oxidation than graphite or graphitized soot.

haiwang@stanford.edu

3E02 DETAILED MODELLING OF SOOT OXIDATION BY O₂ AND OH IN LAMINAR DIFFUSION FLAMES

Ali Khosousi, Seth Benjamin Dworkin, Ryerson University, Canada

A detailed knowledge of soot formation and oxidation processes is desired to reduce the soot emissions in combustion devices. Soot oxidation is one of the most complex processes in the numerical modeling of soot. In this work, the oxidation of soot has been numerically studied in laminar ethylene/air co-flow diffusion flames. There has been disagreement in the literature over the rates of soot oxidation by O₂ molecules and OH radicals. A sensitivity analysis has been performed on the roles of O₂ and OH in various parts of the diffusion flame. A new oxidation model is developed based on the observation that soot ageing reduces surface reactivity and is primarily based on temperature and residence time. Using this new model, it is now possible to capture the correct behavior of both smoking and non-smoking flames in various flame configurations. Along with a detailed sectional soot model, the new oxidation rates predict the correct soot volume fractions, smoke emission characteristics, and primary particle diameters for different flames without any variation in model parameters between cases.

seth.dworkin@ryerson.ca

3E03 RATE COEFFICIENTS AND PRODUCT BRANCHING RATIOS FOR THE OXIDATION OF PHENYL AND NAPHTHYL RADICALS: A THEORETICAL RRKM-ME STUDY

V.V. Kislov¹, R.I. Singh², D.E. Edwards^{2,3}, A.M. Mebel¹, M. Frenklach^{2,3}

¹Florida International University, United States ²University of California at Berkeley, United States

³Lawrence Berkeley National Laboratory, United States

Theoretical VRC-TST/RRKM-ME calculations were performed to evaluate total rate coefficients and product branching ratios for the oxidation of phenyl and 1- and 2-naphthyl radicals with O₂ at temperatures relevant to combustion (1500, 2000, and 2500 K) and pressures of 0.01, 0.1, 1.0, and 10 atm. The results give the rate coefficients in the range of 3.0–5.5 × 10⁻¹¹ cm³ molecule⁻¹ s⁻¹ with slightly positive temperature dependence, activation energies varying within 2.3–3.3 kcal/mol, and preexponential factors of 7–10 × 10⁻¹¹ cm³ molecule⁻¹ s⁻¹. The dominant reaction channel in all three cases is elimination of the oxygen atom from peroxy complexes formed at the initial O₂ addition step and leading to the phenoxy and naphthoxy radical products. The contribution of this channel increases with temperature. Chemically-activated phenoxy and naphthoxy radicals either decompose to the cyclopentadienyl+CO and indenyl+CO products, respectively, or undergo thermal equilibration. The relative yields of the decomposition/equilibration products strongly depend on temperature and pressure in the way that a temperature growth favors decomposition, whereas an increase in pressure favors equilibration. At the lowest temperature considered, 1500 K, the reactions also yield significant amounts of pyranil+CO (phenyl+O₂) or 1-benzopyranil+CO (1-naphthyl+O₂). A comparison of the phenyl+O₂ and naphthyl+O₂ reactions reveals that although the general trends in the oxidation kinetics of phenyl and naphthyl radicals are similar, the size and especially the position of the radical site in the aromatic moiety may affect the details of the mechanism and relative product yields.

mebela@fiu.edu

3E04 SOOT NANOSTRUCTURE EVOLUTION IN PREMIXED FLAMES BY HIGH RESOLUTION ELECTRON TRANSMISSION MICROSCOPY (HRTEM)

B. Apicella¹, P. Pr  , M. Alf  , A. Ciajolo¹, V. Gargiulo¹, C. Russo¹, A. Tregrossi¹, D. Deldique³, J.N. Rouzaud³

¹IRC-CNR, Italy ²GEPEA, France ³Laboratoire de G  ologie de l'Ecole Normale Sup  rieure, France

HRTEM fringe analysis by means of our “Analyse Plan” approach has been applied to soot sampled along the axis of sooting premixed benzene and ethylene flame, in order to follow more in detail the evolution of soot properties along the soot formation region. A new HRTEM image analysis procedure, based on mathematical morphology, was also applied for extracting parameters related to the geometry of the individual fringes: length, tortuosity, and local curvature radii, which are correlated with the defective nature of soot structure. Their trends, along with the percentage of nearly-straight fragments also reported in the work, clearly show a structure improvement resulting in a better stacking of longer and more planar layers with aging for both the fuels. The nanostructural ordering occurs faster for benzene with respect to ethylene but reaches similar features at the end of the flame. These findings are in agreement with H/C ratio and optical properties evolution of soot. In order to follow quantitatively the structural change with aging and fuel nature, aromatic structures have been proposed on the basis of the fringe length distribution. The method, already applied by Mathews et al., was used to assign aromatic sizes to the extracted HRTEM fringes, assuming that the aromatic fringes are in the shape of parallelograms. The distributions obtained were compared with elemental analysis and specific absorption properties to give a view of the structural properties evolution of soot during its formation.

Raman evaluation of in-plane layer length, La, has been also carried out for a comparison with the data obtained by the HRTEM image analysis. The agreement found is very satisfying, considering the different physical approaches of the two techniques.

apicella @irc.cnr.it

3E05 MORPHOLOGY OF NASCENT SOOT IN ETHYLENE FLAMES

Marina Schenk¹, Sydney Lieb², Henning Vieker¹, Andr   Beyer¹, Armin G  lzh  user¹, Hai Wang³, Katharina Kohse-H  inghaus¹

¹Bielefeld University, Germany ²University of Southern California, United States ³stanford University, United States

Because of their significant impact on climate, environment and health, reducing the emission of soot from combustion processes remains a problem that requires detailed understanding of its formation as well as of the principles that govern how the result in terms of size, morphology, and chemical reactivity of soot particles depends upon the formation process. Especially very small, below ten nanometer-sized particles in the early stages of the soot nucleation process are interesting targets for more detailed inspection, to reveal useful insight and to guide further model development. In this study, Helium-Ion Microscopy (HIM) is applied as an imaging technique new to combustion studies to analyze the morphology of soot particles > 2nm and to determine their geometrical characteristics. For this analysis, a series of premixed ethylene flames are investigated. Mobility size measurements from an earlier investigation have been compared with the particle sizes determined by HIM. Observed particle shapes and geometrical statistics suggest that in all of the flames under investigation, nascent soot possesses no well-defined morphologies. Additionally, investigations have

been made using X-Ray Photoelectron Spectroscopy (XPS) to obtain more information on the chemical characteristics of these particles.

kkh@uni-bielefeld.de

3E06 PROBING THE SMALLEST SOOT PARTICLES IN LOW-SOOTING PREMIXED FLAMES USING LASER-INDUCED INCANDESCENCE

Henrik Bladh¹, Nils-Erik Olofsson¹, Thomas Mouton², Johan Simonsson¹, Xavier Mercier², Alessandro Faccineto², Per-Erik Bengtsson¹, Pascale Desgroux²

¹Lund University, Sweden ²PC2A – CNRS Université Lille 1, France

In this work we investigate nascent soot particles by analyzing laser-induced incandescence (LII) signals obtained in low-sooting premixed flames. The analysis covers two data sets obtained in separate experimental campaigns.

The first data set was obtained in a previous work (Mouton et al. Appl. Phys. B, vol.112 (2013) 369-379) in methane/oxygen/nitrogen flames (equivalence ratio range $1.95 < F < 2.32$) stabilized at 26.6 kPa whereas the second was obtained in this work in atmospheric ethylene/air flames ($1.77 < F < 2.00$). Both studies show similar trends, i.e. a gradual change of the fluence curves (evolution of the LII signal as function of the laser fluence) from the well-known Sshaped curve for mature soot found at high Heights Above the Burner (HAB) and high equivalence ratio to a nearly linear behavior for nascent soot found at low HAB and reduced equivalence ratio. With this change comes a decrease in the LII decay time (and hence inferred particle size) which appears to be almost constant with HAB in flames having the lowest equivalence ratio at which the incandescence signal could be detected.

In these flames, so-called nucleation flames, the stability of the particle size with HAB suggests that recently nucleated particles have undergone very slow surface growth and coagulation. Existence of such nucleation flames is of great interest for improving the theoretical description of the nucleation step. Experimental results are analyzed by using a theoretical model for LII to determine the particle diameter evolution throughout the flame at various experimental conditions. We highlight the size difference from nascent soot particles up to mature soot, giving insight into the particle nucleation and the surface growth processes as a function of reaction time and flame conditions.

henrik.bladh@forbrf.lth.se

3E07 FURTHER EXPERIMENTAL AND MODELLING EVIDENCES OF SOOT FRAGMENTATION IN FLAMES

Mariano Sirignano, Andrea D'Anna, Università degli Studi di Napoli Federico II, Italy

Particle oxidation is one of the steps still not completely understood in particle formation in combustion. Most of the approach are based on semi-empirical reaction rates to account for this process. A correct evaluation of oxidation is mandatory to predict the final amount of the particles emitted in diffusion flames. Fragmentation has been recently proposed to be a controlling step in determining the global soot burn out as well as the size of particles emitted.

In order to systematically study the oxidation and fragmentation of soot particle in diffusion flames, counterflow configuration has been chosen. In situ optical diagnostics have been adopted, namely laser induced incandescence and elastic light scattering. MultiSectional approach has been adopted to predict combustion-generated particles. Two counterflow diffusion flames has been chosen, a Soot Formation (SF) and a Soot Formation/Oxidation (SFO) flame. In the first one soot oxidation is absent, whereas in the latter soot oxidation is the peculiar process.

Experimental data supported by model predictions clearly show the role of fragmentation in controlling the final burn-out and the size distribution of particle in flame. In particular, in SF flame, where no soot oxidation occurs, large particles are formed. On the contrary, in the SFO flame, the evaluation of mean diameter of soot particles shows that when fragmentation is active coagulation is less effective, aggregates are rather formed and primary particle with small size are mostly formed.

marianosirignano@yahoo.it

3E08 EXPERIMENTAL STUDY OF SOOT SIZE DECREASE WITH PYROLYSIS TEMPERATURE RISE

A.Emelianov¹, A.Eremin¹, E. Gurentsov¹, E. Mikheyeva^{1,2}, M. Yurischev¹

¹Joint Institute for High Temperatures Russian Academy of Sciences, Russia ²Bauman Moscow State Technical University, Russia

Simultaneous measurements of the temperature dependences of the sizes, growth rate and relative yield of soot particles are carried out at shock wave pyrolysis of various carbon bearing species (carbon suboxide – C_3O_2 , acetylene – C_2H_2 and benzene – C_6H_6). In all studied substances in the temperature range from 1800 – 2000 K to 2500 – 3000 K a sharp fall in particle size, accompanied by a sharp increase in the rate of their formation, was observed. Analysis of the data obtained showed that the decrease of particle size, and decrease in total time of their formation with the temperature rise, obey the similar exponential dependences which are well correlated with an increase in the rate of decomposition of the initial carbon bearing molecules. It is established that the observed decrease in the total time of particle growth with temperature increase is caused by a decrease in their final size, and the decrease of extinction at 633 nm, reflects not a reduction of particle yield, but a decrease in the extinction coefficient at reduction of particle size. Extinction

measurements on a shorter wavelength (220 nm and 248 nm) indicated an approximately constant yield of the condensed phase in the specified temperature range.

eremin@ihed.ras.ru

3E09 INFLUENCE OF SULPHUR ADDITION ON EMISSIONS OF POLYCYCLIC AROMATIC HYDROCARBONS DURING BIOMASS COMBUSTION

T. Streibel, F. Mühlberger, R. Geißler, M. Saraji-Bozorgzad, T. Adam, R. Zimmermann, University of Rostock, Germany

Emissions of Polycyclic Aromatic Hydrocarbons (PAH) in the flue gas of a bark fuelled combustion facility were monitored in real time by time-of-flight mass spectrometry combined with resonance-enhanced multiphoton ionization. Sampling and on-line analysis could be maintained up to more than six hours consecutively, providing an insight in the aromatic profile of gaseous emissions as a function of varying combustion conditions. Naphthalene concentrations were quantified by determining a response factor of the ionization signal relative to toluene, which served as an external standard. Limits of detection of 1 ppb could be achieved with a time resolution of ten seconds. The emission of PAH occurred in peaks displaying exceeding levels of concentration. Between such emission peaks PAH concentration could drop to ground level near the limit of detection. Addition of sulphur to the combustion chamber – either as ammonium sulphate solution or elemental sulphur pellets – caused a significant decrease in the number of emission peaks, yielding an overall diminishment of average PAH concentration up to 88 %. This was accompanied by a simultaneous decrease in concentration of carbon monoxide and volatile organic compounds, indicating an improvement in combustion quality after sulphur injection.

thorsten.streibel@uni-rostock.de

3F01 ON THE DYNAMICS OF SPRAY FLAMES IN TURBULENT FLOWS

Yuval Dagan¹, Eran Arad², Yoram Tambour¹

¹Israel Institute of Technology, Israel ²RAFAEL, Israel

Unsteady turbulent spray-flame propagation was computationally investigated, employing the same flow configuration used in previous studies for analyzing the structure of gaseous turbulent flames. The presence of a recirculation zone, which is common in jet engine combustion chambers, has a significant role in spray and flame dynamics, diverting the flame in a cyclic motion. Two repetitive developmental stages of flame structures were identified and analyzed. Droplet grouping was found in the vicinity of large vertical structures, and flames surrounding groups of droplets were identified. Back-flow of droplets was found to have ligament structures, similar to those found in turbulent shear flow. The local statistics of fuel droplet dispersion is discussed. A new approach is used to investigate spray flame propagation by reducing the dimensionality of the problem, revealing low frequency flame repetitive motions, while retaining its turbulent characteristics.

yuvalda@technion.ac.il

3F02 REACTION ZONE VISUALISATION IN SWIRLING SPRAY N-HEPTANE FLAMES

R. Yuan¹, J. Kariuki¹, A. Dowul², R. Balachandran², E. Mastorakos¹

¹University of Cambridge, United Kingdom ²University College London, United Kingdom

Joint PLIF measurements of CH₂O and OH were performed in a swirl-stabilized nheptane spray flame at conditions close to extinction. Simulations of laminar counterflow heptane flames at different strain rates showed that the heat release could be approximately represented by the product CH₂OxOH, but also that this product cannot visualise the heat release at the lean side of stoichiometry. The simulations suggest that the outline of CH₂O regions in PLIF images could be an approximate indicator of the stoichiometric mixture fraction *iso*-line. Due to the intense turbulence and local extinction, individual PLIF images show a very variable behaviour. They indicate rich zones, reaction sheet breaks, lift-off, and they suggest that this flame is mostly of non-premixed character. The mean heat release rate as represented here is consistent with inverse Abel-transformed OH* chemiluminescence imaging. The usefulness of this technique for spray flames is discussed.

ry235@cam.ac.uk

3F03 ANALYSIS OF SEGREGATION AND BIFURCATION IN TURBULENT SPRAY FLAMES: A 3D COUNTERFLOW CONFIGURATION

Aymeric Vié¹, Benedetta Franzelli¹, Yang Gao², Tianfeng Lu², Hai Wang¹, Matthias Ihme¹

¹Stanford University, United States ²University of Southern California, United States

Spray combustion is encountered in a wide range of industrial applications. The understanding of such combustion processes is of primary importance. In the present work, direct numerical simulations of a 3D turbulent counterflow spray configuration are conducted. Primary focus is on the impact of the coupling between turbulence, mixing and evaporation, and combustion. By considering different initial droplet diameters and through comparisons with a

gaseous combustion configuration at the some operating condition, it is shown that the preferential concentration can lead to conditions of locally high mixture-fraction composition. In addition, the strain rate variability introduces a subcritical bifurcation of the spray flame structure, which includes premixed-diffusion and diffusion-diffusion combustion modes for operating conditions that are highly sensitive to the strain rate.

aymeric.vie@stanford.edu

3F04 DROPLET/LIGAMENT MODULATION OF LOCAL SMALL-SCALE TURBULENCE AND SCALAR MIXING IN A DENSE FUEL SPRAY

J. Shinjo^{1,2}, J. Xia², A. Umemura³

¹Japan Aerospace Exploration Agency, Japan ²Brunel University, United Kingdom ³Nagoya University, Japan

In this study, the modulation of turbulence and scalar mixing by finite-size droplets/ligaments in a dense fuel spray is investigated using a DNS (Direct Numerical Simulation) dataset. Ejected from a spray nozzle with a high speed, a liquid-fuel jet deforms and the fuel spray is atomized into many ligaments and droplets. During these processes, the gas flow becomes turbulent due to droplet/ligament dynamics. At the same time, droplet evaporation and mixing with ambient air are affected by the small-scale gas turbulence. An understanding of the mixing characteristics in the dense spray zone is important for modeling spray combustion. In a region where the droplet number density is relatively low, a universal feature of isotropic turbulence was found, although the alignments of strain eigenvectors with vorticity and the mixture fraction gradient are slightly modulated by the presence of droplets, which is a characteristic of particle-laden flows. In gas-phase regions close to droplet surfaces, where the dissipation rate of turbulent kinetic energy is strongly increased, the alignments are more modulated, especially those of the scalar gradient with strain eigenvectors. This can also be seen in the topology similarity among energy dissipation, enstrophy and scalar dissipation in the near field of droplet/ligament surfaces. For the first time, it is found that droplets whose size is comparable to turbulence scales do affect the mixing characteristics in a realistic turbulent spray. This finding has shed new light upon the modeling of flow turbulence and scalar mixing in an evaporating and atomizing fuel spray.

Junji.Shinjo@brunel.ac.uk

3F05 EVIDENCE FOR SUPERCRITICAL MIXING LAYERS IN THE ECN SPRAY A

Zachary Falgout¹, Mattias Rahm¹, Zhenkan Wang², Mark Linne¹

¹Chalmers University, Sweden ²Lund University, Sweden

Prior work on an engine combustion network Diesel fuel injector led to the conclusion that the jet was transitionally supercritical under Diesel engine conditions (pressure and temperature). We report initial experiments aimed at observing the thickened turbulent mixing layer that would result if the jet were transitionally supercritical. We have applied ballistic imaging to the same Diesel fuel injector, under similar conditions, and we find that the images do indicate a structural change when going from subcritical to supercritical conditions. Under subcritical conditions we observe a well-defined liquid/gas interface, surface wave structure, and formation of ligaments and voids. Under supercritical conditions the interface transitions into a continuous, turbulent mixing layer. Images of this layer include the cellular structure characteristic of gas jets. These changes are consistent with experimental literature on cryogenic supercritical jets and with DNS modeling of supercritical mixing layers.

mark.linne@chalmers.se

3F06 NON-EQUILIBRIUM GAS-LIQUID INTERFACE DYNAMICS IN HIGH-PRESSURE LIQUID INJECTION SYSTEMS

Rainer N. Dahms, Joseph C. Oefelein, Sandia National Laboratories, United States

The transition of classical spray atomization processes to single-phase continuous dense-fluid mixing dynamics is poorly understood. Recently, a theory has been presented that established, based on a Knudsen-number criterion, that the development of such mixing layers is initiated because the multicomponent two-phase interface becomes much wider than the mean free molecular path. This shows that the transition to mixing layers occurs due to interfacial dynamics and not, as conventional wisdom had suggested, because the liquid phase has heated up to supercritical temperatures where surface tension forces diminish. In this paper we focus on the dynamics of this transition process, which still poses many fundamental questions. We show that such dynamics are dictated by substantial statistical fluctuations and the presence of significant interfacial free energy forces. The comprehensive analysis is performed based on a combination of non-equilibrium mean-field thermodynamics and a detailed modified 32-term Benedict-Webb-Rubin mixture state equation. Statistical fluctuations are quantified using the generally accepted model of Poisson-distributions for variances systems with a small number of molecules. Such fluctuations quantify the range of pressure and temperature conditions under which the gradual transition to dense-fluid mixing dynamics occurs. The interface begins to deteriorate as it broadens substantially, and the related interfacial free energy forces do not instantly diminish only because vapor-liquid equilibrium conditions do not apply anymore. Instead, such forces are shown to gradually decrease and to diminish once the interface

enters the continuum regime. At this point the interfacial region becomes a continuous gas-liquid mixing layer that is significantly affected by single-phase real-fluid thermodynamics and transport properties.

Rndahms@sandia.gov

3F07 VISUALIZATION OF MILD COMBUSTION FROM JETS IN CROSS-FLOW

J. Sidey, E. Mastorakos, University of Cambridge, United Kingdom

The behaviour of methane jet flames autoigniting in a turbulent cross-flow at MILD combustion conditions is examined experimentally. The methane jet was injected orthogonally into a turbulent, low oxygen ($X_{O_2} < 8\%$) cross-flow at high temperatures in a cylindrical quartz tube. Regardless of cross-flow conditions, the methane jet autoignited and a flame was stabilized in a wide region clearly separated from the injection nozzle. OH* chemiluminescence images show that OH* intensity was not significantly diminished by changing X_{O_2} , but the size of the reacting region, as well as its location, was noticeably sensitive to X_{O_2} . Cross-flows enriched with additional air sustained methane jet flames with larger reactive regions than those diluted with N₂ or composed of pure hot products. Additional cross-flow dilution with N₂ shifted the reaction further downstream, an observation supported by the imaging of individual autoignition kernels. Mean OH-PLIF shows OH radical presence in areas devoid of heat release, as indicated by the time-averaged OH* chemiluminescence images. In all cases, OH-PLIF instantaneous images show regions with wide OH distributions, but sharp gradients, similar to those evident in traditional combustion regimes. The data interpretation is supported by laminar non-premixed flame calculations that demonstrate some differences and similarities between MILD and conventional flames.

jams4@cam.ac.uk

3F08 SUBGRID SCALE MODELLING FOR MILD COMBUSTION

Y. Minamoto, N. Swaminathan, University of Cambridge, United Kingdom

A simple closure for filtered reaction of a reaction progress variable is analysed in this study using explicitly filtered DNS data of turbulent MILD combustion of methane for Large Eddy Simulation (LES). The conditional averages of major and minor species mass fractions, and reaction rate constructed from the DNS data along with those obtained using flamelet and Perfectly Stirred Reactor (PSR) models suggest that the PSR can serve as a good canonical reactor for MILD combustion modelling. The flamelet predictions of reaction rate are observed to be poor because it does not include effects of flame interactions, which are abundant in the MILD combustion. The PSR solution obtained over a wide range of residence time along with presumed beta sub-grid PDF seems a reasonable closure for the filtered reaction rate for the LES filter size greater than three flame thermal thicknesses. Both spatial variations and joint PDF of modelled and DNS values of filtered reaction rates are analysed.

ym270@cam.ac.uk

3F09 SCALING FOR HIGH INTENSITY SWIRL BASED ULTRA-LOW EMISSION FLAMELESS COMBUSTOR OPERATING WITH LIQUID FUELS

V. Mahendra Reddy^{1,2}, Amit Katoch¹, William L. Roberts², Sudarshan Kumar¹

¹Indian Institute of Technology Bombay, India ²King Abdullah University of Science and Technology, Saudi Arabia

Flameless combustion offers many advantages over conventional combustion, particularly uniform temperature distribution and lower emissions. In this paper, a new strategy is proposed and adopted to scale up a burner operating in flameless combustion mode from a heat release density of 5.4 to 21 MW/m³ (thermal input 21.5 – 84.7 kW) with kerosene fuel. A swirl flow based configuration was adopted for air injection and pressure swirl type nozzle with an SMD 35-37 μm was used to inject the fuel. Initially, flameless combustion was stabilized for a thermal input of 21.5 kW ($\dot{Q} = 5.37$ MW/m³). Attempts were made to scale this combustor to higher intensities *i.e.* 10.2, 16.3 and 21.1 MW/m³. However, an increase in fuel flow rate led to incomplete combustion and accumulation of unburned fuel in the combustor. Two major difficulties were identified as possible reasons for unsustainable flameless combustion at the higher intensities (i) A constant spray cone angle and SMD increases the droplet number density (ii) Reactants dilution ratio (R_{dil}) decreased with increased thermal input. To solve these issues, a modified combustor configuration, aided by numerical computations was adopted, providing a chamfer near the outlet to increase the R_{dil} . Detailed experimental investigations showed that flameless combustion mode was achieved at high intensities with an evenly distributed reaction zone and temperature in the combustor at all heat intensities. The emissions of CO, NO_x and HC for all heat intensities ($\Phi = 1 - 0.6$) varied between 11 - 41, 6 - 19 and 0 - 9 ppm, respectively. These emissions are well within the range of emissions from other flameless combustion systems reported in the literature. The acoustic emission levels were also observed to be reduced by 8-9 dB at all conditions.

sudar@aero.iitb.ac.in

3F10 EFFECT OF HYDROGEN ADDITION ON THE FLAME STRUCTURE OF NATURAL-GAS JET-IN-HOT-COFLOW FLAMES

L.D. Arteaga Mendez, E.H. van Veen, M.J. Tummers, D.J.E.M. Roekaerts, Delft University of Technology, The Netherlands

The extension of flameless combustion technology to non-traditional hydrogen containing industrial fuels can produce important benefits if the typical performance levels obtained with traditional hydrocarbon fuels can be also achieved. Measurements of the flame luminescence, the velocity field and the instantaneous temperatures were conducted in four flames with different natural-gas/hydrogen fuel mixtures (with a similar jet Reynolds number) in a jet-in-hot-coflow burner that mimics heat and exhaust gas recirculation in flameless combustion. The results show major changes in the structure of the flame stabilization mechanism when the hydrogen content of the fuel is increased. By increasing the hydrogen concentration in the fuel, the typical autoignition kernels observed in natural-gas flames are not detectable anymore. The position of the first ignition kernels are substantially shifted upstream until the flame stabilizes through flame propagation. Temperatures higher than adiabatic are observed at the lean side of the fuel jet only in the hydrogen containing flames suggesting that preferential diffusion plays an important role in the stabilization mechanism of hydrogen enriched hydrocarbon containing fuels.

L.D.ArteagaMendez@tudelft.nl

3F11 NUMERICAL SIMULATION OF THE DELFT-JET-IN-HOT-COFLOW (DJHC) FLAME USING CONDITIONAL SOURCE-TERM ESTIMATION

J.W. Labahn, D. Dovizio, C.B. Devaud, University of Waterloo, Canada

RANS simulations of the Delft-Jet-in-Hot-Coflow (DJHC) flame operating in the Moderate and Intense Low Oxygen Dilution (MILD) combustion mode, are performed using the Conditional Source-term Estimation (CSE) approach. The non-premixed CSE formulation is extended, by introducing a second mixture fraction. Two flames are simulated, DJHC-I 4100 and DJHC-I 8800. Detailed chemistry tabulations and radiation are included. The objective of the current study is to assess the capabilities of CSE to accurately reproduce the velocity field, temperatures and lift-off height using the DJHC experimental conditions. The present RANS-CSE predictions for the axial velocity and turbulent kinetic energy agree well with the experimental data for both flames. For DJHC-I 4100, the radial CSE temperature predictions are in very good agreement with the experiments. The current CSE performs better compared to previous RANS and LES simulations. This is explained by the inclusion of radiation in the present work. For the second flame, a good agreement is achieved, in particular in the second half of the flame in the radial direction. A temperature overprediction is observed near the centreline. At the last axial location, CSE overpredicts the temperatures for most parts of the flame. These discrepancies are explained by some inaccuracies in the turbulent mixing due to RANS. The trend of lift-off height decreasing with increasing Reynolds number is well reproduced. However, the lift-off height appears to be lower than the experimental value. The present predictions are shown to be independent of the number of CSE ensembles. Further improvement is expected with LES for the turbulent flow and mixing fields. A third conditioning variable may also be considered to improve the lift-off height predictions.

cdevaud@uwaterloo.ca

3G01 EFFECT OF AN EXTERNAL ELECTRIC FIELD ON THE PROPAGATION VELOCITY OF PREMIXED FLAMES

M. Sánchez-Sanz¹, D. Murphy², C. Fernandez-Pello²

¹Universidad Carlos III de Madrid, Spain ²The University of California-Berkeley, United States

There have been many experimental investigations into the ability of electric fields to enhance combustion by acting upon ion species present in flames. In this work, we examine this phenomenon using a one-dimensional model of a lean premixed flame under the influence of a longitudinal electric field. We expand upon prior two-step chain-branching reaction laminar models with reactions to model the creation and consumption of both a positively-charged radical species and free electrons. Also included is the electromotive force in the conservation equation for ion species and the electrostatic form of the Maxwell equations in order to resolve ion transport by externally applied and internally induced electric fields. The numerical solution of these equations allows us to compute changes in flame speed due to electric fields. Further, the variation of key kinetic and transport parameters modifies the electrical sensitivity of the flame. From changes in flame speed and reactant profiles we are able to gain novel, valuable insight into how and why combustion can be controlled by electric fields.

mssanz@ing.uc3m.es

3G02 ELECTROMAGNETICALLY INDUCED VORTEX IN LAMINAR COFLOW DIFFUSION FLAMES BY APPLYING AC ELECTRIC FIELD

Yuan Xiong, Min Suk Cha, Suk Ho Chung, King Abdullah University of Science and Technology, Saudi Arabia

Experiments were performed applying sub-critical high-voltage Alternating Current (AC) to the nozzle of laminar propane coflow diffusion flames. Light scattering, laser-induced incandescence and laserinduced fluorescence techniques

were used to identify the soot zone, and the structures of OH and Polycyclic Aromatic Hydrocarbons (PAHs). Particle image velocimetry was adopted to quantify the velocity field. Under certain AC conditions of applied voltage and frequency, the distribution of PAHs and the flow field near the nozzle exit were drastically altered, leading to the formation of toroidal vortices. Increased residence time and heat recirculation inside the vortex resulted in appreciable formation of PAHs and soot near the nozzle exit. Decreased residence time along the jet axis through flow acceleration by the vortex led to a reduction in the soot volume fraction in the downstream sooting zone. Electromagnetic force generated by AC was proposed as a physical mechanism for the formation of the toroidal vortex. The onset conditions for the vortex formation supported the role of an electromagnetic force acting on charged particles in the flame zone.

min.cha@kaust.edu.sa

3G03 INFLUENCE OF ELECTRIC FIELDS ON PREMIXED LAMINAR FLAMES: VISUALIZATION OF PERTURBATIONS AND POTENTIAL FOR SUPPRESSION OF THERMOACOUSTIC OSCILLATIONS

*Johannes Kuhl, Gordana Jovicic, Lars Zigan, Stefan Will, Alfred Leipertz
Friedrich-Alexander Universität Erlangen-Nürnberg, Germany*

In this experimental study chemiluminescence of the flame and laser-based measurements, namely Planar Laser Induced Fluorescence (PLIF) and Particle Image Velocimetry (PIV), were used to characterize the interactions of electric fields with laminar premixed flames. Transient DC electric fields were applied with different frequencies (1-200 Hz) to a laminar flame for the investigation of the changes occurring in the flow field and the flame structure. For various low frequencies similar behaviour was observed. After the activation of the electric field the flow field changes inducing a disturbance at the flame root which travels as a wave like oscillation towards the flame tip until stationary conditions are reached. For higher frequencies different behaviour was revealed since the process cannot establish a steady state anymore. For 100 and 200 Hz the time between activation and deactivation of the electric field is too short as compared to the flame response time. Therefore, only quasi-stationary conditions of the oscillation can be reached. From this changed response behaviour a limiting frequency for technical application in the range of 100 Hz was derived.

The potential of electric fields to suppress acoustic flame instabilities was studied for a flat flame. Acoustic oscillations were generated by an injector with different injection frequencies. Depending on the electric field strength the duration of flame oscillation could be reduced by up to 54 %, so the flame returns quicker to its initial condition.

Lars.Zigan@cbi.uni-erlangen.de

3G04 PARTIAL OXIDATION OF METHANE IN A TEMPERATURE-CONTROLLED DIELECTRIC BARRIER DISCHARGE REACTOR

Xuming Zhang, Min Suk Cha, King Abdullah University of Science and Technology, Saudi Arabia

We studied the relative importance of the reduced field intensity and the background reaction temperature in the partial oxidation of methane in a temperature-controlled dielectric barrier discharge reactor. We obtained important mechanistic insight from studying high-temperature and low-pressure conditions with similar reduced field intensities. In the tested range of background temperatures ($297 < T < 773$ K), we found that the conversion of methane and oxygen depended on both the electron-induced chemistry and the thermochemistry, whereas the chemical pathways to the products were overall controlled by the thermo-chemistry at a given temperature. We also found that the thermo-chemistry enhanced the plasma-assisted partial oxidation process. Our findings expand our understanding of the plasma-assisted partial oxidation process and may be helpful in the design of cost-effective plasma reformers.

min.cha@kaust.edu.sa

3G05 AN EXPERIMENTAL INVESTIGATION OF OIL GASIFICATION PROCESS BY MICROWAVE INDUCED NON-EQUILIBRIUM PLASMA COMBUSTION

*Tsuyoshi Yamamoto¹, Takahiro Tsuboi¹, Yoshiho Iwama¹, Ryo Tanaka²
¹Kyushu University, Japan ²Aichi Electric Co., Ltd., Japan*

In order to utilize low grade fuel effectively, microwave induced non-equilibrium plasma of the glow charge type has been applied to spray combustion of the electrical insulation oil. This study is focused on developing a spray combustion method that employs microwave induced non-equilibrium plasma for spray combustion of the electrical insulation oil. The spray combustion experiment has been carried out in a quartz reaction tube with creating microwave induced non-equilibrium plasma of the glow charge type. A lot of O radicals and H radicals are generated by the electron impact dissociation reactions, $O_2 + e \rightarrow 2O + e$ and $C_mH_n + e \rightarrow C_mH_{n-1} + H + e$ (hydrocarbon C_mH_n is produced by vaporization of insulation oil) under spray combustion by microwave induced non-equilibrium plasma. Additionally, a lot of OH radicals is produced by the $O + C_mH_n$ and $O + H$ reactions. Because O radical and OH radical play an important role in the combustion reaction and work as a combustion reaction promoter, the ignition and combustion of insulation oil are enhanced under microwave induced non-equilibrium plasma. As a result, the flammability limit of combustion of insulation oil is expanded the rotational temperature increases under microwave induced non-equilibrium plasma. The

calorific value of exhaust gas increases under spray combustion by non-equilibrium plasma, because the exhaust gas volume and the mole fractions of combustible gas such as H₂ and CO are increased.

yamamoto@chem-eng.kyushu-u.ac.jp

3G06 PLASMA ASSISTED COMBUSTOR DYNAMICS CONTROL

Wooyung Kim, Jordan Snyder, Jeffrey Cohen, *United Technologies Research Center, United States*

The primary purpose of the current research is to demonstrate and interpret the effectiveness of implementing a plasma discharge to improve combustor dynamics and flame stability. Specifically, a Nano-Second Pulsed Plasma Discharge (NSPD) was applied to a premixed methane/air dump combustor for mitigation of dynamic combustion instabilities with a minimal NO_x penalty. As a result, up to ~ 25 dB noise reduction was observed in the presence of the NSPD. High speed imaging suggests that the NSPD relocated the flame stabilization point from the outer recirculation zone to the center zone. Due to the highly non-equilibrium temperature characteristic of the NSPD, the incremental increase of emissions in the presence of the discharge was minimal, typically around 0.5 EINO_x, while the increase of combustion efficiency could be significant and on the order of ~ 10%. A new control algorithm that measured pressure oscillation amplitude, and actuated with plasma power was developed. This algorithm does not require knowledge/measurement of pressure oscillation phase, and therefore, avoids challenges associated with convective and actuator phase delays. The impact of NSPD on swirlstabilized flames was also investigated for swirl numbers from 0 – 0.33. It is shown that the relative effect of NSPD for dynamics reduction decreases with increasing swirl due to the inherent decrease in nascent flame dynamics. All observations in the current work suggest that the flame shape plays a central role in determining the degree of plasma effectiveness and that any noisy, outer recirculation zone stabilized flames will be significantly improved by this implementation of NSPD. Potential impacts for advanced combustor concepts with wider operability are also discussed.

kimw@utrc.utc.com

3G07 *IN SITU* SPECIES DIAGNOSTICS AND KINETIC STUDY OF PLASMA ACTIVATED ETHYLENE PYROLYSIS AND OXIDATION IN A LOW TEMPERATURE FLOW REACTOR

Joseph K. Lefkowitz¹, Mruthunjaya Uddi^{1,2}, Bret C. Windom^{1,3}, Guofeng Lou^{1,4}, Yiguang Ju¹

¹Princeton University, United States ²Massachusetts Institute of Technology, United States

³University of Colorado Colorado Springs, United States ⁴University of Science and Technology Beijing, China

In situ measurements by mid-IR laser absorption spectroscopy of C₂H₄/Ar pyrolysis and C₂H₄/O₂/Ar oxidation activated by a nanosecond repetitively pulsed plasma have been conducted in a low temperature flow reactor (below 500 K) at a pressure of 60 Torr for both a continuously pulsed plasma discharge mode and a burst mode with 150 pulses. The measurements of the *in situ* diagnostics are validated and complemented by gas chromatography in the continuous discharge mode. A recently developed kinetic mechanism (HP-Mech) for plasma activated C₂H₄ oxidation is assembled. The experiments of plasma activated pyrolysis show that the formation of acetylene by direct electron impact dissociation and dissociation by excited and ionized argon collision reactions is the major fuel consumption pathway. Plasma activated C₂H₄ oxidation experiments show that there exist three fuel consumption pathways, 1) a plasma activated low temperature fuel oxidation pathway via RO₂ chemistry; 2) a direct fragmentation pathway via collisional dissociation by electrons, ions, and electronically excited molecules; and 3) a high temperature oxidation pathway by plasma generated radicals. It is found that the plasma activated low temperature oxidation pathway is dominant and leads to a large amount of formaldehyde formation with less acetylene and negligible large hydrocarbon molecules as compared to the pyrolysis experiment. The results also indicate that the latter two fuel consumption pathways are strongly dependent on O₂ and Ar concentrations due to their effect on the production of atomic oxygen and excited Ar. Although the current model improves the overall prediction over USC-Mech II for plasma activated pyrolysis and oxidation, both models fail to predict quantitatively the H₂O and CH₄ formation. The present data provide good targets for future model development in plasma-assisted combustion.

jlefkowi@Princeton.edu

3G08 TIME-RESOLVED RADICAL SPECIES AND TEMPERATURE DISTRIBUTIONS IN AN Ar-O₂-H₂ MIXTURE EXCITED BY A NANOSECOND PULSE DISCHARGE

Z. Yin, Z. Eckert, I.V. Adamovich, W.R. Lempert, *The Ohio State University, United States*

Temperature and absolute concentrations of OH and H are measured by UV Rayleigh scattering, Laser-Induced Fluorescence (LIF), and Two-Photon Absorption LIF (TALIF), respectively, in an Ar-O₂-H₂ (80:20:2) mixture at P=40 torr and T₀=300 K. The mixture is excited by a 50-pulse burst of a repetitive nanosecond pulse filament discharge, operated at 100 kHz pulse repetition rate and 5 Hz burst repetition rate. One-dimensional radial distributions of temperature and species concentrations across the filament during and after the discharge burst are obtained from Rayleigh scattering and fluorescent images of the laser beam, taken by an Intensified Charge-Coupled Device (ICCD) camera. Both temperature and species concentration profiles are found to expand with time, with peak centerline values of T_{peak}≈1200 K,

$[H]_{\text{peak}} \approx 6.0 \cdot 10^{15} \text{ cm}^{-3}$, and $[OH]_{\text{peak}} \approx 1.0 \cdot 10^{15} \text{ cm}^{-3}$. Secondary maxima in OH distributions are detected near the periphery of the filament after a few tens of discharge pulses. Experimental results are compared with predictions of a plasma-assisted combustion chemistry model. The model reproduces trends in time evolution of radial distributions of temperature, as well as OH and H concentrations. Based on rate of species production analysis, the secondary peaks in OH radial distributions are caused by radial diffusion of H atoms from the central region of the discharge filament, with subsequent formation of HO_2 and OH via reactions $\text{H} + \text{O}_2 + \text{M} \rightarrow \text{HO}_2 + \text{M}$ and $\text{H} + \text{HO}_2 \rightarrow \text{OH} + \text{OH}$ in the low-temperature peripheral regions. The results demonstrate significant potential of the present approach for quantitative, time- and spatially-resolved studies of coupled radical reaction kinetics and diffusion over a wide range of temperatures, pressures, and mixture compositions.

yin.67@osu.edu

3G109 NANOSECOND PLASMA ENHANCED $\text{H}_2/\text{O}_2/\text{N}_2$ PREMIXED FLAT FLAMES

Sharath Nagaraja¹, Ting Li², Jeffrey A. Sutton², Igor V. Adamovich², Vigor Yang¹
¹Georgia Institute of Technology, United States ²Ohio State University, United States

The effect of nanosecond pulsed plasma discharges on a laminar, lean ($\phi = 0.5$) premixed $\text{H}_2/\text{O}_2/\text{N}_2$ flame is studied at low pressure (25 torr), using a novel plasma-flame facility, non-intrusive laser diagnostics, and high-fidelity numerical simulations. Spatially-resolved quantitative OH mole fraction and temperature measurements are performed with and without a burst of 200 nanosecond discharge pulses using laser-induced fluorescence. Measured temperatures increase by ~20% in both the pre-heat and post-flame zones with the use of the plasma discharge. In addition, OH mole fractions increase by 100 - 500% in the preheat zone and an average increase of 40% in the post-flame gases. Simulations are conducted with a one-dimensional, multi-scale, pulsed-discharge model with detailed plasma-combustion kinetics to develop additional insight into the complex plasma and flame interactions. Good agreement between measured and predicted OH and temperature profiles provides confidence in the model framework. The reduced electric field, E/N , during each pulse varies inversely with number density. A significant portion of the input energy is expended to electron impact ionization in the high temperature regions downstream of the flame because of high E/N in this region (700-1000 Td). Lower E/N values (100-700 Td) in the lower-temperature preheat regions, promote efficient generation of radicals and excited species via electron impact processes, as well as by collisional quenching of excited states. The plasma action results in a significant increase in O and H densities, with the peak values increasing by a factor of 6 and 4 respectively. With the plasma on, species and temperature profiles move upstream (i.e. closer to the burner) by approximately 0.2 cm. Simulations show that electron impact dissociation and excitation processes in the plasma have a major impact on the observed temperature and species profile displacement, such that Joule heating alone cannot account for it.

sharath@gatech.edu

3G110 EFFECT OF NON-EQUILIBRIUM PLASMA ON TWO-STAGE IGNITION OF *n*-HEPTANE

Sharath Nagaraja, Wenting Sun, Vigor Yang, Georgia Institute of Technology, United States

The effect of pulsed nanosecond dielectric barrier plasma discharges on the ignition characteristics of *n*-heptane and air mixtures is investigated through self-consistent simulations in a plane-to-plane geometry at reduced pressures (20.3 kPa). A plasma-fluid formulation is developed with ions and neutral species at gas temperature, and electrons in non-equilibrium. The work makes use of an optimized chemical kinetics mechanism consisting of 166 species and 611 reactions, obtained by combining a reduced *n*-heptane kinetic model, a non-equilibrium plasma chemistry scheme, and a NO_x kinetic model. The catalytic effect from plasma-generated radicals on the first stage of the *n*-heptane ignition process has been identified. Production of radicals such as O, H and OH from the plasma initiates and accelerates the H abstraction of fuel molecules, and dramatically reduces the induction time of the exothermic cycle ($\text{RH} \rightarrow \text{R} \rightarrow \text{RO}_2 \rightarrow \text{OROOH}$) by a factor of 10. Furthermore, the plasma action on low temperature chemistry is found to be nearly independent of the equivalence ratio and more pronounced at lower temperatures (550 - 650 K). A staggered application of nanosecond voltage pulses (2 - 4 pulses at the beginning and 20 - 30 pulses after the first stage heat release) is shown to be optimal, resulting in a reduction of the ignition delay by approximately a factor of 2. NO production from the plasma via electron impact and quenching processes at low temperatures plays an important role in promoting chain-branching reactions and contributes to shortening the ignition delay by approximately 10%.

sharath@gatech.edu

3G111 PLASMA ASSISTED COMBUSTION: EFFECTS OF O_3 ON LARGE SCALE TURBULENT COMBUSTION STUDIED WITH LASER DIAGNOSTICS AND LARGE EDDY SIMULATIONS

A. Ehn¹, J. Zhu¹, P. Petersson¹, Z. Li¹, M. Aldén¹, C. Fureby², T. Hurtig², N. Zettervall², A. Larsson², J. Larfeldt³
¹Lund University, Sweden ²Swedish Defence Research Agency – FOI, Sweden ³Siemens Industrial Turbomachinery AB, Sweden

In plasma-assisted combustion, electric energy is added to the flame where the electric energy will be transferred to kinetic energy of the free electrons that, in turn, will modify the combustion chemical kinetics. In order to increase the understanding of this complex process, the influence of one of the products of the altered chemical kinetics, ozone (O_3),

has been isolated and studied. This paper reports on studies using a low-swirl methane (CH_4) air flame at lean conditions with different concentrations of O_3 enrichment. The experimental flame diagnostics include Planar Laser Induced Fluorescence (PLIF) imaging of Hydroxyl (OH) and formaldehyde (CH_2O). The experiments are also modeled using Large Eddy Simulations (LES) with a reaction model based on a skeletal CH_4 -air reaction mechanism combined with an O_3 sub-mechanism to include the presence of O_3 in the flame. This reaction mechanism is based on fundamental considerations including reactions between O_3 and all other species involved. The experiments reveal an increase in CH_2O in the low-swirl flame as small amounts of O_3 is supplied to the CH_4 -air stream upstream of the flame. This increase is well predicted by the LES computations and the relative radical concentration shift is in good agreement with experimental data. Simulations also reveal that the O_3 enrichment increase the laminar flame speed, s_u , with $\sim 10\%$ and the extinction strainrate, σ_{ext} , with $\sim 20\%$, for 0.57% (by volume) O_3 . The increase in σ_{ext} enables the O_3 seeded flame to burn under more turbulent conditions than would be possible without O_3 enrichment. Sensitivity analysis indicates that the increase in σ_{ext} due to O_3 enrichment is primarily due to the accelerated chain-branching reactions $\text{H}_2 + \text{O} \rightleftharpoons \text{OH} + \text{H}$, $\text{H}_2\text{O} + \text{O} \rightleftharpoons \text{OH} + \text{OH}$ and $\text{H} + \text{O}_2 \rightleftharpoons \text{OH} + \text{O}$. Furthermore, the increase in CH_2O observed in both experiments and simulations suggest a significant acceleration of the chain-propagation reaction $\text{CH}_3 + \text{O} \rightleftharpoons \text{CH}_2\text{O} + \text{H}$.

andreas.ehn@forbrf.lth.se

3G12 SELF-SUSTAINING *N*-HEPTANE COOL DIFFUSION FLAMES ACTIVATED BY OZONE

Sang Hee Won¹, Bo Jiang^{1,2}, Pascal Diévert¹, Chae Hoon Sohn^{1,3}, Yiguang Ju¹

¹Princeton University, United States ²Nanjing University of Aeronautics & Astronautics, China ³Sejong University, Korea

A novel method to establish self-sustaining cool diffusion flames with well-defined boundary conditions has been experimentally demonstrated by using ozone into the oxidizer stream in counterflow configuration. It is found that the formation of atomic oxygen via the decomposition of ozone dramatically shortens the induction timescale of low temperature chemistry, extending the flammable region of cool flames, and enables the establishment of self-sustaining cool flames at pressure and timescales at which normal cool flames may not be observable. The present method, for the first time, provides an opportunity to study cool flame dynamics, structure, and chemistry simultaneously in well-known flame geometry. Extinction limits of *n*-heptane/oxygen cool diffusion flames are measured. A cool diffusion flame diagram for four different flame regimes is experimentally measured. Numerical simulations show that the extinction limits of cool diffusion flames are strongly governed by species transport and low temperature chemistry activated by ozone decomposition. The structure of cool diffusion flame is further investigated by measuring the temperature and species distributions with a micro-probe sampling technique. It is found that the model over-predicts the rate of *n*-heptane oxidation, the heat release rate, and the flame temperature. Measurements of intermediate species, such as CH_2O , acetaldehyde, C_2H_4 , and CH_4 indicate that the model over-predicts the QOOH thermal decomposition reactions to form olefins, resulting in substantial over-estimation of C_2H_4 , and CH_4 concentrations. The new method and data of the present study will contribute to promote understandings of cool flame chemistry.

sangwon@Princeton.EDU

THURSDAY PLENARY LECTURE: DEVELOPMENTS IN INTERNAL COMBUSTION ENGINES AND IMPLICATIONS FOR COMBUSTION SCIENCE AND FUTURE TRANSPORT FUELS

G.T. Kalghatgi, Aramco, Saudi Arabia

Changes in engine technology, driven by the need to increase the efficiency of the SI engine and reduce NO_x and soot from diesel engines, and in transport energy demand will have a profound effect on the properties, specifications and production of future fuels. The expected increase in global demand for transport energy is significantly skewed towards heavier fuels like diesel and jet fuel while the demand for gasoline might decrease. Abnormal combustion such as knock and preignition will become more likely as Spark-Ignition (SI) engines develop to become more efficient and fuel antiknock quality will become more important. In current and future SI engines, for a given RON (Research Octane Number), a fuel of lower MON (Motor Octane Number) has better antiknock quality. Current fuel specifications in several parts of the world assume that MON contributes to antiknock quality and will need to be revised as the mismatch with engine requirements widens. The primary challenge for diesel engines is to reduce emissions of soot and NO_x while maintaining high efficiency. This becomes much easier if such engines are run on fuels of extremely low cetane. In the long term compression ignition engines are likely to use fuels with RON in the range of 70-85 (Cetane number $< \sim 30$) but with no strict requirements on volatility. Such fuels would require less processing in the refinery than today's fuels and also help mitigate the expected demand imbalance in favour of heavier fuels. Such an engine/fuels system will be at least as efficient as today's diesel engine but could be significantly cheaper. The review concludes with a list of issues for combustion science that are relevant to this fuel and engine development.

gautam.kalghatgi@aramco.com

4A01 IMPACT OF HEAT LOSS ON V TO M SHAPE TRANSITION OF CONFINED SWIRLING FLAMES

T.F. Guiberti^{1,2}, D. Durox^{1,2}, P. Scoufflaire^{1,2}, T. Schuller^{1,2}

¹Ecole Centrale Paris, France ²CNRS, France

Shape transitions of swirling flames are often observed in combustion chambers operated at fixed flow conditions. These transitions may alter pollutant emissions, heat fluxes to the chamber walls or the system stability. In adiabatic combustors, transitions of a V to a M swirling flame are controlled by the dynamics of stretched flame elements propagating through the reactants diluted by the burnt products in the outer shear layer of the swirling combustible jet in contact with the hot outer recirculation zone. The impact of H₂ concentration in the fuel and of heat loss at the chamber walls modifying the temperature in the outer recirculation zone are analyzed in this study for lean premixed CH₄/H₂/air flames. Laser induced OH fluorescence in different planes and particle imaging velocimetry are used to determine the probability of V to M shape transitions when the hydrogen concentration or the temperature of the combustor walls are modified. The wall temperatures are determined by laser induced phosphorescence and the temperature in the outer recirculation zone is inferred from thermocouple measurements. It is found that the probability of stabilizing a M flame increases with the H₂ concentration. For the same laminar burning velocity, the mixture featuring a higher extinction limit to strain rate has a higher probability to take a M shape. When combustion is initiated with cold chamber walls, the V to M flame transition probability is reduced compared to a situation with hot walls. During thermal transient and at steady state, it is shown that the evolution of the chamber wall temperature is an important factor controlling these shape transitions due to its impact on the temperature of burnt gases in the outer recirculation zone. This study confirms the high sensitivity to heat transfer to the combustion chamber walls in the stabilization of swirling flames.

thibault.guiberti@ecp.fr

4A02 UNBURNED MIXTURE FINGERS IN PREMIXED TURBULENT FLAMES

Andrei N. Lipatnikov¹, Vladimir A. Sabelnikov², Shinnosuke Nishiki³, Tatsuya Hasegawa⁴

¹Chalmers University of Technology, Sweden ²ONERA - The French Aerospace Lab., France

³Kagoshima University, Japan ⁴Nagoya University, Japan

Data obtained in 3D direct numerical simulations of statistically planar, 1D premixed turbulent flames indicate that the global burning velocity, flame surface area, and the mean flame brush thickness exhibit significant large-scale oscillations with time. Analysis of the data shows that the oscillations are caused by origin, growth, and subsequent disappearance of elongated channels filled by unburned gas. The growth of such an Unburned Mixture Finger (UMF), which deeply intrudes into combustion products, is controlled by a physical mechanism of flame-flow interaction that has not yet been highlighted in the turbulent combustion literature, to the best of the present authors knowledge. More specifically, the fingers grow due to strong axial acceleration of unburned gas by local pressure gradient induced by heat release in surrounding flamelets. Under conditions of the present DNS, this physical mechanism plays an important role by producing at least as much flame surface area as turbulence does when the density ratio is equal to 7.5. Although, similarly to the Darrieus-Landau (DL) instability, the highlighted physical mechanism results from the interaction between a premixed flame and pressure field, it is argued that the UMF and the DL instability are different manifestations of the aforementioned interaction. Disappearance of an UMF is mainly controlled by the high-speed self-propagation of strongly inclined flame fronts (cusps) to the leading edge of the flame brush, but significant local increase in displacement speed due to large negative curvature of the front plays an important role also.

lipatn@chalmers.se

4A03 MODELLING OF MEAN FLAME SHAPE DURING PREMIXED FLAME FLASHBACK IN TURBULENT BOUNDARY LAYERS

A. Gruber¹, A.R. Kerstein¹, D. Valiev⁴, C.K. Law^{2,3}, H. Kolla⁴, J.H. Chen⁴

¹SINTEF Energy Research, Norway ²Princeton University, United States ³Tsinghua University, China

⁴Sandia National Laboratories, United States

Direct numerical simulations of freely-propagating premixed flames in the turbulent boundary layer of fully-developed turbulent channel flows are used for a priori validation of a new model that aims to describe the mean shape of the turbulent flame brush during flashback. Comparison with the DNS datasets, for both fuel-lean and fuel-rich mixture conditions and for Damköhler numbers lower and larger than unity, shows that the model is able to capture the main features of the flame shape. Although further a priori and a posteriori validation is required, particularly at higher Reynolds numbers, this new simple model seems promising and can potentially have impact on the design process of industrial combustion equipment.

andrea.gruber@sintef.no

4A04 IMPACT OF FUEL COMPOSITION ON THE RECIRCULATION ZONE STRUCTURE AND ITS ROLE IN LEAN PREMIXED FLAME ANCHORING

Seunghyuck Hong, Santosh J. Shanbhogue, Ahmed F. Ghoniem, Massachusetts Institute of Technology, United States

We investigate the dependence of the Recirculation Zone (RZ) size and structure on the fuel composition using high-speed Particle Image Velocimetry (PIV) and chemiluminescence measurements for C₃H₈/H₂/air lean premixed flames

stabilized in a backward-facing step combustor. Results show an intricate coupling between the flame anchoring and the RZ structure and length. For a fixed fuel composition, at relatively low equivalence ratios, the time-averaged RZ is comprised of two counter rotating eddies: a Primary Eddy (PE) between the shear layer and the bottom wall; and a Secondary Eddy (SE) between the vertical step wall and the PE. The flame stabilizes downstream of the saddle point of the dividing streamline between the two eddies. As equivalence ratio is raised, the flame moves upstream, pushing the saddle point with it and reducing the size of the SE. Higher temperature of the products reduces the velocity gradient in the shear layer and thus the reattachment length. As equivalence ratio approaches a critical value, the saddle point reaches the step and the SE collapses while the flame starts to exhibit periodic flapping motions, suggesting a correlation between the RZ structure and flame anchoring. The overall trend in the flow field is the same as we add hydrogen to the fuel at a fixed equivalence ratio, demonstrating the impact of fuel composition on the flow field. We show that the reattachment lengths (L_R), which are shown to encapsulate the mean RZ structure, measured over a range of fuel composition and equivalence ratio collapse if plotted against the strained consumption speed (S_c). Results indicate that for the flame to remain anchored, the RZ structure should satisfy $(L_{R, \text{isothermal}} S_c) / (L_{R, \text{reacting}} U_\infty) \sim 0.1$. If this criterion cannot be met, the flame blows off, flashes back or becomes thermoacoustically unstable, suggesting a Damköhler-like criterion for aerodynamic flame stabilization in backward-facing step flows.

ghoniem@mit.edu

4A05 FUEL EFFECTS ON LEADING POINT CURVATURE STATISTICS OF HIGH HYDROGEN CONTENT FUELS

Andrew Marshall, Julia Lundrigan, Prabhakar Venkateswaran, Jerry Seitzman, Tim Lieuwen,
Georgia Institute of Technology, United States

Fuel composition has significant influences on the turbulent flame speed of mixtures with strong stretch sensitivity. These fuels effects are associated with reactant thermal-diffusive properties and stretch sensitivities, causing local variations in the burning rate along the flame front. This study is motivated by leading point descriptions of the turbulent flame speed, which argue that S_T is controlled by the flame characteristics at its positively curved leading edge. It has been argued that the leading edge of the flame approaches “critically stretched” values in thermo-diffusively unstable flames, implying that the appropriate laminar flame speed to parameterize the turbulent flame speed is the maximum flame speed across all potential values of flame stretch, $S_{L, \text{max}}$, as opposed to its unstretched value, $S_{L,0}$. This paper describes an experimental investigation of the characteristics of the flame leading point in high stretch sensitivity flames to assess this hypothesis more fully. Measurements of the flame curvature were obtained with a Low Swirl Burner (LSB) for several H_2/CO mixtures at velocities from 30-50 m/s. These data show that the leading point conditioned curvature statistics are a strong function of the turbulence intensity of the flow. Counter to our expectations, however, the measurements show relatively weak influences of fuel composition on the leading point curvature of the turbulent flame front. As such, these results do not seem consistent with prior arguments that the increased turbulent flame speeds seen with increasing hydrogen content are the result of increasing flame curvature/stretch rates, and therefore $S_{L, \text{max}}$ values, at the flame leading points. Additional analysis is needed to understand the physical mechanisms through which the turbulent flame speed is altered by differential diffusion effects.

andrew.marshall@gatech.edu

4A06 TURBULENCE-FLAME INTERACTION AND FRACTAL CHARACTERISTICS OF H_2 -AIR PREMIXED FLAME UNDER PRESSURE RISING CONDITION

Basmil Yenerdag¹, Naoya Fukushima¹, Masayasu Shimura¹, Mamoru Tanahashi¹, Toshio Miyauchi²
¹Tokyo Institute of Technology, Japan ²Meiji University, Japan

Direct Numerical Simulation (DNS) of turbulent premixed flames in a constant volume vessel is conducted to investigate turbulence-flame interaction and fractal characteristics under pressure rising condition. DNS is conducted for hydrogen-air mixture with decaying homogeneous isotropic turbulence of which Reynolds number based on Taylor micro scale is 97:1. The detail kinetic mechanism including 12 reactive species and 27 elementary reactions is used to represent the hydrogen-air flames. Even for pressure rising process, the local heat release rate, the flame curvature and the tangential strain rate can be scaled by the maximum laminar heat release rate corresponding to instantaneous mean pressure, the Kolmogorov length scale and the ratio of the turbulent intensity to the Taylor micro scale in the unburned mixture. These facts show very quick response of flame characteristics to the pressure change. In the propagation process, flame displacement speed is very high compared to open flames due to the expansion of the burned gas. The compression of the unburned mixture due to the high displacement speed increases pressure in the vessel and induces slow decaying or increasing of turbulent Reynolds number even for no mean flow. It is clarified that fractal dimension of the flame surface do not show any dependence on pressure increase. The inner cutoff obtained in pressure rising condition shows good agreement with the expression proposed in our previous study where the ratio of the diameter of coherent fine scale eddy, which is an universal fine scale structure of turbulence, to the laminar flame thickness is used as an important parameter.

ybasml@navier.mes.titech.ac.jp

4A07 THREE-DIMENSIONAL TOPOLOGY OF TURBULENT PREMIXED FLAME INTERACTION

R.A.C. Griffiths^{1,2}, J.H. Chen³, H. Kolla³, R.S. Cant², W. Kollmann¹

¹University of Cambridge, United Kingdom ²University of California Davis, United States ³Sandia National Laboratories, United States

The topology of turbulent premixed flames is analysed using data from Direct Numerical Simulation (DNS), with emphasis on the statistical geometry of flame–flame interaction. A general method for obtaining the critical points of line, surface and volume fields is outlined, and the method is applied to isosurfaces of reaction progress variable in a DNS configuration involving a pair of freely-propagating hydrogen–air flames in a field of intense shear-generated turbulence. A complete set of possible flame–interaction topologies is derived using the eigenvalues of the scalar Hessian, and the topologies are parameterised using a pair of shape factors. The frequency of occurrence of each type of topology is evaluated from the DNS dataset for two different Damköhler numbers. Different types of flame–interaction topology are found to be favoured in various regions of the turbulent flame, and the physical significance of each interaction is discussed.

racg3@cam.ac.uk

4A08 FLAME STRUCTURE ANALYSIS FOR CATEGORIZATION OF LEAN PREMIXED CH₄/AIR AND H₂/AIR FLAMES AT HIGH KARLOVITZ NUMBERS: DIRECT NUMERICAL SIMULATION STUDIES

Henning Carlssona, Rixin Yu, Xue-Song Bai, Lund University, Sweden

This paper presents direct numerical simulation studies of lean CH₄/air and H₂/air flames at high Karlovitz numbers utilizing detailed chemical kinetic mechanisms. Identical Karlovitz numbers are applied to the two flames; however, as the interaction of high turbulence intensity small scale structures with the reaction zones is investigated, a significant difference in the effect of the turbulence structures on the inner reaction layer is observed. The heat release rate layer as well as layers of different species reaction rates are found to be more distributed for the H₂/air flame compared with the CH₄/air flame, flowing to a smaller Kolmogorov length scale and differential diffusion effects. A modified, species specific Karlovitz number is proposed, where the chemical time scale in the definition is a characteristic species specific chemical time scale, which is obtained from stationary 1D simulations. The difference between the two flames for different intermediate species corresponds well to the difference in species specific Karlovitz numbers obtained. A validation study of the species specific Karlovitz number is also conducted, where a chemical time scale after the reaction zone has been affected by turbulence for different intermediate species is quantified from instantaneous data sets. In the preheat zone and reaction zone of the flame, the ratio between the laminar and turbulent chemical time scales of intermediate species corresponds well to the species specific Karlovitz numbers for the two different flames.

Henning.Carlsson@energy.lth.se

4B01 NUMERICAL STUDY OF UNSTABLE HYDROGEN/AIR FLAMES: SHAPE AND PROPAGATION SPEED

Christos E. Frouzakis¹, Navin Foglia², Ananias G. Tomboulides³, Christos Altantzis⁴, Moshe Matalon²

¹Swiss Federal Institute of Technology, Switzerland ²University of Illinois at Urbana-Champaign, United States

³University of Western Macedonia, Greece ⁴Massachusetts Institute of Technology, United States

Extensive 2-D numerical simulations with detailed chemistry and transport are performed to investigate the effect of equivalence ratio and domain size on the initial amplification of flame front perturbations and the long-term propagation of hydrogen/air premixed flames. Equivalence ratios in the range $0.5 \leq \phi \leq 2.0$ are considered in order to study the stabilizing and destabilizing influence of hydrodynamic and thermodiffusive processes. The numerical data are used to extract the range of unstable wavenumbers and the maximum amplification rate, which are found to increase with decreasing equivalence ratio from rich ($\phi = 2.0$) to lean ($\phi = 0.5$). The numerical dispersion relations are compared with linear stability theory, and, with the exception of the leanest mixture, are found to be in good agreement. The nonlinear dynamics depend strongly on ϕ and the domain size and the flame shape is characterized by a single-cusp structure, which is either stably propagating with a constant speed (stoichiometric and rich mixtures) or are contaminated by small cells which form on the cusp sides, propagate along the front and annihilate at the cusp. In the latter case, the flame propagates with a speed which varies in time.

frouzakis@lav.mavt.ethz.ch

4B02 PULSATING INSTABILITY IN H₂-AIR PARTIALLY PREMIXED FLAMES

Fan Yang, Wenjun Kong, Chinese Academy of Sciences, China

Steady/unsteady hydrogen–air Partially Premixed Flames (PPFs) in counterflow configuration were computationally studied with detailed chemistry and transport, and the pulsating instability of PPFs was observed. During the PPFs oscillation, the pulsating instability for the premixed flame is caused by a large overall activation energy (E_a) and a slow O₂ diffusion process ($Le > 1$). The nonpremixed flame undergoes forced oscillation caused by oscillated H₂ diffusion flux from the premixed flame zone. In H₂–air PPFs, premixed/nonpremixed flame structures and the interactions between them are controlled by the equivalence ratio (ϕ) and global strain rate (a). The two factors also control the stability

boundary. Large ϕ and/or a retard the occurrence of pulsating instability. This result is attributed to increasing ϕ and/or a , which causes the two flames to move closer, intensifying the conduction heat flux from nonpremixed flame to premixed flame. The temperature in strengthened premixed flame is not sensitive to the perturbation of chemical heat release, on the other hand, the competition between $\text{H} + \text{O}_2 \leftrightarrow \text{OH} + \text{O}(\text{R1})$ and $\text{H} + \text{O}_2 + \text{M} \leftrightarrow \text{HO}_2 + \text{M}(\text{R9})$ decreases, which leads to smaller E_a . Thus, the chemical reactions are also not sensitive to the perturbation of flame temperature.

yangfan@iet.cn

4B03 MINOR-SPECIES STRUCTURE OF PREMIXED CELLULAR TUBULAR FLAMES

Carl A. Hall¹, Waruna D. Kulatilaka², Naibo Jiang², James R. Gord³, Robert W. Pitz¹

¹Vanderbilt University, United States ²Spectral Energies, LLC, United States ³Wright-Patterson Air Force Base, United States

Quantitative spatially resolved measurements of atomic hydrogen and hydroxyl radicals are reported of cellular phenomena in lean laminar premixed hydrogen–air tubular flames. Femtosecond Two-Photon Laserinduced Fluorescence (fs-TPLIF) enables photolytic-interference-free measurement of H atoms. Quenching corrections are calculated from temperature and major-species measurements determined by spontaneous Raman scattering. In the sub-unity Lewis number, highly stretched and curved premixed flame structure, the strong effect of thermal-diffusive imbalance is observed through clear local extinction (dearth of H atoms) and highly curved reaction cells. Peak H-atom number densities of $5 \times 10^{15} \text{ cm}^{-3}$ and peak OH number densities of $9 \times 10^{15} \text{ cm}^{-3}$ are found but remain approximately the same value despite doubling the flame stretch from 200 to 400 s^{-1} . Comparisons to non-cellular tubular flame numerical predictions show that the cellular transition increases temperature and local equivalence ratio but lowers peak number densities of H and OH. For cellular instabilities in the tubular flame, the thermal-diffusive imbalance maintains a similar local flame structure (i.e., same curvature and peak values of H, OH, T, and local equivalence ratio) that is insensitive to stretch rate.

Carl.A.Hall@Vanderbilt.edu

4B04 FLAMES IN CONTEXT OF THERMO-ACOUSTIC STABILITY BOUNDS

Maarten Hoeijmakers¹, Viktor Kornilov¹, Ines Lopez^{1,2}, Philip de Goey¹, Henk Nijmeijer¹

¹Eindhoven University of Technology, Netherlands ²Marcus Wallenberg Laboratory, Sweden

Bounds are derived for the acoustic losses such that a thermoacoustic system with a given flame can be guaranteed to be stable. The analysis is based on the flame's acoustic input-to-output properties represented by its scattering matrix. The developed analytical and numerical techniques allow estimating the maximum reflection coefficients (equivalently - acoustic losses) which are sufficient to ensure stable operation of a given burner. It is shown that the calculated numerical upper-bound is less conservative than the analytical one. The frequency dependence of the required acoustic losses provides i) a thermoacoustic signature of the flame and ii) guidelines for the proper design of the up- and downstream acoustics from the flame. The method is illustrated on two burners/flames of premixed multiple Bunsen type. The frequency dependence of the upper bounds allows to identify those frequency ranges where the flame is more likely to cause instability of the complete system.

p.g.m.hoeijmakers@tue.nl

4B05 TIME-DOMAIN ANALYSIS OF THERMO-ACOUSTIC INSTABILITIES IN A DUCTED FLAME

T. Sayadi¹, V. Le Chenadec^{2,3}, P. Schmid¹, F. Richecoeur^{2,3}, M. Massot^{2,3,5}

¹Imperial College London, United Kingdom ²EM2C, CNRS, France ³École Centrale Paris, France ⁵CNRS, France

The present study focuses on a time-domain approach for investigating the response of laminar premixed flames to acoustic flow perturbations. This alternative perspective has recently been found to facilitate the analysis and interpretation of thermo-acoustic instabilities by providing a more intuitive description of the interaction of the acoustics with the heat release rate. A framework is first introduced to generate accurate time-series that provide a complete description of the thermo-acoustic system. Advantages include the flexibility to account for different models (delayed, local, and non-local terms), as well as the separation of numerical and modeling errors. Advanced dynamical system techniques are then employed to analyze the low-amplitude (linear) and finite-amplitude (nonlinear limit-cycle) regimes. These techniques are found to accurately characterize the transition between the two regimes, and give access to the coupled dynamics of complex limit-cycles. This information forms the basis for an effective use of system reduction techniques. The presented capabilities are found to yield physical insight with relative ease, and are expected to yield interesting results by revisiting existing experimental and numerical strategies for the study of thermo-acoustic instabilities.

sayadi@ladhyx.polytechnique.fr

4B06 THE RESPONSE OF A HARMONICALLY FORCED PREMIXED FLAME STABILIZED ON A HEATCONDUCTING BLUFF-BODY

Kushal S. Kedia, Ahmed F. Ghoniem, Massachusetts Institute of Technology, United States

The objective of this work is to investigate the unsteady response of a bluff-body stabilized laminar premixed flame to harmonic inlet velocity excitation. A time series analysis was performed to analyze the physical sequence of events at a fixed longitudinal forcing frequency of 100 Hz for cases with (1) two different equivalence ratios and (2) two different thermal properties of the stabilizing bluff-body. It was observed that conjugate heat exchange between the heat

conducting bluff-body and the surrounding reacting flow has a crucial impact on the dynamic response. The flame area and anchoring location, the net conjugate heat transfer and the total heat release underwent significant oscillations. The latter was mean shifted and had multiple frequencies. The burning velocity varied significantly along the flame length and the recirculation zone underwent complex changes in its shape and size during an unsteady cycle. The lower equivalence ratio case exhibited vortex shedding after an initial symmetric response with periodic flame extinction and re-ignition along its surface, unlike the higher equivalence ratio case. The metal/ceramic bluff-body showed a net heat transfer directed from/to the bluff-body, to/from the reacting flow during an unsteady cycle, resulting in a significantly different flame response for the two otherwise equivalent cases.

kushal@mit.edu

4B07 THERMO-ACOUSTIC INSTABILITIES IN LEAN PREMIXED SWIRL-STABILIZED COMBUSTION AND THEIR LINK TO ACOUSTICALLY COUPLED AND DECOUPLED FLAME MACROSTRUCTURES

*Soufien Taamallah, Zachary A. LaBry, Santosh J. Shanbhogue, Ahmed F. Ghoniem
Massachusetts Institute of Technology, United States*

We investigate the onset of thermo-acoustic instabilities and their link to the flame macrostructure configurations under acoustically coupled and decoupled conditions. Methane/hydrogen mixtures are used to explore the role of the fuel in changing the flame macrostructure, as determined by chemiluminescence, as the equivalence ratio ϕ varies. We observe four different configurations: a columnar flame (I); a bubble-columnar flame (II); a single conical flame (III); and a double conical flame (IV). We also observe different dynamic modes in the lean regime, $\phi \in [0.5-0.75]$, that correspond to different flame configurations. By changing the combustor length without affecting the underlying flow, the lower resonant frequency modes of the geometry are suppressed allowing for the decoupling of heat release fluctuations and the acoustic field over a range of equivalence ratio. We find that the same flame macrostructures observed in the long, acoustically coupled combustor arise in the short, acoustically decoupled combustor and transition at similar equivalence ratios in both combustors. The onset of the first fully unstable mode in the long combustor occurs at the same equivalence ratio as the flame transitions from configuration III to IV. In the acoustically decoupled case, this transition occurs gradually starting with the intermittent appearance of a flame in the outer recirculation zone. Spectral analysis of this phenomenon, referred to as "flame flickering" shows the existence of an unsteady event occurring over a narrow frequency band centered around 28 Hz. This frequency is shown to be associated with the advection azimuthally of the flame around the burner centerline. Changes in the fuel composition, by adding hydrogen, do not affect the correspondence between the dynamic modes and the flame macrostructures, but shift the transition points between the different configurations.

sofiene@mit.edu

4B08 STABILITY ANALYSIS OF A SWIRLED SPRAY COMBUSTOR BASED ON FLAME DESCRIBING FUNCTION

C. Mirat^{1,2}, D. Durox^{1,2}, T. Schuller^{1,2}

¹CNRS, France ²Ecole Centrale Paris, France

Stability analysis exploiting the Flame Describing Function (FDF) of premixed swirling flames was recently shown to capture the main features of the variety of dynamical states observed in premixed combustors. Confrontations of experimental data gathered at limit cycles of thermo-acoustic instabilities in non-premixed systems with predictions based on the analysis of the flame response to externally forced perturbations remain rare and difficult to carry out. In this study, self-sustained combustion oscillations observed at limit cycles in a swirled combustor equipped with liquid fuel injectors are analyzed with the help of FDF. It is first shown that flames stabilized at globally lean conditions burn in a non-premixed mode with non-sooty and sooty regimes. Their unsteady response is then characterized by exploiting the OH* chemiluminescence signal. The FDF of these non-premixed two-phase flow flames features a distinct response compared to lean swirling premixed flames. The gain and phase lag of these FDF is a strong function of the perturbation level. The phase lag increases with the perturbation level for the non-sooty flames and decreases in sooty cases. The sooty flames have also a much lower cutoff frequency. It is then shown that these features are essential to reproduce the correct instability bands and oscillation frequencies at limit cycles. In the sooty-flame regime combustion is always stable. A linear analysis in the non-sooty case fails to capture low frequency instability that have the largest oscillation levels. The FDF enables in both cases to reproduce the correct dynamical state. It is further concluded that the OH* chemiluminescence signal may safely be used to infer the acoustic response of these spray flames at globally lean conditions.

clement.mirat@ecp.fr

4B09 COMBINED EFFECT OF SPATIAL AND TEMPORAL VARIATIONS OF EQUIVALENCE RATIO ON COMBUSTION INSTABILITY IN A LOW-SWIRL COMBUSTOR

Shigeru Tachibana¹, Kota Kanai², Seiji Yoshida¹, Kazuo Suzuki¹, Tetsuya Sato²

¹Japan Aerospace Exploration Agency, Japan ²Waseda University, Japan.

In this experimental study, the combined effect of the fuel inhomogeneity and flow dynamics on the combustion instability is firstly reported in the low-swirl combustor configuration. The experiment is performed using a gas-turbine

model combustor (~60kW) with a low-swirl injector. Detailed measurements are performed in 4 fuel split (to upstream/downstream injections) conditions while keeping the total equivalence ratio constant. It is shown that the combustion stability is very sensitive to the fuel split parameter which determines the local equivalence ratio distribution. Most of the global heat-release oscillations is generated in the flame-to-wall impingement zone in a manner that satisfies the Rayleigh criterion. The driving force of the instability is considered the periodic interaction between the traveling vortex shed from the injector rim and stationary vortex below the flame-to-wall impingement point as reported in the previous study on homogeneous mixture flame. However, the strength of the instability is modified sensitively by changing the local equivalence ratio distribution. Additionally, it is shown that, in the strongest oscillation case, temporal variations of the equivalence ratio provide a positive contribution in the thermoacoustic coupling mechanism.

tachibana.shigeru@jaxa.jp

4C01 LAMINAR FLAME SPEEDS, COUNTERFLOW IGNITION, AND KINETIC MODELING OF THE BUTENE ISOMERS

Peng Zhao¹, Wenhao Yuan², Hongyan Sun¹, Yuyang Li^{1,2}, Andrew P. Kelley¹, Xiaolin Zheng³, C. K. Law^{1,4}

¹Princeton University, United States ²University of Science and Technology of China, China ³Stanford University, United States

⁴Tsinghua University, China

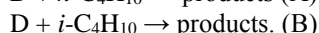
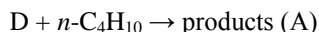
Laminar flame speeds and ignition temperatures of nonpremixed counterflow were measured experimentally for the butene isomers at normal and elevated pressures. Results show that the flame speed increases in the order of isobutene, trans-2-butene, and 1-butene. Furthermore, isobutene has the highest ignition temperature, while those of trans-2-butene and cis-2-butene are quite similar to each other and are slightly higher than that of 1-butene. These results indicate that the reactivities of the butene isomers increase in the order of isobutene, 2-butene, and 1-butene, which in turn implies that short alkenes with straight-chain structures and/or with the double bond situated closer to the end of the chain are more reactive than the other isomers. Furthermore, the critical reaction paths of butene isomer oxidation were analyzed and a new kinetic model was developed with updated rate coefficients from *ab initio* calculation and kinetic theories. Simulations with the present kinetic model agree well with the measured flame speeds as well as the ignition temperatures for all the isomers.

cklaw@princeton.edu

4C02 HIGH TEMPERATURE RATE CONSTANTS FOR H/D + *n*-C₄H₁₀ AND *i*-C₄H₁₀

S.L. Peukert, R. Sivaramakrishnan, J.V. Michael, Argonne National Laboratory, United States

The reactions of D/H with *n*-C₄H₁₀ and *i*-C₄H₁₀ have been studied with both shock-tube experiments and *ab initio* transition state theoretical calculations. D-atom profiles were measured behind reflected shock waves using D-atom atomic resonance absorption spectrometry (ARAS) in mixtures with C₂D₅I (D-atom precursor, <1 ppm) and the alkane of interest in excess (>200 ppm), over the Trange 1063 – 1327 K, at pressures \cong 0.5 atm. D-atom depletion in the present experiments is sensitive only to the reactions,



Simulations of the measured D-atom profiles allow for determinations of total rate constants for the processes (A) and (B). The experimental rate constants are well represented by the Arrhenius equations,

$$k_A = 2.11 \times 10^{-9} \exp(-5661 \text{ K/T}) \text{ cm}^3 \text{ molecules}^{-1} \text{ s}^{-1} \quad (1074\text{-}1253 \text{ K})$$

$$k_B = 2.57 \times 10^{-9} \exp(-5798 \text{ K/T}) \text{ cm}^3 \text{ molecules}^{-1} \text{ s}^{-1} \quad (1063\text{-}1327 \text{ K})$$

The title reactions have also been characterized using electronic structure theory at the CCSD(T)/CBS//M06-2X/cc-pvtz level of theory. Over the T-range of the present experiments, the *ab initio* based Transition State Theory (TST) kinetics predictions for the isotope effects, k_D/k_H , are near unity. The theoretical predictions are in good agreement with the experimental results and can be represented by the modified Arrhenius equations,

$$k_{A,\text{THEORY}} = 6.677 \times 10^{-17} T^{2.118} \exp(-2700 \text{ K/T}) \text{ cm}^3 \text{ molecules}^{-1} \text{ s}^{-1} \quad (500\text{-}2000 \text{ K})$$

$$k_{B,\text{THEORY}} = 5.627 \times 10^{-20} T^{2.934} \exp(-1225 \text{ K/T}) \text{ cm}^3 \text{ molecules}^{-1} \text{ s}^{-1} \quad (500\text{-}2000 \text{ K})$$

To our knowledge, the present experiments are the first direct measurements for the title reactions and the rate constants from this combined experimental/theoretical effort are recommended for use in combustion modeling. Results from the present studies on *n*-C₄H₁₀ and *i*-C₄H₁₀ along with prior studies on C₂H₆ and C₃H₈ suggest the applicability of rate rules for H + Alkanes that are based on generic primary, secondary, and tertiary abstraction sites.

jmichael@anl.gov

4C03 EXPERIMENTAL AND KINETIC MODELING STUDY OF TRANS-2-BUTENE OXIDATION IN A JET-STIRRED REACTOR AND A COMBUSTION BOMB.

Yann Fenard¹, Philippe Dagaut¹, Guillaume Dayma¹, Fabien Halter^{1,2}, Fabrice Foucher²

¹CNRS-INSIS, France ²University of Orléans, France

Butenes are intermediates ubiquitously formed by decomposition and oxidation of larger hydrocarbons (e.g. alkanes) or alcohols present in conventional or reformulated fuels. This study provides new complementary data for the

oxidation of trans-2-butene. The oxidation of trans-2-butene was studied for measuring stable species concentration profiles during the oxidation of the fuel at atmospheric pressure, over a range of equivalence ratios ($0.5 \leq \phi \leq 2$), and temperatures (900-1450K). A combustion bomb apparatus was used to determine laminar flame velocities of trans-2-butene in air at 1 atm, 300K, and for equivalence ratios of 0.8-1.4. The oxidation of trans-2-butene was simulated under these experimental conditions using an extended detail chemical kinetic reaction mechanism (201 species involved in 1788 reactions). This mechanism is based on a previously proposed scheme for the oxidation of hydrocarbons. Good agreement with experimental data presented in this article was obtained which significantly improves kinetic modeling ability. The structure of a trans-2-butene premixed low pressure flat flame recently published was also successfully modeled. Sensitivity and reaction pathways analyses were performed to get insights into the processes involved in the oxidation of trans-2-butene.

dagaut@cnrs-orleans.fr

4C04 EXPERIMENTAL AND MODELLING STUDY OF SPECIATION AND BENZENE FORMATION PATHWAYS IN PREMIXED 1-HEXENE FLAMES

A. Nawdiyal¹, N. Hansen², T. Zeuch³, L. Seidel¹, F. Mauß¹

¹Brandenburg University of Technology, Germany ²Sandia National Laboratories, United States

³Georg-August-Universität Göttingen, Germany

An existing detailed and broadly validated kinetic scheme is augmented to capture the flame chemistry of 1-hexene under stoichiometric and fuel rich conditions including benzene formation pathways. In addition, the speciation in a premixed stoichiometric 1-hexene flame (flat-flame McKenna-type burner) has been studied under a reduced pressure of 20-30 mbar applying flame-sampling molecular-beam time-of-flight mass spectrometry and photoionization by tunable vacuum-ultraviolet synchrotron radiation. Mole fraction profiles of 40 different species have been measured and validated against the new detailed chemical reaction model consisting of 275 species and 3047 reversible elementary reactions. A good agreement of modelling results with the experimentally observed mole fraction profiles has been found under both stoichiometric and fuel rich conditions providing a sound basis for analyzing benzene formation pathways during 1-hexene combustion. The analysis clearly shows that benzene formation via the fulvene intermediate is a very important pathway for 1-hexene, which is different to previous findings based on the same kinetic model for fuel rich C₂-C₄ flames.

fmauss@tdtvt.de

4C05 DISSOCIATION OF ORTHO-BENZYNE RADICALS IN THE HIGH TEMPERATURE FALL-OFF REGIME

Patrick T. Lynch^{1,2}, Christopher J. Annesley¹, Robert S. Tranter¹

¹Argonne National Laboratory, United States ²University of Michigan-Dearborn, United States

The decomposition of *ortho*-benzyne radicals (*o*-C₆H₄), generated from the dissociation of a new precursor, fluorobenzene (C₆H₅F), has been investigated in a diaphragmless shock tube in a combined laser schlieren densitometry, LS, ($P_2 = 30 \pm 2, 59 \pm 3, 121 \pm 5$ Torr, $2050 < T_2 < 2980$) / time-of-flight mass spectrometry, TOF-MS ($P_3 = 1150 \pm 200$ Torr, $2300 < T_3 < 2800$ K) study. The LS density gradient profiles were simulated, and excellent agreement was found between simulations and experimental profiles. Rate coefficients for $C_6H_5F \rightarrow o-C_6H_4 + HF$, $o-C_6H_4 \rightarrow C_4H_2 + C_2H_2$, and $o-C_6H_4 \rightarrow C_6H_3 + H$ were obtained. Good agreement with C. Xu et al. [*Proc. Combust. Inst.*, 31 (2007) 231-239] with respect to the *o*-benzyne dissociation branching ratio was found. However a strong pressure dependence was also observed in *o*-benzyne dissociation which was not seen by Xu et al. For $o-C_6H_4 \rightarrow C_4H_2 + C_2H_2$: $k_{2a,120Torr} = (1.2 \pm 0.4) \times 10^{63} T^{-14.27} \exp(-52710/T)$ $k_{2a,60Torr} = (1.4 \pm 0.5) \times 10^{60} T^{-13.595} \exp(-50538/T)$, $k_{2a,30Torr} = (4.0 \pm 1.3) \times 10^{57} T^{-13.015} \exp(-48628/T) s^{-1}$. The inclusion of high temperature *o*-benzyne abstraction reactions is necessary to simulate the reacting system, and we report estimates of the rate of $o-C_6H_4 + C_6H_5F$.

tranter@anl.gov

4C06 PRODUCTION OF MAJOR REACTION PRODUCTS IN THE INITIAL STEPS OF THE THERMAL DECOMPOSITION OF NAPHTHALENE. EXPERIMENTAL SHOCK-TUBE RESULTS AND COMPUTER SIMULATION

Alexander Laskin, Carmen Tamburu, Faina Dubnikova, Assa Lifshitz, The Hebrew University of Jerusalem, Israel

Initial steps in the thermal decomposition of naphthalene were studied behind reflected shocks in a pressurized driver single pulse shock tube over the temperature range 1350-1650 K and densities of $\sim 3 \times 10^{-5}$ mol/cm³. The present manuscript concentrates on the initial steps in the decomposition of naphthalene, rather than its function in producing molecules having more rings toward the formation of PAH etc. For the purpose of studying the low extent of decomposition, relatively low temperatures were used where the extent of reaction is small so as to prevent a secondary or higher generation of reactions that might obscure the initial decomposition process to take place.

Five major decomposition products that were found in the post shock mixtures of naphthalene were acetylene, diacetylene, benzene, phenyl acetylene, and acenaphthylene. Products that did not exceed 1% at their highest concentration were not considered both in the product distribution map as well as in the computer simulation. These were methane,

ethylene, allene + propyne, methyl naphthalene, and indene. Indene, with somewhat higher than 1% at its maximum, could not be computer simulated with reasonable agreement. The total disappearance rate of naphthalene, in terms of a first-order rate constant is given by $k_{\text{total}} = 7.33 \times 10^{13} \exp(-364 \times 10^3/RT) \text{ s}^{-1}$ where R is expressed in units of joule/(K.mol). A concise kinetics scheme containing 18 species and 25 elementary reactions accounts for the observed major decomposition products with reasonable agreement. The kinetics scheme, as well as results of the computer simulation and the sensitivity analysis are shown.

assa.lifshitz@mail.huji.ac.il

4C07 EXPERIMENTAL AND MODELING STUDY OF FUEL INTERACTIONS WITH AN ALKYL NITRATE CETANE ENHANCER, 2-ETHYL-HEXYL NITRATE

S.S. Goldsborough^{1,2}, M.V. Johnson¹, C. Banyon¹, W.J. Pitz³, M.J. McNenly

¹Argonne National Laboratory, United States ²University of Illinois, United States

³Lawrence Livermore National Laboratory, United States

This study investigates the autoignition behavior of two gasoline surrogates doped with an alkyl nitrate cetane enhancer, 2-Ethyl-Hexyl Nitrate (2EHN) in order to better understand dopant interactions with the fuels, including influences of accelerating kinetic pathways and enhanced exothermicity. A Primary Reference Fuel (PRF) blend of *n*-heptane/iso-octane, and a Toluene Reference Fuel (TRF) blend of *n*-heptane/iso-octane/toluene are used where the aromatic fraction of the latter is set to 20% (liquid volume), while the content of *n*-heptane is adjusted so that the overall reactivity of the undoped fuels is similar, with a RON of ~91, CN ~25. Doping levels of 0.1, 1.0 and 3.0% on a liquid volume basis are used where tests are conducted within a rapid compression machine at a compressed pressure of 21 bar, covering temperatures from 675 to 1025 K with stoichiometric fuel-oxygen ratios at an oxygen concentration of 11.4%.

At the experimental conditions, it is found that the doping effectiveness of 2EHN is fairly similar between the two fuels, though 2EHN is more effective in the aromatic blend at the lowest temperatures, while it is slightly more effective in the non-aromatic blend at intermediate temperatures. Kinetic modeling of the experiments indicates that although some of the reactivity trends can be captured using a detailed model, the extents of predicted cetane enhancement are too large, while the differences in fuel interactions between the two fuels lead to excessive stimulation of the non-aromatic blend. The kinetic model indicates that the CH₂O and CH₃O₂ chemistry are very sensitive to the dopant at all conditions. The 2EHN decomposition is only important at low temperatures. At higher temperature, dopant-derived 3-heptyl radicals are predicted to play an important role stimulating ignition. Finally, nitrogen chemistry becomes important only at the highest doping levels, primarily through the formation of methyl nitrite and nitric acid.

scott.goldsborough@anl.gov

4C08 IGNITION DELAY TIMES OF CONVENTIONAL AND ALTERNATIVE FUELS BEHIND REFLECTED SHOCK WAVES

Yangye Zhu, Sijie Li, David F. Davidson, Ronald K. Hanson, Stanford University, United States

The auto-ignition characteristics of two distillate jet fuels and fifteen alternative fuels (including fuel blends) were investigated using shock-tube/laser-absorption methods. Ignition delay times were measured behind reflected shock waves over a range of temperatures, 1050-1520K, and equivalence ratios, 0.25-2.2, in two pressure and mixture regimes: for fuel/air mixtures at 2.07-8.27 atm, and for fuel/4%Oxygen(O₂)/Argon(Ar) mixtures at 15.9-44.6 atm. In both pressure ranges, the ignition delay times of the alternative fuels and the blends with conventional fuels were found to be similar to those of conventional fuels but with some small systematic differences manifesting the different fuel types. In particular, for alternative aviation fuels, alcohol-to-jet fuels were found to be generally less reactive than Fischer-Tropsch paraffinic kerosenes or hydro-processed renewable jet fuels. Comparisons were also made of the ignition delay time data with detailed kinetic modeling for selected fuels. These comparisons show that existing multi-component surrogate/mechanism combinations can successfully predict the behavior of these fuels over the conditions studied. For those fuels lacking kinetic models, the current ignition delay time measurements provide useful target data for development and validation of relevant surrogate mixtures and reaction mechanisms.

dfd@stanford.edu

4C09 EXPERIMENTAL AND MODELING STUDY OF BURNING VELOCITIES FOR ALKYL AROMATIC COMPONENTS RELEVANT TO DIESEL FUELS

Marco Mehl¹, Olivier Herbine², Patricia Dirrenberger², Roda Bounaceur², Pierre-Alexandre Glaude², Frédérique Battin-Leclerc², William J. Pitz¹

¹Lawrence Livermore National Laboratory, United States ²CNRS, Université de Lorraine, France

Aromatic species represent a significant fraction (about one third by weight) of both diesel and gasoline fuels. Much of the aromatics in diesel and gasoline are alkyl-benzene species. Although toluene, the lightest of the alkyl-benzenes, has been the subject of extensive literature investigations, very little experimental data are available for heavier alkyl benzenes relevant to diesel fuel.

In this work, the burning velocity of ethyl-, *n*-propyl- and *n*-butyl-benzenes were measured in a premixed flat-flame burner using the heat flux method. The burning velocities were measured as a function of the equivalence ratio at atmospheric pressure and for two unburned gas temperatures (358 and 398K). These new experiments are compared with burning velocities for toluene previously measured by the authors. The comparisons showed that ethyl-benzene has the highest flame speed, followed by *n*-propyl- and *n*-butyl-benzenes which have similar burning velocities. Toluene has the lowest flame speed. Excellent agreement was observed between the new measurements and simulations using a recently published LLNL kinetic mechanism for alkyl-benzenes.

Based on the strong correlation between experiments and calculations, different aspects contributing to the burning speed of the fuels (thermal effects, kinetics,...) were analyzed using the model. A sensitivity analysis was used to determine the reaction rate constants that are most important in determining the flame speed. Reaction path analysis and species profiles in the flame were used to identify the key reaction paths that lead to increase and decrease in the burning velocities. Contrary to what is generally observed for alkanes whose flame speed is controlled by small radical fragments, the flame speed of aromatics is influenced by fuel specific intermediates such as phenyl, benzyl, or even heavier species. The new experimental data and modeling insight generated by this work will support the development of models for heavier alkyl-aromatics of great relevance to diesel fuel.

mehl6@llnl.gov

4D01 A DETAILED NUMERICAL SIMULATION OF SPHERICALLY SYMMETRIC *N*-BUTANOL DROPLET COMBUSTION AND COMPARISONS WITH EXPERIMENTAL DATA

E.A Fahd¹, Y.C. Liu², C.T. Avedisian², F.L. Dryer³, T.I. Farouk¹

¹University of South Carolina, United States ²Cornell University, United States ³Princeton University, United States

Recent interest in alternative and bio-derived fuels has emphasized butanol over ethanol as a result of its higher energy density, lower vapor pressure and more favorable gasoline blending properties. Numerous efforts have examined the combustion of butanol from the perspective of low dimensional gas-phase transport configurations that facilitate modeling and validation of combustion kinetics. However, fewer studies have focused on multiphase butanol combustion, and none have appeared on isolated droplet combustion that couples experiments with detailed modeling of the droplet burning process. This paper presents the first coupled experimental and detailed numerical modeling study of isolated droplet burning characteristics of *n*-butanol. The experiments are conducted in an environment that simplifies the transport process to one that is nearly one-dimensional as promoted by burning in a reduced gravity environment. Measurements of the evolution of droplet diameter (initial values between 0.56 mm and 0.57 mm), flame standoff ratio and burning rate are made in the standard atmosphere under reduced gravity and the data are compared to the detailed numerical simulation. The detailed model is based on a comprehensive time-dependent, spherically-symmetric droplet combustion simulation that includes spectrally resolved radiative heat transfer, multi-component diffusive transport, full thermal property variations and detailed chemical kinetic. The simulations are carried out using both a large order kinetic mechanism (284 species, 1892 reactions) and a reduced order mechanism (44 species, 177 reactions). The results show that the predicted burning history and flame standoff ratios are in good agreement with the measurements for both the large and reduced order mechanisms. Additional simulations are conducted for varying oxygen concentration to determine the limiting oxygen index and to elucidate the kinetic processes that dictate the extinction of the flame at these low oxygen concentrations.

tfarouk@sc.edu

4D02 AUTOIGNITION BEHAVIOR OF A SPHERICAL CLUSTER CONSISTED OF A CENTER FINE DROPLET AND SURROUNDING TWELVE FINE DROPLETS

H. Kataoka, H. Yamashita, J. Tada, Y. Oka, Y. Morinaga, M. Itai, D. Segawa, T. Kadota, Osaka Prefecture University, Japan

Autoignition behavior of spherical clusters of pure droplets were experimentally examined near the ignition limit. The fuels with the melting points little above room temperatures were selected as the test fuel. The three-dimensional droplet clusters with HCP structure were selected as the test clusters, which consisted of a center droplet and surrounding twelve droplets (thirteen droplets in total). The initial diameters of the droplets were much reduced from the authors' previous studies. The results showed that the ignition delay of the three-dimensional droplet clusters also had a minimum at a certain droplet spacing, which has been predicted by Niioka and coworkers as a result of rate-controlling process transition between reaction and evaporation. Autoignition of the droplet clusters could be achieved for the center fine droplet, which is out of ignition limit when isolated, in combination with finer surrounding droplets.

segawa@me.osakafu-u.ac.jp

4D03 FERROFLUID DROPLET VAPORIZATION UNDER VERY LARGE MAGNETIC POWER: EFFECTS OF PRESSURE AND EFFECTIVE THERMAL CONDUCTIVITY OF LIQUID

Cesar F.C. Cristaldo, Maycol M. Vargas, Fernando F. Fachini, Instituto Nacional de Pesquisas Espaciais, Brazil

The aim of current analysis is to measure the influence of the effective thermodynamic and transport coefficient and of the transient process of mass and energy accumulation in the gas phase (pressure effect) on the heating and

vaporization of a single ferrofluid droplet. Ferrofluids under external alternating magnetic field heat up themselves due to the magnetic Brownian relaxation mechanism. Under the condition of very large magnetic power, the magnetic heat source together with the heat transfer from the gas phase impose a thermal boundary layer adjacent to the droplet surface in the liquid side and temperature presents a maximum inside the droplet, not at the surface. Since the transport coefficient increases significantly with a dispersion of a small quantity of nanoparticles, the heat transfer from the thermal boundary layer to the droplet core increases, then the temperature of that region increases faster than that for cases without nanoparticle dispersion. The temperature inside the thermal boundary layer increases slower because of the heat transfer to the droplet core as well as to the droplet surface. Therefore, the boiling condition which is found inside the thermal boundary layer is reached later when considering effective thermal conductivity. The droplet vaporization rate is augmented by the heat transfer from the thermal boundary layer to the droplet surface. In addition, the strong dependence of the magnetic relaxation mechanism on temperature imposes a dependence of the vaporization rate on the initial condition of the problem.

cristaldo@lcp.inpe.br

4D04 THE ROLE OF MICRO-CONVECTION INDUCED BY SUPPORT FIBER IN DROPLET COMBUSTION PROCESSES

Y.C. Liu¹, Y. Xu¹, M.C. Hicks², C.T. Avedisian¹

¹Cornell University, United States ²NASA Glenn Research Center, United States

This study reports experimental evidence of gas phase micro-convection induced by support fibers used in droplet combustion experimentation. Soot aggregates formed during combustion of *n*-octane and *n*-decane droplets (initial diameters ranging from 0.5 mm to 5 mm) provide natural seeds to reveal the thermal and flow asymmetries involved. The experiments are carried out in an environment that reduces the influence of forced and buoyant convection for both free-floating (unsupported) and fiber-supported droplets. Under these conditions, the soot trapping patterns (due to a balance of thermophoretic and flow-induced drag) would be spherical. However, this situation is only observed for unsupported droplets, or for fiber-supported droplets when the fiber diameter is small relative to the droplet diameter. For $D_o < 1$ mm a ground based drop tower employed two 15 μ m diameter SiC fibers to fix the droplet's position during burning; unsupported droplets were also examined. For $D_o > 1$ mm the International Space Station provided capabilities for anchoring test droplets onto a single 80 μ m SiC fiber, as well as for deploying unsupported droplets. Results clearly indicate that a non-symmetric gas flow field exists in some cases (i.e., for $1 \text{ mm} < D_o < 3 \text{ mm}$, with an 80 μ m fiber) near to where the fiber enters the droplet. This gas motion (over and above that due to evaporation) originates from the presence of the fiber that induces an asymmetric temperature field by exchanging heat with the surrounding gas, which thereby is considered to induce a Marangoni flow field inside the droplet and, thus, gas motion along the droplet surface. The thermal asymmetry is revealed by soot aggregates being positioned in highly non-symmetric configurations. For very small or no fibers present (unsupported droplet) spherical soot shells are found suggesting that no thermal asymmetries exist.

yl677@cornell.edu

4D05 MULTISTAGE OSCILLATORY "COOL FLAME" BEHAVIOR FOR ISOLATED ALKANE DROPLET COMBUSTION IN ELEVATED PRESSURE MICROGRAVITY CONDITION

T.I. Farouk¹, M.C. Hicks², F.L. Dryer³

¹University of South Carolina, United States ²NASA Glenn Research Center, United States ³Princeton University, United States

Recently, large diameter, isolated *n*-heptane droplet experiments under microgravity conditions (aboard the International Space Station) exhibited "Cool Flame" burning behavior, resulting from a heat loss mechanism that extinguishes hot combustion and a transition into a sustained, low temperature second stage combustion. In atmospheric pressure air, a single combustion mode transition to "Cool Flame" burning is followed by diffusive extinction. But with increasing pressure, *multiple cycles* of hot initiation followed by transition to "Cool Flame" burning are observed. This paper reports experimental observations that characterize the transition time histories of this multi-cycle, multi-stage behavior. Transient spherically-symmetric droplet combustion modeling that considers multi-stage detailed kinetics, multi-component diffusion, and spectral radiation is applied to analyze the experimental observations. The simulations indicate that as parameters change the chemical time scales dictating low temperature degenerate chain branching, multiple hot/cool flame burning transitions are induced by increasing the cool flame burning heat generation rate compared to the diffusive loss rate. The balance of these terms in the negative temperature coefficient kinetic regime defines whether reactions accelerate into re-ignition of a hot flame event, burn quasi-steadily in the cool flame mode, or diffusively extinguish. The rate of reactions controlling ketohydroperoxide formation and destruction are shown to be key for re-ignition of hot combustion from the cool flame mode. Predictions are found to be in good agreement with the experimental measurements. Modeling is further applied to determine how these observations are dependent on initial experimental conditions, including pressure, and diluent species.

tfarouk@sc.edu

4D06 NUMERICAL MODELING OF AUTO-IGNITION OF ISOLATED FUEL DROPLETS IN MICROGRAVITY
Alberto Cuoci, Alessio Frassoldati, Tiziano Faravelli, Eliseo Ranzi, Politecnico di Milano, Italy

In this work we present and apply a mathematical model to simulate the auto-ignition of isolated fuel droplets burning in microgravity conditions. The aim is to demonstrate and explain the fundamental role of the low-temperature mechanisms on the auto-ignition process. Several efforts have been already devoted to the numerical modeling of droplets with complex chemistry, but only a few of them accounted also for the low-temperature mechanisms. Therefore, deeper theoretical investigations are still required.

Thus, in order to better clarify the importance of the low-temperature chemistry, a detailed kinetic scheme (with hundreds of species and thousands of reactions) was adopted to model the spontaneous ignition of isolated droplets of *n*-heptane, *n*-decane and *n*-dodecane in air, in a wide range of operating conditions (with environment temperatures from 600 K to 1100 K and pressures from 1 bar to 20 bar).

The model was able to correctly identify the typical auto-ignition regimes of *n*-alkane oxidation. The comparison with the experimental measurements available in the literature was satisfactory: Both first-stage and total induction times were reasonably captured by the numerical simulations. The simulations confirmed that the low-temperature chemistry plays a role of paramount importance in the auto-ignition process. In particular, the competition between low- and high-temperature mechanisms was found to explain the different types of auto-ignition which can be experimentally observed.

alberto.cuoci@polimi.it

4D07 ANALYSIS OF HIGH-PRESSURE DIESEL FUEL INJECTION PROCESSES USING LES WITH REAL-FLUID THERMODYNAMICS AND TRANSPORT

Guilhem Lacaze¹, Antony Misdariis², Anthony Ruiz¹, Joseph C. Oefelein¹

¹Sandia National Laboratories, United States ²Renault SAS, France

Imaging has long shown that under some high-pressure conditions, the presence of discrete two-phase flow processes becomes diminished. Instead, liquid injection processes transition from classical sprays to dense-fluid jets with no drops present. When and how this transition occurs, however, was not well understood until recently. In this paper, we summarized a new theoretical description that quantifies the effects of real fluid thermodynamics on liquid fuel injection processes as a function of pressure at typical Diesel engine operating conditions. We then apply the Large Eddy Simulation (LES) technique coupled with real-fluid thermodynamics and transport to analyze the flow at conditions when cylinder pressures exceed the thermodynamic critical pressure of the injected fuel. To facilitate the analysis, we use the experimental data posted as part of the Engine Combustion Network (see www.sandia.gov/ECN); namely the "Spray-A (*n*-dodecane)" case. Calculations are performed by rigorously treating the experimental operating conditions and relevant thermo-physical gas-liquid mixture properties. Details related to the transient mixing field are presented with emphasis on the state of the mixing field prior to auto-ignition. The analysis reveals the profound effect of supercritical fluid phenomena on the instantaneous three-dimensional structure of the compressed liquid core and related multicomponent mixing layer dynamics.

gnlacaz@sandia.gov

4D08 LARGE EDDY SIMULATION OF DILUTE ACETONE SPRAY FLAMES USING CMC COUPLED WITH TABULATED CHEMISTRY

S. Ukai, A. Kronenburg, O.T. Stein, Universität Stuttgart, Germany

A Conditional Moment Closure (CMC) method has been coupled to a Large Eddy Simulation (LES) for the modelling of turbulent spray flames. The present study presents an extension to CMC (CMCe) that remedies some inconsistencies of an earlier LES-CMC study. Here, the CMC approach is coupled with a chemistry table that allows for spatial and temporal variations of the tabulated chemical composition and ensures a reasonably accurate computation of the chemical source term of the LES-filtered reaction progress variable despite large fluctuations around the conditional means computed by the CMC equation. CMCe is validated by comparison with experimental results of two dilute acetone spray flames with pre-evaporation. Temperature predictions and axial spray velocities are markedly improved, especially along the centerline, while the velocity RMS shows reasonable agreement.

kronenburg@itv.uni-stuttgart.de

4E01 SPECIES MEASUREMENTS IN A NITROGEN-DILUTED, ETHYLENE AIR DIFFUSION FLAME USING DIRECT SAMPLING MASS SPECTROMETRY AND TUNABLE DIODE LASER ABSORPTION SPECTROSCOPY

Hilary R. Melroy, Erin M. Adkins, Maya J. Pause, J. Houston Miller, The George Washington University, United States

Tunable Diode Laser Absorption Spectroscopy combined with extractive sampling is used to quantify fuel and acetylene concentrations in a 32% ethylene-diluted, nitrogen diffusion flame. Additional major species concentrations are determined using quartz microprobe, direct-sampling mass spectrometry. Quantification of these mass spectra used a multilinear regression technique anchored by computed nitrogen concentration profiles in a simulation from Yale

University. Because of the overlap in mass spectra features for ethylene, nitrogen, and carbon monoxide, both optical and mass spectrometric techniques are required to determine the suite of major species in this flame system. Good agreement is observed between these experimental measurements and numerical simulation of this flame system. Probe clogging in these sooting flames remains a challenge for all probe techniques and additional, non-intrusive optical diagnostics must be applied to characterize flame regions with substantial soot formation.

Hrmelroy@gwmail.gwu.edu

4E02 LOCAL GAS HEATING IN SOOTING FLAMES BY HEAT TRANSFER FROM LASER-HEATED PARTICLES INVESTIGATED USING ROTATIONAL CARS AND LII

*Emil Nordström, Nils-Erik Olofsson, Johan Simonsson, Jonathan Johnsson, Henrik Bladh, Per-Erik Bengtsson
Lund University, Sweden*

Soot particles strongly absorb radiation in visible and infrared spectral regions, and their interaction with laser light during laser diagnostic interrogation leads to particle heating and often to subsequent sublimation. Consequently, laser-heated particles transfer heat to the ambient gas leading to local gas heating, a process that has received minor attention so far in the diagnostic community. In the present work, this specific local gas heating is measured in a pump-probe-type experiment. A 1064-nm laser beam heated the soot particles in a particle-laden flame with known soot volume fraction, and a two-beam rotational coherent anti-Stokes Raman spectroscopy (CARS) setup was used to probe the local gas temperature on time scales from nanoseconds to milliseconds. The particle temperatures were simultaneously probed using a two-color laser-induced incandescence (2C-LII) setup. The results show that laser heating of soot particles from flame temperatures to sublimation temperatures leads to local gas heating of ~100 K at a soot volume fraction of 4 ppm, in good agreement with theoretical predictions. The implication of these results to the application of various laser diagnostic techniques is discussed.

emil.nordstrom@forbrf.lth.se

4E03 SINGLE-SHOT, TIME-RESOLVED PLANAR LASER-INDUCED INCANDESCENCE (TR-LII) FOR SOOT PRIMARY PARTICLE SIZING IN FLAMES

Z.W. Sun, D.H. Gu, G.J. Nathan, Z.T. Alwahabi, B.B. Dally, The University of Adelaide, Australia

Two dimensional measurements of the size of soot primary particles, in both laminar and unsteady sooty C₂H₄/air flames, have been demonstrated in the present work. This is achieved using single-shot, Time-Resolved Laser-Induced Incandescent (TR-LII) technique. The soot primary size is determined from the ratio of different signals obtained from four sequential images together with a theoretical relationship of the LII temporal decays. A laser power of 0.30 J/cm² was chosen for its relevance to application in turbulent sooty flames. Planar measurements are firstly demonstrated in a flat laminar flame and the results are found to be in good agreement with time-resolved single-point-measurements using a photomultiplier tube. A typical uncertainty of ± 9 nm is estimated in the single-shot, planar measurements. Finally, planar measurements in an unsteady sooty flame reveal that the size of soot primary particles is very sensitive to local flame conditions.

Zhiwei.sun@adelaide.edu.au

4E04 A NEW DIAGNOSTIC FOR VOLUME FRACTION MEASUREMENT OF METAL-OXIDE NANOPARTICLES IN FLAMES USING PHASE-SELECTIVE LASER-INDUCED BREAKDOWN SPECTROSCOPY

*Yiyang Zhang¹, Shuiqing Li¹, Yihua Ren¹, Qiang Yao¹, Stephen D. Tse²
¹Tsinghua University, China ²The State University of New Jersey, United States*

A new diagnostic has been developed for measuring nanoparticle volume fraction by using phase-selective Laser-Induced Breakdown Spectroscopy (LIBS) for TiO₂ nanoparticles generated during flame synthesis. The volume fraction is determined from Ti atomic spectra by exciting all the nanoparticle-phase matter to the plasma state, while keeping the gas-phase unexcited, based on the selectivity of breakdown thresholds between gas phase and particle phase. The measurement is performed with no detection delay, as no Bremsstrahlung background is detected. The nonvisible nanoplasmas are likely confined around each nanoparticle, differing from the continuously expanding plasmas produced in conventional LIBS. The intensity of the atomic spectra increases proportionally with laser fluence and reaches a saturation regime above 35 J/cm², facilitating the measurement of volume fraction. It is found that smaller nanoparticles decrease in absorption efficiency due to the size-dependent band gap. Nevertheless, this effect diminishes for nanoparticle sizes above 8 nm. In the saturation regime, a fairly-good linear relation exists between signal intensity and nanoparticle volume fraction, for volume fractions above 140 ppb. Benefitting from locally-confined nanoplasmas without detectable sparks, two-dimensional planar measurements of TiO₂ nanoparticle volume fraction is accomplished, resulting in the visualization of the rapid formation of nanoparticles across the flame sheet and conservation of their volume fraction in the post-flame. When an impinged-upon substrate is added, the two-dimensional phase-selective LIBS imaging shows good resolution of nanoparticle volume fraction variation in the boundary layer, influenced by diffusion and thermophoresis.

lishuiqing@mail.tsinghua.edu.cn

4E05 LASER-BASED *IN-SITU* MEASUREMENT AND SIMULATION OF GAS-PHASE TEMPERATURE AND IRON ATOM CONCENTRATION IN A PILOT-PLANT NANOPARTICLE SYNTHESIS REACTOR

Omid M. Feroughi¹, Sebastian Hardt¹, Irenaeus Wloka², Tim Hülser³, Hartmut Wiggers², Thomas Dreier¹, Christof Schulz¹

¹University of Duisburg-Essen, Germany ²Institute of Energy and Environmental Technology e.V. (IUTA), Germany

A scaled-up flame reactor for nanoparticle synthesis was investigated through a combination of *in-situ* Laser-Induced Fluorescence (LIF) measurements and Computational Fluid Dynamics (CFD) simulations with detailed chemistry. Multi-line NO-LIF was used for imaging gas-temperature and Fe-LIF for measurement of iron atom concentration. Despite the challenging environment of production reactors in an industrial environment, various conditions for stable flames with different gas flows with and without adding Fe(CO)₅ as precursor for the synthesis of iron-oxide nanoparticles were investigated. In contrast to previous measurements in laminar lab-scale flames, a second mechanism for forming iron oxide nanoparticles was found via intermediate formation of iron clusters and elemental iron particles in hot, oxygen-free gas streams followed by subsequent oxidation.

thomas.dreier@uni-due.de

4E06 NUMERICAL AND EXPERIMENTAL INVESTIGATION OF THE PROCESS STEPS IN A SPRAY FLAME REACTOR FOR NANOPARTICLE SYNTHESIS

C. Weise¹, J. Menser¹, S.A. Kaiser¹, A. Kempf^{1,2,3}, I. Wloka¹

¹University of Duisburg-Essen, Germany ²CENIDE, Germany ³CCSS, Germany

The synthesis of titanium dioxide nanoparticles from Titanium Tetraisopropoxide (TTIP) in a nanoparticle spray flame reactor was investigated. The nanoparticle properties are affected by different processes that are analysed by experiment and simulation: a) the break up of the liquid jet from the spray nozzle, b) the combustion of the spray and in the pilot flame and c) the formation and growth of the nanoparticles. The spray process of the injected liquid was analysed by Volume of Fluid (VOF) calculations and validated by shadowgraphy imaging which provided the size distribution and the mean velocity of the droplets. The spray angle was determined by a side illuminated long exposure image of the spray. The resulting spray properties (droplet sizes, velocity, and spray angle) served as injector boundary conditions for the downstream combustion simulations. Spray and gas phase of the flame were simulated using an Euler-Lagrange approach, turbulence was modeled by the RNG k-epsilon model, and turbulent combustion was described as a Partially Stirred Reactor (PaSR). For the formation and growth of the nanoparticles within the synthesis reactor, the population balance equation was solved coupled to the spray combustion using a monodisperse model. The findings from experiment and simulation are discussed in terms of flow, species, temperature, and nanoparticle formation inside the reactor. The effect of the spray droplet properties as droplet size, angle, mean velocity and the dispersion behavior on the nanoparticle synthesis process are investigated and discussed, confirming the observation that this type of spray reactor is a robust design overall.

claudia.weise.ivg@uni-due.de

4E07 THERMAL AND ELECTROLYTIC DECOMPOSITION AND IGNITION OF HAN-WATER SOLUTIONS

Prashant Khare¹, Vigor Yang², Grant A. Risha³, Richard A. Yetter⁴

¹Georgia Institute of Technology, United States ²Pennsylvania State University, United States

Thermal and electrolytic decomposition and ignition of water solutions of Hydroxyl Ammonium Nitrate (HAN, [NH₃OH]⁺[NO₃]⁻) are investigated. Experiments are conducted to demonstrate the feasibility of electrolytic ignition for HAN-based ionic liquid propellants. As a consequence of electrolysis, the propellant decomposes to NH₂OH, HNO₃, HONO, HNO, N₂O, N₂, NO, NO₂, H₂O, H₂(g), and O₂(g). These species then initiate a series of gas phase reactions, governed by the H-O-N kinetics scheme, and lead to ignition. Electrochemical mechanisms are established and incorporated into an existing chemical kinetics scheme for thermal decomposition of HAN-water solutions. The analysis treats the liquid and gas phases separately, and matches their respective processes at the interfacial boundary to determine the overall decomposition and ignition characteristics. Results are benchmarked against experimental data for the species evolution in the condensed phase, as well as laser-induced ignition delay of 13M HAN-water solution. The effects of electric current (0-2.5A), propellant volume (0.1-0.3cc), initial temperature (300-450K), and HAN concentration (9-13M) on the ignition behaviors are investigated systematically. The ignition delay decreases with increasing electric current as a power-law function: $\tau_{\text{ign}} = A I^{-n}$, where $A = 3.95$ and $n = 0.95$ for a 0.1cc 13M HAN-water solution at an initial condition of 300K and 1atm. The exponent n and coefficient A are decreasing functions of the initial temperature. For a given power, decreasing the initial volume of HAN-water solution increases the current density available for electrolysis, and expedites the ignition process. The work represents the first theoretical study of its kind on this topic.

vigor.yang@aerospace.gatech.edu

4E08 HYPERGOLIC IGNITION AND FLAME STRUCTURES OF HYDRAZINE/NITROGEN TETROXIDE CO-FLOWING PLANE JETS

Hiroumi Tani¹, Hiroshi Terashima², Mitsuo Koshi³, Yu Daimon¹

¹Japan Aerospace Exploration Agency, Japan ²The University of Tokyo, Japan ³Yokohama National University, Japan

Hydrazine (N₂H₄)/Nitrogen Tetroxide (NTO) co-flowing plane jets were simulated to explore the hypergolic ignition processes and flame structures in N₂H₄/NTO bipropellant thrusters. The Navier-Stokes equations with a detailed

chemical kinetics mechanism were solved in a manner of direct numerical simulation to reveal the influence of the distinct chemical reaction, i.e. hydrogen abstraction by Nitrogen Dioxide (NO_2) and the thermal decomposition of N_2H_4 . In the ignition processes, the hydrogen abstraction sequence played a significant role in preheating the mixture gases. Further, the ignition eventually occurred in the region where both N_2H_4 and NTO were supplied for preheating. Hence, the ignition position and delay strongly depended on the fluid-mixing conditions. After the flames reached a steady state, the combustion flames uniquely comprised two types of flames, the outer diffusion flame and the inner decomposition flame. The outer diffusion flame came from the oxidization by NTO. The inner decomposition flame was caused by a high rate of heat release of the thermal decomposition of N_2H_4 and the heat transfer from the outer diffusion flame. Because of the decomposition flame, the decomposition products such as NH_3 and H_2 were the major constituents of the downstream combustion gases.

tani.hiroumi@jaxa.jp

4F01 EFFECT OF GRAVITY ON PUFFING PHENOMENON OF LIQUID POOL FIRES

Hiroki Abe, Akihiko Ito, Hiroyuki Torikai, Hirosaki University, Japan

The flame characteristics of the pool fires such as flame height and oscillation frequency change depending on the gravity. To improve our understanding of the effects of gravity on flame characteristics, we conducted an experimental investigation on small-scale pool fires under the normal gravity to low gravity. The drop tower at Hirosaki University in Japan was used to obtain arbitrary low gravity acceleration. The gravitational acceleration was changed from 1G to 0.55G. Our experiments include analyses of flame height and oscillation frequency of puffing phenomenon caused by the buoyancy under the low gravity environments with a high-speed camera. To clarify the factor of puffing occurrence, the experiments were performed using the eleven different size of fuel pan with three different kinds of fuels. It is found that the flame height and puffing frequency declined with decreasing of gravity, and the fuel pan size occurring puffing phenomenon increases with decreasing gravity. The puffing phenomenon is suppressed with the decreasing gravity. The puffing frequency under low gravity environments was summarized by the relationship between the Strouhal number and Froude number. The occurrence of puffing phenomenon, namely puffing-limit, was summarize by the relation between the $(H/D)_{\text{limit}}$ and Grashof number, and found it was summarized on the single curve.

aito@cc.hirosaki-u.ac.jp

4F02 EVOLUTION OF HEAT FEEDBACK IN MEDIUM POOL FIRES WITH CROSS AIR FLOW AND SCALING OF MASS BURNING FLUX BY A STAGNANT LAYER THEORY SOLUTION

Longhua Hu, Junjun Hu, Shuai Liu, Wei Tang, Xiaozheng Zhang, University of Science and Technology of China, China

This paper quantifies experimentally the evolution of heat feedbacks through overall conduction, convection and radiation in medium square pool fires (10~25 cm) with horizontal cross air flows ranged in 0~3.0 m/s. Ethanol and heptane are used as representative fuels producing typically less-sooty and sooty flames. Results show that the overall conduction heat feedback flux through the four sides increases with cross air flow speed, being more prominent for smaller pools than for larger ones. And the rate of overall conduction heat feedback increment is more prominent for heptane, of which the rate of increase with flow speed nearly 2 times that of ethanol. Meanwhile, the radiation heat feedback declines with cross air flow speed, with its contribution fraction nearly negligible at larger flow speeds for both fuels. The convection feedback fraction increases with cross air flow speed. Its increment is more prominent (a) for heptane (increasing fast with flow speed to be even the dominate one) than ethanol (increasing slowly with flow speed; being nearly constant and maintaining to be the dominant one); and (b) for larger pools than for smaller ones. The changing of dominant heat feedback mechanism with cross air flows, results in the change of the scaling behavior of the mass burning flux with pool size. A stagnant layer solution theory is then proposed, by including fuel mass transfer number B , to describe the change of mass burning flux of different size pool fires with cross air flow speed for different fuels in relative strong cross air flows [as indicated by Froude number ($\text{Fr} = u/[gd]^{1/2}$) larger than about unity]. Experimental data are shown to be well collapsed and correlated by the proposed theory.

hlh@ustc.edu.cn

4F03 BUOYANT POOL FIRES UNDER IMPOSED CIRCULATIONS BEFORE THE FORMATION OF FIRE WHIRLS

Jiao Lea, Naian Liu, Kohyu Satoh, University of Science and Technology of China, China

This paper presents the first comprehensive experimental study on the dynamical behaviors of small scale buoyant pool fires under imposed circulation before the formation of fire whirls. A rotating screen facility was used for experiments. It was found that as the screen rotated slowly, the original vertical buoyant pool fire inclined with a certain angle (α) and revolved around the facility central axis steadily. The deviation of the flow field from axial symmetry is proved to be induced by the additional Coriolis force in the rotating coordinates. The correlation $\tan \alpha \sim p^* \text{Fr}_0 \text{Fr}_r$ is proposed to couple the inclination angle to the screen angular speed and fire characteristics. The correlation agrees well with the experimental data in this work. The flame revolution was entirely dominated by aerodynamics and its angular speed was strictly equal to that of the screen. It was found that the inclined flame surface was steady at the base and the

oscillation originated at a higher position due to suppression of vorticity generation. The nominal averaged pulsation frequency of the inclined flame was always larger than that of the free buoyant fire. The flame inclination and the change of pulsation mode can affect the flame heights and lengths significantly. At a critical screen angular speed, the inclined flame became vertical again with self-swirling and the fire whirl formed finally.

liunai@ustc.edu.cn.

4F04 TREATMENT OF LOCAL EXTINCTION IN CFD FIRE MODELING

A.Yu. Snegirev, A.S. Tsoy, St.-Petersburg State Polytechnic University, Russia

A simplified approach capturing the major flame extinction mechanisms has been formulated and calibrated against the measurement data for critical strain rates of laminar diffusion counter-flow flames with fuel and (or) oxidizer streams diluted by nitrogen. The model is based on the perfectly stirred reactor concept, thereby assuming rapid reactant mixing in the reaction zone, where reactants are delivered at stoichiometric proportions. Model simplicity is achieved by considering the single-step global reaction model. Advancing previous studies, we demonstrate that this model is able to replicate critical strain rates at extinctions of both counter- and co-flow flames in a range of experimental configurations including opposed gaseous streams and evaporating liquid pool with a normally impinging oxidizer stream, in the entire range of gaseous diluent concentration enabling flaming combustion. The model correctly predicts the minimum extinguishing concentrations of different inert diluents (argon, nitrogen, water vapor and carbon dioxide) used in practice of fire suppression. The algorithm is simple and computationally affordable enough to be incorporated in a CFD fire model. The proposed algorithm can be used for any practical fuel, as soon as the global kinetic model of fuel oxidation is calibrated using the procedure developed in this work.

a.snegirev@phmf.spbstu.ru

4F05 NUMERICAL SIMULATION OF UNDER-VENTILATED LIQUID-FUELED COMPARTMENT FIRES WITH FLAME EXTINCTION AND THERMALLY-DRIVEN FUEL EVAPORATION

S. Vilfayeau¹, N. Ren², Y. Wang², A. Trouvé¹

¹University of Maryland, United States ²FM Global, United States

Compartment fires exhibit unique features associated with smoke accumulation and restricted air ventilation. The objective of the present study is to evaluate the ability of CFD-based fire models to simulate these features and in particular the effects of flame extinction that results from under-ventilated fire conditions. The study is performed using FireFOAM; FireFOAM is an advanced fire modeling software developed by FM Global and is based on a general-purpose open-source software called OpenFOAM. A new flame extinction model based on the concept of a critical value of the flame Damköhler number is incorporated into FireFOAM. The performance of the extinction model is evaluated via comparisons with a previously developed experimental database corresponding to a reduced-scale, heptane-fueled, compartment fire configuration. The numerical simulations also include a description of fuel evaporation driven by the computed gas-to-liquid heat feedback. Comparisons between experimental data and numerical results provide a suitable test bed to evaluate the ability of CFD-based fire models to describe the transition from over- to under-ventilated fire conditions, as well as the transition from extinction-free conditions to conditions in which the flame experiences partial or total quenching.

atrouve@umd.edu

4F06 APPLICATION OF A SUBGRID SOOT-RADIATION MODEL IN THE NUMERICAL SIMULATION OF A HEPTANE POOL FIRE

Prateep Chatterjee, Yi Wang, Karl V. Meredith, Sergey B. Dorofeev, FM Global, United States

Predictions of temperature, soot volume fraction and incident radiant flux are presented from large-eddy simulations of a medium-scale heptane pool fire. A subgrid soot-radiation model, which is based on the laminar smoke point concept, is applied to provide local emission from the turbulent flame-sheet. A local absorption coefficient is estimated using the local emission, mesh resolved temperature and its modeled subgrid variance. Absorption-emission calculations are conducted with the solution of the Radiative Transport Equation (RTE). The results obtained for the fire including velocity, temperature, volumetric emission and soot concentration distributions are compared with general observations from the experiment. Radial profiles of temperature and soot volume fraction are also compared with experimental data at several heights above the burner. Predicted temperature profiles are found to generally agree with the experimental data. Soot volume fraction predictions show similar trends as experimental measurements with positive and negative deviations. Incident radiation at an axial location away from the fire shows good agreement between the model and the experiment.

prateep.chatterjee@fmglobal.com

4F07 ESTIMATION OF LOCAL MASS BURNING RATES FOR STEADY LAMINAR BOUNDARY LAYER DIFFUSION FLAMES

Ajay V. Singh, Michael J. Gollner, University of Maryland, United States

A thorough numerical and experimental investigation of laminar boundary-layer diffusion flames established over the surface of a condensed fuel is presented. By extension of the Reynold's Analogy, it is hypothesized that the non-dimensional temperature gradient at the surface of a condensed fuel is related to the local mass-burning rate through some constant of proportionality. First, this proportionality is tested by using a validated numerical model for a steady flame established over a condensed fuel surface, under free and forced convective conditions. Second, the relationship is tested by conducting experiments in a free-convective environment (vertical wall) using methanol and ethanol as liquid fuels and PMMA as a solid fuel, where a detailed temperature profile is mapped during steady burning using fine-wire thermocouples mounted to a precision two-axis traverse mechanism. The results from the present study suggests that there is indeed a unique correlation between the mass burning rates of liquid/solid fuels and the temperature gradients at the fuel surface. The correlating factor depends upon the Spalding mass transfer number and gas-phase thermo-physical properties and works in the prediction of both integrated as well as local variations of the mass burning rate as a function of non-dimensional temperature gradient. Additional results from precise measurements of the thermal field are also presented.

mgollner@umd.edu

4F08 NUMERICAL MODELING OF MELTING AND DRIPPING PROCESS OF POLYMERIC MATERIAL SUBJECTED TO MOVING HEAT FLUX: PREDICTION OF DROP TIME

Yangkyun Kim, Akter Hossain, Yuji Nakamura, Hokkaido University, Japan

Numerical simulations are carried out in order to predict drop-size and -time of molten polymer during fire. Mass, momentum and energy conservation equations are solved in a 2-D system based on a fixed grid by means of a finite volume method. The Volume of Fluid (VOF) method and the Enthalpy-Porosity method are applied to model the deformable polymer-air interface and the melting processes, respectively. Results successfully show the dynamic behavior of the molten polymer and the effect of the deformation on the melting process. It is found that the total heat flux at the melting front which directly controls melting speed is linearly correlated with the length of the melting front during frequent accumulation and dripping of molten polymer even if the inclination angle is varied. Drop-size and -time can be estimated by a simple force balance equation at the polymer-air interface, and show a linear correlation with a modified inverse Bond number and with a combined Capillary number and modified Bond number, respectively.

yuji-mg@eng.hokudai.ac.jp

4G01 SOOTING LIMITS AND PAH FORMATION OF *N*-HEXADECANE AND 2,2,4,4,6,8,8-HEPTAMETHYLNONANE IN A MICRO FLOW REACTOR WITH A CONTROLLED TEMPERATURE PROFILE

Hisashi Nakamura, Satoshi Suzuki, Takuya Tezuka, Susumu Hasegawa, Kaoru Maruta, Tohoku University, Japan

Sooting limits of *n*-hexadecane (*n*-cetane)/air and 2,2,4,4,6,8,8-heptamethylnonane (*iso*-cetane)/air mixtures were investigated using a micro flow reactor with a controlled temperature profile at equivalence ratios, ϕ , of 1.5-4.5, inlet mean flow velocities, U_0 , of 10-100 cm/s and atmospheric pressure. Result for *n*-Cetane showed wider ϕ and U_0 region of the soot formation than that for *iso*-cetane. Temperature dependence of mole fractions of polycyclic aromatic hydrocarbons (PAHs) were investigated for *n*-cetane/air and *iso*-cetane/air mixtures at $\phi=4.0$, $U_0=2.0$ cm/s and atmospheric pressure by gas sampling and analysis. At all temperature conditions studied, *n*-cetane showed higher mole fractions of PAHs than *iso*-cetane. However, *iso*-cetane showed higher mole fractions of small alkylbenzenes (toluene, xylene isomers, and ethylbenzene) than *n*-cetane. Numerical simulation showed the opposite tendency, namely, *iso*-cetane showed higher/lower mole fraction of benzene/toluene than *n*-cetane. The species measurement showed branched-chain unsaturated species, 2,4,4-Trimethyl-1-Pentene (TMP1), was observed in the *iso*-cetane case at low temperature in which the significant formation of PAHs were not observed, but TMP1 was not observed in the *n*-cetane case. Considering the molecular structures of the two fuels, branched-chain unsaturated radicals would be formed in the *iso*-cetane case while those would not be formed in the *n*-cetane case. The branched-chain unsaturated radicals would play an important role for the formation of the small alkylbenzenes. The capabilities of the micro flow reactor to examine the difference in sooting limits and the PAH formation between rich *n*-cetane/air and *iso*-cetane/air mixtures were successfully demonstrated.

nakamura@edyn.ifs.tohoku.ac.jp

4G02 EFFECT OF RADICAL QUENCHING ON CH₄/AIR FLAMES IN A MICRO FLOW REACTOR WITH A CONTROLLED TEMPERATURE PROFILE

Yuta Kizakii, Hisashi Nakamura, Takuya Tezuka, Susumu Hasegawa, Kaoru Maruta, Tohoku University, Japan

The effect of radical quenching on CH₄/air flames was investigated using a micro flow reactor with a controlled temperature profile experimentally and numerically. To evaluate the radical quenching, two methods were employed in this study; changing the inner diameter of the reactor at atmospheric pressure, d ; and changing pressure in the reactor, P . The

stabilized flame locations were measured and gas sampling analysis was conducted. The results were compared with two-dimensional computation including detailed gas-phase kinetics with/without a radical quenching surface reaction mechanism.

At atmospheric pressure, there was no significant difference in the flame locations between the inert and quench wall cases at $d = 2.0$ and 1.5 mm. The measured flame location agreed with the computational flame locations. Thus the effect of radical quenching on the flame locations were negligible. The measured CO mole fraction agreed with the computed CO mole fraction without radical quenching on the wall, whereas significant amount of CO was predicted if radical quenching effect is considered. At reduced pressures, the experimental flame location agreed with the computational flame locations in the inert wall case at all pressure conditions. However, computations with radical quenching at $P = 0.1$ and 0.05 atm showed that flames blew out to the downstream. The measured CO mole fractions of burned gas were higher than those in the computation of the inert wall cases at $P = 0.5$, 0.1 and 0.05 when the equivalence ratio, $\phi > 1$. The differences are larger at lower pressure conditions. It can be concluded that the present surface reactions mechanism overestimates the radical quenching effect. Radical quenching can be negligible at atmospheric pressure but it can not be negligible at reduced pressures.

kizaki@edyn.ifs.tohoku.ac.jp

4G03 CHARACTERISTICS OF *N*-BUTANE WEAK FLAMES AT ELEVATED PRESSURES IN A MICRO FLOW REACTOR WITH A CONTROLLED TEMPERATURE PROFILE

Shogo Kikui, Taiki Kamada, Hisashi Nakamura, Takuya Tezuka, Susumu Hasegawa, Kaoru Maruta, Tohoku University, Japan

The very first successful experiments at elevated pressures up to 12 atm by "in-pressure-chamber"-type micro flow reactor with controlled temperature profile are demonstrated. *N*-Butane was applied to the micro flow reactor and the ignition characteristics at pressures of 1-12 atm were investigated by observing weak flames. Among three kinds of the separated weak flames which can be observed by the present reactor, the blue flame was only observed at higher pressures than 2 atm and the cool flame was only observed at higher pressures than 3 atm. This interprets the multi-stage oxidation for *n*-butane was confirmed experimentally and computationally. The positions of the blue and cool flames shifted towards the lower temperature side along with the increase of pressure in the experiment. Computation results reproduced the experimental tendency of the blue and cool flames. Wall temperature of the position of the cool flame in the experiment agreed with that in the computation at all pressures studied, and that at 10 atm agreed with the compressed temperature in which the cool flame was observed in rapid compression machine at compressed pressure at 10 bar. The computational weak flame structure at 1 atm with that of 10 atm was compared. The high-temperature oxidation is important at 1 atm while the low temperature oxidation is important at high pressures. At 10 atm, most of the fuel is consumed at the cool flame. The separated cool flames were found at 12 atm and four-stage oxidation was produced in the computation. Rate of production analysis indicated that the first cool flame was formed by fuel oxidation through low-temperature oxidation and the second cool flame was formed by reaction of peroxy radicals with H_2O_2 .

kikui@edyn.ifs.tohoku.ac.jp

4G04 DIRECT NUMERICAL SIMULATION OF MICRO COMBUSTION IN A NARROW CIRCULAR CHANNEL WITH A DETAILED KINETIC MECHANISM

Eriko Miyata¹, Naoya Fukushima¹, Yoshitugu Naka¹, Masayasu Shimura¹, Mamoru Tanahashi¹, Toshio Miyauchi²
¹Tokyo Institute of Technology, Japan ²Meiji University, Japan

Direct Numerical Simulation (DNS) of micro combustion in a narrow circular channel is conducted for methane-air mixture. The narrow circular channel of which radius 0.5 mm is supposed to have wall temperature gradient in the streamwise direction. To represent methane--air reaction, a detailed kinetic mechanism (GRI-Mech 3.0) including 53 species and 325 elementary reactions is adopted. DNSs are conducted with different inlet temperature and wall temperature gradient, and unsteady phenomena in the micro combustion in a narrow channel are discussed. Similar to the previously reported experiment, unsteady behavior of the flame such as the oscillating flame and the Flame Repetitive Extinction and Ignition (FREI) can be obtained depending on the inlet temperature and the wall temperature gradient. To investigate FREI mechanism, thermal energy budget of the mixture is introduced and evaluated in one cycle of both FREI and oscillating flame. It has shown that FREI possesses the negative phase in the thermal energy budget, which suggests that the definition of the origin of FREI is given by the thermal energy budget of the mixture. It is also shown that the amplitude and frequency of FREI can be scaled by introducing the thermal thickness based on the wall temperature gradient, inlet mass flow rate of the mixture and the thickness of the corresponding steady flame of the inlet mixture.

nfukushim@navier.mes.titech.ac.jp

4G05 CHARACTERISTICS OF OPPOSED FLOW PARTIALLY PREMIXED FLAMES IN MESOSCALE CHANNELS AT LOW STRAIN RATES

Min Jung Lee, Moon Soo Cho, Nam Il Kim, Chung-Ang University, Republic of Korea

This study investigates Opposed Flow Partially Premixed Flames (OFPPFs) in mesoscale horizontal channels. Flame stabilization conditions and behaviors were experimentally investigated for methane and propane, based on experimental parameters including flow velocity, nozzle distance, nozzle width, channel gap, and the equivalence ratios of the mixtures. Various flame structures were formulated, as Partially Premixed Flames (PPFs) can intrinsically formulate three flame branches: Lean Premixed Flame (LPF), Non-Premixed Flame (NPF), and Rich Premixed Flame (RPF), depending on flow conditions. Three extinction limits were obtained: Higher Strain Rate (HSR), Lower Strain Rate (LSR), and flashback. The HSR extinction limits were extended through premixing and the increase of channel gap scale. In this study, some distinctive flame characteristics were found in LSR conditions, which were the main focus of investigation. More specifically, flame oscillation was affected by the premixing, and the trends of LSR extinction limits were opposite in lean and rich sides regarding to the premixing. Flame oscillation phenomena were induced by the self-propagation of a flame skirt, and their periodic motions can be explained by the transient variation of gas concentrations along the stream. The LSR extinction characteristics of PPFs can be explained by variation in thermal thickness or effective heat loss. These results not only help us understand flame characteristics in mesoscale combustion spaces, but also provide important clues regarding the structure of ordinary opposed flow flames.

nikim@cau.ac.kr

4G06 EXPERIMENTAL AND NUMERICAL INVESTIGATIONS ON PREMIXED CH₄/AIR COMBUSTION IN A MESOSCALE CHANNEL WITH CAVITIES

Jianlong Wan, Aiwu Fan, Yi Liu, Hong Yao, Wei Liu, Huazhong University of Science and Technology, China

Behaviors of premixed CH₄/air flame in mesoscale channels with and without cavities were experimentally investigated. No stable symmetric flame was observed in the channel without cavities and flame is prone to inclining and pulsating. In contrast, flame can be effectively anchored by the recirculation zone and low velocity zone in the channel with cavities. When the inlet velocity is increased sufficiently high, curved fluctuating flames appear. Blow-off limit of the channel with cavities is 0.8 m/s, 1.4 m/s and 1.8 m/s for the equivalence ratio of 0.8, 0.9 and 1.0 respectively, which is several times larger than the corresponding burning velocity of incoming CH₄/air mixture. These indicate that the cavities have a strong ability to extend the operational range of inlet velocity. Numerical simulation was performed to help analyzing the flame fluctuating and blow-off mechanisms. Results show that the combustion flow structure is quite different from an isothermal flow. The intensive shear stresses in the reaction zone may lead to flame fluctuation. In addition, numerical results reveal that a large shear stress exists at the transition point between the ramped cavity wall and the downstream inner wall, which results in flame splitting at high inlet velocity, and eventually leads to flame blow-off. In summary, the combustion behaviors in the mesoscale channel with cavities strongly depend on the interactions between the reaction zone and flow field.

faw@hust.edu.cn

4G07 AN EXPERIMENTAL AND NUMERICAL INVESTIGATION OF PREMIXED SYNGAS COMBUSTION DYNAMICS IN MESOSCALE CHANNELS WITH CONTROLLED WALL TEMPERATURE PROFILES

Andrea Brambilla^{1,2}, Marco Schultze¹, Christos E. Frouzakis², John Mantzaras¹, Rolf Bombach¹, Konstantinos Boulouchos²

¹Paul Scherrer Institute, Switzerland ²Swiss Federal Institute of Technology, Switzerland

The dynamics in H₂/CO/O₂/N₂ premixed combustion was investigated experimentally and numerically in a 7-mm height mesoscale channel at atmospheric pressure, fuel-lean equivalence ratios 0.20 to 0.42, volumetric CO:H₂ ratios 1:1 to 20:1 and wall temperature profiles in the range 550 to 1320 K. Experiments were performed in an optically-accessible channel-flow reactor and involved high speed (up to 1 KHz) planar laser induced fluorescence (LIF) of the OH radical and thermocouple measurements of the upper and lower channel wall temperatures. Simulations were carried out with a transient 2-D code using an elementary syngas reaction mechanism and detailed species transport. Demarcation of the experimentally-observed parameter space separating stationary and oscillatory combustion modes indicated that the former were favored at the higher wall temperatures and higher CO:H₂ volumetric ratios, while the latter predominately appeared at the lower wall temperatures and lower CO:H₂ ratios. The numerical model reproduced very well all stationary combustion modes, which included V-shaped and asymmetric (upper or lower) modes, in terms of flame shapes and flame anchoring positions. Simulations of the oscillatory flames, which appeared in the form of ignition/extinction events of varying spatial extents, were very sensitive to the specific boundary conditions. The predictions qualitatively reproduced the flame topology, the ignition sequence (including the reverting from upper asymmetric to lower asymmetric flame propagation), and the range of measured oscillation frequencies.

ioannis.mantzaras@psi.ch

4G08 ANALYSIS OF THE FLAME STRUCTURE FOR LEAN METHANE-AIR COMBUSTION IN POROUS INERT MEDIA BY RESOLVING THE HYDROXYL RADICAL

B. Stelzner¹, Ch. Keramiotis², S. Voss¹, M.A. Founti², D. Trimis^{1,3}

¹TU Bergakademie Freiberg, Germany ²National Technical University of Athens, Greece

³Karlsruhe Institute of Technology, Germany

The increasing need for more efficient and less emissive technologies has shifted the focus of combustion research towards technologies involving combustion in porous inert media. Although burners of this type have started to be examined and characterized over the past years, nonintrusive experimental methods are needed to describe the actual processes taking place inside the porous structure. In the present work, the technique of Laser Induced Fluorescence (LIF) is employed to visualize the flame zone, utilizing the excitation and subsequent detection of the hydroxyl radical (OH). In order to perform the measurements inside the porous combustion zone, optical access along the porous structure for the laser beam to reach the probe volume and furthermore, to allow a sufficient amount of fluorescence to reach the detector was realized by a thin gap of a similar size as the porous cavity size. The optical gap size and positioning was chosen, in order to yield the most suitable configuration for a sufficient signal to noise ratio without significant disturbance of the combustion process in the porous reaction zone. The experiments were conducted over an area of various thermal loads and excess air ratios for methane/air combustion. The main scope of this work is to demonstrate how the flame structure is influenced by the thermal load and the equivalence ratio. Moreover, an experimental characterization of the wide, stable operating conditions of the porous burner is given, along with the description of the flame zone inside the porous matrix.

bjoern.stelzner@iwtt.tu-freiberg.de

4H01 PROPAGATION MECHANISMS OF SUPERSONIC COMBUSTION WAVES

M. Kellenberger, G. Ciccarelli, Queen's University, Canada

The propagation mechanism of a supersonic combustion wave in an obstructed channel is investigated using high-speed schlieren photography. Experiments were carried out in a 2.54 cm wide by 7.82 cm tall cross-section channel with fence-type obstacles mounted on the top and bottom channel surfaces equally spaced at 7.82 cm. Tests were carried out with stoichiometric hydrogen-oxygen mixtures over an initial pressure range of 8 to 30 kPa. The results indicate that the traditional quasi-detonation propagation regime can be broken down into four propagation modes, where only two of the modes involve detonation propagation. For very reactive mixtures, a sustained detonation propagates through the channel with some weakening during diffraction around obstacles. For conditions closer to the DDT limit, the generation of a Mach stem propagating along the centerline of the channel and behind the lead shock wave dictates whether a detonation is initiated. The Mach stem is produced by the interaction of two blast waves formed by ignition of the compressed thin layer of unburned mixture on the upstream side of the top and bottom obstacle faces. The Mach stem initially forms in the thick turbulent flame, and it propagates into the unburned gas ahead of the flame. A local explosion occurs in the compressed (by the leading shock wave), unburned gas that either drives a blast wave or a detonation wave ahead, overtaking the lead shock wave. The upper limit for choked flame propagation (average velocity below the products speed of sound) was found to correspond to $d/\lambda=1.6$ and the limit for detonation initiation was found to be $d/\lambda=3$. Based on these results, the use of the term quasi-detonation to describe supersonic combustion wave propagation between the traditional DDT limits, based on the upper limit of the choked flame regime, is not accurate.

kellenbergerm@me.queensu.ca

4H02 THE EFFECT OF TRANSVERSE SHOCK PROPAGATION ON THE SHOCK-TO-DETONATION TRANSITION PROCESS FOR AN INSENSITIVE EXPLOSIVE

Eric K. Anderson, Tariq D. Aslam, Scott I. Jackson, Los Alamos National Laboratory, United States

The one-Dimensional (1D) shock-to-detonation transition process has been studied extensively for PBX 9502, resulting in a good ability to predict the time or distance to detonation over a range of planar input shock pressures. The results are often represented as run distance or time versus input shock pressure on Pop-plots. In practice, however, input shocks to explosives are often not 1D. Instead, they may be oblique or non-planar. Here, we present results from a series of experiments in which a PBX 9502 slab was bonded on one side to a PBX 9501 slab. The faster detonation in the PBX 9501 slab drove an oblique shock in the PBX 9502. The result was a two-Dimensional (2D) shock structure consisting of a region of delayed reaction, referred to as an initiating layer, immediately adjacent to the PBX 9501/9502 interface, and a transition to detonation further from the interface. The initiating layer thickness varied with the input shock pressure, which was controlled by the thickness of the PBX 9501 layer. The results of nine such tests are presented in run-time vs. input-shock-pressure space and compared to Pop-plots generated with data from 1D experiments. Good agreement was observed, with the 2D results showing similar run-times to detonation but more scatter for a given input shock pressure. Thus, the transverse component of the initiating shock appears to have no measurable effect on the initiation physics due to the good correlation between the 1D and 2D data.

eanderson@lanl.gov

4H03 AN EXPERIMENTAL STUDY ON THE ONSET PROCESSES OF DETONATION WAVES DOWNSTREAM OF A PERFORATED PLATE

Hui Qin¹, John H.S. Lee², Zhenguo Wang¹, Zhuang Fengchen³

¹Science and Technology on Scramjet Laboratory, China ²McGill University, Canada ³Academy of Equipment, China

Steadily propagating detonation waves in a rectangular tube were destroyed by a perforated plate assembled perpendicular to the flow path, whereafter the re-initiation of detonation waves were investigated, which bypasses the turbulent acceleration process of DDT and illustrates only the onset process of detonation waves. Onset of detonation were effected in $C_2H_2+2.5O_2+70\%Ar$ and H_2+N_2O mixtures. The formation of cellular detonation waves were observed via Schlieren pictures and smoked foils. The different patterns of formation of detonation were analyzed in details. It could be concluded that there are apparently two types for the formation of detonation wave. In stable mixtures, the detonation wave could gradually transient to CJ detonation via multi local explosions in the reaction zone in the core flow. While in unstable mixtures, any local perturbation, mostly perturbations at the boundary layer, would result in an abruptly amplified local explosion, which originate an overdriven detonation wave that decay to CJ detonation afterward. With the concurrently obtained Schlieren pictures and smoked foils, the detailed wave structure evolutions during the onset process were formulated, which revealed the homogeneity of the apparently different onset regimes.

h.qinnudt@gmail.com

4H04 DETONATION LIMITS IN ROUGH WALLED TUBES

Amanda Starr¹, John H.S. Lee¹, H.D. Ng²

¹McGill University, Canada ²Concordia University, Canada

The present paper reports the results of a study of detonation limits in rough tubes. Detonation velocity is measured by photodiodes and ionization probes spaced at 10 cm intervals along the length of the tube. Smoked foils inserted into the core of the rough tube is used to register the structure of the detonation wave. Pressure transducers are also used to obtain the pressure profile. The results indicate that in rough tubes, the detonation velocity is generally lower than the corresponding values for smooth tubes. The velocity decreases slowly at first and then more rapidly as the limit is approached. The velocity variation is generally continuous and at the limits, the failure velocity is of the order of $0.4 V_{CJ}$ for all cases. The detonation limits in rough tubes are found to be wider than for a smooth tube. This indicates that the turbulence generated by the wall roughness facilitates the propagation of the detonation and extend the limits. Smoked foil records show that the in the core of the rough tube the detonation front has a cellular structure corresponding to the usual cellular structure due to instability of the detonation. Thus the intrinsic unstable cellular structure is quite robust and retains its global characteristics in spite of the large perturbation generated by the rough wall. The detonation in the core of the rough tube goes from multi-headed to single headed as the limit is approached. Past the single headed spin, the low velocity detonation has no cellular structure but consists of interacting weak transverse waves from the rough wall. The averaged pressure of the low velocity detonation front corresponds to about the constant volume explosion pressure, in accord with the velocity of the low velocity detonation.

amanda.starr@mail.mcgill.ca

4H05 EFFECT OF SPATIAL HETEROGENEITY ON NEAR-LIMIT PROPAGATION OF A STABLE DETONATION

Jianling Li¹, Xiaocheng Mi², Andrew J. Higgins²

¹China Academy of Engineering Physics, China ²McGill University, Canada

The effect of introducing a spatial heterogeneity into an explosive medium is studied computationally by examining the detonation velocity near the limit to propagation in a thin explosive layer. The explosive system studied is an ideal gas with a single exothermic reaction governed by a pressure-dependent reaction rate (p^n) with a pressure exponent of $n = 3$. A pressure-dependent reaction rate, rather than the usual exponential dependence of reaction on temperature of Arrhenius kinetics, is used so that the detonation wave is stable in the homogeneous case and can be modelled with simple, analytical techniques, and thus the effect of introducing heterogeneity can be clearly identified. The two-dimensional slab of explosive is bounded by a layer of inert gas with the same thermodynamic properties as the explosive. The heterogeneity is introduced into the explosive via a large-amplitude, two-dimensional sinusoidal ripple in density in the initialization of the simulation, while maintaining a constant pressure. The computational simulations are initialized with a ZND solution for the ideal CJ detonation, and the detonation is allowed to propagate into the explosive layer. The simulations show that the detonation in the heterogeneous media exhibits a cellular-like structure of complex shock interactions. The detonation is able to propagate into a significantly thinner layer of explosive and can exhibit a greater velocity than the corresponding homogeneous case. A parametric study of varying the wavelength of the sinusoid shows the existence of an optimal size of heterogeneity corresponding to a wavelength that is approximately 40 times the half reaction zone length of the ideal CJ detonation. As the wavelength is decreased to the size of the reaction zone length, the behavior reverts back to the homogeneous case. Wavelengths of heterogeneity significantly larger than the optimal case are deleterious to the propagation of the detonation wave.

xiaocheng.mi@mail.mcgill.ca

4H06 EFFECTS OF POROUS WALLED TUBES ON DETONATION TRANSMISSION INTO UNCONFINED SPACE

Navid Mehrjoo¹, Yuan Gao², Charles Basenga Kiyanda¹, Hoi Dick Ng¹, John H.S. Lee²

¹Concordia University, Canada ²McGill University, Canada

Experiments were carried out to investigate the failure mechanisms in the critical tube diameter phenomenon for stable and unstable mixtures. It was previously postulated that in unstable mixtures where the detonation structure is highly irregular, the failure during the diffraction is caused by the suppression of the instability responsible for the generation of local explosion centers. In stable mixtures, typically with high argon dilution and where the detonation is characterized by very regular cell, the failure is driven by the excessive global front curvature above which a detonation cannot propagate. To discern these two failure mechanisms, porous wall tubes are used to attenuate the transverse instability before the detonation emerges into the unconfined space. Porous sections with length L/D from 0 to 3.0 are used with two confined tube diameters $D = 12.7$ and 15.5 mm. The present results show that when porous wall tubes are used, the critical pressure for unstable $C_2H_2 + 2.5O_2$ and $C_2H_2 + 5 N_2O$ mixtures increases significantly. In contrast, for stable argon diluted $C_2H_2 + 2.5 O_2 + 70\%$ mixtures, the results with porous wall tubes exhibit little variation up to $L/D = 2.5$. For $L/D > 2.5$ a noticeable increase in critical pressure for argon diluted mixtures is also observed. This is dominantly caused by the slow mass divergence through the porous material inducing a curvature on the detonation front even before it emerges into the open area. The present experiment again demonstrates the importance of the transverse wave instability for typical hydrocarbon mixtures in critical situations such as the critical tube diameter experiment. For special cases such as highly argon diluted mixtures, the instability does not play a significant role in the failure and the propagation is controlled dominantly by the global curvature effect and the shock-ignition mechanism.

kiyanda@encs.concordia.ca

4H07 QUALITATIVE MODELING OF THE DYNAMICS OF DETONATION WITH LOSSES

Luiz M. Faria, Aslan R. Kasimov, King Abdullah University of Science and Technology, Saudi Arabia

We consider a simplified model for the dynamics of one-dimensional detonations with generic losses. It consists of a single partial differential equation that reproduces, at a qualitative level, the essential properties of unstable detonation waves, including pulsating and chaotic solutions. Here, we investigate the effects of shock curvature and of friction losses on the detonation dynamics in order to capture the main features of curved detonations and detonations propagating in obstructed media. To calculate steady-state solutions, a new approach to solving the detonation eigenvalue problem is introduced that avoids the well-known numerical difficulties, associated with the presence of a sonic point in the solution. By using unsteady numerical simulations of the simplified model, we also explore the nonlinear stability of the steady-state solutions.

aslan.kasimov@kaust.edu.sa

4H08 MODELLING OF DEFLAGRATION TO DETONATION TRANSITION USING FLAME THICKENING

S Yu, S Navarro-Martinez, Imperial College, United Kingdom

This paper presents a new model to capture Deflagration to Detonation Transition using a Flame Thickening approach. Two approaches have been implemented. One, where the thickening is applied to the reactive scalar only and other where all equations are transformed. A flame sensor is used to maintain the transformation close to the flame. The results show that detonation can be captured with relatively coarse meshes and dynamic choice of the thickening factor.

navarro@imperial.ac.uk

FRIDAY PLENARY LECTURE: CHEMICAL KINETIC AND COMBUSTION CHARACTERISTICS OF TRANSPORTATION FUELS

Frederick L. Dryer, Princeton University, United States

Internal combustion engines running on liquid fuels will remain the dominant prime movers for road and air transportation for decades, probably for most of this century. The world's appetite for liquid transportation fuels derived from petroleum and other fossil resources is already immense, will grow, will at some future time become unsustainable, and will become infeasible in the very long term. Alternative liquid fuels to augment and eventually replace petroleum derived fuels must necessarily involve approaches that result in comparatively much lower net carbon cycle emissions from the transportation sector, most likely through a combination of carbon sequestration and renewable fuel production. The successful growth and establishment of a *sustainable, profitable* alternative fuels industry will be best facilitated by approaches that *integrate* alternative products into the evolving petroleum derived fuel streams, i.e. gasolines, diesel, and jet fuels, with synergistic evolution of and integration with the refining and liquid fuel distribution infrastructure already present.

The emergence of low temperature combustion strategies, particularly those implementing dual fuel methods to achieve Reaction Controlled Compression Ignition (RCCI), offer potential to significantly improve operating efficiency and reduce emissions with minimal aftertreatment. Along with the evolution of other competing combustion engine

operating approaches, a clear understanding of fuel property influences on combustion behaviors will be important to achieving projected engine performance and emissions. Not only must petroleum derived fuels themselves be modified over time, but the effects of blending any proposed alternative fuel candidates with these fuels must be understood. Predicting the physical and chemical effects of real fuels on energy conversion system performance and emissions is a daunting problem, even for petroleum derived real fuels, since each is composed of several hundred to a thousand or more species typically belonging to one of five organic classes (n-paraffins, iso-paraffins, cyclo-paraffins, olefins, aromatics). And it is the global combustion response functions to varying the composition of these mixtures, inclusive of those occurring by blending petroleum derived fuel with alternative fuel candidates that are of interest in optimizing fuel properties for specific combustion applications.

This paper will present an overview of progress on and emerging tools for evaluating and emulating the physical and chemical kinetic related properties of real fuels and alternative fuel candidates on combustion behavior. New analytical and statistical methods can provide important insights as to how the molecular structures found in a fuel contribute to the physical and chemical kinetic properties relevant to combustion energy conversion processes. Results can in turn assist in screening candidate alternative fuels for more detailed study.

fldryer@Princeton.EDU

5A01 PREDICTION OF NO_x IN PREMIXED HIGH-PRESSURE LEAN METHANE FLAMES WITH A MMC-PARTIALLY STIRRED REACTOR

B. Sundaram¹, A.Y.Klimenko¹, M.J.Cleary², U. Maas³

¹The University of Queensland, Australia ²The University of Sydney, Australia ³Karlsruhe Institute of Technology, Germany

The Multiple Mapping Conditioning (MMC) method is used to extend the stochastic PDF approach to the flamelet regimes of premixed combustion. MMC permits for a desired degree of flamelet-like conditions while reflecting the fluctuating nature of turbulent flames and preserving the integrity and universality of the chosen mixing model. The model is implemented in the context of the Partially Stirred Reactor (PaSR), which is therefore generalised to have a wider range of applicability. A stochastic formulation of original MMC is deployed, where mixing of particle scalar values is conditioned on a Markovian reference variable which emulates an implied particle position relative to a flame. The model interactions with the reference variable are controlled through the flamelet localness parameter, λ , which is also related to the ratio of diffusive to convective time scales. The model is implemented in a Monte Carlo numerical scheme using detailed GRI3.0 chemical kinetics without adjustments of kinetic coefficients. Predictions of NO_x emissions are validated against experimental data for a lean premixed high-pressure combustor in which reactions fall between the flamelet and distributed regimes. There is good agreement between model predictions and experimental data.

brruntha.sundaram@uqconnect.edu.au

5A02 IMPACTS OF TURBULENCE-CHEMISTRY INTERACTION AND LOW TEMPERATURE IGNITION ON PREMIXED *N*-HEPTANE/AIR FLAMES

Bret Windom^{1,2}, Sang Hee Won¹, Bo Jiang^{1,3}, Yiguang Ju¹, Stephen Hammack⁴, Timothy Ombrello⁵, Campbell Carter⁵

¹Princeton University, United States ²University of Colorado, United States

³Nanjing University of Aeronautics & Astronautics, China ⁴University of Illinois at Urbana Champaign, United States

⁵Wright-Patterson AFB, United States

Turbulent burning velocities, flashback, and auto-ignition of turbulent *n*-heptane/air flames have been experimentally investigated with kHz-rate Planar Laser-Induced Fluorescence (PLIF) imaging. Using a Reactor-Assisted Turbulent Slot (RATS) burner and varying mixture equivalence ratios and mean jet velocities, turbulent flame structures and dynamics are investigated at two reactor temperatures, 450 and 650 K, with and without low-temperature ignition, respectively. Depending on the flow velocity and reactor temperature, two distinctive turbulent premixed flame regimes, namely, a Chemically-Frozen (CF) regime and a Low-Temperature-Ignition (LTI) regime are observed. For the CF regime, the measured turbulent burning velocities demonstrate a near-linear relationship with the turbulent intensity fluctuations, whereas for the LTI regime, the turbulent burning velocities are found to be nonlinearly accelerated with the progression of low-temperature chemistry. With the onset of LTI, calculations show dramatic changes in mixture composition, laminar flame speed, and mixture Lewis number. Using a scaling analysis, relative contributions of transport, represented by the mixture Lewis number, and chemistry, represented by the laminar burning velocity, on the observed nonlinear increase of LTI turbulent burning speeds are evaluated. The analysis suggests that the increase of turbulent burning velocities for the LTI regime is attributed to both the increase of the laminar burning velocity and the decrease of the mixture Lewis number. It is found that the influence of increased laminar burning velocity due to the change of chemistry becomes more dominant with increasing equivalence ratio. At LTI conditions, accelerated flame propagation driven flashback and pre-flame auto-ignition, are identified and discerned using kHz-rate OH PLIF while increasing the mixture equivalence ratio from fuel lean to rich.

sangwon@princeton.edu

5A03 TURBULENT TRANSPORT IN PREMIXED FLAMES APPROACHING EXTINCTION
K.H.H. Goh, P. Geipel, R.P. Lindstedt, Imperial College, United Kingdom

The turbulent transport in premixed flames approaching extinction has been characterised in terms of statistical properties using an opposed jet burner featuring fractal grid generated turbulence. The burner was used in a symmetric twin flame configuration featuring pre-vaporised cyclopentane and JP-10 (exo-tetrahydrodicyclopentadiene) at equivalence ratios of 0.75 and 0.85. The choice of fuels follows from the practical importance of JP-10 as an aviation fuel with cyclic C₅ compounds appearing as breakdown products. The bulk velocity was set to 3.0 m/s resulting in a turbulent Reynolds number of 120. The obtained data includes conditional velocity statistics, flame curvature information and scalar fluxes. The conversion between conventionally and Favre averaged statistics follows the Bray-Moss-Libby theory and the assumption that finite reaction interface thickness effects can be neglected. The impact of deviations from the latter on statistics is explored and results suggest that the effect is modest for interface thicknesses less than 20% of the turbulent flame brush. The experimental data obtained is sufficient to enable terms up to and including triple correlations to be evaluated in closed form. The work also clearly illustrates the rapid transition from non-gradient to gradient turbulent transport as the extinction limit is approached. The latter confirms that the change of flame propagation mode is related to the disappearance of the conventional premixed turbulent flame with a transition to a flameless oxidation mode required to support combustion in leaner mixtures.

p.lindstedt@imperial.ac.uk

5A04 PROPAGATION, DISSIPATION, AND DISPERSION OF DISTURBANCES ON HARMONICALLY FORCED, NON-PREMIXED FLAMES
Nicholas Magina, Vishal Acharya, Tao Sun, Timothy Lieuwen, Georgia Institute of Technology, United States

This paper describes the dynamics of non-premixed flames responding to bulk velocity fluctuations, and compares the dynamics of the flame sheet position and spatially integrated heat release to a similarly excited premixed flame. Bulk axial or transverse excitation, in either case, leads to the excitation of wrinkles on the flame that propagate axially. Inclusion of axial diffusion in the non-premixed case, and burning velocity stretch sensitivity in the premixed case, causes wrinkle dissipation and dispersion. There are important differences in spatially integrated unsteady heat release dynamics between premixed and non-premixed flames. For general Strouhal numbers, mass burning rate fluctuations are the dominant contributor to non-premixed flame heat release fluctuations, while area fluctuations are the dominant contributor to premixed flame heat release fluctuations. Moreover, the heat release response of non-premixed flames rolls off much slower with frequency, $O(St^{-1/2})$ compared to $O(St^{-1})$ for premixed flames, and, hence, are more sensitive to flow perturbations than premixed flames at high Strouhal numbers. The asymptotic tendencies of the non-premixed flame, however, are largely controlled by the near burner exit region with high transverse gradients and, thus, are expected to be quite sensitive to burner exit details and finite chemistry effects.

narthurm@gatech.edu

5A05 IRREVERSIBLE ENTROPY PRODUCTION RATE IN HIGH-PRESSURE TURBULENT REACTIVE FLOWS
Giulio Borghesi, Josette Bellan, California Institute of Technology, United States

A Direct Numerical Simulation (DNS) database is created describing high-pressure reactive flows for studying the flow characteristics and the irreversible entropy production rate that must be modeled by Subgrid-Scale (SGS) models in Large Eddy Simulation. The governing equations are the continuity, momentum, total energy and species transport equations complemented by a real-gas equation of state. The molecular transport model is based on complete mass-diffusion and thermal-diffusion matrices having elements computed according to all-pressure mixing rules. The mixture viscosity and thermal conductivity are calculated from the individual species values, valid at high pressures, by using all-pressure mixing rules. The reaction is a one-step process and the values of different coefficients in the reaction rate ensure that it gives physically-correct trends for autoignition. The DNS is performed for a temporal mixing layer. Three realizations are computed and examined to reveal the influence of the initial pressure p_0 and of Exhaust Gas Recirculation (EGR). It is found that the main flame is of diffusion type, flanked by premixed flames. As p_0 increases, the most intensive premixed-flame regions draw closer to the diffusion flame. Additionally to the well-known advantage of EGR, we found that it promotes the development of reverse diffusion which is a molecular process inducing the formation of strong species gradients that in turn induce turbulence production, i.e. the formation of dynamic small scales. Analysis of the irreversible entropy production rate revealed that its four modes — due to viscosity, mass diffusivity, thermal conductivity and reaction — operate in different spatial regions of the flow where different phenomena occur. Increasing p_0 and lack of EGR both result in an increase in the magnitude of the irreversible entropy-production rate. For the Reynolds number values achievable in DNS, the reaction mode dominates in magnitude all other modes of the irreversible entropy-production rate.

Josette.Bellan@jpl.nasa.gov

5A06 SOUND GENERATION BY PREMIXED FLAME ANNIHILATION WITH FULL AND SIMPLE CHEMISTRY

C. Jiménez¹, A. Haghiri², M.J. Brear², M. Talej³, E. R. Hawkes³

¹Centro de Investigaciones Energéticas, Spain ²University of Melbourne, Australia ³University of New South Wales, Australia

This paper presents a numerical study of sound generation by premixed laminar flame annihilation with full and simple chemistry. Planar annihilation is examined from lean ($\phi=0.5$) to rich ($\phi=3$) conditions, which correspond to (effective) Lewis numbers ranging from 0.5 to 2.0 respectively. The full chemistry simulations use a well known detailed mechanism for hydrogen-air mixtures [1, 2]. The simple chemistry simulations are tuned such that the freely propagating laminar flame speed matched those from the detailed chemistry simulations at the same equivalence ratio.

These simulations examine two, related issues. First, they are used to confirm whether the Lewis number plays a significant role in the sound generation process, as our previous, simple chemistry studies have found [3, 4]. More generally, these simulations seek to determine whether the use of simple chemistry to model sound generation is reasonable. The importance of the Lewis number is confirmed, and the use of simple chemistry is found to be reasonable in some cases.

a.haghiri@student.unimelb.edu.au

5A07/ 5A08 TOPICAL REVIEW: PARTIAL PREMIXING AND STRATIFICATION IN TURBULENT FLAMES

A.R. Masri, The University of Sydney, Australia

This paper reviews recent advances in understanding the structure of turbulent partially premixed and stratified flames. The term “partially premixed” refers here to compositionally inhomogeneous mixtures that include flammable as well as non-flammable fluid while “stratified” combustion refers to a reacting front propagating through a range of compositions within the flammable limits. An overview of relevant laminar flame concepts is first introduced. In laminar partially premixed flames, the interaction between rich and lean mixtures is significant so that CO and H₂ diffuse from the rich to the lean side and oxygen may leak out of the reaction zone leading to improvement in the flame’s resistance to extinction by straining. In lean back-supported laminar stratified flames, the influx of heat and radicals into the lean fluid results in higher flame speeds, broader reaction zones, and extended flammability limits compared to homogeneous counterparts. The situation in rich stratified flames is more complex due to the combined fluxes of heat as well as reactive species such as hydrogen and carbon monoxide.

Turbulent partially premixed flames are ubiquitous in practical combustion systems and stratified flames are now employed to extend the operating range of lean-burn engines without compromising efficiency and emissions. Detailed measurements in burners representative of those found in gas turbine combustors show that partial premixing at the lifted flame base increases with instability and the relative proportion of premixed and non-premixed events varies in time. Imposing concentration gradients for the reactants issuing at the jet exit plane improves the flame stability which is maximised at some optimum level of inhomogeneity. Highly resolved measurements in turbulent stratified flames show that the mass fractions of CO and H₂ increase with stratification; a result that is consistent with laminar flame studies. Such experiments are, however, very difficult and require multi-level conditioning of the data. The paper concludes with a brief review of potential numerical approaches employed in the calculations of turbulent flames with inhomogeneous conditions. A key challenge here is to reproduce the effects of increasing levels of stratification and/or inhomogeneity on the compositional structure of turbulent flames.

assaad.masri@sydney.edu.au

5A09 IMAGING MEASUREMENTS AND LES-CMC MODELING OF A PARTIALLY-PREMIXED TURBULENT DIMETHYL ETHER/AIR JET FLAME

Bruno Coriton¹, M. Zendehele², S. Ukai², A. Kronenburg², O.T. Stein², Seong-Kyun Im³, Mirko Gamba³, Jonathan H. Frank¹

¹Sandia National Laboratories, United States ²Universität Stuttgart, Germany ³Stanford University, United States

Turbulent Dimethyl Ether (DME) jet flames provide a canonical flame geometry for studying turbulence-flame interactions in oxygenated fuels and for developing predictive models of these interactions. The development of accurate models for DME/air flames would establish a foundation for studies of more complex oxygenated fuels. We present a joint experimental and computational investigation of the velocity field and OH and CH₂O distributions in a piloted, partially-premixed turbulent DME/air jet flame with a jet exit Reynolds number, Re_D , of 29,000. The turbulent DME/air flame is analogous to the well-studied, partially-premixed methane/air jet flame, *Sandia Flame D*, with identical stoichiometric mixture fraction, $\zeta_{st} = 0.35$, and bulk jet exit velocity, $V_{bulk} = 45.9$ m/s. The results of the LES-CMC simulations performed on an intermediate size grid of 1.3 million cells are in good agreement with Particle Image Velocimetry (PIV) and simultaneous CH₂O and OH Laser-Induced Fluorescence (LIF) imaging measurements. LES-CMC simulations employing two different chemical reaction mechanisms show approximately a factor of two difference in the peak CH₂O mole fractions, whereas OH mole fractions are in good agreement between the two mechanisms. The simultaneous OH-LIF and CH₂O-LIF measurements show a wide range of separation distances between the spatial distributions of these intermediate species, indicating that the consumption rates of formaldehyde by OH in a turbulent DME/air jet flame may be highly intermittent with significant departures from flamelet models.

jhfrank@sandia.gov

5A10 THE INFLUENCE OF COMBUSTION SGS SUB-MODELS ON THE RESOLVED FLAME PROPAGATION. APPLICATION TO THE LES OF THE CAMBRIDGE STRATIFIED FLAMES

R. Mercier, T. Schmitt, D. Veynante, B. Fiorina

¹Ecole Centrale Paris, France ²CNRS, France

In Large Eddy Simulation (LES) of premixed and stratified combustion, the overall prediction of the flame consumption speed depends on various SubGrid Scale (SGS) submodels such as the flame wrinkling, the fuel stratification or heat losses. The objective of this study is to investigate the LES sensitivity to the submodeling strategies. Different heat losses and SGS flame wrinkling models are presented in the context of the Filtered TABulated Chemistry for LES (F-TACLES) formulation. LES of the non-adiabatic non-swirling bluff-body stabilized Cambridge flames (SwB burner) are presented. In this complex configuration, both flame brush and flow dynamics are influenced by flame consumption speed submodels. First, accounting for heat losses impacts the prediction of both velocity and temperature of the Inner Recirculation Zone (IRZ). Second, model constants involved into SGS wrinkling submodels have a great impact on the mean flame brush position. The non-adiabatic formulation combined with a dynamic estimation of the SGS wrinkling model constant appears to be a very attractive approach and gives a very good prediction of both the mean flame location and the IRZ flow dynamics.

renaud.mercier@graduates.centraliens.net

5A11 LARGE EDDY SIMULATION OF A PARTIALLY-PREMIXED GAS TURBINE MODEL COMBUSTOR

Yee Chee See¹, Matthias Ihme²

¹University of Michigan, United States ²Stanford University, United States

Large-Eddy Simulations (LES) of a dual-swirl Gas Turbine Model Combustor (GTMC) are performed. The burner was experimentally studied by Meier, and operates under partially-premixed combustion conditions. Two different LES-combustion formulations are employed to separately investigate modeling strategies for the combustion-regime representation and the turbulence/chemistry interaction. A prior model analysis was conducted to examine the accuracy of describing the turbulent combustion regime inside this burner in terms of premixed or non-premixed flamelet solutions. Modeling results from three different LES-computations are compared with measurements for velocity, temperature, and species-mass fractions of CO₂, CO, and H₂. Overall, the simulation results, obtained with a non-premixed Flamelet/Progress-Variable (FPV) model and a premixed-based filtered tabulated chemistry LES (F-TACLES) formulation, are in good agreement with experimental data. By extending the FPV-model, it is shown that the flow-field structure exhibits sensitivity to the representation of the turbulence/chemistry interaction. This is a result of the flame-wrinkling at the lifted flame base in the nozzle-near region. Discrepancies among the different models are analyzed, and the sensitivity of the simulation results to the mesh-resolution, subgrid-closure models, and model-representations are discussed.

mihme@stanford.edu

5A12 HIGH-SPEED TOMOGRAPHIC PIV MEASUREMENTS OF STRAIN RATE INTERMITTENCY AND CLUSTERING IN TURBULENT PARTIALLY-PREMIXED JET FLAMES

Bruno Coriton, Jonathan H. Frank, Sandia National Laboratories, United States

The effects of combustion on the strain rate field in turbulent jets was studied using 10 kHz Tomographic Particle Image Velocimetry (TPIV). We compared strain rate measurements in a well-studied, turbulent partially-premixed methane/air jet flame (*Sandia Flame C*) to measurements in a turbulent non-reacting air jet and a jet flame with significantly greater probability of localized extinction and intermittent blowoff. Since the jet exit Reynolds number of approximately 13,000 was nearly identical in the three jets, differences in the strain rate fields could be attributed to the presence (or absence) of a flame and its burning stability. Spatiotemporal characteristics of the strain rate field were analyzed. Overall, the strain rate norm was larger in the flames than in the non-reacting jet with the most stable flame having the largest values. In all three jets, the compressive strain rate was on average the largest of the three principal strain rates. At high strain rates, the ratios of the compressive and extensive strain rate to the intermediate strain rate were similar to those found in isotropic incompressible turbulent flows. The three-dimensional velocity measurements were used to analyze the spatial distribution of strain rate clusters, defined as singly-connected groups of voxels where the strain rate magnitude exceeded a threshold value. The presence of a stable flame significantly attenuated the number of clusters of intermediate strain rate. Strain rate bursts, corresponding to sudden increases in the number of clusters, were identified in the three jets. The largest bursts in the non-reacting jet and the unstable flame contained twice as many clusters as in the stable flame. The temporal intermittency of the most intense strain rate clusters was analyzed using the time-series measurements. Clusters with strain rates greater than five times the standard deviation of the strain rate norm were highly intermittent.

jhfrank@sandia.gov

5A13 SCALAR STRUCTURE OF TURBULENT PARTIALLY-PREMIXED DIMETHYL ETHER/AIR JET FLAMES

F. Fuest¹, G. Magnotti², R.S. Barlow², J.A. Sutton¹

¹The Ohio State University, United States ²Sandia National Laboratories, United States

This work presents results of temperature and major species measurements from two turbulent piloted, partially-premixed Dimethyl Ether (DME)/air jet flames with Reynolds numbers of 30,750 and 61,500. These results are intended to provide a first set of multi-scalar data from a new flame series for the investigation of turbulence-chemistry interaction and the validation of turbulent combustion models using a complex, oxygenated fuel, DME. The current work investigates two Reynolds number cases from the complete DME flame series (five flames) that were formulated to be similar to the well-known Sydney/Sandia piloted jet burner flame series A-F using methane fuels. The flame structure is examined using ensemble mean and rms radial profiles at various axial positions downstream of the nozzle exit as well as statistics conditioned on mixture fraction. Finally, selected results of the two cases are compared to the original methane-based configurations. Finite-rate chemistry effects such as local extinction and re-ignition and their impact on the scalar flame structure are found to be different in the DME/air jet flames as compared to the methane-based jet flames.

fuest.1@osu.edu

5B01 FLAME DYNAMICS OF EQUIVALENCE RATIO OSCILLATION IN A STAGNATING LAMINAR LEAN METHANE/AIR PREMIXED FLAME

Hisashi Tomita¹, Abdul Rahman Mohd Rosdzimin², Sotaro Miyamae¹, Takeshi Yokomori¹, Toshihisa Ueda¹

¹Keio University, Japan ²Universiti Pertahanan Nasional, Malaysia

This study investigates the effect of fuel concentration oscillation on the laminar stagnating premixed flame by both experiment and numerical simulation. The numerical analysis is conducted by ANSYS FLUENT 14.5. The equivalence ratio oscillation in experiments is formed by a novel oscillator with two cylinder piston units which produce alternative ejection of leaner and richer pre-mixture. The velocity fluctuation is well suppressed by installing screens on the burner exit. The fuel concentration variation between stagnation plate and exit of burner is visualized and analyzed by acetone UVIF (Ultra-Violet Light Induced Fluorescence) in the isothermal condition. The frequency of the oscillator is varied in the range of 2 ~ 20 Hz. In this case, wavelength of the oscillation is much longer than the flame thickness. The flame oscillates periodically with a fuel concentration oscillation and the amplitude of the flame oscillation attenuates with an increase in the frequency of the fuel concentration oscillation when the frequency exceeds 5 Hz, which corresponds to the Strouhal number is unity, for experiment. It indicates that the Strouhal number distinguishes quasi-steadiness for $St < 1$ and unsteadiness for $St > 1$. The flame oscillation makes a closed cycle pattern. This can be explained as a variation in a back support effect to the flame. The numerical results show the similar trend for the response of the flame for the fuel concentration oscillation. The present study elucidated that the flame motion is clearly affected by the fuel concentration oscillation even in the case of low frequency oscillation, in other words, the oscillation wavelength is much longer than the flame thickness due to the back support effect.

hisashi.t.k8k8s-5@a2.keio.jp

5B02 IMPACT OF CHEMISTRY MODELS ON FLAME-VORTEX INTERACTION

Simon Lapointe, Brock Bobbitt, Guillaume Blanquart, California Institute of Technology, United States

In numerical simulations of turbulent combustion, accurate modeling of the fuel chemistry is a critical component of capturing the relevant physics. Various chemical models are currently being used including detailed chemistry, tabulated chemistry, one-step chemistry, and rate-controlled constrained-equilibrium. However, the differences between these models and their impacts on the fluid dynamics are not well understood. Towards that end, the interaction between a laminar premixed hydrogen-air flame and a two-dimensional monopole vortex is investigated through simulations using the four previously-mentioned chemistry models. In these simulations, the flame speed, viscosity, diffusivity, conductivity, heat capacity, density ratio, and initial vortex characteristics are virtually identical providing a comparison of the effects of each chemical model alone. The results with each model are compared by considering the evolution of the flame structure and the characteristics of the vortex. All four models predict very similar results for the interaction with a small, fast vortex. In the interaction with a large, slow vortex, results from one-step chemistry are different due to a different flame thickness. The large, fast vortex case showcases differences in the flame structure and larger discrepancies between the modeling approaches.

slapoint@caltech.edu

5B03 STRUCTURE AND STABILITY OF PREMIXED FLAMES STABILIZED BEHIND THE TRAILING EDGE OF A CYLINDRICAL ROD AT LOW LEWIS NUMBERS

V.N. Kurdyumov¹, Y. Shoshin², L.P.H. de Goey²

¹CIEMAT, Spain ²Technische Universiteit Eindhoven, The Netherlands

Premixed flames stabilized behind the trailing edge of a semi-infinity cylindrical rod placed coaxially in a circular channel were investigated numerically within the diffusive-thermal model. Apart from the inverted flames, or V-flames,

widely reported in the literature, the other kind of flames was observed for the Lewis number lower than unity. The main characteristic of such flames is confinement in the interior of a recirculating vortex formed behind the trailing edge. For a fixed Reynolds number, the flames of this kind exist within a finite range of the Damköhler number. Once the Damköhler number is fixed, they are observed for the Reynolds numbers above a critical value with no limit on large Re . Global linear stability analysis of the axisymmetric steady-state solutions of both kinds was performed. The ranges of the parameters where the axisymmetry-breaking bifurcation arises and the oscillatory behavior takes place were found. The results of the stability analysis were successfully compared with the direct two- and three-dimensional numerical simulations.

vadim.k@ciemat.es

5B04 THE INFLUENCE OF CARBON MONOXIDE AND HYDROGEN ON THE STRUCTURE AND EXTINCTION OF NONPREMIXED AND PREMIXED METHANE FLAMES

Vaishali Amin¹, Georg Katzlinger^{1,2}, Priyank Saxena³, Kalyanasundaram Seshadri¹, Ernst Pucher²

¹University of California at San Diego, United States ²Vienna University of Technology, Austria

³Solar Turbines Inc., United States

An experimental and computational study is carried to elucidate the influence of Carbon Monoxide (CO) addition to nonpremixed methane (CH₄) flames. A Burke-Schumann (flame-sheet) formulation is applied to laminar counterflow diffusion-flame experiments, reported here, in which CO was added to either methane-nitrogen mixtures or oxygen-nitrogen mixtures at normal atmospheric pressure, with both feed streams at normal room temperature. Experimental conditions were adjusted to fix selected values of the stoichiometric mixture fraction and the adiabatic flame temperature, and the strain rate was increased gradually until extinction occurred. At the selected sets of values, the strain rate at extinction was measured as a function of the CO concentration in the fuel or oxidizer stream. It was found that with increasing amounts of CO in the oxidizer stream, the strain rate at extinction first increased and then decreased. With increasing amounts of CO in the fuel stream the strain rate at extinction remained the same exhibiting neither an increase nor a decrease. This experimental result was also in close agreement with computational predictions employing detailed chemistry. A numerical investigation is carried out to characterize the influence of hydrogen and carbon monoxide on the structure and burning velocities of stoichiometric premixed methane flames. The mass fraction of the reactants in the mixture are so chosen that the adiabatic temperature is constant. The flame speed increases when hydrogen is added to the reactant stream. For CO addition the flame speed first increases and then decreases.

seshadri@ucsd.edu

5B05 FUNDAMENTAL PHYSICS OF FLAME DEVELOPMENT IN AN AUTOIGNITING DUAL FUEL MIXTURE

Zhiyan Wang¹, John Abraham^{1,2}

¹Purdue University, United States ²University of Adelaide, Australia

Computations are carried out of n -heptane/methane-air mixing layers under high-pressure and high-temperature conditions to provide insight into the fundamental physics of flame propagation in a lean premixed low cetane number fuel/air system when ignited by autoignition of a high cetane number fuel. Mixing layer thickness, pressure, and premixed fuel/air temperature and equivalence ratio are varied to understand the dependence on these variables of the characteristic time required for steady premixed flame propagation to be achieved. It is shown that the characteristic time has three components: time for autoignition to occur, time for peak temperature to be achieved following autoignition, and time for steady flame propagation in the premixed fuel/air mixture to be achieved. The autoignition time correlates well with pressure and temperature as documented in the literature. The time to achieve peak temperature is relatively short, but correlates with mixing layer thickness and premixed equivalence ratio. The time to achieve steady propagation correlates with mixing layer thickness and laminar flame speed.

wang1695@purdue.edu

5B06 MULTI-SCALE MODELING OF DYNAMICS AND IGNITION TO FLAME TRANSITIONS OF HIGH PRESSURE STRATIFIED N -HEPTANE/TOLUENE MIXTURES

WeiQi Sun¹, Sang Hee Won¹, Xiaolong Gou², Yiguang Ju¹

¹Princeton University, United States ²Chongqing University, China

The transitions from ignition to flames as well as the combustion dynamics in stratified n -heptane and toluene mixtures are numerically modeled by a correlated dynamic adaptive chemistry method coupled with a multi-timescale method (CO-DAC/MTS) in a one-dimensional constant volume chamber. The study attempts to answer how the kinetic difference between n -alkanes and aromatics leads to different ignition to flame transitions and knocking-like acoustic wave formation at low temperature and engine pressure conditions with fuel stratification. It is found that the Low Temperature Chemistry (LTC) and fuel stratification of n -heptane leads to the formation of multiple ignition fronts. Four different combustion wave fronts, a Low Temperature Ignition (LTI) front followed by a High Temperature Ignition (HTI) front, a premixed flame front, and a diffusion flame front, are demonstrated. The fast LTI and HTI wave front propagation leads to a shock-like strong acoustic wave propagations, thus strongly modifying the dynamics of the subsequent diffusion and

premixed flame fronts. On the other hand, for the toluene mixture, due to the lack of LTC, only two combustion wave fronts are formed, a HTI front and a premixed flame front, exhibiting stable flow field and no formation of shock-like acoustic wave. The dynamics of transition from combustion to shock waves is further analyzed by using a modified Burgers' equation. The analysis for *n*-heptane/air mixture indicates that both the onset of LTI and the strong dependency of HTI on the equivalence ratio can either promote or attenuate the transition from strong acoustic wave to shock wave. However, the toluene/air mixture exhibits no coupling with acoustic wave, suggesting that the rich LTC reactivity with fuel stratification, specific to the *n*-alkane chemistry, can lead to knocking and acoustic formation.

yju@Princeton.EDU

5B07 HIGH TEMPERATURE OXIDATION OF FORMALDEHYDE AND FORMYL RADICAL: A STUDY OF 1,3,5-TRIOXANE LAMINAR BURNING VELOCITIES

Jeffrey Santner, Francis M. Haas, Frederick L. Dryer, Yiguang Ju, Princeton University, United States

Few studies of formaldehyde flames are available, especially above vacuum pressures due to the difficulties and hazards associated with producing formaldehyde vapor. This work experimentally and numerically investigates the flame properties of formaldehyde (CH_2O) and formyl radical (HCO) at high O_2 loadings and both atmospheric and reduced pressure by measuring and modeling the laminar burning rates of 1,3,5-trioxane/ O_2/N_2 mixtures. Trioxane is shown to decompose nearly exclusively into high concentrations of formaldehyde early in the flame structure before subsequent flame chemistry reactions occur. Kinetic model predictions show that the flame properties are controlled by CH_2O and HCO kinetics. Laminar burning rate predictions of several combustion kinetic models vary significantly in comparison to experimental data and each other; however, all simulations show that the present observations are particularly sensitive to the competition between reactions $\text{HCO} + \text{M} = \text{H} + \text{CO} + \text{M}$ (R3) and $\text{HCO} + \text{O}_2 = \text{HO}_2 + \text{CO}$ (R4). Monte Carlo optimization of these rate coefficients allows interpretation of the measured flame speeds as indirect rate coefficient measurements at flame relevant temperatures. Although results from simple A-factor optimization agree well with the present measurements, three-parameter optimization is shown to be necessary in order to accurately model kinetics across a wide temperature range, including high temperature flames and low temperature direct rate measurements. A-factor and three-parameter optimization both show that a reduced k_3/k_4 branching ratio over the temperature range from 1100 - 1700 K improves model predictions compared to present measurements.

jsantner@princeton.edu

5B08 A STUDY OF PROPAGATION OF SPHERICALLY EXPANDING AND COUNTERFLOW LAMINAR FLAMES USING DIRECT MEASUREMENTS AND NUMERICAL SIMULATIONS

Jagannath Jayachandran¹, Alexandre Lefebvre², Runhua Zhao¹, Fabien Halter³, Emilien Varea², Bruno Renou², Fokion N. Egolfopoulos¹

¹University of Southern California, United States ²CORIA, CNRS, France ³Université d'Orléans, France

Spherically expanding and counterflow flame configurations are used extensively to determine laminar flame speeds. Even though significant advances have been made over the years with both the theoretical and experimental aspects of these standard experiments, discrepancies persist in reported laminar flame speed data raising the question of accuracy and consistency. Among the probable reasons that the discrepancy among reported data is that laminar flame speed is a derived and not a directly measured physical quantity, leaving thus room for interpretations that typically introduce additional uncertainties. In the present investigation, a combined experimental and modeling study was carried out for first time in both configurations. Ethylene and *n*-heptane flames were considered and the flow velocities were measured using particle image velocimetry in both spherically expanding and counterflow flames. The accuracy and consistency of the results were assessed by comparing directly measured and directly computed physical properties. It was shown that the directly measured data in both configurations are consistent based on comparisons against the results of direct numerical simulations. It was shown also, that notable uncertainties are introduced when extrapolations and density corrections are implemented in spherically expanding flames.

jjayacha@usc.edu

5B09 COMPARATIVE STUDY ON THE LAMINAR FLAME SPEED ENHANCEMENT OF METHANE WITH ETHANE AND ETHYLENE ADDITION

S. Ravi, T.G. Sikes, A. Morones, C.L. Kee, E.L. Petersen, Texas A&M University, United States

A systematic analysis of the flame speed enhancement effects of ethane and ethylene addition to methane was performed. Flame speeds of outwardly propagating spherical flames were measured in a high-pressure, cylindrical flame speed vessel using schlieren photography. It was ensured that the measured data were outside the ignition- and chamber-confinement-affected radii. The unstretched, unburnt flame speeds were obtained using nonlinear extrapolation methods from the experimentally determined stretched flame speeds. The AramcoMech 1.3 kinetics mechanism was validated against flame speeds of ethane, ethylene, and acetylene over a wide range of pressures and equivalence ratios. Good agreement between the measured data and those reported in the literature was seen. The model agreed closely with the

measurements at fuel-lean conditions, but a slight over prediction was observed for the fuel-rich cases. Flame speeds of 80/20 and 60/40 (by volume) CH₄/C₂H_x mixtures in air and in air with excess nitrogen were measured over a wide range of fuel concentrations. In all cases, the addition of ethylene increased the flame speed more than did an equivalent addition of ethane. The Arrhenius effect (predominantly kinetic effect) was the principal driver for flame speed enhancement of methane with ethane/ethylene addition. Sensitivity analysis revealed that thermal and diffusive pathways were equally contributing to the flame speed enhancement of CH₄/C₂H₆ mixtures, but the latter played a comparatively minor role in the C₂H₄-based blends.

sri327@gmail.com

- 5B10 LAMINAR FLAME SPEEDS OF *N*-DECANE, *N*-BUTYLBENZENE, AND *N*-PROPYLCYCLOHEXANE MIXTURES
Andrea Comandini, Thomas Dubois, Nabih Chaumeix, INSIS, CNRS, France

In the present investigation new experimental data on laminar flame speeds of *n*-decane, *n*-butylbenzene, and *n*-propylcyclohexane single- and multi-component mixtures are presented. The experiments have been conducted in a spherical bomb heated to 403 K and at an initial pressure of 1 bar. The comparison between the results indicates that the flame speeds of the multi-component mixtures are influenced by the corresponding components for most of the stoichiometric conditions considered, although on the rich side the experimental curves are mainly affected by the compound with the fastest propagation speed. The experimental results were also used to validate a comprehensive kinetic model which extends the chemistry of the JetSurF 2.0 model to include the aromatic compounds up to *n*-butylbenzene. The simulations well reproduce the experimental measurements over a wide range of conditions. Additional sensitivity and rate of production analyses were performed to clarify how the specific structures of the fuels (one linear alkane, one cyclic alkane, and one aromatic) influence the formation of several intermediate compounds relevant to the flame propagation properties.

andrea.comandini@cnrs-orleans.fr

- 5C01 MEASUREMENTS AND MODELLING OF HCN AND CN SPECIES PROFILES IN LAMINAR CH₄/O₂/N₂ LOW PRESSURE FLAMES USING LIF/CRDS TECHNIQUES
Nathalie Lamoureux, Hilal El Merhubi, Laurent Gasnot, Coralie Schoemaeker, Pascale Desgroux CNRS, Université Lille1, France

In the present work, absolute mole fraction profiles of CN and HCN were jointly performed in low pressure (5.3 kPa) premixed CH₄/O₂/N₂ flames of various equivalent ratios (ϕ = 0.8-1.25). These species were the missing link in the database comprising CH, NCN, NCO and NO species previously acquired in Lille to improve detailed mechanisms of prompt-NO formation. For that purpose, LIF and pulsed CRDS techniques were implemented to measure in the flames absolute mole fraction of CN by probing the B-X(1,0) vibrational band around 356 nm. Thanks to this combination, the detection limit as low as tenth of ppbv that was necessary to measure CN in lean flame condition could be achieved. HCN molecules were measured by using *cw*-CRDS technique around 1.5 μ m (in the (200)-(000) vibrational band) after gas probe sampling. The required sensitivity equal to 15 ppbv of HCN was achieved using a long absorption cell (about 1 m). These CN and HCN profiles are simulated by considering two detailed mechanisms of prompt-NO formation from literature (Konnov0.6 (Combust. Flame 156 (2009) 2093-2105) and GDFkin@3.0_NCN (Combust. Flame 157 (2010) 1929-1941)).

nathalie.lamoureux@univ-lille1.fr

- 5C02 TOWARDS SIMULTANEOUS CALIBRATION-FREE AND ULTRA-FAST SENSING OF TEMPERATURE AND SPECIES IN THE INTRAPULSE MODE
Robin S.M. Chrystie, Aamir Farooq, King Abdullah University of Science and Technology, Saudi Arabia

We report on exploiting the down-chirp phenomenon seen in Quantum Cascade Lasers (QCLs), when modulated with long pulses, for the purpose of performing calibration-free and temporally resolved measurements. Intrapulse spectra of a native species (e.g. H₂O), common to combustion environments, were generated near λ =7.62 μ m at repetition rates as high as 3.125 MHz. Two-line absorption spectroscopy was employed to infer calibration-free temperature from the chirp-induced intrapulse spectra. We demonstrate the ease at which accurate temperatures and H₂O compositions can be achieved using simple and compact QCLs operated in the intrapulse mode. The sensor is also applicable to other species, and has the potential to be integrated into commercial technologies.

robin.chrystie@cantab.net

5C03 HIGH-TEMPERATURE *ISO*-BUTENE ABSORPTION DIAGNOSTIC FOR SHOCK TUBE KINETICS USING A PULSED QUANTUM CASCADE LASER NEAR 11.3 μm

R.M. Spearrin, S. Li, D.F. Davidson, J.B. Jeffries, R.K. Hanson, Stanford University, United States

A high-bandwidth absorption sensing technique for *iso*-butene (iC_4H_8) was developed to measure transient species concentration behind reflected shock waves for combustion kinetics studies. Direct measurements of iC_4H_8 were enabled by monitoring absorption in the infrared near 11.3 μm using a novel pulsed External-Cavity Quantum Cascade Laser (ECQCL) with a repetition rate of 600 kHz. Optimal wavelength selection for high-temperature combustion gases was first determined by a spectral survey at 1000 K near the peak of the absorption band (878 cm^{-1} to 892 cm^{-1}) using the ECQCL. Absorption cross section measurements of iC_4H_8 at 881.4 cm^{-1} , the selected high-temperature wavelength, were then conducted from 800 K to 1800 K behind reflected shocks to characterize temperature dependence at modest pressures (4 – 8 atm). The species-specific technique was subsequently demonstrated by time-resolved (100 kHz) measurements of *iso*-butene decay during thermal decomposition (1280 – 1480 K). First-ever shock tube measurements of iC_4H_8 yields from *iso*-octane pyrolysis (1070-1300 K) were also produced, with a detection limit of ~ 100 ppm. Experimental results were compared to recent kinetic models to illustrate the potential of this diagnostic for analyzing combustion chemistry.

spearrin@stanford.edu

5C04 EARLY FLAME PROPAGATION IN A SPARK-IGNITION ENGINE MEASURED WITH QUASI 4D-DIAGNOSTICS

B. Peterson, E. Baum, B. Böhm, A. Dreizler, Technische Universität Darmstadt, Germany

This paper presents the first results towards experimentally resolving the local three-dimensional (3D) flame propagation and turbulence-chemistry-interaction in a spark-ignition engine using temporally resolved multi-planar laser diagnostics. The experimental method utilizes simultaneous dual-plane OHLIF (OH-LIF) and stereoscopic PIV (SPIV) to locally resolve 3D flame displacement speed during the early flame development when less than 5% of the mass has been consumed. OH-LIF is used to track the reaction-zone position and flame normal direction in 3D space, while SPIV measures the convection of the identified flame contours. Based on the vectorial difference of the 3D convection and absolute propagation of the reaction-zone, the 3D displacement speed (s_T) is calculated. An instantaneous flame realization shows a large dynamic range of local s_T and local flow transport, while also revealing the importance to resolve these quantities in 3D. Several flame-flow configurations are realized along a flame surface and each uniquely defined the local flame transport along the individual flame realization. A detailed uncertainty and sensitivity analysis is performed, confirming the validity of the s_T distribution resolved for the methodology and operating conditions. A discussion on the different mechanisms leading to the large distribution of s_T for the given operations is included and testifies to complex nature of the in-cylinder flame development in this early stage. The limitations of the presented methodology are discussed particularly in the need for improved spatial resolution and additional volumetric information. The merits and limitations of the presented work provides an improved understanding of what is further needed to better resolve local 3D flame transport in engines for both experimental and numerical methodologies.

peterson@csi.tu-darmstadt.de

5C05 CALIBRATION-FREE, HIGH-SPEED, IN-CYLINDER LASER ABSORPTION SENSOR FOR CYCLE-RESOLVED, ABSOLUTE H_2O MEASUREMENTS IN A PRODUCTION IC ENGINE

O. Witzel¹, A. Klein¹, C. Meffert², C. Schulz², S. A. Kaiser², V. Ebert^{1,3}

¹Physikalisch-Technische Bundesanstalt, Germany ²University of Duisburg-Essen, Germany ³TU Darmstadt, Germany

The performance of a hygrometer based on calibration-free direct Tunable Diode Laser Absorption Spectroscopy (dTDLAS) for in-cylinder H_2O measurements is demonstrated in a nearly unmodified production internal combustion engine. The H_2O concentration is a proxy for the residual-gas fraction remaining in the cylinder after intake-valve closure. One challenge for in-cylinder measurements, especially in multi-cylinder engines, is to obtain optical access to the combustion chamber. The measurements here were performed in the flywheel-side cylinder of a four-cylinder engine with small access ports that were previously designed for endoscopic imaging. Due to their position these ports prohibit the usual collinear arrangement of the optical elements typical for line-of-sight measurement techniques. Therefore, we developed a new "angled" fiber-optical interface, which allows a trans-illumination of the engine at a 90° angle. The optical fiber interface uses a scattering target inside the combustion chamber with its 84 mm bore achieving an absorption length of about 70 mm. With this arrangement, crank-angle resolved measurements of the H_2O concentration during early compression could be monitored with a temporal resolution of 250 μs and a H_2O precision of 0.074 vol.%. This allows detailed analysis of single engine cycles as needed for residual-gas investigations. Measurements with various loads (25 - 100 Nm) and speeds (1400 - 3700 rpm) were performed, over which the residual-gas fraction was expected to vary significantly. We measured H_2O concentrations between 3.3 and 5.0 vol.%. The results were compared with a simple model of residual gas content and were found to agree within the combined uncertainty of both methods, which gives an indication that dTDLAS can be used to validate more complex engine models beyond what is possible by pressure-trace analysis.

volker.ebert@ptb.de

5C06 INFRARED LASER ABSORPTION SENSORS FOR MULTIPLE PERFORMANCE PARAMETERS IN A DETONATION COMBUSTOR

C.S. Goldenstein, R.M. Spearrin, J.B. Jeffries, R.K. Hanson, Stanford University, United States

Laser absorption sensors for temperature and H₂O near 1.4 and 2.5 μm , CO₂ near 2.7 μm , and CO near 4.8 μm were developed, validated, and deployed in an ethylene-fueled pulse detonation combustor (PDC). Each sensor was fiber-coupled to enable remote light delivery to the PDC and photovoltaic detectors were mounted directly to the PDC for improved light collection. Measurements were acquired simultaneously along two orthogonal lines-of-sight (LOS) in both the PDC combustion chamber and the throat of a converging-diverging nozzle located at the PDC exit. Measurements in the nozzle throat were combined with a choked flow assumption to calculate the time-resolved enthalpy flow rate exiting the PDC. All sensors used first-harmonic-normalized wavelength-modulation spectroscopy with second-harmonic detection (WMS-2f/1f) to account for non-absorbing transmission losses (e.g., from beamsteering, soot, and window fouling) and emission. Furthermore, strong midinfrared absorption transitions were used to enable improved measurement accuracy and precision. These sensors were validated in non-reactive shock tube experiments at temperatures and pressures up to 2700 K and 50 atm. There, these sensors exhibited a nominal accuracy of 3 to 5% with bandwidths from 4.5 to 10 kHz. Measurements in the PDC indicated peak temperatures near 3500 K with nearstoichiometric proportions of H₂O and incomplete conversion of CO to CO₂. The stagnation enthalpy flow rate was highly transient, but repeatable with peak flow rates near 25 MW.

csgolden@stanford.edu

5C07 FAST SOLVERS FOR LARGE KINETIC MECHANISMS USING ADAPTIVE PRECONDITIONERS

Matthew J. McEnly, Russell A. Whitesides, Daniel L. Flowers, Lawrence Livermore National Laboratory, United States

The adaptive preconditioners developed in this paper substantially reduce the computational cost of integrating large kinetic mechanisms using implicit ordinary differential equation (ODE) solvers. For a well-stirred reactor, the speedup of the new method is an order of magnitude faster than recent approaches based on sparse linear system solvers. Moreover, the new method is up to three orders of magnitude faster than traditional implementations of the ODE solver where the Jacobian information is generated automatically via divide differences, and the factorization relies on standard, dense matrix operations. Unlike mechanism reduction strategies, the adaptive preconditioners do not alter the underlying system of differential equations. Consequently, the new method achieves its performance gains without any loss of accuracy to within the local error controlled by the ODE solver. Such speedup allows higher fidelity mechanism chemistry to be coupled with multi-dimensional fluid dynamics simulations.

mcenly1@llnl.gov

5C08 VALIDATING AND EXPLOITING PREDICTIVE MODELS BY INCORPORATING AN INSTRUMENTAL MODEL

Devin R. Yeates¹, Wenjun Li², Phillip R. Westmoreland², William Speight¹, Trent Russi¹, Andrew Packard¹, Michael Frenklach^{1,3}

¹University of California at Berkeley, United States ²North Carolina State University, United States

³Lawrence Berkeley National Laboratory, United States

A paradigm is described and demonstrated for rigorously evaluating model-versus-data agreement while extracting new insights for improving the model and experiment. “Bound-to-Bound DataCollaboration” (B2B-DC) is augmented with an Instrumental Model, integrating uncertainty quantification of the reactor model, chemical model, and data analysis. The subject of analysis is a fuel-lean C₂H₂/O₂/Ar premixed laminar flat flame, mapped with VUV-photoionization molecular-beam mass spectrometry at the Advanced Light Source of Lawrence Berkeley National Laboratory. Experimental signals were modeled with a CHEMKIN flame code augmented with an Instrumental Model. Consistency of the model and raw experimental data are determined as a quantitative measure of their agreement. Features of the mole-fraction profiles are predicted for O, OH, C₂H₃, and background contributions to H₂O measurements. Also computed are posterior distributions of the initial targets and model parameters, as well as their correlations. This approach to model-versus-data assessment promises to advance the science and practical utility of modeling, establishing validity rigorously while identifying and ranking the impacts of specific model and data uncertainties for model and data improvements.

myf@me.berkeley.edu

5C09 DETERMINING PREDICTIVE UNCERTAINTIES AND GLOBAL SENSITIVITIES FOR LARGE PARAMETER SYSTEMS: A CASE STUDY FOR N-BUTANE OXIDATION

Éric Hébrard¹, Alison S. Tomlin², Roda Bounaceur¹, Frédérique Battin-Leclerc¹

¹CNRS, Université de Lorraine, France ²University of Leeds, United Kingdom

A global sampling approach based on low discrepancy sequences has been applied in order to propose error bars on simulations performed using a detailed kinetic model for the oxidation of *n*-butane (including 1111 reactions). A two parameter uncertainty factor has been assigned to each considered rate constant. The cases of ignition and oxidation in a

Jet-Stirred Reactor (JSR) have both been considered. For the JSR, not only the reactant mole fraction has been considered, but also that of some representative products. A temperature range from 500 to 1250 K has been studied, including the Negative Temperature Coefficient (NTC) region where the predictive error bars have been found to be the largest. It is this temperature region where the highest number of reactions play a role in contributing to the overall output errors. A global sensitivity approach based on High Dimensional Model Representations (HDMR) has then been applied in order to identify those reactions which make the largest contributions to the overall uncertainty of the simulated results. The HDMR analysis has been restricted to the most important reactions based on a non-linear screening method, using Spearman Rank Correlation Coefficients at all studied temperatures. The final global sensitivity analysis for predicted ignition delays illustrates that the key reactions are mainly included in the primary mechanism, for temperatures from 700 to 900 K, and in the C₀-C₂ reaction base at higher temperatures. Interestingly, for predicted butane mole fractions in the JSR, the key reactions are almost exclusively from the reaction base, whatever the temperature. The individual contribution of some key reactions is also discussed.

Frederique.Battin-Leclerc@univ-lorraine.fr.

5C10 UNCERTAINTY ANALYSIS OF THE KINETIC MODEL PREDICTION FOR HIGH-PRESSURE H₂/CO COMBUSTION

Xiaoyu Li¹, Xiaoqing You¹, Fujia Wu², Chung K. Law^{1,2}

¹Tsinghua University, China ²Princeton University, United States

Recent studies showed that current H₂/CO kinetic models failed to match the measured laminar flame speeds of H₂/O₂/CO₂ mixtures at high pressures. To explore the source of discrepancy, we performed uncertainty analysis using the DataCollaboration method, and obtained dataset inconsistency if these measured values were included. We then conducted experiments at similar conditions and found that our new measured values are consistent with other data in the dataset. Our uncertainty analyses suggest two approaches to improve the model prediction performance: by reducing the uncertainties of model parameters directly, and by designing and conducting experiments that can effectively constrain the model predictions.

xiaoqing.you@tsinghua.edu.cn

5C11 OPTIMIZATION OF A HYDROGEN COMBUSTION MECHANISM USING BOTH DIRECT AND INDIRECT MEASUREMENTS

T. Varga^{1,2}, T. Nagy¹, C. Olm^{1,2}, I.Gy. Zsély¹, R. Pálvölgyi¹, É. Valkó^{1,2}, G. Vincze¹, M. Cserhádi¹, H.J. Curran³, T. Turányi¹

¹Eötvös University, Hungary ²Institute of Materials and Environmental Chemistry, Hungary

³National University of Ireland, Ireland

The Kéromnès *et al.* (2013) mechanism for hydrogen combustion has been optimized using a large set of indirect experimental data, consisting of ignition measurements in shock tubes (655 datapoints in 54 datasets) and rapid compression machines (166/9), and flame velocity measurements (475/72), covering wide ranges of temperature (800 K - 2300 K), pressure (0.1 bar - 65 bar) and equivalence ratio ($\phi = 0.2 - 5.0$). According to the sensitivity analysis carried out at each experimental datapoint, 30 Arrhenius parameters and 2 third body collision efficiency parameters of 11 elementary reactions could be estimated using these experimental data. 1749 directly measured rate coefficient values in 56 datasets belonging to the 11 reaction steps were also utilized. Prior uncertainty ranges of the rate coefficients were determined from literature data. The results of mechanism optimization are a new hydrogen combustion mechanism, a set of new recommended rate parameters with their covariance matrix, and temperature-dependent posterior uncertainty ranges of the rate coefficients. The obtained optimized mechanism was tested together with 13 recent hydrogen combustion mechanisms and proved to be the best one.

turanyi@chem.elte.hu

5C12 HYDROGEN OXIDATION AT HIGH PRESSURE AND INTERMEDIATE TEMPERATURES: EXPERIMENTS AND KINETIC MODELING

Hamid Hashemi¹, Jakob M. Christensen¹, Sander Gersen², Peter Glarborg¹

¹Technical University of Denmark, Denmark ²DNV-GL Oil & Gas, The Netherlands

Hydrogen oxidation at 50 bar and temperatures of 700-900 K was investigated in a high pressure laminar flow reactor under highly diluted conditions. The experiments provided information about H₂ oxidation at pressures above the third explosion limit. The fuel-air equivalence ratio of the reactants was varied from very oxidizing to strongly reducing conditions. The results supplement high-pressure data from RCM (900-1100 K) and shock tubes (900-2200 K). At the reducing conditions ($\phi = 12$), oxidation started at 748-775 K while it was shifted to 798-823 K for stoichiometric and oxidizing conditions ($\phi = 1.03$ and 0.05). At very oxidizing conditions (O₂ atmosphere, $\phi = 0.0009$), the temperature for onset of reaction was reduced to 775-798 K. The data were interpreted in terms of a detailed chemical kinetic model. The reaction mechanism was based on recent work of Burke and coworkers, updating the rate constants for OH + OH, HO₂ + OH, and HO₂ + HO₂ based on recent determinations. The modeling predictions were in good agreement with the

measurements in the flow reactor. The predicted H_2 oxidation rate was sensitive to the rate of the $HO_2 + OH$ reaction, particularly at lean conditions, and the present data support recent values for the rate constant. In addition to modeling of the present experiments, the mechanism was evaluated against literature data, including ignition delay time measurements in rapid compression machines and shock tubes. The model was used to analyze the complex dependence of the ignition delay for H_2 on temperature and pressure.

pgl@kt.dtu.dk

5C13 THE REACTIONS SUPPORTING OR OPPOSING THE DEVELOPMENT OF EXPLOSIVE MODES:
AUTO-IGNITION OF A HOMOGENEOUS METHANE/AIR MIXTURE

Dimitris J. Diamantis¹, Dimitris Kyritsis^{2,3}, Dimitris A. Goussis⁴

¹Independent Contractor, Greece ²University of Illinois at Urbana-Champaign, United States

³Khalifa University of Science, United Arab Emirates ⁴National Technical University, Greece

The development of time scales that characterize the initiation of an auto-ignition processes is supported by specific reactions and is opposed by some others. An algorithmic tool which identifies these two sets of reactions is validated on the basis of the auto-ignition of a homogeneous stoichiometric methane/air mixture at 50 bar and 1100 K. It is shown that this process is characterized by two time scales, the fastest of which relates to the generation of the required for ignition radical pool and the temperature increase. This time scale associates mainly to carbon chemistry, except the very last period of its presence where it relates to hydrogen/oxygen-chemistry. The analysis allows for the quantitative assessment of several chemical phenomena that have been associated with the abnormal long ignition delay of methane, such as the formation of C_2H_6 and the relative importance of the formation of CH_2O and CH_3O as means of consumption of CH_3 radicals. The identification of the reactions supporting or opposing the initiation of the auto-ignition is most useful when it is desired to control the ignition process.

dagoussi@mail.ntua.gr

5D01 IMPROVING ION CURRENT OF SPARKPLUG ION SENSORS IN HCCI COMBUSTION USING SODIUM, POTASSIUM, AND CESIUM ACETATES: EXPERIMENTAL AND NUMERICAL MODELING

R.H. Butt, Y. Chen, J.H. Mack, S. Saxena, R.W. Dibble, J.-Y. Chen, University of California, Berkeley, United States

Measuring the ion current with a sparkplug ion sensor in a Homogeneous Charge Compression ignition (HCCI) engine can be used to investigate the ion chemistry in the cylinders during combustion. HCCI engines are similar to a well-stirred reactor and operate at lean equivalence ratios (ϕ). Under these conditions, the ion current becomes increasingly indistinguishable from background noise. This paper investigates various fuel additive effects on ion signal at low ϕ 's, determines side effects of metal acetate addition, and validates a numerical model. The fuel additives added to ethanol were sodium acetate (NaOAc), potassium acetate (KOAc), and Cesium Acetate (CsOAc). Concentration levels ranging from 0.5-4.9 mmol/L of metal acetate-in-ethanol are investigated over ϕ 's 0.11, 0.22, 0.28, and 0.32. The engine operated under naturally aspirated conditions and maintained a constant timing of 2.5 degrees After Top-Dead-Center (ATDC) at the Crank Angle Degree (CAD) where 50% of the heat release occurs (CA50). CsOAc consistently produced the strongest ion signals, followed by KOAc and NaOAc, which NaOAc had the weakest effect on ion signal. No distinguishable ion signals were measured at $\phi = 0.11$, but significant ion signal improvements occurred at $\phi = 0.22$ using the fuel additives. However, the addition of the metal acetates decreased Heat Release Rates (HRR) and peak cylinder pressures. Although CsOAc produced the largest signal improvements, it also had the largest decrease in HRR and peak cylinder pressure. Additionally, a single-zone engine model that simulates the chemical kinetics and ion chemistry of KOAc addition is presented and validated with the experimental results.

rhbutt@berkeley.edu

5D02 INVESTIGATION OF *ISO*-OCTANE COMBUSTION IN A HOMOGENEOUS CHARGE COMPRESSION IGNITION ENGINE SEEDED BY OZONE, NITRIC OXIDE AND NITROGEN DIOXIDE

J-B. Masurier^{1,2}, F. Foucher¹, G. Dayma², P. Dagaut²

¹Univisity Orléans, France ²ICARE, France

The Homogeneous Charge Compression Ignition (HCCI) engine is well known as an alternative engine which could replace conventional engines (Spark Ignition (SI) and Combustion Ignition (CI) engines) in order to meet pollutant requirements and reduce fuel consumption. However, controlling this kind of combustion remains difficult and represents a real challenge. The present investigation focussed on the use of different oxidizing chemical species (ozone, nitric oxide and nitrogen dioxide) which can modify the kinetic mechanism governing HCCI combustion. Experiments were conducted on a single cylinder HCCI engine fuelled with *iso*-octane, for constant engine parameters and for oxidizing species concentrations varying from 0 up to 100 ppm. These experimental results are coupled with kinetic analyses in a homogeneous constant volume reactor performed with a detailed kinetic mechanism. The effects of ozone, nitric oxide and nitrogen dioxide were initially studied and compared when they separately seed the intake of the engine. Results showed that all the molecules improve HCCI *iso*-octane combustion. The highest effect on CA50 phasing was observed for ozone

while the lowest was for nitrogen dioxide. These results were confirmed and explained by a kinetic interpretation. HCCI experiments were then carried out with ozone and nitric oxide injected together in the intake of the engine. Experimental results show a combustion enhancement when these two molecules are present but a delay in CA50 phasing was observed for low ozone concentrations and a constant nitric oxide concentration until the ozone concentration becomes higher. A kinetic interpretation, through two-step computations, showed that there is a strong oxidizing reaction between nitric oxide and ozone, yielding nitrogen dioxide. Therefore, the presence of nitrogen dioxide can explain the CA50 delay observed due to its low effect among all the oxidizing chemical species studied.

jean-baptiste.masurier@cnrs-orléans.fr

5D03 IN-CYLINDER SOOT PRECURSOR GROWTH IN A LOW-TEMPERATURE COMBUSTION DIESEL ENGINE: LASER-INDUCED FLUORESCENCE OF POLYCYCLIC AROMATIC HYDROCARBONS

C.A.J. Leermakers¹, M.P.B. Musculus²

¹Eindhoven University of Technology, Netherlands ²Sandia National Laboratories, United States

The growth of Poly-cyclic Aromatic Hydrocarbon (PAH) soot precursors are observed using a two-laser technique combining Laser-Induced Fluorescence (LIF) of PAH with Laser-Induced Incandescence (LII) of soot in a diesel engine under Low-Temperature Combustion (LTC) conditions. The broad mixture distributions and slowed chemical kinetics of LTC "stretch out" soot-formation processes in both space and time, thereby facilitating their study. Imaging PAH-LIF from pulsed-laser excitation at three discrete wavelengths (266, 532, and 633 nm) reveals the temporal growth of PAH molecules, while soot-LII from a 1064-nm pulsed laser indicates inception to soot. The distribution of PAH-LIF also grows spatially within the combustion chamber before soot-LII is first detected. The PAH-LIF signals have broad spectra, much like LII, but typically with a color temperature that is far too hot for laser-heated soot. Quantitative natural-emission spectroscopy also shows a broad emission spectrum, presumably from PAH chemiluminescence, temporally coinciding with of the PAH-LIF.

mpmuscu@sandia.gov

5D04 TWO-TRACER LIF IMAGING OF PREFERENTIAL EVAPORATION OF MULTI-COMPONENT GASOLINE FUEL SPRAYS UNDER ENGINE CONDITIONS

L.M. Itani^{1,2,3}, G. Bruneaux^{1,2}, A. Di Lella³, C. Schulz²

¹IFPEN, France ²University of Duisburg-Essen, Germany ³Ecole Centrale Paris, France

A Laser-Induced Fluorescence (LIF) technique capable of assessing the effects of preferential evaporation of multi-component fuels was developed based on the simultaneous detection of two aromatic fluorescence tracers with complementary evaporation characteristics. Preferential evaporation is determined from the LIF-signal intensity ratio measured within two distinct spectral bands. A scheme to determine the measurement accuracy and precision was established by characterizing the collection setup through determining the ratio of LIF intensities collected within two identical spectral bands. Measurements were performed in a high-pressure, high-temperature vessel equipped with a hollow-cone injector. Experimental conditions were chosen that are representative for engine environments and favor preferential evaporation. The analysis of the preferential evaporation was based on the comparison of instantaneous and mean images of LIF ratios obtained at various temperatures. Inhomogeneous distributions of the fuel volatility classes as a consequence of preferential evaporation were observed and two-dimensionally imaged at ambient temperatures up to 550 K.

gilles.bruneaux@ifpen.fr

5D05 DETERMINATION OF SOOT ONSET AND BACKGROUND PARTICULATE LEVELS IN A SPARK-IGNITION ENGINE

Mitchell D. Hageman, Stephen S. Sakai, David A. Rothamer, University of Wisconsin-Madison, United States

An experimental method utilizing premixing of the air and fuel well upstream of the intake port in conjunction with careful exhaust sample conditioning was developed to study the onset of sooting in spark-ignition engines. By fully premixing the air-fuel mixture upstream of the intake port, it was possible to create a fully Premixed and Pre-Vaporized (PMPV) fuel-air charge and to eliminate liquid fuel in-cylinder. A baseline Particle Size Distribution (PSD) was demonstrated using multiple fuels including gasoline, methanol, and E100. The baseline particulate level was shown to be insensitive to fuel composition and equivalence ratio below a critical value of the equivalence ratio or C/O ratio, indicating that the baseline PSD is not the result of fuel carbon, but instead is the result of other particulate sources, e.g., engine oil and engine wear particles. With the baseline particle levels established the PMPV technique was applied to determine the local enrichment needed to generate significant soot above the baseline particle size distribution. The critical equivalence ratio for onset of sooting under PMPV operation was determined to be between 1.345 and 1.349 ($C/O_c = 0.461-0.462$). The results, interpreted based on the literature on laboratory premixed flames, indicate that soot first forms by the walls at the end of combustion or slightly after during the expansion stroke. The results give for the first time an indication of the level

of local-enrichment that would be expected to cause a significant increase in soot production in spark-ignition direct-injection engines operating on gasoline at moderate engine load and speed conditions.

rothamer@wisc.edu

5D06 STUDY ON THE PHASE RELATION BETWEEN ION CURRENT SIGNAL AND COMBUSTION PHASE IN A HCCI COMBUSTION ENGINE

Guangyu Dong¹, Yulin Chen², Zhijun Wu¹, Liguang Li¹, Robert Dibble²

¹Tongji University, China ²University of California-Berkeley, United States

Ion sensing technology has been identified as a promising approach to achieve cycle resolved combustion phasing in HCCI engines, however, the essential mechanism governing the phase relationship between ion current signal and combustion phasing is not fully revealed yet. This paper investigates the fundamental processes affecting the relationship between ion signal and combustion phasing using a Computational Fluid Dynamics (CFD) model of a HCCI engine. Numerical analysis of the flame ionization process and experimental results indicate that the phase of the ion current signal is mainly affected by the ion formation and recombination rate of H_3O^+ ions, but the combustion phase is strongly affected by both mixture specific heat and chemical kinetics. Given the similar combustion boundary conditions, the fuels like ethanol and gasoline, have similar ion producing capability. However, the specific heat of ethanol-air mixtures varies more rapidly than gasoline-air mixtures as the equivalence ratio is changed. As a result, a more remarkable phase difference between the ion current and combustion phasing can be found in an ethanol-fueled HCCI engine as the mixture is made leaner. For the fuels with different octane number, such as gasoline and diesel, their combustion boundary conditions are different in HCCI engines, and they have very different ion production capability as well. Because of the low intake temperature and high compression ratio, a very low ion production rate can be found in the diesel flame, with the ion recombination rate being even lower. Thus, the crank angle position with maximum ion concentration appears much later in diesel engine comparing with it in a gasoline engine. As a result, the phase difference between the ion signal and combustion phase is much longer in the diesel flame than the flames from high octane fuels.

G.Dong@brighton.ac.uk

5D07 TURBULENCE-CHEMISTRY INTERACTIONS IN A HEAVY-DUTY COMPRESSION-IGNITION ENGINE

V. Raj Mohan, D.C. Haworth, The Pennsylvania State University, United States

The influences of unresolved turbulent fluctuations in composition and temperature (Turbulence-Chemistry Interactions - TCI) on heat release, flame structure, and emissions are explored in unsteady Reynolds-averaged simulations for a heavy-duty diesel engine at four operating conditions. TCI are isolated and quantified by comparing results from a transported Probability Density Function (PDF) method with those from a model that neglects the influence of fluctuations on local mean reaction rates (a Well-Stirred-Reactor - WSR - model). The simulations feature standard fuel-spray and turbulence models, skeletal-level gas-phase chemistry, and a semi-empirical two-equation soot model. Computed pressure and heat-release traces, turbulent flame structure, and emissions from the WSR and PDF models show marked differences, with the PDF-model results being in closer agreement with experiment. The soot results are especially striking. Computed soot levels from the PDF model are within a factor of five of the measured engine-out particulate matter, and computed soot levels from the WSR and PDF models differ by up to several orders of magnitude. The results show that TCI are important in compression-ignition engines, and that accurate accounting for turbulent fluctuations is at least as important as accurate kinetic rate parameters in the gas-phase chemistry and soot models.

dch12@psu.edu

5D08 LES PREDICTION AND ANALYSIS OF KNOCKING COMBUSTION IN A SPARK IGNITION ENGINE

A. Robert^{1,2}, S. Richard¹, O. Colin¹, L. Martinez¹, L. de Francqueville¹

¹IFP Energies nouvelles, France ²PSA Peugeot Citroën, France

Highly boosted Spark Ignition (SI) engines are more and more attractive for car manufacturers in terms of efficiency and CO₂ emissions. However, thermodynamic conditions encountered in these engines promote the occurrence of abnormal combustions like knock or super-knock, which are experimentally difficult to analyse due to the risks of engine damages. The Reynolds Averaged Navier-Stokes (RANS) method mainly used in industry for piston engines is not the most appropriate as knock does not always affect the mean cycle captured by RANS. Using an accurate LES compressible code and improved versions of ECFM-LES (Extended Coherent Flame Model) and TKI (Tabulated Kinetics of Ignition) models allowing a full uncoupling of flame propagation and auto-ignition reaction rates, this work demonstrates for the first time that LES is able to describe quantitatively knocking combustion in a realistic downsized SI engine configuration. Contrary to previous studies, a quantified knock analysis is conducted based on a specific post-processing of both numerical and experimental data. LES is able to predict the in-cylinder pressure variability, the knock occurrence frequency and the mean knock onset crank angle for several spark timings. A 3D analysis also demonstrates that knock occurs at random locations, mainly at the exhaust valves side. Knock intensity is found proportional to the fresh gases mass

burned by auto-ignition at low knock intensities, while an exponential increase at the highest intensities suggests the influence of additional factors like the knock location in the cylinder or complex behaviour of knocking combustion.

olivier.colin@ifpen.fr

5D09 COMBINED EFFECTS OF FLOW/SPRAY INTERACTIONS AND EGR ON COMBUSTION VARIABILITY FOR A STRATIFIED DISI ENGINE

Wei Zeng¹, Magnus Sjöberg¹, David Reuss^{1,2}

¹Sandia National Laboratories, United States ²University of Michigan, United States

This study investigates combustion variability for a stratified-charge Direct-Injection Spark-Ignited (DISI) engine, operated with near-TDC injection of E70 fuel and a spark timing that occurs during the early part of the fuel injection. Using EGR, low engine-out NO_x can be achieved, but at the expense of increased combustion variability at higher engine speeds. Initial motored tests at different speeds reveal that the in-cylinder gas flow becomes sufficiently strong at 2000 rpm to cause significant cycle-to-cycle variations of the spray penetration. Hence, the fired tests focus on operation at 2000 rpm with N₂ dilution ([O₂] = 19% and 21%) to simulate EGR. In-cylinder flow, spray, and early-flame measurements are correlated to reveal their effect on the combustion variability.

Results reveal two types of flow/spray-interactions that predict the likelihood of a partial burn. 1) Proper flow direction before injection with a more collapsed spray leads to high kinetic energy of the flow during injection, thus generating a rapid early burn, which ensures complete combustion, regardless of the EGR level. 2) Improper flow direction and less collapsed spray generate low flow energy during the early phase of combustion. For this second type of flow/spray-interaction, application of EGR results in a partial-burn frequency of 30%, whereas without EGR, early combustion is shown to be insensitive to flow variations. Flame-probability maps illustrate that the partial-burn cycles for operation with EGR have a weak flame development in that the flame does not develop uniformly and reliably from the spark plug. Without EGR, the flame development is more repeatable regardless of the type of flow/spray-interaction, at the expense of higher NO_x emissions.

wzeng@sandia.gov

5D10 INFLUENCE OF FLOW AND IGNITION FLUCTUATIONS ON CYCLE-TO-CYCLE VARIATIONS IN EARLY FLAME KERNEL GROWTH

Cecile Pera¹, Vincent Knop¹, Julien Reveillon²

¹IFP Energies Nouvelles, France ²CORIA, France

Engine Cycle-to-Cycle Variations (CCVs) constitute a restriction for numerous concepts aimed at improving fuel consumption in spark-ignited engines. In consequence, engine CCV modeling has become an active research topic. Nevertheless, few fundamental studies have thus far examined the individual influences of the key parameters. In the present study, we performed Direct Numerical Simulations (DNSs) of early flame kernel growth with semi-detailed chemistry solving to identify the controlling parameters of heat release fluctuations that are relevant to engine CCVs. Our objective was to assess how certain turbulence and flame parameters - namely turbulent flow motion pattern, turbulence intensity, integral length scale, mixture strength and initial kernel size - influence combustion variability. Two extreme mixture conditions were selected (stable operation at stoichiometry and unstable operation at the lean flammability limit), and computation conditions were derived from actual low load engine operating points. Results provide a classification of the key parameters, indicating initial kernel size and turbulent flow motion pattern as the main contributors. Additionally, DNSs highlighted the crucial role of mixture strength in the occurrence of local flame quenching and in the related amplification of heat release fluctuations.

cecile.pera@ifpen.fr

5D11 SIMULTANEOUS FORMALDEHYDE PLIF AND HIGH-SPEED SCHLIEREN IMAGING FOR IGNITION VISUALIZATION IN HIGH-PRESSURE SPRAY FLAMES

S.A. Skeen, J. Manin, L.M. Pickett, Sandia National Laboratories, United States

The low- and high-temperature auto-ignition events in a high-pressure (60 bar) spray of *n*-dodecane have been observed simultaneously by high-speed Schlieren imaging and formaldehyde (CH₂O) Planar Laser-Induced Fluorescence (PLIF). We used high-speed Schlieren imaging at 150 kHz to visualize the temporal progression of the fuel vapor penetration as well as the low- and high-temperature ignition events, while formaldehyde fluorescence was induced by a pulsed (10 ns), 355-nm planar laser sheet at a select time during the same injection. Fluorescence from Polycyclic Aromatic Hydrocarbons (PAH) was also observed and was distinguished from formaldehyde PLIF both temporally and spatially. A characteristic feature previously recorded in Schlieren images of similar flames, in which refractive index gradients significantly diminish, has been confirmed to be coincident with large formaldehyde fluorescence signal during low-temperature ignition. Formaldehyde persists upstream of the lift-off length and forms rapidly near the injector following the end of injection. The consumption of formaldehyde coincides with the position and timing of high-

temperature ignition and low-density zones that are clearly evident in the Schlieren imaging. After the end of injection, the formaldehyde that formed upstream of the lift-off length is consumed as a high-temperature ignition front propagates back toward the injector tip. Information obtained from the simultaneous application of these two diagnostics enables more effective use of high-speed Schlieren imaging as a tool to investigate transient events in high-pressure spray combustion.

sskeen@sandia.gov

5D12 SPRAY-INDUCED TEMPERATURE STRATIFICATION DYNAMICS IN A GASOLINE DIRECT-INJECTION ENGINE

Brian Peterson¹, Elias Baum¹, Benjamin Böhm¹, Volker Sick², Andreas Dreizler¹

¹Technische Universität Darmstadt, Germany ²The University of Michigan, United States

Simultaneous applications of high-speed toluene-LIF thermometry and PIV at kHz rates were utilized to investigate the evolution of gas temperature stratification imposed from direct-injection of liquid fuel within a motored SIDI engine. Temperature imaging was based on the two-color detection method that measures the LIF signal ratio from two separated wavelength ranges to enable LIF temperature imaging within inhomogeneously mixed systems. It was observed that cold gases associated with evaporative cooling exist within the regions of dense liquid fuel droplet clouds. As droplets disperse, the cold-gas regions expand and relative temperatures as low as -50K exist. Average temperature gradients between cold- and bulk-gases are up to 30 K/mm and gradients persist but drop in magnitude throughout compression as cold- and bulk-gases mix. Relative temperature PDFs at CAD resolution show the nature of temperature stratification during compression. Temperature stratification is greatest as the fuel disperses within the FOV producing large areas of cold-gases with relative temperatures as low as -50K. Individual temperature images and 2D PDFs of identified cold-gas regions reveal that local regions of cold-gas imposed from evaporative cooling can last up to 30 CAD after fuel injection for the given operating conditions. The time-resolved imaging study show the mechanics of localized evaporative cooling and bulk-flow motion-driven mixing that over time reduces temperature gradients but does not completely homogenize the temperature fields.

peterson@csi.tu-darmstadt.de

5D13 SPRAY-COMBUSTION INTERACTION MECHANISM OF MULTIPLE-INJECTION UNDER DIESEL ENGINE CONDITION

Khanh Cung¹, Abdul Moiz¹, Jaclyn Johnson¹, Seong-Young Lee¹, Chol-Bum Kweon², Alessandro Montanaro³

¹Michigan Tech University, United States ²U.S. Army Research Laboratory, United States ³CNR, Italy

Multiple-injection has shown significant benefits in the reduction of combustion emissions and soot formation. However, there is need to understand the secondary flow-induced air-fuel mixture formation and subsequent combustion mechanism under multiple-injection. An experiment was performed by changing the dwell time between the pilot and main injections under the conditions of 23 kg/m³ ambient density with 0% O₂ (non-combusting) and 15% O₂ (combusting) ambient conditions, at injection pressure of 120 MPa. A hybrid shadowgraph and Mie scattering imaging technique in a nearly simultaneous mode along the same line of sight was used to visualize the spray and flame luminosity. Pilot-main spray flame properties including ignition delay, ignition location, and lift-off length were characterized from experimental images. CFD simulation of pilot-main spray combustion has been performed under the same experimental conditions to provide additional insights on combustion process. The air-fuel mixing field, and ignition process followed by main injection flame structure is significantly altered at different dwells. Spray to flame interaction mechanism model has been established for the development of optimal multiple-injection scheme for low soot formation and emission.

sylee@mtu.edu

5E01 SURFACE REACTIVITY OF HOMOGENOUS POLYCYCLIC AROMATIC HYDROCARBON NANO-CLUSTERS

Dongping Chen, Jethro Akroyd, Sebastian Mosbach, Markus Kraft, University of Cambridge, United Kingdom

A scheme to characterise surface atoms is proposed to probe molecular representations of homogenous pyrene and coronene clusters. The concept of solvent-excluded surface, which is widely used for proteins, forms the basis of this scheme. The scheme is used to provide insights into the surface reactivity in terms of the surface availability of active atoms and sites for different gaseous species. It was found that the surface availability of active sites varies with gaseous species, system temperature and particle size. The number of active sites available for a small gaseous species is always greater than that for a large species. Surface exposure increases with an increase in temperature and an obvious enhancement exists when transforming to liquid-like configurations. The surface availability decreases with increasing particle size following a linear relation with reciprocal size. The upper bound of parameter α , which is used in the soot literature to empirically quantify surface reactivity, was further estimated from the surface availability of hydrogen atom in the context of HACA mechanism and was well below 0.1 for reactions between mature soot particles and acetylene. By exploring one particular pocket on the surface of a coronene cluster with 100 molecules, it was noted that it is feasible for both oxygen and acetylene molecules to penetrate inside the cluster. This fact indicates that the surface reactions occurring

on particles are not limited to the actual boundary of the configuration but also certain regions beyond the boundary via surface pockets.

mk306@cam.ac.uk

5E02 TOWARDS A PREDICTIVE MODEL FOR POLYCYCLIC AROMATIC HYDROCARBON DIMERIZATION PROPENSITY

Jeffrey S. Lowe, Jason Y.W. Lai, Paolo Elvati, Angela Violi, University of Michigan, United States

Soot particles are an important pollutant formed as the result of incomplete combustion. Particle nucleation significantly impacts the formation and morphology of soot particles, yet remains a key knowledge gap. To elucidate the process of nucleation, we have investigated the thermodynamic stability of dimers of polycyclic aromatic hydrocarbons, towards developing a more comprehensive model for PAH clustering behavior. Using a computational methodology based on molecular dynamics and well-tempered Metadynamics, we quantified the impact of morphological parameters on homo-molecular dimerization, as well as the relative size of monomers on the stability of hetero-molecular dimers. The results illustrated the substantial impact of PAH mass and geometry on the stability of homo-molecular and hetero-molecular dimers at flame temperatures. In particular, dimer stability was found to depend most strongly on monomer mass, followed by open surface area. Additionally, hetero-molecular dimer stability was found to be largely determined by the size of the smallest monomer. Identifying relationships between PAH morphology and thermodynamic stability is a significant step towards a more comprehensive understanding physical interactions between PAH. Altogether, this work presents a framework for elucidating the clustering behavior of arbitrary PAHs and will greatly impact understanding and modeling of particle nucleation and growth.

avioli@umich.edu

5E03 REACTION PATHWAYS FOR THE GROWTH OF POLYCYCLIC AROMATIC HYDROCARBONS DURING THE SUPERCRITICAL PYROLYSIS OF *N*-DECANE, AS DETERMINED FROM DOPING EXPERIMENTS WITH 1- AND 2-METHYLNAPHTHALENE

Subramanian V. Kalpathy, Nimesh B. Poddar, Sean P. Bagley, Mary J. Wornat, Louisiana State University, United States

In order to investigate growth mechanisms of Polycyclic Aromatic Hydrocarbons (PAH) that can lead to solids formation in the pre-combustion environments of future high-speed aircraft, we have performed supercritical pyrolysis experiments with the model alkane fuel *n*-decane (critical temperature, 344.5°C; critical pressure, 20.7 atm), to which 2-methylnaphthalene and 1-methylnaphthalene, two two-ring products of *n*-decane pyrolysis, have each been added as a dopant (each dopant concentration, 8.8 mg/g *n*-decane). The experiments are conducted in an isothermal, silica-lined stainless-steel flow reactor at 570°C, 94.6 atm, and 133 sec, conditions of incipient solids formation. Analyses of the PAH products by high-pressure liquid chromatography with diode-array ultraviolet-visible absorbance and mass-spectrometric detection reveal vast differences in the growth behavior of the two dopants. In the case of 2-methylnaphthalene, growth is virtually limited to the two- and three-ring PAH that result from 2-naphthylmethyl's reactions with methyl, ethylene, propene, and 1-butene — all abundant in the *n*-decane pyrolysis environment. In the case of 1-methylnaphthalene, the methyl group's attachment to a carbon that is just-adjacent to a "valley" carbon of the naphthalene structure permits 1-naphthylmethyl's reaction with ethylene to form phenalene, an unstable C₁₃H₁₀ PAH that readily loses hydrogen to form the resonance-stabilized phenalenyl radical. This radical sets in motion a sequence for PAH growth that involves reactions of the C₂-C₄ 1-alkenes with both phenalenyl-type radicals and arylmethyl radicals (whose methyl group is attached to a carbon that is just-adjacent to a valley carbon) — producing unsubstituted PAH and methylated PAH of successively higher ring number. As a consequence of these reactions, even though the dopant 1-methylnaphthalene undergoes only 4.5 % conversion, it selectively increases (by up to a factor of four) the yields of many of *n*-decane's favored four- to eight-ring PAH products — demonstrating the prevalence of the arylmethyl/alkene/phenalenyl reaction mechanism in the supercritical *n*-decane pyrolysis environment.

mjwornat@lsu.edu

5E04 THE IMPORTANCE OF REVERSIBILITY IN MODELING SOOT NUCLEATION AND CONDENSATION PROCESSES

N.A. Eaves¹, M.J. Thomson¹, S.B. Dworkin²

¹University of Toronto, Canada ²Ryerson University, Canada

Given the upcoming EURO 6 regulations, which include limits on particle number density (and hence size) for soot emissions from land vehicles, soot models must be capable of accurately predicting soot particle sizes. Previous modeling work has demonstrated the importance of the relative strengths of nucleation and condensation in predicting soot primary particle size; however, fundamental models still rely on tunable constants for modeling both processes, which limits predictive capability. Recent investigations into nucleation and condensation processes suggest that both processes are not thermodynamically favored to occur from 5-ringed PAHs, yet 5-ringed PAHs have been experimentally observed in

abundance within nascent soot particles. This contradiction leads to the understanding that nucleation and condensation from 5-ringed PAHs is plausible, although they are likely highly reversible processes.

A fundamental reversible model for nucleation and condensation is developed through the use of statistical mechanics and the results from several recent works. The inclusion of reversibility in the nucleation and condensation subroutines enables the model to accurately reproduce all relevant soot morphological parameters determined experimentally for the atmospheric pressure, laminar, ethylene-air Santoro flame. The developed reversible model represents an advancement in fundamental soot formation modeling by replacing tunable constants with fundamental physics.

thomson@mie.utoronto.ca

5E05 DAMKÖHLER NUMBER EFFECTS ON SOOT FORMATION AND GROWTH IN TURBULENT NONPREMIXED FLAMES

Antonio Attili¹, Fabrizio Bisetti¹, Michael E. Mueller², Heinz Pitsch³

¹King Abdullah University of Science and Technology, Saudi Arabia ²Princeton University, United States

³Aachen University, Germany

The effect of Damköhler number on turbulent nonpremixed sooting flames is investigated via large scale direct numerical simulation in three-dimensional *n*-heptane/air jet flames at a jet Reynolds number of 15000 and at three different Damköhler numbers. A reduced chemical mechanism, which includes the soot precursor naphthalene, and a high-order method of moments are employed. At the highest Damköhler number, local extinction is negligible, while flame holes are observed in the two lowest Damköhler number cases. Compared to temperature and other species controlled by fuel oxidation chemistry, naphthalene is found to be affected more significantly by the Damköhler number. Consequently, the overall soot mass fraction decreases by more than one order of magnitude for a fourfold decrease of the Damköhler number. On the contrary, the overall number density of soot particles is approximately the same, but its distribution in mixture fraction space is different in the three cases. The total soot mass growth rate is found to be proportional to the Damköhler number. In the two lowest Da number cases, soot leakage across the flame is observed. Leveraging Lagrangian statistics, it is concluded that soot leakage is due to patches of soot that cross the stoichiometric surface through flame holes. These results show the leading order effects of turbulent mixing in controlling the dynamics of soot in turbulent flames.

antonio.attili@kaust.edu.sa

5E06 SOOT PRECURSOR FORMATION AND LIMITATIONS OF THE STABILOMER GRID

K.O. Johansson¹, J.Y.W. Lai², S.A. Skeen¹, D.M. Popolan-Vaida³, K.R. Wilson³, N. Hansen¹, A. Violi², H.A. Michelsen¹

¹Sandia National Laboratories, United States ²University of Michigan, United States

³Lawrence Berkeley National Laboratory, United States

We have performed flame-sampling aerosol mass spectrometry with vacuum-ultraviolet photoionization of an Ar-diluted C₂H₂/O₂ flame using a near-atmospheric pressure (700 Torr) opposed-flow burner. We recorded aerosol mass spectra at different distances from the fuel outlet for fixed ionization energies and in a fixed position while tuning the photoionization energy. Recorded mass spectra contain a wide variety of peaks, highlighting the importance of small building blocks and showing a variety of chemical species that extends beyond the traditional classification of PAH species based on thermodynamic stability. In addition, we performed stochastic simulations of PAH growth in the flame in order to elucidate the chemical composition of species associated with peaks in the measured mass spectra. These simulations were conducted using a stochastic nanoparticle simulator (SNAPS). Synthesis of experimental and simulated results showed that peaks in the observed mass spectra generally consisted of a mixture of PAH isomers. At $m/z = 154$ and 202 , for example, experiments and simulations suggested that additional isomers than biphenyl and pyrene are important. Furthermore, the results highlight the importance of odd-carbon numbered species and complex growth paths. It is clear from the experimental results that species of higher masses can build up concentration ahead of species of lower masses. Our experimental results show, for example, that the peak at $m/z = 278$ appears ahead of the peak at $m/z = 202$.

hamiche@sandia.gov

5E07 INVESTIGATION OF SOOT FORMATION IN PRESSURIZED SWIRL FLAMES BY LASER MEASUREMENTS OF TEMPERATURE, FLAME STRUCTURES AND SOOT CONCENTRATIONS

Klaus Peter Geigle, Markus Köhler, William O'Loughlin, Wolfgang Meier, Institut für Verbrennungstechnik, Germany

Soot formation and oxidation were investigated in swirl flames operated with ethylene/air at elevated pressure in a gas turbine model combustor with optical access. Coherent anti-Stokes Raman scattering was used for temperature measurements, laser-induced incandescence for soot concentration and laser-induced fluorescence for the determination of OH radical distributions. A major focus of the experiments was the investigation of the influence of the injection of secondary oxidation air into the fuel-rich product gas of the primary combustion zone. Soot is mainly present in tiny filament-like regions left without OH signal. In the 3 bar flame with oxidation air injection these are found in a region

separating the primary combustion zone fed by combustion air and ethylene, and the secondary combustion induced by oxidation air and Unburned Hydrocarbons (UHC) that are transported into the inner recirculation zone. The different behavior of flames with and without oxidation air is most pronounced in the inner recirculation zone that is strongly influenced by the oxidation air admixture. This is reflected by changed OH distributions, mean temperatures and shape of the temperature pdfs resulting in significantly different soot distributions. The combined temperature statistics and correlated OH and soot distributions acquired at 3 and 5 bar are well suited to support the understanding of soot formation and oxidation and are expected to be valuable input to soot model validation.

klauspeter.geigle@dlr.de

5E08 SIMULTANEOUS PLANAR MEASUREMENTS OF TEMPERATURE AND SOOT VOLUME FRACTION IN A TURBULENT NON-PREMIXED JET FLAME

S.M. Mahmoud, G.J. Nathan, P.R. Medwell, B.B. Dally, Z.T. Alwahabi, The University of Adelaide, Australia

New measurements are reported of the soot-temperature interaction in a turbulent non-premixed ethylene-hydrogen-nitrogen attached jet flame with an exit Reynolds number of 15,000. Spatially resolved, two-dimensional temperature and soot volume fractions were measured simultaneously using Non-linear excitation regime Two-Line Atomic Fluorescence (NTLAF) and Laser-Induced Incandescence (LII) techniques, respectively. The soot-temperature correlation is presented and analyzed through representative images of single-shot simultaneous temperature and soot volume fraction at various heights, as well as through joint Probability Density Functions (PDFs) of Soot Volume Fraction (SVF) and temperature. A strong influence of temperature on SVF is found, which is consistent with current understanding of their inter-dependence. Axial and radial plots of mean SVF categorized into temperature bands of 300K are also reported. These reveal that, while the mean SVF is a function of both temperature and axial distance, the joint pdf depends only weakly on radial distance. The study highlights the value of the simultaneous measurements for understanding soot behavior in a turbulent environment and for model development and validation.

saleh.mahmoud@adelaide.edu.au

5E09 SIMULTANEOUS INSTANTANEOUS MEASUREMENTS OF SOOT VOLUME FRACTION, PRIMARY PARTICLE DIAMETER, AND AGGREGATE SIZE IN TURBULENT BUOYANT DIFFUSION FLAMES

Brian M. Crosland¹, Kevin A. Thomson², Matthew R. Johnson¹

¹Carleton University, Canada ²National Research Council of Canada, Canada

Understanding the mechanisms of soot formation, growth, oxidation, and emission is important for diverse reasons including better combustor design, quantifying soot's contribution to climate change, and mitigating air quality concerns. Instantaneous soot measurement in turbulent flames is difficult, and has mostly been restricted to high-momentum jet flames and pool fires. The current work partially fills this gap by presenting simultaneous measurements of soot volume fraction (f_v), effective aggregate radius of gyration (R_{gml}), and primary particle diameter (d_p) in combination with separately-acquired measurements of mean gas velocity, within a range of turbulent buoyant non-premixed jet flames burning a fuel mixture representative of associated gas flares in the upstream oil and gas industry. Fifteen cases comprising six possible nozzle exit velocities and four nozzle diameters were studied. Soot intermittency and histograms of f_v and d_p support the suggestion that reduced f_v near the flame tip results from increased soot intermittency rather than reduced local f_v . Furthermore, the data indicate that oxidation of mature soot structures occurs rapidly and completely, and is insensitive to the local f_v . For most conditions studied, centerline f_v shows self-similar behavior when scaled by measured flame height in the axial direction. The more buoyancy-dominated flames show a marked increase in peak f_v that occurs lower in flame-length-normalized coordinates, while the more momentum-dominated flames show a decreased peak f_v that occurs higher in flame-length-normalized coordinates. Low in the flame, soot is only present in an annular region where f_v , d_p , and R_{gml} all grow. Once soot is present on the centerline, d_p growth slows and d_p is relatively constant at all radial locations and all conditions higher in the flame. Aggregate size continues to grow steadily with increased flame height and correlates well with residence time when adjusted to account for differing flow fields close to the burner outlet.

Matthew.Johnson@Carleton.ca

5E10 COMPARISON OF ONE-DIMENSIONAL TURBULENCE AND DIRECT NUMERICAL SIMULATIONS OF SOOT FORMATION AND TRANSPORT IN A NONPREMIXED ETHYLENE JET FLAME

David O. Lignell, Garrison C. Fredline, Adam D. Lewis, Brigham Young University, United States

Accurate models of soot formation in turbulent flames are important for correctly predicting and simulating flames and fires. Modeling soot formation and transport is challenging due to the complex chemical formation processes, and differential diffusion of soot relative to a flame. Direct Numerical Simulations (DNS) have highlighted the importance of such transport on soot concentrations, however DNS is computationally expensive. The One-Dimensional Turbulence (ODT) model is able to resolve a full range of length and timescales and solves the evolution of diffusive and reactive scalars in the natural physical coordinate. We present results of soot formation in ODT and compare the model to simulation results from DNS in a temporally-evolving planar ethylene jet flame where the same transport, thermodynamic, and kinetic

models are applied. Good agreement is found for the jet evolution in terms of the mixture fraction profiles. Conditional soot statistics (mean and fluctuations) are presented, along with joint soot-mixture fraction PDFs that illustrate the location and motion of soot in the mixture fraction coordinate. Good qualitative agreement between the models is found and the soot behavior is similar. While the ODT cannot capture three-dimensional flow structures, the ODT simulations are less computationally expensive than the DNS suggesting its use in conjunction with DNS for parametric study, model validation, and investigation at parameter ranges not currently available to DNS.

davidlignell@byu.edu

5E11 TIME-RESOLVED SPATIAL PATTERNS AND INTERACTIONS OF SOOT, PAH AND OH IN A TURBULENT DIFFUSION FLAME

B. Franzelli^{1,2}, P. Scoufflaire^{1,2}, S. Candel^{1,2}

¹Ecole Centrale Paris, France ²CNRS, France

Soot control raises important fundamental issues and industrial challenges, which require a comprehensive understanding of processes governing its formation, interactions and destruction in turbulent flames. A physical insight of the soot space-time evolution in a turbulent diffusion flame is reported in this article obtained by combining three simultaneous high sampling rate imaging diagnostics operating at a frame rate of 10 kHz: light scattering from soot particles, Planar Laser Induced Fluorescence (PLIF) of the OH radical (a marker of the flame region) and planar laser induced fluorescence of Polycyclic Aromatic Hydrocarbons (PAHs), classically identified as soot precursors. Images issued from these diagnostics provide a spatially resolved information on the production of soot, its interaction with the turbulent flow and its link with the flame surface and with soot precursors regions. It is shown in particular that soot pockets are highly distorted by turbulent eddies forming a characteristic layered pattern. Information on soot-OH-PAH correlation deduced from the high speed imaging could be employed to verify the adequacy of models devised to represent soot dynamics in direct or large eddy simulations of turbulent flames.

benedetta.franzelli@ecp.fr

5E12 FURTHER DETAILS ON PARTICLE INCEPTION AND GROWTH IN PREMIXED FLAMES

Mario Commodo¹, Gabriella Tessitore², Gianluigi De Falco², Annalisa Bruno³, Patrizia Minutolo¹, Andrea D'Anna²

¹CNR, Italy ²Università degli Studi di Napoli Federico II, Italy ³ENEA, Italy

Soot inception in flames still remains mostly unknown. What are, if any, the differences of inception particles in non sooting and sooting flame is still not well ascertained. Moreover, it is not still understood if particle nucleation is governed primarily by coagulation or by a different composition/aromatization of inception particles.

In this work the initial particle growth occurring in premixed non-sooting flames of ethylene has been investigated. On line size-selected photoionization efficiency of inception particles produced in various flames has been measured. Structural/chemical differences of inception and grown particles have been additionally investigated by off-line cyclic voltammetry, Raman, light absorption, and XRD. The aromaticity of primary particles slightly increases when moving from flames in which the particle size distribution remains nearly constant and mono-modal, to flames in which particle coagulation gives rise to the formation of a second mode. Only in Mode II particles, $d \approx 10\text{nm}$, the first appearance of three-dimensional aromatic domains is observed.

In this light, two additional aromatization processes occur during the first stages of particle dynamic preceding soot inception: a slight aromatization of incipient particles with an increase of in plane aromatic islands and the formation of aromatic plane stacks in coagulated primary particles. This second type of coagulating-aromatization process explains the closure of the band gap towards the typical values observed in soot.

minutolo@irc.cnr.it

5E13 EFFECTS OF AROMATIC CHEMISTRY-TURBULENCE INTERACTIONS ON SOOT FORMATION IN A TURBULENT NON-PREMIXED FLAME

Y. Xuan, G. Blanquart, California Institute of Technology, United States

In this paper, Large Eddy Simulations (LES) have been performed on an ethylene/air piloted turbulent non-premixed sooting jet flame to quantify the importance of aromatic chemistry-turbulence interactions. Aromatic species are of primary importance since their concentrations control directly the soot nucleation rates. In the current work, the chemistry-turbulence interactions for benzene and naphthalene are taken into account by solving transport equations for their mass fractions. A recently developed relaxation model is used to provide closure for their chemical source terms. The effects of turbulent unsteadiness on soot yield and distribution are highlighted by comparing the LES results with a separate LES using tabulated chemistry for all species including the aromatic species. Results from both simulations are compared to experimental measurements. Overall, it is shown that turbulent unsteady effects are of critical importance for not only the accurate prediction of inception locations, but also the magnitude and fluctuations of soot.

yxuan@caltech.edu

5F01 RATE-RATIO ASYMPTOTIC ANALYSIS OF THE STRUCTURE AND MECHANISMS OF EXTINCTION OF NONPREMIXED CH₄/N₂-O₂/N₂O/N₂ FLAMES

Kalyanasundaram Seshadri¹, Xue-Song Bai², Forman Williams¹

¹University of California at San Diego, United States ²Lund University, Sweden

Rate-ratio asymptotic analysis is carried out to elucidate the influence of nitrous oxide on the structure and critical conditions for extinction of nonpremixed methane flames. Steady, axisymmetric, laminar flow of two counterflowing streams toward a stagnation plane is considered. One stream is made up of a mixture of methane and nitrogen. The other stream is a mixture of oxygen, nitrous oxide, and nitrogen. A reduced mechanism of five global steps is employed in the analysis. Chemical reactions are presumed to take place in a thin reaction zone that is established in the vicinity of the stagnation plane. On either side of this thin reaction zone, the flow field is inert. These inert regions are called outer zones. Methane and nitrous oxide are completely consumed in the reaction zone, while oxygen is presumed to leak through the reaction zone. In the reaction zone, chemical reactions are presumed to take place in two layers---the inner layer and the oxidation layer. In the inner layer fuel (methane) is consumed and the intermediate species hydrogen and carbon monoxide are formed. These intermediate species are oxidized in the oxidation layer to water vapor and carbon dioxide. Radicals are produced in the oxidation layer from chain-branching reactions that consume hydrogen. Asymptotic analysis gives the scalar dissipation rate at extinction. Critical conditions for extinction predicted by the analysis agree well with previous experimental data. Nitrous oxide is found to have an inhibiting effect on the flame, promoting extinction. The inhibiting effect is attributed to the competition between the net reaction of nitrous oxide with hydrogen to form water vapor and nitrogen and the chain-branching reaction between oxygen and hydrogen that produces radicals.

seshadri@ucsd.edu

5F02 SUPERCRITICAL PYROLYSIS OF *N*-DODECANE WITH COLLOIDAL PLATINUM-DECORATED GRAPHENE SHEETS

Hyung Sub Sim¹, Richard A. Yetter¹, Daniel M. Dabbs², Ilhan A. Aksay²

¹The Pennsylvania State University, United States ²Princeton University, United States

The present work aims to understand the fundamental effects of graphene-based nanostructured materials on the thermal decomposition of a fuel under supercritical conditions. The supercritical pyrolysis of *n*-dodecane (*n*-C₁₂H₂₆) containing Functionalized Graphene Sheets (FGS) with and without platinum nanoparticles was studied in a high pressure flow reactor over the temperature range of 480 - 530°C and at a constant pressure of 4.75 MPa. With the addition of the Platinum-decorated FGS (Pt-FGS) particles, it was found that conversion rates are higher than those of pure *n*-C₁₂H₂₆. At a low loading concentration of 50 ppmw Pt-FGS in the fuel mixture (resulting in 10 ppmw Pt being added to the *n*-C₁₂H₂₆), the well-dispersed Pt nanoparticles can play an important role in catalyzing supercritical *n*-C₁₂H₂₆ pyrolysis, producing higher hydrogen and low molecular weight species compared to those in pure *n*-C₁₂H₂₆. Moreover, the yields of specific pyrolysis products changed with the addition of the Pt-FGSs as a function of temperature and time, leading to the conclusion that the activity of the particles on the product distribution could be controlled.

hys5109@psu.edu

5F03 A DETAILED KINETIC STUDY OF THE THERMAL DECOMPOSITION OF TETRAETHOXYSILANE

Daniel Nurkowski, Philipp Buerger, Jethro Akroyd, Markus Kraft, University of Cambridge, United Kingdom

This work presents a detailed kinetic modelling study of the thermal pyrolysis of Tetraethoxysilane (TEOS). A chemical mechanism is proposed based on an analogy between the hydrocarbon branches attached to the central silicon atom and an existing mechanism for the decomposition and combustion of ethanol. Important reaction pathways are identified through element flux and sensitivity analyses. It was found that the key reaction routes are the step-wise four-centre molecular decomposition of TEOS to form silanols and ethylene: Si(OH)_n(OC₂H₅)_m → Si(OH)_{n+1}(OC₂H₅)_{m-1} + C₂H₄ (*n*+*m* = 4) and the barrier-less C-C bond cleavage of the ethoxy branches: Si(OH)_n(OC₂H₅)_m → Si(OH)_n(OC₂H₅)_{m-1}(OCH₂)+CH₃ (*n*+*m* ≤ 4). Rate constants were calculated using conventional and variational transition state theories (TST and VTST) for all the reactions in the first route and for the methyl radical removal from Si(OH)₃(OC₂H₅) in the second route. The calculated results are similar to the rate constants of the corresponding ethanol reactions, providing support for the analogy with the ethanol decomposition. Simulations using the proposed mechanism are shown to be consistent with experimental data for the decomposition of TEOS.

mk306@cam.ac.uk

5F04 SIMULATIONS OF HETEROGENEOUS PROPELLANT COMBUSTION: EFFECT OF PARTICLE ORIENTATION AND SHAPE

Mathieu Plaud, Stany Gallier, Matthieu Morel, SAFRAN-Herakles, France

In this paper we have developed a direct numerical simulation approach to study the combustion of ammonium perchlorate-based heterogeneous solid propellants. Oxidizer particles are first supposed to be spheroidal and the effect of

their orientation on the burning rate is examined. Particles aligned normal to the combustion surface are found to burn faster than when aligned parallel while randomly-oriented particles generally burn at an intermediate rate, at least for moderate aspect ratio. Simulations also show that the burning rate of random spheroids is relatively independent of the aspect ratio. Finally, the effect of particle shape is investigated using superellipsoidal particles but is here found to be limited for the chosen propellant and pressure.

mathieu.plaud@herakles.com

5F05 EXPERIMENTAL INVESTIGATION OF CELLULAR INSTABILITY IN AMMONIUM PERCHLORATE (AP) AND FINE AP-BINDER MIXTURES

Niharika Gurram, S.R. Chakravarthy, Indian Institute of Technology Madras, India

This paper examines scanning electron micrographs for the size of cells that appear on the burning surfaces of (1) single crystals and pressed pellets of Ammonium Perchlorate (AP), and (2) mixtures of fine AP particles with polymeric binder, quenched by rapid depressurization at different pressures. While the cellular structures in self-deflagration of AP are well known yet unexamined quantitatively, those on fine AP/binder mixtures are examined in the context of their mid-pressure extinction leading to plateau burning rate behaviour of propellants containing them. The results are an experimental validation of the theoretical predictions of Margolis and Williams based on diffusional-thermal coupling in the intrinsic stability of combustion of premixed solids.

src@ae.iitm.ac.in

5F06 FLAME STRUCTURE AND PARTICLE COMBUSTION REGIMES IN PREMIXED METHANE-IRON-AIR SUSPENSIONS

Philippe Julien, Sam Whiteley, Samuel Goroshin, Michael J. Soo, David L. Frost, Jeffrey M. Bergthorson, McGill University, Canada

Flame structures and particle combustion regimes are studied in hybrid fuel mixtures of methane and iron using a modified Bunsen burner with two different oxidizing environments. The first is a stoichiometric methane-air mixture, in which the iron reacts with the hot gaseous combustion products in a kinetically-controlled regime; the second is a lean methane-oxygen-nitrogen mixture, allowing iron to react with the excess oxygen in a diffusion-controlled regime. The particle seeding concentration is monitored using laser attenuation and varies from 0 – 350 g/m³. Burning velocities are obtained from flame photographs and condensed phase temperatures are determined from particle emission spectra via polychromatic fitting of the spectra to Planck's law of blackbody radiation. High-speed imaging is also used to qualitatively characterize the different flame structures. Results are also compared to a methane flame seeded with inert silicon carbide particles instead iron. It is shown that, independent of the combustion regime, a critical concentration of iron powder is required to form a coupled flame front in the combustion products of the methane flame. Furthermore, after the dust flame formation, a double front structure separated by a dark zone is observed in the kinetic regime, whereas the two flames overlap and form a single Bunsen cone in the case of the diffusion regime.

philippe.julien@mail.mcgill.ca

5F07 COMPUTER MODELLING OF NANO-ALUMINIUM AGGLOMERATION DURING THE COMBUSTION OF COMPOSITE SOLID PROPELLANTS

Kishor Balbudhe, Aviral Roy, S.R. Chakravarthy, Indian Institute of Technology Madras, India

Previously reported computer modelling of agglomeration of micrometre-sized aluminium particles during the combustion of composite solid propellants fails when applied to nano-aluminium particles because of the enormous number of the latter particles. A modified algorithm for three-dimensional casting and burning of composite propellants containing nano-aluminium particles on the computer is developed in the present work. In this, a regular grid is constructed overlaying the computer cast of coarse and fine Ammonium Perchlorate (AP) particles in the propellant, and the nano-aluminium particles are placed at randomly selected grid points outside of previously placed AP particles. Moreover, this is done one grid layer at a time in the burning direction to save computer memory. Further, since the burning surface is regressed at known burning rates over a larger step size than the above grid spacing, all the nano-aluminium particles located at grid points within one step of surface regression are lumped together and represented by an equivalent micrometre-sized particle. The agglomeration algorithm previously reported is then applied to this representative computer propellant cast. Results are compared with previously reported experimental data for two propellants with different coarse AP particles, one of them at three pressures. The predicted agglomerate size distribution agrees well with the experimental data.

src@ae.iitm.ac.in

5F08 GAS-SURFACE THERMOCHEMISTRY AND KINETICS FOR ALUMINUM PARTICLE COMBUSTION

Julien Glorian¹, Laurent Catoire², Stany Gallier³, Nathalie Cesco¹

¹CNES, France ²ENSTA ParisTech, France ³SAFRAN-HERAKLES, France

Quantum chemical calculations have been used to investigate possible reactions on aluminum surface in the Al/H/C/O/N system. Transition states or barrierless reaction paths have been identified for essentially all feasible

adsorption/desorption reactions in this system involving atoms and diatomic homonuclear molecules. Structures, energies, and vibrational frequencies for reactants, products and transition states in this system are presented and compared to available experimental data. These results provide a basis for the estimation of reaction rate parameters for this system using Transition State Theory (TST) and related unimolecular reaction rate theories, and thereby constructing a reaction mechanism useful for detailed chemical kinetic modeling of aluminum particle combustion in propellant environment. In the few cases where previous experimental or theoretical results have been published, the present work is consistent with these studies.

julien.glorian@ensta-paristech.fr

5F09 QUENCHING DISTANCE OF FLAMES IN HYBRID METHANE-ALUMINUM MIXTURES

Jan Palecka, Philippe Julien, Samuel Goroshin, Jeffrey M. Bergthorson, David L. Frost, Andrew J. Higgins
McGill University, Canada

Quenching distances for laminar flames in hybrid methane-aluminum fuel mixtures (16.3% O₂/8.1% CH₄/75.6% N₂/Al) was experimentally measured at different concentrations of aluminum suspensions with the aluminum particles having an average size of about $d_{32} = 5.6 \mu\text{m}$. Experiments were performed with freely propagating flames in a 48-mm-inner-diameter Pyrex glass tube. A set of parallel equidistant metal plates was installed at about 50 cm from the open tube end, forming parallel channels. The flame was initiated at the upper open tube end and propagated downwards. Benchmark experiments performed with an inert Silicon Carbide (SiC) powder suspension in the same gaseous mixture have demonstrated a steady increase of the quenching distance from about 3.5 mm for an unseeded methane flame to about 9.5 mm for a flame seeded with 270 g/m³ of SiC. At higher SiC concentrations, the flame failed to propagate down the tube. Coupled aluminum-methane flame fronts only appeared above a threshold aluminum concentration around 300 g/m³. Below this concentration, the appearance and quenching behaviors of the methane flame seeded with reactive aluminum and inert SiC dusts were similar. The coupled aluminum-methane flame demonstrated two quenching modes. At concentrations below 400 g/m³, the aluminum flame decoupled from the methane flame and quenched while the methane flame still propagated. The quenching of a decoupled methane flame in a narrow channel resembles the quenching behavior of the inert powder-seeded flame. At concentrations above 400 g/m³, only a coupled aluminum-methane flame could be observed to propagate, or be extinguished, as a whole and exhibited a weaker dependence of the quenching distance on aluminum concentration. These results were interpreted in terms of models for binary fuel mixtures wherein the second fuel to react is completely decoupled, separated by a fixed distance, or merged with the initial flame front.

samuel.goroshin@mcgill.ca

5F10 COMBUSTION CHARACTERISTICS OF MONODISPERSED ALUMINUM NANOPARTICLE STREAMS IN POST FLAME ENVIRONMENT

Chengdong Kong, Qiang Yao, Dan Yu, Shuiqing Li, Tsinghua University, China

The combustion characteristics of monodispersed Aluminum (Al) nanoparticles are investigated in the post flame region of a non-premixed flat flame burner. The dispersion and feeding of nanoparticles are fulfilled by a self-developed jet collision nebulizer connected to a diffusion dryer. The mobility diameter of the fed nano-Al particles is measured as mean of 191 nm, while the primary particle has a size of 92nm from TEM images. The dispersed nano-Al particles exhibit a red-color mild flame, differing from those burning aluminum microparticles. The temperature of nano-Al flame is found to be only 165K higher than the ambient. The characteristic burning time, derived from the flame images, decreases as the ambient temperature increases. It obeys well with an Arrhenius-type exponential formula. The burning nano-Al particles are thermophoretically sampled along the different heights above the burner for further analysis. Hollow structure of product is observed, indicating the outward diffusion of aluminum across the oxide shell during the combustion. A single-particle combustion model based on the ionic diffusive mechanism is developed to predict the burning time after the validation by both Al/O ratio and oxide shell thickness.

yaoq@tsinghua.edu.cn

5G01 RADICAL QUENCHING ON METAL SURFACE IN A METHANE-AIR PREMIXED FLAME

Yu Saiki¹, Yuji Suzuki²

¹Nagoya Institute of Technology, Japan ²The University of Tokyo, Japan

In order to quantify radical quenching on metal surfaces, a methane-air premixed flame formed in narrow quartz channels is investigated. Stainless steel321 (SUS321) and Inconel600 are chosen as metal surface materials for their high oxidation/heat resistivity. Thin films of SUS321 and Inconel600 are deposited on quartz substrates using a vacuum arc plasma gun to realize equivalent thermal boundary condition with different surface reactions. In addition to the metal surfaces, two types of alumina thin films are prepared using Atomic Layer Deposition (ALD) and sputtering techniques to explore the surface roughness effect. OH-PLIF and numerical simulation with detailed chemistry are employed to examine the near-wall flame structures. When the wall temperature is higher than 1073 K, OH* concentrations near the SUS321/Inconel600 surfaces are significantly lower than that near the quartz surface. Based on the PLIF data, the initial

sticking coefficient S_0 associated with radical adsorption is estimated to be 0.1 and 0.01 for the metal and quartz surfaces, respectively, indicating stronger radical quenching effect on these metal surfaces. On the other hand, OH^* profile near the sputtered-alumina surface, which has larger roughness, is in good accordance with that near the ALD-alumina surface. This implies that the radical adsorption is independent on surface roughness or surface defects. A series of numerical simulation is also carried out to examine the effect of S_0 on flame characteristics in micro-scale channels. It is found that the value of S_0 becomes of great importance for initiation temperature of the gas-phase reaction and effective heat release rate.

saiki.yu@nitech.ac.jp

5G02 THERMAL AND CHEMICAL STRUCTURES FORMED IN THE MICRO BURNER OF MINIATURIZED HYDROGEN-AIR JET FLAMES

Akter Hossain, Yuji Nakamura, Hokkaido University, Japan

The thermal and chemical structure formed in the micro burner leading to the unique stability mechanism of miniaturized jet diffusion flame via excess heat recirculation through the burner wall, is studied numerically. 2-D axis-symmetric heat and mass transport processes with chemical reactions are considered in gas phase, while the heat transport process is considered in solid phase. Burner materials and the fuel ejecting velocities are considered as main numerical parameters in order to examine the role of the burner on the thermal and chemical structure in the burner. A skeletal reaction mechanism consists of twelve steps chemical reactions and nine species is applied to consider the radical generation/consumption/transport in the burner. It is found that the tiny flame is stabilized even with extra-ordinary small Reynolds number, at which the extinction is generally experienced, when the low conductivity burner is adopted. This is due to the effective usage of the transferred heat from the flame to the burner to improve the stability flowing to 1) preheating the incoming fuel, 2) the least heat loss from the flame toward the burner tip, 3) enhancing the reactivity inside the burner. In such low Reynolds number jet flow with the low conductive burner, ambient air can easily diffuse back into the burner via diffusion and oxidative reactions at the vicinity of the burner tip is then promoted. Accordingly, the flame structure is dramatically modified beyond the typical 1-D flame to lead the stability. It is suggested that the further chemical process can be enhanced in the micro burner, at which the least dynamic disturbance is expected, by considering the catalytic reaction at the inner burner surface or using oxygenated fuel likely alcohol or ether.

yuji-mg@eng.hokudai.ac.jp

5G03 EXPERIMENTAL AND THEORETICAL STUDY ON THE INTERACTION BETWEEN TWO IDENTICAL MICRO-SLOT DIFFUSION FLAMES: BURNER PITCH EFFECTS

Akihiro Kosugi¹, Naoki Sato², Kazunori Kuwana¹, Taro Hirasawa², Yuji Nakamura³

¹Yamagata University, Japan ²Chubu University, Japan ³Hokkaido University, Japan

This paper studies the interaction between two identical micro-slot flames. First, we experimentally found that a change in burner pitch alters the flame shape and the total heat release rate. Total heat release rate has a local maximum and a local minimum, and the critical burner pitch at which two flames touch each other is identified as a representative parameter that characterizes flame interaction. Then, a simple analytical model was developed to predict the critical burner pitch. The model yields the critical burner pitch as a function of the stoichiometric value of mixture fraction. Lastly, CFD simulations under a wide range of conditions were conducted to validate the model prediction.

kuwana@yz.yamagata-u.ac.jp

5G04 FUNDAMENTAL INVESTIGATION ON THE FUEL- NO_x EMISSION OF THE OXY-FUEL COMBUSTION USING A TUBULAR FLAME BURNER

Daisuke Shimokuri, Shinichi Fukuba, Satoru Ishizuka

Hiroshima University, Japan

The fuel- NO_x emission from the oxy-fuel combustion has been experimentally investigated using $\text{CH}_4/\text{O}_2/\text{CO}_2$ mixture as a model of the oxy-fuel combustion with FGR, and using NH_3 as a model of fuel-N. With a tubular flame burner, effects of the oxygen concentration, fuel-N concentrations, equivalence ratio and the preheating temperature have been systematically investigated. Results showed that, under the non-preheating conditions, Fuel- NO_x concentrations were strongly dependent on the oxygen concentrations and the equivalence ratio. However, under the preheating conditions, the NO_x concentration approached to the same values for all O_2 concentration conditions, and hence, the effects of O_2 seemed to become less by the preheating. It was also found that relatively large amount of NO_2 was emitted in the fuel-lean condition when both of O_2 concentration and the preheating temperature are low. NO_2 was decreased with increase in the oxygen concentration and the preheating temperature, however, at least 45 ppm was detected, which is 5~7% of NO_x . The effects of the preheat temperature on the fuel- NO_x emission of the oxy-fuel combustion was investigated with simulation. Results showed that, preheating under the low O_2 concentration condition leads to an evident increase of the O radical due to the limitation of the H radical formation in the oxy-fuel combustion. This results in the increase of the HNO and eventually NO concentration. On the other hand, under the high O_2 concentration conditions, NO_x was not increased by the preheating. under the high O_2 conditions, the preheating leads to an increase of H radical as well as O radical because the

flame temperature is high, and the H radical limitation become moderate due to the abundant O and OH radical, and thus, the NH formation was enhanced which resulted in the reduction of the HNO, and hence, the saturation of the NO concentrations.

cri@hiroshima-u.ac.jp

5G05 THE CHEMICAL ROLE OF CO₂ IN PYRITE THERMAL DECOMPOSITION

Weizhi Lv¹, Dunxi Yu¹, Jianqun Wu¹, Lian Zhang², Minghou Xu¹

¹Huazhong University of Science and Technology, China ²Monash University, Australia

The transformation of pyrite (FeS₂) is critical to ash slagging in oxy-fuel combustion but has little been explored. The chemical role of CO₂, the dilution gas in oxy-fuel boilers, on pyrite decomposition was investigated in this work. Pyrite samples of 63-75 μm were decomposed at temperatures between 948 and 1073 K, and in high-purity CO₂ or N₂ in a novel Thermo-Gravimetric Reactor (TGR) under isothermal conditions. Sample weight loss with respect to time was recorded online and time-resolved data on the evolution of gas products were obtained by Fourier Transform Infrared Spectroscopy (FT-IR). The solid products were characterized by X-Ray Diffraction (XRD). The results show that pyrrhotite is the only iron product detected in either CO₂ or N₂, but the pyrrhotite from CO₂ contains less sulfur than that from N₂. Pyrite decomposition in CO₂ is noticeably faster and has lower activation energies than that in N₂. These effects of CO₂ are chemical in nature and are evidenced by the evolution of SO₂, CO and COS in addition to sulfur vapor. Based on the data of both solid and gas products, pyrite decomposition in either CO₂ or N₂ is divided into three distinct stages. However, different from N₂, CO₂ is found to participate in pyrite decomposition at each stage. A reasonable mechanism is proposed to account for the chemical role of CO₂ in pyrite decomposition.

yudunxi@hust.edu.cn

5G06 EXPERIMENTAL INVESTIGATION OF STRUCTURE AND STABILIZATION OF SPRAY OXYFUEL FLAMES DILUTED BY CARBON DIOXIDE

G. Cleon, D. Honoré, C. Lacour, A. Cessou, CORIA- CNRS, France

Oxycombustion diluted by recirculating flue gases is one of the most advanced innovating combustion technique to adapt Carbon Capture and Storage (CCS) to industrial combustion plants. The dilution by flue gases with a large amount of CO₂ impacts the flame behavior in terms of combustion efficiency, pollutant emission, radiative transfer and flame stabilization. The present paper investigates, at lab-scale, the effect of CO₂ dilution on a spray oxyfuel flame in terms of flame structure and stabilization. A burner is well designed such that the boundary conditions may be accurately measured and be suitable to provide a confident database. A central spray of ethanol is surrounded by a O₂-CO₂ coflow. The coflow is modular to investigate the effect of CO₂ content separately from the coflow velocity. Size-classified Phase Doppler Anemometry characterizes the spatial non-homogeneity in size and velocity. The average flame structures are observed by OH* chemiluminescence and complementary instantaneous flame observations by OH Planar Laser Induced Fluorescence. Three types of flames are observed with a trailing flame exhibiting a double structure specific to two-phase combustion and linked to the competition between vaporization, chemical and mixing time scales. The amount of CO₂ in the oxidant affects strongly the flame structure and stabilization. It modifies drastically the chemical time, the flame temperature, and thus the vaporization time and the size dispersion. The outer flame of the double structure is always diffusion-like while the inner flame changes from diffusion-like to premixed-like when the vaporization time shortens. This investigation shows the additional effects of CO₂ dilution on spray combustion.

armelle.cessou@coria.fr

5G07 LARGE EDDY SIMULATION OF COAL COMBUSTION IN A LARGE-SCALE LABORATORY FURNACE

M. Rabaçal^{1,2}, B.M. Franchetti³, F. Cavallo Marincola³, F. Proch², M. Costa¹, C. Hasse⁴, A.M. Kempf²

¹University of Lisbon, Portugal ²Universität Duisburg-Essen, Germany

³Imperial College London, United Kingdom ⁴Technische Universität Bergakademie Freiberg, Germany

A detailed Large Eddy Simulation (LES) of pulverised coal combustion in a large-scale laboratory furnace is presented. To achieve a detailed representation of the flow, mixing and particle dispersion, a massively parallel LES was performed. Different phenomenological network models were applied and compared to each other in order to obtain the most adequate devolatilization kinetic data for the LES. An iterative procedure allowed to optimise the devolatilization kinetic data for the studied coal and operating conditions. The particle combustion history is studied by analysing particle instantaneous properties giving a perspective on coal combustion that currently is not available by other means than LES. Predicted major species and temperature were compared with measurements and good agreement was obtained. The finely resolved near burner region revealed that the flame is stabilised very close to the burner. Furthermore, two distinct zones of CO₂ production were found - one in the Internal Recirculation Zone (IRZ) due to gaseous combustion, and one downstream of the vortex breakdown, due to intense char combustion. It was found that particle properties are inhomogeneous within the IRZ, whereas in the External Recirculation Zone (ERZ) and downstream of the vortex breakdown they were found to be homogeneous.

miriamrabacal@ist.utl.pt

5G08 USE OF SYNTHETIC OXYGEN CARRIERS FOR CHEMICAL LOOPING COMBUSTION OF VICTORIAN BROWN COAL

S. Rajendran¹, S. Zhang², R. Xiao², S. Bhattacharya¹

¹Monash University, Australia ²Southeast University, China

Chemical Looping Combustion (CLC) is a promising alternative technology for inherent capture of CO₂ at a lower cost and energy penalty relative to other Carbon Dioxide Capture and Storage (CCS) options. This paper details the use of iron oxide based synthetic oxygen carriers composed of 20% CuO, Mn₂O₃ and NiO impregnated on Fe₂O₃ in CLC with Victorian brown coal as a fuel. The investigation used a variety of experimental equipment and instruments - a fluidized bed reactor, Thermogravimetric Analyser (TGA) and Temperature Programmed Reduction (TPR) unit. The oxygen carrier samples were characterized using X-Ray Diffraction (XRD), Scanning Electron Microscope (SEM) and Accelerated Surface Area and Porosimetry (ASAP). The characterization also included in-situ high temperature XRD using synchrotron radiation to study the changes in the lattice parameter and crystal size of the oxygen carrier with temperature in a CLC-like environment. It was observed that the synthetic oxygen carriers exhibited better performance over Fe₂O₃ with the sample impregnated with NiO having highest CO₂ conversion efficiency. The synchrotron based high temperature in-situ XRD study showed an increase in the crystal size of the oxygen carrier after one redox cycle which was also observable from the SEM micrographs of the used samples due to coalescence of the grains. Thermochemical modelling was carried out to generate an Ellingham diagram which supported the findings from the in-situ XRD which showed that CO initiated the reduction of Fe₂O₃ at 650°C. The synthetic oxygen carriers demonstrated enhanced reactivity towards the fuel relative to pure Fe₂O₃, however viability of their use in larger scale will depend on the economics of their production

sankar.bhattacharya@monash.edu

5G09 COMBUSTION KINETICS AND PARTICLE FRAGMENTATION OF RAW AND TORRIFIED BIOMASS IN A DROP TUBE FURNACE

F.F. Costa, Gongliang Wang, M. Costa, University of Lisbon, Portugal

This study focuses on the combustion kinetics and particle fragmentation of raw and torrefied biomass in a Drop Tube Furnace (DTF). Two biomass fuels were studied, namely pine shells and olive stones, which have been torrefied in a nitrogen inert atmosphere at 280-300°C. Both the raw and torrefied biomass fuels were then burned in the DTF. The data reported includes gas temperatures and particle burnout measured along the DTF for five furnace temperatures (900, 950, 1000, 1050 and 1100°C). In addition, measurements of Particulate Matter (PM) concentrations and size distributions were made for all the biomass fuels at 1100°C in the middle and near the exit of the DTF. The results showed that: 1) The high heating value of the torrefied biomass fuels are higher than those of the raw biomass fuels; specifically, for pine shells it increased by 25% and for olive stones by 18%; 2) in contrast with the torrefied olive stones, the torrefied pine shells require similar residence times to attain overall burnout values comparable to those of the untreated material; 3) the kinetic data for both fuels, raw and torrefied, indicates that the torrefaction reduces the activation energy of the present biomass chars; and 4) torrefaction does not promote particle fragmentation even for biomass fuels that present high tendency for it.

mcosta@tecnico.ulisboa.pt

5G10 IGNITION BEHAVIORS OF PULVERIZED COAL PARTICLES IN O₂/N₂ AND O₂/H₂O MIXTURES IN A DROP TUBE FURNACE USING FLAME MONITORING TECHNIQUES

Chun Zou, Lei Cai, Di Wu, Yang Liu, Siliang Liu, Chuguang Zheng, Huazhong University of Science and Technology, China

Oxy-steam combustion technology is regarded to be the next generation of oxy-fuel combustion technology. Because the physical and chemical properties of steam are very different from that of CO₂ or N₂, especially its reactivity, the ignition characteristics of coal in oxy-steam combustion are expected to be different from those in conventional combustion or O₂/CO₂ recycled combustion. This paper presents experimental investigations of the ignition behaviors of coal in O₂/N₂ and O₂/H₂O atmospheres using different oxygen fractions (21%, 30%, 35%, 40% and 50%). Ignition experiments were performed in a drop tube furnace. The ignition behaviors were recorded using a high-speed camera and a two-color pyrometer. According to the images of the ignition, the pulverized coals ignite homogeneously in all cases. The ignition of pulverized coal in the O₂/H₂O atmospheres occurs sooner than in the O₂/N₂ atmospheres at identical oxygen fractions. A high concentration of steam may enhance the steam gasification reaction (C+H₂O→CO+H₂) and the steam shift reaction (CO+H₂O→CO₂+H₂) in O₂/H₂O atmospheres. These two reactions can form a large amount of H₂ and CO in O₂/H₂O atmospheres in the gaseous mixture around the coal particle. This result is beneficial to reducing the ignition delay times of volatiles mixtures in O₂/H₂O atmospheres.

zouchun@hust.edu.cn

- 5H01 INFLUENCE OF HYDRODYNAMIC INSTABILITIES ON THE PROPAGATION MECHANISM OF FAST FLAMES
L. Maley, R. Bhattacharjee, S. Lau-Chapdelaine, M.I. Radulescu, University of Ottawa, Canada

The present work investigates the structure of fast supersonic turbulent flames typically observed as precursors to the onset of detonation. These high speed deflagrations are obtained after the interaction of a detonation wave with cylindrical obstacles. Two mixtures having the same propensity for local hot spot formation were considered, namely hydrogen-oxygen and methane-oxygen. It was shown that the methane mixture sustained turbulent fast flames, while the hydrogen mixture did not. Detailed high speed visualizations of nearly two-dimensional flow fields permitted to identify the key mechanism involved. The strong vorticity generation associated with shock reflections in methane permitted to drive jets. These provided local enhancement of mixing rates, sustenance of pressure waves, organization of the front in stronger fewer modes and eventually the transition to detonation. In the hydrogen system, for similar thermo-chemical parameters, the absence of these jets did not permit to establish such fast flames. This jetting slip line instability in shock reflections (and lack thereof in hydrogen) was correlated with the value of the isentropic exponent and its control of Mach shock jetting instability.

matei@uottawa.ca

- 5H02 IGNITION AND SUPERSONIC COMBUSTION BEHAVIOR OF LIQUID ETHANOL IN A SCRAMJET MODEL COMBUSTOR WITH CAVITY FLAME HOLDER

Shinji Nakaya¹, Yuta Hikichi¹, Yoshiki Nakazawa¹, Kazuki Sakaki¹, Minh Choi¹, Mitsuhiro Tsue¹, Michikata Kono¹, Sadatake Tomioka²

¹The University of Tokyo, Japan ²Japan Aerospace Exploration Agency, Japan

Supersonic combustion behavior of ethanol at Mach 2 and stagnation temperature of 1800 to 2400K was investigated experimentally. Liquid or gaseous ethanol was injected into a scramjet model combustor with a cavity flame holder. Ethanol flow rates were varied and the minimum equivalence ratio for supersonic combustion was obtained based on the statistic of the Weibull distribution. CH chemiluminescences were measured by a video camera with an optical filter and pressures were measured by pressure transducers on the upper wall of the combustor. Ethanol droplet diameters were also measured by a laser diffraction spray analyzer. The induction time of the fuel breakup, vaporization and ignition delay was estimated using a measured Sauter mean diameter. When ignition and supersonic combustion were realized, two combustion modes, intensive and transient combustions, were observed, which were classified by pressure gains over the cavity. Ignition for liquid ethanol injections was observed at the stagnation temperature of 2200K. An increase in the stagnation temperature resulted in a decrease in the minimum equivalence ratio for supersonic combustion. In the case of the gaseous ethanol injections, supersonic combustion was realized at the stagnation temperature of 2000K. When combustion behavior for liquid and gaseous ethanol injections was compared, the penetration height was set to be equal by changing the pressure of nitrogen gas. A change in the penetration height for liquid ethanol injections was proportional to the dynamic pressure ratio of the fuel injection and the main air flow, and no ignition was observed when the penetration height exceeded a threshold. The combustion behavior in the present study was explained well by results of the analytical cavity residence time and induction time for fuel breakup, vaporization and ignition.

tsnakaya@mail.ecc.u-tokyo.ac.jp

- 5H03 SIMULTANEOUS GAS DENSITY AND FUEL CONCENTRATION MEASUREMENTS IN A SUPERSONIC COMBUSTOR USING LASER INDUCED BREAKDOWN

Hyungrok Do¹, Campbell D. Carter², Qili Liu¹, Timothy M. Ombrello², Stephen Hammack³, Tonghun Lee³, Kuang-Yu Hsu⁴

¹University of Notre Dame, United States ²Wright-Patterson Air Force Base, United States

³University of Illinois at Urbana-Champaign, United States ⁴Innovative Scientific Solutions, Inc., United States

Laser-induced breakdown is used for quantitative gas property measurements (gas density and ethylene fuel concentration) in a cavity flameholder in a supersonic crossflow. A plasma discharge is produced by a focused laser beam (Nd:YAG, 532 nm) in the cavity to measure gas properties at the location of the plasma and to ignite cavity flames. Plasma energy (PE), defined by the laser pulse energy absorbed/scattered in the plasma, and plasma emission spectra are recorded for estimating gas density and species concentration, respectively. To obtain correlations of PE vs. gas density and emission spectra vs. fuel concentration, calibration experiments are conducted using a variable-pressure (0 – 900 mbar)/temperature (300 – 900 K) chamber and a Hencken burner installed in a variable-pressure (50 – 900 mbar) combustion chamber. Total measurement time is sufficiently short, ≤ 80 ns after laser arrival at the probe region, to capture the high intensity portion of the emission and to minimize effects of probe displacement (in the high-speed flow). Specifically, the laser pulse energy incident and transmitted (through the plasma) are measured, and the plasma emission spectra are captured during a 50-ns gate, after an approximate 30-ns time delay (relative to onset of emission from the probe volume) to avoid broadband thermal emission from the plasma.

hdo3@nd.edu

5H04 A COMPUTATIONAL STUDY OF SUPERSONIC COMBUSTION IN STRUT INJECTOR AND HYPERMIXER FLOW FIELDS

C. Fureby¹, K. Nordin-Bates¹, K. Petterson¹, A. Bresson², V. Sabelnikov²

¹FOI, Sweden ²ONERA, France

Achieving sufficiently high combustion efficiency and stability in supersonic combustion is extremely challenging and is highly dependent on the fuel-injection and mixing strategies adopted. A viable approach is the strut injector, which provides some recirculation, thereby facilitating flame stabilization in the strut-wake. In this investigation we examine in detail the flow, mixing, self-ignition and flame stabilization mechanism of conventional and alternating-wedge injection struts. In order to analyze these, we consider NAL's supersonic combustor, equipped with two conventional two-stage injection struts, and an alternating-wedge injection strut, in conjunction with ONERA's vitiation air heater. In this investigation we combine experimental data, including spontaneous flame images, wall-pressure and Planar Laser Induced Fluorescence (PLIF) images of Hydroxyl (OH) with computational results, using finite-rate chemistry Large Eddy Simulation (LES) and skeletal hydrogen-air reaction mechanisms. The spontaneous flame images and the computational flame structures for both injector-strut types agree well qualitatively, demonstrating that computations capture the overall features of the experiments. Detailed comparisons between experimental data and computational results for the wall pressure and for mean and rms OH-PLIF cross-sections show acceptable agreement, indicating that the LES results can be used to further examine the intrinsic features of the flame structure and the stabilization mechanism. These results indicate significant differences in flow and flame structures between the two two-stage injection struts and the alternating-wedge injection strut tested. More specifically, the longitudinal vorticity introduced by the alternating-wedge injection strut increases the combustion efficiency but marginally decreases the flame stability marginally. For two-stage injection struts combustion consists of auto-ignition pockets surrounded by self-igniting fronts embedded in a background of non-premixed flames or stirred reactors, whereas for the alternating- wedge injection strut vigorous combustion is observed proceeding through a multi-mode (auto-ignition, non-premixed, premixed) combustion event.

fureby@foi.se

5H05 DIRECT NUMERICAL SIMULATION OF SUPERSONIC COMBUSTION WITH THERMAL NONEQUILIBRIUM

Heeseok Koo¹, Venkat Raman², Philip L. Varghese²

¹Seoul National University, Korea ²The University of Texas at Austin, United States

Flow inside the combustor of a scramjet engine is likely to be in thermal nonequilibrium due to upstream shock-based compression. Given the short flow-through timescales in such engines, the flow will not reach equilibrium in the combustor. Since the distribution of energy in the internal modes affects chemical reactions, nonequilibrium could have significant impact on ignition and flame stabilization inside scramjet combustors. In this study, Direct Numerical Simulation (DNS) is used to understand the impact of thermal nonequilibrium on flame structure in a supersonic flow. The operating conditions correspond to the HyShot II scramjet experiment. A two-temperature model along with detailed chemical kinetics is used to model supersonic combustion. It is observed that when vibrational temperature is lower than translational temperature, there is significant delay in flame ignition. In addition, combustion reactions are weaker leading to reduced heat release. The vibrational temperature exhibits a broad dissipation structure compared to a conserved scalar, but contains thin dissipation elements near the shear layer between the fuel and oxidizer. There is a small improvement in turbulent mixing with nonequilibrium, primarily due to reduced viscosity arising from lower translational temperature in the domain. Overall, thermal equilibrium occurs over time scales longer than the integral scale, indicating that nonequilibrium will play a crucial role in the internal structure of the flame.

heeseokkoo@gmail.com

5H06 LARGE EDDY SIMULATIONS OF THE HIFIRE SCRAMJET USING A COMPRESSIBLE FLAMELET/PROGRESS VARIABLE APPROACH

Amirreza Saghafian, David A. Philips, Lee Shunn, Frank Ham, Cascade Technologies Inc., United States

In this study, Large Eddy Simulations (LES) of supersonic combustion using a Compressible Flamelet-Progress Variable (CFPV) approach are performed for the HIFiRE scramjet at Mach 8 flight conditions. The LES results show good agreements with the ground test experimental measurements. The combustion model is based on an efficient flamelet-based approach, where a detailed chemistry mechanism is used in a pre-processing step. In the CFPV model, compressibility corrections are devised based on assumed functional forms of important thermo-chemical quantities. Specifically, the source term of the progress variable is rescaled with the local density and temperature in the LES, leading to significantly improved predictions. A modified equilibrium wall-model, capable of predicting the viscous heating, is used in the viscous near-wall region. Temperature near the wall increases significantly due to viscous heating, enhancing the reaction rates and heat-release. This is shown to be a crucial step for accurately predicting the pressure rise in the combustor.

shunn@cascadetechnologies.com

5H07 THE EXPERIMENTAL AND MECHANISM STUDY OF NOVEL HETEROGENEOUS FENTON-LIKE REACTIONS USING $\text{Fe}_{3-x}\text{Ti}_x\text{O}_4$ CATALYSTS FOR Hg^0 ABSORPTION

Changsong Zhou¹, Lushi Sun¹, Jun Xiang¹, Song Hu¹, Sheng Su¹, Anchao Zhang²
¹Huazhong University of Science and Technology, China ²Henan Polytechnic University, China

The novel heterogeneous Fenton-like $\text{Fe}_{3-x}\text{Ti}_x\text{O}_4$ catalysts, prepared by co-precipitation method, have been used for Hg^0 absorption in a self-designed bubbling reactor system. The catalysts characterized by X-Ray Diffraction (XRD), X-ray Photoelectron Spectroscopy (XPS) and Scanning Electron Microscope (SEM) suggest that Ti successfully entered the structure of $\text{Fe}_{3-x}\text{Ti}_x\text{O}_4$ catalysts and Ti enriched on the surface of $\text{Fe}_{3-x}\text{Ti}_x\text{O}_4$. The important factors of H_2O_2 concentration and Ti content in $\text{Fe}_{3-x}\text{Ti}_x\text{O}_4$ are considered for Hg^0 absorption. The results show that $\text{Fe}_{3-x}\text{Ti}_x\text{O}_4$ can effectively decompose H_2O_2 generating highly reactive $\cdot\text{OH}$ radicals, and oxidize Hg^0 to Hg^{2+} in Fenton-like solutions. The mechanism model of Hg^0 absorption by heterogeneous Fenton-like reaction is preliminary established. Theoretical calculated results with the model are in good agreement with the experimental results, indicating that Hg^0 absorption is simultaneously controlled by solid-liquid surface oxidation and gas-liquid film oxidation, which are helpful to further explore the mechanism of Hg^0 absorption by heterogeneous Fenton-like reaction.

sunlushi@hust.edu.cn

5H08 HG OXIDATION REACTION MECHANISM OF Fe_2O_3 WITH H_2S : COMPARISON BETWEEN THEORY AND EXPERIMENTS

Lucheng Xue, Ting Liu, Xin Guo, Chuguang Zheng, Huazhong University of Science and Technology, China

A group of adsorption experiments were performed to clarify the mechanism of elemental mercury adsorption on Fe_2O_3 in the presence of H_2S . The roles of H_2S and Fe_2O_3 playing in the heterogeneous reaction were respectively discussed. A probable pathway of Hg^0 adsorption on Fe_2O_3 with H_2S was proposed in previous computational research. Corresponding experiments were designed to compare with theoretical results. The H_2S adsorption experiments and subsequent temperature programmed desorption analysis of derived sample indicate that H_2S can be adsorbed on the surface of Fe_2O_3 , which is in accordance with the computational results. Significantly high Hg^0 removal efficiency of H_2S adsorbed Fe_2O_3 verifies the strong interaction between gaseous mercury and adsorbed sulfur species which is inferred in the theoretical study. Combining experimental and computational results together, the Eley-Rideal mechanism with H_2S pre-adsorption can be determined.

guoxin@mail.hust.edu.cn

5H09 ANALYSIS OF MERCURY SPECIES OVER $\text{CuO-MnO}_2\text{-Fe}_2\text{O}_3/\gamma\text{-Al}_2\text{O}_3$ CATALYSTS BY THERMAL DESORPTION

Pengying Wang¹, Song Hu¹, Jun Xiang¹, Sheng Su¹, Lushi Sun¹, Fan Cao¹, Xi Xiao¹, Anchao Zhang²
¹Huazhong University of Science and Technology, China, ²Henan Polytechnic University, China

The efficiency of the $\text{CuO-MnO}_2\text{-Fe}_2\text{O}_3/\gamma\text{-Al}_2\text{O}_3$ (CMFA) catalysts on mercury oxidation and the effects of individual flue gas (O_2 , HCl , NO , SO_2) were investigated in our previous study. To elucidate the mercury oxidation mechanism, a Thermal Desorption (TD) method was applied in this study to analyze the characteristics of the mercury species formed on the CMFA catalysts. A series of pure mercury compounds mixed with fresh CMFA were first studied for qualitative calibration. Then, the TD method was employed to identify the Hg species on used CMFA catalysts pretreated under different operation conditions. The formation of HgO , HgCl_2 , $\text{Hg}(\text{NO}_3)_2$ and HgSO_4 during the oxidation process was confirmed and the reaction pathway proposed. The mercury species present were mainly HgCl_2 after CMFA catalysts were used to oxidize Hg^0 under simulated flue gas conditions. HgO and HgSO_4 were found to exist in very low concentrations. This has shown that the TD method is an efficient technique for mercury speciation on the catalyst surface.

husong_hust@hotmail.com

5H10 INSIGHTS INTO THE MECHANISM OF HETEROGENEOUS MERCURY OXIDATION BY HCl OVER VO_x/TiO_2 CATALYST: PERIODIC DENSITY FUNCTIONAL THEORY STUDY

Bingkai Zhang¹, Jing Liu¹, Guoliang Dai², Ming Chang³, Chuguang Zheng¹
¹Huazhong University of Science and Technology, China ²Suzhou University of Science and Technology, China
³Wuhan University of Technology, China

The Selective Catalytic Reduction (SCR) for the reduction of NO_x can enhance the oxidation of elemental mercury, which is regarded as a low-cost option for mercury control in coal-fired power plants. First-principles calculations based on the density functional theory and the periodic slab models were used to gain a fundamental understanding of mercury oxidation mechanism across VO_x/TiO_2 SCR catalyst. The adsorption of Hg^0 , HCl , HgCl , and HgCl_2 on $\text{VO}_x/\text{TiO}_2(001)$ surface were studied. The energy profile of the oxidation reaction and the structures of related transition states and intermediates were examined. The results show that Hg^0 is mainly physically absorbed on vanadyl-oxygen sites of the $\text{VO}_x/\text{TiO}_2(001)$ surface with an adsorption energy of -27.93 kJ/mol. HCl is chemisorbed on vanadyl-oxygen sites of $\text{VO}_x/\text{TiO}_2(001)$ surface, and can undergoes dissociation process with an energy barrier of 101.53 kJ/mol to form the vanadium oxy-chloride complex which is essential in Hg^0 oxidation reaction on $\text{VO}_x/\text{TiO}_2(001)$ surface. The mercury

oxidation reaction occurs through an Eley-Rideal mechanism in which Hg reacts with HCl that has previously been adsorbed and dissociated on $\text{VO}_x/\text{TiO}_2(001)$ surface to form surface HgCl , and then surface HgCl reacts with HCl to form HgCl_2 , finally HgCl_2 desorbs from the $\text{VO}_x/\text{TiO}_2(001)$ surface. In the whole Hg oxidation reaction, the formation of HgCl_2 is the rate-determining step based on its high energy barrier.

liujing27@mail.hust.edu.cn

5H11 RELEASE OF ORGANIC SULFUR AS SULFUR-CONTAINING GASES DURING LOW TEMPERATURE PYROLYSIS OF SEWAGE SLUDGE

Shuai Liu¹, Mengmeng Wei¹, Yu Qiao¹, Zhenle Yang¹, Ben Gui¹, Yun Yu², Minghou Xu¹

¹Huazhong University of Science and Technology, China ²Curtin University, Australia

This study reports the release of five sulfur-containing odorants (H_2S , SO_2 , COS , CS_2 and CH_3SH) during sewage sludge pyrolysis. Pyrolysis experiments using both the raw sewage sludge sample and seven sludge samples loaded with various organic sulfur compounds were performed to understand the effect of organic sulfur type on the release of sulfur-containing gases. It was observed that the formation of H_2S as the predominant odorant significantly increases at temperatures above 150°C . Aliphatic and aromatic sulfur compounds were found to be the main two organic sulfur sources for the release of sulfur-containing gases. The release of sulfur-containing gases from aliphatic sulfur greatly increases at 250°C , whereas significant sulfur-containing gases are released from aromatic sulfur at a relatively high temperature of $350 - 450^\circ\text{C}$. It was also found that sulfonic acid and thiophene in sludge do not significantly affect the release of sulfur-containing gases.

yuqiao@hust.edu.cn

5H12 CATALYTIC ROLE OF CONDITIONER CaO IN NITROGEN TRANSFORMATION DURING SEWAGE SLUDGE PYROLYSIS

Huan Liu, Qiang Zhang, Hongyun Hu, Peng Liu, Xiaowei Hu, Aijun Li, Hong Yao, University of Science and Technology, China

Thermal disposal of sewage sludge is likely to cause serious nitrogen related environmental pollution since it contains considerable amounts of nitrogen, whose species are quite different from that in coal. Considering that lime (CaO) is a widely applied chemical conditioner for sewage sludge dewatering, this study investigated the catalytic role of conditioner CaO in nitrogen transformation during sewage sludge pyrolysis in a drop-tube/fixed-bed furnace at 873 K , 973 K and 1073 K , respectively. Model compounds were also used to further clarify the mechanisms involved. According to the results, conditioner CaO increased the fraction of more stable protein-N as well as amine-N. The solid phase reactions produced CaC_xN_y , thus enhancing the nitrogen retention in char. Correspondingly, decreased relative ratio of nitrates-N/nitrites-N and oxygenated organics in sludge conditioning contributed to the less NO emission. Meanwhile, conditioner CaO promoted the conversion of HCN to NH_3 , as well as the deamination of proteins, amine, and other N-containing compounds in tar and char, leading to increased NH_3 generation. Subsequently, CaC_x , the decomposition product of CaC_xN_y , captured NH_3 , driving down the final production of NH_3 . In addition, $\text{Ca}(\text{OH})_2$ hindered the transformation of nitrile-N in char to HCN , decreasing HCN generation. CaO reacted with HCN , further reducing its releasing amount. CaC_xN_y derived from different sources decomposed to produce a very large amount of N_2 . These indicate that reusing conditioner CaO is a promising strategy for reducing the productions of NO_x precursors efficiently and increasing the formation of non-polluting N_2 dramatically.

hyao@mail.hust.edu.cn

5H13 SPECIATION TRANSFORMATION OF ARSENIC DURING MUNICIPAL SOLID WASTE INCINERATION

Hongyun Hu¹, Huan Liu¹, Juan Chen¹, Aijun Li¹, Hong Yao¹, Fiona Low², Lian Zhang²

¹Huazhong University of Science and Technology, China ²Monash University, Australia

The release of Arsenic (As) during Municipal Solid Waste (MSW) incineration results in a new sources of anthropogenic arsenic contamination. Arsenic toxicity depends not only on the quantity but also on its speciation. At high temperatures, arsenic is predominantly present as vapors ($\text{As}_2\text{O}_3(\text{g})$) and its speciation transformation is determined by the interactions between $\text{As}_2\text{O}_3(\text{g})$ and inorganic compounds. In this study, synchrotron X-ray Absorption Near-Edge Structure (XANES) was used to investigate the speciation transformation of arsenic during MSW combustion and flue gas cooling process. However, arsenates in various forms are hardly distinguished by using XANES alone. Considering that various arsenates are of different thermal stability, the thermal stability of arsenic in MSW incineration fly ash was examined to provide detailed information regarding arsenic speciation in the ash samples. To further understand the relationships between arsenic and inorganic compounds, the sequential extraction procedures of arsenic in the ash were conducted. The results show that the oxidation of $\text{As}_2\text{O}_3(\text{g})$ during MSW combustion is incomplete and is continuously performed in flue gas cooling process. The physical adsorption of $\text{As}_2\text{O}_3(\text{g})$ is favored at low temperature by ash particles, especially by the injection of CaO in the flue gas. Various kinds of arsenates are formed due to the interactions between $\text{As}_2\text{O}_3(\text{g})$ and Ca, Fe and/or Al compounds. Some of the arsenates are thermally unstable and are decomposed when the fly ash was heated at

1323 K. Part of arsenic is stabilized in the ash matrix including some un-oxidized As(III) which remained stable even when the ash was heated at 1323 K.

hyao@mail.hust.edu.cn

MONDAY Work-in-Progress Posters

- W1P001: EFFECTS OF BURNING RENEWABLE FUELS IN A VARIABLE GEOMETRY LOW SWIRL INJECTOR OPERATED IN A BOILER ENVIRONMENT
Vincent G. McDonnell, Nathan Kirksey
- W1P002: OXYGEN-ENRICHED CO-COMBUSTION OF BIOMASS FOR CCS APPLICATIONS
William Nimmo, Mohamed Pourkashanian, Sam Pickard
- W1P003: EFFECT OF CATALYTIC PRE-COMBUSTION ON FLAME STABILITY IN HIGHLY CONCENTRATED CO₂
Toshinori Nagai, Takeshi Yokomori
- W1P004: SIMPLE METHODOLOGY FOR CONSTRUCTING OVERALL REACTION MECHANISMS USING A MICRO FLOW REACTOR WITH A CONTROLLED TEMPERATURE PROFILE
Shogo Onishi, Kaoru Maruta, Hisashi Nakamura, Takuya Tezuka, Susumu Hasegawa
- W1P005: FORMALDEHYDE ENHANCEMENT BY OZONE ADDITION IN CH₄/AIR PREMIXED FLAMES
Wubin Weng, Elna Nisson, Andreas Ehn, Zhihua Wang, Zhongshan Li
- W1P006: AN EXPERIMENTAL STUDY OF THE EFFECT OF HYDROGEN ADDITIVE ON A PRIMARY REFERENCE FUEL HCCI COMBUSTION
Hyunsoo An, Seunghyeon Lee, Kwangmin Chun, Soonho Song
- W1P007: MODELING REGENERATION RATES OF SUPPORTED PARTICLES IN CHEMICAL LOOPING COMBUSTION SYSTEMS
Eli A. Goldstein, Reginald E. Mitchell, Turgut M. Gur
- W1P008: THE ROLE OF CO₂ AND H₂O ON IGNITION CHEMISTRY OF SIMPLE HYDROCARBONS
Pino Sabia, Mara de Joannan, Marco Lubrano Lavadera, Raffaele Ragucci
- W1P009: CHARACTERIZATION OF LITHIUM COMBUSTION FOR THE USE AS ENERGY CARRIER IN A RENEWABLE ENERGY CYCLE
Julia Koppmann, Andreas Brockhinke, Regina Brockhinke
- W1P010: EXERGY ANALYSIS ON EFFECTIVE UTILIZATION OF METHANE/AIR AND METHANE/O₂ COMBUSTION
Tsukasa Hori, Akeshi Kegasa, Akane Nagasaki, Yosuke Shiraga, Yoshinori Hisazumi
- W1P011: ELECTRIC FIELD EFFECTS ON CO EMISSION FROM NON-PREMIXED QUENCHING FLAMES
Yu-Chien (Alice) Chien, David Escofet Martin, Derek Dunn-Rankin
- W1P012: FLOW AND ELECTRICAL CHARACTERISTICS OF COUNTERFLOW NONPREMIXED LAMINAR FLAMES WITH DC ELECTRIC FIELDS
Daegeun Park, Min Suk Cha, Suk-Ho Chung
- W1P013: APPLICATION OF A COMPREHENSIVE MODEL FOR THE TRANSPORT OF ELECTRONS AND CHARGED SPECIES IN PREMIXED FLAMES WITH AN EXTERNAL ELECTRICAL FIELD
Jie Han, Fabrizio Bisetti, Mani Sarathy, Tiernan Casey, Paul G. Arias, Hong G. Im, Jyh-Yuan Chen
- W1P014: FLAME-ASSISTED FUEL CELL FURNACE FOR MICRO COMBINED HEATING AND POWER (FFH microCHP)
Ryan Milcarek, Jeongmin Ahn, Kang Wang
- W1P015: INTEGRATED ANAEROBIC DIGESTER AND FUEL CELL POWER GENERATION SYSTEM FOR COMMUNITY USE
Ryan Falkenstein-Smith, Kang Wang, Jeongmin Ahn
- W1P016: THE CHARACTERISTICS OF ADDING CARBON DIOXIDE IN A COFLOW ON LIFTOFF METHANE DIFFUSION FLAME
Yung-Sheng Lien, Yei-Chin Chao
- W1P017: THE DEVELOPMENT OF A NOVEL MICROWAVE-PLASMA STABILIZATION MECHANISM FOR FLAME STABILIZATION
Hong Yuan Li, Yueh Heng Li, Yei Chin Chao
- W1P018: THE EFFECTS OF UNBURNED-GAS TEMPERATURE ON INTRINSIC INSTABILITIES OF 3-D PREMIXED FLAMES
Satoshi Kadowaki, Takuto Yanagioka, Wataru Yamazaki, Hideaki Kobayashi
- W1P019: EFFECT OF HYDROGEN ADDITION ON OH DISTRIBUTION OF INVERSE DIFFUSION FLAME BURNING LPG FUEL
Jing Miao
- W1P020: EXPERIMENTAL STUDY ON FLAMMABILITY OF R1234ze IN THE PRESENCE OF MOISTURE
Tei Saburi, Akira Matsugi, Hiroumi Shiina, Akifumi Takahashi, Yuji Wada
- W1P021: AIR/STEAM BLOWN GASIFICATION OF LIGNIN FROM BIO-REFINERY PROCESS OF PULP MILL
Jihong Moon, Suji Jeon, Jeongjun Yoon, Uendo Lee, Byunghwan Um
- W1P022: OXIDATION AND IGNITION STUDY OF 2-METHYL HEXANE IN A MICRO FLOW REACTOR WITH CONTROLLED TEMPERATURE PROFILE
Muneeb Khurshid, Hisashi Nakamura, Kaoru Maruta, S. Mani Sarathy
- W1P023: OH-LIF MEASUREMENT OF H₂/O₂/N₂ FLAMES IN A MICRO FLOW REACTOR WITH A CONTROLLED TEMPERATURE PROFILE
Takashige Shimizu, Takuya Tezuka, Susumu Hasegawa, Hisashi Nakamura, Kaoru Maruta
- W1P024: LES MODELLING OF MESOCOMBUSTION CHAMBERS WITH ARRHENIUS COMPLEX CHEMISTRY
Pierre Benard, Vincent Moureau, Ghislain Lartigue, Yves D'Angelo

- W1P025: EXPERIMENTAL STUDY ON MESO-SCALE TUBE COMBUSTORS WITH MULTI-JET-MODE ELECTROSPRAY
Naoyuki Hatakedda, Fudhail BinAbdulMunir, Masato Mikami, Takehiko Seo
- W1P026: OBSERVATIONS OF THE PROPAGATION OF LEAN PREMIXED FLAMES IN MESO-SCALE TUBES
Chris Lawn, Hamisu Adamu Dandajeh
- W1P027: COMBUSTION CHARACTERISTICS OF N-HEPTANE DROPLET IN A MESO-SCALE TUBE
Junwei Li
- W1P028: EXPERIMENTAL AND NUMERICAL STUDY OF MILD COMBUSTION IN A CYCLONIC BURNER
Giancarlo Sorrentino, Pino Sabia, Mara de Joannon, Raffaele Ragucci, Antonio Cavaliere, Ugur Goktolga, Jeroen van Oijen, Philip de Goey
- W1P029: INFLUENCE OF PREMIXING AND RESIDENCE TIME ON MILD COMBUSTION IN A REVERSE FLOW CONFIGURATION
Stephan Kruse, Emilien Varea, Veronika Wassmuth, Heinz Pitsch
- W1P030: CHARACTERISTICS OF THE MICROWAVE INDUCED FLAMES ON THE STABILITY AND EMISSIONS
Young Hoon Jeon, Eui Ju Lee
- W1P031: EFFECT OF FLUE GAS AND DEPOSIT COMPOSITION ON CORROSION AND DEPOSITION IN OXY-FUEL ENVIRONMENTS
William Nimmo, Mohamed Pourkashanian, Toor-E-Aiman Rizvi
- W1P032: COMPARISON OF THERMODYNAMICAL POTENTIALS OF OXY-FUEL COMBUSTION, NORMAL AIR-COMBUTION AND REGENERATIVE COMBUSTION
Kenichi Sato, Osamu Fujita
- W1P033: COMBUSTION OF LIGNITE AND ITS CHARS IN AIR AND OXY CONDITIONS
Michal Ostrycharczyk, Jakub Dlugosz, Halina Pawlak-Kruczek, Jacek Zgora
- W1P034: OXY-FUEL COMBUSTION PERFORMANCE EVALUATION IN A 250 KW TEST FACILITY
William Nimmo, Janos Szuhanski, Sandy Black, Mohamed Pourkashanian
- W1P035: COMBUSTION CHARACTERISTICS OF OXY-FUEL STAGED COMBUSTION WITH A RAPIDLY-MIXED TYPE TUBULAR FLAME BURNER
Akane Nagasaki, Akeshi Kegasa, Tsukasa Hori, Yosuke Shiraga, Hiroki Shibagaki
- W1P036: CHARACTERISTICS OF EXHAUST EMISSION OF LAMINAR INVERSE DIFFUSION FLAMES ON OXY-FUEL COMBUSTION
Tomohiro Yamanaka, Nichiki Okada, Shuhei Yoneyama, Takeshi Yokomori
- W1P037: TRANSIENT PLASMA: A UNIQUE TOOL FOR REDUCING SOOT AND NO_x
Bikau Shukla, Kian Eiszadeh-Far, William Schroeder, Daniel Singleton, Martin Gundersen, Fokion N. Egolfopoulos
- W1P038: FUEL-RICH PARTIAL OXIDATION BY REACTIVE VOLATILIZATION
Will Northrop
- W1P039: A THERMAL PARTIAL OXIDATION “SWISS-ROLL” FUEL REFORMER
Chien-Hua Chen, Howard Pearlman, Paul D. Ronney, Shrey Trivedi, Andrew Lawson, Swapnil Desai, Srushti Koli
- W1P040: THE COMBUSTION CHARACTERISTICS OF PREMIXED PROPANE/AIR FLAME IN MOVING CERAMIC GRANULAR BED
Ian Shou-Yin Yang, De-Li Hsu
- W1P041: EXPERIMENTAL AND NUMERICAL INVESTIGATIONS OF METHANE THERMAL PARTIAL OXIDATION IN A SMALL-SCALE POROUS MEDIA REFORMER
Alexandra Loukou, Miguel Mendes
- W1P042: A DISCRETE QUASI THREE-DIMENSIONAL MODEL OF GAS COMBUSTION IN POROUS MEDIA
Fedir Sirotkin, Sergey Minaev, Roman Fursenko
- W1P043: POROUS INSERTS FOR PASSIVE CONTROL OF NOISE AND THERMO-ACOUSTIC INSTABILITIES IN LDI COMBUSTION
Ajay K. Agrawal, Joseph Meadows
- W1P044: THERMAL TRANSPIRATION BASED PUMPING AND PROPULSION DEVICE
Shirin Jouzdani, Ryan Falkenstein-Smith, Jeongmin Ahn, Pingying Zeng
- W1P045: FORMATION OF SYNTHESIS GAS BY SUPER ADIABATIC FLAME FOR HIGH TEMPERATURE FUEL CELLS
Pil Hyong Lee, Chun Loon Cha, Sang Soon Hwang
- W1P046: FLAMELESS COMBUSTION OF LIQUID FUEL FOR GAS TURBINE
Chun Loon Cha, Pil Hyong Lee, Ho Yeon Lee, Sang Soon Hwang
- W1P047: THE APPLICATION TO SMOKE TUBE AND FLUE BOILER COMBUSTION OF NEW ENERGY SAVING TECHNIQUE USING ELECTRO-MAGNETIC WAVE IN THE RANGE OF FAR INFRARED RAY
Satoshi Okajima
- W1P048: GENERATION OF HYDROTHERMAL FLAMES IN A MOBILE SUPERCRITICAL WATER OXIDATION REACTOR
Sivamohan N. Reddy, Sonil Nanda, Janusz Kozinski, Michael C. Hicks, Uday G. Hegde
- W1P049: CO-GENERATION OF HYDROGEN AND ELECTRICITY FROM SOLID FUELS IN A NOVEL CARBON FUEL CELL
David Johnson, S. Michael Stewart, Brandon Loong, Turgut M. Gur, Reginald E. Mitchell

- W1P050: A CERAMIC-MEMBRANE-BASED METHANE COMBUSTION REACTOR WITH TAILORED FUNCTION OF SIMULTANEOUS SEPARATION OF CARBON DIOXIDE FROM NITROGEN
Pingying Zeng, Kang Wang, Ryan Falkenstein-Smith, Jeongmin Ahn
- W1P051: CONTROL OF BUOYANCY-DRIVEN INSTABILITY IN LIFTED FLAMES BY AC ELECTRIC FIELDS
Minkuk Kim, Suk-Ho Chung
- W1P052: PT-NANOPARTICLES: SYNTHESIS, CHARACTERIZATION AND TESTING IN A CATALYTIC FLOW REACTOR WITH APPLICATION TO MICROCOMBUSTORS
Smitesh Bakrania, Howard Pearlman, James Applegate, Dylan McNally, Marika Agnello, Brigitte Pastore
- W1P053: PLIF MEASUREMENT OF OH GENERATED WITH PULSED ARC DISCHARGE FOR RADICAL QUENCHING STUDY
Sui Wan, Yuji Suzuki, Weirong Lin
- W1P054: SPECTROSCOPIC ANALYSIS OF THE RESPONSE OF A LAMINAR PREMIXED FLAME TO EXCITATION BY NANOSECOND GLOW DISCHARGES
Deanna Lacoste, Jonas Moeck
- W1P055: ION MEASUREMENTS IN PREMIXED METHANE-OXYGEN FLAMES
Awad Alquaity, Nadim Hourani, May Chahine, Mani Sarathy, Aamir Farooq
- W1P057: CHARACTERISTICS OF NON-PREMIXED OXYGEN ENRICHED FLAMES FROM A SWIRL BURNER WITH A RADIAL FUEL INJECTION
Toufik Boushaki, Nazim Merlo, Christian Chauveau, Iskender Gökalp, Stephanie de Persis
- W1P058: REALIZATION OF THE EFFECT OF SELF-DILUTION CHARACTERISTICS IN CONFINED FLAMES ON NO_x ABATEMENT
Kapuruge Don Kunkuma Amila Somarathne, Susumu Noda
- W1P059: INVESTIGATION OF WALL THERMAL CONDUCTIVITY EFFECTS ON COMBUSTION STABILITY IN MESO-SCALE TUBE COMBUSTORS WITH WIRE MESH
Fudhail BinAbdulMunir, Naoyuki Hatakeda, Takehiko Seo, Masato Mikami
- W1P060: INFLUENCE OF SIMULATED CONCENTRATED SOLAR RADIATION ON A LAMINAR SOOTY FLAME
Xue Dong
- W1P061: JOINT INFLUENCE OF IGNITION ENERGY AND GAS DYNAMICS ON COMBUSTION IN A CONSTANT VOLUME COMBUSTION CHAMBER APPLIED TO AIR-BREATHING PROPULSION
Bastien Boust, Marc Bellenoue, Julien Sotton
- W1P062: STRUCTURE OF METHANE INVERSED DIFFUSION FLAMES WITH SIMULATED PRE-HEATED CO-FLOW COMBUSTION PRODUCTS
Zakaria Movahedi, Xisheng Zhao, Andrzej Sobiesiak
- W1P063: LASER IGNITION OF METHANE HYDRATES
Michela Vicariotto
- W1P064: AMMONIA/AIR FLAMES IN A MICRO FLOW REACTOR WITH A CONTROLLED TEMPERATURE PROFILE
Hisashi Nakamura, Takuya Tezuka, Susumu Hasegawa, Kaoru Maruta
- W1P065: OSCILLATION OF OPPOSED FLOW FLAMES WITHIN A MESOSCALE CHANNEL AT LOW STRAIN RATE CONDITIONS
Min Jung Lee
- W1P066: DEVELOPMENT AND COMBUSTION CHARACTERIZATION OF AN INDUSTRIAL SIZE FLOW BLURRING INJECTOR
Ajay K. Agrawal, Yonas Niguse
- W1P067: COMPARISON OF BIOMASS PULVERISED FUEL IGNITION BEHAVIOUR IN AIR AND OXYGEN/CARBON DIOXIDE MIXTURES USING A 20-L SPHERE APPARATUS
Ignacio Trabadela, Hannah Chalmers, Jon Gibbins
- W1P068: AN EXPERIMENTAL STUDY ON LOW NO_x PETROLEUM COKES COMBUSTION SYSTEM
Sewon Kim, Changyeop Lee, Minjun Kwon
- W1P069: BIODIESEL FUEL REFORMING BY OZONE-RICH AIR AND NUMERICAL SIMULATION OF COMBUSTION PROCESSES
Takaaki Morimune
- W1P070: PARTICLES EMISSION FROM PASSENGER CAR ENGINE USING COMMERCIAL DIESEL AND FISCHER-TROPSCH FUELS
Azhar Malik
- W1P071: A COMPUTATIONAL INVESTIGATION OF THE RELATIONSHIP BETWEEN FLAME LIFT-OFF HEIGHT AND SOOT CONCENTRATION IN DIESEL JETS
May Yen, Vinicio Magi, John Abraham
- W1P072: EXPERIMENTS AND COMPUTATIONAL MODELING OF NATURAL GAS/DIESEL DUAL FUEL COMBUSTION WITH EXPLORATION OF UNCONTROLLED COMBUSTION RATES
Andrew Hockett, Anthony Marchese, Greg Hampson, Jason Barta, Marc Baumgardner, Nolan Polley
- W1P073: NUMERICAL STUDY ON EFFECTS AND DESIGNING LIMITATIONS OF VALVE TIMING IN THE DUAL FUEL ENGINE THAT IS MODIFIED FROM DIESEL ENGINE
Jungkeun Cho, Sangjun Park, Jungsoo Park, Soonho Song

- W1P074: TOWARDS A BETTER UNDERSTANDING OF HOW POST-INJECTIONS AFFECT SOOT OXIDATION USING LASER DIAGNOSTICS IN AN OPTICAL DIESEL ENGINE
Jacqueline O'Connor, Mark Musculus
- W1P075: A NUMERICAL STUDY ON PREDICTION OF THE PERFORMANCE AND NO_x EMISSIONS IN A LIGHT-DUTY DIESEL ENGINE WITH SYNGAS ADDITION
Sangjun Park, Jungsoo Park, Soonho Song, Kwang Min Chun
- W1P076: CHARACTERIZATION OF GASEOUS AND PARTICULATE EMISSIONS FROM THE COMBUSTION OF CELLULOSIC BIOMASS BASED OXYGENATED COMPONENTS IN A COMPRESSION IGNITION ENGINE
Tim Vaughn, Aaron Drenth, Arunachalam Lakshminarayanan, Daniel Olsen, Matthew Ratcliff, Robert McCormick, Anthony John Marchese
- W1P077: RECESSION OF SECOND-STAGE IGNITION AFTER END-OF-INJECTION IN DIESEL-LIKE SPRAYS
Benjamin Knox, Caroline Genzale
- W1P078: SOOT LUMINOSITY AND LASER-INDUCED INCANDESCENCE OF DIESEL SPRAY COMBUSTION: CHARACTERISTICS AND CORRELATION ANALYSIS
Seong-Young Lee, Anqi Zhang, Jeffrey Naber, Luigi Allocca, Alessandro Montanaro
- W1P079: EFFICIENT IMPLEMENTATION OF DETAILED SOOT MODELS IN INTERNAL COMBUSTION ENGINE SIMULATIONS
Zhaoyu Luo, Mandhapat P. Raju, Tom Malewicki, Peter Kelly Senecal, Harry Lehtiniemi, Cathleen Perlman, Fabian Mauß, Tushar Shethaji, Yuanlong Li
- W1P080: INVESTIGATING PHYSICAL CONDENSATION PROCESSES IN ADVANCED LOW TEMPERATURE COMBUSTION ENGINES
Lu Qiu, Rolf D. Reitz
- W1P081: MECHANISMS OF PRESSURE WAVE GENERATIONS IN END-GAS AUTOIGNITION: COMPRESSIBLE FLOW SIMULATIONS WITH DETAILED CHEMISTRY
Hiroshi Terashima, Mitsuo Koshi
- W1P082: NEXT GENERATION KNOCK CHARACTERIZATION
Howard Levinsky, Sander Gersen, Martijn Van Essen, Gerco van Dijk
- W1P083: ROLE OF KINETICS IN HCCI COMBUSTION
Mattia Bissoli, Alessio Frassoldati, Alberto Cuoci, Tiziano Faravelli, Eliseo Ranzi, G. Natta
- W1P084: A NEW FUEL INDEX FOR LTC ENGINES BASED ON OPERATING ENVELOPES IN LIGHT-DUTY DRIVING CYCLE SIMULATIONS
Kyle Niemeyer, Shane Daly, William Cannella, Chris Hagen
- W1P087: KINETIC AND NUMERICAL STUDY ON THE EFFECTS OF DTBP ADDITIVE ON THE REACTIVITY OF METHANOL AND ETHANOL
Hu Wang, Rolf D. Reitz, Mingfa Yao, Ming Jia
- W1P088: HIGH-SPEED OPTICAL CHARACTERIZATION OF TRANSIENT INJECTION EVENTS IN AN ENGINE
Nicholas Neal, David Rothamer
- W1P089: TIME-SERIES ANALYSIS OF RADICAL EMISSIONS USING A SPARK PLUG WITH OPTICAL FIBER
Nobuyuki Kawahara, Shota Hashimoto, Eiji Tomita
- W1P090: EFFECTS OF HYDROGEN AS AN ADDITIVE ON EMISSION GAS OF TURBO GASOLINE DIRECT INJECTION ENGINE
Joonsuk Kim, Jungmin Seok, Soonho Song
- W1P091: RESEARCH IDENTIFICATION ON MIXTURE COMBUSTION CREATED BY TWO GDI INJECTORS IN SI ENGINE
Ireneusz Pielecha, Przemyslaw Borowski, Jakub Czajka, Wojciech Cieslik, Wojciech Bueschke, Krzysztof Wislocki
- W1P092: THERMODIFFUSIVE EFFECTS IN SPARK-IGNITION ENGINES
Pierre Brequigny, Christine Mounaim-Rousselle, Fabien Halter, Thomas Dubois
- W1P093: INVESTIGATION OF PARTIALLY PREMIXED COMBUSTION IN A LIGHT DUTY ENGINE USING MULTIPLE INJECTIONS
Zhenkan Wang, Slavey Tanov, Richter Mattias, Johansson Bengt, Marcus Aldén
- W1P095: EFFECTS OF BOOST PRESSURE AND INTAKE TEMPERATURE ON THE EMISSION OF A CNG-FUELED HCCI ENGINE FOR ELECTRIC GENERATOR
Hyunwoo Song, Soonho Song
- W1P096: EXPERIMENTAL PERFORMANCE AND EMISSION CHARACTERISTICS OF A SPLIT-CYCLE ENGINE FUELLED WITH NATURAL GAS
Iain Cameron, Andrzej Sobiesiak
- W1P097: EXPLORING THE DYNAMICS OF CYCLE-TO-CYCLE VARIABILITY USING MANY HIGH-DIMENSIONAL SINGLE-CYCLE SIMULATIONS
Charles E.A. Finney, Miroslav K. Stoyanov, K. Dean Edwards, C. Stuart Daw
- W1P098: OPTICAL CHARACTERIZATION OF STRATIFIED COMBUSTION IN A DIRECT-INJECTED GASOLINE ENGINE
Mats Andersson, Lars Christian Riis Johansen, Eugenio de Benito, Stina Hemdal
- W1P099: EFFECT OF SPLIT MICRO-PILOT FUEL INJECTION ON ENGINE PERFORMANCE, EXHAUST EMISSIONS, FLAME DEVELOPMENT AND OPERATION RANGE OF PREMIER COMBUSTION IN A DUAL FUEL ENGINE USING NATURAL GAS
Cagdas Aksu, Eiji Tomita, Nobuyuki Kawahara, Kazuya Tsuboi, Shun Nanba, Morio Kondo
- W1P100: INVESTIGATION OF THE COMBUSTION AND SOOTING BEHAVIOR OF ETHANOL-BLENDED DISI-SPRAYS IN A CONSTANT-VOLUME CHAMBER
Stefan Will, Michael Storch, Lars Zigan, Michael Wensing

- W1P101: DIRECT NUMERICAL SIMULATIONS OF THE EFFECTS OF NTC REGIME ON THE IGNITION OF A LEAN *N*-HEPTANE/AIR MIXTURE WITH TEMPERATURE AND COMPOSITION INHOMOGENETIES
Chun Sang Yoo, Minh Bau Luong, Gwang Hyeon, Yu Ulsan, Suk-Ho Chung
- W1P102: ASSESSMENT OF CONDITIONAL MOMENT CLOSURE FOR MODELLING AUTO-IGNITION IN COMPOSITIONALLY STRATIFIED *N*-HEPTANE/AIR MIXTURES USING DIRECT NUMERICAL SIMULATION
James Behzadi, Mohsen Talei, Evatt Hawkes, Tommaso Lucchini, Gianluca D'Errico, Sanghoon Kook
- W1P103: DNS ASSESSMENT OF FLAMELET MODELS FOR LES OF DIESEL JETS
Muhsin Ameen, Vinicio Magi, John Abraham
- W1P104: SIMULATIONS OF AUTOIGNITION-ASSISTED FLAME PROPAGATION IN RCCI-BASED ENGINES
Ankit Bhagatwala, Ramanan Sankaran, Sage Kokjohn, Jacqueline H. Chen
- W1P105: LARGE EDDY SIMULATION OF AN INTERNAL COMBUSTION ENGINE USING AN EFFICIENT IMMersed BOUNDARY TECHNIQUE
Thuong Nguyen, Andreas Kempf, Fabian Proch, Irenaeus Wlokas
- W1P106: PENETRATION OF FLAME AND BURNT GASES INTO THE TOP-LAND CREVICE – LARGE-EDDY SIMULATION AND EXPERIMENTAL HIGH-SPEED VISUALIZATION
Sebastian Kaiser, Peter Janas, Martin Schild, Andreas Kempf
- W1P107: INVESTIGATION OF ROLE OF PLASMA FOR LASER-INDUCED BREAKDOWN IGNITION IN FUEL-RICH PREMIXED ETHANOL SPRAY FLOW
Takehiko Seo, Yuki Ishimura, Masato Mikami
- W1P108: TRANSIENT PLASMA DISCHARGE IGNITION FOR INTERNAL COMBUSTION ENGINES
Si Shen, Kanchana Gunasekera, Jie Yang, Jonathan Flamenco, Paul D. Ronney
- W1P109: THE EFFECT OF DISCHARGE-INDUCED RADICALS ON FLAME KERNEL FORMATION: A COMPREHENSIVE SPARK IGNITION MODEL
Seong-Young Lee, Anqi Zhang, Xiucheng Zhu, Jeffrey Naber
- W1P110: AN ANALYSIS OF ION CURRENT IN A CONSTANT-VOLUME COMBUSTOR
Seiya Hitomi, Yoshiki Noguchi, Ralph Aldredege, Yuki Tsuzuki
- W1P111: RCM CHARACTERIZATION INITIATIVE: TOWARDS HARMONIZING IGNITION DATA
Guillaume Vanhove, Scott Goldsborough, Chih-Jen Sung, Henry Curran, Margaret Wooldridge
- W1P112: COMPUTATIONAL INVESTIGATION OF SYNGAS AUTOIGNITION BEHAVIOR AT HIGH PRESSURE AND LOW TEMPERATURE CONDITIONS IN THE PRESENCE OF THERMAL INHOMOGENETIES
Pinaki Pal, Andrew Mansfield, Margaret Wooldridge, Hong Im
- W1P113: IGNITION OF COMBUSTIBLE MIXTURES BY A SURFACE NANOSECOND DISCHARGE IN A RAPID COMPRESSION MACHINE
Mohamed A. Boumehdi, Sergey Stepanyan, Sergey Shcherdanev, Svetlana Starikovskaya, Pascale Desgroux, Guillaume Vanhove
- W1P114: LARGE-EDDY-SIMULATION OF RICH-QUENCH-LEAN COMBUSTOR
Masahiro Uchida, Shintaro Ito
- W1P115: THE INTERACTION BETWEEN PILOT AND MAIN FLAMES IN A DUAL SWIRL COMBUSTOR
Taejoon Park, Keeman Lee, Dongsoo Noh
- W1P116: COMBUSTION INSTABILITY MODE IN DUAL SWIRL GAS TURBINE MODEL BURNER BY HS-PLIF AND CHEMILUMINESCENCE MEASUREMENT
Keeman Lee, Inchan Choi
- W1P117: DYNAMICAL STRUCTURE OF THERMOACOUSTIC COMBUSTION OSCILLATIONS IN A LABORATORY-SCALE GAS-TURBINE MODEL COMBUSTOR
Yuta Okuno, Shohei Domen, Hiroshi Gotoda
- W1P118: INVESTIGATION OF TURBULENT COMBUSTION IN A GAS TURBINE COMBUSTOR BY THE SCALE-ADAPTIVE SIMULATION METHODS
Seyfettin Ertan Hataysal, Ahmet Yozgatligil
- W1P119: FLAMEHOLDING PROPENSITIES OF SMALL FEATURE STABILIZED HYDROGEN AND NATURAL GAS FLAMES AT HIGH TEMPERATURES AND PRESSURES
Vincent G. McDonell, Elliot Sullivan-Lewis
- W1P120: ACTIVE COMBUSTION CONTROL OF AUGMENTOR INSTABILITY
Kenneth Yu, Sammy Park
- W1P121: COMBUSTION INSTABILITY ANALYSIS FOR PARTIALLY PREMIXED SWIRLING SYNGAS BURNERS
Youngjun Shin, Kiyoung Jung, Seungtaek Oh, Yongmo Kim
- W1P122: CORRELATION OF DEFECTS IN AIRCRAFT ENGINES BY OPTICAL MEASURING EXHAUST GASES AND NUMERICAL ANALYSIS
Christoph Hennecke, Friedrich Dinkelacker
- W1P123: EVALUATION OF CFD MODELS TO PREDICTING NO_x EMISSIONS IN A GAS TURBINE COMBUSTOR
Fulin Lei
- W1P124: DEVELOPMENT OF A HYBRID-MODEL FOR CH₄ EMISSIONS IN BIOGAS ENGINES
Kalyan Kuppa, Ansgar Ratzke, Friedrich Dinkelacker

- W1P125: APPLICATION OF A CHEMICAL REACTOR NETWORK FOR PREDICTION OF NO_x EMISSIONS FROM PREMIXED NATURAL GAS AND HYDROGEN ENRICHED FLAMES STABILIZED WITH A LOW-SWIRL BURNER
Vincent G. McDonnell, Andres Colorado
- W1P126: CHARACTERIZING NO_x EMISSION BEHAVIOR IN THE WAKE OF SINGLE REACTING AIR JET IN RICH CROSSFLOW NEAR THE WALL
Vincent G. McDonnell, Howard Lee
- W1P127: COMPARING NO_x AND SOOT FORMATION FOR ALTERNATIVE AVIATION FUELS
Shazib Vijlee, Stefan Bjornsson, Arshiya Chime, Garrett Allawatt, John Kramlich, Ann Mescher, James Hermanson, Philip C. Malte
- W1P128: SURROGATE MODELING OF JET FUELS FOR STUDY OF AUTOIGNITION CHARACTERISTICS AT LOW TEMPERATURE AND LEAN OPERATING REGIMES
Anna Oldani, Daniel Valco
- W1P129: INFLUENCE OF FUEL INJECTION ON THE SHAPE OF A TURBULENT SWIRLING FLAME USING TWO-PHASE FLOW LARGE EDDY SIMULATION
Benoit Cheneau, Sébastien Ducruix, Aymeric Vié
- W1P130: LARGE EDDY SIMULATION AND EXPERIMENTAL STUDIES ON LOW-SWIRL COMBUSTION IN A LEAN PREMIXED MULTI-NOZZLE CAN COMBUSTOR
Weijie Liu, Bing Ge, Yinshen Tian, Shusheng Zang, Shilie Weng
- W1P131: EXTINCTION AT THE FLAME TIP IN LEAN PREMIXED BURNER WITH SWIRLING FLOW
Yuichi Ichikawa
- W1P132: IMPACT SENSITIVITY ESTIMATION OF ENERGETIC MATERIALS
Aurelien Demenay, Laurent Catoire, Guy Jacob
- W1P133: REACTIVITY TRENDS IN FURAN AND ALKYL FURAN COMBUSTION
Mazen Eldeeb, Ben Akih-Kumgeh
- W1P134: PREVENTING FUEL TANK OXYGEN INGRESS FOR A BIMODAL CNG INTERNAL COMBUSTION ENGINE
Chris Hagen, Zachary Taie
- W1P135: TOWARDS PREDICTION OF HIGH FREQUENCY INSTABILITIES IN COMBUSTION CHAMBERS OF LIQUID PROPELLANTS ROCKET ENGINES
Marie Theron, Francoise Baillot, Cindy Merlin, Gerard Ordonneau
- W1P136: PECULARITIES OF THE INFLUENCE OF THE STRUCTURE OF THE SOLID-FUEL MIXTURE GLYCIDYL AZIDE POLYMER/RDX ON THE THERMAL EFFICIENCY OF A ROCKET ENGINE
Sergey Futko, A.V. Luikov
- W1P137: COMBUSTION VISUALIZATION OF ETHANOL/LIQUID OXYGEN ROCKET ENGINE COMBUSTOR WITH 2D PINTLE INJECTOR
Kazuki Sakaki, Shinji Nakaya, Mitsuhiro Tsue, Tetsuo Hiraiwa
- W1P138: LARGE EDDY SIMULATIONS OF A NATURALLY UNSTABLE TRANSCRITICAL COAXIAL INJECTOR
Thomas Schmitt, Axel Coussement, Sébastien Ducruix, Sébastien Candel, Yoshio Nunome
- W1P139: EFFECTS OF POTASSIUM AND ZIRCONIUM ADDITIVES ON THE INFRARED RADIATION SIGNATURE IN ROCKET MOTOR PLUME
Mintaek Kim, Soonho Song, Kwangmin Chun
- W1P140: TEMPERATURE SENSITIVITY OF COMPOSITE PROPELLANTS CONTAINING NOVEL NANO-ADDITIVE CATALYSTS
Andrew Demko, James Thomas, Catherine Dillier, Eric L. Petersen, David Reid, Sudipta Seal, Thomas Sammet
- W1P141: IMPLEMENTING NANO-SIZED ADDITIVES INTO COMPOSITE SOLID PROPELLANTS
Catherine Dillier, Andrew Demko, James Thomas, Thomas Sammet, Eric L. Petersen, Kevin Grossman, David Reid, Sudipta Seal
- W1P142: DIFFERENTIAL WEIGHT MEASUREMENTS DURING COMBUSTION OF METHANE HYDRATES
Joan Santacana Vall, Sunny Karnani, Derek Dunn-Rankin

TUESDAY Work-in-Progress Posters

- W2P001: COMBUSTION REGIMES OF LOW-LEWIS-NUMBER STRETCHED PREMIXED FLAMES
Roman Fursenko, Sergey Minaev, Hisashi Nakamura, Takuya Tezuka, Susumu Hasegawa, Tomoya Kobayashi, Koichi Takase, Masato Katsuta, Masao Kikuchi, Kaoru Maruta
- W2P002: LAMINAR BURNING VELOCITY AND MARKSTEIN NUMBER OF SPHERICALLY PROPAGATING AMMONIA/AIR PREMIXED FLAMES
Takashi Goto, Akihiro Hayakawa, Rentaro Mimoto, Taku Kudo, Hideaki Kobayashi
- W2P003: MARKSTEIN LENGTH IN OUTWARDLY PROPAGATING SPHERICAL FLAMES
Hao Yu, Zheng Chen, Emilien Varea, Bruno Renou, Fabien Halter, Yiguang Ju
- W2P004: TOWARD AN ACCURATE DETERMINATION OF THE LAMINAR BURNING VELOCITY OF HIGHLY CO₂ DILUTED MIXTURE
Alexandre Lefebvre, Bruno Renou, Vincent Modica, Fabien Halter, Mourad Boukhalfa
- W2P005: MEASUREMENTS AND NUMERICAL STUDY OF LAMINAR BURNING VELOCITIES OF ISO-BUTANOL AND ETHANOL BLENDS
Florian Rau, Christian Hasse, Sandra Hartl, Stefan Voss, Dimosthenis Trimis

- W2P006: LAMINAR BURNING VELOCITIES OF METHANE, METHANOL AND ETHANOL: A COMPARATIVE STUDY MADE WITH FOUR HEAT FLUX BURNER SETUPS
Stefan Voss, Alexander Konnov, Vladimir Alekseev, Florian Rau, Evgeniy Volkov, Philip de Goey, Roy Hermanns, Richard Haas-Wittmuess
- W2P007: HYDROUS ETHANOL LAMINAR BURNING VELOCITY MEASUREMENTS WITH CONSTANT VOLUME BOMB METHODS
Nathan Hinton
- W2P008: BURNING VELOCITY VS. FLAME STRETCH IN BUNSEN JET FLAMES OF METHANE – AIR MIXTURES
Gabriel Garcia-Soriano, Sergio Margenat, Francisco J. Higuera, Jose Castillo, Pedro Garcia-Ybarra
- W2P009: PREMIXED FLAME PROPAGATION BETWEEN TWO CLOSELY SPACED PARALLEL PLATES
Daniel Fernandez-Galisteo, Paul D. Ronney
- W2P010: MEASUREMENTS OF LAMINAR FLAME SPEEDS OF ALTERNATIVE GASEOUS FUEL MIXTURES
Samer Ahmed, Ahmed Ibrahim, Othman Abulaban
- W2P011: EXPERIMENTAL AND NUMERICAL STUDY OF FLAME SPEED FOR *ISO*-OCTANE/*N*-DECANE/AIR PREMIXED FLAMES AT HIGH PRESSURE
Kiyong Lee, Sugak Lee
- W2P012: EFFECTS OF ELECTRIC FIELDS ON LAMINAR COFLOW NORMAL AND INVERSE DIFFUSION FLAMES
May Chahine
- W2P013: PROPAGATING NONPREMIXED EDGE FLAMES IN A COUNTERFLOW ANNULAR JET BURNER WITH ELECTRIC FIELDS
Manh-Vu Tran, Min Suk Cha
- W2P014: MODELING THE INFLUENCE OF MAGNETIC FIELD GRADIENT ON THE DIFFUSION FLAMES OF LAMINAR JET FLOW
Fang Yue, Pei Fang Fu, Qian Wang, Zhong Qi Fu
- W2P015: LASER IGNITION AND FLAME DEVELOPMENT IN PREMIXED CONVENTIONAL AND ALTERNATIVE FUEL MIXTURES
Luke Thompson, Bader Almansour, Subith Vasu, Joseph Lopez, Leonid Glebov
- W2P016: A STUDY OF COMBUSTION CHARACTERISTICS IN PREMIXED IMPINGING FLAMES OF SYNGAS(H_2/CO)/AIR
Byeonggyu Jeong, Keeman Lee
- W2P017: ANALYSIS OF 2- AND 3-METHYL HEPTANE COMBUSTION USING SYNCHROTRON PHOTOIONIZATION MASS SPECTROMETRY
Hatem Selim, Arnas Lucassen, Nils Hansen, Mani Sarathy
- W2P018: AUTOIGNITED NON-PREMIXED LAMINAR LIFTED FLAMES OF *ISO*-OCTANE IN HEATED COFLOW AIR
Saeed AlNoman, Sang-kyu Choi, Suk-Ho Chung
- W2P019: COMBUSTION INSTABILITIES: CHEMILUMINESCENCE AS SENSOR FOR MODEL PREDICTIVE CONTROL
Raimund Noske, Andreas Brockhinke
- W2P020: EXPERIMENTAL STUDY OF THE CHEMICAL STRUCTURES OF LAMINAR PREMIXED FLAMES OF DIMETHOXYMETHANE AND DIMETHYL CARBONATE
Bin Yang, Wenyu Sun, Nils Hansen, Arnas Lucassen, Kai Moshhammer, Katharina Kohse-Höinghaus, Chung King Law
- W2P021: STRUCTURE OF PREMIXED FUEL-RICH $CH_4/O_2/N_2/CO_2$ AND $C_3H_8/O_2/N_2/CO_2$ FLAMES STABILIZED ON A FLAT BURNER AT ATMOSPHERIC PRESSURE
Andrey Shmakov, Denis Knyazkov, Oleg Korobeinichev, Tatiana Bolshova, Artem Dmitriev, Alexey Lobasov, Dmitry Sharaborin
- W2P022: FLAME EXTINCTION LIMIT AND FLAME STRUCTURE CHANGE OF A PREMIXED MICROFLAME
Manabu Fuchihata, Tamio Ida, Kazunori Kuwana, Satoru Mizuno
- W2P023: INTERNAL STRUCTURE AND PHYSICAL INTERPRETATION OF A FLAME FRONT THICKNESS
Jury Kryzhanovskiy
- W2P024: MEASUREMENT AND ANALYSIS OF THE DISTRIBUTED TRANSFER FUNCTION FOR NON-PREMIXED FLAMES
Liyue Jing, Min Zhu
- W2P025: DYNAMICS OF COLLIDING SPHERICAL FLAMES: MORPHOLOGY, CORNER DYNAMICS, AND FLAME-GENERATED VORTICITY
Sheng Yang, Swetaprovo Chaudhuri, Delin Zhu, Chung King Law
- W2P026: BEHAVIOR OF METHANE TORCH UNDER ACOUSTIC ACTION
Victor Golub, Mikhail Krivokorytov
- W2P027: THE EFFECTS OF THERMAL EXPANSION AND GRAVITY ON THE PROPAGATION AND STABILITY OF TRIPLE FLAMES
Philip Pearce, Joel Daou
- W2P028: DNS OF SPHERICAL FLAME PROPAGATION IN A NON-UNIFORM CONCENTRATION OF FUEL
Shinnosuke Nishiki
- W2P030: THERMO-DIFFUSIONAL EFFECTS ON LAMINAR PREMIXED FLAMES OF MULTICOMPONENT FUELS
Christodoulos Xiouris, Tailai Ye, Shyam Menon, Fokion N. Egolfopoulos

- W2P031: IGNITION OF *N*-HEXANE-AIR MIXTURES BY MOVING HOT SPHERES
Stephanie Coronel, Joseph Shepherd
- W2P032: LAMINAR FLAME SPEED MEASUREMENTS OF SYNTHETIC GAS BLENDS WITH AND WITHOUT IMPURITIES
Charles Keese, Eric L. Petersen
- W2P033: NUMERICAL INVESTIGATION OF THE STAGNATING LAMINAR PREMIXED METHANE/AIR FLAME WITH FUEL CONCENTRATION OSCILLATION USING A FOUR-STEP REACTION MECHANISM
Sotaro Miyamae, Mohd Rosdzimin Abdul Rahman, Hisashi Tomita, Takeshi Yokomori, Toshihisa Ueda
- W2P034: DYNAMIC BEHAVIOR OF BUNSEN FLAME WITH A VERTICALLY IMPINGING VORTEX TUBE
Natsumi Yamane, Takeshi Yokomori, Toshihisa Ueda, Akihiro Tanaka
- W2P035: PREMIXED LAMINAR FLAMES OF METHYL PENTANOATE AND METHYL HEXANOATE: AN EXPERIMENTAL AND KINETIC MODELING STUDY
Oleg Korobeinichev, Ilya Gerasimov, Charles K. Westbrook, Denis Knyazkov, Andrey Shmakov, Tatiana Bolshova, Nils Hansen, Guillaume Dayma, Bin Yang
- W2P036: EFFECT OF WALL HEAT LOSSES ON FLAME PROPAGATION IN MICRO-CHAMBERS
Orlando Ugarte, Berk Demirkok, V'yacheslav Akkerman, Damir Valiev, Vitaly Bychkov
- W2P037: NUMERICAL STUDY OF INFLUENCE OF WALL TEMPERATURE AND SURFACE REACTION ON FLAME-WALL INTERACTION OF A METHANE-AIR MIXTURE
Naoki Hayashi, Yamashita Hiroshi
- W2P038: EFFECT OF PRESSURE ON HYDROGEN/OXYGEN COUPLED FLAME-WALL INTERACTION
Raphael Mari, Benedicte Cuenot, Florent Duchaine
- W2P039: NUMERICAL MODELING FOR COMBUSTION PROCESSES IN TWO-LAYER POROUS BURNERS
Jaehyeon Kim, Youngjun Shin, Yongmo Kim
- W2P040: INSTABILITY AND TRANSITION TO BALL-LIKE FLAMES OF PREMIXED COUNTERFLOW LOW-LEWIS-NUMBER FLAMES
Tomoya Kobayashi, Koichi Takase, Hisashi Nakamura, Takuya Tezuka, Susumu Hasegawa, Masato Katsuta, Masao Kikuchi, Kaoru Maruta
- W2P041: UPWARD PROPAGATION OF VERY LEAN METHANE-AIR FLAMES IN VERTICAL TUBES
Victor Muntean, Francisco J. Higuera
- W2P042: THERMAL DIFFUSION AND COMBUSTION MODELING
Nancy Brown, Aurore Loisy
- W2P043: A STUDY OF THE EFFECTS OF C=C DOUBLE BOND AND ITS POSITION ON SOOT FORMATION IN LAMINAR COFLOW DIFFUSION FLAMES OF SURROGATES FOR B100 BIODIESEL
Mohammad Reza Kholghy, Jason Weingarten, Murray Thomson
- W2P044: EFFECT OF OXY-ENRICHED OXIDIZER AND N₂O ADDITION ON CHARACTERISTICS OF LAMINAR METHANE JET DIFFUSION FLAME
Hsien-Tsung Lin, Yueh-Heng Li, Guan-Bang Chen, Tsarng-Sheng Cheng, Yei-Chin Chao
- W2P045: FLAME STRUCTURE AND LUMINOUS CHARACTERISTICS OF DOUBLE DIFFUSION FLAME
Kotaro Moriyama, Takeshi Yokomori, Hiromichi Yamada
- W2P046: DILUTION EFFECTS ON THE FLAMMABILITY LIMITS OF OPPOSED-JET SYNGAS DIFFUSION FLAMES
Hsin-Yi Shih, Jou-Rong Hsu, Chi-Rong Liu
- W2P047: EXPERIMENTAL AND THEORETICAL STUDY OF DIETHYL CARBONATE IN A NONPREMIXED OPPOSED-FLOW DIFFUSION FLAME
Juan David Ripoll Sepulveda
- W2P048: EXTINCTION PROPERTIES OF LAMINAR SYNGAS COUNTERFLOW DIFFUSION FLAMES
Amrit Sahu, Rayavarapu V. Ravikrishna
- W2P049: MOMENTUM AND BUOYANCY DRIVEN LAMINAR DIFFUSION FLAME CHARACTERISTICS AT PRESSURES OF 45-100 KPA
Jun Fang, Jing-Wu Wang
- W2P050: STABILIZING MECHANISM OF DIFFUSION MICROFLAME IN HIGH OXYGEN AMBIENT COFLOW
Taro Hirasawa, Akter Hossain, Naoki Sato, Yuji Nakamura
- W2P051: DIFFUSION FLAME IN A POROUS CHAMBER
Max Endo Kokubun, Fernando Fachini, Moshe Matalon
- W2P053: AUTOMATIZED CHOICE OF AN OPTIMAL PROGRESS VARIABLE FOR CHEMISTRY TABULATION – A CONSTRAINED CONTROL APPROACH
Danny Messig, Uwe Prüfert, Christian Hasse, Sandra Hartl, Franziska Hunger, Michael Eiermann
- W2P054: EXPERIMENTAL STUDY ON ULTRALEAN PREMIXED SWIRLING FLAMES OF METHANE-AIR AND HYDROGEN-AIR
Akane Uemichi, Takumi Hattori, Hiroki Aizawa, Makihiro Nishioka

- W2P055: INFLUENCES OF PERIODIC FUEL CONCENTRATION OSCILLATION TO LAMINAR BUNSEN FLAME
Taichi Minowa, Kei Ito, Abdul Rahman Mohd Rosdzimin, Toshihisa Ueda, Takeshi Yokomori
- W2P056: THE EFFECT OF HEAT LOSS ON LEAN CH₄/O₂/Xe COUNTERFLOW PREMIXED SLOT-JET BURNER FLAMES
Koichi Takase, Hisashi Nakamura, Kaoru Maruta
- W2P057: DYNAMICAL BEHAVIOUR OF FLAME FRONT INSTABILITY WITH RADIATIVE HEAT LOSS
Kazuhiro Ueda, Yuta Okuno, Hiroshi Gotoda
- W2P058: CHARACTERISTICS OF AMMONIA/N₂/O₂ LAMINAR FLAME IN OXYGEN-ENRICHED AIR CONDITION
Hiroyuki Takeishi, Jun Hayashi, Kimio Iino, Fumiteru Akamatsu
- W2P059: EXPERIMENTAL AND MODELING STUDIES OF ETHYL VALERATE FLAMES AT LOW PRESSURE
Véronique Dias, Haddy Mbuyi Katshiatschia, Hervé Jeanmart
- W2P060: EFFECT OF AIR TEMPERATURE ON FLAME BASE POSITION OF MINIATURE JET FLAMES
Takato Chujo, Tsuneyoshi Matsuoka, Susumu Noda, Taro Hirasawa, Yuji Nakamura
- W2P061: PILOTED IGNITION OF CLEAR AND BLACK PMMA CYLINDERS
Shmuel Link, Carlos Fernandez-Pello
- W2P062: ON CELLULAR INSTABILITY IN LEAN PREMIXED HYDROGEN-METHANE-AIR FLAMES AT ELEVATED PRESSURES
Ekenechukwu Okafor, Yukihide Nagano, Toshiaki Kitagawa
- W2P063: 2D-INSTABILITY OF HYDROGEN FLAMES
Mike Kuznetsov, Jorge Yanez, Joachim Grune, Antonio Souto-Iglesias
- W2P064: FLAME INSTABILITY OF LEAN HYDROGEN-AIR MIXTURES IN A SMOOTH VERTICAL CHANNEL WITH OPEN END
Mike Kuznetsov, Jorge Yanez, Joachim Grune, Antonio Souto-Iglesias
- W2P065: INFLUENCE OF THE BURNER RIM THICKNESS ON THE STABILITY OF CH₄/O₂/CO₂ NON-PREMIXED FLAME
Shuhei Yoneyama, Takeshi Yokomori
- W2P066: NUMERICAL STUDY OF INTERACTION BETWEEN DARRIEUS-LANDAU INSTABILITY AND SPATIALLY PERIODIC SHEAR FLOW
Damir Valiev, Andrea Gruber, Chung King Law, Jacqueline H. Chen
- W2P067: ADVANCED COMBUSTION VIA MICROGRAVITY EXPERIMENTS: PLANNED INTERNATIONAL SPACE STATION RESEARCH ON GASEOUS FLAMES
Dennis Stocker, Fumiaki Takahashi, J. Mark Hickman, Andrew Suttles
- W2P068: DYNAMICS OF BLUFF-BODY STABILIZED HYDROGEN/AIR PREMIXED FLAME IN A MICRO-CHANNEL
Bok Jik Lee, Chun Sang Yoo, Hong Im
- W2P069: LAMINAR FLAME SPEEDS OF GASOLINE SURROGATES MEASURED WITH THE FLAT FLAME METHOD
Ying-Hao Liao, William Roberts
- W2P070: ANALYZING WATER-LADEN NON-PREMIXED COUNTERFLOW FLAMES USING GENERALIZED SHVAB-ZEL'DOVICH VARIABLES
Vinicius Sauer, Derek Dunn-Rankin
- W2P071: IMPACT OF FLAMELET CONFIGURATIONS ON CHEMISTRY TABULATION
Shyam Menon, Runhua Zhao, Jagannath Jayachandran, Fokion N. Egolfopoulos
- W2P072: A NUMERICAL STUDY OF HIGHLY-DILUTED, BURNER STABILIZED DIMETHYL ETHER FLAMES
Daniel Mayer, Kai Moshhammer, Liming Cai, Heinz Pitsch, Katharina Kohse-Höinghaus
- W2P073: EFFECTS OF HEAVY HYDROCARBON DECOMPOSITION ON FUNDAMENTAL FLAME PROPERTIES
Jennifer Smolke, Francesco Carbone, Fokion N. Egolfopoulos, Hai Wang
- W2P074: VALIDATING KINETIC DATA DERIVED FROM 40 MBAR PREMIXED FLAMES WITH SUB-ATMOSPHERIC FLAME PROPAGATION MEASUREMENTS: METHYL FORMATE AND N-BUTANOL
Robert Burrell, Dong Joon Lee, Fokion N. Egolfopoulos
- W2P075: PRESSURE EFFECTS ON THE EXTINCTION OF NON-PREMIXED C₁-C₂ HYDROCARBON FLAMES
Hugo Burbano, Fokion N. Egolfopoulos
- W2P076: FLAME ACCELERATION DUE TO WALL FRICTION: ACCURACY AND INTRINSIC LIMITATIONS OF THE ANALYTICAL FORMULATION
Berk Demirgok, V'yacheslav Akkerman, Hayri Sezer
- W2P077: THE EFFECT OF MIXTURE FRACTION ON EDGE FLAME PROPAGATION SPEED
Philip Wang, Richard Boles, Paul D. Ronney, David Matinyan, Wenyu Li, Hatsachai Praphanphap, Jesse Piotrowicz, Hang Song
- W2P078: EXPERIMENTAL AND NUMERICAL INVESTIGATION OF FREELY PROPAGATING LEAN ETHYLENE/AIR FLAMES
Erica Belmont, Timothy Ombrello, Michael Brown, Campbell D. Carter, Janet L. Ellzey

- W2P079: TEMPERATURE AND FLOW FIELD EFFECTS ON FLAME IGNITION IN THE COUNTERFLOW CONFIGURATION
Abtin Ansari, Francesco Carbone, Fokion N. Egolfopoulos
- W2P080: LOW-TEMPERATURE COMBUSTION CHEMISTRY – DETAILED SPECIATION EXPERIMENTS
Daniel Felsmann, Kai Moshhammer, Christian Hemken, Katharina Kohse-Höinghaus
- W2P081: EFFECTS OF THERMAL DISSOCIATION OF FUELS ON THE CHARACTERISTICS OF LAMINAR LIFTED FLAMES
Min Jung Lee
- W2P082: A MIXING MODEL FOR LAMINAR FLAME SPEED CALCULATION OF LEAN H₂/CO/AIR MIXTURES BASED ON ASYMPTOTIC ANALYSES
Yang Zhang, Hairui Yang, Hai Zhang, Yuxin Wu, Qing Liu
- W2P083: H₂ CONTENT AND DILUTION EFFECTS ON THE EXTINCTION LIMITS OF LEAN PREMIXED H₂/CO/AIR FLAMES
Yang Zhang, Hai Zhang
- W2P084: COMPARISON OF A MULTI-ZONE COMBUSTION MODEL WITH OPTICAL AND TRANSIENT PRESSURE METHODS FOR THE MEASUREMENT OF LAMINAR FLAME SPEED USING A SPHERICAL CONSTANT VOLUME REACTOR
Amir A.M. Oliveira, Ricardo Hartmann, Eduardo Hartmann, João Monteiro, Edmilsson Oliveira, Mauro Rocha, Leonel Cancino
- W2P085: NUMERICAL SIMULATIONS OF PREMIXED FLAME IGNITION IN PERIODICAL VORTEX FLOWS
Evgenii Sereshchenko, Roman Fursenko, Sergey Minaev, Shengyang (Steven) Shy, Kaoru Maruta
- W2P086: THEORETICAL CRITERION OF THE STABILITY OF FLAME PROPAGATION
Yuanxiang Sun
- W2P087: A SELF-SUSTAINING THERMAL CRACKING CONVERSION PROCESS TO TURN POLYETHYLENE RESIDUES INTO A NOBLE HYDROCARBON
Joao Vitor Ferreira Duque
- W2P088: COMBUSTION OF PULVERIZED OLIVE CAKE IN VERTICAL FURNACE FOR HEAT AND POWER GENERATION.
N. Mrad-Koched, A.E. Elorf, B. Sarh, I. Gökalp, B. Izrar, M. Asbik, J. Chaoufi, A. Idlimam
- W2P089: A SCIENTIFIC BASIS FOR THE DEVELOPMENT OF THE NEXT GENERATION OF BIODUST BURNERS
Joakim Johansen, Peter A. Jensen, Sønnik Clausen, Alexander Fateev, Karsten Nielsen, Jesper Thomsen, Rasmus Gadsbøl, Reginald E. Mitchell, Roman Weber, Marco Mancini, Maria Tonell, Jimmy Andersen, Lisbeth Myllerup, Peter Glarborg
- W2P090: ADVANCED CONTROL METHODOLOGY FOR BIOMASS COMBUSTION
Stefan Bjornsson, Igor Novosselov, Philip C. Malte, Riley Gorder
- W2P091: A FUNDAMENTAL STUDY ON GROUP COMBUSTION PHENOMENON OF SOLID FUEL IN A TURBULENT REACTING FLOW
Jaeyong Jeong, Jihong Moon, Uendo Lee, Won Yang, Joohyang Yang, Changkook Ryu
- W2P092: THE EFFECT OF JET MIXING IN A NATURAL DRAFT RESIDENTIAL LOG WOOD STOVE ON THE REDUCTION OF PARTICULATE MATTER AND GASEOUS EMISSIONS
Smail Kalla, Alain De Champlain
- W2P093: IN-FIELD MEASUREMENT OF COMBUSTION EMISSION FROM SOLID FUEL COOK-STOVES
Jin Dang, Derek Dunn-Rankin, Rufus Edwards, Andy Dang
- W2P094: SCALING OF 100 KW CHEMICAL LOOPING COMBUSTION SYSTEM AND PERFORMANCE WITH DIFFERENT FLUIDIZING GASES
Matthew Hamilton, JoAnn S. Lighty, Kevin J. Whitty
- W2P095: NUMERICAL AND EXPERIMENTAL STUDY ON COAL AND BIOMASS CO-FIRING IN THE FLUIDIZED BED UNDER O₂/CO₂ ATMOSPHERES
Lingling Zhao, Bo Fang, Qing Jia
- W2P096: HUMAN FECES AS FEEDSTOCK FOR GASIFICATION: CHARACTERIZATION OF GASEOUS AND SOLID PRODUCT
Marcio Ferreira Martins, Bianca Medeiros
- W2P097: MODELING OF COMBUSTION AND REACTIONS IN A BED OF SOLID PARTICLES
Hyunjun Ahn, Sangmin Choi
- W2P098: SO₃ AND Hg EMISSIONS FROM A VICTORIAN BROWN COAL DURING OXY-FUEL FLUIDIZED BED COMBUSTION
Bithi Roy, Luguang Chen, Sankar Bhattacharya, Sharmen Rajendran
- W2P100: A STUDY OF THE EFFECT OF AGGLOMERATION DUE TO UTILIZATION OF BIOMASS AND LOW GRADE COAL ON THE BED OF A PILOT SCALE 350KW FLUIDIZED BED COMBUSTOR SYSTEM
Stephen Chilton, William Nimmo, Mohamed Pourkashanian
- W2P101: EXPERIMENTS AND MODELING OF ADVECTIVE OUTPUT FROM POROUS COMBUSTORS USING RECLAIMED FUEL SOURCES
Anthony Terracciano, Subith Vasu, Nina Orlovskaya

- W2P102: PM REMOVAL EFFICIENCY FROM STATIONARY DIESEL GENSETS EQUIPPED WITH AFTERMARKET PARTICULATE CONTROL DEVICES
Tiffany Yelverton, Amara Holder, Jelica Pavlovic
- W2P103: APPLICATION OF CENTRAL COMPOSITE DESIGN FOR THE STUDY OF NO_x EMISSION PERFORMANCE OF A LOW NO_x BURNER
Marcin Damian Dutka, Mario Ditaranto, Terese Løvås
- W2P104: AN EXPERIMENTAL STUDY ON THE COMBUSTION CHARACTERISTICS OF PYROLYSIS OIL DERIVED FROM WASTE TIRE
Myung Chul Shin, Jin Ki Lee, Jong Ho Lee, Su Jin Kim, Hoon Huh
- W2P105: REMOVAL OF PARTICULATE MATTER FROM THE EXHAUST GAS OF A DOMESTIC BIOMASS BOILER USING A SMALL-SCALE ELECTROSTATIC PRECIPITATOR
Enrique Granada, Ivan Iglesias, David Patino, Jacobo Porteiro, Araceli Regueiro
- W2P106: FINE PARTICULATE FORMATION AND ASH DEPOSITION DURING PULVERIZED COAL COMBUSTION OF HIGH-SODIUM LIGNITE IN A DOWN-FIRED FURNACE
Qian Huang, Gengda Li, Qing Liu, Shuiqing Li, Qiang Yao
- W2P107: EFFECTS OF FUEL-SIDE AND OXIDIZER-SIDE DILUTION ON FLAME STRUCTURES AND NO_x FORMATION CHARACTERISTICS OF TURBULENT SYNGAS NONPREMIXED FLAMES
Sangwoon Park
- W2P108: EXPERIMENTAL AND NUMERICAL STUDY OF NO_x EMISSION CHARACTERISTICS IN CH₄/AIR NON-PREMIXED FLAMES WITH EXHAUST GAS RECIRCULATION
Chang-Eon Lee, Wheesung Oh, Seungro Lee, Byeonghun Yu
- W2P109: EXPERIMENTS AND SIMULATIONS OF NO_x FORMATION IN THE COMBUSTION OF HYDROXYLATED FUELS
Myles Bohon, Mariam El-Rachidi, Mani Sarathy, William Roberts
- W2P110: THEORETICALLY STUDY OF MERCURY SPECIES ADSORPTION MECHANISM ON MnO₂(110) SURFACE
Bingkai Zhang
- W2P111: CHARACTERISTICS OF COMBUSTION AND CRITICAL SPACE HEATING RATES IN MESO-SCALE COMBUSTORS
Katsuo Asato
- W2P112: DETONATION WAVE PROPAGATION IN CHANNELS OF ARBITRARY RADIUS OF CURVATURE
Jeong-Yeol Choi, Tae-Young Kim
- W2P113: NUMERICAL INVESTIGATIONS OF DETONATION PROPAGATION IN A TWO-DIMENSIONAL SMALL CURVED CHANNEL
Yuta Sugiyama, Akiko Matsuo, Yoshio Nakayama
- W2P114: NUMERICAL MODELING OF SUPERSONIC COMBUSTION WAVE PROPAGATION IN AN OBSTRUCTED CHANNEL
Mark Kellenberger, Gaby Ciccarelli, Mobin Khakbazzaboli
- W2P115: EXPLOSION FLAME ACCELERATION OVER OBSTACLES: EFFECTS OF SEPARATION DISTANCE FOR A RANGE OF SCALES
A.M. Na'inna, H.N. Phylaktou, G.E. Andrews
- W2P116: TRANSITION FROM DEFLAGRATION TO DETONATION OF METHANE-OXYGEN BLENDS IN NARROW CHANNEL
Victor Golub, Sergey Golovastov
- W2P117: PROPAGATION AND MORPHOLOGY OF PREMIXED FLAME FRONTS IN OBSTRUCTED TUBES
Orlando Ugarte, Berk Demirgok, V'yacheslav Akkerman, Damir Valiev, Satyanaryanan Chakravarthy, Amit Kumar, Vitaly Bychkov
- W2P118: ANALYSIS OF ETHYLENE-OXYGEN COMBUSTION IN MICRO-PIPES
V'yacheslav Akkerman, Berk Demirgok, Orlando Ugarte, Damir Valiev, Chung King Law, Vitaly Bychkov, Ming-Hsun Wu
- W2P119: EXPERIMENTAL STUDY ON REFLECTED SHOCK BIFURCATION
Urszula Niedzielska, Remy Mével, Joseph E. Shepherd, Andrzej Teodorczyk
- W2P120: AUTO-IGNITION IN BOUNDARY LAYER
Edyta Dzieminska, Makoto Asahara, A. Koichi Hayashi
- W2P121: EFFECT OF CHEMICAL KINETICS IN THE EXPANSION FLOW OF A HYDROGEN-AIR ROTATING DETONATION ENGINE
Douglas A. Schwer, K. Kailasanath
- W2P122: SELF-SUSTAINING MECHANISM OF CONTINUOUS ROTATING DETONATION WAVE
Shijie Liu
- W2P123: FLIGHT DEMONSTRATION OF A ROTAR-VALVED FOUR-CYLINDER PULSE DETONATION ROCKET ENGINE "TODOROKI II"
Ken Matsuoka, Tomohito Morozumi, Shunsuke Takagi, Jiro Kasahara, Akiko Matsuo, Ikko Funaki

- W2P124: KINETIC AND GASDYNAMIC ASPECTS OF DDT IN DIFFERENT GEOMETRIES
Mike Kuznetsov
- W2P125: NUMERICAL SIMULATION OF DUST EXPLOSION IN 20L CHAMBER
Zdzislaw Salamonowicz, Rafal Matuszkiewicz
- W2P126: CORRELATION BETWEEN SHOCK STRENGTH AND DUST ENTRAINMENT HEIGHT
Eric L. Petersen, Amira Chowdhury, Sam Mannan, Howard Johnston
- W2P127: OPEN VOLUME DETONATION EXPERIMENTS WITH MIXTURES OF PROPANE-BUTANE, ACETYLENE AND PROPANE-BUTANE-ACETYLENE IN AIR
Andrey Gavrikov
- W2P128: DETONATION IN SUPERSONIC RADIAL OUTFLOW
Aslan Kasimov
- W2P129: PREVENTION AND PROTECTION OF EXPLOSIONS OF HYDROGEN-AIR PREMIXTURES
Satoshi Kadowaki
- W2P130: DETERMINATION OF TEMPERATURE IN LOW ENERGY SPARK DISCHARGES BY OPTICAL EMISSION SPECTROSCOPY
Stefan Essmann, Detlev Markus, U. Maas
- W2P131: ASSESSMENT AND IMPLEMENTATION OF A MARKSTEIN NUMBER BASED TURBULENT BURNING VELOCITY CORRELATION FOR SIMULATING INDUSTRIAL GAS EXPLOSIONS IN COMPLEX GEOMETRIES
Gordon Atanga, Trygve Skjold, Helene Pedersen
- W2P132: THERMAL DEFORMATION OF PLASTIC SHEETS AFTER A GAS EXPLOSION
Takashi Tsuruda
- W2P133: PASSIVE SCALAR-BASED ANALYSIS OF CAVITY-STABILIZED JET COMBUSTION IN A SUPERSONIC COMBUSTOR
Hongbo Wang
- W2P134: A COMPRESSIBLE LEM-LES STRATEGY (CLEM-LES) FOR MODELLING SUPERSONIC AND TURBULENT COMBUSTION
Brian Maxwell, Matei Radulescu, Sam Falle
- W2P135: COMBUSTOR PERFORMANCE COMPARISON IN DUAL-MODE SCRAMJET
Camilo Aguilera Muñoz, Kenneth Yu
- W2P136: INTERACTION BETWEEN PRE-COMBUSTION GAS INJECTION FROM A RAMP INJECTOR AND INCIDENT SHOCKWAVE IN SUPERSONIC FLOW
Tatsuya Yamaguchi, Yoshitaka Iwamura, Taku Kudo, Akihiro Hayakawa, Hideaki Kobayashi
- W2P137: SUPERSONIC COMBUSTION MODELLING USING THE CONDITIONAL MOMENT CLOSURE APPROACH
Mark Picciani
- W2P138: AN ANALYSIS OF THE SUPPRESSION OF PREMIXED FLAMES
Jenny Chao, Sergey B. Dorofeev
- W2P139: ON THE STRUCTURE OF SELF-SIMILAR DETONATION WAVES IN TNT CHARGES
Allen Kuhl, John Bell, Vincent Beckner, Kaushik Balakrishnan

WEDNESDAY Work-in-Progress Posters

- W3P001: EXPERIMENTAL INVESTIGATION OF ATOMIZATION AND COMBUSTION PERFORMANCE OF RENEWABLE BIOFUELS
Vincent G. McDonell, Adam Silver
- W3P002: SPHERICAL FLAME INITIATION AND PROPAGATION IN A LIQUID FUEL MIST WITH FINITE-RATE EVAPORATION
Wang Han, Zheng Chen
- W3P003: SINGULARLY PERTURBED HOMOTOPY ANALYSIS METHOD APPLIED TO THERMAL EXPLOSION OF POLYDISPERSE FUEL SPRAY
O'Phir Nave, Vladimir Gol'dshtein
- W3P004: EXPERIMENTAL STUDY OF THE INTERACTION BETWEEN AN ETHANOL SPRAY AND A TURBULENT FLAME FRONT
Luis Fernando Figueira da Silva, Juan Jose Cruz Villanueva
- W3P005: SPRAY FLAME STRUCTURE ANALYSIS IN A LAB-SCALE BURNER USING LARGE EDDY SIMULATION AND DISCRETE PARTICLE SIMULATION
Damien Paulhiac, Benedicte Cuenot, Elonore Riber
- W3P006: EFFECT OF FUEL-SPRAY OSCILLATIONS AND DROPLET GROUPING IN THE FORMATION OF MULTIPLE FLAMES
David Katoshevski, Barry Greenberg
- W3P007: PLANAR LASER-INDUCED FLUORESCENCE SPECTROSCOPY AND SIMULATIONS OF IGNITION AND COMBUSTION OF FREELY FALLING ALKANE,

ALCOHOL, AND METHYL ESTER DROPLETS

Torben Grumstrup, Anthony John Marchese, Azer Yalin, Frederick L. Dryer, Tanvir Farouk

W3P008: SIMULATING FLAME-SPREAD BEHAVIOR OF RANDOMLY DISTRIBUTED DROPLET CLOUDS BASED ON PERCOLATION THEORY AND MICROGRAVITY EXPERIMENT OF DROPLET ARRAY

Herman Saputro, Masato Mikami, Takehiko Seo

W3P009: BURNING CHARACTERISTICS OF BIODIESEL MIXED WITH ALCOHOL IN MICROGRAVITY CONDITION

Kuo-Long Pan, Jia-Jun Yao

W3P010: LES OF THE SYDNEY SPRAY FLAME SERIES WITH PFGM/ATF AND DIFFERENT SUB-GRID MODELS

Andreas Rittler, Fabian Proch, Andreas Kempf

W3P011: OXYGEN LEWIS NUMBER EFFECTS ON REDUCED GRAVITY COMBUSTION OF METHANOL DROPLETS

Chang Vang, Benjamin D. Shaw

W3P012: INVESTIGATION OF THE LAMINAR BURNING VELOCITY OF ETHANOL AND HEXANE/AIR AEROSOLS

Laurence Bernard, Dan Pugh, Daniel de la Rosa

W3P013: A MONOTONIC MIXTURE FRACTION DEFINITION FOR THE FLAMELET FORMULATION OF SPRAY FLAMES

Benedetta Franzelli, Aymeric Vié, Matthias Ihme

W3P014: COMPUTATIONAL MODELING OF UNSUPPORTED AND FIBER-SUPPORTED *N*-HEPTANE DROPLETS IN REDUCED GRAVITY

Narugopal Ghata, Benjamin D. Shaw

W3P015: AUTOIGNITION OF UNSTEADY LIQUID FUEL SPRAY IN CONSTANT VOLUME COMBUSTION CHAMBER

Nimal Naser, Seung Yeon Yang, Suk-Ho Chung

W3P016: EFFECTS OF AMBIENT PRESSURE ON ATOMIZATION BEHAVIOR OF AIRBLAST ATOMIZER

Kodai Kato, Soichiro Suzuki, Taku Kudo, Soichiro Kato, Mitsunori Itoh, Masahiro Uchida, Akihiro Hayakawa, Hideaki Kobayashi

W3P017: SPRAY IGNITION IN SUPERCRITICAL ENVIRONMENTS

Lukasz Kapusta, Ireneusz Pielecha, Jakub Czajka, Krzysztof Wislocki, Andrzej Teodorczyk

W3P018: LES OF A PARTIALLY PREMIXED SPRAY FLAME USING AN ADAPTATIVE-DYNAMIC ATF MODEL COUPLED TO FGM

Fernando Luiz Sacomano Filho, Mouldi Chrighi, Amsini Sadiki, Johannes Janicka

W3P019: A COMPUTATIONAL MODELING OF DROPLET EVAPORATION INDUCED BY A LOCALIZED HEAT SOURCE

Jaeheon Sim, Hong Im, Suk-Ho Chung

W3P020: TEMPERATURE IMAGING OF TURBULENT DILUTE ACETONE SPRAY FLAMES USING TWO-LINE ATOMIC FLUORESCENCE

Paul Medwell, Assaad Masri, Phuong Xuan Pham, Bassam Dally, Graham Nathan

W3P021: QUANTIFIED MEASUREMENT OF DROPLET EVAPORATION RATES OF A TWO COMPONENT MIXTURE

Chris Hagen, Nicholas Olson

W3P022: EXTINCTION OF COOL-FLAMES SUPPORTED BY *N*-ALKANE DROPLETS IN MICROGRAVITY

Vedha Nayagam, Daniel Dietrich, Michael C. Hicks, Forman Williams

W3P023: TRANSPORTED PDF MODELING OF AN ETHANOL SPRAY IN HOT-DILUTED COFLOW FLAME

Likun Ma, Hugo Correia Rodrigues, Bertrand Naud, E.H. van Veen, Mark Tummers, Dirk Roekaerts

W3P024: STOCHASTIC EVAPORATION MODELLING FOR PRESUMED-PDF SPRAY COMBUSTION SIMULATIONS

Edward Richardson, Tomas Matheson

W3P025: FLAME SPREAD OF A LINEAR *N*-DECANE DROPLET ARRAY WITH PARTIAL PREVAPORIZATION IN MICROGRAVITY

Masao Kikuchi

W3P026: MODULATION OF TURBULENT PROPERTIES IN A SPRAY FLAME BURNING *N*-HEPTANE

Abouelmagd Abdelsamie, Dominique Thévenin

W3P027: EFFECTS OF HYDROGEN OR METHANE ADDITION ON THE COUNTERFLOW SPRAY DIFFUSION FLAME: SPRAY-FLAMELET MODEL FOR BIPHASIC AND MULTI-COMPONENT FUEL

Fernando Fachini, Daniela Maionchi

W3P028: A NOVEL APPROACH TO ASSESS DIESEL SPRAY MODELS USING LIQUID-PHASE EXTINCTION AND X-RAY RADIOGRAPHY MEASUREMENTS

Gina Magnotti, Caroline Genzale

W3P029: INTERMITTENT PRODUCTION OF OH ON A SWIRL-STABILIZED PULSED SPRAY FLAME

Newton Fukumasu, Guenther Krieger

- W3P030: EVAPORATION MODEL OF HYPERGOLIC FUEL DROPLETS
Yu Daimon, Hideyo Negishi, Hiroumi Tani, Yoshiki Matsuura, Hiroshi Terashima, Mitsuo Koshi
- W3P031: SIMULATIONS OF *N*-HEPTANE COOL FLAMES IN ZERO GRAVITY
Fumiaki Takahashi, Viswanath R. Katta
- W3P032: INVESTIGATION OF GLYCEROL ATOMIZATION IN THE NEAR-FIELD OF A FLOW-BLURRING INJECTOR USING TIME-RESOLVED PIV AND HIGH-SPEED FLOW VISUALIZATION
Ajay K. Agrawal, Lulin Jiang
- W3P033: EFFECTS OF DROPLET INTERACTION AND AMBIENT-GAS COMPOSITION ON SPONTANEOUS IGNITION OF FUEL DROPLETS
Osamu Moriue, Kota Yone, Takeru Iwamoto, Hideki Hashimoto, Eiichi Murase
- W3P034: CHARACTERISTICS OF LASER-INDUCED BREAKDOWN IGNITION IN DIFFERENT ETHANOL SPRAY CONCENTRATION
Yuki Ishimura, Takehiko Seo, Masato Mikami
- W3P035: AN EXPERIMENTAL STUDY OF COMBUSTION CHARACTERISTICS OF PARTICLE-ADDED DIESEL FUEL
Mohsen Ghamari, Jared Becker, Albert Ratner
- W3P036: THERMAL DECOMPOSITION OF *N*-PENTANOL AT VARIOUS PRESSURES: FLOW REACTOR PYROLYSIS AND KINETIC MODELING STUDY
Yuyang Li, Gao Wang, Long Zhao, Zhanjun Cheng, Lidong Zhang, Fei Qi
- W3P037: UNCERTAINTY ANALYSIS OF VARIOUS THEORETICAL TREATMENTS ON ETHANOL DECOMPOSITION
Feng Zhang, Lili Xing, Shuang Li, Zhaohui Wang, Bin Yang
- W3P038: AN EXPERIMENTAL AND KINETIC MODELING STUDY OF 2-METHYLBUTANOL COMBUSTION
Sungwoo Park, Ossama Mannaa, Rafik Bougacha, Aamir Farooq, Suk-Ho Chung, Mani Sarathy
- W3P039: INVESTIGATION OF THE PERFORMANCE OF SEVERAL METHANOL COMBUSTION MECHANISMS
Carsten Olm, Robert Palvolgyi, Tamás Varga, Eva Valko, Henry Curran, Tamas Turanyi
- W3P040: LAMINAR BURNING VELOCITIES OF $C_2H_5OH+O_2$ IN DIFFERENT BATH GASES AND AN INVESTIGATION OF THE GENERAL PERFORMANCE OF SEVERAL ETHANOL COMBUSTION MECHANISMS
Carsten Olm, Jenny Naucélér, Alexander Konnov, Sandra Hartl, Christian Hasse, Florian Rau, Tamas Turanyi
- W3P041: RATE CONSTANT CALCULATIONS OF THE H-ATOM ABSTRACTION REACTIONS OF OXYGENATED FUELS WITH HO_2 RADICALS
Jorge Mendes, Chong-Wen Zhou, Henry Curran
- W3P042: THEORETICAL STUDY OF LOW-TEMPERATURE OXIDATION CHEMISTRY OF *ISO*-BUTANOL
Nathan Yee, Shamel Merchant, William Green
- W3P043: EXPERIMENTAL AND KINETIC MODELING STUDY OF TERT-BUTANOL PYROLYSIS
Fei Qi, Jianghuai Cai, Wenhao Yuan, Lili Ye, William Green
- W3P044: EXPERIMENTAL AND NUMERICAL STUDY OF 1-PENTANOL IN A SHOCK TUBE AT HIGH TEMPERATURE
Damien Nativel, Romain Grosseuvres, Andrea Comandini, Nabiha Chaumeix
- W3P045: THEORETICAL INVESTIGATION OF LOW-TEMPERATURE COMBUSTION CHEMISTRY OF THE ISOPENTANOL: MASTER EQUATION ANALYSIS OF MULTI-ENERGY WELL REACTIONS OF HYDROXYL ISOPENTYLPROXY RADICALS
Harish Chakravarty, Akira Matsugi
- W3P046: INVESTIGATION OF THE REACTIVITY OF ENOLS IN THE GAS PHASE BASED ON AB INITIO MO CALCULATION
K. Yasunaga, S. Takada, H. Yamada, K.P. Somers, J.M. Simmie, H.J. Curran
- W3P047: KINETICS FOR $OH + CH_3OH$: ISOTOPIC LABELING STUDIES REVEAL MECHANISTIC FEATURES OF CH_2OH DECOMPOSITION
Nicole J. Labbe, Sebastian L. Peukert, Stephen J. Klippenstein, Joe V. Michael, Raghu Sivaramakrishnan
- W3P048: KINETIC MODELING STUDY OF PROPANAL OXIDATION AT HIGH TEMPERATURE
Xingjia Man
- W3P049: PYROLYSIS OF CYCLOHEXANONE IN A HEATED MICRO-REACTOR
Jessica Porterfield, Zeynep Serinyel, Barney Ellison, David Robichaud, John Daily, Aristotelis Zaras
- W3P051: AN EXPERIMENTAL AND KINETIC MODELING STUDY OF NITROETHANE PYROLYSIS AT LOW PRESSURE: COMPETITION REACTIONS IN THE PRIMARY DECOMPOSITION
Kuiwen Zhang
- W3P052: LEAN METHANE/PROPANE IGNITION AT HIGH PRESSURES: COMPARISON OF CHEMICAL KINETIC MECHANISMS
Robert Pachler, Franz Winter

- W3P053: SITE-SPECIFIC RATE CONSTANT MEASUREMENTS FOR PRIMARY AND SECONDARY H- AND D- ABSTRACTION BY OH RADICALS: PROPANE AND *N*-BUTANE
Ehson Fawad Nasir, Jihad Badra, Aamir Farooq
- W3P054: INVESTIGATION OF ETHANE PYROLYSIS AND OXIDATION AT HIGH PRESSURES USING GLOBAL OPTIMIZATION BASED ON SHOCK TUBE DATA
Viktor Samu, Tamas Varga, Kenneth Brezinsky, Aleksandr Fridlyand, Tamas Turanyi
- W3P055: IGNITION DELAY TIME MEASUREMENTS AND MODELING OF PENTANE ISOMERS
Olivier Mathieu, Claire Gregoire, Brandon Marks, Rachel Archuleta, Eric L. Petersen, John Bugler, Henry Curran
- W3P058: AN EXPERIMENTAL STUDY OF *ISO*-BUTENE AND 1,3-BUTADIENE IGNITION DELAY TIME AT ELEVATED PRESSURES
Yang Li, Chong-Wen Zhou, Eoin O'Connor, Henry Curran
- W3P059: KINETICS OF HOMOALLYLIC/HOMOBENZYLIC REARRANGEMENTS REACTIONS UNDER COMBUSTION CONDITIONS
Feng Zhang, Zhaohui Wang, Lidong Zhang
- W3P060: THERMAL DECOMPOSITION OF STYRENE: AN AB INITIO/MASTER EQUATION STUDY
Edward Ross, Gabriel da Silva
- W3P061: THE ROLE OF THE FULVENALLENYL RADICAL IN THE FORMATION OF POLYCYCLIC AROMATIC HYDROCARBONS DURING AROMATIC FUEL COMBUSTION: AN AB INITIO/MASTER EQUATION STUDY
Edward Ross, Gabriel da Silva
- W3P062: AUTOMATIC GENERATION OF KINETIC MODELS FOR THE OXIDATION OF LARGE ALKYL BENZENES
Valerie Warth, Roda Bounaceur, Pierre-Alexandre Glaude, Olivier Herbinet, Frederique Battin-Leclerc
- W3P063: KINETICS OF THE SELF-REACTION OF CYCLOPENTADIENYL RADICALS
Vadim D. Knyazev, Konstantin Popov
- W3P064: EXPERIMENTAL AND KINETIC MODELING STUDY OF DIMETHYL CARBONATE
Erjiang Hu, Lun Pan, Zihang Zhang, Zuohua Huang
- W3P065: A HIGH-PRESSURE AUTO-IGNITION STUDY OF METHANE IN A HIGH-PRESSURE SHOCK TUBE
Alan Keromnes, Benoîte Lefort, Luis Le Moyne
- W3P066: SHOCK-TUBE STUDY OF THE IGNITION OF FUEL-RICH CH₄/AIR AND CH₄/ADDITIVE/AIR MIXTURES OVER A WIDE TEMPERATURE RANGE AT HIGH PRESSURE
Jürgen Herzler, Mustapha Fikri, Christof Schulz
- W3P067: PARTIAL OXIDATION OF METHANE AT ELEVATED PRESSURES AND EFFECTS OF PROPENE AND ETHANE AS ADDITIVE
Tina Kasper, Fikri Sen, Burak Atakan, Ulf Bergmann
- W3P068: MODELING THE MULTIPLE-WELL, MULTIPLE-PATH UNIMOLECULAR DECOMPOSITION OF SMALL RADICAL INTERMEDIATES A COMPARISON BETWEEN CANTHERM, MULTIWELL, AND VARIFLEX
Enoch Dames, Shamel Merchant, C. Franklin Goldsmith, William Green
- W3P069: CLOUDFLAME: A HYBRID CLOUD SYSTEM FOR COMBUSTION KINETICS SIMULATION
Mani Sarathy
- W3P070: OPENSMOKE++: AN OBJECT-ORIENTED FRAMEWORK FOR THE NUMERICAL MODELING OF REACTING SYSTEMS WITH DETAILED KINETIC MECHANISMS
Alberto Cuoci, Alessio Frassoldati, Mattia Bissoli, Alessandro Stagni, Tiziano Faravelli
- W3P071: AN ADAPTIVE METHODOLOGY FOR THE EFFICIENT IMPLEMENTATION OF DETAILED CHEMISTRY IN SIMULATIONS OF TURBULENT COMBUSTION
Perrine Pepiot, Stephen B. Pope, Youwen Liang
- W3P072: STRATEGIES FOR ACCELERATING COMBUSTION SIMULATIONS WITH GPUS
Kyle Niemeyer, Chih-Jen Sung
- W3P073: RMG-PY: THE PYTHON VERSION OF REACTION MECHANISM GENERATOR
Richard West, Joshua Allen, Pierre Bhoorasingh, Connie Gao, William Green
- W3P074: EXPERIMENTAL AND MODELING INVESTIGATION OF THE OXIDATION OF DIMETHYL ETHER IN A JET-STIRRED REACTOR WITH CRDS DIAGNOSTIC
Olivier Herbinet, Anne Rodriguez, Ophélie Frottier, Baptiste Sirjean, René Fournet, Christa Fittschen, Frédérique Battin-Leclerc
- W3P075: HIGH AND LOW TEMPERATURE OXIDATION OF METHYL-STEARATE-OLEATE AND -LINOLEATE IN JSR
Olivier Herbinet, Anne Rodriguez, Frédérique Battin-Leclerc, Alessio Frassoldati, Tiziano Faravelli, Eliseo Ranzi
- W3P076: A DETAILED KINETIC MODEL FOR METHYL BUTANOATE OXIDATION

Mickael Matrat, Laurent Catoire, Guillaume Dayma, Philippe Dagaut

- W3P077: EXPERIMENTAL AND KINETIC MODELING STUDY OF 2-METHYLFURAN PYROLYSIS AT VARIOUS PRESSURES
Yuyang Li, Zhanjun Cheng, Lili Xing, Yizun Wang, Wenhao Yuan, Zhandong Wang, Fei Qi
- W3P078: UNCERTAINTY PROPAGATION AND GLOBAL SENSITIVITY ANALYSIS FOR THE EVALUATION OF MECHANISMS DESCRIBING LOW TEMPERATURE DME OXIDATION
Alison Tomlin, Michal Vasinek, Vaclav Nevrlý, Jakub Dlabka, Edirin Agbro
- W3P079: GLOBAL UNCERTAINTY PROPAGATION AND SENSITIVITY ANALYSIS IN THE $\text{CH}_3\text{OCH}_2 + \text{O}_2$ SYSTEM: COMBINING EXPERIMENT AND THEORY TO CONSTRAIN KEY RATE COEFFICIENTS IN DME COMBUSTION.
Alison Tomlin, Robin Shannon, Michael Pilling, Mark Blitz, Paul Seakins, Struan Robertson
- W3P080: EXPERIMENTS AND MODELING OF A LARGE OXYGENATED MOLECULE: TRI-PROPYLENE GLYCOL MONOMETHYL ETHER (TPGME)
Ultan Burke, William Pitz, Henry Curran
- W3P081: OXIDATION PATHWAYS OF CINEOLE
Connie Gao, Adam Scheer, Aaron Vandeputte, Jorge Aguilera-Iparraguirre, William Green, Craig Taatjes
- W3P082: LOW-TEMPERATURE IGNITION OF DME/AIR MIXTURE AT ATMOSPHERIC PRESSURE: ON THE TRANSITION FROM COOL FLAME TO HOT FLAME
Jian Gao, Liqiao Jiang, Daiqing Zhao, Yuji Nakamura
- W3P083: THERMAL DECOMPOSITION MECHANISM OF 2-METHOXYFURAN
Kimberly Urness, Barney Ellison, John Daily, John Simmie, Tyler Troy, Musahid Ahmed
- W3P084: KINETIC STUDY OF LOW AND INTERMEDIATE TEMPERATURE OXIDATION OF 2-METHYLFURAN AND 2-METHYLFURAN-PRIMARY REFERENCE FUEL BLENDS
Kotaro Tanaka, Naozumi Isobe, Kota Sato, Mitsuru Konno
- W3P085: REVISITING THE LOW TEMPERATURE COMBUSTION OF DIMETHYL ETHER
Ultan Burke, Kieran Somers, Henry Curran
- W3P086: RELATIONSHIP BETWEEN OCTANE NUMBER, CETANE NUMBER, AND METHANE NUMBER: ANALYSIS OF CONSTANT VOLUME COMBUSTION CHAMBER AND VARIABLE COMPRESSION RATIO ENGINE RESULTS
Marc Baumgardner, Anthony John Marchese
- W3P087: A COMPUTATIONAL APPROACH FOR GASOLINE SURROGATE FUEL FORMULATION TO EMULATE PHYSICAL AND CHEMICAL KINETIC PROPERTIES
Ahfaz Ahmed, Gokop Goteng, William Roberts, Mani Sarathy
- W3P088: A COMPARATIVE STUDY OF THE OXIDATION CHARACTERISTICS OF TWO GASOLINE FUELS AND AN *N*-HEPTANE/*ISO*-OCTANE SURROGATE MIXTURE
Tamour Javed, Ehson Fawad Nasir, Aamir Farooq
- W3P089: EFFECTS OF CHEMICAL ADDITIVES ON THE IGNITION DELAY OF *ISO*-OCTANE IN THE RAPID COMPRESSION MACHINE
Seunghyeon Lee, Hyunsoo An, Mintae Kim, Kwang Min Chun, Soonho Song
- W3P090: UNCERTAINTY OF THE RATE PARAMETERS OF SEVERAL IMPORTANT ELEMENTARY REACTIONS OF THE H_2 AND WET CO COMBUSTION SYSTEMS
Tibor Nagy, Éva Valkó, Inez Sedyó, István Gy. Zsély, Michael J. Pilling, Tamas Turanyi
- W3P091: EXPERIMENTAL AND MODELING STUDY ON EFFECT OF DILUENT GASES ON AUTO-IGNITION OF HYDROGEN BEHIND REFLECTED SHOCK WAVE
Yingjia Zhang, Lun Pan, Jiexiang Zhang, Zuohua Huang, Zeimin Tian
- W3P092: COMBUSTION PROPERTIES OF H_2/CO MIXTURES: CONSISTENT CHEMICAL MECHANISM FROM COLLABORATIVE DATA PROCESSING
Uwe Riedel, Nadja Slavinskaya, Jan Hendrik Starcke, W. Matt Speight, Andrew Packard, Michael Frenklach
- W3P093: DEVELOPMENT OF A SYNGAS COMBUSTION MECHANISM BASED ON A HIERARCHICAL OPTIMIZATION APPROACH
Tamas Varga, Carsten Olm, István Gy. Zsély, Éva Valkó, Henry Curran, Tamas Turanyi
- W3P095: SHOCK TUBE STUDY ON THE THERMAL DECOMPOSITION OF HYDROFLUOROCARBONS USING IR LASER ABSORPTION DETECTION OF HF
Akira Matsugi, Hiroumi Shiina
- W3P096: THE IGNITION OF GAS MIXTURE $\text{CH}_3\text{Cl} + \text{Cl}_2$ AFTER BRIEF EXPOSURE TO UV LIGHT
Ildar Begishev, I.S. Nikitin
- W3P097: THE INFLUENCE OF THE GAS MIXTURE ($\text{CH}_3\text{Cl} + \text{Cl}_2$) COMPOSITION ON SPEED AND TEMPERATURE OF THE FLAME
Ildar Begishev, A.K. Belikov, I.R. Begishev
- W3P098: THE LOCATION AND SIZE OF CORE OF PHOTOIGNITION IN MIXTURES ($\text{CH}_3\text{Cl} + \text{Cl}_2$)
Ildar Begishev

- W3P099: A COMPREHENSIVE REACTION MODEL FOR THE Si-H-Cl-C CHEMICAL SYSTEM
Remy Mével, Laurent Catoire
- W3P100: EXPERIMENTAL AND MODELING INVESTIGATION OF *N*-DECANE PYROLYSIS AT SUPERCRITICAL PRESSURES
Zhenjian Jia, Weixing Zhou
- W3P101: EXPERIMENTAL AND KINETIC MODELING STUDY OF *N*-TETRADECANE PYROLYSIS
Yuyang Li, Meirong Zeng, Wenhao Yuan, Yizun Wang, Lidong Zhang, Fei Qi
- W3P102: EXPERIMENTAL AND KINETIC MODELING STUDY OF *N*-PROPYLCYCLOHEXANE COMBUSTION
Fei Qi, Zhandong Wang, Long Zhao, Zhanjun Cheng, Lidong Zhang, Feng Zhang, Yuyang Li
- W3P103: DEVELOPMENT OF RATE RULES FOR THE LOW-TEMPERATURE OXIDATION OF ALKANES
John Bugler, Sinéad Burke, Kieran Somers, Emma Silke, Henry Curran
- W3P104: PARAMETRIC STUDY OF THE LOW TEMPERATURE OXIDATION OF HEXANE IN A FLOW REACTOR
Remy Mével, Jocely Aleka, Karl Chatelain, Joseph Shepherd
- W3P105: THERMAL STABILITY OF *N*-HEXANE-OXYGEN MIXTURES
Remy Mével, Joseph Shepherd
- W3P106: EXPERIMENTAL COMBUSTION STUDY OF LARGE LINEAR AND BRANCHED HYDROCARBONS USING NOVEL MOLECULAR BEAM MASS SPECTROMETRY TECHNIQUES
M. Köhler, P. Oßwald, M. Fischer, P. Hemberger, T. Bierkandt, E. Akyildiz, T. Kasper, U. Riedel
- W3P107: AN INVESTIGATION OF PHASE-CHANGE BEHAVIOR IN RCM EXPERIMENTS WITH LARGE MOLECULAR WEIGHT FUELS
Colin Banyon, S. Scott Goldsborough
- W3P108: QUASI-GLOBAL KINETIC MODELING OF DIFFERENT ALKANE AND ALCOHOL FUELS
Karl Alexander Heufer
- W3P109: IDENTIFICATION AND COMPARISON OF DETAILED CHEMICAL MECHANISMS
Richard West, Esma Goktekin, Anthony Silvi, Victor Lambert
- W3P110: COMBUSTION CHEMISTRY MODEL OF FOUNDATIONAL FUELS
Yujie Tao, Enoch Dames, Gregory Smith, Hai Wang
- W3P111: APPROXIMATE TRAJECTORY OPTIMIZATION ALGORITHM FOR MECHANISM REDUCTION OF *N*-HEPTANE OXIDATION
AiKe Liu, Fan Wang, Xiangyuan Li, Jian-Li Wang
- W3P112: IMPROVING DETAILED KINETIC MODELS OF BIO-OIL GASIFICATION VIA RATE RULE CALCULATIONS
Fariba Seyedzadeh, Richard West
- W3P113: A GROUP ADDITIVE APPROACH FOR HIGH-THROUGHPUT TRANSITION STATE ESTIMATION
Pierre Bhoorasingh, Richard West
- W3P114: RELIABLE FORMATION ENTHALPIES FROM A COMBINATION OF COMPOUND METHOD ATOMISATION ENERGIES
Ultan Burke, Kieran Somers, John Simmie, Henry Curran
- W3P115: COMPARATIVE ANALYSIS OF COMBUSTION CHEMISTRY MODELS USING THE ALTERNATE SPECIES ELIMINATION APPROACH
Nathan Peters, Ben Akih-Kumgeh
- W3P116: FIRST HIGH-TEMPERATURE MEASUREMENT OF THE $\text{HNO} + \text{O}_2$ REACTION RATE CONSTANT BEHIND SHOCK WAVES
Gernot Friedrichs, Nancy Fassheber
- W3P117: KINETICS OF $\text{NO}_2 + \text{N}_2\text{H}_3$ RADICAL-RADICAL REACTION: THEORETICAL AND EXPERIMENTAL STUDIES
Hongyan Sun
- W3P118: AB INITIO KINETICS AND THERMAL DECOMPOSITION MECHANISM OF MONONITROBIURET AND 1,5-DINITROBIURET
Hongyan Sun
- W3P119: IGNITION DELAY TIME AND KINETIC MODELING OF NITROMETHANE-OXYGEN-ARGON MIXTURES
Remy Mével, Karl Chatelain, Laurent Catoire, Joseph Shepherd
- W3P120: CHEMICAL KINETICS OF SILANE-NITROUS OXIDE MIXTURES AT TEMPERATURE BELOW 1700 K
Remy Mével, Florence Falue, Sandra Javoy
- W3P121: THERMAL DECOMPOSITION OF ORGANOPHOSPHORUS AGENTS
Pierre Glaude, Baptiste Sirjean, Maude Ferrari, Adil Khalfa, René Fournet, Laurent Verdier
- W3P122: MICROWAVE INTERFEROMETER FOR IONIZATION KINETICS
Daniel Murphy, Awad Alquaity, Jie Han, Aamir Farooq, Fabrizio Bisetti

- W3P123: A NEW SHOCK-TUBE FACILITY FOR THE STUDY OF HIGH-TEMPERATURE CHEMICAL KINETICS
Jose Vivanco, Eric L. Petersen, James Anderson, Daniel Pastrich, Katherine Latourneau
- W3P124: COMPARING PREDICTIONS AND EXPERIMENTAL DATA FOR FLOW REACTOR STUDIES: COMPUTATIONAL RE-INITIALIZATION
Andrei Kazakov, Marcos Chaos, Joshua Heyne, Frederick L. Dryer
- W3P125: IMPROVED SEMICLASSICAL TUNNELING FORMULA AND ITS APPLICATION TO DEEP TUNNELING
Albert F. Wagner
- W3P126: SIMULATIONS OF INTERNALLY EXCITED MOLECULES IN DENSE GASES
Albert F. Wagner
- W3P127: GLOBAL SENSITIVITY ANALYSIS WITH SMALL SAMPLE SIZES
Michael Davis, Wei Liu, Raghu Sivaramakrishnan
- W3P129: USING DIFFERENTIAL ENTROPY AS A DATA DISCRIMINATION TOOL AT THE DEVELOPMENT OF DETAILED REACTION MECHANISMS
József Bruck, Tamas Varga, István Gy. Zsély, Tamas Turanyi
- W3P130: GENERATION OF SKELETAL KINETIC MECHANISMS THROUGH REACTING FLUX ANALYSIS AND SENSITIVITY ANALYSIS
Alessandro Stagni, Alessio Frassoldati, Alberto Cuoci, Tiziano Faravelli, Eliseo Ranzi
- W3P131: MONTE CARLO SIMULATIONS FOR UNCERTAINTY ANALYSIS IN MODELING SINGLE PULSE SHOCK TUBE DATA
Aleksandr Fridlyand, S. Scott Goldsborough, Kenneth Brezinsky
- W3P132: A SEGMENTED KINETIC INVESTIGATION ON SULFATION OF CONDENSED POTASSIUM CHLORIDE IN SO₂/O₂/H₂O AT 523K-1023K
Zhongfa Hu, Xuebin Wang, Yibin Wang, Shuanghui Deng, Houzhang Tan
- W3P133: ESTABLISHMENT OF KINETIC PARAMETERS OF PARTICLE REACTION FROM A PERFECTLY STIRRED FLUIDIZED BED REACTOR
Anna Massmeyer, Herman Hausteijn, Benjamin Gövert, Reinhold Kneer
- W3P134: INITIAL STAGES OF THE PYROLYSIS OF POLYETHYLENE
Vadim D. Knyazev, Konstantin Popov
- W3P135: COMPUTATIONAL FLUID DYNAMICS ANALYSIS OF DIFFERENT GEOMETRIES FOR A JET STIRRED REACTOR FOR BIOFUEL RESEARCH
Amir A.M. Oliveira, Amir DeToni, Leandro Oliveira, Leonel Cancino, Edmilsson Oliveira, Mauro Rocha
- W3P136: APPLICATION OF BIOMASS-COAL CO-COMBUSTION FOR ELECTRIC GENERATION IN CHINA
Yaohui Si, Haiping Yang, Zhi Li, Qing Yang, Hanping Chen
- W3P137: EFFECTS OF FLUE GAS ADDITION ON THE PREMIXED OXY-METHANE FLAMES IN ATMOSPHERIC CONDITION
Guan-Bang Chen, Yueh-Heng Li, Fang-Hsien Wu, Yei-Chin Chao
- W3P138: STRUCTURE OF PREMIXED AMMONIA/AIR FLAMES AT ATMOSPHERIC PRESSURE - LASER DIAGNOSTICS AND KINETIC MODELLING
Christian Brackmann, Vladimir Alekseev, Bo Zhou, Emil Nordström, Bengtsson Per-Erik, Li Zhongshan, Marcus Aldén, Konnov Alexander
- W3P139: IMPROVED KINETIC MODEL AND HCCI ENGINE SIMULATIONS OF DIISOPROPYL KETONE IGNITION
Ghazal Barari, Subith Vasu

THURSDAY Work-in-Progress Posters

- W4P001: SPECTROSCOPY OF TRACERS FOR TWO-DIMENSIONAL LIF MEASUREMENTS OF OIL FILM THICKNESS AND FUEL-OIL INTERACTION IN INTERNAL COMBUSTION ENGINES
Daniel Fuhrmann
- W4P002: SIMULTANEOUS MEASUREMENTS OF H₂O₂ AND H₂O CONCENTRATION DISTRIBUTIONS USING PHOTOFRAGMENTATION LASER-INDUCED FLUORESCENCE
Kajsa Larsson
- W4P003: CO AND CO₂ FOLLOWED BY LASER-INDUCED FLUORESCENCE DURING CATALYTIC OXIDATION OF CO
Johan Zetterberg, Sara Blomberg, Johan Gustafson, Christian Brackmann, Edvin Lundgren
- W4P004: CHOOSING THE OPTIMAL FUEL TRACER FOR LIF IMAGING IN DIFFERENT USE-CASE SCENARIOS
Sebastian Kaiser, Martin Goschütz, Martin Schild, Daniel Fuhrmann, Christof Schulz

- W4P005: EFFECT OF FLAME FLUCTUATIONS ON MULTI-LINE NO-LIF GAS-PHASE TEMPERATURE IMAGING
Omid Feroughi, Helmut Kronemayer, Thomas Dreier, Christof Schulz
- W4P006: COLLISIONAL QUENCHING OF FORMALDEHYDE LASER-INDUCED FLUORESCENCE
Jonathan H. Frank, Erxiong Huang, Bruno Coriton
- W4P007: SIMULTANEOUS HIGH-SPEED FORMALDEHYDE FLUORESCENCE AND THREE-DIMENSIONAL VELOCIMETRY IN LIFTED, NON-PREMIXED JET FLAMES
Prabhakar Venkateswaran, James Michael, Harish Subramani, Suresh Roy, James Gord, Terrence R. Meyer
- W4P008: INVESTIGATION OF PS-PFLIF FOR DETECTION OF HYDROGEN PEROXIDES IN LAMINAR FLAMES
Malin Jonsson, Kajsa Larsson, Jesper Borggren, Marcus Aldén, Bood Joakim
- W4P009: MECHANISM OF PHASE-SELECTIVE LASER-INDUCED BREAKDOWN SPECTROSCOPY IN HETEROGENEOUS COMBUSTION
Yihua Ren, Yiyang Zhang, Shuiqing Li
- W4P010: MECHANISM FOR LASER-INDUCED FLUORESCENCE SIGNAL GENERATION FROM ABLATION SEEDED, PLANAR FLAME THERMOMETRY
Dahe Gu, Zhiwei Sun, Paul Medwell, Zeyad Alwahabi, Bassam Dally, Graham Nathan
- W4P011: LASER-BASED *IN-SITU* MEASUREMENT OF GAS-PHASE TEMPERATURE AND *ISO* CONCENTRATION IN A LOW-PRESSURE NANOPARTICLE SYNTHESIS REACTOR USING LASER-INDUCED FLUORESCENCE
Omid Feroughi, Andreas Langer, Thomas Dreier, Christof Schulz
- W4P012: DEVELOPMENT OF A CONTINUOUS-WAVE CAVITY RING-DOWN SPECTROMETER FOR THE STUDY OF ACETYLENE IN SOOTING FLAMES.
Gordon Humphries, Iain Burns, Michael Lengden
- W4P014: A NEW FAST TIME-RESPONSE PULSED CRDS SENSOR FOR SENSITIVE DETECTION OF ETHYLENE
Awad Alquaity, Ettouhami Essebbar, Aamir Farooq
- W4P015: SIMULTANEOUS IMAGING OF MIXTURE FRACTION, VELOCITY, AND SOOT VOLUME FRACTION IN A SOOTING JET FLAME
Okjoo Park, Ross Burns, Oliver Buxton, Noel Clemens
- W4P016: SIMULTANEOUS HIGH-SPEED 2D MIXTURE FRACTION AND 3D VELOCITY FIELD IMAGING IN GAS-PHASE TURBULENT JETS
Michael Papageorge, Jeffrey A. Sutton
- W4P017: DESIGN AND DEVELOPMENT OF A MID-INFRARED CARBON MONOXIDE SENSOR FOR A HIGH-PRESSURE COMBUSTOR RIG
Alejandro Camou, Gabriel Cruz, James Anderson, Eric L. Petersen, David M. Cusano
- W4P018: SIMULTANEOUS MEASUREMENT OF CO AND TEMPERATURE USING TDLAS AT 2.3 μM
Majed Alrefae, Weichao Wang, Aman Satija, Anup Sane, Jay P. Gore
- W4P019: TEMPERATURE IMAGING IN LOW-PRESSURE FLAMES USING DIODE LASERS
Jesper Borggren, Iain Burns, Zongshan Li, Anna-Lena Sahlberg, Marcus Aldén
- W4P020: TEMPERATURE MEASUREMENTS IN COMBUSTION SYSTEM USING H_2O ABSORPTION SPECTROSCOPY
Sewon Kim, Changyeop Lee, Miyoung Yoo
- W4P021: DESIGN AND VALIDATION OF LED-BASED ABSORPTION SENSOR FOR SIMULTANEOUS DETECTION OF CO AND CO_2
Kyle Thurmond, Subith Vasu, William Partridge, Raynella Connatser
- W4P022: SIMULTANEOUS MEASUREMENT OF CO AND CO_2 CONCENTRATIONS USING FIBER LASER INTRACAVITY ABSORPTION SPECTROSCOPY
Sergey Cheskis, Igor Rahinov, Alexey Fomin, Tatiana Zavlev
- W4P023: HIGH-SPEED 1D RAMAN/RAYLEIGH SCATTERING IMAGING IN TURBULENT H_2/N_2 FLAMES
Kathryn Gabet, Frederik Fuest, Jeffrey A. Sutton
- W4P024: PICOSECOND PHOTODISSOCIATION OF METHANE/AIR MIXTURES AT ATMOSPHERIC PRESSURES
Malin Jonsson, Jesper Borggren, Kajsa Larsson, Marcus Aldén, Bood Joakim
- W4P025: NON-INTRUSIVE *IN-SITU* DETECTION OF METHYL CHLORIDE IN HOT GAS FLOWS USING INFRARED DEGENERATE FOUR-WAVE MIXING
Anna-Lena Sahlberg, Jianfeng Zhou, Zhongshan Li, Marcus Aldén
- W4P026: IR CROSS-SECTIONS, LINE STRENGTHS, AND COLLISION BROADENING COEFFICIENTS OF PROPANAL IN GAS PHASE- A MAJOR BIOFUELS COMBUSTION INTERMEDIATE
Batikan Koroglu, Zachary Loparo, Robert Peale, Subith Vasu
- W4P027: TWO-DIMENSIONAL MULTI-ANGLE LIGHT SCATTERING (2D-MALS) OVER A WIDE ANGULAR RANGE
Stefan Will, Michael Altenhoff, Franz Huber
- W4P028: MEASUREMENTS OF PR:YAG PHOSPHOR LUMINESCENCE AT ELEVATED TEMPERATURE
Dustin Witkowski, David Rothamer

- W4P029: LASER DIAGNOSTICS ON METHANE HYDRATES
David Escofet Martin, Jeff Botimer, Derek Dunn-Rankin, Peter Taborek, Sunny Karnani
- W4P030: THE ROLE OF CO₂ ON CHEMILUMINESCENCE SENSORS FOR ACTIVE CONTROL
Julia Krüger, Katharina Kohse-Höinghaus, Andreas Brockhinke
- W4P031: FLAME CHEMILUMINESCENCE MEASUREMENT FOR REAL TIME AIR/FUEL RATIO CONTROL
Jin Ki Lee, Myung Chul Shin, Se Won Kim
- W4P032: CHARACTERIZING A MINIATURE SHOCK TUBE WITH SYNCHROTRON X-RAY DENSITOMETRY
Robert Tranter, Christopher Annesley, Alan Kastengren, Patrick Lynch
- W4P033: PROBING OPTICALLY DENSE GASES WITH X-RAY ABSORPTION AND FLUORESCENCE OF ARGON
Robert Tranter, Alan Kastengren, Christopher Annesley, Patrick Lynch, King Yiu Lam
- W4P034: SYNCHROTRON VUV BEAMLINE/ENDSTATIONS DEDICATED TO COMBUSTION RESEARCH AT TAIWAN LIGHT SOURCE
Fei Qi, Zhouyue Zhou, Jiuzhong Yang, Yuyang Li, Yin-Yu Lee, Huang-Wen Fu, Di-Jing Huang
- W4P035: DIAGNOSTICS OF GLIDING ARC FOR PLASMA-ASSISTED COMBUSTION
Jiajian Zhu, Jinlong Gao, Andreas Ehn, Zhongshan Li, Marcus Aldén, Mirko Salewski, Frank Leipold, Yukihiro Kusano
- W4P036: NON-CONTACT WALL TEMPERATURE MEASUREMENT USING MEMS WIRELESS SENSOR
Min Hyeok Lee, Yuji Suzuki
- W4P037: COMPARISON OF PHOTOPHYSICAL PROPERTIES OF SELECTED AROMATIC AND KETONE FLUORESCENCE TRACERS
Omid Feroughi, Thorsten Benzler, Thomas Dreier, Christof Schulz
- W4P038: DETERMINATION OF THE WOBBE INDEX OF NATURAL GASES BY SPEED OF SOUND
Inchul Choi, Gwang-Jung Kim
- W4P039: INVESTIGATION ON MINIMUM IGNITION ENERGY OF MIXTURES OF A-PINENE BENZENE/AIR
Bruno Coudour
- W4P040: DUAL-GATE OPTICAL KERR EFFECT BALLISTIC IMAGING FOR DENSE SPRAY MEASUREMENTS
David Sedarsky, Said Idlahcen, Claude Roze
- W4P041: DEVELOPMENT OF A PHOTOACOUSTIC DETECTION SCHEME FOR SOOT MEASUREMENT
Gordon Humphries, John Black, Iain Burns, Jaclyn Dunn, Michael Lengden
- W4P042: RAYLEIGH *SLIP* FOR HIGH BACKGROUND NOISE THERMOMETRY
Nathan Kempema, Marshall B. Long
- W4P043: REAL TIME PARTICULATE MASS FLOW APPROXIMATION IN BIOMASS COOKSTOVES USING A GRAVIMETRIC SAMPLING SYSTEM
Kevin Dischino, John Mizia
- W4P044: NOVEL DENSITY MEASUREMENT METHOD UNDER SUB- AND SUPERCRITICAL CONDITIONS: VALIDATION AND APPLICATION TO RP-3
Jianli Wang, Quan Zhu, Xiangyuan Li
- W4P045: CHARACTERIZATION OF ORGANIC COMPOUNDS IN CIGARETTE SMOKE BY SOFT IONIZATION MASS SPECTROMETRY
Kenichi Tonokura, Rumiko Hayashi
- W4P046: MICROSTRUCTURE AND ELECTROMAGNETIC PROPERTIES OF COAL CHARs
Haiyu Liu, Liang Xu, Yan Jin, Baoguo Fan, Yanxia Yang
- W4P047: FLAMMABILITY LIMITS DETERMINATION BY A SEMI-EMPIRICAL EQUILIBRIUM METHOD: PURE COMPOUNDS IN AIR AT ATMOSPHERIC PRESSURE AND MODERATE TEMPERATURES
Andres Armando Mendiburu Zevallos, Joao Andrade de Carvalho Jr., Christian Coronado
- W4P048: EXTINGUISHING PERFORMANCE OF PLANT BIOMASS FOAM EXTINGUISHING METHOD
Yuji Kudo, Kuya Yamamoto
- W4P049: EXPERIMENTAL STUDY OF EXTINGUISHMENT OF A CONFINED PROPANE/AIR DIFFUSION FLAME BY WATER MIST
Akira Yoshida, Naoto Ohashi, Hiroyoshi Naito
- W4P050: MEASUREMENT OF SUPPRESSION EFFECTIVENESS OF WATER MIST WITH VARYING DIAMETER USING COUNTERFLOW METHANE/AIR DIFFUSION FLAMES
Akira Yoshida, Shuhei Hashizume, Hiroyoshi Naito
- W4P051: EXPERIMENTAL AND NUMERICAL STUDY OF LAMINAR FLAME SPEED RETARDATION BY WATER MIST
Akira Yoshida, Toichiro Okawa, Wataru Ebina, Hiroyoshi Naito

- W4P052: COMBUSTION BEHAVIOR OF FIRE WHIRL FORMED ON FUEL CONTAINER
Genichiro Kushida, Masayuki Mizuno
- W4P053: FLAME SPREAD OVER THIN SOLID FUELS ON OPEN AND CLOSED CHANNELS
Bruna Comas, Toni Pujol
- W4P054: EFFECT OF PRESSURE AND OXYGEN CONCENTRATION ON THE FLAME SPREAD LIMITS OF FIRE RESISTANT FABRICS
Danielle Kirchmeyer
- W4P055: THE EXPERIMENTAL STUDY OF FLAME SPREAD RATE NEAR EXTINCTION LIMIT ON ETFE INSULATED WIRE
Ken Mizutani, Andres Osorio, Carlos Fernandez-Pello, Osamu Fujita
- W4P056: AN OBSERVATION OF PULSATING FLAME SPREAD ON COMBUSTION PROCESS OF A SOLID
Tadafumi Daitoku, Takashi Tsuruda
- W4P057: COMBUSTION CHEMISTRY AND PYROLYSIS KINETICS OF PINE NEEDLES FIRE SPREAD ACROSS A FOREST FUEL BED
Oleg Korobeinichev, Alexander Tereshchenko, Alexander Paletsky, Andrey Shmakov, Munko Gonchikzhapov, Inna Shundrina, Lilia Kataeva, Dmitriy Maslennikov, Yury Naganovsky, Naian Liu
- W4P058: AN EXPERIMENTAL STUDY ON FLAME SPREAD OVER SOLID SURFACE WETTED WITH COMBUSTIBLE LIQUID-EFFECTS OF GASIFICATION PROPERTIES OF COMBUSTIBLE LIQUIDS
Takeshi Suzuki
- W4P059: ENSEMBLE-BASED DATA ASSIMILATION FOR REGIONAL-SCALE SIMULATIONS OF WILDFIRE SPREAD
Melanie Rochoux, Sophie Ricci, Benedicte Cuenot, Arnaud Trouvé
- W4P060: COMPUTATIONAL SMOULDERING WILDFIRES: DEPTH OF BURN AND SUPER CRITICAL MOISTURE AT THE IN-DEPTH FIRE SPREAD OVER PEAT SOILS
Xinyan Huang, Guillermo Rein
- W4P061: EFFECT OF $K_4[Fe(Cn)_6]$ AEROSOL ON CH_4 /AIR AND H_2 /AIR FLAMES SPEED
Andrey Shmakov, Anatoly Chernov, Tatiana Bolshova, Oleg Korobeinichev
- W4P062: EFFECT OF DISTANCE BETWEEN DOUBLE TWO-DIMENSIONAL IMPINGING OXIDIZER JETS ON BURNING RATE OF SOLID COMBUSTIBLES
Tsuneyoshi Matsuoka, Kyohei Kamei, Susumu Noda, Harunori Nagata
- W4P063: SUPPRESSION MODELING ADAPTED FOR THE EDC MODEL IN SIERRA/FLUID MECHANICS/FUEGO
Alexander Brown, Flint Pierce, John Hewson
- W4P064: FLAME SUPPRESSION VIA OXIDIZER DILUTION IN A TURBULENT SLOT BURNER: EXPERIMENT AND LES
James White, Eric Link, Sebastien Vilfayeau, Andre Marshall, Peter B. Sunderland, Arnaud Trouvé, Yi Wang, Ning Ren
- W4P065: SKELETAL MECHANISM FOR FLAMES INHIBITION BY TRIMETHYLPHOSPHATE
Tatiana Bolshova, Vladimir Shvartsberg, Oleg Korobeinichev, Andrey Shmakov
- W4P066: APPLICATION OF THE METHOD OF OPPOSED FLOW DIFFUSION FLAMES FOR THE STUDY OF THE MECHANISM OF TPP FLAME RETARDANCY FOR UHMWPE
Oleg Korobeinichev, Alexander Paletsky, Munko Gonchikzhapov, Andrey Shmakov, Alexander Tereshchenko, Inna Shundrina, Naian Liu
- W4P067: INVESTIGATION ON FLAMMABILITY LIMITS OF FUEL VAPORS AT ELEVATED TEMPERATURES
Marcin Grabarczyk, Rafal Porowski, Andrzej Teodorczyk
- W4P068: ON THE EFFECT OF HARDWOOD PALLETS ON THE FIRE GROWTH BEHAVIOR OF RACK STORAGE FIRES A NUMERICAL AND EXPERIMENTAL STUDY
Jaap de Vries
- W4P069: ASSESSING THE IGNITION OF WILDLAND FUELS EXPOSED TO TIME-VARYING HEAT FLUX PULSES
Rory Hadden, Claire Belcher, Guillermo Rein
- W4P070: EFFECTS OF SEASON AND HEATING MODE ON IGNITION AND BURNING BEHAVIOR OF TEN LIVE FUEL SPECIES MEASURED IN A FLAT-FLAME BURNER SYSTEM
Thomas H. Fletcher, Jonathan R. Gallacher, Victoria Lansinger, Sydney Hansen, David R. Weise
- W4P071: EFFECTS OF SEASON ON IGNITION OF LIVE WILDLAND FUELS USING THE FIST APPARATUS
Sara McAllister, David Weise
- W4P072: MODELING OF SPOT-FIRE IGNITION OF NATURAL FUEL BEDS BY HOT PARTICLES
Casey Zak, James Urban, Mario Sanchez-Sanz, Carlos Fernandez-Pello
- W4P073: IGNITION BEHAVIOR OF PMMA PYROLYSIS GAS BY LASER-INDUCED BREAKDOWN SPARKS
Yoshinari Kobayashi, Rihito Takimoto, Shinji Nakaya, Mitsuhiro Tsue

- W4P074: SMOULDERING COMBUSTION CHARACTERISTICS OF PHASE CHANGE MATERIALS WHEN EXPOSED TO RADIANT HEAT FLUX
Martyn McLaggan, Rory Hadden, Martin Gillie
- W4P076: SOOT PRODUCTION AND TEMPERATURE MEASUREMENTS IN CANDLE FLAMES
Maria Thomsen, Andres Fuentes, Pedro Reszka, Rodrigo Demarco, Jean-Louis Consalvi
- W4P077: BEHAVIOUR OF AERONAUTICAL COMPOSITE MATERIALS SUBMITTED TO SEVERE FIRE CONDITIONS
Sachin Dahikar, Jean-Michel Most
- W4P078: CHANGE IN THE EXTINCTION LIMIT OF ELECTROLYTE FOR Li-ION BATTERIES BY ADDITION OF PHOSPHORUS BASED FLAME RETARDANT
Masaya Inatsuki, Osamu Fujita, Katsunori Nishimura
- W4P079: LARGE-SCALE SPACECRAFT FIRE SAFETY TESTS
David Urban, Gary Ruff, Grunde Jomaas, Paul Ferkul, James S. T'ien, Carlos Fernandez-Pello, Jose Torero, Guillaume Legros, Christian Eigenbrod, Sandra Olson, Nickolai Smirnov, Osamu Fujita, Adam Cowland, Sebastian Rouvreau, Balazs Toth, Olivier Minster
- W4P080: A BURNING RATE EMULATOR FOR MICROGRAVITY STUDIES
James G. Quintiere
- W4P081: POLYMETHYLMETHACRYLATE COMBUSTION IN A SIMULATED MICROGRAVITY ENVIRONMENT
Garrett Bornand, Fletcher J. Miller, Gregory Sullivan
- W4P082: SIMULATING SPRAY-PLUME INTERACTION IN A FIRE ENVIRONMENT
Karl Meredith, Xiangyang Zhou
- W4P083: EFFECTS OF CONVECTION ON COMBUSTION BEHAVIOR OF METHANE HYDRATE
Genichiro Kushida, Kento Sakata
- W4P085: TRANSPORT AND CONCENTRATIONS OF EMISSIONS IN A RESIDENCE FROM A COOKSTOVE
Jennifer Jones, Daniel Murphy, Carlos Fernandez-Pello
- W4P086: TOWARDS PREDICTIVE SCENARIO OF METHANE AND COAL DUST EXPLOSION IN A MINING ACCIDENT
V'yacheslav Akkerman, Ali S. Rangwala, Vitaly Bychkov
- W4P087: COMPUTATIONAL MODELING OF POLYMETHYLMETHACRYLATE COMBUSTION IN A NARROW CHANNEL APPARATUS
Garrett Bornand, Fletcher J. Miller
- W4P089: COMBUSTION SYNTHESIS OF GRAPHENE FILMS
Nikolay Prikhodko, Zulkhair Mansurov, Bakhytzhana Lesbayev, Moldir Auyelkhankyzy
- W4P090: STUDY OF THE EVOLUTION OF SOOT PARTICLE SIZE DISTRIBUTIONS IN PREMIXED ISO-OCTANE/ETHANOL FLAMES
Isabel Frenzel, Steffen Salenbauch, Christian Hasse, Dimosthenis Trimis
- W4P091: SOOT SIZE IN ELEVATED PRESSURE DIFFUSION FLAMES
Scott Steinmetz, Nick Eaves, Seth Dworkin, Murray Thomson, Tiegang Fang, William Roberts
- W4P092: SOOTING TENDENCIES OF C₄ – C₇ UNSATURATED ESTERS IN NONPREMIXED COFLOW FLAMES
Dhrubajyoti Das, Charles Stewart McEnally, Lisa D. Pfefferle
- W4P093: OXIDATION OF SOOT: KINETIC MONTE CARLO SIMULATIONS OF GRAPHENE-EDGE GROWTH AND OXIDATION
Ravi Singh, Michael Frenklach
- W4P094: MECHANISM OF GRAPHENE FORMATION IN FLAMES
Zulkhair Mansurov, Moldir Auelkhankyzy, Nikolay Prikhodko, Michael Frenklach, Raja Singh
- W4P095: MODELING FOR SOOT FORMATION PROCESSES OF LAMINAR ETHYLENE/AIR COUNTERFLOW DIFFUSION FLAME
Namsu Kim, Yongmo Kim, Tae Hoon Kim
- W4P096: EXPERIMENTAL STUDY OF SOOT OXIDATION BY OH
Isabel Jaramillo, Hossein Ghiassi, Paulo Perez, JoAnn S. Lighty
- W4P097: SOOT OXIDATION BY OH: THEORY DEVELOPMENT, MODEL, AND EXPERIMENTAL VALIDATION
Isabel Jaramillo, Hossein Ghiassi, JoAnn S. Lighty
- W4P098: EXPERIMENTAL AND KINETIC MODELING STUDY OF STYRENE COMBUSTION
Yuyang Li, Wenhao Yuan, Philippe Dagaut, Jiuzhong Yang, Fei Qi
- W4P099: STOCHASTIC SIMULATION OF POLYCYCLIC AROMATIC HYDROCARBON GROWTH IN OXYGENATED FUEL FLAMES
Tyler Dillstrom, Jason Lai, Paolo Elvati, Angela Violi
- W4P100: MOLECULAR DYNAMICS SIMULATIONS ON THE FORMATION OF INCIPIENT CARBONACEOUS NANOPARTICLES AT FLAME CONDITIONS
Salvatore Iavarone, Andrea D'Anna, Mariano Sirignano

- W4P101: APPLICATION OF DIRECT MONTE CARLO SIMULATION FOR MORPHOLOGY OF AGGREGATES AND PARTICLE SIZE DISTRIBUTIONS: COMPARISON OF THE CLUSTER-CLUSTER AGGREGATION MODEL WITH THE STOCHASTIC MODEL
Kiminori Ono
- W4P102: HOW MOLECULAR STRUCTURE AFFECTS POLYCYCLIC AROMATIC HYDROCARBON DIMERIZATION
Jeffrey Lowe, Paolo Elvati, Angela Violi
- W4P103: CHARACTERIZATION OF SOOT GROWTH PROCESSES AND MORPHOLOGY IN A TURBULENT NON-PREMIXED FLAME USING MONTE CARLO METHODS
Ahmed Abdelgadir
- W4P104: REVISITING APPROACHES TO OBTAINING TRANSPORT PROPERTIES OF PAH AND FULLERENES
Christopher Pope
- W4P105: AN UPDATED KINETIC MECHANISM FOR DIMETHOXYMETHANE OXIDATION UNDER HIGH-PRESSURE CONDITIONS
Lorena Marrodán, Eduardo Royo, Ángela Millera, Rafael Bilbao, Maria Alzueta
- W4P106: NEW IDENTIFICATIONS OF POLYCYCLIC AROMATIC HYDROCARBONS IN PRODUCTS OF SUPERCRITICAL *N*-DECANE PYROLYSIS
Nimesh Poddar, Subramanian V. Kalpathy, Mary Julia Wornat
- W4P107: POLYCYCLIC AROMATIC HYDROCARBON (PAH) AND SOOT FORMATION IN THE PYROLYSIS OF DIMETHOXYMETHANE
Fausto Viteri, Rafael Bilbao, Ángela Millera, Maria Alzueta
- W4P108: THE EFFECTS OF TEMPERATURE ON THE YIELDS OF PRODUCTS FROM PROPYLENE PYROLYSIS
Eva Caspary, Nimesh Poddar, Mary Julia Wornat
- W4P109: NEW IDENTIFICATIONS OF POLYCYCLIC AROMATIC HYDROCARBONS IN PRODUCTS OF COAL SOOT EXTRACTS
Matthew Skapura, Nimesh Poddar, Mary Julia Wornat
- W4P110: EXPERIMENTAL AND MODELLING STUDY OF DIMETHYL CARBONATE OXIDATION AND ITS INTERACTION WITH NO
Maria Abian, Pablo Salinas, Ángela Millera, Rafael Bilbao, Maria Alzueta
- W4P111: SOOTING LIMITS OF NONPREMIXED *N*-HEPTANE, *N*-BUTANOL, AND METHYL BUTANOATE FLAMES: EXPERIMENTAL DETERMINATION AND MECHANISTIC ANALYSIS
Sili Deng, Jeremy Koch, Michael Mueller, Chung King Law
- W4P112: STRAIN RATE EFFECT ON SOOTING CHARACTERISTICS IN LAMINAR COUNTERFLOW DIFFUSION FLAMES
Yu Wang, Suk-Ho Chung
- W4P113: SUPERCRITICAL PYROLYSIS OF 1-OCTENE
Elizabeth Hurst, Subramanian V. Kalpathy, Mary Julia Wornat
- W4P114: DQMOM APPROACH FOR POLY-DISPERSED SOOT FORMATION PROCESSES IN TURBULENT NON-PREMIXED ETHYLENE/AIR FLAME
Taehoon Kim, Yongmo Kim
- W4P115: SOOTING BEHAVIOR OF HYDROCARBONS IN A MICRO FLOW REACTOR WITH A CONTROLLED TEMPERATURE PROFILE
Ajit Kumar Dubey, Kaoru Maruta, Hisashi Nakamura, Takuya Tezuka, Susumu Hasegawa
- W4P116: EFFECT OF TEMPERATURE AND RESIDENCE TIME ON SOOT FORMATION DURING PYROLYSIS OF ASPHALTENE
Vinoj Kurian, Nirlipt Mahapatra, Ben Wang, Frans Martens, Rajender Gupta
- W4P117: MODELING SOOT FORMATION IN PREMIXED FLAMES USING A CONDITIONAL QUADRATURE METHOD OF MOMENTS (CQMOM) APPROACH
Steffen Salenbauch, Alberto Cuoci, Isabel Frenzel, Dimosthenis Trimis, Tiziano Faravelli, Christian Hasse
- W4P118: SOOT INTERNAL NANO-STRUCTURE AND ITS EFFECTS ON SOOT SURFACE REACTIVITY AND TRANSITION FROM COALESCENCE COLLISIONS TO AGGLOMERATION
Mohammad Reza Kholghy, Murray Thomson
- W4P119: A STUDY OF SOOT PROPERTIES AT DIFFERENT STAGES IN THE SOOT FORMATION PROCESS IN PREMIXED ONE-DIMENSIONAL FLAT FLAMES BY LASER HEATING AND LIGHT SCATTERING
Nils-Erik Olofsson, Johan Simonsson, Sandra Török, Henrik Bladh, Per-Erik Bengtsson
- W4P121: SOOTING TENDENCY OF SURROGATES FOR THE AROMATIC FRACTIONS OF DIESEL AND GASOLINE IN A WICK-FED DIFFUSION FLAME
Maria Botero, Markus Kraft, Sebastian Mosbach, Jethro Akroyd
- W4P122: SOOT CHARACTERISATION OF *N*-HEPTANE/TOLUENE MIXTURES IN A WICK-FED DIFFUSION FLAME
Maria Botero, Sebastian Mosbach, Jethro Akroyd, Markus Kraft
- W4P123: SOLID-LIQUID TRANSITIONS IN HOMOGENOUS OVALENE, HEXABENZOCORONENE AND CIRCUMCORONENE CLUSTERS FROM MOLECULAR DYNAMICS SIMULATION

Dongping Chen, Jethro Akroyd, Sebastian Mosbach, Markus Kraft

- W4P124: ADHESIVE AND ATTRACTIVE FORCES OF FLAME-FORMED CARBON NANOPARTICLES BY ATOMIC FORCE MICROSCOPY
Gianluigi De Falco, Mario Commодо, Patrizia Minutolo, Andrea D'Anna
- W4P125: OPTICAL PROPERTIES OF MATURE SOOT
Elizabeth Rieken, Hope Michelsen, Ronald Hanson
- W4P126: LARGE-EDDY SIMULATION OF PARTIAL OXIDATION REFORMING OF TAR IN SYNGAS FROM WOODY BIOMASS USING FLAMELET MODEL
Noriaki Nakatsuka, Hiroaki Watanabe, Ryoichi Kurose
- W4P127: COMBUSTION AND SECTIONAL SOOT MODELING FOR SPRAY SIMULATIONS
Damien Aubagnac-Karkar, Olivier Colin
- W4P128: THE EFFECT OF ETHANOL ADDITION ON POLYAROMATIC HYDROCARBON FORMATION INVESTIGATED THROUGH DETECTION OF NATURALLY OCCURRING IONS IN FLAMES
Tina Kasper, Thomas Bierkandt, Denis Knyazkov, Oleg Korobeinichev, Erdal Akyildiz
- W4P129: EFFECT OF WATER MIST ADDITION ON AGGREGATION OF PM FROM A DIFFUSION FLAME
Yoshihiro Kobayashi
- W4P130: SEMI-VOLATILE NANOPARTICLE NUCLEATION AND GROWTH IN LOW TEMPERATURE COMBUSTION EXHAUST
Will Northrop, Glenn Lucachick
- W4P131: A NUMERICAL STUDY ON THE SENSITIVITY OF LARGER POLY-AROMATIC HYDROCARBONS IN NUCLEATION PROCESSES OF SOOTING FLAMES
Prabhu Selvaraj, Paul Arias, Yang Gao, Sungwoo Park, Hong Im, Mani Sarathy, Tianfeng Lu
- W4P132: SOOT FORMATION IN A LAMINAR ETHYLENE DIFFUSION FLAME
Edward Yapp, Markus Kraft, Jethro Akroyd, Sebastian Mosbach, Anthony Knobel, Alastair Smith, Dongping Chen, Erin Adkins, Houston Miller
- W4P133: PRODUCTION AND OXIDATION OF CARBON PARTICLES USED FOR A SOLAR ABSORPTION MEDIUM
Lee Frederickson, Fletcher J Miller, Mario Leoni
- W4P134: AN EXPERIMENTAL AND MODELING STUDY OF SOOT FORMATION IN PROPENE FLAMES
Chiara Saggese, Joaquin Camacho, Tiziano Faravelli, Hai Wang
- W4P135: SIZE EVOLUTION OF SOOT FORMED IN PREMIXED C₆ HYDROCARBON FLAMES
Joaquin Camacho, Hai Wang, Sydnie Lieb
- W4P136: EXTINCTION MEASUREMENTS FOR DETERMINATION OF OPTICAL BAND GAPS FOR SOOT IN NITROGEN-DILUTED, ETHYLENE/AIR NON-PREMIXED FLAMES
Erin Adkins, Houston Miller
- W4P137: SOOT FORMATION IN NONPREMIXED BIODIESEL FLAMES
J.F. Correa-Pugliese, S. McCollam, Wilson Merchan-Merchan
- W4P138: ANALYSIS OF SOOT MORPHOLOGY IN A CO-FLOW NONPREMIXED METHANE OXY-FLAME
J.F. Correa-Pugliese, A.D. Ngo, D. Orr, Wilson Merchan-Merchan
- W4P139: THE ROLE OF ALKYL AROMATICS ON PARTICLE FORMATION IN DIFFUSION FLAMES
Marielena Conturso, Mariano Sirignano, Andrea D'Anna
- W4P140: CARBON PARTICLE BEHAVIOR IN FLAMES EXPOSED TO AN ELECTRIC FIELD
Jesse Tinajero, Derek Dunn-Rankin

FRIDAY Work-in-Progress Posters

- W5P001: DNS OF A LEAN PREMIXED CH₄-H₂/AIR SLOT FLAME
Donato Cecere, Eugenio Giaomazzi, Franca Rita Picchia, Nunzio Maria Salvatore Arcidiacono
- W5P002: DIRECT NUMERICAL SIMULATION AND REACTION RATE MODELLING OF PREMIXED TURBULENT FLAMES
Haiou Wang, Kun Luo, Jianren Fan
- W5P003: A STUDY OF CONDITIONAL SCALAR DISSIPATION RATE IN A PREMIXED HYDROGEN FLAME USING CHEMICAL EXPLOSIVE MODE ANALYSIS
Michael Kuron, Zhuyin Ren, Jacqueline H. Chen, Tianfeng Lu
- W5P004: TURBULENCE-CHEMISTRY INTERACTIONS ON STATISTICALLY PLANAR H₂-AIR PREMIXED FLAMES USING DIRECT NUMERICAL SIMULATION
Paul Arias, Hong Im, Swetaprovo Chaudhuri, Chung King Law

- W5P005: TRANSFORMATION OF TURBULENCE IN PREMIXED TURBULENT COMBUSTION
Brock Bobbitt, Guillaume Blanquart
- W5P006: MODELLING TURBULENCE-CHEMISTRY INTERACTION IN PREMIXED FLAMES WITH A STRAINED FLAMELET MODEL
Konstantin Kleinheinz, Philipp Trisjono, Evatt Hawkes, Heinz Pitsch
- W5P007: PROPAGATION OF THE ENSEMBLE AVERAGED FLAME FRONT IN TURBULENT FLOW
Dong-Hyuk Shin, Edward Richardson, Tim Charles Lieuwen
- W5P008: STRUCTURE AND PROPAGATION OF TURBULENT METHANE/AIR PARTIALLY PREMIXED FLAME: A DNS STUDY
Vivianne Holmén, Henning Carlsson, Bai Xuesong, Rixin Yu
- W5P009: A DNS STUDY OF IGNITION OF LEAN PRF/AIR MIXTURES WITH TEMPERATURE INHOMOGENEITIES UNDER HIGH PRESSURE AND INTERMEDIATE TEMPERATURE
Chun Sang Yoo, Minh Bau Luong, Seung Oook Kim, Jacqueline H. Chen
- W5P010: A CONDITIONALLY-AVERAGED DYNAMIC SUB-GRID MODEL FOR TURBULENT NON-PREMIXED COMBUSTION
Graham Hendra, W. Kendal Bushe
- W5P011: APPLICATION OF COHERENT STRUCTURE METHOD FOR SIMULATION OF TURBULENT PREMIXED LABORATORY-SCALED FLAMES IN CFMLES FRAMEWORK
Luka Perkovic, Neven Duic, Peter Priesching
- W5P012: THE UNIFORM CONDITIONAL MOMENT CLOSURE MODEL FOR PREMIXED COMBUSTION OF A TURBULENT ENCLOSED METHANE JET
Carlos Velez, Subith Vasu, Scott Martin
- W5P013: PREDICTION OF A TURBULENT ENCLOSED PREMIXED HYDROGEN FLAME WITH THE UNIFORM CONDITIONAL MOMENT CLOSURE MODEL
Carlos Velez, Subith Vasu, Scott Martin, Aleks Jemcov
- W5P014: FOLDS AND POCKETS IN THE PROPAGATION OF PREMIXED TURBULENT FLAMES
Navin Fogla, Francesco Creta, Moshe Matalon
- W5P015: THE DAMKÖHLER-SHELKIN PARADOX IN THE THEORY OF TURBULENT FLAME PROPAGATION
Vladimir Zimont
- W5P016: GENERAL CORRELATION OF TURBULENT BURNING VELOCITY OF VARIOUS MIXTURES AT HIGH PRESSURE UP TO 3.0 MPa
Jinhua Wang, Wu Jin, Meng Zhang, Zuohua Huang, Hideaki Kobayashi
- W5P017: TURBULENT DISPLACEMENT SPEEDS OF A NATURAL GAS SURROGATE WITH HYDROGEN ADDITION
Anibal Morones Ruelas, Sankaranarayanan Ravi, Eric L. Petersen, Felix Guethe
- W5P018: DISTRIBUTED REACTIONS IMAGED IN HIGH REYNOLDS NUMBER PREMIXED TURBULENT COMBUSTION
Aaron Skiba, Timothy Wabel, Jacob Temme, James Driscoll
- W5P019: ZIMONT SCALE VORTEX INTERACTIONS WITH PREMIXED FLAMES
Runhua Zhao, Nicole Aeina, Vyaas Gururajan, Fokion N. Egolfopoulos
- W5P020: ON THE ROLE OF INTERMEDIATE SPECIES IN TURBULENT PREMIXED COMBUSTION OF PROPANE AND PROPANOL ISOMERS AT HIGH PRESSURE
Tomohiro Uchida, Shungo Souyoshi, Shun Nakajima, Thwe Thwe Aung, Taku Kudo, Akihiro Hayakawa, Satoshi Kadowaki, Hideaki Kobayashi
- W5P021: INVESTIGATIONS OF THE INFLUENCE OF TURBULENT LENGTH SCALES ON PREMIXED FLAMES BY AN ACTIVE GRID BURNER
Markus Höllermann, Christoph Hennecke, Friedrich Dinkelacker
- W5P022: AN EXPERIMENTAL STUDY OF TURBULENT PREMIXED C₁-C₈ HYDROCARBON FLAMES IN A STAGNATION FLOW CONFIGURATION
Jennifer Smolke, Francesco Carbone, Fokion N. Egolfopoulos
- W5P023: SYSTEMATIC INVESTIGATION OF PREMIXED METHANE IMPINGING FLAMES
Jin Fu
- W5P024: HEAT RELEASE RATE MEASUREMENTS ON METHANE, SIMULATED BIOGAS AND SYNGAS TURBULENT FLAMES
Irfan Mulla, Aadil Dowlut, Satyanarayanan Chakravarthy, Ramanarayanan Balachandran, N. Swaminathan
- W5P025: TURBULENT FLAME EXTINCTION PREDICTION IN PARTIALLY PREMIXED COUNTER FLOW FLAMES
William Calhoon, Jr.
- W5P026: NUMERICAL SIMULATIONS OF HIGHLY TURBULENT COUNTERFLOW FLAMES (TCFS) IN NON-PREMIXED AND PREMIXED MODES
Ranjith Tirunagari, Stephen B. Pope
- W5P028: AN EFFICIENT TRANSPORTED FDF AND FLAMELET HYBRID APPROACH FOR LARGE EDDY SIMULATION
Martin Rieth, Jyh-Yuan Chen, Fabian Proch, Andreas Kempf

- W5P029: IMPROVED POLLUTANT AND EXTINCTION PREDICTION IN LARGE EDDY SIMULATION OF TURBULENT PILOTED JET DIFFUSION FLAMES
Seung Hyun Kim
- W5P030: FULLY CONSERVATIVE KINETIC ENERGY PRESERVING SCHEMES FOR HIGH REYNOLDS NUMBER TURBULENT COMBUSTION
Ayaboe Edoh
- W5P031: MULTI-ENVIRONMENT PROBABILITY DENSITY FUNCTION APPROACH FOR TURBULENT STRATIFIED BLUFF-BODY FLAMES
Sangtae Jeon, Yongmo Kim
- W5P032: TEMPERATURE AND OH FIELD MEASUREMENTS IN TURBULENT PREMIXED AND STRATIFIED METHANE/AIR FLAMES
M. Mustafa Kamal
- W5P033: STABILITY CHARACTERISTICS OF PARTIALLY PREMIXED FLAMES
Mohamed Senosy, Mohy Mansour, Assaad Masri, Mohamed Zayed, Mrinal Juddoo
- W5P034: LINE RAMAN/RAYLEIGH MEASUREMENTS IN PARTIALLY PREMIXED SLOT BURNER FLAMES FOR CONSERVED AND REACTION SCALAR GRADIENT MEASUREMENTS
Stephan Kruse, David Broll, Emilien Varea, Mohy Mansour, Ayman Elbaz, Gerd Gruenefeld, Heinz Pitsch
- W5P035: EFFECT OF THERMAL BOUNDARY CONDITIONS ONTO THE FLAME STABILIZATION OF A TURBULENT PREMIXED STRATIFIED FLAME
Anja Ketelheun, Guido Kuenne, Amer Avdic, Matthias Euler, Andreas Dreizler, Johannes Janicka
- W5P036: THE ROLE OF TEMPERATURE, MIXTURE FRACTION, AND SCALAR DISSIPATION RATE ON AUTO-IGNITION OF A TRANSIENT METHANE JET IN A HOT COFLOW
Christoph Arndt, Michael Papageorge, Frederik Fuest, Jeffrey A. Sutton, Wolfgang Meier
- W5P037: STRUCTURE AND STABILIZATION OF A HYDROGEN-RICH TRANSVERSE JETS IN A VITIATED TURBULENT FLOW
Sgouria Lyra, Benjamin Wilde, Hemanth Kolla, Tim Charles Lieuwen, Jacqueline H. Chen
- W5P038: PREMIXED FLAME KERNEL PROPAGATION IN HIGH SPEED CHANNEL FLOWS WITH MODERATE TURBULENCE AND COMPRESSIBILITY
Nathan Grady, Robert Pitz, Bradley Ochs, Suresh Menon, David Scarborough, Tom Slais
- W5P039: TURBULENT FLAMMABILITY AND EXTINCTION STUDIES APPLIED TO PREMIXED CONFINED MIXTURES BETWEEN BIOADDITIVES AND PRF GASOLINE FUELS
Ricardo Hartmann, Robert A. Schiessl, Amir A.M. Oliveira, U. Maas
- W5P040: DYNAMICS OF AN OSCILLATING MIXTURE OF REACTING FLUIDS
Martin Jurisch, William Jones, Andrew Marquis
- W5P042: OH-ZONE STRUCTURE OF SWIRLED, STRONGLY-PULSED TURBULENT JET DIFFUSION FLAMES
Ying-Hao Liao, Jim Hermanson
- W5P043: STRAIN RATES AND REACTION ZONE STRUCTURES IN SYNGAS TURBULENT NON-PREMIXED JET FLAMES NEAR EXTINCTION
Jeongjae Hwang, Taesung Kim, Jisu Yoon, Youngbin Yoon
- W5P044: STATISTICS OF UNSTEADY EXTINCTION USING A SIMPLE STOCHASTIC MODEL
John Hewson
- W5P045: TURBULENT COMBUSTION SUBGRID CLOSURE OF RANS USING LEM3D
Alan Kerstein, Sigurd Sannan
- W5P046: A STUDY ON COMBINED DIMENSION REDUCTION AND TABULATION FOR TURBULENT PREMIXED FLAME SIMULATIONS
Jeonglae Kim, Stephen B. Pope
- W5P047: JET FLAME SIZE AND FLAME SURFACE DENSITY CORRELATIONS FOR AN EXTENSIVE RANGE OF FUELS AND FLOW RATES
Adriana Palacios, Derek Bradley, Philip Gaskell, Xiao Gu
- W5P048: PARTICLE TIME-TEMPERATURE HISTORIES IN TURBULENT FLAMES STUDIED THROUGH STOCHASTIC MODELING
John Hewson, David Lignell, Guangyuan Sun
- W5P049: TURBULENT COMBUSTION MODELLING FOR SPLIT FUEL INJECTION
Edward Richardson, Dong-hyuk Shin, Nabil Meah, Roderick Johnstone
- W5P050: THE INFLUENCE OF OXYGEN-ENHANCED COMBUSTION METHODS ON NO_x EMISSIONS, IN-FLAME TEMPERATURES AND HEAT FLUX DISTRIBUTION
Petr Belohradsky, Pavel Skryja, Igor Hudak
- W5P051: INVESTIGATION OF PREFERENTIAL DIFFUSION EFFECTS IN TURBULENT LIFTED CH₄/H₂ FLAMES USING LES WITH A NOVEL FGM-PDF MODEL
Ebrahim Abtahizadeh, Jeroen van Oijen, Philip de Goeij
- W5P052: MODELLING LIFTED JET FLAMES IN A HEATED COFLOW USING AN OPTIMISED EDDY DISSIPATION CONCEPT MODEL
Paul Medwell, Michael Evans, Zhao Feng Tian

- W5P053: TOWARDS MILD COMBUSTION UNDER HIGH PRESSURE CONDITIONS
Paul Medwell, Michael Evans, Zhao Feng Tian, Qing Nian (Shaun) Chan, Alessio Frassoldati, Alberto Cuoci, David Blunck, William Roquemore
- W5P054: AERODYNAMIC BEHAVIOR OF DIFFUSION FLAMES IN LOW AND HIGH SWIRL COMBUSTOR
Teresa Parra, Ruben Perez, Francisco Castro
- W5P055: TURBULENT COMBUSTION MODELING OF COMPLEX FUELS USING TABULATED CHEMISTRY FOR LARGE-EDDY SIMULATION
Daniel Mira, Simon Gövert, Mariano Vazquez, Guillaume Houzeaux, Jim Kok
- W5P056: VALIDATION OF THE TURBULENT BURNING SPEED MODEL ON NUMERICAL SIMULATION OF A GAS-TURBINE COMBUSTOR
Kagenobu Murase, Nobuyuki Oshima, Yuta Hamada, Kohshi Hirano, Yoshiharu Nonaka
- W5P057: LARGE EDDY SIMULATION OF PREMIXED FLAME FLASHBACK IN A TURBULENT CHANNEL
Malik Hassanaly, Christopher Lietz, Venkat Raman, Hemanth Kolla, Jacqueline H. Chen, Gruber Andrea
- W5P058: DNS ANALYSIS OF THERMOCHEMICAL EFFECTS ON TURBULENT PREMIXED FLAMES NEARBY A WALL SURFACE
Kazuya Tsuboi, Eiji Tomita, Tatsuya Hasegawa
- W5P059: EXPERIMENTAL INVESTIGATION OF BOUNDARY LAYER FLASHBACK IN H₂/CH₄-AIR SWIRL FLAMES
Dominik Ebi, Noel Clemens
- W5P060: LOW LEWIS NUMBER FLAME PROPAGATION IN NARROW CHANNELS
Jonathan Gross, Daniel Fernandez-Galisteo, Xiaojun Pan, Paul D. Ronney
- W5P061: EXPERIMENTAL AND NUMERICAL INVESTIGATION OF THE PREMIXED FLAME PROPAGATION ACROSS THE VARIED COMPOSITION FIELD IN A STRAIGHT RECTANGULAR CHANNEL
Zakaria Movahedi, Andrzej Sobiesiak, Indika Gallage
- W5P062: MODEL-BASED IMAGING OF INFRARED RADIATION INTENSITY FROM A TURBULENT NONPREMIXED JET FLAME AND PLUME
Brent Rankin, Matthias Ihme, Jay P. Gore
- W5P063: CONDITIONAL ANALYSIS OF A HIGH SPEED LIFTED JET FLAME
Tai Jin, Kun Luo, Jianren Fan
- W5P064: PREMIXED FLAME KERNEL PROPAGATION AND INTERACTION WITH A SHOCK WAVE IN A SUPERSONIC TURBULENT CHANNEL FLOW
Bradley Ochs, John Berlette, David Scarborough, Suresh Menon, Nathan Grady, Robert Pitz
- W5P065: NUMERICAL ANALYSIS OF IGNITION AND FLAME STABILIZATION IN AN *N*-HEPTANE SPRAY FLAME
Zhuyin Ren, Zhen Lu, Lei Zhou, Tianfeng Lu, Kai Hong Luo
- W5P066: TRANSIENT SIMULATIONS OF AN *N*-HEPTANE SPRAY FLAME WITH DYNAMIC ADAPTIVE CHEMISTRY
Zhuyin Ren, Zhen Lu, Lei Zhou, Tianfeng Lu, Kai Hong Luo
- W5P067: ADOPTION OF ANALYTICAL DESIGN METHODS FOR THE DESIGN OF HIGH-PRESSURE COMBUSTION CHAMBERS IN LOW-POWER EVAPORATING BURNERS
Volodymyr Ilchenko, Vitali Dell
- W5P068: FLOW STRUCTURE MEASUREMENT DOWNSTREAM OF AXIAL GUIDE VANE SWIRLER
Jiri Vondal, Jiri Hajek
- W5P069: SOOT PARTICLE SIZE DISTRIBUTION MEASUREMENTS ALONG THE CENTERLINE OF A PILOTED TURBULENT NON-PREMIXED FLAME AT ATMOSPHERIC PRESSURE
Wesley Boyette, Snehaunshu Chowdhury, William Roberts
- W5P070: SIMULATION OF INSTANTANEOUS COAL GASIFICATION FLAMES WITH ONE DIMENSIONAL TURBULENCE MODEL
Yuxin Wu, Philip Smith, Hai Zhang, Alan Kerstein
- W5P071: NUMERICAL INVESTIGATION ON DEVOLATILIZED SUBSTANCES IN A COAL COMBUSTION FLAME USING LES
Hiroaki Watanabe, Seongyool Ahn, Tetsuya Shoji, Nozomu Hashimoto, Kenji Tanno
- W5P072: OBSERVATION AND QUANTIFICATION OF COMBUSTION BEHAVIOR OF A SINGLE COAL PARTICLE ENTRAINED INTO HOT GAS FLOW
Hookyung Lee, Sangmin Choi
- W5P073: SOOT PARTICLE GROWTH IN A COMBUSTION FIELD FORMED BY SMALL PULVERIZED COAL JET BURNER
Nozomu Hashimoto, Jun Hayashi, Noriaki Nakatsuka, Hirofumi Tsuji, Satoshi Umemoto, Kazuki Tainaka, Fumiteru Akamatsu, Hiroaki Watanabe, Hisao Makino
- W5P074: CHARACTERISTICS OF NO REDUCTION BY CHAR LAYER IN FIXED-BED COAL COMBUSTION
Hailiang Du
- W5P075: INFLUENCE OF ASH COMPOSITION Fe₂O₃ ON COAL PYROLYSIS IN A TUBULAR REACTOR
Qinhui Wang, Yukun Yang, Mengxiang Fang, Jinsong Zhou, Zhongyang Luo

- W5P076: THE TRANSITION OF HETEROGENEOUS-HOMOGENEOUS IGNITIONS OF DISPERSED COAL PARTICLE STREAMS
Ye Yuan, Shuiqing Li
- W5P077: ENHANCEMENT OF GASIFICATION REACTIVITY OF LOW-RANK COAL THROUGH HIGH TEMPERATURE TREATMENT
Xian Li, Ryuichi Ashida, Kouichi Miura, Hong Yao
- W5P078: DETERMINING THE OPTIMUM COAL CONCENTRATION IN A GENERAL TANGENTIAL-FIRED FURNACE WITH RICH-LEAN BURNERS: FROM A BENCH-SCALE TO A PILOT-SCALE STUDY
Xuebin Wang, Houzhang Tan, Shien Hui, Tongmo Xu
- W5P079: SIMULTANEOUS MEASUREMENTS OF MIE SCATTERING, PAHS LASER INDUCED FLUORESCENCE AND SOOT LASER INDUCED INCANDESCENCE TO LAB-SCALE PULVERIZED COAL JET FLAMES
Jun Hayashi, Noriaki Nakatsuka, Nozomu Hashimoto, Kazuki Tainaka, Hirofumi Tsuji, Hiroaki Watanabe, Hisao Makino, Fumiteru Akamatsu
- W5P080: EFFECT OF COAL RANK ON PCI COMBUSTION ZONE IN BLAST FURNACE
JinHo Kim
- W5P081: EFFECT OF NEW AUXILIARY AIR INJECTION ON WATER-WALL WASTAGE IN PULVERIZED COAL BOILER
Ho Lim
- W5P082: THE SEPARATE PHYSICO-CHEMICAL EFFECTS OF CARBON DIOXIDE ON COAL CHAR COMBUSTION IN O₂/CO₂ ENVIRONMENTS
Yuegui Zhou
- W5P083: EVALUATION OF ASH FREE COAL COMBUSTION CHARACTERISTICS IN A DROP TUBE FURNACE
Sang-In Kim
- W5P084: COMBUSTION BEHAVIOR OF PULVERIZED PETROLEUM COKE IN BOILER SYSTEM
Chun Loon Cha, Ho Yeon Lee, Pil Hyong Lee, Sang Soon Hwang
- W5P085: CFD SIMULATION OF CO-COMBUSTION OF SOLID RECOVERED FUEL AND COAL IN A CEMENT CALCINER
Hrvoje Mikulcic, Eberhard von Berg, Milan Vujanovic, Peter Priesching, Reinhard Tatschl, Neven Duic
- W5P086: EXPERIMENTAL DETERMINATION OF THE KINETICS OF PRESSURIZED OXY-FUEL CHAR COMBUSTION
Ethan Hecht, Manfred Geier, Christopher R. Shaddix
- W5P087: EFFECT OF DEVOLATILIZATION PROCESS ON PM10 FORMATION DURING OXY-FUEL COMBUSTION OF A BITUMINOUS COAL
Jingying Xu, Chang Wen, Dunxi Yu
- W5P088: SELF-IGNITION OF H₂/O₂ /CO₂ IN THE FIXED-BED CATALYTIC REACTOR
Chih-Yung Wu, Ian Shou-Yin Yang, Qin Hui Zeng, Yu Shun Hong
- W5P089: NUMERICAL STUDY AND APPLICATION TO THE ACTUAL BOILER OF A NEW LOW-NO_x COAL-FIRED BURNER BASED ON THE LOW-NO_x PRINCIPLE
Keigo Matsumoto, Koutaro Fujimura, Kazuhiro Domoto, Ryuichiro Tanaka, Tomonori Saeki, Munehiro Kakimi
- W5P090: TOWARDS UNDERSTANDING THE IMPACT ON CHAR SURFACE AREA WHEN COAL AND BIOMASS ARE CO-FIRED IN GASIFICATION ENVIRONMENTS
Matthew Tilghman, Reginald E. Mitchell
- W5P091: EFFECT OF TORREFACTION ON PHYSICAL PROPERTIES AND CONVERSION BEHAVIOR OF HIGH HEATING RATE CHAR OF FOREST RESIDUE
Tian Li, Manfred Geier, Liang Wang, Xiaoke Ku, Berta Matas-Guell, Terese Løvås, Christopher R. Shaddix
- W5P092: COAL AND BIOMASS HYBRID FUEL FOR IMPLEMENTATION OF RPS IN COAL POWER PLANT
Se-Joon Park, Dong-Wook Lee, Jong-Soo Bae, Young-Joo Lee, Ju-Hyoung Park, Jai-Chang Hong, Jeong-Geun Kim, Young-Chan Choi
- W5P093: AN EXPERIMENTAL STUDY OF THE PYROLYSIS AND COMBUSTION CHARACTERISTICS OF COAL AND PINE SAWDUST BLENDS
Zhezi Zhang, Guangjun Lu, Mingming Zhu, Pengfei Liu, Setyawati Yani, Fangqin Cheng, Dongke Zhang
- W5P094: DEVELOPMENT OF A TIER 4 SEMI-GASIFIER BIOMASS COOKSTOVE THROUGH THE APPLICATION OF FUNDAMENTAL COMBUSTION SCIENCE
Jessica Tryner, Torben Grumstrup, Azer Yalin, Morgan DeFoort, Anthony John Marchese
- W5P095: FINE ASH PARTICLE EMISSIONS FROM COMBUSTION OF COALS AND BIOMASS PROCESS RESIDUES
Feyza Kazanc, Yiannis Levendis, Amanda Ruscio
- W5P096: AN EXPERIMENTAL AND KINETIC INVESTIGATION INTO THE PYROLYSIS OF PINE SAWDUST HEATED AT VARIOUS HEATING RATES
Zhezi Zhang, Dongke Zhang, Mingming Zhu, Wenchao Wan, Pengfei Liu, Yii Leng Chan
- W5P097: PARAMETRIC STUDY OF BIOMASS GASIFICATION IN A PILOT-SCALE GASIFIER
Yunye Shi, Tejasvi Sharma, Guiyan Zang, Albert Ratner
- W5P098: BIO-OILS PRODUCED BY STEAM ASSISTED PYROLYSIS OF ARUNDO DONAX AND AXYLAN, CELLULOSE AND LIGNIN MIXTURE: A PRELIMINARY STUDY ON SALT EFFECT
V. Gargiulo, P. Giudicianni, M. Alfé, R. Ragucci

- W5P099: EULERIAN-LAGRANGIAN SIMULATION OF BIOMASS GASIFICATION IN A HIGH-TEMPERATURE ENTRAINED FLOW REACTOR: EFFECTS OF BIOMASS TYPE AND PARTICLE SIZE
Xiaohe Ku, Tian Li, Terese Løvås
- W5P100: UNDERSTANDING THE REDUCTION OF PARTICULATE EMISSIONS IN BIOMASS COOKSTOVES
Kathleen Lask, Cristian Birzer, Paul Medwell, Ashok Gadgil
- W5P101: UNDERSTANDING THE PRIMARY AND SECONDARY PYROLYSIS MECHANISMS OF CELLULOSE, LIGNIN AND WOOD WITH LASER-INDUCED FLUORESCENCE
Alba Dieguez-Alonso, Andres Anca-Couce, Nico Zobel, Frank Behrendt
- W5P102: THE OIL COMBUSTION AT THE SURFACE OF WATER
Zulhair Mansurov, Nikolay Prikhodko, Gauhar Smagulova, Bakhytzhhan Lesbayev
- W5P103: SYNTHESIS OF HYBRID COAL CONTAINING GLYCEROL AND ITS COMBUSTION CHARACTERIZATION
Jong-Soo Bae, Young-Joo Lee, Dong-Wook Lee, Se-Joon Park, Ju-Hyoung Park, Jai-Chang Hong, Joeng-Geun Kim, Young-Chan Choi
- W5P104: INFLUENCE OF COMBUSTION PARAMETERS ON FOULING AND BOTTOM ASH AFTER COMBUSTION OF WOOD PELLET IN AN EXPERIMENTAL LOW-POWER BOILER
Enrique Granada, Lara Febrero, Raquel Perez, Araceli Regueiro
- W5P105: A COMPARATIVE STUDY OF BOTTOM ASH AND FOULING FROM WOODY BIOMASS COMBUSTION IN AN EXPERIMENTAL PILOT BOILER
Enrique Granada, Lara Febrero, David Patino, Pablo Eguia, Araceli Regueiro
- W5P106: EFFECTS OF AIRFLOW ENTRANCE CONDITIONS ON GASIFICATION PROCESS
Ching-Po Lin, Hsiao-Kang Ma, Chun-Hao Peng, Hsin-Luen Tsai Tsai
- W5P107: EFFECTS OF COAL-CHAR HEATING RATES AND SIZES ON KINETICS OF STEAM AND CO₂ GASIFICATION
Jaya Raman, I. Gökalp
- W5P108: PYROLYSIS AND GASIFICATION CHARACTERISTICS OF SEWAGE SLUDGE AND BIOMASS
Jaya Raman, I. Gökalp
- W5P109: GASIFICATION OF MIXING FUELS ON DOWNDRAFT GASIFIER
Howping Wu
- W5P110: NUMERICAL ANALYSIS OF HYDROGEN INHIBITION DURING COAL GASIFICATION
Jonas Krueger
- W5P111: FILTRATION COMBUSTION OF CARBON AND INERT MATERIAL CHARGED IN INTERMITTENT LAYERS
Eugene Salgansky
- W5P112: A THEORETICAL ANALYSIS OF TRANSIENT OXIDATION OF MAGNETITE TO HEMATITE IN CHEMICAL LOOPING COMBUSTION
Tianxiang Li, Yunqing Han, Kunlei Liu, Kozo Saito
- W5P113: NUMERICAL STUDY OF SUGARCANE BAGASSE GASIFICATION IN A FLUIDIZED BED REACTOR
Albino Leiroz, Gabriel Verissimo, Jean de Pinho, Manuel Cruz
- W5P114: COMBUSTION BEHAVIOR OF AQUEOUS HAN SOLUTIONS CONTAINING METHANOL AND NANOPARTICLE ADDITIVES
Kenneth McCown, Gabriel Homan-Cruz, Eric L. Petersen
- W5P115: TURBULENT FLAME PROPAGATION IN DUST CLOUDS
Trygve Skjold
- W5P116: CATALYTIC BEHAVIOR OF FLAME-MADE PD/TiO₂ NANOPARTICLES IN METHANE OXIDATION AT LOW TEMPERATURES
Fang Niu, Shuiqing Li, Yichen Zong, Qiang Yao
- W5P117: LAMINAR FLAME SPEEDS OF AN AEROSOL MIXTURE CONTAINING NANO-ALUMINUM IN CH₄/O₂/N₂
Travis Sikes, Eric L. Petersen, M.S. Mannan
- W5P118: PERFORMANCE OF A MECHANICALLY ALLOYED AL-CUO THERMITE FOR APPLICATIONS IN DRUG DELIVERY AND CELLULAR TRANSFECTION
Geoffrey Maines, Matei Radulescu, Kadeem Dennis, Julian Lee
- W5P119: ASSEMBLY OF NANOTHERMITE VIA ELECTROPHORETIC DEPOSITION OF ALUMINUM NANOPARTICLES ON COPPER OXIDE NANOWIRES
Ming-Hsun Wu, Hendrik Hartono
- W5P120: SYNTHESIS OF SrSiO₃-SiO₂ AND ZrO₂-SiO₂ CORE-SHELL PARTICLES BY FLAME SPRAY PYROLYSIS
Takuro Kusunoki, Hiroshi Hasegawa, Toshihisa Ueda, Takeshi Yokomori
- W5P121: ROLE OF FLAME STOICHIOMETRY ON PHASE STABILITY OF NANOCRYSTALLINE TiO₂ SYNTHESIZED IN PREMIXED FLAME STABILIZED ON A ROTATING

SURFACE

Ruxiao An, Hai Wang

W5P122: FUNDAMENTAL STUDY OF FLAME SYNTHESIS OF TiO₂ NANOPARTICLES BY MOLECULAR DYNAMICS SIMULATION

Kai Luo, Qian Mao

W5P123: MULTI-VARIABLE MEASUREMENT BASED ON DUAL THERMOPHORETIC SAMPLING WITH DIFFERENT TIME INTERVALS DURING FLAME SYNTHESIS NANOPARTICLES

Zuwei Xu, Haibo Zhao

W5P124: SINTERING AND GROWTH OF ALUMINA NANOPARTICLES USING MOLECULAR DYNAMICS SIMULATIONS

Alauddin Ahmed, Paolo Elvati, Nathan Taylor, Richard Laine, Angela Violi

W5P125: HYBRID ROCKET BURNING RATE ENHANCEMENT BY NANO-SCALE ADDITIVES IN HTPB FUEL GRAINS

James Thomas, Eric L. Petersen, John Desain, Brian Brady

W5P126: COMBUSTION OF MECHANICALLY ALLOYED Al/Mg POWDER WITH WATER

Evgeny Shafirovich, Daniel Rodriguez, Aly Yasmine, Mirko Schoenitz, Edward L. Dreizin

W5P127: TEMPERATURE DEPENDENCE OF FLAME PROPAGATION OVER METHANE HYDRATE SURFACE UNDER A NATURAL CONVECTION

Tomoki Yoshioka, Takeshi Yokomori, Ryo Ohmura, Toshihisa Ueda, Masanori Suemitsu

W5P128: POOL FIRE EXTINCTION BY A CARBON DIOXIDE HYDRATE

Hiroataka Nakano, Kosuke Sasakura, Ryo Ohmura, Takeshi Yokomori, Toshihisa Ueda

W5P129: MECHANISMS OF THERMITE REACTIONS IN THE MIXTURES OF MAGNESIUM WITH LUNAR AND MARTIAN REGOLITH SIMULANTS

Evgeny Shafirovich, Armando Delgado

W5P130: ON SOME FEATURES OF HETEROGENEOUS COMBUSTION IN POROUS MEDIA UNDER FREE CONVECTION

Nickolay Lutsenko

WORK-in-PROGRESS POSTER AUTHORS

<i>Author.....Paper #</i>	<i>Author.....Paper #</i>	<i>Author.....Paper #</i>	<i>Author.....Paper #</i>
Abdelgadir, A. W4P103	Aleka, J. W3P104	Aubagnac-Karkar, D. W4P127	Bernard, L. W3P012
Abdelsamie, A. W3P026	Alekseev, V. W2P006, W3P138	Auelkhankyzy, M. W4P089,	Bhagatwala, A. W1P104
Abian, M. W4P110	Alfe, M. W5P098 W4P094	Bhattacharya, S. W2P098
Abraham, J. W1P071, W1P103	Allawatt, G. W1P127	Aung, T.T. W5P020	Bhoorasingh, P. W3P073,
Abtahizadeh, E. W5P051	Allen, J. W3P073	Avdic, A. W5P035 W3P113
Abulaban, O. W2P010	Allocca, L. W1P078	Badra, J. W3P053	Bierkandt, T. W3P106, W4P128
Adkins, E. W4P132, W4P136	Almansour, B. W2P015	Bae, J.-S. W5P092, W5P103	Bilbao, R. W4P105,
Aeina, N. W5P019	AlNoman, S. W2P018	Baillot, F. W1P135 W4P107, W4P110
Agbro, E. W3P078	Alquaity, A. W1P055,	Bakrania, S. W1P052	BinAbdulMunir, F. W1P025,
Agnello, M. W1P052 W3P122, W4P014	Balachandran, R. W5P024 W1P059
Agrawal, A.K. W1P043,	Alrefae, M. W4P018	Balakrishnan, K. W2P139	Birzer, C. W5P100
..... W1P066, W3P032	Altenhoff, M. W4P027	Banyon, C. W3P107	Bisetti, F. W1P013, W3P122
Aguilera-Iparraguirre, J. .. W3P081	Alwahabi, Z. W4P010	Barari, G. W3P139	Bissoli, M. W1P083, W3P070
Ahmed, A. W3P087	Alzueta, M. W4P105,	Barta, J. W1P072	Bjornasson, S. .. W1P127, W2P090
Ahmed, A. W5P124 W4P107, W4P110	Battin-Leclerc, F. W3P062,	Black, J. W4P041
Ahmed, M. W3P083	Ameen, M. W1P103 W3P074, W3P075	Black, S. W1P034
Ahmed, S. W2P010	An, H. W1P006, W3P089	Baumgardner, M. W1P072,	Bladh, H. W4P119
Ahn, H. W2P097	An, R. W5P121 W3P086	Blanquart, G. W5P005
Ahn, J. W1P014, W1P015,	Anca-Couce, A. W5P101	Becker, J. W3P035	Blitz, M. W3P079
..... W1P044, W1P050	Andersen, J. W2P089	Beckner, V. W2P139	Blomberg, S. W4P003
Ahn, S. W5P071	Anderson, J. W3P123, W4P017	Begishev, I. W3P096,	Blunck, D. W5P053
Aizawa, H. W2P054	Andersson, M. W1P098 W3P097, W3P098	Bobbitt, B. W5P005
Akamatsu, F. W2P058,	Andrews, G.E. W2P115	Behrendt, F. W5P101	Bohon, M. W2P109
..... W5P073, W5P079	Annesley, C. W4P032, W4P033	Behzadi, J. W1P102	Boles, R. W2P077
Akih-Kumgeh, B. W1P133,	Ansari, A. W2P079	Belcher, C. W4P069	Bolshova, T. W2P021,
..... W3P115	Applegate, J. W1P052	Belikov, A.K. W3P097 W2P035, W4P061, W4P065
Akkerman, V. W2P036,	Archuleta, R. W3P055	Bell, J. W2P139	Borggren, J. W4P008,
..... W2P076, W2P117,	Arcidiacono, N.M.S. W5P001	Bellenoue, M. W1P061 W4P019, W4P024
..... W2P118, W4P086	Arias, P.G. W1P013,	Belmont, E. W2P078	Bornand, G. W4P081, W4P087
Akroyd, J. W4P121, W4P122, W4P131, W5P004	Belohradsky, P. W5P050	Borowski, P. W1P091
..... W4P123, W4P132	Arndt, C. W5P036	Benard, P. W1P024	Botero, M. W4P121, W4P122
Aksu, C. W1P099	Asahara, M. W2P120	Bengt, J. W1P093	Botimer, J. W4P029
Akyildiz, E. W3P106, W4P128	Asato, K. W2P111	Bengtsson, P.-E. W3P138,	Bougacha, R. W3P038
Aldén, M. W1P093, W3P138,	Asbik, M. W2P088 W4P119	Boukhalfa, M. W2P004
..... W4P008, W4P019,	Ashida, R. W5P077	Benzler, T. W4P037	Boumehdi, M.A. W1P113
..... W4P024, W4P025, W4P035	Atakan, B. W3P067	Bergmann, U. W3P067	Bounaceur, R. W3P062
Aldredege, R. W1P110	Atanga, G. W2P131	Berlette, J. W5P064	Boushaki, T. W1P057

<i>Author</i>	<i>Paper #</i>
Boust, B.	W1P061
Boyette, W.	W5P069
Brackmann, C.	W3P138,
.....	W4P003
Bradley, D.	W5P047
Brady, B.	W5P125
Brequigny, P.	W1P092
Brezinsky, K. ...	W3P054, W3P131
Brockhinke, A.	W1P009,
.....	W2P019, W4P030
Brockhinke, R.	W1P009
Broll, D.	W5P034
Brown, A.	W4P063
Brown, M.	W2P078
Brown, N.	W2P042
Bruck, J.	W3P129
Bueschke, W.	W1P091
Bugler, J.	W3P055, W3P103
Burbano, H.	W2P075
Burke, S.	W3P103
Burke, U.	W3P080,
.....	W3P085, W3P114
Burns, I.	W4P012,
.....	W4P019, W4P041
Burns, R.	W4P015
Burrell, R.	W2P074
Bushe, W.K.	W5P010
Buxton, O.	W4P015
Bychkov, V.	W2P036, W2P117,
.....	W2P118, W4P086
Cai, J.	W3P043
Cai, L.	W2P072
Calhoon Jr., W.	W5P025
Camacho, J.	W4P134, W4P135
Cameron, I.	W1P096
Camou, A.	W4P017
Cancino, L.	W2P084, W3P135
Candel, S.	W1P138
Cannella, W.	W1P084
Carbone, F.	W2P073,
.....	W2P079, W5P022
Carlsson, H.	W5P008
Carter, C.D.	W2P078
Casey, T.	W1P013
Caspary, E.	W4P108
Castillo, J.	W2P008
Castro, F.	W5P054

<i>Author</i>	<i>Paper #</i>
Catoire, L.	W1P132, W3P076,
.....	W3P099, W3P119
Cavaliere, A.	W1P028
Cecere, D.	W5P001
Cha, C.L.	W1P045,
.....	W1P046, W5P084
Cha, M.S.	W1P012, W2P013
Chahine, M.	W1P055, W2P012
Chakravarthy, S.	W2P117,
.....	W5P024
Chakravarty, H.	W3P045
Chalmers, H.	W1P067
Chan, Q.N.	W5P053
Chan, Y.L.	W5P096
Chao, J.	W2P138
Chao, Y.-C.	W1P016, W1P017,
.....	W2P044, W3P137
Chaos, M.	W3P124
Chaoufi, J.	W2P088
Chatelain, K.	W3P104, W3P119
Chaudhuri, S. ...	W2P025, W5P004
Chaumeix, N.	W3P044
Chauveau, C.	W1P057
Chen, C.-H.	W1P039
Chen, D.	W4P123, W4P132
Chen, G.-B.	W2P044, W3P137
Chen, H.	W3P136
Chen, J.H.	W1P104, W2P066,
.....	W5P003, W5P009,
.....	W5P037, W5P057
Chen, J.-Y.	W1P013, W5P028
Chen, L.	W2P098
Chen, Z.	W2P003, W3P002
Cheneau, B.	W1P129
Cheng, F.	W5P093
Cheng, T.-S.	W2P044
Cheng, Z.	W3P036,
.....	W3P077, W3P102
Chernov, A.	W4P061
Cheskis, S.	W4P022
Chien, Y.-C.	W1P011
Chilton, S.	W2P100
Chime, A.	W1P127
Cho, J.	W1P073
Choi, I.	W1P116
Choi, I.	W4P038
Choi, J.-Y.	W2P112

<i>Author</i>	<i>Paper #</i>
Choi, S.	W2P097, W5P072
Choi, S.-K.	W2P018
Choi, Y.-C.	W5P092, W5P103
Chowdhury, A.	W2P126
Chowdhury, S.	W5P069
Chrigui, M.	W3P018
Chujo, T.	W2P060
Chun, K.M.	W1P006,
.....	W1P075, W1P139, W3P089
Chung, S.-H. ...	W1P012, W1P051,
.....	W1P101, W2P018, W3P015,
.....	W3P019, W3P038, W4P112
Ciccarelli, G.	W2P114
Cieslik, W.	W1P091
Clausen, S.	W2P089
Clemens, N.	W4P015, W5P059
Colin, O.	W4P127
Colorado, A.	W1P125
Comandini, A.	W3P044
Comas, B.	W4P053
Commodo, M.	W4P124
Connatser, R.	W4P021
Consalvi, J.-L.	W4P076
Conturso, M.	W4P139
Coriton, B.	W4P006
Coronado, C.	W4P047
Coronel, S.	W2P031
Correa-Pugliese, J.F.	W4P137,
.....	W4P138
Coudour, B.	W4P039
Coussement, A.	W1P138
Cowlard, A.	W4P079
Creta, F.	W5P014
Cruz, G.	W4P017
Cruz, M.	W5P113
Cuenot, B.	W2P038,
.....	W3P005, W4P059
Cuoci, A.	W1P083, W3P070,
.....	W3P130, W4P117, W5P053
Curran, H.	W1P111,
.....	W3P039, W3P041,
.....	W3P046, W3P055,
.....	W3P058, W3P080, W3P085,
.....	W3P093, W3P103, W3P114
Cusano, D.M.	W4P017
Czajka, J.	W1P091, W3P017
da Silva, G.	W3P060, W3P061

<i>Author</i>	<i>Paper #</i>
da Silva, L.F.F.	W3P004
Dagaut, P.	W3P076, W4P098
Dahikar, S.	W4P077
Daily, J.	W3P049, W3P083
Daimon, Y.	W3P030
Daitoku, T.	W4P056
Dally, B.	W3P020, W4P010
Daly, S.	W1P084
Dames, E.	W3P068, W3P110
Dandajeh, H.A.	W1P026
Dang, A.	W2P093
Dang, J.	W2P093
D'Angelo, Y.	W1P024
D'Anna, A.	W4P100,
.....	W4P124, W4P139
Daou, J.	W2P027
Das, D.	W4P092
Davis, M.	W3P127
Daw, C.S.	W1P097
Dayma, G.	W2P035, W3P076
de Benito, E.	W1P098
de Carvalho Jr., J.A.	W4P047
De Champlain, A.	W2P092
De Falco, G.	W4P124
de Goey, P.	W1P028,
.....	W2P006, W5P051
de Joannon, M.	W1P008,
.....	W1P028
de la Rosa, D.	W3P012
de Persis, S.	W1P057
de Pinho, J.	W5P113
de Vries, J.	W4P068
DeFoort, M.	W5P094
Delgado, A.	W5P129
Dell, V.	W5P067
Demarco, R.	W4P076
Demenay, A.	W1P132
Demirgok, B.	W2P036,
.....	W2P076, W2P117, W2P118
Demko, A.	W1P140, W1P141
Deng, S.	W3P132
Deng, S.	W4P111
Dennis, K.	W5P118
D'Errico, G.	W1P102
Desai, S.	W1P039
Desain, J.	W5P125
Desgroux, P.	W1P113

<i>Author</i>	<i>Paper #</i>
DeToni, A.	W3P135
Dias, V.	W2P059
Dieguez-Alonso, A.	W5P101
Dietrich, D.	W3P022
Dillier, C.	W1P140, W1P141
Dillstrom, T.	W4P099
Dinkelacker, F.	W1P122, W1P124, W5P021
Dischino, K.	W4P043
Ditaranto, M.	W2P103
Dlabka, J.	W3P078
Dlugosz, J.	W1P033
Dmitriev, A.	W2P021
Domen, S.	W1P117
Domoto, K.	W5P089
Dong, X.	W1P060
Dorofeev, S.B.	W2P138
Dowlut, A.	W5P024
Dreier, T.	W4P005, W4P011, W4P037
Dreizin, E.L.	W5P126
Dreizler, A.	W5P035
Drenth, A.	W1P076
Driscoll, J.	W5P018
Dryer, F.L.	W3P007, W3P124
Du, H.	W5P074
Dubey, A.K.	W4P115
Dubois, T.	W1P092
Duchaine, F.	W2P038
Ducruix, S.	W1P129, W1P138
Duic, N.	W5P011, W5P085
Dunn, J.	W4P041
Dunn-Rankin, D.	W1P011, W1P142, W2P070, W2P093, W4P029, W4P140
Duque, J.V.F.	W2P087
Dutka, M.D.	W2P103
Dworkin, S.	W4P091
Dzieminska, E.	W2P120
Eaves, N.	W4P091
Ebi, D.	W5P059
Ebina, W.	W4P051
Edoh, A.	W5P030
Edwards, K.D.	W1P097
Edwards, R.	W2P093

<i>Author</i>	<i>Paper #</i>
Egolfopoulos, F.N.	W1P037, W2P030, W2P071, W2P073, W2P074, W2P075, W2P079, W5P019, W5P022
Eguia, P.	W5P105
Ehn, A.	W1P005, W4P035
Eiermann, M.	W2P053
Eigenbrod, C.	W4P079
Eisazadeh-Far, K.	W1P037
Elbaz, A.	W5P034
Eldeeb, M.	W1P133
Ellison, B.	W3P049, W3P083
Ellzey, J.L.	W2P078
Elorf, A.E.	W2P088
El-Rachidi, M.	W2P109
Elvati, P.	W4P099, W4P102, W5P124
Essebbar, E.	W4P014
Essmann, S.	W2P130
Euler, M.	W5P035
Evans, M.	W5P052, W5P053
Fachini, F.	W2P051, W3P027
Falkenstein-Smith, R.	W1P015, W1P044, W1P050
Falle, S.	W2P134
Falue, F.	W3P120
Fan, B.	W4P046
Fan, J.	W5P002, W5P063
Fang, B.	W2P095
Fang, J.	W2P049
Fang, M.	W5P075
Fang, T.	W4P091
Faravelli, T.	W1P083, W3P070, W3P075, W3P130, W4P117, W4P134
Farooq, A.	W1P055, W3P038, W3P053, W3P088, W3P122, W4P014
Farouk, T.	W3P007
Fassheber, N.	W3P116
Fateev, A.	W2P089
Febrero, L.	W5P104, W5P105
Felsmann, D.	W2P080
Ferkul, P.	W4P079
Fernandez-Galisteo, D.	W2P009, W5P060

<i>Author</i>	<i>Paper #</i>
Fernandez-Pello, C.	W2P061, W4P055, W4P072, W4P079, W4P085
Feroughi, O.	W4P005, W4P011, W4P037
Ferrari, M.	W3P121
Fikri, M.	W3P066
Filho, F.L.S.	W3P018
Finney, C.E.A.	W1P097
Fischer, M.	W3P106
Fittschen, C.	W3P074
Flamenco, J.	W1P108
Fletcher, T.H.	W4P070
Fogla, N.	W5P014
Fomin, A.	W4P022
Fournet, R.	W3P074, W3P121
Frank, J.H.	W4P006
Franzelli, B.	W3P013
Frassoldati, A.	W1P083, W3P070, W3P075, W3P130, W5P053
Frederickson, L.	W4P133
Frenklach, M.	W3P092, W4P093, W4P094
Frenzel, I.	W4P090, W4P117
Fridlyand, A.	W3P054, W3P131
Friedrichs, G.	W3P116
Frottier, O.	W3P074
Fu, H.-W.	W4P034
Fu, J.	W5P023
Fu, P.F.	W2P014
Fu, Z.Q.	W2P014
Fuchihata, M.	W2P022
Fuentes, A.	W4P076
Fuest, F.	W4P023, W5P036
Fuhrmann, D.	W4P001, W4P004
Fujimura, K.	W5P089
Fujita, O.	W1P032, W4P055, W4P078, W4P079
Fukumasu, N.	W3P029
Funaki, I.	W2P123
Fursenko, R.	W1P042, W2P001, W2P085
Futko, S.	W1P136
Gabet, K.	W4P023
Gadgil, A.	W5P100
Gadsbøl, R.	W2P089

<i>Author</i>	<i>Paper #</i>
Gallacher, J.R.	W4P070
Gallage, I.	W5P061
Gao, C.	W3P073, W3P081
Gao, J.	W3P082
Gao, J.	W4P035
Gao, Y.	W4P131
Garcia-Soriano, G.	W2P008
Garcia-Ybarra, P.	W2P008
Gargiulo, V.	W5P098
Gaskell, P.	W5P047
Gavrikov, A.	W2P127
Ge, B.	W1P130
Geier, M.	W5P086, W5P091
Genzale, C.	W1P077, W3P028
Gerasimov, I.	W2P035
Gersen, S.	W1P082
Ghamari, M.	W3P035
Ghata, N.	W3P014
Ghiassi, H.	W4P096, W4P097
Giaomazzi, E.	W5P001
Gibbins, J.	W1P067
Gillie, M.	W4P074
Giudicianni, P.	W5P098
Glarborg, P.	W2P089
Glaude, P.-A.	W3P062, W3P121
Glebov, L.	W2P015
Gökalp, I.	W1P057, W2P088, W5P107, W5P108
Goktekin, E.	W3P109
Goktolga, U.	W1P028
Goldsbrough, S.S.	W1P111, W3P107, W3P131
Gol'dshtein, V.	W3P003
Goldsmith, C.F.	W3P068
Goldstein, E.A.	W1P007
Golovastov, S.	W2P116
Golub, V.	W2P026, W2P116
Gonchikzhapov, M.	W4P057, W4P066
Gord, J.	W4P007
Gorder, R.	W2P090
Gore, J.P.	W4P018, W5P062
Goschütz, M.	W4P004
Goteng, G.	W3P087
Goto, T.	W2P002
Gotoda, H.	W1P117, W2P057
Gövert, B.	W3P133

<i>Author</i>	<i>Paper #</i>
Govert, S.	W5P055
Grabarczyk, M.	W4P067
Grady, N.	W5P038, W5P064
Granada, E.	W2P105,
.....	W5P104, W5P105
Green, W.	W3P042, W3P043,
.....	W3P068, W3P073, W3P081
Greenberg, B.	W3P006
Gregoire, C.	W3P055
Gross, J.	W5P060
Grosseuvres, R.	W3P044
Grossman, K.	W1P141
Gruber, A.	W2P066, W5P057
Gruenefeld, G.	W5P034
Grumstrup, T. ..	W3P007, W5P094
Grune, J.	W2P063, W2P064
Gu, D.	W4P010
Gu, X.	W5P047
Guethe, F.	W5P017
Gunasekera, K.	W1P108
Gundersen, M.	W1P037
Gupta, R.	W4P116
Gur, T.M.	W1P007, W1P049
Gururajan, V.	W5P019
Gustafson, J.	W4P003
Haas-Wittmuess, R.	W2P006
Hadden, R.	W4P069, W4P074
Hagen, C.	W1P084,
.....	W1P134, W3P021
Hajek, J.	W5P068
Halter, F.	W1P092,
.....	W2P003, W2P004
Hamada, Y.	W5P056
Hamilton, M.	W2P094
Hampson, G.	W1P072
Han, J.	W1P013, W3P122
Han, W.	W3P002
Han, Y.	W5P112
Hansen, N.	W2P017,
.....	W2P020, W2P035
Hansen, S.	W4P070
Hanson, R.	W4P125
Hartl, S.	W2P005,
.....	W2P053, W3P040
Hartmann, E.	W2P084
Hartmann, R. ...	W2P084, W5P039
Hartono, H.	W5P119

<i>Author</i>	<i>Paper #</i>
Hasegawa, H.	W5P120
Hasegawa, S. ...	W1P004, W1P023,
.....	W1P064, W2P001,
.....	W2P040, W4P115
Hasegawa, T.	W5P058
Hashimoto, H.	W3P033
Hashimoto, N.	W5P071,
.....	W5P073, W5P079
Hashimoto, S.	W1P089
Hashizume, S.	W4P050
Hassanally, M.	W5P057
Hasse, C.	W2P005, W2P053,
.....	W3P040, W4P090, W4P117
Hatakeda, N.	W1P025, W1P059
Hataysal, S.E.	W1P118
Hattori, T.	W2P054
Haustein, H.	W3P133
Hawkes, E.	W1P102, W5P006
Hayakawa, A.	W2P002,
.....	W2P136, W3P016, W5P020
Hayashi, A.K.	W2P120
Hayashi, J.	W2P058,
.....	W5P073, W5P079
Hayashi, N.	W2P037
Hayashi, R.	W4P045
Hecht, E.	W5P086
Hegde, U.G.	W1P048
Hemberger, P.	W3P106
Hemdal, S.	W1P098
Hemken, C.	W2P080
Hendra, G.	W5P010
Hennecke, C.	W1P122, W5P021
Herbinet, O.	W3P062,
.....	W3P074, W3P075
Hermanns, R.	W2P006
Hermanson, J. ..	W1P127, W5P042
Herzler, J.	W3P066
Heufer, K.A.	W3P108
Hewson, J.	W4P063,
.....	W5P044, W5P048
Heyne, J.	W3P124
Hickman, J.M.	W2P067
Hicks, M.C.	W1P048, W3P022
Higuera, F.J.	W2P008, W2P041
Hinton, N.	W2P007
Hiraiwa, T.	W1P137
Hirano, K.	W5P056

<i>Author</i>	<i>Paper #</i>
Hirasawa, T.	W2P050, W2P060
Hiroshi, Y.	W2P037
Hisazumi, Y.	W1P010
Hitomi, S.	W1P110
Hockett, A.	W1P072
Holder, A.	W2P102
Holmén, V.	W5P008
Höltermann, M.	W5P021
Homan-Cruz, G.	W5P114
Hong, J.-C.	W5P092, W5P103
Hong, Y.S.	W5P088
Hori, T.	W1P010, W1P035
Hossain, A.	W2P050
Hourani, N.	W1P055
Houzeaux, G.	W5P055
Hsu, D.-L.	W1P040
Hsu, J.-R.	W2P046
Hu, E.	W3P064
Hu, Z.	W3P132
Huang, D.-J.	W4P034
Huang, E.	W4P006
Huang, Q.	W2P106
Huang, X.	W4P060
Huang, Z.	W3P064,
.....	W3P091, W5P016
Huber, F.	W4P027
Hudak, I.	W5P050
Huh, H.	W2P104
Hui, S.	W5P078
Humphries, G.	W4P012,
.....	W4P041
Hunger, F.	W2P053
Hurst, E.	W4P113
Hwang, J.	W5P043
Hwang, S.S.	W1P045,
.....	W1P046, W5P084
Hyeon, G.	W1P101
Iavarone, S.	W4P100
Ibrahim, A.	W2P010
Ichikawa, Y.	W1P131
Ida, T.	W2P022
Idlachen, S.	W4P040
Idlimam, A.	W2P088
Iglesias, I.	W2P105
Ihme, M.	W3P013, W5P062
Iino, K.	W2P058
Ilchenko, V.	W5P067

<i>Author</i>	<i>Paper #</i>
Im, H.G.	W1P013, W1P112,
.....	W2P068, W3P019,
.....	W4P131, W5P004
Inatsuki, M.	W4P078
Ishimura, Y.	W1P107, W3P034
Isobe, N.	W3P084
Ito, K.	W2P055
Ito, S.	W1P114
Itoh, M.	W3P016
Iwamoto, T.	W3P033
Iwamura, Y.	W2P136
Izrar, B.	W2P088
Jacob, G.	W1P132
Janas, P.	W1P106
Janicka, J.	W3P018, W5P035
Jaramillo, I.	W4P096, W4P097
Javed, T.	W3P088
Javoy, S.	W3P120
Jayachandran, J.	W2P071
Jeanmart, H.	W2P059
Jemcov, A.	W5P013
Jensen, P.A.	W2P089
Jeon, S.	W1P021
Jeon, S.	W5P031
Jeon, Y.H.	W1P030
Jeong, B.	W2P016
Jeong, J.	W2P091
Jia, M.	W1P087
Jia, Q.	W2P095
Jia, Z.	W3P100
Jiang, L.	W3P032
Jiang, L.	W3P082
Jin, T.	W5P063
Jin, W.	W5P016
Jin, Y.	W4P046
Jing, L.	W2P024
Joakim, B.	W4P008, W4P024
Johansen, J.	W2P089
Johansen, L.C.R.	W1P098
Johnson, D.	W1P049
Johnston, H.	W2P126
Johnstone, R.	W5P049
Jomaas, G.	W4P079
Jones, J.	W4P085
Jones, W.	W5P040
Jonsson, M.	W4P008, W4P024
Jouzdani, S.	W1P044

<i>Author</i>	<i>Paper #</i>
Ju, Y.	W2P003
Juddoo, M.	W5P033
Jung, K.	W1P121
Jurisch, M.	W5P040
Kadowaki, S.	W1P018,
.....	W2P129, W5P020
Kailasanath, K.	W2P121
Kaiser, S.	W1P106, W4P004
Kakimi, M.	W5P089
Kalla, S.	W2P092
Kalpathy, S.V.	W4P106,
.....	W4P113
Kamal, M.M.	W5P032
Kamei, K.	W4P062
Kapusta, L.	W3P017
Karnani, S.	W1P142, W4P029
Kasahara, J.	W2P123
Kasimov, A.	W2P128
Kasper, T.	W3P067,
.....	W3P106, W4P128
Kastengren, A.	W4P032,
.....	W4P033
Kataeva, L.	W4P057
Kato, K.	W3P016
Kato, S.	W3P016
Katoshevski, D.	W3P006
Katshiatshia, H.M.	W2P059
Katsuta, M.	W2P001, W2P040
Katta, V.R.	W3P031
Kawahara, N. ...	W1P089, W1P099
Kazakov, A.	W3P124
Kazanc, F.	W5P095
Keese, C.	W2P032
Kegasa, A.	W1P010, W1P035
Kellenberger, M.	W2P114
Kempema, N.	W4P042
Kempf, A.	W1P105, W1P106,
.....	W3P010, W5P028
Keromnes, A.	W3P065
Kerstein, A.	W5P045, W5P070
Ketelheun, A.	W5P035
Khakbazbaboli, M.	W2P114
Khalfa, A.	W3P121
Kholghy, M.R.	W2P043,
.....	W4P118
Khurshid, M.	W1P022

<i>Author</i>	<i>Paper #</i>
Kikuchi, M.	W2P001,
.....	W2P040, W3P025
Kim, G.-J.	W4P038
Kim, J.	W1P090
Kim, J.	W2P039
Kim, J.	W5P046
Kim, J.	W5P080
Kim, J.-G.	W5P092, W5P103
Kim, M.	W1P051
Kim, M.	W1P139, W3P089
Kim, N.	W4P095
Kim, S.	W1P068, W4P020
Kim, S.H.	W5P029
Kim, S.-I.	W5P083
Kim, S.J.	W2P104
Kim, S.W.	W4P031
Kim, S.O.	W5P009
Kim, T.	W5P043
Kim, T.H.	W4P095, W4P114
Kim, T.-Y.	W2P112
Kim, Y.	W1P121, W2P039,
.....	W4P095, W4P114, W5P031
Kirchmeyer, D.	W4P054
Kirksey, N.	W1P001
Kitagawa, T.	W2P062
Kleinheinz, K.	W5P006
Klippenstein, S.J.	W3P047
Kneer, R.	W3P133
Knobel, A.	W4P132
Knox, B.	W1P077
Knyazev, V.D.	W3P063,
.....	W3P134
Knyazkov, D.	W2P021,
.....	W2P035, W4P128
Kobayashi, H.	W1P018,
.....	W2P002, W2P136,
.....	W3P016, W5P016, W5P020
Kobayashi, T.	W2P001,
.....	W2P040
Kobayashi, Y.	W4P129
Kobayashi, Y.	W4P073
Koch, J.	W4P111
Köhler, M.	W3P106
Kohse-Höinghaus, K.	W2P020,
.....	W2P072, W2P080, W4P030
Kok, J.	W5P055
Kokjohn, S.	W1P104

<i>Author</i>	<i>Paper #</i>
Kokubun, M.E.	W2P051
Koli, S.	W1P039
Kolla, H.	W5P037, W5P057
Kondo, M.	W1P099
Konno, M.	W3P084
Konnov, A.	W2P006,
.....	W3P040, W3P138
Kook, S.	W1P102
Koppmann, J.	W1P009
Korobeinichev, O.	W2P021,
.....	W2P035, W4P057, W4P061,
.....	W4P065, W4P066, W4P128
Koroglu, B.	W4P026
Koshi, M.	W1P081, W3P030
Kozinski, J.	W1P048
Kraft, M.	W4P121, W4P122,
.....	W4P123, W4P132
Kramlich, J.	W1P127
Krieger, G.	W3P029
Krivokorytov, M.	W2P026
Kronemayer, H.	W4P005
Krueger, J.	W5P110
Krüger, J.	W4P030
Kruse, S.	W1P029, W5P034
Kryzhanovskiy, J.	W2P023
Ku, X.	W5P091, W5P099
Kudo, T.	W2P002, W2P136,
.....	W3P016, W5P020
Kudo, Y.	W4P048
Kuene, G.	W5P035
Kuhl, A.	W2P139
Kumar, A.	W2P117
Kuppa, K.	W1P124
Kurian, V.	W4P116
Kuron, M.	W5P003
Kurose, R.	W4P126
Kusano, Y.	W4P035
Kushida, G.	W4P052, W4P083
Kusunoki, T.	W5P120
Kuwana, K.	W2P022
Kuznetsov, M.	W2P063,
.....	W2P064, W2P124
Kwon, M.	W1P068
Labbe, N.J.	W3P047
Lacoste, D.	W1P054
Lai, J.	W4P099
Laine, R.	W5P124

<i>Author</i>	<i>Paper #</i>
Lakshminarayanan, A.	W1P076
Lam, K.Y.	W4P033
Lambert, V.	W3P109
Langer, A.	W4P011
Lansinger, V.	W4P070
Larsson, K.	W4P002,
.....	W4P008, W4P024
Lartigue, G.	W1P024
Lask, K.	W5P100
Latourneau, K.	W3P123
Law, C.K.	W2P020,
.....	W2P025, W2P066,
.....	W2P118, W4P111, W5P004
Lawn, C.	W1P026
Lawson, A.	W1P039
Lavadera, M.L.	W1P008
Le Moyne, L.	W3P065
Lee, B.J.	W2P068
Lee, C.	W1P068, W4P020
Lee, C.-E.	W2P108
Lee, D.J.	W2P074
Lee, D.-W.	W5P092, W5P103
Lee, E.J.	W1P030
Lee, H.	W1P126
Lee, H.	W5P072
Lee, H.Y.	W1P046, W5P084
Lee, J.	W5P118
Lee, J.H.	W2P104
Lee, J.K.	W2P104, W4P031
Lee, K.	W1P115,
.....	W1P116, W2P016
Lee, K.	W2P011
Lee, M.H.	W4P036
Lee, M.J.	W1P065, W2P081
Lee, P.H.	W1P045,
.....	W1P046, W5P084
Lee, S.	W1P006, W3P089
Lee, S.	W2P011
Lee, S.	W2P108
Lee, S.-Y.	W1P078, W1P109
Lee, U.	W1P021, W2P091
Lee, Y.-Y.	W4P034
Lee, Y.-J.	W5P092, W5P103
Lefebvre, A.	W2P004
Lefort, B.	W3P065
Legros, G.	W4P079
Lehtiniemi, H.	W1P079

<i>Author.....Paper #</i>	<i>Author.....Paper #</i>	<i>Author.....Paper #</i>	<i>Author.....Paper #</i>
Lei, F. W1P123	Liu, K. W5P112	Man, X. W3P048	Maxwell, B. W2P134
Leipold, F. W4P035	Liu, N. W4P057, W4P066	Mancini, M. W2P089	Mayer, D. W2P072
Leiroz, A. W5P113	Liu, P. W5P093, W5P096	Mannaa, O. W3P038	McAllister, S. W4P071
Lengden, M. W4P012, W4P041	Liu, Q. W2P082, W2P106	Mannan, M.S. W5P117	McCollam, S. W4P137
Leoni, M. W4P133	Liu, S. W2P122	Mannan, S. W2P126	McCormick, R. W1P076
Lesbayev, B. W4P089, W5P102	Liu, W. W1P130	Mansfield, A. W1P112	McCown, K. W5P114
Levendis, Y. W5P095	Liu, W. W3P127	Mansour, M. W5P033, W5P034	McDonell, V.G. W1P001,
Levinsky, H. W1P082	Lobasov, A. W2P021	Mansurov, Z. W4P089, W1P119, W1P125,
Li, G. W2P106	Loisy, A. W2P042 W4P094, W5P102 W1P126, W3P001
Li, H.Y. W1P017	Long, M.B. W4P042	Mao, Q. W5P122	McEnally, C.S. W4P092
Li, J. W1P027	Loong, B. W1P049	Marchese, A.J. W1P072,	McLaggan, M. W4P074
Li, S. W2P106, W4P009,	Loparo, Z. W4P026 W1P076, W3P007,	McNally, D. W1P052
..... W5P076, W5P116	Lopez, J. W2P015 W3P086, W5P094	Meadows, J. W1P043
Li, S. W3P037	Loukou, A. W1P041	Margenat, S. W2P008	Meah, N. W5P049
Li, T. W5P091, W5P099	Løvås, T. W2P103,	Mari, R. W2P038	Medeiros, B. W2P096
Li, T. W5P112 W5P091, W5P099	Marks, B. W3P055	Medwell, P. W3P020,
Li, W. W2P077	Lowe, J. W4P102	Markus, D. W2P130 W4P010, W5P052,
Li, X. W5P077	Lu, G. W5P093	Marquis, A. W5P040 W5P053, W5P100
Li, X.-Y. W3P111, W4P044	Lu, T. W4P131,	Marrodán, L. W4P105	Meier, W. W5P036
Li, Y. W1P079 W5P003, W5P065, W5P066	Marshall, A. W4P064	Mendes, J. W3P041
Li, Y. W3P036,	Lu, Z. W5P065, W5P066	Martens, F. W4P116	Mendes, M. W1P041
..... W3P077, W3P101,	Lucachick, G. W4P130	Martin, D.E. W1P011, W4P029	Menon, S. W2P030, W2P071
..... W3P102, W4P034, W4P098	Lucassen, A. W2P017, W2P020	Martin, S. W5P012, W5P013	Menon, S. W5P038, W5P064
Li, Y. W3P058	Lucchini, T. W1P102	Martins, M.F. W2P096	Merchan-Merchan, W. W4P137,
Li, Y.-H. W1P017,	Luikov, A.V. W1P136	Maruta, K. W1P004, W4P138
..... W2P044, W3P137	Lundgren, E. W4P003 W1P022, W1P023,	Merchant, S. W3P042, W3P068
Li, Z. W1P005, W3P138	Luo, K. W5P002, W5P063 W1P064, W2P001, W2P040,	Meredith, K. W4P082
..... W4P019, W4P025, W4P035	Luo, K. W5P122 W2P056, W2P085, W4P115	Merlin, C. W1P135
Li, Z. W3P136	Luo, K.H. W5P065, W5P066	Maslennikov, D. W4P057	Merlo, N. W1P057
Liang, Y. W3P071	Luo, Z. W1P079	Masri, A. W3P020, W5P033	Mescher, A. W1P127
Liao, Y.-H. W2P069, W5P042	Luo, Z. W5P075	Massmeyer, A. W3P133	Messig, D. W2P053
Lieb, S. W4P135	Luong, M.B. W1P101, W5P009	Matalon, M. W2P051, W5P014	Mevel, R. W2P119,
Lien, Y.-S. W1P016	Lutsenko, N. W5P130	Matas-Guell, B. W5P091 W3P099, W3P104,
Lietz, C. W5P057	Lynch, P. W4P032, W4P033	Matheson, T. W3P024 W3P105, W3P119, W3P120
Lieuwen, T.C. .. W5P007, W5P037	Lyra, S. W5P037	Mathieu, O. W3P055	Meyer, T.R. W4P007
Lighty, J.S. W2P094,	Ma, H.-K. W5P106	Matinyan, D. W2P077	Miao, J. W1P019
..... W4P096, W4P097	Ma, L. W3P023	Matrat, M. W3P076	Michael, J. W4P007
Lignell, D. W5P048	Maas, U. W2P130, W5P039	Matsugi, A. W1P020,	Michael, J.V. W3P047
Lim, H. W5P081	Magi, V. W1P071, W1P103 W3P045, W3P095	Michelsen, H. W4P125
Lin, C.-P. W5P106	Magnotti, G. W3P028	Matsumoto, K. W5P089	Mikami, M. W1P025,
Lin, H.-T. W2P044	Mahapatra, N. W4P116	Matsuo, A. W2P113, W2P123 W1P059, W1P107,
Lin, W. W1P053	Maines, G. W5P118	Matsuoka, K. W2P123 W3P008, W3P034
Link, E. W4P064	Maionchi, D. W3P027	Matsuoka, T. W2P060, W4P062	Mikulcic, H. W5P085
Link, S. W2P061	Makino, H. W5P073, W5P079	Matsuura, Y. W3P030	Milcarek, R. W1P014
Liu, A.K. W3P111	Malewicki, T. W1P079	Mattias, R. W1P093	Miller, F.J. W4P081,
Liu, C.-R. W2P046	Malik, A. W1P070	Matuszkiewicz, R. W2P125 W4P087, W4P133
Liu, H. W4P046	Malte, P.C. W1P127, W2P090	Mauss, F. W1P079	

<i>Author.....Paper #</i>	<i>Author.....Paper #</i>	<i>Author.....Paper #</i>	<i>Author.....Paper #</i>
Miller, H. W4P132, W4P136	Naber, J. W1P078, W1P109	Niu, F. W5P116	Palacios, A. W5P047
Millera, Á. W4P105, W4P107, W4P110	Nagai, T. W1P003	Noda, S. W1P058, W2P060, W4P062	Paletsky, A. W4P057, W4P066
Mimoto, R. W2P002	Nagano, Y. W2P062	Noguchi, Y. W1P110	Palvolgyi, R. W3P039
Minaev, S. W1P042, W2P001, W2P085	Naganovsky, Y. W4P057	Noh, D. W1P115	Pan, K.-L. W3P009
Minowa, T. W2P055	Nagasaki, A. W1P010, W1P035	Nonaka, Y. W5P056	Pan, L. W3P064, W3P091
Minster, O. W4P079	Nagata, H. W4P062	Nordström, E. W3P138	Pan, X. W5P060
Minutolo, P. W4P124	Nagy, T. W3P090	Northrop, W. W1P038, W4P130	Papageorge, M. W4P016, W5P036
Mira, D. W5P055	Naito, H. W4P049, W4P050, W4P051	Noske, R. W2P019	Park, D. W1P012
Mitchell, R.E. W1P007 W1P049, W2P089, W5P090	Nakajima, S. W5P020	Novosselov, I. W2P090	Park, J. W1P073, W1P075
Miura, K. W5P077	Nakamura, H. .. W1P004, W1P022, W1P023, W1P064, W2P001, W2P040, W2P056, W4P115	Nunome, Y. W1P138	Park, J.-H. W5P092, W5P103
Miyamae, S. W2P033	Nakamura, Y. W2P050, W2P060, W3P082	Ochs, B. W5P038, W5P064	Park, O. W4P015
Mizia, J. W4P043	Nakano, H. W5P128	O'Connor, E. W3P058	Park, S. W1P120
Mizuno, M. W4P052	Nakatsuka, N. W4P126, W5P073, W5P079	O'Connor, J. W1P074	Park, S. W1P073, W1P075
Mizuno, S. W2P022	Nakaya, S. W1P137, W4P073	Oh, S. W1P121	Park, S. W2P107
Mizutani, K. W4P055	Nakayama, Y. W2P113	Oh, W. W2P108	Park, S.-J. W5P092, W5P103
Modica, V. W2P004	Nanba, S. W1P099	Ohashi, N. W4P049	Park, S. W3P038, W4P131
Moeck, J. W1P054	Nanda, S. W1P048	Ohmura, R. W5P127, W5P128	Park, T. W1P115
Montanaro, A. W1P078	Naser, N. W3P015	Okada, N. W1P036	Parra, T. W5P054
Monteiro, J. W2P084	Nasir, E.F. W3P053, W3P088	Okafor, E. W2P062	Partridge, W. W4P021
Moon, J. W1P021, W2P091	Nathan, G. W3P020, W4P010	Okajima, S. W1P047	Pastore, B. W1P052
Morimune, T. W1P069	Nativel, D. W3P044	Okawa, T. W4P051	Pastrich, D. W3P123
Moriue, O. W3P033	Natta, G. W1P083	Okuno, Y. W1P117, W2P057	Patino, D. W2P105, W5P105
Moriyama, K. W2P045	Naucér, J. W3P040	Oldani, A. W1P128	Paulhiac, D. W3P005
Morozumi, T. W2P123	Naud, B. W3P023	Oliveira, A.A.M. W2P084, W3P135, W5P039	Pavlovic, J. W2P102
Mosbach, S. W4P121, W4P122, W4P123, W4P132	Nave, O. W3P003	Oliveira, E. W2P084, W3P135	Pawlak-Kruczek, H. W1P033
Moshhammer, K. W2P020, W2P072, W2P080	Nayagam, V. W3P022	Oliveira, L. W3P135	Peale, R. W4P026
Most, J.-M. W4P077	Neal, N. W1P088	Olm, C. W3P039, W3P040, W3P093	Pearce, P. W2P027
Mounaim-Rousselle, C. ... W1P092	Negishi, H. W3P030	Olofsson, N.-E. W4P119	Pearlman, H. W1P039, W1P052
Moureau, V. W1P024	Nevrly, V. W3P078	Olsen, D. W1P076	Pedersen, H. W2P131
Movahedi, Z. ... W1P062, W5P061	Ngo, A.D. W4P138	Olson, N. W3P021	Peng, C.-H. W5P106
Mrad-Koched, N. W2P088	Nguyen, T. W1P105	Olson, S. W4P079	Pepiot, P. W3P071
Mueller, M. W4P111	Niedzielska, U. W2P119	Ombrello, T. W2P078	Perez, P. W4P096
Mulla, I. W5P024	Nielsen, K. W2P089	Onishi, S. W1P004	Perez, R. W5P104
Muñoz, C.A. W2P135	Niemeyer, K. W1P084, W3P072	Ono, K. W4P101	Perez, R. W5P054
Muntean, V. W2P041	Niguse, Y. W1P066	Ordonneau, G. W1P135	Perkovic, L. W5P011
Murase, E. W3P033	Nikitin, I.S. W3P096	Orlovskaya, N. W2P101	Perlman, C. W1P079
Murase, K. W5P056	Nimmo, W. W1P002, W1P031, W1P034, W2P100	Orr, D. W4P138	Peters, N. W3P115
Murphy, D. W3P122, W4P085	Nishiki, S. W2P028	Oshima, N. W5P056	Petersen, E.L. .. W1P140, W2P032, W2P126, W3P055, W3P123, W4P017, W5P017, W5P114, W5P117, W5P125
Musculus, M. W1P074	Nishimura, K. W4P078	Osorio, A. W4P055	Peukert, S.L. W3P047
Myllerup, L. W2P089	Nishioka, M. W2P054	Oßwald, P. W3P106	Pfefferle, L.D. W4P092
Na'Inna, A.M. W2P115	Nisson, E. W1P005	Ostrycharczyk, M. W1P033	Pham, P.X. W3P020
		Pachler, R. W3P052	Phylaktou, H.N. W2P115
		Packard, A. W3P092	Picchia, F.R. W5P001
		Pal, P. W1P112	

<i>Author</i>	<i>Paper #</i>
Picciani, M.	W2P137
Pickard, S.	W1P002
Pielecha, I.	W1P091, W3P017
Pierce, F.	W4P063
Pilling, M.J.	W3P079, W3P090
Piotrowicz, J.	W2P077
Pitsch, H.	W1P029,
.....	W2P072, W5P006, W5P034
Pitz, R.	W5P038, W5P064
Pitz, W.	W3P080
Poddar, N.	W4P106,
.....	W4P108, W4P109
Polley, N.	W1P072
Pope, C.	W4P104
Pope, S.B.	W3P071,
.....	W5P026, W5P046
Popov, K.	W3P063, W3P134
Porowski, R.	W4P067
Porteiro, J.	W2P105
Porterfield, J.	W3P049
Pourkashanian, M.	W1P002,
.....	W1P031, W1P034, W2P100
Prahanphap, H.	W2P077
Priesching, P. ...	W5P011, W5P085
Prikhodko, N.	W4P089,
.....	W4P094, W5P102
Proch, F.	W1P105,
.....	W3P010, W5P028
Prüfert, U.	W2P053
Pugh, D.	W3P012
Pujol, T.	W4P053
Qi, F.	W3P036, W3P043,
.....	W3P077, W3P101,
.....	W3P102, W4P034, W4P098
Qiu, L.	W1P080
Quintiere, J.G.	W4P080
Radulescu, M. ..	W2P134, W5P118
Ragucci, R.	W1P008,
.....	W1P028, W5P098
Rahinov, I.	W4P022
Rahman, M.R.A.	W2P033
Rajendran, S.	W2P098
Raju, M.P.	W1P079
Raman, J.	W5P107, W5P108
Raman, V.	W5P057
Rangwala, A.S.	W4P086
Rankin, B.	W5P062

<i>Author</i>	<i>Paper #</i>
Ranzi, E.	W1P083,
.....	W3P075, W3P130
Ratcliff, M.	W1P076
Ratner, A.	W3P035, W5P097
Ratzke, A.	W1P124
Rau, F.	W2P005,
.....	W2P006, W3P040
Ravi, S.	W5P017
Ravikrishna, R.V.	W2P048
Reddy, S.N.	W1P048
Regueiro, A.	W2P105,
.....	W5P104, W5P105
Reid, D.	W1P140, W1P141
Rein, G.	W4P060, W4P069
Reitz, R.D.	W1P080, W1P087
Ren, N.	W4P064
Ren, Y.	W4P009
Ren, Z.	W5P003,
.....	W5P065, W5P066
Renou, B.	W2P003, W2P004
Reszka, P.	W4P076
Riber, E.	W3P005
Ricci, S.	W4P059
Richardson, E.	W3P024,
.....	W5P007, W5P049
Riedel, U.	W3P092, W3P106
Rieken, E.	W4P125
Rieth, M.	W5P028
Rittler, A.	W3P010
Rizvi, T.-E.-A.	W1P031
Roberts, W.	W2P069,
.....	W2P109, W3P087,
.....	W4P091, W5P069
Robertson, S.	W3P079
Robichaud, D.	W3P049
Rocha, M.	W2P084, W3P135
Rochoux, M.	W4P059
Rodrigues, H.C.	W3P023
Rodriguez, A. ...	W3P074, W3P075
Rodriguez, D.	W5P126
Roekaerts, D.	W3P023
Ronney, P.D.	W1P039,
.....	W1P108, W2P009,
.....	W2P077, W5P060
Roquemoire, W.	W5P053
Rosdzimin, A.R.M.	W2P055
Ross, E.	W3P060, W3P061

<i>Author</i>	<i>Paper #</i>
Rothamer, D.	W1P088, W4P028
Rouvreau, S.	W4P079
Roy, B.	W2P098
Roy, S.	W4P007
Royo, E.	W4P105
Roze, C.	W4P040
Ruelas, A.M.	W5P017
Ruff, G.	W4P079
Ruscio, A.	W5P095
Ryu, C.	W2P091
Sabia, P.	W1P008, W1P028
Saburi, T.	W1P020
Sadiki, A.	W3P018
Saeki, T.	W5P089
Saggese, C.	W4P134
Sahlberg, A.-L.	W4P019,
.....	W4P025
Sahu, A.	W2P048
Saito, K.	W5P112
Sakaki, K.	W1P137
Sakata, K.	W4P083
Salamonowicz, Z.	W2P125
Salenbauch, S. ..	W4P090, W4P117
Salewski, M.	W4P035
Salgansky, E.	W5P111
Salinas, P.	W4P110
Sammet, T.	W1P140, W1P141
Samu, V.	W3P054
Sanchez-Sanz, M.	W4P072
Sane, A.	W4P018
Sankaran, R.	W1P104
Sannan, S.	W5P045
Saputro, H.	W3P008
Sarathy, M.	W1P013,
.....	W1P022, W1P055,
.....	W2P017, W2P109, W3P038,
.....	W3P069, W3P087, W4P131
Sarh, B.	W2P088
Sasakura, K.	W5P128
Satija, A.	W4P018
Sato, K.	W1P032
Sato, K.	W3P084
Sato, N.	W2P050
Sauer, V.	W2P070
Scarborough, D.	W5P038,
.....	W5P064
Scheer, A.	W3P081

<i>Author</i>	<i>Paper #</i>
Schiessl, R.A.	W5P039
Schild, M.	W1P106, W4P004
Schmitt, T.	W1P138
Schoenitz, M.	W5P126
Schroeder, W.	W1P037
Schulz, C.	W3P066, W4P004,
.....	W4P005, W4P011, W4P037
Schwer, D.A.	W2P121
Seakins, P.	W3P079
Seal, S.	W1P140, W1P141
Sedarsky, D.	W4P040
Sedyó, I.	W3P090
Selim, H.	W2P017
Selvaraj, P.	W4P131
Sen, F.	W3P067
Senecal, P.K.	W1P079
Senosy, M.	W5P033
Seo, T.	W1P025,
.....	W1P059, W1P107,
.....	W3P008, W3P034
Seok, J.	W1P090
Sepulveda, J.D.R.	W2P047
Sereshchenko, E.	W2P085
Serinyel, Z.	W3P049
Seyedzadeh, F.	W3P112
Sezer, H.	W2P076
Shaddix, C.R. ...	W5P086, W5P091
Shafirovich, E.	W5P126,
.....	W5P129
Shannon, R.	W3P079
Sharaborin, D.	W2P021
Sharma, T.	W5P097
Shaw, B.D.	W3P011, W3P014
Shcherdanev, S.	W1P113
Shen, S.	W1P108
Shepherd, J.E.	W2P031,
.....	W2P119, W3P104,
.....	W3P105, W3P119
Shethaji, T.	W1P079
Shi, Y.	W5P097
Shibagaki, H.	W1P035
Shih, H.-Y.	W2P046
Shiina, H.	W1P020, W3P095
Shimizu, T.	W1P023
Shin, D.-H.	W5P007, W5P049
Shin, M.C.	W2P104, W4P031
Shin, Y.	W1P121, W2P039

<i>Author</i>	<i>Paper #</i>
Shiraga, Y.	W1P010, W1P035
Shmakov, A.	W2P021,
.....	W2P035, W4P057,
.....	W4P061, W4P065, W4P066
Shoji, T.	W5P071
Shukla, B.	W1P037
Shundrina, I.	W4P057, W4P066
Shvartsberg, V.	W4P065
Shy, S.	W2P085
Si, Y.	W3P136
Sikes, T.	W5P117
Silke, E.	W3P103
Silver, A.	W3P001
Silvi, A.	W3P109
Sim, J.	W3P019
Simmie, J.	W3P083,
.....	W3P046, W3P114
Simonsson, J.	W4P119
Singh, R.	W4P093
Singh, R.	W4P094
Singleton, D.	W1P037
Sirignano, M.	W4P100, W4P139
Sirjean, B.	W3P074, W3P121
Sirotkin, F.	W1P042
Sivaramakrishnan, R.	W3P047,
.....	W3P127
Skapura, M.	W4P109
Skiba, A.	W5P018
Skjold, T.	W2P131, W5P115
Skryja, P.	W5P050
Slais, T.	W5P038
Slavinskaya, N.	W3P092
Smagulova, G.	W5P102
Smirnov, N.	W4P079
Smith, A.	W4P132
Smith, G.	W3P110
Smith, P.	W5P070
Smolke, J.	W2P073, W5P022
Sobiesiak, A.	W1P062,
.....	W1P096, W5P061
Somarathne, K.D.K.A.	W1P058
Somers, K.P.	W3P085,
.....	W3P046, W3P103, W3P114
Song, H.	W2P077
Song, H.	W1P095

<i>Author</i>	<i>Paper #</i>
Song, S.	W1P006,
.....	W1P073, W1P075, W1P090,
.....	W1P095, W1P139, W3P089,
Sorrentino, G.	W1P028
Sotton, J.	W1P061
Souto-Iglesias, A.	W2P063,
.....	W2P064
Souyoshi, S.	W5P020
Speight, W.M.	W3P092
Stagni, A.	W3P070, W3P130
Starcke, J.H.	W3P092
Starikovskaya, S.	W1P113
Steinmetz, S.	W4P091
Stepanyan, S.	W1P113
Stewart, S.M.	W1P049
Stocker, D.	W2P067
Storch, M.	W1P100
Stoyanov, M.K.	W1P097
Subramani, H.	W4P007
Suemitsu, M.	W5P127
Sugiyama, Y.	W2P113
Sullivan, G.	W4P081
Sullivan-Lewis, E.	W1P119
Sun, G.	W5P048
Sun, H.	W3P117, W3P118
Sun, W.	W2P020
Sun, Y.	W2P086
Sun, Z.	W4P010
Sunderland, P.B.	W4P064
Sung, C.-J.	W1P111, W3P072
Suttles, A.	W2P067
Sutton, J.A.	W4P016,
.....	W4P023, W5P036
Suzuki, S.	W3P016
Suzuki, T.	W4P058
Suzuki, Y.	W1P053, W4P036
Swaminathan, N.	W5P024
Szuhanski, J.	W1P034
Taatjes, C.	W3P081
Taborek, P.	W4P029
Taie, Z.	W1P134
Tainaka, K.	W5P073, W5P079
Takagi, S.	W2P123
Takada, S.	W3P046
Takahashi, A.	W1P020
Takahashi, F.	W2P067, W3P031

<i>Author</i>	<i>Paper #</i>
Takase, K.	W2P001,
.....	W2P040, W2P056
Takeishi, H.	W2P058
Takimoto, R.	W4P073
Talei, M.	W1P102
Tan, H.	W3P132, W5P078
Tanaka, A.	W2P034
Tanaka, K.	W3P084
Tanaka, R.	W5P089
Tani, H.	W3P030
Tanno, K.	W5P071
Tanov, S.	W1P093
Tao, Y.	W3P110
Tatschl, R.	W5P085
Taylor, N.	W5P124
Temme, J.	W5P018
Teodorczyk, A.	W2P119,
.....	W3P017, W4P067
Terashima, H.	W1P081, W3P030
Tereshchenko, A.	W4P057,
.....	W4P066
Terracciano, A.	W2P101
Tezuka, T.	W1P004,
.....	W1P023, W1P064,
.....	W2P001, W2P040, W4P115
Theron, M.	W1P135
Thévenin, D.	W3P026
Thomas, J.	W1P140,
.....	W1P141, W5P125
Thompson, L.	W2P015
Thomsen, J.	W2P089
Thomsen, M.	W4P076
Thomson, M.	W2P043,
.....	W4P091, W4P118
Thurmond, K.	W4P021
Tian, Y.	W1P130
Tian, Z.	W3P091
Tian, Z.F.	W5P052, W5P053
T'ien, J.S.	W4P079
Tilghman, M.	W5P090
Tinajero, J.	W4P140
Tirunagari, R.	W5P026
Tomita, E.	W1P089,
.....	W1P099, W5P058
Tomita, H.	W2P033
Tomlin, A.	W3P078, W3P079
Tonell, M.	W2P089

<i>Author</i>	<i>Paper #</i>
Tonokura, K.	W4P045
Torero, J.	W4P079
Török, S.	W4P119
Toth, B.	W4P079
Trabadela, I.	W1P067
Tran, M.-V.	W2P013
Tranter, R.	W4P032, W4P033
Trimis, D.	W2P005,
.....	W4P090, W4P117
Trisjono, P.	W5P006
Trivedi, S.	W1P039
Trouvé, A.	W4P059, W4P064
Troy, T.	W3P083
Tryner, J.	W5P094
Tsai Tsai, H.-L.	W5P106
Tsuboi, K.	W1P099, W5P058
Tsue, M.	W1P137, W4P073
Tsuji, H.	W5P073, W5P079
Tsuruda, T.	W2P132, W4P056
Tsuzuki, Y.	W1P110
Tummers, M.	W3P023
Turanyi, T.	W3P039,
.....	W3P040, W3P054,
.....	W3P090, W3P093, W3P129
Uchida, M.	W1P114, W3P016
Uchida, T.	W5P020
Ueda, K.	W2P057
Ueda, T.	W2P033, W2P034,
.....	W2P055, W5P120,
.....	W5P127, W5P128
Uemichi, A.	W2P054
Ugarte, O.	W2P036, W2P117,
.....	W2P118
Ulsan, Y.	W1P101
Um, B.	W1P021
Umemoto, S.	W5P073
Urban, D.	W4P079
Urban, J.	W4P072
Urness, K.	W3P083
Valco, D.	W1P128
Valiev, D.	W2P036, W2P066,
.....	W2P117, W2P118
Valkó, E.	W3P039, W3P090,
.....	W3P093
Vall, J.S.	W1P142
van Dijk, G.	W1P082
van Essen, M.	W1P082

<i>Author.....Paper #</i>	<i>Author.....Paper #</i>	<i>Author.....Paper #</i>	<i>Author.....Paper #</i>
van Oijen, J. W1P028, W5P051	Wang, J. W4P044	Wu, F.-H W3P137	Yokomori, T. ... W1P003, W1P036,
van Veen, E.H. W3P023	Wang, J. W5P016	Wu, H. W5P109 W2P033, W2P034, W2P045,
Vandeputte, A. W3P081	Wang, J.-L. W3P111	Wu, M.-H W2P118, W5P119 W2P055, W2P065, W5P120,
Vang, C. W3P011	Wang, K. W1P014, W1P015,	Wu, Y. W2P082, W5P070 W5P127, W5P128
Vanhove, G. W1P111, W1P113 W1P050	Xing, L. W3P037, W3P077	Yone, K. W3P033
Varea, E. W1P029, W2P003,	Wang, L. W5P091	Xiouris, C. W2P030	Yoneyama, S. ... W1P036, W2P065
..... W5P034	Wang, P. W2P077	Xu, J. W5P087	Yoo, C.S. W1P101, W2P068,
Varga, T. W3P039W3P054,	Wang, Q. W2P014	Xu, L. W4P046 W5P009
..... W3P093, W3P129,	Wang, Q. W5P075	Xu, T. W5P078	Yoo, M. W4P020
Vasinek, M. W3P078	Wang, W. W4P018	Xu, Z. W5P123	Yoon, J. W1P021
Vasu, S. W2P015, W2P101,	Wang, X. W3P132, W5P078	Xuesong, B. W5P008	Yoon, J. W5P043
..... W3P139, W4P021,	Wang, Y. W3P077, W3P101	Yalin, A. W3P007, W5P094	Yoon, Y. W5P043
..... W4P026, W5P012, W5P013	Wang, Y. W3P132	Yamada, H. W2P045, W3P046	Yoshida, A. W4P049, W4P050,
Vaughn, T. W1P076	Wang, Y. W4P064	Yamaguchi, T. W2P136 W4P051
Vazquez, M. W5P055	Wang, Y. W4P112	Yamamoto, K. W4P048	Yoshioka, T. W5P127
Velez, C. W5P012, W5P013	Wang, Z. W1P005	Yamanaka, T. W1P036	Yozgatligil, A. W1P118
Venkateswaran, P. W4P007	Wang, Z. W1P093	Yamane, N. W2P034	Yu, B. W2P108
Verdier, L. W3P121	Wang, Z. W3P037, W3P059	Yamazaki, W. W1P018	Yu, D. W5P087
Verissimo, G. W5P113	Wang, Z. W3P077, W3P102	Yanagioka, T. W1P018	Yu, H. W2P003
Vicariotto, M. W1P063	Warth, V. W3P062	Yanez, J. W2P063, W2P064	Yu, K. W1P120, W2P135
Vié, A. W1P129, W3P013	Wassmuth, V. W1P029	Yang, B. W2P020, W2P035,	Yu, R. W5P008
Vijlee, S. W1P127	Watanabe, H. .. W4P126, W5P071, W3P037	Yuan, W. W3P043, W3P077,
Vilfayeau, S. W4P064 W5P073, W5P079	Yang, H. W2P082 W3P101, W4P098
Villanueva, J.J.C. W3P004	Weber, R. W2P089	Yang, H. W3P136	Yuan, Y. W5P076
Violi, A. W4P099, W4P102,	Weingarten, J. W2P043	Yang, I. S.-Y ... W1P040, W5P088	Yue, F. W2P014
..... W5P124	Weise, D. W4P070, W4P071	Yang, J. W1P108	Zak, C. W4P072
Viteri, F. W4P107	Wen, C. W5P087	Yang, J. W2P091	Zang, G. W5P097
Vivanco, J. W3P123	Weng, S. W1P130	Yang, J. W4P034, W4P098	Zang, S. W1P130
Volkov, E. W2P006	Weng, W. W1P005	Yang, Q. W3P136	Zaras, A. W3P049
von Berg, E. W5P085	Wensing, M. W1P100	Yang, S. W2P025	Zavlev, T. W4P022
Vondal, J. W5P068	West, R. W3P073, W3P109,	Yang, S.Y. W3P015	Zayed, M. W5P033
Voss, S. W2P005, W2P006 W3P112, W3P113	Yang, W. W2P091	Zeng, M. W3P101
Vujanovic, M. W5P085	Westbrook, C.K. W2P035	Yang, Y. W4P046	Zeng, P. W1P044, W1P050
Wabel, T. W5P018	White, J. W4P064	Yang, Y. W5P075	Zeng, Q.H. W5P088
Wada, Y. W1P020	Whitty, K.J. W2P094	Yani, S. W5P093	Zetterberg, J. W4P003
Wagner, A.F. ... W3P125, W3P126	Wilde, B. W5P037	Yao, H. W5P077	Zevallos, A.A.M. W4P047
Wan, S. W1P053	Will, S. W1P100, W4P027	Yao, J.-J W3P009	Zgora, J. W1P033
Wan, W. W5P096	Williams, F. W3P022	Yao, M. W1P087	Zhang, A. W1P078, W1P109
Wang, B. W4P116	Winter, F. W3P052	Yao, Q. W2P106, W5P116	Zhang, B. W2P110
Wang, F. W3P111	Wislocki, K. W1P091, W3P017	Yapp, E. W4P132	Zhang, D. W5P093, W5P096
Wang, G. W3P036	Witkowski, D. W4P028	Yasmine, A. W5P126	Zhang, F. W3P037, W3P059,
Wang, H. W1P087	Wlokas, I. W1P105	Yasunaga, K. W3P046 W3P102
Wang, H. W2P073, W3P110,	Wooldridge, M. W1P111,	Ye, L. W3P043	Zhang, H. W2P082, W2P083,
..... W4P134, W4P135, W5P121 W1P112	Ye, T. W2P030 W5P070
Wang, H. W2P133	Wornat, M.J. ... W4P106, W4P108,	Yee, N. W3P042	Zhang, J. W3P091
Wang, H. W5P002 W4P109, W4P113	Yelverton, T. W2P102	Zhang, K. W3P051
Wang, J. W2P049	Wu, C.-Y W5P088	Yen, M. W1P071	

<i>Author.....</i>	<i>Paper #</i>
Zhang, L.	W3P036, W3P059, W3P101, W3P102
Zhang, M.	W5P016
Zhang, Y.	W2P082, W2P083
Zhang, Y.	W3P091
Zhang, Y.	W4P009
Zhang, Z.	W5P093, W5P096
Zhang, Z.	W3P064
Zhao, D.	W3P082
Zhao, H.	W5P123
Zhao, L.	W2P095
Zhao, L.	W3P036, W3P102
Zhao, R.	W2P071, W5P019
Zhao, X.	W1P062
Zhou, B.	W3P138
Zhou, C.-W	W3P041, W3P058
Zhou, J.	W4P025
Zhou, J.	W5P075
Zhou, L.	W5P065, W5P066
Zhou, W.	W3P100
Zhou, X.	W4P082
Zhou, Y.	W5P082
Zhou, Z.	W4P034
Zhu, D.	W2P025
Zhu, J.	W4P035
Zhu, M.	W2P024
Zhu, M.	W5P093, W5P096
Zhu, Q.	W4P044
Zhu, X.	W1P109
Zigan, L.	W1P100
Zimont, V.	W5P015
Zobel, N.	W5P101
Zong, Y.	W5P116
Zsély, I.G.	W3P090, W3P093, W3P129

W1P001 EFFECTS OF BURNING RENEWABLE FUELS IN A VARIABLE GEOMETRY LOW SWIRL INJECTOR OPERATED IN A BOILER ENVIRONMENT

Vincent G. McDonell, Nathan Kirksey, University of California, Irvine, United States

At the University of California, Irvine Combustion Laboratory a low swirl injector with a variable blockage is being used in a boiler to fire varying compositions of renewable fuels. The goal is to develop a relationship between the emissions and stability of the burner to the blockage and fuel composition. To change the geometry of the injector, or the swirl number, an adjustment is made to the blockage in the center of the injector. In order to determine how the flowfield or turbulence levels have changed with the different blockages a method of laser imaging called reactive particle image velocimetry is used. From the developed vector fields a wealth of information can be gathered, including: the turbulence intensity, the flame height, and the turbulent flame speed. Compiling all this information results in a turbulence level for each blockage, as well as, changing flame heights; in addition, the turbulent flame speeds for the differing fuel compositions can be determined as a by-product. Current research aims to investigate the improvements on stability of the flame resulting from adjustments to the blockage on the low swirl injector. The idea is that by using a larger blockage, which will lower the injector speed, it will bring a slower burning biogas fuel closer to the injector point thus improving stability. Another important tool used when determining stability is a fiber optic probe. The probe can measure the flame luminosity and fluctuations in real time to give feedback in regards to the stability. As a flame is leaned or moved closer to blowoff the flickering increases while the luminosity decreases this can be correlated to the stability of the flame through the use of the fiber optic probe. Emissions data is an essential part of the testing, as such; an emission analyzer tracks the changes in emissions due to the wide variety of blockages, fuels, and equivalence ratios present during the testing. Lastly, the current development is in developing a speed of sound gas composition sensor. This sensor was used to correctly identify binary hydrocarbon mixtures in the past; the future goal is to outfit the device with more sensors in order to identify almost any fuel composition for use as an indicator for industrial applications. Industrial boilers operating on landfill gas do not know the composition of the fuels they are burning during the majority of their operation; this sensor would be a low cost device to ensure proper tuning of the boiler for emissions and stability depending on the actual fuel composition.

mcdonell@uci.uci.edu

W1P002 OXYGEN-ENRICHED CO-COMBUSTION OF BIOMASS FOR CCS APPLICATIONS

William Nimmo, Mohamed Pourkashanian, Sam Pickard, Leeds University, United Kingdom

Biomass combustion and Carbon Capture and Storage (CCS) individually represent significant options for decarbonising the power generation sector and when combined may permit a carbon-neutral or even carbon-negative process. Despite this potential, little research has been published that examines the combustion of biomass in atmospheres with application in CCS processes. This work reports on laboratory-scale and bench-scale testing of biomass and coal combustion in atmospheres enriched in O₂ and CO₂ which are relevant for retrofitting power stations for oxyfuel combustion. At bench-scale, thermogravimetric analysis shows substituting N₂ as the combustion diluent with CO₂ has little impact on the combustion properties of the fuels but that increasing the O₂ concentration accelerates combustion of coal and biomass chars. Results from cofiring three biomasses with coal at 20kW scale suggest substitution of N₂ with CO₂ significantly reduces temperatures, carbon burnout and emissions of NO while combustion in O₂-enriched conditions has the opposite effects. Emissions of NO and SO₂ were found to reduce compared to air in combustion atmospheres enriched with O₂ and CO₂ while combustion temperatures and carbon burnout slightly increased.

Comparing a typical oxyfuel combustion atmosphere (30% O₂ in CO₂) with combustion in air finds that the former is more reactive for all fuels during both the combustion of volatiles and char oxidation stages during Thermo-Gravimetric Analysis (TGA) and that the elevated [O₂] particularly accelerated the char-oxidation stage of the combustion process. Little difference was observed when N₂ was replaced with CO₂ as the diluent since at temperatures typical in TGA gasification reactions have little impact and the increased heat capacity of the atmosphere is negated by the TGA control system. Unstaged cofiring (15%th) of each of the biomasses at 20kW scale showed that the heat capacity of the fluid was important and temperatures in CO₂-enriched combustion atmospheres were lower than those that were N₂-based, delaying combustion and reducing NO emissions. O₂-enrichment and biomass blending were both observed to improve carbon burnout with the former tending to increase NO emissions, while biomass blending tended to effect slight reductions compared to coal firing mainly due to changes to local [O₂] and temperatures near the burner. Emissions of SO₂ were reduced during cofiring and during combustion in atmospheres enriched with CO₂ and O₂ though a full sulphur balance could not be performed to suggest further reasons for this. SEM images of ash samples support the relative combustion efficiencies with a increasing tendency for smaller, spherical particles in the ash with increasingly efficient combustion observed during O₂-enrichment.

w.nimmo@leeds.ac.uk

W1P003 EFFECT OF CATALYTIC PRE-COMBUSTION ON FLAME STABILITY IN HIGHLY CONCENTRATED CO₂

Toshinori Nagai, Takeshi Yokomori, Keio University, Japan

Oxy-fuel combustion attracts attention as an effective solution of reducing CO₂ emission. However, highly concentrated CO₂ destabilizes the combustion. In this study, the catalytic pre-combustion was used for the improvement of

the flame stability in highly concentrated CO₂. The experiments and numerical calculation were performed to elucidate the influence of the catalytic pre-combustion on the flame stabilization. The burner consisted simply of a Pt catalyst pipe with 5 mm in diameter confined by a quartz tube with 40 mm in diameter. The CH₄/O₂/CO₂ mixture was jetted out from the Pt catalyst pipe. The mixture inlet velocity V and equivalence ratio f were varied. For comparison, the CH₄/O₂/N₂ mixture was also used. The volumetric ratio of O₂ to CO₂ (or N₂) was 3:7. The O₂/CO₂ (or N₂) mixture flowed at 0.2 m/s in the circumference of the jet. In the numerical calculation, a two-dimensional axisymmetric model was implemented into the CFD code ANSYS-Fluent 14.0. Gas phase and surface reaction mechanisms consisted of 57 reactions involving 18 species and 24 reactions involving 11 species, respectively. In addition, DO model was adopted as a radiation model and the emissivity of the gas phase was calculated with WSGG model. The thermal conduction of the catalyst was also taken into account. In the experiment, the blow off velocity of the flame stabilized at the downstream of the catalyst typically increased with increasing the equivalence ratio. The blow off velocity in the CH₄/O₂/CO₂ mixture showed lower than that in the CH₄/O₂/N₂ mixture even with and without the catalytic combustion. The blow off velocity with the catalytic combustion was lower than that without the catalytic combustion at the lower equivalence ratio. This is because the catalytic combustion consumed reactants, so that the reactants were insufficient to sustain the flame at the downstream side of the catalyst. On the other hand, the blow off velocity with the catalytic combustion is higher than that without the catalytic combustion at the higher equivalence ratio. This is because the high temperature mixture including the high reactivity intermediates such as CO and H₂ generated by the catalytic combustion stabilized the gas phase reaction. These results show that the catalytic combustion can effectively act on the flame stabilization at the higher equivalence ratio.

toshinori.nagai@z6.keio.jp

W1P004 SIMPLE METHODOLOGY FOR CONSTRUCTING OVERALL REACTION MECHANISMS USING A MICRO FLOW REACTOR WITH A CONTROLLED TEMPERATURE PROFILE

Shogo Onishi, Kaoru Maruta, Hisashi Nakamura, Takuya Tezuka, Susumu Hasegawa, Tohoku University, Japan

Multi-dimensional combustion simulations play an important role in developing engines and combustors. However, the computational cost of simulation with chemical reactions is proportional to the cube of the number of species. Therefore, there is a demand for the construction of chemical reaction mechanisms which are able to obtain reasonable answer with small simulation cost. The objective of this study is to develop simple methodology for constructing overall reaction mechanisms of ethanol/air for the engineering-purpose combustion simulation of ethanol scramjet engines operated under reduced pressure conditions.

The construction of overall reaction mechanisms was made by fitting for the dependence of inlet mean flow velocity on the weak flame location in the author's original flow reactor. Weak flame is characterized as the initiation of ignition while itself is observed as stable flames. This unique characteristic of the weak flames was employed for the construction of overall reaction mechanisms in this study. The dependence of inlet mean flow velocity on the weak flame location was obtained by experiments and computations using detailed reaction mechanisms for a stoichiometric ethanol/air mixture at 0.3 atm, which is the representative pressure condition in scramjet engines considered. Overall reaction mechanism constructed by fitting for the computational results was labeled as "Mmfr" and that for the experimental results was labeled as "Mmfr-exp". In addition to them, the construction of overall reaction mechanisms was made by fitting for the dependence of initial mixture temperature on ignition delay time labeled as "Mig" and laminar flame speed as "MSI" obtained by detailed mechanism for a stoichiometric ethanol/air mixture at 0.3 atm.

The developed overall reaction mechanisms were tested by 2-D simulation for the supersonic combustion field of the vertical ethanol injection. For reference, an overall reaction mechanism used in a commercial software (FLUENT 6.3) shown in "Mflu" was also employed. The combustion completeness was defined as the ratio of amount of burned ethanol to amount of input ethanol.

The figure shows combustion incompleteness as a function of total temperature of the airstream for all overall reaction mechanisms used. The different target of the constructions shows different response of the total temperature on combustion incompleteness. The simulation using detailed reaction mechanisms will be conducted and compared with the present result in future.

s.onishi@edyn.ifs.tohoku.ac.jp

W1P005 FORMALDEHYDE ENHANCEMENT BY OZONE ADDITION IN CH₄/AIR PREMIXED FLAMES

Wubin Weng¹, Nisson Elna², Andreas Ehn², Zhihua Wang¹, Zhongshan Li²
¹Zhejiang University, China ²Lund University, United Kingdom

Plasma assisted combustion is one of the most promising technology which can lower ignition threshold and extend flame stability range. It is particularly useful for modern gas turbines, which operates under extremely lean condition to reduce NO_x emission. Compared to other plasma-generated species, for example singlet oxygen, ozone has a relatively long lifetime (half-life in excess of 30-40 min at ambient condition) which might be very practical. In order to understand the combustion enhancement effect by ozone, experiments on laminar burning velocity enhancements have previously been studied. Using chemical kinetics modeling, it has been shown that the ozone decomposition in the pre-heat zone of the flame can initiate and accelerate the chain-branching reactions. In the present study formaldehyde (CH₂O), as one of the important intermediate species in the pre-heat zone of a flame, was investigated by both experiment and simulation methods in methane/air laminar premixed flames under atmospheric conditions. The formaldehyde concentration profiles

in the flames were measured with CH₂O-PLIF. The experimental results showed that the formaldehyde concentration was enhanced significantly with ozone addition. When 4500 ppm of ozone was added, the formaldehyde concentration in Bunsen type laminar flame was enhanced about 58.5% at fuel-rich condition and about 15.5% at stoichiometric condition. In the simulation work, the most recent ozone sub-mechanism was coupled with GRI-mech 3.0 kinetic mechanism. It showed that, with 4500 ppm ozone addition, the formaldehyde concentration was enhanced about 48.1% at rich condition ($\phi=1.4$) and about 14.7% in stoichiometric mixture, which is in very good agreement with the experimental results. According to the simulation results, an early production of CH₂O was found with ozone addition, especially in rich conditions. These reactions occurred at relatively low temperature, around 500 K. In order to isolate these reactions from the flame, experiments with preheated unburnt mixtures were carried out. It was found that a larger amount of formaldehyde was produced in the zone far from the flame as the preheating temperature was increased. It indicated that the combustion enhancement with ozone can be caused by the additional reaction of ozone at relatively low temperature. Simulations showed that CH₃O is the key specie for production of formaldehyde at lower temperatures, early in the pre-heat zone of the laminar flame it occur via decomposition of CH₃O, and in the pre-heated gas mixture via reaction of CH₃O with O₂.

wubin.weng@forbrf.lth.se

W1P006 AN EXPERIMENTAL STUDY OF THE EFFECT OF HYDROGEN ADDITIVE ON A PRIMARY REFERENCE FUEL HCCI COMBUSTION

Hyunsoo An, Seunghyeon Lee, Kwangmin Chun, Soonho Song, Yonsei University, Korea

Gasoline Homogeneous Charge Compression Ignition (HCCI) combustion enables internal combustion engines to achieve higher thermal efficiency and lower NO_x emissions than conventional gasoline and diesel engines. To operate an HCCI engine stably, combustion control is crucial. One of the methods to control HCCI combustion is using additives. In this study, hydrogen was used as an additive. Using a Rapid Compression Machine(RCM), an experimental tool that can simulate the single compression stroke of an internal combustion engine, ignition delay times of blended hydrocarbons(*n*-heptane + *iso*-octane) were measured over a various range of equivalence ratio($\phi=0.3, 0.35, 0.4$), octane number(0, 50, 100), and percentage of heat value of H₂ additive for fuel(0.5, 10%). When hydrogen was added to the mixture of hydrocarbon, there was a significant increase in the ignition delay. As the amount of hydrogen was increased, ignition delay was also increased especially at low temperature region. In addition, as the octane number was increased, the effect of hydrogen was larger; hydrogen increased the ignition delay. These phenomena were explained based on the chemical kinetic analysis; hydrogen consumes a radical that is related to the ignition delay of hydrocarbon fuels. However, with the results we gained so far, we cannot present a specific mechanism and reaction path for low temperature chemical reaction when hydrogen is added. Thus, our future work includes sensitivity analysis of ignition delay to figure out a specific mechanism and reaction path when hydrogen is added.

dksgustn@yonsei.ac.kr

W1P007 MODELING REGENERATION RATES OF SUPPORTED PARTICLES IN CHEMICAL LOOPING COMBUSTION SYSTEMS

Eli A. Goldstein, Reginald E. Mitchell, Turgut M. Gur, Stanford University, United States

A model that predicts copper oxidation rates of spray-granulated particles in air the reactor of Chemical Looping Combustion (CLC) systems is presented. The model solves the necessary equations that describe both oxygen transport through pores within the particle as well as the chemical rate equations describing oxide layer growth. Oxide layer growth is described by Wagner's Oxidation Theory, which states that the flux of interstitial and vacancy defects in the Cu₂O (cuprous oxide) and CuO (cupric oxide) oxide layers control the oxidation rate. In order to validate this model, Cu/ZrO₂ spray granulated particles were oxidized in a TGA at temperatures between 600 to 900°C and 21% O₂ and the measured conversion was compared to the model output. With reasonable agreement obtained between the model and the experiments, the model was then exercised to show the influence of characteristic morphological parameters including particle diameter, copper loading, and characteristic copper diameter on the oxygen carrier oxygen transport capacity and particle reaction time. Based on these findings, an optimal particle design has been proposed.

eagoldst@stanford.edu

W1P008 THE ROLE OF CO₂ AND H₂O ON IGNITION CHEMISTRY OF SIMPLE HYDROCARBONS

*Pino Sabia, Mara de Joannon, Marco Lubrano Lavadera, Raffaele Ragucci
Istituto di Ricerche sulla Combustione – CNR, Italy*

It is currently unquestionable that the use of new combustion technologies based on dilution and pre-heating of fuel and/or oxidant, such as MILD combustion, is among the most favorable methods to reducing the formation or to eliminate classes of pollutants. This is related to the peculiar reacting zone established from pre-heated and diluted reactants, characterized by relatively low, nearly homogeneous temperature and concentration distributions. These features also imply a strong flexibility with respect to the fuel thus allowing the use of low calorific values mixtures with high efficiency. In this framework MILD combustion appears to be one of the most suitable modes to recover energy from biofuels. The high content of diluent species, deriving either from presence of diluent in low calorific values fuels or from

recirculation of flue gases to reach MILD combustion regime, namely H_2O and/or CO_2 makes the role of these species relevant in the oxidation chemistry in such a non-standard condition.

The aim of the present work is to highlight the effect of the H_2O and CO_2 on ignition kinetics of two reference fuels. More specifically, ignition delay time has been evaluated from experimental point of view in a tubular flow reactor using propane and a model gas surrogating the gaseous fraction of biomass pyrolysis products containing C1-C2 species (biogas), CO and CO_2 . The experimental analysis has been carried out at atmospheric pressure and inlet temperature ranging from 1000K to 1300K in presence of high dilution of either N_2 , or CO_2 or H_2O . In particular, different dilution levels (90-97%) and C/O ratio (0.05-1.5) have been analyzed. It has been found that for a fixed inlet temperature the ignition delay time measured in presence of CO_2 or H_2O is longer than the one measured using nitrogen as diluent and the extent of increase depends on fuel and diluent itself. However, such an increase of ignition delay does not prevent the use of MILD combustion processes, even if they rely on massive CO_2 and H_2O recirculation, in practical applications. Numerical simulations for studying the evolution both of propane and the model gaseous fuel oxidation process in the same working conditions of experimental tests have been carried out by means of several kinetic models available in literature. It has been shown that models significantly underestimate ignition delay values. Thus, a detailed kinetic analysis has been carried out with the aim to evidence the main routes in which CO_2 and H_2O could interfere with. CO_2 and H_2O can modify the evolution of the combustion process for both kinetic and thermodynamic reasons. Beside a different heat capacity of such species, they can be involved in direct or indirect way in the fuel oxidation reaction. The numerical analysis has evidenced the complex effect of the diluent typology on evolution of chemical process that depends on the temperature range considered. More specifically, it has been shown that CO_2 and H_2O strongly alter the competition between the oxidation and recombination/pyrolytic reaction channels also acting on H_2/O_2 oxidation systems.

ragucci@irc.cnr.it

W1P009 CHARACTERIZATION OF LITHIUM COMBUSTION FOR THE USE AS ENERGY CARRIER IN A RENEWABLE ENERGY CYCLE

Julia Koppmann, Andreas Brockhinke, Regina Brockhinke, Bielefeld University, Germany

For environmental reasons, there is an increasing demand to use solar and wind power plants for the generation of electricity. However, as their output fluctuates strongly depending on weather conditions, adequate energy storage systems are a necessity. Batteries and fuel cells do not scale up well to the desired capacities due to high mass-to-storage ratios, short life cycles or the need to store inflammable gases. An alternative is to use excess electrical energy to produce energy-dense solid combustibles and use them for storage.

In a joint venture of two universities and industry, we investigate the potential of lithium metal as energy carrier in such an energy cycle. Using lithium has several advantageous aspects: It is liquid at moderate temperatures, which allows adapting established spray combustion techniques. All main combustion products are solid salts, which can be stored until stranded renewable energy is available for their electrolytic regeneration. Additionally, lithium combustion opens pathways for the formation of valuable products like acetylene (C_2H_2) and ammonia (NH_3). Previous investigations analyzed the exothermic reaction of lithium with oxygen to lithium oxide (Li_2O). In carbon dioxide (CO_2) Li_2O , lithium carbonate (Li_2CO_3) and lithium carbide (Li_2C_2) are formed. The formation of Li_2CO_3 releases carbon monoxide (CO), which is an important synthesis gas. Additionally, lithium reacts with the otherwise inert nitrogen (N_2) forming lithium nitride (Li_3N). Further reactions allow formation of NH_3 , thereby opening an alternative to the energy-intensive Haber-Bosch process.

We have characterized these reaction pathways under laboratory conditions varying atmosphere, pressure and temperature determining lithium flame temperatures and product compositions. Spectroscopic and mass spectrometric methods were combined to shed light on this combustion process, which is of interest for both fundamental research and application.

julia.koppmann@uni-bielefeld.de

W1P010 EXERGY ANALYSIS ON EFFECTIVE UTILIZATION OF METHANE/AIR AND METHANE/ O_2 COMBUSTION

Tsukasa Hori, Akeshi Kegasa, Akane Nagasaki, Yosuke Shiraga, Yoshinori Hisazumi, Osaka University, Japan

Numerous efforts have been conducted to save energy and to reduce nitrogen oxides, such as oxy-fuel combustion, high temperature combustion and mild combustion. These energy saving effects are evaluated by the amount of energy consumption based on the first law of thermodynamics. When we use exergy that is based on the second of thermodynamics, new insights on the energy saving of a combustion system may be obtained. In this study, an estimation method of the combustion loss including dissociation of species at high adiabatic flame temperature is developed by use of the exergy. Next, an exergy balance of a heating furnace is calculated to examine the energy saving effects with preheating unburned fuel and oxidants. The fuel is methane, while oxidants are air and O_2 . The chemical species considered are 53 species listed in GRI-Mech 3.0, and the overall exergy is defined as the sum of the physical and chemical exergies. The environmental temperature and pressure used as a reference condition of exergy estimation are 25°C and 101.325 kPa, respectively. The combustion is assumed to proceed in an equilibrium and adiabatic condition. For simplicity, heat recirculation is assumed, but material recirculation is not considered. It is found that the combustion losses of 30% and 17% are calculated for the methane/air and methane/ O_2 combustion, respectively, at an equivalence ratio ϕ of unity and an

unburned gas temperature of 25°C. Preheating of the unburned gas and increasing of the equivalence ratio ($\phi < 1$) lead to the reduction in the combustion loss, because the adiabatic flame temperature increases due to decreasing nitrogen and excess O₂ in oxidant, which are not consumed in the combustion reaction. The minimum combustion loss occurs when the unburned gas temperature is raised by a preheating to realize the isothermal combustion. In this condition, the combustion loss is approximately 8% ($\phi < 1$) both for methane/air and methane/O₂ combustion. The dissociation increases with rising adiabatic flame temperature. That influences on the adiabatic flame temperature significantly, but mostly does not influence on the combustion loss estimation. Next, the exergy balance was calculated for an adiabatic heating furnace with some different premixed gas compositions and object temperatures. It is found that the effective exergy of object in the case of methane/O₂ combustion is higher than that in the case of methane/Air combustion in the high object temperature. Moreover, the maximum effective exergies of the object occur at the object temperature of 840 K and 1260 K for the methane/air and methane/O₂ combustions without preheating the unburned gas, respectively.

thori@ed.jrl.eng.osaka-u.ac.jp

W1P011 ELECTRIC FIELD EFFECTS ON CO EMISSION FROM NON-PREMIXED QUENCHING FLAMES

Yu-Chien (Alice) Chien, David Escofet Martin, Derek Dunn-Rankin, University of California, Irvine, United States

This research examines the potential for controlling the release of carbon monoxide from surface-impinging diffusion flames by using electric fields. While CO can be desirable in some SYNGAS processes it is usually a dangerous emission from forest fires, gas heaters, gas stoves, or furnaces where insufficient oxygen available in the core reaction does not fully oxidize the fuel to carbon dioxide and water. Electrical aspects of flames, specifically, the production of chemi-ions in hydrocarbon flames and the use of convective flows driven by these ions has been investigated in a wide range of applications. This poster examines these effects when a flame is impinging on a nearby surface. In particular, electric fields are used to control combustion as flames are partially extinguished. Several examinations and observations are involved, including Schlieren images of hot gas flows, CO emission variations, OH chemiluminescence, and OH planar laser induced fluorescence. We measure the changes in CO emission as correlated with variations in flame structure observed as a function of burner-to-plate distance and electrical potential applied to the flame. The results show that while both affect the CO emission, the burner-to-plate distance dominates. The CO release correlates strongly with changes in location and extent of high concentration regions of OH in the surface-impinging diffusion flame.

chieny@uci.edu

W1P012 FLOW AND ELECTRICAL CHARACTERISTICS OF COUNTERFLOW NONPREMIXED LAMINAR FLAMES WITH DC ELECTRIC FIELDS

Daegeun Park, Min Suk Cha, Suk-Ho Chung, King Abdullah University of Science and Technology, Saudi Arabia

We studied the effects of DC (Direct Current) electric fields on counterflow nonpremixed flames with emphasis on flow-field modification and electrical currents. High voltage and ground terminals from a DC power supply (upto ± 20 kV) were connected to a lower (fuel) and an upper (oxidizer) nozzle, respectively. Uniform electric fields were assumed in a gap between the two nozzles, because perforated plates were installed at each exit of the nozzle. As a result of DC, flames moved toward the lower potential side due to ionic wind, because the number of positive ions is greater than that of negative ions. To further investigate a generation of ionic wind and consequent flow modification, we adopted 2-D Mie scattering of Ar-ion laser with seed particles (~ 3 μ m, TiO₂). As a result, bi-directional ionic winds from a reaction zone could be identified, which blew to the both lower and upper nozzle at the same time. As a consequence of electrically induced axial velocity component from a reaction zone, two separate stagnation planes could be observed, which means well understood flow-fields in a counterflow burner are drastically changed with DC electric fields. Thus, DC electric fields also change a strain rate and the axial location of stoichiometry, which are important parameters to characterize a nonpremixed flame in a counterflow geometry. To find a correlation between aforementioned flow modification and electrical aspect of the flames, total electrical currents due to flow of ions in the flames with biased voltages, which are external applied voltage, were measured. The trend of electrical currents along with applied voltage demonstrated a typical feature showing an electric field intensity controlled regime and ion generation limit regime. Interestingly, the critical voltage to show double stagnation planes corresponded to that for the onset of ion generation limit regime (showing saturated electrical current) in the measurement of electrical currents. The values of saturated electrical currents were characterized for various flame conditions, such as adiabatic flame temperatures, fuels, and strain rate. And, the relation between the measured critical electrical currents for generating the double stagnation planes and calculated rate of ion generation was also discussed. Detailed explanations for flame behavior, electrical currents, and flow characteristics with DC electric fields are discussed in the poster.

daegeun.park@kaust.edu.sa

W1P013 APPLICATION OF A COMPREHENSIVE MODEL FOR THE TRANSPORT OF ELECTRONS AND CHARGED SPECIES IN PREMIXED FLAMES WITH AN EXTERNAL ELECTRICAL FIELD

Jie Han¹, Fabrizio Bisetti¹, Mani Sarathy¹, Tiernan Casey², Paul G. Arias¹, Hong G. Im¹, Jyh-Yuan Chen²

¹King Abdullah University of Science and Technology, Saudi Arabia ²University of California, Berkeley, United States

Electrically-enhanced combustion has been shown to improve combustion efficiency and reduce pollutant emissions.

The ionic wind, which is related to the flux of charged species induced by the electric field, is believed to play a key role. The charged species flux consists of a Fickian diffusion term due to the concentration gradient and a drift diffusion term due to the electric field. Diffusivity and mobility are transport properties appearing in the fluxes. In the case of ion/neutral and electron/neutral pairs, the Lennard-Jones potential does not describe the interaction properly due to quantum mechanic effects and does not account for the polarization of neutrals induced by the ion charge. In this work, we apply a comprehensive modeling strategy for the diffusivity and mobility of charged species in premixed flames, thereby enabling the accurate simulation of ionic wind effects. In particular, the concept of common mean energy of electrons is adopted to compute electron drift velocity at arbitrary electric field in any gas mixture. It has an obvious advantage over solving the Boltzmann equation directly because it is possible to tabulate electron mobility in binary gases before the simulation. The (n,6,4) potential is used for ion-neutral interactions. The main difficulty in applying the (n,6,4) potential is the lack of polarizability data. We overcome this difficulty by consulting the Computational Chemistry Comparison and Benchmark Data Base (CCCBDB), which has been updated in recent years. Finally, a comprehensive kinetic and transport model for electrons and ions is applied to premixed flames, while an external electrical field is imposed along the flow direction. The results detail the distribution of electrons and ions in the premixed flames and the effects of ionic wind on the flow field.

jie.han@kaust.edu.sa

W1P014 FLAME-ASSISTED FUEL CELL FURNACE FOR MICRO COMBINED HEATING AND POWER (FFF MICROCHP)
Ryan Milcarek, Jeongmin Ahn, Kang Wang, Syracuse University, United States

Increased electricity consumption in the United States has been a growing problem that is only expected to increase in the future. Combating this problem will require new applications of fuel cell technologies that efficiently convert fuels to electrical and thermal energy. In this project, we propose to integrate Flame-assisted Fuel Cells (FFCs) in a gas-fired up-flow furnace to enable the generation of both electricity and heat from the fuels, transforming the furnace into a FFC micro CHP system (FFF- μ CHP). The FFCs will be integrated with the furnace in-shot burners in a modified setup to allow staged combustion with a slightly rich 1st stage (FFC), then a leaner 2nd stage to complete combustion in the flues. This Rich Quick Lean (RQL) combustion process will simultaneously produce the heat needed for the heat exchanger and for SOFC operation. The system will extract ~ 1 kWe of power from a 60,000-100,000 Btu/h furnace. The application of this technology in a typical residential size furnace has the potential of making this a commercially viable option for households.

To achieve the goal of the proposed research project, three specific research objectives will be accomplished: 1) examine and characterize the partially combusted products from a typical furnace in-shot burner; 2) fabricate and test planar FFCs using model fuels of the in-shot burner exhaust to investigate its electrochemical behaviors and 3) fabricate, test and evaluate tubular FFCs performance. We will examine and characterize in order to quantify the operating temperature, the composition of the exhaust and the operating window of the furnace to ensure compatibility with FFC operation; investigate how FFCs behave in model fuels comparable to the exhaust of an in-shot burner; and demonstrate the feasibility of the FFC- μ CHP power generation system.

The main benefits of the FFF- μ CHP system result from the increased efficiency of CHP systems compared to traditional power plant electricity generation. Furthermore, heating will still be provided for the residential market through a combination of heat from the electrochemical reactions in the FFCs and the heat from combustion in the burners. This system is not meant to create a new CHP market. Rather, this system will take the existing furnace market and improve it by adding the benefits of CHP in a residential environment.

The use of such systems in a residential environment will reduce the electricity needed from power plants for this sector. The electricity generated by this system has several immediate uses within a house without ever creating a need for energy storage. Additionally, energy can be stored in a battery for use during morning or evening hours when more electricity is used for lights, stoves and other household appliances. This stored energy has the potential of offsetting the traditional peak hours of electricity consumption. By storing energy for peak periods, the load on the grid will be significantly reduced, which will further lessen the need for additional power plants and the associated infrastructure. Savings will also occur in the typical household utility bill because household electricity is often billed based upon on-peak or off-peak hours of operation. Besides producing high efficiency electricity and heat, the FFF- μ CHP will also save industrial facilities in demand related charges by offsetting the load during peak hours of operation. These savings are typically on the order of 10-14 \$/kW for an industrial facility which is a large portion of their electricity bill. At the same time, the total chemical energy of the fuel is used more efficiently because it is being used for heating near the site of electricity generation.

rjmilcar@syr.edu

W1P015 INTEGRATED ANAEROBIC DIGESTER AND FUEL CELL POWER GENERATION SYSTEM FOR COMMUNITY USE

Ryan Falkenstein-Smith, Kang Wang, Jeongmin Ahn, Syracuse University, United States

The purpose of this project is to evaluate the feasibility of integrating an Anaerobic Digester (AD) system with a Flame-assisted Fuel Cell (FFC) power generation system that can demonstrate a sustainable alternative energy system in a STEM education environment. The fabrication process for both a YSZ-SDC (Yttria Stabilized Zirconia- Samaria Doped

Ceria) double layer FFC and a SDC single layer FFC using tape casting techniques is reported. In order to find the optimal performance of the fabricated FFCs an electrochemical performance test is investigated while varying the biogas composition, flow rate, and air intake.

The performance of the FFC was measured using a Solartron 1287 potentiostat in combination with a 1260A frequency response analyzer. While monitoring the power density and voltage under a current density change, methane to CO₂ ratio, flow rate, and equivalence ratio were all modified to produce a wide range of power generating and Open circuit Voltage (OCV) values. After running the experiments using YSZ-SDC FFC, the same tests were run using an SDC FFC under the same modified conditions.

Although YSZ-SDC FFC generated some power, the SDC FFC proved to be a higher performing cell under the scaled methane ratio gas composition. The SDC FFC maximum power density achieved was at 748 mWcm⁻² and an OCV of 0.856 V. This was under the operating conditions of a 6:4 methane to CO₂ ratio, a 500 ml/min flow rate, and equivalence ratio of 5. Therefore in order to power an LED light for a substantial amount of time, it would be most effective to place 2 to 3 SDC single layer cells in stacked formation.

rlfalken@syr.edu

W1P016 THE CHARACTERISTICS OF ADDING CARBON DIOXIDE IN A COFLOW ON LIFTOFF METHANE DIFFUSION FLAME

Yung-Sheng Lien, Yei-Chin Chao, National Cheng Kung University, Taiwan

Experimental and numerical study on the effects of CO₂/O₂ in coflow to a liftoff CH₄ diffusion flame are essentially studied. The interesting point is when the ratio of CO₂/O₂ coflow was 80%/20%. In general speaking, methane diffusion flame is not easy to liftoff stably. Some reasonable explanations are mainly due to carbon dioxide has high heat capacity. One of the interesting findings is the methane diffusion could not liftoff stably under coflow is N₂/O₂ (air) rate of 79%/21%. But the calculated and experimental results show that methane diffusion flame can liftoff stably under coflow was composed of ratio of CO₂/O₂ was 80%/20%. For coflow at CO₂/O₂ rate is 80%/20%, the liftoff methane diffusion flame is stabilized on the lean side of methane stoichiometric conour. It can be explained by the reaction rate profiles at liftoff flame base that CO₂ comes from coflow will be dissociated by flame temperature and follow the endotherml reaction in front of liftoff flame base and then enter liftoff flame. But at the liftoff methane diffusion flame (exothermic) and (endotherml) produce a lot of CO and CO₂ radical pools at the same time. The net heat release in the flame zone will play an important role in sustain the liftoff methane diffusion flame and the exothermic effect is stronger than endotherml one. It is believed that the main reason to sustain the liftoff methane diffusion flame.

yslien0214@gmail.com

W1P017 THE DEVELOPMENT OF A NOVEL MICROWAVE-PLASMA STABILIZATION MECHANISM FOR FLAME STABILIZATION

Hong Yuan Li, Yueh Heng Li, Yei Chin Chao, National Cheng Kung University, Taiwan

Recently, electric and microwave/plasma aspects of combustion receive intensive attention, especially for flame stabilization and fuel economy for the increasing global concerns of energy and climate. In this research, a novel low power concentrated-microwave/plasma jet burner system is first proposed and developed for fundamental studies of the stabilization mechanism of the methane/air premixed flames. The control parameters and operation characteristics of the integrated microwave burner system is further investigated. The microwave energy is enhanced and applied to the combustion system by means of a rectangular resonant cavity. In order to concentrate the microwave energy and enhance the absorption of microwave energy by the flame, a novel design of centralized microwave burner is used to incorporate microwave (2.45 GHz) electromagnetic energy directly into the reaction zone of a premixed laminar methane-air flame for flame enhancement. The experiments show that the current microwave/plasma setup can effectively stabilize lean and sub-limit lean methane-air flames with reasonably low input microwave power. The chemiluminescence and optical emission spectral results show that with the onset of a low-power plasma induced by microwave, a significant rise in coupling efficiency as well as excited state species of the incoming premixed stream, such as N₂ and O₂, leading to profound active combustion radicals of CH*, O*, H* and OH* for significant enhancement of flame stabilization can be observed. The stabilization process and mechanism of the methane-air flame enhanced by microwave-plasma is also discussed in this study.

calibuk88@mail.ncku.edu.tw

W1P018 THE EFFECTS OF UNBURNED-GAS TEMPERATURE ON INTRINSIC INSTABILITIES OF 3-D PREMIXED FLAMES

Satoshi Kadowaki¹, Takuto Yanagioka¹, Wataru Yamazaki¹, Hideaki Kobayashi²

¹Nagaoka University of Technology, Japan ²Tohoku University, Institute of Fluid Science, Japan

We studied numerically the effects of unburned-gas temperature on intrinsic instabilities of 3-D premixed flames. A sinusoidal disturbance with sufficiently small amplitude was superimposed on a planar flame to obtain the relation

between the growth rate and wave number, i.e. the dispersion relation. As the unburned-gas temperature became higher, the growth rate increased and the unstable range widened, which was due to the increase of the burning velocity of a planar flame. At sufficiently small wave numbers, the obtained numerical results were consistent with the theoretical solutions. As the Lewis number became smaller, the growth rate increased and the unstable range widened, which was due to diffusive-thermal effects. The growth rate and wave number were normalized by the burning velocity of a planar flame and preheat zone thickness. The normalized growth rate decreased and the normalized unstable range narrowed with an increase of unburned-gas temperature. This was because thermal-expansion effects became weaker owing to the decrease of the temperature ratio of burned and unburned gases. To clarify the characteristics of cellular flames generated by intrinsic instability, we superimposed a disturbance with the critical wave number. The superimposed disturbance evolved, and a hexagonal cellular flame formed. The behavior of cellular flames became milder as the unburned-gas temperature became higher, even though the growth rate increased. The burning velocity of a cellular flame normalized by that of a planar flame decreased, which was due to the weakness of thermal-expansion effects.

kadowaki@mech.nagaokaut.ac.jp

W1P019 EFFECT OF HYDROGEN ADDITION ON OH DISTRIBUTION OF INVERSE DIFFUSION FLAME BURNING LPG FUEL

Jing Miao, The Hong Kong Polytechnic University, China

OH distribution inside LPG Inverse Diffusion Flame (IDF) with various hydrogen percentages has been examined. The result indicates the effect of hydrogen addition on flame structure and fluid dynamics of LPG inverse diffusion flame. OH Planar Laser-Induced Fluorescence (OH-PLIF) was used to collect OH information. Experiment was done with various overall equivalence ratios and hydrogen percentages. The range of overall equivalence ratio is from 0.5 to 1.5 with a difference of 0.1. And the hydrogen percentages varies from 0% to 100%. The typical OH profile of LPG IDF contains zero-OH-hollow in the bottom centre of the flame. And under high Reynolds number (Re_{air} larger than 3000) and low equivalence ratio ($\phi < 1$) the OH profile shows an open tip, which may indicate poor combustion and large amount of unburnt fuel. Hydrogen addition in the fuel side can significantly narrow the open tip and enlarge the OH profile, hence larger burning area and longer residence time for the fuel. The effect of hydrogen is substantial when H₂% exceeds 60%. The OH profile can also be enlarged by increasing overall equivalence ratio. However, the influence of equivalence ratio is not as strong as that of hydrogen addition. Pure hydrogen IDF have a OH profile in "M" shape, which is totally different from that of LPG-IDF or even 10%LPG-90%H₂ IDF.

harmony_mj@126.com

W1P020 EXPERIMENTAL STUDY ON FLAMMABILITY OF R1234ze IN THE PRESENCE OF MOISTURE

*Tei Saburi, Akira Matsugi, Hiroumi Shiina, Akifumi Takahashi, Yuji Wada
National Institute of Advanced Industrial Science and Technology, Japan*

National Institute of Advanced Industrial Science and Technology Flammability characteristics of 1,3,3,3-tetrafluoropropene (R1234ze) in the presence of moisture were experimentally determined by an ignition test using a large volume spherical vessel. HydroChloroFluoroCarbons (HCFCs) and HydroFluoroCarbons (HFCs) were used as alternative refrigerants for Chlorofluorocarbons (CFCs). Ozone Depletion Potentials (ODPs) of HCFCs are much lower than that of CFCs, although they are still not zero. Also, HCFCs and HFCs were found to be Greenhouse Gas (GHG) and cause global warming. In the context of environmental protection, next-generation refrigerants with zero ODP and lower Global-Warming Potential (GWP) are expected to be utilized and to be spread throughout. However, these next-generation refrigerants exhibit a mild flammability and ASHRAE (2010) added an optional 2L subclass to the existing Class 2 (lower flammability) to classify the safety of refrigerants. Thus, evaluating the combustion safety of A2L refrigerants in the event of leakage into the atmosphere owing to an accident is necessary. In previous study, the flammable behaviors of difluoromethane (R32, CH₂F₂) and 2,3,3,3-tetrafluoropropene (R1234yf, CH₂=CFCF₃) were evaluated. Since it often reaches over 30 degrees C temperature and 80% humidity in Japan due to the hot and humid climate, the effects of temperature and humidity on the flammable behaviors were investigated. These effects on the flammable behavior of R1234ze are also important issue. In this study, the flammable behavior of R1234ze refrigerants in the presence of moisture was experimentally investigated by ignition tests of fuel/Air mixture gases with an electric discharge in a large spherical combustion vessel (1m in diameter). The moisture was added to the mixture gas by a bubbler on a circulation loop and the humidity in the mixture gas was conditioned. The operation temperature was maintained by a jacket heater, which covered the entire area of the vessel. The mixture gas was ignited with an electric discharge at a certain fuel-air equivalent ratio under dry and wet condition. The pressure profile was measured using a pressure transducer and the flammable behavior was observed by a high-speed video camera. Burning velocity, peak pressure and deflagration index KG were estimated and the dependency on temperature and humidity were discussed.

t.saburi@aist.go.jp

W1P021 AIR/STEAM BLOWN GASIFICATION OF LIGNIN FROM BIO-REFINERY PROCESS OF PULP MILL

*Jihong Moon¹, Suji Jeon¹, Jeongjun Yoon¹, Uendo Lee, Byunghwan Um²
¹Korea Institute of Industrial Technology, Korea ²Hankyong University, Korea*

Bio-refinery process is a promising option which produces bio-energy and sustainable eco-products simultaneously. The main process of pulp bio-refinery process is similar to existing petrochemical refinery process and it is composed of separation, liquid extraction, and fermentation by using the black liquor of a pulp mill. During the process, lignin is generated by hydrolysis and filtration of black liquor as a main byproduct and it can be used as fuel for supplying energy to run the bio-refinery process. For converting lignin into useful energy, thermo-chemical process is more efficient and faster than bio-chemical process which is hard to decompose lignin. As a representative thermochemical conversion process, air and steam gasification of the lignin was investigated in this study. A tube furnace was used to examine the characteristics of air/steam blown gasification of lignin from pulp bio-refinery process and the results were compared with those from conventional biomass fuel; wood pellet. The results suggest the details of lignin gasification characteristics and important parameters to design lignin gasification system for integrating it with the other bio-refinery process of pulp mill.

mjh5635@kitech.re.kr

W1P022 OXIDATION AND IGNITION STUDY OF 2-METHYL HEXANE IN A MICRO FLOW REACTOR WITH CONTROLLED TEMPERATURE PROFILE

Muneeb Khurshid¹, Hisashi Nakamura², Kaoru Maruta², S. Mani Sarathy¹

¹King Abdullah University of Science and Technology, Saudi Arabia ²Tohoku University, Japan

The Primary Reference Fuels (PRFs), *n*-heptane and *iso*-octane, are commonly used as fuel surrogates in combustion studies to emulate physical and chemical properties of a more complex real fuel. However, simple surrogate systems do not accurately represent real fuel in terms of its physical and chemical properties. Thus, more components need to be added to the surrogate fuel in order for it to match real fuel properties. 2-methyl hexane (2MH) is a candidate component to represent *iso*-paraffinic contents in real gasoline fuels. However, to use such complex surrogate system, it is required to understand detailed ignition and combustion chemistry of the individual component.

In the current study, we investigate combustion and ignition characteristics of a stoichiometric mixture of 2MH/air using a Micro Flow Reactor (MFR) with a controlled temperature profile. This kind of set up has already been used in studying combustion properties of other PRF mixtures and pure components. Three different flame regimes were observed depending on the mixture flow velocity at the inlet of the reactor; normal stable flames were observed at high velocity region, Flames with Repetitive Extinction and Ignition (FREI) at intermediate velocity, and weak flames in low velocity regions. Since weak flames represent auto ignition behavior of a fuel, they were further investigated in detail.

Computational results showed three distinctive Heat Release Rate (HRR) peaks appear in experimental conditions at atmospheric pressure. The HHR peak at low temperature corresponds to a cool flame regime, the one at intermediate temperatures represents a blue flame, and the high temperature HHR peak signifies the presence of hot flame. At atmospheric pressure, a significantly strong hot flame was observed, while a faint blue flame was observed and no cool flame was noticed. This qualitatively agrees with the computational results, as the high-temperature HHR peak was significantly stronger than low and intermediate temperature HHR peaks. As the reaction pressure was increased up to 5 atmospheres, a cool flame appeared, a blue flame became significant and the hot flame was broadened. This suggests that the first two oxidation reactions are more significant at elevated pressures and long residence time.

Gas sampling was also conducted and samples were analyzed using Gas Chromatography (GC). Further experiments carried out by coupling MFR with Molecular Beam Mass Spectrometry (MBMS) provide more detailed analytical data on the reaction species. Results of the chemical analysis are then utilized to improve current mechanisms and models of 2MH.

muneeb.khurshid@kaust.edu.sa

W1P023 OH-LIF MEASUREMENT OF H₂/O₂/N₂ FLAMES IN A MICRO FLOW REACTOR WITH A CONTROLLED TEMPERATURE PROFILE

Takashige Shimizu, Takuya Tezuka, Susume Hasegawa, Hisashi Nakamura, Kaoru Maruta, Tohoku University, Japan

Combustion and ignition characteristics of H₂/O₂/N₂ flames were investigated experimentally and numerically using a micro flow reactor with a controlled temperature profile. H₂/O₂/N₂ mixture (H₂:O₂:N₂=2:1:7 in molar ratio) was supplied to the reactor which is a quartz tube with the inner diameter of 2 mm and a stationary temperature gradient (300-1300 K).

In our past study, two kinds of flame responses were observed experimentally for H₂/O₂/N₂ mixtures by OH chemiluminescence using an UV CCD camera. One is the stable flat flame (Normal flame) which was observed in the high flow velocity region. Another is the unstable flame called Flames with Repetitive Extinction and Ignition (FREI) which was observed in the intermediate flow velocity region. However, a stable flame with weak luminescence (Weak flame), which was observed in low velocity conditions for hydrocarbon fuels in our past study, could not be observed in the previous experiment for H₂/O₂/N₂ mixture at the low flow velocity. There would be still open question whether there is no weak flame of H₂/O₂/N₂ mixture or the previous experiment by OH chemiluminescence was not able to capture the weak flame. Therefore, OH-LIF measurement was conducted to investigate H₂/O₂/N₂ weak flames in detail in this study.

The OH-LIF measurement was conducted at flow velocities from 5 to 0.3 cm/s and stable luminescence from weak flames were observed at flow velocities less than 3 cm/s. The flame location shifted to the higher temperature region as the flow velocity was decreased from 3 to 1 cm/s, while the flame location shifted to the lower temperature region as the velocity was decreased from 1 to 0.3 cm/s.

1-D computations were also carried out in this study using several detailed mechanisms (GRI3.0, San Diego Mech., Princeton H₂-O₂ Model and Aramco Mech 1.3.). The position of the rise in the computational OH profile was compared

with that in the measured luminosity profile. All mechanisms predicted that the flame location shifted to the higher temperature region with the decrease of flow velocity less than 10 cm/s. This tendency was observed in the experiment at flow velocities from 3 to 1 cm/s but the experiment showed the different tendency at velocities less than 1 cm/s. The position of the rise in the computational OH profile using GRI3.0 showed a better agreement with that in the measured luminosity profile compared with the other mechanisms employed.

shimizu@edyn.ifs.tohoku.ac.jp

W1P024 LES MODELLING OF MESOCOMBUSTION CHAMBERS WITH ARRHENIUS COMPLEX CHEMISTRY

Pierre Benard, Vincent Moureau, Ghislain Lartigue, Yves D'Angelo, CNRS - Saint Etienne du Rouvray Cedex, France

In the past decade, much effort has been devoted to the investigation of combustion at the centimeter scale, or meso-scale combustion. As a portable source of heat or mechanical work, or as thermo-electric power generators, light small-sized devices would allow new applications requiring a few up to 100W. However, as the characteristic length of the object decreases, scaling issues may lead to unsustainable heat loss, more intricate flame topology and combustion regimes and/or incomplete combustion. Small scale can significantly affect flame stability, overall efficiency and pollutant formation.

In the present study, a quasi-cubic meso-scale 0.64 cm³ air/methane whirl flow combustion chamber, with no moving parts, is analyzed by means of well-resolved LES. The computations include a semi-detailed chemical kinetics mechanism (by Coffee, involving 13 species and 38 reactions) and complex transport. The resolution takes place on unstructured meshes of ~35 million elements. To reduce the computation wall-time, a dynamic load balancing strategy on the species source terms was implemented in the low Mach number LES/DNS code YALES₂. This allows to perform massively parallel computations up to 32k processors.

One dimensional benchmarking as well as 3D computations show that combustive flow structure, flame topology and global efficiency are quite in line with previous experimental and less detailed numerical modeling. Combustion is stabilized by a Central Recirculation Zone (CRZ) and mainly takes place in the pre-mixed lean regime.

We consider a methane/air case with 87W injected chemical power. The computations suggest a quite poor chemical conversion ratio of 55%, computed as the ratio of the heat release on the injected power. Incomplete combustion zones are identified leading to low combustion efficiency. As the wall boundary condition is set isothermal, wall heat loss are also estimated. Around 60% of the heat release is lost at the wall while the remainder corresponds to the outlet heat flux.

In order to improve the global performance, hydrogen enrichment was also tested. This showed an improved chemical conversion ratio, around 66%. But most of this additional power is lost at the walls. It can be explained by a too restrictive residence time and non-optimal combustion chamber geometry. However, hydrogen enrichment showed a positive effect on the pollutant emissions.

Within the framework of thermo-electric applications, this preliminary study is aimed at gathering and assessing modeling tools and efficient specific numerical strategies for shape and set-up optimization of the combustion chamber.

pierre.benard@coria.fr

W1P025 EXPERIMENTAL STUDY ON MESO-SCALE TUBE COMBUSTORS WITH MULTI-JET-MODE ELECTROSPRAY

Naoyuki Hatakeda, Fudhail BinAbdulMunir, Masato Mikami, Takehiko Seo, Yamaguchi University, Japan

In recent years, micro-combustors with liquid hydrocarbon fuels have attained a great interest among researchers in the combustion field. This surge in interest is mainly due to the high-energy density of liquid fuels. To have a feasible liquid fuel micro-combustor, a stable flame is essentially required. However, it is difficult to achieve a stable flame inside a micro-combustor due to the high heat loss. In order to ensure that the combustion of liquid fuel can be implemented in micro channels, the fuel needs to be pre-vaporized over a short period of time. Thus, an electrospray technique needs to be utilized. Although the multi-jet electrospray mode can generate finer droplets than the other electrospray modes, only few investigations have been performed so far in this particular spray mode and no investigations have employed this mode to micro- and meso-scale combustion. In this paper, the focus is mainly on two parts. The first part is on the multi-jet electrospray mode, which produces a large number of fuel jets from a single capillary, resulting in fine droplet generation. The effects of applied voltage to the capillary and fuel flow rate on the jet characteristics were investigated by visualizing jets and sprays. Laser tomography and a nano flash shadow graphy were utilized. The capillary diameter and the distance between the capillary and the grounded wire mesh were also varied. The liquid fuel used was a mixture of 70 vol% *n*-heptane and 30 vol% ethanol. The results show that the multi-jet electrospray mode is stable at high applied voltages and low flow rates. In order to successfully employ this type of electrospray mode in meso-scale tube combustors, a small capillary diameter is needed. Furthermore, the distance between the capillary and the wire mesh should be within a certain range so that uniform spray behavior and a large number of jets can be generated. By having this range of distance, wall wetting phenomenon can also be eliminated. The second focus of this research is to investigate the effect of the meso-scale tube combustor structures on the combustion stability. For this specific reason, the flame stabilization limit inside a cylindrical tube with inner diameter of 3.5 mm and wall thickness of 0.7 mm were examined. At the preliminary stage, a gaseous fuel was used. Then, the experiment was expanded to include the liquid fuel. The experimental results show that stable flame can be achieved in meso-scale tube combustors by employing the multi-jet-mode electrospray technique with appropriate structures.

W1P026 OBSERVATIONS OF THE PROPAGATION OF LEAN PREMIXED FLAMES IN MESO-SCALE TUBES

Chris Lawn, Hamisu Adamu Dandajeh, Queen Mary University of London, United Kingdom

It has long been known that premixed flames in meso-scale tubes can propagate against mixture velocities that are considerably greater than the adiabatic burning velocity. Experiments in with horizontal tubes have explored the multiple-flame regime in which there is sometimes a sudden increase in flame speed as the lean equivalence ratio is increased. At ratios approaching stoichiometric, the flame speed depends on the flow rate, and the maximum flame speeds at a 'positive propagation limit' are greater than the adiabatic burning velocity. Numerical simulations in the literature have shown that this could be due to preheating of the mixture incident on the flame by radiation from the post-flame region, or by conduction through the tube wall. In the experiments reported here on 3 mm, 4 mm and 5 mm quartz tubes, no such limit was observed, probably because the tubes were vertical. Instead, the flames became stationary as the flow rate was increased, and maintained that condition up to an extinction limit. Methane and propane fuels behaved similarly and the displacement speeds were almost independent of the equivalence ratio in the range 0.6 to 0.9. The heating of a 3 mm diameter tube to 400 K upstream of the flame front enhanced this effect and allowed propane flame displacement speeds in excess of 300 cm/s to be sustained. There was an inverse relationship of the achievable displacement speed to the diameter of the tube. Consideration of the magnitude of the terms in the energy equation for the tube wall suggests that heating of the wall ahead of the flame by radiation from the wall behind it does increase the mixture preheat significantly and hence the burning velocity. This effect is supplemented by the increase in the reacting area of the mushroom-shaped flames, and by the flow redirection around them.

c.j.lawn@qmul.ac.uk

W1P027 COMBUSTION CHARACTERISTICS OF *N*-HEPTANE DROPLET IN A MESO-SCALE TUBE

Junwei Li, Beijing Institute of Technology, China

N-heptane droplet combustion in a small tube (inner diameter, 4mm) was experimentally investigated. In the case of no heating, *n*-heptane droplets accumulate on the wall and the flame stays at the tube exit. However, when heated, at or less than 30ul/min, liquid *n*-heptane is vaporized in the needle and the flame position is dependent on the airflow velocity. At or greater than 80ul/min, the droplet falls on the hot wall and there is a strong interaction between droplets and flame. To stabilize the flame, a recuperator was used to recover the waste heat. It is found that a self-excited oscillation of combustion in the tube is generated. As it increases, frequency of the temperature oscillation increases, but the amplitude decreases.

david78lee@gmail.com

W1P028 EXPERIMENTAL AND NUMERICAL STUDY OF MILD COMBUSTION IN A CYCLONIC BURNER

Giancarlo Sorrentino¹, Pino Sabia², Mara Joannon², Raffaele Ragucci², Antonio Cavaliere¹, Ugur Goktolga³, Jeroen van Oijen³, Philip de Goey³

¹*University Federico II of Naples, Italy* ²*Istituto di Ricerche sulla Combustione-CNR, Italy*

³*Eindhoven Univ. of Technology, Netherlands*

Cyclonic mixers could represent a very effective system in realizing mixing processes in very short time and compact size while allowing for a reasonable long residence time for the development of combustion reactions. This is particularly of interest in the case of high inlet temperature and diluted conditions, typical of MILD and HiTAC combustion, where the fast mixing process is a need, chemical kinetics and fluid-dynamical characteristic times are comparable and the residence time plays a central role in the achievement of satisfying reaction progress. In addition this configuration can be of interest also for more fundamental studies since it allows a very detailed control of the fluid-dynamic process and the study of the interaction of fluid-dynamics and chemical kinetics in well defined conditions. For these reasons a lab-scale facility has been designed and built. The core of the facility is a rectangular prismatic chamber with a typical volume of 2 cubic dm. Oxidant/diluent (preheated up to 1400K) and fuel streams, independently adjustable, are injected from two opposite sides of the chamber allowing for the realization of various cyclonic flowfields. Inlet temperatures (up to 1400K), equivalence ratio (lean to rich mixtures), residence times and mixture dilution levels are the main operating parameters of the system. Temperature measurements, sampling and inline chemical analysis as well as optical access are built-in. The main reaction chamber is made of an easily machinable refractory material thus allowing for the realization of different geometries. A detailed numerical simulation of fluid dynamics and reactive processes in the chamber is currently under development and will allow for a side-by-side analysis of the numerical and experimental results. For the time being, numerical simulations are based on RANS in which combustion chemistry is accounted for by the flamelet-generated manifold (FGM) approach. RANS results will give clues about more detailed LES studies.

g.sorrentino@unina.it

W1P029 INFLUENCE OF PREMIXING AND RESIDENCE TIME ON MILD COMBUSTION IN A REVERSE FLOW CONFIGURATION

Stephan Kruse, Emilien Varea, Veronika Wassmuth, Heinz Pitsch, RWTH Aachen University, Germany

Based on exhaust gas recirculation and hence on dilution of fresh gases, MILD (Moderate or Intense Low oxygen Dilution) combustion can significantly reduce nitric oxides and carbon monoxide emissions, as it has already been applied in furnace systems under atmospheric pressure. Besides MILD combustion, several similar concepts based on the principle of air dilution have been investigated such as FLameless OXidation (FLOX), High Temperature Air Combustion (HiTAC) and Colorless Distributed Combustion (CDC). MILD combustion could also be an auspicious technology to reduce pollutant emissions at higher pressure in gas turbines.

Reduction of emissions is challenging since NO_x and CO emissions evolve in opposite trends. NO_x emissions decrease with lower temperature or residence time, whereas CO emissions decrease with longer residence time (oxidation of CO to CO_2). Therefore, in MILD combustion, the key issue is the trade-off between the mixing process of burnt gas, fresh air, and fuel in the combustion chamber and the residence time. The mixing process has to be fast enough to be completed before the combustion process begins.

To improve mixing and characteristic time scales, different combustor designs have been developed. A swirl combustor presented by Khalil and Gupta allows good mixing due to high turbulence level, but low residence times cause an increase in CO emissions. A straight flow design related to typical gas turbines is used by Lückerrath et al. and Sadanandan et al. The recirculation of burnt and fresh gases is realized by high air and fuel inlet velocities resulting in low emissions under high pressure.

In this study, a combustion chamber based on the reverse flow configuration is used. The outlet of the burnt products and the inlet of fresh gases are located at the same side of the combustor enhancing the mixing process. Similar configurations based on this flow concept have been used in different studies by Arghode and Gupta and by Bobba et al. Besides differences in the chamber dimensions and the closed end design, the main difference remains in the nozzle arrangement. In this work, fuel and air enter the combustion chamber through two concentric nozzles located at the bottom of the chamber. The fuel nozzle exit has a diameter of $D_{\text{fuel}} = 2 \text{ mm}$ and is 35 mm upstream of the air nozzle orifice in standard configuration. This results in a partially premixed air/fuel flow at the chamber entrance. The degree of premixing can be varied by adjusting the distance of air and fuel nozzle exit. The air nozzle has a standard diameter of $D_{\text{air}} = 10 \text{ mm}$, and can be decreased to change the gas inlet velocities. The combustor has a square cross section with a side length of 58 mm and it is 200 mm long. Quartz glass windows allow for optical access at various heights of the chamber along the centerline. For the experiments, air inlet temperature is kept constant at 873 K to be in the range of relevant gas turbine combustor inlet temperatures (700-900 K).

In this study, the effect of combustor inlet velocity, which influences residence time and mixing, as well as the effect of premixing between fuel and air on NO_x and CO emissions is investigated. In order to evaluate the pressure influence, the measurements are performed at ambient pressure and at a pressure of 5 bar. The emissions are analyzed by a sensor in the exhaust tube based on the potentiometry technique. For the detection of the flame structure OH^* -chemiluminescence measurements are performed utilizing an intensified CCD-camera (pco dicam) equipped with a Nikkor 105 mm UV-lens. To carefully investigate the influence of different exit velocities on flow field and hence on exhaust gas recirculation, PIV measurements are performed. The PIV system consists of a Quantel Brilliant B Twin-Laser (2*400 mJ), light sheet optics and an Andor-Zyla CMOS (2560*2160 p²) camera equipped with a Nikkor 105 mm lens. The magnification ratio is 29.05 p/mm.

First, the inlet velocity is increased by decreasing the air nozzle diameter and keeping the flow rates constant resulting in higher recirculation rates and lower residence time. The higher velocities indicate a significant decrease in emissions. In a second step, to evaluate the pressure influence, air nozzle diameters are adjusted to match the same exit velocities compared with the ambient pressure investigation. Due to changes in the chemical pathways of NO_x formation, the increased pressure leads to higher NO_x emission. In a third step, the influence of premixing of fuel and air on MILD combustion is investigated for three different nozzle configurations. The fuel nozzle is located 0 mm, 35 mm and 70 mm upstream the air nozzle, indicating the non-premixed, partial premixed and premixed case, respectively. The results indicate that the nozzle distance of 35 mm exhibits a wider joint low CO and NO_x emission region, due to a better flame stability limit in the lean side.

s.kruse@itv.rwth-aachen.de

W1P030 CHARACTERISTICS OF THE MICROWAVE INDUCED FLAMES ON THE STABILITY AND EMISSIONS

Young Hoon Jeon, Eui Ju Lee, Pukyong National University, Korea

The use of electromagnetic energy and non-equilibrium plasma for enhancing ignition and combustion stability are receiving increased attention recently. The conventional technologies have adapted the electrical devices to make the electromagnetic field, which resulted in various safety issues such as high-maintenance, additional high-cost system, electric shock and explosion. Therefore, an electrodeless microwave technology has an advantage for economic and reliability compared with conventional one because of no oxidation. However, the application of microwave has been still limited because of lack of interaction mechanism between flame and microwave. In this study, an experiment was performed with jet diffusion flames induced by microwaves to clarify the effect of microwave on the combustion stability and pollutant emissions such as soot formation and NO_x .

The burner used in this experiment consisted of coaxial tubes, where 7.5mm of inner diameter for fuel and 20mm of outer diameter for oxidizer. Methane was used as a fuel and compressed air was used as an oxidizer, of which flow rates were controlled by using MFC (Mass Flow Controller). Schematic waveguide system was designed to provide for more

efficient coupling of the microwave power into the flame. As increasing the electric field strength and minimizing the losses by the wall are minimized, it ensures that practically all of the power delivered from the source passes into the flame. Microwaves produces a standing wave within the waveguide WR-430 (10.92cm x 5.46cm), and the flame experiences a sinusoidal time-varying electric field at a frequency of 2.45 GHz. The sliding short was used to control the location of the standing wave such that a field maximum is coincident with the location of the laminar flame burner. The 3-stub tuner also served as a means to match the phase of the incident wave with the standing wave. Directional coupler would be represented through the power monitor to absorb incident wave and reflected wave, which provides approximate microwave power.

The results show that the induced microwave enhances the flame stability and blowout limit. The unstable lifted rotating flames under high fuel/oxidizer velocity is changed to stable attached flames as a high microwave applied to the flames, which results from the abundance of radical pool. However, NO_x emission was increased monotonically with increasing the microwave power but NO_x emission decrease at the power of 0.2 kW. The effects might be attributed to the heating of combustion field and thermal NO_x mechanism will be prevailed. Soot particle was examined at the post flame region by TEM grid. The morphology of soot particle sampled in the microwave induced flames was similar to the incipient soot that is not agglomerated and contain a lots of liquid phase hydrocarbon such as PAH, which soot particle formed near reaction zone is oxidized on the extended yellow flame region and hence only unburned young particles are emitted on the post flame region.

younghun2434@naver.com

W1P031 EFFECT OF FLUE GAS AND DEPOSIT COMPOSITION ON CORROSION AND DEPOSITION IN OXY-FUEL ENVIRONMENTS

William Nimmo, Mohamed Pourkashanian, Toor-E-Aiman Rizvi, University of Leeds, United Kingdom

The global increase in demand for electricity, along with stringent emission regulations, poses several operational and economic problems for the power industry. One such problem is the corrosion and deposition encountered by boiler heat transfer surfaces.

This study is based on investigating the fireside corrosion behaviour of waterwall and superheater boiler tube materials, under simulated oxy-fuel environments, with and without the influence of coal and biomass ash deposits. A custom-built laboratory scale corrosion rig with the ability to simulate a range of flue gas compositions and temperatures, in addition to generating a heat flux through the specimen, was set up for this purpose. Initially, a series of experiments were performed to evaluate the influence of increasing the SO_2 content (1000,2000,3000 vppm) of the simulated gas, while keeping the molar concentration of other constituents ($\text{O}_2 \sim 3\%$, $\text{CO}_2 \sim 70\%$, $\text{H}_2\text{O} \sim 10\%$, $\text{HCl} \sim 250\text{vppm}$) fairly constant. The gas temperature was maintained at $900 \pm 50^\circ\text{C}$ with an exposure time of up to 350hrs. Pre and post exposure thickness measurements were used to determine the rate of metal loss and the corroded specimen were analyzed using SEM/EDX analysis.

Furthermore, the properties of a high sulphur coal (potland burn UK) and four biomass samples (pine wood, peanut shells, sunflower husk and miscanthus) were evaluated in order to predict their fusion and deposit forming tendencies in combustion systems. This entailed a series of ash fusion tests, simultaneous thermal analysis (STA) of fuel ashes using Netzsch STA 449 coupled with a Netzsch QMS(Quadrupole Mass Spectrometer) 403C Aeolos equipment, calculation of empirical indices and predicting ash melting behaviour with the help of the thermodynamic equilibrium software Factsage 6.3.

w.nimmo@leeds.ac.uk

W1P032 COMPARISON OF THERMODYNAMICAL POTENTIALS OF OXY-FUEL COMBUSTION, NORMAL AIR-COMBUSTION AND REGENERATIVE COMBUSTION

Kenichi Sato, Osamu Fujita, Hokkaido University, Japan

Possibility of the high combustion efficiency using the oxy-fuel combustion technology has been studied from the thermodynamic point of view. The energy consumption and the change in entropy were calculated for the case of the normal air combustion, regenerative combustion, and the oxy-fuel combustion. The energy consumption and the change in entropy were compared and discussed for three cases. For the oxy-fuel combustion, the energy required to produce the pure oxygen from the air was considered. Regenerative combustion was the case in consideration of a heat recovery.

The industrial furnaces that use the normal air combustion, the regenerative combustion, and the oxy-fuel combustion. The materials are heated up in the furnaces. In these figures, T_{in} is the inlet temperature, T_{out} is the outlet temperature, and T_f is the furnace temperature. For the normal air combustion which is no thermal recycling, the furnace temperature is controlled by the air flow rate. The regenerative combustion is the thermal recycling system. The air used for the combustion is heated up by the high temperature exhaust gas. The heat recovery efficiency is the very important parameter to evaluate the thermal efficiency of the regenerative combustion. The furnace temperature is controlled by the air flow rate. For the oxy-fuel combustion, the fuel and oxygen are burned at the stoichiometric ratio. A part of the exhaust gas is recirculated into the furnace and mixed with the burned gas of the stoichiometric oxygen and fuel. The furnace temperature is controlled by the amount of the recirculated exhaust gas. For the oxy-fuel combustion, the energy required to produce the pure oxygen was considered as $0.3\text{Wh/m}^3_{\text{N}}$ as a base condition.

The heat recovery efficiency of the regenerative combustion at the entropy equivalent points of the oxy-fuel

combustion and the regenerative combustion for a certain value of the outlet gas temperature. η_{RC} is the heat recovery efficiency of the regenerative combustion at entropy equivalent point. For the oxy-fuel combustion, five cases are shown in the figure. In Fig.2, the word “consider” means that the heat capacity of the working fluid is considered. Upper side of each curve is an area where regenerative combustion is thermally better than oxy-fuel combustion. On the other hand, the lower side of each curve is an area where oxy-fuel combustion is thermally better than regenerative combustion. When the energy to produce the pure oxygen is not considered, the oxy-fuel combustion is thermally better than the regenerative combustion except for the higher heat recovery efficiency. If the energy to produce the pure oxygen is considered, η_{RC} decreases with decrease in outlet temperature or increase in the difference between the outlet temperature and furnace temperature. When the difference between the outlet temperature and furnace temperature decrease, oxy-fuel combustion is advantageous compared to the regenerative combustion.

The thermodynamical potential of the oxy-fuel combustion is higher than that of the normal air combustion when the exhaust gas temperature is high. The thermodynamical potential of the regenerative combustion depends on the efficiency of the heat recovery of the regenerative system. When the exhaust gas temperature is high, thermodynamical potential of the oxy-fuel combustion could be higher than that of the regenerative combustion according to the heat recovery efficiency practically attained in industry.

k-sato@mech-hm.eng.hokudai.ac.jp

W1P033 COMBUSTION OF LIGNITE AND ITS CHARS IN AIR AND OXY CONDITIONS

Michał Ostrycharczyk, Jakub Dlugosz, Halina Pawlak-Kruczek, Jacek Zgora, Wrocław University of Technology, Poland

Oxy combustion has been one of the proposed clean coal technologies. It is also a very promising method of carbon dioxide emissions reduction from power plants fired with fossil fuels. This technology is advantageous for retrofitting existing units from conventional combustion to oxy-combustion. But the differences (fluid dynamics, ignition, heat release and heat transfer rates) between air and oxy gases composition lead to different combustion process behaviour. The following work in progress focuses on investigations of the predried lignite with various moisture contents during fast pyrolysis in carbon dioxide and nitrogen atmospheres (laboratory scale isothermal flow reactor). Additionally the combustion of chars in oxy and air environment were also studied. Significant influence on both these processes have CO_2 and H_2O gasification reactions and the homogenous water shift reactions. The objective of the research was to determine the effect of atmosphere (oxy and air combustion environments) on C, H, and N elements speciation from the solid and gas phase in the pyrolytic stage. In the conducted tests, composition of pyrolytic gas was analysed (CH_4 , CO , H_2) with special regard to N – gas components (NO_x , HCN , NH_3). Also, the total fuel mass loss and fractional mass loss of C, H, and N during the pyrolysis process were determined. The solid phase (char) was characterized by ultimate analysis, SEM and by mercury porosimetry technique. Furthermore characterisation of NO_x emission intensity from char combustion obtained in N_2 and CO_2 atmosphere were also performed.

Authors studied lignite with three different moisture content (14%, 7%, 1.5% by mass). Results showed that CO_2 environment has more significant effect on the mass loss than it is in the case with moisture content in N_2 atmosphere. Mass loss and porosity of char obtained from CO_2 atmosphere were higher than in the case of chars obtained from N_2 atmosphere, which may be attributed to the CO_2 gasification reaction of fuel C taking place in both external and internal surface areas. This effect is stronger for lignite with the higher moisture content (i.e. for 14% moisture content in comparison to 1.5%). The analysis of TFN compounds shows that for the lignite with high volatile matter content, the pyrolysis atmosphere has big effect on amount and composition of TFN. In presence of high concentration of CO compound (CO_2 environment) the higher NO_x and lower HCN were obtained in comparison to the N_2 atmosphere. An additional objective was to determine the NO_x emission intensity from the combustion of raw lignite and its chars obtained in CO_2 and N_2 environments. The results exhibited that NO_x emission from raw lignite combustion is lower in air and oxy atmospheres than from its chars combustion. In spite of relatively low content of N-fuel in char from CO_2 atmosphere, the emission intensity of NO_x from both air and oxy combustions is higher in comparison to raw lignite combustion. The level of NO_x emission intensity from combustion of char produced in CO_2 atmosphere slightly depends on the combustion atmosphere because NO_x emission intensity during oxy combustion in $\text{O}_2/\text{CO}_2 = 25/75\%$ is similar to raw lignite. It might have been caused by lower reactivity of the char obtained in CO_2 environment and less N-fuel share in char.

michal.ostrycharczyk@pwr.wroc.pl

W1P034 OXY-FUEL COMBUSTION PERFORMANCE EVALUATION IN A 250 KW TEST FACILITY

William Nimmo, Janos Szuhanski, Sandy Black, Mohamed Pourkashanian, University of Leeds, United Kingdom

In order to help mitigate the effects of climate change, and to enable the UK government to meet its ambitious goal of achieving an 80% reduction in greenhouse gas emissions (based on 1990 levels), the UK power generation industry has been set challenging targets for reducing their CO_2 emissions. Carbon Capture and Sequestration (CCS), which has been endorsed by both the IEA and the UK Government, will form an essential part of the strategy to achieve substantial CO_2 reductions by 2050. Oxy-coal combustion, which can be retrofitted, is one of the leading CCS technologies. This poster presents the results of programme of experimental work undertaken at a 250 kW Combustion Test Facility (CTF), located at the UKCCSRC PACT facilities in Sheffield, UK. The CTF consists of a down fired cylindrical furnace fitted with a 250 kW Doosan Power Systems Low- NO_x burner, capable of burning pulverised coal and biomass, under both air and oxy-firing conditions. Coal was fired in air, establishing a baseline study, and under oxy-fuel conditions at different

O₂ enrichment levels. The excess air was kept at the same level for all cases. Burner Measurement ports. A variety of measurement techniques were used in order to build up a comprehensive picture of the combustion process. Suction pyrometry was used for in-flame temperature measurements, in-flame species concentrations (O₂, CO, CO₂, SO₂ and NO_x) were measured using gas sampling methods, and flue gas emissions and burnout were also monitored. However, since matching the flame temperature and radiative heat transfer properties of oxy-fuel flames to air-fired ones are especially important when considering a boiler retrofit, particular attention was given to the heat transfer performance of the resulting flames. A Medtherm digital heat flux probe was used to measure both total surface incident radiation and total surface heat flux along the length of the furnace at different axial positions from the burner.

The experiments have also provided comprehensive, detailed data sets for the validation of modified Computational Fluid Dynamics (CFD) models developed for oxy-fuel combustion. This will help to enable computational modeling techniques to be used more effectively in the design of newly built oxy-fuel furnaces, as well as in predicting the impact of retrofit conversion of the existing fleet of coal fired power plants.

w.nimmo@leeds.ac.uk

W1P035 COMBUSTION CHARACTERISTICS OF OXY-FUEL STAGED COMBUSTION WITH A RAPIDLY-MIXED TYPE TUBULAR FLAME BURNER

Akane Nagasaki¹, Akeshi Kegasa¹, Tsukasa Hori¹, Yosuke Shiraga², Hiroki Shibagaki¹

¹Osaka University, Japan ²OSAKA GAS CO., LTD, Japan

Recently, a swirl-type tubular flame, which is formed by inletting fuel and oxidizer tangentially through narrow slots cut axially on a combustion tube, has been remarked as a combustion technology having thermal and aerodynamic advantages. The flame is highly adiabatic because burned gas flows inside the tubular flame and unburned mixture outside. Especially, a rapidly-mixed type tubular flame where fuel and oxidizer are supplied separately is safe from a backfire. Therefore, since a high temperature field could be built in the burner safely by a combination of oxy-fuel combustion and adiabatic tubular flame, the combustion technology may be applicable to high temperature furnaces. As an application, we consider applying this technology to a so-called in-flight melting of glass. The in-flight melting is a new technology of glass production. Granulated raw materials are melted during falling, where the particles are in full contact with the flame. Significant energy saving effects in the glass melting process will be expected, because the in-flight melting could make the fusion time shorter and the furnace size smaller dramatically.

In this study, we have performed oxy-fuel combustion using a rapidly-mixed type tubular flame burner. Following phenomena may generate problems when applying the tubular flame to the in-flight melting, firstly, oscillation combustion at near stoichiometric ratio, secondly, attached flames on the burner slots which may cause overheating of the burner, and finally, luminous flames which might make soot mixed into the glass particles. In order to avoid these problems, combustion characteristics were investigated experimentally by using a rapidly-mixed type tubular flame burner divided in two axially. The oscillation combustion did not occur in the burner, but the flames were attached to the slots under almost all conditions, and it caused overheating of the burner. Rich-lean combustion and two staged combustion were experimented and conditions that could avoid above three problems were found by diluting the mixture with carbon dioxide. On the other hand, attached flame conditions were examined theoretically and a concept of non-dimensional flame length was advocated and inspected experimentally. After the condition suitable for the in-flight melting was settled, we performed a melting experiment of glass particles and confirmed the melting.

nagasaki@ed.jrl.eng.osaka-u.ac.jp

W1P036 CHARACTERISTICS OF EXHAUST EMISSION OF LAMINAR INVERSE DIFFUSION FLAMES ON OXY-FUEL COMBUSTION

Tomohiro Yamanaka, Nichiki Okada, Shuhei Yoneyama, Takeshi Yokomori, Keio University, Japan

In recent years, CCS (Carbon Capture and Storage) has been attracted attention as the key technologies to reduce the levels of CO₂ emission from the combustion. In this technology, there are several options to capture and sequester CO₂. Oxy-fuel combustion is one of the leading options because it can be operated in retrofitted power plants. Although some authors reported that the abundant presence of CO₂ affects the combustion characteristics, the details of them have not been clarified yet. Therefore, in order to apply oxy-fuel combustion to the industrial scenes, further fundamental studies are needed. In some of industrial burners, there is a situation where the oxidizer jet is surrounded by fuel. In non-premixed turbulent flames, furthermore, some of flame segments are also under the same situation. In this study, therefore, we adopted the co-flowing laminar Inverse Diffusion Flames (IDFs) which was formed where oxidizer is surrounded by fuel, and the characteristics of exhaust emission of IDFs on oxy-fuel combustion were investigated experimentally and numerically. Local gas sampling near the flame was achieved by the fine quartz suction probe, and the sampling gas was analyzed by the gas chromatography. Chemiluminescence spectra of IDFs were also measured using a spectroscope to understand the characteristics of chemical reactions. Numerical calculation was performed using Open FOAM with GRI-Mech 3.0 mechanism. In addition, the chemiluminescence reactions with respect to CO₂^{*}, CH₂O^{*} and OH^{*} were also added for the comparison with the experimental results. Experiments and numerical calculations were carried out under CO₂ and N₂ dilutions. The flame temperature in CO₂ dilution was lower than that of N₂ dilution owing to the high specific heat of CO₂. OH^{*} chemiluminescence was weaker and HCO^{*}, CH₂O^{*} and CO₂^{*} chemiluminescences were stronger in CO₂ dilution than that in N₂ dilution. This result suggests that the abundant presence of CO₂ affected the chemical

reactions in CO₂ dilution. CO was mainly produced at the downstream of the reaction surface surrounded with the soot radiation region. The amount of CO in CO₂ dilution was larger than that in N₂ dilution even though the flame temperature was lower in CO₂ dilution than in N₂ dilution. This result suggests that CO was produced by not only oxidation of fuel but also CO₂ decomposition due to the abundant presence of CO₂.

tomohiro.yamanaka@z8.keio.jp

W1P037 TRANSIENT PLASMA: A UNIQUE TOOL FOR REDUCING SOOT AND NO_x

Bikau Shukla¹, Kian Eisazadeh-Far², William Schroeder¹, Daniel Singleton¹, Martin Gundersen¹, Fokion N. Egolfopoulos¹

¹University of Southern California, United States ²Tula Technology Inc., United States

Reducing environmental pollutants (Soot & NO_x) emission from combustion sources has been a challenge for combustion scientists, engineers, and engine manufacturers. According to Environmental Protection Agency (EPA) report, while modern engine has reduced emission substantially, emissions from diesel engines such as on-road buses & trucks, off-road farm & construction vehicles, and non-road marine engines are still causing an estimated 6% of lung cancer deaths in the US and UK. Nanosecond pulsed discharge non-equilibrium Transient Plasma (TP) appears as a powerful tool for lowering emissions. As ethylene is produced as a major component from the decomposition of real fuels, in this study, TP was discharged into a sooty flame of ethylene using a TP pulsar developed at USC and soot volume fraction was measured by laser extinction technique. Similarly, for the examination of TP effect on NO_x, exhaust from a Kubota diesel engine was passed through a shell with volumetric TP discharge. Results showed that TP reduces soot by ~30% and NO_x by ~90%. Effect of TP on emission of CO, CO₂ and hydrocarbons including PAHs is under progress. To understand and optimize the efficiency of TP, a comparative study on combustion initiation by TP and a regular spark was performed using a constant volume combustion chamber and a counter flow configuration coupled with optical shadowgraph. Results showed that TP induces ignition from the tip of an electrode where the electric field and electron densities are the highest, however, a spark initiates ignition from the hot region between the two electrodes. Discharges in only air suggested that ignition initiated by TP is at least partly non-thermal and driven by the production of active species. Then, detailed ignition studies on both premixed and non-premixed flames of a variety of fuels ranging from hydrogen to heavy fuels including US Navy diesel F-76 and a bunker fuel IFO380 in different experimental systems such as constant volume chamber, opposed-jets, pool burner, and spray burner were also performed. Noticeably, single pulsed TP discharge was found sufficient to ignite all flames without any thermal support. Finally, TP seems highly efficient for reducing emission by enhancing combustion efficiency while geometry of electrodes and location of discharge affect its efficiency significantly.

bikaushu@usc.edu

W1P038 FUEL-RICH PARTIAL OXIDATION BY REACTIVE VOLATILIZATION

Will Northrop, University of Minnesota, United States

This poster describes our current progress on a project to investigate reactive volatilization, a unique method for evaporating and partially oxidizing liquid fuels at high equivalence ratio ($\phi > 4$) without soot formation. A fuel reforming device based on the reactive volatilization concept could be used with internal combustion engines to improve catalytic after treatment regeneration or for controlling the reactivity of fuels to increase engine efficiency and reduce emissions. High equivalence ratio operation leads to high reforming efficiency especially when combined with engine exhaust thermal recuperation strategies.

Here, we expand on previously reported work, presenting modeling results from an opposed flow reactive volatilization reactor. In this reactor, fuel reforming at high ϕ is accomplished by vaporizing and reacting fuel through conductive and radiative heat transfer from catalytic oxidation sustained on a porous catalytic screen. We present a 1-D model that uses the classical opposed flow diffusion flame formulation with modified boundary conditions accounting for liquid vaporization on the fuel side and heterogeneous catalytic oxidation reaction on the air side. A multi-component vaporization model and catalytic oxidation kinetics have been added to our previously reported work. Our modeling results show that partial oxidation reforming reactions are primarily occurring at the surface of the porous wall and that carbon formation is suppressed by gas-phase pyrolysis reactions. We find that the gas-phase reactions, although much slower than catalytic oxidation, lead to significant unsaturated hydrocarbon concentrations which are advantageous for altering ignition properties in engine applications.

We also present the status of our efforts to construct an opposed-flow reactor to experimentally examine the reactive volatility concept. This reactor, based on radial counter flow burners described in the literature, incorporates a catalytic screen and liquid reservoir. Diagnostics include fast-response thermocouples, axial gas sampling for gas chromatography analysis, and optical accessibility for applying techniques like Filtered Rayleigh Scattering for temperature measurement and planar laser-induced fluorescence for measuring radical concentration. The reactor is in the design phase and is expected to be completed within the coming year. Experimental data from the setup will be used to validate our modeling activities and for improving the general understanding of homogeneous reaction kinetics in fuel-rich environments.

wnorthro@umn.edu

W1P039 A THERMAL PARTIAL OXIDATION “SWISS-ROLL” FUEL REFORMER

Chien-Hua Chen¹, Howard Pearlman¹, Paul D Ronney², Shrey Trivedi¹, Andrew Lawson², Swapnil Desai², Srushti Koli²

¹Advanced Cooling Technologies, Inc., United States ²University of Southern California, United States

A compact, non-catalytic, Thermal Partial Oxidation (TPOX) based reformer based on the Swiss-roll concept (recirculating spiral heat exchanger) has been developed to provide hydrogen rich SYNGAS to solid oxide fuel cells (SOFC). The Swiss-roll reformer is highly effective at recuperating heat from the exiting reformat stream and transferring it to the inlet fuel-air stream, thus enabling superadiabatic temperatures to be achieved within the reformer. The basic concept of superadiabatic temperature is the temperature superposition of from heat recirculation and chemical reaction. Without heat recirculation, the reaction temperature increases due to the chemical heat release associated with the partial oxidation process. With heat recirculation, the reactant temperature increases due to the chemical heat release and heat recirculation from the hot reformat stream. The superadiabatic reaction temperatures and long residence time in the preheated inlet channel allow the reformat composition to approach the equilibrium state (the maximum SYNGAS yield can be achieved) without the need for catalysts. The reaction is self-sustained (does not require external energy sources other than for startup) and stabilized in the center reaction zone for a wide range of operating conditions. To date, fuel flexibility has been demonstrated using rich propane, n-heptane, and JP-8-air premixtures.

Using a six-turn Swiss-roll reformer having dimensions 5 cm in height and 8 cm wide, representative results for three different fuels at the same equivalence ratio ($\Phi = 3$) and flow conditions ($Re = 157$) are shown in Table 1, noting that higher hydrocarbons (C_6 and above) were not measured. H_2 and CO are the primary species. Further testing is now being done to better to evaluate the effect of inlet flow conditions and mixture composition on the SYNGAS yields, potential production of aromatics and soot formation.

chien-hua.chen@1-act.com

W1P040 THE COMBUSTION CHARACTERISTICS OF PREMIXED PROPANE/AIR FLAME IN MOVING CERAMIC GRANULAR BED

Ian Shou-Yin Yang, De-Li Hsu, National Formosa University, Taiwan

Experimental measurement was employed to investigate the combustion characteristics of premixed propane/air flame in Moving Ceramic Granular Bed (MCGB). The CGB has physical properties of porous and therefore it accumulates heat; thus, in combustion wave propagation in a CGB, the flame demonstrates mild combustion because of changes to heat transfer mechanism. Additionally, under certain operating conditions, premixed flames become flameless. This study investigated the heat transfer mechanisms effects the premixed C_3H_8 /air flame characteristics of flow rate and granular velocity in moving ceramic granular bed by experimental method and theoretical analysis. The temperature and thermal wave propagation speed of premixed flame were conducted the combustion phenomenon's in difference granular velocity. The results indicated MCGB burner enhance the heat transfer effect of the thermal wave propagation speed and decrease the flame temperature that is for the heat transfer characteristics to make the effective thermal conductivity decrease. But firing rate flux affected flame temperature increase, and thermal wave propagation speed of flame decrease that cause the heat transfer mechanisms change of MCGB. Radiation and conduction effect of heat transfer mechanism of CGB is mainly dominated the heat transfer in low firing rate flux condition. The effect of thermo-radiation increases with the firing rate flux.

ianyong@nfu.edu.tw

W1P041 EXPERIMENTAL AND NUMERICAL INVESTIGATIONS OF METHANE THERMAL PARTIAL OXIDATION IN A SMALL-SCALE POROUS MEDIA REFORMER

Alexandra Loukou, Miguel Mendes, TU Bergakademie, Germany

This study investigates SYNthesis Gas (SYNGAS) production from preheated, rich methane/air mixtures. The examined process relies on non-catalytic partial oxidation within a small-scale porous media based reactor, intended for Solid Oxide Fuel Cell applications. Unlike other porous media based reformers, an important feature of the examined reactor is the ability to operate on the basis of stationary flames. Flame stabilization is achieved using a two-section reactor design. The two sections differ only in terms of geometry, whereas the same porous medium is installed in both of them. The first one has a conical shape that induces a continuous change in the cross-sectional area and hence, in the axial flow velocity of the incoming reactants. In this manner, stationary flames can be sustained at positions where flow velocity equals the mixture's burning velocity. The second section is cylindrical and it provides residence time for post-flame, slow, reforming reactions.

For the current study, the porous medium was created as packed bed of Al_2O_3 Raschig rings (62% open porosity). Process characteristics like temperature profiles within the porous zone and exhaust SYNGAS compositions, are experimentally and numerically investigated under conditions that can be encountered in SOFC based systems. Soot particle size distributions within the generated SYNGAS are also measured with the technique of Scanning Mobility Particle Sizing. The process is simulated with a quasi-1D numerical model that uses the volume-averaged approach, solves both the gas- and solid-phase energy balances explicitly, and accounts for the radiative heat transport in the solid-phase. Peak temperatures measured within the porous zone provide evidence of superadiabatic combustion, which is also confirmed by the numerically predicted temperature profiles. SYNGAS compositions reveal a maximum reforming efficiency of 65% based on H_2 and CO, while the soot limit of the process lies at an equivalence ratio of 2.2.

W1P042 A DISCRETE QUASI THREE-DIMENSIONAL MODEL OF GAS COMBUSTION IN POROUS MEDIA

Fedir Sirotkin, Sergey Minaev, Roman Fursenko, Far Eastern Federal University, Russia

A discrete quasi three-dimensional model of gas combustion in porous media is proposed. The porous media is represented as the set of randomly placed solid grains which are connected through the artificial solid plate to mimic thermal conductivity between grains. The propagation of the combustion wave is simulated in the frame of thermal-diffusion model with the prescribed old computed preliminary using Lagrangian particles method. Dependencies of combustion wave velocity on the inlet gas velocity for different equivalence ratios and porosities are obtained and compared with the continuous one-dimensional thermal-diffusion model. Our results imply that the same propagation in the porous media can be considered as a collective process, when the actual combustion wave can be represented by a set of individual flame fronts propagating in the mutually connected micro-channels of the different diameter. The discrete structure of the combustion wave is most prominent when the inlet velocities are small and the flame propagation is accomplished with pulsations of flame front fragments. When the inlet velocities are high enough, the propagation of the combustion wave is much more regular. Our model describes the flame anchoring phenomena when the combustion wave is stabilized inside of the porous media for a range of inlet velocities.

sirotkin.f.v@gmail.com

W1P043 POROUS INSERTS FOR PASSIVE CONTROL OF NOISE AND THERMO-ACOUSTIC INSTABILITIES IN LDI COMBUSTION

Ajay K. Agrawal, Joseph Meadows, University of Alabama, United States

In this study, ring-shaped porous inserts made from high-strength, temperature resistant ceramic materials are stacked on the dump plane of a combustor to create different geometric configurations with the goal to favorably influence emissions and acoustics in LDI combustion. Porous inserts with converging, diverging, and hyperbolic configurations are considered in this study. Kerosene fuel atomized by an air-blast injector is introduced in the swirl-stabilized combustor operated at atmospheric pressure. Emissions and acoustics measurements are obtained for different heat release rates and atomizing air to liquid mass ratios. Results show negligible effects of porous inserts on NO_x and CO emissions or the flame structure. Porous inserts are however very effective in reducing acoustic power throughout the frequency range, thereby suppressing both noise and thermo-acoustic instabilities for different operating conditions. The measured trends in acoustic absorption are predicted using a simplified thin-layer model of porous materials. Detailed velocity and heat release measurements are needed to accurately quantify interactions between porous insert and the flow field.

aagrawal@eng.ua.edu

W1P044 THERMAL TRANSPIRATION BASED PUMPING AND PROPULSION DEVICE

Shirin Jouzdani, Ryan Falkenstein-Smith, Jeongmin Ahn, Pingying Zeng, Syracuse University, United States

Recently there has been a generated interest in mesoscale or microscale propulsion and pumping devices have many potential applications for small air or space reconnaissance vehicles. This study examines the successful development of a combustion-driven thermal transpiration-based combustor and a self-sustaining gas pump and propulsion systems, having no moving parts and using readily storable hydrocarbon fuel. This was achieved by developing microscale or mesoscale propulsion and pumping systems, applicable to either space or air breathing vehicles, by using an entirely different principle based on the process of thermal transpiration. Since only thermal power and not electrical power is required for thermal transpiration, it is possible in principle to use heat release from a chemical or nuclear process rather than electrical resistive heating to provide the thermal power. In fact, by exploiting a catalytic reaction process integrated with the outlet side of the thermal transpiration device it is possible in principle to produce a self-sustaining propulsion system that has no moving parts, no supplemental working or pressurization fluids, very low mass and integrates pressurization and thrust generation into one device.

A cubic combustor was designed to house the thermal transpiration membrane and develop into a self-sustaining gas pump system. Fuel/Air would feed through an inlet into a mixing chamber that would flow into the thermal guard containing the thermal transpiration membrane. This configuration allowed both fuel and air to be transpired through the membrane meaning it was not possible for any reactant flow to occur as a result of the fuel supply pressure and only the membrane could draw reactants into the device.

A 1-D propulsion device using Aerogel instead of glass microfibers filters was also studied. The pressure difference between two chambers was established through the attachment of a bubble meter and measured with sensitive pressure transducers. The temperature gradient between both chambers would be created through heating wires which subsequently would be measured by thermo couples. Aerogel substance is used as a membrane between two sides of the chamber. The use of a porous substance such as aerogel as the transpiration membrane and a pressure gradient served as the two requirements in order to successfully achieve thermal transpiration.

sjouzdani@syr.edu

W1P045 FORMATION OF SYNTHESIS GAS BY SUPER ADIABATIC FLAME FOR HIGH TEMPERATURE FUEL CELLS

Hydrogen has been considered to be the fuel of the future because it contains more energy per unit mass than any other fuel and generates minimum emissions when it burned and essentially no emissions when it is electro-chemically converted to electricity in fuel cell systems. For the projected demand in hydrogen, simple and efficient processes of hydrogen generation from various feed stock should be engineered. One of such solutions is a direct thermal partial oxidation of hydrocarbon by super adiabatic flame under rich and ultra-rich condition without platinum catalyst. Commercial thermal partial oxidation reformer is 100mm long, 50mm diameter and 31 holes separated by SiC walls. The flow holes have a radius of 4mm each and are divided by 1mm thick SiC walls. The fuel and air flow rate were metered using MFC and MFC controller that directed the two separate flow rated streams into a fuel/air mixing chamber. 99.995% pure methane gas and compressed dry air were used in the experiments. The data acquisition systems consisted of 8 K-type thermocouples system used to monitor the thermal partial oxidation temperature front location along the axis of the reformer. The formation of the synthesis gases is analyzed using a HP 6890 series GC (Gas Chromatography). Temperature profiles obtained from the super adiabatic flame of rich methane air mixtures at equivalence ratios of 2.0. Comparison of experimental and computational simulation temperature curve for reformer under ultra rich equivalence ratio and different inlet mixture gas velocity. Computational simulation and experimental results follow similar trends, although experiments predict temperatures that are lower than the ones observed in computational simulation results. Experimental results of hydrogen and carbon monoxide yield versus the different equivalence ratio and inlet mixture gas velocity. The percent hydrogen and carbon monoxide yield increases with increasing equivalence ratio. At increased equivalence ratio, synthesis gas yields vary from 7.47% to 10.20% for hydrogen and 7.11% to 9.20% for carbon monoxide.

meman80@incheon.ac.kr

W1P046 FLAMELESS COMBUSTION OF LIQUID FUEL FOR GAS TURBINE

Chun Loon Cha, Pil Hyong Lee, Ho Yeon Lee, Sang Soon Hwang, Incheon National University, Korea

Flameless combustion, well known as MILD combustion or CDC (Colorless Distributed Combustion), is considered as one of the promising technology for achieving low NO_x and CO emissions and improve thermal efficiency of combustion system.

In this paper, the effects of air injection condition on formation of flameless combustion of liquid fuel were analyzed using three-dimensional numerical simulations for application of gas turbine combustor. Especially, effect of air injection diameter was investigated to elucidate the evaporation rate of liquid fuel, gaseous fuel/air mixing and gas recirculation on effective formation of flameless combustion at relatively lower heat intensity of 5 MW/m³ atm and $\Phi=0.8$. In the first part of investigation, an experimental spray penetration length measured at EHPC (Eindhoven High Pressure Cell) was compared with calculated penetration length to verify the accuracy of liquid spray model used in Fluent.

Results show that the spray model tends to overestimate spray penetration length a little bit at the beginning of the spray but the spray model acts well to predict the spray pattern accurately after 1ms. Also the flameless combustion results show that the local high temperature region was decreased and flame temperature was spatially uniformly distributed due to higher recirculation rate of burnt gas. The gap of recirculation ratio at between minimum and maximum air injection velocity had seven times higher recirculation than at minimum velocity. The maximum velocity was observed when air injection diameter was 2mm. Analyzing the mixing effect by entrainment rate, it was also found that the evaporation length of liquid fuel was decreased when the recirculation ratio was increased. Fast evaporation made the liquid fuel to the gaseous fuel, so the air/fuel mixture was quickly formed. Therefore recirculation ratio, mixing and dilution effects are very important factors to perform liquid fuel flameless combustion system.

clcha@incheon.ac.kr

W1P047 THE APPLICATION TO SMOKE TUBE AND FLUE BOILER COMBUSTION OF NEW ENERGY SAVING TECHNIQUE USING ELECTRO-MAGNETIC WAVE IN THE RANGE OF FAR INFRARED RAY

Satoshi Okajima, Infield Capital, United States

The energy saving mechanism on fossil fuel combustion can be determined by two concepts: increasing the flame temperature established in the combustion chamber and increasing the temperature exchange efficiency at the heat exchange region of combustors.

In order to achieve the energy saving mechanism on fossil fuel combustion, we have developed two techniques using the electro-magnetic wave in the regime of far infrared ray. One is the flame temperature rise method, which is caused by excited reaction between active chemical species in flame and chemical species in flame and electro-magnetic wave in the regime of far infrared ray. Other is the spectrum heat absorption method at heat exchange region, which is produced by absorption of spectrum emitted from the combustion flame through the radiation materials developed in the study. The effectiveness of these techniques for practical boilers is verified using the smoke tube and flue boiler. The fuel used is Town gas 13A, boiler capacity is 6 ton/h, and the vapor pressure is 0.8MPa. The results under electro-magnetic combustion show the increased boiler efficiency and the fuel reduction rate of greater than 10%.

sofireuperg@yahoo.co.jp

W1P048 GENERATION OF HYDROTHERMAL FLAMES IN A MOBILE SUPERCRITICAL WATER OXIDATION REACTOR

Sivamohan N. Reddy¹, Sonil Nanda¹, Janusz A. Kozinski¹, Michael C. Hicks², Uday G. Hegde²

¹York University, Canada ²NASA Glenn Research Center, United States

Supercritical water (pressure > 22.1 MPa and temperature > 374°C) possesses attractive solvation capabilities to dissolve organic compounds and permanent gases (e.g., CO₂, O₂, N₂, CO, CH₄ and H₂). This enables Supercritical Water (SCW) to be used as an environmental friendly medium for the oxidation of complex and recalcitrant molecules to simple gases. The oxidation of organic compounds to produce H₂, CO, CO₂ and H₂O makes SCW oxidation process an optimal technology for toxic waste remediation.

The introduction of hydrothermal flames results in complete conversion of complex organics. Moreover, the reaction rates are high and reactions are completed in milliseconds. A highly reactive environment of hydrothermal flames degrades the recalcitrant molecules into simple gases. However, the generation and stability of hydrothermal flames in SCW medium is the most crucial phase during the oxidation reaction. An organic solvent with appropriate concentration in the presence of oxidant in SCW generates hydrothermal flames.

Ignition of hydrothermal flames depends on various parameters such as temperature, pressure, oxidant, oxidant temperature and flow rate, feed concentration and reactor configuration. Flames in SCW can be generated in two modes, namely premixed and diffusion-limited. The design of the equipment plays a major role for the generation and sustainability of hydrothermal flames. Organic solvents, including both primary and secondary alcohols, could be used as fuels for the reaction and air serves as the oxidant. Although, oxygen is an efficient oxidant, yet risks associated with its flammability in extremely high pressure and temperature environments of SCW precludes its wide usage. The ignition of hydrothermal flames was studied in a mobile SCW flame reactor designed by National Aeronautics and Space Administration (NASA) at Glenn Research Center, USA. The reactor is currently being used in the Department of Earth and Space Science and Engineering at York University, Canada in collaboration with NASA. The flame reactor has capabilities to investigate the impact of temperature, pressure, oxidant flow rate and temperature, and feed concentration on the ignition of hydrothermal flames. Initial research by NASA using this SCWO setup was focused on ignition of flames and thermal distribution studies in microgravity. Buoyant forces play a significant role in the temperature distribution profile making the SCW reactions distinct at ground level and zero gravity. The current research at York University deals with the evaluation of various parametric impacts on the temperature distribution and ignition of hydrothermal flames for studying chemical reactions such as combustion, gasification and pyrolysis. Optimization of the process parameters will be illustrated with regards to the ignition and stability studies of flames in SCW in order to implement them for treating biogenic waste materials.

janusz.kozinski@lassonde.yorku.ca

W1P049 CO-GENERATION OF HYDROGEN AND ELECTRICITY FROM SOLID FUELS IN A NOVEL CARBON FUEL CELL

David Johnson, S. Michael Stewart, Brandon Loong, Turgut M. Gür, Reginald E. Mitchell, Stanford University, United States

The work presented addresses three key aspects of the future energy landscape, namely advanced conversion of solid fuels (coal and biomass), hydrogen production, and CO₂ mitigation and capture. Our novel Steam-Carbon-Air Fuel cell (SCAFC) utilizes the chemical energy stored in carbonaceous fuels to electrochemically break down steam to produce hydrogen and electricity.

The electrochemical conversion of carbon into CO₂ enables higher conversion efficiencies than what is possible with conventional chemical conversion processes. A recent modeling study of the SCAFC from our group shows that the system is capable of reaching efficiencies above 78%. The fact that the oxidizers and the carbonaceous fuel are physically separated by an impermeable electrolyte provides two important benefits. First, unlike steam reforming, the hydrogen produced in the steam domain is carbon-free and hence does not contain trace amounts of CO, which acts as a poison for the catalyst in PEM fuel cells. Second, the nitrogen in the air stream never enters the carbon stream and hence a concentrated exhaust stream of CO₂ is produced. Consequently, the CO₂ stream can readily be sequestered and stored or sold as a marketable product.

The SCAFC combines a Steam-Carbon Fuel Cell (SCFC) with an Air-Carbon Fuel Cell (ACFC) in a coupled fuel cell in which a carbon bed is sandwiched between the two electrolytes creating a common anode chamber. On the cathode surface in the steam domain, steam is electrochemically split into hydrogen and oxygen ions. In a conventional steam electrolyzer this is a thermodynamically unfavorable process with an Open-Circuit Voltage (OCV) of 1.23 V. In the SCAFC, due to the presence of the carbon bed in the anode chamber, this becomes a thermodynamically favorable process with an OCV of 0.5 V at 900°C. In the anode chamber, the carbonaceous fuel undergoes dry gasification via the reverse Boudouard reaction, forming CO that gets oxidized at the anode surfaces. The CO₂ formed on the anode surfaces can then once again gasify the carbon forming a self-sustained "CO shuttle" mechanism. The SCFC is by itself endothermic and would require an external heat input. By integrating with the exothermic ACFC, the heat input is eliminated, and a flexibility of choosing between hydrogen or electricity production is gained, as the electricity of the ACFC can be used to overdrive the SCFC, boosting hydrogen production.

A finite element model of the SCAFC is further expanded and refined to take into account conductive, convective and radiative heat transfer effects along with electrochemistry at the electrodes, heterogeneous chemistry in the carbon

bed, and mass transport in the gas phase. The kinetic parameters needed to describe the half-cell reactions are derived experimentally as are the kinetic parameters that describe the heterogeneous reaction rates. The model is used to map out the operating space for hydrogen production, power output and efficiency.

Carbonaceous fuels, and in particular coal, contains sulfur, and sulfur containing species like H_2S and COS are known to rapidly degrade the performance of typical catalysts in SOFCs. Integrating *in situ* sulfur removal in our SCAFC concept would provide a significant breakthrough in clean coal utilization and change the landscape for clean coal power production as well as production of carbon-free hydrogen. Our lab has a dual approach to dealing with sulfur contaminants that involves identification of potent sulfur sorbents that would dramatically reduce the concentration of the sulfur containing species in the gas stream, and the development of sulfur-tolerant anode catalysts that have a high activity for CO oxidation in the presence of sulfur containing species. Progress in both these areas will be presented.

daviduj@stanford.edu

W1P050 A CERAMIC-MEMBRANE-BASED METHANE COMBUSTION REACTOR WITH TAILORED FUNCTION OF SIMULTANEOUS SEPARATION OF CARBON DIOXIDE FROM NITROGEN

Pingying Zeng, Kang Wang, Ryan Falkenstein-Smith, Jeongmin Ahn, Syracuse University, United States

There is increasing pressure for the industry to reduce carbon dioxide emissions from combustion processes, resulting in an increased interest in the development of methods to sequester and recycle the carbon dioxide from flue gases. One potential technology is a ceramic membrane catalytic reactor, which produces pure oxygen and simultaneously conducts oxy-fuel combustion; thus, CO_2 in the product stream could be successfully separated from the nitrogen in air. The ceramic membranes exploited here are oxygen semi-permeable, dense ceramic membranes based on the composite oxides with mixed oxygen ionic and electronic conductivity at high temperatures; they have received considerable attention during the past decade. This work investigates the performance of a perovskite-type $\text{SrSc}_{0.1}\text{Co}_{0.9}\text{O}_{3-\delta}$ (SSC) membrane reactor for the catalytic combustion of methane. For this purpose, the mixed ionic and electronic conducting SSC oxygen-permeable planar membrane was prepared by a dry-pressing technique, and the SSC powder catalyst was spray coated on the permeation side of the membrane. Then, the prepared SSC membrane with the catalyst was used to perform the catalytic combustion of methane. The oxygen permeability of the membrane reactor was studied. Also, the methane conversion rates and CO_2 selectivity at various test conditions were reported.

The CO_2 selectivity was calculated based on the GC analysis results of exhaust compositions. And it was found that both the increases of temperature and methane flow rate have a positive effect on the CO_2 selectivity and that the highest CO_2 selectivity obtained in this study is about 85%. Since we have demonstrated that the application of a disk-shaped SSC membrane as methane combustion reactor is feasible, future research should focus on the improvement of the performance by selecting more favorable catalysts and more favorable membrane configurations such as a hollow fiber membrane.

pizeng@syr.edu

W1P051 CONTROL OF BUOYANCY-DRIVEN INSTABILITY IN LIFTED FLAMES BY AC ELECTRIC FIELDS

Minkuk Kim¹, Suk-Ho Chung²

¹Korea Institute of Machinery and Materials, Korea ²University of King Abdullah Science & Technology, Saudi Arabia

The feasibility of adopting AC electric fields as a means to control flame instability has been tested in a coflow jet configuration. A propane fuel diluted by nitrogen was used to make a naturally oscillating lifted flame due to buoyancy-driven instability. And high voltage was supplied to a center nozzle and a ground mesh was installed on top of acrylic-cylinder such that electric field was applied to the flame. Variation in edge height with AC frequency was observed first for a fixed voltage. Four different modes (I-IV) were identified based on flame responses to the applied AC frequency. In the high frequency mode (I), the mean position of oscillating edge height is insensitive to the AC frequency, while the amplitude decreases as the AC frequency decreases. Consequently, a stationary lifted flame can be obtained in the range of frequency from 1100 to 670 Hz (mode II). When the frequency is less than mode II, flame oscillates again. The mean edge height continuously decreases in modes III and IV (symmetric and asymmetric flame, respectively), although the flame remains oscillating with the amplitude reasonably insensitive to the AC frequency. The mean edge height becomes even smaller than the minimum edge height of the naturally oscillating flame, marked with the vertical arrow. AC voltage also is effective on the stability of oscillating flame. A stability map was obtained in terms of AC voltage and frequency. In general, the boundaries of AC frequency for each mode are increasing with increasing AC voltage. The stationary lifted flame can be obtained in the voltage and frequency ranges of 400 - 700 V and 350 - 5000 Hz, respectively. Various flame behaviors during the transition period were investigated by using phase diagram analysis. Our results indicate that electric fields can be a viable option in controlling flame instability.

mkkim@kimm.re.kr

W1P052 PT-NANOPARTICLES: SYNTHESIS, CHARACTERIZATION AND TESTING IN A CATALYTIC FLOW REACTOR WITH APPLICATION TO MICROCOMBUSTORS

Smitesh Bakrania¹, Howard Pearlman², James Applegate¹, Dylan McNally¹, Marika Agnello¹, Brigitte Pastore¹

¹Rowan Univeristy, United States ²Advanced Cooling Technologies, Inc., United States

Microreactors with catalyst coatings have been explored to sustain combustion in sub-millimeter size channels for

micropower generation. In this work, we synthesized nano-sized platinum particles, characterized the particles using XRD, TEM and SEM and coated cordierite substrates with loosely supported Pt particles having different mass loadings. The catalyst was then tested in a bench-scale flow reactor with premixed methanol-air subject to a range of flow conditions. Room temperature light-off was observed followed by sustained combustion. The bulk temperature and stable gas species concentrations were measured as a function of mass loading and flow conditions. The effects of sintering were also qualitatively assessed by SEM imaging of the catalysts following sustained combustion. A brief description of the catalyst synthesis methodology, the particle characterization work, and the flow reactor results are presented below.

Platinum nanoparticle synthesis and characterization: Platinum (Pt) nanoparticles are synthesized via an ethylene glycol (99.8% anhydrous) based colloidal solution using hexachloroplatinic acid (H_2PtCl_6) as the precursor and PolyVinylPyrrolidone (PVP) as the stabilizer. Particles were cleaned using methanol, followed by deionized water while centrifuging between cleanings. X-ray diffraction analysis confirmed the presence of metallic platinum; Scherrer analysis indicated an average crystallite size $d_{\text{XRD}} = 8.9 \text{ nm}$.

Catalyst Preparation and Testing: The Pt particles were deposited on a cordierite substrate (900 cells/in having a channel width of $\sim 800 \mu\text{m}$ square channels) using a draw-coating method. The mass loading was controlled by the number of coated sides. A thin film of soft agglomerates formed on the cordierite substrate. The catalyst activity was then evaluated at different flow conditions. As noted, room temperature ignition was achieved and steady-operating temperatures in the range of $250\text{--}850^\circ\text{C}$ were measured. Multiple repeat tests were also conducted to ensure reproducibility of the results and assess any adverse effects due to restructuring/sintering of the catalyst (loss of available surface area). In addition, the effect of sintering on catalyst structure was assessed by SEM characterization of the cordierite surface following controlled heating at temperatures up to 1000°C . While SEM characterization studies on the post-reaction catalysts following repeat tests at reasonably high operating temperatures ($\sim 500^\circ\text{C}$ and higher) show evidence of sintering, the associated loss of surface area was found to have minimal effect on the overall catalyst activity, for the range of conditions tested.

Application: This work continues to explore fuel alternatives and microcombustor designs. Regarding application, the catalytic combustor was integrated with commercial thermoelectric generator modules to produce electrical power. The device has an overall efficiency (chemical energy to electricity) of 0.1%. More information on microcombustor performance will be presented.

bakrania@rowan.edu

W1P053 PLIF MEASUREMENT OF OH GENERATED WITH PULSED ARC DISCHARGE FOR RADICAL QUENCHING STUDY

Sui Wan, Yuji Suzuki, Weirong Lin, The University of Tokyo, Japan

Radical quenching by surface reaction has been proved to be responsible for the flame quenching near hot wall surface. However, experimental data for chemical quenching mechanisms are limited, partially because absorption spectra among various chemical species in flame are overlapped, which makes Laser-Induced Fluorescence (LIF) measurements difficult. In the present study, instead of using actual flame, we propose on-demand radical generation based on pulsed arc discharge in order to examine the wall chemical effect. As our first step, we employ electron-impact water dissociation in humid nitrogen to generate OH radical. In the present experimental setup, a pair of tungsten electrodes is fixed inside a quartz chamber, and a 5 kV pulsed voltage is applied between the electrodes to generate non-equilibrium plasma. A polished transparent quartz plate is used as a substrate, on which a 2-mm-thick black quartz (Nb-doped) layer is fusion-bonded on the backside for infra-red light heating. To examine the wall chemical effect of quartz and alumina surfaces, 100-nm-thick 2 mm-wide alumina strips are patterned onto the quartz surface. The distance from the electrode edge to the wall is 0.7 mm. It is found that, with a discharge current of 19.5 mA, the OH intensity generated with the arc discharge is as large as that in the actual methane-air flame, showing the capability of the pulsed discharge for supplying OH as a substitution of actual flames. The OH concentration increases with the wall temperature from 300°C to 700°C . Thus, the wall thermal effect plays a dominant role in near-wall OH field at low wall temperature. OH distributions 0.2 mm above the patterned alumina-quartz wall show that, at 500°C , the fluorescence intensity profiles on different wall materials overlap each other, indicating that the wall chemical effect is negligible. However, as the wall temperature increases, difference between the OH distributions over alumina and quartz surfaces increases, which is attributed to the wall chemical effect. The wall-normal OH molar fraction χ_{OH} normalized with its maximum value is compared with the simulation results for the present configuration. It is found that the experimental data of χ_{OH} on the alumina and quartz surfaces are in accordance with the simulation results for $S_0 = 0$ and 0.01, respectively. These results are consistent with our previous study using a methane-air flame, showing the validity of the proposed method for the wall chemical effect studies.

swan@mesl.t.u-tokyo.ac.jp

W1P054 SPECTROSCOPIC ANALYSIS OF THE RESPONSE OF A LAMINAR PREMIXED FLAME TO EXCITATION BY NANOSECOND GLOW DISCHARGES

Deanna Lacoste¹, Jonas Moeck²

¹Laboratoire EM2C, France ²TU Berlin, Germany

Recently, Nanosecond Repetitively Pulsed (NRP) discharges were successfully applied to turbulent premixed flame configurations to control combustion instabilities. Full suppression of instabilities was achieved but, due to strongly coupled plasma–flame interaction mechanisms, detailed understanding of this effect is still lacking. The strong action of the plasma on flame stability has been attributed to coupled thermal and chemical activation of the fluid. Understanding which of these effects is dominant for the response of the flame is necessary to further improve the capabilities of plasma-assisted combustion in view of technical applications. In order to distinguish the individual effects, another regime of NRP discharges is considered here: the glow regime. The NRP glow regime is known for its reduced thermal impact, while offering a high level of chemical activation. However, since the energy deposition of this plasma is low, a noticeable effect can only be achieved for laminar flames. Therefore, in the present study, the response of a laminar lean premixed flame to excitation by NRP glow discharges is investigated. Since in combustion instabilities, one key factor is the response of the flame to acoustically induced velocity fluctuations, the two types of forcing are compared. Finally, in order to provide additional understanding of the chemical activation by NRP glow discharges, a spectroscopic analysis is conducted. The results validate the low thermal effect of the discharges, with a maximum of 100 K gas heating in the plasma region. The spectroscopic analysis shows the production of excited nitrogen ($N_2(C)$), ions (N_2^+), and an increase in the density of OH^* . In contrast, the density of CH^* appears to be insensitive to activation by NRP glow discharges. A possible mechanism for the plasma action is a significant local increase of the burning velocity due to the chemical effect of NRP glow discharges.

deanna.lacoste@ecp.fr

W1P055 ION MEASUREMENTS IN PREMIXED METHANE-OXYGEN FLAMES

Awad Alqaity, Nadim Hourani, May Chahine, Mani Sarathy, Aamir Farooq
King Abdullah University of Science and Technology, Saudi Arabia

Ions are formed as a result of chemi-ionization processes in combustion systems. Flame is a weak plasma containing various ions in low concentrations. In the past decade, there has been an increased interest in studying flame ion chemistry due to the adverse environmental effects of combustion exhaust and the potential of using external electric fields to actively control combustion processes for reduced emissions and increased efficiency. Electric field assisted combustion has been shown to reduce emissions, improve combustion efficiency, and extend the operability of combustion devices. Nevertheless, the progress is restrained due to the limited understanding of the flame ionization processes and the lack of experimental data on the evolution and distribution of ionic species in the flame. In order to predict the effect of external electric fields on combustion plasma, the first step is to gain a good understanding of ion chemistry in flames by measuring flame ion concentration profiles.

In this work, a Molecular Beam Mass Spectrometer (MBMS) is utilized in conjunction with a Langmuir probe to measure ion concentration profiles in premixed methane-oxygen-argon burner stabilized flames, as a function of height above the burner. MBMS is a widely used technique for measuring species concentration profiles in premixed flames. Its high sensitivity and ability to differentiate ions from neutrals make this technique attractive for studying ion chemistry in flames. Herein, a modified Hiden HPR-60 MBMS system equipped with a triple filter quadrupole detector (EQP) is used. A commercially available water-cooled 6 cm diameter McKenna burner (Holthuis & Associates) was used to produce methane-oxygen flat flame with argon as the diluent gas. Lean, stoichiometric and rich flames at atmospheric pressure were used to study the dependence of ion chemistry on equivalence ratio of premixed flames. The relative ion concentration profiles were compared qualitatively with previous methane-oxygen studies and showed good agreement. Information on the total positive ion concentration obtained using the Langmuir probe will be combined with mass spectrometric measurements to convert the relative ion concentrations to an absolute scale. The above study is expected to improve the understating of ion chemistry and the data collected herein will serve as a benchmark for testing of numerical models for simulating flame ion chemistry.

awad.alqaity@kaust.edu.sa

W1P057 CHARACTERISTICS OF NON-PREMIXED OXYGEN ENRICHED FLAMES FROM A SWIRL BURNER WITH A RADIAL FUEL INJECTION

Toufik Boushaki, Nazim Merlo, Christian Chauveau, Iskender Gökalp, Stephanie de Persis, ICARE – CNRS, France

This work investigates the combustion characteristics of methane - oxygen enriched air turbulent non-premixed swirling flames. The burner configuration consists of two concentric tubes with a swirler placed in the annular part supplying the oxidant flow rate. The radial fuel injection mode is chosen to enhance the air-fuel mixing with the expectation that a partially premixed flame arises whilst the reactants are initially non-premixed. The idea of oxygen enrichment of the air is related to the augmentation of the CO_2 concentration in the flue gases to enable membrane capture of CO_2 . Stereo-Particle Image Velocimetry is used to analyse the flow fields. The measurements are performed for oxygen concentrations ranging from 21% to 30%, with swirl numbers from 0.8 to 1.4 and global equivalence ratios from 0.8 to 1. The results show that combustion noticeably affects the swirling motion and that azimuthal velocities rapidly decrease along the axial axis. Besides the recirculation mass flow ratio dramatically increases compared to non reactive cases. Increasing global equivalence ratios increase the recirculation mass flow ratio contrary to oxygen enrichment effects. Fuel is injected into the highest turbulence level regions where the local mixing is enhanced supporting the idea of a shift from a non-premixed flame towards a partially premixed one. The exhaust gas compositions are measured using gas analysers. It is observed that NO_x emissions decrease when the global equivalence ratio increases suggesting that CO_2 in the

recirculated burned gases could be responsible for NO_x destruction at relatively high oxygen enrichment rates. Globally, the results show that the developed and characterized novel burner configuration has a good potential to be used to stabilize non-premixed fuel and oxidant streams as partially premixed low emission flames with an increased concentration of CO_2 in the flue gases, by combining enhanced mixing and moderate oxygen enrichment of the air.

toufik.boushaki@cns-orleans.fr

W1P058 REALIZATION OF THE EFFECT OF SELF-DILUTION CHARACTERISTICS IN CONFINED FLAMES ON NO_x ABATEMENT

Kapuruge Don Kunkuma Amila Somarathne¹, Susumu Noda²

¹Tohoku University, Miyagi ²Toyohashi University of Technology, Japan

The present study describes a numerical evaluation for characterizing the effect of self-dilution in confined flames, in terms of the furnace geometry and the global equivalence ratio, on the NO_x emission properties. In confined flames, the recirculation vortex, which is generated between flame and the furnace wall, leads to self-dilution of the combustion mixture. Therefore, the enhancement of the self-dilution should lead to a peak temperature reduction in the furnace and consequently, considerable thermal NO_x abatement. The self-recirculation characteristics of a small cylindrical furnace configuration that has been proposed for placement in a large industrial furnace room has paved the way for combining the dilution and pre-heating phenomena. In the present study, the flame self-dilution is quantitatively evaluated, and the EINO_x characteristics of confined flames are demonstrated to exhibit a linear reduction with the increase in flame dilution. Hence, the increase in the dilution factor as a dominant parameter, which controls the characteristics of confined flames, is very important for NO_x abatement. In addition, an investigation of flame structures in confined flames in the mixture fraction domain verifies that the effect of self-dilution has a significant influence on maximum temperature reduction and thus NO_x abatement in the flame.

kunkuma@flame.ifs.tohoku.ac.jp

W1P059 INVESTIGATION OF WALL THERMAL CONDUCTIVITY EFFECTS ON COMBUSTION STABILITY IN MESO-SCALE TUBE COMBUSTORS WITH WIRE MESH

Fudhail Bin Abdul Munir, Naoyuki Hatakeda, Takehiko Seo, Masato Mikami, Yamaguchi University, Japan

In the last two decades, with the continued depletion of energy resources and the need for better power sources for small scale devices, researchers have become increasingly interested in meso and micro-scale combustion. The combustion stability of a meso-scale combustor depends on a few parameters. To improve the design of combustors, it is essential to fundamentally understand the determinant factors for the stability and efficiency of meso and micro-scale combustors. In this research, the effects of wall thermal conductivity on the flame characteristics and stability of meso-scale tube combustors with stainless steel wire mesh were numerically and experimentally examined. The main purpose of the numerical simulation is to provide basic understanding of how heat is conducted from the burned gas to the unburned gas region. The wall thermal conductivity surrounding the unburned gas region was varied in both numerical and experimental work. Cylindrical tubes with an inner diameter of 3.5 mm and a wall thickness of 0.7 mm were used. The wire mesh was located between the unburned and burned gas region of the combustor. In the experiment, the equivalence ratio and mixture flow velocity were varied and the effects in terms of flame stabilization limits were recorded. The wall temperatures of the combustors were also measured and the results are presented in the paper. Generally, the pattern of the wall surface temperature obtained from numerical calculation is consistent with the experimental results. Furthermore, the results obtained from the experiment show that the combustion stability can be significantly enhanced by optimizing the wall thermal conductivity in the unburned gas region.

fudhail@utem.edu.my

W1P060 INFLUENCE OF SIMULATED CONCENTRATED SOLAR RADIATION ON A LAMINAR SOOTY FLAME

Xue Dong, The University of Adelaide, Australia

The use of Concentrated Solar Radiation (CSR), though has the potential to be the dominant source of sustainable energy in the long term, remains significantly more expensive than many alternative energy sources. One approach to reduce the cost of solar thermal energy is to combine it with established technologies utilising fossil fuels. However, there is a need to study the potential thermodynamic synergies to quantify the benefit of this hybrid system. In this work, the influence on the soot distribution in a laminar diffusion flame, caused by the introduction of high-flux, broad-band radiation with a similar spectrum to the solar spectrum is reported. This investigation differs from a previous investigation, both in being broad-band as distinct from single-wavelength, and in irradiating the entire flame instead of only a small fraction. In the current experiment, a high flux solar simulator, comprising a 6kW Metal Halide Lamp, an elliptical reflector, a water-cooled secondary concentrator and tertiary concentrator was used to generate a radiant flux of 2.4 MW/m^2 peak and 1 MW/m^2 on average within a target of 55 mm diameter. Measurements of Soot Volume Fraction (SVF) were performed with and without the introduction of the simulated CSR, using Laser Induced Incandescence (LII), in a laminar ethylene non-premixed flame of 60 mm in height, similar to that used by Santoro et al. The introduction of CSR was found to cause a large change in SVF distribution within the flame, with the SFV increasing by approximately 40% along the flame central line beyond $\text{HAB}=10$ mm. In addition, the zone of inception was caused to move upstream

significantly. Furthermore, the radially integrated SVF at all flame heights is increased by 30 – 50% beyond HAB = 30 mm. The significant increase of soot formation by CSR indicates that, there is a strong heating effect, as well as potential photo-chemical effect of CSR on the laminar diffusion flame.

xue.dong@adelaide.edu.au

W1P061 JOINT INFLUENCE OF IGNITION ENERGY AND GAS DYNAMICS ON COMBUSTION IN A CONSTANT VOLUME COMBUSTION CHAMBER APPLIED TO AIR-BREATHING PROPULSION

Bastien Boust, Marc Bellenoue, Julien Sotton, PPRIME, France

Increasing the efficiency of aeronautical engines is a major concern in order to reduce their fuel consumption, pollutant emissions and environmental impact. For this purpose, alternative combustion modes are currently investigated such as constant volume combustion or detonation, thus leading to a potential gain in efficiency up to 20%. Compared to the conventional engine cycle based on isobaric combustion (Joule-Brayton cycle), the implementation of an isochoric combustion (Humphrey cycle) is a deep change that raises new concerns. To that extent, each of the successive phases of the cycle (intake, combustion, exhaust) deserve scientific investigations, especially concerning air-fuel mixing, ignition, flame propagation, heat losses and transient flow dynamics.

The present study addresses some specific aspects of constant volume combustion occurring during the operation of an original combustor based on rotary valves for intake and exhaust. The air-fuel mixture is prepared upstream of the combustion chamber, introduced through the intake valves and spark-ignited inside the combustion chamber. The cycle is operated at a rate of 40 Hz, which creates high instantaneous flow rates during intake and exhaust. The resulting internal flow field exhibits locally high velocity magnitudes and gradients, with a large spectrum of turbulent flow structures. In this study, the process of constant volume combustion is characterized using time-resolved diagnostics that quantify the thermodynamic properties of the cycle (dynamic pressure, transient heat flux), and the propagation of combustion (chemiluminescence, tomography, PIV). This characterization provides a comprehensive insight in the cycle dynamics as far as intake, ignition and flame propagation are concerned. However, the stabilization of the combustion cycle proves to be sensitive to the local conditions at ignition point, possibly leading to misfire or late combustion. In order to better understand this phenomenon, the spark energy and the ignition phasing have been varied. This study indicates that the successful operation of the combustor requires an increased spark energy or a delayed ignition, thus pointing out the crucial influence of the local flow field on ignition: advection velocity, turbulence intensity, or turbulence scales. Further analyses of the PIV measurements are currently being carried out to better understand the joint influence of ignition energy and gas dynamics on the ignition and combustion phases.

bastien.boust@ensma.fr

W1P062 STRUCTURE OF METHANE INVERSED DIFFUSION FLAMES WITH SIMULATED PRE-HEATED CO-FLOW COMBUSTION PRODUCTS

Zakaria Movahedi, Xisheng Zhao, Andrzej Sobiesiak, University of Windsor, Canada

Flameless oxidation is a mode of combustion which is characterized by the large extended reaction zone with no definitely visible flame and more uniform heat transfer to the load. Inside a furnace, the three-way process mixing of fuel, air jets and combustion products which have cooled down by heat transfer to the load creates the flameless oxidation regime. This prompted our previous studies of the structure of co-axial non-premixed diffusion flames with inversed flow arrangement of methane and air, surrounded by a co-flow of combustion products from a premixed flat flame. It was found that the temperature of co-flowing flat flame combustion products (around 1800K) is much too high to promote fuel reformation and setting-up the flameless oxidation. The objective of the study is to identify the operating conditions that could lead to fuel reformation and flameless oxidation. In this investigation the co-flow is that of simulated combustion products composed of 7.57% of CO, 4.27% of O₂ and 88.16% of N₂. In addition the temperature of the co-flowing combustion products can be varied to provide the suitable conditions for fuel reformation and subsequent flames oxidation. In experiments, the flame structure is determined by CH* chemiluminescence imaging and temperature profiles from thermocouple measurements. The CH* signal is imaged through a 10 nm bandpass optical filter centered at 430 nm (Andover Corp. 430FS10-50) with a 90mm macro lens (Tamron) onto an intensified CCD camera (Cooke Corp. DiCAM-Pro). Temperature measurements are obtained with the use of R type 0.003 inch thermocouples.

The numerical simulation is conducting with STAR-CCM+. The GRI-MECH 3.0 chemical kinetics mechanism has been used along with standard thermodynamics and mass, momentum and energy transport equations. Calculations for two different compositions of co-flowing combustion products have been performed; with the actual flat flame combustion products containing water vapor and the simulated combustion products without water vapor. Numerical simulation results from 2-D axisymmetric geometry conducted by STAR-CCM+ are compared with those from the experimental CH* imaging and temperature measurement.

movahedz@uwindsor.ca

W1P063 LASER IGNITION OF METHANE HYDRATES

Michela Vicariotto, University of California, United States

Methane hydrates, also known as clathrates, are solid compounds formed by water molecules enclosing gaseous

methane; they are naturally formed in arctic permafrost and marine sediments, where pressure and temperature create thermodynamically favorable conditions. Many studies have been carried out in the past to prevent the formation of clathrates in gas pipelines while, more recently, research started focusing also on the energy release during combustion of those methane hydrates.

Experiments of methane hydrates combustion at higher pressure than ambient have been completed using a glow igniter to start the process, but the physical igniter can disrupt the flame once the hydrate is burning. Laser induced ignition of such compounds at high pressures is an interesting alternative to conventional ignition sources due to its non-intrusive nature. Furthermore, changes in geometries of the samples could be easily managed thanks to the flexibility in positioning of the ignition location.

To investigate the possibility of igniting methane hydrates with a laser source, we first carried out some introductory analysis of air breakdown using a Q-switched 532 nm, 300mJ Nd:YAG laser, including a determination of the damage threshold of sapphire windows that will be used in the high pressure hydrate combustion experiments. Since the procedure of forming and growing hydrates samples is difficult and slow preliminary experiments were carried out using Sterno gel-fuel. The results show that ignition occurs with a single shot only if there is a relatively warm layer of gases around the sample. Both in the case of gel-fuels and methane hydrate, the sample needs to be heated, once a layer of ignitable gases is released ignition with a single pulse is possible. While in the case of a glow or flame igniter some dissociation of the hydrate occurs allowing the methane to react with the air, when using a laser single pulse it is necessary to have an ignitable mixture around the sample prior to ignition.

In this regard, the poster also shows the results of gas chromatography used to determine the stoichiometry of the layer of air/methane mixture around the hydrate. Gas samples are taken at different times while measuring the temperature of the hydrate surface and immediate surrounding to observe the relation between the release of methane and the temperature increase due to the warming of the clathrate in the ambient environment.

michela.vicariotto@gmail.com

W1P064 AMMONIA/AIR FLAMES IN A MICRO FLOW REACTOR WITH A CONTROLLED TEMPERATURE PROFILE

Hisashi Nakamura, Takuya Tezuka, Susumu Hasegawa, Kaoru Maruta, Tohoku University, Japan

Combustion and ignition characteristics of ammonia/air mixtures were investigated by a micro flow reactor with a controlled temperature profile. A quartz tube with the inner diameter of 2 mm was employed as a reactor channel and the wall-temperature profile from room temperature to 1300 K was formed by a hydrogen/air flat-flame burner. Figure 1 shows flame images for stoichiometric ammonia/air mixtures at various inlet mean flow velocities. Three kinds of flame responses were observed likewise the case of hydrocarbon fuels: normal flames in the high flow velocity regime; *Flames with Repetitive Extinction and Ignition* (FREI) in the moderate flow velocity regime and weak flames in the low flow velocity regime. Compared to flame responses for stoichiometric methane/air mixture, positions of normal flames and extinction points in FREI for the ammonia case are located in the higher temperature region than those of methane while the ignition properties, that is, positions of ignition in FREI and weak flames of the ammonia case is located in the similar temperature region to that of methane. The range of the flow velocity of FREI/weak flames for stoichiometric ammonia/air mixtures is narrower/wider than that for stoichiometric methane/air mixtures. Due to very low reactivity of ammonia, fundamental experimental data have not been obtained enough so far. The micro flow reactor was able to obtain combustion and ignition characteristics in the simple system.

Two representative flow velocities were selected for the comparison between computation and experiment; 40 cm/s for normal flames and 10 cm/s for weak flames. Four chemical kinetics were employed for the computation (GRI3, UCSD, Lindstedt and Tian). Only Lindstedt mechanism reproduced normal flames at 40 cm/s and all the mechanisms failed to reproduce weak flames at 10 cm/s.

Species measurement will be conducted and ammonia oxidation kinetics will be further validated using the experimental data in the future.

nakamura@edyn.ifs.tohoku.ac.jp

W1P065 OSCILLATION OF OPPOSED FLOW FLAMES WITHIN A MESOSCALE CHANNEL AT LOW STRAIN RATE CONDITIONS

Min Jung Lee, Korea Advanced Institute of Science and Technology, Korea

Recently, interests on combustion phenomena within narrow combustion spaces in terms of mesoscale combustion were increased with the development of practical small combustion systems or basic reactors. In the early study of mesoscale combustion, flame stabilization at low strain rate was an important issue. However, the use of diverse burner configurations hindered a clear understating of mesoscale combustion phenomena, and it was difficult to be directly compared with their results each other. Therefore, some basic configurations were necessary for the evaluation of characteristic length scales in previous reference database regarding mesoscale combustion phenomena. More recently, an opposed flow burner installed within a mesoscale channel was suggested as a basic configuration as shown in Fig. 1 and the flame stabilization characteristics were evaluated for non-premixed and partially premixed conditions. Especially, the stabilization characteristics of the Lower Strain Rate (LSR) were obtained, and these results could be compared with the micro-gravity experimental results.

In their results, the flame oscillation was observed when the strain rate was sufficiently low as shown in Fig. 2 and it

was considered as a main extinction phenomenon for the LSR condition. The structure of an oscillatory flame was divided into two regions corresponding to a flame core and a pair of oscillatory regions. Moreover, the oscillation frequency was changed by the strain rate and the equivalence ratios from both nozzle sides. The edge flame propagation and the burned gas dilution effect were considered as a driving force and a damping force, respectively. Though they could explain a basic mechanism regarding the flame oscillation and the frequency change, flame oscillation mechanism is still remained unclear. Therefore, in this study, the analytical model for the flame oscillation and the quantitative prediction of oscillation frequency would be introduced.

For this, two simple analytical theories were concerned. One is a function of 2-dimension mixture fraction and the other is a mixing layer of burned gas produced from the core region. The first was used to calculate the non-reactive flow which represents a flame location and a fuel concentration gradient determining edge flame propagation velocity at the outmost of the flame. The second was used to consider a dilution effect on the propagating edge flame. From this study, an advanced analytical model of the flame oscillation at LSR condition would be suggested.

limjer@kaist.ac.kr

W1P066 DEVELOPMENT AND COMBUSTION CHARACTERIZATION OF AN INDUSTRIAL SIZE FLOW BLURRING INJECTOR

Ajay K. Agrawal, Yonas Niguse, University of Alabama, United States

Flow-Blurring (FB) atomization, a recently discovered twin fluid atomization concept, has been reported as effective method for producing fine spray of liquids with wide range of viscosities. Recent experimental combustion investigations by our research group, using a burner of 7-kW capacity, and spray experiments using laser techniques have showed that FB injector's atomization capability is superior when compared to other similar techniques, such as air blast. Despite these favorable results, however, scalability of the injector has not been tested; hence its potential use for large capacity industry-scale systems is yet to be proved. The objective of this study is, therefore, to demonstrate scalability of the injector by conducting experiments on a scaled-up version of the injector with 60-kW capacity. The injector was investigated for combustion performance by operating it in a swirl stabilized dual fuel burner system, using diesel and vegetable oil (soybean oil) as fuels. Constant velocity criterion was used to scale dimensions of the new injector and cross sections of the dual fuel burner system, including the swirler. Results showed that the scaled-up injector's performance is comparable to the smaller scale system in terms of flame quality, emission levels and static stability. Photographic flame comparisons at different Air to Liquid Ratios (ALR) showed good flame quality characterized by complete blue color at the higher ALRs of above 2.8. Emission measurements also showed a general trend of lower CO and NO_x levels at higher ALRs, replicating the performance of the small scale injector. The injector preformed robustly with uncompromised stability for the range of firing rates above 40% of its capacity.

aagrawal@eng.ua.edu

W1P067 COMPARISON OF BIOMASS PULVERISED FUEL IGNITION BEHAVIOUR IN AIR AND OXYGEN/CARBON DIOXIDE MIXTURES USING A 20-L SPHERE APPARATUS

Ignacio Trabadela, Hannah Chalmers, Jon Gibbins, University of Edinburgh, United Kingdom

Results for ignition behaviour of pulverised biomass fuels in a 20 Litre (L) spherical combustion chamber are presented and discussed. Four types of biomass currently used in UK utility pulverised fuel boilers have been tested for ignition behaviour in air, so at 21%v/v O₂, and also, to assess relative performance under oxy-fuel combustion conditions, in a 21%v/v O₂, balance carbon dioxide (CO₂) balance mixture (21Oxy) and a 25%v/v O₂ mixture (25Oxy) respectively. Peak pressures (P_{max}) during constant volume ignition and combustion with 2500J and 5000J igniters were measured and recorded. The pressure ratios (P/R), defined as the ratio of the maximum pressure (P_{max}) to the pressure at the start of ignition (P₀) for each test are reported. A P/R above a threshold of 2.5 is taken as an indication of positive ignition. All four biomass types ignited nearly as readily in 25Oxy as in air at a range of fuel concentrations. Ignition was much less readily achieved in 21Oxy for all fuel concentrations and peak pressures were also generally lower. Results were more erratic with 2500J igniters compared to 5000J igniters, suggesting a relatively stronger ignition source is required with these biomass samples than with pulverised coals previously tested; this is tentatively attributed to larger particle sizes and higher moisture contents. Implications for pulverised fuel oxy-fuel combustion applications are: 1) a Primary Recycle (PR) stream with 21%v/v O₂ would give improved Pulverised Fuel (PF) milling safety when compared to air firing but reduced ignitability in the burners; 2) a 25%v/v O₂ primary stream would approach air behaviour in mills and burners. These preliminary results suggest that approximately 25%v/v O₂ may give air-like performance in oxy-fuel pulverised coal plants using oxy-biomass.

i.trabadela@ed.ac.uk

W1P068 AN EXPERIMENTAL STUDY ON LOW NO_x PETROLEUM COKES COMBUSTION SYSTEM

Sewon Kim, Changyeop Lee, Minjun Kwon, Korea Institute of Industrial Technology, Korea

This work is to study the emission characteristics of noble petroleum cokes burner and the application of reburn technology in order to reduce NO_x emissions. In this study, petroleum cokes are used as a fuel to the industrial boiler. Petroleum cokes have high heat value, but their ignitability is very low because of their high fixed carbon content.

In this study, both petroleum cokes and light oil are used as fuels at a ratio of 9 to 1. The burner is designed as an air-staged type, and the oil nozzle is installed at the center of the burner. The 1st annular air nozzle is installed around the oil nozzle. This 1st air flow solves the high temperature problem at the flame front region. Petroleum cokes are then fed using carrier air in the second annulus. The 2nd and 3rd air nozzles are installed outside of the petroleum cokes nozzle comprising third and fourth annulus, and swirlers are installed at the 2nd and 3rd air nozzle. So the degree of turbulence is increased.

Reburn technology is applied to reduce the NO_x in this experimental system. Light oil is used as a reburn fuel, and injected at fuel rich zone in the furnace, and they are injected at three different positions in the furnace. The burner is operated at maximum 1 MW.

As mentioned above, the burner is operated in mixed firing condition using petroleum cokes and light oil at a ratio of 9 to 1 respectively. The results show that petroleum cokes and light oil combustion is quite stable. In addition, the burner operated at very high fuel rich conditions to minimize fuel NO_x. The low NO_x emission characteristics of this combustion system are experimentally investigated, and it is shown that very low NO_x concentrations emissions are achieved in this system.

swkim@kitech.re.kr

W1P069 BIODIESEL FUEL REFORMING BY OZONE-RICH AIR AND NUMERICAL SIMULATION OF COMBUSTION PROCESSES

Takaaki Morimune, Shonan Institute of Technology, Japan

We experimentally evaluate a performance and exhaust emissions of a single-cylinder, four stroke direct-injection type diesel engine with no modifications operating on BDF (Biodiesel Fuel made from rice oil) and diesel blending reformed by ozone-rich air generated by corona discharge ozonizer. The effects of ozone on the exhaust emissions such as NO_x, CO, THC, smoke and pressure indicator diagram in cylinder are compared with the case of base oil. It is expected that the flammable ozonide is generated in double bond of fatty acid contained in BDF by fuel reforming. Also discussed are the ozone suitable content within the bio-fuel, as well as practical use for ozone treated process of bio-fuel.

On the other hand, combustion simulation of DI diesel engine fueled by BDF, gas oil and diesel blending reformed by ozone is presented using Wiebe combustion model. Ignition delay prediction is based on the work of Arai et al (JSME,1984) and is calculated by using in-cylinder temperature, pressure at the start of injection. Eichelberg's heat transfer model is employed in cylinder wall. The Wiebe parameters for premixed, diffusive and post combustion duration are determined by curve fitting technique with measured in-cylinder pressure. Cylinder pressure at each crank angle is computed by using Runge-Kutta method in ordinary differential equations. Then the engine parameters such as heat release rate and indicated work are calculated.

We found that (1) the NO_x, CO, THC concentrations and smoke emissions of ozone-treated BDF are lower than base fuel in almost all load range, (2) ignition delay of ozone-treated BDF is shortened compared with the case of base fuel especially in the low load condition, (3) ozone-treated B50 and Blend50 are effective for combustion, while the effects of ozone on gas oil cannot be observed, (4) triple Wiebe thermodynamic modeling can predict engine performances fueled with gas oil, BDF and diesel blending.

morimune@mech.shonan-it.ac.jp

W1P070 PARTICLES EMISSION FROM PASSENGER CAR ENGINE USING COMMERCIAL DIESEL AND FISCHER-TROPSCH FUELS

Azhar Malik, Norwegian University of Science and Technology, Norway

The use of biofuels in commercially available engines is subject to uncertainties regarding performance, emissions and durability despite their potential to net reduction of CO₂. Differences in fuel characteristics complicate the use of biofuel in modern IC engines. Further insight of combustion process and optimization of engine performance in relation to gaseous and particles emission is therefore needed.

Experimental tests have been carried out on an engine from small passenger car at idle and part load conditions. Gaseous and particle emissions were monitored in a series of tests. In most of the cases Diesel Oxidation Catalyst (DOC) was also installed in the absence of particle filter to study the oxidation capacity with use of different fuels. Test with FT fuel (biomass origin) exhibited almost no change of NO_x at all tested loads, although the reduction in CO and HC was visible. It can be suggested that other strategies such as EGR and injection timing may prove more effective. Particles emission was measured by using the Scanning Mobility Particle Sizer (SMPS) consisting of a Differential Mobility Analyzer (DMA) and a Condensation Particle Counter (CPC). Due to very high concentration of particles from cylinder chamber and variation of exit temperature, the exhaust was diluted with a preheated-air mixed at similar temperatures. The dilution was employed between 5 to 20 times depending on the engine run conditions. Particle emissions at idle conditions were also compared for FT fuel from biomass and commercially available FT fuel (coal origin). It is found that there is no difference of concentration and mean size of particles in this case, with the exception of nucleated particle (10-20nm) present in commercial FT exhaust. The latter represented the particles generated due to additives present in commercial FT fuel. In the case of diesel at idle conditions, particles were dominated by relatively larger size (45nm). At low and medium loads (40-80Nm @1500rpm and 80Nm @2500rpm), the generated particles size distribution ranged between 80-100nm with concentration 1-3e7 particles/cc. The size and concentration of particles distribution was greatly affected by the extent of dilution and mixing temperature.

The investigation of particles emitted from IC engines using biofuels is ongoing and will be further developed by applying kinetic models and available mechanisms.

azhar.malik@ntnu.no

W1P071 A COMPUTATIONAL INVESTIGATION OF THE RELATIONSHIP BETWEEN FLAME LIFT-OFF HEIGHT AND SOOT CONCENTRATION IN DIESEL JETS

May Yen, Vinicio Magi, John Abraham, Purdue University, United States

In this work, computations of reacting diesel jets, including soot and NO, are carried out for a wide range of conditions by employing a RANS model in which an Unsteady Flamelet Progress Variable (UFPV) submodel is employed to represent turbulence/chemistry interactions. As reported in prior work, the UFPV model predicts the ignition delay and flame lift-off height within about 25% (majority of the cases are within 10%) of reported measurements (www.sandia.gov/ecn/). The flame is found to stabilize at the location where the ignition scalar dissipation rate is equal to the local scalar dissipation rate at the stoichiometric mixture fraction. It has been suggested that larger lift-off height enables greater fuel/air mixing upstream of the lift-off height which, in turn, leads to reduced formation rates of soot. In this work, we assess the capability of the model to predict this relationship.

A soot model which includes a detailed kinetic mechanism that accounts for nucleation of soot precursors and surface growth via a hydrogen abstraction and carbon addition mechanism, and soot PAH condensation, coagulation, and oxidation is used, and NO is modeled using the kinetics from a sub-mechanism of GRI-Mech 3.0. Tracer particles are used to track the residence time of the injected mass in the jet. For the soot and NO species, this residence time is used to track the progress of reaction. The computed conditions reflect changes in injection pressure, chamber temperature, oxygen concentration, and density, and orifice diameter. Note that the cases selected are identical to those which were modeled in the earlier study of Bajaj et. al. Measured soot volume fractions are available for some of the cases. Computed and measured soot volume fractions differ by less than one order of magnitude across the range of conditions considered. In some of the cases, the agreement is within a factor of two. Taking all the cases together, the soot concentration normalized with mass injected is found to correlate with the lift-off height normalized for effects of increasing orifice diameter and increasing ambient density. Analysis of the entrained mass upstream of the lift-off height confirms that this correlation arises from the variation in the entrained mass normalized by the mass injected.

While the quantitative trends in the measured distribution of soot in the jets, e.g. correlation with oxygen concentration and ambient density, are preserved by the computed results, the computed soot distribution is spatially concentrated upstream of the measured results. To provide further insight into this discrepancy, computed results in a steady lifted ethylene jet under atmospheric conditions were compared with measured results. A steady flamelet progress variable model was employed. The soot distribution is again found to be upstream of the measured distribution. Interestingly, this is consistent with the findings in a prior work using a somewhat different kinetic model for soot. This suggests a gap in our understanding of soot kinetics or in the modeling of the turbulence/chemistry interactions and is the subject of our continuing work.

myen@purdue.edu

W1P072 EXPERIMENTS AND COMPUTATIONAL MODELING OF NATURAL GAS/DIESEL DUAL FUEL COMBUSTION WITH EXPLORATION OF UNCONTROLLED COMBUSTION RATES

Andrew Hockett¹, Anthony Marchese¹, Greg Hampson², Jason Barta², Marc Baumgardner¹, Nolan Polley²

¹Colorado State University, United States ²Woodward Inc, United States

Natural gas substitution into diesel engines has the potential to provide cleaner combustion than conventional diesel, while retaining the high efficiencies associated with the diesel engine. Moreover, with natural gas being less expensive than diesel fuel, there is an economic motivation to maximize the substitution percentage of natural gas. However, the substitution percentage is often limited by uncontrolled fast combustion or engine knock. To increase natural gas substitution percentage and develop robust control strategies for dual fuel engines, a greater understanding of the in-cylinder dual fuel combustion process is needed. This poster presents the results of a three dimensional computational model for natural gas/diesel dual fuel combustion using the CONVERGE™ commercial code, which includes spray breakup physics and a new chemical kinetic mechanism. The spray model has been validated against experimental data from the Engine Combustion Network. The chemical kinetic mechanism was reduced from the a recent detailed natural gas mechanism of Curran et. al. (methane through pentane) combined with the 88 species skeletal heptane mechanism of Yoo et. al. using the direct relation graph method. The final 86 species reduced mechanism was compared against fully detailed mechanisms for natural gas and heptane using constant volume ignition delay and adiabatic HCCI simulations. The dual fuel engine simulations were compared against experimental data acquired from a GM 1.9 liter turbocharged 4-cylinder common rail diesel engine, which was modified to accommodate port injection of natural gas. Experiments were conducted over a range of diesel injection timing and natural gas to diesel mass ratios. The results show that the model accurately predicts the start of combustion timing, pressure rise rate, peak pressure, heat release rate shape, and combustion duration. The model was then used to extrapolate results at conditions of uncontrolled combustion by using higher substitution rates of natural gas, a more reactive mixture using propane addition, and higher intake temperature. These additional results indicate the onset of uncontrolled fast combustion towards the end of the combustion duration. This behavior can be identified in pockets of natural gas between premixed propagating flames from adjacent diesel sprays

and in the natural gas between the propagating flames and the walls of the piston bowl.

andrew.hockett@gmail.com

W1P073 NUMERICAL STUDY ON EFFECTS AND DESIGNING LIMITATIONS OF VALVE TIMING IN THE DUAL FUEL ENGINE THAT IS MODIFIED FROM DIESEL ENGINE

Jungkeun Cho, Sangjun Park, Jungsoo Park, Soonho Song, Yonsei University, Korea

Recently a growing interest in the environmental problems along with a number of regulations are requiring improvements in many sectors of power plant fields. Among those sectors, the thermal power plants in the islands that mainly use diesel engines also should be improved in environmental issues.

Many researchers have provided several solutions, and one of them is the dual fuel engine which uses diesel and natural gas. In order to actualize this solution, converting the existing diesel engine to dual fuel engine is presented as a practical method. In this case, a number of detailed designs of the various elements, such as valve timing, should be modified to convert diesel engine to dual fuel engine. However, there are not enough researches on these fields. Thus, in this study, the research on the dual fuel engine that is based on diesel engine will be conducted by changing the valve timing and 1D commercial engine simulation program (GT-Power) will be used.

The object of this study is to define effects of the valve timing in dual fuel engine that is converted from diesel engine and define limitations on design according to the effects. Building and validating the simulation model of the existing diesel engine will be the first step of this study. Modifying the diesel engine model to dual fuel engine model will be the next step. Using the modified model, the effects and the limitations on design will be discussed on this study with the results of changes in cylinder pressure, performance of the engine, volumetric efficiency and etc in accordance with the change of valve timing. Especially, the valve timing will be adjusted to change the valve overlap. The valve overlap has close connection with combustion in internal combustion engine, because an increase of cylinder pressure and a decrease of volumetric efficiency can be occurred by shortening valve overlap region which can affect the whole engine performance.

jkcho2000@yonsei.ac.kr

W1P074 TOWARDS A BETTER UNDERSTANDING OF HOW POST-INJECTIONS AFFECT SOOT OXIDATION USING LASER DIAGNOSTICS IN AN OPTICAL DIESEL ENGINE

Jacqueline O'Connor¹, Mark Musculus²

¹The Pennsylvania State University, United States ²Sandia National Laboratories, United States

While modern heavy-duty diesel engines typically use after treatment systems to meet pollution emissions targets for soot, in-cylinder soot reduction techniques remain important to decrease the after treatment burden as regulatory requirements become increasingly stringent. In particular, post-injections—short, close-coupled fuel injections after the main fuel delivery – have been shown to decrease engine-out soot emissions in a variety of engine architectures and over a range of operating conditions. Although many studies show that post injections can be beneficial for soot reduction, there is very little direct evidence of how post injections decrease soot. In this study, we use multiple laser/optical imaging diagnostics to probe the interaction between the post injection and the soot from the main injection in a heavy-duty diesel optical engine. Images of high-speed Natural Soot Luminescence (soot-NL) and Planar Laser-Induced Incandescence of soot (soot-PLII) show that the post injection directly interacts with the main-injection soot, with significant and repeatable differences in the structure of the main-injection soot during the interaction event. Later in the cycle, the soot from the main injection is not visible throughout the depth of the combustion chamber, providing compelling evidence that it is greatly decreased as a result of the interaction with the post injection, consistent with exhaust soot measurements. Simultaneous soot-PLII and Planar Laser Induced Fluorescence of OH (OH-PLIF) imaging show that during the early stages of the post injection, the post jet has a similar structure to the main injection: ignition near the injector orifice followed by a jet with a core of soot surrounded by a diffusion flame. During this initial period, significant OH-PLIF signal is measured in the main-injection mixture, indicating that oxidation of both fuel, and likely soot, is occurring as a result of OH produced by the post injection and transported into the residual main-injection mixture and products. During the remainder of the interaction of the post jet with the main-injection soot, significant OH-PLIF signal remains in the interaction region and continues later into the cycle compared to a the main injection only. We will discuss this ongoing work and possible mechanisms by which post injections are likely oxidizing soot.

jxo22@engr.psu.edu

W1P075 A NUMERICAL STUDY ON PREDICTION OF THE PERFORMANCE AND NO_x EMISSIONS IN A LIGHT-DUTY DIESEL ENGINE WITH SYNGAS ADDITION

Sangjun Park, Jungsoo Park, Soonho Song, Kwang Min Chun, Yonsei University, Korea

Facing the restricted emission regulations, emission reduction technologies have become a main issue for the diesel engine system. Following those research trends, clean combustion with various fuel compositions, such as dual-fuel, has been grown as the future technology considering engine performances and emission characteristics.

SYNGAS (SYNthesis Gas) which consists of hydrogen and carbon monoxide is used as a fuel additive on internal combustion engines. Most of previous researches have introduced the effects of SYNGAS addition on engine performance

and emission using engine bench test fueling with conventional fossil fuel. However, it is difficult to control the various engine parameters because there are complex interactions between each parameter. Therefore, numerical analysis could be more effective method to handle wide ranges of parameters reducing time and cost problems.

The goal of this study is to construct the 1-dimensional engine model and to predict the fundamental effects of SYNGAS addition on diesel engine. The engine model is constructed by commercial engine analysis tool, GT-POWER. It can evaluate the performance and NO_x emission of diesel engine without SYNGAS and predict effects of SYNGAS addition on combustion and emission describing lean operation. After conducting parametric study, performance compensation has to be performed under various conditions. In our future work, optimized results will be suggested by controlling the engine parameters.

psjrukka@yonsei.ac.kr

W1P076 CHARACTERIZATION OF GASEOUS AND PARTICULATE EMISSIONS FROM THE COMBUSTION OF CELLULOSIC BIOMASS BASED OXYGENATED COMPONENTS IN A COMPRESSION IGNITION ENGINE

Tim Vaughn¹, Aaron Drenth¹, Arunachalam Lakshminarayanan¹, Daniel Olsen¹, Matthew Ratcliff², Robert McCormick², Anthony John Marchese¹

¹Colorado State University, United States ²National Renewable Energy Laboratory, United States

Recent studies suggest that by the year 2030 the U.S. will be capable of annually producing 1.3 billion tons of sustainable forest and agricultural waste as well as perennial crops that can be processed into biofuel. This vast quantity of biomass can potentially yield up to 45 billion gallons/year of liquid transportation fuels, which is far greater than that available from conversion of vegetable oil, animal fat or via fermentation of starch-derived sugars. However, processes such as fast pyrolysis of whole biomass or base-catalyzed depolymerization of the lignin fraction produce complex mixtures of oxygenated compounds including acids, phenolics, furans, aryl ethers, and carbonyl compounds that must be upgraded to be suitable for blending with petroleum and processing in a refinery. Complete removal of these oxygenated compounds is exceedingly energy intensive and it is likely that upgraded pyrolysis oils will contain up to 2% oxygen content to be economically viable. The purpose of this study was to evaluate the effect of the presence of oxygenated chemical components indicative of those present in upgraded pyrolysis oil on diesel engine performance and emissions. Engine testing was performed by blending 10 different oxygenated components with certification ULSD diesel fuel and quantifying the performance and emissions from the combustion of these fuels in a 4-cylinder, turbocharged, 4.5 L John Deere PowerTech Plus common rail, direct injection diesel engine that meets Tier 3 emissions specifications. The properties of the oxygenated fuel components were fully characterized in accordance with ASTM diesel fuel standards. Gaseous emissions measurements included CO, CO₂, NO, NO₂, and total hydrocarbons. Particulate measurements included total PM mass emissions.

t.vaughn@colostate.edu

W1P077 RECESSION OF SECOND-STAGE IGNITION AFTER END-OF-INJECTION IN DIESEL-LIKE SPRAYS

Benjamin Knox, Caroline Genzale, Georgia Institute of Technology, United States

Significant unburned hydrocarbon emissions under low-temperature operating conditions have recently been linked to the end-of-injection transient in diesel injectors. Excessive unburned hydrocarbon emissions undermine the benefits that low-temperature strategies can provide, namely very low soot and NO_x emissions. After end-of-injection, a lifted flame is observed to remain relatively far downstream of the injector leaving a large region of unburned fuel-air mixture upstream. Failure of the lifted flame to propagate back towards the injector and thus consume the unburned fuel-air mixture has been suggested to be the consequence of locally enhanced entrainment, termed an “entrainment wave”, following the end-of-injection transient. The entrainment wave produces very lean mixtures upstream of the lifted flame that are incapable of supporting second-stage ignition. Our recent modeling efforts have shown that the entrainment wave magnitude can be controlled by modifying the end-of-injection transient. For example, a longer end-of-injection transient duration will result in a lower entrainment wave magnitude and a reduction of over-lean mixtures upstream of the lifted flame that allows for recession of second-stage ignition and reduction of unburned hydrocarbons.

To complement our modeling efforts, we have developed a novel experimental method for rapid control of the end-of-injection transient through pressure modulation. The end-of-injection transient can be selected to last anywhere from a typical duration of approximately 100 microseconds to a very long duration of 2 milliseconds. Rapid control of the pressure applied to the injector inlet, while keeping the injector energized and thus the nozzle orifices open, allows the fuel injection rate during end-of-injection to be modified. Quantification of the modified fuel injection rate is obtained with a commonly used impingement technique that is designed to measure the rate of momentum of the spray.

Once the modified fuel injection rates during end-of-injection have been measured, global spray mixing parameters, i.e. vapor penetration and spreading angle, will be measured in a nominally-quiescent high-temperature/pressure optically-accessible chamber using high-speed Schlieren imaging to characterize the affected fuel-air mixing fields. Validation of our model-predicted global spray mixing parameters to those measured in the experiment will thus enable more information to be extracted about how the mixing field is affected by the end-of-injection transient duration. Then, the experimental temporal and spatial characteristics of low and high-temperature combustion will be found using a combination of high-speed natural luminosity and chemiluminescence imaging measurements. By performing these measurements, we hope to validate the observation of model-predicted second-stage ignition recession with longer end-of-

injection transient durations.

By complementing our experimental efforts with a model, we intend on providing a physical link between the end-of-injection transient duration and unburned hydrocarbon emissions. Information obtained from this work may then be used to inform the combustion community on the optimized end-of-injection transient duration for the reduction of unburned hydrocarbons.

bknex3@gatech.edu

W1P078 SOOT LUMINOSITY AND LASER-INDUCED INCANDESCENCE OF DIESEL SPRAY COMBUSTION: CHARACTERISTICS AND CORRELATION ANALYSIS

Seong-Young Lee¹, Anqi Zhang¹, Jeffrey Naber¹, Luigi Allocca², Alessandro Montanaro²

¹Michigan Technological University, United States ²Istituto Motor-CNR, Italy

Understanding of soot formation and oxidation within the transient diesel spray flame with laser-based diagnostics (such as Laser-Induced Incandescence, LII) is significantly limited due to its low-frequency and high-cost operation. On the other hand, thanks to the advanced high-speed camera technology, visualization of broadband soot luminosity of diesel spray combustion with fine temporal resolution is readily realized. Both signals are believed to be originated from the existence of soot, while the LII shows planar soot field and high-speed imaging provides volume integrated soot luminosity.

In the current work, diesel spray test was performed using ULSD #2 fuel of different injection pressures spraying into ambient density of 25.4 kg/m³ under the ambient temperature of 900 K with 15% O₂ environment. Instantaneous LII signal and high-speed series of soot luminosity have been obtained from the same spray combustion event for each test run. Characteristics of soot structures resulted from both techniques are discussed and analyzed.

A novel, comprehensive IXT contour plot was introduced to illustrate both temporal and spatial information of soot field intensity in spray combustion. The horizontal axis of the contour indicates the time scale after the start of injection and vertical axis indicating the axial location from injector tip. The colored contour demonstrates the radial integrated soot luminosity. Plenty of information including soot field movement, stabilization and distribution can be extracted. Correlation analysis was performed on both 2D and 3D basis. Image processing techniques such as three-point Abel inversion and volumetric integration were adopted to convert the images to the same format. A weak image correlation was recognized for the two imaging techniques. It was found that the presence of turbulence, acquisition wavelength and soot temperature distribution can affect the correlation results.

sylee@mtu.edu

W1P079 EFFICIENT IMPLEMENTATION OF DETAILED SOOT MODELS IN INTERNAL COMBUSTION ENGINE SIMULATIONS

Zhaoyu Luo¹, Mandhapati P. Raju¹, Tom Malewicki¹, Peter Kelly Senecal¹, Harry Lehtiniemi², Cathleen Perlman², Fabian Mauß³, Tushar Shethaji³, Yuanlong Li³

¹ Convergent Science, Inc, United States ² Loge AB, Sweden ³ Caterpillar, Inc., United States

High-fidelity soot models can reveal detailed soot information in flame simulations, but the complexity of the models renders them computationally impractical for three dimensional engine simulations with detailed chemistry. In the present study, a detailed soot model, where the soot Particle Size Distribution Function (PSDF) is treated using a sectional method was implemented into CONVERGE CFD solver. The detailed soot model is based on the sectional method. It considers detailed PAH formation kinetics for particle inception. During the oxidation of the fuel, i.e., *n*-heptane, aromatic species are formed in the gas phase and grow to large PAHs. Species with more than four rings can combine and inception soot particles. They can further condense on the soot particle surface which will contribute to the soot growth process. All processes affecting soot growth, oxidation, and dynamics of the particle size distribution function are considered: surface growth by the simple hydrogen abstraction acetylene addition mechanism HACA with separate ring closure, oxidation by O₂ and OH, condensation of PAH onto the soot particle surface, and coagulation between soot particles of different size classes. All of these processes can be calculated from the Smoluchowski equation. The use of detailed soot models requires higher order PAH chemistry in the chemical reaction mechanism, thereby increasing the size of the mechanism. Thus, there is a need for acceleration of chemistry calculations. Three different acceleration strategies have been applied in the solver to speed up the calculations. The first strategy is to use adaptive zoning. It groups the combustion cells with similar physical and thermodynamic properties into zones in each discrete time step. As such, the chemistry solver will solve the temperature and species concentrations for each zone instead of invoking chemistry at each and every cell. Since the detailed soot sectional model is closely related to the temperature and gas phase mixture in the system, the same two-dimensional zoning strategy, in which the zoning is done based on two variables of the temperature and the gas phase equivalence ratio of the cells, was applied to each soot section. For each zone, the average temperature, pressure and the gas composition are determined to specify the thermodynamic state of the mixture in that zone. The second strategy is to construct the Jacobian matrix based on analytically computed derivatives. A hybrid approach is used in the present study to assemble the Jacobian matrix. While the Jacobian entries corresponding to the gas phase chemistry are evaluated analytically, the entries corresponding to the soot variables are evaluated using numerical finite difference approach. Since there are only a limited number of species that are coupled with the soot model, the gas chemistry and soot phase are assumed to be decoupled for the Jacobian evaluation. This assumption can increase the sparsity of the Jacobian matrix

which can help speed up the calculations and be taken advantage by the iterative solver. The third strategy is to solve the linear system of chemical reactions using the GMRES based iterative solver with a suitable pre-conditioner. An incomplete LU (ILU) factorization is used as a pre-conditioner for the Jacobian matrix. The proposed acceleration strategies were tested in a 0-D homogenous system and a 3-D diesel engine sector. A skeletal mechanism for n-heptane with comprehensive PAH reaction path, which consists of 121 species and 593 reactions, was employed in the present study. Cyclopenta[c,d]pyrene (A4R5) was used as soot precursor for the gas phase chemistry. The detailed soot model was fully coupled with the gas phase chemistry and solved by the chemistry solver SAGE of CONVERGE. It was observed that the computational time of the simulations can be reduced by a factor of more than 6 while very good agreement in important soot parameters such as soot number density and mass fraction was retained in the simulations when the proposed acceleration strategy was applied, which makes it possible to apply the detailed soot model in practical engine simulations. The detailed soot model was further validated with shock-tube speciation and ECN spray bomb experiments, and it was found that the simulations can well predict the experiments.

zhaoyu.luo@convergecf.com

W1P080 INVESTIGATING PHYSICAL CONDENSATION PROCESSES IN ADVANCED LOW TEMPERATURE COMBUSTION ENGINES

Lu Qiu¹, Rolf D. Reitz²

¹Engine Research Center, United States ²University of Wisconsin, United States

Advanced low temperature combustion strategies, such as Reactivity Controlled Compression Ignition (RCCI), have been developed to reduce undesired emissions and increase engine thermal efficiency. Recent experimental work has further shown that more than 90% of the particulate matter from RCCI combustion consists of organic species, which is drastically different from the situation in conventional diesel combustion, favoring elemental carbon formation. This distinctive character is believed to be related to condensation processes of large hydrocarbon species that cannot stably exist in the gas phase. Rather, at certain conditions the heavy gaseous species can condense, which becomes responsible for the organic fraction in the particulate matter. In this work, condensation of gaseous fuels is investigated in a low temperature combustion engine fueled with double direct-injected diesel and premixed gasoline. Possible condensation is predicted by a recently developed phase equilibrium solver, which performs phase stability tests considering real gas effects. The simulations show that indeed fuel condensation events are predicted to occur. The first two condensation events are found within the direct-injected sprays where the evaporative cooling reduces the local temperature until phase separation occurs. A third condensation event is predicted to occur in the crevice-wall region during the late stages of the expansion stroke, where the continuous expansion sends the local fluid into the two-phase region again. Condensation was not found to greatly affect the average cylinder pressure or temperature mainly because, before the main combustion event, the condensed phase is converted back to the vapor phase due to compression and/or first stage heat release. However, condensed fuel is seen to exist and affect the emission predictions, including engine-out particulate matter and unburned hydrocarbons.

lqiu4@wisc.edu

W1P081 MECHANISMS OF PRESSURE WAVE GENERATIONS IN END-GAS AUTOIGNITION: COMPRESSIBLE FLOW SIMULATIONS WITH DETAILED CHEMISTRY

Hiroshi Terashima¹, Mitsuo Koshi²

¹University of Tokyo, Japan ²Yokohama National University, Japan

Knocking is a severe pressure oscillation caused by flame propagation and end-gas autoignition in spark-assisted engines. The risk of severe knocking prevents increasing compression ratios and thus higher operation efficiency. In the present study, knockings of n-butane and n-heptane premixed gases in a one-dimensional space, i.e., flame propagation, end-gas autoignition, and pressure oscillations, are directly simulated using a compressible flow solver with detailed chemistry. The compressible Navier-Stokes (N-S) equations are solved in a time splitting form, i.e., the fluid and chemical reaction parts are solved separately in time. To efficiently handle stiff chemistry of reaction equations, a robust and fast explicit time integration method (ERENA) developed by the author's group is introduced. For the N-S equations (fluid part), a species bundling is introduced to efficiently calculate diffusion coefficients. The present approach, thus, greatly enhances computational efficiency. The detailed mechanisms, in which n-butane consists of 113 species and n-heptane consists of 373 species, can be directly applied.

A length of 4 cm is used. While one initial pressure of 5 atm is set, several temperatures between 500 and 1000 K are considered. An initial hot spot of 1400 K is introduced at the left boundary to initiate flame propagation. Adiabatic wall condition is used at the right boundary. An equivalence ratio is 1.0. Current findings are as follows. The flame speeds are determined by the expansions of hot spot ignition and dynamically changing end-gas conditions, which are not associated to laminar flame speeds. Rapid heat release comparable to sound speed in end-gas regions produces disparity of pressure distributions, leading to the generation of severe pressure waves; otherwise severe knocking never happens. An origin of knocking is at the wall in case of adiabatic conditions. Negative Temperature Coefficient (NTC) region greatly influence the knocking occurrences, e.g., knocking of n-heptane at the initial temperature of 750 K occurs earlier than 800 K. More detailed discussions, e.g., how knocking intensity is determined, would be made in a final presentation.

W1P082 NEXT GENERATION KNOCK CHARACTERIZATION

Howard Levinsky¹, Sander Gersen², Martijn van Essen², Gerco Van Dijk²
¹University of Groningen, Netherlands ²DNV GL, Netherlands

The globalization of the gas market is increasing the diversity of the supply of natural gases. As a rule, "new" gases have different chemical compositions than the gases traditionally distributed. However, different compositions can have different combustion properties, which can lead to unacceptable changes in the safety or fitness-for-purpose of end-use equipment. Gas-fuelled reciprocating internal combustion engines are known to be sensitive to variations in fuel composition because of the possible occurrence of engine knock, caused by autoignition of unburned fuel mixture, the so-called end gas, ahead of the propagating flame in the cylinder. Mild engine knock increases pollutant emissions, while severe knock can cause engine failure or physically damage the engine, and should thus be avoided. Rather than rely on the empirical methods using gas mixtures and "standard" engines traditionally employed for this purpose, we have developed a method to characterize the knock resistance of gases based on the combustion properties of the fuel mixtures. The core of the method is the computation of the autoignition process during the compression and burn periods of the engine cycle. The chemical mechanism used to compute autoignition has been tested against experimentally determined autoignition delay times for a broad range of gaseous fuels measured in our Rapid Compression Machine (RCM) at conditions relevant to spark-ignited gas engines. In addition to the effects on autoignition itself, the effects of fuel composition on the in-cylinder pressure and temperature conditions relevant for knocking, such as changes in the combustion rate are also incorporated in the method. Comparison between predicted and measured pressure profiles shows that the model accurately predicts the changes in the in-cylinder pressure when varying the fuel composition in our high-speed medium Brake Mean Effective Pressure (BMEP) engine.

To rank the knock resistance of different gases for the lean-burn, spark-ignited gas engine used in this study a propane-based scale (Propane Knock Index, PKI) is developed. In this scale, the knock resistance for a given gaseous fuel mixture is expressed as an equivalent fraction of propane in methane under the same engine conditions. We demonstrate the veracity of the knock model by comparing the predictions of autoignition of the end gas using the model for a wide variety of fuel compositions, expressed as the computed PKI, with the Knock-Limited Spark Timing (KLST) measured in the DNV GL engine for the following mixtures: Dutch Natural Gas (DNG), DNG/C₂H₆/C₃H₈, DNG/H₂, DNG/C₂H₆/C₃H₈/H₂, CH₄/C₂H₆, CH₄/C₃H₈, CH₄/*i*-C₄H₁₀, CH₄/*n*-C₄H₁₀, CH₄/C₂H₆/C₃H₈ and CH₄/C₃H₈/N₂. The predicted ranking of knock resistance of these mixtures is shown to be in excellent agreement with the KLST measurements. Comparing the predictions of the new method with the ranking obtained using the methods currently in industrial use, such as the AVL methane number, shows superior performance of the PKI for this engine.

Howard Levinsky

levinsky@dnvgl.com

W1P083 ROLE OF KINETICS IN HCCI COMBUSTION

Mattia Bissoli, Alessio Frassoldati, Alberto Cuoci, Tiziano Faravelli, Eliseo Ranzi, G. Natta, Politecnico di Milano, Italy

The ever increasingly requests of fuel efficiency and reduction of pollutants emissions make HCCI a possible solution in the field of IC engines. This work presents the last improvements of a recent multi-zone quasi-dimensional model developed for describing the HCCI combustion in a four-stroke single cylinder engine. The reacting volume is discretized into several concentric sub-domain called zones, each of which is treated as a well-mixed reactor with time variable volume. Neighboring zones can interact through laminar and turbulent diffusive fluxes of heat and mass. The model takes into account also the effects of the residual burned gasses, which remain trapped in the cylinder between two cycles. Initially, all the zones have the same thickness, which depends on the number of sub-domain selected by the user. During the cycle, the size of each zone changes according to density variations due to the heat released, and the geometrical constrain. In fact, the sum of zone volumes is also dictated by the compression ratio and the piston position. Turbulence effects are evaluated by following the approach of Yang and Martin, where a simplified solution of a 1-D energy equation allows to estimate the turbulent viscosity. A similar approach is applied to the boundary layer to calculate the heat transfer to the cylinder walls, following the work of Han and Reitz. This new model allows to improve the description of the near-wall phenomena, which are very important in the HCCI combustion. The turbulence and the wall-heat transfer models were validated against CFD simulations, showing good agreement in terms of temperature, heat release and heat exchanged, both in non-reactive and reactive cases. With all these features, the multi-zone model is reliable, efficient and predictive: no additional information about the physic of the system are required, and all the properties are directly evaluated. The capacity of the model in predicting pollutant formation and emission were validated in comparison with the experimental data deriving from the HCCI combustion of *n*-heptane and different bio-fuels [4]. With *n*-heptane and methyl-decanoate the composition profiles show that both the low and high temperature ignitions are well captured, as well as their duration.

The kinetic mechanism adopted is the last version of the scheme developed by Ranzi et al. (<http://creckmodeling.chem.polimi.it/>), composed by 460 species and 16000 reactions. It allows to describe the oxidation of hydrocarbons up to jet fuels and diesel, plus bio-fuels like alcohols and methyl-esters. The lumped approach, coupled with the concepts of hierarchy and modularity, allows containing the dimension of the scheme.

A single simulation of 10 engine cycles with 15 zones requires from 5 to 10 hours on a last generation pc. The model also includes all the main tools for kinetic analysis, like rate of production and sensitivity analysis. This tool allows to make a further step in understanding the chemistry ruling the HCCI engines.

mattia.bissoli@polimi.it

W1P084 A NEW FUEL INDEX FOR LTC ENGINES BASED ON OPERATING ENVELOPES IN LIGHT-DUTY DRIVING CYCLE SIMULATIONS

Kyle Niemeyer¹, Shane Daly¹, William Cannella², Chris Hagen¹

¹Oregon State University, United States ²Chevron Energy Technology Company, United States

Low-Temperature Combustion (LTC) engine concepts such as Homogeneous Charge Compression Ignition (HCCI) offer the potential of improved efficiency and reduced emissions of NO_x and particulates. However, engines can only successfully operate in HCCI mode for limited operating ranges that vary depending on the fuel composition. Unfortunately, traditional ratings such as octane number poorly predict the autoignition behavior of fuels in such engine modes, and metrics recently proposed for HCCI engines have areas of improvement when wide ranges of fuels are considered. In this study, a new index for ranking fuel suitability for LTC engines was defined, based on the fraction of potential fuel savings achieved in the FTP-75 light-duty vehicle driving cycle. Driving cycle simulations were performed using a typical light-duty passenger vehicle, providing pairs of engine speed and load points. Separately, naturally aspirated HCCI engine simulations were performed for a variety of fuels in order to determine the operating envelopes for each. These results were combined to determine the varying improvement in fuel economy offered by fuels, forming the basis for a fuel performance index. Results showed that, in general, lower octane fuels performed better, resulting in higher LTC fuel index values; however, octane number alone did not predict fuel performance.

Kyle.Niemeyer@oregonstate.edu

W1P087 KINETIC AND NUMERICAL STUDY ON THE EFFECTS OF DTBP ADDITIVE ON THE REACTIVITY OF METHANOL AND ETHANOL

Hu Wang¹, Rolf D. Reitz¹, Mingfa Yao², Ming Jia³

¹University of Wisconsin, United States ²Tianjing University, China ³Dalian University of Technology, China

A numerical investigation was conducted to study the effects of Di-Tert-Butyl Peroxide (DTBP) additive on the reactivity of methanol and ethanol fuels. First, a reduced Primary Reference Fuel (PRF)-methanol-ethanol-DTBP mechanism was proposed to simulate the Homogeneous Charge Compression Ignition (HCCI) combustion processes of PRF and alcohol-DTBP fuels. Effective combustion phasing maps were generated for the alcohol-DTBP fuels, and the agreement between experimental and simulation results was reasonably good. Then, the reasons for the enhancement of reactivity by DTBP addition to both methanol and ethanol fuels were explored kinetically. It was found that both thermal and chemical effects contribute to the reactivity enhancement, and this could be attributed to the heat released in the DTBP decomposition process and to the reactive radicals generated through the $\text{CH}_3\text{OCH}_2\text{OCH}_3 \rightarrow \text{CH}_3\text{O} + \text{CH}_2\text{O} \rightarrow \text{CH}_3\text{O} + \text{H} + \text{OH}$ pathway. The major reason for the different response of DTBP between methanol and ethanol was found to be due to the higher DTBP content in methanol-DTBP mixtures under the current conditions, and this was further confirmed by the fact that the effects of DTBP addition on methanol and ethanol reactivity were quite similar if the same absolute DTBP mass was added to these two alcohols. However, the reactions $\text{CH}_3 + \text{HO}_2\text{CH}_2 + \text{O}_2$ and $\text{CH}_3\text{O}_2 + \text{CH}_2\text{CH}_2\text{O}$ also contributed to the somewhat lower reactivity of ethanol-DTBP mixtures.

gwrets@gmail.com

W1P088 HIGH-SPEED OPTICAL CHARACTERIZATION OF TRANSIENT INJECTION EVENTS IN AN ENGINE

Nicholas Neal, David Rothamer, University of Wisconsin, United States

Preliminary experiments studying transient rate-of-injection effects on jet development and combustion for high-pressure diesel injections have been carried out in an optically accessible internal combustion engine. These experiments include measurements and analysis of the dispersion angle, liquid penetration, and jet penetration for transient fuel jets. Much of the existing literature in this field focuses on quasi-steady jets, assuming transient portions of injections to be negligible. While these results are useful for gaining a fundamental understanding of the combustion and mixing processes inherent in compression-ignition engines, they are not entirely representative of the actual conditions often seen in real applications, especially in the case of the small-bore diesel engine. Small-bore engines often use short injection durations (resulting in ramped rate-of-injection profiles) that do not correspond to the conditions under which many of the scaling theories and dependencies set forth in the literature were developed. Additionally, engines operating with multiple in-cylinder injections per cycle will similarly have injections dominated by ramped rate-of-injection profiles. Therefore, there is a strong need to gain an understanding of transient effects on jet/spray development and combustion. Optical measurements were taken for a range of experimental conditions. Multiple densities at a start-of-injection time of 5 crank angle degrees before top-dead-center were used. Injection pressures of 30 and 75 MPa for a six-orifice injector were studied. A standard #2 diesel fuel, a jet fuel (JP-8), and a 50/50 blend of JP-8 and Sasol Iso-Paraffinic Kerosene (IPK) were tested to investigate the influence of fuel properties on the transient injection process. Initial results indicate that jet penetration obeys the same scaling with time as the rate-of-injection profile for the accelerating period of the rate-of-

injection profile, reverting to classic $t^{1/2}$ scaling as the injection profile shifts to a constant rate-of-injection, as evident in the plots above. Figure 1 shows two log-log plots of jet penetration during the initial injection transient for the two injection pressures tested, along with the corresponding ROI plots. For these two cases, penetration scaling with time is seen to change during the accelerating part of the injection process. These changes are seen to correlate changes in the measured ROI. To our knowledge this complex behavior of a multi-hole injector has yet to be documented in the literature. The penetration scaling for each condition has been characterized. The dependence of penetration scaling with ROI will have impacts on the overall jet development and combustion for injections where the transient portion of the injection is significant.

njneal@wisc.edu

W1P089 TIME-SERIES ANALYSIS OF RADICAL EMISSIONS USING A SPARK PLUG WITH OPTICAL FIBER

Nobuyuki Kawahara, Shota Hashimoto, Eiji Tomita, Okayama University, Japan

In this study, radical emissions were observed and analyzed at a combustion process in engine cylinder using time-series of spectroscopic measurement. The chemiluminescence from radical emissions such as OH*(306nm), CH*(431nm) and C₂*(516nm) were detected. Combustion characteristics are understandable using spectroscopic measurement of flame in engine cylinder. An air/fuel ratio correlates to intensity ratio of radical emissions. A broad spectrum owing to thermal radiation from soot is measured when there is luminous flame. The behavior of flame front can be studied from radical emissions due to time tracking using time-series of spectroscopic measurement because of including information of flame front in radical emissions. In Direct-Injection Spark-Ignition (DISI) engine, these combustion characteristics are significant. These cause cyclic variations such as partial burn due to stratified mixture gas. In particular, it is important to understand flame kernel characteristics and propagation in early flame.

A spark plug equipped an optical fiber was developed in this study. A spark plug sensor can be easily applied to practical engines. This sensor has a simple structure and high durability because an optical fiber is just inserted into the spark plug. Therefore, radical emissions were measured by time-series of spectroscopic measurement with this spark plug sensor. A Compression-Expansion Machine (CEM) with visualization piston was used, and a high-speed camera viewed the flame propagation from bottom. The relationship between radical emissions and the flame front of images was investigated.

Using the spark plug sensor, three kinds of spectra can be detected. Firstly, there are radical emissions of the CH* and C₂* in case that a plug sensor detects the flame front. Secondary, the CO-O recombination emission is observed in case of detecting the burned gas. Furthermore, these time-series of spectra are measured when the flame front passes through the measurement area. Thus, the flame kernel characteristics can be investigated. Finally, a broad spectrum that is higher intensity than radical emission is observed when there is the luminous flame in engine cylinder. A new tool was developed, and this tool can investigate propagation characteristics of early flame in engine cylinder using radical emissions.

kawahara@mech.okayama-u.ac.jp

W1P090 EFFECTS OF HYDROGEN AS AN ADDITIVE ON EMISSION GAS OF TURBO GASOLINE DIRECT INJECTION ENGINE

Joonsuk Kim, Jungmin Seok, Soonho Song, Yonsei University, Korea

In these days, a regulation of fuel efficiency and emission gas is the global issue of the engine. So, downsizing through Turbo Gasoline Direct Injection (T-GDI) technology is the general trend of gasoline engines. T-GDI definitely makes high efficiency as compared with a Natural Aspirated Port Fuel Injection conventional gasoline engine (N/A PFI). However, T-GDI has a self-limited problem which is high in-cylinder temperature due to boosting. If T-GDI engine has a same compression ratio of natural aspirated engine, knocking will easily occur. So T-GDI engine has a low compression ratio to avoid knocking. Thus, limitation of increasing thermal efficiency arises.

Hydrogen has features of fast flame speed, low energy density per volume, and low ignition energy. Hydrogen additive and T-GDI engine are well-suited. Because hydrogen prevents knocking on T-GDI that compression ratio can be increased. Moreover, the difficulty of lean burn on gasoline engine can be solved by using hydrogen as an additive. T-GDI also makes up for low power problem of hydrogen.

The objective of this study is to establish fundamental emission characteristics of T-GDI engine with hydrogen additive by finding out the effects of hydrogen additive on emission gas of T-GDI engine. The engine used in this study is a direct fuel injection, four-cylinder, turbo charged SI 2,000cc gasoline engine. Horiba and SMPS are installed at a front muffler to measure emission gas and pure hydrogen is injected in front of intake air intercooler. Generally, engine operates most of time around 2,000 RPM. So the operating condition of engine is set at 2,000 RPM with BMEP 6.9bar. Hydrogen flow rate has 3 cases that hydrogen energy fraction in the intake is constantly kept at 2%, 5% and 8%.

The experimental results indicated that emission gas of T-GDI engine was influenced by hydrogen flow rate. Especially, the number of nitrogen oxides was increased as hydrogen energy fraction was increased.

vtesco@yonsei.ac.kr

W1P091 RESEARCH IDENTIFICATION ON MIXTURE COMBUSTION CREATED BY TWO GDI INJECTORS IN SI ENGINE

In modern Spark Ignition engines, a trend to maximize efficiency of combustion exists. It is possible thanks to a usage of appropriate engine fueling system that is capable of atomizing the divided fuel dose leading to its ignition. New Gasoline Direct Injection systems are used in most of produced SI engines adopted in cars. The authors present the results about mixture combustion created by unconventional supply system with a usage of two GDI injectors.

The research was performed using Rapid Compression Machine. The injection was realized using outward-opening piezoelectric injectors getting empty inside conical stream. Injectors are positioned with right angle between them and with a spark plug amid them. The angle of cone equals 90 degrees, which enables to get connection of fuel streams around spark plug electrodes allowing the ignition of mixture. The optical tests were carried out with the usage of a high-speed camera HSS 5 with the recoding frequency of 10 kHz and image resolution of 512×512 pixels. The combustion processes were recorded using specialist dual optic and two color method. The images were analyzed by LaVision DaVis software. The research on combustion processes was made using different injection strategies: single dose injection, double simultaneous injection and triple sequential injection. The time of injections equals respectively 0.8 ms, 2×0.4 ms and $0.3 + 0.3 + 0.3$ ms. The delay time between the start of injections in sequential injection equals $\Delta t = 0.5$ ms. In all strategies, the same injection pressure equals 20 MPa and close back-pressure in combustion chamber before injection were used. In the analysis of combustion processes, increased intensity of flame radiation in single injection strategy is noticeable. Big local concentration of fuel caused by a single big dose brought High Temperature Combustion on. It is not advantageous for ecology; HTC causes increased production of nitrogen oxides NO_x . In this situation, simultaneous injection strategy is the most advantageous. By obtaining the biggest area of injected fuel and the biggest evaporation, the most homogenous mixture from all three strategy was obtained. The smaller flame radiation is observed in the whole combustion chamber. The research shows that the shortest combustion runs with the usage of double simultaneous injection strategy despite the fact that the biggest increase of flame is for a single dose strategy.

ireneusz.pielecha@put.poznan.pl

W1P092 THERMODIFFUSIVE EFFECTS IN SPARK-IGNITION ENGINES

Pierre Brequigny¹, Christine Mounaim-Rousselle¹, Fabien Halter¹, Thomas Dubois²

¹Université d'Orléans, France ²CRES – Solaize, France

The current decrease in fossil energy resources requires a diversification of the liquid and gaseous fuels potentially consumable in internal combustion engines. The use of these fuels alters the combustion process and the heat released as well. In a Spark Ignition engine, the heat released is mainly piloted not only by the mixture reactivity but also by its sensitivity to stretch effects. Former studies performed with different burner configurations have demonstrated a strong impact of stretch effects on the turbulent flame speed. Only few results can be found in the literature for SI engine configurations. The purpose of the present work is to evaluate stretch effects on the flame front propagation in an optical SI-engine and to investigate the relative importance of these effects depending on the fuel considered.

For this study different fuels and mixture conditions presenting almost equivalent laminar flame speeds and thermodynamical properties have been selected. Four different fuels (Propane, Methane, Isooctane and Butanol) at different equivalence ratios have been studied. Laminar burning speeds measured experimentally at 1 Bar, 400K, reveal quite similar values for all the mixtures selected. Furthermore, Lewis numbers and Markstein lengths, relevant parameters to describe flame-stretch interactions, display different values for all the mixtures selected, corresponding to different sensitivities to stretch effects.

In the first part of this study, the effect of different engine speeds (from 1400 to 2000 rpm), corresponding to different turbulence intensities, has been investigated using direct visualization of the flame propagation. In-cylinder pressure analyses have been performed to determine the heat release rate and the crank angle corresponding to 5% of mass burned. In the same time, direct visualizations of the flame through the piston have been performed using an intensified high-speed video camera. A global flame stretch and an equivalent propagation speed have been defined and evaluated. The obtained results are in good agreement with in-cylinder pressure analyses. An increase of the stretch rate is observed for higher rotation speeds. The combustion process for the mixtures presenting a strong sensitivity to stretch is slowed down compared to non stretch sensitive mixtures and more particularly when the engine speed is increased.

To describe more precisely the flame front structure in terms of curvature and wrinkling, Mie-scattering tomography was performed for the engine operating at 1200 rpm and with an intake pressure of 700 mBar. By using a high speed camera operating at 12500 fps, flame propagation images were acquired through the piston for different lean mixtures fueled with methane, propane and isooctane. The in-cylinder pressure analyses were performed to obtain pressure and temperature conditions when the spark occurs and during the flame visualization. Unstretched laminar burning velocity and Lewis number were evaluated at the engine conditions using the CHEMIN package. During the visualization process, all the mixtures present very similar unstretched laminar burning velocities with different Lewis numbers, thus confirming the pertinent choices of mixtures selected. Using instantaneous binarized flame images, a global flame stretch and an equivalent propagation speed have been defined and estimated. The ranking already observed in the laminar regime is obtained in terms of flame stretch sensitivities. Probability density functions of flame curvature were found to be centered at 0.05 mm^{-1} for the three mixtures whereas differences were observed on the global wrinkling.

Finally, the same mixtures were studied in a spherical turbulent combustion chamber. The chamber provides greater

optical accesses which enables an easier flame front tracking. Moreover initial pressure, temperature and turbulent conditions were fixed during the visualization process. Mie-Scattering Tomography experiments were performed for three different turbulent intensities. The final aim of this work is to predict the influence of the fuel on the heat release rate inside the SI engine regarding turbulence level and its laminar characteristics, i.e. the unstretched laminar burning velocity and the Lewis number or the Markstein length.

pierre.brequigny@etu.univ-orleans.fr

W1P093 INVESTIGATION OF PARTIALLY PREMIXED COMBUSTION IN A LIGHT DUTY ENGINE USING MULTIPLE INJECTIONS

Zhenkan Wang, Slavey Tanov, Richter Mattias, Johansson Bengt, Marcus Aldén, Lund University, Sweden

Because the load range of Homogeneous Charge Compression Ignition (HCCI) is limited and combustion control is difficult, there are reasons to change combustion concept from HCCI to Partially Premixed Combustion (PPC) in internal combustion engine. It has been proven that PPC has the capability of high combustion efficiency with low soot and NO_x emissions, which meets the requirements of extremely restricted emission regulations in the future. High octane number fuels, such as gasoline, give the potential to have longer premix period of fuel and air mixture which could suppress the soot formation without compromising the CO emission levels.

In this work, an optical engine was used to conduct high speed imaging in the combustion chamber so as to visualize the cycle resolved chemiluminescence, which represents the flame formation and development. A quartz piston and cylinder liner was installed in Bowditch configuration to enable optical access. The geometry of the quartz piston crown is based on the standard diesel combustion chamber design for this passenger car engine, including a re-entrant bowl shape. The severe optical distortion caused by the optical piston shape could be minimized through recordings of reference targets and careful image registration. A blended fuel consisting of *n*-heptane and *iso*-octane was used.

By employing different multiple fuel injection strategies, the homogeneity of the fuel distribution and the subsequent combustion could be varied. This was done in order to investigate the spatial properties of PPC ignition and combustion. Furthermore, the work includes investigations of the transition between the conventional Diesel process and HCCI combustion.

zhenkan.wang@forbrf.lth.se

W1P095 EFFECTS OF BOOST PRESSURE AND INTAKE TEMPERATURE ON THE EMISSION OF A CNG-FUELED HCCI ENGINE FOR ELECTRIC GENERATOR

Hyunwoo Song, Soonho Song, Yonsei University, Korea

The air pollution issues due to emission from petroleum fuels are getting serious recently. In that regard, Homogeneous Charge Compression Ignition (HCCI) engine is drawing attention as the upcoming engine operation mode to meet the tight emission regulation. Besides, Compressed Natural Gas (CNG) is treated as a clean fuel, on account of the low carbon monoxide, nitrogen oxide and particulate matter emission by its simple molecular structure and low molecular weight. The objective of this study is to find out the effects of boost pressure and intake temperature on the emission of HCCI engine fueled by CNG. We used 6-cylinder, 6 liter diesel engine equipped with both diesel injector and CNG mixer. Undersized turbocharger was installed to obtain higher peak boost pressure. Meanwhile, unlike the gasoline or diesel HCCI, the engine has to be heated to fire CNG mixture because of the low ignition quality of methane, which is the major ingredient of CNG. So the exhaust gas heat exchanger was located between CNG mixer and turbocharger compressor to heat the mixture. The output power of the engine was controlled by the main throttle body, the one from a 5 liter gasoline engine. Additional throttle body was employed to bypass the heat exchanger for the intake mixture temperature control. The engine was operated only by diesel until the intake temperature gets higher enough to fire the pure CNG mixture. Whole control logic and system was built by NI LabVIEW and DAQ.

Before starting to investigate the effects of boost pressure and intake temperature on emission, the operation range of CNG HCCI should be found. For the system above, the temperature has to be over 170°C to successfully fire the mixture and under 200°C to prevent severe knock. On that range, we varied boost pressure as well as intake temperature, by controlling the engine output power with the main throttle. The experimental results indicated that the nitrogen oxide and hydrocarbon emission increases with higher boost pressure and higher intake temperature. However, the tendency was not proportional for the boost pressure and the times and aspects of peaks were different for the intake temperature.

hws90@naver.com

W1P096 EXPERIMENTAL PERFORMANCE AND EMISSION CHARACTERISTICS OF A SPLIT-CYCLE ENGINE FUELLED WITH NATURAL GAS

Iain Cameron, Andrzej Sobiesiak, University of Windsor, Canada

Spark Ignition (SI) engines fuelled with Compressed Natural Gas (CNG) are characterized by low levels of harmful exhaust emissions and a high knock resistance, but they suffer from mediocre thermal efficiencies. The relatively slow laminar burning velocity of methane, the main constituent in natural gas, is the underlying cause of a drawn out heat release duration when compared with gasoline. Consequently, advanced spark timing must be used to maintain Mean-Best-Torque (MBT) characteristics, which results in higher pumping and heat transfer losses, as well as increased nitrogen-

oxide (NO_x) emissions. The method of fuel delivery (port vs. direct) is a further complication which results in a trade-off between reduced volumetric efficiency and incomplete charge mixing.

It is well known that if levels of turbulence can be increased, the rates of combustion and mixing in engines are enhanced. The difficulty lies in producing adequate small-scale and high intensity turbulence at the correct time; immediately prior to and during combustion. One potential means of accomplishing this task is through the use of split-cycle engine architecture, where one engine cylinder performs the tasks of intake and compression, while a second cylinder is used for combustion and exhaust. The transfer between cylinders occurs through a valved, isobaric, high pressure connecting passage and is timed to occur immediately prior to the start of combustion. The air/fuel mixture is discharged into the combustion chamber under choked flow conditions and is the primary means of turbulence generation. This work focuses on the design, development and testing of a spark-ignited, split-cycle engine fuelled with natural gas whose goal is to overcome the aforementioned challenges associated with using CNG. The engine incorporates reverse poppet valves, which open outward from the cylinder to minimize clearance volumes and create a solid, high intensity jet of flow into the combustion chamber. Fuel is injected directly into the passage connecting the two cylinders, circumventing the issues of fuel displacing intake air and poor gas-jet mixing.

The 10-90% Mass-Fraction-Burn (MFB) durations are compared with those in standard SI-CNG engines, and corresponding performance and emissions levels are reported. Quantification of the turbulence characteristics, (size and intensity), were made using laser-Doppler measurements of a flow discharging through a reverse poppet valve into an optical cylinder, and are presented. The long-term goal of this research is to shift the combustion regime from that of the flamelet regime to a more distributed reaction zone, improving thermal efficiency and reducing NO_x emissions.

cameroni@uwindsor.ca

W1P097 EXPLORING THE DYNAMICS OF CYCLE-TO-CYCLE VARIABILITY USING MANY HIGH-DIMENSIONAL SINGLE-CYCLE SIMULATIONS

Charles E.A. Finney, Miroslav K. Stoyanov, K. Dean Edwards, C. Stuart Daw, Oak Ridge National Laboratory, United States

The full potential of highly dilute operation (with EGR or excess air) of SI engines to increase engine efficiency and reduce NO_x production by lowering the overall in-cylinder temperature is limited in practice by complex combustion dynamics which promote unstable operation and even misfire. As fuel-economy and emissions regulations continue to tighten, the ability to operate the engine at, and even beyond, this edge of stability becomes increasingly important. Because some key features of dilute combustion dynamics can take hundreds or thousands of successive cycles to manifest, the computational time involved in using complex CFD-type models to explore the performance responses pace has limited industry's ability to utilize simulations to optimize engine designs. As a result, past studies have mostly relied upon experimental observations and low-order engine models to examine and understand the physical mechanisms responsible for the instabilities, especially for rarer events occurring over longtime scales. We have implemented a novel approach for utilizing parallel computations to reveal long-timescale features of dilute combustion without the need of thousands of serial cycle-by-cycle CFD simulations. Our approach relies on adaptive hierarchical sparse grid sampling of single-cycle simulations to create meta models that preserve the long-timescale features of interest. We validated them methodology using a simplified combustion model and have demonstrated that this approach can accurately approximate the dominant nonlinear dynamics. Furthermore, we report on the successful implementation of this strategy with a higher-fidelity, multi-scale combustion model (using CONVERGE by Convergent Sciences, Inc.) on high-performance computing resources at the Oak Ridge Leadership Computing Facility.

finneye@ornl.gov

W1P098 OPTICAL CHARACTERIZATION OF STRATIFIED COMBUSTION IN A DIRECT-INJECTED GASOLINE ENGINE

Mats Andersson, Lars Christian Riis Johansen, Eugenio de Benito, Stina Hemdal, Chalmers University of Technology, Sweden

One way to reduce fuel consumption in gasoline engine is to operate the engine in stratified mode at low- and medium-load conditions. In the spray-guided concept the fuel is injected directly into the cylinder late during the compression stroke, with the purpose to create a suitable fuel-air mixture close to the spark plug while the outer parts of the cylinder only contains air. The benefits are globally lean combustion, reduced heat transfer losses and pumping losses since the engine can run with wide-open throttle. Potential problems are emissions and in particular soot particle formation, due to incomplete fuel air mixing creating rich zones.

In order to better understand the fuel mixing and combustion processes, stratified combustion was studied in a single-cylinder engine with optical access. The upper part of the cylinder liner was made of quartz, there were quartz windows in the pent-roof of the cylinder head, and the piston had a large quartz window. The fuel injector, an outwards-opening piezo-actuated injector, and the spark plug were located close to each other at the top of the cylinder head. The spray and combustion were characterized using high-speed video cameras in various configurations. The spray was filmed from below and from the side, indicating the liquid fuel penetration. The ignition and flame was also imaged both from below and the side, and with the use of a color camera the time-evolution and extension of the sooting and non-sooting flames, respectively. Furthermore, a spectrograph was used to obtain time-resolved luminescence spectra from the flame, including emission lines from OH^* , CH^* and C_2^* .

It was found that the timing of fuel injection and the spark, as well as injection strategy had an influence on spray

penetration and on the amount of soot formed. Under certain conditions fuel was deposited on the piston resulting in slowly burning pool fires generating soot also late during the combustion. Under more favorable conditions the soot formed appeared to have oxidized well before the end of combustion.

f3cma@chalmers.se

W1P099 EFFECT OF SPLIT MICRO-PILOT FUEL INJECTION ON ENGINE PERFORMANCE, EXHAUST EMISSIONS, FLAME DEVELOPMENT AND OPERATION RANGE OF PREMIER COMBUSTION IN A DUAL FUEL ENGINE USING NATURAL GAS

Cagdas Aksu¹, Eiji Tomita¹, Nobuyuki Kawahara¹, Kazuya Tsuboi¹, Shun Nanba¹, Morio Kondo²

¹Okayama University, Japan ²Mitsui Engineering and Shipbuilding Co., Ltd, Japan

Previous studies focusing on dual fuel combustion indicated that it is possible to utilize auto ignition of end-gas mixtures without encountering knocking; a third heat release peak that indicates auto ignition of end-gas region was observed at absence of pressure fluctuations. This phenomenon is named as -PREmixed Mixture Ignition in the End-Gas Region (PREMIER) combustion in later studies. This combustion mode has improved thermal efficiency and HC and CO emission characteristics in exchange for deterioration in NO_x emissions. A major limitation is its limited operation range: PREMIER combustion occurs as a precursor of knocking and in the vicinity of upper operation range in dual fuel operation mode. Split pilot injection is expected to be a possible solution that can extend operation range of both dual fuel combustion and PREMIER combustion.

In this study, the effect of split pilot fuel injection and injection pressure on operation range, performance and exhaust characteristics of a direct injection gas engine with micro pilot fuel injection and operation range of PREMIER combustion is investigated experimentally and visually. Cylinder pressure versus crank angle data was collected in order to obtain indicated performance data, and in-cylinder images were recorded for observing progress of combustion. Pilot fuel is injected at 40 and 80 MPa pressures with minimum achievable injection rates of 0.6 and 1.2 mg/cycle with split injection that provide 1.2% and 2.4% of total energy input through a direct injection injector with three Ø1mm holes aligned at 120° from each other. Natural gas is mixed with intake air and its flow rate is adjusted in order to keep total equivalence ratio at 0.6. Experiments were carried out at 1000 rpm with 101 kPa intake pressure throughout the study.

Performance characteristics with 40MPa injection pressure indicate that PREMIER combustion is achievable at only a single operation condition, which was widened to a range of 2 degrees of crank angle via split fuel injection by both suppressing knocking at upper operation range and promoting end-gas auto ignition at the lower operation range. Suppressing knocking allowed a maximum of 1.38% improvement in thermal efficiency at upper operation range due advanced first injection timing, and 2.83% at lower operation range by promoting regular dual fuel combustion to PREMIER combustion. Time-resolved in-cylinder images showed that split injection can fasten or delay ignition delay of pilot fuel and control overall reaction rate. The improvement in thermal efficiency is accompanied by rapid increase in NO_x emissions, and slight deteriorations in CO and HC emissions. Increasing injection pressure to 80MPa improved CO and HC emissions over 40 MPa injection pressure without any negative impact on NO_x emissions. Cylinder images showed signs of deeper penetration and better atomization, which is expected to be an indicator that combustion is closer to completeness.

cagdasaksu@gmail.com

W1P100 INVESTIGATION OF THE COMBUSTION AND SOOTING BEHAVIOR OF ETHANOL-BLENDED DISI-SPRAYS IN A CONSTANT-VOLUME CHAMBER

Stefan Will, Michael Storch, Lars. Zigan, Michael Wensing, LTT Erlangen, Germany

For future CO₂- reductions of Spark Ignition (SI) engines, the combination of modern engine operation concepts, e.g. Direct Injection (DI), and the use of biofuels such as ethanol is essential. However, DI concepts have the drawback of higher particulate matter emission as compared to port fuel injection. Especially when driven with biofuels, the operation of Direct Injection Spark Ignition Engines (DISI) requires a deeper insight into particulate formation processes. A spray combustion investigation within an optically accessible constant volume chamber at stratified engine operation was conducted to study soot formation of ethanol blended fuels. The work has focused on the influence of gas temperature, gas pressure and ignition timing on the combustion behavior of ethanol, isooctane and its blends E85 and E20 at cold start conditions. For this purpose the injection chamber was equipped with a spark plug and an ignition power amplifier. A high-speed camera in combination with an image stereoscope and a set of 2 different cut-off filters (525 nm cut-off wavelength) was used in order to investigate the combustion processing two different wavelength regions simultaneously. With this setup, premixed and sooting combustion regions can be visualized. Furthermore, the separation of bright spots in the sooting combustion regions gives insight into liquid fuel combustion (combustion of dense droplet clouds), which is a significant source of soot formation at late injection timing conditions.

The study reveals that depending on the operation conditions either the chemical (e.g. reaction kinetics) or the physical properties (especially enthalpy of evaporation) of the fuel dominate the combustion and sooting behavior. The results of this study can be used to identify sources of soot formation during spray formation and air-fuel mixing of ethanol blended fuels in DISI engines with charge stratification.

Stefan.Will@lth.uni-erlangen.de

W1P101 DIRECT NUMERICAL SIMULATIONS OF THE EFFECTS OF NTC REGIME ON THE IGNITION OF A LEAN *N*-HEPTANE/AIR MIXTURE WITH TEMPERATURE AND COMPOSITION INHOMOGENEITIES

Chun Sang Yoo¹, Minh Bau Luong¹, Gwang Hyeon¹, Yu Ulsan¹, Suk-Ho Chung²

¹National Institute of Science and Technology, Korea ²University of King Abdullah Science & Technology, Saudi Arabia

The effect of the mean temperature lying in/near/outside the Negative Temperature Coefficient (NTC) regime on the ignition of a lean *n*-heptane/air mixture with stratifications in temperature and equivalence ratio at elevated pressure has been investigated using Direct Numerical Simulations (DNSs) with a 58-species reduced mechanism. 2-D DNSs are performed by varying key parameters: initial mean temperature, T_0 , and the variance of temperature and equivalence ratio (T' and ϕ') together with three different T - ϕ correlations: 1) baseline cases with only either T' or ϕ' , 2) negatively-correlated and 3) uncorrelated T - ϕ cases. It is found that for T_0 in the NTC regime, fuel stratification becomes more effective than thermal stratification in controlling the ignition delay and mitigating the Heat Release Rate (HRR); whereas, for a higher T_0 relative to the NTC temperature regime, thermal stratification plays a predominant role over fuel stratification in enhancing the temporal advancement and distribution of the overall combustion. In general, the overall combustion occurs quickly and the mean HRR increases more slowly with a reduced peak Pressure Rise Rate (PRR) as ϕ' is increased for the cases with only ϕ' and the uncorrelated T - ϕ cases regardless of T_0 . For the cases with only T' , however, depending sensitively on T_0 , the ignition delays are retarded for low T_0 , while advanced for high T_0 with increasing T' . In the same way, the corresponding ignition delays of the negatively-correlated cases are retarded further with increasing ϕ' for low and high T_0 . For intermediate T_0 in the NTC regime, the overall combustion becomes more advanced and is temporally more distributed with increasing ϕ' regardless of the correlation of T - ϕ fields. Chemical explosive mode and Damköhler number analyses reveal that for all the cases except the negative-correlated cases of low and high T_0 , a mixed mode of spontaneous ignition and deflagrative combustion coexists during the ignition process. It is also verified that the deflagration mode prevails at the reaction fronts for large ϕ' and/or T' and hence, the combustion occurs subsequently, rendering more distributed over time. On the contrary, the spontaneous ignition mode becomes predominant for the cases with small T' and/or ϕ' , especially for the cases of low and relatively high T_0 with the negative T - ϕ correlations. As such, volumetric auto-ignition occurs nearly throughout the whole domain, causing an excessive HRR. However, for high T_0 outside the NTC region, even with small T' , a sequential ignition event still occurs as deflagrative combustion mode, resulting in distributed HRR and PRR. These results suggest that a harmonious combination of initial mean temperature and an appropriate level of stratification in temperature and composition with a well-designed T - ϕ field can promisingly prevent an excessive PRR under high-load conditions and regulate effectively the timing of combustion in the Homogeneous Charge Compression-Ignition (HCCI) engines

csyoo@unist.ac.kr

W1P102 ASSESSMENT OF CONDITIONAL MOMENT CLOSURE FOR MODELLING AUTO-IGNITION IN COMPOSITIONALLY STRATIFIED *N*-HEPTANE/AIR MIXTURES USING DIRECT NUMERICAL SIMULATION

James Behzadi¹, Mohsen Talei², Evatt Hawkes¹, Tommaso Lucchini³, Gianluca D'Errico³, Sanghoon Kook¹

¹The University of New South Wales, Australia ²University of Melbourne, Australia ³Politecnico di Milano, Italy

A spatially zero-dimensional Conditional Moment Closure (CMC) model is implemented in OpenFOAM and used to model ignitions relevant to Stratified Charge Compression Ignition (SCCI) engines. To investigate the model performance, comparisons are made to a set of Direct Numerical Simulation (DNS) data. The DNS model ignition of stratified *n*-heptane/air mixtures in two-dimensional flows using a reduced 58 species chemical mechanism.

The DNS and CMC are compared for four test cases having different initial levels of stratification. The mean temperatures for all four CMC test cases are in good agreement with the DNS. Furthermore, for low levels of mixture stratification, the conditional temperature from the CMC model closely matches the DNS. However, the deviations of CMC from DNS become more prominent as the level of stratification increases.

Two closure tests are devised to assess the range of validity for the CMC model using the DNS data. Closure-test 1 aims to analyse the validity of first order closure hypothesis for the reaction rate source term of the CMC model. Closure-test 2 is performed to investigate whether the CMC equation is closed for the cases under study. The tests provide insight into the validity scope of the model before attempting to apply them in full HCCI engine simulations.

J.Behzadi@unsw.edu.au

W1P103 DNS ASSESSMENT OF FLAMELET MODELS FOR LES OF DIESEL JETS

Muhsin Ameen, Vinicio Magi, John Abraham, Purdue University, United States

Large-Eddy Simulations (LES) of reacting diesel jets is challenging because the combustion process is fundamentally unsteady and turbulence scales vary over orders of magnitude. The accuracy of Large Eddy Simulations (LES) of reacting jets, in general, depends strongly on the accuracy of the turbulent sub-grid scale combustion models. In a general sense, the filtered reaction rate term can be assumed to be the convolution of the local and instantaneous reaction rate with the joint Probability Density Function (PDF) of the scalar variables at that point and time. In prior work, flamelet models, Conditional Moment Closure (CMC) models, and transported Filtered Density Function (FDF) models have been employed. In this study, we employ Direct Numerical Simulations (DNS) to assess the flamelet-based model for the

filtered reaction rate term. In flamelet-based models, the assumption is that the flame thickness is much shorter than the turbulence length scales, and the effect of the turbulence is to locally stretch and wrinkle the flame. If this is the case, the local and instantaneous reaction rates and/or scalar variables can be obtained separately by solving a set of equations for transport in the flamelet. These variables can be tabulated in a library or obtained through interactive simulations and then convolved with an appropriate PDF to obtain the filtered terms. In practice, simplifications are made so that the number of independent variables is reduced. For example, in a common implementation of the approach, three parameters, the mixture fraction Z , the scalar dissipation rate χ , and the progress variable Λ , are assumed to be the independent variables. The accuracy of the flamelet assumption and the simplifications, however, need to be assessed. This is especially important when employing the model for LES of reacting diesel jets where unsteady ignition is an important part of the combustion process. In other words, statistical steady state assumptions cannot be made.

The DNS studies are performed for a turbulent reacting mixing layer with *n*-heptane, which is chosen to be a surrogate for diesel, and air separated by a mixing layer. The initial temperature, pressure and turbulence scales are chosen to be similar to the conditions found inside diesel engines. The validity of the flamelet model is first evaluated by comparing the flame development predicted by DNS with that predicted using the flamelet assumption. In flamelet models, the dependence of χ on Z is assumed to have a constant functional relationship, usually an error function, which remains unchanged during the flame development process. It is also assumed that each flamelet is identified by the value of the stoichiometric scalar dissipation rate, χ_{st} . The DNS results show that the chemical reactions cause significant increase in the local scalar dissipation rate near the flame. This increase leads to significant differences in the flame development predicted by DNS as compared to that by the flamelet model. This difference in the unsteady flame development can be a source of error during ignition and flame development. The steady-state flame structure predicted by the model agrees closely with that predicted by DNS.

The filtered scalar dissipation rate χ has to be modeled. Its modeling is not clear. In this work, four models are evaluated for χ : a turbulent diffusivity-based model, the k - ϵ model, the Strain Rate Tensor (SRT) model and the Sub-Filtered Kinetic Energy (SKE) model. It is found that the SRT model is the best choice when considering the performance and ease of implementation in LES codes. In addition to the assessment of the structure of the flame and χ , it is important to determine if the assumptions made about PDF are accurate. Usually, the PDFs are constructed a priori under the assumption that the variables are statistically independent. For the PDF of χ , it is found that an exponential PDF works well for low values of χ and the lognormal PDF works well for large values of χ . This PDF requires the variance of χ . The DNS data has been employed to derive a model for the variance of χ . Modeling the filtered progress variable, the variance of the progress variable, and its PDF is in progress.

nameen@purdue.edu

W1P104 SIMULATIONS OF AUTOIGNITION-ASSISTED FLAME PROPAGATION IN RCCI-BASED ENGINES

Ankit Bhagatwala¹, Ramanan Sankaran², Sage Kokjohn³, Jacqueline H. Chen¹

¹Sandia National Laboratories, United States ²Oak Ridge National Laboratory, United States ³University of Wisconsin, United States

Single fuel premixed compression-ignition strategies are operationally limited to low loads due to difficulties controlling combustion phasing and heat release rate which, in turn, affects the pressure rise rate. Dual fuel strategies such as Reactivity-Controlled Compression Ignition (RCCI) use in-cylinder blending of two fuels with different autoignition characteristics to control combustion phasing and heat release rate. In a typical RCCI engine, a homogeneous charge of a low-reactivity fuel (e.g., gasoline) is created using port-fuel-injection or early direct-injection. Later in the compression stroke, a high-reactivity fuel (e.g., diesel fuel) is injected into the combustion chamber using direct-injection. This in-cylinder blending process allows the ratio of the two fuels and the local stratification to be controlled on a cycle-to-cycle basis. The combustion phasing is controlled by the overall fuel reactivity (i.e., the ratio of the two fuels) and the combustion duration is controlled by the level of spatial stratification in the two fuels. RCCI experiments in an optical engine have shown that ignition occurs in the region containing the highest concentration of high-reactivity fuel. The ignition zone then grows for several crank angles and merges with other local ignition zones following the gradient in fuel reactivity. The mechanism controlling the local growth of the auto-ignited zones is unclear.

The goal of this study is to shed light on the relative roles of autoignition and premixed flame propagation under RCCI conditions. Premixed flame propagation has been shown to occur in RCCI engine simulations and is conjectured to occur in real engines. However, since it has proved difficult to observe or measure these flames in engine experiments due to a lack of spatial resolution, high-fidelity simulations are currently the only means to study this phenomenon. It is important to quantify the characteristics and likelihood of flame propagation from a modeling point of view since different models are used to describe flame versus autoignition. One and two-dimensional direct numerical simulations with a primary Reference Fuel (PRF), a mixture of *iso*-octane and *n*-heptane with detailed chemistry have been carried out. Parametric variations in fuel concentration, rate of compression and temperature stratification have been studied and the results suggest that the energy release characteristics of RCCI engines are dominated by a combination of local autoignition and premixed flame propagation. Once autoignition establishes an ignition zone, the region quickly transitions to a flame propagation (diffusion driven) event. However, surrounding the local propagating flames, other autoignition events occur establishing new local flame zones creating what could be described as a autoignition-assisted flame propagation event.

abhagat@sandia.gov

W1P105 LARGE EDDY SIMULATION OF AN INTERNAL COMBUSTION ENGINE USING AN EFFICIENT IMMERSED BOUNDARY TECHNIQUE

Thuong Nguyen, Andreas Kempf, Fabian Proch, Irenaeus Wlokas, University of Duisburg-Essen, Germany

High resolution Large Eddy Simulations (LES) are presented for the flow and combustion in an Internal Combustion Engine (ICE). The Favre-filtered Navier-Stokes equations are solved for the compressible flow employing a finite volume method on Cartesian grids. Stationary parts of the engine are described by the computationally efficient Immersed Boundary (IB) method; moving immersed boundaries are represented by Lagrangian particles that describe the valve and piston. The operations calculating the particle motion are simple to implement, cause a low number of operations and are easy to parallelize - in particular on an isotropic and i,j,k-countable computational grid, where only few hashing operations are required to calculate the logical particle location. Non-reflecting boundary conditions are used at the intake and exhaust ports. Combustion is described by a Flame Surface Density (FSD) model with an algebraic reaction rate closure.

A total of three test-cases is investigated on different grids with up to hundreds of million cells to evaluate the impact of cell size and filter width. The results are compared to the available measurements of the corresponding optically accessible internal combustion engine investigated by the Dreizler group of Darmstadt University.

During gas exchange, the flow is driven mainly by the piston and the valve motion. The pressure and the velocity profiles in this operating state show good results for all applied grid resolutions. The low deviation in the kinetic energy evaluated on the various grids confirms the robustness of the method.

A good overall agreement was found between the measurements and the simulation for velocities, the pressure measured in the motored case was also captured by the simulation. The simulation of the fired engine showed a well-captured flame propagation. The flame front geometry obtained in the simulation shows a remarkable similarity to the experiment in terms of the volume of the flame kernel, its level of corrugation, and its propagation speed. The pressure was however predicted during the late combustion phase, as the large crevice of the optical engine traps a large mass of unburned reactants, keeping the overall pressure very low.

Overall, the strategy of using Lagrangian particles for describing the moving parts of an engine on a simple structured grid with isotropic LES filtering and a central discretisation scheme is shown to be accurate and of high algorithmic efficiency, permitting efficient parallel simulations on thousands of processor cores.

nguyen.thuong@uni-due.de

W1P106 PENETRATION OF FLAME AND BURNT GASES INTO THE TOP-LAND CREVICE – LARGE-EDDY SIMULATION AND EXPERIMENTAL HIGH-SPEED VISUALIZATION

Sebastian Kaiser, Peter Janas, Martin Schild, Andreas Kempf, University of Duisburg-Essen, Germany

In spark-ignited internal combustion engines, the top-land crevice (the space between cylinder and piston above the top-most piston ring) is known to be the source of unburned hydrocarbon emissions. This is because the flame cannot propagate entirely into the crevice, leaving unburnt mixture behind. Many implementations of optical access in single-cylinder research engines require enlarging the crevice volume many times beyond that of a production engine. On one hand, such top-land crevices are not representative of production geometries, on the other the optical access to this area is excellent, and therefore, the possibility exists to study the phenomena in this area in detail.

In fact, high-speed imaging of combustion clearly shows a luminous front with an irregular pattern, subject to cyclic variability, penetrating into the top-land crevice. With surprising similarity, large-eddy simulations with a progress-variable model of combustion show the same phenomenon. The fact that a front is seen in the crevice does not necessarily mean that high-temperature reactions are occurring. It could simply be that hot gases (with luminosity from hot reaction products) are being pushed into the crevice by volume expansion due to combustion in the main chamber. Nevertheless, the phenomenon is interesting and lends itself to experimental and numerical investigation. Thus, for further discussion, this poster presents preliminary data from both optical engine and large-eddy simulation.

The simulations are performed with OpenFOAM, using an implicit pressure-based algorithm. The mesh is based on hexahedral cells with an average cell size of 1 mm in the combustion chamber and 0.125 mm inside the crevice volume. The sub-grid stresses are calculated with the standard Smagorinsky model. Combustion is modeled with the algebraic Flame Surface Density model (FSD) proposed by Weller. In order to stop the flame from burning inside the crevice volume, the reaction source term of the Favre-filtered transport equation for the progress variable is set to 0 there, and only the convective and diffusive transport are applied. This remaining convective transport of the progress variable accounts for the hot gases pushed into the crevice gap – leading to a remarkable qualitative similarity between experiment and simulation.

sebastian.kaiser@uni-due.de

W1P107 INVESTIGATION OF ROLE OF PLASMA FOR LASER-INDUCED BREAKDOWN IGNITION IN FUEL-RICH PREMIXED ETHANOL SPRAY FLOW

Takehiko Seo, Yuki Ishimura, Masato Mikami, Yamaguchi University, Japan

As combustion technology of the IC engine has been developed to reduce pollutant emissions and improve thermal efficiency, ignition using the spark plug has become difficult. Laser-induced breakdown ignition is a promising ignition

method using high energy density plasma generated by converging laser beam as ignition source. In previous study, many plasmas were generated by fuel droplets and the volumetric ignition had been suggested in fuel spray flow. However, the ignition mechanisms have not been clarified. In present study, ignition experiments were conducted in fuel-rich premixed ethanol spray flow under atmospheric pressure, the relationships of the growth of flame kernel and plasmas in ethanol premixed spray flow were investigated to clarify the ignition mechanisms. The third harmonic of the Q-switched Nd:YAG laser was used as a laser source. Ethanol spray generated with the ultrasonic nebulizer was supplied around the focal position. Total equivalence ratio of fuel-rich premixed ethanol spray flow was controlled by the flow rate of air as the carrier gas for spray. Schlieren image of flame kernels and plasmas were taken by high-speed CMOS camera. Some plasmas generated by the existence of the ethanol droplets inside the premixed flow could be seen. However, the generated plasmas did not always contribute to ignition. In addition, it was found that there are some plasmas inhibiting the growth of the flame kernels.

tseo@yamaguchi-u.ac.jp

W1P108 TRANSIENT PLASMA DISCHARGE IGNITION FOR INTERNAL COMBUSTION ENGINES

Si Shen, Kanchana Gunasekera, Jie Yang, Jonathan Flamenco, Paul D. Ronney, University of Southern California, United States

The use of non-thermal Transient Plasma Ignition (TPI) as an alternative to Spark Ignition (SI) for internal combustion engines was investigated for possible benefits of increasing engine efficiency. Bench tests in quiescent and turbulent constant-volume combustion chambers showed typically 3x shorter ignition delays and pressure rise times with TPI than with SI, as well as higher maximum pressures in constant-volume combustion chambers. These results suggest the possibility of using transient plasma discharges to enhance performance of combustion engines. In this work the feasibility of employing TPI in low turbulent internal combustion engines is assessed.

For on-engine testing a 2000 Ford Ranger 2.5 liter dual-plug engine was used. One cylinder was fitted with the TPI electrode in one plug port. The other spark plug port was fitted with a modified spark plug containing a Kistler pressure transducer. An optical encoder was used to measure crank angle information and in concert with the cylinder pressure data to create P-V diagrams. A disc-shaped electrode (courtesy of Transient Plasma Systems, Inc.) was used for the TPI testing. Results obtained at varying engine load, intake pressure, equivalence ratio and ignition timing showed an increase in burning rates with TPI, which was attributed to its multi-site ignition compared to single-point ignition with conventional sparks. With this motivation we were encouraged to reverse-engineer the #1 cylinder to produce very low in-cylinder turbulence (which would normally cause poor performance due to slow burn) and use TPI to “restore” the lost burning rate. This low-turbulence cylinder was accomplished via smoothing the intake port; removing most of the intake valve guide boss; reducing the degree of bending in the intake port to reduce swirl and adding grooves to the intake valve seat, just downstream of the ring of contact between the valve and the cylinder head. This combination of TPI + low turbulence was found to result in approximately the same burning rate as with spark ignition + conventional turbulence, but with less heat loss and thus higher indicated thermal efficiency, with no increase in engine emissions. It is concluded that low-turbulence, TPI-ignited engines may provide a simple, practical alternative to HCCI, DISC and other advanced engine concepts for some applications.

sishen0525@gmail.com

W1P109 THE EFFECT OF DISCHARGE-INDUCED RADICALS ON FLAME KERNEL FORMATION: A COMPREHENSIVE SPARK IGNITION MODEL

Seong-Young Lee, Anqi Zhang, Xiucheng Zhu, Jeffrey Naber, Michigan Technological University, United States

Fuel-lean and dilute combustion is believed to be beneficial for spark-ignition engine efficiency, while it makes the ignition more difficult and causes potential problems. Understanding of electrical discharge as an ignition source started decades ago. It has been well understood that three distinct phases, the breakdown, arc and glow phases, can be recognized from the very transient discharge process. The high-power discharge ionizes a small fraction of gas within the spark plug gap and forms a plasma channel, which is of high temperature and energy level and serves as ignition source. It is a key question in spark ignition that how much electrical energy was used effectively for combustion initiation. In terms of spark ignition modeling, most of current models considered the thermal effect of the plasma channel as the energy source. Efforts have been made in this study to obtain a more detailed description of this ignition source by means of experiments and numerical simulation. Spectroscopy measurements of the plasma channel indicate the existence of several radicals that would also be active in the initial combustion processes. These radical effects are combined with thermal effect as energy source in a 3-D CFD model using CONVERGE code. This model has also considered reaction mechanism and local turbulence in the vicinity of the spark plug. Several validation and application conditions are followed to access the model performance.

sylee@mtu.edu

W1P110 AN ANALYSIS OF ION CURRENT IN A CONSTANT-VOLUME COMBUSTOR

Seiya Hitomi¹, Yoshiki Noguchi¹, Ralph Aldredege², Yuki Tsuzuki²

¹Ryukoku University, Japan ²University of California, United States

To know the combustion state of the car engine which senses an ion current in the combustion reaction. Ion current is

generated by the ion which is a kind of chemical species in the combustion reaction. Figure 1 also shows the ion current waveform obtained by using the ion probe.

There are three peaks of the ion current. Peak I is the ion current that occurs when the piston of the engine comes to top dead center. Peak II is the ion current that occurs when the piston moves to the bottom dead center from the top dead center. Then, at the end of the peak of II, small peak once again exists. I named this the peak II'. Peak III is the ion current that occurs after the piston reaches the bottom dead center and the exhaust valve opens. Since the ion current waveform of peak I and II are already known.

Peak I is the noise at the time of the ignition and Peak II occurs after the combustion reaction, which means after the flame has arrived. However, peak II' is detected again at the end of the peak II. But we do not know the cause of peak II'. The ion current peak III is generated after completion of the combustion reaction. Also the cause of peak III is unknown. The purpose of this research is to find the cause of the ion current waveform of II' first.

To experiment with a real engine is difficult. Therefore, I will use a constant volume combustor. Since this can keep the volume constant, the combustor makes the experiment easier.

Shape of the combustion chamber has length of 55mm, width of 95mm, and thickness of 30mm. Quartz glass of thickness 20mm is attached to both sides of the combustion chamber, so it is possible to check the state of flame propagation from outside. I use an ion probe to detect the ion current in the flame.

In addition, I will also use simulation software. I will be using both simulation and experiment to approach the investigation of the causes of peak II'. The simulation software used is the Open Form.

Ion probe can detect the flame surface because ion concentration is high only around the flame. By analyzing the ion current waveform, the ion distribution in the flame front can be seen. It is also possible to see the shape and behavior of the flame when the flame passes through the ion probe.

The simulation result of the pressure when the flame arrives at the ion probe indicates the change appears in the pressure before and after the flame. The pressure on the left side of the flame is greater than the pressure exerted on the right hand side of the flame.

And the simulation results of the flame position indicates that after the flame arrives at the ion probe, the speed of the flame is slow and stagnation in the vicinity of the ion probe by the pressure from the results of simulation. When the pressure of the constant-volume combustor is high, flame is stagnation in the ion probe vicinity and think peak II' can be detected.

y-noguch@rins.ryukoku.ac.jp

W1P111 RCM CHARACTERIZATION INITIATIVE: TOWARDS HARMONIZING IGNITION DATA

Guillaume Vanhove¹, Scott Goldsborough², Chih-Jen Sung³, Henry Curran⁴, Margaret Wooldridge⁵

¹Université de Lille 1 Villeneuve d'Ascq, France ²Argonne National Laboratory, United States

³University of Connecticut, United States ⁴National University of Ireland, Ireland ⁵University of Michigan, United States

Rapid Compression Machines (RCMs) have become widely-used experimental platforms employed to acquire fundamental insight into fuel ignition and pollutant formation chemistry, as well as fluid dynamics – chemistry interactions, especially at conditions that are relevant to current and future combustion engines, such as low temperature combustion regimes. Initially configured using simple mechanical designs, they enabled some of the first detailed studies of autoignition and flame propagation at elevated pressure and moderate temperature conditions, and the results facilitated insight into the processes controlling single-stage and multi-stage ignition, and other complex chemical phenomena like negative temperature coefficient behavior.

RCMs have evolved into sophisticated apparatuses that can be used to create and maintain well-controlled, elevated temperature and pressure environments representative of conditions found in combustion engines (e.g. $T = 600$ to 1100 K, $P = 5$ to 80 bar) where the chemically-active period leading to auto- and assisted-ignition can be monitored and probed via advanced *in situ* and *ex situ* diagnostics. The operational range of RCMs is complementary to other laboratory platforms such as shock tubes and flow reactors, and datasets acquired with RCMs are often utilized as validation targets for chemical kinetics and fluid dynamics – chemistry interaction models, quantitative understanding of fuel reactivity and towards the development of reduced-order models for engine system simulations.

There are currently more than twenty laboratories worldwide that utilize RCMs for investigations of gas-phase processes, including autoignition, Homogeneous Charge Compression Ignition (HCCI) and spark-assisted compression ignition, and development of novel ignition technologies. A wealth of fundamental and applied knowledge has been generated using RCM-based experimental methods. A review of recent literature indicates that there has been significant growth over the past two decades in the number of investigations conducted with RCMs, as well as associated model development and validation based on RCM datasets. This has been primarily driven by the evolving needs of the combustion engine community where an understanding of low and intermediate temperature fuel chemistry and related phenomena has become essential.

Even after many years of development however, opportunities still exist for improving the methods for reporting and representing RCM data, such as quantifying facility-dependent effects like heat transfer, and formulating alternative approaches for comparing RCM data with datasets from other devices such as shock tube and flow reactors. These opportunities represent the principal motivation for this characterization initiative. A primary goal of this initiative is to provide methods for interpreting and reporting data from ignition studies conducted using diverse RCM technologies. To achieve this goal, a combination of experimental and modeling procedures has been adopted:

Twelve international research groups have acquired ignition data for *iso*-octane at similar state and mixture conditions in the form of pressure time histories at reactive and non-reactive conditions; Detailed chemical kinetic simulations will be conducted using a variety of approaches; Modeling is undertaken with help from CFD codes, in order to provide information on the aerodynamic conditions after compression for a number of RCMs and the interaction of these with ignition chemistry; Additional analyses of the data will help understand the uncertainties of RCM data and will guide improved methods for reporting experimental and modeling results.

Other groups working on ignition experiments are welcome to join the initiative. In particular, experimental data at comparable mixture composition and state conditions are most welcome.

guillaume.vanhove@univ-lille1.fr

W1P112 COMPUTATIONAL INVESTIGATION OF SYNGAS AUTOIGNITION BEHAVIOR AT HIGH PRESSURE AND LOW TEMPERATURE CONDITIONS IN THE PRESENCE OF THERMAL INHOMOGENEITIES

Pinaki Pal¹, Andrew Mansfield¹, Margaret Wooldridge¹, Hong Im²

¹University of Michigan, United States ²King Abdullah University of Science and Technology, Saudi Arabia

The study aims to improve our understanding of SYNGAS combustion under high pressure (up to 30 bar) and moderate/low temperature ($T < 1000$ K) conditions, applicable to modern gas turbines using high hydrogen content fuels derived from coal or alternative sources. In particular, there is a marked discrepancy between ignition delay times predicted by zero-dimensional chemical kinetic models and experimental measurements. Recent experimental studies have suggested that the resultant SYNGAS ignition regime is connected to thermal non-uniformities in the unburned gas. The objective of the present study is to computationally investigate the effects of thermal inhomogeneities on SYNGAS ignition characteristics at conditions relevant to gas turbine operation. A simple one-dimensional model incorporating detailed chemistry and transport is employed to analyze the ignition behavior. Parametric studies considered are the molar $H_2:CO$ ratio of 0.7:1, the overall equivalence ratios of $\phi = 0.1$ and 0.5, the mean temperature of 900-1100 K, and a pressure range of 3-20 atm. A sinusoidal temperature profile with varying levels of root-mean-square fluctuation is set as initial condition, thereby resulting in different magnitudes of imposed thermal gradient. Compression heating effects are taken into account by specifying periodic boundary conditions.

The results show that an ignition kernel first develops at the location of highest temperature near the center of the domain. Subsequently combustion waves emanate from this location. As the fronts propagate, the remaining charge gets heated up by compression, thereby accelerating the ignition of the end-gas mixture. At high temperatures, the reaction front is observed to be chemistry-controlled (spontaneous ignition front) with front speed much higher than the laminar flame speed at the mean state condition. As the mean temperature is lowered, however, molecular transport becomes more important (deflagrative front). The critical mean temperature separating the regions of the two distinct ignition modes is computed using a predictive criterion that incorporates the effect of chemical kinetics, thermo-physical properties and device-dependent thermal characteristics on the autoignition behavior. Non-dimensional criteria based on the front speed and Damkohler number are also identified. It is also found that the front behavior may shift back from deflagrative to spontaneous ignition regime at sufficiently low temperatures. This is attributed to passive scalar dissipation, which modifies the statistics of the pre-ignition temperature field, by way of dissipating fluctuations before any significant reaction occurs. Mixing has a pronounced effect when the mixing time scale is of the same order of the homogeneous ignition delay at the mean condition. The present work is currently being extended to investigate the effect of localized thermal hot spots on SYNGAS autoignition behavior. Subsequently, 2D Direct Numerical Simulations (DNS) will be employed to understand the statistical effects of turbulent fluctuations in temperature and/or scalar fields on SYNGAS ignition characteristics at high pressure and low temperature conditions.

pinaki@umich.edu

W1P113 IGNITION OF COMBUSTIBLE MIXTURES BY A SURFACE NANOSECOND DISCHARGE IN A RAPID COMPRESSION MACHINE

Mohamed A. Boumehdi¹, Sergey Stepanyan¹, Sergey Shcherdanev¹, Svetlana Starikovskaya¹, Pascale Desgroux², Guillaume Vanhove²

¹University of Pierre and Marie Curie, France ²Université de Lille, France

Recently, pulsed nanosecond discharges are intensively studied as an efficient tool to ignite combustible mixtures at low initial temperatures or under lean conditions. Low temperature non-equilibrium plasmas provide, locally or distributed in space, an additional density of active species and supplementary gas heating due to the relaxation of the electronically excited states.

A nanosecond Surface Dielectric Barrier Discharge (SDBD) was used to initiate combustion at moderate to high pressures in a Rapid Compression Machine (RCM) at the University of Lille. The discharge has a quasi-uniform radial geometry and was located in the proximity of the end plate of the combustion chamber of the RCM. Experiments were performed for methane, *n*-butane and *n*-heptane/ O_2 mixtures diluted by Ar or N_2 for core gas temperatures at the end of compression respectively ranging from 620 to 1000 K.

For the experiments carried out with methane and *n*-butane containing mixtures, a significant decrease of the ignition delay time is observed when the energy deposit in the discharge reaches a given value. Under this energy value, the system behaves as in the AutoIgnition (AI) conditions. The existence of a Minimal Ignition Energy (MIE) depending on the initial conditions was therefore demonstrated. The effect of the voltage (amplitude and polarity) on the electrode on

the ignition delay for Plasma Assisted Ignition (PAI) was studied. Under these conditions, it was shown that when the deposited energy increases, the heat release rate increases. These results were correlated with high speed imaging experiments, showing the propagation of the flame front from the electrode towards the piston.

For *n*-heptane mixtures, a modification of the ignition behavior by the discharge has been demonstrated. When the discharge energy increases, the reactive system evolves from a situation where no ignition is observed, to a plasma induced cool flame occurring tens of ms after the discharge and followed by ignition and finally, to fast ignition as in the other mixtures at high energy values. To our knowledge, this is the first experimental observation of a plasma initiated cool flame.

sergey.stepanyan@lpp.polytechnique.fr

W1P114 LARGE-EDDY-SIMULATION OF RICH-QUENCH-LEAN COMBUSTOR

Masahiro Uchida, Shintaro Ito, IHI Corporation, Japan

Rich-Quench-Lean (RQL) combustion concept is frequently used in power generation and aviation gas turbines. The prediction of RQL combustor performance is more complex than for other combustion concepts such as Lean-Direct-Injection because of non-linear interaction of different combustion behaviors in rich and lean zones. Verification and validation of LES for the RQL combustion concept will promote the use of LES in the development of new combustors. Lab scale experiments with a kerosene-fueled, single-swirler combustor were conducted to obtain gas concentration profiles in both zones. The results show that CO concentrations in the rich zone are 6 vol% or more. LES computations with simplified chemistry show that the choice of the chemistry has a strong impact on the CO concentration profiles. Results with two and four step chemistry predict 2% or less CO concentration in the rich zone, while results with a ten step mechanism including NO_x show good agreement with the experimental results.

masahiro_uchida_1@ihi.co.jp

W1P115 THE INTERACTION BETWEEN PILOT AND MAIN FLAMES IN A DUAL SWIRL COMBUSTOR

Taejoon Park¹, Keeman Lee¹, Dongsoo Noh²

¹Sunchon National University, Korea ²Korea Institute of Energy Research, Korea

The lean premixed combustion has advantage of reducing NO_x emission by a low flame temperature. But lean premixed flame behavior has flashback and lean blow-off which are determined by turbulent burning velocity and mixture composition. One of methodology to expand stable region is to produce combustion configuration with partially premixed flame (pilot) and premixed flame (main) at the same time.

In this study, the various flame behavior and interaction between pilot flame and main flame in a dual swirl combustor of micro gas turbine for a distributed power generation have been investigated. A burner concept indicating a combustion of swirling jet partially premixed and premixed flames was adopt to achieve high flame stability as well as clean combustion. Pilot swirl angles were systematically varied as three cases (15°, 30°, 45°) under the condition of fixed main swirl angle as a 45°. The results show that the variation of pilot swirl angle and total heat release rate affected in the significant change in flame shape and emission characteristics due to the change in recirculating flow pattern of swirling flow field. Thus, pilot swirl angle of 15° produced more NO_x emission compared to the 30° and 45°, which were confirmed by ICCD images with the distribution of high OH* chemiluminescence intensities at the flame base. To analyze the changes of combustion field with respective to the pilot swirl angles, the measured CH* chemiluminescence images were also compared with the numerical result (R1 reaction rate). The used numerical reaction model was the Eddy Dissipation Concept (EDC) with 3 reaction steps.

In case of pilot swirl angle of 15° (Image-(a)), the overall flame including main and pilot flame was reacted at over the nozzle throat due to the low swirl intensity. Also, high R1 reaction rate was mainly distributed at flame base in numerical result. For pilot swirl angle of 30° (Image-(b)), overall flame was reacted under the nozzle throat, and high R1 reaction rate continuously distributes from burner exit. But, the pilot flame of swirl angle 45° (Image-(c)) was reacted at end of fuel nozzle due to the high swirl intensity. And, it could see that high R1 reaction rate in numerical result doesn't continuously distribute from burner exit. Which are because high reaction rate was mostly distributed by main premixed flame.

To confirm this phenomenon, numerical analysis of flame temperatures was systematically conducted by dividing the combustion configurations into three cases, that is, only pilot flame (case1), pilot flame with swirling air of main burner (case 2) and pilot and main flame (case 3). Case1, case2 and case3 were similar in temperature distribution trend at pilot swirl angle of 15° and 30°. But pilot swirl angle of 45° wasn't similar in other swirl angles. Whereas the pilot swirl angle of 15° and 30° was mostly burned by pilot flame, the pilot swirl angle of 45° was mostly burned by main flame.

tjpark@scnu.ac.kr

W1P116 COMBUSTION INSTABILITY MODE IN DUAL SWIRL GAS TURBINE MODEL BURNER BY HS-PLIF AND CHEMILUMINESCENCE MEASUREMENT

Keeman Lee, Inchan Choi, Sunchon National University, Korea

The stabilization of turbulent flames is the most important problem of the gas turbine combustor. Especially thermo-acoustic instabilities are common phenomena existing in combustion chambers, when the combustions are under the

condition of lean premixed combustion to reduce the emission of NO_x . Combustion instability is a serious obstacle for the lean premixed combustion of gas turbines and can even cause fatal damage to the combustor and entire system. Thus the improved understanding of mechanisms of combustion instability is necessarily required in the design and operation of gas turbine combustor.

The present study described the experimental investigations of combustion instability mode in a lean premixed dual swirl combustor for micro-gas turbine system. When such the instability occurs, a strong coupling between pressure oscillations and unsteady heat release excites a self-sustained acoustic wave which results in a loud, annoyed sound and may also lead a structural damage to the combustion chamber. The detailed period of flame behavior and heat release in combustion instability mode have been examined by flame tomography with high speed CH PLIF system and CH^* chemiluminescence measurement using a high speed ICCD camera operated at 10kHz and 6kHz each.

The swirling CH_4/air flame was investigated with overall equivalence ratio of 1.1 to lean blowout limit of methane fuel. Experiment results showed that the unstable flame behavior not heat release oscillations had a different frequency with 200Hz (Fig.1) and this frequency was corresponded with about 1/2 sub-harmonic of resonance frequency to coincide with large amplitude acoustic pressure frequency driven by heat release oscillations (Fig.2). This is very interesting finding that have not reported yet from other previous works. Therefore, when the thermo-acoustic instability with Rayleigh criterion occurs, the fact that the period between heat release and flame behavior is different each other was proposed through this work for the first time.

This result provides the information which could be newly added in the combustion instability mechanism involving a resonant feedback between the unstable heat release and system acoustics for gas turbine with lean premixed combustion.

kmlee@snu.ac.kr

W1P117 DYNAMICAL STRUCTURE OF THERMOACOUSTIC COMBUSTION OSCILLATIONS IN A LABORATORY-SCALE GAS-TURBINE MODEL COMBUSTOR

Yuta Okuno, Shohei Domen, Hiroshi Gotoda, Ritsumeikan University, Japan

Of current interest in modern combustion physics and related branches of nonlinear science is to obtain a better understanding of nonlinear process underlying combustion instability. Gotoda has relatively recently conducted the experimental investigation on nonlinear dynamics of the pressure fluctuations in a lean premixed gas-turbine model combustor from a viewpoint of chaos theory. They reported that the pressure fluctuations near blowout are ascribed to stochastic process with self-affine structure, while those are ascribed to low-dimensional chaotic oscillations. On the basis of the nonlinear nature of the pressure fluctuations extracted by nonlinear time series analysis, two of authors have clearly showed the availability of chaos theory to the early detection and suitable control of combustion instability. These studies focused on analyzing the pressure fluctuations, but the dynamical structure of the OH^* chemiluminescence intensity, which is an important indicative of the heat release ration fluctuations, remains to be fully elucidated in the present-day combustion research area. In this Work-In-Progress section, we mainly investigate the dynamical structure of the OH^* chemiluminescence intensity fluctuations using the colored version of the recurrence plots.

rm0002hk@ed.ritsumei.ac.jp

W1P118 INVESTIGATION OF TURBULENT COMBUSTION IN A GAS TURBINE COMBUSTOR BY THE SCALE-ADAPTIVE SIMULATION METHODS

Seyfettin Ertan Hataysal¹, Ahmet Yozgatligil²

¹Tusas Engine Industries, Turkey ²Middle East Technical University, Turkey

A Scale Adaptive Simulation (SAS) method proposed by Menter and Egorov is applied to the combustion in a realistic prototype combustor in this study. SAS model dynamically adjusts the turbulence scales by using the Von Karman length scale. By utilizing this approach, it is possible to obtain detailed transient field results in unsteady regions of the flow field and classical RANS solutions in stable flow regions. Non-premixed combustion model with tabulated chemistry for the kerosene is utilized for liquid kerosene combustion. A flamelet library is prepared for the composition of the chemical species and temperature inside the domain for the changing turbulence character. Injection, turbulent mixing and evaporation of the liquid droplets are also modeled inside the combustor. The modeling outputs are compared with the experimental results of a prototype combustor which are also presented in this study. Experiments give out extensive output about the transient temperature values at the exit section. Furthermore, the transient distribution of the major species like CO_2 and H_2O are presented at the exit section. A combustion efficiency calculation is also given for the model and experimental cases. Experiments are performed for different fuel air ratios and as a result different operating points of the chamber are investigated throughout the study. Time averaged and instantaneous point wise measurements are served for changing values of fuel air ratio. The experimental results are compared with the output of the SAS analysis. A further investigation is performed by comparing the test case with the classical URANS results. Comparison of the URANS, SAS and experiment values are presented in this study. The advantages and shortcomings of the methods are evaluated and discussed in the context.

sehataysal@gmail.com

W1P119 FLAMEHOLDING PROPENSITIES OF SMALL FEATURE STABILIZED HYDROGEN AND NATURAL GAS

FLAMES AT HIGH TEMPERATURES AND PRESSURES

Vincent G. McDonell, Elliot Sullivan-Lewis, University of California, United States

To increase efficiency, gas turbines are being operated at increasingly high pressure ratios and high combustor inlet temperatures. Lean-premixed operation of gas turbines is extensively used to reduce the emissions of nitrogen oxides from combustion. Furthermore, hydrogen containing fuels are gaining interest because they can be generated from low cost feedstock (coal and biomass) and because of potential environmental benefits. However, simultaneously increasing combustor inlet temperatures and pressures while premixing the fuel and air upstream of the combustion chamber leads to a significant risk of flashback, which occurs when the flame from the combustion chamber propagates upstream into the engines premixing zone. This can render the engine inoperable due to hardware damage. Preventing damage associated with flashback is a significant concern for lean premixed gas turbines, especially when the fuel has a high hydrogen content. Engine damage from flashback can be avoided in two ways: combustors that prevent flashback from occurring can be used, or upstream hardware that will not allow a flame to anchor should a flashback occur can be implemented. An experiment was constructed to determine the flameholding tendencies of hydrogen and natural gas at elevated temperatures and pressures, similar to those found in the premixing passageways of a gas turbine. Tests were conducted at pressures up to 9 atm, temperatures up to 750K, and free stream velocities up to 100 m/s. Flames were stabilized in the wakes of small bluff body and wall features that are typical of premixer passage ways (spokes, steps, etc). In addition to performing experiments with hydrogen, natural gas was tested in order to compare with existing experimental work performed with hydrocarbons. The results of these experiments were analyzed to produce correlations that predict the point of flame extinction.

mcdonell@ucicl.uci.edu

W1P120 ACTIVE COMBUSTION CONTROL OF AUGMENTOR INSTABILITY

Kenneth Yu, Sammy Park, University of Maryland, United States

Active combustion control experiments were performed in a model augmentor operating at a naturally unstable combustion mode. The model augmentor consisted of a two-dimensional v-gutter flame-holder placed in a rectangular test section, which was attached to the exit of a primary burner through an acoustic isolator. The augmentor has a Reynolds number of 15,000, a thermal output of 100 kW, and an inlet temperature of 500 K. The objectives were to examine the effect of the primary burner, which could interact with the augmentor instability, and to assess the practicality of using alternative fuels for active control. By parametrically varying both the inlet velocity and the augmentor equivalence ratio, an augmentor stability map was constructed for various primary burner equivalence ratios. A naturally unstable operation at 25 m/s and augmentor equivalence ratio of 0.65 was selected for further active control testing. Schlieren images and CH* chemiluminescence of unstable augmentor operation exhibit a 'flapping' motion of the v-gutter wake and large-scale vortices in the shear layers, which occur at the instability frequency. Furthermore, the phase-averaged data reveal changes to the flame length consistent with the flapping motion. The active control system in this study followed a typical approach of using a closed-loop pulsed secondary fuel injection. Preliminary testing using the controlled secondary fuel injection showed effective damping of the flame motion. The optimized timing of secondary fuel injection is relatively insensitive to the alternative fuel type, as long as the actuator fuel spray characteristics are comparable. Additional testing and analyses are being conducted for selected conditions. Lastly, an investigation is currently in progress to test the feasibility of using secondary injection of air for augmentor instability suppression.

yu@umd.edu

W1P121 COMBUSTION INSTABILITY ANALYSIS FOR PARTIALLY PREMIXED SWIRLING SYNGAS BURNERS

Youngjun Shin, Kiyoun Jung, Seungtaek Oh, Yongmo Kim, Hanyang University, Korea

SYNthesis GAS (SYNGAS) is a mixture of hydrogen and carbon monoxide and can be obtained from natural gas, coal, petroleum, biomass and even organic waste. SYNGAS is less expensive and can be used for clean combustion resulting in a significant reduction in pollutant emissions. One promising application of SYNGAS as a direct fuel in Integrated Gasification Combined Cycle (IGCC) units used to generate electricity from coal, petroleum coke or heavy residuals. The composition of SYNGAS fuels can vary greatly depending on the source and the processing technique. The variability in SYNGAS composition substantially modifies stationary and non-stationary combustion processes such as pollutant emissions, flame structures, flame stabilization (flame liftoff, blowout, and flashback). The high temperatures involved in hydrogen combustion can lead to high NO_x emissions. To control the NO_x emission in the non-premixed gas turbine combustor, the SYNGAS is burned with the high levels of N₂ or steam dilution. In the optimal design analysis of the SYNGAS-fuelled combustion systems, the very reliable numerical and physical models are need to realistically represent physical processes involved in the turbulent SYNGAS flames. Since the caloric heating value of the SYNGAS is relatively low, the SYNGAS flames with the high volumetric flow rate in IGCC gas turbine combustor are highly susceptible to flame instabilities as well as combustion instabilities. Thus, flame stabilization and combustion instabilities are a main concern especially in the low-emission SYNGAS combustors.

The present study has been mainly motivated to investigate the flame-acoustics interaction in the turbulent partially premixed flames encountered in the actual IGCC SYNGAS diffusion-type combustors. Special emphasis is given on the effects of pressure and wall cooling. To validate the prediction capability of the present LES-based combustion model, the

partially premixed burner devised at University of Twente has been chosen as the benchmark case. Computations are made for two example cases including 40kW/ air factor 1.4 and 60kW/ air factor 1.25. In terms of the 1st and 2nd longitudinal mode, the natural frequencies are slightly overestimated. However, numerical results clearly indicate that the present approach yields the reasonably good conformity with experimental data such as FFT results and self-excited combustion instability dynamics. Next, we numerically simulate the combustion dynamics in the SYNGAS partially premixed swirl burner experimentally studied at SNU. Computations are performed for two pressure conditions (1atm, 15atm) and two thermal boundary conditions (adiabatic and non-adiabatic wall). Based on numerical results, the detailed discussions are made for the effects of pressure and heat losses on flame structure and flame-acoustics interaction, and driving mechanism of combustion instability in the SYNGAS swirl combustor.

spoonbill85@gmail.com

W1P122 CORRELATION OF DEFECTS IN AIRCRAFT ENGINES BY OPTICAL MEASURING EXHAUST GASES AND NUMERICAL ANALYSIS

Christoph Hennecke, Friedrich Dinkelacker, Leibniz Universität Hannover, Germany

The inspection of aircraft engines is a complex and time-consuming process, often requiring disassembling the engine or extensive boroscopic examinations. Detecting failures in the combustion chamber of an aircraft engine during the operating time may improve the resource management and the availability of the system. Aim of the ongoing research project is to find an approach to evaluate the state of the jet engine by analyzing the temperature and emissions field in the exhaust jet, as shown in Figure 1. For this new method the major assumptions are: impacts caused by defects propagate to the engine's exhaust, these effects can be measured outside the engine in the exhaust gases and by an inverse correlation using numerical approaches the sources of defects may be located. The temperature profile of the exhaust jet is measured with spatial resolution by an appropriate optical measurement technique, backward oriented schlieren, whereas the emissions field will be evaluated by the tunable diode laser absorption spectroscopy. The connection between failures and measurable exhaust gas pattern is done numerically. The current work focuses on this inverse approach. The feasibility of this approach is shown for a pilot scaled combustor, which provides optical access. It consists of an atmospheric tubular combustor with a premixed swirl burner with a maximum output of 450 kW. As a typical error in jet engines is related to faulty supply of cooling air generated from liner failures, the current study focuses on this aspect. It is observed that it is possible to determine the position and strength of an assumed defect from temperature profiles which also provide information about the type of failure.

The current CFD simulations are performed as RANS simulations using the extended coherent flame model, however due to the high swirl and transient nature of the flow field, hybrid RANS/LES models are preferred to achieve better accuracy at optimum computational capacity, what is part of the future work.

Hennecke@itv.uni-hannover.de

W1P123 EVALUATION OF CFD MODELS TO PREDICTING NO_x EMISSIONS IN A GAS TURBINE COMBUSTOR

Fulin Lei, Institute of Engineering Thermophysics, China

Integrated Gasification Combined Cycle (IGCC) is a promising way for future power generation, thus the study of SYNGAS turbine combustors is of great importance. CFD simulation provides an effective approach to predicting and analyzing the surface temperature and the emissions of combustors, which will aid to the improved design of combustors. Because the flow field in the combustor is complex, it is necessary to evaluate the suitability of different models for the CFD simulation of SYNGAS combustors.

A standard methane swirl flame configuration at Sydney University, whose flow pattern is similar to the SYNGAS combustor, is numerically studied using four different turbulence models including standard κ - ϵ , realizable κ - ϵ , RNG κ - ϵ and Reynolds Stress Model (RSM), coupled with non-premixed combustion model of the assumed-shape Probability Density Function (PDF) of mixture fraction and GRI-Mech 2.11 skeleton kinetic mechanism. The calculated profiles of velocity and temperature by different turbulence models are compared with the experimental data, and the realizable κ - ϵ model shows the best agreement, although it under predicts slightly the dissipation rate of velocity.

According to the theory of κ - ϵ model, the constants of source terms in the ϵ equation affect the velocity dissipation rate. Base on the ϵ equation of realizable κ - ϵ model, increasing the constant of C_2 in source term will lead to the increase of the velocity dissipation rate. Different C_2 values of 1.9, 2.0 and 2.1 are used in the simulations, and the calculated results of velocity, mixture fraction and temperature with $C_2=2.0$ show better agreements with experimental data.

An experimental study on a scaled turbine combustor of SYNGAS is conducted to verify the above conclusion. The liner surface temperatures and the NO_x emissions of the combustor calculated using the modified realizable κ - ϵ model coupled with the EDC (Eddy Dissipation Concept) combustion model and a detailed SYNGAS kinetic mechanism agree well with the experimental measurements. It can be concluded that the modified model is suitable for the CFD simulation of combustion characteristics and NO_x emissions in the SYNGAS turbine combustor.

leifulin@iet.cn

W1P124 DEVELOPMENT OF A HYBRID-MODEL FOR CH₄ EMISSIONS IN BIOGAS ENGINES

Kalyan Kuppa, Ansgar Ratzke, Friedrich Dinkelacker, Leibniz Universität Hannover, Germany

Gas engines show a huge potential for the reduction of CO₂ emissions. However, Unburnt HydroCarbon (UHC) emission can be a significant greenhouse gas contribution for gas engines. Aim of the ongoing research project is the development of a calculation procedure to quantify the local UHC sources in the burning chamber which is also applicable for complex three dimensional geometries and which regards the local flow and turbulence conditions. A direct integration of the reaction rate calculation into the CFD flow calculation is not possible. Hence, a hybrid-model is proposed to integrate the detailed reaction kinetics via separate sub models coupled with CFD.

Block (I) includes 1-D reaction kinetic simulations performed using the chemistry solver Cosilab, the GRI 3.0 mechanism is used. A database for laminar flame speeds is created relevant to gas engine conditions, i.e, pressure: 1 bar to 180 bar, temperature: 300 K to 1500 K, equivalence ratios: 1.1 to 0.4 and the Exhaust Gas Recirculation rates (EGR): 0% to 30 %. This laminar flame speed data-base is used to compute the turbulent flame propagation. Different combustion models are tested, it is observed that the AFSW (Algebraic Flame Surface Wrinkling model) provides better results compared to the other tested combustion models for the engine conditions. The AFSW model is implemented through a user defined function in ANSYS Fluent for the CFD simulations. Block (II) includes a computational model implemented to determine the distance at which the flame quenches on the cold walls during the numerical simulation. This model is developed by Ratzke and is based on the experimental work done by Boust. The distance for post-quench oxidation of the boundary fuel after the flame quench is calculated through the 0-D perfectly stirred reactors simulations in block (III), the GRI 3.0 Mechanism is used for the kinetic simulations. The diffusion is taken into account solving the Fick's diffusion equation. The 0-D simulations are performed for the ranges of temperatures between that of the flame and the cold wall, pressures, equivalence ratios and EGR for the engine conditions. A function is developed to calculate the UHC layer thickness on the wall boundaries based on the above models. The validation experiments are currently planned at the Institute of Internal Combustion Engines TU Munich.

kuppa@itv.uni-hannover.de

W1P125 APPLICATION OF A CHEMICAL REACTOR NETWORK FOR PREDICTION OF NO_x EMISSIONS FROM PREMIXED NATURAL GAS AND HYDROGEN ENRICHED FLAMES STABILIZED WITH A LOW-SWIRL BURNER

Vincent G. McDonell, Andres Colorado, University of California, United States

Fuel-flexibility and ultra-low NO_x emissions have become a critical requirement of next-generation gas turbines. Low Swirl Burners (LSB) are emerging as a technology that is able to meet those requirements. Since the burner supports ultra-lean mixtures while also lacking a significant post flame flow recirculation zone, nitrogen originated emissions produced in the flame are extremely low. This paper addresses the numerical prediction of NO_x emissions from a LSB using a Chemical Reactor Network (CRN). The CRN is considered a simplified, but analogous, representation of the fluid-dynamics of the system. Also a parametric analysis of the effect of the Exhaust Gas Recirculation (EGR) and heat losses from the flame on the NO_x emissions is presented. Two fuel compositions are analyzed, (1) pure methane which represents the composition of a typical Natural Gas (NG), and (2) a highly reactive mixture of 90% H₂ - 10% CH₄. Since the prediction based on a CRN is a kinetic based approach, several reaction mechanisms, including the GRI_{mech} 3.0, USC_{mech} II, Konnov 0.5, and Galway III were tested in order to understand the sensitivity of the methodology to the mechanism used. The results obtained with the CRN indicate that most of the NO_x is formed through the N₂O route for the LSB, regardless of the fuel composition or the reaction mechanism used. The CRN predicts trends similar to those observed experimentally, regardless of the reaction mechanism. However, Galway III and GRI_{mech} 3.0 are able to more accurately predict the experimental results for NG, and the USC_{mech} II is more precise for the hydrogen blend. The results also show that fuel enrichment with hydrogen promotes the production of NO_x through the Zeldovich, NNH and N₂O routes while hindering the prompt route, when compared to the NG flames.

mcdonell@uci.cl.uci.edu

W1P126 CHARACTERIZING NO_x EMISSION BEHAVIOR IN THE WAKE OF SINGLE REACTING AIR JET IN RICH CROSSFLOW NEAR THE WALL

Vincent G. McDonell, Howard Lee, University of California, United States

The NO_x emission behavior was investigated in the wake of single reacting air jet in rich crossflow near the wall for its characterization. Various analyses of the overall RQL combustor design to optimize mixing while minimizing NO_x emissions have been carried out in the past. Few studies (Vardakas et al. 1999 & Leong et al. 2000) in particular have found the highest NO_x was found in the wake of the air jet entering the rich crossflow. However, a lack of information exists regarding the details of an individual air jet reacting in the RQL combustor, especially NO_x emission behavior in that region. The images of reacting jet were obtained in two different angles: side view and frontal view. The images from both angles exhibit edges emitting the highest intensity. The highest light intensity can be seen at the leading shear layer of the jet from the side view and at the circumferential edge from the frontal view. The local equivalence ratio analyses of the reacting jet using the cassegrain optical system suggest that the regions emitting the highest intensity are reacting near stoichiometric conditions. The NO_x emission levels are dependent upon reaction temperature primarily through the thermal NO_x mechanism. The determination of local equivalence ratio within the jet, and identification of the regions where the reaction is occurring at near stoichiometric conditions, would give insight into the nature of NO_x formation via thermal NO_x mechanism for the jet in crossflow system. The NO_x emission level was measured using water-cooled probe in the

wake of the jet entrance where the probe was moved across the jet. The NO_x data demonstrate the two peaks in NO_x level. These peaks align with the edge of the jet that were found to be reacting near stoichiometric conditions. The coincidence of peak NO_x level and region of stoichiometric condition suggests the high NO_x was produced via thermal NO_x mechanism. The two peaks in NO_x emission curve is found fairly near downstream of the jet injection, only up to 2 to 3 jet diameters in distance. These results suggest that the thermal NO_x mechanism plays a big role in NO_x emission level in short downstream of jet injection. Although high NO_x peaks disappear far downstream of jet injection, barring any NO_x re-burn, it can be concluded that thermal NO_x mechanism has a big impact on high NO_x level in the wake of the jet.

mcdonell@ucicl.uci.edu

W1P127 COMPARING NO_x AND SOOT FORMATION FOR ALTERNATIVE AVIATION FUELS

Shazib Vijlee, Stefan Bjornsson, Arshiya Chime, Garrett Allawatt, John Kramlich, Ann Mescher, James Hermanson, Philip Malte
University of Washington, United States

In this poster, we compare the formation of oxidizes of nitrogen (NO_x) and black carbon particulate (soot) for alternative aviation fuels. Fischer-Tropsch fuels made from natural gas and coal, and hydro-processed bio-fuels made from fatty acid esters of camelina seed and tallow are tested. JP-8 is used as the reference fuel. The alternative fuels are composed mainly of various alkane isomers, with lesser amounts of normal and cyclo alkanes present. Additionally, the alternative fuels are blended with aromatics. Both a petroleum-based aromatic mixture and a bio-based aromatic of 1, 3, 5 trimethyl benzene are used. The NO_x experiments are conducted in a conical, single-jet stirred reactor operated fuel lean at atmospheric pressure and approximately 2.3 ms residence time. The liquid fuels are vaporized and premixed in a staged, two-temperature zone premixer. For each fuel, NO_x is measured as a function of the measured-corrected combustion temperature, over the range from about 1700 to 2000K. Generally, the aromatic 1,3,5 trimethyl benzene (TMB) shows the greatest NO_x and HP tallow the least, with a ratio of about 1.3. At a common temperature of 1900K, from highest to lowest NO_x : 1,3,5 trimethyl benzene > HP camelina \approx FT coal \approx JP-8 \approx petroleum aromatics > FT natural gas > HP tallow. Generally, jet fuel contains about 20% aromatic content, in order to promote seal swell and lubricity. Blending of the alternative fuels with 20% petroleum aromatics shows interesting behavior: a decrease in NO_x for FT coal and a substantial increase for HP tallow. Chemical kinetic modeling is underway on these trends. Sooting threshold measurements are conducted for these fuels using atmospheric pressure Bunsen and Meker burners. Fuel vaporization and premixing are done by passing heated air into a gauze constructed of steel and glass wool, into which the liquid fuel is injected by a syringe pump. Sooting tendency is determined by measuring the fuel-air equivalence ratio for the initial appearance of yellow tips. The alkane fuels show soot downstream of the blue luminous flame zone, whereas the aromatic (TMB) shows soot forming close to or in the flame zone. 2,2,4 trimethyl pentane (isooctane) is also used in these experiments. Sooting tendency varies as: TMB > isooctane with 20% TMB > JP-8 \approx HP camelina > isooctane. Additional experiments and chemical kinetic interpretation are underway. Soot concentration measurements are being developed. Project goals are to correlate and predict NO_x and soot tendencies for alternative aviation fuels as a function of fuel composition. NO_x and soot behavior as a function of aromatic type and concentration (up to about 20%) may be important for fuel development. This research is supported by the state of Washington JACATI program.

malte@u.washington.edu

W1P128 SURROGATE MODELING OF JET FUELS FOR STUDY OF AUTOIGNITION CHARACTERISTICS AT LOW TEMPERATURE AND LEAN OPERATING REGIMES

Anna Oldani, Daniel Valco, University of Illinois at Urbana, United States

Recently published surrogate models are evaluated for their predictive capabilities of autoignition characteristics for conventional jet fuels. Computational simulation results are compared with experimentally obtained data from Rapid Compression Machine (RCM) tests for conventional jet fuel, Jet A and JP-8. Evaluation of these surrogate models aids in identifying differences in chemical kinetics mechanisms, helping to establish model validity across operating conditions of interest.

Autoignition characteristics are evaluated at compressed pressures, P_c , of 20 bar, compressed temperatures, T_c , of 600 to 800K, and equivalence ratios, Φ , of 0.25, 0.5, and 1.0 in air, representing lean to stoichiometric conditions in the low temperature combustion regime. This is an extension from previous work, which primarily focuses on an intermediate to high temperature range and richer mixtures.

A background on the chemical characteristics of alternative jet fuels is given, focusing on bio-based jet fuels. These fuels are referred to as Hydrotreated Renewable Jet (HRJ) fuels, also termed Hydroprocessed Esters and Fatty Acids (HEFA). HRJ fuels compared with traditional jet fuel have higher paraffinic and lower aromatic content, leading to enhanced ignition. Well-developed surrogate models for conventional jet fuels with an understanding of relevant chemical features will help build robust surrogate models for available alternative jet fuels.

Three chemical kinetic mechanisms are evaluated: the Ranzi mechanism from the CRECK modeling group at Politecnico di Milano, the Aachen mechanism from the Institut für Technische Verbrennung at Aachen University, and the Dooley mechanism from Princeton University. The mechanisms are evaluated using the multi-component surrogate models published for each mechanism under the stated operating conditions.

The influence of equivalence ratio and compressed temperature on the first-stage and overall ignition delay is evaluated, helping to understand key factors impacting the autoignition process. Of particular interest is the study of first

stage ignition effects on the overall ignition delay and the resulting reaction for low temperature and lean combustion conditions. These conditions represent the limits of engine operating conditions. Mechanism model validation in these non-ideal regimes will then lead to the development of optimized next generation alternative fuels, capable of performing at all operating conditions. Continuing this work to understand the roles chemical features play in influencing a fuel's ignition characteristics will facilitate the development of surrogate models. These more robust models can then be used to examine alternative jet fuel performance at target engine operating conditions.

oldani1@illinois.edu

W1P129 INFLUENCE OF FUEL INJECTION ON THE SHAPE OF A TURBULENT SWIRLING FLAME USING TWO-PHASE FLOW LARGE EDDY SIMULATION

Benoit Cheneau¹, Sébastien Ducruix¹, Aymeric Vié²

¹Ecole Centrale Paris, France ²Stanford University, United States

A laboratory-scale two-stage swirling burner fueled with liquid dodecane is studied numerically using large eddy simulations. The first stage corresponds to a central, primary, pilot injection zone, while the second one is associated to a peripheral, secondary, multipoint injection zone. For a chosen lean operating point, fuel is injected alternatively through these two different injection devices, highlighting a dramatic influence of the fuel distribution on the flame stabilization process. When fuel is injected through the multipoint stage, evaporation and mixing are enhanced and a partially premixed mixture enter the combustion chamber. The flame then takes an 'M' shape, mainly controlled by the large inner and outer recirculation zones associated with this highly swirling flow and in which trapped burnt gases guarantee permanent ignition of the fresh mixture entering the chamber. The situation is much more complicated when fuel is solely injected through the central pilot nozzle. Due to the large amount of liquid present in the pilot zone, premixing is hardly possible and the flame is mainly stabilized in a diffusion regime. This is only possible thanks to a complex situation in this region, where hot evaporated fuel is trapped in front of the nozzle by the large central recirculation zone and oxygen is mainly coming from this recirculation zone. In that case, the flame takes a 'V' shape, with a stabilization point deep inside the injection device. Both flame shapes are analyzed in the mixture fraction phase space, highlighting the different regions of the stabilization process and confirming both scenarios.

benoit.cheneau@ecp.fr

W1P130 LARGE EDDY SIMULATION AND EXPERIMENTAL STUDIES ON LOW-SWIRL COMBUSTION IN A LEAN PREMIXED MULTI-NOZZLE CAN COMBUSTOR

Wei jie Liu, Bing Ge, Yinshen Tian, Shusheng Zang, Shilie Weng, Shanghai Jiao Tong University, China

Large-Eddy Simulations (LES) and laser diagnostic experiments of low-swirl lean premixed methane/air flames in a multi-nozzle can combustor are presented. OH Planar Laser Induced Fluorescence (PLIF) is used to observe flame shapes and identify main reaction zones. The flows and flames are studied at different equivalence ratios ranging from 0.5 to 0.8, while the inlet velocity is fixed at 6.2 m/s. Results show that the neighboring swirling flows interact with each other, generating a highly turbulent mixing zone where intensive reactions take place. The center flow is confined and distorted by the neighboring flows, resulting in instabilities of the center flame. Mean OH radical images reveals that the center nozzle flame is extinguished when equivalence ratio is equals to 0.5, which is successfully predicted by LES. In addition, NO_x emissions show log-linear dependency on the adiabatic flame temperature, while the CO emissions remain lower than 10 ppm. NO_x emissions for multi-nozzle flame are less sensitive to the flame temperature than those for single nozzle.

zhanshen@sjtu.edu.cn

W1P131 EXTINCTION AT THE FLAME TIP IN LEAN PREMIXED BURNER WITH SWIRLING FLOW

Yuichi Ichikawa, Osaka University, Japan

Lean premixed combustion is one of the most promising approaches to reduce nitrogen oxide (NO_x) emission. However, the flame upstream propagation in unburned gas, which is called flashback, is a big issue in premixed burners. In this study, we present characteristics of unsteady flame behavior in a lean premixed burner with swirling flow. A variable swirler is used in order to investigate the flame behavior in the cylindrical glass under different swirl intensity. The characteristics of flame behavior interacting with flow fields in the cylindrical glass have been studied by applying high-speed Particle Image Velocimetry (PIV) measurement. In our PIV measurement, the burnable olive oil was used as a tracer, and both of flow fields and detailed flame shapes can be measured. Disagreement in flame tip shapes is clarified between chemiluminescence images and olive oil particle images at blow-off limit with swirl intensity, S fixed at 0.63. This disagreement suggests the existence of a high temperature zone upstream the flame tip. It can be considered that the high temperature zone consists of the burned gas remained after flame extinction. At $S = 0.63$, reverse flow region exists along the central axis of the cylindrical glass. Therefore, axial velocity gradient in radial direction is steep. As the result, flame extinction occurs at flame tip because of flame stretch caused by steep velocity gradient. However, flame extinction cannot be seen under other conditions of swirl intensity.

ichikawa@tran.mech.eng.osaka-u.ac.jp

W1P132 IMPACT SENSITIVITY ESTIMATION OF ENERGETIC MATERIALS

Aurelien Demenay, Laurent Catoire, Guy Jacob, ENSTA Paristech, France

In the past ten years, scientists have done research to design new energetic materials having great energetic potential. Nevertheless, a good knowledge of molecules properties is necessary to manage such compounds. More specifically, sensitivity and performance were the mainly properties studied over the past twenty years. Sensitivity refers to the degree of response of an energetic material caused by external stimuli (impact, shock, electrostatic discharge, heat and friction). The ease of energetic materials manipulation is limited because of potential hazards due to the high energy molecules. Therefore, empirical and semi-empirical methods are preferentially used in order to predict properties of newly designed energetic materials. The development of these methods is supported by growth of computer power. In that way the purpose of this work is to establish correlation between experimental $h_{50\%}$ value (height at which an energetic material decomposes with a probability equal to 50%) and molecules properties. Models must classify energetic compounds according to their impact sensitivity degree for all families such as nitroaromatic, nitramine, nitroaliphatic, pyridine, pyrazole, imidazole, furazan, etc.

Starting with available experimental $h_{50\%}$ data, a basis set (54 compounds) and a validation set (about 300 molecules) have been created. Both sets include different chemical families as cited above. The correlation chosen is the following:

$$h_{50\%} = A.[P1]^{\alpha}.[P2]^{\beta}.[P3]^{\gamma}.[P4]^{\delta}$$

-P1, P2, P3 et P4 : Properties involve

- A, α , β , γ et δ : Constants determined by the predictive tool

Many properties must be considered due to the complexity of studied compounds. For example, physicochemical, structural, crystallographic or electronic parameters have been examined. Four main properties have been highlighted to model the phenomenon of impact sensitivity. First, the number of nitro groups (n_{NO_2}) inducing an increase of the energetic potential of materials must be considered. Secondly the oxygen balance (OB_{100}) that indicates the degree to which an explosive can be oxidized is regarded. Thirdly, the melting temperature (T_m) is included because an energetic material quickly decomposes through liquid then gaseous state. Finally, the balance parameter (v) is found important. This parameter is a statistical quantity associated to the electrostatic potential which itself refers to the electronic charges distribution within the molecule. This property is essential to identify sites where nucleophilic and electrophilic attack can potentially occur.

OB_{100} and n_{NO_2} have been determined from molecule chemical structures whereas T_m and v require specific calculation methods. v has been calculated thanks to Gaussian 09W software using semi-empirical DFT/6-31G(d,p) method. The melting temperature T_m has been calculated from the Hukkerikar and Gani group contribution method that estimates physical and thermodynamical properties of pure organic compounds.

Evaluation of correlation is done using three well known energetic compounds (PETN, RDX and TNT). This way, molecules are sorted in four classes of sensitivity as presented below. The correlation quality is characterized by a good classification in one of these classes.

High sensitivity < PETN < sensitive < RDX < low sensitivity < TNT < insensitive

Correlation established with the basis set and the four parameters mentioned above provide good estimation of impact sensitivity. Currently, efforts are made to calculate molecule properties from the validation set. Then the same work will be done for electrostatic discharge, shock and heat sensitivities.

This work will be completed with detailed decomposition mechanisms generation for energetic molecules such as RDX, CL-20, NTO, BTTN and TMETN which are often found in propellants composition. This will lead us to estimate decomposition temperature of energetic molecules.

aurelien.demenay@ensta-paristech.fr

W1P133 REACTIVITY TRENDS IN FURAN AND ALKYL FURAN COMBUSTION

Mazen Eldeeb, Ben Akih-Kumgeh, Syracuse University, United States

Bio-derived furans have attracted attention as alternative transportation fuels. Their physical properties are comparable with those of gasoline and their energy densities are higher than those of short-chain alcohols. There is ongoing research, with initial positive results, regarding the feasibility of furan production from sugar-containing second generation biomass and system-level tests of their combustion in research engines.

From a fundamental perspective, the ignition behavior and laminar burning velocities of these furan fuels are being investigated alongside with chemical kinetic model development. However, these studies have only focused on the investigation of individual furans. Quantifying reactivity trends among the various furans could aid in the development of fuel formulations with improved combustion dynamics and lower emissions. It could also provide general insight on the role of substitution on the reactivity of furans.

In this work, a systematic investigation of the ignition behavior of furan and the substituted furans, 2-Methyl Furan (2-MF) and 2,5-Dimethyl Furan (DMF), is presented. Ignition delay times are measured over a temperature range of 981 K to 1552 K for lean, stoichiometric, and rich mixtures of fuel, oxygen and argon. The experiments are carried out in a newly constructed shock tube facility. The results of the 2,5-dimethyl furan ignition are further compared with those of the gasoline surrogate, *iso*-octane. The structure-reactivity trends provide some insight on the complexity of furan combustion and also provide experimental data which can contribute toward further understanding of furans combustion.

W1P134 PREVENTING FUEL TANK OXYGEN INGRESS FOR A BIMODAL CNG INTERNAL COMBUSTION ENGINE

Chris Hagen, Zachary Taie, Oregon State University, United States

We have created a bimodal Compressed Natural Gas (CNG) internal combustion engine which can compress residential natural gas from approximately atmospheric pressure at the home to US CNG on-vehicle storage pressures (250 bar). This engine acts both as a refueling compressor and as a power producing device for vehicle locomotion. This is to say, one cylinder of this engine acts as a compressor at times and at other times combusts as normal.

One of the challenges of this engine is determining the sequence of events for switching from combustion mode to compression mode. As one might imagine, it is undesirable to compress atmospheric oxygen into a CNG tank (even though it would be unlikely for the mixture equivalence ratio to go under the rich limit). The work here describes approaches to mitigate undesirable in-tank fuel air mixing during mode switching.

Processes will be model numerically to determine expected results and experiments will be conducted using a fast oxygen sensor in the fuel line.

chris.hagen@oregonstate.edu

W1P135 TOWARDS PREDICTION OF HIGH FREQUENCY INSTABILITIES IN COMBUSTION CHAMBERS OF LIQUID PROPELLANTS ROCKET ENGINES

Marie Theron¹, Francoise Baillo², Cindy Merlin, Gerard Ordonneau⁴

¹CNES, France ²CORIA, CO., France ³SNECMA Vernon, France ⁴Office National d'Etudes et de Recherche Aéronautiques, France

High Frequency (HF) instabilities have frequently been encountered in past developments of Liquid Rocket Engines (LREs), causing highly destructive damages. Such instabilities result from the complex interaction between several physical phenomena: resonant coupling can occur between propellants injection, flame dynamics and acoustic modes (mainly transverse) in the combustion chamber and possibly in the injection cavities. The complete interaction mechanism between all physical phenomena has not yet been fully understood, despite decades of intensive research. In Europe, these research activities are currently being continued in the frame of the French-German research group: REST (Rocket Engine STability research initiative), involving partners from space industry, research institutes as well as academic laboratories. REST program is translated on French side by CNES Liquid Propulsion R&D program on HF instabilities, involving CORIA, EM2C, ONERA and SNECMA as main partners.

Research activities aim at a deeper understanding of physical mechanism at stake in the HF instabilities source mechanism(s), thanks to improved modeling of most relevant physical processes and of their cross-couplings and interactions with acoustics. Both 3D CFD and low-order models are being developed; small-scale and intermediate-scale experiments have also been specifically developed as a support for models formulation and/or validation. Final objective of this research is to build validated numerical tools for the prediction of HF instabilities in LREs, useful to ensure design of new liquid propulsion combustion devices free of HF instabilities in a near future.

Main targets for application of this research work are hydrogen/oxygen cryogenic thrust chambers equipped with coaxial injection elements, at medium to high combustion chamber pressures (meaning inner oxygen jet injection ranging from subcritical to transcritical/supercritical regime).

Large-Eddy Simulations (LES) of transcritical coaxial jet flames are carried out to investigate the impact of HF transverse acoustic modulations on flame dynamics. Numerical results are validated against experimental results obtained in a multi-injector combustor on Mascotte test bench equipped with a Very High Amplitude Modulator (VHAM). In parallel, a low-order modeling tool, STAHF (STability High Frequency), which solves the acoustic wave equation by using the acoustic pressure modal decomposition of Culick et al., is developed. In this problem, the key element is to obtain a suitable representation of the unsteady heat release rate under high amplitude transverse acoustic oscillations: advanced models for source terms and damping coefficients are being developed and implemented in STAHF. These models are validated on acoustically modulated test-cases: Mascotte experimental test results in reactive conditions and TPC (Transparent Pressurized Cavity) tests results in non-reactive conditions.

The behavior of the inner dense oxygen jet plays a key role in the flame dynamics behavior under high amplitude transverse acoustic oscillations : an experimental test set-up has been developed at CORIA to study the influence of a high-frequency transverse acoustic field on the atomization of air-assisted water jets in rocket engine representative aerodynamic regimes ; in parallel, large eddy simulations of transcritical round jets are carried out to study the detailed behavior of the jet under acoustic oscillations for different acoustic modes/frequencies and injector locations in the acoustic field by EM2C. Despite differences in the jets thermodynamic regime (subcritical vs. transcritical) between experimental and numerical test cases, major experimental features can be retrieved in numerical simulations results, for e.g. the flattening of a jet placed at a velocity anti-node into a liquid sheet normal to the acoustic axis. In a near future, large eddy simulations of coaxial jets in subcritical conditions under high amplitude transverse acoustic oscillations will also be performed and validated against CORIA non-reactive and Mascotte VHAM subcritical and reactive experimental results; these simulations will rely on a new atomization model under development at ONERA.

Finally, possible injection cavities/injectors/combustion chambers coupling effects will be studied both experimentally, in an evolved version of the TPC experiment and in the CORIA experiment. Results analysis should be helpful to define injector impedance models to be implemented later on in STAHF low order modelling tool.

W1P136 PECULARITIES OF THE INFLUENCE OF THE STRUCTURE OF THE SOLID-FUEL MIXTURE GLYCIDYL AZIDE POLYMER/RDX ON THE THERMAL EFFICIENCY OF A ROCKET ENGINE

Sergey Futko, A.V. Luikov, Heat and Mass Transfer Institute NAS Belarus, Russia

Solid-fuel mixtures Glycidyl Azide Polymer (GAP)/RDX have found wide application as promising solid rocket fuels in which the content of GAP is about 5–30 mass% and which burn in the combustion chamber of the rocket engine at pressures of the order of 30–100 atm.

With the help of thermodynamic calculations for a wide range of solid-fuel mixtures Glycidyl Azide Polymer (GAP)/RDX with a component ratio from 100% GAP/0% RDX to 0% GAP/100% RDX we have found that dependence of theoretical thermal efficiency of a rocket engine on RDX content in such mixtures has non-monotonous character with two distinct peaks at 26.9 and 60.8 mass% of RDX in GAP respectively. After the second maximum thermal efficiency undergoes rapid decrease with increase in RDX content. It is shown that the first peak corresponds to the condition of equality of molar fractions of C and N atoms in mixture composition. For the second peak the same condition is fulfilled for C and O atoms in solid fuel mixture.

Detailed analysis revealed that this point divides naturally all possible GAP/RDX mixtures into two regions of compositions: up to the mass fraction of RDX 60.8% the solid-fuel mixture retains the similarity of properties of the GAP as a monofuel (relatively low combustion temperatures, light combustion products, the formation of a considerable quantity of synthesis gas H_2 , CO and solid carbon Cs), and a mixture with a larger fraction of RDX in the GAP is characterized by the properties of RDX as a monofuel (high adiabatic combustion temperatures, relatively large molecular weight of combustion products, and the formation of H_2O and CO_2).

It is shown that a mixture of 60.8 mass% of RDX in GAP corresponds to the structural change in the solid-fuel mixture GAP/RDX from predominantly amorphous to polycrystalline structure, and is a phase transition point. This point is also pressure-independent and corresponds to the minimum point on the curve of the combustion velocity of the mixture as a function of its composition. It is expected that analogous results, with necessary modifications, hold true also for a wider class of solid fuel mixtures of the type of polymeric binder/explosive.

foutko@itmo.by

W1P137 COMBUSTION VISUALIZATION OF ETHANOL/LIQUID OXYGEN ROCKET ENGINE COMBUSTOR WITH 2D PINTLE INJECTOR

Kazuki Sakaki, Shinji Nakaya, Mitsuhiro Tsue, Tetsuo Hiraiwa, Japan Aerospace Exploration Agency, Japan

The rocket engine with deep throttling capability is a key technology for future space transportation system such as orbital transfer vehicles and landers of the planet exploration probe which require propulsion systems with wide thrust range. One of the most important components of the rocket engine with deep throttling capability is propellant injection system. Combustion oscillation is induced under deep throttling condition with conventional propellant injection systems such as coaxial injector or impinging injector due to the deterioration of atomization and mixing performance. Pintle injector is one the most promising candidates for the rocket engines with wide operation range due to its simple structure and combustion stability under deep throttling condition. However, the number of researches on pintle injector is limited due to the difficulty of observation and reduction of the test scale. Detail phenomena of pintle injector are not clarified due to the lack of established measurement method for pintle injector. Therefore, a combustion test of a ethanol/liquid oxygen rocket engine is carried out with a planar pintle injector in a rectangular combustor which has pintle like geometry and enables optical access. Fundamental combustion characteristics such as characteristic exhaust velocity efficiency are acquired at the combustion pressure of 0.45 MPa and O/F=1.25 to 1.80. The minimum C^* efficiency is 77.5% at O/F=1.25 and the maximum C^* efficiency is 85% and C^* efficiency increases with an increase in O/F. The combustion stability is evaluated in terms of Coefficient of Variance (CoV) which is a ratio of the standard deviation to average combustion pressure. CoV of all the test cases are below 5%. However, CoV increases in the decrease of O/F and there is a possibility that combustion is unstable under fuel rich condition. Flame structure at 0.45MPa and O/F=1.75 are observed. Luminous flame is not observed in almost all the region except for the vicinity of the faceplate. Two ignition modes were observed. One is hard start mode which has strong pressure peak on ignition and the other is a smooth start mode which has no pressure peak on ignition. The peak pressure of the hard start cases has a tendency to be large with the decrease in O/F. Strong luminous flame is observed during ignition transition phase. The flow field of a combustion chamber with pintle injector has two large recirculation zones which contribute the combustion stability of pintle injectors. The combustion chamber used in this research can simulate one of the recirculation zones called upper recirculation zone which is formed in the vicinity of the injector face. Intermittent reaction was observed in the upper recirculation zone. However, the other recirculation zone called core recirculation zone which is formed at the top of the injector body is not simulated appropriately due to the existence of the lower wall of the combustor.

6961404203@mail.ecc.u-tokyo.ac.jp

W1P138 LARGE EDDY SIMULATIONS OF A NATURALLY UNSTABLE TRANSCRITICAL COAXIAL INJECTOR

Thomas Schmitt¹, Axel Coussement¹, Sébastien Ducruix¹, Sébastien Candel¹, Yoshio Nunome²

¹EM2C, France ² Japan Aerospace Exploration Agency, Japan

Understanding the flame dynamics in combustion chamber is still a wide field of research. In some cases instabilities can occur leading to degraded operating conditions or even damage to the system. When considering liquid rocket engines, the power developed inside the combustion chamber will lead in general to the destruction of the engine if strong instabilities take place. In order to avoid this, expensive and extensive experimental tests are still needed. The numerical tool can be a very interesting alternative, but validation and modeling efforts are still required. Stable transcritical flames and transcritical flames modulated by large amplitude transverse acoustic waves were successfully simulated recently. However, the ability of computer codes to predict naturally unstable cases must still be verified.

In this context, the JAXA has recently developed an original experimental configuration: depending on the injection conditions and the geometry of the injectors, the transcritical flame can be made unstable. It is therefore a potentially rich and unique configuration for validation of the numerical tool.

In this study two cases have been simulated using the AVBP-RG solver jointly developed by CERFACS and EM2C. The first case corresponds to experimentally stable injection conditions, while the other one features large pressure oscillations in the combustion chamber. First numerical results indicate a more dynamic behavior of the unstable case compared with the stable case. Our objective is to present the current state of our simulations and on-going analysis.

thomas.schmitt@ecp.fr

W1P139 EFFECTS OF POTASSIUM AND ZIRCONIUM ADDITIVES ON THE INFRARED RADIATION SIGNATURE IN ROCKET MOTOR PLUME

Mintaek Kim, Soonho Song, Kwangmin Chun, Yonsei University, Korea

The spectral characteristics of Infrared Radiation (IR) signature emitted from rocket plume are used for detection, tracking, and identification of the target. To increase the survivability of tactical missile by avoiding the detection, it is essential to make a missile with low IR radiation signature. The spectral characteristics of IR radiation signatures are determined by the propellant composition that many studies are being conducted to analyze the detailed information of radicals and molecules contained in the IR radiation signature and devise a method to lower the IR intensity emitted from rocket plume. The rocket exhaust plume is formed due to the combustion of fuel-rich products (CO and H₂). The oxidative reaction of CO and H₂ with oxygen in the ambient air produces CO₂ and H₂O which results in the afterburning of propellant. CO₂ and H₂O are known to emit the IR radiation that the intensity of IR radiation is increased as the amount of CO₂ and H₂O increases. According to previous studies, certain metal-containing additives are known to act as suppressants of spontaneous ignition of hydrocarbon flames by retarding the chemical reaction of propellants. Among various additives, it was found that potassium acts as an afterburning suppressant and zirconium as an afterburning stabilizer.

The objective of this study is to find out the effects of potassium and zirconium additives on the IR radiation signature emitted from rocket motor plume. The experiments were held with the propellants of different additive amounts. The IR radiation signature of 4 inch standard rocket motor was measured at the static firing test using the Fourier Transform IR (FT-IR) spectroradiometer. This equipment is capable of measuring the spectral emission ranges from 2 μm to 6 μm (Middle InfraRed; MIR) with a maximum scan rate of 34 scan/s. Using IR spectroscopy, combustion-products formed in a process of afterburning and spectral characteristics of IR radiation signatures were both experimentally measured. The experimental results indicated that the IR intensity differs due to the various amounts of potassium and zirconium additives. The increased potassium lowers the amount of combustion-products and significantly lowers the IR intensity as a consequence.

mintaek.kim@yonsei.ac.kr

W1P140 TEMPERATURE SENSITIVITY OF COMPOSITE PROPELLANTS CONTAINING NOVEL NANO-ADDITIVE CATALYSTS

Andrew Demko¹, James Thomas¹, Catherine Dillier¹, Eric L. Petersen¹, David Reid², Sudipta Seal², Thomas Sammet¹

¹Texas A&M University, United States ²University of Central Florida, United States

A primary focus for the development of solid propellant has been to introduce different additives to the propellant to tailor its burning behavior for specific applications. Often the propellant is used in systems where it experiences harsh environments, such as extreme temperatures and impact loading. Thus, the propellant is subjected to less-than-ideal environments for combustion. This brings rise to the issue of how safe the propellants are to handle, as well as to manufacture, in addition to the effect of temperatures and pressures on the burning rate.

Composite solid propellants have been altered through the use of various additives to tailor their strength or burning behavior. The effect of such additives on the temperature sensitivity of propellants requiring durability in harsh environments such as extreme hot and cold temperatures is of interest. Research at Texas A&M University has shown that the inclusion of nano-additives manufactured using novel techniques, such as titania and cerium oxide, will increase the burning rate of Ammonium Perchlorate (AP) and Hydroxyl Terminated PolyButadiene (HTPB) composite propellants. Metal oxides can be synthesized using various techniques, changing their morphology to tailor their burning behavior. The propellant's burning rate is proportional to pressure raised to a power according to the classical burning rate relationship with empirical coefficients a (pre-exponent or temperature coefficient) and n (pressure exponent).

The authors have refined techniques for mixing laboratory-scale samples over several years. Hand mixing propellant batches has the advantage of being small enough that many parameters can be tested quickly while retaining the ability to

test many variations of composite propellants with novel ingredients. The present poster is concerned with testing AP/HTPB propellants with different nano-sized catalytic additives (and additive formulation techniques) at various initial temperatures. Titania nanoadditives are the focus, where the three different manufacturing techniques described earlier are included: spray-dried particles; wet-mixed particles; and *in situ* grown particles. Temperatures ranging from -60°C to 100°C were targeted to examine the temperature sensitivity of the propellants with various additives; elevated pressures in the range of 3.5 to 15.5MPa (500-2250 psi) were considered. The intent is to show how different additives alter the temperature sensitivity in addition to the increased burning rate. In addition, the results of safety tests to simulate different harsh scenarios the propellant might be subjected will be described. Additional safety tests were also designed to illustrate possible hazards from the storage and manufacturing safety for each of the propellants.

ardemko21@neo.tamu.edu

W1P141 IMPLEMENTING NANO-SIZED ADDITIVES INTO COMPOSITE SOLID PROPELLANTS

Catherine Dillier¹, Andrew Demko¹, James Thomas¹, Thomas Sammet¹, Eric L. Petersen¹, Kevin Grossman², David Reid², Sudipta Seal²
¹Texas A&M University, United States ²University of Central Florida, United States

Recent advancements in chemical synthesis techniques have allowed for the production of improved solid rocket propellant nano-scale additives. These additives show larger burning rate increases in composite propellants compared to previous generations of additives. In addition to improving additive effectiveness, novel synthesis methods can improve manufacturability, reduce safety risks, and maximize energy efficiency of nano-scale burning rate enhancers. One of these novel synthesis methods, termed nano-assembly, has recently been developed in our laboratory.

Nano-assembly directly synthesizes TiO₂ (Titania) in the binder of an Ammonium Perchlorate Composite Propellant (APCP). This new method is the latest incarnation of an increasingly effective series of procedures for introducing catalytic nanoparticles into a solid propellant matrix. It has been shown to increase the efficiency of Titania as a burning rate catalyst in APCPs, with increases in burning rates as high as 67.7% at additive mass loadings of less than 0.5% in non-aluminized, ammonium perchlorate-based propellants over the pressure spectrum of 500 psi to 2250 psi. In similarly formulated aluminized propellants, increases in burning rate as high as 73.0% have also been shown. Additionally, compared to commercial nano-particles, the nano-assembled particles have been shown to produce a significant increase in burning rate.

This increase in burning rate is primarily due to the minimization of particle/agglomerate diameter. Minimizing the particle/agglomerate diameter increases the surface area-to-mass ratio of the propellant which has been shown to increase the catalytic activity during ammonium perchlorate decomposition and APCP combustion. Overall, nano-assembly greatly improves the burning rates of composite propellants. It also allows for control of surface chemistry dispersion, and particle topography in such a way as to tailor performance in a propellant by assembling the particles from the bottom up. Finally, by synthesizing the particles directly in the propellant binder, safety and health risks associated with the handling of “dry” nanoparticles are mitigated. Hence nano-assembly improves manufacturability, reduces safety risks, and maximizes energy efficiency of nano-scale burning rate enhancers. This poster provides recent advances in this area, including its use with particles other than Titania.

cdillier2301@tamu.edu

W1P142 DIFFERENTIAL WEIGHT MEASUREMENTS DURING COMBUSTION OF METHANE HYDRATES

Joan Santacana Vall, Sunny Karnani, Derek Dunn-Rankin, University of California, United States

Methane clathrates (or methane hydrates) are ice-like crystalline solids composed of water and methane. Produced at elevated pressures and reduced temperatures when the methane concentration exceeds the solubility limit of water – conditions typically found along continental shelves and arctic permafrost – methane hydrates, in their entirety, represent the largest hydrocarbon source found on Earth. To better understand the implications of directly utilizing methane hydrates, this poster describes the formation and combustion behavior of methane hydrates.

Many factors play a significant role in producing a uniform methane hydrate sample, including the precise control of temperature, pressure, and the required time for the methane hydrate sample to form. When clathration occurs, pressure in the surrounding environment drops as the methane in the gas phase is taken up by the structure, and temperature increases because the process is slightly exothermic. Managing these effects during hydrate formation is important for reproducible results. Combustion studies presented consist of differential weight measurements of the hydrate sample and the water melted during combustion. The measurement provides the dissociation/melting rate and time history of water melted and evaporated from burning hydrate samples. These measurements provide an estimate of the amount of hydrate water that is evaporated into the fuel stream. Experimental results describe the major elements of the hydrate combustion process. These experiments provide insight into the different elements that influence hydrate formation and combustion, including sample size, sample subcooled temperature level, surfactant content, and initial clathrate percentage. The results show the same trends of combustion behavior as expected from theoretical and numerical calculations. Furthermore, it is concluded that for atmospheric pressure, free convective burning, approximately half of the heat of combustion goes to the environment and the other half to the hydrate. These results incorporate different types of methane hydrate, based on the phase diagram, and a sufficient number of samples to ensure consistency of the results.

jsantaca@uci.edu

W2P001 COMBUSTION REGIMES OF LOW-LEWIS-NUMBER STRETCHED PREMIXED FLAMES

Roman Fursenko¹, Sergey Minaev², Hisashi Nakamura³, Takuya Tezuka³, Susumu Hasegawa³,
Tomoya Kobayashi³, Koichi Takase³, Masato Katsuta⁴, Masao Kikuchi⁴, Kaoru Maruta³

¹Khristianovich Institute of Theoretical and Applied Mechanics, Russia ²Far Eastern Federal University, Russia

³Tohoku University, Japan

The dynamic behavior and 3D spatial structure of low-Lewis-number counterflow premixed flames are studied numerically and experimentally. Numerical simulations are performed in the frame of thermo-diffusive model with one-step chemical reaction. Our numerical and experimental data show that under microgravity conditions there is a big diversity of combustion regimes: planar and cellular continuous flames; sporadic combustion waves and worm-like flames. The regions of the existence of different combustion regimes are determined. We conclude that in the range of high stretch rates, the cellular flames exist at relatively high equivalence ratios whereas the planar twin flames are observed for leaner mixtures. Both experiments and simulations show that, for the small stretch rates, the continuous cellular flame transforms to the sporadic combustion wave when the equivalence ratio decreases. The sporadic combustion wave can be represented by the set of moving ball-like flames which exist beyond the flammability limits calculated by 1D model. The extension of 1D flammability limits may be associated with spatial structure of sporadic wave and the flame curvature effects peculiar to the flame ball-like structures. A new non-stationary combustion regime with relatively long lifetime is distinguished. In this regime, one or several moving worm-like flames form before extinction. The numerical results allow us to distinguish the main physical processes governing flame behavior. We conclude that the diffusive-thermal instability is responsible for the behavior of low-Lewis-number counterflow premixed flames.

roman.fursenko@gmail.com

W2P002 LAMINAR BURNING VELOCITY AND MARKSTEIN NUMBER OF SPHERICALLY PROPAGATING AMMONIA/AIR PREMIXED FLAMES

Takashi Goto, Akihiro Hayakawa, Rentaro Mimoto, Taku Kudo, Hideaki Kobayashi, Tohoku University, Japan

Ammonia has high capability to retain hydrogen and potential as hydrogen carrier. It is possible to use existing ammonia storage apparatus and carriage infrastructure, and it is easier to deal with ammonia than hydrogen. Although ammonia has been manufactured by the Haber-Bosch process up to the present, a new process for producing ammonia from solar energy is being studied. Ammonia as hydrogen energy carrier is useful not only for hydrogen automobile engines and fuel cell but also for direct combustion. Ammonia is one of the carbon-free fuels, and carbon dioxide is not emitted when ammonia burns. In addition, direct combustion of ammonia has advantages of being able to divert existing combustors, such as gas turbines and industrial furnaces. However, in general, ammonia had not been considered as a fuel because of its lower calorific value, lower laminar burning velocity, narrower flammability and so on. Therefore, few fundamental studies on ammonia flames have been conducted, especially on pure ammonia/air flames. The authors present in the oral session of the 35th symposium about NO_x formation characteristics of ammonia/air premixed laminar flames for various equivalence ratios and pressure conditions using the high-pressure combustion test facility. Takizawa and Pfahl investigated stretched laminar burning velocity of ammonia/air flames from spherically propagating flames, and showed the laminar burning velocity of ammonia/air flames to be less than 10 cm/s for all examined equivalence ratios. The purpose of this study is to evaluate the unstretched laminar burning velocity and Markstein numbers of ammonia/air premixed flames from spherically propagating laminar flame.

Experiments were carried out using a constant volume combustion chamber, whose volume is approximately 23 liters. Mixture was ignited by electric spark at the center of the chamber. Two spark electrodes of 1.5 mm in diameter were inserted in the chamber. Spark gap was set to 2 mm, and the spark energy could be 2.8 J. The initial mixture temperature was set to ambient temperature. Flame propagation was observed using Schlieren photographs up to 60 mm in diameter. As will be noted from Schlieren images of stoichiometric ammonia/air premixed flame at initial mixture pressure of 0.1 MPa, Ammonia/air premixed flame was gradually moving upward, and eventually changed to warped shape. Additionally, the unstretched laminar burning velocity of ammonia/air premixed flames was proven to be much lower than that of hydrocarbon as shown in the previous studies and numerical simulations. It is presumed that the change in the shape of ammonia/air premixed flame was caused by the slow laminar burning velocity.

tgoto@flame.ifs.tohoku.ac.jp

W2P003 MARKSTEIN LENGTH IN OUTWARDLY PROPAGATING SPHERICAL FLAMES

Hao Yu¹, Zheng Chen¹, Emilien Varea², Bruno Renou², Fabien Halter³, Yiguang Ju⁴

¹Peking University, China ²CORIA – INSA de Rouen, France ³PRISME, Université d'Orléans, France

⁴Princeton University, United States

Markstein length is an important parameter of a combustible mixture. The emphasis of this poster is spent on answering two questions: whether the Markstein length relative to burned gas can be converted to the Markstein length relative to unburned gas by multiplying the density ratio; and whether the Markstein length depends on flame geometry. It is shown that, in previous studies the Markstein length relative to unburned gas in OPF was not measured or calculated and the reduced Markstein length was wrongly considered to be the Markstein length relative to unburned gas. In this study, the Markstein length relative to unburned gas in OPF is obtained for the first time from

simulation with detailed chemistry for CH₄/air and C₃H₈/air mixtures. Finally, a correlation is proposed to obtain, at least approximately, the Markstein length/number relative to unburned gas in OPF experiments.

yuhao8987568@163.com

W2P004 TOWARD AN ACCURATE DETERMINATION OF THE LAMINAR BURNING VELOCITY OF HIGHLY CO₂ DILUTED MIXTURE

Alexandre Lefebvre, Bruno Renou, Vincent Modica, Fabien Halter, Mourad Boukhalfa, CNRS, France

The reduction of pollutant emissions and energy diversification become a world challenge which requires new combustion methods and new combustibles. Many ways are explored involving combustion of mixtures containing a large amount of CO₂ or H₂O. Then new kinetic models have to be developed and validated. One of the validation steps is based on the unstretched Laminar Burning Velocity (LBV) which reflects the reactivity and dynamics of the flame, and has to be therefore accurately determined. For this purpose, spherical expanding flame has been extensively used due to its simple implementation and the large thermodynamic conditions accessible. The classical technique used in this configuration consists in recording the flame front propagation and defines the LBV, noted SI°, as the product between the density ratio and the propagation speed extrapolated at zero stretch rate. This method requires several assumptions on mixture properties and extrapolation models. However recent numerical works challenge these assumptions and conclude on significant uncertainty due to radiation phenomena, diffusivity effects and stretch response modeling, which are relevant for CO₂ or H₂O diluted mixtures. The aim of the present study is to investigate the influence of radiation flux on the laminar burning velocity.

A collaborative work with F.N. Egolfopoulos team has lead to the conclusion that an efficient comparison between experiments and simulations should be done by directly comparing raw measurements with direct computed physical properties. It was made possible by using a recent technique based on tomographic records which allows to determine the stretched flame displacement speed relative to the fresh gases, Un, without any assumptions. Besides, Jayachandran have numerically demonstrated that this speed is not influenced by radiative effects compared to the propagation speed. The mixture CH₄ / (0.3O₂ + 0.5CO₂ + 0.2He) reported in the well documented numerical and experimental work has been used in this work. Experimental measurements have been performed on a wide range of equivalence ratios and pressures. Results denote a discrepancy between the extrapolated velocities SI° and Un°, such as SI° < Un°. This discrepancy is different with the equivalence ratio, decreases with the pressure and may be associated to radiative heat losses, extrapolation model or the chemical equilibrium of the burned gases. In order to explain this difference, 1D and 3D direct numerical simulations with complex chemistry and three radiation models: adiabatic, optically thin and statistical narrow-band based correlated-k are in progress. Comparison with experimental results will enable to analyze each assumption of the classical measurement method SI° and highlight the physical effects responsible of the apparent discrepancy. The impact of the extrapolation models unavoidable for the two quantities, SI and Un, will be also quantify. Finally, an analysis on the radiation models will be performed.

lefebvre@coria.fr

W2P005 MEASUREMENTS AND NUMERICAL STUDY OF LAMINAR BURNING VELOCITIES OF *ISO*-BUTANOL AND ETHANOL BLENDS

Florian Rau, Christian Hasse, Sandra Hartl, Stefan Voss, Dimosthenis Trimis, Technische Universität, Germany

The reduction of emissions from the traffic sector is of great priority as they account for about 23% of the world's total energy-related GHG emissions. The substitution of conventional fuels with biogenic ones like ethanol and butanol, is regarded as a one of the most promising mitigation strategies. Alcohols can be easily blended with gasoline in mixtures that have high octane number and high calorific value. Thus, the currently established method to use biogenic fuels is by creating blends with gasoline, in proportions that depend mainly on local market restrictions. In order to improve the acceptance in the automotive sector and to increase the number of applications for such fuels, a more precise characterization of their combustion properties is essential.

In this work in progress, laminar burning velocities for *iso*-octane/ethanol and *iso*-octane/*iso*-butanol blends are measured for combustion with air, using the Heat Flux Burner method. The aim of the work is to investigate the influence of alcohol addition in these blends. The conventional Heat Flux Burner test-rig configuration has been adapted so as to include a fuel conditioning system and to have an automated measurement procedure. In order to minimize pre-reactions in the fuel conditioning pathway a direct evaporator unit is used. The measurements are taken for variations of the equivalence ratio at constant atmospheric pressure and mixture temperatures that range from 298 K to 373 K. Numerical calculations are also performed using an 1D model and different available reaction mechanisms, suitable for modeling *iso*-octane, ethanol and *iso*-butanol oxidation chemistry. The performance of the different kinetic schemes is evaluated against the obtained experimental data.

florian.rau@iwtt.tu-freiberg.de

W2P006 LAMINAR BURNING VELOCITIES OF METHANE, METHANOL AND ETHANOL: A COMPARATIVE STUDY MADE WITH FOUR HEAT FLUX BURNER SETUPS

Stefan Voss¹, Alexander Konnov², Vladimir Alekseev², Florian Rau¹, Evgeniy Volkov³, Philip de Goey³, Roy Hermanns⁴, Richard Haas-Wittmuess⁴

Laminar burning velocity is a fundamental property of a reactive fuel-oxidizer mixture, varying with its composition, pressure and initial temperature. Furthermore, it can be used for reaction mechanism validation and is often needed for design of industrial burners. There are several experimental methods to measure laminar burning velocity, e.g., the Bunsen flame method, the expanding spherical flame method, the counterflow flame method and the flat flame burner method, which also includes the Heat Flux method. In this study, the Heat Flux method was applied to measure the laminar burning velocities of methane, methanol and ethanol. In order to improve the method and to determine possible systematic uncertainties, several sets of experiments were carried out and compared. The measurements were performed by four different groups from Eindhoven University of Technology, Lund University, OWI-Oel-Waerme Institut GmbH and TU Bergakademie Freiberg. The investigated range of equivalence ratios was from 0.7 to 1.4. All mixtures had initial temperature of 298 K, except for ethanol, in which case a higher temperature of 318 K was set in order to avoid condensation. The observed discrepancy between the measured values is discussed.

stefan.voss@iwtt.tu-freiberg.de

W2P007 HYDROUS ETHANOL LAMINAR BURNING VELOCITY MEASUREMENTS WITH CONSTANT VOLUME BOMB METHODS

Nathan Hinton, University of Oxford, United Kingdom

The increased use of ethanol as a blending component with gasoline, or as a fuel alone, has made it important to consider the efficiency of its production. When ethanol is produced by fermentation the presence of the azeotrope at 96.5% ethanol by volume (95.6% by mass) limits the purity that can be obtained by simple distillation. The cost of manufacturing pure ethanol is about double the cost of manufacturing 90% ethanol by volume. Studies into the feasibility, energy savings and engine performance of hydrous ethanol have been carried out in the literature. To use hydrous ethanol in blends with gasoline such as E85 (85% ethanol and 15% unleaded gasoline by volume), phase stability of the blend must be considered, due to the immiscibility of gasoline and water. Johansen and Schramm have examined the miscibility of such blends with respect to flex fuel applications. Therefore, it is of interest to obtain data regarding to the fundamental property of burning velocity of hydrous ethanol, for use in engine modeling. Burning velocity measurements have been made from two methods using a constant volume combustion bomb, over a range of initial temperatures, pressures and equivalence ratios, for hydrous ethanol mixtures containing up to 40% water by volume. The combustion bomb has a diameter of 160mm and is fitted with 40mm diameter quartz windows to allow imaging of the initial stages of flame propagation using a schlieren photography system and high speed camera, and a pressure transducer to measure the pressure rise in the vessel during combustion. The premixed mixture of fuel and air is ignited using a pair of an electrodes forming a spark gap at the centre of the vessel.

The initial stages of combustion can be shown to be taking place at conditions of constant pressure, and so schlieren imaging of the flame front allows for a constant pressure analysis of flame speed. Due to the small radius of curvature of the flame at initial conditions, the flames are highly stretched, so a linear extrapolation of the flame speed to conditions of zero stretch is used, to obtain values for laminar burning velocity and Markstein length, as performed in many existing studies such as that of Bradley.

Once the flame has passed beyond the field of view, combustion can no longer be considered to be taking place at constant pressure, so a constant volume combustion analysis is performed. By combining the pressure record with a model for constant volume combustion it is possible to determine the burning velocity following the method of Lewis and von Elbe. Considering isentropic compression of the unburned gas, this method allows burning velocity to be measured for a wide range of temperature and pressure of the unburned gas from a single experiment. Data accumulated from a number of experiments over a range of initial temperatures, pressures volume fractions of water and equivalence ratios is combined and fitted to a 14 term correlation to express the effect of these parameters. A quadratic dependence of the temperature and pressure exponent upon equivalence ratio has been used, as in the work of Konnov. Correlation coefficients are obtained and compared with the results from flame front imaging techniques, showing a good agreement, not seen in previous presented data such as that of. The results showed the burning velocity to increase with temperature and decrease with pressure. For the case of water addition, a non-linear decrease in burning velocity with increasing volume fraction of water. The peak burning velocity is seen to occur rich of stoichiometric, which is consistent with existing literature data for ethanol.

nathan.hinton@eng.ox.ac.uk

W2P008 BURNING VELOCITY VS. FLAME STRETCH IN BUNSEN JET FLAMES OF METHANE – AIR MIXTURES

Gabriel Garcia-Sergio Margenat, Francisco Higuera, Jose Castillo, Pedro Garcia-Ybarra, National University of Distance Education (UNED), Spain

An experimental setup has been devised for the simultaneous measurement of the distributions of burning velocity and stretch a Bunsen flame front. Methane-air mixtures have been investigated and the relation between burning velocity and stretch has been experimentally determined along the front, from the lower quasi-conical region up to the tip. At the lower region of weak stretch, the results agree with the theoretical predictions of the linear theory. Approaching the flame tip, the observed burning velocity is respectively larger than the linear prediction. On the other

hand, for a given mixture ratio, the burning velocity at the tips of flames of different heights follows a well defined power law in a log-log plot with respect to the tip curvature. The possible occurrence of flame quenching at the tip has been examined. Numerical calculations have also been performed to analyze the intensity of the chemical reaction around the tip.

gabrielgs@dfmf.uned.es

W2P009 PREMIXED FLAME PROPAGATION BETWEEN TWO CLOSELY SPACED PARALLEL PLATES

Daniel Fernandez-Galisteo¹, Paul D. Ronney²

¹CIEMAT, Spain ²University of Southern California, United States

We study numerically the propagation of slow quasi-isobaric premixed flames between two closely spaced parallel plates. The formulation is based on an averaging of the conservation equations in the direction perpendicular to the plates. Time-dependent computations were conducted using simplified Arrhenius chemistry. The effects of thermal expansion, buoyancy, Lewis number and heat and momentum losses on the flame dynamics were studied. The simulations showed qualitative similarities with the dynamics investigated experimentally, including cellular-like wrinkled structures. Computed average propagation rates were consistent with measured values.

d.galisteo@ciemat.es

W2P010 MEASUREMENTS OF LAMINAR FLAME SPEEDS OF ALTERNATIVE GASEOUS FUEL MIXTURES

Samer Ahmed, Ahmed Ibrahim, Othman Abulaban, Qatar University, Qatar

Global warming and the ever increasing emission levels from combustion engines have forced the engine manufacturers to look for alternative fuels for better engine performance and low emissions. Gaseous fuel mixtures such as biogas, SYNGAS, and Liquefied Petroleum Gas (LPG) are new alternative fuels that have great potential to be used with combustion engines. In the present work, alternative fuel mixtures, mainly LPG (60% butane, 20% *iso*-butane and 20% propane) and methane with percentages of other gases and fuels such as hydrogen, oxygen, carbon dioxide and nitrogen, will be studied to observe how the change in the fuel composition affects the combustion characteristics of the fuel, specially the Laminar Flame Speed (S_L). The test rig used in this work consists of a 4.5-m long optical-quality quartz tube with 1-in diameter. The inlet of the tube is attached to a mixing chamber to supply the fuel-air mixture at atmospheric conditions with a laminar flow at $Re = 1000$. The flame is ignited at the inlet of the tube and S_L is measured by two methods simultaneously in order to confirm the results; two type-k thermocouples fixed at the inlet and exit of the tube, and a high speed camera. The thermocouple signals detected by a digital oscilloscope with 1 MHz sampling rate. The time between the two peaks of the signals is used to calculate the flame speed. Instantaneously, high speed camera images of the same ignition events were used also to calculate S_L of the same fuel mixture. S_L of CH_4 -air mixture has been measured first to validate the results of the present test rig. Results of both methods show excellent agreement with literature and with each other. Preliminary results of CH_4 /LPG-air mixtures show that S_L of a mixture of these two fuels with any percentage is higher than S_L of both pure fuels separately. Moreover, increasing the percentage of LPG in the mixture from 20% to 60% increases S_L considerably, especially around stoichiometric condition, around stoichiometric condition. The reason is not clear at this stage; however, it can be related to the expected increase in flame temperature with the increase of LPG percentage in the mixture. This may lead to change the production and consumption rate of the molar fraction of H, O, OH and CH_3 radicals in the reaction zone.

sahmed@qu.edu.qa

W2P011 EXPERIMENTAL AND NUMERICAL STUDY OF FLAME SPEED FOR *ISO*-OCTANE/*N*-DECANE/AIR PREMIXED FLAMES AT HIGH PRESSURE

Kiyong Lee, Sugak Lee, Andong National University, Korea

A comprehensive experimental and numerical study has been conducted to investigate flame speed of premixed flames for mixture of *iso*-octane and *n*-decane at high pressure. Spherically expanding flames are used to measure flame speeds, which are derived from the corresponding laminar flame speeds at zero stretch. The classical shadowgraph technique is used to detect the reaction zone. Data are obtained for an initial temperature of 462K, initial pressures from 5 to 10 atm, and equivalence ratios varying from $\phi=0.8$ to 1.4. A short kinetic mechanism for premixed *iso*-octane/*n*-decane/air flames at high pressure is developed with a reduction method of Simulation Error Minimization Connectivity Method (SEM-CM). Flame speeds are calculated and compared with those from full mechanism and experiments. In summary both the various experimental data and numerical results are in an overall good agreement.

kylee@anu.ac.kr

W2P012 EFFECTS OF ELECTRIC FIELDS ON LAMINAR COFLOW NORMAL AND INVERSE DIFFUSION FLAMES

May Chahine, King Abdullah University of Science and Technology, Saudi Arabia

Electric field assisted combustion has demonstrated over many years of studies a promising effect on the flame propagation speed, jet flame stabilization, and emission reduction. A previous study has been carried out to study the

effect of an Alternating Current (AC) electric field on a laminar diffusion flame formed by a central circular jet of propane and a coaxial jet of air. This study has made in evidence the presence of a pair of vortices induced by high voltage alternating current on laminar overventilated normal coflow diffusion flame. This study has been extended to the case of underventilated normal diffusion flame. An interest was also accorded to the overventilated and underventilated inverse diffusion flame where air is injected at the center and the coflow consisted of a jet of propane. Various laser diagnostic methods (OH and PAH Planar Laser Induced Fluorescence, Particle Image Velocimetry and Mie scattering) were used to analyze the flame and flow field structures. Certain AC conditions induced a change in the distribution of Polycyclic Aromatic Hydrocarbons (PAHs), OH radicals, soot particles and flow field. In some cases, this change was the result of formation of a pair of counter rotating toroidal vortices near the nozzle. The underventilated and overventilated normal diffusion flames showed the same changes under the effect of electric field according to OH and PAH profile. The OH profile remained unchanged while the PAHs were shifted toward the nozzle exit. An outer recirculating vortex was visible with naked eyes. While for the two cases of inverse diffusion flame, the signal of OH and PAH was stronger in the absence of electric field and the recirculation zones were identified at the top of the flame. Further studies with continuous wave Argon-ion laser and particle image velocimetry will confirm the effect of the electric field on the recirculation zones. A magnetic field induced due to displacement currents in time varying electric field was the physical mechanism to explain the formation of the recirculation vortices.

may.chahine@kaust.edu.sa

W2P013 PROPAGATING NONPREMIXED EDGE FLAMES IN A COUNTERFLOW ANNULAR JET BURNER WITH ELECTRIC FIELDS

Manh-Vu Tran, Min Suk Cha, King Abdullah University of Science and Technology, Saudi Arabia

We developed a counterflow annular jet burner having 2-mm-wide three co-annular slots. A central slot is for fuel and oxidizer, inner and outer slots for sheath flow of nitrogen. Because a diameter of the central annular slot is 193 mm, a length of the slot is 606 mm. Unlike a flame in a finite length 2D slot burner, a flame with the counterflow annular burner is subjected to a pure one dimensional strain, which is the radial direction in a cylindrical coordinate with (r, theta). In addition, when a flame stabilizes, there are no flame edges along the angle (theta) due to its back-to-back configuration. In this way, more precise measurements of edge flame behaviors will be realized. In this study, propagation speeds of nonpremixed flames were investigated experimentally. CH₄/N₂-O₂/N₂ mixtures were tested, and the effects of electric fields were also investigated applying Alternating Current (AC) as well as positive and negative Direct Current (DC) between upper and lower burners. While the counterflow annular burner was energized with high voltages, a mixture was ignited with a short-pulsed, (O(1) ms), spark. Two high-speed cameras were used to determine a propagation speed of flame, and the detailed shapes of flame edges were captured with an ICCD camera and optical filters. Results showed that both flame propagation speed and flame front shape are affected much for applied electric fields of which direction was orthogonal to that of edge flame propagation.

manhvu.tran@kaust.edu.sa

W2P014 MODELING THE INFLUENCE OF MAGNETIC FIELD GRADIENT ON THE DIFFUSION FLAMES OF LAMINAR JET FLOW

Fang Yue, Pei Fang Fu, Qian Wang, Zhong Qi Fu, Huazhong University of Science and Technology, China

Numerical simulations of axisymmetric laminar hydrogen diffusion flames with/without magnetic gradients are performed, focusing on the flow behavior driven by magnetic convection. It is revealed that magnetic convection is induced by magnetic buoyancy forces due to the inhomogeneity of magnetic susceptibility around the diffusion flame. An interesting quasi-hemispherical structure of diffusion flames on the ground is discovered under, which indicates an isolation of gravity effects on diffusion flames by magnetic field. Furthermore, to investigate the potential magnetic direct influence on radical distributions and chemical kinetics, radical drift motion driven by magnetic gradients is proposed and modeled based on kinetic theory of gases and magnetic force equations. And following theoretical calculations under ordinary magnetic conditions shows a negligible effect of radical drift on laminar jet diffusion flames.

koer.yue@foxmail.com

W2P015 LASER IGNITION AND FLAME DEVELOPMENT IN PREMIXED CONVENTIONAL AND ALTERNATIVE FUEL MIXTURES

Luke Thompson, Bader Almansour, Subith Vasu, Joseph Lopez, Leonid Glebov, University of Central Florida, United States

Laser ignition is one of the most promising ignition techniques with lower ignition energies and ability to ignite leaner mixtures over conventional spark plug ignitions. The recently constructed high-pressure, high-temperature, constant-volume facility at UCF is highly optically accessible, with four windows for Schlieren photography, laser ignition, and more. A pulsed Nd:YAG laser (Quanta-Ray Lab-190) was used to explore the ignition characteristics of methane/air, isooctane/air, and Diisopropyl Ketone (DIPK)/air mixtures. Testing was carried out under various initial temperatures (300-500 K), pressures (1-10 atm), and equivalence ratios (0.4-1.4). High speed Schlieren imaging was

recorded using a He-Ne laser and Phantom v12.1 camera (21000 frames per second), which used to observe flame initiation and flame propagation. The images were post-processed to yield flame speeds as well as unstretched laminar burning velocities. For high pressure cases, flame front wrinkling was observed along with a decrease in flame front thickness compared to smooth laminar flames at atmospheric conditions (Image). Ignition near the lean limit for methane was also conducted and found to be consistent with previous studies. Laser characterization was achieved (using Princeton Instruments ICCD camera) which yielded a non-ideal beam profile and slight pulse to pulse inconsistencies with regards to plasma formation and pulse energy. However, consistency was great enough to allow for reliable ignition studies. Other laser-induced phenomena were examined, including characterization of the resulting shock wave. Ignition testing was performed slightly above the energy threshold for plasma formation. Results from modeling of ignition experiments using detailed mechanisms will be presented as well.

lukezt@knights.ucf.edu

W2P016 A STUDY OF COMBUSTION CHARACTERISTICS IN PREMIXED IMPINGING FLAMES OF SYNGAS(H_2/CO)/AIR

Byeonggyu Jeong, Keeman Lee, Sunchon National University, Korea

Because the SYNGAS fuels which are mainly composed of H_2 and CO , are having a characteristic of low emissions due to the considerable hydrogen contents, they are in the spotlight as a clean fuel of an alternative to conventional hydrocarbon fuels. The staged combustion which reacts with rich conditions has been suggested as most effective way of reducing the NO_x emission for the SYNGAS fuel combustion, maintaining other pollutants at low levels. On the other hand, industrial systems have been used an impinging jet combustion technology in which flames in the combustion chamber are made to impinge directly on — collide directly with — heated objects or heat exchanger for the purpose of homogeneous heating and an improvement in thermal and discharge performance. Therefore, studies of such impinging jet combustion technology can use the role of heated objects or the heat exchanger as the impinging plate to get the quantitative information of transmitted heat with ease.

In present study, the characteristics of flame shape, laminar burning velocity, emissions and heat flux of stagnation point in premixed impinging jet flame of SYNGAS fuel with 10% hydrogen content were experimentally investigated. Also, the adiabatic temperature and burning velocity are calculated by Chemkin package with USC-II mechanism. The wide equivalence ratios (0.8~5.0) and dimensionless separation distance (2.0~5.0) with a fixed Reynolds number (1800) are main parameters in this work. Different flame shapes and colors were observed for different impingement conditions. The experimental results of burning velocity by flame surface area have a consistent with previous works and numerical simulation of this work. The inner flame length could be predicted with the ratio of mixture velocity and burning velocity from a simple formulation by the laminar burning velocity definition. It has been observed that the heat fluxes at stagnation point are directly affected by the flame shape including the separation distance. The emission results in impinging flame of SYNGAS fuel show that the characteristics of NO_x emission traced well with adiabatic temperature trend and CO emission due to fuel rich condition increased continuously with respect to the equivalence ratio. It is expected that the present study will help burner designers select appropriate burner for obtaining more uniform heat flux distribution in flame impingement heat transfer applications.

jbg0928@scnu.ac.kr

W2P017 ANALYSIS OF 2- AND 3-METHYL HEPTANE COMBUSTION USING SYNCHROTRON PHOTOIONIZATION MASS SPECTROMETRY

Hatem Selim¹, Arnas Lucassen², Nils Hansen², Mani Sarathy¹

¹King Abdullah University of Science and Technology, Saudi Arabia ²Sandia National Laboratories, United States

The need to enhance the combustion efficiency in engines while following the strict environmental safety regulations presents a significant challenge. This tradeoff dictates researchers to come up with alternatives and additives to the typical engine fuels. 2-methyl heptane has always been an important component in numerous engine fuels such as JP-4, FACE, and S-8. However, the amount of research devoted to the investigation of 2-methyl heptane combustion remains insufficient. In this on-going research we investigate the low pressure combustion of 2-methyl heptane (C_8H_{18-2}) and one of its isomers, 3-methyl heptane (C_8H_{18-3}).

These experiments were performed at the Advanced Light Source (ALS) at Lawrence Berkeley National Laboratory. The ALS provides monochromatic tunable synchrotron radiation in the vacuum UV range which is used for photoionization. The experimental setup consists of a laminar premixed flame stabilized on a McKenna burner, which is placed in a low-pressure chamber. Gas sampling from the flame, molecular beam formation, and photoionization take place respectively before the sampled gas is directed into a time of flight mass spectrometer with a mass resolution of $m/\Delta m \sim 3500$. Combustion of both 2- and 3-methyl heptane took place at pressure of 20 torr and stoichiometric conditions with 50% of dilution with argon.

The results showed similar trends of the major species (H_2 , CO , CO_2 , H_2O , O_2 , Ar , and fuel) in both flames. Similarly, small intermediate hydrocarbons, e.g. C_2H_2 , C_2H_4 , and C_3H_8 , found to have comparable profiles. However, starting from C_4 the comparison of intermediate hydrocarbons proved to be far different, where the location of the methyl group played a pivotal role. For instance, in case of 2-methyl heptane, the formation of *iso*-butene was significantly evident, while 2-butene was the dominant species in case of 3-methyl heptane, yet the formation of 1-

butene was not affected significantly. Both 1,3 butadiene and 1-butyne were formed in both flames, but in the C₈H₁₈-3 flame 1-butyne mole fraction was one order of magnitude higher. This is emanated from the fact that β -scission bond dissociation can form two C₄ radicals, where both can form 1-butyne. This is not valid in the C₈H₁₈-2 flame. With the help of energy scans the isomers of C₅ to C₇ were also clearly identified. However, some of the isomers were not easy to separate to quantify their mole fractions due to their close ionization threshold.

hatem.selim@kaust.edu.sa

W2P018 AUTOIGNITED NON-PREMIXED LAMINAR LIFTED FLAMES OF *ISO*-OCTANE IN HEATED COFLOW AIR

Saeed AlNoman¹, Sang-kyu Choi^{1,2}, Suk-Ho Chung¹

¹King Abdullah University of Science and Technology, Saudi Arabia ²Korea Institute of Machinery & Materials, Korea

The stabilization characteristics of laminar nonpremixed jet flames of pre-vaporized *iso*-octane, which is one of the primary reference fuels, have been studied experimentally in heated coflow air. Various characteristics of axisymmetric laminar non-premixed jet flames were analyzed, including non-autoignited and autoignited nozzle-attached and lifted flames. For relatively low initial temperatures ($T_0 < 900$ K), an external ignition source was required to stabilize a flame. At low jet velocities, the flame was attached to the nozzle. As the jet velocity increased, the flame lifted-off and lifted flames with tribrachial-edge structure consisting of lean and rich premixed wings and a trailing diffusion flame was observed. The flame lift-off height increased as the jet velocity increased till the flame blew-out. When the initial temperature was over the autoignition temperature ($T_0 \geq 900$ K), autoignited lifted flames can be stabilized without requiring an external ignition source.

Two distinct lifted flames were investigated including those with tribrachial-edge and with mild combustion. Autoignited flames were attached to the nozzle for low jet velocity and then lifted-off for higher velocities. For highly diluted fuels, autoignited lifted flames with mild combustion were observed. Flame lift-off heights were measured and compared with existing *n*-heptane data. It was found that the lift-off height for *iso*-octane was larger than that for *n*-heptane for all flame structures and regimes. A transition behavior from the nozzle-attached flame to the lifted tribrachial-edge flame and then to the mild combustion was also observed in the autoignition regime.

For non-autoignited lifted flames, the flame propagation speed for *iso*-octane was smaller which resulted in higher lift-off height. Successful correlations were obtained for the lift-off height with the ratio of fuel jet velocity to the stoichiometric laminar burning velocity, which is due to the balance mechanism between the local flow velocity and the flame propagation speed. For the auto ignited flames with tribrachial edge structure, the lift-off height for *iso*-octane was higher. This can be attributed to the longer ignition delay time for *iso*-octane when compared to *n*-heptane. The correlations of lift-off height with the computed adiabatic ignition delay time for current pre-vaporized liquid fuels were not successful, while successful correlations were obtained for gaseous fuels in previous studies. The result suggests that the ignition delay time is much less sensitive to initial temperature in the atmospheric pressure condition, as compared to the prediction based on existing kinetic mechanisms. For the mild combustion case, weak dependence on the calculated ignition delay time was also found.

seed.noman@kaust.edu.sa

W2P019 COMBUSTION INSTABILITIES: CHEMILUMINESCENCE AS SENSOR FOR MODEL PREDICTIVE CONTROL

Raimund Noske, Andreas Brockhinke, Bielefeld University, Germany

Modern low-pollutant gas power plants have to run under very lean or low temperature combustion conditions. One of the major issues relevant for the development and operation of these gas turbines is the occurrence of combustion instabilities. These instabilities are based on the coupling of a periodically fluctuating heat release with the acoustic field of the burner chamber. Some consequences of these oscillations are a lower performance and a more rapid deterioration of hot burner parts, making combustion instabilities a very costly phenomenon.

In order to control this problem, a detailed knowledge of the flame behavior and its underlying chemistry is needed. We developed a modular system with rectangular geometry featuring a slit flame holder, a speaker for control purposes and several measuring ports for microphones and optical measurements. This burner is designed to exhibit self-excited oscillations under selected operating conditions. The local heat release fluctuations as well as the reaction zone position were determined by chemiluminescence measurements of OH in the A-X band.

Based on the detailed flame characterization and an acoustic model of the burner chamber, a Model Predictive Controller (MPC) was developed. The MPC critically depends on real-time, accurate sensor information to predict the system behavior. We use the flame chemiluminescence as a fast and inexpensive technique in conjunction with pressure measurements as sensors for the current combustion conditions. This enables the MPC to predict the system behavior, calculate the optimal control signal for the actuator and thus to stabilize the oscillating flame in less than 200 ms, with the speed limited dominantly by the actuator system.

rnoske@uni-bielefeld.de

W2P020 EXPERIMENTAL STUDY OF THE CHEMICAL STRUCTURES OF LAMINAR PREMIXED FLAMES OF DIMETHOXYMETHANE AND DIMETHYL CARBONATE

Bin Yang¹, Wenyu Sun¹, Nils Hansen², Arnas Lucassen¹, Kai Moshhammer³, Kohse-Hoinghaus³, Chung King Law⁴

Among numerous oxygenate fuels, DiMethoxy-Methane (DMM) and DiMethyl Carbonate (DMC) draw particular attention. Due to the lack of C-C bond in chemical structures and relatively high oxygen fractions, they have great potential to reduce particulate emissions. To apply these two fuels to practical diesel engines, we need to better understand their high temperature oxidation chemistry. Previous work have developed detailed kinetic model for both DMM and DMC, but the validation by experimental results is still largely lacking, especially for the case of DMC. In 2005 Glaude built a mechanism which can predict combustion behaviour for both DMM and DMC based on experimental results of an opposed diffusion flame. Only temperature and mole fraction profiles of 8 species were provided by that specific experiment. And no other experimental results for neat DMC flames have been available by so far.

In the present work, low-pressure premixed laminar DMM and DMC flames with equivalence ratio of 1 were investigated. The detailed chemical structures of these flames have been measured with a high mass resolution mass spectrometry using vacuum ultraviolet light as the ionization source. Species identification is the key first-step in the mole fraction measurement. CH_3O (methoxy radical, $m/z = 31$) is a reactive radical that rarely observed in hydrocarbon flames. However, it's supposed to be a significant intermediate in DMM and DMC flames. The PIE spectrum for $m/z=31$ of DMC flame confirms the formation of this radical. At about 10.72 eV an obvious threshold can be observed, which matches the ionization energy of CH_3O , confirming the formation of this radical. About 30 combustion intermediates and products in total were well identified and their mole fractions enable validation and improvement of the proposed reaction mechanism.

The results obtained show that with the mechanism by Glaude the modelling results could well reproduce the flame structure of DMM thus the sub-mechanism for DMM was further validated. While in the case of DMC, the model well predicted mole fractions of the major species, but the prediction for several intermediate species such as CH_3OCHO and CH_3OH were not satisfactory compared to that of DMM. This demonstrated that in the sub-mechanism for DMC the reactions need update and some rate constants for DMC reactions need reestimation. The revised mechanism is still in progress.

byang@tsinghua.edu.cn

W2P021 STRUCTURE OF PREMIXED FUEL-RICH $\text{CH}_4/\text{O}_2/\text{N}_2/\text{CO}_2$ AND $\text{C}_3\text{H}_8/\text{O}_2/\text{N}_2/\text{CO}_2$ FLAMES STABILIZED ON A FLAT BURNER AT ATMOSPHERIC PRESSURE

Andrey Shmakov¹, Denis Knyazkov¹, Oleg Korobeinichev¹, Tatiana Bolshova¹, Artem Dmitriev², Alexey Lobasov², Dmitry Sharaborin²

¹Voevodsky Institute of Chemical Kinetics and Combustion, Russia ²Kutateladze Institute of Thermophysics, Russia

The reduction of pollutant emissions from combustion of fossil fuels is the world's largest problem. One of the alternative methods of solving this problem is using the technology of recirculation of flue gas, the main component of which is CO_2 . Previous studies have shown that the replacement of N_2 with CO_2 influences significantly on combustion efficiency of hydrocarbons. The effects of CO_2 on the burning velocity, composition of final products, and other combustion characteristics of hydrocarbon/air mixtures were extensively studied. Nevertheless, the influence of CO_2 addition on the chemical structure of premixed hydrocarbon/air flames at atmospheric pressure was not investigated earlier. An important issue, in particular, is the influence of replacement of N_2 with CO_2 in the fresh combustion mixture on soot formation in the flame. The goal of this work is to study the effect of replacement of part of N_2 with CO_2 in fuel-rich CH_4/air and $\text{C}_3\text{H}_8/\text{air}$ mixtures on chemical kinetics in premixed flame stabilized on a flat burner at 1 atm by measurement and numerical simulation of its thermal and chemical structure.

Fuel-rich ($\phi=1.2$) $\text{CH}_4/\text{O}_2/\text{N}_2=0.111/0.186/0.703$, $\text{C}_3\text{H}_8/\text{O}_2/\text{N}_2=0.048/0.2/0.752$ and $\text{CH}_4/\text{O}_2/\text{N}_2/\text{CO}_2=0.111/0.186/0.553/0.15$, $\text{C}_3\text{H}_8/\text{O}_2/\text{N}_2/\text{CO}_2=0.048/0.2/0.602/0.15$ flames were stabilized on a flat burner 16 mm in diameter at 1 atm. The burner surface was kept at 95°C. The linear velocity of the fresh mixture on the burner surface was 16.0 cm/s for the $\text{CH}_4/\text{O}_2/\text{N}_2$ flame, 40.2 cm/s for the $\text{C}_3\text{H}_8/\text{O}_2/\text{N}_2$ flame and 7.25 cm/s for the $\text{CH}_4/\text{O}_2/\text{N}_2/\text{CO}_2$ flame, 20.1 cm/s for the $\text{C}_3\text{H}_8/\text{O}_2/\text{N}_2/\text{CO}_2$ flame.

The concentration profiles of the combustion products were measured using quadrupole mass spectrometer coupled with molecular-beam sampling system. Sampling was performed using a quartz probe with the orifice diameter of 0.08 mm and inner angle of 40 degrees. The mass spectrometer was equipped with improved ion source with a narrow spread of electron energies (± 0.25 eV). The mass peaks corresponding to H_2 (2 a.m.u.) were measured at electron energies of 16.65 eV; H_2O and CO_2 (18 and 44 a.m.u.) at 15.4 eV; CH_4 and CO (15 and 28 a.m.u.) at 14.35 eV; CH_3 (15 a.m.u.), C_2H_3 (vinyl, 27 a.m.u.), $\text{C}_2\text{H}_6+\text{CH}_2\text{O}$ (30 a.m.u.), O_2 (32 a.m.u.), C_3H_3 (propargyl, 39 a.m.u.), C_3H_8 (44 a.m.u.), C_3H_4 (allene+propyne, 40 a.m.u.), C_2H_4 (28 a.m.u.), C_2H_2 (26 a.m.u.) at 13.2 eV. Gas-dynamic perturbations of the flame by a probe were taken into account by shifting the obtained profiles upstream.

Temperature profiles were measured using Pt/Pt+10%Rh thermocouple made of wires 0.02 mm in diameter and coated with SiO_2 . To take into account the thermal disturbances induced in flames by a sampling nozzle temperature profiles were measured by a thermocouple, the junction of which was placed at the distance 0.2 mm from the probe's orifice. The flame structure was simulated using Premix code from the Chemkin-II collection of codes and Konnov's

mechanism for hydrocarbons combustion. Experimentally measured temperature profiles were used as input data for the modeling.

The results of measurements indicate that the replacement of 15% of N_2 with CO_2 in $CH_4/O_2/N_2$ and $C_3H_8/O_2/N_2$ flames leads to reducing the post-flame temperature and decreasing maximum mole fraction of ethylene, vinyl, propargyl, allene, propyne and other intermediate hydrocarbon species in the reaction zone. Addition of CO_2 to fuel-rich methane and propane flames is shown to result in considerable reduction of mole fraction of soot precursors. Konnov's chemical kinetic mechanism, in general, adequately reproduces the experimental profiles for major flame species, however, noticeable discrepancies take place between measured and calculated mole fraction profiles for some combustion intermediates. Analysis of the results of calculating the structure of the flame under study and of the literature data has shown the effect of reducing the concentration of intermediate combustion products with partial replacement of N_2 with CO_2 to be connected with the increase of the reaction rate $CO_2+H \rightarrow CO+OH$, resulting in the growth of the ratio of OH/H in the zone of reactions in rich flames. The increase of OH concentration results in acceleration of the transformation of intermediate carbon-containing species into the final products of combustion, thus reducing the probability of soot formation.

shmakov@kinetics.nsc.ru

W2P022

FLAME EXTINCTION LIMIT AND FLAME STRUCTURE CHANGE OF A PREMIXED MICROFLAME

Manabu Fuchihata¹, Tamio Ida¹, Kazunori Kuwana², Satoru Mizuno¹

¹Kinki University, Japan ²Yamagata University, Japan

A methane-air laminar premixed microflame stabilized by an annular pilot flame was observed. The flame is formed even on a main burner whose diameter is 0.4 mm. However, the shape of the flame formed on the main burner whose diameter is less than 1 mm or at around the lowermost flow rate is nearly spherical. It is similar to the appearance of a micro diffusion flame. The flame is not considered a typical laminar propagating flame, because a typical laminar propagating flame has a structure, the thickness of which is more than around 0.5 mm. The flame structure change and the uppermost and the lowermost flow rates that the flame could be formed stably were observed. Consequently, it is supposed that the flame formed on a burner with a submillimeter diameter is dominated by the diffusion mixing of the main premixture flow and the pilot flow. The flame extinction limit and the flame structure change-point are dominated by the condition of the diffusion mixing and the no flame distance around the burner port. The flame condition could be categorized by several non-dimensional parameters, which are the ratio of mean flow velocity to mean diffusion velocity, the ratio of burner diameter to no flame distance, and Damköhler number for diffusion mass transport.

fuchihata@mech.kindai.ac.jp

W2P023

INTERNAL STRUCTURE AND PHYSICAL INTERPRETATION OF A FLAME FRONT THICKNESS

Jury Kryzhanovskiy, Kiev Institute of Nuclear Research, Ukraine

The new interpretation of the concept of the thickness of a normal flame front, λ_n , and interconnection between the flame front propagation rate, U_n , and the specific volume intensity of combustion, ω_n , was presented. So $\omega_n = U_n / \lambda_n$ for normal flame front, and for any flame $\omega_f^L = \omega_f^T = \Pi U_n / (d_0 + \Pi \lambda_n)$. Independence of ω_f^L , U_n and λ_n upon flow regime has been shown. For the laminar flame front thickness at standard pressure and initial temperature of mixture is obtained, $\lambda_n = (D_{LP}^c / U_n)(T/T_0)^{1.5}$, where D_{LP}^c is diffusivity of the limiting reaction product (LP). The new interpretation of the Peclet number, Pe_f , for flame was tested, $Pe_f = d_0 U_n / D^c = d_0 / \lambda_n$. Test results allow drawing a conclusion about existence of three typical zones within flame front thickness (OA, AB and BC) and about new legitimacies for each zone. If an average reaction rate in a flame front, K , we can define using equation, $\omega_n = U_n / \lambda_n = 1/\tau_f = K / C_{LP}^{max}$, then for the local values K the following we have: $K_{OA} \neq f(T_0)$; $K_{AB} \sim T_0^{-1}$; $K_{BC} \sim T_0^{0.5}$; $K_{AB}/K_{OA} \sim T_0^{-1}$. To the each LP concentration the certain temperature in a flame front corresponds irrespective of concentration of reactants. Researches of the laminar flame front structure for the purpose of its detailing have been made. The measurement of \tilde{N}_2 and NO concentrations and temperatures within a laminar flame front of methane-air mixture at various initial temperatures and excess-air factors has been fulfilled. In this paper is carried out the analysis of profiles of temperature change and \tilde{N}_2 concentration change within the laminar flame front thickness. It was revealed that the typical break of a \tilde{N}_2 concentration profile for hydrocarbon-air mixtures is a necessary condition for existence of a self-spreading wave of reaction. It was revealed hydrogen burns out as if it was in the free molecular state at burning of hydrocarbons. Explanation of these results demands improvement of a nowadays understanding of combustion process.

ju.kryzhanovskiy@gmail.com

W2P024

MEASUREMENT AND ANALYSIS OF THE DISTRIBUTED TRANSFER FUNCTION FOR NON-PREMIXED FLAMES

Liyue Jing, Min Zhu, Tsinghua University, China

The combustion oscillation for non-premixed methane-air coflow flame is investigated with experiments and theoretical analyses. The one-dimensional distributed Flame Transfer Function (FTF) is employed to understand the

response of non-premixed flame to external acoustic forcing. Analytically, the general distributed FTF is based on conservation equations and influenced by temperature transfer function and the velocity transfer function. The distributed FTF for an ideal two-dimensional flame is calculated with Green's function method. Experimentally, a non-premixed methane-air coflow flame is generated and forced sinusoidally by loudspeakers mounted on the air flow over a range of frequencies (20Hz~80Hz). The two-microphone technique and CH* chemiluminescence intensity measurement are used to determine the inlet-velocity perturbations and heat release oscillation, which are the input and output to the transfer function. A Cassegrain optical system is used to improve the spatial resolution so that the local, temporal intensity of chemiluminescence can be measured. The system collects the light emitted from a control volume with diameter of 3mm. A guide rail controlled by a stepper motor is applied to make the Cassegrain optical system move along the axial direction. The axisymmetric images of CH* chemiluminescence at different phases in a period captured by ICCD are Abel inverted to obtain the radial profile of the flame structures. The flame flickering phenomenon is also discussed in this paper and the results show that this phenomenon disappears when the air flow rate exceeds a critical number, hence the flame is in the condition of convective instability. In this case we impose the external perturbations to get the distributed FTF. The experimental and analytical results are compared and show that in the frequency domain, the amplitude of the distributed FTF has two peaks, and the angle of the distributed FTF has a nearly π shift through between two peaks. The flame surface is split periodically and the split parts move downstream and gradually decay by diffusion process. The analytical results show that the π shift in angle is caused by hot spot crossing the flame surface, from the fuel-rich zone to the fuel-lean zone. A global FTF is obtained after we integrate the amplitude of the distributed FTF along the centerline and shows that the non-premixed flame system has a low-pass characteristic.

jingliuyue@126.com

W2P025 DYNAMICS OF COLLIDING SPHERICAL FLAMES: MORPHOLOGY, CORNER DYNAMICS, AND FLAME-GENERATED VORTICITY

Sheng Yang, Swetaprovo Chaudhuri, Delin Zhu, Chung King Law, Princeton University, United States

The collision of two identical spherical flames was studied for its relevance in flame interactions in various practical situations including those within turbulent flames. Experimentally, premixtures of fuel (H_2 , C_3H_8) and oxidizer were ignited by two synchronized sparks in a closed chamber under atmospheric pressure, with the subsequent flame-front evolution tracked by a Schlieren system with high-speed camera, as well as computationally simulated.

Results show that development of the morphology of flame collision can be distinguished in three stages: largely independent propagation, strong interaction with flattened interfaces, and corner dynamics after merging of the interfaces. It is further demonstrated that propagation of the flame corner is controlled by the three interacting mechanisms of preferential diffusion, kinematic restoration, and repulsion due to thermal expansion, that vorticity of considerable strength is generated downstream of the corner flame segment, and that the kinetic energy of the flame-generated vorticity is substantial as compared to those of the Kolmogorov eddies such that it could have strong influence on the turbulence energy spectrum.

shengy@princeton.edu

W2P026 BEHAVIOR OF METHANE TORCH UNDER ACOUSTIC ACTION

Victor Golub¹, Mikhail Krivokorytov²

¹*Joint Institute for High Temperatures of the Russian Academy of Sciences, Russia*

²*Moscow Institute of Physics and Technology, Russia*

In this work an experimental research on the behavior of the methane torch under acoustic action was carried out with using of shadow visualization techniques and StereoPIV. It was found that asymmetric mode of instability grows up under acoustic action in internal fuel jet and leads to significant changes in flame shape such as the flame bifurcation. In our experiments we measured the nitrogen oxides concentration in combustion products of detached flame under acoustic action and found that it reduced by half at some resonant frequency of excitation.

victor.v.golub@gmail.com

W2P027 THE EFFECTS OF THERMAL EXPANSION AND GRAVITY ON THE PROPAGATION AND STABILITY OF TRIPLE FLAMES

Philip Pearce, Joel Daou, University of Manchester, United Kingdom

We investigate the effect of thermal expansion and gravity on the propagation of a triple flame in a horizontal channel with porous walls, where the fuel and oxidiser concentrations are prescribed. The triple flame therefore propagates in a direction perpendicular to the direction of gravity. In order to investigate the characteristics of a horizontally propagating triple flame subject to the effect of gravity, it is imperative to first understand the stability of the "strongly burning" diffusion flame, which forms one of the triple flames branches. Steadily propagating triple flames are only expected for parameter values for which the diffusion flame exists and is stable. We therefore begin with a thorough investigation of the effects of thermal expansion and gravity on the stability of a planar diffusion

flame, using a linear stability analysis and numerical simulations of the full governing equations. The planar Burke–Schumann diffusion flame, which has been previously considered unconditionally stable in studies disregarding gravity, is shown to become unstable when the Rayleigh number (which governs gravitational strength) exceeds a critical value¹. The effects of compressibility and finite chemistry on the stability of a planar diffusion flame are tested to provide a full characterisation of the parameter space for which a planar diffusion flame exhibits buoyancy-driven instabilities. For parameter values where the planar diffusion flame is stable, the shape, propagation speed and stability of a triple flame is investigated.

It is found that the system exhibits hysteresis if the Rayleigh number is large enough and the flame-front thickness is small enough. The solutions on the middle branch of hysteresis curves are found to be unstable to small perturbations. Finally, it remains to investigate the behaviour of triple flames for parameter values where the planar diffusion flame is unstable. When the Rayleigh number is large enough, a diffusion flame forms cellular structures, while the fluid forms convection rolls. It is expected that these could affect the propagation of a triple flame, depending on how fast the triple flame propagates.

philip.pearce@maths.manchester.ac.uk

W2P028 DNS OF SPHERICAL FLAME PROPAGATION IN A NON-UNIFORM CONCENTRATION OF FUEL

Shinnosuke Nishiki, Kagoshima University, Japan

In recent years, the computer has been developed dramatically, but, DNS of engine combustion is impossible in realistically. This work is trying DNS of spherical flame propagation. Especially, this poster will show DNS of spherical flame propagation in a non-uniform concentration of fuel gas without turbulence. The numerical domain of 15mm³ is filled by a non-uniform concentration of fuel gas. The grid interval is 0.015625 mm, and the total grid number is about 880 million point (9603). The numerical domain is separated into 60 parts, and 960 cores (60 node X 16 cores) are employed for the DNS.

The ignition is carried out by giving the spherical high-temperature region at the center of computational domain. The initial ambient pressure is 0.1MPa and the temperature is 300K. The Le number is set 3 different values of 1.0, 0.75 and 0.5. The DNS result shows that a spherical flame propagates rapidly in the low Le number case. Even there is no turbulent flow, wrinkled flames are formed by the effect of the Lewis number and the difference of local flame speed. And the integrated reaction rate in the whole of the domain is larger as Le is small.

This indicates a non-uniform concentration of fuel gas condition accelerates combustion in an engine. And this effect should be incorporated into the combustion modeling. For the combustion modelling, DNS will be continued with beneficial improvement in the future.

nishiki@mech.kagoshima-u.ac.jp

W2P030 THERMO-DIFFUSIONAL EFFECTS ON LAMINAR PREMIXED FLAMES OF MULTICOMPONENT FUELS

Christodoulos Xiouris, Tailai Ye, Shyam Menon, Fokion N. Egolfopoulos, University of Southern California, United States

In premixed flames the relative importance of mass and heat diffusivity is manifested by the Lewis number, which is an important parameter affecting burning rates and flame stability. Most of the formulations existing in the literature are derived for single component fuels. However practical fuels are composed of multiple components and as a result the traditional single component Lewis number definition may not be adequate for a variety of conditions. In this investigation, the effect of distinctly different mass diffusivities on the dynamics of stretched flames of multicomponent fuels was studied and the performance of various Lewis number formulations was evaluated.

Flames of propane-hydrogen-air mixtures were studied at various pressures in different configurations using experimental and computational techniques. The shadowgraph technique was implemented to extract Markstein lengths, Lewis numbers, and observe the onset of thermal-diffusional instabilities, in spherically expanding flames under constant pressure conditions. Linear and non-linear extrapolation techniques were used to extract the aforementioned characteristic quantities.

Direct numerical simulations were performed also using detailed chemistry in various one-dimensional flow configurations in order to capture the corresponding changes on burning intensity and flame morphology, due to the very distinct diffusivities of the mixture components.

xiouris@usc.edu

W2P031 IGNITION OF N-HEXANE-AIR MIXTURES BY MOVING HOT SPHERES

Stephanie Coronel, Joseph Shepherd, California Institute of Technology, United States

Assessing the risk of accidental ignition of flammable mixtures is an issue of obvious importance in industry and aviation. In aircraft, potential ignition sources include: lightning strikes, sparks from electrical equipment, electrostatic discharge in fuel tanks, and overheated pumps. In the case of a lightning strike, hot particles are often ejected from the surface that is struck. Such hot particles represent a potential ignition hazard if they are ejected into the flammable vapor space of a fuel tank. Quantifying the ignition hazard of aviation fuels as a function of particle material, temperature, size and velocity is a key issue for both engineering design and safety analyses. In this work, ignition of n-hexane-air mixtures is investigated using falling hot spheres of various materials, diameters and surface

temperatures. Metallic and ceramic spheres of 1.5-4 mm diameters are heated using electrical current and a high power CO₂ laser and injected with an average velocity of 2.3 m/s into a premixed n-hexane-air mixture at an initial temperature and pressure of 298 K and 100 kPa, respectively. The surface temperature of the spheres plausible for ignition upon entering the flammable gas mixture is greater than 1000 K, based on two-color pyrometry temperature measurements. The ignition tests were performed in a 22 L, closed, cylindrical, stainless steel combustion vessel that is first evacuated then filled with the flammable mixture to within 0.01 kPa using the method of partial pressures. Schlieren optics are used to visualize the hot sphere wake and the propagating flame in the case of ignition. The temperature of the sphere is measured during heating, immediately before it is released and begins to fall, and immediately before it enters the flammable mixture. Statistical tools were used to calculate probability distributions as a function of surface temperature and the results were compared for different mixture compositions and sphere diameters. The high-speed experimental visualizations indicate that ignition occurs in the vicinity of the separation point of the boundary layer on the sphere when the sphere surface temperature is near the ignition threshold. The images also indicated that the resulting flames can be either stabilized on the sphere or propagating away from the sphere depending on the laminar burning speed relative to the sphere speed.

coronel@caltech.edu

W2P032 LAMINAR FLAME SPEED MEASUREMENTS OF SYNTHETIC GAS BLENDS WITH AND WITHOUT IMPURITIES

Charles Keesee, Eric L. Petersen, Texas A&M University, United States

New Laminar Flame Speed measurements have been taken for a wide range of synthetic gas, i.e., SYNGAS, mixtures. SYNGAS continues to remain an attractive fuel source; however its composition can vary greatly depending on its feedstock and the process used to gasify it. These experiments encompassed a wide range of SYNGAS mixtures beginning with two baseline mixtures. The first of these baseline mixtures is a bio-SYNGAS with a 50/50 H₂/CO split. The second baseline mixture is a coal SYNGAS with a 40/60 H₂/CO split. Experiments have been conducted over a range of equivalence ratios from $\phi = 0.5$ to $\phi = 3$. All experiments were conducted at initial conditions of 1 atm and 300 K. Upon completion of the baseline experiments, additional hydrocarbons and other impurities were added to the fuel mixture keeping the H₂/CO ratio locked for the bio-SYNGAS and coal SYNGAS mixtures. The addition of these light hydrocarbons makes the mixtures more realistic, as SYNGAS is rarely just H₂ and CO, while allowing the effect on the overall flame speed of each additional component to be studied individually. These flame speed experiments and mixtures therein are based off of earlier research from our group that focused on ignition delay times, which also included a numerical analysis of the laminar flame speed at gas turbine conditions in Mathieu.

It has been shown that addition of hydrocarbons to SYNGAS mixtures have significant effects on the combustion properties. These effects are seen even with small concentrations of hydrocarbons. Experiments were conducted using the Stainless Steel, constant-volume bomb at Texas A&M University. The vessel has an internal diameter of 31.8 cm and an internal length of 28 cm. Optical access was obtained through two fused quartz windows 12.7 cm in diameter. Experimental data were collected using a Z-type Schlieren setup and a high-speed camera. The images were processed using a MATLAB-based edge detection program. The vessel was filled using the partial pressure method monitored with a 0-1000 Torr pressure transducer.

keeseec1@neo.tamu.edu

W2P033 NUMERICAL INVESTIGATION OF THE STAGNATING LAMINAR PREMIXED METHANE/AIR FLAME WITH FUEL CONCENTRATION OSCILLATION USING A FOUR-STEP REACTION MECHANISM

Sotaro Miyamae, Mohd Rosdzimin Abdul Rahman, Hisashi Tomita, Takeshi Yokomori, Toshihisa Ueda, Keio University, Japan

The responses of stagnating laminar premixed methane/air flames under fuel concentration oscillation was numerically investigated using a one-step overall reaction mechanism and a four-step reaction mechanism that included CO and H₂ formation.

The four-step reaction mechanism is 1. $\text{CH}_4 + 1/2\text{O}_2 \rightarrow \text{CO} + 2\text{H}_2$, 2. $\text{CH}_4 + \text{H}_2\text{O} \rightarrow \text{CO} + 3\text{H}_2$, 3. $\text{H}_2 + 1/2\text{O}_2 \rightleftharpoons \text{H}_2\text{O}$, 4. $\text{CO} + \text{H}_2\text{O} \rightleftharpoons \text{CO}_2 + \text{H}_2$ in this research. The analysis was conducted in an axi-symmetric stagnation flow field. The methane/air mixture with sinusoidal equivalence ratio oscillations ($\phi(t) = \phi_m + \phi_A \sin \omega t$) was issued from the burner exit with 1.0 m/s uniform velocity profiles. The flame motion was numerically investigated for three different oscillation cases namely: lean ($\phi_m = 0.75$, $\phi_A = 0.1$), rich ($\phi_m = 1.15$, $\phi_A = 0.15$) and lean-rich crossover case ($\phi_m = 1.0$, $\phi_A = 0.3$). The frequency of the equivalence ratio oscillation was varied from 2 Hz to 50 Hz. For the steady state condition, the results of the one-step overall reaction mechanism and the four-step reaction mechanism show nearly the same characteristics in the lean region, while it shows that the much difference for the flame location and the flame displacement speed. When the equivalence ratio is oscillated, the flame location and the flame displacement speed oscillated. The variation in flame location and the flame displacement speed did not follow those for the steady state condition and made a limit cycles. This was due to the back support effect. The cycles were significantly inclined from the steady state condition at higher frequencies. In the lean condition, the limit cycle was inclined similarly for both the one-step and four-step reaction mechanisms. However, the limit cycle for the four-step reaction was more inclined than that for the one-step reaction in the rich condition. These results show that the formation of CO and H₂ played an

important role in the rich condition. The amplitude of the flame location oscillation did not change when the frequency of equivalence ratio oscillation was less than 8 Hz, while it decreased monotonically when it exceeded 8 Hz. Here 8 Hz corresponds to the Strouhal number (St) is unity. This result indicates that the flame was in a quasi-steady state when $St=1.0$.

croro.so.0627@a5.keio.jp

W2P034 DYNAMIC BEHAVIOR OF BUNSEN FLAME WITH A VERTICALLY IMPINGING VORTEX TUBE

Natsumi Yamane, Takeshi Yokomori, Toshihisa Ueda, Akihiro Tanaka, Keio University, Japan

The flame tip motion of Bunsen flame with a vertically impinging vortex tube has been investigated experimentally focusing on the rotational frequency, the flame stretch and the Lewis number effect. The experimental equipment consists of a burner (ID=12 mm) and a rotating inner tube (D=4 mm). When the inner tube is rotated, a vortex tube is formed along the centerline of the burner. To discuss the effect of Lewis number Le , lean methane/air mixture ($Le \ll 1$), rich methane/air mixture ($Le > 1$), lean propane/air mixture ($Le > 1$) and rich propane/air mixture (Le) were used. The mean velocity U is varied from 0.5 m/s to 1.4 m/s and the rotational frequency N is varied up to 6,000 rpm. When U is gradually decreased keeping equivalence ratio ϕ and N constant, the conical flame tip around the centerline of the vortex tube starts to move toward the unburned side due to the effect of the centrifugal force and finally the curvature of the flame tip is reversed and the convex flame is formed. In the case of the rich propane/air mixture (Le), when $N=0$, the flame tip is weakened. As ϕ is increased, the tip opening and the polyhedral flame can be observed. When the convex flame is formed with increasing N , the flame tip is intensified and the flame edge is weakened. In the case of lean propane/air mixture ($Le > 1$), on the other hand, the flame edge of the convex flame is intensified. For the methane/air mixture, the flame tip varies inversely. These can be explained by the Lewis number effect. The convex flame ratio which is defined as the rate of formation of convex flame per unit time is found to increase as U is decreased, or N is increased. To normalize the effect of the rotational frequency, Swirl number S which is defined as the ratio of the angular momentum to the axial momentum is introduced. The convex flame ratio becomes a function of S regardless of U and N for each ϕ . Modified Swirl number S' which is taking account of the flame stretch is also introduced. The convex flame ratio becomes a function of S' regardless of ϕ except for the rich propane/air flame for $\phi > 1.3$. In this case, the polyhedral flame and the tip opening are observed and the flame stretch cannot be defined.

natsumi0825@z2.keio.jp

W2P035 PREMIXED LAMINAR FLAMES OF METHYL PENTANOATE AND METHYL HEXANOATE: AN EXPERIMENTAL AND KINETIC MODELING STUDY

Oleg Korobeinichev¹, Ilya Gerasimov¹, Charles K. Westbrook², Denis Knyazkov¹, Andrey Shmakov¹, Tatiana Bolshova¹, Nils Hansen³, Guillaume Dayma⁴, Bin Yang⁵

¹Institute of Chemical Kinetics and Combustion, Russia ²Lawrence Livermore National Laboratory, United States

³Sandia National Laboratories, United States ⁴CNRS-INSIS, France ⁵Tsinghua University, China

Detailed chemical structures of stoichiometric and rich premixed laminar flames of methyl pentanoate and methyl hexanoate were investigated over a flat burner at 20 torr and for methyl pentanoate at 1 atm. Molecular beam mass spectrometry was used with tunable synchrotron Vacuum UltraViolet (VUV) photoionization for low pressure flames of both methyl pentanoate and methyl hexanoate, and soft electron-impact ionization was used for atmospheric pressure flames of methyl pentanoate. Mole fraction profiles of temperatures and stable and intermediate species, as well as temperature profiles, were measured in the flames. A detailed chemical kinetic reaction mechanism for high temperature studies of small alkyl ester flames was extended to include combustion of methyl pentanoate and methyl hexanoate, and the resulting model was used to compute mole fraction profiles in each flame and compare computed values with experimentally measured values. Reaction pathways for both fuels were identified, with good agreement between measured and computed species profiles. Implications of these results for future studies of larger alkyl ester fuels are discussed.

korobein@kinetics.nsc.ru

W2P036 EFFECT OF WALL HEAT LOSSES ON FLAME PROPAGATION IN MICRO-CHAMBERS

Orlando Ugarte¹, Berk Demirgok¹, V'yacheslav Akkerman¹, Damir Valiev², Vitaly Bychkov³

¹West Virginia University, United States ²Princeton University, United States ³Umea University, Sweden

Boundary conditions often play the dominant role in the evolution of the combustion processes in micro-burners. In particular, wall friction presumably constitutes the main reason of spontaneous flame acceleration and subsequent Deflagration-to-Detonation Transition (DDT) in narrow channels and pipes. This phenomenon has been intensively studied, computationally and analytically, during the last decade. However, the researchers have focused on the mechanistic scenario of the combustion intensification, induced by wall friction, while the thermal effects at the walls were usually omitted. Specifically, the tube walls were modeled as adiabatic ones in order to distinguish wall friction and wall heat losses. However, the effect is of crucial importance for micro-burners: the processes can be diminished or even quenched because of the energy elimination from the reaction zone.

With this project, we initiate a systematic investigation of the effect of heat losses on the shape and propagation velocity of combustion fronts in micro-burners. Specifically, we compare the roles of adiabatic and isothermal walls by means of direct numerical simulations of the hydrodynamic and combustion equations in various configurations. The parametric study includes channels/tubes with both ends open, and with one end closed, with different radii; slip and non-slip walls, and different isothermal wall temperatures. Ideally-slip walls do not result in a noticeable flame corrugation, except for the effect of intrinsic combustion instabilities. In this configuration, the competition between the instabilities, promoting the flame propagation, and wall heat losses is studied. In contrast, nonslip walls strongly corrugate the flame shape, leading to unlimited in time flame acceleration. The latter is diminished by the heat losses to the wall.

In general, isothermal walls provide weaker flame acceleration as compared to adiabatic ones. Such a result has generally been expected from the primary viewpoint. However, what is interesting is the comparison between isothermal walls at different temperatures. A priori, one can suggest that hot walls facilitate combustion as compared to the cold ones, but our simulations demonstrate the opposite tendency: the higher the temperature of the isothermal walls, the slower the flame propagation. This intriguing effect can be elucidated by the radial heat transfer in the fresh gas, namely, higher wall temperatures will preheat the unburnt fuel and consequently reduce the thermal expansion which drives flame acceleration, reducing the flame front velocity. Consequently, the larger flame velocities should occur when heat is not lost at the boundaries at all, namely, in the adiabatic case. Nevertheless, in spite of the slower flame acceleration with hot walls, the DDT event is anticipated to occur earlier in this case.

ougartea@mix.wvu.edu

W2P037

NUMERICAL STUDY OF INFLUENCE OF WALL TEMPERATURE AND SURFACE REACTION ON FLAME-WALL INTERACTION OF A METHANE-AIR MIXTURE

Naoki Hayashi, Yamashita Hiroshi, Nagoya University, Japan

Flame-wall interaction is an important phenomenon on combustors. Especially, the wall effect on the flame characteristics in a small scale combustor becomes larger than those on normal scale ones due to their large surface-to-volume ratio. The wall effects are caused by heat loss and surface reaction. The surface reaction on many common materials may weaken or quench the flames, although those for a catalytic wall can strengthen the flames. In this study, the influence of the surface reaction and the heat loss on a non-catalytic wall is investigated using numerical simulation.

A two-dimensional slit burner between two parallel plates was modeled. The distance between the two parallel plates is changed, and “quenching distance”, which is defined as the distance between wall when the flame quenches or blows off, is obtained for both active and inert wall conditions, whether the surface reactions are considered or not. The wall temperature is also changed from 500 to 1200 K.

As a result, the quenching distance for the active wall conditions is larger than that for inert wall conditions, and the main reason of “the quenching” is heat loss to the wall, but the surface reaction affect the flame behavior in the immediate vicinity (less than quenching distance) of the wall.

hayashi@mech.nagoya-u.ac.jp

W2P038

EFFECT OF PRESSURE ON HYDROGEN/OXYGEN COUPLED FLAME-WALL INTERACTION

Raphael Mari, Benedicte Cuenot, Florent Duchaine, CERFACS, France

The design and optimization of liquid-fuel rocket engines is a major scientific and technological challenge. One particularly critical issue is the heating of solid parts that are subjected to extremely high heat fluxes when exposed to the flame. As the chamber pressure is usually much larger than the critical pressure of the mixture, supercritical flow behaviors add even more complexity to the thermal problem. When simulating such phenomena, these thermodynamic conditions raise both modeling and numerical specific issues. In the present work, the interactions of Hydrogen/Oxygen supercritical flames with solid walls are studied in conjugate heat transfer simulations, to evaluate the resulting heat flux to the wall and wall temperature, and to study their sensitivity to high pressure and real gas thermodynamics. This high temperature variation occurs in a very thin layer, less than 1mm, leading to very strong temperature gradients and making experimental observation of FWI quite difficult. A fully parallel environment for conjugate heat transfer has been set up, based on a reacting flow solver and a heat conduction solver that can exchange data at their interface. The wall heat flux and temperature are measured over a pressure range from 1 to 100 bar where real gas effects are important. At low pressure, results are found in good agreement with previous studies in terms of wall heat flux and quenching distance, and the wall stays close to isothermal. By changing the fluid transport properties and the flame characteristics, increasing the pressure modifies the heat exchange with the wall that experiences significant heating.

mari@cerfacs.fr

W2P039

NUMERICAL MODELING FOR COMBUSTION PROCESSES IN TWO-LAYER POROUS BURNERS

Jaehyeon Kim, Youngjun Shin, Yongmo Kim, Hanyang University, Korea

Combustion technology in the inert porous media has gained the certain popularity due to its high power density, high power dynamic range and low pollutant emission. In the porous burners, a porous inert medium is used to sustain the stable flame and enhance the combustion efficiency within the solid matrix. The heat release arising from the gaseous combustion is partly utilized to heat the porous matrix in the flame zone. Consequently, in the upstream preflame zone, the porous solid is heated through radiation and conduction and the unburned reactants are be preheated. This regenerative heat feedback mechanism yields several desirable features of the porous medium flame burner such as the reduction of pollutant (CO , NO_x , UHC) emission, enhancement of flame stabilization, effective mixing of the combustion gases, increase of combustion efficiency, and extension of flammability limits.

Depending on the flame stabilization location, the combustion types for the porous burners have been largely classified by the surface flame mode and the radiant flame mode. In the surface flame mode, the mixing and the flow uniformity is enhanced by passing through the solid matrix and the flame is anchored at the surface of solid matrix without propagating into the solid medium. On the other hand, at the radiant mode, the flame is submerged in the solid matrix and the solid medium is exposed to the high-temperature environment. Even if the submerged flame burner has the material limitation for applying commercial burners, the porous burners with the submerged flame has various advantages. The combustion processes with the porous media significantly modify the flame characteristics by increasing the flame speed and the volumetric energy release rates as well as by decreasing the flame length. These unique flame features allow the porous burner to be compactly made as well as to reduce NO_x and CO emission. Moreover, the solid matrix enhances the flame stabilization characteristics such as the anti flashback and the extended lean flammability limit as well as the uniformity of the heat release rate distribution by effectively spreading the flame. Among the various types of the submerged flame burner, the two-sectional porous burner yields the best performance in terms of flame stabilization and pollutant formation characteristics. In the two layered porous burner, the first layer representing the upstream preheating zone has the much lower porosity while the second layer including the premixed flame zone has the much higher porosity.

The performance of the porous burners in terms of heat transfer, flame stability and pollutant formation is substantially influenced by the choice of porous configuration including cellular foams and honeycomb monoliths. Reticulated foams are the most commonly used materials in porous burners due to the inherent advantages such as enhanced mixing, reduced weight, and low pressure loss. On the other hand, honeycomb monoliths are also suitable for the preheating zone of a porous burner owing to low thermal conductivity and limited radiative heat transfer which potentially prevent the flashback.

The present study has numerically investigated the effects of porous configuration on the combustion characteristics of the porous burner. The two-dimensional model with the detailed chemistry and variable transport properties has been applied to numerically investigate the combustion processes and flame dynamics in the bilayer porous burner. Computations are made for two porous configurations including cellular foams and honeycomb monoliths. Based on numerical results, the comparative performances are discussed in terms of heat transfer, flame stability and pollutant emission.

kjh6781@gmail.com

W2P040 INSTABILITY AND TRANSITION TO BALL-LIKE FLAMES OF PREMIXED COUNTERFLOW LOW-LEWIS-NUMBER FLAMES

Tomoya Kobayashi¹, Koichi Takase¹, Hisashi Nakamura¹, Takuya Tezuka¹, Susumu Hasegawa¹, Masato Katsuta², Masao Kikuchi², Kaoru Maruta¹

¹Tohoku University, Japan ²Japan Aerospace Exploration Agency, Japan

To develop clean and efficient combustors, knowledge on combustion limits and near limit phenomena is essential. Past studies have succeeded in clarifying the combustion limits of the planar propagating flame and the flame ball, observed in quiescent low-lewis-number mixtures. However, knowledge on the relationship between these two flames as well as their interactions and stabilities remains incomplete. In a recent study by Takase, the transition from planar flames to ball-like flames was experimentally and numerically shown in the counterflow field at low stretch rates for $\text{CH}_4/\text{O}_2/\text{Xe}$ mixtures. In this study, $\text{CH}_4/\text{O}_2/\text{CO}_2$ mixtures were used to assess the effect of radiation reabsorption on the transition.

Counterflow experiments under normal gravity and microgravity were conducted for stretch rates $1.6\sim 210\text{ s}^{-1}$. Microgravity environments were obtained by parabolic flights on an aircraft. The C-shaped extinction curve was obtained for stretch rates $4.9\sim 210\text{ s}^{-1}$ which has a turning point at stretch rate 11.9 s^{-1} and equivalence ratio 0.473. However, a break of the C-shaped extinction curve was observed at stretch rates below 4.9 s^{-1} along the extinction branch of the C-curve. In this region, transition from planar flames to ball-like flames were observed. Pulsating flames and cellular flames were also observed and a regional diagram of stretch rate and equivalence ratio was made for all observed flame types.

Computations were performed for ideal counterflow flames and ideal flame balls using optically thin radiation models to identify the possibility of transition from planar flames to flame balls. The computed flame temperature of flame balls was higher than that of the counterflow flame at low equivalence ratios. This indicates that if the stretch rate and the equivalence ratio were both sufficiently low, transition from a planar flame to a flame ball may occur in near limit conditions.

UPWARD PROPAGATION OF VERY LEAN METHANE-AIR FLAMES IN VERTICAL TUBES

Victor Muntean, Francisco J. Higuera, Technical University of Madrid, Spain

An experimental investigation of lean methane-air flame fronts propagating upward in a vertical tube has been carried out. During the propagation of the flame the tube is open at the lower end and closed at the upper end. The velocity of the flame front has been measured with an array of photodiodes set along the tube wall and, independently, from photographic records. A PIV system triggered by a photodiode signal has been used to measure the velocity of the flow induced by the flame front in a vertical plane through the axis of the tube. The shape of the luminous region of the flame front, assumed axisymmetric, has been extracted from the recorded images. For the lean mixtures considered in the present work the velocity of the flame front has been found to be independent of the equivalence ratio. As expected, the shape and velocity of a very lean flame front, and the velocity of the fresh gas ahead of the front, are dominated by the buoyancy force and are similar to those of a bubble rising in the tube. The vortical flow of the burnt gas behind the flame front is more complex than the flow of the gas in a rising bubble. As pointed out by various authors before this flow features a region of low velocity relative to the front whose size scales with the radius of the tube and increases when the equivalence ratio decreases. The result can be explained by the competition of two opposing mechanisms. On one hand, as for a bubble, the combination of buoyancy and shear stress acting across the flame front tends to drive the flow of the burnt gas relative to the flame upward around the axis of the tube and downward away from the axis. On the other hand, contrary to a bubble, the gas crosses the flame front and speeds up downward due to the thermal expansion.

The second mechanism dominates for vigorous flames and causes an intense downward flow of the burnt gas relative to the flame front. The first mechanism comes into play when the equivalence ratio, and thus the mass flux across the flame, decrease, and leads to the region of low velocity mentioned above and even to recirculation of the burnt gas. A large residence time of the hot burnt gas in the low velocity region enhances radiation losses from the CO_2 and H_2O present in the gas. Even though the concentrations of these species are far too small for radiation losses to affect the propagation of a planar flame with the same equivalence ratio, order-of-magnitude estimates and numerical computations show that their effect is of the right order to cause extinction at the flammability limit measured in a standard flammability tube.

A simple model based on a combination of experimental results and conservation laws has been proposed to study the effect of radiation losses. Energy and species conservation equations are posited for a narrow stream tube surrounding the axis of the tube and containing the tip of the flame front, where extinction is first observed to occur. Diffusion across the boundary of the stream tube is left out, an optically thin gas is assumed to compute the radiation losses, and the gas velocity that appears in these equations is taken from the PIV measurements. Results for a single overall Arrhenius reaction show the computed location and thickness of the flame compare well with the observed luminous region and the region of increasing velocity in the measured axial velocity profile, which is associated to the thermal expansion of the gas in the flame. The computed temperature displays a marked fall behind the flame due to the radiation losses, with final combustion temperatures smaller than the adiabatic flame temperature by an amount of the order of the Frank-Kamenetskii temperature, and thus able to cause extinction. Inspection of the terms of the energy equation reveals that, in stark contrast with a planar flame, convection may be very small in the low velocity region, leaving an approximate balance of conduction and radiation in this large region. This makes the heat conduction flux from the flame toward the burnt gas larger than for a planar flame by a factor of the order of the ratio of the tube radius to the flame thickness. The proposed model also allows to include more realistic kinetic schemes and radiation laws.

victor.muntean@upm.es

THERMAL DIFFUSION AND COMBUSTION MODELING

Nancy Brown, Aurore Loisy, Lawrence Berkeley National Laboratory, United States

We evaluated the suitability of seven intermolecular potentials and the accuracy of five approximations for computing Thermal Diffusion Factors (TDFs) for eight experimentally studied binary mixtures. We also considered three Lennard-Jones potentials and four modified Buckingham exponential potentials with increasing repulsive character; all potentials except one have the $(1/r^6)$ attractive term. The approximations considered are the Chapman and Cowling, Kihara, Hirschfelder, and the TRANLIB mixture and multi-component methods. Experimental data for these systems were assembled and evaluated by inter-comparison. Quoted TDF experimental error values appear to be larger than the literature quoted values. Calculated values of the TDF were compared with experimental values and with each other using a variety of statistical metrics for individual mixtures and for the ensemble of mixtures. The TDFs were sensitive to the potential shape. The modified Buckingham exp potentials were deemed unsuitable due to the large variability in their computed deviation (with respect to experimental values) distributions even though median deviations often fell within acceptable ranges. The LJ 9-6 potential was the most suitable, and it gave low values of the root-mean-square deviation for four of the approximations used for computing TDFs. The LJ 12-6 potential performed acceptably except for the Kihara approximation. The LJ 28-7 potential is not suitable for the mixtures studied. A synergy between the approximation and the potential was evident: use of the best potential

removed differences between approximations. The TRANLIB mixture approximation was mislabeled in the manual; it only should be applied to isotopic mixtures, and is inaccurate for other binary mixtures. The TRANLIB multi-component approximation works best for the best potential, and should be evaluated for more complex mixtures.

njbrown@lbl.gov

W2P043 A STUDY OF THE EFFECTS OF C=C DOUBLE BOND AND ITS POSITION ON SOOT FORMATION IN LAMINAR COFLOW DIFFUSION FLAMES OF SURROGATES FOR B100 BIODIESEL

Mohammad Reza Kholghy, Jason Weingarten, Murray Thomson, University of Toronto, Canada

Biodiesel produced from vegetable oils, animal fats, or algae is a sustainable renewable fuel with more oxygen content and less aromatic compounds compared to the pure petrodiesel resulting in up to 80% reduced soot emissions from diesel engines. However, soot formation in biodiesel combustion has yet to be studied fundamentally. Results of engine experiments vary in quantitative details and even the laboratory studies about the effects of oxygenated fuels on soot formation are not conclusive. Westbrook showed that biodiesel significantly reduces the concentrations of soot precursors in the premixed combustion and the presence and the number of C=C double bonds change the low temperature reactivity of the fuel. Kholghy studied the effects of ester moiety on soot formation in a laminar coflow diffusion flame of a surrogate for B100 biodiesel with detailed chemistry coupled to the soot aerosol dynamics. The surrogate consisted of 50% *n*-decane and 50% methyl-octanoate to represent methyl-oleate. However the surrogate did not contain any double bonds. In the current study combustion of five decene isomers, i.e. 1-decene to 5-decene and *n*-decane in a laminar coflow flame are simulated to investigate the effects of the C=C double bond and its position on soot formation. It is observed that both the presence and position of the C=C double bond have significant effects on the radial profiles of soot volume fraction. However, the effects of the position of the C=C double bond are dominant. Radial profiles of soot for 5-decene and *n*-decane are similar but the sooting tendencies of decene isomers increase significantly as the C=C double bond becomes closer to the end of the carbon chain resulting in the following sequence of sooting tendencies: 1-decene>2-decene>3-decene>4-decene>5-decene. Maximum for 1-decene is 2.95 ppm which is three times higher than the maximum for 5-decene. C=C double bond in methyl-octanoate is located in the middle of the alkyl carbon chain which is most similar to the position of the double bond in 5-decene. Because *n*-decane and 5-decene show similar sooting tendencies it is concluded that the mixture of 50% *n*-decane/50% methyl-octanoate used in well represents the sooting characteristics of methyl-oleate.

mrk6785@gmail.com

W2P044 EFFECT OF OXY-ENRICHED OXIDIZER AND N₂O ADDITION ON CHARACTERISTICS OF LAMINAR METHANE JET DIFFUSION FLAME

Hsien-Tsung Lin¹, Yueh-Heng Li¹, Guan-Bang Chen¹, Tsarng-Sheng Cheng², Yei-Chin Chao¹

¹National Cheng Kung University, Taiwan ²Chung Hua University, Taiwan

Effective control of flame states will help to improve thermal efficiency and reduce emissions on new energy conversion devices. In order to avoid the combustion instability during lean operation for low fuel consumption, the strong oxidizer concept, such as employing oxy-enriched conditions and nitrous oxide (N₂O) to enhance combustion, is proposed in this study. The objective of this work is to theoretically and experimentally investigate the flame behaviors of oxidizer addition to methane diffusion flames by varying the ratio of oxidizer jet velocity to that of the fuel jet ($R=V_1/V_2$), carried out on a triple port burner. The theoretical results show that the stream velocities, fuel and oxidizer concentrations and stream temperatures are important parameters for flame structures. The experiment results reveal that the formation of the particular double flame structure: an inner Inverse Diffusion Flame (IDF) and an outer Normal Diffusion Flame (NDF) can be observed only by using N₂O as an oxidizer and oxy-enriched conditions of $\Omega \geq 35\%$. It is conjectured that by increasing the oxygen content the local heat release rate rises to a critical condition so that the induced Partially Premixed Flame (PPF) propagates rapidly upstream to form the inner IDF and plenty of soot will suddenly increase due to the change of local velocity field and temperature. If the *R* value increases continuously, the open flame tip phenomenon of IDF and NDF can be observed, this is because the fuel is consumed locally by the considerable amount of oxidizers. In addition, it shows that two types of IDF formation are observed by varying the oxygen concentration and stream velocity. Furthermore, before the formation of IDF, N₂O addition to the flame strongly favors soot formation compared to the mixture of oxygen and nitrogen. Besides, it is found that when N₂O is used as the oxidizer operating condition of the *R* value of IDF are quite similar to that for $\Omega=70\%$.

htlin7747@gmail.com

W2P045 FLAME STRUCTURE AND LUMINOUS CHARACTERISTICS OF DOUBLE DIFFUSION FLAME

Kotaro Moriyama, Takeshi Yokomori, Hiromichi Yamada, Keio University, Japan

In order to meet requirements for saving fossil fuel, the improvement in thermal efficiency of the burner is needed. We focused the radiative heat transfer on combustion to lead the improvement in thermal efficiency. It is well-known that soot in combustion enhances the radiative heat transfer significantly, due to its solid radiation. However, soot is one of main pollutants. To realize the high radiative heat transfer without exhausting soot into the atmosphere, Double Diffusion Flame (DDF) was investigated in this study. The double diffusion flame is consisted of outer

Normal Diffusion Flame (NDF) and inner Inverse Diffusion Flame (IDF) by using coaxial triple port burner which has three concentric tubes. The oxidizer flows from the inner and outer tubes, and fuel (CH_4) flows in the middle tube between these oxidizer tubes. The experimental study was made to investigate the flame structure and the luminous intensity of DDF for various flow velocities V_{in} and O_2 concentrations x_o of inner oxidizer. A numerical simulation was also conducted to discuss the relationship between the inner oxidizer condition and the flame luminous intensity, based on the behavior of C_2H_2 which was one of major precursors of soot. As a result, four types of flame structures were observed; 1) a single cone shaped flame (only NDF), 2) a double cone shaped flame (NDF and IDF), 3) an enveloped shaped flame (IDF penetrates NDF), and 4) a double flame (NDF and lifted IDF). As increasing V_{in} at $x_o > 21\%$, the luminous intensity showed the peculiar variation, that is, the intensity decreased in the range of low V_{in} , increased in the range of middle V_{in} and decreased again in the range of high V_{in} . Based on the numerical results, this variation can be explained as follows. The first decreasing of luminous intensity at low V_{in} is caused by fuel dilution and reduction of soot formation. On the other hand, the increasing of luminous intensity at middle V_{in} is caused by preheating unburned fuel from IDF and increasing C_2H_2 formation which leads to soot production. At high V_{in} , inner IDF approaches outer NDF so that the soot production and the luminous region are reduced, resulting in the decrease of luminous intensity. Consequently, DDF has a suitable flow condition to allow the high luminous intensity.

k.moriyama@z5.keio.jp

W2P046 DILUTION EFFECTS ON THE FLAMMABILITY LIMITS OF OPPOSED-JET SYNGAS DIFFUSION FLAMES
Hsin-Yi Shih, Jou-Rong Hsu, Chi-Rong Liu, Chang Gung University, Taiwan

SYNGAS which is mainly composed of H_2 and CO has been recognized as a viable energy source and an attractive fuel, particularly for stationary power generation with IGCC (Integrated Gasification Combined Cycle) technology. There is considerable variation of H_2/CO ratio with the rest being primarily N_2 , CO_2 , and H_2O . These three diluents may be present or introduced in the SYNGAS mixture during the gasification and refining processes. The practical facilities may also use CO_2 or H_2O as the diluents to control soot and NO_x emission. In addition, to prevent explosions or accident fire from occurring, N_2 is the most commonly used diluents, while CO_2 and H_2O are the most efficient fire-extinguishing agents. The study of the dilution effects on the combustion and extinction of SYNGAS fuels are then important for the combustion applications. The dilution effects on the flame can be categorized as inert effect, thermal/diffusion effect, chemical effect, and radiation effect. In this work, we attempt to provide much clearer insights into how the diluents affect SYNGAS combustion and its extinction limits by those individual effects.

A computational tool, OPPDIF coupled with narrowband radiation model, is used to study 1-D counterflow SYNGAS diffusion flames with fuel side dilution gases such as CO_2 , H_2O and N_2 . In order to distinguish the inert, thermal, chemical, and radiation effects, five artificial and chemically inert species XH_2 , XCO , XCO_2 , XH_2O and XN_2 , which have the same physical and chemical properties as their counterparts are assumed. By comparing the realistic and hypothetical flames, the individual effects on flame structures, chemical reactions and extinction limits are revealed. The computed extinction boundaries are constructed with strain rates and the percentages of diluents (CO_2 , H_2O , N_2) as the coordinates. The inversely U-shaped curves divide flammable and non-flammable ranges. The dilution percentages drop drastically for quenching limits at lower strain rates compared to those for blow off limits at higher strain rates, indicating the significance of radiation effect than chemical effect from the diluents for low-stretched flames. More importantly, the limiting dilution percentages for quenching extinction drop the most with H_2O dilution, but it decreases the most with CO_2 dilution for blow off extinction. A crossover of extinction boundaries between CO_2 and H_2O dilutions are found and the reasons require further dilution analysis. Results show, for equal-molar SYNGAS fuel ($\text{H}_2/\text{CO}=1$) at strain rate of 1000 s^{-1} , the peak flame temperature drops the most for CO_2 -diluted flames, and the least for H_2O dilution. For CO_2 dilution, the thermal/diffusion, chemical and radiation effects all favor flame extinction, and thermal/diffusion effect actually contributes the most with higher heat capacity. Flame goes out earlier due to lower flame temperature at very high CO_2 dilution percentage. As for H_2O dilution, flame extinction is assisted by chemical and radiation effects, especially from chemical effect, but the thermal/diffusion effect can extend the extinction dilution percentage. On the other hand, the analysis for equal-molar SYNGAS fuel ($\text{H}_2/\text{CO}=1$) at strain rate of 0.1 s^{-1} indicates that the peak flame temperature drops the most for H_2O -diluted flames, followed by CO_2 and then N_2 dilution. The extinction dilution percentage with N_2 -diluted SYNGAS fuel is the highest, and it is least with H_2O dilution. The shift of the lowest extinction dilution percentage from CO_2 to H_2O dilutions at lower strain rate is due to the radiation effect. Normally, CO_2 gases are more active in radiation participation than H_2O . However, adding H_2O can produce more OH radicals through the reactions of $\text{H}_2\text{O}+\text{H}\rightarrow\text{H}_2+\text{OH}$ and $\text{H}_2\text{O}+\text{O}\rightarrow\text{OH}+\text{OH}$. This actually leads to the promotion of CO_2 production rate through $\text{CO}+\text{OH}\rightarrow\text{H}+\text{CO}_2$. Therefore, the H_2O -diluted flame has larger amounts of radiatively species including CO_2 , CO and H_2O , despite CO_2 gases is more radiative and less reactive than H_2O . With H_2O addition, the flame temperature before extinction is highest due to chemical effect, but the lowest extinction dilution percentage at lower strain rates attributes to the radiation effect.

hyshih@mail.cgu.edu.tw

W2P047 EXPERIMENTAL AND THEORETICAL STUDY OF DIETHYL CARBONATE IN A NONPREMIXED
 OPPOSED-FLOW DIFFUSION FLAME
Juan David Ripoll Sepulveda, Antioquia University, Colombia

Green oxygenates additives have been shown to reduce soot emissions in combustion systems. Diethyl carbonate is an oxygenate candidate as additive in gasoline and diesel because its high content of oxygen and good miscibility. Ethanol and CO₂ produced by fermenting different raw materials in Colombia are converted to diethyl carbonate using Ni/Cu as catalyst, it may become economically feasible to produce DEC for extensive use as an additive. Furthermore DEC has key chemical kinetic features because of leads to the formation of moiety ROC=O with R= alkyl chain, this moiety appears in the chemistry of all biodiesel fuels due to their ethyl ester groups presents in the molecular structure. Species concentrations were measured across opposed non-premixed diffusion flame of diethyl carbonate. Measures were repeated for mixtures of propane and oxygenated hydrocarbon in order to investigate synergistic effects. The experiments were conducted at atmospheric pressure by withdrawing samples from the flame using a modified quartz microprobe coupled to an online gas chromatograph, major and minor species was determined and theoretical studies of breakdown kinetic mechanism proposed for diethyl carbonate were carried out using "ab initio" quantum chemical methods at the MP2/6-311++g** level of theory. Thermodynamic and kinetic parameters for unimolecular reactions and the key reaction path for bimolecular hydrogen abstraction reactions was determined in order to develop a chemical kinetic mechanism for DEC. This results are being used to gain insights into the combustion of DEC under conditions in the flame and to simulate the same process using Opposed Diffusion Flame (OPPDIF) code. The mechanism proposed and the kinetic parameters calculated for the studied reactions agree well with the available experimental results.

jdripoll@gmail.com

W2P048

EXTINCTION PROPERTIES OF LAMINAR SYNGAS COUNTERFLOW DIFFUSION FLAMES

Amrit Sahu, Rayavarapu V. Ravikrishna, Indian Institute of Science, India

This work presents experimental data on global and local extinction strain rates of SYNGAS diffusion flames. Two different composition of SYNGAS with different calorific values have been considered for the study. The compositions of SYNGAS are chosen based on the composition of commonly available SYNGAS fuels generated from gasification of coal or biomass. The results presented for the first time for SYNGAS diffusion flames would prove to be a valuable addition to literature since extinction strain rates or stretch rates are one of the fundamental properties of any fuel. The global extinction strain rates for 20%-20% H₂/CO SYNGAS and 8%-32% H₂/CO SYNGAS at burner (L/D) standoff were found to be 1713 sec⁻¹ and 848 sec⁻¹ respectively which are very close to the near extinction local strain rate values obtained using the PIV technique. Simulations of the counterflow diffusion flame using OPPDIF have also been conducted to predict the local extinction strain rate. The predicted extinction strain rates using various mechanisms available in the literature when compared with measurements showed discrepancies as high as 25% indicating need for refinement of chemical kinetic models for SYNGAS combustion.

rockinabs4u@gmail.com

W2P049

MOMENTUM-AND BUOYANCY-DRIVEN LAMINAR DIFFUSION FLAME CHARACTERISTICS AT PRESSURES OF 45-100 KPA

Jun Fang, Jing-wu Wang, University of Science and Technology of China, China

Buoyancy and momentum are two major driving forces affecting the behavior of diffusion flames that have not been fully interpreted in sub-atmospheric environments. In this work, the properties of Buoyancy (B)- and Momentum (M)-driven methane laminar diffusion flames at 45–100 kPa were investigated. With increasing fuel source Froude number, Fr_{fs}, flame temperature decreases and radiant fraction increases for B- and M-driven flames; B-driven temperature is generally lower while its radiant fraction is larger. With increasing air pressure, B-driven flame temperature decreases while M-driven flame temperature first increases and then decreases with a maximum at about 70 kPa; radiant fraction increases for both B- and M-driven flames. Flame length measurements showed that with increasing Fr_{fs}, dimensionless flame length lF/d increases for B- and M-driven flames, but lF/d of B-driven ones are far smaller than those of M-driven. With increasing air pressure, B-driven flame lengths decrease slightly, while those of M-driven ones decrease more below 70 kPa, and then stay nearly constant at 70–100 kPa, which agree well with theoretical predictions. For flame oscillation, Strouhal and fuel Froude numbers have the relationship for B- and M-driven flames. With increasing Fr_{fs}, flickering frequency increases and that of B-driven flames is generally smaller than that of M-driven. Air pressure affects flame frequency with the relationship (for B-driven, for M-driven). For M-driven flames, a turning point for flame temperature and length at about 70 kPa merits additional study.

This work provides new findings about the effects of Froude number and low air pressure on flame characteristics and data that validate numerical models of diffusion flames, which will increase understanding of the behavior of unwanted fires in high-altitude environments and spacecraft.

fangjun@ustc.edu.cn

W2P050

STABILIZING MECHANISM OF DIFFUSION MICROFLAME IN HIGH OXYGEN AMBIENT COFLOW

Taro Hirasawa¹, Akter Hossain², Naoki Sato², Yuji Nakamura¹

¹Chubu University, Japan ²Toyohashi University of Technology, Japan

Small-scale jet diffusion flames under the conditions of $Re = O(1\sim 2)$ and $Fr \gg 1$, so called microflames, are in spherical shape even under normal gravity and shown to be dominated by diffusion. Since microflames have features of high heat release density and low soot emission, they have potential to be utilized in new type of burners and combustors. For the wide range of utilization, it is necessary to understand their basic combustion characteristics, like flame stabilizing mechanism. Since the microflames are diffusion flame, they are supposed to be sensitive to the ambient oxygen fraction but its effect on flame stabilization have not been understood. In the present study, the effect of oxygen fraction in ambient coflow on the stabilization of microflame has been investigated experimentally and numerically. A microflame is established where methane issues from the inner tube with 0.7 mm ID at the velocity of 48 cm/s and the coflow mixture of oxygen and nitrogen issues from the outer coaxial tube with 6.0 mm ID at the velocity of 10 cm/s. The oxygen mole fraction in ambient coflow is ranged from 0.20 to 0.49. Positions of the flame base, i.e., reaction kernel are measured in experiments as high emission spot of CH^* observed near the edge. The burner tip temperature is investigated to estimate quenching effect. In numerical simulation, two-dimensional transient transport equations (mass, momentum, energy, and species) that consider the buoyancy effect are solved. The conjugate boundary condition is applied to account for the heat conduction within burner. Both in experimental and numerical results, it is observed that there are two distinct stabilizing mechanisms depending on the applied oxygen fraction in ambient coflow. At higher oxygen region where Damköhler-number is large enough, the flame base position is determined by coactive mechanisms of the increasing quenching zone and the outward shift of the stoichiometric contour line of mixture fraction. At lower oxygen region, on the other hand, where Damköhler-number is not large enough, the flame base position shifts from the position determined by the coactive mechanisms to the downstream by advection.

txhirasawa@isc.chubu.ac.jp

W2P051

DIFFUSION FLAME IN A POROUS CHAMBER

Max Endo Kokubun¹, Fernando Fachini¹, Moshe Matalon²

¹Instituto Nacional de Pesquisas Espaciais, Brazil ²University of Illinois at Urbana-Champaign, United States

We analyze a steady planar diffusion flame established inside an inert porous chamber. Gas and solid phases are coupled through the heat exchange. The influence of porosity and heat exchange (which depends on the injection velocity) on the flame structure and extinction limits is analyzed. The existence of two distinct extinction points for low and high injection velocities (high and low heat exchange, respectively) is observed, as in non-confined problems with heat losses. However, differently from those cases, the extinction point associated with low injection velocity (high heat exchange) has a low Damköhler number. This happens because the injection velocity modifies the stoichiometric (leading-order) flame temperature. For low enough velocities the heat exchange is high, and differently than in premixed flames, the flame temperature drops below its "adiabatic" value. This feature may lower pollutant emissions.

max.akira@gmail.com

W2P053

AUTOMATIZED CHOICE OF AN OPTIMAL PROGRESS VARIABLE FOR CHEMISTRY TABULATION – A CONSTRAINED CONTROL APPROACH

Danny Messig, Uwe Prüfert, Christian Hasse, Sandra Hartl, Franziska Hunger, Michael Eiermann, TU Bergakademie, Germany

In those TCI models chemical look-up table construction strategies are based on the definition of a valid progress variable. This poster deals with the problem to find a valid progress variable. We reformulate it as a nonlinear optimization problem. For that, we state an algorithm to find a valid progress variable, which is also optimal in the sense that the gradients of the tabulated quantities are minimized.

danny.messig@iec.tu-freiberg.de

W2P054

EXPERIMENTAL STUDY ON ULTRALEAN PREMIXED SWIRLING FLAMES OF METHANE-AIR AND HYDROGEN-AIR

Akane Uemichi¹, Takumi Hattori², Hiroki Aizawa², Makihiro Nishioka²

¹The University of Tokyo, Japan ²University of Tsukuba, Japan

Methane-air and hydrogen-air premixed flames around their lean flammability limits were experimentally investigated by using an original swirl burner equipped with a downstream holder that inhibits backflow of unburned gas. It was found that without preheating of the premixed gas, ultralean flames of methane-air and hydrogen-air were obtained; the leanest extinction limits are equivalence ratios 0.465 for methane-air and 0.081 for hydrogen-air. In our recent detailed-chemistry numerical studies on Rotating Counterflow Twin Flames (RCTF), stable ultralean flame was obtained successfully, and its combustion mechanism was identified. There is a possibility that the upstream tip of the present cone-shaped very lean swirl flame has almost the same flame structure and velocity field as the rotating counterflow twin flame of the same equivalence ratio. Indeed, the measured maximum flame temperature of the present hydrogen-air swirl flame is more than 200 K higher than its adiabatic flame temperature, which is one of the peculiarities of ultralean hydrogen-air RCTF. Although the flow field was not measured in the present experiment, there must be a large recirculation zone of the burned gas surrounded by the flame surface and the downstream holder,

since the self-propagation speed of flame near the lean flammability limit is almost zero. This recirculation zone causes a counterflow of burned gas and unburned gas at the flame tip similarly to an ultralean RCTF, which suggests that the mechanism of ultralean combustion can be common between the present swirling flame and RCTF.

uemichi@fiv.t.u-tokyo.ac.jp

W2P055 INFLUENCES OF PERIODIC FUEL CONCENTRATION OSCILLATION TO LAMINAR BUNSEN FLAME

Taichi Minowa, Kei Ito, Abdul Rahman Mohd Rosdzimin, Toshihisa Ueda, Takeshi Yokomori, Keio University, Japan

Time variations of flame height and flame luminosity of the methane / air laminar Bunsen flame with periodic equivalence ratio oscillation were experimentally investigated. The amplitude of the equivalence ratio oscillation, the oscillating frequency and the mean value of equivalence ratio oscillation were varied. The flame motion was recorded by a high-speed camera with the frame rates 250 or 500 fps. The influence of the amplitude of the equivalence ratio oscillation ϕ_a was investigated by varying $\phi_a = 0 \sim 0.20$, keeping the oscillating frequency $f = 10$ Hz and the mean equivalence ratio $\phi_m = 1.40$ constant. Amplitudes of variations of the flame height and the flame luminosity increased with increasing ϕ_a . At the same time, it was found that the phase of the maximum flame height shifted backward with increasing ϕ_a . This seems to be due to the phase shift of burning velocity oscillation by the interaction between the instantaneous flame velocity and the fuel concentration gradient of the premixed mixture. Furthermore, it was observed that there was a phase lag between the variation of the flame height and that of the flame luminosity. The influence of the oscillating frequency f was investigated by varying $f = 5 \sim 40$ Hz, keeping $\phi_m = 1.40$ and $\phi_a = 0.20$ constant. Amplitudes of flame height and flame luminosity decreased with increasing f . This seems to be due to the attenuation of the equivalence ratio oscillation because of the increase in the transport by the molecular diffusion relative to that by the convective transport. These results suggest that the molecular diffusion of fuel plays an important role to explain the influences of the periodic fuel concentration oscillation.

m-taichi@a3.keio.jp

W2P056 THE EFFECT OF HEAT LOSS ON LEAN $\text{CH}_4/\text{O}_2/\text{Xe}$ COUNTERFLOW PREMIXED SLOT-JET BURNER FLAMES

Koichi Takase, Hisashi Nakamura, Kaoru Maruta, Tohoku University, Japan

Recent microgravity experiments show that the formation of ball-like flame was observed on the center of low-speed and low-Lewis-number counterflow field, near the stagnation plane. Axisymmetric 2-D computation revealed that obtained ball-like flame is allied to an ideal flame ball. Besides, the formations of curved flames on the low-Lewis-number slot-jet counterflow field have been observed experimentally. This experimental slot-jet burner has the walls at the burner edges to stabilize the curved flame. However, the walls are expected to act as heat dissipater when the speed of counterflow is extremely low and may affect the shape of observed flame.

The objective of this research is to computationally clarify the effect of heat loss through the walls on the edges of slot-jet burner by the 3-D computation of low-Lewis-number counterflow premixed flames using slot-jet burner. Two rectangular nozzles of 3 cm in height and 1 cm in width are used as a slot-jet counterflow burner and the distance of two nozzles is 3 cm. Two kinds of thermal boundary conditions at slip walls are adopted on the upper and lower edges of slot-jet burner. One is adiabatic wall and another is fixed wall temperature at 300 K. CH_4/O_2 mixture was used and Xenon (Xe) is adopted as inert species to decrease the Lewis number, Le . The dilution ratio (The ratio of molar fraction of O_2 to that of Xe) is fixed to 0.141 ($Le \sim 0.5$). The focus is on the low-Lewis-number counterflow flame under the interaction of convective, diffusive and radiative effects. At equivalence ratio of 0.40 and stretch rate of 3.2 s^{-1} , the twin planar flames were obtained with the adiabatic wall. Whereas, a flame with convex curvature on the flame-edge and concave curvature at the center, was obtained. The reaction rate at the edge of flame is higher than that at the center of flame more than two times. Therefore, it is implied that the heat loss through the burner walls play an important role in the formation of curvature flame. Future investigation plans to clarify the regime of low-speed slot-jet $\text{CH}_4/\text{O}_2/\text{Xe}$ counterflow premixed flame and the effect of interaction between the convective, diffusive and radiative effects.

takase@edyn.ifs.tohoku.ac.jp

W2P057 DYNAMICAL BEHAVIOUR OF FLAME FRONT INSTABILITY WITH RADIATIVE HEAT LOSS

Kazuhiro Ueda, Yuta Okuno, Hiroshi Gotoda, Ritsumeikan University, Japan

We conduct a detailed and systematic study of the dynamical behavior of flame front instability in a diffusion flame with radiative heat loss preceding to flame extinction by making use of time series based on chaos theory. One of author (Combust Theory Modell. 14, 479, 2010; Chaos 22, 033106, 2012) recently reported two main findings on the dynamical behavior and its nonlinear nature: one is that the dynamical behavior of flame front temperature fluctuations undergoes an interesting transition from steady-state to chaos with increasing the Damköhler number via the period-doubling cascade process known as Feigenbaum scenario. The other is that the short-term predictability and long-term unpredictability nature of chaotic dynamics can be quantified by a global nonlinear predictor such as a generalized radial basis function network. These studies have focused on the dynamical behavior of flame front temperature fluctuations, but not yet dealt with the fuel mass fraction fluctuations. In this Work-In-Progress session,

we present the possible route to chaos for the fuel mass fraction fluctuations and its dynamical properties from a viewpoint of chaos theory.

rm0001xp@ed.ritsumei.ac.jp

W2P058 CHARACTERISTICS OF AMMONIA/N₂/O₂ LAMINAR FLAME IN OXYGEN-ENRICHED AIR CONDITION

Hiroyuki Takeishi¹, Jun Hayashi¹, Kimio Ino², Fumiteru Akamatsu¹

¹Osaka University, Japan ²Taiyo Nippon Sanso Co. Ltd, Japan

This study focused on the combustion characteristics of ammonia for clarifying the effect of the oxygen-enriched combustion on the flammable region, the laminar burning velocity and the flame temperature of an ammonia/N₂/O₂ laminar premixed flame. Recently, the world's energy demand has been increasing because of economic development and population growth in developing countries. In addition, anxieties regarding fossil fuel depletion and global warming have arisen worldwide (IEA, 2011). At present, 81% of the world's total primary energy demand is supplied by combustion of fossil fuel (IEA, 2011). Additionally, fossil fuels are limited resources. Therefore, alternative fuels without CO₂ emission in combustion process are now getting attentions and they are required to be used more efficiently. This study focused on ammonia fuel as one of the alternative fuels. Ammonia is produced on a large scale easily by using the Haber–Bosch process and be transported easily.

Additionally, ammonia fuel emits no CO₂ during the combustion process. One of the problems of ammonia fuel is lower combustion quality than that of fossil fuel. In this study, laminar burning velocity was used as one of the means to evaluate the combustion quality. In the previous study, it is known that the laminar burning velocity of ammonia/air premixed flame was about 6 cm/s at near stoichiometric condition. This laminar burning velocity is very low compared with that of other fossil fuels. Therefore it is necessary to increase the combustion quality for the utilization of ammonia fuel in combustion systems. In this study, the oxygen-enriched combustion was applied to an ammonia/N₂/O₂ premixed flame for achieving higher combustion quality and the effects of the oxygen-enriched combustion on the laminar burning velocity of an ammonia/N₂/O₂ premixed flame were evaluated experimentally. Also, the flammable conditions and the flame temperature were measured experimentally. Results showed that the laminar burning velocity was improved as O₂ concentration increased. In addition, the laminar burning velocity of an ammonia/N₂/O₂ premixed flame becomes the same order of laminar burning velocities of methane and propane premixed flame in O₂ enriched condition (O₂: 30%). Also, the temperature of ammonia flame zone was about 1900 °C under O₂ enriched condition (O₂: 30%).

htakeishi@combu.mech.eng.osaka-u.ac.jp

W2P059 EXPERIMENTAL AND MODELING STUDIES OF ETHYL VALERATE FLAMES AT LOW PRESSURE

Véronique Dias, Haddy Mbuyi Katshiatshia, Hervé Jeanmart, Université Catholique de Louvain, Belgium

The increasing demand of energy, the decreasing availability of fossil fuels, and the climate changes are important challenges of this century. To alleviate these issues, scientists propose to diversify the energy mix including a major contribution from biomass, also in the form of biofuels. The present work considers specific biofuels: esters with pentanoate as the principal radical. They can be produced as follows. Levulinic acid is produced by the acid hydrolysis of lignocellulosic biomass. Then, the esters are produced, combining the acids and an alcohol, by hydrogenation and esterification. Some of these esters, the methyl and ethyl valerate (C₆H₁₂O₂ and C₇H₁₄O₂), can be used as fuels in a spark ignition engine. The heavier ones, propyl and butyl valerate (C₈H₁₆O₂ and C₉H₁₈O₂), can be used in a diesel engine. Those molecules can also be used in Homogeneous Charge Compression Ignition engines. Recently, Dayma studied experimentally the ethyl valerate combustion at high pressure (10 atm) in a jet stirred reactor, and the laminar burning velocities in a spherical combustion chamber. According to the experimental results, they elaborated a mechanism containing 524 species and 2431 reactions. However, the validation this mechanism at low pressure is an important step to predict the different pathways of the ethyl valerate combustion at different equivalence ratios.

Thus, this study focuses on ethyl valerate (C₇H₁₄O₂) combustion. Specifically, we analyzed experimentally the structure of premixed flat flames of ethyl valerate/O₂/Ar at different equivalence ratios, at 55 mbar. The flames are stabilized on a Spalding-Botha type burner at low pressure to accurately measure the mole fraction profiles of species produced and consumed during the combustion. The chemical compounds have been identified and calibrated by gas chromatography. Three premixed flames (lean, stoichiometric, and rich) have been studied at the same pressure by keeping the total flow rate of the reactants constant. However, working with esters required some modifications of the experimental setup. We had to adapt an evaporation system for the ester, so that they can be fed into the combustion chamber in gaseous phase. The experimental set up is composed of an Evaporation System (EV), a Combustion Chamber (CC), a Compression System (CS) and a Gas Chromatography (GC). The combustion chamber is connected to the evaporation system which is composed of two mass flow meters and an evaporator. The first flow meter is used for the liquid and has a capacity of 110g/h and the second one, is used for the argon, as a gas vector, with a maximum flow of 2ln/min. The liquid and the gas are mixed and evaporate in the evaporator at 200°C. To keep the ethyl valerate in the gaseous phase, a heated ribbon (250°C) is used between the EV and the combustion chamber. The other gaseous reactants are also heated to 90°C using water into to avoid condensation of ester in the mixing volume before the CC. The sampling system is composed by a quartz nozzle, a heated ribbon and a compression system. The quartz nozzle is

placed into the CC and has a diameter of 0.2 mm. Sample is collected by moving the burner which is horizontal to the nozzle. Sampling in the flame is done through a quartz nozzle. To keep the sample at high temperature and to avoid condensation, a ribbon heats up the sampling line (200°C). As the experiments are performed at low pressure (55mbar) and as the GC is working at atmospheric pressure, a compression system is required to increase the pressure of the sampled gas before its injection. Pressure controllers and thermocouples are used before and after the compression system to assess the pressure and the temperature before injecting sample into the GC. The pressure before and after the compression system are 20 mbar and 1700mbar, respectively. The compression is nearly isothermal at a temperature of 72°C. The cylinder of the compression system is also heated at 130°C to avoid condensation of the ester during compression. The GC is used to analyze the sample collected (fresh and burned gas) and has three columns (CP SIL CB₅ for the hydrocarbon compounds and Molseive in series with RTX1 for the permanent gases).

It is envisioned that the kinetic model elaborated by Dayma will complete the "UCL" mechanism already validated against several hydrocarbons and oxygenated species flames. Moreover, it will be exploited in related combustion modeling efforts. In particular, the mechanism could be coupled to Computational Fluid Dynamics (CFD) tools in order to study the performance of esters within an Homogeneous Charge Compression Ignition (HCCI) engine.

Veronique.Dias@uclouvain.be

W2P060

EFFECT OF AIR TEMPERATURE ON FLAME BASE POSITION OF MINIATURE JET FLAMES

Takato Chujo¹, Tsuneyoshi Matsuoka¹, Susumu Noda¹, Taro Hirasawa², Yuji Nakamura¹

¹Toyohashi University of Technology, Japan ²Chubu University, Japan

Since the combustion is enable to convert the chemical energy to thermal energy in convenient way yet generate a high power than a battery, combustion technology could be utilized to the miniature power source of unmanned robots operating in hazardous environments at which the human activity is no longer possible (e.g. radiative environment delivered by damaged nuclear power plant). For this purpose, the combustion for such device must be easily controllable and stable against disturbance in small scale. Hence, the stability of a miniature flame must be understood well from fundamental point of view. As one example, there is a millimeter-size of diffusion flame so-called "microflame", which is formed over a fine needle burner when a small amount of fuel is supplied. As the scale is reduced, the thermal and chemical interactions between the flame and the burner must be enhanced, so that effect of such interaction on the flame stability is a research target. To separate the thermal and chemical effects intentionally, this study utilize the high-temperature combustion technique. The flame shape especially near the burner edge was experimentally observed. The flame-base positions are compared to ones in other situations such as high oxygen concentration in ambient flow (Hirasawa Proc. ECM 2013) to find out a similarity rule of the effects of oxygen concentration and temperature on the stability of microflame. Methane gas was issued through stainless straight burner with 0.7 mm inner diameter and 1.0 mm outer diameter. Surrounding air flow was straightened and supplied into a combustion chamber. Direct flame images under various air temperature conditions showed that the flame size got smaller and its shape approached to semi-spherical as the air temperature increased. It is found that, for any flow rate, the flame-base position suddenly closes toward the burner when the temperature becomes higher then turns into toward the edge. The similar tendency was observed in Hirasawa's experiments under various oxygen fractions. Reactivity modeling would be possible to describe/predict the flame base location, namely, the thermal interaction between the flame and the burner in various (potential) conditions to be utilized in the power device.

t113126@edu.tut.ac.jp

W2P061

PILOTED IGNITION OF CLEAR AND BLACK PMMA CYLINDERS

Shmuel Link, Carlos Fernandez-Pello, University of California, Berkeley, United States

The piloted ignition of cylindrical samples of clear and black PMMA was investigated with the intent to better understand the effect of in-depth radiation absorption on the ignition process of solid fuels. The experiment consisted of 7.62 cm length 1.27 cm diameter PMMA samples that were placed axially at the center of a 7 cm diameter flow duct. The samples were then uniformly heated with quartz halogen lamps with between 10 and 30 kW/m² of incident radiant flux. Both temperature and mass data was collected from which time to ignition and mass flux at ignition was subsequently determined. Clear samples were seen to exhibit a longer ignition delay time than black samples of similar geometry when subjected to similar heat fluxes. Yet, both clear and black samples exhibit similar mass fluxes at ignition. It is hypothesized that this difference in ignition delay is caused by in-depth radiation absorption in the clear samples, while the black samples absorb most of the thermal energy within a thin layer close to the surface of the samples. These differences in thermal radiation absorption between the clear and black samples lead to differing rates of pyrolysis generation throughout the samples leading to differing times at which a sufficient mass flux of pyrolyzate for ignition can be achieved. The observation that similar mass fluxes must be achieved for ignition to occur confirms the concept of a critical mass flux at ignition. Comparison with the experimental results of piloted ignition of flat PMMA samples show that piloted ignition times are shorter for cylinders while the mass flux at ignition is similar, supporting the present models of piloted ignition

slink@berkeley.edu

ON CELLULAR INSTABILITY IN LEAN PREMIXED HYDROGEN-METHANE-AIR FLAMES AT ELEVATED PRESSURES

Ekenechukwu Okafor, Yukihide Nagano, Toshiaki Kitagawa, Kyushu University, Japan

Hydrogen addition to natural gas in spark ignition engines is considered one of the possible means of enhancing the burning velocity, reducing CO₂ emission and increasing the thermal efficiency through robust lean operation. This may increase the tendency of the flames to be unstable because lean hydrogen flames tend to be more unstable than lean methane flames. Flame instability may be further intensified by an increase in pressure. Therefore, a proper understanding of the effects of hydrogen concentration and mixture pressure on the stability of H₂-CH₄ flames may be useful in modeling of the turbulent flames.

Experimental and theoretical studies on lean premixed hydrogen-methane-air flames were conducted to investigate these effects on flame front instability. The experiments were conducted in a 35 liter constant volume chamber at a mixture temperature of 350 K and mixture pressures of 0.10, 0.25 and 0.50 MPa. The mole fraction of hydrogen in the binary fuel was varied from 0 (methane only) to 1.0 (hydrogen only) at equivalence ratio of 0.8. The unstretched laminar burning velocity, the Markstein number and the critical Peclet number for the onset of flame front instability were obtained from the experiments. The Markstein number and the critical Peclet number were further evaluated analytically. The two parameters are functions of the effective Lewis number, the Zeldovich number and the thermal expansion ratio.

For fixed mixture pressures, the Markstein number and the critical Peclet number decreased non-monotonically with an increased in hydrogen fraction due primarily to the influence of the effective Lewis number, which decreased and then increased as hydrogen fraction increased. A comparison of the morphology of the flames at same values of a non-dimensional stretch rate showed that the propensity of the flames to be unstable supported the trends in the Markstein number and the critical Peclet number. The results suggest that a mixture of hydrogen and methane with hydrogen mole fraction of 0.7 may be more unstable than a pure hydrogen flames at equivalence ratio of 0.8. It was concluded that the variation in the propensity of the flames to be unstable with hydrogen fraction was controlled mainly by thermo-diffusive effects. For fixed hydrogen fractions, the flames became more unstable with increase in mixture pressure and the scale of flame wrinkling decreased. The thermal expansion ratio proved to be insensitive to pressure variation; however, the flame thickness decreased with increase in mixture pressure thereby suggesting an enhancement of hydrodynamic instability. The Markstein number decreased mainly due to increase in the Zeldovich number with increase in mixture pressure. The Markstein number turned negative at higher pressures when the critical effective Lewis number, which increased with mixture pressure, became larger than the pressure insensitive effective Lewis number. Hence, increase in mixture pressure may intensify flame instability due also to an increase in the destabilizing influence of thermo-diffusive effects.

kenevidson@yahoo.com

2D-INSTABILITY OF HYDROGEN FLAMES

M. Kuznetsov¹, J. Yanez¹, J. Grune², A. Souto-Iglesias³

¹Karlsruhe Institute of Technology, Germany ²Pro-Science GmbH, Germany

³Naval Architecture Department, Technical University of Madrid, Spain

To date, very limited knowledge is available on how hydrogen behaves in two-dimensional planar geometry as much focus were given towards hydrogen flame behavior in one – dimensional tube and three – dimensional spherical geometry. The focus of this work is to investigate how flame behaves in a planar 2D-geometry and particularly, how the intrinsic instabilities of hydrogen flame affects its propagation in such geometry. A series of experiments in 2D-geometry with hydrogen – air and hydrogen – oxygen mixtures were conducted in between two transparent glass plates at ambient conditions. Different configurations with respect to hydrogen concentration and layer thickness were implemented. Shadowgraph method, with the help of a high – speed camera, was used to visualize the flame propagation. Flame instabilities give rise to the development of a cellular structure on the surface of the flame. The cellular structure results in an increase of flame surface area and hence, promotes higher rate of fuel consumption. This results in Flame Acceleration (FA), which in turn could lead to the transition from Deflagration to Detonation (DDT). Formation of the cellular structure was analyzed and the stretched-free laminar burning velocity was determined. Thermo-diffusion and Landau – Darrieus instabilities were leading to formation of double-modes cellular structure of the flame surface.

An analysis with the Sivashinski-Michelson equation was performed in order to describe the experimental results and its dynamic development in terms of the basic physical properties of combustible mixtures. It was found, that the burning velocity increased by the factor of $X = 1.2-1.5$ due to the flame instability. This value was proportional to the flame area amplification rather close to experimental data. The characteristic time of flame development with a cellular structure due to Landau-Darrieus instability was found to be much longer than the corresponding one for thermo-diffusion instability for lean mixtures. Also, we correlated the time required for instability development as a function of the mixture reactivity.

kuznetsov@kit.edu

W2P064

FLAME INSTABILITY OF LEAN HYDROGEN-AIR MIXTURES IN A SMOOTH VERTICAL CHANNEL WITH OPEN END

Mike Kuznetsov¹, Jorge Yanez¹, Joachim Grune², Antonio Souto-Iglesias³

¹Karlsruhe Institute of Technology, Germany ²Pro-Science GmbH-Germany ³Technical University of Madrid- Spain

This work addresses the experimental investigation and analytical interpretation of a flame suffering the acoustic-parametric instability excited by the pulses generated by the own flame. The research was carried out for lean hydrogen-air mixtures under flame propagation in a smooth channel with open end. It was found that very lean mixtures with hydrogen concentration less than 14% H₂ generate acoustic oscillations due to the flame instabilities which in turn significantly influence the propagation of the flame. Above concentrations of 14% H₂ the flame becomes relative stable to self-generated acoustic perturbations. It was also found that external polychromatic sound generator with a dominant frequency of 1000 Hz inhibits the instabilities and results in a reduced flame propagation velocity. Numerical solutions of the Searby and Rochwerger analytical formulation for the acoustic-parametric instability were utilized to analyze the experiments and to study the influence of different parameters on the existence of spontaneous transition from the acoustic to the parametric instability.

kuznetsov@kit.edu

W2P065

INFLUENCE OF THE BURNER RIM THICKNESS ON THE STABILITY OF CH₄/O₂/CO₂ NON-PREMIXED FLAME

Shuhei Yoneyama, Takeshi Yokomori, Keio University, Japan

Oxy-fuel combustion is one promising approach for carbon dioxide emission reduction. Because of the destabilization of the flame by a flame temperature reduction in oxy-fuel combustion, understanding the stabilization mechanism of the flame is one of key issues to design the burner. The purpose of this study is to investigate the influence of burner rim thickness on the stabilization mechanism of methane non-premixed flame under various diluted conditions with CO₂. The non-premixed flame was stabilized on a two-dimensional Wolfhard-Parker burner with a variable partition wall (burner rim) thickness between the fuel and oxidizer jets. The burner rim thickness δ was changed from 0.5 mm to 6.0 mm. The lifted flame height and the stability limit were investigated experimentally. As increasing the velocity at fuel and oxidizer concentrations 35 %, the lifted flame appeared and then the blowout occurred for $\delta = 0.5, 2.0$ mm in CO₂, while the flame base remained anchored in the wake region and a blow off occurred suddenly for $\delta = 2.5, 6.0$ mm. Moreover, the blow off limit for the thick burner rim was larger than that for the thin burner. Those results suggest that the flame was stabilized by the recirculation zone in the wake region for the thick burner rim. Comparing between the diluted conditions with CO₂ and N₂, the stability limit in CO₂ was smaller than in N₂ and the lifted flame was not observed for any burner rim thicknesses in N₂. It is suggested that the flame stabilization was influenced by not only the reduction of the flame temperature due to high specific heat but also the aerodynamical modification in the CO₂ diluted condition.

shuhei-yoneyama@z8.keio.jp

W2P066

NUMERICAL STUDY OF INTERACTION BETWEEN DARRIEUS-LANDAU INSTABILITY AND SPATIALLY PERIODIC SHEAR FLOW

Damir Valiev¹, Andrea Gruber², Chung King Law³, Jacqueline H. Chen¹

¹Sandia National Laboratories, United States ²SINTEF Energy Research, Norway ³Princeton University, United States

It was recently shown that DL instability has a role in boundary layer flashback of premixed turbulent flames, actively contributing to flame acceleration through flame corrugation that, in turn, results in the creation of near-wall regions of flow reversal ahead of the flame sheet. The flame in the boundary layer behaves in a laminar fashion modulated by weak, highly anisotropic velocity fluctuations. It is seen that the flame acquires a corrugated shape with the characteristic time and length scales that can be correlated with the structures in the boundary layer. The oncoming prolonged velocity streaks with alternating regions of relatively high and low velocities interact with the initially planar flame. The observed flame shape evolution suggests that the streaky structure of the flow triggers the corresponding unstable wavelength of Darrieus-Landau (DL) instability, resulting in the flame acceleration and subsequent upstream propagation of a corrugated flame.

Recent experimental investigations have confirmed the existence of the above mentioned flow reversal regions in both swirling and non-swirling configurations, with flame propagation upstream with velocities approximately two times larger than the laminar burning velocity. Several previous studies focused on the interaction of weak, homogeneous isotropic turbulence and DL instability. In Refs. it was found that the effect of DL instability may be dominant when the turbulence intensity is low. In Ref. it was found that a planar flame that is subjected to oncoming periodic shear flow can propagate with increased velocities in the absence of thermal expansion. However, there still remain many open questions regarding the interaction of anisotropic velocity fluctuations and flames with realistic expansion. We perform a detailed investigation of the role of DL instability on the regime of laminar flame front propagation subjected to external forcing by a spatially periodic shear flow that resembles the turbulent boundary layer's streaky pattern. The present study is focused on identifying conditions for which either intrinsic flame spatial scales or streaky structure spatial scales would be dominant in the process. The parametric study is focused on the variation of flame

configuration and propagation speed dependent upon the amplitude and spatial scale of the oncoming periodic shear flow.

dvaliev@princeton.edu

W2P067 ADVANCED COMBUSTION VIA MICROGRAVITY EXPERIMENTS: PLANNED INTERNATIONAL SPACE STATION RESEARCH ON GASEOUS FLAMES

Dennis Stocker¹, Fumiaki Takahashi², J. Mark Hickman¹, Andrew Suttles¹

¹NASA Glenn Research Center, United States ²Case Western Reserve University, United States

The Advanced Combustion via Microgravity Experiments (ACME) project currently consists of five independent experiments that will be conducted on the International Space Station (ISS), where the environment provides longer residence times and larger length scales, yielding a broad range of flame conditions which are beneficial for simplified analysis. ACME's primary objective is to enable improved efficiency and reduced emissions in practical combustion processes on Earth, for example through the development and verification of improved computational models. More specifically, the current goals are to enhance our understanding of flame stability and extinction limits, soot control and reduction, oxygen-enriched combustion which could enable practical carbon sequestration, combustion at fuel lean conditions where both optimum performance and low emissions can be achieved, the use of electric fields for combustion control, and materials flammability. To accomplish these objectives, the planned studies will be conducted with variety of laminar gaseous diffusion flames including for example gas-jet, co-flow, and spherical flames. The detailed design of the modular ACME hardware, e.g., with exchangeable burners, has been completed and integrated testing of the engineering hardware will soon begin. On-orbit testing is expected to start in 2016.

dennis.p.stocker@nasa.gov

W2P068 DYNAMICS OF BLUFF-BODY STABILIZED HYDROGEN/AIR PREMIXED FLAME IN A MICRO-CHANNEL

Bok Jik Lee¹, Chun Sang Yoo², Hong Im¹

¹King Abdullah University of Science and Technology, Saudi Arabia

²Ulsan National Institute of Science and Technology, Korea

Towards the development of combustion-based micro-device for power generation, there have been efforts to understand the combustion characteristics of premixed flame in small-scale combustors, in particular for the flame stability. Recent experimental study reported that the blow-off limit of hydrogen/air premixed flame in a micro-combustor can be significantly extended using a bluff body flame stabilizer. In the present study, a high-fidelity reacting flow simulation is used to investigate the onset of instability of hydrogen/air premixed flames in a micro-channel. A two-dimensional computational domain is set for a channel of 1 mm height and 10 mm length, with a square cylinder of size 0.5 mm by 0.5 mm acting as a flame holder located at station 2.25 mm. Non-reflecting characteristic boundary conditions are applied both inflow and outflow boundary in order to accurately capture the occurrence of thermo-acoustic instability. A series of simulations at different mean inflow velocities are conducted while the equivalence ratio of the hydrogen/air mixture is fixed at 0.5. Non-reacting flows are also simulated as a reference condition to understand the fluid-dynamic nature of the flows under given conditions.

The results show that the stabilized flame remains symmetric behind the bluff body when the vortex shedding from the bluff body is symmetric under non-reacting condition, observed at lower inlet velocities. As the inflow velocity is increased, the vortex shedding becomes unstable in non-reacting flows, in which case the stabilized flame also undergo instability behind the bluff body. Transition of a symmetric stabilized flame to an asymmetric unstable flame is observed at the velocity of 20 m/s for the configuration under study. When the instability is triggered, the combustion characteristics exhibit complex behavior as the fluctuation frequency becomes comparable to that of the fundamental mode in the channel. At higher inlet velocities, strong asymmetric shedding of vortices occurs in non-reacting flows. Under these conditions, flames are not stabilized and are blown out eventually. The detailed mechanism of instability and blow-off of flames is also examined by using the Chemical Explosive Mode Analysis (CEMA).

bjlee.snu@gmail.com

W2P069 LAMINAR FLAME SPEEDS OF GASOLINE SURROGATES MEASURED WITH THE FLAT FLAME METHOD

Ying-Hao Liao¹, William Roberts²

¹University of Washington, United States ²King Abdullah University of Science and Technology, Saudi Arabia

Adiabatic laminar flame speed is a fundamental characteristic of each combustible mixture and is invaluable both for design of combustion devices and for understanding of underlying combustion chemistry, validation of models, formulation of surrogate fuels, etc. Surrogate fuel mixtures vary in complexity, and multi-component surrogate mixtures are required for applications being dependent upon fuel chemistry such as emission and soot formation, or applications involving special type of flames such as lean premixed flames. In the present work, the Primary Reference Fuels (PRF), mixtures of *n*-heptane and *iso*-octane, Toluene Reference Fuels (TRF), mixtures of toluene and PRF, and ethanol reference fuels, mixtures of ethanol and PRF, are used as gasoline surrogate components.

The current work presents the flat flame method, which produces a one-dimensional flat flame free of stretch, to measure the laminar flame speed of the gasoline surrogates at atmospheric pressure over equivalence ratios of $\Phi = 0.7 - 1.4$ and a range of unburned gas temperatures of $T_u = 298 - 400$ K. To determine the laminar flame speed, a technique with heat extraction through the cooling water, similar to that described by Botha and Spalding (1954), was employed and the adiabatic laminar flame speed was obtained by extrapolation. In general, there is a good agreement between the present measurements and the data from literature, particularly for lean and stoichiometric mixtures. Deviations are observed for rich mixtures, where the present measurements are generally lower than most of the reported data in literature. The deviation is possibly due to the cellular flame structure that leads to smaller heat loss, resulting in lower measured flame speeds. In the present work, the maximum accessible equivalence ratio of heavy hydrocarbon fuels at 298 K is around $\Phi = 1.3$ due to the appearance of cellular flames, which was also observed in literature using the similar technique. On the other hand, the minimum accessible equivalence ratio of these fuel mixtures at room temperature is around $\Phi = 0.8$ due to the flame stabilization limitation. A wider range of equivalence ratios could be covered when the initial temperature of the mixture is increased.

In the current study, the tertiary mixtures of toluene reference fuels (5% – 15% of toluene and RON's of 86-96) exhibit comparable laminar flame speeds, regardless of the blend concentration and the octane ratings. Similarly, the laminar flame speeds for the ethanol-blended PRF's (5%-15% ethanol and RON's of 85-95) are generally insensitive to the blend concentrations and RON's. Overall, the PRF's and their tertiary blends in the present work show similar peak flame speeds, regardless of the blend compositions, blend concentrations, and RON's. The temperature of the unburned fuel mixture has an impact on the adiabatic laminar flame speed; that is, in a logarithmic scale, the laminar flame speed is a linear function of the unburned gas temperature for any given equivalence ratio. For a TRF mixture (17.6% of n-heptane, 77.4 % of iso-octane, and 5% toluene, resulting in an octane rating of RON = 85), the adiabatic laminar flame speed is found to be slightly higher, around 2 to 4 cm/s, than that of iso-octane at any given temperature and equivalence ratio.

liaoyh@uw.edu

W2P070 ANALYZING WATER-LADEN NON-PREMIXED COUNTERFLOW FLAMES USING GENERALIZED SHVAB-ZEL'DOVICH VARIABLES

Vinicius Sauer, Derek Dunn-Rankin, University of California, Irvine, United States

The present work analyzes a methane-air counterflow diffusion flame with and without the addition of water vapor to the fuel inlet stream, away and close to the maximum water capacity limit of the flame. The chemical reaction between fuel and oxidizer is assumed to be infinitely fast, and the formulation developed by Liñán, based on the combination of energy and species conservation equations, is used to eliminate the reaction terms. The resulting formulation, namely, mixture fraction and excess-enthalpy conservation equations, is solved numerically together with the momentum and continuity equation. Two methodologies are considered, with one based on a similarity transformation, which allows the problem to be treated as one-dimensional in space, and the other using the Finite Volume Method to solve the two-dimensional system of conservation equations. Simple mathematical relations are used to model the thermodynamic and transport properties dependence on temperature. The solutions are compared to each other and to experimental data available in the literature. The numerical solutions show the impact of water addition on the temperature and major species profiles, position of the flame and physical characteristics of the flame. The comparison with experimental measurements can show the viability of the generalized Shvab-Zel'dovich variables to provide a computationally fast characterization of these water-laden non-premixed flames. Counterflow, non-premixed flames, infinitely fast chemistry, similarity solution, finite volume method

vsauer@gmail.com

W2P071 IMPACT OF FLAMELET CONFIGURATIONS ON CHEMISTRY TABULATION

Shyam Menon, Runhua Zhao, Jagannath Jayachandran, Fokion N. Egolfopoulos, University of Southern California, United States

Flamelet approaches utilizing tabulated chemistry are widely used in large eddy simulations of turbulent combustion. However, there is no clear consensus regarding the choice of the flame configuration that should be used in flamelet approaches. In this investigation, counterflow twin flames, counterflow reactants to products flames, and spherically expanding flames were utilized to assess the effect of choice of these positively stretched flames on the tabulation of chemistry. The numerical simulations were carried out for methane/air flames at standard conditions using detailed description of chemical kinetics and molecular transport. Additionally, the effects of equivalence ratio, Lewis number, and reactant differential diffusion were investigated.

A key requisite to developing chemistry tabulation using stretched flamelets is a tabulation parameter to quantify the stretch effects. In past studies, the H mass fraction has been suggested as a tabulation parameter. However, in the present study it was determined that in the twin-flame configuration, the variation of H mass fraction with stretch rate can be non-monotonic and thus it cannot be used as a tabulation parameter. Analysis showed that transport as well as kinetic effects for near-extinction conditions, cause this non-monotonic behavior. On the other hand, the variation of the H mass fraction with stretch rate is monotonic in the other two configurations. The variations of OH and CO mass fractions with stretch rate were found to be similar to H in most but not all cases.

Comparisons of the source terms of the progress variable in the three configurations revealed about 5-10% differences at the location of peak reaction rate and 20-60% in the post-flame region at high stretch rates. On the other hand, differences in temperature predictions in the three configurations were found to be only 2-5%. The differences observed for source term of the progress variable indicate that to the first order, laminar flame speeds as well fuel consumption and heat release rates predicted by tabulated chemistry calculations utilizing different flame configuration could differ. A major concern however, is that counterflow reactants to products flames can sustain small but finite reaction rates at stretch rates that are much higher compared to twin-flames. This suggests that in an actual turbulent flow field the choice of flame configuration for chemistry tabulation could result in vastly different answers. To further test these observations, a model opposed-jet flame problem was investigated numerically using calculations incorporating detailed chemistry as well as calculations using tabulated chemistry utilizing flamelets generated from different configurations. Significant differences were observed at conditions of high stretch close to extinction.

smenon@princeton.edu

W2P072

A NUMERICAL STUDY OF HIGHLY-DILUTED, BURNER STABILIZED DIMETHYL ETHER FLAMES

Daniel Mayer¹, Kai Moshhammer², Liming Cai¹, Heinz Pitsch¹, Katharina Kohse-Höinghaus²

¹ RWTH Aachen University, Germany ² Bielefeld University, Germany

Recently, a new burner was designed to enable investigations of one-dimensional, premixed flames at atmospheric pressure with a temperature in the burnt gases near 1500K. It consists of a matrix burner plate with alternating fuel and oxidizer feeds that, because of the small scale nozzles, mix quite rapidly. In this work, we examine the burner with regard to the validity of the one-dimensional assumption for the investigated flames. For this purpose, experiments and multidimensional numerical simulations were performed. Experimental measurements were conducted using molecular beam mass spectrometry for species concentrations. Temperatures were obtained from their dependence on the sampling rate following. Numerical simulations are performed using the FlameMaster software package for one-dimensional cases, and an in-house code is applied to simulate the three-dimensional geometry. In all simulations, the chemistry is described by a detailed chemistry approach based on a mechanism featuring 32 species and 133 elementary reactions reduced from the detailed mechanism of Fischer. Three flames were studied with lean, stoichiometric, and rich equivalence ratios of $\phi = \{0.85, 1.0, 1.2\}$. To achieve low burnt temperatures of $T_{\text{burnt}} \approx 1500$ K, all flames were diluted with 90% argon by volume. The experimental results are compared to several 1D simulations with various unburnt temperature boundary conditions. For the simulations, first, the unburnt temperature T_{unburnt} is set to the measured temperature closest to the burner surface; second, T_{unburnt} is chosen such that the position of the CO peak of simulation and experiment match; and third, the experimental temperature profile is prescribed in the whole simulation domain without solving the energy equation. The comparison shows that the 1D simulation predicts the experimental results reasonably well, if the experimentally obtained temperature profile is prescribed in the simulation domain or if the boundary condition is adjusted such that the flame front positions match. Differences are found in the mole fractions of CO₂ and CO for the rich flame, and differences in the mole fractions of methyl and formaldehyde are found for the two other flames with $\phi = \{0.85, 1.0\}$. This motivates detailed 3D simulations to enable the further analysis. The temperature boundary conditions in the experiment are highly complex due to significant heat loss to the burner. Therefore, 3D simulations with constant temperatures are prescribed at the boundaries. The 3D simulations are then used as substitutes for the experiments with slightly different operating points and are compared to 1D simulations. In contrast to the comparison with the experimental results, 1D simulations predict the methyl and formaldehyde mole fractions found in the 3D simulation accurately. This indicates that the differences between measured and computed mole fractions of these species are not a result of the three-dimensionality of the experimental flame and might be attributed to the chemical mechanism. An advanced analysis of the 3D simulation results based on the mixture fraction reveals that the three-dimensional flame topology affects the CO to CO₂ conversion in the rich flame. The conclusion is that lean up to stoichiometric flames in this burner can be modeled as one-dimensional, while for rich flames three-dimensional effects need to be considered. The results of this study are of interest regarding the validity of the experimental results as verification data in the development of future chemical reaction mechanisms.

d.mayer@itv.rwth-aachen.de

W2P073

EFFECTS OF HEAVY HYDROCARBON DECOMPOSITION ON FUNDAMENTAL FLAME PROPERTIES

Jennifer Smolke¹, Francesco Carbone¹, Fokion N. Egolfopoulos¹, Hai Wang²

¹ University of Southern California, United States ² Stanford University, United States

Partial reaction of atmospheric-pressure *n*-dodecane/air mixtures was modeled under isobaric and adiabatic conditions for initial temperatures between 1000 and 1300 K, and equivalence ratios of 0.7, 1.0, and 1.4. To examine the impact of fuel decomposition on fundamental flame properties, the partially reacted mixture was used to determine mass burning rates and extinction strain rates. Results were compared to those of unreacted *n*-dodecane/air mixture with an identical total enthalpy. It was determined that the partial reaction leads to endothermic fuel decomposition that is to a large extent decoupled from the subsequent oxidation of decomposition products, including mainly C₂-C₄ alkenes, hydrogen and methane. The difference in the mass burning rates with and without partial reaction is generally

small and does not exceed 17% at the highest extent of fuel decomposition. The extinction strain rates exhibit differences up to 160% compared to the baseline *n*-dodecane/air mixtures, and this difference also increases with the extent of fuel decomposition. Sensitivity coefficients of mass burning rates and extinction strain rates to kinetic rate parameters and binary diffusion coefficients were calculated and the controlling mechanisms of the observed behaviors were identified.

smolke@usc.edu

W2P074

VALIDATING KINETIC DATA DERIVED FROM 40 MBAR PREMIXED FLAMES WITH SUB-ATMOSPHERIC FLAME PROPAGATION MEASUREMENTS: METHYL FORMATE AND *N*-BUTANOL

Robert Burrell, Dong Joon Lee, Fokion N. Egolfopoulos, University of Southern California, United States

Development of kinetic models for the high temperature oxidation of structurally complex fuel molecules, such as methyl formate and the butanol isomers, often relies on kinetic data derived from low-pressure (~ 40 mbar) premixed flames. Broadening of the flame thickness at these pressures permits probing of species profiles with acceptable spatial resolution. However, recent studies suggest that the effect of the probe's presence in the flame has not been sufficiently quantified and may affect the reported data. Flame measurements for methyl formate and the butanol isomers in counterflow at pressures approaching 40 mbar may serve as a complementary data set. However, to the authors' knowledge no such data exists.

In order to assess the viability of using counterflow flames, a parametric computational study was performed to quantify the uncertainty of particle-based methods for flow field characterization in laminar counterflow flames, especially Particle Image Velocimetry (PIV) and Laser Doppler Velocimetry (LDV). These methods are frequently used to determine global flame properties such as laminar flame speeds and ignition/extinction states. Given the notable dependence of these flame properties on flame chemistry, uncertainties in velocity field measurements at reduced pressures may propagate intolerable uncertainty into kinetic information derived under such conditions. This study was performed using an opposed jet code modified to model the multiphase, particle-seeded flow environment of PIV and LDV laminar flame measurements. Results informed a complementary experimental study of the low-pressure flame propagation of methyl formate.

Laminar flame speeds of methyl formate and *n*-butanol flames were measured at sub-atmospheric pressures and elevated unburned mixture temperatures in the counterflow configuration. The methyl formate data were modeled using two recently developed kinetic models that have been tested successfully against a variety of data. Predicted laminar flame speeds for both models were found to deviate significantly from the data, especially for fuel rich mixtures. Furthermore, it was shown that the discrepancies grow at lower pressures despite sensitivity analysis suggesting similar rate-controlling steps. On the other hand, reaction path analysis revealed that branching ratios for the fuel consumption kinetics of one radical species produced directly from the fuel might have a strong effect on the overall reactivity. The variation of laminar flame speed with pressure revealed a notably different behavior between experiments and simulations and as a result different overall reaction orders.

roeburrell@gmail.com

W2P075

PRESSURE EFFECTS ON THE EXTINCTION OF NON-PREMIXED C₁-C₂ HYDROCARBON FLAMES

Hugo Burbano, Fokion N. Egolfopoulos, University of Southern California, United States

Validation of chemical kinetic models in a wide range of pressures is essential, given the complex effects of pressure on chain mechanisms that are controlled by two- and three-body reactions and which can affect the flame dynamic behavior and structure at engine-like conditions. Due to the hierarchical nature of hydrocarbons combustion kinetics and the fast decomposition rates of large molecular weight fuels, H₂/CO/C₁-C₂ kinetics are controlling to large extent various flame phenomena including propagation and extinction. It is known also that compared to kinetics, reactant diffusion can have a comparable or even greater effect on the flame behavior especially under near-extinction conditions. While the extinction strain rates, of non-premixed counterflow flames of various hydrocarbons have been measured at atmospheric pressures, the number of data available at high pressures is limited.

In the present study, locally measured extinction strain rates of laminar non-premixed counterflow C₁-C₂ hydrocarbon flames were determined for pressures ranging from 0.5 to 7 atm in a newly developed high-pressure facility. The experiments were simulated using two recently developed kinetic models and detailed description of molecular transport. In general, experimental and computed extinction strain rates are in good agreement for CH₄ flames at all pressures and for C₂ flames up to 2.0 atm. At higher pressures, predictions obtained using both kinetic models over-predict considerably the data for C₂ flames. It was determined through sensitivity analysis to kinetics, that uncertainties associated with the HO₂ chemistry could be responsible for the observed over-predictions. Selected HO₂-related kinetic rates were modified and closer agreements were realized. Furthermore, sensitivity analysis on transport coefficients revealed that the extinction strain rate exhibits higher sensitivity to fuel diffusivity compared to kinetics. Modifications in the fuel Lennard-Jones parameters resulted also in significant improvements in predicting the extinction data.

The present findings along with those available in the literature on experiments and modeling of fundamental combustion data, further emphasize the need for minimizing the uncertainties of the chemistry of foundational fuels and in particular the kinetics of HO₂ that have a dominant effect on any combustion process under high-pressure

conditions. Additionally, uncertainties exist in the transport coefficients of fuels as simple as C_2 hydrocarbons, whose diffusion has a first order effect on critical flame phenomena such as extinction and ignition. Finally, failure to predict data for C_2 -hydrocarbon flames can have major implications regarding the ability to predict soot formation.

burbano@usc.edu

W2P076

FLAME ACCELERATION DUE TO WALL FRICTION: ACCURACY AND INTRINSIC LIMITATIONS OF THE ANALYTICAL FORMULATION

Berk Demirkok, V'yacheslav Akkerman, Hayri Sezer, West Virginia University, United States

The analytical formulations on accelerative premixed flame propagation induced by wall friction in two-dimensional (2D) channels and cylindrical tubes are revisited. Namely, with the approximations of (i) near-isobaric combustion process; (ii) Landau limit of zero flame thickness; and (iii) plane-parallel, flame-generated flow, nonlinear equations are derived, in 2D and cylindrical configurations, and solved, computationally and analytically. The equations couple the flame acceleration rate to the Reynolds number, related to the flame propagation, and the thermal expansion of the burning matter. While the original theories provide the analytical formulas for the basic flame and flow characteristics (such as the flame acceleration rate, the flame shape and propagation speed as well as the flame-generated flow velocity), in this study, the accuracy of the approaches adopted is verified computationally, and the intrinsic limitations and validity domains of the formulations are identified. Specifically, the error diagrams are presented to demonstrate how the accuracy of the formulations depends on the expansion factor and Re .

It is shown that the two-dimensional theory is accurate enough for a wide range of parameters (though, while the main characteristics of the flame acceleration are predicted very well at large expansion factor and Re , the accuracy deteriorates otherwise). In contrast, the zeroth-order approximation for the cylindrical configuration appeared to be quite inaccurate and had to be revisited. It is subsequently demonstrated that the first-order approximation for the cylindrical geometry is pretty accurate for realistically large thermal expansions and Reynolds numbers. Consequently, unlike the zeroth-order approach, the first-order formulation can constitute a backbone for the comprehensive theory of the flame acceleration and detonation initiation in cylindrical tubes. Cumulatively, the accuracy of the formulations deteriorates with the reduction of Re and the thermal expansion.

bedemirkok@mix.wvu.edu

W2P077

THE EFFECT OF MIXTURE FRACTION ON EDGE FLAME PROPAGATION SPEED

Philip Wang, Richard Boles, Paul D. Ronney, David Matinyan, Wenyu Li, Hatsachai Praphanphap, Jesse Piotrowicz, Hang Song, University of Southern California, United States

Flames in strongly turbulent flows are subject to local extinction and re-ignition that may affect their heat release rates, extinction conditions, and unburned hydrocarbon emissions. The interaction of flames with turbulence is an extremely complicated problem hence simpler, tractable model systems are needed to develop a fundamental understanding of these local extinction and re-ignition events. As a consequence, so-called “edge flames” separating regions of burning and non-burning portions of a flame surface has been studied by many researchers. The most important property of edge flames is the speed (U_{edge}) it moves relative to the unburned gases in the direction parallel to the flame sheet. U_{edge} can be positive, negative or zero depending on the mixture strength and global strain rate (σ).

While some experimental studies of non-premixed edge flames have been conducted, one aspect that has not received attention in prior literature is the effect of the stoichiometric mixture fraction (Z_{st}). With the growing popularity of unconventional combustion systems such as oxy-fuel combustion, massive exhaust gas recirculation, etc., values of Z_{st} may be very different from those of conventional fuel-air mixtures. With this motivation, the effect of Z_{st} and σ on U_{edge} was measured for several fuel/oxidant/diluent combinations using a counter-flow slot-jet burner. It was found that for conditions with fuel Lewis number (Le_{fuel}) ≈ 1 and oxidant Lewis number (Le_{O_2}) ≈ 1 (e.g. CH_4 - O_2 - N_2 mixtures) with fixed Z_{st} , U_{edge} is negative for sufficiently large or small σ and positive at intermediate σ , and that U_{edge} increases monotonically with increasing Z_{st} for both positive and negative values of U_{edge} . In contrast, for $Le_{fuel} > 1$ and $Le_{O_2} \approx 1$ with fixed σ , U_{edge} exhibits a minimum at $Z_{st} \approx 0.2$.

These results indicate that varying Z_{st} has both chemical and Lewis number effects on non-premixed edge flame speeds. For $Le_{fuel} \approx Le_{O_2} \approx 1$, chemical effects dominate over the whole range of Z_{st} whereas for $Le_{fuel} > 1$ and $Le_{O_2} \approx 1$, Lewis number effects become important at low Z_{st} . Consequently, the near-extinction behavior of highly turbulent non-premixed flames may depend critically on the fuel type (i.e. Lewis number), the extent of dilution of both fuel and air, and the local strain rate at the flame front.

philipwang1989@gmail.com

W2P078

EXPERIMENTAL AND NUMERICAL INVESTIGATION OF FREELY PROPAGATING LEAN ETHYLENE/AIR FLAMES

Erica Belmont¹, Timothy Ombrello², Michael Brown², Campbell D. Carter², Janet L. Ellzey¹

¹University of Texas at Austin, United States ²US Air Force Research Laboratory, United States

A lean ethylene flame, hydrodynamically stabilized on a Hencken flat flame burner, is characterized at low pressures by measurement of major reactant and product species. Extractive sampling and absorption spectroscopy are used to obtain spatially-resolved species profiles of oxygen, ethylene, carbon monoxide, carbon dioxide and water. Experimental results are compared to one-dimensional numerical flame simulations performed using PREMIX and C₃ hydrocarbon reaction kinetics mechanisms. Hydroxyl-Radical Planar Laser Induced Fluorescence (OH PLIF) imaging of probe intrusion into the flame, and the resultant impact on flame front distortion was also performed.

This study demonstrates the viability of the Hencken burner for flat flame measurements. This type of burner supports hydrodynamically stabilized flames and little heat loss to the burner, producing a flame that nearly approaches a freely propagating adiabatic flame. Thus, the use of a Hencken-style burner for fundamental flame studies may be advantageous over the more commonly utilized heat flux burner, where internal cooling is utilized to anchor the flame, because a freely propagating adiabatic flame is readily numerically modeled; only an upstream, unburned reactant temperature is required instead of a full measured temperature profile, which can introduce significant error.

erica.belmont@mail.utexas.edu

W2P079 TEMPERATURE AND FLOW FIELD EFFECTS ON FLAME IGNITION IN THE COUNTERFLOW CONFIGURATION

Abtin Ansari, Francesco Carbone, Fokion N. Egolfopoulos, University of Southern California, United States

The counterflow configuration is widely used to study the ignition of premixed and non-premixed flames. It has been reported in past studies that under ideal conditions i.e. top hat exit temperature and velocity profiles, ignition initiates at the centerline close to the stagnation plane and numerical simulations have been subsequently performed using (quasi) one-dimensional stagnation flow codes. However, based on recent experimental evidence, it appears that ignition can also be initiated away from the centerline. The temperature and velocity profiles of the counterflow field were measured before ignition in different separation distances and strain rates. Shadowgraph technique was utilized to further verify the qualitative conditions of the field. In order to capture the ignition state position and the subsequent edge flame propagation, both shadowgraph and flame visualization method was used by utilizing a high-speed camera. Particle image velocimetry was used to characterize the flow field. It was shown that under certain conditions, the temperature profiles exhibit a significant radial variation very close to the stagnation plane. The higher peripheral temperatures due to this non-uniformity could explain why off-center ignition takes place. The prediction of such behavior is of significant importance since it cannot be modeled by the routinely used one-dimensional codes.

abtinans@usc.edu

W2P080 LOW-TEMPERATURE COMBUSTION CHEMISTRY – DETAILED SPECIATION EXPERIMENTS

Daniel Felsmann, Kai Moshhammer, Christian Hemken, Katharina Kohse-Höinghaus, Bielefeld University, Germany

For the next decades, combustion will remain a dominant source of energy worldwide. It is therefore desirable to investigate and design efficient and clean combustion technologies. One of the most promising but challenging approaches is Low-Temperature Combustion (LTC), which shows great potential regarding increased efficiency and thus reduced CO₂ emission as well as reductions in NO_x and soot. These advantages make LTC an interesting target for the development of, e.g., cleaner engines. For practical conditions, exhaust gas recirculation and dilution are used to achieve LTC, with the drawbacks of a different emission spectrum and potentially destructive instabilities, however. To overcome such disadvantages, a deeper understanding of the related combustion processes is mandatory, including detailed information on the chemical reaction mechanisms under LTC conditions.

Here we present results from ongoing research projects using a flow reactor and a partially premixed low-temperature burner, each coupled to an Electron-Ionization Time-Of-Flight Molecular-Beam Mass Spectrometer (EI-TOF-MBMS). With this technique it is possible to simultaneously detect almost all chemical compounds formed in the combustion process, including radicals and peroxy species, to obtain a quantitative overview of the species involved in the combustion reactions. Experiments with the flow reactor give access to detailed low-temperature kinetics under flameless oxidation conditions over a wide range of parameters (stoichiometry, dilution, preheating temperature), while the burner experiments concentrate on selected flames to extend the field of parameters. This powerful combination of experimental targets provides insight into details of the chemistry which may eventually support a more reliable understanding of low-temperature combustion. Results from these full speciation experiments may be especially valuable for critical inspection of current models and their further development. To illustrate the potential of these methods, exemplary results of both experiments and preliminary modeling approaches will be presented.

daniel.felsmann@uni-bielefeld.de

W2P081 EFFECTS OF THERMAL DISSOCIATION OF FUELS ON THE CHARACTERISTICS OF LAMINAR LIFTED FLAMES

Min Jung Lee, Korea Advanced Institute of Science and Technology, Korea

Characteristics of flame stabilization mechanism of laminar lifted flames have been investigated during last decades. Through these studies, it was shown that flame front has an edge flame structure that has a propagation

velocity faster than laminar burning velocity. In many studies, sub-millimeter nozzles have been used, and it has been usually accepted that Schmidt number is the criterion of the existence of lifted stable flames. Recently, the studies on edge flame propagation and flame stabilization have been extended to high temperature combustion in order to achieve a higher thermal efficiency, and it was found that the flame stabilization condition is affected by ignition temperature if the environment temperature is sufficiently high. However, there is a possibility that the fuels passing through fuel nozzles, which were exposed to the high temperature environment, may suffer a portion of thermal dissociation before the fuel reaches its self ignition condition. In this study, therefore, the thermal dissociation and the flame ignition were decoupled by employing a separated heating part at the far upstream of the fuel streams and the flame stabilization characteristics were compared without elevating the environment temperature for various fuels (methane, propane, and DME). As a result, it was shown that the flame stabilization characteristics are significantly affected by thermal dissociation. There were at least two effects. One is the variation of the fuel composition that results in variation of Schmidt number and stoichiometry location. The other is the variation of fuel volume flow rate that can shift the velocity distribution at the downstream. A more detailed experimental investigation and a new analytical prediction are being investigated.

limjer@kaist.ac.kr

W2P082 A MIXING MODEL FOR LAMINAR FLAME SPEED CALCULATION OF LEAN H₂/CO/AIR MIXTURES BASED ON ASYMPTOTIC ANALYSES

Yang Zhang, Hairui Yang, Hai Zhang, Yuxin Wu, Qing Liu, Tsinghua University, China

Nowadays, laminar flame speed can be precisely calculated using the CHEMKIN-based 1-D PREMIX code or other software coupled with detailed chemistry mechanisms and transport data. However, this kind of calculation is costly in engineering CFD modeling. Alternatively, mixing models are proposed to predict laminar flame speed of a fuel blend from that of individual component.

In this work, several existing mixing models for laminar flame speed calculation of fuel blends were validated for H₂/CO flames against the experimental data reported in literature. Results show that Di Sarli's model and Hirasawa's model remarkably under-predicted's of lean premixed H₂/CO/air flames. Chen's model predicted well the experimental data, but it is inconvenient to use for an arbitrarily given fuel blend because it introduced a parameter that had to be pre-determined with a set of experimental data. This work proposed a mixing model derived through asymptotic analysis coupled with a 3-step chemistry mechanism reduced from Li's C1 mechanism. The model predicted well against the experimental data over wide ranges of equivalence ratios (0.6-1.0), fuel compositions (1 % - 100 % H₂ in the fuel blend), and unburned gas temperatures (ambient to 600 K), and its predictions also agreed well with the detailed simulation results with Li's mechanism over a wide range of pressures (ambient to 20 atm). The proposed mixing model can be cost-effectively used in engineering CFD modeling for laminar flame speed calculation of lean premixed H₂/CO/air flames. The proposed model needs to be improved for more accurate predictions at higher unburned gas temperatures (> 600 K), and validations against the experimental data at elevated pressure are needed to be performed for both the proposed model and detailed chemistry mechanisms as well.

yang-zhang05@mails.tsinghua.edu.cn

W2P083 H₂ CONTENT AND DILUTION EFFECTS ON THE EXTINCTION LIMITS OF LEAN PREMIXED H₂/CO/AIR FLAMES

Yang Zhang, Hai Zhang, Tsinghua University, China

The extinction limits of lean premixed H₂/CO/air flames were studied in the counterflow twin-flame configuration at ambient pressure and unburned gas temperature, over a wide range of H₂/CO ratios, and with N₂ and CO₂ dilutions.

In order to overcome the difficulty in defining the onset of flame front of a weak counterflow premixed flame from the DPIV measured axial velocity profiles, the location with minimum velocity gradient was used alternatively. This proposed method is convenient and with satisfied accuracy. The measured extinction limits and simulation results at the same conditions agreed well with each other. The extinction limits of lean premixed H₂/CO/air flames increased with the H₂ content and equivalence ratio. The extinction stretch rate increased with the H₂ content when the local flame speed was kept the same. Besides the change of flame speed, the change of chemical kinetic also causes the variation of extinction limit of SYNGAS flames with the presence of H₂ content. In addition, flame temperature at extinction was found to be roughly an only function of equivalence ratio, indicating that the extinction was determined by the competition of chain branching and termination reactions.

The dilution effect of CO₂ was more profound to flame extinction than that of N₂. Analyses showed that the disparity in K_{ext}'s between N₂ dilution and CO₂ dilution was mainly because N₂ and CO₂ played different roles in the chemical kinetics rather than the changes in diffusivity and flame temperature. The dilution of CO₂ enhanced the third-body reaction $H + O_2 (+ M) = HO_2 (+ M)$, and weakened the reaction $CO + OH = CO_2 + H$ more significantly than the dilution of N₂, resulting in a lower extinction limit.

yang-zhang05@mails.tsinghua.edu.cn

COMPARISON OF A MULTI-ZONE COMBUSTION MODEL WITH OPTICAL AND TRANSIENT PRESSURE METHODS FOR THE MEASUREMENT OF LAMINAR FLAME SPEED USING A SPHERICAL CONSTANT VOLUME REACTOR

Amir A.M.Oliveira¹, Ricardo Hartmann¹, Eduardo Hartmann¹, João Monteiro¹, Edmilsson Oliveira², Mauro Rocha², Leonel Cancino¹

¹Universidade Federal de Santa Catarina, Brazil ²Petrobras/R&D Center, Brazil

Constant volume reactors have been extensively used to measure laminar flame speeds. The method is fast and economic, since only small amounts of fuel are needed, and allows for measurements at relatively high pressures. The application of the method usually relies on modeling in order to estimate the unstretched flame speed, either from the transient pressure curve using curve fit or a two-zone thermodynamic model, or from the optically recorded time variation of the flame radius. Detailed direct measurement of the flow speed at the surface of spherical flames as well as direct numerical simulation of a cylindrical flame propagation have provided additional insight on the conditions behind and at the flame front. Detailed analysis evidences that the flame speed in closed reactors is affected by curvature effects at small radii and by confinement effects at large radii. Curvature effects are enhanced as the fuel Lewis number departs from unity. While this effect is not easily accounted for in the analysis of measurements, the effect of confinement may be accounted for by considering the isentropic compression of the unburned mixture. However, the burned mixture is also compressed as the flame propagates outwardly, generating an additional flow component in the burned side of the flame. This effect can also be quantified and suggests the possibility of using a multi-zone method to estimate the local flame speed from the pressure transient data.

In this work a constant pressure reactor is presented and the flame speed for hydrocarbon mixtures is estimated from the transient pressure measurement and the high speed recording of the flame using the Schlieren method. The stainless-steel reactor has an inner diameter of 150 mm and optical access through two opposite quartz windows with 100 mm diameter. It is rated for 350 bar maximum pressure at 500 K. A spark plug centered in the reactor ignites the mixture with a controlled amount of energy. The flame front is recorded with a MotionPro Y7.2 high speed camera at 4000 fps. Dynamic pressure is measured with a Kistler Type 6041B piezo-electric sensor. The mixture composition is prepared using static capacitive manometers. Measurements for methane and natural gas were performed from 0.3 to 10 bar (absolute) at 300 K. The propagation of uncertainties indicate an accuracy of ± 0.06 in the equivalence ratio and ± 0.5 cm/s in the laminar flame speed. Three methods for estimating the laminar flame speed are compared. The first uses a cubic approximation of the transient flame development at the low pressures. The second is the basic optical method, using an algorithm that automatically curve-fits a disk in the image of the flame surface and follows the radius of the disk with time. Finally, the multi-zone method divides the volume into a number of onion shells and burns them sequentially. All the three methods are applied to the same set of measurements, their consistency is assessed and their results are compared to the literature.

amir.oliveira@gmail.com

NUMERICAL SIMULATIONS OF PREMIXED FLAME IGNITION IN PERIODICAL VORTEX FLOWS

Evgenii Sereshchenko¹, Roman Fursenko², Sergey Minaev¹, Shenqyang (Steven) Shy³, Kaoru Maruta⁴

¹Far Eastern Federal University, Russia ²Khrstianovich Institute of Theoretical and Applied Mechanics, Russia

³National Central University, Taiwan ⁴Tohoku University, Japan

The ignition process in prescribed flow field modeling turbulent flow was investigated in the frame of 2D thermal-diffusion model. Initial conditions were represented by a fixed size square domain δ filled with hot combustion products. The numerical simulations start with respectively low initial temperature T_{ini} and after the flame extinction, the initial temperature is increased by a constant increment and the calculations with new initial conditions are performed. This procedure repeats until the flame ignition occurs at some critical temperature. This temperature is referred as the ignition temperature T_{ign} for a given initial size of the initial hot domain. The minimum ignition energy is determined as product of ignition temperature and squared domain size $E_{ign} = T_{ign} \cdot \delta^2$. The dependencies of minimum ignition energy on turbulence intensity, eddies size and Lewis number in the flow field consists of time-independent, space-periodic array of large-scale vorticities were obtained. Analysis of time-dependency of maximal gas temperature allows us to give qualitative explanation of ignition temperature behavior under variation of different parameters. It was found that in the case of fixed value of flow-intensity, there is a critical eddies size corresponding to the maximal ignition energy. This critical wave number is almost independent on flow-intensity and corresponds to the eddy size about 15–30 thermal thicknesses for mixtures with equivalence ratios 0.57–0.9. The numerical results shows that in large-scale eddies flow, the minimum ignition energy is almost constant until the turbulent intensity exceeds some critical value, then the abrupt linear increase of ignition energy is observed. Such behavior resembles previous experimental observations. The ignition process in the flow field, which is pre-calculated in the frame of the two-dimensional Euler equation for freely decaying turbulence, is also studied. It was found that behavior of the minimum ignition energy/turbulent intensity curves strongly depends on the location of the igniting hotspot. At some initial conditions, these curves resemble the dependencies previously obtained within the model with spatially-periodic vertical flow.

s_evgeniy@yahoo.com

W2P086

THEORETICAL CRITERION OF THE STABILITY OF FLAME PROPAGATION

Yuanxiang Sun, Beijing Institute of Technology, China

The criterion for the shift of lamellar flame to turbulent flame is very important in engineering. So far, the research works of the field is not perfect. In this paper, the Lyapunov stability theory is used to obtain a criterion for the stability of flame propagation.

Take a straight pipe, the right side of the pipe is opening, the left is closed. Discuss a single reaction channel and a single reaction medium in case of $A \rightarrow B$. Then the unsteady flow of the combustion flame meets N-S equations. According to the definition of Reynolds number and the relationship between Reynolds number and the N-S equation, we can know that local Reynolds number Re is defined as: D is the characteristic length. Take the critical Reynolds number for steady spread of flame as, stability analysis is carried out on the Reynolds number. If adding a small disturbance to the system, after a long enough time, flame propagation is still spreading in the form of laminar flow. In other words, any point on the surface of the flame array at any time, the Reynolds number is not more than the critical Reynolds number, the stability is proved.

Suppose is incremental, the perturbation equations of the unsteady combustion flame one-dimensional unsteady Navier-Stokes equations are: Add perturbation incremental to the time derivative of Reynolds number, we get : According to Lyapunov stability theory, we obtain: In this case, the lamellar flame is stable. The above criterion is the theoretical criterion of the stability of flame propagation under the critical Reynolds number. In other words, when, the flame fronts will be unstable, front instability speed up the flame. Further instability of the flame forms turbulent flame.

sun_yuan_xiang@hotmail.com

W2P087

A SELF-SUSTAINING THERMAL CRACKING CONVERSION PROCESS TO TURN POLYETHYLENE RESIDUES INTO A NOBLE HYDROCARBON

Joao Vitor Ferreira Duque, Federal Institute of Espirito Santo, Brazil

The huge varieties of products consumed are produced from various types of plastics, generating a considerable amount of environmental and socioeconomic problems due to their incorrect and irresponsible disposal. This study proposes a self-sustaining thermal cracking conversion process, as an alternative, to turn the polyethylene (PE) residue into a noble hydrocarbon. For that, a detailed thermo chemical characterization was performed. Elemental analysis detected only amounts of carbon and hydrogen. From the proximate analysis, due to lack of standards for this specific waste material, was possible to determine, only, the amount of moisture and ash. Volatile material was obtained by difference, up to 98 wt. %. The PE calorific value was between 31 – 49 MJ kg^{-1} . The ThermoGravimetry Analysis (TGA), between 30 – 700 °C, and at four heating rates (2, 20, 40 and 100 K min^{-1}), and under two atmospheres, one inert (N_2) and another oxidant (air) was carried out. The results show agreement with proximate analysis for ash and moisture. Also, the TGA reveals that the PE sample can be converted into one to three mechanism steps, depending on the number of recycle steps and on the type. The Differential Scanning Calorimetry (DSC) was carried out for PE samples and for the product recovered from the process. From the data obtained in the DSC, the Arrhenius kinetic parameters were established for an overall reaction mechanism for PE pyrolysis. It was established that activation energies to melt the PE is between 24 – 76 KJ mol^{-1} , and for the degradation in one step mechanisms was between 79 – 201 KJ mol^{-1} . The DSC for the product recovered indicates that almost all quantity produced can be used as fuel. This information could be ratified by carry out the analysis of its calorific value, around 35.2 MJ Kg^{-1} . Finally, we suggest that the PE co-combustion with a carbonaceous material in a reactive porous media can reach temperatures enough to convert all PE into a noble hydrocarbon, and ensuring a self-sustaining process.

joaovitorduque@gmail.com

W2P088

COMBUSTION OF PULVERIZED OLIVE CAKE IN VERTICAL FURNACE FOR HEAT AND POWER GENERATION.

*N. Mrad-Koched¹, A.E. Elorf¹, B. Sarh¹, I. Gökalp¹, B. Izrar¹, M. Asbik², J. Chaoufi³, A. Idlimam⁴**¹Université d'Orléans, France ²Université Moulay Ismaïl Meknès, Morocco ³Université Ibn Zohr Agadir, Morocco,**⁴Ecole Normale Supérieure, Africa*

The depletion of fossil fuels and also the increase of environmental pollutions have caused an interest for the development of alternative resources of energy. Biomass received attention at a global scale because it is renewable, widely dispersed and has a large resource base such as agricultural residues, animal wastes, forestry and wood processing residues and municipal and industrial wastes. Combustion of biomass is a promising technology being researched by the “Institut de Combustion Aerothermique Reactivite et Environnement”. The project developed in the laboratory, called «VERA», is focused on the Olive Cake (OC) as an agricultural waste biomass for heat and power generation. Olive cake is a by-product of olive oil production process and is a solid material consisting of seed particles and the fleshy parts of olive. OC waste has high energy content and has the advantage of not containing sulphur and, hence, reduces the impact on the environment. However, OC has disadvantages as a source of energy such as high moisture content, a low bulk density and a nonhomogeneous form. The VERA project is based on a combination of successive processes to overcome these disadvantages, starting with solar drying of the OC for further

reduce the moisture content, then extracting residual oil, thereafter the combustion of pulverized solid fraction in vertical furnace and finally the cogeneration of heat and power. The goal of the project is to optimize energy obtained with minimum flue gas emissions. The optimization is based on experimental and numerical investigations. Numerical simulations are performed using the CFD commercial software ANSYS FLUENT and ASPEN PLUS software. We present in this summary the CFD simulation of pulverized OC combustion in a 3D furnace using RANS methods for turbulent flow. Air is introduced through the lower base of the furnace. The particles of OC are injected perpendicularly to the central axis of furnace near the lower base. The mean size particle diameter is 100 μ m. The OC is represented in the model as a solid hydrocarbon material containing moisture and ash, which undergoes drying, pyrolysis, and char combustion. The individual component concentrations for a certain species of interest are derived from the predicted mixture fraction, the high temperature yield is volatiles 68.82 %, char 15.64%, ash 9.01 % and moisture 6.53%. In addition to this predictive analysis, ultimate analysis of OC was performed and according to these data, the Probability Density Function (PDF) integration process was created. Eulerian/Lagrangian approach is used to describe the flow particle motion. The gases released in the devolatilization process are assumed to be CO, CH₄, CO₂, H₂ and H₂O. Mathematical models used in this study involved the k- ϵ model of turbulent flow, the PDF/mixture fraction model of nonpremixed combustion and P⁻¹ radiation model. The result obtained concern the temperature profile in furnace, as well as the gaseous combustion emission.

Brahim.Sarh@cnsr-orleans.fr

W2P089 A SCIENTIFIC BASIS FOR THE DEVELOPMENT OF THE NEXT GENERATION OF BIODUST BURNERS

Joakim Johansen¹, Peter A. Jensen¹, Sønnik Clausen¹, Alexander Fateev¹, Karsten Nielsen¹, Jesper Thomsen¹, Rasmus Gadsbøl¹, Reginald E. Mitchell², Roman Weber³, Marco Mancini³, Maria Tonell⁴, Jimmy Andersen⁵, Lisbeth Myllerup⁶, Peter Glarborg¹

¹Technical University of Denmark, DTU, Germany ²Stanford University, United States

³Clausthal University of Technology, Germany ⁴COWI, Germany ⁵DONG Energy, Germany

⁶Burmeister and Wain Energy, Germany

In recent decades, central power and heat production through thermal conversion of biomass has gained ground concurrently with the political agenda. The development of high efficiency biomass plants are required in order to balance the fluctuating power production from wind mills and other alternative energy sources, while still striving towards a CO₂-neutral emission profile. In addition, the thermal plants are a necessary need in the provision of district heating. Development and implementation of high efficiency and flexible biomass combustion technology is arguably the best near-term solution to provide stable and CO₂-neutral centralized power and district heating.

This work aims to establish a scientific basis for the development of a new generation of biomass burners designed to facilitate high efficiency and fuel flexibility combined with good particle burn-out and stable flame capabilities of 100 % biodust fuelled plants. The work links fuel properties to flame properties, considering both fluid dynamic effects due to the differences in particle characters and chemical effects due to changes in chemical composition and chemical kinetics. The work is made up of three complementary modules: Fuel characterization: Studying the development of both woody and annual crops as they undergo devolatilization and combustion at high heating rates and short residence times (6-200 ms) in laboratory (500mW) and pilot (15kW) scale. The fuels are characterized by simple global kinetics and morphology studies for easy implementation to numerical modeling. Full-scale measurements: In-flame full-scale measurements from two different biodust fired combined heat and power plants in Denmark. These include local gas phase temperatures, composition, LDA velocimetry, and imaging in the visual and infra-red spectrum. These measurements are central in evaluating and developing large scale flame simulations.

Computational Fluid Dynamics: CFD is used as the main tool for evaluating the experimental results in lab-, pilot-, and full-scale and to expand the experimental matrix beyond what is possible in the test facilities.

jjoha@kt.dtu.dk

W2P090 ADVANCED CONTROL METHODOLOGY FOR BIOMASS COMBUSTION

Stefan Bjornsson¹, Igor Novosselov¹, Philip C. Malte¹, Riley Gorder²

¹University of Washington, United States ²Enertech, Inc., United States

Small-scale biomass furnaces are considered a significant source of Particulate Matter (PM) emission. Well-proven and established particle emission reduction technologies are prohibitively expensive at small-scale, and are only economically viable for medium- to large-scale furnaces. The biomass combustion process depends on multiple factors such as fuel composition, format, placement in the combustion furnace and air distribution. As a result, meeting stricter emission regulations and efficiency standards is a challenge for operation on diverse fuel types. We present the first phase of a study on inexpensive combustion control system for biomass furnaces operated with a variety of fuels. The system measures major combustion species in the exhaust and utilizes a predictive chemical kinetic model to gain insight into the combustion process in real-time. The model uses a Chemical Reactor Network (CRN) to simulate wood pyrolysis and tar formation, flame zone combustion, post-flame zone combustion and burnout in a biomass furnace. The CRN model has been shown to simulate smoldering, ignition and flaming combustion. The model agrees with experimental data obtained for a small-scale wood furnace for temperature, CO and combustion generated

aerosols. Utilizing the model, the control system can potentially improve combustion efficiency and reduce emissions of particulate matter, CO, and unburned hydrocarbons that have been linked to detrimental health effects and urban and rural air pollution.

stefanbj@uw.edu

W2P091 A FUNDAMENTAL STUDY ON GROUP COMBUSTION PHENOMENON OF SOLID FUEL IN A TURBULENT REACTING FLOW

Jaeyong Jeong¹, Jihong Moon¹, Uendo Lee¹, Won Yang¹, Joohyang Yang², Changkook Ryu²

¹Korea Institute of Industrial Technology, Korea ²Sungkyunkwan University, Korea

A fundamental study was conducted to investigate the group combustion phenomenon of solid fuels in a turbulent reacting flow. A Group Combustion Simulator (GCS) was designed for simulating sequential reactions of solid particles in a large Pulverized Coal (PC) boiler. The GCS is composed of a solid feeder, high temperature air supplier, long tube reactor, and several particle collection systems. In a PC boiler, solid fuels are subjected to various reaction steps such as drying, devolatilization, ignition, combustion and reduction. During the burning process, each reaction step is significantly dependent on the reactants and operating conditions: fuel properties, air temperature, local equivalence ratio, residence time, turbulence intensity and interactions between solid particles. In this study, the effects of aforementioned parameters were examined in a separate way by using the GCS. The combustion characteristics of coal and biomass were investigated and the effect of co-combustion was also tested for different coal-to-biomass ratio. In addition, the experimental results were compared with numerical simulations of similar configurations. The results suggest important parameters for optimizing solid combustions and help to understand the complex nature of group combustion phenomena of solid particles in a turbulent reacting flow.

freeze@kitech.re.kr

W2P092 THE EFFECT OF JET MIXING IN A NATURAL DRAFT RESIDENTIAL LOG WOOD STOVE ON THE REDUCTION OF PARTICULATE MATTER AND GASEOUS EMISSIONS

Smail Kalla, Alain De Champlain, University Laval, Canada

The residential wood stove produces fine particles and hazardous organic compounds causing air quality problems. There is a need to decrease the particle and gaseous emissions from wood combustion in small scale appliances. The purpose of this study is to improve understanding of the relationship between mixing chemical kinetics and pyrolysis efficiency by using the theory of multiple and intersecting jets in a combustion chamber of a wood stove with natural draft. Also, this study is to verify a new concept of log burning wood and was motivated by the need to improve the mixing and pyrolysis efficiency of natural draft residential wood stoves. Four different secondary air injection systems and various primary air distribution patterns in the combustion chamber were investigated using Computational Fluid Dynamic (CFD) in an attempt to eliminate the existing particulate emissions problems and at the same time obtain optimum combustion conditions which would minimize potential emissions of toxic pollutants.

The approach used in this study is firstly to achieve isothermal numerical simulations by CFD of four configurations of air supply system and evaluate the allocation of quantities of air between the primary and secondary zone, the flow momentum, the residence time and the rate of turbulence (Ret). Secondly, it is to carry out a measurement campaign to evaluate the distribution of the air in the firebox and the influence of the theory of multiple intersecting jets on reduction of particulate emissions. The Organic Gaseous Carbon (OGC) was analyzed with a Flame Ionization Detector (FID) that was calibrated against propane. Volatile Organic Compounds (VOCs) are measured with a Fourier Transform Infrared analyzer (FTIR, Gasmet Technologies Ltd.). We paid particular attention to the orientation of the holes tubes secondary zone, which is an important factor in reducing particulate emissions. In effect, the tubes are provided with a row of holes, which are initially oriented horizontally, the angle between the hole and the horizontal is zero. In addition, the penetration of the jets creates a complex flow that ensures good mixing between the pyrolysis gas produced in the primary zone and the secondary zone air. The J parameter represents the ratio between the amount of movement of an end of the jet hole of the tube and the average moving amount of the overall flow. Indeed, increasing J creates increased turbulence which results in a reduction of the mixing time compared to the time of chemical reaction (or chemical kinetics), this leads us to a very small Damköhler; synonymous with a good mix. The exhaust gas was measured continuously with a combination of gas analyzers for Carbon Monoxide (CO), Carbon Dioxide (CO₂) and Oxygen (O₂). CO/CO₂ ratio was used as control criterion. The study underline that the distribution of air between the primary and secondary zone by increasing jet penetrations in a secondary zone has a significant impact on reducing particulate matter emissions. Increasing the residence time of the flue gas and optimizing the air delivery system a 48 % reduction of particulate emissions rate was achieved in the combustion chamber of the stove. We have significantly reduced the rate of emission and we got a very good result in making independent secondary area of the position of the load in the primary zone. However, we have conducted simulations by changing the angle of the holes with respect to the horizontal; the stove initial value of J is 3. In the new configurations of the holes the value of J is increase from 3 to 6 in the high pyrolysis case. In a low pyrolysis case, the value of J is increase from 20 to 120 for the modified stove. Several studies show that more parameter J is high, best is mixing rate. The predominance of equivalence ratio \hat{O} underlines the importance of the degree of mixing

between the air and the pyrolysis gases during the combustion process. The combustion efficiency and the good balance between the air and the pyrolysis gas are improved when the number of secondary tube zone jets and the turbulence increases.

smail.kalla@gmc.ulaval.ca

W2P093 IN-FIELD MEASUREMENT OF COMBUSTION EMISSION FROM SOLID FUEL COOK-STOVES

Jin Dang¹, Derek Dunn-Rankin¹, Rufus Edwards¹, Andy Dang²

¹University of California, Irvine, United States ²San Diego State University, United States

Combustion of solid fuel makes considerable contribution to worldwide Greenhouse Gas (GHG) and aerosol emissions. Significant impact on climate and global atmosphere changes. However, there remain large gaps in knowledge regarding the emission from resident household. Without accurate information, this contribution to overall emission might be underestimated since there are large population, especially in the developing countries, using cook-stove with solid fuel (wood, animal dung, coal etc.). This research characterizes the emission of PM_{2.5}, carbon dioxide, carbon monoxide and methane from solid fuel burning cook-stoves in Nepal and China (Yunnan province and Tibet area). The real time monitoring of PM_{2.5}, carbon dioxide and carbon monoxide concentration is conducted in field. Gravimetric PTFE filter analysis is used to study the accumulate PM_{2.5}. Gas Chromatography (GC) is utilized to analyze the gas compounds from the in-field emission gas sample. These comprehensive measurement conducted in a number of randomly selected local households to acquire statistical significance.

dangjl@uci.edu

W2P094 SCALING OF 100 KW CHEMICAL LOOPING COMBUSTION SYSTEM AND PERFORMANCE WITH DIFFERENT FLUIDIZING GASES

Matthew Hamilton, JoAnn S. Lighty, Kevin J. Whitty, The University of Utah, United States

One promising technology for capturing CO₂ while minimizing the energy penalty is Chemical Looping Combustion (CLC) and the subset Chemical Looping with Oxygen Uncoupling (CLOU), which uses metal oxide particles as an oxygen carrier to separate oxygen from atmospheric air. In the CLC and CLOU processes a dual fluidized bed system is used to transfer the oxygen carrier from an air reactor to a fuel reactor. In the air reactor, the oxygen carrier is oxidized using atmospheric air and then is transferred to the fuel reactor, where the oxygen carrier is reduced either directly as the oxidizer in the combustion process or by releasing oxygen which is used as the oxidizer in the combustion process. The fuel reactor exhaust is predominantly CO₂ and H₂O. The hydrodynamics of integrating two fluidized beds is complex and worthy of study. Our overall research plan is to build a scaled cold-flow unit to represent our approximately 100 kW Process Development Unit (PDU), which is under construction. The PDU can be operated in different modes, including CLC, CLOU, or as a dual bed gasifier. Finding the most economical manner to study the fluid dynamics of the PDU is the driving force for this study. This poster shows the scaling of a hot 100 kW CLOU system to a cold-flow unit with 93% helium and 7% air as the fluidizing gas by applying Glicksman simplified scaling laws. The scaling was validated using Barracuda-VRM for the cold-flow unit. Since helium is expensive, the desire is to use 100% compressed air in the cold-flow unit for studies. The results show that using air to fluidize the system resulted in similar overall circulation rates, but with a more dilute particle axial concentration profile. The similarity within the results indicates that we can use different gases within our cold-flow unit without significant differences in the results.

matthewanthonyhamilton@gmail.com

W2P095 NUMERICAL AND EXPERIMENTAL STUDY ON COAL AND BIOMASS CO-FIRING IN THE FLUIDIZED BED UNDER O₂/CO₂ ATMOSPHERES

Lingling Zhao, Bo Fang, Qing Jia, Southeast University, China

Oxy-fuel fluidized bed combustion technology is considered to be one of the most promising technologies to reduce the CO₂ emissions from power plants. At present, the technology still has a lot of basic uncertainties required in-depth studies, especially in application for co-firing of coal and biomass, in which few investigations are reported. This paper focuses on results of co-firing coal and biomass under oxy-fuel combustion conditions in a 6 kWth fluidized bed combustor. Maintaining the same thermal input, CFD was used as a predictive tool to examine the effects of firing coal, co-firing biomass with coal under O₂/CO₂ atmosphere. Hydrodynamics, heat transfer, composition concentration, and char gasification in fluidized bed were investigated. Compared with coal combustion, the hydrodynamics and temperature profiles of biomass co-firing are not affected much when maintaining the same thermal input. The temperature of biomass co-firing at the bottom of dense-phase zone, which is mainly char combustion area, 10K lower than coal combustion. More O₂ and H₂O and less CO₂ outlet concentration were investigated when biomass co-firing. Char combustion rate and gasification rate of biomass co-firing are all less than coal combustion in the combustor. The experimental study of biomass co-firing under 21O₂/79CO₂ atmosphere is used to validate the CFD modeling.

zhao_lingling@seu.edu.cn

W2P096 HUMAN FECES AS FEEDSTOCK FOR GASIFICATION: CHARACTERIZATION OF GASEOUS AND SOLID PRODUCT

Marcio Ferreira Martins, Bianca Medeiros, Federal University of Espirito Santo, Brazil

The context of the present work permeates through the problems caused by the human excreta. This paper looks more closely at human feces such as a potential feedstock for gasification. A series of thermochemical characterization was carried out. The methodology has consisted of produce samples from human feces according to three kinds of diets: rich in fats, in carbohydrates, and in fruits/vegetables. As the samples have large moisture content, about 75 wt. %, they were pre-dried to measure its Calorific Value (HCV).

For Elemental, ThermoGravimetry (TG) and Differential Scanning Calorimetry (DSC) analyses, the samples were exposed to the environment humidity before the tests. These results served as the basis for the gasification trials carried out in experimental cell previously developed and finely instrumented. The HCV for human feces rich in fats, carbohydrates and fruits/vegetables are 26.9, 23.0 and 19.8 MJ kg⁻¹ respectively. In order to establish a comparison, the HCV for other animals were also determined. By using HCV to estimate the amount of energy that can be used for produce work, the calculation shows that one person excreting an average 30 g day⁻¹ in dry basis, the correspondent energy available is about 700 kJ day⁻¹. By considering the Brazilian population the quantity of human excreta produced is close to 5721 ton day⁻¹ (in dry basis) equivalent to an energetic potential of 1,302 MW. The thermochemical characterization shows that feces rich in fats have more Carbon and Hydrogen – respectively 52.16 and 8.05 wt. % - than the one rich in carbohydrates and fruits/vegetables. Otherwise, for Nitrogen, about 3.94 wt. % while for the rich in carbohydrates and fruits/vegetables were close to 5.0 and 4.57 wt. % respectively. Other compounds like sulfur and phosphorus have less than 0.01 wt. %. From TGA, an alternative proximate analysis was established for those samples rich in fats, carbohydrates and fruits/vegetables: Ash content was up to 15, 13 and 7 wt. %; The moisture content was 8, 6 and 13 wt. %; Volatile matter quantified about 38, 35 and 47 wt. %; and finally, Fixed Carbon around 39, 46, 33 wt. %, respectively. From DSC analysis, the heat necessary for devolatilization reactions was determined between 506 to 340 kJ kg⁻¹. The gasification trials were carried out with samples with average particle diameter of 5 mm and 10 wt. % of moisture. The trials were run with an air flow rate of 0.676 kg h⁻¹. This corresponds to a Darcy velocity of 0.024 m s⁻¹ at 20.0 °C, or 0.173 m s⁻¹ at 1000 °C. The temperature level obtained, inside the reactor, was close to 900 °C. With an oxidation front velocity between 1.3 and 1.7 mm min⁻¹, the experiments spent around 5 hours. The flue gas measured contains as major components CO₂, CO and H₂, 18, 8 and 4 vol. %, respectively. At the end of the trials tar and ash were recovered.

marcio.martins@ufes.br

W2P097 MODELING OF COMBUSTION AND REACTIONS IN A BED OF SOLID PARTICLES

Hyungjun Ahn, Sangmin Choi, Korea Advanced Institute of Science and Technology, Korea

Solid particle bed reactors have been widely applied in the industrial fields and applications for physical or chemical processing of solid materials. Among the types of solid beds, packed bed type reactors are of interest for this study. In the solid bed homogeneous and heterogeneous physical and chemical reactions, as well as mass and heat transfer, take place simultaneously. Regarding the harsh operating conditions and limit of measurable parameters in experiments, numerical modeling has been utilized as the effective approach for the studies of solid bed processes. Common United States ge of modeling results may include obtaining overall process parameters, such as temperature distribution in the bed or component profiles for the process operation. A number of previous studies are based on the similar procedure and outline of solid bed modeling for coal gasifiers, catalytic reactors, waste incinerators, sintering beds, and so forth. Generally, in the bed process modeling, several assumptions are adopted to simplify bed structure to the unsteady one-dimensional condition. The simplification is based on the porous media approximation, which regards the bed as a continuum of solid and gas phase. As solid bed usually consists of randomly packed particles of multiple components which may have distribution in size, the entire bed is characterized with representative particle mean size and shape, as well as bed porosity. The entire bed is considered to be a combination of small segmented areas whose properties are assumed to be uniform within a segment. Regarding the porous media approximation, generally the particles are considered to have high thermal conductivity and small size that are enough for the assumption of locally isothermal condition. Solid-gas reactions may be assumed to initiate at the dense particle surface and progress inward depends on the effect of diffusion and chemical reaction rate, as shrinking-core type models describe.

Based on reviewing the modeling procedure of solid bed processes, current work tries to discuss certain circumstances which may necessitate additional considerations with regard to size and thermal characteristics of particles as well as the progress of particle reactions. For instance, iron ore pellets, agglomerated fine ore grains and binders to have typical size of 9 to 15mm and particle porosity of 25 to 30%, are subject to induration process to increase their strength. Previous models of pellet indurator, which is straight-grate moving bed type reactor, have also been conducted with the same ground for simplification and discretization as described above. Given that typical pellet induration processes focus mostly on the bed thermal profile and may not include serious particle reactions, it appears that the porous media approximation is acceptable for the purpose of estimating overall process parameters. However, iron ore pellet size is reported to be large for isothermal assumption in practice, which requires determination of representative temperature for a modeling segment or how seriously take the impact of intra-particle temperature

gradient on particle reactions. In addition, as a pellet is a porous particle which consists of small grains, progress of reaction may take different forms depends on the effects of chemical reaction, pore diffusion, external mass transfer, and diffusion through product layer of each grain. Moreover, if the iron ore pellet contains carbon component to augment reduction reactions, the particle reaction may not be modeled properly with the shrinking-core models. With the features above, additional consideration to the previous simplifications can be addressed with regard to the numerical modeling of solid particle bed process.

aj1983@kaist.ac.kr

W2P098 SO₃ AND Hg EMISSIONS FROM A VICTORIAN BROWN COAL DURING OXY-FUEL FLUIDIZED BED COMBUSTION

Bithi Roy, Luguang Chen, Sankar Bhattacharya, Sharmen Rajendran, Monash University, Australia

In reducing CO₂ emissions from power generation utilizing different grades of coal, Oxy-fuel Fluidized Bed (Oxy-FB) combustion has emerged as a promising technology. The advantages of this technology include fuel flexibility, uniform temperature distribution, small unit size, low operating costs, reduced NO_x formation, potential for in-bed SO₂ capture via the addition of sorbents and low air in-leakage. In oxy-fuel combustion, however, it is important to know the extent of SO₃ formation in flue gas as SO₃ can corrode air-heater and economizer surfaces. On the other hand, the fate of mercury (Hg) is also an important consideration for the design and operation of oxy-fuel combustors as apart from being harmful to the health and environment, there are also implications for CO₂ transport and storage. Though a number of studies have been performed to investigate the fate and mechanism of SO₃ formation, and the mercury speciation during oxy-fuel combustion, studies on SO₃ formation and mercury emissions from brown coal or lignite during Oxy-FB combustion are very limited. Since Victoria has an abundant resource of brown coal which is expected to last for over 500 years at current consumption rate, this study investigates, for the first time, the SO₃ and Hg emissions using one Victorian brown coal (Loy Yang) in a 10 kWth fluidized bed unit under oxy-fuel combustion conditions. From the experimental results it was observed that compared to air combustion, SO₃ concentrations and Hg⁰ emissions were higher by 6.7% and 28% respectively during oxy-fuel combustion at similar oxygen (21% v/v) concentrations in the feed gas. Moreover, the addition of steam (12% v/v) in the combustion environment was found to increase the SO₃ formation by 7% and Hg⁰ emissions by 32.6%. These experiments showed clearly that SO₃ emissions significantly increased by 38% from 9 mg/MJ to 14.5 mg/MJ and Hg⁰ emissions increased by 32% from 13 µg/m³N to 19 µg/m³N, when the oxygen concentration in the feed gas was increased from 15% (v/v) to 30% (v/v) in the combustion atmosphere. Around 83% of total gaseous mercury released as Hg⁰, with the rest emitted as Hg₂⁺. Therefore, to control this harmful Hg⁰, mercury removal system, such as particulate control unit (e.g. electrostatic precipitator) or selective catalytic reduction unit, will need to be considered to avoid the corrosion in boiler and CO₂ separation units during oxy-fuel fluidized-bed combustion using this coal.

bithi.roy@monash.edu

W2P100 A STUDY OF THE EFFECT OF AGGLOMERATION DUE TO UTILIZATION OF BIOMASS AND LOW GRADE COAL ON THE BED OF A PILOT SCALE 350KW FLUIDIZED BED COMBUSTOR SYSTEM.

Stephen Chilton, William Nimmo, Mohamed Pourkashanian, Leeds University, United Kingdom

Fluidised bed and recirculating fluidised bed combustion of biomass is an increasingly attractive alternative to fossil fuels for power generation at a scale of 30 to 50 MW as evidenced by the new build in the UK. This is due to the ability of a fluidised bed combustion system to efficiently utilise lower grade fuels which would have historically being branded as unacceptable low calorific value; such as lignite's or biomass. However, there are a number of problems that need to be resolved related to the operation of the plant coupled with the nature of the biomass being burned. In particular, the composition of the ash and the propensity to initiate agglomeration in the bed which can ultimately lead to de-fluidisation and shut-down. The work presented here represents preliminary results from an on-going study of the combustion of a range of biomass fired at 100%. The 350KW fluidised bed rig has a number of screw feeders and operational variables in order to test fire a number of different types of biomasses and fuels. Post-run, the bed material was examined and analysed using SEM/EDX, XRF techniques in addition to observation of sand agglomeration caused by ash sintering of ash particles. The effect of biomass type, bed depth, temperature and fluidising velocity were studied with respect to gaseous emissions in addition to bed effects.

pm08s2c@leeds.ac.uk

W2P101 EXPERIMENTS AND MODELING OF ADVECTIVE OUTPUT FROM POROUS COMBUSTORS USING RECLAIMED FUEL SOURCES

Anthony Terracciano, Subith Vasu, Nina Orlovskaya, University of Central Florida, United States

Combustion with a high surface area continuous solid immersed within the flame, referred to as combustion in porous media, is an innovative approach to combustion. Within the flame, the solid phase acts as an internal regenerator distributing heat from the combustion byproducts to the upstream reactants. Heat redistribution from the solid phase enables a flammability limits far beyond those of conventional flames, while offering dramatically reduced emissions of NO_x and CO, greatly increased burning velocities, and enables radiative output from the solid phase

within the combustion chamber. Experimental operation of the combustor under lean methane mixtures were used to determine the appropriate length of the combustion media and materials selection to optimize output. Operation of the combustor using kerosene gave key information on the considerations for use of liquid fuels. Furthermore, a reactor network model of the combustion phenomena was developed within CHEMKIN-PRO employing the GRI 3.0 mechanism, validated using data gathered from operation of the combustor on methane. Further investigations utilizing abstractions from the model are conducted to examine the effects of exhaust gas recirculation as a tool for the reduction of NO_x and CO emissions and the implementation of staged reactor inlets to a single phase porous media to optimize combustion efficiency. The overall goal of efforts documented here are used to construct a streamlined set of design principles, and characterization of the flame's behavior when operating using fuel mixtures of low heating values, as is common in reclaimed fuels, aiding in the development of future combustors for lean burn applications in open flow systems.

antwan718@gmail.com

W2P102 PM REMOVAL EFFICIENCY FROM STATIONARY DIESEL GENSETS EQUIPPED WITH AFTERMARKET PARTICULATE CONTROL DEVICES

Tiffany Yelverton¹, Amara Holder¹, Jelica Pavlovic²

¹US Environmental Protection Agency, United States ²JRC, European Commission, Italy

For years, finding ways to mitigate or eliminate Particulate Matter (PM) emissions from combustion sources has been a focus of research and regulatory communities in an effort to improve human and environmental health. More recently, attention has been focused on how diesel particulate emissions, particularly the strongly light absorbing fraction (i.e. Black Carbon, BC), may impact global climate. Utilizing three stationary diesel gensets (230kW, 400kW, and 600kW) of varying engine displacement (from 8.8-27 L) and physical size, the present study aims to quantify the efficiency of Aftermarket Active and Passive Diesel Particulate Filters (A-DPF and P-DPF, respectively) and a Diesel Oxidative Catalyst (DOC) at controlling PM by comparing to the emissions of an uncontrolled genset. While the main function of a DOC is to oxidize hydrocarbons and CO in the engine exhaust, it has been suggested by manufacturers that a co-benefit for PM removal exists as well. A suite of instruments (Aethalometer, Scanning Mobility Particle Sizer, Photoacoustic Soot Spectrometer) and filter methods (elemental / organic carbon, EC/OC analysis) are used to characterize the PM and removal efficiency from these controlled and uncontrolled diesel gensets.

Several measures of PM or subsets of PM were analyzed (BC and EC), and as such it is important to consider each of these in determining the efficiency of overall particle removal. Table 1 shows the average percent removal and standard deviation, for each of these PM measures, across all three gensets, and for each control device. Both the P-DPF and A-DPF have very high average percent removal efficiencies for PM, BC, and EC across gensets, while the DOC had minimal average removal for several cases. Both BC and EC removal followed a similar trend, but under some controlled conditions the Total Carbon (TC) particulate emissions had as much as 50% OC, indicating changes in the particulate composition with the addition of aftermarket controls or changes in load, as all tests were steady-state.

Particle concentrations were also significantly reduced with the DPFs, with a greater than 97% reduction in particle concentrations with the P-DPF and greater than 82% reduction by the A-DPF. The DOC exhibited much lower particle reductions, reducing the particle concentration by only 5 to 35%, depending upon the genset or load. The single scattering albedo (ratio of light scattering to light extinction) of PM was slightly decreased from the P-DPF and A-DPF compared to the uncontrolled case. The lower albedos suggest that particles that are emitted from a DPF have different physical and chemical characteristics from those emitted from uncontrolled engines, in agreement with the changes of the OC content of these particles.

Overall, use of a DPF resulted in significant PM removal, while a DOC resulted in statistically insignificant removal. Further, based upon increased OC/TC fraction of the particles emitted, coupled with changes in single scatter albedo, it is suggested that the chemical composition of the particles is altered when an aftermarket control device is used.

Table 1: Control device average PM, BC, and EC removal
 Average PM % Removal Average BC % Removal Average EC % Removal

50% Load P-DPF 98 ± 1.7 99 ± 1.9 99 ± 1.7 A-DPF 80 ± 16 84 ± 12 87 ± 5.1 DOC 8.0 ± 12 16 ± 7.9 4.2 ± 9.5
 90% Load P-DPF 96 ± 3.3 99 ± 1.2 99 ± 1.3 A-DPF 80 ± 18 81 ± 12 86 ± 9.0 DOC 23 ± 22 19 ± 21 26 ± 9.7

yelverton.tiffany@epa.gov

W2P103 APPLICATION OF CENTRAL COMPOSITE DESIGN FOR THE STUDY OF NO_x EMISSION PERFORMANCE OF A LOW NO_x BURNER

Marcin Damian Dutka¹, Mario Ditaranto², Terese Løvås¹

¹Norwegian University of Science and Technology, Norway ²SINTEF Energy Research, Norway

In this study, the influence of various factors on Nitrogen Oxides (NO_x) emissions of a low NO_x burner is investigated using a central composite design approach to an experimental matrix. Four factors have been analysed in terms of their impact on NO_x formation: hydrogen fraction in the fuel (0%–15% mass fraction in hydrogen-enriched methane), amount of excess air (5%–30%), burner head position (20–25 mm from the burner air outlet) and secondary fuel fraction provided to the burner (0%–6%). The measurements were performed at a constant thermal load equal to

25 kW. Response surface methodology and central composite design were used to develop a second-degree polynomial model of the burner NO_x emissions. The significance of the tested factors over their respective ranges has been evaluated using the analysis of variance and by the consideration of the coefficients of the model equation. Results show that hydrogen addition to methane leads to increased NO_x emissions in comparison to emissions from pure methane combustion. Hydrogen content in a fuel is the strongest factor affecting NO_x emissions among all the factors tested. Lower NO_x formation because of increased excess air was observed when the burner was fuelled by pure methane, but this effect diminished for hydrogen-rich fuel mixtures. NO_x emissions were slightly reduced when the burner head was shifted closer to the burner air outlet, whereas a secondary fuel stream provided to the burner was found to have no impact on NO_x emissions over the investigated range of factors.

marcin.d.dutka@ntnu.no

W2P104 **AN EXPERIMENTAL STUDY ON THE COMBUSTION CHARACTERISTICS OF PYROLYSIS OIL DERIVED FROM WASTE TIRE**

Myung Chul Shin, Jin Ki Lee, Jong Ho Lee, Su Jin Kim, Hoon Huh, Korea Institute of Industrial Technology, Korea

In this study, the combustion characteristics of pyrolysis oil derived from waste tire in an industrial system for waste tire treatment by pyrolysis are investigated to reduce NO_x emissions. An industrial scale, 1MWth, burner with internal mixing type nozzle for the oil spray is designed and tested to investigate the effects of burner operating parameters on the flame and NO_x emission characteristics. The sprayed oil is mixed with the combustion air which is passed on the swirler at the inner annulus and additional air through the swirler outside is supplied. The swirled primary air and fuel are operated at fuel rich conditions to provide reducing conditions of the NO mainly formed by fuel NO mechanism. The combustion air through the swirler outside diffuses into the flame downstream to provide complete combustion. The burner operation parameters at this experiment are heat input and overall equivalence ratio. The pollutant emission characteristics are measured at various burner operating conditions over a broad range of burner equivalence ratio.

It is experimentally found that the N wt% of pyrolysis oil is the important parameter for NO_x emission. After ignition and flame stabilization, the NO_x level is about 350ppm @ 4% O₂. It's so high compared with an ordinary heavy oil because the N wt% of pyrolysis oil is about 3wt% as a result of ultimate analysis. We consider that it's necessary to apply burner design for reducing fuel bound NO emissions. So we currently approach to optimize primary tangential air momentum and to modify burner design to apply forced induced flue gas recirculation. We estimate that these are the effective methods to suppress the fuel and thermal NO formation simultaneously.

mcshin@kitech.re.kr

W2P105 **REMOVAL OF PARTICULATE MATTER FROM THE EXHAUST GAS OF A DOMESTIC BIOMASS BOILER USING A SMALL-SCALE ELECTROSTATIC PRECIPITATOR**

Enrique Granada, Ivan Iglesias, David Patino, Jacobo Porteiro, Araceli Regueiro, University of Vigo, Spain

Electrostatic Precipitators (ESP), developed in the early 1900s, have been used in many industries for the high efficiency collection of Particulate Matter (PM). In spite of being a relatively well-known technology, just a few models for small heating applications has been commercialised so far.

In this work, a prototype for cleaning exhaust gas from a domestic biomass boiler is presented. The chimney is electrically grounded and used as collection electrode, while a wire supplied with high voltage is inserted in the tube to work as discharge electrode. To guarantee a uniform distribution of the electric field, a structure made of insulating material is added to keep the wire centred and tight.

A 3D model of the ESP is simulated using commercial CFD Fluent software to predict the performance of the prototype. Discrete Phase Model (DPM) and k-ε turbulent model, along with programmed User Defined Functions (UDF), are utilised to determine the main processes involved (gas flow, electrical conditions and particle trajectories) as well as the interactions between them. Data obtained from experimental tests is taken into account to create a realistic poly-disperse distribution of particles. In order to make tests under controllable conditions, the ESP is used to clean the exhaust gas of a diesel engine. Particle size distribution of emissions from both biomass combustion and diesel engines are known to be similar, having most of these particles a diameter under 1 micron. Experimental setup has a control panel that allows regulation of the engine and displays temperatures in different parts of the equipment as well as a smoke meter to measure opacity. Particle concentration is calculated using a correlation that relates Filter Smoke Number (FSN) and smoke emissions. Collection efficiencies and electrical characteristics obtained experimentally are compared to determine the point of optimal operation.

egrana@uvigo.es

W2P106 **FINE PARTICULATE FORMATION AND ASH DEPOSITION DURING PULVERIZED COAL COMBUSTION OF HIGH-SODIUM LIGNITE IN A DOWN-FIRED FURNACE**

Qian Huang, Gengda Li, Qing Liu, Shuiqing Li, Qiang Yao, Tsinghua University, China

A kind of newly explored lignite, rich in Alkali and Alkaline Earth Metal (AAEM) elements, causes severe fouling/slagging problems in stationary combustion systems. In this paper, the ash deposition propensity as well as its

relation to AAEM-rich fine particulates was investigated in a 25kW self-sustained, down-fired furnace. The high content AAEM (mainly calcium) species in this Zhundong lignite results in the molten slag near the burner inlet, differing from other case burning High-Ash-Fusion (HAF) bituminous coal. By collecting ash deposits under 800 C, it is found that the ash deposition tendency of Zhundong lignite is dramatically higher than those of the contrast coal fuels with different ranks and even herbaceous biomass. It is attributed to the formation of large amounts of ultrafine PM0.2 during the combustion of Zhundong lignite, which is almost 4-6 times of those from contrast coals. The mechanism of fine particulate in enhancing ash deposition are interpreted as in two aspects, the forming of a sticky inner layer on the bare tube surface and the forming of “glue” bridges between the bulk ash particles.

hqqh91@qq.com

W2P107 EFFECTS OF FUEL-SIDE AND OXIDIZER-SIDE DILUTION ON FLAME STRUCTURES AND NO_x FORMATION CHARACTERISTICS OF TURBULENT SYNGAS NONPREMIXED FLAMES
Sangwoon Park, Hanyang University, Korea

Synthesis Gas (SYNGAS) is a mixture of hydrogen and carbon monoxide and can be obtained from natural gas, coal, petroleum, biomass and even organic waste¹. SYNGAS regarded as a source of environmentally clean fuels has the potential to become a major fuel in the production of essentially pollution-free energy. The use of synthesis gas has several advantages because SYNGAS is less expensive and can be used for clean combustion resulting in a considerable reduction of pollutant emissions. Recently, SYNGAS finds the promising application in Integrated Gasification Combined Cycle (IGCC) units which has the higher efficiency as well as the lower emission of carbon dioxide and nitrogen oxide. To control the NO_x emission in the nonpremixed SYNGAS combustor, the SYNGAS is usually burned with the high levels of N₂ or steam dilution. This is particularly important in the case of gas turbine combustors highly optimized to meet low emissions.

In these aspects, the present study has been mainly motivated to numerically investigate the effects of the fuel-side and oxidizer-side dilution on the precise structure and NO_x formation characteristics of the turbulent SYNGAS nonpremixed flames encountered at the actual IGCC SYNGAS combustor. The turbulence-chemistry interaction is represented by the transient flamelet model. In context with the transient flame model, the NO concentration is obtained directly from the flamelet calculation based on the full NO_x chemistry and the radiative heat loss is taken into account through the flamelet energy equation. The example cases include the nonpremixed SYNGAS jet flames with the fuel-side nitrogen dilution and the nonpremixed SYNGAS swirling flames with the N₂ or H₂O dilution at fuel-side or oxidizer-side.

Numerical results for the nonpremixed nitrogen-diluted SYNGAS jet flames indicate that the local scalar dissipation rates near nozzle are quite high due to the intense turbulent mixing and they decrease rapidly along the axial distance. At the further downstream locations, the levels of scalar dissipation rates are lower than the upstream level by several orders of magnitude. The faster fuel injection velocity condition corresponding to the higher nitrogen dilution case yields the much higher level of the local scalar dissipation rate by an order of magnitude especially near the injector region. The 10% dilution case has the minimum level of the domain-averaged scalar dissipation rate along the axial direction. These features directly stems from the smaller global strain rate corresponding to the lowest fuel jet velocity corresponding to the 10% dilution condition. In terms of the convective residence time, the 10% dilution case with the lowest jet velocity has the longest flight time of flamelets. Next, the Eulerian particle flamelet model has been applied to numerically simulate the NO_x formation characteristics of the SYNGAS swirl combustor. By increasing the dilution level in the fuel side or oxidizer side, the peak temperature is noticeably decreased and the NO_x emission is progressively reduced. Compared to the N₂ dilution, the NO_x formation is more effectively suppressed by H₂O dilution. However, more study is required to determine the optimum combustion condition for minimizing pollutant (NO_x, CO) emission in the fuel-side and oxidizer-dilution procedures.

avenue-84@hanmail.net

W2P108 EXPERIMENTAL AND NUMERICAL STUDY OF NO_x EMISSION CHARACTERISTICS IN CH₄/AIR NON-PREMIXED FLAMES WITH EXHAUST GAS RECIRCULATION
Chang-Eon Lee, Wheesung Oh, Seungro Lee, Byeonghun Yu, Inha University, Korea

We examined the characteristics of NO_x emission for CH₄/air non-premixed flames using the Exhaust Gas Recirculation (EGR) methods, which are the Air-Induced EGR method (AI-EGR) and Fuel-Induced EGR method (FI-EGR). First, coaxial non-premixed flames was verified the characteristics of NO_x with various EGR ratios and EGR methods. The non-premixed mode in the variable EGR hybrid combustion system was used for this experiment. Second, the two-dimensional (2-D) commercial program ANSYS FLUENT with GRI-2.11 detailed reaction mechanism was used to verify the distributions of flame temperature and the mole fraction of the NO emission. Finally, in terms of a practical combustion system, swirl non-premixed flames were tested to investigate the characteristics of NO_x emission. Our experimental results show that the NO_x emission index (EI NO_x) decreased with increasing EGR ratio. In the range needed to form a stable flame, the reduction rate of EI NO_x for the FI-EGR method was approximately 29% when the EGR ratio was 20%, and the reduction rate for the AI-EGR method was approximately 28% with 25% of the EGR ratio. According to the flame structure based on numerical results, high temperature regions for the FI-EGR method were narrower and lower than those for the AI-EGR method at the same

EGR ratio. Furthermore, based on the experimental results for swirl flames, the reduction rate of EI NO_x for the FI-EGR method was approximately 61% with 15% of the EGR ratio, while the maximum reduction rate for AI-EGR method was approximately 45% with 25% of the EGR ratio. Consequently, we verified that the FI-EGR method was more effective than the AI-EGR method in reducing NO_x emission for non-premixed flames with EGR. We expect that the results of this study will provide fundamental information relating to hybrid combustion systems, which can be used in the design of combustion systems in the future.

chelee@inha.ac.kr

W2P109 EXPERIMENTS AND SIMULATIONS OF NO_x FORMATION IN THE COMBUSTION OF HYDROXYLATED FUELS

*Myles Bohon, Mariam El-Rachidi, Mani Sarathy, William Roberts,
King Abdullah University of Science and Technology, Saudi Arabia*

With considerable interest in the combustion of oxygenated fuels, either as primary fuels or as fuel additives, it is important to understand the influence that these fuels have on emissions formation. This work therefore attempts to investigate the influence of molecular structure in hydroxylated fuels (i.e. fuels with one or more hydroxyl groups), such as alcohols and polyols. In this work, the fuels studied are the lower alcohols (methanol, ethanol, and n-propanol), two diols (1,2-ethanediol and 1,2-propanediol), and one triol (1,2,3-propanetriol); all of which are liquid at room temperature and span a wide range of thermophysical properties. Experimental measurements of NO/NO₂, CO, and CO₂ stack emissions and flame temperature profiles utilizing a rake of translating thermocouples were obtained in globally lean, swirling, liquid atomized spray flames inside a refractory combustion chamber as functions of the atomizing air flow rate and swirl number. These experiments show significantly reduced NO_x formation with increasing fuel oxygen content despite similarities in the flame temperature profiles. Measurements of the spray droplet size distribution were conducted to provide insight into the influence of the wide range of fuel characteristics on the spray – namely large differences in volatility, viscosity, surface tension and energy density. Additionally, simulations were conducted using these fuels under a wide range of conditions in a model, perfectly stirred reactor as functions of the equivalence ratio, temperature, and residence to provide further insight in the conditions similar to those measured within the combustion region. A detailed high temperature chemical kinetic model for NO_x formation from hydroxylated fuels was developed based on recent alcohol combustion models and extended to include polyol combustion chemistry. Lastly, an analysis of the variations in the reaction pathways are performed to better understand the causes for a reduction in NO_x formation with increasing oxygen content.

mdbohon@gmail.com

W2P110 THEORETICALLY STUDY OF MERCURY SPECIES ADSORPTION MECHANISM ON MnO₂(110) SURFACE

Bingkai Zhang, Huazhong State Key Laboratory of Coal Combustion, China

MnO₂-based sorbents have been considered as potential materials for Hg removal because of their regeneration and high activity. First-principles calculations based on the density functional theory and the periodic slab models were used to gain a fundamental understanding of mercury adsorption mechanism on MnO₂(110) surface. The adsorption energies and adsorption structures of mercury species (Hg⁰, HgC₁ and HgC₁₂) on MnO₂(110) surface were calculated. The electronic structural changes of surface system before and after adsorption were investigated to better understand the surface reactivity. The potential energy diagram of different pathways of mercury species adsorption on surface were given in order to elucidate the mechanism of adsorption process. In addition, thermodynamic data based on statistical thermodynamic partition functions for mercury species adsorption were also calculated. The results show that Hg⁰ is strongly adsorbed on oxygen and manganese sites of MnO₂(110) surface with chemisorption. The energy diagrams of HgC₁ and HgC₁₂ adsorption and possible desorption show that HgC₁ and HgC₁₂ can exist stably on the surface because the desorption and dissociation are highly endothermic, yet there is still a possibility that HgC₁ dissociates and Hg desorbs from the surface. The trends of equilibrium constant suggest that mercury species adsorptions on MnO₂(110) surfaces are favorable at low temperature and HgC₁₂ is more easily captured than Hg⁰ under high temperature.

zhangkai0503@126.com

W2P111 CHARACTERISTICS OF COMBUSTION AND CRITICAL SPACE HEATING RATES IN MESO-SCALE COMBUSTORS

Katsuo Asato, Gifu University, Japan

The characteristics of meso-scale combustors with high-speed flame propagation in a rotating flow and heat-recirculating combustion were examined. Heat-recirculation rates increased and heat-loss rates decreased with an increase in the Reynolds number. The flame blew out before approaching the limit of flame stabilization, calculated by considering the preheated temperature of the unburned mixture. Therefore, an improved method of flame stabilization is needed in order to achieve greater combustion intensity. The Space-Heating Rates (SHR) depend only on the residence time (τ_b) of the mixture in the combustor and are in inverse to τ_b , regardless of the volume and scale of the combustor or type of fuel used. The characteristics of SHR in meso-scale combustors are in some ways similar to

those of gas turbine combustors with various kinds of scales and fuels. The non-dimensional space-heating rate remains almost constant regardless of fuel types, volume and scale of the combustor, or velocity of the mixture. This means that the critical combustion intensity can be determined if the scale of combustor is given.

asato@gifu-u.ac.jp

W2P112 DETONATION WAVE PROPAGATION IN CHANNELS OF ARBITRARY RADIUS OF CURVATURE
Jeong-Yeol Choi, Tae-Young Kim, Pusan National University, Korea

During the last decade the research efforts Pulse Detonation Engine (PDE) has lead the activities of detonation studies. There were a lot of studies on the detonation propagations for the variety of applications. For the development of the PDE, acceleration of detonation initiation has been a key issue to enhance the PDE operation frequency since the higher operation frequency is a desperate performance parameter that makes the PDE useful. As a mean of enhancing the detonation initiation, Frolov, employed the coil shape tube and U-bend tubes. As an alternative way of using detonation wave for aerospace propulsion, continuous detonation wave propagation in a annular channel has been considered recently by adopting the old concepts suggested by Nicholls and Voitsekhovskii in 1960's. Daniau considered it for the rocket applications with name of CDWRE(Continuous Detonation Wave Rocket Engine). A numerical study was done for this application. Milanowski also considered nearly same idea for air-breathing application with name of RDE (rotating detonation engine). These concepts have same flow feature of detonation wave propagation in tubes or channels with large curvature. During last several years a lot of experimental and numerical studies have been carried out for these concepts, and the RDE is more widely accepted to encompass these concepts of the pressure gain combustor.

Gas turbine is the one of the major application of the RDE concept, where the circular configuration is essential for the rotating machine, but the configuration of RDE can be further extended to arbitrary shaped closed channel if the RDE is used as a stand-alone propulsion device, or at least the application is not limited by the rotating component such as turbine. If the combustor cross section is not limited to the circular shape, the vehicle designer could have much more flexibility for propulsion system installation. Therefore, detonation wave propagating in several type of non-circular channel is demonstrated in this study. In addition to the demonstration of detonation wave propagation, further investigation will be discussed for the critical condition of the successful detonation transmission from one direction to the other direction, since a curved element is an essential part connecting different directions, as an extension of the previous study for the effect of curvature.

Choi, Jeong-Yeol (aerochoi@pusan.ac.kr)

W2P113 NUMERICAL INVESTIGATIONS OF DETONATION PROPAGATION IN A TWO-DIMENSIONAL SMALL CURVED CHANNEL
Yuta Sugiyama, Akiko Matsuo, Yoshio Nakayama, National Institute of Advanced Industrial Science and Technology, Japan

Detonations with curved shock front propagating in a small curved channel are numerically investigated using two-dimensional Navier-Stokes equations with a two-step reaction model of Korobeinikov. This study clarifies the effect of the ratio of outer and inner radii R_{out}/R_{in} on detonation propagation in a small curved channel, whose width is equivalent to cell width. The time evolutions of the simulation results are utilized to reveal the propagation mechanism of detonation with curved shock front. Detonations propagate at a constant velocity that depends on R_{out}/R_{in} . In cases that R_{out}/R_{in} is larger than 3, a shock front contains Mach reflection near the outer wall with a curved incident shock wave near the inner wall. The shock structure has the similar characteristics of the pseudo shock wave. shock angle between the inner wall and the triple point does not depend on R_{out}/R_{in} when distance R is normalized with respect to R/R_{in} .

yuta.sugiyama@aist.go.jp

W2P114 NUMERICAL MODELING OF SUPERSONIC COMBUSTION WAVE PROPAGATION IN AN OBSTRUCTED CHANNEL
Mark Kellenberger, Gaby Ciccarelli, Mobin Khakbazbaboli, Queen's University, United Kingdom

Explosions almost universally start by the ignition of a flame from a weak ignition source, such as a weak electrical spark or mixture contact with a hot surface. A common scenario for detonation initiation is via flame acceleration in an obstructed volume leading to Deflagration-to-Detonation Transition (DDT). The mechanisms involved in flame acceleration and DDT has been studied extensively in ducts equipped with repeated obstacles. Experiments were performed to investigate the propagation of a supersonic combustion wave in a 2.54 cm wide by 7.82 cm tall cross-section channel with fence-type obstacles mounted on the top and bottom channel surfaces equally spaced at 7.82 cm. High-speed Schlieren photography was used to capture the progression of the combustion wave through the channel. Tests were carried out in hydrogen-air mixtures at an initial pressure of 101 kPa. Numerical simulations were performed with Open Foam to compare with the experimental images of the interaction of the combustion wave with the obstacles. Unlike the experiments where DDT occurred following flame acceleration, in the simulations a stable 2-dimensional detonation was transmitted into an obstacle field. Therefore, the complexity of modeling compressible turbulent combustion that is important in the flame acceleration stage is not required. The idea

is that the simulations are compared to the experiments when the quasi-steady explosion front propagation is established in both cases. The simulations were carried out with a stoichiometric hydrogen-air mixture using a detailed reaction mechanism and a single-step reaction model. The experiments show that a combustion wave propagates in the quasi-detonation regime. The high-speed video shows that a combustion wave undergoes a cycle of detonation initiation and failure. The detonation initiation process occurs as a result of the formation of a Mach stem at the channel centerline as a result of the collision of blast waves originating from local explosions at the obstacle corners. These explosions occur when the decoupled shock wave propagates into the corner formed where the obstacle attaches to the channel top and bottom plate. The numerical simulation with full chemistry results in detonation initiation when the shock wave reflects off the obstacle surface and then fails over the next few obstacles. For the single-step reaction different detonation propagation mechanisms are activated depending on the reactivity of the mixture. For all simulations the normalized activation energy (based on CJ detonation post-shock temperature) was 8.5, and the mixture reactivity was varied via the pre-exponential factor. For the least reactive a detonation wave is not initiated and the supersonic combustion wave propagates at an average velocity just above the products speed of sound. For more reactive mixtures detonation initiation and failure is observed.

kellenbergerm@me.queensu.ca

W2P115 EXPLOSION FLAME ACCELERATION OVER OBSTACLES: EFFECTS OF SEPARATION DISTANCE FOR A RANGE OF SCALES

A.M. Na'inna, H.N. Phylaktou, G.E. Andrews, University of Leeds, United Kingdom

The influence of obstacle separation distance on explosion flame acceleration was studied for 10% methane-air mixtures using two 20% blockage obstacles in a 162mm diameter 4.5 m long tube with ignition on the centre of the closed end and flame propagation towards the open end. Sets of two identical flat-bar obstacles with variable number and width of bars were investigated, so that the turbulent length scale b was varied from 6 to 26 mm (for the same fixed blockage ratio). The spacing between the obstacles was varied from 0.25 m to 2.75 m by changing the position of the second obstacle in 0.25m increments. The downstream obstacle experienced the accelerated flame after the first obstacle with associated higher unburned gas approach velocities. The second obstacle effect was evaluated by comparison to the single obstacle results. It was observed that the maximum overpressure increased with the reduction in number of flat-bars (i.e. with increasing b). A maximum overpressure of 129 kPa at 2.25 m obstacle spacing was achieved with 1-flat-bar obstacles, followed by 118 kPa and 110kPa for 2 and 4-flat-bars respectively at 1.25 m and 0.5 m obstacle separation for the same obstacle blockage. Reducing the obstacle length scale reduced the separation distance for the worst case, due to the peak turbulence position scaling with obstacle scale. The flame speeds were also measured and these were 300 - 350 m/s after the second obstacle for the worst case spacing.

Pm08amn@leeds.ac.uk

W2P116 TRANSITION FROM DEFLAGRATION TO DETONATION OF METHANE-OXYGEN BLENDS IN NARROW CHANNEL

Victor Golub, Sergey Golovastov, Joint Institute for High Temperatures of the Russian Academy of Sciences, Russia

The formation of detonation of methane-oxygen mixtures in a narrow channel with a prechamber was experimentally investigated. The effect of the geometrical parameters of the prechamber on the deflagration-to-detonation transition in the channel of subcritical diameter has been investigated. Several scenarios of combustion propagation were observed in the narrow channel with the prechamber and a non-dimensional criterion defining these scenarios was proposed. This criterion defines the effectiveness of the prechamber effect on the deflagration-to-detonation transition in subcritical channels and takes into account the energy release in the prechamber and relative distance passed by the flame front in the prechamber.

victor.v.golub@gmail.com

W2P117 PROPAGATION AND MORPHOLOGY OF PREMIXED FLAME FRONTS IN OBSTRUCTED TUBES

Orlando Ugarte¹, Berk Demirgok¹, V'yacheslav Akkerman¹, Damir Valiev², Satyanaryanan Chakravarthy³, Amit Kumar³, Vitaly Bychkov⁴

¹West Virginia University, United States ²Princeton University, United States ³Indian Institute of Technology Madras, India

⁴Umea University, Sweden

Bychkov have recently revealed a physical mechanism of extremely fast flame acceleration and Deflagration-to-Detonation Transition (DDT) in obstructed tubes and channels. Namely, the acceleration is driven by an intensive jet-flow, generated by the delayed combustion process in the space between the obstacles. The acceleration rate is Reynolds-independent and the detonation can be attained in a very short time interval. In the present work, this mechanism is compared to other conventional scenarios of the flame acceleration, including those driven by wall friction and a "finger" flame shape. A threshold blockage ratio, at which the obstacle-based mechanism dominates, is identified, and it is shown how such a cutoff quantity depends on the variety of combustion and fluid characteristics.

We are performing a comprehensive parametric study of the phenomenon that includes analytical, computational, and experimental efforts. In particular, extensive fully-compressible numerical simulations of the

combustion and hydrodynamic equations are performed to support a novel experimental facility developed at IIT Madras. Various thermal-chemical options, configurations and boundary conditions are implemented in the simulations. The geometry is characterized by two-dimensional channels and cylindrical tubes of different radii, including one and both ends open. The “mechanical” boundary conditions include slip and non-slip walls; the “thermal” conditions include adiabatic and isothermal walls, and various wall temperatures are tested in the latter case. The variety of fuels is represented by the variations of the thermal expansion coefficient. The computational simulations are coordinated with an asymptotic analysis predicting the evolution of the main combustion characteristics such as the acceleration rate, the flame tip position, the instantaneous burning rate and the DDT locus. We thereby describe several stages of the evolution of the combustion intensification process, namely, an initially exponential acceleration; its moderation because of the gas compression effect; eventual saturation to quasi-steady fast flame propagation with a near-sonic speed; and the detonation initiation by an accelerating flame.

ougartea@mix.wvu.edu

W2P118

ANALYSIS OF ETHYLENE-OXYGEN COMBUSTION IN MICRO-PIPES

V'yacheslav Akkerman¹, Berk Demircok¹, Orlando Ugarte¹, Damir Valiev², Chung King Law², Vitaly Bychkov³, Ming-Hsun Wu⁴

¹West Virginia University, United States ²Princeton University, United States ³Umea University, Sweden

⁴National Cheng Kung University, Taiwan

Recent analytical and experimental studies have identified several stages of flame propagation in micro-tubes. This includes the occurrence of spontaneous flame acceleration, due to wall friction, and the deflagration-to-detonation transition event. However, in contrast to the theoretical prediction of an exponential acceleration of laminar flames at the initial, quasi-incompressible regime of burning, the experiments on stoichiometric ethylene-oxygen flames in near/sub-millimeter tubes have demonstrated a number of specific effects (such as a moderation of the flame acceleration, with a subsequent saturation of the flame velocity to a near-sonic, steady value, which can be interpreted as the Chapman-Jouguet deflagration speed). In order to elucidate these observations, and to reconcile the experimental data with the analytical predictions, the role of gas compression in the acceleration process has been analyzed. In particular, we have extended the incompressible analytical formulation on flames in tubes to incorporate small but finite gas compression, by employing expansion in the initial Mach number up to first-order terms.

In general, in this work we investigate – computationally, analytically and experimentally – the propagation of premixed stoichiometric ethylene-oxygen flames in cylindrical pipes of sub/near-millimeter radii. Various stages of the flame evolution are identified and scrutinized, namely: (i) quasi-isobaric, exponential acceleration; (ii) its subsequent slowdown to a weaker trend; (iii) eventual saturation to a steady or quasi-steady fast near-sonic deflagration. In particular, the dynamics and morphology of the flame front, its propagation velocity and acceleration rate are determined. Eventually, due to viscous heating, the entire process can be followed by (iv) the detonation initiation ahead of the flame front.

To be specific, the present study focuses, mostly, on the computational component of this research. The latter constitutes the numerical solution of the hydrodynamics and combustion equations including transport processes (heat conduction, diffusion and viscosity) and chemical kinetics represented by one-step Arrhenius reaction, namely, the equations of continuity and Navier-Stokes, as well as that of the energy and species balance. The computational platform is based on a fully-compressible, finite-volume Navier–Stokes solver, with the accuracy of the numerical scheme being second-order in time, fourth-order in space for the convective terms; and second-order in space for the diffusive term. The solver is robust and pretty accurate, having been successfully utilized in numerous aero-acoustic and combustion applications. The code is adapted for parallel computations and it employs a self-adaptive structured computational grid, which makes the platform perfect, in particular, for the fundamental studies of flame hydrodynamics in combustion tubes. The solver is available in the two-dimensional (Cartesian and cylindrical-axisymmetric) versions, as well as in the fully three-dimensional Cartesian version, but the present work, obviously, utilizes the cylindrical-axisymmetric version of the solver. While the majority of the experimental measurements lie beyond the validity domain of the analytical formulation, the computational platform allows reconciling both investigations. Indeed, the computational simulations are compared to both the theoretical formulation and the experiments, with good agreement in both cases. Consequently, the overall study bridges the gap between the experiments and the analytical formulation.

Vyacheslav.Akkerman@mail.wvu.edu

W2P119

EXPERIMENTAL STUDY ON REFLECTED SHOCK BIFURCATION

Urszula Niedzielska¹, Remy Mével², Joseph E. Shepherd², Andrzej Teodorczyk¹

¹Warsaw University of Technology, Poland ²California Institute of Technology, United States

Shock tube experiments on ignition delay time and species evolution in fuel-oxidizer-diluent mixtures are now a standard approach in combustion studies. Although the theory is conceptually simple, actual flows in shock tubes have a number of nonideal effects that can complicate the interpretation of ignition data. In an effort to avoid these issues, most studies use highly diluted mixtures and careful attention to operating parameters in an effort to minimize nonideality. However, in some instances it is desirable to work with undiluted mixtures or mixtures with a substantial

fraction of polyatomic species such as N_2O , CO_2 or hydrocarbon fuels. For these cases, the interaction of the reflected shock wave with the boundary layer behind the incident shock can create substantial flow nonuniformity that will significantly affect the data. This is manifested by the creation of an oblique shock precursor running into the boundary layer region ahead of the main reflected shock wave, usually termed "shock bifurcation".

Empirical models and experimental data on shock bifurcation in selected mixtures are available but there are few systematic studies of the onset and growth of the bifurcation region as a function of gas molecular structure and incident shock wave strength, particularly for less dilute mixtures with polyatomic species. In order to improve the models and extent the experimental database, a series of experiments are in progress in our laboratory. Measurements in three gas systems over a range of incident shock Mach numbers have been carried out in the Caltech 6-in shock tube to obtain systematic data on pressure time histories in the region near the end wall of the shock tube.

Air, argon and carbon dioxide test gases were investigated for incident shock Mach numbers ranging from 1.5 to 2.5 and an analysis of the results has been conducted to determine the extent of the bifurcation zone.

We found that by supplementing the pressure data with a laser light deflection measurements, it is possible to determine the extent of the bifurcation zone. In agreement with previous studies, the bifurcation zone is found to increase with increasing difference between the ideal reflected shock pressure P_5 and boundary layer stagnation pressure P_{0BL} . Representative results for all three mixtures and a progress report on the analysis of the onset and growth of the bifurcation zone will be provided in the poster presentation.

uniedz@itc.pw.edu.pl

W2P120

AUTO-IGNITION IN BONDARY LAYER

Edyta Dzieminska¹, Makoto Asahara², A. Koichi Hayashi²

¹Sophia University, Japan ²Aoyama Gakuin University, Japan

Analysis has been done numerically and it seeks to demonstrate physics of the interaction in a matter of fluid dynamic and thermodynamic view. Flame propagates and produces shock waves which interact with a boundary layer causing auto-ignition in a vicinity of the wall. From the process of the auto-ignition a new flame is developed and it propagates along the wall with more than local sound speed, which makes it a fast flame, and triggers DDT in consequence.

The fluid dynamic and thermodynamic interactions are discussed and it is clear that they lead towards an auto-ignition. We should be able to determine the location of the auto-ignition. It is unlikely to show an exact point although it is possible to estimate the location area of the auto-ignition.

The wall was chosen for the measurement as this is the hottest place in the boundary layer formed due to adiabatic conditions. Nevertheless, in experiments an auto-ignition also appears in the boundary layer but it cannot be said whether it takes place on the wall or just inside of the boundary layer. Taking a close look it can be effortlessly spotted that temperature rise is not just a steep apex.

It is possible to recognize reaction zone with OH production which drastically increases when chemical reactions take place. The beginning of the auto-ignition can be estimated at $9.777 \mu\text{s}$ while a new flame development based on temperature and OH distribution at $9.786 \mu\text{s}$. When the mixture ignites, a reaction zone is formed in the boundary layer on the wall. The maximum OH production is 0.0048 kg/m^3 but $0.006 \mu\text{s}$ later it drastically jumps to 0.13 kg/m^3 . It is merit to notice that the OH production on the wall is identical with that of the first grid line above the bottom wall and the center of the reaction zone is slightly moving towards the downstream.

An auto-ignition is always clearly recognized on a distance versus time plot, so called x-t diagram. Shock waves, an auto-ignition, and a newly developed flame can be easily spotted. The similar structure to ours was shown by Gaydon in theoretical study. Their simplified structure presents a spontaneous ignition which developed ahead of the propagating flame behind the leading shock wave. It catches up with the shock front in almost no time and goes to detonation.

edyta.d@sophia.ac.jp

W2P121

EFFECT OF CHEMICAL KINETICS IN THE EXPANSION FLOW OF A HYDROGEN-AIR ROTATING DETONATION ENGINE

Douglas A. Schwer, K. Kailasanath, Naval Research Laboratory, United States

Rotating Detonation Engines (RDEs) represent a novel approach to using the high efficiency detonation thermal cycle for propulsion and gas generators. Because of the intense pressures, temperatures, time and length scales within the detonation wave, use of detailed kinetic mechanisms with respect to RDEs has been limited to very small scale calculations or idealized detonation wave calculations. However, understanding the exhaust species concentrations in propulsion devices is important for both performance considerations and understanding pollutant formation. The approach presented in this article uses an induction time parameter model for modeling chemistry within the detonation wave, and a detailed kinetic model used in the expansion flow of a baseline RDE configuration. An 8-10 cm diameter hydrogen/air RDE calculation is done with and without expansion flow kinetics to examine the effect of this chemistry on performance of the RDE. Adding expansion flow chemistry had almost no effect on the detonation characteristics or cellular structure, as expected. Results show that overall radical concentrations in the exhaust are substantially lower than assuming no reactions past the CJ point, although along the slip line temperatures remain high

enough that radical concentrations also remain high, in some small areas higher than CJ point mole fractions. The performance of a baseline hydrogen/air RDE increased from 4940 s to 5000 s with expansion flow chemistry, due to recombination of radicals and more production of H₂O resulting in additional heat release.

doug.schwer@nrl.navy.mil

W2P122 SELF-SUSTAINING MECHANISM OF CONTINUOUS ROTATING DETONATION WAVE

Shijie Liu, National University of Defense Technology, China

Continuous Rotating Detonation Engine (CRDE) is a promising engine concept, which can operate continuously with just one ignition, producing a roughly steady thrust. A CRDE ground test system has been designed and constructed, and a series of tests have been carried out. Based on the PCB results, flow-field structure in CRDE is constructed. The features include a upstream detonation wave and a downstream oblique shock wave emanating from its bottom end. The detonation wave propagation velocity deficits are calculated, and a critical value of 15-16.5% is obtained. When the velocity deficit is less than the critical value, the reactants are mainly consumed by the upstream detonation wave. Otherwise, further heat release may occur when the un-consumed products encounter the downstream shock wave. So CRDE can be self-sustained even with a much larger propagation velocity deficit. Influences of the lateral expansion effect on the detonation wave in CRDE have been analyzed theoretically. Detonation wave in CRDE is confined by the high-temperature, low-density combusted products in the axial direction, which has a weak confinement effect. So the detonation wave is influenced significantly by the lateral expansion effect, which may produce a majority of the propagation velocity deficit.

lsjnudt@gmail.com

W2P123 FLIGHT DEMONSTRATION OF A ROTAR-VALVED FOUR-CYLINDER PULSE DETONATION ROCKET ENGINE "TODOROKI II"

Ken Matsuoka¹, Tomohito Morozumi², Shunsuke Takagi¹, Jiro Kasahara¹, Akiko Matsuo³, Ikkoh Funaki⁴

¹Nagoya University, Japan ²University of Tsukuba, Japan ³Keio University, Japan

⁴Japan Aerospace Exploration Agency, Japan

The thrust in real flight condition using the pure detonation engine has not yet been demonstrated. In addition, the challenge in making practical use of a PDE is to increase the thrust-to-weight ratio. We constructed a rotary-valved four-cylinder pulse detonation rocket engine system "Todoroki II" for the flight demonstration. Total length and weight were 1910 mm and approximately 32.5 kg with LC₂H₄-LN₂O propellant and helium gas as purge gas, respectively. The inner diameter and length of each detonation tube were 37 mm and 800 mm, respectively. We investigated the thrust performance of the PDRE system by ground test, and confirmed the stable valve and PDE operation and continuous supplying of oxidizer, as designed. Propellant-based specific impulse of 131 s, time-averaged thrust of 256 N and thrust-to weight ratio of 0.8 were achieved. Moreover, we carried out the flight test using the newly-developed launch-recovery system. The rolling by rotation of the rotary valve and the significant vibration by intermittent detonation was not confirmed and we validated the detonation engine thrust in real flight condition (6-degree-of-freedom condition). The time-averaged thrust in flight duration was estimated at $F_{exp} = 254$ N. The experimental propellant-based specific impulse was estimated at 113 s and 86% of the ground test. It was due mainly to miss fire cycle confirmed by high speed camera.

matsuoka@nuae.nagoya-u.ac.jp

W2P124 KINETIC AND GASDYNAMIC ASPECTS OF DDT IN DIFFERENT GEOMETRIES

Mike Kuznetsov, Karlsruhe Institute für Technologie, Germany

The problem of the Deflagration-to-Detonation Transition (DDT) and a key role of shock waves, boundary layer and turbulence in the detonation preconditioning process is well known but still not resolved in the combustion theory. The ignition, flame propagation with flow ahead of the flame, shock waves generation with turbulent boundary layer behind the shock is the sequence of principal events leading to the deflagration-to-detonation transition in smooth channels.

An overview of DDT phenomena in linear (1D), planar (2D) and torus geometries will be presented in current work in order to demonstrate an effects of gasdynamics and kinetics on the detonation onset. A specific effect of geometry connected with boundary layer phenomena and shock-flame interaction will also be analyzed. It will also be demonstrated that detonation preconditioning history, starting from the ignition, plays an important role on the success of the detonation transition. For instance, a recently developed concept of shockless flame acceleration and detonation transition will for the first time be presented. An effect of turbulence and different instabilities on flame acceleration with respect to detonation preconditioning will be considered in this work. An importance of detailed chemistry on reliability of DDT theory and numerical simulations will be shown. The main idea of this work is to accumulate still unresolved key aspects of the DDT mechanism to be analyzed experimentally and theoretically for the nearest future.

kuznetsov@kit.edu

W2P125 NUMERICAL SIMULATION OF DUST EXPLOSION IN 20L CHAMBER

The paper presents experimental and numerical validation of combustion process of coal and flour dust dispersed in a spherical chamber of 20 cubic decimetres volume. The aim of the study is to validate the numerical simulation results in relation to experimental data obtained on the test stand. To perform numerical simulations, a Computational Fluid Dynamics code FLUENT was used. Geometry of the computational domain was built in compliance with EN 14460. Numerical simulations were divided into two main steps. First one consist in dust dispersion process, where influence of standardized geometry was verified. Second part of numerical simulations investigated dust explosion characteristics in compliance with EN 14034. After several model modifications, outcomes of the numerical analysis shows positive agreement with both, explosion characteristics for different dust concentration levels and maximum pressure increase obtained on the test stand.

zsalamonowicz@sgsp.edu.pl

W2P126

CORRELATION BETWEEN SHOCK STRENGTH AND DUST ENTRAINMENT HEIGHT

Eric L. Petersen, Amira Chowdhury, Sam Mannan, Howard Johnston, Texas A&M University, United States

Secondary dust explosion is a serious industrial issue because it occurs under conditions corresponding to an increased quantity and concentration of dispersed combustible dust when compared with the primary explosion. The problems of lifting and dispersing of a dust layer behind a propagating shock wave must therefore be understood to ensure safety regarding secondary dust explosion hazards. A new shock-tube facility was developed recently by the authors for the study of shock waves over dust layers. This facility utilized an existing 10-cm square shock tube driven section and modified it to provide a new test section with optical access and a removable bottom plate onto which the a dust layer can be placed. A shadowgraph system with a high-speed camera is employed for visualizing the dust layer height as a function of time. For the present experiments, the driven gas was pure nitrogen (rather than air) to prevent any combustion of the powder when exposed to the shock wave (incident or reflected); the driver gas was compressed air.

A study was performed using this new facility to demonstrate the capabilities of the new facility and to compare results with experimental trends formerly established in the literature. Limestone dust with a layer thickness of 3.2 mm was subjected to Mach numbers 1.10, 1.23, 1.32, and 1.40, and a high-speed (15,000 fps) shadowgraph setup was used for flow visualization. Dust layer rise height was graphed with respect to shock wave propagation time, and a new correlation was developed between the shock strength and the dust entrainment height. These results are in agreement with trends found in the literature, where there is a linear trend between dust growth rate and shock Mach number. Also, new data were collected for image analyses over longer periods than found in prior works where the longer observation time and higher framing rates led to the discovery of trends not previously observed in earlier studies, namely a clear transition between a linear-growth regime and a low-growth regime. A plot of the dust layer height as a function of shock Mach Number and time shows first a linear trend of dust height with time. A correlation of this linear trend, as a function of incident-shock Mach Number, is provided in this poster.

epetersen@tamu.edu

W2P127

OPEN VOLUME DETONATION EXPERIMENTS WITH MIXTURES OF PROPANE-BUTANE, ACETYLENE AND PROPANE-BUTANE-ACETYLENE IN AIR

Andrey Gavriko, National Research Center Kurchatov Institute, Russia

Liquefied Petroleum Gas, also called LPG or simply propane-butane, is a flammable mixture of hydrocarbon gases, mostly consisted of propane (90%). LPG is one of the most environmentally friendly fossil fuels available. It is cleaner burning than petrol, diesel, wood, coal and fuel oil. LPG is used as a fuel in a range of applications including heating and cooking appliances, industrial applications, in vehicles and as a propellant and refrigerant. When the risks are properly identified and managed, LPG can be safely used as a fuel source for many applications. But the problem of propane and LPG safety is very important for development of production, transportation and its safe use in industry and for domestic purposes.

The paper presents results of large scale detonation experiments with propane-butane – air and propane-butane – acetylene – air mixtures in open volume. Experiments were carried out in different geometries. In most experiments vertical cylindrical volume covered with polyethylene film was used. Bottom of the cylinder was located at the height of 0.5 m above ground. The total volume of the cylinder varied from 23.5 to 25.3 m³, concentration of propane-butane varied from 4.1% to 4.9%. Additional experiments with acetylene – air and acetylene – propane – air mixtures were performed. Initial temperature in all experiments was 300K and initial pressure – 1 atm. Registration system consisted of 24 pressure sensors and 9 light sensors which were located on 3 rays at a distance from 0 to 20 meters from central axes of cylinder. Detonation was observed in all experiments. Detailed experimental diagnostics, including gas component chromatography and fast video recording were used in each experiment.

Experiments showed that parameters of detonation wave obtained are lower than theoretical values by 5-10%. Mixture of acetylene with air is the most dangerous because of the highest values of detonation wave speed and pressure. But stoichiometric acetylene-air mixture contains highest amount of fuel by mass and content in mixture that

results in lower TNT equivalent than ordinary propane-butane mixture. Large scale experimental results obtained in a series can be used for verification of numerical and analytical models and improvement of CFD tools.

gavrikovandrey@yandex.ru

W2P128

DETONATION IN SUPERSONIC RADIAL OUTFLOW

Aslan Kasimov, King Abdullah University of Science and Technology, Saudi Arabia

We consider supersonic two-dimensional flow of an ideal reactive mixture emanating radially out from a central source. The flow is described by reactive Euler equations with either one-step Arrhenius kinetics or one-step two-stage reduced chemistry for hydrogen-oxygen mixture. It is found that the flow configuration admits a steady-state circular self-sustained detonation as a possible solution. We compute the structure of such a solution and investigate its dependence on the flow conditions at the source. To understand the stability of the steady solutions, we perform two-dimensional numerical simulations that begin with the steady-state solution as the initial condition.

aslan.kasimov@kaust.edu.sa

W2P129

PREVENTION AND PROTECTION OF EXPLOSIONS OF HYDROGEN-AIR PREMIXTURES

Satoshi Kadowaki, Nagaoka University of Technology, Japan

We pay attention to hydrogen as one of alternative fuel for heat engines because of no emission of carbon dioxide or particulates. The characteristic features of hydrogen have a strong tendency to cause explosions, including detonations and deflagrations. To avoid explosions, it is significant to adopt the concept of system safety. The system safety is defined as the application of engineering and management principles, criteria, and techniques to achieve acceptable risk within the constraints of operational effectiveness and suitability, time, and cost throughout all phases of the system life-cycle. Based on the concept of system safety, we shall perform the risk reduction of hydrogen explosion. The basic principles of explosion prevention and protection are that the first step is prevention and the second step is protection. The explosion prevention is to avoid or reduce explosive atmospheres and to avoid any possible effective ignition source. The protection is to halt the explosion and/or limit the range to a sufficient level by protection methods. The risk reduction is achieved by applying the prevention and/or protection principles.

Achieving the risk reduction in accordance with the prevention and protection principles, the knowledge on hydrogen explosion is necessary. Thus, it is indispensable to perform the experiments of explosions of hydrogen-air premixtures to elucidate the characteristics of hydrogen explosion. The present experiments are performed using the closed combustion chamber whose volume is approximately 73L. Hydrogen-air premixtures are prepared in the combustion chamber, and the equivalence ratios are 0.5 and 1.0. The initial temperature and pressure of premixtures are 298K and 101kPa, respectively. Explosion behavior is observed by schlieren photography through quartz windows with 300mm diameter and recorded by Photron high-speed video camera operated at 10000 f/s with 1024×1024 pixel image resolution. The propagation velocity increases with time because of the evolution of disturbances on flame fronts and of the increase of flame-surface area.

kadowaki@mech.nagaokaut.ac.jp

W2P130

DETERMINATION OF TEMPERATURE IN LOW ENERGY SPARK DISCHARGES BY OPTICAL EMISSION SPECTROSCOPY

Stefan Essmann¹, Detlev Markus¹, U. Maas²

¹Physikalisch-Technische Bundesanstalt, Germany ²Karlsruhe Institute of Technology, Germany

Much empirical knowledge has been gathered about the ignition of flammable gas/air mixtures by low energy electrical spark discharges. However, the detailed underlying physical and chemical processes are not yet fully understood. There is a lack of quantitative knowledge of the loss processes in particular. Especially in safety engineering applications where the spark energies are near the Minimum Ignition Energy (MIE) a better understanding is needed. A physicochemical numerical model considering detailed chemical kinetics, transport phenomena of neutral species, ions, and electrons, as well as electrodynamic modeling of the interaction between a spark and the fuel/air mixture is currently under development. In order to devise such a model, detailed experiments are needed, which both guide the modeling and allow a verification of the model.

In this study, the plasma temperature of spark discharges at atmospheric pressure is determined by spectrally analyzing the light emitted by the discharges using a spectrometer and an intensified CCD camera. Radiative transmissions in the second positive system of nitrogen N₂ C-B are used for comparison between the experimental spectra and the spectra simulated with the software Specair. From the best fit the rotational and vibrational temperatures of the plasma can be derived. Temperatures are determined for spark energies in the low energy range near the minimum ignition energy. The effects of spark energy and electrode gap width on the plasma temperature are analyzed. Using the temperatures found in this study a numerical model is employed in order to calculate the initial phase of flame propagation. Experimental data on the flame front propagation of flammable mixtures ignited by low energy capacitance sparks is available from earlier studies and is used to validate the numerical model.

stefan_essmann@yahoo.de

W2P131 ASSESSMENT AND IMPLEMENTATION OF A MARKSTEIN NUMBER BASED TURBULENT BURNING VELOCITY CORRELATION FOR SIMULATING INDUSTRIAL GAS EXPLOSIONS IN COMPLEX GEOMETRIES

Gordon Atanga¹, Trygve Skjold², Helene Pedersen²

¹GexCon US Inc, United States ²University of Bergen, Norway

The use of Computational Fluid Dynamics (CFD) for modelling gas explosion scenarios in industrial plants is a challenging task, involving multi-scale modelling of highly transient phenomena from complex initial and boundary conditions. Although the predictive capability of current turbulence and combustion models has significantly improved in recent years, several issues are still pending. One relevant example involves the optimization of safety gaps between process units in onshore processing facilities, such as large offshore installations, floating processing facilities, and onshore process plants.

The Laminar Burning Velocity (SL), which is the elemental unit in the description of key complex combustion phenomena (e.g. flame extinction/ignition, instabilities, stabilization, etc.), is pivotal in turbulent combustion modelling. A scatter in the earlier measured values for SL of up to ± 25 cm/s has been reduced to ± 2 cm/s with the recent understanding of the non-linear nature of stretch on SL. It is therefore imperative to work with stretch-free laminar burning velocities in conjunction with turbulent velocity correlations. Most correlations for turbulent burning velocity (ST) fall short of including critical phenomena related to flow and combustion. A simple correlation, yet with high predictive potential, has recently been proposed by Bradley and co-workers in terms of the strain rate Markstein number (Masr) : $u_t/u'_k = \alpha K^\beta$; for $K > 0.05$ where α and β are constants expressed by first order expressions in terms of the strain rate Markstein number and the Karlovitz stretch factor (K). Its predictive potential stem from the fact that Masr not only represent a physico-chemical property of the mixture, but also a viable measure of its sensitivity to stretch (flame curvature and flow field strain). The difficulty here is to establish an appropriate set of input data, that is, tabulated strain rate Markstein numbers for the relevant fuel mixtures over the entire equivalence ratio of interest.

The goal of the present study is to compute laminar burning velocities for several fuels, such as hydrogen, methane and propane, over the entire flammable concentration range. The numerical experiments describe spherical flame propagation, in order to eliminate the effect of stretch. Masr values are then extracted using both linear and non-linear methods described in the literature. After implementing the above correlation in the RANS based solver FLACS, the performance of the model system will be assessed by comparing simulation predictions to results from large-scale experiments.

gordon@gexcon.com

W2P132 THERMAL DEFORMATION OF PLASTIC SHEETS AFTER A GAS EXPLOSION

Takashi Tsuruda, Akita Prefectural University, Japan

A series of tsunami waves damaged nuclear reactors of Fukushima Daiichi Nuclear Power Plant on March 11, 2011. The explosion of unit 4 occurred during its outage when maintenance works had been carried out with various combustible materials in the plant. Combustible materials in the nuclear power plants were always controlled to minimize fire and explosion hazards. If a gas explosion occurred, the hot combustion product heats combustible materials in a short period. The heating rate is much faster than the flammability test. Combustible materials are treated as thermally thin, that the temperature in the combustible material is at a constant value in the cross section. For a gas explosion heating, the heating period is same order of the thermal wave travel time from the surface to the center of the combustible material. The current knowledge of the non-steady heat transfer of a gas explosion heating is still insufficient to understand the thermal deformation of combustible materials. A series of explosion tests has been carried out to investigate the thermal deformation of combustible materials with a small experimental chamber.

TTsuruda@akita-pu.ac.jp

W2P133 PASSIVE SCALAR-BASED ANALYSIS OF CAVITY-STABILIZED JET COMBUSTION IN A SUPERSONIC COMBUSTOR

Hongbo Wang, National University of Defense Technology, China

A passive scalar-based approach for studying complex combustion phenomena has been proposed in the context of nonequilibrium chemistry. Based on mixture fracture concept widely used for the description of nonpremixed combustion, transport equations for passive scalars have been derived and solved together with the conventional large eddy simulation governing equations. These passive scalars are readily utilized to trace the mass transport in simulations of complicated reacting flows, regardless of turbulence and chemistry models. The approach is used to study the cavity-stabilized H_2 jet combustion in a supersonic combustor, where characteristics of the mass transfer into and out of the cavity are captured, revealing the spatiotemporal dynamics of the cavity-stabilized supersonic combustion. The cavity-stabilized jet combustion is found to consist of three key parts: a reservoir for hot and activated products within the cavity acting as an ignition source, the fuel-rich premixed combustion under/within the fuel jet promoted by the forced ignition of the reservoir, and downstream diffusion flames stabilized by the premixed combustion. The stabilization mechanism is consistent with a degraded triple flame.

W2P134

A COMPRESSIBLE LEM-LES STRATEGY (CLEM-LES) FOR MODELLING SUPERSONIC AND TURBULENT COMBUSTION

Brian Maxwell¹, Matei Radulescu¹, Sam Falle²¹University of Ottawa, Canada ²University of Leeds, United Kingdom

A turbulent combustion model based on the Linear Eddy Model for Large Eddy Simulation (LEM-LES) has been developed to study highly compressible and reactive flows involving very rapid transients in pressure and energy. The model is treated as a one-dimensional sample of a diffusion-reaction system within each multi-dimensional LES cell. This reduces the expense of solving a complete multi-dimensional problem through Direct Numerical Simulation (DNS) while preserving micro-scale hot spots and their physical effects on ignition. Thus, the model provides a high resolution closure for the unresolved chemical reaction terms in the governing, LES-filtered, reactive Navier-Stokes equations. Furthermore, the current approach features a Lagrangian description of fluid particles on the sub-grid for increased accuracy. Additional closure for the unresolved turbulent viscosity is provided by a one-equation Localized Subgrid Kinetic Energy Model (LKM). Finally, Adaptive Mesh Refinement (AMR) is carefully implemented for increased computational efficiency. Recently, this modelling strategy has been validated for various 1-D test cases. This includes laminar and turbulent flame propagation as well as laminar detonation initiation and propagation. In the current work, the model is extended to treat two-dimensional unsteady and turbulent detonation propagation, in a narrow channel, which involves a premixed methane-oxygen mixture at low pressures. The results have shown that the detonation propagates at an average velocity that corresponds to the theoretical Chapman-Jouguet (CJ) velocity. Furthermore, the two-dimensional cellular structure captured resembles that obtained through higher resolution DNS. Finally, three specific major limitations of the model are revealed. They are, namely; 1) the model does not capture well flame propagation near walls and in zero-velocity regions, 2) for multi-dimensional flow, the flow velocity must be predominantly aligned with the grid in order to minimize spurious diffusive errors, and 3) AMR must be carefully implemented in order to avoid errors associated with refinement. Despite these limitations, however, the model's use can be justified for modelling detonation waves that travel predominantly in a planar direction at sufficiently high velocities. In summary, the CLEM-LES is a fully conservative, high resolution, turbulent combustion model that reduces the complexities of a multi-dimensional problem to one-dimension and is able to handle highly compressible flows.

bmaxw005@uottawa.ca

W2P135

COMBUSTOR PERFORMANCE COMPARISON IN DUAL-MODE SCRAMJET

Camilo Aguilera Muñoz, Kenneth Yu, University of Maryland, United States

An experimental study was performed to assess the effect of fuel injection on propulsion performance in a laboratory-scale dual-mode scramjet combustor, which uses hydrogen fuel and a cavity flame-holder. The testing was conducted with Mach 2 airflow at the isolator entrance, simulating the total enthalpy of a Mach 4.7 flight condition. Two different injector configurations were compared – a baseline configuration using normal transverse fuel injection, and a fin-guided configuration using a mixing-enhancement fin placed just upstream of the injector. Both configurations were tested over an overall equivalence ratio ranging between 0.04 and 0.20. Fuel injection and mixing in both configurations were characterized using planar Mie-scattering images of the cross stream, schlieren images along the stream, and shock-induced pressure rise measurements. The results showed that the fin-guided injection allowed an additional 60~90% recovery of the stagnation pressure loss caused by jet-induced shocks in the baseline configuration. The combustion characteristics were also studied by correlating schlieren images, OH* chemiluminescence data, and the wall pressure measurements along the stream-wise direction. At moderate equivalence ratios between 0.08 and 0.12, a clear difference in combustion mode was observed between the two configurations (Fig. 1). While the baseline configuration operated in a thermally-choked combustion mode with a concentrated heat release near the flame-holder, the fin-guided configuration allowed a supersonic combustion mode operation with an axially distributed heat release zone. As expected, the baseline configuration at thermally-choked mode reached significantly higher pressures than the fin-guided configuration operating at supersonic combustion mode. An analytical comparison of propulsion performance showed that a supersonic-combustion-mode operation would be preferable for a high-efficiency high-compression-ratio inlet, while a thermally-choked-mode operation would yield a better propulsion performance in case of a less efficient inlet with a relatively low compression ratio. These results highlight a complexity associated with determining an optimal mode of operation in a dual-mode scramjet combustor.

camilo986@gmail.com

W2P136

INTERACTION BETWEEN PRE-COMBUSTION GAS INJECTION FROM A RAMP INJECTOR AND INCIDENT SHOCKWAVE IN SUPERSONIC FLOW

Tatsuya Yamaguchi, Yoshitaka Iwamura, Taku Kudo, Akihiro Hayakawa, Hideaki Kobayashi, Tohoku University, Japan

A SCRAMJET engine is expected as a propulsion system for a hypersonic airplane. Because of short residence time of inlet air, mixing and combustion should be completed in the combustor within millisecond time scale. In

addition, the interaction between shockwaves and combustion region must be revealed. Ramp injector is expected as a promising injection method which can introduce streamwise vortices for mixing enhancement and reduce the total pressure loss. The aim of this study is to investigate the interaction between pre-combustion gas injection from a ramp injector and an incident shockwave in supersonic flow by experiments and numerical simulations. The incident shockwave is formed by a shock generator, which has turning angle of 6 degrees, and introduced into region downstream of the ramp injector. H_2 /Air mixture with equivalence ratio of 3.6 is ignited in the pre-combustion chamber before injection. The Mach number, total pressure, and total temperature of the inlet air are 2.5, 0.5 MPa, 673 K, respectively. Those properties of pre-combustion gas are 1.0, 0.6 MPa, 1500K, respectively.

In this study, when the incident shockwave was introduced, combustion region was confirmed by flame emission (Image), which shows that combustion was enhanced in the downstream of the shockwave. Wall pressure measurement and numerical simulation (Image) indicates that high pressure region formed near the wall in the downstream of the reflected shockwave increases reaction rate between hydrogen and air. Numerical simulation (Table 1) also shows that baroclinic torque generated by pressure gradient of incident shockwave and density gradient between inlet air and injection gas facilitates mixing by increasing streamwise vorticity. Wall pressure measurement (Image) also shows that shockwave entering into high temperature and low sonic speed zone like combustion region changes the shock angle to fulfill the relational equation among turning angle, shock angle and Mach number.

yamaguchi@flame.ifs.tohoku.ac.jp

W2P137

SUPERSONIC COMBUSTION MODELLING USING THE CONDITIONAL MOMENT CLOSURE APPROACH

Mark Picciani, Cranfield University, United Kingdom

This work presents a novel algorithm for supersonic combustion modelling. The method involved coupling the Conditional Moment Closure (CMC) model to a fully compressible, shock capturing, high-order flow solver, to model a reacting hydrogen-air, supersonic lifted jet. The objective is to extend this algorithm to study the flow within a scramjet combustor. The Compressible High Order Combustion (CHOC) code is a finite volume, single block, structured code. It is based on the Godunov method with 5th order MUSCL reconstruction and low Mach number correction, with the HLLC approximate Riemann solver used to evaluate the local Riemann problem at the CFD and CMC cell interfaces. An explicit second order Runge-Kutta TVD method is used to advance the solution in time. The algorithm is applied to the supersonic reacting case of ONERA specifically the LAERTE jet. The results showed the method was able to successfully capture chemical non-equilibrium effects, as the lift-off height and autoignition time were reasonably captured. A lift-off height of about 0.165-0.183m was calculated based on peak gradient of OH production, which compares to an experimental lift-off height of about 0.170m. Distributions of reactive scalars are difficult to assess as experimental data was deemed to be very inaccurate by the publishers. If experimental errors were quantified, a better conclusion on the accuracy of the results of the simulations could have been made. As a consequence, published numerical results for the same test case were utilised to aid in analysing the results of the presented simulations. The temperature from the simulations are slightly lower than the presumably overestimated experimental results suggesting that the current results could in fact be similar to the experimental conditions. Additionally, the effect of CMC grid was analysed. It was shown that too coarse of a CMC grid can cause un-realistic combustion behaviour through the onset of large discontinuities at the CMC cell interfaces. Refining the CMC grid removed the non-physical behaviour, but still showed miniature discontinuities at the CMC cell interfaces when cross-stream averaging was applied. To achieve a smoother solution, further refinement of the CMC grid is hypothesised to be needed. However, further refinement begins to deviate from the primary advantage of CMC, and therefore could represent a practical limitation of this method in supersonic flows. It is also unclear if more accurate modelling of CMC terms is required and is in fact, the cause of these miniature discontinuities. The primary conclusions from the study were that the CMC method is feasible to model supersonic combustion, as good agreement was obtained from the limited data available. The present work does not confirm, or refute, the detailed accuracy of the proposed method as concluding this requires better analysis and data. It does however, give confirmation to its feasibility and application, and gives rise to potential modelling uncertainties and areas of improvement both in the CHOC code, and also the CMC method. Potential drawbacks of the methods are also presented, such as CMC resolution issues, but it is uncertain whether these limitations are a function of the model or of the manner in which the model has been used. These vague conclusions also illustrate the need for more reliable, simple experimental data for supersonic reacting flows.

m.a.picciani@cranfield.ac.uk

W2P138

AN ANALYSIS OF THE SUPPRESSION OF PREMIXED FLAMES

Jenny Chao, Sergey B. Dorofeev, FM Global Research, United States

The use of an explosion suppression system as a means for explosion protection has become fairly popular in industrial settings, particularly when alternative protection methods such as explosion venting cannot be easily applied. In general, an explosion suppression system is comprised of a detector (such as a pressure transducer or an infrared sensor) that detects an accidental explosion at the incipient stage of flame growth and then triggers a high-pressure discharge of suppressant (such as sodium bicarbonate) in order to quench the expanding flame ball and inert the remaining explosive mixture. Depending on different factors such as the time of suppressant injection, the amount

of suppressant injected, and the distribution of suppressant concentration in the protected enclosure, an explosion suppression system can potentially reduce damaging overpressures (that are otherwise generated by an accidental explosion) to levels within the strength of the protected enclosure. Manufacturers of explosion-suppression systems use proprietary models and computer codes to design a configuration for a specific scenario that will result in acceptable reduced overpressures. Although these models are developed based on results from large-scale tests by the manufacturers, it is not clear how to verify the designed reduced overpressure for different explosion-suppression systems and how to evaluate the overall performance of these systems.

Therefore, in the present study, an attempt is made to understand the physical mechanisms that control the suppression of a premixed flame in order to be able to evaluate the efficacy of an overall explosion-suppression system. A parametric series of experiments were performed at different scales on the suppression of propane-air and cornstarch-air flames using sodium bicarbonate as an example suppressant. The effects of vessel volume, system-activation pressure, suppressant-injection location, number of injection locations, and suppressant concentration on the reduced overpressure were investigated. In general, it was found that lower system-activation pressures resulted in lower reduced overpressures. As well, multiple injection locations were much more effective in reducing the overpressure compared to a single injection location (for the same total amount of suppressant); however, direct suppressant injection from a single location onto the growing flame ball was shown to be just as effective. From the experimental results, there was no clear indication how the results should be scaled to full-volume systems. In order to synthesize the large volume of experimental data that was obtained, a simple model is developed to describe the suppression of a spherically-expanding premixed flame. From the conservation of mass, assuming isentropic compression, an expression can be used to characterize the pressure development in the vessel due to flame propagation and suppressant injection. If the injected suppressant is approximated as a hemisphere, the flame surface area, A_f , is given by $4\pi R_f^2 - A_{cap}$ where A_{cap} is the surface area of the spherical cap resulting from the intersection of a hemispherical suppressant cloud with a spherical flame and represents the portion of the flame quenched by the suppressant. The mass flow rate of the suppressant injected into the protected volume is dm/dt and can be determined from isentropic choked flow from a finite volume where stagnation conditions do not remain constant. The results of this simple model are then compared to the experimental results.

jenny.chao@fmglobal.com

W2P139

ON THE STRUCTURE OF SELF-SIMILAR DETONATION WAVES IN TNT CHARGES

Allen Kuhl, John Bell, Vincent Beckner, Kaushik Balakrishnan, Lawrence Berkeley National Laboratory, United States

A phase plane method is proposed to model flow fields bounded by constant-velocity detonation waves propagating in TNT charges. Similarity transformations are used to formulate the problem in the phase plane of non-dimensional sound speed: Z versus non-dimensional velocity: F . The formulation results in two coupled ordinary differential equations that are solved simultaneously. The solution corresponds to an integral curve $Z(F)$ in the phase plane, starting at the Chapman-Jouguet (CJ) point and terminating at singularity A—the sonic point within the wave. The system is closed by computing thermodynamic variables along the expansion isentrope passing through the CJ point—forming, in effect, the complete equation of state of the thermodynamic system. The CJ condition and isentropic states were computed by the thermodynamic code Cheetah. Solutions were developed for planar, cylindrical and spherical detonations. Species profiles were also computed; carbon graphite was found to be the predominant component (~10 moles/kg). This illustrates the unique contribution of this work—the coupling of a complete equation of state (including species compositions) for the detonation products at high densities (~ 1.6 g/cc) with the similarity field. Previous solutions employed a constant-gamma assumption, which is appropriate for detonations in gases but not in solids.

KUHL2@LLNL.GOV

W3P001 **EXPERIMENTAL INVESTIGATION OF ATOMIZATION AND COMBUSTION PERFORMANCE OF RENEWABLE BIOFUELS**

Vincent G. McDonell, Adam Silver, University of California, Irvine, United States

This poster presents results from an experimental investigation of the macroscopic and microscopic atomization behavior of B99-biodiesel, ethanol, B99-ethanol blends, methanol, and an F-76-Algae biodiesel blend. In addition, conventional F-76 and Diesel #2 sprays are characterized as a base case to compare with. The experimental spray apparatus consists of a plain air-blast atomizer mounted on a traverse. The breakup characterization of each fuel is conducted under the same air flow conditions in order to simulate use as a drop in source to existing gas turbines with only slight modifications. For this study, a Phase Doppler Particle Analyzer and Laser Doppler Velocimetry system is employed to gain information on drop size, SMD, velocity, and volumetric flux distribution across the spray plume. A Vision Research Phantom high speed camera is used to gather high speed cinematography of the sprays for use in observing breakup characteristics and providing additional insight. The results illustrate how the fuel type impacts the atomization and spray characteristics. A variety of B99-ethanol fuel blends are used which illustrate a tradeoff between lower density, surface tension, and viscosity with a decrease in the air to liquid ratio. Future work will entail swirl stabilized combustion of each fuel in order to compare with non-reacting flow results. Reacting flow measurements will include NO_x , SO_x , and CO emissions, lean blow off limits, and flame luminosity.

mcdonell@ucicl.uci.edu

W3P002 **SPHERICAL FLAME INITIATION AND PROPAGATION IN A LIQUID FUEL MIST WITH FINITE-RATE EVAPORATION**

Wang Han, Zheng Chen, Peking University, China

Droplet vaporization might have a great impact on fundamental spray combustion processes such as ignition, flame propagation and extinction. In this study, spherical spray flame initiation and propagation through a fuel-rich/lean pre-mixture containing fuel droplet with finite-rate evaporation are analyzed using the large-activation-energy asymptotic method. Thermal-diffusive model with constant density is employed and the spherical flame is assumed to propagate in a quasi-steady state. Analytical correlations describing the change of spherical spray flame propagation speed with flame radius are derived. The droplet vaporization parameters (initial droplet load, δ , and vaporization Damköhler number, Da), Lewis number and ignition power are included in these correlations. Therefore, the present model can predict the evolution of ignition kernel and propagating spherical spray flame. Based on these correlations, spherical spray flame initiation and propagation are investigated and the impact of droplet vaporization on critical ignition condition and spherical flame propagation is assessed.

whan@pku.edu.cn

W3P003 **SINGULARLY PERTURBED HOMOTOPY ANALYSIS METHOD APPLIED TO THERMAL EXPLOSION OF POLYDISPERSE FUEL SPRAY**

Ophir Nave, Vladimir Gol'dshtein, Ben Gurion University, Israel

In this paper we discuss the new Homotopy Perturbation Method (HPM) combined the Homotopy Analysis Method (HAM) and the Method of Invariant Manifolds (MIM). The HAM method is used for slow subprocesses only after a decomposition of the original process to slow and fast subprocesses with the help of the MIM method. For a good accuracy we used the first approximation of a corresponding invariant manifold in the sense of a corresponding small parameter. The HAM method was introduced recently by the authors and their collaborators as an attempt to avoid main problems of the HPM method for slow-fast models. With the help of the HAM method we investigate the problem of thermal explosion in two-phase polydisperse combustible mixtures of gas and fuel droplets. The size distribution of the fuel droplets is modeled as a continuous function in the form of an exponential distribution and is found from the solution of the kinetic equation for the probability density function. The system of the polydisperse fuel spray takes into account the effects of the thermal radiation and convection. By applying the HAM, we derived an analytical solution of the system and we compared our results with the numerical solutions.

naveof@cs.bgu.ac.il

W3P004 **EXPERIMENTAL STUDY OF THE INTERACTION BETWEEN AN ETHANOL SPRAY AND A TURBULENT FLAME FRONT**

Luis Fernando Figueira da Silva, Juan Jose Cruz Villanueva, PUC-Rio, Brazil

The objective of this study is to characterize the direct interaction between a turbulent flame stabilized by a bluff body and the associated spray. This characterization is performed by using a 283.56 nm laser beam to excite the OH radical fluorescence, which marks the reaction zone in the flame, whereas the second harmonic of a Nd:YAG laser is used to generate the Mie scattering signal of the spray droplets. The spray is operated both at the design point and at off design situations by varying the ethanol flow rate. The effect of different air velocities is also investigated. The turbulent Reynolds number is circa 2300 at the bluff body region. The obtained results show that the instantaneous flame front remains mostly continuous, but corrugated by turbulence. The flame front is closed at the vicinity of the bluff body for the smaller flow rates of ethanol. The increase of air velocity increases the flame thickness, which is attributed to a larger

turbulent diffusivity at higher air Reynolds numbers, and is accompanied by higher averaged OH fluorescence intensity. The Mie scattering signal shows that the air velocity influences the geometry when the air flow velocity is increased. All studied cases are shown to lead to strong flame/spray interactions. Indeed, a large number of droplets are found to pass through the flame, indicating that ethanol is not completely evaporated or burned. Thus, the particular regime of combustion obtained seems to be the percolation one, which will be the subject of future studies.

luisfer@esp.puc-rio.br

W3P005 SPRAY FLAME STRUCTURE ANALYSIS IN A LAB-SCALE BURNER USING LARGE EDDY SIMULATION AND DISCRETE PARTICLE SIMULATION

Damien Paulhiac, Benedicte Cuenot, Elonore Riber, CERFACS, France

The numerical study of an academic lab-scale spray burner using Large Eddy Simulation (LES) coupled with a Discrete Particle Simulation (DPS) is presented. The objectives of this study are first, to validate subgrid-scale models for two-phase turbulent flow and combustion, and second, to bring new insight on two-phase flame structure in a complex geometry representative of industrial systems. The configuration is an experiment characterized by a strong interaction between the liquid disperse phase and the reaction zone, as is also observed in most industrial combustion chambers. This strong interaction leads to complex spray burning modes that raise additional modeling issues. The comparison with measurements confirms the capability of LES - DPS to reproduce the velocity field in both non-reacting and reacting cases with good quantitative accuracy. Experimental and numerical images of the spray flame are also in good agreement. The detailed analysis of the spray flame shows that both partially premixed and diffusion flames are present, depending on the possible pre-evaporation of the droplets. In addition, and as observed in the experiment, single droplet combustion occurs downstream the main flame front. This combustion mode leads to small diffusion flames around the droplets that can not be resolved in the simulation and require a specific modelling approach. An extended two-phase combustion model that takes into account single droplet combustion is finally presented with first validation tests.

paulhiac@cerfacs.fr

W3P006 EFFECT OF FUEL-SPRAY OSCILLATIONS AND DROPLET GROUPING IN THE FORMATION OF MULTIPLE FLAMES

David Katoshevski¹, Barry Greenberg²

¹Ben-Gurion University of the Negev, Israel ²Israel Institute of Technology, Israel

The sensitivity to the vaporization Damkohler number of the behavior of a co-flow laminar spray diffusion flame in an oscillating flow field is investigated. Droplet grouping induced by the host gas flow oscillations is accounted for. The effect of droplet grouping is described through a specially constructed model for the vaporization Damkohler number that responds to the proximity of the droplets as they cluster due to the spray-flow oscillations. A formal analytical solution is developed for Schwab-Zeldovitch parameters through which the dynamics of the spray flame front shapes and thermal fields are deduced. Computed results based on the solutions demonstrate how strongly the vaporization Damkohler number including droplet grouping effects impacts on the type of primary homogeneous flame formed and on the possible existence of multiple flame sheets as a result of dynamic changes from under- to over-ventilated flames as the flow field oscillates. A further subtle, allied phenomenon that produces isolated regions of high fuel vapor concentrations is fuel droplet enrichment that stems from the combination of droplet grouping and the oscillating droplet and host gas flow fields. Such regions also lead to the formation of multiple flames under certain operating conditions. The Burke-Schumann laminar spray flame configuration is considered, in which fuel vapor and droplets flow in an inner duct and air flows in outer duct. Under appropriate operating conditions, after diffusive mixing of the two streams, a laminar spray diffusion flame is maintained. The model and the evolution of the flame with/without the grouping effect of the fuel-droplets, as well as the multi-flame situation will be presented.

davidk@bgu.ac.il

W3P007 PLANAR LASER-INDUCED FLUORESCENCE SPECTROSCOPY AND SIMULATIONS OF IGNITION AND COMBUSTION OF FREELY FALLING ALKANE, ALCOHOL, AND METHYL ESTER DROPLETS

Torben Grumstrup¹, Anthony John Marchese¹, Azer Yalin¹, Frederick L. Dryer², Tanvir Farouk³

¹Colorado State University, United States ²Princeton University, United States ³University of South Carolina, United States

In emission measurement studies, diesel engines fueled by fatty-acid methyl ester biodiesel often exhibit slightly increased production of oxides of nitrogen (NO_x) in comparison to petroleum diesel. A number of explanations for this increase have been proposed by the research community. One theory, which has been supported by optical engine test results, suggests that the presence of oxygen atoms in the methyl ester fuel molecule results in a leaner premixed autoignition zone, thereby increasing in-cylinder temperatures and promoting thermal NO_x production. Other experiments have suggested that the unsaturated methyl esters in biodiesel cause an increase in CH radical production (and/or other potential precursors such as C_2O) which in turn increases prompt NO_x formation.

In the present study, these hypotheses are explored experimentally and computationally by considering the ignition and combustion of single, isolated alkane, alcohol and methyl ester droplets. Experiments were conducted in

which the Planar Laser-induced Fluorescence (PLIF) spectroscopy technique was applied to burning liquid fuel droplets in free-fall. A monodisperse stream of droplets was generated by a piezoelectric device and passed through an electrically heated coil where they autoignited. A pulsed laser beam from a Nd:YAG-pumped dye laser (10 Hz, ~10 ns width) was formed into a sheet and passed through the droplet flame. The dye laser was tuned to excite hydroxyl (OH) at 282.9 nm and Nitric Oxide (NO) at 226.0 nm. The resulting fluorescence was imaged by a Cooke Corporation DiCam Pro ICCD digital camera. Bandpass filters were utilized to reject laser light scattering while admitting fluorescence wavelengths. Due to the small fluorescence signal, many fluorescence images were averaged together to create a useful average image; approximately 250 and 1000 images were averaged for OH and NO spectroscopy, respectively.

Finally, pixel intensities of the averaged fluorescence image were integrated about the droplet center to create radial profiles of OH and NO concentration. Profiles were generated for a number of oxygenated fuels and one pure hydrocarbon: methanol, ethanol, 1-propanol, methyl butanoate, methyl decanoate, and *n*-heptane.

To quantitatively interpret the contribution of thermal and prompt NO_x mechanisms on NO_x formation in the vicinity of igniting liquid droplets, simulations were conducted with an independently-developed comprehensive numerical model developed at Princeton University. The transient, spherically symmetric droplet combustion model features detailed gas-phase kinetics, spectrally resolved radiant heat transfer, and multi-component gas transport. Mass and energy conservation is solved in both the gas and liquid phase. The heat transfer within the droplet is of "finite" conduction prescribed by the liquid phase thermal conductivity. Chemical kinetic mechanisms were created by appending NO_x chemical kinetics to the respective fuel mechanisms.

The fuels for which simulations have thus far been conducted are: methanol, methyl butanoate, and *n*-heptane. In the computations, non-oxygenated (heptane) and oxygenated (methyl butanoate, methanol) fuel droplets are introduced into a hot (1150 K) air ambient whereupon the liquid vaporizes, thus producing a stratified fuel/air mixture that thermally autoignites after an ignition delay period. The computational results suggest that NO_x formation in stratified fuel/air mixture in the vicinity of a cold liquid droplet is influenced greatly by the detailed full NO_x chemistry (prompt, thermal, and N₂O) and cannot be fully explained by considering only the thermal NO_x route. The computations also suggest, however, that the stoichiometry of the premixed autoignition zone in the laminar gas phase surrounding a spherical droplet differs from that observed in turbulent diesel spray ignition.

tpg460@gmail.com

W3P008 SIMULATING FLAME-SPREAD BEHAVIOR OF RANDOMLY DISTRIBUTED DROPLET CLOUDS BASED ON PERCOLATION THEORY AND MICROGRAVITY EXPERIMENT OF DROPLET ARRAY

Herman Saputro, Masato Mikami, Takehiko Seo, Yamaguchi University, Japan

It is difficult to conduct the experiment on large-scale droplet cloud combustion because the buoyancy effect is significant in normal gravity. Experiments on the flame-spread characteristics of droplet-array and droplet-cloud elements have been conducted in microgravity, but the findings have not fully elucidated the spray combustion phenomenon because the number of droplets is limited in the experiments. This research presents the numerical simulation of 2-Dimensional (2D) and 3-Dimensional (3D) flame-spread behavior in large scale droplet clouds in which the droplets are distributed randomly. The numerical simulation was calculated using the percolation approach and considering the flame-spread characteristics of droplet array obtained in microgravity experiments, especially the flame-spread-limit distance (S/d_0) limit. The Occurrence Probability of Group Combustion (OPGC) was calculated as a function of the mean droplet spacing (S/d_0) m without and with two-droplet interaction. The results show that OPGC rapidly decreases with increasing (S/d_0) m around a specific value and this critical threshold separates the droplet clouds into two types: dilute spray and dense spray. The critical mean droplet spacing (S/d_0) critical increases with the two-droplet interaction and is greater for the 3D droplet cloud than for 2D one. (S/d_0) critical was also discussed considering the influence of the lattice size (NL/d_0), lattice point interval (L/d_0).

hermansaputro@yahoo.com

W3P009 BURNING CHARACTERISTICS OF BIODIESEL MIXED WITH ALCOHOL IN MICROGRAVITY CONDITION

Kuo-Long Pan, Jia-Jun Yao, National Taiwan University, Taiwan

By using a drop tower that can support a free-falling process of 0.68s, we have studied combustion characteristics of biodiesel droplets mixed with various alcohols in microgravity environment. By using two hot wires to ignite a droplet with fixed diameter around 535 μm, we have observed various combustion phenomena of fuel droplets made of single and binary components in reduced gravity, including the evolutions of droplet diameter, burning rate, micro-explosion, and extinction. In particular, we studied the propensity to microexplosion of binary fuels containing premixed liquids of biodiesel and ethanol. To minimize experimental uncertainty, we used the powerful built-in function of an image processing software, Matrox Inspector 8.0, to measure the boundaries. It was found that when a droplet of biodiesel mixed with alcohol was deployed onto the cross section of two ceramics fibers, non-uniform sites similar to liquid bubbles occurred. In this situation, whether under the condition of normal gravity or reduced gravity, micro-explosion was always generated while burning. Occurrence of such non-uniform phenomena was related to the relative humidity of the environment. With increasing of relative humidity, the bubble-like sites became bigger. At the same relative humidity, the bubbles became smaller as the carbon number of alcohol increased. Furthermore, with increase of

the alcohol concentration, the size of liquid bubbles became bigger. It was also found that the bubble-like sites inside the droplet diminished with time. After the bubbles vanished, no micro-explosion was ever observed during burning.

panpeter@ntu.edu.tw

W3P010 LES OF THE SYDNEY SPRAY FLAME SERIES WITH PFGM/ATF AND DIFFERENT SUB-GRID MODELS
Andreas Rittler, Fabian Proch, Andreas Kempf, University of Duisburg-Essen, Germany

The Sydney spray flame series is investigated by Large Eddy Simulation (LES). Combustion is modeled by the Premixed Flamelet Generated Manifold approach (PFGM), which is combined with the Artificially Thickened Flame Method (ATF). The dilute ethanol and acetone spray flames, stabilised by a coaxial pilot flame, have been experimentally investigated by Masri and coworkers at the University of Sydney. Of the available fuel and mass flow combinations, we have chosen the ethanol flames referred as "EtF₃, EtF₆ and EtF₈", with the same ethanol mass flow rate but different carrier gas mass flow rates in the central stream.

The simulations are performed with the LES inhouse code PsiPhi. Grids with three different resolutions (from 3 to 24 million cells) are used to investigate the influence of the filter width. The gas and spray phases are described by an Euler/Lagrange approach. The phases are fully coupled by the exchange of mass and momentum. Nicoud's σ -model is used to determine the turbulent Sub-Grid-Scale (SGS) stresses. One dimensional simulations of premixed freely propagating flames with a detailed reaction mechanism were performed a priori to tabulate the combustion variables as a function of two controlling variables ($\Phi=f(Z, Y_p)$). The Favre filtered mixture fraction (Z) and progress variable (Y_p) are the determining quantities. A thickening factor is applied to the transport equation of the progress variable to resolve the thin reaction zone of the flame (typically ~ 0.1 - 0.5 mm) on the computational grid, and a flame sensor indicates the burning region and determines the use of the thickening factor.

The sub-grid distributions of Z and Y_p are modeled with (a) a presumed beta filtered density function (β -fdf) and (b) a Top-Hat function (TH). In the β -fdf approach, the two-dimensional look-up table ($\Phi = f(Z, Y_p)$) is extended to a third dimension by using either the mixture fraction variance (Z''^2) or the progress variable variance ($Y_p''^2$) as a third control variable. Albeit, in the TH approach the two-dimensional look-up table is a priori integrated over a third control variable (Z''^2 or $Y_p''^2$), or over a third and fourth control variable (Z''^2 and $Y_p''^2$). With the TH approach, the look-up table remains two-dimensional. The variances Z''^2 and $Y_p''^2$ are determined with either an algebraic gradient model or with a transport equation model. First, the influence of the mixture fraction variance ($\Phi=f(Z, Y_p, Z''^2)$) and the progress variable variance ($\Phi=f(Z, Y_p, Y_p''^2)$) on the simulation results is investigated separately. Subsequently, the joint impact of Z''^2 and $Y_p''^2$ is investigated with the TH model ($\Phi=f(Z, Y_p, Z''^2, Y_p''^2)$). The results obtained with the different sub-grid models are compared against the available experimental data and reference simulations without any Sub-Grid Model.

Generally, the particle statistics are in good agreement with the experimental evidence. The results obtained with the TH and the β -fdf model are comparable. It must be stressed that the influence of the sgs models for the mixture fraction and the progress variable was found to be small for the investigated spray flames series. We have therefore set up a more sensitive test case to amplify and show the differences in the models, which are presented in the poster.

andreas.rittler@uni-due.de

W3P011 OXYGEN LEWIS NUMBER EFFECTS ON REDUCED GRAVITY COMBUSTION OF METHANOL DROPLETS
Chang Vang, Benjamin D. Shaw, University of California, United States

Reduced-gravity combustion experiments of individual methanol droplets were conducted on the International Space Station in air/xenon and air/helium environments at 1 atm and 0.7 atm and about 298 K. Droplet diameters were initially in the 2-4mm range. The present study investigates the flammability and extinction of methanol droplets under these conditions. Droplet diameter histories, burning rate histories, and radiometer data are evaluated. The experimental results show that the Limiting Oxygen Index (LOI) for methanol droplets in air/xenon ambients is appreciably smaller than in air/helium ambients. This discrepancy between the two ambients is due to differences in transport properties and simplified theory for prediction of the LOI is developed in terms of the oxygen Lewis number. Additionally, the radiometer data show fluctuations for methanol droplets with initial diameters greater than 3mm; these fluctuations correlate with flame shape oscillations.

clvang@ucdavis.edu

W3P012 INVESTIGATION OF THE LAMINAR BURNING VELOCITY OF ETHANOL AND HEXANE/AIR AEROSOLS.
Laurence Bernard¹, Dan Pugh², Daniel De La Rosa²
¹University of Bergen, Norway ²University of Cardiff, United Kingdom

Combustion of droplets is of significant research interest for a wide range of applications such as furnaces, gas turbines or engines. In addition, aerosol explosions represent a hazard in the process industry, with actual methods for preventing the effects of such accidents still qualitative, and rely on correlations used for gas explosions. It is of prime importance to investigate the mechanisms underlying aerosol explosions to evaluate this hazard and develop models to quantify and predict the consequences.

To this end, the presented poster work details an experimental apparatus consisting of a cloud chamber/

combustor, tested and benchmarked with prevaporized ethanol and *n*-hexane/air mixtures and, used for the generation of ethanol and *n*-hexane mists. The measurement of spherically expanding ethanol and *n*-hexane/air flames, quantified by a Schlieren optical technique is detailed. The work outlines the benchmarking study of the laminar burning velocity and Markstein length of vaporized fuels and the first results in the investigation of laminar burning velocity in mists.

laurence.bernard@gexcon.com

W3P013 A MONOTONIC MIXTURE FRACTION DEFINITION FOR THE FLAMELET FORMULATION OF SPRAY FLAMES

Benedetta Franzelli, Aymeric Vié, Matthias Ihme, Stanford University, United States

Compared to gaseous combustion, spray flames represent a considerably more complex combustion system, which requires the consideration of competing processes between evaporation, mixing and chemical reaction. Because of this complexity, the analysis of spray flames in canonical combustion configurations, such as counterflow flames, represents a viable approach to obtain physical insight into the behavior of these flames.

Laminar gaseous diffusion flames are typically examined in composition space by introducing the mixture fraction Z_g as an independent variable. This quantity is defined with respect to the composition of the gas phase and provides a unique relation to the distance along the flame-normal direction. Such a description allows to obtain a state-space representation of the flame structure that is independent of spatial coordinates. Many turbulent combustion models rely on such a representation, by assuming that a turbulent flame is composed of a collection of laminar flames, called flamelets. Extending this mixture fraction concept to spray flames is desirable to enable the modeling of turbulent spray flames. Unfortunately, the classical mixture fraction definition is not anymore monotonic due to evaporation so that the structure of spray flames cannot be solved in the classical mixture fraction formulation, except for pre-evaporated spray flames. Because of this, spray flames are commonly represented in physical space and then transformed into mixture fraction space, for example by separating the purely gaseous region of the flame from the evaporation zone. Although feasible, this approach introduces undesirable model complexities, thereby preventing the use of analysis tools that have been developed for mixture fraction formulations. Furthermore, this approach does not allow for a theoretically consistent extension of turbulent flamelet combustion models to spray flames.

By addressing these issues, this poster presents recent work on the theoretical development of a spray flamelet formulation that extends the classical flamelet concept for gaseous diffusion systems. The key idea of this approach consists in identifying a unique and monotonic representation of a mixing-describing coordinate for spray flames. This new mixture fraction coordinate, referred to as effective mixture fraction, is then used to extend Peters' flamelet theory, utilizing the same assumptions that were introduced for gaseous flames. In the absence of a liquid spray phase, this new formulation reduces to the classical mixture fraction definition for gaseous systems, thereby ensuring consistency. The validity of this approach is demonstrated in an application to an axisymmetric mono-disperse counterflow spray flame.

This new formulation represents a theoretical tool for the asymptotic analysis of spray flames in composition space. Moreover, it can be considered as the theoretical basis for one-dimensional spray flamelet formulations.

benedetta.franzelli@ecp.fr

W3P014 COMPUTATIONAL MODELING OF UNSUPPORTED AND FIBER-SUPPORTED *N*-HEPTANE DROPLETS IN REDUCED GRAVITY

Narugopal Ghata, Benjamin D. Shaw, University of California, United States

A detailed numerical investigation of unsupported and fiber supported *n*-heptane droplet combustion in reduced gravity is done in the current study. A compact *n*-heptane mechanism consisting of 20 species and 21 reactions is incorporated to model both high temperature and low temperature reactions. The Volume-Of-Fluid (VOF) method is employed to capture the liquid-gas interface for transient two-phase multidimensional flows. The calculations also include variable thermo-physical properties of the liquid and gas phases.

The reaction mechanism is validated for the ignition delay time. The ignition delay times computed in this study agree the experimental results of Tanabe. Computed burning rates and flame stand-off ratios for both unsupported and fiber-supported droplets have been validated with data from drop tower experiments. The present computational results agree well with the experimental results.

The present study has explored influences of heptane pyrolysis on soot shell locations for the first time with a Computational Fluid Dynamics (CFD) analysis that includes a detailed gas-phase reaction mechanism with high and low temperature chemistry. The results show that soot shells should exist at radial locations where heptane pyrolysis first becomes significant, leading to local variations in the temperature gradient, which determines thermophoretic particle velocities. Calculated soot shell radii compare well with available experimental data.

nghata@ucdavis.edu

W3P015 AUTOIGNITION OF UNSTEADY LIQUID FUEL SPRAY IN CONSTANT VOLUME COMBUSTION CHAMBER

Nimal Naser, Seung Yeon Yang, Suk-Ho Chung, University of King Abdullah Science & Technology, Saudi Arabia

Autoignition behavior of unsteady spray at relatively low temperature conditions was investigated for the primary reference fuels of *n*-heptane and *iso*-octane and diesel fuels. The KAUST-research ignition quality tester (KR-IQT, AET

Ltd.) was used to measure Ignition Delay (ID) and Derived Cetane Number (DCN). A unique feature was that the chamber pressure and temperature could be controlled. A pneumatically-driven mechanical pump delivered liquid fuel to a single-hole S-type pintle nozzle, through which the fuel was injected into the pressurized chamber. The injection pressure was fixed at 18 MPa for all test conditions. KR-IQT has additional capability of temperature swing that enables ignition delay time measurement in a continuous temperature range. This was made possible by heating the combustion chamber to a desired temperature and then switching off the electrical heaters. This resulted in gradual temperature drop in the combustion chamber and the continuous injection of fuel into the combustion chamber provided ignition delay as a function of temperature.

The conventional method specified in the IQT software determined the Start of Ignition (SoIgn) at the point where the difference in the chamber pressure and the initial chamber pressure exceeded a certain preset value, typically 138 kPa, comparisons were also made with Bogin et al. that uses 256 kPa for SoIgn determination, twice the value used by IQT to account for the intermediate heat release of fuels. These definitions, however, could result in an erroneous result for the fuels exhibiting intermediate heat release characteristics, such as *iso*-octane, having two-stage ignition behavior, especially under relatively low temperature conditions. The conventional definition of ID in IQT experiments exhibits that ID decreases as the temperature decreases at a certain temperature range, exhibiting the behavior of the Negative Temperature Coefficient (NTC). A close investigation of the pressure traces show that the pressure rise by the first stage ignition exceeds the preset values of the pressure difference.

A new method in determining SoIgn is introduced and applied in the present study. To isolate the effect of the intermediate heat release, the start of ignition is defined by the point of intersection of two slopes, the first being the maximum slope during which the chamber pressure increases steeply and the other being the slope of the chamber pressure curve at the pressure recovery point, which is defined as the point where the chamber pressure recovers the initial pressure after drop in pressure due to evaporative cooling as liquid fuel is injected. The result clearly demonstrates that the seemingly NTC behavior was due to inaccurate definition of SoIgn for the *iso*-octane fuel having intermediate heat release behavior.

nimal.naser@kaust.edu.sa

W3P016 EFFECTS OF AMBIENT PRESSURE ON ATOMIZATION BEHAVIOR OF AIRBLAST ATOMIZER

Kodai Kato¹, Soichiro Suzuki¹, Taku Kudo¹, Soichiro Kato², Mitsunori Itoh², Masahiro Uchida², Akihiro Hayakawa¹, Hideaki Kobayashi¹

¹Tohoku University, Japan ²IHI Corporation, Japan

Airblast atomizer has several advantages, rapid mixing of fuel and air, high degree of homogeneity and fine spray in wide operating range as fuel injector of gas turbine combustor. However, that atomization mechanism and the effects of ambient pressure are not fully clarified. For developing a high performance airblast atomizer, it is important to reveal the effects of ambient pressure on these. In this study, the effects of ambient pressure on atomization process and characteristics of typical type airblast atomizer were experimentally investigated from droplet diameters, spray structure and behavior of atomization. In addition, a two-dimensional atomizer was used to observe detailed atomization process of airblast atomizer, whose structure is simulating an airblast atomizer. Further, the effects of liquid properties on atomization characteristics were also investigated using water and kerosene model solution as a liquid for spray.

The high-speed back light imaging was used to observe atomization processes of a typical type airblast atomizer at several pressures between 0.1 MPa and 0.7 MPa. Phase Doppler Particle Analyzer (PDPA) and Particle Imaging Velocimetry (PIV) were performed to measure droplet diameters and spray structure. In the present experiment, air flow velocity and mass Air Liquid Ratio (ALR) set constant. Kerosene model solution is a mixture of liquid and polyvinyl alcohol.

A spray structure was generated in a cone shape which consisted of several regions characterized by air flow. At atmospheric pressure, large recirculation zone was observed inside of the cone (IC) and large high shear zone (high velocity zone) was along the cone. At high pressure of 0.5 MPa, small eddies were inside of the cone and high shear zone became small. These could be explained kinetic viscosity of surrounding air change with increasing pressure.

From PDPA data, pressure dependences of droplet diameters were different in each region. In addition, these tendencies were changed by properties of a liquid for spray. These result indicated that pressure dependence of droplet diameters were strongly affected air flow structure and liquid properties. Therefore, it is required to understand detailed change of air flow structure with increasing pressure and the effects of liquid properties on atomization.

kodai.kato@flame.ifs.tohoku.ac.jp

W3P017 SPRAY IGNITION IN SUPERCRITICAL ENVIRONMENTS

Lukasz Kapusta¹, Ireneusz Pielecha², Jakub Czajka², Krzysztof Wislocki², Andrzej Teodorczyk¹

¹Warsaw University of Technology, Poland ²Poznan University of Technology, Poland

In this study, process of spray ignition of a liquid fuel which is of crucial importance in terms of energy conversion efficiency in internal combustion engines was under investigation. The main aim of this research was to elucidate if the ignition properties of a fuel injected into environments of parameters exceeding its critical values differ from those obtained for subcritical region. However, in this research the focus was on backpressure, specifically on its influence on auto-ignition process in terms of exceeding the critical pressure of the injectant. Therefore the fuel was

injected into environments of pressure below, around and exceeding its critical value while the temperature was kept far above the critical temperature of the injected liquid.

The research was conducted in a rapid compression machine equipped with piston with transparent crown. *N*-hexane was chosen as the injectant due to its relatively low critical point parameters and the fact that it remains in liquid form under ambient conditions. *N*-hexane was injected into environments composed of air. *N*-hexane was introduced into the RCM by gasoline outward opening pintle injector under pressure of 20 MPa. The injector was mounted centrally on the top of the head.

The ignition data was analyzed in terms of ignition delay. The process of ignition was observed in two ways: by the pressure measurement in the combustion chamber and by visual observation of the combustion chamber by means of high speed camera through transparent window in the piston crown. However, the quantitative analysis was based on monitoring the pressure rise. For monitoring the pressure evolution in the chamber, the AVL IndiCom 621 equipped with piezoelectric sensor was used. The pressure recording frequency was of 5 kHz. The ignition delay was determined by pressure rise according to tangential method. The ignition delay determined that way included both physical delay and chemical delay.

Number of studies already showed that ignition delay is influenced by backpressure due to higher energy entrainment into the fuel jet. However, there arises a question whether there is a change in the energy exchange between the liquid jet and the surrounding air when the conditions become supercritical. This question seems to be important, especially taking into account that physical delay is influenced by atomization, evaporation and fuel vapor-air mixing which are different in supercritical environments than in subcritical ones. The ignition delay in supercritical environments is expected to decrease more than in subcritical ones due to the lack of latent heat and, as a result, lack of evaporation.

Lukasz.Kapusta@itc.pw.edu.pl

W3P018

LES OF A PARTIALLY PREMIXED SPRAY FLAME USING AN ADAPTATIVE-DYNAMIC ATF MODEL COUPLED TO FGM

Fernando Luiz Sacomano Filho, Mouldi Chrigui, Amsini Sadiki, Johannes Janicka, Technische Universität Darmstadt, Germany

Turbulent spray flames are strongly affected by the unsteady stratification of the reactive mixture, which is originated by the turbulent dispersion of evaporating droplets. This mixture stratification allows the simultaneous appearance of different combustion regimes into the flow, delivering highly complex flame structures. The correct reproduction of these phenomena is indispensable to predict the behaviour of turbulent spray flames through numerical simulations.

To investigate the behaviour of the propagation of partially pre-vaporized spray flames, this work presents an Eulerian-Lagrangian spray module relying on the Artificially Thickened Flame (ATF) framework coupled to the Flamelet Generated Manifold (FGM) chemistry reduction method. The unsteadiness arisen from turbulent dispersion of evaporating droplets are captured by the Large Eddy Simulation (LES) method and an evaporation model based on the non equilibrium approach. In order to avoid the presence of different combustion regimes in the reaction domain, the lean partially pre-vaporized spray flame configuration measured experimentally by Pichard et al., which behaves more like a premixed flame, is used to validate the proposed module.

The modified turbulence-flame interaction created by the ATF is recovered through the usage of the efficiency function proposed by Charlette et al.. Modifications due to the presence of the spray are carried out on the computation of this efficiency function. The dynamic thickening approach is used to defined where the transported scalar quantities shall be thickened, whereas the grid adaptive method is employed to define the thickening factor. Considering that, to predict the flame propagation, the correct computation of the flame speed shall be done; a detailed *n*-heptane mechanism including 88 species and 387 elementary reactions is adopted.

The validation of the spray quantities is performed through comparisons with experimental data through radial profiles of: droplets mean velocities and their fluctuations, liquid volumetric fluxes and droplets characteristic diameters. Accordingly, the flame structure is validated through comparisons of mean contour profiles of a reaction progress variable defined experimentally. Qualitative analyzes include the investigation of turbulent flame propagation for two flames with two different global equivalence ratios (0.72 and 0.79), respectively. The effects of the presence of the spray on the efficiency function are also analysed.

The validation process was successfully done. The reaction progress variable contours are reproduced in good agreement with experimental measurement. The spray characteristics e.g. droplet diameters and volume flux show minimal discrepancies compared with measured data. The spray presence on the efficiency function shown to make small influence on the computation of the flame structure. The qualitative analysis show that, as experimentally observed, the increase of the global equivalence ratio reduces the flame length, for lean flames.

Even though some effects were neglected, it is suitable for future investigations to include the SGS dispersion modelling and the evaporative cooling in the chemistry computations.

fernando.sacomano@gmail.com

W3P019

A COMPUTATIONAL MODELING OF DROPLET EVAPORATION INDUCED BY A LOCALIZED HEAT SOURCE

Droplet evaporation by a localized heat source was numerically investigated as an attempt to understand the mechanism of the fuel vapor jet ejection, which was observed experimentally during the flame spread through a droplet array under microgravity conditions. The phenomenon was believed to be mainly responsible for the enhanced flame spread rate at microgravity conditions. An Eulerian-Lagrangian method was implemented in order to effectively capture the interfacial dynamics between liquid droplet and surrounding air. The numerical algorithm utilizes the stationary Eulerian grids to describe the flow field, and moving Lagrangian surface meshes to treat the phase boundaries. Temperature-dependent surface tension and a new local phase change model were employed for modeling thermo-capillary effect and non-uniform droplet evaporation by a local heating. It was found that the temperature difference by a localized heating creates a surface tension gradient along the droplet surface, inducing surface movement. Subsequently, the outer shear flow and internal flow circulation inside the droplet, commonly referred to as the Marangoni convection, are created. The outer shear flow around the droplet transports the fuel vapor to the cold wake region of the droplet, resulting in a fuel vapor ejection. A parametric study demonstrated that, at realistic droplet combustion conditions, the Marangoni effect indeed produces a sufficiently large level of convective flow and following fuel vapor jet, which can enhance flame spread rate by transporting fuel vapor and heat to cold regions. The present study confirmed that the Marangoni effect by a local temperature gradient is the key mechanism to understand the fuel vapor jet ejection observed experimentally.

Jaeheon.Sim@kaust.edu.sa

W3P020 TEMPERATURE IMAGING OF TURBULENT DILUTE ACETONE SPRAY FLAMES USING TWO-LINE ATOMIC FLUORESCENCE

Paul Medwell¹, Assaad Masri², Phuong Xuan Pham², Bassam Dally¹, Graham (Gus) Nathan¹

¹University of Adelaide, Australia ²University of Sydney, Australia

Diagnostic capabilities in spray flows are gradually evolving but remain limited due to inherent difficulties imposed by the presence of droplets and/or liquid filaments. Dense sprays are extremely hard to probe and techniques such as ballistic imaging and X-ray radiography are just starting to make advances in measuring the structure of the sprays and the mass depletion from the liquid core. Dilute spray flames are relatively easier but still challenging, particularly with respect to measuring details of the mixing and reactive fields. Laser-Induced Fluorescence (LIF) techniques have previously been applied to image selected species such as OH, CH₂O, or fuel vapour. These measurements, while qualitative, reveal interesting information about the structure and evolution of reaction zones. However, measurements of critical parameters such as mixture fraction and temperature remain elusive. This study addresses one of these problems by introducing an approach to measure temperature in turbulent dilute spray flames.

Measurement of temperature in flows laden with solid particles or droplets is very difficult. Standard techniques, such as Rayleigh scattering, are no longer applicable due to corruption by Mie scattering. Coherent Anti-Stokes Raman Spectroscopy (CARS) has established capabilities for accurate measurements of temperature in flames containing soot and more recently in spray flames. Notwithstanding recent developments in CARS, which are yet to be fully exploited, a key limitation of this technique, however, lies in its ability to provide single-point measurements rather than large-scale planar information. Thermometry based on multi-line fluorescence from molecular species such as NO offer capability for two-dimensional imaging, but these methods remain limited to time-averaged measurements. Two-Line Atomic Fluorescence (TLAF) techniques can fill this gap, as demonstrated recently through imaging of instantaneous planar temperature fields in turbulent flames containing soot. The extension of TLAF to the non-linear excitation regime, so called NTLAF, has enabled instantaneous temperature imaging in turbulent non-premixed gaseous flames and flames containing soot. The objective of this study is to extend such capabilities to turbulent dilute spray flames.

With spray flames, there is an opportunity to seed the liquid fuel with indium chloride and thus avoid the need for introducing an additional stream as required for turbulent gaseous flames. Although the NTLAF technique is generally immune from interferences due to soot scattering, it is unclear whether interference from the fuel droplets in spray flames will allow the seeding advantages to be realised. Hence, research is required to determine whether the signal-to-noise ratio is sufficiently high for reliable single-shot data and whether good quality measurement is possible in the region immediately around an evaporating droplet. The aim of the current study is, therefore, to assess, for the first time, the feasibility of conducting instantaneous single-shot temperature imaging in turbulent spray flames using the NTLAF technique.

The liquid-fuel spray flames have been demonstrated to be highly effective for seeding indium required for NTLAF measurements. The detected fluorescence signal is found to be immune to scattering/interference from the spray droplets and vapour. The dilute spray burner is ideally suited to NTLAF thermometry with potential for additional simultaneous measurements via other laser diagnostic techniques. Reliable NTLAF temperature measurements are reported in the reaction zone and these are in excellent agreement with thermocouple measurements.

paul.medwell@adelaide.edu.au

W3P021 QUANTIFIED MEASUREMENT OF DROPLET EVAPORATION RATES OF A TWO COMPONENT MIXTURE

Chris Hagen, Nicholas Olson, Oregon State University, United States

In this work we are using an FTIR to measure the evaporation rate of a suspended binary mixture droplet. The intent here is to devise a method that may be useful to calibrate fuel evaporation models. It is hoped that this information will be used to learn more about distillate fuels injected into small internal combustion engines.

The procedure involves taking a background spectrum using the FTIR (considered the incident light, I_0). Next, a droplet is suspended in the instrument beam path and another spectrum is captured (considered as transmitted light, I). The Beer-Lambert law will be applied to determine the path averaged concentration of the evaporated components. Of course beam steering and droplet absorption will be considered. This measurement will be repeated at the scan rate of the instrument to provide a time resolved record of droplet shrinkage.

The components of the droplet will be selected such that their volatilities and absorption spectra are sufficiently different in order to definitely separate the components temporally and optically.

chris.hagen@oregonstate.edu

W3P022 EXTINCTION OF COOL-FLAMES SUPPORTED BY *N*-ALKANE DROPLETS IN MICROGRAVITY

Vedha Nayagam¹, Daniel Dietrich¹, Michael C. Hicks¹, Forman Williams²

¹NASA Glenn Research Center, United States ²University of California, United States

Ongoing droplet-combustion experiments in the International Space Station have shown for the first time that large *n*-alkane droplets can continue to burn quasi-steadily and subsequently extinguish abruptly, controlled by low-temperature Negative-Temperature-Coefficient (NTC) chemistry, without a visible flame. In this study we report recent experimental observations of *n*-decane, *n*-octane, and *n*-heptane droplets of varying initial droplet sizes burning in microgravity under a range of ambient oxygen and diluent (helium or carbon dioxide) concentrations at 0.5, 1.0 and 2.0 atmospheric pressures. The oxygen concentration in these tests varied in the range of 14% to 30% by volume. It is shown that all three normal alkanes exhibit a quasi-steady “cool-flame” burning mode, followed by cool-flame extinction at a finite droplet diameter. Results for droplet burning rates in both the hot-flame and cool-flame regimes as well as droplet extinction diameters at the end of each stage are presented. An aerosol cloud was found to form in most cases slightly prior to or following the cool-flame extinction, likely by the condensation of unburned fuel vapor that leaks through the cool flame. Time histories of radiant emission from the burning droplet, captured using broadband and narrowband radiometers, help identify the precise time at which cool-flame extinction occurs. It is shown that the measured residence time at cool-flame extinction (extinction diameter squared divided by the burning-rate constant) for all three normal alkanes follow a similar trend, and can be correlated against the oxygen molar concentration, which is inversely proportional to the chemical time in the NTC region. The correlation is based on the idea that the effective unimolecular activation energy for high-temperature alkyl radical removal is about $\frac{3}{4}$ the unimolecular activation energy for kretohydroperoxide decomposition.

v.nayagam@grc.nasa.gov

W3P023 TRANSPORTED PDF MODELING OF AN ETHANOL SPRAY IN HOT-DILUTED COFLOW FLAME

Likun Ma¹, Hugo Correia Rodrigues¹, Bertrand Naud², E.H. van Veen¹, Mark Tummers¹, Dirk Roekaerts¹

¹Delft University of Technology, The Netherlands ²CIEMAT, Spain

MILD Combustion, also known as flameless combustion, is attracting wide scientific interest due to its potential of high efficiency and low NO_x emission. Delft Spray-in-Hot-Coflow (DSHC) burner has been used to create an experimental database for studying of the fundamental aspects of flameless oxidation of light oils. The hot diluted coflow of the DSHC flame, which is aimed at mimicking the recirculated combustion products in large scale flameless combustion furnace, is generated by secondary burner matrix. This makes the DSHC flame different in many ways from the conventional spray flame. The in-house hybrid finite volume/ transported PDF code 'PDFD' is used to model the DSHC flame. The continuous phase is described by a joint velocity-scalar PDF, and the dispersed phase is described by a joint PDF of droplet position, velocity, temperature, diameter, and the gaseous properties 'seen' by the droplet. Due to the high-dimensionality, the joint PDFs are solved by a Monte Carlo particle method. In contrast with more standard Eulerian-Lagrangian approach, in PDFD, both the gas phase and the dispersed phase evolution are defined by Lagrangian equations, therefore we refer it as 'Lagrangian-Lagrangian' approach. To overcome the bias error due to the limited number of computational particles in the Monte Carlo method, the mean velocities and Reynolds stresses are calculated using a Finite-Volume (FV) method, in which the Reynolds Averaged Navier Stokes (RANS) equations are solved. A consistent combination of the Generalised Langevin Models (GLM) for Lagrangian particle velocity evolution and Eulerian Reynolds-stress turbulence models is used. The evolution of gas phase composition is described by a Flamelet Generated Manifold (FGM) and IEM micro-mixing model. The detailed ethanol high-temperature oxidation mechanism by Marinov containing 57 species and 383 reactions is used for the generation of an FGM lookup table with 'Chem1D' code, which is developed in Eindhoven University of Technology. The droplet heating and evaporation processes are described by 'parabolic temperature profile model' with modified Nusselt and Sherwood numbers taking into account the effect of Stefan flow.

This modeling approach was validated by comparison with experimental measurements. Spray behavior is successfully reproduced, the predicted droplet mean axial and radial velocity profiles for all droplet size classes are in very good agreement with the experimental data at various axial locations. Droplet Sauter Mean Diameter and droplet number density have been accurately predicted comparing to the experiment results. Gas phase velocity and temperature

also match well with experimental data. Though the temperature in the spray region has been slightly over-predicted due to the fact that the absence of enthalpy information in the current 2D FGM table prohibits the consideration of the heat loss by droplet evaporation. Important characteristics of the DSHC flame such as flame lift-off and dual flame front have been successfully captured by the current simulation. Further improvement will be focused on the coupling between dense and dilute spray region as well as better models for local flame structure, such as the spray flamelet.

malikun-2005@hotmail.com

W3P024 **STOCHASTIC EVAPORATION MODELLING FOR PRESUMED-PDF SPRAY COMBUSTION SIMULATIONS**

Edward Richardson, Tomas Matheson, University of Southampton, United Kingdom

The evaporation of liquid fuel sprays determines the distribution of fuel vapour and the mode of combustion in aeronautical gas turbines and direct injection internal combustion engines. Accurate evaporation rate modelling is therefore necessary for useful predictions of combustor performance, including flame stability and pollutant production.

The evaporation rates of individual droplets depend on the temperature, composition and relative velocity that the droplets 'see' in the surrounding fluid. Due to the presence of thin flame fronts in turbulent combustion, the 'seen' temperature, and hence evaporation rate, can vary significantly between similar droplets. However spray combustion models usually compute droplet evaporation rates using an estimate for the local mean gas phase properties. This study develops evaporation modelling which overcomes this limitation.

A new stochastic evaporation model is presented in the context of presumed-pdf modelling. The method samples the composition seen by a given droplet from the presumed joint-pdf of composition at the droplet location. In order to account for possible correlations between progress variable and mixture fraction, the joint-pdf is constructed using a copula from two beta-distributed marginal pdfs for mixture fraction and for normalised progress variable. We use a flamelet generated manifold to relate mixture fraction and progress variable to composition and temperature. The impact of considering the (co-)variances of mixture fraction and progress variable on the evaporation rate, and on global flame structure are analysed in Reynolds-averaged simulations of a laboratory spray flame.

e.s.richardson@soton.ac.uk

W3P025 **FLAME SPREAD OF A LINEAR *N*-DECANE DROPLET ARRAY WITH PARTIAL PREVAPORIZATION IN MICROGRAVITY**

Masao Kikuchi, Japan Aerospace Exploration Agency, Japan

In this study, flame spread characteristics of a linear *n*-decane droplet array with partial prevaporization is investigated in microgravity for obtaining fundamental insight on flame propagation mechanism among partially prevaporized fuel spray. In the experiments, multiple *n*-decane droplets are generated and sustained at intersections of fine X-shaped SiC fibers (14 micrometer in diameter) simultaneously, by supplying fuel from the tips of fine glass needles. Then, the array is inserted into the combustion chamber which was preheated at a desired high-temperature. In the combustion chamber, activation delay time of the igniter wire at an edge droplet was employed to control the degree of partial prevaporization of the array prior to flame spread. After ignition of the edge droplet, subsequent flame spread behaviors along the array are observed by various cameras. The merit of microgravity environment for the current study is symmetric formation of fuel vapor as well as flame around the axis of the array, even for relatively large diameter droplets. It enables detail observation of the phenomena as well as comparison with numerical simulation. The experimental parameters include initial droplet diameter, droplet interval, ambient temperature, and prevaporization time. In our past research, it was found that flame structure changes with increase of the degree of prevaporization of the array. Occurrence of triple flame structure at the propagating flame front was also recognized. In addition, the relation between the flame travelling speed (flame spread rate) and the degree of prevaporization was obtained.

kikuchi.masao@jaxa.jp

W3P026 **MODULATION OF TURBULENT PROPERTIES IN A SPRAY FLAME BURNING *N*-HEPTANE**

Abouelmagd Abdelsamie, Dominique Thévenin, University of Magdeburg, Germany

The final objective of the current work is to investigate turbulent spray flames at high droplet density, quantifying possible modifications of the turbulent properties. As a first step, the modification of turbulence statistics (kinetic energy, dissipation rate spectrum, the auto-ignition process and the resulting flame structure are investigated in decaying turbulence by Direct Numerical Simulation (DNS) considering *n*-heptane liquid droplets. The droplets, being smaller than the grid resolution, are modeled as point droplets, while the Navier-Stokes equations are solved in the low-Mach number regime. Detailed models are employed to describe chemical reaction and molecular transport in the gas phase. Existing publications on the subject can be roughly categorized into four groups. First, those investigating in 3D the two-way coupling of a non-reactive turbulent flow with droplets. The second group examined reacting cases but using a single-step reaction mechanism. A third approach takes into account detailed chemistry but only 2D turbulent flows, while, in the last case, both 3D flows and detailed chemistry are considered, like in. However, even with this highest level of detail, the resulting turbulence statistics have never been examined in detail yet. In the current DNS, the continuous (gas) phase is simulated in a standard manner (Eulerian frame) whereas the discontinuous (droplet) phase is tracked in a Lagrangian frame. Two-way coupling interaction between both phases is quantified via the

exchange of mass, momentum and energy. The impact of different parameters is investigated, in particular: initial temperatures, equivalence ratio/droplet mass fraction, droplet size, turbulence level (with a Taylor Reynolds number up to 80). For the figures shown in the uploaded file, *n*-heptane droplets at 300 K are initially randomly distributed in isotropic turbulence. A fully periodic domain containing hot air at 1000 K is simulated. The Stokes drag force is dominant in the droplet momentum equation, whereas the evaporation process is computed by using a variable Spalding mass transfer number and an infinite conduction model inside the droplet. The in-house 3D DNS solver DINOSOARS is used for all simulations. An implicit time integration scheme is used for the chemistry source term. All kinetic and transport properties are handled in DINOSOARS using Cantera 1.8 and Eglib 3.4. A skeletal mechanism accounting for 29 species and 52 reactions is used for *n*-heptane combustion. Very complex flame structures are obtained, highlighting the need for powerful analysis tools. The resulting turbulence statistics and the analysis of the data will be shown on the poster.

abouelmagd.abdelsamie@ovgu.de

W3P027 EFFECTS OF HYDROGEN OR METHANE ADDITION ON THE COUNTERFLOW SPRAY DIFFUSION FLAME: SPRAY-FLAMELET MODEL FOR BIPHASIC AND MULTI-COMPONENT FUEL

Fernando Fachini¹, Daniela Maionchi²

¹Instituto Nacional de Pesquisas Espaciais, Brazil ²Universidade Federal de Mato Grosso, Brazil

This work presents an extended analysis of the external structure of multi-phase and multi-component fuel counterflow diffusion flame (multi-component spray-flamelet). The model assumes part of the main fuel, ethanol (C_2H_6O) or *n*-heptane (C_7H_{16}), in liquid phase (droplets) and part in gas phase with addition of methane (CH_4) or hydrogen (H_2). The droplets vaporize completely before the stagnation point and there is no relative velocity between the droplets and the gas phase. The multi-component fuel spray-flamelet is described by means of the Schvab-Zel'dovich-Linan formulation. The model exhibits a more general spray combustion parameter that combines the chemical reaction, flow field and spray properties. The aim of the analysis is to identify how the external structure of the spray-flamelet is affected by addition of a small amount of methane or hydrogen in a spray of ethanol or *n*-heptane. The droplets are described by a uniform mono-sized distribution. For fixed spray combustion parameter and dimensionless incoming condition, the results point out that by substituting part of the main fuel by methane or hydrogen does not affect significantly the position and temperature of the flame. The small differences are due to the Lewis number. Consequently, the re-scaled species mass fraction of the main fuel and dimensionless temperature show a quasi-universal behavior for the external structure of the spray-flamelet. The description of temperature and fuel mass fraction in terms of the mixture fraction is non linear. To avoid that it is included the gradient of mixture fraction.

fachiniff@gmail.com

W3P028 A NOVEL APPROACH TO ASSESS DIESEL SPRAY MODELS USING LIQUID-PHASE EXTINCTION AND X-RAY RADIOGRAPHY MEASUREMENTS

Gina Magnotti, Caroline Genzale, Georgia Institute of Technology, United States

Spray model predictions are a critical component of engine CFD simulations since the spray physics will dictate boundary conditions for fuel-air mixing and subsequent combustion processes. However, given the current capability of spray diagnostics, it is not possible to validate the fundamental mechanisms governing spray breakup under diesel relevant conditions. As a result, there are many different physically-based spray breakup models that have been employed in the literature. Most models are indirectly validated against global spray parameter measurements, such as liquid penetration and vapor penetration. Though some have been validated against quantitative local droplet size measurements, these measurements are limited to the periphery of the spray and have been largely conducted under a limited range ambient density conditions. Due to the lack of high-fidelity quantitative measurements of desired spray parameters, robust validation of spray morphology predictions has not been possible. Questions therefore remain about the ability of current spray models to faithfully represent and predict the correct spray structure over a range of ambient and injection conditions.

Recent advances in spray diagnostics have resulted in a large improvement in quantitative experimental characterization of spray parameters; examples include x-ray radiography measurements, which is an absorption-based technique that quantifies projected mass density throughout the spray, and liquid-phase extinction measurements, which can quantify the optical thickness. Both measurements are coupled functions of droplet size and number density. Although each of these measurements has a coupled dependence on these parameters, simultaneously validating model predictions against these measurements in overlapping regions of the spray shows promise of decoupling their dependencies and providing a more detailed validation of the spray morphology.

In the current work, we explore the use of light propagation and x-ray radiography models in CFD spray simulations to assess spray morphology predictions. Using CONVERGE, we compare predictions of optical thickness and projected mass density against available quantitative liquid-phase extinction and x-ray radiography measurements, respectively, among three different physically-based spray breakup models: Kelvin-Helmholtz (KH), Kelvin-Helmholtz Rayleigh-Taylor (KH-RT), and Kelvin-Helmholtz-Aerodynamics Cavitation Turbulence (KH-ACT). The model predictions of droplet size and number density distributions throughout the spray are compared and spray breakup

statistics and their relative impact on the spray structure is evaluated. Recommendations are then provided for future modeling and experimental endeavors to help guide best modeling practices under diesel-relevant conditions.

gina.magnotti@gatech.edu

W3P029 **INTERMITTENT PRODUCTION OF OH ON A SWIRL-STABILIZED PULSED SPRAY FLAME**

Newton Fukumasu, Guenther Krieger, Polytechnic School of the University of Sao Paulo, Brazil

Combustion of fuel droplets in engines and gas-turbines are applied to generate power and, in those systems, instabilities may arise from the interaction between the evaporation, mixing and combustion of the droplets and the surrounding air. In this work, laser diagnostic techniques are applied to analyze combustion instabilities near the burner for an open pulsed ethanol spray flame. Fuel droplet diameter and velocity distributions are acquired by Phase Doppler Interferometry (PDI) across the flame. The interaction between the OH profile, the swirling flow and the spatial evolution of fuel droplets is analyzed by both time resolved Mie scattering and high repetition rate planar Laser Induced Fluorescence of OH. Velocity fields at planes parallel to the exit of the burner are obtained by time resolved Particle Image Velocimetry for the cold flow. The burner, constituted by a swirler mixer and an automotive port fuel injector, was positioned in an open space with quiescent air. The fuel injection frequency was defined as 400Hz, which produces a dilute spray susceptible to the recirculating air. The resulting flame presented a small chemiluminescent region lifted from the burner. The spatial evolution of the OH profile and the velocity field suggest that the lifted behavior is produced by a complex periodic mixing behavior between evaporating droplets and turbulent structures from the swirling flow, which produces regions with intermittent combustion near the burner.

fukumasu@gmail.com

W3P030 **EVAPORATION MODEL OF HYPERGOLIC FUEL DROPLETS**

Yu Daimon¹, Hideyo Negishi¹, Hiroumi Tani¹, Yoshiki Matsuura², Hiroshi Terashima³, Mitsuo Koshi³

¹Japan Aerospace Exploration Agency, Japan ²IHI Aerospace, Japan ³University of Tokyo, Japan

Bipropellant rocket engines have been used in spacecraft propulsion systems for several decades. These engines have shown high reliability and good achievements in past missions. On the other hand, developments of the bipropellant rocket engines rely mainly on trial-and-error approaches supported by extensive experimental tests. Therefore, it takes a long time and high cost for the experimental tests. From the physics point of view, the mechanisms and interactions occurring in the rocket thrust chamber are manifold and fairly complex. During the first process in the sequence of the phenomena, the fuel and the oxidizer are injected from an injector faceplate, and they collide with each other. After that, primary atomization occurs from the edge of a liquid sheet that is generated by the collision of jets. Some liquid particles of fuel and oxidizer break up again due to secondary atomization. Almost simultaneously, the liquid particles evaporate and generate gaseous fuel and oxidizer. Finally, the gaseous fuel and oxidizer react and are transformed into combustion gas. The characteristics time of the evaporation in these processes significantly affects to the combustion efficiency of the bipropellant rocket engines. Therefore, an accuracy of the evaporation model is very important to predict the thrust performance in the numerical simulation of the bipropellant rocket engine.

In order to support design and optimization of the bipropellant rocket engine, the simulation tools, which is predict thrust and heat load based on three-dimensional combustion simulations with a theoretical atomization model for the unlike doublet impinging jet, has been developed in Japan Aerospace Exploration Agency/JAXA's Engineering Digital Innovation Center (JAXA/JEDI). This simulation tools include an atomization, a evaporation, a combustion, and a film cooling models. In this study, the evaporation model is evaluated for the experimental data for single droplets.

At first, the two kinds of evaporation models were evaluated for the experimental data of the heptane single droplet evaporation. The evaporation model, which takes into account the non-equilibrium of mass transfer, could reproduce the evaporation rate of the experimental data very well. For the next step, this evaporation model applied for the simulation of the hydrazine and MMH single droplet evaporation, respectively. The hydrazine and MMH have decomposition reactions. Therefore, the reaction model should be taken into account to reproduce the actual evaporation rate. The effect of reaction was clarified for the evaporation rate using the global and the detailed chemical reaction set. In these simulations, the difference for the evaporation rate between the global and the detailed chemical reactions was small because the amount of fuel is a few against for the ambient gas. In the future work, the simulation of the evaporation of the liquid droplet groups will be performed. As a final goal, the applicable evaporation model will be specified for hypergolic fuel spray combustion.

daimon.yu@jaxa.jp

W3P031 **SIMULATIONS OF *N*-HEPTANE COOL FLAMES IN ZERO GRAVITY**

Fumiaki Takahashi¹, Viswanath R. Katta²

¹Case Western Reserve University, United States ²Innovative Scientific Solutions, Inc., United States

Numerical simulations of gaseous *n*-heptane diffusion flames in zero gravity have been performed to study the two-stage combustion leading to a "cool flame", which has been discovered in the droplet combustion experiment in the International Space Station. The time-dependent, two-dimensional numerical code, which includes a detailed reaction mechanism (127 species and 1130 reactions), diffusive transport, and a gray-gas radiation model, revealed the flame

structure, radiative flame extinction, and subsequent cool-flame formation. *N*-heptane at boiling point (372 K) issued from an axisymmetric fuel source consisted of (1) a single porous cylinder (4 mm dia. \times 2 mm ht.), (2) concentrically superimposed two cylinders (4 mm dia. \times 1.33 mm ht. and 1.33 mm dia. \times 4 mm ht.), or (3) three cylinders (4 mm dia. \times 0.67 mm ht., 2.5 mm dia. \times 2 mm ht., and 1 mm dia. \times 4 mm ht.). The fuel velocity (0.1 to 1 cm/s) and the pre-ignition injection period were varied. The stoichiometric fuel-air mixture was ignited above and below the fuel source on the axis. The ignition kernel grew and propagated around the fuel source to form a growing spherical flame. The maximum temperature decreased due to the radiative heat loss, and the flame extinction occurred at \sim 1200 K several seconds after ignition. As the remaining hot zone cooled down, the cool flame with the maximum temperature of 740-780 K became apparent at a closer proximity to the fuel source. The volume of the fuel discharged before ignition plays an important role in the initial flame growth and radiative extinction, leading to the cool flame as a result of the negative temperature coefficient in the low-temperature chemistry.

fumi3g@gmail.com

W3P032 INVESTIGATION OF GLYCEROL ATOMIZATION IN THE NEAR-FIELD OF A FLOW-BLURRING INJECTOR USING TIME-RESOLVED PIV AND HIGH-SPEED FLOW VISUALIZATION

Ajay K. Agrawal, Lulin Jiang, University of Alabama, United States

Glycerol with its very high viscosity and high vaporization and auto-ignition temperatures has been effectively atomized at room temperature and cleanly combusted by using a novel Flow Blurring (FB) injector without any combustor hardware modification. Present study quantitatively reveals the details of glycerol atomization by the FB injector. Time-resolved Particle Image Velocimetry (PIV) with exposure time of 1 μ s and framing rate of 15 kHz is utilized to probe the near injector region of the spray at spatial resolution of 16.83 μ m per pixel. PIV results describe the flow structure in terms of the instantaneous and mean velocity fields, turbulent kinetic energy, and histograms of axial velocity. In addition, high-speed imaging (75 kHz) coupled with backside lighting is applied to reveal the glycerol breakup process at exposure time of 1 μ s and spatial resolution of 7.16 μ m per pixel. Results show that glycerol atomization can be categorized as bubble-explosion atomization and atomization by Rayleigh-Taylor instabilities. FB atomization of glycerol results in a collection of fast-moving droplets and slow-moving streaks at the injector exit. By interacting with the high-velocity atomizing air, the relatively thin long streaks first disintegrate into shorter streaks, and then, into small droplets. Thus, within a short distance downstream of the injector exit, most of the glycerol is atomized into fine droplets with diameter range of about 8 to 21 μ m, indicating excellent atomization of glycerol by the FB injector.

aagrawal@eng.ua.edu

W3P033 EFFECTS OF DROPLET INTERACTION AND AMBIENT-GAS COMPOSITION ON SPONTANEOUS IGNITION OF FUEL DROPLETS

Osamu Moriue, Kota Yone, Takeru Iwamoto, Hideki Hashimoto, Eiichi Murase, Kyushu University, Japan

Spontaneous ignition of fuel droplets in hot ambient gas was experimentally studied. Fuel was *n*-decane, and initial droplet diameter was 1 mm. First, a suspended droplet pair inserted into hot air was studied in microgravity, and the effect of droplet interaction was examined. Pressure was 0.3 MPa, and air temperature was between 620 K and 700 K. Thus, the ambient conditions were in the range where two-stage ignition, i.e., cool-flame appearance and subsequent hot-flame appearance, occurs. The previous studies with thermocouple measurement showed that the mutual cooling effect of two droplets was dominant before cool-flame appearance, while the effect of duplicated fuel sources was dominant after cool-flame appearance. This is supposed to be related to locations of cool flame and hot flame appearances. In the present study, interferometry was applied to qualitatively observe density field around a droplet pair, and the location of heat release by cool-flame or hot-flame was evaluated. Cool flame appeared on the outer side of the pair, and hot flame appeared on the inner side of the pair. The results indicate that temperature distribution is important before cool-flame appearance, while fuel-concentration distribution is important after cool-flame appearance, which corresponds with the discussion in the previous studies. Next, a suspended isolated droplet inserted into hot ambient gas was studied in normal gravity, and the composition of the gas was varied. Substitution of nitrogen of air by carbon dioxide delayed vaporization and hot-flame appearance in the examined ambient conditions.

moriue@mech.kyushu-u.ac.jp

W3P034 CHARACTERISTICS OF LASER-INDUCED BREAKDOWN IGNITION IN DIFFERENT ETHANOL SPRAY CONCENTRATION

Yuki Ishimura, Takehiko Seo, Masato Mikami, Yamaguchi University, Japan

Laser-induced ignition is a new ignition method that employs non-contact ignition. This method has a great potential to improve the thermal efficiency of conventional internal combustion engines because this ignition method is free from both the heat loss to the electrode and the electrode interference to spray. Moreover, an arbitrary ignition position can be selected in the combustion chamber. Numerous researches on laser-induced ignition and breakdown of gaseous fuels have been conducted. There are very limited investigations on the laser-induced breakdown ignition in fuel spray. For an application to spray guided direct injection engines, it is necessary to investigate the characteristics of

laser-induced breakdown ignition in the fuel spray. In this study, we experimentally investigated the effects of the spray concentration on the breakdown and ignition characteristics. The laser ignition characteristics were quantitatively evaluated by using ignition probability.

A laser-induced plasma was generated by focusing the laser beam of 355 nm with energy adjustment. Slightly rich ethanol spray/air mixture was supplied around the focal position. An ultrasonic nebulizer generated the ethanol spray. The number density of droplets in the ethanol spray was controlled by the flow rate of air as the carrier gas for spray. The plasma generation and the flame propagation in ethanol spray were recorded by using a high-speed camera with a Schlieren optics system.

The results show that there is a difference between the energy required for generation of plasma and ignition. The generated plasma does not always contribute to ignition. The probability of the laser-induced breakdown increases with the laser beam energy and the spray concentration. The probability of ignition also increases with the laser beam energy. However, there is an inverse relationship between the ignition probability and the spray concentration. The plasma generated in the spray loses heat by the large heat capacity of the droplet and latent heat of evaporation of the droplet. When the spray concentration is higher, the probability that droplets exist around the plasma is higher, resulting in greater heat loss to droplets and the lower ignition probability. Therefore, the optimal spray concentration possibly exists.

t002ve@yamaguchi-u.ac.jp

W3P035 AN EXPERIMENTAL STUDY OF COMBUSTION CHARACTERISTICS OF PARTICLE-ADDED DIESEL FUEL
Mohsen Ghamari, Jared Becker, Albert Ratner, University of Iowa, United States

The majority of modern transportation energy is consumed via combustion of liquid hydrocarbon fuels. Manufacturers and consumers are consistently looking for ways to optimize the efficiency of fuel combustion in terms of cost, emissions and consumer safety. Experimental research has shown that the addition of long chained polymers to hydrocarbon fuel imparts non-newtonian characteristics to the emulsified fluid. This results in a suppressed splashing behavior upon spilling over a surface. This has led to a study to not only optimize the emulsion ratio but to characterize the properties of the emulsified fuel (including ignition, extinction and burning rate). This is done to investigate how the modified fuels will impact commercial automotive engines as it relates to their performance and emissions. Experiments are conducted using micro-sized droplets tethered to ceramic fibers. Through a series of synchronous events, droplets are first ignited using electrical hot wire and data is acquired through the use of high speed photography and Schlieren imaging. Time variations regarding droplet diameter and intensity of emitted soot in Schlieren images are used to characterize the sample size. Residual soot aggregates attached to the support fiber are also collected to be analyzed using SEM technique.

jaredmbecker@gmail.com

W3P036 THERMAL DECOMPOSITION OF *N*-PENTANOL AT VARIOUS PRESSURES: FLOW REACTOR PYROLYSIS AND KINETIC MODELING STUDY
Yuyang Li, Gao Wang, Long Zhao, Zhanjun Cheng, Lidong Zhang, Fei Qi, University of Science and Technology of China, China

As prospective biofuels, long chain alcohols like *n*-butanol and *n*-pentanol have a lot of advantages over ethanol, such as higher energy density, better miscibility with practical fuels, lower water absorption, and higher suitability for conventional engines. Compared with *n*-butanol, the combustion research of *n*-pentanol is very insufficient. Most previous combustion experiments on *n*-pentanol were focusing on the measurements of global combustion parameters, such as ignition delay times, laminar flame speeds and engine performances. This work presents the first experimental investigation on the *n*-pentanol pyrolysis at various pressures and reports a detailed pyrolysis model of *n*-pentanol.

Synchrotron vacuum ultraviolet photoionization mass spectrometry was used to detect pyrolysis species and measure their mole fraction profiles. Detailed descriptions of the synchrotron beamlines and pyrolysis apparatus used in this work have been reported elsewhere. The pyrolysis of 3% *n*-pentanol in Ar was investigated from 810 to 1410 K at 30, 150 and 760 Torr. More than 20 pyrolysis species were detected, especially some radicals such as methyl, propargyl and allyl radicals and unstable intermediates like ethenol and 2-propen-1-ol. A detailed pyrolysis model of *n*-pentanol with 162 species and 1141 reactions was developed and validated against the experimental results, and was used to understand the thermal decomposition processes of *n*-pentanol. The model was based on our recently reported models of butanol isomers, and the sub-mechanism of *n*-pentanol was constructed in this work.

The present model can get reasonable prediction on the mole fraction profiles of *n*-pentanol and its major pyrolysis products, as shown in Fig. 1. The ROP analysis and sensitivity analysis (Image) demonstrate the importance of unimolecular decomposition reactions and H-atom abstraction reactions by H and OH attack in the primary decomposition of *n*-pentanol. The unimolecular decomposition reactions have very large sensitivities to the consumption of *n*-pentanol, because these reactions are the most important chain initiation steps under the investigated conditions. Due to the high carbon fluxes from the H-atom abstraction reactions, C₅H₁₀OH radicals play significant roles in the decomposition processes of *n*-pentanol. These C₅H₁₀OH radicals mainly decompose through β -scission reactions, especially β -C-C scission reactions. Specific products of most C₅H₁₀OH radicals were observed, such as ethenol, 2-propen-1-ol, 1-butene and propene, which provide validation to the pathways initiated from the H-atom abstraction of *n*-pentanol. Ethenol also plays a crucial role in the formation of acetaldehyde which is an important oxygenated pollutant

relevant to alcohol combustion.

yuygli@ustc.edu.cn

W3P037 UNCERTAINTY ANALYSIS OF VARIOUS THEORETICAL TREATMENTS ON ETHANOL DECOMPOSITION

Lili Xing¹, Shuang Li¹, Feng Zhang¹, Zhaohui Wang¹, Bin Yang²

¹University of Science and Technology of China, China ²Tsinghua University, China

The random sampling high dimensional model representation (RS-HDMR) approach was used to reveal the important source and the variation of uncertainty for the rate constants of C-C bond dissociation and H₂O elimination of ethanol computed by canonical variational transition state theory. Proper qualitative and quantitative uncertainty evaluation is strongly recommended for theoretically investigation on kinetics of unimolecular decomposition with competing pathways.

7 main parameters (such as the energy parameters, the collisional parameters et al.) were selected for further study according to the test results. The calculations were performed at temperatures (1000-2000 K) and three pressures (0.1 atm, 1 atm, 10 atm) respectively. For each (T, P), we randomly generated 5000 samples and then calculated the corresponding rate constants, where the step number has been checked for convergence. We deduced the uncertainty factors of these two rate constants and the uncertainty source of ethanol decomposition can be divided into three parts: energy parameters, collision parameters and competition relationship.

The uncertainty at high pressure limit is only determined by energy parameters and independent with reaction type. The expression of uncertainty factor was provided quantitatively. The collision parameters are playing an increasingly important role with the decreasing pressure. The rate constant of minor channel shows larger uncertainty than that of major channel at both low and high pressures due to the impact of competing relationship.

The uncertainty propagation of the selected input parameters rate constants provided valid uncertainty information for the sensitivity and uncertainty analysis of chemical model and proper uncertainty evaluation is strongly recommended for theoretically investigation on the temperature and pressure dependent kinetics for complex reaction systems.

feng2011@ustc.edu.cn

W3P038 AN EXPERIMENTAL AND KINETIC MODELING STUDY OF 2-METHYLBUTANOL COMBUSTION

Sungwoo Park, Ossama Mannaa, Rafik Bougacha, Aamir Farooq, Suk-Ho Chung, Mani Sarathy

King Abdullah University of Science and Technology, Saudi Arabia

The need to reduce emissions in practical engines has spurred the interest in alternative fuels, and the use of bio-derived oxygenated fuels have been considered as potential alternative fuels to reduce fossil fuel consumption and minimize NO_x and particulate emissions. However, these oxygenated fuels have different combustion chemistry that needs to be evaluated in practical applications.

Ethanol has been used as fuel extender for petroleum fuels. Due to disadvantages of ethanol such as high O/C ratio, high hygroscopicity and low energy density, the focus of alcohol combustion chemistry research is shifting now to linear and branched C₄ and C₅ alcohols. Over the last few years, extensive combustion studies on butanol isomers have been conducted, but there have been limited studies on C₅ alcohol family including *n*-pentanol, *iso*-pentanol (3-methylbutanol), and 2-methylbutanol.

The purpose of the current study is to provide a detailed chemical kinetic model for 2-methylbutanol including high- and low-temperature reactions with new experimental data, including ignition delay times and flame speeds, for a better understanding the combustion characteristics of higher alcohols. The proposed model is based on previous *iso*-pentanol modeling study and a similar methodology was used to develop a detailed model for 2-methylbutanol.

The present model for the 2-methylbutanol is validated against a wide range of experimental data covering low- and high-temperature oxidation conditions. Ignition delay times were measured for 2-methylbutanol over a temperature range of 800–1300 K, pressures at 20 and 40 atm, and equivalence ratios of 0.5, 1.0 and 2.0 in air using a High Pressure Shock Tube (HPST) at KAUST. The present model is validated against the high-pressure autoignition experimental data by running homogeneous batch reactor simulations. Overall, the proposed model for 2-methylbutanol is in good agreement with the experimental data over the whole temperature region. The present model is also validated against laminar burning velocities. The laminar flame speeds of 2-methylbutanol/air mixtures at 353K and pressures of 1, 2 and 5 atm were measured using the spherically propagating flame in a constant volume chamber at KAUST. The predictions show good agreement with experimental data. In addition, reaction path and temperature A-factor sensitivity analyses were conducted for identifying key reactions in the combustion of 2-methylbutanol.

sungwoo.park@kaust.edu.sa

W3P039 INVESTIGATION OF THE PERFORMANCE OF SEVERAL METHANOL COMBUSTION MECHANISMS

Carsten Olm¹, Robert Palvolgyi¹, Tamás Varga¹, Eva Valko¹, Henry Curran², Tamas Turanyi¹

¹Eötvös University (ELTE), Hungary ²National University of Ireland, Ireland

Methanol is widely used as an important alternative fuel and feedstock in various industrial processes. Even though substantial efforts have been made to understand its combustion characteristics, large differences in reactivity

predictions of various methanol reaction mechanisms can be observed. While in most experimental and computational studies the agreement between measurements and simulations is characterized by figures, in which the experimental data and the simulation results are plotted together, a quantitative and wide-ranging evaluation with respect to methanol combustion has not yet been performed. The measured values coming from different types of experiments may have different orders of magnitude and different units. Thus, a direct comparison of the deviations corresponding to the different types of experiments would be meaningless. In the present work, a sum-of-squares based objective function suggested by Turányi and co-workers was used that accounts for these difficulties. A MATLAB code was developed which allows for automatic simulations using the CHEMKIN-II and OpenSMOKE++ solver packages. The code also evaluates the value of the objective function for each reaction mechanism to facilitate a direct comparison of the performances of the different mechanisms. A large set of experimental data was accumulated for the combustion of methanol including ignition measurements in shock tubes and RCMs, burning velocity measurements, concentration–time profiles in flow reactors and jet-stirred reactors (~1500 data points in total), covering wide regions of temperature, pressure and mixture composition and measured in different bath gases. All data were encoded in PrIME file format, an XML scheme used for the systematic storage of combustion experiments.

This poster presents the comparison of the performance of 11 recently published methanol combustion mechanisms based on these experimental data. It is a part of a systematic evaluation of kinetic mechanisms for a range of combustion systems, such as hydrogen, syngas and ethanol, and can be considered as an important step towards a better understanding of more complex C/H/O combustion systems.

carsten.olm@googlemail.com

W3P040 LAMINAR BURNING VELOCITIES OF C₂H₅OH+O₂ IN DIFFERENT BATH GASES AND AN INVESTIGATION OF THE GENERAL PERFORMANCE OF SEVERAL ETHANOL COMBUSTION MECHANISMS

Carsten Olm¹, Jenny Nauclér², Alexander Konnov², Sandra Harlt¹, Dr.-Ing. Christian Hasse³, Florian Rau³, Tamas Turanyi¹
¹Eötvös University (ELTE), Hungary ²Lund University, Sweden ³TU Bergakademie Freiberg, Germany

Ethanol is widely used as a renewable alternative fuel and as a gasoline additive. The combustion characteristics of this fuel were frequently investigated, both in experimental and computational studies. However, the details of the underlying chemistry are still not fully understood and there is a large scatter among the predictions of kinetic mechanisms that were developed to describe ethanol combustion. Due to the lack of experimental data available from literature at particular conditions of interest, new measurements of laminar burning velocities using the heat flux method were carried out. Mixtures of C₂H₅OH+O₂+Ar at initial temperatures ranging from 298 to 348 K were measured at Lund University for different equivalence ratios and various oxygen ratios in the oxidizer mixture (12 to 20 %). At TU Bergakademie Freiberg, C₂H₅OH+air flames diluted with 5% and 10% H₂O were measured at 298 K and 373 K. The comparison of these data with simulations indicated room for substantial improvement of kinetic schemes for ethanol combustion.

The agreement between measurements and simulations is typically characterized by figures, in which the experimental data and the simulation results are plotted together. However, a quantitative measure has to be applied to make these comparisons objective, such as a sum-of-squares objective function based method suggested by Turányi and co-workers. A MATLAB code was written which allows automatic simulations using the CHEMKIN-II and OpenSMOKE++ solver packages and evaluations of the objective function. A large set of experimental data was compiled for the combustion of ethanol, such as burning velocity measurements (including the above presented and further data from the literature), ignition measurements in shock tubes and RCMs, and concentration–time profiles in flow reactors and jet-stirred reactors (~1600 data points in total). This poster presents the comparison of the performance of 14 published ethanol combustion mechanisms based on these experimental data.

carsten.olm@googlemail.com

W3P041 RATE CONSTANT CALCULATIONS OF THE H-ATOM ABSTRACTION REACTIONS OF OXYGENATED FUELS WITH HO₂ RADICALS

Jorge Mendes, Chong-Wen Zhou, Henry Curran, National University of Ireland, Ireland

Oxygenated fuels generated from biomass have received considerable interest in recent years. Alcohols, esters, ethers and ketones are among some promising biofuel candidates. Over the last few decades, the combustion community has developed significant knowledge on the fundamental reactions and associated rate constants for hydrocarbon fuels; however, much less is known about oxygenated compounds. High-level theoretical calculations of the H-atom abstraction reactions by OH and HO₂ radicals are important in order to predict the reactivity and product formation of these fuels. This work serves to help generate rate constant rules for H-atom abstraction by HO₂ radicals from large oxygenated biofuel molecules, and other biofuel candidates, which may be used as possible future fuel for transport and energy generation. High-level ab initio and chemical kinetic calculations have been performed to determine the influence of the functional group of oxygenated species, such as esters¹, ethers², aldehydes, ketones^{3,4}, alcohols⁵, and acids, on the rate constants for H-atom abstraction by HO₂ radicals, under combustion relevant conditions. We have determined that abstraction from the carbon atoms adjacent to the functional group (α'/α) was slower for ketones and esters and faster for alcohols and ethers, when comparing to alkanes. Overall, we found that the further the abstraction occurs from the functional group, the more similar are our calculated rate constants for oxygenated species when

compared to those calculated for alkanes.

Rate constants for abstraction of a hydrogen atom by an HO_2 radical from either side of the functional group on ketones and esters are very similar. However, for ethers the rate constants for abstraction at the α' and α positions are calculated to be faster than for ketones and esters due to the electron lone pair on the oxygen atom being delocalized to the adjacent C–H anti-bonding orbital (α - $\sigma^*(\text{CH})$). This weakens the adjacent C–H bond which, consequently, lowers the energy required for abstraction.

Abstraction of a hydrogen atom by HO_2 radicals at the α'/α and β'/β positions are the most influenced by the hydrogen bond interactions that occur between the radical and the functional group. At the γ position, abstraction of a H-atom by an HO_2 radical is less influenced by these interactions and only when abstracting a H-atom at the δ position are the rate constants the most similar to alkanes.

j.mendesferreira1@nuigalway.ie

W3P042 THEORETICAL STUDY OF LOW-TEMPERATURE OXIDATION CHEMISTRY OF *ISO*-BUTANOL

Nathan Yee, Shamel Merchant, William Green, Massachusetts Institute of Technology, United State

The efficient use of novel biofuels in internal combustion engines, particularly those relying on compression ignition, critically depends on understanding the fundamental autoignition chemistry. *Iso*-Butanol is a promising candidate as a next-generation biofuel. Numerous companies, such as Gevo, Inc and Butmax, are already setting up industrial-level production plants, making *iso*-butanol a viable fuel to enter the marketplace soon. Whereas its high-temperature ($T > 1000$ K) oxidation is well understood, the low temperature ($T < 850$ K) oxidation chemistry of *iso*-butanol remains underexplored. Recent experimental works (Pan et al., Weber et al.) have also indicated that most chemical kinetic models in literature are unable to accurately predict ignition delays in the intermediate-low temperature regime. In the current work, we present detailed insight into the fundamental low-temperature chemistry of *iso*-butanol. We calculate the relevant stationary points on the potential energy surface for the α -, β -, and γ -*iso*-hydroxybutyl radicals with O_2 at the CCSD (T) level and perform master-equation calculations on these surfaces. From the master-equation calculations we have obtained (T, P)-dependent product branching ratios for the $\text{R}+\text{O}_2$ reactions and compared them with published low temperature, low pressure experimental branching ratios (Welz et al.). Unlike O_2 reacting with alkanes, the predominant reaction for alcohols is α -*iso*-hydroxybutyl + O_2 yielding HO_2 . However, competing channels yielding OH are much more conducive to ignition. We discuss the competition between these channels and its impact on low temperature autoignition of *iso*-butanol.

nyee@mit.edu

W3P043 EXPERIMENTAL AND KINETIC MODELING STUDY OF TERT-BUTANOL PYROLYSIS

Fei Qi¹, Jianghuai Cai², Wenhao Yuan¹, Lili Ye¹, William Green²

¹University of Science and Technology of China, China ²Massachusetts Institute of Technology, United States

Using biofuels as alternatives fuels can offset the CO_2 emission and reduce the climatic impact. Butanols are of increasing interest as alternatives to petroleum-based transportation because they offer higher energy density, better miscibility with practical fuels, lower water absorption than ethanol. Tert-Butanol has the most complex branched structure among four butanol isomers, thus it has been used as an octane booster to prevent knock in spark-ignition engines.

In this work, the pyrolysis of tert-butanol in a flow reactor was studied using Synchrotron Vacuum Ultraviolet Photoionization Mass Spectrometry (SVUV-PIMS), which were carried out at the National Synchrotron Radiation Laboratory in Hefei, China. Temperature ranges of 850 ~ 1550 K at pressures of 5, 30, 150 and 760 Torr were selected to investigate the pyrolysis chemistry of tert-butanol. About 20 species were identified in the experiment and their mole fractions versus temperature and pressure were quantified. A model consisting of 186 species and 1319 reactions was developed base on our previous butanol models. The pyrolysis species profiles measured in the present work are used to validate the model. The simulation was carried out using Plug Flow Reactor module in Chemkin-Pro software. The experimental and simulated results of some selected species were presented in Figure 1. Sensitivity analysis shows that H_2O elimination and C-C scission reactions are very important to the decomposition of tert-butanol. Moreover, the mole fractions of primary products are also very sensitive to rate constants of the unimolecular reactions. For example, the H_2O elimination reaction of tert-butanol is the most sensitive reaction to the mole fractions of iC_4H_8 at different pressures, as shown in Fig. 2. ROP analysis shows that tert-butanol mainly decomposes through reaction sequence $\text{tC}_4\text{H}_9\text{OH}/\text{tC}_4\text{H}_8\text{OH} \rightarrow \text{iC}_4\text{H}_8 \rightarrow \text{iC}_4\text{H}_7 \rightarrow \text{aC}_3\text{H}_4 \rightarrow \text{pC}_3\text{H}_4$ at both low and high pressures. The difference is that unimolecular reactions of tert-butanol are more important at low pressure than high pressure. This reaction sequence produces most of the hydrocarbon species in tert-butanol pyrolysis. Moreover, reaction sequence $\text{tC}_4\text{H}_9\text{OH} \rightarrow \text{CH}_3\text{COHCH}_3 \rightarrow \text{CH}_3\text{COCH}_3$ also contributes approximately 10% of tert-butanol decomposition. The oxygenated species CH_2CO and CO are the follow-up products of this reaction sequence.

fqi@ustc.edu.cn

W3P044 EXPERIMENTAL AND NUMERICAL STUDY OF 1-PENTANOL IN A SHOCK TUBE AT HIGH TEMPERATURE

Damien Nativel, Romain Grosseuvres, Andrea Comandini, Nabih Chaumeix, ICARE – CNRS, France

Due to increase of greenhouse gases and the finite quantity of fossil energies, alternative fuels are the focus of many current research programs. Moreover, European regulation imposes a proportion of 20 % of biofuel in conventional fuels. Currently, ethanol is widely used as biofuel but it has several drawbacks such as a low energy density and source of supply. For those reasons, heavier alcohols are foreseen, they are less hygroscopic and have higher energy densities. Among all the heavier alcohols, 1-pentanol seems to be a good candidate. A better understanding of its decomposition at engine like combustion conditions is a requirement, as a first step, in order to construct a detailed kinetic mechanism that will describe its combustion.

In the present study, new experimental data on 1-pentanol in shock tube are provided. The decomposition of 1-pentanol was studied behind a shock wave at high temperature. The implementation of a rapid sampling system on the shock tube was carried out. Previously, the shock tube was characterized at 363K in order to know reaction time and pressure profiles behind a reflected shock wave. The experiments were performed at 10 bars and over a temperature range from 800 to 1600K. The shock tube was initially heated at 363K and the mixture was composed with 100ppm of fuel diluted in argon. Stable species (CH_4 , C_2H_6 , C_3H_8 , C_2H_4 , C_3H_6 , 1- C_4H_8 , C_2H_2 , propadiene, propyne, acetaldehyde, C_4H_6 , C_4H_2 , 1- C_5H_{10}) from 1-pentanol decomposition were sampled from the shock tube and analyzed by Gas Chromatography. Two detectors were used to identify and quantify the species, respectively a Mass Spectrometer and a Flame Ionization Detector. The species profiles were simulated based on Togbé. Mechanism and present a reasonable agreement with the simulation.

damien.nativel@cnrs-orleans.fr

W3P045 THEORETICAL INVESTIGATION OF LOW-TEMPERATURE COMBUSTION CHEMISTRY OF THE SOPENTANOL: MASTER EQUATION ANALYSIS OF MULTI-ENERGY WELL REACTIONS OF HYDROXYL ISOPENTYLPEROXY RADICALS

Harish Chakravarty¹, Akira Matsugi²

¹Max Planck Institute for Chemistry, Germany ²National Institute of Advanced Industrial Science and Technology, Japan

Isopentanol is potential next generation biofuels for advanced HCCI engines at low temperatures and high pressures. Isopentanol exhibits higher HCCI reactivity over ethanol or gasoline. In spite of lots of theoretical and experimental investigations on the kinetics of the peroxy chemistry of alcohol based biofuels, there is no comprehensive report available to the best of our knowledge on theoretical low temperature peroxy chemistry of isopentanol. Present study investigates, detailed potential energy surface of the reactions of α , β , γ and γ -hydroxyisopentyl radicals with O_2 calculated at the B3LYP/cc-pVTZ and CBS-QB₃ level of theory for lowest energy conformers, and refined at the CCSD(T)/cc-pV ∞ Z//B3LYP/cc-pVTZ levels of theory. All quantum chemical calculations have been performed using the Gaussian 09 suite of programs. Calculations of hindered rotor partition function for low frequency torsional modes were performed employing the 1D Schrödinger equations. Conventional transition state theory calculations have been performed to evaluate the temperature dependent high pressure limit rate constants of all oxidation reaction pathways. Rate constants of barrierless entrance channels were determined at CASPT2 (7e,5o)/aug-cc-pVDZ//UB3LYP/cc-pVTZ level of theory coupled with variational transition state theory. High-level ab initio results were employed in RRKM analysis coupled with steady state master equation analysis with single exponential down model for collisional energy transfer probability and collision frequency using Lennard-Jones model (L-J model) to determine the temperature and pressure dependent rate coefficients in modified Arrhenius form for chemical activation reactions in the 300-2500K temperature and 0.1-100atm pressure range relevant for combustion modeling. Thermochemical parameters of all species involved in elementary reaction channels in complex systems were determined at CBS-QB₃ level of theory.

Detailed kinetic model has been developed and optimized on the basis of available reaction mechanisms of isopentanol and further refined for the kinetics of low temperature combustion reactions pertinent to peroxy chemistry calculated from present theoretical and computational analysis. Chemical kinetic simulations have been performed to predict ignition delay times using isothermal batch reactor module as implemented in Chemkin-II software package. Generally, complete model exhibits good agreement for ignition delays times with previously published work in the literature. Present theoretical investigation reveals that high pressure rate coefficients are adequate to explain the low temperature RO_2 chemistry in most ignition conditions. Major objective of the present investigation was to calculate the temperature and pressure dependent rate coefficients of peroxy chemistry of isopentanol and to develop and refine detailed chemical kinetic model to explain its ignition kinetics under low-temperature combustion conditions and validate against literature experimental results. These results will be presented in detail at symposium.

hkchakravarty@gmail.com

3P046 INVESTIGATION OF THE REACTIVITY OF ENOLS IN THE GAS PHASE BASED ON AB INITIO MO CALCULATION

K. Yasunaga¹, S. Takada¹, H. Yamada¹, K.P. Somers², J.M. Simmie², H.J. Curran²

¹National Defense Academy, Japan ²NUI Galway, Ireland

Enols have been observed as common intermediates in hydrocarbon oxidation. To reduce the use of fossil fuels, biofuels have attracted considerable attention. Several studies have been performed to elucidate the combustion properties of the butanol isomers and higher alcohols. In our previous work, we studied the pyrolysis of the butanol isomers in a single-pulse shock tube, where acetaldehyde, propionaldehyde and acetone were detected as products. These

aldehydes and ketone were thought to be produced via the tautomerization of enols generated from the pyrolysis of alcohols. To describe the combustion of alcohols accurately, the reaction mechanisms of aldehydes, ketones and enols should be established.

In the present work, we carried out Ab initio MO calculations to estimate the thermochemical properties and kinetic parameters for the tautomerization of enols. The enthalpies of formation estimated based on isodesmic reactions are shown in Table 1 together with those from the NIST database. The enthalpy of formation of isobutyraldehyde estimated in the present work shows good agreement with those in the NIST database. However, discrepancies were confirmed in the case of enols.

Bond Dissociation Energies (BDE) of enols were also estimated, and those of 1-butene-1-ol are shown in Figure 1 as a representative of all enols considered in the present work. The BDE of the O–H bond in *n*-butanol is 439 kJ mol⁻¹, the BDE of the O–H bond of 1-butene-1-ol (335 kJ mol⁻¹) is much weaker than that of butanol (439 kJ mol⁻¹), because the radical produced in the abstraction of hydrogen atom of O–H bond in enols form resonant structures. The rate constants of tautomerization of enols were also estimated, and it is found that those for the tautomerizations propen-2-ol to acetone and 1-butene-2-ol to 2-butanone are faster than the cases of the other enols due to the relatively lower activation energies of these reactions. Details of the present work will be described in the poster.

yasunagasedy@yahoo.co.jp, yasunaga@nda.ac.jp

W3P047 KINETICS FOR OH + CH₃OH: ISOTOPIC LABELING STUDIES REVEAL MECHANISTIC FEATURES OF CH₂OH DECOMPOSITION

Nicole J. Labbe, Sebastian L. Peukert, Stephen J. Klippenstein, Joe V. Michael, Raghu Sivaramakrishnan
Argonne National Laboratory, United States

Methanol (CH₃OH), the simplest alcohol, is an important molecule in combustion not only because of its potential to be a neat alternative transportation fuel but it also is a prominent intermediate in the combustion of a variety of oxygenated fuels. Due to its implications in combustion, methanol has been the subject of numerous high temperature studies over the past 30-40 years. Despite this, only recent experimental and theoretical studies (from our laboratory) have been instrumental in providing a complete understanding of the mechanistic features related to its high temperature decomposition. While these thermal decompositions act as initiations, subsequent propagation steps that involve H-atom abstractions are often the dominant channels for fuel destruction and also appear as sensitive reactions in ignition.

H-atom abstraction by OH from CH₃OH is one of the important propagation steps of relevance not only in combustion but also in atmospheric chemistry. Measurements of H/D-atoms (using the ARAS technique) that results from shock heating mixtures of deuterated CH₃OH and TBHP (Tert-ButylHydroPeroxide as a thermal source for OH) were used to probe the kinetics of OH + CH₃OD/CD₃OH. *H*-atom profiles were used to obtain total rate constants for OH + CD₃OH. While kinetics simulations (based on input from ab-initio/theoretical kinetics) for *H/D*-atom profiles reveals that site-specific abstraction rate constants at the CH₃ and OH site in CH₃OH are indeterminate in these experiments (because of the sequence of reactions CH₂OH→CH₃O→Products); the *H/D*-atom profiles provide some constraints for the abstraction branching ratios in the title reaction. Furthermore the measurements also provide some insights into mechanistic features of CH₂OH decomposition.

raghu@anl.gov

W3P048 KINETIC MODELING STUDY OF PROPANAL OXIDATION AT HIGH TEMPERATURE

Xingjia Man, Xi'an Jiaotong University, China

Measurement of ignition delay times were conducted for propanal-O₂ mixtures diluted in argon at temperatures from 1050 to 1800 K, pressures from 1.2 to 16.0 atm, fuel concentrations of 0.5%, 1.25%, 2.0%, and equivalence ratios of 0.5, 1.0 and 2.0. A detailed kinetic model consisting of 250 species and 1479 reactions was developed and validated using the present experimental results and the literature data of shock tube under other conditions. Further validation of the kinetic mechanism was carried out by comparing the simulated results with measured JSR data and laminar flame speeds, and reasonable agreements were achieved under all test conditions. Kinetic analysis was performed using present model to provide an insight into the main reaction pathways and key reactions for the propanal oxidation in both low- and high-pressure.

xingjiaman@stu.xjtu.edu.cn

W3P049 PYROLYSIS OF CYCLOHEXANONE IN A HEATED MICRO-REACTOR

Jessica Porterfield¹, Zeynep Serinyel², Barney Ellison¹, David Robichaud³, John Daily¹, Aristotelis Zaras²
¹University of Colorado at Boulder, United States ²LRGP – CNRS, France ³NREL, United States

Photoionization mass spectrometry has been used to study the initial thermal decomposition products of cyclohexanone using a heated microtubular reactor.

Biofuels derived from upgrading bio-oil are important in the development of renewable transportation fuels. There are a number of methods used in upgrading bio-oil that produce cyclic ketones, and understanding the pyrolysis of these compounds is important for incorporation of these fuels into existing petroleum infrastructure. We are currently characterizing the initial thermal products of the pyrolysis of cyclohexanone using PhotoIonization Mass Spectrometry

(PIMS) and matrix isolation infrared spectroscopy. Pyrolysis at 1200 K has been carried out at 260 ppm cyclohexanone in H_2 . The dilute gas mixture was pulsed through a resistively heated silicon carbide tube (1 mm ID). Upon exiting the reactor, the gas entered a vacuum chamber ($1 \rightarrow 10^{-6}$ Torr) where it rapidly expanded and cooled, quenching further reaction chemistry. The resulting thermal products were ionized and studied with time-of-flight PIMS (see below). We believe the cyclohexanone is tautomerizing to 1-cyclohexenol and undergoing a retro Diels-Alder reaction to form 1,3-Butadiene-2-ol ($CH_2=C(OH)CH=CH_2$) and ethylene ($H_2C=CH_2$). Further work needs to be done to characterize these species in the infrared as a compliment to the PIMS data. Pyrolysis will be carried out in Ar and products will be deposited onto a cryogenically frozen window (C_6I , 20 K) and studied with FTIR spectroscopy.

jessica.porterfield@colorado.edu

W3P051 AN EXPERIMENTAL AND KINETIC MODELING STUDY OF NITROETHANE PYROLYSIS AT LOW PRESSURE: COMPETITION REACTIONS IN THE PRIMARY DECOMPOSITION

Kuiwen Zhang, National University of Ireland, Galway, Ireland

The pyrolysis of nitroethane has been investigated over the temperature range of 682-1423 K in a plug flow reactor at low pressure. The major species in the pyrolysis process have been identified and quantified using tunable synchrotron vacuum ultraviolet photoionization mass spectrometry and molecular-beam sampling techniques. From ab initio calculations for nitroethane decomposition, the rate constants for the primary pyrolysis of nitroethane have been generated for the conditions of the present work, and adopted in a detailed chemical kinetic model which contains 118 species and 719 reactions. The model was validated against the experimental results with satisfactory agreement in general. The results indicate that both the concerted molecular elimination and C-N bond rupture are significant in the primary pyrolysis of nitroethane, with the latter channel dominating at high temperatures. The results indicate that decomposition of nitroethane on the reactor wall to form CH_2CHNO and CH_3CNO constitutes a minor consumption pathway, and this step has only a small impact on the overall behavior. Further investigations will be carried out on the pyrolysis of nitroethane at different pressures, too.

KUIWEN.ZHANG@nuigalway.ie

W3P052 LEAN METHANE/PROPANE IGNITION AT HIGH PRESSURES: COMPARISON OF CHEMICAL KINETIC MECHANISMS

Robert Pachler, Franz Winter, Vienna University of Technology, Austria

As a result of the importance of CO_2 reduction and worldwide increasing fuel prices, renewable energy sources like biogas, are becoming more and more important. In order to increase the calorific values e.g. propane is added and mixed with the biogas produced. To study the ignition behavior of the propane enriched biogas, two recently published mechanisms were chosen to perform a parameter variation study using COSILAB software. These mechanisms cover C_1 - C_3 fuel combustion: NUIG NGM 3, SAN DIEGO.

Simplified chemical kinetic mechanisms play an important role for CFD simulations. To develop a new highly economic engine, e.g. lean biogas-fueled internal combustion engines at high pressure conditions, chemical kinetic simulation tool are inevitable. Due to the fact, commonly published mechanisms are validated only up to 30atm, there is no experience available. For this reason Rapid Compression Machine (RCM) experiments were performed to investigate the simulated ignition behavior at high pressures of 80-120bar, temperatures from 800K to 1000K and an air-to-fuel ratio from 1.9.

Ignition delay times, obtained from a zero - dimensional chemical kinetic simulation, were compared to the measurements. The investigations were adopted at described conditions.

robert.pachler@tuwien.ac.at

W3P053 SITE-SPECIFIC RATE CONSTANT MEASUREMENTS FOR PRIMARY AND SECONDARY H- AND D- ABSTRACTION BY OH RADICALS: PROPANE AND N-BUTANE

Ehson Fawad Nasir¹, Jihad Badra², Aamir Farooq¹

¹King Abdullah University of Science and Technology, Saudi Arabia ²Saudi Aramco, Saudi Arabia

The site-specific rate constants for hydrogen (H) and deuterium (D) abstraction by hydroxyl (OH) radicals were determined experimentally by monitoring the reaction of OH with two normal and six deuterated alkanes. The reaction of OH with the propane isotopes: propane (C_3H_8), propane 2,2 D2 ($CH_3CD_2CH_3$), propane 1,1,1-3,3,3 D6 ($CD_3CH_2CD_3$), and propane D8 (C_3D_8) and the butane isotopes: *n*-butane ($n-C_4H_{10}$), butane 2,2-3,3 D4 ($CH_3CD_2CD_2CH_3$), butane 1,1,1-4,4,4 D6 ($CD_3CH_2CH_2CD_3$), and butane D10 (C_4D_{10}) was investigated behind reflected shock waves over 840 – 1470 K and 1.2 – 2.1 atm. Previous low temperature data were combined with the current high temperature measurements to generate three-parameter fits which were then used to determine the site-specific rate constants. Two primary ($P_{1,H}$ and $P_{1,D}$) and four secondary ($S_{00,H}$, $S_{00,D}$, $S_{01,H}$, and $S_{01,D}$) H- and D- abstraction rate constants, where the subscripts refer to the number of carbon (C) atoms connected to the Next-Nearest-Neighbor (N-N-N) C atom, are obtained. The modified Arrhenius expressions for the six site-specific abstractions by OH radicals are:

$$P_{1,H}=1.90 \times 10^{-18} T^{2.00} \exp(-340.87 \text{ K/T}) \text{ cm}^3 \text{ molecule}^{-1} \text{ s}^{-1} \text{ (210-1294 K)}$$

$$P_{1,D}=2.72 \times 10^{-17} T^{1.60} \exp(-895.57 \text{ K/T}) \text{ cm}^3 \text{ molecule}^{-1} \text{ s}^{-1} \text{ (295-1317 K)}$$

$$\begin{aligned}
S_{00,H} &= 4.40 \times 10^{-18} T^{1.93} \exp(121.50 \text{ K/T}) \text{ cm}^3 \text{ molecule}^{-1} \text{ s}^{-1} \text{ (210-1294 K)} \\
S_{00,D} &= 1.45 \times 10^{-20} T^{2.69} \exp(282.36 \text{ K/T}) \text{ cm}^3 \text{ molecule}^{-1} \text{ s}^{-1} \text{ (295-1341 K)} \\
S_{01,H} &= 4.65 \times 10^{-17} T^{1.6} \exp(-236.98 \text{ K/T}) \text{ cm}^3 \text{ molecule}^{-1} \text{ s}^{-1} \text{ (235-1407 K)} \\
S_{01,D} &= 1.26 \times 10^{-18} T^{2.07} \exp(-77.00 \text{ K/T}) \text{ cm}^3 \text{ molecule}^{-1} \text{ s}^{-1} \text{ (294-1412 K)}
\end{aligned}$$

ehsonfawad.nasir@kaust.edu.sa

W3P054 INVESTIGATION OF ETHANE PYROLYSIS AND OXIDATION AT HIGH PRESSURES USING GLOBAL OPTIMIZATION BASED ON SHOCK TUBE DATA

Viktor Samu¹, Tamas Varga¹, Kenneth Brezinsky², Aleksandr Fridlyand², Tamas Turanyi¹

¹Eötvös University (ELTE), Hungary ²University of Illinois at Chicago, United States

Tranter et al. conducted a series of experiments of ethane oxidation and pyrolysis covering a wide range of temperature (800 K – 1500 K) and pressure (5 bar – 1000 bar) in a high pressure shock tube. The oxidation and pyrolysis of ethane were carried out behind reflected shock waves, and the concentrations of the reaction products were measured by gas chromatography. The results of these experiments were re-evaluated by optimizing selected rate parameters of the NUIG C5 combustion mechanism. For faster calculations, this mechanism was truncated first by eliminating the reactions of five carbon atom species. Using local sensitivity analysis at the condition of each experiment, 20 reactions steps were selected, which are important for the quantitative reproduction of the experimental results. Direct experimental data and results of theoretical calculations were searched for in the literature for these elementary reactions. A hierarchical optimization strategy was designed based on the sensitivity calculations. Arrhenius parameters (A, n, E) of the selected reaction steps were optimized using not only the experimental data of Tranter et al., but also the results of direct measurements related to these reactions. The obtained mechanism with the optimized rate parameters described the experiments of Tranter et al. much better than the original mechanism. The parameter estimation procedure provided new, temperature dependent uncertainty limits for the rate coefficients of relatively well known reactions, like $\text{C}_2\text{H}_6 + \text{H} = \text{C}_2\text{H}_5 + \text{H}$ and $\text{C}_2\text{H}_6 + \text{M} = \text{C}_2\text{H}_6 + \text{M}$, and also gave new recommended Arrhenius parameters and uncertainty estimations for reactions with few previous experimental and theoretical investigations, like the steps $\text{C}_2\text{H}_3 + \text{O}_2 = \text{CH}_2\text{CHO} + \text{O}$ and $\text{CH}_3 + \text{HO}_2 = \text{CH}_3\text{O} + \text{OH}$.

samu.viktor@gmail.com

W3P055 IGNITION DELAY TIME MEASUREMENTS AND MODELING OF PENTANE ISOMERS

Olivier Mathieu¹, Claire Gregoire¹, Brandon Marks¹, Rachel Archuleta¹, Eric L. Petersen¹, John Bugler², Henry Curran²

¹Texas A&M University, United States ²National University of Ireland, Galway, Ireland

Pentane isomers (*n*-pentane, *iso*-pentane (2-methyl-butane), and *neo*-pentane (2,2, dimethyl-propane) combustion chemistry is of interest because pentanes are components of gas-turbine and gasoline engine fuels and are intermediate species in the oxidation of higher-order hydrocarbons. Although the combustion of pentanes was examined in several studies in Rapid Compression Machine (RCM), shock-tube, well-stirred reactor, and an annular flow reactor, some conditions remain unexplored.

The present study expands on the current knowledge of *n*-pentane, *iso*-pentane, and *neo*-pentane combustion by investigating conditions not reported in the literature and which may be of interest to engine designers. Ignition delay time data from mixtures of the various pentanes in air were collected experimentally via shock tube and RCM for mixtures over wide ranges of equivalence ratios, pressures (1, 10, and 20 atm), and temperatures (640-1550 K). Shock-tube experiments were performed on the high-pressure shock tube at Texas A&M University, and all RCM experiments were performed at the National University of Ireland Galway's Combustion Chemistry Centre (NUIG). These data were used to improve the detailed kinetics mechanism developed at NUIG. The purpose of this study was to verify and adjust the chemical kinetic mechanism based on experimental results.

Experimentally, the pentane isomers present similar ignition delay times at high temperature. Noticeable differences are however visible for intermediate (in the Negative Temperature Coefficient (NTC) region) and low temperatures, where the branched isomers showed longer ignition delay times than *n*-pentane. The ignition delay time decreases as pressure increases for all isomers. Ignition delay times were well predicted for all isomers throughout the temperature range.

olivier.mathieu@tamu.edu

W3P058 AN EXPERIMENTAL STUDY OF ISOBUTENE AND 1,3-BUTADIENE IGNITION DELAY TIME AT ELEVATED PRESSURES

Yang Li¹, Chong-Wen Zhou¹, Eoin O'Connor², Henry Curran¹

¹National University of Ireland, Galway, Ireland ²Galway-Mayo Institute of Technology, Ireland

Isobutene is an important intermediate of the pyrolysis and oxidation of branched alkanes such as *iso*-octane. The oxidation or combustion of Ethyl Tert-Butyl Ether (ETBE) and Ethyl Tert-Butyl Ether (ETBE), which are used as octane enhancer worldwide, also produce significant amount of isobutene. While 1,3-butadiene is also an intermediate in the combustion of higher order hydrocarbons, and is emitted to the environment from the exhaust of automotive engines, biomass combustion and industrial on-site uses, which is involved in the formation of polycyclic aromatic hydrocarbons,

soot, and tropospheric ozone. Therefore, it is necessary to study the oxidation of isobutene and 1,3-butadiene to build their chemical kinetic model. Despite these importance, there is a lack of experimental data available in the literature for both of them at low and intermediate temperatures (700-1200K) and high pressures (≥ 10 atm). In this study, Rapid Compression Machine (RCM) and Shock Tube (ST) ignition delay time measurements were performed for both isobutene and 1,3-butadiene fuel/air mixtures at equivalence ratios of 0.3, 0.5, 1.0, and 2.0. The wide range of experimental conditions included temperatures from 760 to 1500 K at pressures of approximately 10, 30, and 50 atm. Experimental results of these 2 fuels were compared based on different equivalence ratios and different pressures respectively.

As to the results of isobutene ignition delay time measurement, for several pressures and equivalence ratios, the ST and RCM meet at nearly coincident temperatures, with remarkable agreement between the two techniques, and all results got from RCM showed an excellent coalescence with those from ST which were quite linear. As to the effect of pressure on ignition, it is apparent that reactivity increases with increasing pressure, as a decrease in ignition delay time with an increase in pressure at constant temperature was observed. NTC behavior wasn't pointed out along with temperature increasing. As to the effect of equivalence ratio on ignition, at these particular high pressures (30 and 50atm) and relatively low temperature conditions (≤ 950 K), fuel-rich mixtures are most reactive while fuel-lean mixtures are slowest to ignite at constant temperature. While at relatively high temperature conditions (≤ 1000 K), there appears to be a lesser dependence of ignition delay time on equivalence ratio. Moreover, under the pressure condition of 10atm and relatively high temperature conditions (≥ 1100 K), there appears to be no dependence on equivalence ratio with all mixtures igniting at about the same time when at the same temperature and pressure. These experimental results above will be used to validate detailed chemical kinetic models of them.

y.li9@nuigalway.ie

W3P059 KINETICS OF HOMOALLYLIC/HOMOBENZYLIC REARRANGEMENTS REACTIONS UNDER COMBUSTION CONDITIONS

Feng Zhang, Zhaohui Wang, Lidong Zhang, University of Science and Technology of China, China

Homoallylic/homobenzylic radicals refer to typical radicals with the radical site located at the β position from the vinyl/phenyl group and are largely involved in combustion systems[1], such as the pyrolysis or oxidation of alkenes, cycloalkanes and aromatics. Therefore, it's significant to carry out investigations of Homoallylic/homobenzylic radicals.

The homoallylic/homobenzylic rearrangement, called 1,2-vinyl/phenyl migration, is a peculiar reaction type for homoallylic/homobenzylic radicals. The 1,2-vinyl migration is regarded as taking place by a two-step sequence: (1) ring closure of an allylcarbiny radical to form a cyclopropylcarbiny radical, and (2) ring opening of the formed radical to yield an allylcarbiny radical of rearranged structure. With the help of rate constant calculations, the competitions between this reaction mechanism and other possible reaction pathways under combustion temperatures (500-2000 K) were evaluated. The 1,2 vinyl/phenyl migration is the most favored reaction channel for R1/R2 compared with other competing reactions at least under 1500K due to its low energy barrier and it still has ~20% contribution even at 2000 K.

Analogous rearrangements, like 1,3 and 1,4 vinyl/phenyl migrations are also evaluated with the help of rate constants of elementary reactions. Results indicates that the reaction mechanisms of 1,3- or 1,4-vinyl/phenyl migration for radicals with similar structures are not favored under combustion temperatures.

Our studies suggest that the homoallylic/homobenzylic rearrangements have great influence on the unimolecular reaction of such radicals with homoallylic/homobenzylic structures, which are extremely needed in the kinetic models of combustion systems involving such homoallylic/homobenzylic radicals.

feng2011@ustc.edu.cn

W3P060 THERMAL DECOMPOSITION OF STYRENE: AN AB INITIO/MASTER EQUATION STUDY

Edward Ross, Gabriel da Silva, University of Melbourne, Australia

Styrene is a key intermediate formed during the combustion of the xylene compounds, a type of aromatic compound found in gasoline. Styrene itself can undergo further decomposition at high temperatures, with experimental studies showing that it predominantly decomposes to benzene and acetylene ($C_6H_6 + C_2H_2$). Although mechanisms have been proposed in order to explain the decomposition process, this following work is the first of its kind to use ab initio quantum chemistry methods to elucidate the decomposition mechanism of styrene.

The Gaussian-4 (G4) composite method was used to determine structures and energies for each of the intermediates and transition states involved in the decomposition mechanism. It was found that there exist three distinct decomposition channels, each of which contributes under combustion-relevant conditions. The most energetically favourable pathway was the dissociation to benzene and vinylidene, the latter being a carbene isomer of acetylene. This pathway was found to have a barrier height of 84.9 kcal/mol and consists of a series of ring opening/closing steps that involve the formation of a seven-membered ring structure. It was also discovered that styrene can surmount a 94.7 kcal/mol barrier to produce phenylacetylene plus molecular hydrogen ($C_8H_6 + H_2$) via a two-step hydrogen migration/elimination process. Furthermore, styrene can also isomerise to o-xylene and benzocyclobutene before dissociating to benzyne and ethene ($C_6H_4 + C_2H_4$) after overcoming a 95.6 kcal/mol energy barrier.

The constructed mechanism was then used to conduct an RRKM/Master Equation study in order to examine the kinetics of styrene decomposition. According to the simulations, negligible decomposition of styrene was observed to

occur below 1800K. Above this value, it was found that the pathway to form $C_6H_6 + C_2H_2$ was the most favourable, accounting for 95% of the styrene dissociation. The Troe falloff method was used to obtain rate expressions for each of the dissociation channels, which were found to accurately represent the data obtained from the RRKM/Master Equation simulations. For completeness, a two-parameter Arrhenius expression was also obtained for the isomerisation process from o-xylylene to styrene, since this represents one of the main styrene formation processes found in aromatic combustion.

elross@student.unimelb.edu.au

- W3P061 THE ROLE OF THE FULVENALLENYL RADICAL IN THE FORMATION OF POLYCYCLIC AROMATIC HYDROCARBONS DURING AROMATIC FUEL COMBUSTION: AN AB INITIO/MASTER EQUATION STUDY
Edward Ross, Gabriel da Silva, University of Melbourne, Australia

The fulvenallenyl radical (C_7H_5) is a Resonance Stabilised Radical (RSR) which is present in appreciable quantities during the combustion of aromatic fuels. By virtue of its structural similarity to the propargyl (C_3H_3) and cyclopentadienyl (C_5H_5) radicals, it has been postulated that the fulvenallenyl radical can undergo reactions with other RSRs, and thus contribute to the formation of Polycyclic Aromatic Hydrocarbon (PAH) molecules during aromatic fuel combustion. Although a recent kinetic study has incorporated several such reactions in their model, uncertainties abound in the rate expressions for these reactions since these are estimations based on the kinetics for the self-addition of propargyl radicals. This study examines the kinetics of the reaction between the fulvenallenyl and propargyl radical to form naphthalene by first investigating the reaction mechanism using ab initio quantum chemistry methods. Both the M06-2X and G₃X-K methods were used in calculations. It was found that only two out of the eight possible addition sites between the two radicals directly lead to subsequent isomerisation and formation of naphthalene and the naphthyl radicals. The first involves direct addition of the acetylenic end of the propargyl radical to the β -carbon on the CCH_2 side chain, followed by isomerisation to naphthalene via fulvalene. The acetylenic end of the propargyl radical can also add to the ring on the carbon atom adjacent to the CCH_2 side chain, followed by a series of H-transfer and ring closing/opening steps to form naphthalene via azulene, another bicyclic PAH molecule. Once formed, naphthalene can then lose a hydrogen at either the α or β site to form the corresponding naphthyl radical. A total of three different formation mechanisms with a barrier height below the initial entrance channel were found, with the fulvalene pathway being the most energetically favourable (25.0 kcal/mol below the entrance channel). The two other pathways that take place via azulene have barriers of 8.8 and 13.2 kcal/mol below the entrance channel respectively.

An RRKM/Master Equation study was then performed on the resulting mechanism to determine the kinetics of the reaction between 300-2000K and 0.01-100 atm. At low temperatures, quenching of the initial adduct dominates due to the high-pressure limit being attained, even at the lower end of pressures examined in this study. At high temperatures, the formation of naphthalene and the naphthyl radicals was found to compete with dissociation back to the original radical reactants. A three-parameter Arrhenius fit was used to determine separate rate expressions for the formation of naphthalene, naphthyl radicals and fulvalene as well as the dissociation to form the original reactants.

elross@student.unimelb.edu.au

- W3P062 AUTOMATIC GENERATION OF KINETIC MODELS FOR THE OXIDATION OF LARGE ALKYL BENZENES
Valerie Warth¹, Roda Bounaceur¹, Pierre-Alexandre Glaude¹, Olivier Herbinet², Frederique Battin-Leclerc¹
¹LRGP – CNRS, France ²Universite de Lorraine, France

Among automotive fuels, diesel fuels are a complex mixture of hundreds components consisting of alkanes, alkylcyclohexanes, alkyldecalines, alkylbenzenes (approximately 10%) and polycyclic naphthoaromatic compounds, which contain from 10 to 20 carbon atoms. Because of the difficulty to consider the chemistry of a real diesel fuel as the sum of all its components due to the complexity of the mixture, surrogate fuels have been suggested: e.g. a mixture of *n*-hexadecane, heptamethylnonane, 1-methylnaphthalene and *n*-decylbenzene. However, while some kinetic models are available for the three first proposed surrogate compounds, no model has been yet proposed for alkylbenzenes larger than butylbenzene. In the present study, a new version of the software EXGAS (EXGAS-alkylbenzenes) has been developed in order to automatically generate model for the oxidation of large alkylbenzenes. A comprehensive and validated reaction base containing the reactions of the light aromatic species involving less than two carbon atoms on the side chain (benzene, toluene, ethylbenzene, styrene, oxygenated intermediates...) is included in each generated mechanism. For alkylbenzene reactant with an alkyl chain containing more than two atoms of carbon, a primary and a lumped secondary mechanism are generated based on generic reactions which have been defined following our previous modeling work on butylbenzene. The algorithm of generation of the primary mechanism follows the scheme of chain reactions in oxidation. Most of the generic reactions are similar to those used for alkanes, only the ipso-additions (addition-elimination on the aromatic ring) are specific to aromatic compounds. The generated models have been validated by simulating experimental results obtained in a jet-stirred reactor for butylbenzene and hexylbenzene and a priori prediction of the reactivity of decylbenzene has been given.

valerie.warth@univ-lorraine.fr

- W3P063 KINETICS OF THE SELF-REACTION OF CYCLOPENTADIENYL RADICALS
Vadim D Knyazev, Konstantin Popov, Catholic University of America, United States

Self-reactions of hydrocarbon radicals are important steps in the pyrolysis and combustion of hydrocarbon fuels. At the same time, such reactions are difficult to study experimentally and reliable information on their kinetics available in the literature is rather sparse.

In the current work in progress, the kinetics of the self-reaction of cyclopentadienyl radicals is being studied experimentally over the temperature interval 298 – 600 K and at bath gas (He) densities of $(3 - 12) \times 10^{16}$ molecule cm^{-3} by the Laser Photolysis / Photoionization Mass Spectrometry technique. Cyclopentadienyl radicals are produced by 248-nm laser photolysis of cyclopentadiene. Initial concentrations of the cyclopentadienyl radicals are determined using the measured fraction of cyclopentadiene decomposed during the photolysis. The kinetics of cyc-C₅H₅ decay is monitored in real time and the values of the rate constant of the self-reaction reaction are determined from the [cyc-C₅H₅] temporal profiles.

Preliminary results indicate that the values of the rate constant obtained in the experiments are rather large compared with those of the self-reactions of alkyl radicals, similar to the value of the collision frequency. C₁₀H₁₀ is observed as the recombination product.

Knyazev@cua.edu

W3P064

EXPERIMENTAL AND KINETIC MODELING STUDY OF DIMETHYL CARBONATE

Erjiang Hu, Lun Pan, Zihang Zhang, Zuohua Huang, Xi'an Jiaotong University, China

Dimethyl carbonate (CH₃OCOOCH₃, DMC) is an attractive oxygenated fuel because of its very high weight percent of oxygen. Diesel engine studies have shown that dimethyl carbonate addition to the fuel can significantly reduce smoke emissions. However, the chemical mechanism responsible for this decrease is still not well understood. Ignition delay times of dimethyl carbonate were measured in a shock tube for the first time at T = 1100-1600 K, p = 1.2-10.0 atm, fuel concentration = 0.5-2.0%, and f = 0.5-2.0. A chemical kinetic model was developed and can well predict measured ignition delay times. Further validation of the proposed kinetic model was made on the basis of the opposed flow diffusion flame data. Reasonable agreements were also achieved under the literature conditions. Reaction pathway analysis shows that the DMC molecule is primarily consumed through the H-abstraction. Sensitivity analysis provides some key fuel-species reactions at high temperature ignition.

hujiang@mail.xjtu.edu.cn

W3P065

A HIGH-PRESSURE AUTO-IGNITION STUDY OF METHANE IN A HIGH-PRESSURE SHOCK TUBE

Alan Keromnes, Benoîte Lefort, Luis Le Moyne, University of Burgundy, France

Fundamental data such as ignition delay times and species profiles at practical conditions are invaluable for the improvement and extension of chemical kinetics models to engine applications. High pressure shock tubes are ideal to study such measurements and have been used during last decade. A major challenge for kinetic modeling is pressure dependence of branching fractions for the most sensitive reactions; it is why more experimental results are needed at high pressure. A 9m long high-pressure shock tube with an inner diameter of 50 mm has been designed and validated during this study. The shock tube is designed to reach 40 bar after the reflected shock wave and can be heated up to 473 K. A double-diaphragm section divides the tube into a 4 m long driver section and a 5 m driven section.

The shock tube has been validated by reproducing previously published experimental results on methane by Zhang et al. and results show a very good agreement. The experimental study extends the ignition delay time results to pressure up to 40 bar. The experiments were performed using a lean mixture with an equivalence ratio of 0.5. All gases used for the experiments had a purity of 99.9 % or higher. The ignition delay times recorded show a strong dependence on the compressed pressure. The ignition delays decrease with increasing pressure. The temperature both impacts the ignition delay which reduces with increasing temperature.

alan.keromnes@u-bourgogne.fr

W3P066

SHOCK-TUBE STUDY OF THE IGNITION OF FUEL-RICH CH₄/AIR AND CH₄/ADDITIVE/AIR MIXTURES OVER A WIDE TEMPERATURE RANGE AT HIGH PRESSURE

Jürgen Herzler, Mustapha Fikri, Christof Schulz, University of Duisburg-Essen, Germany

Flexibility between the conversion and storage of energy will be an important aspect in future energy systems, especially when considering the fluctuating availability of renewable energies. In times of low demand but high availability of energy, an interesting concept is the use of external mechanical or electrical energy in Internal Combustion Engines (ICEs) to convert “cheap” chemicals (e.g., natural gas) into higher-value chemicals so that most of the exergy of the cheap fuels is stored. This production of chemicals typically proceeds at fuel-rich conditions, far away from current operating regimes of ICEs. A fundamental understanding of the chemical kinetics under these conditions and the availability of validated reaction mechanisms for these fuel-rich conditions are essential for the successful implementation of such processes. However, most of the reaction mechanisms published in the literature are validated preferentially for lean and stoichiometric mixtures, because these conditions are important in ICEs and gas turbines.

To test the performance of existing reaction mechanisms under fuel-rich conditions, we measured the ignition delay times of CH₄/air and CH₄/additive/air mixtures at fuel-rich ($F = 2$) and engine-typical conditions ($p = 30$ bar) and

compared the results with the predictions of literature mechanisms. A very good agreement was found using the mechanisms of Herzler and Naumann and Yasunaga. Additives (ethanol, dimethyl ether, propene) were used to reduce the ignition delay times of CH₄ so that engines can be used in the HCCI mode without preheating the reactants.

juergen.herzler@uni-due.de

W3P067 PARTIAL OXIDATION OF METHANE AT ELEVATED PRESSURES AND EFFECTS OF PROPENE AND ETHANE AS ADDITIVE

Tina Kasper, Fikri Sen, Burak Atakan, Ulf Bergmann, University of Duisburg-Essen, Germany

Partial homogeneous oxidation of methane within stationary engines may be one concept for conversion of available energy to alternatively mechanical energy, heat, and additional useful chemicals like syngas, formaldehyde, methanol or higher hydrocarbons (e.g. ethene).

These thermochemical conversion reactions are investigated experimentally using a flow reactor. Methane oxidation is studied under fuel-rich conditions (stoichiometry=20) at high pressures (6 bar) and high temperatures (T_{max} = 1030K) for long residence times in a tubular reactor. The gas composition after passage through the reactor is determined by time-of-flight mass spectrometric analysis for different reactor temperatures. Through variation of reactor temperature an overview of the maximum mole fractions of target chemicals, the temperature of observed reaction onset and the optimal temperature to increase target yields can be determined.

The experimental results are compared to kinetic simulations of neat methane conversion in the reactor setup using two literature mechanisms to assess how well the data are reproduced for these uncommon reaction conditions. Both mechanisms have not been optimized for this use and the simulation deviate significantly in the predicted initiation temperature and absolute species mole fractions. The experimentally observed initiation temperatures fall between the simulation results. Absolute mole fractions exhibit differences between experiment and simulation that are as large as the deviations between the two mechanisms. In summary, the comparisons of experimental data and the results of the simulation of the experiment with these two mechanisms identify a need for further improvements of the experiments as well as the reaction mechanisms.

Given the low reactivity of methane at temperatures below 1000K the addition of additives to the gas mixture seems to be a viable way to reduce the initiation temperatures and make partial oxidation reactions more attractive for the production of base chemicals. The potential for activating the conversion reactions with ethane and propene as additives is investigated. Methanol is chosen as one target compound. Its yield is increased by both additives. In addition, propene as additive reduces the temperature of reaction onset in the experiments. Simulations of these experiments capture general trends correctly, e.g. lower initiation temperature with use of propene additive, but reproduce absolute mole fractions values poorly. This work emphasizes the need for better chemical models and accurate validation data to progress model based planning of thermochemical conversion reactions and to develop the ability to predict target chemical yields.

tina.kasper@uni-due.de

W3P068 MODELING THE MULTIPLE-WELL, MULTIPLE-PATH UNIMOLECULAR DECOMPOSITION OF SMALL RADICAL INTERMEDIATES – A COMPARISON BETWEEN CANTHERM, MULTIWELL, AND VARIFLEX

Enoch Dames¹, Shamel Merchant¹, C. Franklin Goldsmith², William Green¹

¹Massachusetts Institute of Technology, United States ²Brown University, United States

Three commonly utilized rate theory packages (Rice–Ramsperger–Kassel–Marcus (RRKM) theory and Master Equation solvers) are used to investigate the unimolecular decomposition of CH₂OH, CH₃O, CH₃CHOH, and C₂H₅O. These systems, with varying possibilities for isomerization and dissociation to bimolecular products, also have pressure-dependent kinetics. In the cases of methoxy and ethoxy, comparisons of simulation results are made with available experimental data over a wide range of pressures. Comparisons between analogous high-pressure limit rate coefficients, density of states, microcanonical rate coefficients, rates in the falloff regime, and product branching fractions reveal an array of differences between Cantherm, Multiwell, and Variflex predictions. In some cases, absolute differences in species properties (e.g., the density of states) between the three packages can be large, but the consequences of these differences can be reduced due to error cancellation in computed rate coefficients. Because focus of this work is to compare simulation results with equal input parameters, the rigid rotor harmonic oscillator assumption is used to describe molecular internal degrees of freedom. However, differences in and consequences of how internal hindered rotors are treated across the three packages is also highlighted. This work is part of an ongoing effort to delineate differences across rate theory packages for atmospheric and combustion-related kinetics.

enoch.dames@gmail.com

W3P069 CLOUDFLAME: A HYBRID CLOUD SYSTEM FOR COMBUSTION KINETICS SIMULATION

Mani Sarathy, King Abdullah University of Science and Technology, Saudi Arabia

The kinetics and combustion communities use various computational simulation applications (e.g., CHEMKIN, Cantera, OpenSMOKE) and platforms (Windows, Linux, Macintosh). Some problems hindering the sharing of scientific results for collaboration among researchers in the community are the lack of standardized input data (kinetics

mechanism, thermodynamic, boundary conditions, transport), machine-readable data, and collaborative systems for simulation. The Process Informatics Model (PrIme) introduced a cyberinfrastructure for modeling and analysis of combustion kinetics, as well as data standards and workflows for linking simulation with data. In this research, the PrIme infrastructure is extended to design and implement a platform-independent cyberinfrastructure called CloudFlame that enables improved automation of combustion simulations. CloudFlame is a hybrid cloud system consisting of public and private clouds using the PrIme web portal to provide computational power, a digitized data warehouse, and kinetics automation workflow for researchers. We demonstrate that chemical kinetics data stored in the PrIme hierarchical binary XML data format (HDF5) consisting of element data, species data, and reaction data can be automatically converted to data formats compatible with combustion simulation applications. Using the data that are generated, an automated workflow securely transfers files between public and private servers, and then calls the application programming interfaces of the simulation application (e.g., CHEMKIN-PRO) to run the pre-processing, calculations, and post-processing stages. The simulation results are again securely transferred back to the public cloud where comparisons are performed against the archived data in warehouses stored on both PrIme and CloudFlame servers. The result of using this system by researchers at the Clean Combustion Research Center at King Abdullah University of Science & Technology and its collaborating partners indicated a significant improvement in flexibility and portability of kinetics data and increased efficiency, scalability, and accessibility to computational resources using the hybrid PrIme-CloudFlame infrastructure. This operational hybrid cloud system presents a new paradigm for collaboration in combustion and kinetics research, enabling future advances in computational chemistry, kinetic model development, experimental data management, uncertainty quantification, and reactive flow simulation.

mani.sarathy@kaust.edu.sa

W3P070 **OPENSMOKE++: AN OBJECT-ORIENTED FRAMEWORK FOR THE NUMERICAL MODELING OF REACTING SYSTEMS WITH DETAILED KINETIC MECHANISMS**

Alberto Cuoci, Alessio Frassoldati, Mattia Bissoli, Alessandro Stagni, Tiziano Faravelli, Politecnico di Milano, Italy

Realistic numerical simulations of combustion phenomena necessarily require not only accurate, detailed modeling of fluid dynamic aspects, but also a detailed characterization of the chemical reactions and the physical and chemical properties of the species involved. In recent years many efforts were devoted to the development of very complex kinetic mechanisms, consisting of thousands of reactions and species, with a very high level of accuracy and excellent predictive capabilities. However, the computational cost of simulations performed using such large mechanisms can be prohibitive, even for ideal systems (batch, plug-flow, perfectly-stirred reactors, etc.) or one-dimensional laminar flames (flat premixed flames, counter-flow diffusion flames, etc.). Moreover, the huge number of species and reactions makes very difficult and complicated to recognize the main chemical paths and to interpret the numerical results from a kinetic point of view.

The considerations reported above suggest the need of computational tools able to manage large kinetic schemes, with the following features:

1. Efficiency: the calculations have to be fast, i.e. proper numerical technique have to be adopted to reduce the computational cost, without loss of accuracy;
2. User-friendly interface: i.e. the user must be able to easily incorporate them in new or existing numerical codes, to perform also complex operations (reduction of species, stiffness analysis, etc.)
3. Availability of tools to perform kinetic analyses: Reaction Path Analysis, Sensitivity Analysis, Rate Production Analysis, etc. in order to better understand the results of the numerical simulations. This work describes a suite of numerical tools, known as OpenSMOKE++, designed to provide a flexible, extensible framework for numerical simulations involving thermodynamics, transport processes, and chemical kinetics. The proposed framework is specifically conceived to manage very large detailed kinetic mechanisms (thousands of species and reactions). The OpenSMOKE++ framework strongly relies on the Computation Cost Minimization (CCM) techniques, i.e. a set of strategies that expedite the numerical simulations with little or no accuracy loss through optimization of the computation sequence. Moreover, since it is based on the most modern features of C++ (template- and meta- programming, polymorphism, policies, etc.), the OpenSMOKE++ framework can be easily incorporated in new or existing numerical codes to efficiently evaluate thermodynamic properties, transport properties, and homogeneous and heterogeneous kinetics rates. In order to better show the generality and the potential applications of the proposed framework, a series of illustrative examples is presented, with particular emphasis about the numerical performances with respect to existing tools currently used by the combustion community.

alberto.cuoci@polimi.it

W3P071 **AN ADAPTIVE METHODOLOGY FOR THE EFFICIENT IMPLEMENTATION OF DETAILED CHEMISTRY IN SIMULATIONS OF TURBULENT COMBUSTION**

Perrine Pepiot, Stephen B. Pope, Youwen Liang, Cornell University, United States

The development of validated, predictive, multi-scale combustion modeling capabilities has been recognized as a key step to optimize the design and operation of evolving fuels in advanced engines for transportation applications. Owing to the increased sensitivity of new energy systems to the chemical processes, being able to accurately capture chemical kinetics, and how they interact with flow dynamics is key in developing these capabilities. Our understanding

of chemical kinetics has exploded over the past two decades, leading to the development of ever growing detailed kinetic schemes for a wide range of molecular species pyrolysis and oxidation, mostly for combustion applications. With more accurate rate rules and improved mechanistic considerations, some of the latest published mechanisms are approaching 104 species and as many reactions. However, these advances in chemical kinetics and detailed model development have to be integrated with Computational Fluid Dynamics (CFD) tools to fully realize their potential in terms of improved understanding and optimization of practical energy conversion devices. The real challenge then is to maximize the level of chemical detail that can be afforded in CFD so that meaningful and reliable data are obtained for advanced design purposes.

In this work, we propose and assess the performance of a novel adaptive chemistry strategy specifically designed for LES/particle PDF simulations of non-premixed turbulent flames. For a given reactive flow configuration, thermodynamic conditions can vary widely in space and time, and in any small range of temperature and compositions, many species have negligible concentration, and only a few are chemically active. The short-term trajectories, in composition space, of the particles used to sample the local gas mixture can therefore be described using many fewer species and reactions than the original, comprehensive model.

Our approach relies on an a priori partitioning of the composition space into a user-specified number of regions, over which suitable reduced chemical representations and chemical models are identified. A computational particle in the LES/PDF simulation evolves according to, and carries only the variables present in, the reduced representation corresponding to the composition space region it belongs to. This region is identified using a low-dimensional binary tree search algorithm, thereby keeping the run-time overhead associated with the adaptive approach to a minimum. An overview of the adaptive strategy is presented, with details being provided for the major components of the algorithm. The adaptive treatment of the chemistry is then implemented within the ISAT/RCCE framework validated previously by Hiremath et al. [Hiremath, Ren & Pope, Combust. Flame, 2011]. A proof-of-concept of the combined adaptive chemistry and tabulation strategy is presented in different configurations, including the simpler partially stirred reactor (PaSR) with pair-wise mixing configuration. Even in the stringent PaSR case, results indicate that for a similar overall computational cost, using a set of reduced models adaptively using the proposed strategy increases accuracy by up to an order of magnitude compared to a non-adaptive approach that is, using a single reduced chemical model valid over the entire composition space.

pp427@cornell.edu

W3P072 STRATEGIES FOR ACCELERATING COMBUSTION SIMULATIONS WITH GPUS

Kyle Niemeyer¹, Chih-Jen Sung²

¹Oregon State University, United States ²University of Connecticut, United States

Combustion simulations with detailed chemical kinetics require the integration of a large number of ordinary Differential Equations (ODEs), with at least one ODE system per spatial location solved every time step. This task is well-suited to the massively parallel processing capabilities of Graphics Processing Units (GPUs), where individual GPU threads concurrently integrate independent ODE systems for different spatial locations. However, the typical high-order implicit algorithms used in combustion modeling applications (e.g., VODE, LSODE) to handle stiffness involve complex logical flow that causes severe thread divergence when implemented on GPUs, thus limiting the performance. Alternate algorithms are therefore needed.

We will demonstrate that standard explicit integrators such as the fifth-order Runge–Kutta–Cash–Karp (RKCK) algorithm can be used in the case of nonstiff chemical kinetics. When implemented on GPUs, we demonstrate a performance speedup of up to 126 times over the same algorithm executed on a single CPU with a nine-species hydrogen oxidation mechanism. In the case of moderate stiffness, the second-order stabilized Runge–Kutta–Chebyshev (RKC) method can be used. The GPU-based RKC algorithm performed 64 times faster than the same algorithm executed a CPU for an ethanol oxidation mechanism with 57 species; in addition, GPU-RKC outperformed a six-core parallel CPU version of VODE by a factor of 57 with the well-known GRI-Mech 3.0 methane oxidation mechanism (53 species). However, in the case of more severe stiffness, the performance of GPU-RKC degraded below that of VODE on six CPUs, demonstrating the need for a stiff integrator appropriate for GPU acceleration. Pending results, we will also demonstrate that specialized GPU-based stiff integrators can replace standard implicit algorithms even in the case of severe stiffness.

Kyle.Niemeyer@oregonstate.edu

W3P073 RMG-PY : THE PYTHON VERSION OF REACTION MECHANISM GENERATOR

Richard West¹, Joshua Allen², Pierre Bhoorasingh¹, Connie Gao², William Green²

¹Northeastern University, United States ²Massachusetts Institute of Technology, United States

The open-source software project Reaction Mechanism Generator (RMG) has been generating detailed kinetic models for hydrocarbon combustion since its launch in 2003, with continued development over the decade adding many new features. In recent years a new version has been written, in the Python programming language, with the design aims of facilitating future development. RMG-Py has new capabilities, and an interactive website allowing easy estimation of thermochemical and kinetic parameters, interrogation and modification of the databases, and visualization of results.

RMG-Py is an open source project developed collaboratively on GitHub. Current features include: rate-based

model expansion; thermodynamics estimation using group additivity or, optionally, on-the-fly semi-empirical quantum chemistry calculations; extensible libraries, to allow model expansion from a known seed mechanism, or inclusion of trusted thermodynamic and kinetic data; kinetics estimates via functional-group interpolation or group-additive estimates; pressure-dependent reaction network master-equation calculations based on Modified Strong Collision or Reservoir State methods; simultaneous mechanism generation for several conditions of interest; transport properties estimation; pruning of minor species to keep memory requirements in check.

r.west@neu.edu

W3P074 **EXPERIMENTAL AND MODELING INVESTIGATION OF THE OXIDATION OF DIMETHYL ETHER IN A JET-STIRRED REACTOR WITH CRDS DIAGNOSTIC**

Olivier Herbinet¹, Anne Rodriguez², Ophélie Frottier², Baptiste Sirjean², René Fournet¹, Christa Fittschen³, Frédérique Baatin-Leclerc²

¹Université de Lorraine, France ²LRGP – CNRS, France ³Université de Lille, France

Due to the current issue concerning the growing primary energy demand, not to mention a general interest in sustainable development, bio-fuels became very fashionable in recent years. They are subject to a lot of research on combustion with the characterization of the reactivity and pollutant emissions. The molecule of Dimethyl Ether (DME) has led to a strong interest in the field of combustion. Corresponding to the simplest linear ether (CH₃-O-CH₃), it has a high cetane value (55-60) and a low toxicity. Promising studies have highlighted key-strengths of this molecule as an additive agent or even an alternative diesel fuel. Among these advantages, we find a particularly significant decrease in the formation of soot and NO_x particles. Several experimental and theoretical studies have investigated the combustion of DME, using various equipments (jet-stirred reactor, shock-tube, counterflow diffusion flame, variable-pressure flow reactor) and under different conditions. Even if they bring essential information, they are unable to predict a single valid model for all circumstances. The objective of this study is to investigate DME oxidation with a different approach in order to complete existing experimental data sets, and subsequently better understand its reaction chemistry.

This was done with several experiments carried out in a jet-stirred reactor operating at 800 Torr, 500-1100 K, and at different equivalence ratios: 0.25, 1 and 2. Reaction products have been analyzed using two complementary methods: Gas Chromatography (GC) and Cavity Ring-Down Spectroscopy (CRDS). GC is efficient in separating compounds and allows to analyse a wide range of products like CO, CO₂, hydrocarbons, CH₃CHO and CH₃OCHO ; while CRDS is an absorption spectroscopic technique which allows to analyze species such as CH₂O, H₂O and H₂O₂ (undetected by GC).

Significant differences were observed when comparing experimental results to data computed with a model from the literature, especially at low-temperature (500-750 K) where the reactivity was over-predicted. A new model was developed and quantum mechanics calculations have been performed to improve the set of kinetic parameters used in this new model.

olivier.herbinet@univ-lorraine.fr

W3P075 **HIGH AND LOW TEMPERATURE OXIDATION OF METHYL-STEARATE, -OLEATE AND -LINOLEATE IN JSR**

Olivier Herbinet¹, Anne Rodriguez², Frédérique Battin-Leclerc², Alessio Frassoldati³, Tiziano Faravelli³, Eliseo Ranzi³

¹Université de Lorraine, France ²LRGP – CNRS, France ³Politecnico di Milano, Italy

The attention towards biodiesel combustion is increasing worldwide due to the interest in renewable energy. The five major components of typical biodiesel fuels are both saturated and unsaturated methyl-esters, specifically methyl-palmitate, -stearate, -oleate, -linoleate and -linolenate. The degree of unsaturation of these molecules has a noticeable influence on the combustion characteristics and emissions. The combustion of large saturated methyl-esters is very similar to the one of methyl-decanoate, while large unsaturated methyl esters are significantly less reactive at low and intermediate temperatures. The ignition times of the four methyl esters in the NTC region follow the same order as their cetane numbers. In this work, we present new experimental data on the oxidation of large methyl-esters at high and low temperature. The experiments, performed in a Jet Stirred Reactor (JSR) at 800 Torr and temperatures 500-1050 K, refer to mixtures of benzene (92% mol) and methyl-esters (8%), such as stearate, oleate, linoleate. The residence time is 2 s and the initial total fuel mole fraction is 0.5%. The reactivity of benzene can be considered negligible below 900 K under these conditions.

Due to the size and complexity of the molecules, the detailed kinetic mechanism of Westbrook et al., able to describe the high and low temperature reactivity of the five components biodiesel fuels, contains more than 4800 species and ~20,000 reactions. Saggese et al. developed a model of these biodiesel fuels starting from the POLIMI kinetic mechanism by introducing new ~60 lumped species and ~2000 reactions. The limited dimension of the overall kinetic scheme, involving ~420 species, allows an easier application of the model for practical applications. Due to the lack of experimental data, Saggese et al. only theoretically showed that large differences in the ignition delay times of biodiesel fuels components exist at low and intermediate temperatures and that the lumped and detailed mechanisms predicted the same trends, but with a larger effect of the presence of unsaturations in the case of the detailed model. The new experimental measurements presented in this work, which include a detailed analysis of the intermediate products, are compared to the lumped POLIMI_1311 kinetic mechanism (<http://creckmodeling.chem.polimi.it>).

The comparison showed that the lumped model is able to correctly characterize the effect of the different degree of unsaturation on the low temperature oxidation of methyl-esters. Nevertheless, the comparisons showed that this kinetic model overestimates the reactivity at very low temperatures. For this reason we revised the model in order to improve the predictions of the low temperature reactivity of the system. The revision of the kinetic scheme was performed adopting proper simplifications in order to maintain the lumped structure of the mechanism and limit the total number of species. The model was also further validated using recent experimental data, such as the ignition delay times of methyl-esters at 7 atm, and the oxidation of stoichiometric mixtures of *n*-decane with methyl-palmitate methyl-oleate at ~1 atm.

olivier.herbinet@univ-lorraine.fr

W3P076 A DETAILED KINETIC MODEL FOR METHYL BUTANOATE OXIDATION

Mickael Matrat¹, Laurent Catoire¹, Guillaume Dayma², Philippe Dagaut²

¹ENSTA Paristech, France ²Centre National de la Recherche Scientifique, France

2nd generation biofuel, mainly originated from non food lignocellulosic materials, could potentially be an interesting solution for supplying a non negligible amount of biofuel (e.g. biooil or biodiesel) to replace crude oil derivatives. Unsaturated or saturated methyl and ethyl esters are potential future biodiesel but their higher oxygen content impacts their reactivity. Therefore, investigating these new species that differ from the current diesel structure is a challenge but necessary. New pollutants can be emitted and combustion characteristics may be different. The objective here is to obtain an oxidation mechanism for methyl levulinate. Because of the lack of experimental results, methyl butanoate has been chosen for testing the capabilities of a mechanism generator (RMG, in development at MIT) that could help developing levulinates mechanisms. Methyl butanoate may present the same reactivity due to the ester function and many experimental studies are available for testing the mechanism generated. In order to test the sub-mechanism, the methyl propenoate and methyl formate, two intermediate species from the methyl butanoate oxidation, have been chosen. New experimental data for methyl butanoate and methyl propenoate measured in a jet stirred reactor at 10 bar and for different equivalence ratios will also be compared to the model. The detailed kinetic model generated includes 11890 reactions and 272 species. Initial model did not predict well the different sets of data and refinement based on sensitivity analysis and rates of production lead to about 30 rates replacement with existing data or slight adjustments within the existing uncertainty factor when existing. In addition, five reactions were added to better simulate methyl formate ignition delays. The final mechanism successfully models several set of data of lean and rich compositions and in different conditions (1-10 bar, $\approx 700 - 1900$ K) for three molecules, namely methyl butanoate, propenoate and formate. Two examples are given in Figure 1. A first mechanism is also generated for methyl levulinate based on the changes required to generate a methyl butanoate oxidation model.

mickael.matrat@ensta-paristech.fr

W3P077 EXPERIMENTAL AND KINETIC MODELING STUDY OF 2-METHYLFURAN PYROLYSIS AT VARIOUS PRESSURES

Yuyang Li, Zhanjun Cheng, Lili Xing, Yizun Wang, Wenhao Yuan, Zhandong Wang, Fei Qi

University of Science and Technology of China, China

As a new kind of biofuels, furan and its derivatives, such as 2-methylfuran (MF) and 2,5-dimethylfuran (DMF), have received more and more attentions because of the rapid consumption of fossil fuels and the novel production methods from biomass. Understanding the combustion chemistry of furan and its derivatives is crucial for their practical utilization, and requires thorough detection of their combustion products which can provide solid validation for their combustion models. This work presents a new experimental study of MF pyrolysis at 30, 150 and 760 Torr using synchrotron vacuum ultraviolet photoionization mass spectrometry, and reports a modified pyrolysis model of MF.

The experimental work was performed at National Synchrotron Radiation Laboratory, Hefei, China. Rate constants of several radical attack reactions of MF and some reactions of small hydrocarbons in the MF model developed by Somers were updated according to the validation against the present and previous pyrolysis data of MF. The simulation was carried out using Plug Flow Reactor module in Chemkin-Pro software.

Based on the Rate Of Production (ROP) and sensitivity analyses, main pathways in the decomposition of MF and the growth of aromatics are determined. The unimolecular decomposition to produce 1-butyne + CO and acetyl + propargyl, H-atom abstraction to produce 2-furanylmethyl radical, ipso-substitution by H to produce furan, and H-atom attack to produce $\text{CH}_2\text{CHCHCO} + \text{CH}_3$ and $\text{C}_4\text{H}_7 + \text{CO}$ are concluded to dominate the primary decomposition of MF. Further decomposition of 2-furanylmethyl radical leads to great production of vinylacetylene. Many large aromatic hydrocarbons, including benzene, benzyl radical, toluene, phenylacetylene, styrene, indenyl radical, indene, naphthalene, and so on, are also detected. It is observed that at the same conversion of fuels, the concentrations of benzene and toluene in the pyrolysis of MF is slightly higher than those in the pyrolysis of DMF. Based on the ROP analysis, it is concluded that the higher concentrations of benzene and toluene in the MF pyrolysis than in the DMF pyrolysis under the similar conditions mainly result from the greater formation of propargyl radical and 1,3-butadiene.

yuygli@ustc.edu.cn

W3P078 UNCERTAINTY PROPAGATION AND GLOBAL SENSITIVITY ANALYSIS FOR THE EVALUATION OF

MECHANISMS DESCRIBING LOW TEMPERATURE DME OXIDATION

Alison Tomlin¹, Michal Vasínek², Vaclav Nevrlý², Jakub Dlabka², Edirin Agbro¹

¹Leeds University, United Kingdom ²Technical University of Ostrava, Czech Republic

Cleaner combustion devices based on the utilization of oxygenated fuels provide promising options for the development of lower carbon strategies in the transportation and energy sectors in the near future. The high heating value, high cetane number and the ability of Dimethyl Ether (DME) to provide low gaseous and particulate emissions makes it a suitable substitute for most existing direct injection diesel engines. NO_x emissions when using DME may also be lower than with diesel since ignition delays are shorter. The ability of combustion models to predict emissions properties and ignition delays is therefore critical to designing practical combustion devices in order to use DME optimally. This relies on the availability of accurate and robust detailed chemical kinetic models for DME oxidation. Several DME oxidation mechanisms have recently been proposed that could potentially fulfil this purpose¹⁻³, although the mechanisms may display either mechanistic, or parametric differences. It is therefore useful to perform an evaluation of such mechanisms, to explore any major differences between them, and to evaluate how inherent uncertainties in their input data may impact on their predictive capability with respect to available target experimental data. Liu et al. for example highlight the over-prediction of key intermediates HO₂ and H₂O₂ by current schemes and suggest that large uncertainties may be present at high pressure³. In this work we perform a global uncertainty propagation of errors within input rate parameterisations for several DME oxidation mechanisms¹⁻³ in order to assess their ability to predict key experimental targets such as oxygenated products within a low temperature atmospheric pressure flow reactor⁴, as well as ignition delays based on recent data obtained within a high pressure Rapid Compression Machine (RCM), within the temperature range (550 K – 700 K). The uncertainty propagation is based on a quasi-random sampling approach where input rate constants are varied based on a uniform distribution in log (k) space within their uncertainty bounds and sample sizes of up to 4096 are utilized to generate predicted target output distributions. A new Graphical User Interface (GUI) has been designed to facilitate global sampling based uncertainty/sensitivity studies within the Cantera software suite and will be illustrated.

Based on current uncertainties within the mechanisms, it is shown that the predicted distributions of key targets for a single experimental target can be wide. Predicted concentrations of CH₂O, CH₃OCHO and H₂O₂ as well as ignition delays may vary over several orders of magnitude for some conditions. However, in all cases the experimental target data is encompassed by the 75th percentile of the predicted output distributions, indicating that the mechanistic formulation of the models is likely to be sound, but that better quantification of key rate data is required. A global sensitivity analysis is then performed in order to highlight the main sources of predictive uncertainty within the schemes. Sensitivities to the key reactions will be demonstrated and we show that the isomerisation step CH₃OCH₂O₂ = CH₂OCH₂O₂H strongly influences the formation of all species at the 550 K as well as ignition delays and methyl formate production over the whole temperature range. At higher temperatures the competition between 2nd O₂ addition to CH₂OCH₂O₂H and its decomposition to OH+CH₂O dominate uncertainties in H₂O₂ predictions, whereas CH₂O prediction is dominated by reactions of OH with DME and CH₂O above 650 K. There are some minor differences between the key product channels between the schemes. Most of the sensitivities are highly nonlinear across the uncertainty range and significant 2nd order interactions between parameters were found. Finally, the impact of new data from a combined experimental/theoretical study⁶ of CH₃OCH₂+O₂ on the prediction of key targets will be explored.

A.S.Tomlin@leeds.ac.uk

W3P079

GLOBAL UNCERTAINTY PROPAGATION AND SENSITIVITY ANALYSIS IN THE CH₃OCH₂ + O₂ SYSTEM: COMBINING EXPERIMENT AND THEORY TO CONSTRAIN KEY RATE COEFFICIENTS IN DME COMBUSTION.

Alison Tomlin¹, Robin Shannon¹, Michael Pilling¹, Mark Blitz¹, Paul Seakins¹, Struan Robertson²

¹Leeds University, United Kingdom ²Accelrys Ltd, Science Park, United Kingdom

Theoretical calculations provide a useful way of estimating rate coefficients for systems over wide ranges of temperatures and pressures, not all of which are accessible from experiments. However, several studies have recently demonstrated that errors in calculated transition state energies, for example, can lead to substantial uncertainties in predicted rate coefficients. These have been suggested to be from a factor of 2 for simple abstraction reactions, up to 5-10 for complex multi-well systems, even when using high levels of theory. When experimental data are available for a system, these can be used to substantially reduce the uncertainties in predicted rate coefficients by constraining the *ab initio* parameters. In this work the CH₃OCH₂ + O₂ system, of relevance to the low temperature combustion of DME, is used to illustrate this point. The input parameters for master equation calculations and their uncertainties are first derived from theory and then subsequently refined through fitting to experimental data using a Levenburg Marquardt algorithm available within the MESMER code. Uncertainties in predicted yields and overall and elementary rate constants are compared for the two approaches. At each stage, a global sensitivity analysis is also performed in order to first demonstrate how particular experiments can help to constrain the input parameters to the master equation, and secondly to explore the causes of remaining uncertainties following the fitting process. The uncertainty and sensitivity analyses are performed both for the conditions of existing experiments, and for conditions under which no experimental data are available, allowing the investigation of conditions relevant to practical combustion devices. Correlations between input parameters, present due to the fitting procedures, are taken into account. For reactions of importance to low temperature

DME oxidation, the uncertainties from the system constrained by experiment are predicted to be between factors of 2-3. However, substantial differences are found between predicted elementary rate constants in this work and those used within currently available mechanisms, suggesting that such parameters should be updated, thereby reducing overall uncertainties within low temperature DME oxidation models.

A.S.Tomlin@leeds.ac.uk

W3P080 EXPERIMENTS AND MODELING OF A LARGE OXYGENATED MOLECULE: TRI-PROPYLENE GLYCOL MONOMETHYL ETHER (TPGME)

Ultan Burke¹, William Pitz², Henry Curran¹

¹National University of Ireland, Ireland ²Lawrence Livermore National Laboratory, United States

TPGME is being considered as a fuel additive due to its soot reduction capabilities. It has been compared previously to a selection of other oxygenated soot reducing compounds and showed favourable trends. These results have led to interest in studying the combustion chemistry of this molecule. From a kinetic modeling point of view its structure provides an interesting challenge. It has primary, secondary and tertiary hydrogen atoms, it has both alcoholic and ether functional groups and it has a high oxygen to carbon ratio.

Ignition delay time measurements behind reflected shock waves were recorded in order to provide validation targets for a lumped kinetic model. No previous experimental data was available for TPGME. Its low vapour pressure is prohibitive when attempting to study it practically, but using a heated shock tube and laser absorption measurements ignition delay times were measured for 0.25% TPGME at $\phi = 0.5$, 1.0 and 2.0 and pressures of 10 and 20 atm covering a temperature range of 990 – 1540 K.

(Image) A lumped approach was taken to building a model for TPGME's oxidation. There are 8 structural isomers of TPGME. Isomer #1 (Image) was chosen to represent of all isomers in order to simplify our modeling efforts. Rate constants were assigned via analogies to similar chemical environments. This initial modeling effort was capable of predicting the experimental data very well.

Further experimental data is needed to continue development of this chemical kinetic model. Low-temperature oxidation and high-temperature pyrolysis data would allow further validation of this model in order to improve its predictive capabilities.

u.burke1@nuigalway.ie

W3P081 OXIDATION PATHWAYS OF CINEOLE

Connie Gao¹, Adam Scheer², Aaron Vandeputte¹, Jorge Aguilera-Iparraguirre¹, William Green¹, Craig Taatjes²

¹Massachusetts Institute of Technology, United States ²Sandia National Laboratories, United States

Recently, direct decomposition of cellulosic biomass by fungi was found to produce significant quantities of cineole (1,3,3-trimethyl-2-oxabicyclo[2,2,2]octane), a saturated cyclic ether and monoterpenoid. This has prompted researchers to consider cineole as a prospective biofuel for use in advanced engines. However, little is known about cineole's fundamental oxidation chemistry and viability as a fuel. In this work, the low temperature (550 – 650 K) oxidation pathways of cineole were explored using a combination of experiment and theory. Chlorine-initiated oxidation using Multiplexed Photoionization Time-Of-Flight Mass Spectrometry (MPIMS) was used to identify products as a function of time, mass, and photoionization energy. Theoretical quantum calculations at the CBS-QB₃ level were performed to elucidate the potential energy surfaces associated with key species and expected pathways. These calculations were incorporated into the Reaction Mechanism Generator (RMG) software package to generate a detailed reaction network for cineole.

The generated model predicts the major products found in experiment and demonstrates similar temperature dependencies in product distribution. Under the studied conditions, cineole's decomposition is initiated by hydrogen abstractions by Cl radical. The resulting alkyl radicals ($m/z = 153$) can add O₂ to form RO₂ or thermally decompose, mainly to acetone ($m/z = 58$) and C₇H₁₁ radicals ($m/z = 95$). One important general oxidation pathway is intramolecular hydrogen abstraction of RO₂ to form a carbon-centered radical, QOOH. These QOOH can undergo ring closure upon ejection of OH to form a cyclic ether moiety, a chain-propagating channel. This cyclic ether formation channel leads to a plethora of products with atomic masses that are 15 amu higher than the primary intermediate radicals, mainly C₇H₁₀O ($m/z = 110$) and C₁₀H₁₆O₂ ($m/z = 168$).

connieg@mit.edu

W3P082 LOW-TEMPERATURE IGNITION OF DME/AIR MIXTURE AT ATMOSPHERIC PRESSURE: ON THE TRANSITION FROM COOL FLAME TO HOT FLAME

Jian Gao¹, Liqiao Jiang², Daiqing Zhao², Yuji Nakamura¹

¹Toyohashi University of Technology, Japan ²Chinese Academy of Sciences, China

Dimethyl Ether (DME: CH₃OCH₃) has been considered as a promising alternative fuel due to its merits of favorable compression ignition property and little soot formation in combustion field. A deep understanding of low-temperature ignition of DME is important in two engineering aspects: the design of engine and the safety for preventing accidental explosions. The ignition of DME exhibits a two-stage mode, which shows complexity due to the existence of

the Negative Temperature Coefficient (NTC) effect. The objective of this study is to clarify the ignition characteristics of DME, and special attention is given to the transition from a cool flame to a hot flame.

Low-temperature (< 550 K) ignition regime of DME/air mixture is experimentally investigated in a laminar flow reactor, which is updated from our previous work. The ignition limit is depicted in the temperature-equivalence ratio (TR, ex - ϕ) plane. It is found that the equivalence ratio has a dramatic impact on the ignition regime: at a specific equivalence ratio ($\phi = 1.6$), cool flames transits to hot flames; while as equivalence ratio increases, the transition is significantly suppressed, resulting in weak flames. To investigate the ignition kinetics, computation is then performed using the plug-flow model based on the latest detailed kinetics by Zhao et al. The Zhao model predicts well the ignition limit, however, fails to predict the transition from a cool flame to a hot flame. Reaction pathway analyses suggest that the competition between the β -scission reaction and the molecular oxygen addition reaction of the methoxy-methyl radical (CH_3OCH_2) could strongly influence the transition. This influence is further investigated via a slight modification of the activation energy of the β -scission reaction of the CH_3OCH_2 radical. Depending on this modification, both the ignition limit and the ignition regimes against equivalence ratio are well predicted: a two-stage ignition regime corresponds to a hot flame in the experiments, and a transition suppressed ignition regime corresponds to a weak flame in the experiments, respectively. In addition, the kinetics model with this modification shows reasonable agreement with shock tube ignition delay results. It is indicated that the modification strongly influences the reactivity in the NTC region, therefore influences the transition to a hot flame. Further investigations determining the rate constants of the reactions of the CH_3OCH_2 radical may be needed to improve the DME oxidation kinetics.

gao@me.tut.ac.jp

W3P083

THERMAL DECOMPOSITION MECHANISM OF 2-METHOXYFURAN

Kimberly Urness¹, Barney Ellison¹, John Daily¹, John Simmie², Tyler Troy³, Musahid Ahmed³

¹University of Colorado at Boulder, United States ²National University of Ireland, Galway, Ireland

³Lawrence Berkeley National Laboratory, United States

Substituted furans including furanic ethers derived from nonedible biomass have been proposed as second-generation biofuels. In order to use these molecules as fuels it is important to understand how they break apart thermally. In this work a series of experiments were conducted to study the unimolecular and low-pressure bimolecular decomposition mechanisms of the smallest furanic ether, 2-methoxyfuran. CBS-QB₃ calculations indicate this substituted furan has an unusually weak O-CH₃ bond, approximately 45 kcal mol⁻¹, thus the first reaction is bond scission resulting in CH₃ and 2-furanyloxy radicals. Final products from the ring opening of the furanyloxy radical include 2 CO, HCCH and H. The decomposition of this molecule was studied over a range of concentrations (0.0025–0.1%) in helium or argon in a heated Silicon Carbide (SiC) microtubular flow reactor (0.66–1 mm i.d., 2.5–3.5 cm long) over a range of reactor wall temperatures from 300 to 1300 K. Inlet pressures are 150 to 300 Torr and the gas mixture emerges as a skimmed molecular beam at a pressure of approximately 10 μ Torr. Products formed at early pyrolysis times (50–200 μ s) are detected by 118.2 nm (10.487 eV) PhotoIonization Mass Spectrometry (PIMS), tunable synchrotron VUV PIMS and matrix infrared absorption spectroscopy. Secondary products resulting from H or CH₃ addition to the parent and radical reactions with 2-furanyloxy include CH₂=CH-CHO, CH₃-CH=CH-CHO, CH₃-CO-CH=CH₂ and furanones; at the conditions in the reactor we estimate these reactions contribute to at most 1-3% of total methoxyfuran decomposition. This work also includes characterization of the 2-furanyloxy radical by the assignment of several intense vibrational bands in an Ar matrix and a low-resolution estimate of the ionization threshold and photoionization efficiency curve of this allylic lactone.

Kimberly.Urness@colorado.edu

W3P084

KINETIC STUDY OF LOW- AND INTERMEDIATE-TEMPERATURE OXIDATION OF 2-METHYLFURAN AND 2-METHYLFURAN-PRIMARY REFERENCE FUEL BLENDS

Kotaro Tanaka, Naozumi Isobe, Kota Sato, Mitsuru Konno, Ibaraki University, Japan

Recently, furan and its derivatives such as 2-methylfuran (MF) and 2,5-DiMethylFuran (DMF) have been produced from residual or nonfood biomass by a catalytic strategy. In addition to offering a novel production process, furans provide certain advantages in terms of their physicochemical properties over ethanol, the chief biofuel in the current market. However, more fundamental studies are required to utilize MF and DMF as alternative fuels. Besides the investigations of MF and DMF combustion charaterers, it is necessary to evaluate the effects of MF or DMF addition on the ignition delay times of Primary Reference fuel (PRF), because the blended fuels of gasoline or diesel with biofuels are already being utilized,. In this study, the autoignition characteristics of MF and MF-PRF blends were studied using a rapid compression machine at an equivalence ratio of 1.0 with an oxygen concentration of 4.1% and 16.4% in nitrogen and argon or nitrogen and carbon dioxide, in the temperature range 694–1063 K and pressure range 21.0–30.1 atm, respectively. The measured ignition delays were simulated using a detailed kinetic model of DMF constructed by Somers et al., which included the MF oxidation mechanism and a detailed kinetic model of MF-PRF blends.

As a result, in the intermediate temperature range, the ignition delays of MF are shorter than those of PRF₉₀. The ignition delays of MF-PRF₉₀ blends become slightly shorter than those of PRF₉₀, which indicates that the MF promotes the ignition in this temperature range. On the other hand, in the low temperature range, the ignition delays of MF are longer than those of PRF₉₀. In the case of MF, ignition does not occur below 846 K. The ignition delays of MF-PRF₉₀

blends become drastically longer than those of PRF₉₀. In the low-temperature range, MF is found to inhibit the PRF₉₀ oxidation. Simulated ignition delays using the existing MF model and MF-PRF model, which is constructed in this study, are in reasonably agreement of those of experiments in the low temperature range. Rate-of-product analysis indicates that the ring-opening reactions of MF followed by H abstraction reactions from MF by radicals, and radical addition reactions to MF are considered to be the key reactions in the MF oxidation mechanism. In the intermediate temperature range, the model does not predict the experimental results well; therefore, further improvement is required.

k_tanaka@mx.ibaraki.ac.jp

W3P085

REVISITING THE LOW TEMPERATURE COMBUSTION OF DIMETHYL ETHER

Ulián Burke, Kieran Somers, Henry Curran, National University of Ireland, Ireland

The combustion of dimethyl ether has been extensively studied due to its ability to act as an ignition enhancer and emissions reducer when blended with fossil fuels, and due to its promise as a neat biofuel. In turn, there are numerous chemical kinetic models in the literature which describe its combustion in flow/stirred reactors, flames, shock tubes etc.

However, in order to reproduce the experiments against which they were validated, the kinetic and thermodynamic parameters applied in current mechanisms can vary significantly from one another, and from experimental/theoretically derived recommendations.

Surprisingly, despite the many DME mechanisms which have arisen since the late 90's, none have attempted to incorporate the theoretical rate constants of Yamada et al. (Int. J. Chem. Kin 32 (7) (2000), 435–452.) for DME low-temperature combustion from early 2000, relying instead on rate constants estimated based on Evans-Polanyi correlations and analogy to alkanes (whose kinetics are also still open to debate). Effectively all the mechanisms in the literature require unreasonable alterations to the rate constant recommended by for the decomposition of O=CH-CH₂-O-CH₂-OOH to an alkoxy and a hydroxyl radical. Virtually all current mechanisms have had to alter the rate constant recommended for the decomposition of CH₃OCH₂ from Li et al. (J. Phys. Chem. A., 108 (11) (2004) 2014–2019.) in order to predict low-temperature/NTC data accurately. These reactions form the cornerstone of any model which aims to predict the low-temperature combustion of DME, yet there is still no consensus on what kinetic parameters are representative of the physical truth.

So despite the mechanism of DME oxidation being well-known, and despite over a decade passing since the still popular Curran/Fischer (Int. J. Chem. Kin 32 (12) (2000), (a) 713–740 (b) 741–759.) mechanism was described, there are still inconsistencies between the mechanisms which are currently in wide-spread use, and the literature rate constants which perhaps best describe the elementary kinetics of low-temperature DME combustion.

Here we present an updated chemical kinetic mechanism for DME pyrolysis and oxidation where the most recent experimental and/or theoretical determinations of elementary reaction kinetics are adopted, where available, into an existing C₀–C₂ chemistry set (AramcoMech 1.3). Whilst initially these updates had a deleterious impact on the predictive capability of the mechanism, minimal alterations were ultimately required to reproduce literature data, which we ultimately attribute to a pressure-dependent treatment of the low temperature combustion kinetics of CH₃OCH₂ radical and its derivatives.

The unimolecular decomposition of the CH₃OCH₂ radical and corresponding low-temperature reactions of RO₂ and QOOH species have been treated as pressure-dependent via QRRK/MSR computations. Non-negligible fall-off is observed in the rate constants for CH₃OCH₂ and CH₂OCH₂OOH radical β-scission reactions, which are of importance in predicting low-temperature combustion properties. RRKM/ME calculations on the decomposition of CH₃OCH₂ radical were also carried out to assess the validity of the QRRK/MSR results, with the two methods diverging by a factor of ~2 in the worst instances. The current work highlights the value which high-level quantum chemistry coupled with RRKM/ME computations would have in removing (a) the remaining uncertainty in the kinetics of the low-temperature oxidation pathways of DME, and (b) the many disparities which exist in current kinetic mechanisms for this supposedly well-understood fuel.

u.burke1@nuigalway.ie

W3P086

RELATIONSHIP BETWEEN OCTANE NUMBER, CETANE NUMBER, AND METHANE NUMBER: ANALYSIS OF CONSTANT VOLUME COMBUSTION CHAMBER AND VARIABLE COMPRESSION RATIO ENGINE RESULTS

Marc Baumgardner, Anthony John Marchese, Colorado State University, United States

The Octane Number (ON), Cetane Number (CN), and Methane Number (MN) metrics have historically been used to characterize the relative reactivity of fuels used in spark ignited and compression ignition engines. The relationship between ON and CN has previously been reported to approximate an inverse proportionality, but a fundamental relationship between the two metrics has yet to be developed. In this study, a phenomenological relationship between these two fuel reactivity scales is presented. The relationship is then compared against experimental results from 18 different liquid fuel blends tested in a Waukesha Fuel Ignition Tester (FIT), a device typically used to measure Derived Cetane Number (DCN), and a Cooperative Fuels Research (CFR) engine. Fuel blends of Primary Reference Fuels (PRFs), toluene/*n*-heptane, ethanol/*n*-heptane, and *n*-butanol/*n*-heptane are examined and the results reveal different reactivity trends for the alcohol fuels compared to the hydrocarbon fuels. Chemical kinetic modeling suggests that differences in the observed alcohol reactivity trends are due in large part to the relatively higher rates of H abstraction by

OH radicals from alcohols compared to traditional fuels. Additionally, a new parameter called knock length is proposed as a more fundamental metric to examine fuels in Spark Ignited (SI) engines as well as a way to investigate results that cannot be explained by either ON or MN scales. The knock length parameter can be calculated directly from 0-D homogeneous ignition delay and 1-D steady laminar flame speed computations using full detailed chemical kinetic mechanisms. As part of the knock length portion of this work, 5 different methane/hydrogen fuel blends were tested in a CFR engine and the experimental results were interpreted using knock length computations using CHEMKIN. The results of this study suggest the potential to use knock length for comparing the reactivity of real fuels across various engine platforms without the use of reference fuels. For example, knock length could be used to compare reactivity differences between liquid and gaseous fuels and could potentially be extended beyond SI engines to dual-fuel applications.

marc.baumgardner@gmail.com

W3P087 **A COMPUTATIONAL APPROACH FOR GASOLINE SURROGATE FUEL FORMULATION TO EMULATE PHYSICAL AND CHEMICAL KINETIC PROPERTIES**

Ahfaiz Ahmed, Gokop Goteng, William Roberts, Mani Sarathy, King Abdullah University of Science and Technology, Saudi Arabia

Gasoline is the most widely used fuel for light duty automobile transportation. Due to its complex nature, studying the fundamental combustion properties of real gasoline fuels is intractable. Therefore, surrogates with simpler molecular composition that represent real fuel behavior in one or more aspects are needed to enable experimental and computational combustion research. This study presents a novel computational approach combining regression modeling with physical and chemical kinetics simulations to formulate surrogates for FACE (Fuels for Advanced Combustion Engines) gasoline A and C. The computational methodology links various simulations executed across software platforms. The regression algorithm implemented in MatLab is linked to Refprop for simulation of distillation curves and calculation of physical properties. The MatLab code generates surrogate compositions at each iteration, which are then automatically inputted to CHEMKIN input files and submitted to homogenous batch reactor simulations for prediction of Research Octane Number (RON). The regression algorithm determines the optimal surrogate composition to match the FACE A and C fuel properties, specifically H/C ratio, density, distillation behavior, carbon types and RON. The palette species and carbon types are selected based on Detailed Hydrocarbon Analysis (DHA) of FACE A and C. The surrogate-fuel properties were compared to the measured real-fuel properties, and a good agreement was observed.

ahfaz.ahmed@kaust.edu.sa

W3P088 **A COMPARATIVE STUDY OF THE OXIDATION CHARACTERISTICS OF TWO GASOLINE FUELS AND AN N-HEPTANE/ISO-OCTANE SURROGATE MIXTURE**

Tamour Javed, Ehson Fawad Nasir, Aamir Farooq, King Abdullah University of Science and Technology, Saudi Arabia

Energy is considered to be the driving force and lifeline for modern economies. World energy consumption is projected to grow by 56 % through 2040 and approximately 80% of this demand will be met by fossil sources (coal, oil, gas) [US EIA 2013]. The demand for petroleum-based liquid fuels and other alternative/renewable liquid fuels is also increasing rapidly to fulfill the requirements of growing transportation sector. Recently, advanced engine concepts (HCCI, PCCI, RCCI etc.) have received special attention due to their promise of decreasing transportation related emissions and increasing engine efficiency. The performance and control of these new engine concepts is closely linked to the chemical kinetics phenomena.

Gasoline is most widely used light duty transportation fuel. Ignition delay times and CO, H₂O, OH and CO₂ species time-histories were measured for two FACE (Fuels for Advanced Combustion Engines) gasoline fuels and one PRF (Primary Reference Fuel) blend behind reflected shock waves. Using these data, it was possible to compare the behavior of the various species for different gasolines and PRF blend. The FACE gasolines chosen for this work are primarily paraffinic and have the same octane rating (RON 84), but contain widely varying amounts of *iso*-/*n*-paraffins and aromatics. Species time-histories and ignition delay times were measured using laser absorption methods over a temperature range of 1350 – 1550 K and pressures near 2 atm. The species time-histories and ignition delay times of the PRF surrogate reasonably duplicated the trends found in measured speciation profiles and ignition delay times of the two widely different FACE fuels. However, when compared to recent gasoline surrogate mechanisms, the simulations did not capture some of the kinetic trends found in the species time-history profiles. To our knowledge, these data provide some of the first shock tube time-history data for gasoline fuels and PRF surrogates and should enable further improvements in detailed gasoline kinetic mechanisms.

tamour.javed@kaust.edu.sa

W3P089 **EFFECTS OF CHEMICAL ADDITIVES ON THE IGNITION DELAY OF ISO-OCTANE IN THE RAPID COMPRESSION MACHINE**

Seunghyeon Lee, Hyunsoo An, Mintaek Kim, Kwang Min Chun, Soonho Song, Yonsei University, Korea

Concerns about global warming due to the increasing amount of CO₂ and lack of fossil fuels are increasing. Transportation sector has a significant impact on the CO₂ and energy consumption. Therefore, engines with high

efficiency and low emissions are gaining more and more attention.

The Homogeneous Charge Compression Ignition (HCCI) engine uses premixed homogeneous charge of the Spark Ignition (SI) engine and compression ignition of the Compression Ignition (CI) engine. It has an advantage of low NO_x and PM emission, and high thermal efficiency. However, controlling combustion timing is hard because it does not have a direct controlling device such as a spark plug or an injector. The ignition delay change of *iso*-octane by chemical additives such as hydrogen, Di-Tert-Butyl Peroxide (DTBP), and 2-Ethylhexyl Nitrate (2EHN) was investigated. Homogeneous charge was made by using the fuel mixing vessel with the magnetic stirrer, and the ignition delay was measured by Rapid Compression Machine (RCM) experiment.

As a result, the ignition delay was increased with hydrogen addition, and decreased with DTBP and 2EHN addition. In the case of hydrogen addition, most of added hydrogen molecules consumed OH radicals by OH+H₂=H+H₂O reaction, so the rate of hydrogen abstraction was decreased due to the smaller amount of OH radical, and ignition delay was increased. DTBP was divided into two tertiary butoxy radicals, and then increased the rate of hydrogen abstraction. Thus, auto-ignition process became slow and ignition delay was decreased. Similarly, 2EHN was divided into NO₂ and alkoxy radical, and this radical makes the overall reaction rate fast. Therefore, the possibility of changing ignition delay by chemical additives was confirmed.

Other species with various chemical additives will also be tested, and chemical kinetic analysis and optical diagnostics will also be conducted to figure out detailed reaction paths.

mechlee@yonsei.ac.kr

W3P090 UNCERTAINTY OF THE RATE PARAMETERS OF SEVERAL IMPORTANT ELEMENTARY REACTIONS OF THE H₂ AND WET CO COMBUSTION SYSTEMS

Tibor Nagy¹, Éva Valkó², Inez Sedyó², István Gy. Zsély², Michael J. Pilling³, Tamas Turanyi²

¹Hungarian Academy of Sciences, Hungary ²Eötvös University, Hungary ³University of Leeds, United Kingdom

Data bases of elementary combustion reactions characterize the uncertainty limits of the rate coefficients with uncertainty parameter *f*. Re-evaluation of the temperature-dependent uncertainty parameter *f* (T) is proposed by considering all available direct measurements and theoretical calculations. A procedure is presented for making function *f* (T) consistent with the recommended Arrhenius expression. It is shown that the corresponding uncertainty domain of the Arrhenius parameters is convex and centrally symmetric around the recommended parameter set. The *f* (T) function can be stored efficiently using the covariance matrix of the Arrhenius parameters. The calculation of the uncertainty of a reverse rate coefficient from the uncertainty of the forward rate coefficient and the uncertainty of the thermodynamic data is discussed. For the rate coefficients of several hundred elementary reactions, a large number of experimental and theoretical determinations is available, and a normal distribution can be assumed for the uncertainty of ln *k*. If little information is available for the rate coefficient, equal probability of the Arrhenius parameters within their domain of uncertainty can be assumed. Algorithms are provided for sampling the Arrhenius parameters with either normal or uniform distributions. A suite of computer codes is presented that allows the straightforward application of these methods. For twenty-one important elementary reactions of the H₂ and wet CO combustion systems, the Arrhenius parameters and 3rd body collision efficiencies were collected from experimental, theoretical and review publications. For each elementary reaction, *k*_{min} and *k*_{max} limits were determined at several temperatures within a defined range of temperature. These rate coefficient limits are used to obtain a consistent uncertainty function *f* (T) and to calculate the covariance matrix of the Arrhenius parameters. Uncertainty ranges for the 3rd body collision efficiencies are also recommended.

tibornagy@chem.elte.hu

W3P091 EXPERIMENTAL AND MODELING STUDY ON EFFECT OF DILUENT GASES ON AUTO-IGNITION OF HYDROGEN BEHIND REFLECTED SHOCK WAVE

Yingjia Zhang, Lun Pan, Jiaxiang Zhang, Zuohua Huang, Zeimin Tian, Xi'an Jiaotong University, China

Dilution strategy is important to control the auto-ignition in Homogeneous Charge Compression Ignition (HCCI) engine, improve the combustion and emissions in Internal Combustion Engine (ICE) with Exhaust Gas Recirculation (EGR) and validate the kinetic mechanisms. In this study, new ignition delay times were measured for hydrogen with diluent gases (Ar, N₂ and CO₂) behind reflected shock conditions: at temperatures of 850 – 1350 K, pressures of 1.2 – 16.5 atm, and equivalence ratios of 0.5, 1.0 and 2.0. Both NUIG H₂-CO Mech and USC 2.0 Mech were evaluated against the measured ignition times, with poor agreement in the cases of N₂ and CO₂ dilutions and fair agreement in the case of Ar dilution. Effects of diluent gases on the shock-pressures and ignition times were then examined through the comparison between simulations and experiments. Thermal and kinetic effects of dilution gases on the auto-ignition of hydrogen were quantified. Results revealed that thermal effects were negligible at high temperature, but it becomes significant with the decrease in temperature. Differences between model predictions and measurements are mainly resulted from the uncertainties of third-body collision efficiencies of reactions H + O₂ (+M) = HO₂ (+M) and H₂O₂ (+M) = OH + OH (+M), especially in the case of CO₂ and N₂ dilutions.

yjzhang_xjtu@mail.xjtu.edu.cn

W3P092 COMBUSTION PROPERTIES OF H₂/CO MIXTURES: CONSISTENT CHEMICAL MECHANISM FROM COLLABORATIVE DATA PROCESSING

Uwe Riedel¹, Nadja Slavinskaya¹, Jan Hendrik Starcke¹, W. Matt Speight², Andrew Packard², Michael Frenklach²

¹German Aerospace Centre, Germany ²University of California at Berkeley, United States

A revision of the DLR H₂/CO kinetic model and related experimental data is presented. The new development employed numerical algorithms and tools of the Bound-to-Bound Data Collaboration (B₂B-DC) module of an automated data-centric infrastructure, Process Informatics Model (PrIme). The uncertainty-quantification framework of B₂B-DC establishes consistency or inconsistency of a data-and-model system, when model parameters and experimental observations used for model validation are known within their respective uncertainties. Applying this to the DLR H₂/CO kinetic model, the influence of parameter and experiment uncertainties on the optimal solution were examined and experimental targets that are most difficult to match as well as model parameter values that are likely to be questionable were identified. Over 100 experimental observations (targets) of H₂/CO ignition delays and laminar flame speeds along with their respective bounding uncertainties were collected from literature and included in the B₂B-DC dataset. After the B₂B-DC analysis of consistency, the H₂/CO data-model system was subjected to model-parameter optimization over the feasible region of the parameter space. Considering the experimental uncertainties along with the parameter uncertainties, the rate coefficients of 12 most influential reactions were optimized. The approach to optimizing combustion models by constraining the optimization not only to parameter uncertainties but also to the uncertainties in experimental data promises the best-fit solution. The predictions calculated with such a model deviate the least from the experimental targets while remaining within their experimental uncertainties. It is anticipated that developed in this way reaction model may offer more reliable predictions for combustion at arbitrary conditions of interest.

Nadja.Slavinskaya@dlr.de

W3P093 DEVELOPMENT OF A SYNGAS COMBUSTION MECHANISM BASED ON A HIERARCHICAL OPTIMIZATION APPROACH

Tamas Varga¹, Carsten Olm¹, István Gy. Zsély¹, Éva Valkó¹, Henry Curran², Tamas Turanyi¹

¹Eötvös University, Hungary ²National University of Ireland, Ireland

An optimized syngas combustion mechanism has been developed using a large set of indirect experimental data, consisting of ignition measurements in shock tubes and rapid compression machines, and flame velocity measurements, covering wide ranges of temperature, pressure, equivalence ratio and H₂/CO ratio. The performance of the mechanism was also tested against concentration profiles measured in flow reactors and jet-stirred reactors.

The starting point of development was the hydrogen and syngas combustion mechanism of Kéromnès, which was recently optimized for hydrogen combustion (Image). According to the sensitivity analysis carried out at each experimental data point, the rate coefficients of 16 elementary reaction steps could be optimized and estimated with acceptable accuracy. 10 of these reaction rates have been determined in, and the previously obtained reaction rates and uncertainties have been utilized in the current optimization. Direct measurements of the 6 new important reactions (H+H+M=H₂+M; CO+O₂=CO₂+O; CO+OH=CO₂+H; HCO+M=H+CO+M; HCO+O₂=HO₂+CO; HCO+H=CO+H₂) were collected and their prior uncertainty ranges were determined based on the literature data.

We used the optimization methodology described in detail by Turányi et al. coupled with a hierarchical optimization strategy using both the indirect and direct experimental data measurements as optimization targets. As a result of optimization, a new syngas combustion mechanism was obtained that is also consistent with the hydrogen combustion experimental data. The performance of the optimized mechanism was compared to those of various recently published syngas combustion mechanisms.

vargatamas@caesar.elte.hu

W3P095 SHOCK TUBE STUDY ON THE THERMAL DECOMPOSITION OF HYDROFLUOROCARBONS USING IR LASER ABSORPTION DETECTION OF HF

Akira Matsugi, Hiroumi Shiina, National Institute of Advanced Industrial Science and Technology, Japan

The global production and consumption of HydroFluoroCarbons (HFCs) is dramatically increasing. Because some of HFCs, particularly those having low global warming potential, are flammable, elucidation of their combustion properties and chemistry is critical to ensure their safe use. Thermal decomposition of HFCs is important initiation reactions in combustion of HFCs, but the kinetic of HFC decomposition is still sparsely understood. In the present study, the rate constants for the thermal unimolecular decomposition of some HFCs have been measured by using a shock tube / laser absorption spectroscopy. The experiment was performed using a double piston-actuated shock tube. The rate constants for the thermal decomposition of HFCs diluted in Ar were measured behind reflected shock waves by monitoring the formation of HF. HF was detected by the IR absorption of R (1) line in the 1-0 fundamental vibrational band near 2476 nm using a distributed feedback laser. The HF concentration was determined using the known line intensity and the line shape parameter determined by monitoring the HF generated from C₂H₅F decomposition. The rate constants for the decomposition of HFCs were determined from the time-concentration profiles of the HF produced. The results for the selected HFCs, including C₂H₅F (HFC-161), CH₃CF₃ (HFC-143a), and CH₂=CFCF₃ (HFO-1234yf) are presented.

W3P096

THE IGNITION OF GAS MIXTURE $\text{CH}_3\text{Cl} + \text{Cl}_2$ AFTER BRIEF EXPOSURE TO UV – LIGHT

Ildar Begishev, I.S. Nikitin, State Fire Academy of EMERCOM of Russia, Russia

Under the action of UV radiation on the mixture ($\text{CH}_3\text{Cl} + \text{Cl}_2$) as a result of photodissociation of chlorine molecules there are formed initial reaction centers- chlorine atoms. In isothermal conditions within a short time, the concentration of chlorine atoms in the system becomes quasi-stationary. Since during the chlorination CH_3Cl chains are not ramified

$$[\text{Cl}]_0 = (W_i/k[M])^{1/2}$$

where W_i – thy rate of initiation, and k – rate constant of the reaction $\text{Cl} + \text{Cl} + \text{M} \rightarrow \text{Cl}_2 + \text{M}$.

After the cessation of initiation the concentration of active particles decreases

$$[\text{Cl}] = ((k[M]/W_i)^{1/2} + k[M]\tau)^{-1}$$

Ignition of the mixture may occur only in the period during which the active particles concentration exceeds the critical value ($[\text{Cl}]_c$)

$$\tau_c \approx [\text{Cl}]_0/[\text{Cl}]_c * (k[M]W_i)^{1/2}$$

According to the previously obtained results of ($\text{CH}_3\text{Cl} + \text{Cl}_2$) mixtures photoignition, the value τ_{lim} was evaluated, which depending on the conditions varies from 0.02 to 0.1 s. The ignition after a short exposure of UV - light was observed in a steel cylindrical vessel with a diameter of 0.05 m and a length of 0.89 m. The $\text{CH}_3\text{Cl} + \text{Cl}_2$ mixture contained in atmospheric pressure and room temperature, was irradiated with a mercury lamp UV-radiation of 1 kW through the quartz glass installed in the end of the vessel. Irradiance was registered at $2 \cdot 10^{21}$ quantum/m²s. The temperature in the vessel was measured by thermocouples ($d = 20 \cdot 10^{-6}$ m), placed at the distances 1)- 0,03; 2)- 0,07; 3)- 0,1; 4)- 0,15; 5)- 0,225; и 6)- 0,795 m along the axis of the vessel.

In (0,14 $\text{CH}_3\text{Cl} + 0,86\text{Cl}_2$) and (0,59 $\text{CH}_3\text{Cl} + 0,41\text{Cl}_2$) mixtures photoignition occurs approximately 0.1 s after the cessation of initiation. In a rich mixture the photosensor disposed near the quartz glass outside of reaction vessel captures the radiation of arising flame.

begishev@mail.ru

W3P097

THE INFLUENCE OF THE GAS MIXTURE ($\text{CH}_3\text{Cl} + \text{Cl}_2$) COMPOSITION ON SPEED AND TEMPERATURE OF THE FLAME

Ildar Begishev, A.K. Belikov, I.R. Begishev, State Fire Academy of EMERCOM of Russia, Russia

The spread of the flame was explored in a cylindrical stainless steel vessel with a diameter 0,05 m and a length of 0,05 m. To initiate the ignition of ($\text{CH}_3\text{Cl} + \text{Cl}_2$) mixture contained in $T_0=293$ K and $P=101$ kPa, it was irradiated with a mercury lamp radiation of 1 kW through the quartz glass installed in the end of the vessel. The flame propagation was monitored by microthermocouples ($d = 20 \cdot 10^{-6}$) placed at various distances along the axis of the vessel. According to the indications of thermocouples the relationship $x = f(\tau)$ was plot, and using it the instantaneous rate of flame propagation was calculated.

The highest speed is typical of (0,33 $\text{CH}_3\text{Cl} + 0,67 \text{Cl}_2$) mixture, which is stoichiometric under the condition of substituting two hydrogen atoms by chlorine in molecule of chloromethane. The high speed in the initial sections are due to propagation of photoignition wave. Mixtures containing 14 and 59 % vol. CH_3Cl are ultimate. Dependence of maximum values of temperature (fixed by thermocouples placed at distances 1 - 0,035; 2 - 0,105; 3 - 0,155; 4 - 0,235; 5 - 0,38; 6 - 0,585; 7 - 0,805 m.) on the concentration of chloromethane has been received. In near thermocouples (1-4), maximum values are also fixed in the mixture (0,33 $\text{CH}_3\text{Cl} + 0,67 \text{Cl}_2$). At the distal thermocouple (7), all the indications are higher, and the maximum value is observed in a mixture of (0,5 $\text{CH}_3\text{Cl} + 0,5 \text{Cl}_2$) which is stoichiometric when one of hydrogen atom is substitute by chlorine. Maximum heating of the same mixture was observed previously in its photoignition in in a short vessel ($l = 0,05$ m).

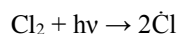
begishev@mail.ru

W3P098

THE LOCATION AND SIZE OF CORE OF PHOTOIGNITION IN MIXTURES ($\text{CH}_3\text{Cl} + \text{Cl}_2$)

Ildar Begishev, State Fire Academy of EMERCOM of Russia, Russia

The photodissociation of chlorine molecules occurs under the action of UV light on the gas mixtures with formation of the initial reaction centers



The rate of initiation of the photochemical reaction (W_i) decreases in the direction of the light flux due to radiation attenuation in an absorbing medium in accordance with the equation $W_i = 2I_0 \epsilon C_{\text{Cl}_2} \exp(-\epsilon C_{\text{Cl}_2} x)$.

The photoignition of the mixture occurs in the region of space where $W_i > W_i^{\text{crit}}$. The photoignition zone size will be determined by the dependence $W_i(x)$. We have previously established critical values of the rate of initiation in mixtures of different composition at $P_0 = 101$ kPa and $T_0 = 293$ K. From the dependence of $W_i(x)$ the distance at which the initiation rate is reduced to the critical values was estimated. Depending on the mixture composition the distance varies from $2,5 \cdot 10^{-2}$ to $8,8 \cdot 10^{-2}$ m.

The experimental studies of temperature fields in photochemical reactions were conducted in a steel cylindrical

vessel with a diameter of 0.05 m and a length of 0.89 m. To initiate the reaction, the $\text{CH}_3\text{Cl} + \text{Cl}_2$ mixture, placed in a box at atmospheric pressure and room temperature, was irradiated with a mercury lamp of 1kW through quartz glass set in the back of the vessel. Incident intensity (I_0) was $2 \cdot 10^{21}$ quantum/m²s. The temperature in the vessel was measured by thermocouples ($d = 20 \cdot 10^{-6}$ m), placed at different distances along the axis of the vessel.

In a mixture with chloromethane of 14 and 25 % vol. concentration the photoignition source due to heat transfer in quartz glass is formed at some distance from it. Primarily, the core is placed at a distance from $3 \cdot 10^{-2}$ to $10 \cdot 10^{-2}$ m. Higher concentration of chlorine in the mixture makes the area of the initial ignition narrower. The dimensions of source are significantly bigger than the calculated values estimated without account of thermal expansion of the reaction mixture.

begishev@mail.ru

W3P099

A COMPREHENSIVE REACTION MODEL FOR THE Si-H-Cl-C CHEMICAL SYSTEM

Remy Mével¹, Laurent Catoire², ¹California Institute of Technology, United States ²ENSTA-ParisTech, France

Silicon-based compounds, such as silicon hydrides, silicon halides, and silicon hydridohalides, are widely used as a source of silicon atoms in a number of industrial processes. A large variety of materials, including SiC , Si_3N_4 and SiO_2 , can be produced from chemical vapor deposition and combustion-based processes. For example, SiH_3Cl and SiH_2Cl_2 can be employed to create epitaxial layer onto electronic devices. Because of a wide range of applications, a deep understanding of the high-temperature kinetics of the Si-H-Cl-C chemical system is required to improve and optimize industrial fabrication processes. The aim of the present study is to develop a comprehensive reaction model able to reproduce available high-temperature data for gaseous mixtures containing Si-H-Cl-C atoms.

Experimental time-resolved profiles of Si, H and Cl obtained during the pyrolysis of different mixtures containing one or several components among Si_2H_6 , SiH_4 , SiCl_4 , SiHCl_3 , HCl , CH_4 , CH_3I , CH_3Cl and $\text{C}_2\text{H}_5\text{I}$, have been collected as a validation database. These experimental data come from Roth's group and have been obtained using the shock-tube technique within the following ranges: $X_{\text{Reactant}} = 0.2\text{--}201$ ppm; $T_5 = 1137\text{--}4525$ K; $P_5 = 72\text{--}172$ kPa. The proposed reaction model includes 311 elementary reactions and 87 chemical species. Silane pyrolysis kinetics was taken from Petersen study and hydrocarbon pyrolysis reactions were taken from Konnov's reaction model. Halogen and silicon hydridohalides reactions, and halogen-hydrocarbon as well as halogen-silicon interactions were compiled from various studies from the literature.

The figures below present typical results obtained in the present study. The proposed reaction model allows to reproduce satisfactorily most of the experimental data available in the literature. In all cases, the main trends are captured by the model. The largest discrepancies were observed for hydrogen atom profiles. In some cases, the concentration is over-estimated by a factor of two. Typical error for silicon and chlorine atoms is on the order of 30%. This seems to indicate that some rate constants relevant for hydrogen atom kinetics might need reappraisal.

mevel@caltech.edu

W3P100

EXPERIMENTAL AND MODELING INVESTIGATION OF *N*-DECANE PYROLYSIS AT SUPERCRITICAL PRESSURES

Zhenjian Jia, Weixing Zhou, Harbin Institute of Technology, China

The pyrolysis kinetics of fuels under supercritical conditions is an important concern for developing regenerative cooling technology of advanced aircraft using hydrocarbon fuels as the primary coolant. *N*-Decane as a component of some jet fuels was studied at the temperature range from 773 to 943 K in a flow reactor under the pressure of 3, 4 and 5 MPa. GC-MS was used to analyze the pyrolysis products, which were mainly alkanes from $\text{C}_1\text{--C}_9$ and alkenes from $\text{C}_2\text{--C}_9$. A kinetic model containing 138 species and 697 reactions has been developed and validated by the experimental results including the distribution of products and the chemical heat sink of fuel. The decomposition pathways of *n*-decane were illustrated through the reaction flux analysis. It is concluded that the $\text{C}_4\text{--C}_9$ alkanes are mainly generated by the recombinations of alkyls, while the small alkanes ($\text{C}_1\text{--C}_3$) are formed by H-abstraction reactions by $\text{C}_1\text{--C}_3$ alkyl radicals. The applicability at supercritical pressure and high fuel concentration condition of previous models was discussed, the performance of the present model in reproducing the experimental data is reasonably well.

jiahcms@gmail.com

W3P101

EXPERIMENTAL AND KINETIC MODELING STUDY OF *N*-TETRADECANE PYROLYSIS

Yuyang Li, Meirong Zeng, Wenhao Yuan, Yizun Wang, Lidong Zhang, Fei Qi, University of Science and Technology of China, China

Long chain normal alkanes with 10 and more carbon atoms are important components in commercial transportation fuels such as gasoline, diesel, kerosene and jet fuels. They are also widely used as major components of surrogate fuels. Compared with *n*-decane and *n*-dodecane, the combustion studies of *n*-tetradecane were very limited and completely focused on the global parameters such as laminar flame speeds and ignition delay times. No measurement on the mole fraction profiles in the gas phase pyrolysis and oxidation of *n*-tetradecane has been performed. The targets of this work are to report the first investigation on the chemical structure of *n*-tetradecane pyrolysis at low and atmospheric pressures and develop a kinetic model of *n*-tetradecane pyrolysis.

The experimental work was performed at National Synchrotron Radiation Laboratory, Hefei, China. Detailed

descriptions of the two beamlines and pyrolysis apparatus used in this work have been reported elsewhere. The pyrolysis of 2% *n*-tetradecane in Ar was investigated from 830 to 1300 K at 30 and 760 Torr. Synchrotron vacuum ultraviolet photoionization mass spectrometry was used to detect the pyrolysis species. Dozens of pyrolysis products of *n*-tetradecane were detected, including alkanes, 1-alkenes, 2-alkenes, dialkenes, alkynes, and free radicals such as methyl radical (CH_3), propargyl radical (C_3H_3) and allyl radical (aC_3H_5) and so on. And their mole fractions were evaluated as functions of temperature. A new pyrolysis model of *n*-tetradecane with 184 species and 925 reactions was developed to reproduce the experimental results. The simulation was carried out using Plug Flow Reactor module in Chemkin-Pro software.

The present model can get reasonable prediction on the profiles of *n*- $\text{C}_{14}\text{H}_{30}$ and its major pyrolysis products. Rate of production analysis shows that the consumption of *n*- $\text{C}_{14}\text{H}_{30}$ is dominated by unimolecular C-C bond dissociation reactions and H-atom abstraction reactions. Based on the sensitivity analysis of *n*- $\text{C}_{14}\text{H}_{30}$ at 30 Torr, 1163 K and 760 Torr, 1017 K, the C-C bond dissociation reactions have the highest sensitivities to the decomposition of *n*- $\text{C}_{14}\text{H}_{30}$ among all types of primary decomposition reactions of *n*- $\text{C}_{14}\text{H}_{30}$ at both 30 Torr and 760 Torr, mainly due to their crucial roles in both the consumption of *n*- $\text{C}_{14}\text{H}_{30}$ and the production of free radicals. Among all H-atom abstraction reactions, the H-atom abstraction reactions by H and CH_3 have the greatest contributions to the consumption of *n*- $\text{C}_{14}\text{H}_{30}$ and are also the major formation source of H_2 and CH_4 . The C_2 and larger alkyl radicals mainly suffer β -scission reactions to produce 1-alkenes (e.g. 1- C_7H_{14}). The subsequent decomposition reactions of C_4 and larger 1-alkenes will lead to the production of smaller radicals (e.g. aC_3H_5), alkenes and dialkenes.

yuygli@ustc.edu.cn

W3P102

EXPERIMENTAL AND KINETIC MODELING STUDY OF *N*-PROPYLCYCLOHEXANE COMBUSTION

Fei Qi, Zhandong Wang, Long Zhao, Zhanjun Cheng, Lidong Zhang, Feng Zhang, Yuyang Li
University of Science and Technology of China, China

Cycloalkanes are an important component family in the gasoline, diesel oils and jet fuels, as well as their surrogates. Thus, their combustion kinetics is crucial for the development of kinetic models of real fuels. As a further step of the systemic study on the combustion of cycloalkanes, the pyrolysis of *N*-PropylCycloHexane (PCH) at 30, 150 and 760 Torr were investigated in a flow reactor using synchrotron vacuum ultraviolet photoionization mass spectrometry. Mole fraction profiles of more than 40 species were quantified, providing new validation data for the kinetic models of PCH.

A detailed kinetic model of PCH combustion was developed and validated against the pyrolysis data in the present work. The developed kinetic model can reproduce the consumption of PCH and the formation of pyrolysis products. Under the pyrolysis conditions of this work, PCH is consumed via both unimolecular decomposition and H-abstraction reactions. The dominant unimolecular decomposition pathway is the loss of *n*-propyl radical to cyclohexyl radical. The contribution of this reaction to PCH consumption decreases as the pressure increases. Products from the ring-opening isomerization of PCH and the dissociation of C_9H_{17} and cyclohexyl radicals constitute the product pool in the PCH pyrolysis.

Furthermore, mole fraction profiles of species measured in the Jet-Stirred Reactor (JSR) oxidation and lean premixed flame of PCH reported in the literature were used for further validation of the present model. Under these oxidation conditions, PCH is mainly consumed by the H-abstraction reactions by OH attack, while the unimolecular reactions of PCH only have little contributions.

fqi@ustc.edu.cn

W3P103

DEVELOPMENT OF RATE RULES FOR THE LOW-TEMPERATURE OXIDATION OF ALKANES

John Bugler, Sinéad Burke, Kieran Somers, Emma Silke, Henry Curran, National University of Ireland, Ireland

Ignition delay times of fuel-'air' *n*-pentane, *iso*-pentane and *neo*-pentane mixtures were measured in a Rapid Compression Machine (RCM). The experimental data were then used to improve the current chemical kinetic models of the isomers. The present study shows ignition delay time data at equivalence ratios of 0.3, 0.5, 1.0 and 2.0 at pressures near 10 and 20 atm across temperatures ranging from 640 to 1020 K.

Rate rules for reaction classes important to low-temperature oxidation, including those related to the Negative Temperature Coefficient (NTC) region and to first-stage ignition, have been updated based on recent quantum-chemically derived rate coefficients from the literature. There have been a variety of systematic studies which have used various computational quantum chemical methods for rate coefficient calculations for reactions relevant to the low-temperature oxidation of alkanes. These studies have calculated high-pressure limit rate coefficients for sets of training reactions with the aim that they can be used directly in chemical kinetic mechanisms for combustion relevant applications. In this work, the rate coefficients from these studies are compared and applied to the mechanisms of the isomers of pentane. Several reaction classes have also been included, and pressure dependency of rate coefficients has also been investigated. Updates to the thermochemistry of the species important in the low-temperature oxidation of hydrocarbons have also been made based on a thorough literature review. The work in this study will provide a systematic evaluation of the rate rules in the literature and their suitability for application to mechanisms for the low temperature oxidation of straight-chain, branched and highly-branched alkanes, and new rate rules are developed which will form the basis for efficient mechanism construction for larger alkanes. This will be particularly important for the

production of gasoline surrogate mechanisms.

When compared to the chemical kinetic models, in general, ignition delay times were well predicted for all of the isomers over all ranges of temperature, pressure and mixture composition. To the authors' knowledge, this study covers compositions and conditions not yet present in the literature, and will expand fundamental knowledge of the combustion kinetics of alkanes.

j.bugler1@nuigalway.ie

W3P104 PARAMETRIC STUDY OF THE LOW TEMPERATURE OXIDATION OF HEXANE IN A FLOW REACTOR

Remy Mével, Jocely Aleka, Karl Chatelain, Joseph Shepherd, California Institute of Technology, United States

The goal of the present study is to characterize in detail the low-temperature oxidation process of a kerosene surrogate over a wide range of conditions, in order to accurately evaluate the effectiveness of alternative inerting strategies for flammable atmospheres in aircraft fuel tanks.

The experimental facility is a flow reactor composed of three parts: an inlet, a quartz reactor and an outlet. The residence time within the reactor is controlled by a mass flow controller from Omega. The quartz tube is located in an oven and has an inner diameter of 2.54 cm and a length of 25 cm. The inlet and outlet are made of stainless steel and have a width of 5.08 cm. The inlet is used to feed the gaseous mixture into the flow reactor and check the initial composition using infrared laser absorption measurements through sapphire windows. At the outlet, sampling and spectroscopic measurements of water and fuel are performed. Both the pressure and the temperature are monitored along the inlet-reactor-outlet assembly. Gaseous samples are analyzed using a gas chromatograph with identification and calibration performed for 26 chemical species.

The evolution of the gas phase composition at the flow reactor exit as a function of temperature was investigated for *n*-hexane based mixtures over the following ranges: $\phi=0.7$ -1.5; $T=450$ -1000 K; $P=40$ -100 kPa; $\tau=2$ -30 s. The figures below illustrate the effect of residence time and pressure on the oxidation regimes. The cool flame region shifts from 600 K to 500 K as the residence time is changed from 2 to 30 s. In the Negative Temperature Coefficient, NTC, region, between 700 and 800 K, significant consumption of the fuel occurs essentially through pyrolysis as demonstrated by the large amounts of non-oxidized species formed. As the pressure is decreased from 100 to 40 kPa, the cool flame region shifts from 500 K to 550-575 K. The NTC region, within $T=650$ -750 K, appears more pronounced at 40 kPa than at 100 kPa. The peak production of hydrogen, alkanes and alkenes is shifted from 800 to 900 K. The temperature at which total oxidation is achieved is shifted from 900 K to above 950 K.

mevel@caltech.edu

W3P105 THERMAL STABILITY OF *N*-HEXANE-OXYGEN MIXTURES

Remy Mével, Joseph Shepherd, California Institute of Technology, United States

Accidental combustion events in fuel tanks and flammable leakage zone are a major concerns in aviation safety. In order to mitigate this risk and fulfill safety regulations, some commercial aircraft use an inerting strategy based on hollow fiber membranes that exhibit selective permeability so that a nitrogen-enriched environment is created in the fuel tank. Although effective, this approach has limitations. The present study examines the alternative strategy of a long duration thermal process close to but below the auto-ignition temperature to create an inert mixture through slow oxidation.

Experiments were performed in a 1.14 L cylindrical cell made of stainless steel. Two 5 cm in diameter, 5 mm thick ZnSn windows are located opposite to each other for optical access. A Frontier Perkin-Elmer Mid-IR FTIR spectrometer is employed to monitor in real-time the evolution of the gas-phase composition. For all experiments, resolution was 1 cm^{-1} and the scanning rate was 0.17 Hz with averaging of three consecutive spectra. The test cell is equipped with 3 pneumatic valves for rapid filling, gas sampling and evacuation. The temperature and pressure inside the cell are monitored with a shielded K-type thermocouple and a pressure transducer. Mica foil-heaters and a heated magnetic stirrer plate are used along with temperature controllers to heat the vessel and maintain the temperature constant. Prior to experiments, the test cell is evacuated to below 2 Pa and heated to the desired temperature. The gas mixture, prepared from research-grade liquid *n*-hexane and gaseous oxygen and nitrogen, is introduced from a 5 L glass into the test cell. Homogeneity of the mixture is ensured by active mixing with a quartz coated magnetic stirrer. Infra-red spectra, temperature and pressure are recorded over 7200s. Experiments were performed for fuel- O_2 mixtures diluted with 89% and 78% nitrogen and an equivalence ratio between 0.67 and 1.35. The temperature and pressure were varied between 420 and 500 K and between 37 and 147 kPa, respectively. The figures below show the evolution of the IR spectrum as a function of time as well as the evolution of CO_2 as a function of temperature. For all conditions studied, no ignition was observed but significant amounts of CO_2 and H_2O were formed. At low temperature, the chemical activity is characterized by a slow and constant reaction rate. At high temperature, the reaction proceeds in two-phases. Initially, rapid production of CO_2 , CO and CH_2O is observed followed by a period of slower production of CO_2 and H_2O .

mevel@caltech.edu

W3P106 EXPERIMENTAL COMBUSTION STUDY OF LARGE LINEAR AND BRANCHED HYDROCARBONS USING NOVEL MOLECULAR BEAM MASS SPECTROMETRY TECHNIQUES

Linear and branched hydrocarbons with chain lengths from C₆ to C₁₄ as prototype Fischer-Tropsch fuels from coal, gas or biomass have become the main target for applications as alternative fuels in aviation as well as mid-term energy storage solutions. Long-term goals include the application of numerical CFD based methods as flexible design tools for fuels or storage media. The CFD approach includes the combination of fluid dynamics with chemical processes, provided by implementation of kinetic models. However, for the development of those chemistry models, experimental data for validation is strongly needed based on the new demands. Molecular Beam Mass Spectrometry (MBMS) has proven to be a reliable and versatile technique in obtaining a vast, quantitative overview of species related information in complex kinetic processes.

Here, we present two novel MBMS approaches to provide quantitative experimental species information for large hydrocarbons from C₈ to C₁₀: the first part deals with a high-temperature flow reactor with coupled MBMS-ToF detection operating at atmospheric conditions, currently under close characterization at the DLR in Stuttgart to provide species profiles as a function of temperature. Initial experimental results from gaseous species (methane) are presented to demonstrate the potential for the first time together with preliminary studies for large hydrocarbons such as *n*-nonane. The second part involves a new approach at the iPEPICO experiment of the Swiss Light Source (SLS) at the Paul Scherrer Institut in Villigen, Switzerland. This powerful tool is a new diagnostic method allowing the investigation of complex chemistry reaction pathways. In the present work, the potential of the iPEPICO system is demonstrated for a premixed low pressure (40 mbar) *iso*-butane/O₂/Ar-flame, stabilized on a McKenna type burner. Experimental results for large hydrocarbons, e.g. *n*-nonane doped into a premixed low pressure (30 mbar) H₂/O₂/Ar-flame at a total equivalence ratio of $\Phi = 1.5$ are presented and discussed.

M.Koehler@dlr.de

W3P107 AN INVESTIGATION OF PHASE-CHANGE BEHAVIOR IN RCM EXPERIMENTS WITH LARGE MOLECULAR WEIGHT FUELS

Colin Banyon, S. Scott Goldsborough, Argonne National Laboratory, United States

Rapid Compression Machines (RCMs) are well-suited for acquiring validation targets for chemical kinetic models at the operating conditions of current and future internal combustion engines. These laboratory devices are able to provide empirical access to the low- to intermediate-temperature (e.g., T = 600–1000 K) kinetics of transportation-relevant fuels at elevated pressure (e.g., p = 10–80 bar), under non-dilute conditions. However, probing the gas-phase chemistry of large molecular weight fuels (e.g., MW > 140) in these devices has historically been challenging due to the in-volatility of constituent or surrogate species, and full boiling range fuels. This challenge has been addressed via heating of the apparatus and accompanying pre-mixing tank, while experiments utilizing fuel aerosols have also been suggested as a viable approach. The effect of phase change during experiments with these large molecular weight fuels using either fuel loading method, on the well-defined “adiabatic core” of the reaction chamber has not been previously assessed. This study attempts to do so where a computational approach is utilized and several representative conditions are investigated. A reduced-order model is extended to facilitate this study, where the multi-phase species and energy transport are taken into account. Simulated stratification profiles are presented for mixtures containing two non-reacting, aerosol-loaded diesel surrogates, *n*-dodecane and *n*-hexadecane. For the conditions explored here, it is found that a thermally and compositionally well-defined “adiabatic core” can be maintained throughout the duration of a typical experiment, e.g., 100 ms. The simulation results presented here also indicate that fuel condensation within the cooler thermal boundary layer may be beneficial during RCM experiments, where condensive heating reduces the boundary thickness and stabilizes the core gas temperature.

colin.banyon@marquette.edu

W3P108 QUASI-GLOBAL KINETIC MODELING OF DIFFERENT ALKANE AND ALCOHOL FUELS

Karl Alexander Heufer, RWTH Aachen University, Germany

Within the Cluster of Excellence „Tailor Made Fuel from Biomass” at RWTH Aachen University novel synthesis and production routes for bio-based fuels are investigated. Detail understanding of combustion chemistry of such tailor-made fuels plays an important role in combustion research area. However, detailed kinetic modeling usually needs a significant amount of effort and time and is not suitable for screening of many bio-fuel candidates within short time. Furthermore, CFD simulation of e.g. combustion engines with full kinetic models cost computational effort. For this reason kinetic models with a small number of reactants and reactions are desirable.

These aspects motivate to develop a quasi-global kinetic model for describing the auto-ignition of various fuels. The approach is based on the idea to combine a C0 base mechanism with some characteristic fuel reactions. In principle this idea has already been described by Westbrook and Dryer for modelling laminar flame speeds but according to the authors knowledge this approach hasn't been applied for autoignition studies. The focus of the present study is the low temperature autoignition of fuels based on the reactions described by Curran et al. as the major pathway towards low temperature chain branching (RH => R => RO₂ QOOH O₂QOOH => Ketone + OH => Decomposition Products + OH). Although this reaction scheme has been reported first for alkane fuels recent studies of biofuels, e.g. butanol, have shown

that this reaction pathway plays a dominant role in the low temperature chemistry also of these fuels. Consequently, this scheme has been implemented as base mechanism for the low temperature kinetic of all fuels of interest focusing in a first step on alkane and alcohol fuels. One of the main differences compared to other global mechanisms is the fact that the proposed model directly includes the most important radicals OH and HO₂ as reactants which play a major role in low temperature chemistry. Preliminary results for *n*-heptane-air mixtures show a very good agreement between the proposed quasi-global model and results from experiment and from a detailed kinetic model.

heufer@pcfc.rwth-aachen.de

W3P109

IDENTIFICATION AND COMPARISON OF DETAILED CHEMICAL MECHANISMS

Richard West, Esma Goktekin, Anthony Silvi, Victor Lambert, Northeastern University, United States

We are developing tools to facilitate identification of chemical species in a kinetic model “Chemkin file”, and then to allow comparison of the models. The tools, built on top of the Python version of Reaction Mechanism Generator software (RMG-Py), will also enable error identification, self-consistency checking, model merging, gap-filling, and facilitate model validation and updating. In recent decades, detailed kinetic models have become integral to combustion research. Progress has been significant and the latest models can explain many complicated combustion phenomena, and allow increasingly accurate engine simulations.

These models can be very large (eg. the LLNL model for 2-methylalkanes has over 7,000 species and 30,000 reactions) and there are now dozens of large published models. Unfortunately, these ever-proliferating detailed kinetic models are incompatible and inconsistent, are seldom compared directly, and often contain undetected mistakes.

Adoption of collaborative optimization, solution mapping, and data curation projects is low, and the preferred publication format remains a “Chemkin file”. This Chemkin format, devised in the 1970’s when input was limited by the width of 80-column punch-cards, forces model-builders to abbreviate species’ names, thereby losing their chemical identity, and to discard other metadata. The main challenge in comparing these models is in recognizing, for example, that the name “C₃KET₁₂” in one model represents 1-hydroperoxypropan-2-one, which another research group may have named “CH₃COCH₂O₂H” in a different model.

We are using our tool to import all the models published in supplementary material to the Proceedings of the 34th Combustion Symposium into a unified and cross-referencable database, and to analyze them to reveal agreements, disagreements, consistencies, and areas for the combustion kinetics community to focus on in the future. If the proceedings are published in time, we will also analyze the current 35th symposium.

r.west@neu.edu

W3P110

COMBUSTION CHEMISTRY MODEL OF FOUNDATIONAL FUELS

Yujie Tao¹, Enoch Dames¹, Gregory Smith², Hai Wang¹

¹Stanford University, United States ²SRI International, United States

Because of the hierarchical nature of hydrocarbon fuels high-temperature oxidation, a reliable foundational fuel chemistry model is crucial to the accuracy of any reaction chemistry model of fuel combustion. The current effort centers on providing a detailed chemical kinetic model with well-quantified and minimized uncertainty for use as a foundation for the combustion of all hydrocarbon fuels at high temperatures. This foundation model describes the combustion kinetics of hydrogen, carbon monoxide, and C₁-4H_xO_y species. The current version is consisted of 291 elementary reactions of 33 species.

The model development effort takes the following steps with an emphasis on uncertainty quantification, propagation and minimization: trial model compilation in which the reaction pathways were analyzed and updated and their rate constants evaluated, validation against experimental targets, rate constant re-evaluation, and constrained rate parameter optimization with uncertainty quantification and minimization. A total of 148 targets were selected for model optimization, including laminar flame speed, shock tube ignition delay and species profile of H₂, H₂O₂, CO, CH₄, CH₂O and C₂H₆ oxidation. Model optimization and uncertainty minimization uses the Method of Uncertainty Minimization by Polynomial Chaos Expansion (MUM-PCE), with response surfaces generated from Sensitivity Analysis-Based (SAB) method as well as Monte Carlo sampling and factorial design. Experimental targets were carefully evaluated with a special attention placed on an assessment of the uncertainties in the initial conditions and their impact on the simulation of flow reactor and shock tube experiments.

This poster will present validation results of the trial and the optimized model and an assessment of the initial conditions and their impact on the simulation of flow reactor and shock tube experiments.

ytao@stanford.edu

W3P111 APPROXIMATE TRAJECTORY OPTIMIZATION ALGORITHM FOR MECHANISM REDUCTION OF *N*-HEPTANE OXIDATION

AiKe Liu, Fan Wang, Xiangyuan Li, Jian-Li Wang, Sichuan University, China

In this work, a novel Approximate Trajectory Optimization Algorithm (ATOA) to generate skeletal mechanisms is presented and validated. To produce a skeletal mechanism with combustion trajectory closely resemble that of the detailed mechanism, we require the relative error of the global species production rate to be smaller than a preset threshold on a set of representative state points. A trajectory approaching process which minimizes global species production rate error is proposed to fulfill this requirement. Many skeletal mechanisms can be generated in this way and iterative improvement algorithm is further adopted to optimize the obtained skeletal mechanism systematically. In the iterative improvement process, a skeletal mechanism is first perturbed and new skeletal mechanism will be achieved based on the trajectory approaching process. Lots of skeletal mechanisms can be produced and the one with minimum number of species and simulation error bellow a given accuracy criteria will be chosen as the optimal skeletal mechanism. This algorithm has been applied to reduce a detailed *n*-heptane oxidation mechanism with 561 species and a 75-species skeletal mechanism has been obtained. This skeletal mechanism is shown to be able to reproduce combustion trajectory of the detailed mechanism under a wide range of parameters and configurations.

cwnu@qq.com

W3P112 IMPROVING DETAILED KINETIC MODELS OF BIO-OIL GASIFICATION VIA RATE RULE CALCULATIONS

Fariba Seyedzadeh, Richard West, Northeastern University, United States

The major challenge in modeling thermal conversion and combustion of biofuels is the presence of a wide range of cyclic oxygenated species and in particular, more attention should be paid to specific reaction classes like primary ring-opening isomerization that can take place through direct C–C or C–O bond breaking. Since manually generating detailed chemical models is effortful and error-prone, it is preferable to use computers instead. In this study, Reaction Mechanism Generator (RMG), an open-source software, has been used to study the main kinetic features of bio-oil pyrolysis and gasification. RMG's kinetics database contains various type of reaction families with relevant reaction recipes to generate an extensive set of elementary reactions. Electronic structure calculations can be used to estimate Arrhenius rate parameters and fill the kinetics database. However, the number of reactions in each reaction family is massive, and applying high-level electronic structure calculations, especially for biofuels molecules that are quite large, would be prohibitively expensive. Alternatively, rate calculations can be performed for a smaller set of reactants belonging to the particular reaction class and, if it is transferable, it can be applied to the whole target reaction class. In order to identify the transferability of the rate rule in a specific reaction class, the role of the different functional groups should be deliberated.

A detailed kinetic model for bio-oil gasification was built in RMG and comparison with experimental data shows that the RMG-built model couldn't predict CO and CO₂ formation properly. Testing the RMG-built model against the wide range of literature data revealed that RMG missed some important primary ring-opening pathways for cyclic oxygenated molecules, via either C–C or C–O bond breaking and simultaneous H-migration. For mechanism generating purposes, new reaction classes for cyclic oxygenated molecules were added into the current RMG database and associated kinetic parameters were determined. In order to investigate if the rate rule can be generalized to the reaction class or not, kinetic parameters of specific reaction groups belong to each reaction class were calculated using the CBS-QB₃ quantum calculations and Transition State Theory (TST). Rate rule calculations were started from xylan, the most relevant component of hemicellulose, whose C–O bond breaking reactions have significant impact on model prediction because of H₂O and CO₂ formation. From literature, proposed transition state geometry of ring opening reaction of xylopyranose, a monomer of xylan, was used as an initial guess for transition state optimization of the rest relevant reactions. There are some significant differences in simulation results between RMG-built models before and after updating the database, specifically in CO and CO₂ predictions. Discrepancies in the models show the important role of specific reaction families and their relevant kinetics parameters when studying thermal conversion and combustion of biofuels.

seyedzadehkhanshan.f@husky.neu.edu

W3P113 A GROUP ADDITIVE APPROACH FOR HIGH-THROUGHPUT TRANSITION STATE ESTIMATION

Pierre Bhoorasingh, Richard West, Northeastern University, United States

We propose an automated procedure to locate transition state geometries using molecular group contributions. Important combustion parameters, such as ignition delay, are very sensitive to the chemistry, and detailed chemical reaction networks help understand such processes. The detailed models are built with automated network generators, such as Reaction Mechanism Generator (RMG), due to their size and complexity. Ideally, trusted thermodynamic and kinetic parameters are used to complete the model, but these are sparse in comparison to the number required. As a result, correlation based estimates are used, but they can be quite approximate. In an effort to improve the thermochemistry, an automated procedure has been implemented in RMG to calculate thermodynamic parameters using semi-empirical quantum calculations (Magoon & Green, 2012). Known bond lengths are used to position the atoms in three-dimensional space using distance geometry, then the geometry is optimized by a quantum chemistry package

which also returns molecular properties. While this has reduced the thermodynamic errors in RMG, the kinetic errors remain.

Kinetic parameters can be calculated via transition state theory, but this first requires location of a transition state geometry. Distance geometry can only be used if interatomic distances at the transition state are known, but they are not; we can now estimate these distances using a group additive approach. The only interatomic distances that undergo appreciable change during a reaction are the ones between the active atoms. By organizing these key distances for known transition states into a tree structure, group values can be determined and used to estimate the distances for unknown transition state geometries. In this poster we demonstrate the ability of this procedure to automatically find unknown transition states.

pbhoorasingh@coe.neu.edu

W3P114 RELIABLE FORMATION ENTHALPIES FROM A COMBINATION OF COMPOUND METHOD ATOMISATION ENERGIES

Ultan Burke, Kieran Somers, John Simmie, Henry Curran, National University of Ireland, Ireland

Mid/high-level quantum chemical methods are recognized as an indispensable tool in determining formation enthalpies ($\Delta_f H^\theta$) of stable and radical molecules due to their decreasing expense, their ability to study experimentally inaccessible molecules, and most importantly, their increasing ability to approach chemical accuracy. Typically, very high-level determinations using CCSDT, Wn, HEAT, or other such methods, are feasible only for systems containing a small number ($\Delta_f H^\theta$ are known, in order to determine $\Delta_f H^\theta$ in instances where "gold standard" methods cannot be employed. If the working reactions and standard $\Delta_f H^\theta$ are well chosen, the uncertainties in the computed $\Delta_f H^\theta$ can rival high-level methods. The atomisation method is also frequently used to determine $\Delta_f H^\theta$, but due to the inherent lack of error-cancellation, uncertainties can be large unless very high-level methods are used.

We recently applied (J. Chem. Thermo., 58 (2013) 117–128.) the isodesmic reaction method to determine formation enthalpies of 40+ stable polyoxygenated furans of interest as platform chemicals and biofuels, using the CBS-QB3, CBS-APNO and G3 methods. Comparison with experiment showed agreement in the majority of instances, giving credence to the thermochemical networks which were hierarchically built. Atomisation energies were also computed which agreed surprisingly well with the isodesmically derived values. We have re-visited the data to rationalize the agreement between the isodesmic and atomisation results, benchmarking the latter against the former, with some interesting trends arising. The computed atomisation formation enthalpies could be correlated the isodesmic values via $\Delta_f H^\theta$ (Atomisation) = $\Delta_f H^\theta$ (Isodesmic) + 0.24 kJ/mol, with $R^2 = 0.99$. Despite this remarkable correlation, if a single molecule were considered, the uncertainty (2σ) in the formation enthalpy of any given compound was much greater in the atomisation $\Delta_f H^\theta$ than the isodesmic $\Delta_f H^\theta$ - up to 26 kJ/mol for the former but only 6 kJ/mol for the latter in the worst instances. The uncertainty in the atomisation results seems to be somewhat overestimated however, certainly in light of the above correlation.

When methods were considered in isolation, atomisation calculations from the CBS-QB3 and G3 methods tended to slightly over-predict the isodesmic formation enthalpies by 0.16 ± 4.4 and 4.17 ± 2.4 kJ/mol respectively, and the CBS-APNO method tended to under-predict by -5.57 ± 4.9 kJ/mol. On average the combination of these three methods tended to agree with the isodesmic values within -0.41 ± 2.2 kJ/mol to 2σ uncertainty—significantly less than the 26 kJ/mol extreme highlighted above. The excellent linearity observed appears to be the result of an error-cancellation effect introduced by using a combination of the CBS-QB3, CBS-APNO and G3 methods, which overcomes the lack of error-cancellation when only a single method was used—some methods tended to consistently over-predict $\Delta_f H^\theta$, others under-predicted $\Delta_f H^\theta$, but the methods tended to compensate well for each others deficiencies. Future studies should assess the applicability of a combination of these, or similar, methods for determining accurate but cost-effective formation enthalpies, by benchmarking their performance against a test-set of well-known (e.g. ATcT, 3rd Millenium Database) stable and radical species.

u.burke1@nuigalway.ie

W3P115 COMPARATIVE ANALYSIS OF COMBUSTION CHEMISTRY MODELS USING THE ALTERNATE SPECIES ELIMINATION APPROACH

Nathan Peters, Ben Akih-Kumgeh, Syracuse University, United States

In recent years, numerous chemical kinetic models have been developed for computational analysis of various combustion processes. Different modeling approaches are taken, sometimes leading to large deviations in model prediction of combustion properties from experimental measurements, as well as deviations among the various models. Comparative analysis of these models is complicated since typical models consist of hundreds of species and thousands of reactions. Identifying specific sub chemistry models that lead to these differences is challenging. A promising approach to identify key kinetic differences appears to be the use of reduced models which retain the predictive ability of their original versions. These reduced models can also be independently employed in further computational analysis of combustion phenomena. In this work, we use the Alternate Species Elimination (ASE) method to derive and compare reduced models for propane and syngas combustion based on selected detailed models from the literature. Chemical species are systematically eliminated and reinstated while changes in a specific combustion property, ignition delay in this case, are recorded. The simulations for this process are carried out in CANTERA and MATLAB. The importance of

a chemical species is revealed through a high ranking of the normalized change in ignition delay time caused by the elimination of the said species. A reduced model is obtained by imposing a reasonable normalized change threshold, below which all species and their reactions are eliminated. Results show a normalized change threshold of 10⁻⁴ retains good predictive ability for both ignition delay and flame speed. In most cases the model is reduced to at least half of the original number of species and at least a third the number of reactions. The average deviation for each reduced model from original simulation results was within 5%. A comparison of the various skeletal models based on the relative rankings and normalized changes reveal underlying differences in modeling approaches and the extent of chemical reactivity of key species. The results show that the approach is useful in revealing differences in chemical kinetic modeling strategies and kinetic parameter assignment.

ndpeters@syr.edu

W3P116 FIRST HIGH-TEMPERATURE MEASUREMENT OF THE HNO + O₂ REACTION RATE CONSTANT BEHIND SHOCK WAVES

Gernot Friedrichs, Nancy Fassheber, Kiel University, Germany

Strategies for reducing NO_x emissions from fossil fuel burning rely on a detailed knowledge of the reaction kinetics of the underlying elementary gas phase reactions. HNO (nitroxyl) represents an important flame species and its intermediate concentrations are closely linked to the resulting NO levels in the exhaust gas. Depending on the combustion conditions, HNO equilibrium reactions such as $\text{HNO} \leftrightarrow \text{H} + \text{NO}$, $\text{HNO} + \text{OH} \leftrightarrow \text{NO} + \text{H}_2\text{O}$, and $\text{H} + \text{HNO} \leftrightarrow \text{NO} + \text{H}_2$ can either increase or reduce NO formation. As most HNO reaction rates have not been measured at combustion temperatures so far, estimated or theoretical values have to be used in NO formation models. These estimates vary strongly depending on the fuel type and the applied kinetic mechanism, respectively. For example, for the reaction $\text{HNO} + \text{O}_2 \rightarrow \text{NO} + \text{HO}_2$, which acts as a major NO source under certain combustion conditions, reported literature data differ by several orders of magnitude.

Here, the first detection of HNO behind shock waves and the first rate constant measurements for the reaction $\text{HNO} + \text{O}_2$ at temperatures between 750 K < T < 1370 K will be presented. The obtained overall rate expression reveals that the reaction is astonishingly fast, even when compared with the highest literature data. This result underlines the high uncertainties of HNO chemistry implementations in current flame models.

We directly observed the reaction $\text{HNO} + \text{O}_2$ behind shock waves by applying the very sensitive absorption based Frequency Modulation (FM) spectroscopy. FM spectra of the electronic A¹A' – X¹A' HNO transition and concentration-time profiles of HNO have been detected at three different wavelengths around 618 nm and 625 nm. HNO mole fractions of about 200 ppm behind reflected shock waves have been generated from the 193 nm UV photolysis of glyoxal/NO mixtures. Glyoxal photolysis provides HCO radicals in high yields whereas HNO is formed by the fast consecutive reaction $\text{HCO} + \text{NO} \rightarrow \text{HNO} + \text{CO}$. By simultaneous modeling of corresponding HNO and HCO concentration-time profiles, which were obtained under similar reaction conditions, the temperature dependent absorption cross section of HNO could be determined as well.

friedrichs@phc.uni-kiel.de

W3P117 KINETICS OF NO₂ + N₂H₃ RADICAL-RADICAL REACTION: THEORETICAL AND EXPERIMENTAL STUDIES

Hongyan Sun, Edwards AFB, United States

The Air Force Research Laboratory is developing new hypergolic fuels which will provide enhanced performance capabilities as well as improved affordability and efficiency. Furthermore, handling of these new hypergolic fuels is expected to have a much smaller logistical footprint due to the fact that they are being designed to be environmentally benign. However, practical realization of these hypergols in spacecraft propulsion systems will only come after attaining a satisfactory understanding of how to optimize their combustion characteristics in relevant operating environments.

The state-of-the-art hypergol combination currently used in the US for many space propulsion applications consists of monomethyl hydrazine, as the fuel, and nitrogen tetroxide, as the oxidizer. Here we report theoretical and experimental results obtained on a prototypical NO₂-radical reaction with N₂H₃. The potential energy surface was investigated by *ab initio* multi-reference second-order perturbation, density functional, quadratic configuration interactions, and coupled-cluster theories. The reaction proceeds via a complex mechanism with submerged energy barriers and relatively large exothermicities. It was found that direct NO₂ addition to the NH site in N₂H₃ forms two isomeric adducts with energy of 38.12 kcal/mol lower than that of the N₂H₃ + NO₂ entrance channel, which is set as a zero energy reference. The isomeric adducts undergo decomposition to trans-HONO + trans-NH=NH and trans-HONO + cis-NH=NH with energy barriers of -9.56 and -4.65 kcal/mol, respectively. Furthermore, the addition adducts undergo decomposition to NO, NNH and H₂O via several steps involving isomerization and molecular elimination. It was also found that the NO₂ can add to the NH₂ site in N₂H₃ to form an unstable adduct which undergoes isomerization to form the NH₂NHONO isomer. The NH₂NHONO isomer has energy of -19.94 kcal/mol and further isomerizes before dissociating to smaller products. Important reaction channels for the NH₂NHONO isomers involve dissociation to NO + NH₂NHO radical products with energy barriers ranging from 5.2 to 13.8 kcal/mol. Dilute mixtures of N₂H₄/NO₂ in nitrogen carrier gas, maintained at 2 Torr and 298 K, were subjected to 193-nm laser photolysis in a flow-tube reactor coupled to an electron-impact ionization mass spectrometer to study the reaction kinetics of N₂H₃ radicals in excess NO₂. Upon photolysis, the reacting gas was mass spectrometrically sampled using a skimmer as the mixture escaped via

a pin-hole inside the flow-tube reactor. The temporal profile of the product, HONO, was determined by direct detection of the ion signal at $m/z = 47$. For each chosen $[\text{NO}_2]$, the observed [HONO] trace could be fitted to a bi-exponential kinetics expression, which yielded a value for the pseudo-first-order rate coefficient, k' , for the reaction of N_2H_3 with NO_2 . A value for the bimolecular rate coefficient, $k = (1.03 \pm 0.29) \times 10^{-11} \text{ cm}^3 \text{ molecule}^{-1} \text{ s}^{-1}$, for this reaction was obtained from the slope of a plot of k' versus $[\text{NO}_2]$. Pressure-dependent rate coefficients of the $\text{N}_2\text{H}_3 + \text{NO}_2$ reaction system were determined by Rice–Ramsperger–Kassel–Marcus (RRKM) theory with multi-well master equation simulations. With the energy transfer probability approximated by $\text{DE}_{\text{down}} = 100 \times (\text{T}/300)^{0.85} \text{ cm}^{-1}$, excellent agreement was observed between the measured value and the computed overall rate coefficient at 298 K and 2 Torr of N_2 . The negative energy barriers and large exothermicities for the various product channels suggest a significant role of this reaction in the early stages of hypergolic ignition of hydrazine and its derivatives.

hongyan.sun.ctr@us.af.mil

W3P118

AB INITIO KINETICS AND THERMAL DECOMPOSITION MECHANISM OF MONONITROBIURET AND 1,5-DINITROBIURET

Hongyan Sun, Edwards AFB, United States

Mononitrobiuret (MNB) and 1,5-Dinitrobiuret (DNB) are, tetrazole-free, nitrogen-rich compounds that have been reported as powerful new explosives. A new ignition mechanism for the thermal decomposition of MNB and DNB is proposed herein. Ignition of MNB and DNB occurs through a multistep reaction process, in which the thermal decomposition of MNB and DNB is initiated by intramolecular H-atom transfer from the central NH group to an adjacent nitro oxygen of the NO_2 group to eliminate an unstable HNNO_2H intermediate that rapidly dissociates to OH, HNNO , NH_2 , NO_2 , N_2O , and H_2O . The radicals produced from HNNO_2H decomposition react further with MNB and DNB via H-abstraction reactions to produce MNB and DNB radicals, which subsequently decompose and oxidize to low-molecular weight intermediates and then final products.

In this work, the potential energy surface for thermal decomposition of the HNNO_2H intermediate was investigated at the $\text{RCCSD(T)/cc-pV}\infty\text{Z//CASPT2/aug-cc-pVDZ}$ level of theory, and pressure-dependent rate coefficients were determined by Rice–Ramsperger–Kassel–Marcus (RRKM) theory with multi-well master equation simulations at the E, J resolved level. Isomerization of HNNO_2H to NH_2NO_2 isomer occurs with an energy barrier of 28.87 kcal/mol, which then dissociates to $\text{NH}_2 + \text{NO}_2$ radicals, while inversion of the aminylene-H has an energy barrier of 30.11 kcal/mol to form another HNNO_2H isomer, which undergoes N-OH bond fission to form OH and trans- HNNO radicals. Furthermore, it also undergoes migration of the aminylene-H to the hydroxyl-O which results in H_2O elimination with an energy barrier of 30.73 kcal/mol and reaction exothermicity of 50.4 kcal/mol. At atmospheric pressure, the result shows that decomposition to $\text{NH}_2 + \text{NO}_2$ is competitive with decomposition to $\text{OH} + \text{trans-HNNO}$ at all temperatures. At ~700 K and above, formation of thermodynamically stable products, $\text{N}_2\text{O} + \text{H}_2\text{O}$, becomes less competitive to the radical channels, and decreases with increasing temperature.

Abstraction of H-atoms from different positions in MNB generates three different MNB radicals, for which the bond dissociation energies for the amine-H in terminal NH group, central NH group and terminal NH_2 group, were respectively computed to be 109.72, 119.51, and 116.59 kcal/mol by $\text{CCSD(T)/cc-pV}\infty\text{Z//B3LYP/6-311++G(d,p)}$ calculations. The energy barriers for the OH radical to abstract each of the different H-atoms in MNB were found to be 10.49, 13.04, 12.30, and 8.85 kcal/mol, which are consistent with the corresponding bond dissociation energies calculated above. The bimolecular rate coefficients for H-abstraction in MNB by OH radicals were also determined in the range 300–2500 K. The H-atoms in DNB have the same bonding environments as that in MNB except for the central amine-H, which is shielded by two $-\text{C}(\text{O})\text{NHNO}_2$ groups. It was found that the abstraction of the central amine-H of DNB occurs once one of the surrounding groups rotates away and makes its bonding moiety the same as that of MNB. This implies that the rate coefficients of $\text{DNB} + \text{OH}$ are similar as those of $\text{MMB} + \text{OH}$.

hongyan.sun.ctr@us.af.mil

W3P119

IGNITION DELAY TIME AND KINETIC MODELING OF NITROMETHANE-OXYGEN-ARGON MIXTURES

Remy Mével¹, Karl Chatelain¹, Laurent Catoire², Joseph Shepherd¹

¹California Institute of Technology, United States ²ENSTA, France

Energetic materials such as nitrogen-containing molecules, commonly used as fuel, fuel additives and propellants, are mainly studied for their capability of releasing large amount of energy. Nitro-alkanes are relatively simple model fuels to study the gas phase combustion kinetics of these compounds. Gas phase detonations in nitro-alkanes exhibit a double cellular structure under certain conditions. Although nitro-methane is the most studied nitro-alkane, there is a limited amount of experimental data in the high-temperature range. The present study aims at providing a comprehensive set of auto-ignition delay time for nitro-methane-oxygen mixtures.

The shock-tube is composed of three parts separated by two diaphragms and is made of stainless steel. The driver section and the driven section are 6.19- and 11.28-m-long, respectively, (i.d. 15.24 cm). The test section is 2.44-m-long (i.d. 7.62 cm) and is linked to a 2.03-m-long cookie-cutter. The driver gas was nitrogen. The test section is equipped with 4 pressure transducers, for shock velocity measurements, and two quartz optical window mounted at 13 mm from the tube end. Two optical fibers are used to collect emission. One of the optical fibers is linked to a single-photomultiplier (Hamamatsu) equipped with a 306+-5 nm band-pass filter for detecting the OH^* radicals. The second fiber is linked to a

dual-photomultiplier (Thorlabs) equipped with a quartz beam splitter and two band-pass filters centered at 410 \pm 5 nm and 430 \pm 5 nm for detecting the CO₂* and CH* emission, respectively. Emission and pressure histories of CH₃NO₂-O₂-Ar mixtures with ϕ =0.75-1.5 were measured behind reflected shock wave in the temperature and pressure ranges 1076-1509 K, 340-410 kPa, respectively. The argon dilution was 97% in all cases. The figures below display an example of experimental signals a) and the evolution of the delay-time with reciprocal temperature b) and c). Delay-times in b) come from Guirguis et al. and were derived on pressure signals. For all equivalence ratios and temperatures, the oxidation of nitro-methane is characterized by two distinct exothermic steps. The first one is taking place very shortly after the reflected shock heating and exhibits a low activation energy whereas the second one has a large activation energy. A comprehensive reaction model has been built and validated against data from the literature. It can reproduce the main trends observed in the present study.

mevel@caltech.edu

W3P120

CHEMICAL KINETICS OF SILANE-NITROUS OXIDE MIXTURES AT TEMPERATURE BELOW 1700 K

Remy Mével¹, Florence Falue², Sandra Javoy²

¹California Institute of Technology, United States ²Université d'Orléans, France

Silane-nitrous oxide mixtures are widely used as a source of silicon atom in the semi-conductors industry to produce thin solid layers of SiO₂. Chemical Vapor Deposition, CVD, processes can be employed to form these protective and/or insulative layers onto the device surface. The utilization of SiH₄ based mixtures is potentially hazardous and can lead to significant material destruction as well as human fatalities. The specific kinetic properties of silane are also relevant to propulsion applications. Despite a number of application of silane-based mixtures, there is a lack of experimental data for these systems. Especially, elementary reaction rate parameters are missing for a large number of reactions. The purpose of the present study is to obtain additional experimental data for reflected shock heated SiH₄-N₂O-Ar mixtures at temperature below 1700 K.

Mixtures were prepared from a mixture containing 1% of SiH₄ in argon. High purity gases, 99.998% and above, were employed. The shock tube used was a 78 mm internal diameter stainless-steel pressure-driven shock tube with a 5.5-m-long driven section and a 3.5-m-long driver section. A turbomolecular pump evacuated the test section to less than 2.10⁻⁴ Pa. The optical detection technique for measuring O atom concentration was an emission line absorption method. A microwave-excited discharge lamp that contained a flowing mixture of 1 % O₂ in He maintained at a pressure of 1.4 kPa was used as light source. A vacuum ultraviolet monochromator was used to isolate the O triplet wavelength, 130.5 nm, and a solar blind photo-multiplier was used to convert vacuum UV photons.

The dynamics of oxygen atom in reflected shock-heated silane-nitrous oxide-argon mixtures was investigated at temperatures between 1353-1885 K and pressures from 212 to 373 kPa. In the 1450-1700 K temperature range, the absorption profiles exhibit unusual complex shapes characterized by an initial rapid rise, a plateau and a second rise. This complex behaviour was attributed to the reaction of disilyne with oxygen atom: Si₂H₂+O=Si₂H+OH. The rate constant of this reaction has been determined by fitting the experimental absorption profiles with computed ones, as illustrated in the figures below.

mevel@caltech.edu

W3P121

THERMAL DECOMPOSITION OF ORGANOPHOSPHORUS AGENTS

Pierre Glaude¹, Baptiste Sirjean¹, Maude Ferrari¹, Adil Khalifa¹, René Fournet¹, Laurent Verdier²

¹CNRS, France ²DGA, France

Organophosphorus compounds are involved in toxic compounds such as pesticides or chemical warfare agents. The understanding of their thermal decomposition and oxidation chemistry is largely limited by the scarcity of thermochemical and kinetic data due to the extreme difficulty to perform experiments with these highly toxic molecules. Literature studies on the decomposition of nerve agent surrogates such as DIMP showed that the preponderant decomposition channels of these molecules occur through pericyclic molecular reactions. Therefore, an accurate determination of the rate parameters of these reactions is critical to describe their thermal decomposition.

A theoretical study of the initial concerted reactions in the decomposition of a series of organophosphorus compounds (sarin, soman, tabun, VX) was performed by means of quantum chemical calculations at the CBS-QB₃ level of theory. For each organophosphorous compound, the potential energy surface of 4-, 5- and 6-centered concerted eliminations were investigated. Based on the calculation of the electronic structures, canonical transition state theory was used to evaluate rate constants. The contributions of hindered internal rotations were corrected in the harmonic vibrational partition functions with the tabulations of Pitzer and Gwinn. The characteristics of internal rotor potentials were determined using scans performed at the B₃LYP/6-31+G(d,p) level of theory.

Theoretical results show that 6-centered eliminations generally face energy barriers of ~40 kcal/mol. Such low activation energies should favor molecular decomposition routes over radical initiation pathways that involve much higher bond dissociation energies. To confirm the critical role of molecular eliminations, a comprehensive chemical kinetic model, including molecular and radical reactions, was developed for the pyrolysis of the toxics. Simulations showed that 6-centered eliminations in these compounds are preponderant over a wide range of conditions.

pierre-alexandre.glaude@univ-lorraine.fr

W3P122 MICROWAVE INTERFEROMETER FOR IONIZATION KINETICS

Daniel Murphy¹, Awad Alquaity², Jie Han², Aamir Farooq², Fabrizio Bisetti²

¹University of California, Berkeley, United States ²King Abdullah University of Science and Technology, Saudi Arabia

The electrical aspects of flames have attracted much interest and study over the years, but there remains considerable uncertainty regarding the processes fundamentally responsible for the various observed phenomena. Detailed physical models will be crucial in developing a clear understanding of these effects, but they must be supported by experimental measurements. Specifically, determination of the chemical kinetics responsible for ionization in flames is necessary. Free electrons, the primary negative charge carrier in flames, have proven difficult to measure accurately and unobtrusively. In this work, we present a Microwave Interferometer (MWI) as a means to measure the number density of electrons in a shock tube for the evaluation of reaction kinetics.

The MWI is fundamentally equivalent to the familiar optical techniques used in combustion. A coherent wave is generated at 94 GHz and then split into a test and reference signal to be sent through and around, respectively, the test section of a shock tube. Subsequent comparison of the two signals resolves the relative phase shift and attenuation of the test signal, from which index of refraction and absorptivity can be determined. Free electrons have the uncommon property of exhibiting an index of refraction below unity and absorptivity that increases non-linearly with their concentration. Both of these effects are increased at low frequency, making microwave systems significantly more sensitive than optical wavelengths. This high sensitivity is critical for combustion experiments due to the low electron densities produced by chemionization.

The present work begins with detailed characterization of the *in situ* spatial response of the MWI in the shock tube by measurement known physical structures (e.g. non-reacting shocks). From those data, signal deconvolution tools are developed to improve spatial resolution beyond apparent limitations imposed by the long wavelengths (~3 mm) and quasi-optical properties of microwave antennae. Ultimately, the MWI is used to measure the formation and decay of electrons in the combustion of various hydrocarbon fuels over a range of equivalence ratios, pressures and temperatures. These results, coupled with simultaneous optical emission and absorption measurements provide a dataset against which proposed ion chemistry mechanisms can be validated and calibrated.

dcmurphy@berkeley.edu

W3P123 A NEW SHOCK-TUBE FACILITY FOR THE STUDY OF HIGH-TEMPERATURE CHEMICAL KINETICS

Jose Vivanco, Eric L. Petersen, James Anderson, Daniel Pastrich, Katherine Latourneau, Texas A&M University, United States

A new stainless steel shock-tube facility designed for the study of chemical kinetics at elevated temperatures and pressures is described. It consists of a helium-driven, single-pulse shock tube capable of using both lexan diaphragms and die-scored aluminum disks of up to 4 mm in thickness. It has a relatively large driven-section inner diameter of 16.2 cm to minimize non-ideal boundary layer effects. Test times around 3 milliseconds are achievable at conditions ranging from temperatures between 600 and 4000 K and pressures between 1 and 100 atm behind the reflected shock wave. The facility includes a new high-vacuum system capable of achieving ultimate pressures on the order of 1×10^{-6} torr, a new gas-delivery system, a shock velocity-measurement scheme, a computer-based data acquisition system and the capability of implementing several optical diagnostics. Applications of the new facility include ignition delay time measurements, measurement of reaction rates coefficients and high-temperature spectroscopy, among others.

Additionally, an overall description of the set up and operation of the facility along with details on the characterization procedure of the shock tube will be provided. These include pressure behavior, vacuum integrity, turnaround times and a thorough study on the velocity behavior of the shock to maximize the accuracy of calculated experimental conditions. Also, in order to validate the facility, demonstrated behavior of standard diluted methane-air and hydrogen-air mixtures will be shown. The first set of new data obtained with the new shock tube for acetylene-air ignition delay times will also be presented.

jv0246681@tamu.edu

W3P124 COMPARING PREDICTIONS AND EXPERIMENTAL DATA FOR FLOW REACTOR STUDIES: COMPUTATIONAL RE-INITIALIZATION

Andrei Kazakov¹, Marcos Chaos², Joshua Heyne³, Frederick L. Dryer³

¹National Institute of Standards and Technology, United States ²FM Global Research, United States

³Princeton University, United States

Flow reactor experiments are frequently modeled as plug flow phenomena. Typically, comparison of the computational predictions with experimental data requires careful considerations and reflection of the experimental conditions upstream of the diagnostic region. The manner in which these upstream conditions are reflected in comparison to the experimental reality introduces uncertainties in terms of utilizing the data for kinetic model development and validation. Moreover, the reaction region itself may be neither adiabatic nor isothermal, requiring experimental characterization of the axial temperature distribution. Flow reactor modeling approaches, including various approximation methods, have recently been discussed in detail. One of the methods, referred to as “computational re-initialization”, avoids the need of considering the impacts of upstream experimental conditions and bypasses the requirement of defining an absolute time scale for comparing predictions and experimental data. The general philosophy of this approach is to utilize measured data at some axial location within the region where plug flow

assumptions are well approximated to estimate concentrations of the remaining species for which the measurements are not available. This provides the complete model initialization for comparing predictions and further experimental data downstream of the initialization location and reaction time scale in the region of interest. This technique has been applied in several specific flow reactor studies previously. High dilution was employed in these experiments, thus eliminating the need to consider changes in the diluent mole fraction and closure in experimental atom conservation consistent with the initial reactor chemical composition supplied to the reactor.

In this poster, we will present a more robust methodology for applying computational re-initialization, and demonstrate the method for reaction systems that are neither adiabatic nor isothermal. Applications will be presented involving the pyrolysis of *iso*-propanol and the oxidation of several fuels, including hydrogen and methane. Uncertainties arising from computational re-initialization, model size, and the importance of adding additional initialization species data will be examined.

andrei.kazakov@nist.gov

W3P125 IMPROVED SEMICLASSICAL TUNNELING FORMULA AND ITS APPLICATION TO DEEP TUNNELING

Albert F. Wagner, Argonne National Laboratory, United States

The analytic multidimensional semiclassical tunneling formula of Miller is qualitatively incorrect for deep tunneling at energies well below the top of the barrier. The origin of this deficiency is that the formula uses an effective barrier weakly related to the true energetics but correctly adjusted to reproduce the harmonic description and anharmonic corrections of the reaction path at the saddle point as determined by second order Vibrational Perturbation Theory (VPT2). We have developed an analytic improved semiclassical formula that correctly includes energetic information and allows a qualitatively correct representation of deep tunneling. This involves constructing of a three segment composite Eckart potential that is continuous everywhere in both value and derivative. This composite potential has an analytic barrier penetration integral from which the semiclassical action can be derived and then used to define the semiclassical tunneling probability. The middle segment of the composite potential by itself is superior to the original formula of Miller et al. because it incorporates the asymmetry of the reaction barrier produced by the known reaction exoergicity.

Recent experimental studies by the Continetti group have concluded that the barrier between HOCO and the dissociated products $\text{H}+\text{CO}_2$ is considerably narrower than that represented in a previously available Potential Energy Surface (PES). We apply the original and improved semiclassical formulas to this PES, two recent PESs, and a partial PES specific to this project. As seen in the figure, the original formula is qualitatively incorrect on three of the four PESs. The improved formula produces tunneling probabilities that, with one exception, are quite similar to POLYRATE and in qualitative agreement with the experimental studies. Unlike many methods that require the calculation of a reaction path, semiclassical tunneling requires only VPT2 calculations at the saddle point that can be readily parallelized and are options in popular electronic structure code packages. For existing PESs, we have a code soon to be distributed that samples a user PES to construct a VPT2 description of a saddle point and thereby enables semiclassical tunneling approaches.

wagner@anl.gov

W3P126 SIMULATIONS OF INTERNALLY EXCITED MOLECULES IN DENSE GASES

Albert F. Wagner, Argonne National Laboratory, United States

At low pressures, the relaxation of vibrationally and rotationally excited molecules by a thermal bath gas is characterized by rates that are directly proportional to pressure because each collision can be considered an isolated event. At higher pressures, collisions are no longer isolated, collision frequencies are not directly proportional to pressure, and the relaxation rates are overestimated by linear extrapolations derived from low pressures results. In order to better understand at what pressures this over-estimation becomes important and what mechanisms might be responsible, we have started a series of molecular dynamics simulations in which diatomic, triatomic, and polyatomic molecules are excited in an argon bath gas at different pressures and the system is followed to times where full thermalization has almost been reached (up to 1000 ps). All Ar atoms and the molecule are explicitly followed and the simulations are contained with either periodic boundary conditions or cell techniques. This approach, while computationally expensive, avoids the isolated binary collision approximation of single collision studies and the assumption of full IVR relaxation between collisions of the successive collisions approximation. In our simulations, the intramolecular potential for the molecules are taken from the literature and pairwise additive potentials are used to represent Ar-Ar and Ar-molecule interactions. Preliminary representative decay curves, on a semi-log scale, are shown in the figure where CH_3NO_2 is excited to approximately 40 kcal/mol above thermal energy in room temperature argon. The results in the figure are normalized to the excess vibrational energy above thermal at $t = 0$. One can see that the vibrational relaxation rate increases with pressure. However, between 75 atm and 150 atm, the rates increase by noticeably less than a factor of two. Furthermore, since two of these decay curves are not linear on a log plot, it is clear that multi-rate relaxation becomes apparent at the higher pressures. Mechanisms for this behavior are being investigated. At the highest pressures, van der Waals clusters of Ar and of $\text{CH}_3\text{NO}_2\text{-Ar}$ become important. Related results with similar methods have been seen by others for C_6F_6 in a N_2 bath.

W3P127 GLOBAL SENSITIVITY ANALYSIS WITH SMALL SAMPLE SIZES

Michael Davis, Wei Liu, Raghu Sivaramakrishnan,
Argonne National Laboratory, United States

A new algorithm for Global Sensitivity Analysis (GSA) has been developed for small sample sizes. It relies on the use of sparse regression, specifically the lasso. Results for butanol speciation and ignition will be presented, as well as extensive tests of the algorithm on ignition of *n*-heptane/methyl butanoate mixtures at low temperatures and high pressures. An example of the accuracy for butanol ignition is presented in the Table where column 2 shows the ranking of the sensitivity of reactions using a sample size of 800 runs with the sparse algorithm versus a full regression with 10,000 runs (column 3). This table demonstrates that the method finds the most sensitive reactions with good accuracy, particularly for sensitivity coefficients greater than 0.01. The mechanism used for the butanol calculations had 1446 reactions, indicating that the sparse GSA can use sample sizes smaller than brute-force local sensitivity analysis, which generally is undertaken with two computer runs per reaction. We have also made comparisons of the sparse GSA with our new algorithm for brute-force local sensitivity analysis which generally requires ~ 1.2 computer runs per reaction.

davis@tcg.anl.gov

W3P129 USING DIFFERENTIAL ENTROPY AS A DATA DISCRIMINATION TOOL AT THE DEVELOPMENT OF DETAILED REACTION MECHANISMS

József Bruck, Tamas Varga, István Gy. Zsély, Tamas Turanyi, Eötvös University (ELTE), Hungary

Development of detailed reaction mechanisms is traditionally based on using rate parameters that had been measured directly or determined in theoretical calculations, and comparing the simulation results based on the obtained mechanism with the outcomes of indirect experiments, like concentration measurements in reactors or flame velocity determinations. At the testing of reaction mechanisms, an important question is the relative weighting of the available experimental data. An alternative approach for mechanism development is the optimization of a detailed reaction mechanism. In this context, weighting of the experimental data used is also an important issue.

To determine the importance of data points, we implemented the approach of Sheen et al, which is based on differential entropy. Differential entropy indicates how much the calculated uncertainty of a rate parameter is affected by the reduction of the experimental error of a given data point. It is calculated from the sensitivity of Shannon entropy with respect to data uncertainty. This approach is conceptually related to Bayesian experimental design, which commonly minimizes Shannon entropy, and hence the model prediction uncertainty, during parameter optimization.

Our calculations were based on the optimized version of the hydrogen combustion mechanism of Kéromnès et al. The analysis included flame velocity data, and ignition delay time data measured in shock tubes and rapid compression machines. Weighting was assigned to the data points according to their information content for the improvement of the hydrogen combustion mechanism. The impact of the differential entropy based data discrimination on parameter estimation results was also investigated.

jozsef.bruck@gmail.com

W3P130 GENERATION OF SKELETAL KINETIC MECHANISMS THROUGH REACTING FLUX ANALYSIS AND SENSITIVITY ANALYSIS

Alessandro Stagni, Alessio Frassoldati, Alberto Cuoci, Tiziano Faravelli, Eliseo Ranzi, Politecnico di Milano, Italy

The use of detailed kinetic mechanisms in multidimensional applications is often limited by the significant computing load, resulting from the high number of involved species and reactions: in particular, when mixtures including large hydrocarbon molecules are concerned, their use in CFD codes is practically impossible with the current available technology. Therefore, reduction techniques have been developed in order to obtain proper skeletal models with the right trade-off between mechanism size and accuracy.

In this work, a two-step procedure to reduce a detailed mechanism to an affordable size for CFD applications is presented. Two different approaches are coupled to this purpose: an analysis of reacting fluxes (RFA) in ideal, plug flow reactors to first cut out the unnecessary species and reactions from the original model, and a sensitivity analysis of the retained reactions with respect to some key species, through which the importance of the remaining species is assessed. Following this methodology, several reduced mechanisms were successfully developed for different starting fuels and fuel surrogates, with a “design” criterion of a maximum 15% error on the ignition delay time in the operating range of temperature, pressure and equivalence ratio. The effectiveness of the proposed approach was validated through a multi-scale benchmark. Starting from laminar flame speed evaluations and species formation in ideal reactors, the comparison between the skeletal models and original mechanisms was carried out in more complex case studies, too, like a quasi-dimensional, multi-zone model of a HCCI engine and a two-dimensional CFD model of a laminar coflow flame. In all the cases, the results proved that the reduced models can be used in place of the original ones without significant errors in the provided output. Finally, the computational benchmarks quantified the time savings in using the reduced models, thus showing the practical advantages in the use of skeletal mechanisms even in the simplest simulations.

alessandro.stagni@polimi.it

W3P131 MONTE CARLO SIMULATIONS FOR UNCERTAINTY ANALYSIS IN MODELING SINGLE PULSE SHOCK TUBE DATA

Aleksandr Fridlyand¹, S. Scott Goldsborough², Kenneth Brezinsky¹

¹University of Illinois at Chicago, United States ²Argonne National Laboratory, United States

When modeling speciation data, such as those from single pulse shock tube experiments, agreement between chemical kinetic models and the data is often only described qualitatively. The models developed are typically adjusted manually, where individual reaction rate constants are adjusted within their known error bounds based on sensitivity analysis. Targets used for model development and refinement are typically only the experimentally measured magnitudes of stable intermediate species and their measured reactivity. The experimental target data, within their bounds of uncertainty, can be readily compared with the nominal model predictions. Unlike the uncertainty bounds on experimental data, error bounds for chemical kinetic models used to simulate the experimental data are difficult to determine due to the large number of rate constants with finite uncertainties that are included in the models.

In this study, simple Monte Carlo simulations were performed in order to sample the range of uncertainty of an automatically generated chemical kinetic model when simulating high pressure single pulse shock tube data. Two simple test cases were examined for uncertainty in the rate constants; $\pm 30\%$ and a factor of 2 uncertainties were applied to all of the Arrhenius pre-exponential factors (A), representing minimum and more reasonable estimates in uncertainty, respectively. Approximately 1000 samples were simulated at each uncertainty level, and the results showed a strong central tendency. It was found that the range of probable outputs of the model at the higher temperatures of the experiments were significantly larger than the estimated systematic error in the experimental results. This leads to the possibility of using single pulse shock tube data in constraining larger chemical kinetic models in order to reduce uncertainty. In addition, it is demonstrated how this simple to apply technique provides a quantitatively meaningful way to evaluate the agreement between single pulse shock tube experiments and chemical kinetic models.

afridly2@gmail.com

W3P132 A SEGMENTED KINETIC INVESTIGATION ON SULFATION OF CONDENSED POTASSIUM CHLORIDE IN $\text{SO}_2/\text{O}_2/\text{H}_2\text{O}$ AT 523K-1023K

Zhongfa Hu, Xuebin Wang, Yibin Wang, Shuanghui Deng, Houzhang Tan, Xi'an Jiaotong University, China

The sulfation of condensed alkali chloride has significant implications for deposition and corrosion on heat transfer surfaces in biomass combustion. In the present work, an investigation on the heterogeneous sulfation of condensed KCl (100-200 μm) was conducted in a fixed bed reactor at 523-1023 K with levels of 0.1%-2% SO_2 , 2.5%-10% O_2 and 5%-15% water vapor. The sulfation rate was determined by measuring the formation of HCl in gas and the content sulfur in solid residues. Results show that the sulfation product is only K_2SO_4 , not other potassium sulfates, and the sulfation rate of KCl within temperature range of 523-1023 K can be divided into three stages: 1) a slow increase of sulfation rate below 723 K, 2) a slight decline at 723-773 K, 3) a rapid increase over 823 K. It should be noted that a transformation in sulfation mechanism takes place between 723 K and 823 K, and the further investigations on the effects of reactant SO_2 , O_2 and water vapor at temperature 723 K and 923 K further proved this changing on reaction mechanism. A reason for this phenomena is that a mixture of KCl and the reaction products K_2SO_4 may form a eutectic at higher temperatures, which was confirmed by the results of SEM and TGA. Based on the experimental results, the kinetic calculation has been performed, and the sulfation reaction rate of condensed potassium chloride can be described by the expression $dX/dt = 5.32 \times 10^{-3} \exp(-2120/T)(1-X)^{2/3} (\text{C}_{\text{O}_2})^{0.27} (\text{C}_{\text{SO}_2})^{0.27} (\text{CH}_2\text{O})^{0.42}$ at 523-723 K, and $dX/dt = 1.20 \times 10^4 \exp(-14180/T)(1-X)^{2/3} (\text{C}_{\text{SO}_2})^{0.92} (\text{C}_{\text{SO}_2})^{0.39} (\text{CH}_2\text{O})^{0.12}$ at 823-1023 K.

634072526@qq.com

W3P133 ESTABLISHMENT OF KINETIC PARAMETERS OF PARTICLE REACTION FROM A PERFECTLY STIRRED FLUIDIZED BED REACTOR

Anna Massmeyer¹, Herman Hausteijn², Benjamin Gövert¹, Reinhold Kneer¹

¹RWTH Aachen University, Germany ²Tel-Aviv University, Israel

A Perfectly Stirred Reactor (PSR) ideally provides homogenous, controlled conditions for process and reaction analysis. Therefore, it forms a basis for model development and validation. A novel method for an experimental study of gas-particle reaction, based on realizing a perfectly stirred reactor as a small scale fluidized bed is presented. The reactor enables high heating rates ($\sim 10,000$ K/s), high temperatures ($T=1073\text{K}-1553\text{K}$), long timescale observation (up to several hours), operation with small fuel particles (~ 100 micron), and accurate control of reaction conditions. Char reaction rates are established from real-time gas products analysis by FTIR spectroscopy, through a detailed data-analysis procedure. For rapid reactions, this iterative procedure employs a particle surface-evolution model, while accounting for sampling system signal attenuation. The validity of the perfectly stirred conditions has been experimentally established, by performing temperature and concentration measurements at different heights inside the bed. The method is employed here for char gasification – the Boudouard reaction. The results are highly consistent for over a wide range of conditions ($T=1073\text{K}-1553\text{K}$, $\text{CO}_2=0-76\%$), enabling the reliable establishment of kinetic parameters. The activation energy as well as order of reaction are comparable to the values found in literature. Hence, the

perfectly stirred fluidized bed reactor presented here, provides a novel method to quantitatively study heterogeneous reaction.

massmeyer@wsa.rwth-aachen.de

W3P134 INITIAL STAGES OF THE PYROLYSIS OF POLYETHYLENE

Vadim D. Knyazev, Konstantin Popov, Catholic University of America, United States

Combustion and flammability of plastics are important topics of practical interest directly related to fire safety and recycling of polymeric materials; pyrolysis of the solid is the initial step of its combustion. Mechanistic modeling of combustion and pyrolysis of polymers is considerably hindered by the lack of kinetic data necessary for the modeling. In virtually all existing models of polymer pyrolysis the majority of kinetic parameters used are derived from the data on chemically similar but smaller species in the gas phase. The use of gas phase rate constants is, generally, not justified without an experimental support for the values used.

In the current work, the kinetics of the formation of liquid phase and gas phase products of polyethylene pyrolysis was studied experimentally in the 400 – 440 K temperature range. Gas Chromatography was used to determine the yields of volatile products and Nuclear Magnetic Resonance spectroscopy was employed to determine the kinetics of the formation of three types of carbon-carbon double bonds and terminal $-CH_3$ groups in the liquid polymer melt phase. Experimental conditions were selected to limit the conversion of polyethylene to less than 1% and thus isolate for study only the initial stages of the overall process, where secondary reactions of pyrolysis products are unimportant.

The results were modeled with a simple mechanism consisting of a limited number of reaction types: C-C bond scission, beta-scission of alkyl radicals, hydrogen atom transfer via abstraction, addition of alkyl radicals to double bonds, and radical recombination. Values and temperature dependences of the rate constants of key reactions were determined and compared to the constants of similar reactions of smaller molecules in the gas phase.

Knyazev@cua.edu

W3P135 COMPUTATIONAL FLUID DYNAMICS ANALYSIS OF DIFFERENT GEOMETRIES FOR A JET STIRRED REACTOR FOR BIOFUEL RESEARCH

Amir A.M. Oliveira¹, Amir DeToni¹, Leandro Oliveira¹, Leonel Cancino¹, Edmilsson Oliveira², Mauro Rocha²

¹Universidade Federal de Santa Catarina, Brazil ²Petrobras, Brazil

Most biofuels are derived from alcohols obtained from biomass fermentation and esters produced from the transesterification of vegetable oils. Their use is growing, from the blending with conventional petroleum-based fuels in amounts up to 20%, to the development of new formulations and additives. While real fuels are very complex mixtures, surrogates offer simpler alternatives that emulate physical and combustion properties, and, as such, have become important research tools. The components of surrogates of biofuels include alcohols, methyl esters, acyclic and cyclic ethers. The development of the chemical kinetics mechanisms for surrogates relies on measurements of important combustion parameters for the pure species and their combinations, under the many different conditions of temperature, pressure and concentrations. This is a very active area of research but, still, few chemical kinetics mechanisms for the oxidation of the pure components are available and the set of available measurements is far from covering the range of conditions found in the applications. This work reports an ongoing effort to develop surrogates for aviation biofuels. Among the target experiments being developed, the jet stirred reactor appear as a very flexible and practical tool for chemical kinetics research. The design idealized by P. Dagaut and co-workers is the most well known. It employs four jets to achieve homogeneous turbulent-mixing within a spherical crystal reactor. In this work, several geometric variations on Dagaut's design were numerically studied to assess the homogeneity of the distribution of temperature and concentration of chemical species across the reactor. Full multicomponent-transport and a RANS turbulent model were used in ANSYS Fluent™. The computational domain was divided from 12 to 25 million tetrahedral volumes. The numerical results revealed the main features of the flow within the feeding system and reactor evidencing the high pressure drop in the jet orifice and flow impingement on the reactor's rear wall in some alternative configurations. The nozzle diameter and angle were found to be the critical factors to ensure mixing. From the simulations, a 7 cm³ spherical crystal reactor was designed and manufactured. The experiment is scheduled to be operational in 2015.

amir.oliveira@gmail.com

W3P136 APPLICATION OF BIOMASS-COAL CO-COMBUSTION FOR ELECTRIC GENERATION IN CHINA

Yaohui Si, Haiping Yang, Zhi Li, Qing Yang, Hanping Chen, Huazhong University of Science and Technology, China

Purpose of the work: There is abundant of biomass resource in China which however is not properly used, large amounts of biomass such as agricultural and forestry waste are frequently simply burned and rot away in the land, causing severe pollution problems and energy wastage. One most typical way of utilizing biomass is to burn it in blends with coal or alone for electric generation and this technique has been tested in many areas in China. In this article, we aim at telling the combustion feature; ash characteristics; chlorine derived corrosion and pollutants status of burning several types of typical local biomass with coal, trying to give an advice on the application of biomass-coal co-combustion in domestic power market.

Approach: In our experiment, biomass samples(cotton stalk, rice husk, sawdust) is mixed with huangling bituminous coal at the ratio of 0%,10%, 20% and 30% and each group is combusted at the temperature of 10500C and 13000C in TG-DTG and drop tube furnace. Firstly, a thermogravimetry analysis is made to analyze the overall combustion feature. During the combustion in drop tube furnace, The excess air coefficient is 1.2 and 1.4 and the feeding speed is 0.3g/min. Then, an infrared gas analyzer is used to detect the gas emissions (CO₂, NO, SO₂, HCl, HF) on line and the concentration of O₂ is also measured by a portable flue gas analyzer. Later, an XRD and SEM-EDX test is made of the ash. A numerical simulation is conducted on a trial running coal and biomass co-combustion power plant to estimate the combustion and pollution status.

Results &Conclusions: A synergy obviously occurs when co-combusting biomass and coal and it facilitates the process of coal combustion. But apparently, the promotion degree depends on the different kinds of coal and biomass.Rice husk has a higher concentration of ash content and alkali metal, in comparison with cotton stalk and sawdust. It advised mix ratio for Rice husk is no more than 10% and the ratio for cotton stalk and sawdust is no more than 20% in co combustion With a higher proportion of biomass mixed in coal, the production of NO_x reduce in both high and low temperature zone, indicating that a lower NO_x emission may be approached with the designed condition and the co-combustion of biomass and coal. As demonstrated in the simulation, with a higher proportion of biomass mixed in coal, the production of NO_x reduce in both high and low temperature zone, indicating that a lower NO_x emission may be approached with the designed condition and the co-combustion of biomass and coal. And also, a weakened tube erosive wear could be seen.

syh850330@gmail.com

W3P137 EFFECTS OF FLUE GAS ADDITION ON THE PREMIXED OXY-METHANE FLAMES IN ATMOSPHERIC CONDITION

Guan-Bang Chen, Yueh-Heng Li, Fang-Hsien Wu, Yei-Chin Chao, NCKU, Taiwan

This numerical study investigates the flame characteristics of premixed methane with various inert gas dilutions in order to simulate oxy-combustion of hydrocarbon fuels with flue gas recirculation system. In general, a flue gas consists of high concentration CO₂/H₂O and high gas temperature. The diluent gas in oxy-combustion has been changed compared with air-combustion, so that the flame behavior and combustion characteristics of oxy-fuel must be influenced. The effect of laminar burning velocity and adiabatic flame temperature on inert gas dilution is discussed via using Chemkin-pro simulation. By observing the resultant flame temperature and species concentration profiles one can identify that the flame location shifts, and the concentration profile of major chemical reaction radicals varies, indicating the change of flame structure and flame chemical reaction paths. The dominant initial consumption reaction step of methane shifts from R53 (H+CH₄CH₃+H₂) to R98 (OH+CH₄CH₃+H₂O) when nitrogen is replaced by the recirculated gases. It is because the chemical effects of the recirculated gases changes the flame reaction pathway, and further affect reaction rate, species and radical concentrations.

gbchen26@gmail.com

W3P138 STRUCTURE OF PREMIXED AMMONIA/AIR FLAMES AT ATMOSPHERIC PRESSURE - LASER DIAGNOSTICS AND KINETIC MODELLING

*Christian Brackmann, Vladimir Alekseev, Bo Zhou, Emil Nordström, Per-Erik Bengtsson, Li Zhongshan, Marcus Aldén, Alexander Konnov
Lund University, Sweden*

Ammonia (NH₃) flame structure has been the subject of many studies. However, previous studies employed oxidizers (O₂/N₂, O₂/Ar, N₂O/Ar) with composition significantly different from that of air, in order to facilitate flame stabilization. Thus, there is a lack of flame structure data for ammonia/air combustion. Therefore, the goal of the present work was to acquire experimental profiles of temperature as well as concentration of O₂ and important intermediates, NH, NO, and OH, in lean, stoichiometric, and rich ammonia/air flames at atmospheric pressure using laser diagnostic methods. Measurements were made on a water-cooled stainless steel porous-plug burner for ammonia/air flames of equivalence ratios (ϕ) of 0.9, 1 and 1.2. Radical species were monitored by Laser-Induced Fluorescence (LIF) whereas profiles of temperature and O₂ concentration were acquired using rotational Coherent Anti-Stokes Raman Spectroscopy (CARS). Fluorescence measurements were made under signal saturation conditions or combined with absorption measurements in order to allow for evaluation of quantitative radical concentrations.

Three mechanisms were compared with the new experimental data: the model of Duynslaegher et al., the model of Shmakov et al., and the mechanism of Mendiara and Glarborg. The impact of uncertainties in equivalence ratio, inlet flow rates and temperatures was evaluated by re-runs of the models, which allowed for estimations of total uncertainties in radical concentrations and flame front positions.

The stoichiometric flame showed a maximum temperature of around 1800 K while the lean and rich flames reached maximum temperatures around 2000 K. Only the model of Mendiara and Glarborg was able to reproduce flames detached from the burner when solving the energy equation. The shapes of the temperature and O₂ profiles were very well reproduced by this model for all flames with good agreement in terms of absolute values and flame front position. In addition, the shape of experimental radical profiles in general showed good agreement with this model. Regarding radical concentration prediction, the performance of models of Mendiara and Glarborg and Shmakov et al. was found to

be similar whereas the model of Duynslaegher et al. showed larger discrepancy with the experiments and the two other models in most cases. For OH and NO prediction, the best agreement with experimental data was observed for the model of Mendiara and Glarborg in the stoichiometric flame. In the lean and rich flames all three models showed a considerable discrepancy for one or both of these radicals and variations of individual rate constants did not improve the agreement sufficiently. Thus, further investigations to determine the accuracy of experimental data, in particular for NO but also NH, are currently in progress in order to clarify whether some structural modifications of the mechanisms are necessary.

christian.brackmann@forbrf.lth.se

W3P139

IMPROVED KINETIC MODEL AND HCCI ENGINE SIMULATIONS OF DIISOPROPYL KETONE IGNITION

Ghazal Barari, Subith Vasu, University of Central Florida, United States

DiIsoPropyl Ketone (DIPK) is considered as a promising biofuel candidate, which is produced using endophytic fungal conversion. In the current study, modeling of DIPK HCCI engine experiments from Sandia is conducted with single-zone engine and multi-zone models using CHEMKIN PRO. Both adiabatic and non-adiabatic single-zone HCCI models are explored. The non-adiabatic model employs the Woschni correlation to account for heat transfer from the Sandia HCCI engine with the coefficients determined by matching the motored pressure trace of the engine. In order for the single-zone model to give accurate compressed-gas pressures and temperatures, the published DIPK kinetic model is improved. The modifications have been done by adding important intermediate species and radical reactions which were not considered in the original reaction mechanism. The corresponding thermodynamic properties for the new species were calculated using the THERM program and rates were either estimated in comparison with similar molecules or calculated using the RMG program. In addition, zero dimensional simulation has been conducted to obtain ignition delay time for the temperature range of 500-1000 K which showed better agreement with the available shock tube experimental data. For the single zone model of HCCI engine, the updated model provides better agreement from BDC to TDC, however, it over predicts the pressure peak as expected. Brute force sensitivity analyses revealed that the most sensitive reaction in which DIPK participates is the H-abstraction reaction from the fuel by HO₂. Discussion is provided on the validity of the DIPK model in comparison with the parametric engine data over a range of temperature, pressure, equivalence ratio, and engine speed. Although ignition timing can be investigated using the single-zone model, heat release rates in HCCI engines is largely controlled by charge non-uniformities. Since the charge in the Sandia HCCI engine was well premixed for these experiments, the heat-release rate is mainly affected by temperature non-uniformities resulting from heat transfer and turbulent convection. Heat release results from multi-zone modeling of the current experiments showed good agreement with the Sandia experimental trends.

gh.barari@knights.ucf.edu

W4P001 SPECTROSCOPY OF TRACERS FOR TWO-DIMENSIONAL LIF MEASUREMENTS OF OIL FILM THICKNESS AND FUEL-OIL INTERACTION IN INTERNAL COMBUSTION ENGINES

Daniel Fuhrmann, University of Duisburg-Essen, Germany

In combustion research, Laser-Induced Fluorescence (LIF) of organic tracers is commonly used to investigate fuel/air mixing. Sprays in internal combustion engines have also been investigated with this method, but liquid films are less explored. The objective of this poster is to present advances in LIF of laser dyes for imaging the thickness of oil films as they occur in the piston ring area of an engine. Tracer-LIF is also investigated to image the interaction between fuel and oil-film residues, which is thought to be relevant to pre-ignition phenomena in direct-injection engines. Although the experiments are dedicated mainly to liquid films, the procedures and challenges in quantifying the measurements are very similar to those in gas-phase experiments, yet there are novel and interesting aspects. Investigations of the dyes used as tracers for oil and fuel are presented. Oil is a rather unconventional solvent for laser dyes, and thus excitation and fluorescence of these dyes in oil is not well known, in particular at elevated temperatures. In addition to dyed oil, we also investigated mixtures of oil, dye, and toluene. Toluene can be used as a tracer for gasoline model fuels. Thus, this liquid system may be relevant to laser-based measurements of fuel contaminations in the lubrication oil.

daniel.fuhrmann@uni-due.de

W4P002 SIMULTANEOUS MEASUREMENTS OF H_2O_2 AND H_2O CONCENTRATION DISTRIBUTIONS USING PHOTOFRAGMENTATION LASER-INDUCED FLUORESCENCE

Kajsa Larsson, Lund Institute of Technology, Sweden

A quantitative measurement of hydrogen peroxide (H_2O_2) and water (H_2O) vapor is demonstrated. The method is based on Photofragmentation Laser-Induced Fluorescence (PFLIF), where a pump pulse (248 nm) dissociates H_2O_2 into two OH fragments whereupon a probe pulse, whose wavelength is tuned to 281.91 nm, i.e. the overlapping Q1 and R2 absorption lines in the $\text{A}_2\text{S}^+ (v=1) \rightarrow \text{X}_2\text{P} (v=0)$ band of OH, induces fluorescence from the OH fragment. The H_2O_2 concentration is determined from the total fluorescence intensity, while the H_2O concentration is extracted from either the spectral or the temporal shape of the OH fluorescence. Given that the $\text{H}_2\text{O}_2/\text{H}_2\text{O}$ vapor is surrounded by a bath gas that has a low cross section for collisional quenching of OH fluorescence, for example argon, the intensity ratio between the fluorescence emitted in the 0-0 and 1⁻¹ band is dependent on the water concentration. Thus, by measuring this ratio the water concentration can be determined. Thus, the concept allows simultaneous measurement of H_2O and H_2O_2 concentrations. Spectrally dispersed fluorescence spectra were recorded in different $\text{H}_2\text{O}_2/\text{H}_2\text{O}$ -mixtures of known compositions. The experimental spectra agree very well with calculated spectra, thus validating the model. Single-shot two-dimensional imaging has been demonstrated using a setup based on two intensified CCD cameras. With the spectral dependence of the OH fluorescence, also follows a temporal dependence of the 0-0 and 1⁻¹ bands. This fact was utilized in the 2-D measurements by capturing different temporal regions of the OH fluorescence using different intensifier gates on the two cameras. Simultaneous single-shot images of H_2O_2 and H_2O , recorded in a mixture containing a $\text{H}_2\text{O}_2/\text{H}_2\text{O}$ concentration gradient, are shown. The quantification relies on calibration measurements performed in different $\text{H}_2\text{O}_2/\text{H}_2\text{O}$ mixtures of known compositions. We believe that the proposed measurement concept could be a valuable tool in various areas where *in-situ* visualization of H_2O_2 and H_2O is of importance, for example in atmospheric science and research on vapor-phase H_2O_2 sterilization in the pharmaceutical and aseptic food-packaging industries.

kajsa.larsson@forbrf.lth.se

W4P003 CO AND CO_2 FOLLOWED BY LASER-INDUCED FLUORESCENCE DURING CATALYTIC OXIDATION OF CO

Johan Zetterberg, Sara Blomber, Johan Gustafson, Christian Brackmann, Edvin Lundgren, Lund University, Sweden

Catalytic oxidation of CO by Pt-group metals is important not only for industrial purposes and exhaust gas treatment but has also an academic value. To increase the understanding of the fundamentals, surface sensitive techniques such as surface X-ray diffraction and X-ray Photoelectron Spectroscopy (XPS) are typically used to determine the active phase. This is done by correlating the surface structure and chemical composition with Mass Spectrometry (MS) data as the sample is heated. The mass spectrometer in these setups are usually connected at the gas outlet from the reactor, and monitors the gas without any spatial resolution and with poor temporal resolution, leaving you vulnerable and blind to from where the gas signal actually originates from. On top of that, the pressure range for e.g. XPS is limited to about 1 torr, a pressure much lower than in real applications.

By using laser diagnostics, these inherent shortcomings can be overcome and *in situ* measurements of the gas phase of both the reactant CO and the product CO_2 can be measured in two dimensions. This gives an opportunity to follow the event both with a high spatial and temporal resolution, directly being able to determine from where the signal arises. Together

with the fact that laser-based techniques are applicable above atmospheric pressure means that it is possible to get gas phase information at real working conditions.

In the CO case, pico-second two-photon laser-induced fluorescence was used to monitor the gas distribution above the catalytic sample, a Pd (110) single crystal. The sample was positioned in a reactor where the temperature, pressure and gasflows could be carefully controlled. The temperature of the sample was then ramped up above the ignition temperature of the catalyst and back again, following the decreasing CO as the Pd (110) crystal becomes active. The same measurement was made, but following the CO₂ instead, using infra-red laser-induced fluorescence. Here, the CO₂ signal should increase as the sample becomes active and the CO is catalytically oxidized. As both measurements were made in 2D, a spatial correlation between the CO and CO₂ could be made. This is the first time both the reactant and the product has been monitored in 2D and in time for catalytic oxidation of CO, following the whole event. The spatially resolved results were also compared to the global gas composition collected by MS at the outlet of the reactor. We see a great promise in optical diagnostic techniques to study catalysis, and when applied at similar or the same conditions as surface sensitive methods a more complete picture of the phenomenon can be given.

johan.zetterberg@forbrf.lth.se

W4P004 CHOOSING THE OPTIMAL FUEL TRACER FOR LIF IMAGING IN DIFFERENT USE-CASE SCENARIOS
Sebastian Kaiser, Martin Goschütz, Martin Schild, Daniel Fuhrmann, Christof Schulz, University of Duisburg-Essen, Germany

Fluorescent “tracers” have been used in a wide range of experiments on liquid and gas-phase heat and mass transfer. For example, in combustion, a model fuel can be doped with a UV-excitable tracer, which then allows visualization of mixing and the temperature distribution in an optically accessible engine. Quantitative application of such tracer-based Laser-Induced Fluorescence (LIF) requires previous in-depth characterization of the photophysical properties of the tracer. At elevated temperatures and pressures this is quite complex. Nevertheless, the “palette” of characterized tracers is continuously expanding. At the same time, the range of available cameras has broadened, with sensors based on different CCD and CMOS technologies available. Thus, for a given experiment, the investigator has considerable freedom in choosing the optimal tracer and detector, depending on the conditions and goals of the experiment.

This poster is intended to complement a submission by T. Benzler. That contribution compares LIF-tracers in terms of their fundamental photophysical properties at elevated temperatures and pressures. The current contribution examines the effect of these properties on different use scenarios, including examples from imaging experiments at room temperature and pressure. Several tracers with very different thermodynamic and photophysical properties are used, as well as different camera systems. In particular, we consider what an optimal candidate would be for tracer-LIF of natural gas in the intake and cylinder of an internal combustion engine, but the results are transferable to other use scenarios.

sebastian.kaiser@uni-due.de

W4P005 EFFECT OF FLAME FLUCTUATIONS ON MULTI-LINE NO-LIF GAS-PHASE TEMPERATURE IMAGING
Omid Feroughi, Helmut Kronmayer, Thomas Dreier, Christof Schulz, University of Duisburg-Essen, Germany

Multi-line NO Laser-Induced Fluorescence (LIF) thermometry is a tool to accurately measure two-dimensional gas-phase temperature distributions in combustion systems through least squares fitting of excitation spectra of thermally populated molecular energy levels. The method yields accurate temperatures in steady systems but has some drawbacks when fluctuations are involved due to the necessity of signal-averaging over time. Deviations also occur when the LIF signal is spatially averaged over regions with steep temperature gradients, e.g., across flame fronts. In the present work these effects are quantified by a theoretical approach of simulating fluctuating NO-LIF excitation spectra. Gaussian temperature distributions as well as linear and bimodal distributions are assumed. Bimodal distributions have the largest effect on the measurements whereas linear and Gaussian distributions have less influence. Temperature fluctuations of less than $\pm 5\%$ result in a negligible error of less than $\pm 1\%$ in temperature for all cases. We find that the deviation of the “measured” temperature to the arithmetic average temperature is negligible for symmetric fluctuations around 900 K. At lower mean temperatures, measurements systematically over-predict the real temperature. At higher mean temperatures the opposite occurs and the temperature is under-predicted. Surprisingly, the influence of fluctuations depends only little on the spectral region used for spectra acquisition as far as investigated.

The results of the theoretical approach can be used to estimate the systematic error on temperature arising from flame fluctuation based on a post-processing algorithm consisting of the statistical analysis of the instantaneous NO-LIF images recorded during LIF-thermometry excitation scans in a pilot-plant nanoparticle-synthesis flame reactor operating with a turbulent jet flame. With a Reynolds number of about 8000, the current jet flame can be considered mildly turbulent and a more detailed characterization of flame properties would be of interest, particularly with respect to an optimum reactor design based on, e.g., comparisons with CFD simulations. For this purpose analyzing turbulent flame fluctuations is one

means to characterize the combustion process. The objective of the examinations is the following: The statistical analysis of the single-shot images helps to quantify the influence of variations in local NO concentration or temperature fluctuations on the determined temperature. In order to obtain the contribution of the NO-concentration fluctuations a temperature-insensitive transition in the NO A–X(0,0) band is selected, for the contribution of temperature fluctuations a temperature-sensitive transition in the same band is selected, respectively.

omid.feroughi@uni-due.de

W4P006 COLLISIONAL QUENCHING OF FORMALDEHYDE LASER-INDUCED FLUORESCENCE

Jonathan H. Frank, Erxiong Huang, Bruno Coriton, Sandia National Laboratories, United States

Formaldehyde is an important intermediate species in hydrocarbon combustion, and its lifetime in turbulent flames can be sufficiently long that it is subject to significant transport by turbulent mixing. For some hydrocarbon fuels, there are significant discrepancies in predictions of formaldehyde concentrations using different chemical mechanisms. Quantitative measurements of formaldehyde concentrations in flames remain a challenge.

Formaldehyde is commonly detected using Laser-Induced Fluorescence (LIF) with UV laser excitation. However, these LIF measurements are often qualitative and only provide a relative measure of formaldehyde distributions because of a lack of information on formaldehyde photo-physics, and in particular the collisional quenching rates. The present study provides measurements of collisional quenching rates of formaldehyde LIF in an isolated, well-controlled system. A quartz cell is filled with a sub-atmospheric pressure mixture of formaldehyde and the quenching partner of interest. Laser-induced fluorescence of formaldehyde is excited by the third harmonic of an injection seeded Nd:YAG laser. The diode seed laser is temperature tuned to $\lambda=354.83$ nm to excite overlapping transitions in the band of the system. The fluorescence emission is imaged onto an intensified CCD camera using a medium-format camera lens, an AR-coated singlet, and a 35-mm format lens. A color glass filter (GG375) in the imaging system blocks elastic scattering from the laser and transmits the formaldehyde LIF signal. The pressure dependence of the collisional quenching rate is determined by measuring the Stern-Volmer relation of formaldehyde LIF signal as a function of the quencher pressure. Quenching rate measurements for major quenching partners in flames will be presented.

jhfrank@sandia.gov

W4P007 SIMULTANEOUS HIGH-SPEED FORMALDEHYDE FLUORESCENCE AND THREE-DIMENSIONAL VELOCIMETRY IN LIFTED, NON-PREMIXED JET FLAMES

Prabhakar Venkateswaran¹, James Michael¹, Harish Subramani¹, Suresh Roy², James Gord³, Terrence R. Meyer¹

¹Iowa State University, United States ²Spectral Energies, LLC, United States ³Wright-Patterson AFB, United States

We report recent measurements designed to elucidate the spatio-temporal characteristics of the stabilization region of CH₄/N₂ lifted, turbulent, non-premixed jet flames. This is accomplished utilizing a pair of burst-mode lasers to perform 10 kHz and greater formaldehyde Planar Laser-Induced Fluorescence (CH₂O-PLIF) simultaneously with tomographic and stereoscopic Particle Image Velocimetry (PIV) measurements in lifted turbulent jet flames. A key development enabling these measurements is the ability to achieve burst-mode laser output with closely-spaced, equal-amplitude pulse pairs from a single laser source for PIV measurements. The burst-mode PIV laser is a custom Nd: YAG-based system consisting of a continuous-wave diode laser seed source and three successive flashlamp-pumped amplifier stages. An arbitrary waveform generator is used to control a high-dynamic-range Acousto-Optic Modulator (AOM) to produce pulse pairs with spacing down to sub-microsecond and with individual 532 nm pulse energies of 50 mJ at a laser repetition rate of 10,000 pulse pairs per second. In this manner, equal pulse amplitudes can be achieved despite the large amplification gain (~108) of the initial seed pulse laser energies of order 10 nJ. The suppression of detrimental Amplified Spontaneous Emission (ASE) is achieved through the use of an intensity-dependent phase conjugate mirror. Depending on the pulse pair repetition rate, for a 10 ms burst-length, this results in 100-500 pulse pairs and energy sufficient for large-sheet PIV and tomographic PIV.

These measurements can be used to develop a detailed picture of the complex flame-turbulence interactions responsible for flame stabilization by ensuring a high degree of image correlation with short time spacing while varying the repetition rate to track the relevant spatio-temporal flow physics under turbulent conditions. This allows simultaneous measurement of the three-dimensional flow field along with high-speed measurement of formaldehyde fluorescence using a second burst-mode laser tuned for ultraviolet excitation at 355 nm. The measurements improve the capability to capture the multi-dimensional and time dynamical features of fluid-flame interactions relevant, for example, to stabilization in turbulent, non-premixed jet flames.

prabs84@gmail.com

W4P008 INVESTIGATION OF PS-PFLIF FOR DETECTION OF HYDROGEN PEROXIDES IN LAMINAR FLAMES

Malin Jonsson, Kajsa Larsson, Jesper Borggren, Marcus Aldén, Bood Joakim, Lund University, Sweden

Photolytic interference is a well-known trouble in laser-diagnostic experiments performed in the UV regime, and Photo Fragmentation Laser-Induced Fluorescence (PFLIF) is no exception. For PFLIF detection of hydrogen peroxides, a problem appears if the photolysis laser creates OH fragments from molecules other than hydrogen peroxides. Even if no OH photo fragments are directly produced, OH may be created by chemical reactions originating from any photo fragment. This is the case for PFLIF detection of hydrogen peroxides in premixed hydrocarbon flames, where hot CO₂ in the product gas is photo dissociated into CO + O whereupon the O atom reacts with H₂O and H₂ producing OH, which hence results in an interfering signal contribution. It has been shown that decreasing the pump-probe delay time can reduce this photochemical interference. However, with nanosecond laser pulses it was not possible to reduce the interference to a level giving satisfactory signal-to-interference ratio. Picosecond laser pulses allow for very short pump-probe delay times, allowing significant suppression of photochemical interferences. In the present work a laser system producing 80-picosecond laser pulses has been used for PFLIF measurements of hydrogen peroxides in premixed flames as well as in free flows of H₂O₂/H₂O vapor. Flame measurements were performed for a set of different pump-probe delay times and for different probe wavelengths, in order to analyze the intensity of the interference vs delay time. At very short delay times (< 10 ns), the OH fragments are expected to be in non-thermal equilibrium. The rotational population dynamics of OH fragments was therefore investigated in pump-probe delay studies of OH fragments created by H₂O₂ photolysis at ambient conditions.

malin.jonsson@forbrf.lth.se

W4P009 MECHANISM OF PHASE-SELECTIVE LASER-INDUCED BREAKDOWN SPECTROSCOPY IN HETEROGENEOUS COMBUSTION

Yihua Ren, Yiyang Zhang, Shuiqing Li, Tsinghua University, China

A novel phase-selective Laser-Induced Breakdown Spectroscopy (LIBS) has been developed for diagnostic in heterogeneous combustion (flame synthesis and coal combustion). In this work, *in situ* diagnostic of phase-selective LIBS on flame-made TiO₂ nanoparticles is demonstrated in a premixed Bunsen flame stabilized by non-premixed flat flames. By selecting the laser power between the gas and particle breakdown thresholds, atoms in particle phase but not gas phase can be excited with characteristic atomic emission spectrum, which has been applied in diagnostic gas-to-particle conversion and particulate volume fraction of pure- or multi- component in one-dimensional or planar measurement. It is found that the light scattering of TiO₂ nanoparticles does not increase proportionally with laser power which is different from Rayleigh signal of gas molecules.

The scattering cross-sections of nanoparticles indicate that the transition point from elastic to inelastic scattering occurs at the laser power about 1mJ/pulse, while the atomic spectrum of Ti at 498.17nm arises at the almost same laser power. Time-resolved measurements of Rayleigh signal and phase-selective LIBS further confirm that the nanoparticles are ablated during the ~10ns pulse of the laser shot. Therefore, it is implied that the electrons are excited to conduction band after two-photon absorption. The free electrons are accelerated by laser field, collide with crystal lattice and transfer energy from the electromagnetic field to the lattice. The crystal lattice is then ablated to disperse atoms. Finally, the atoms are excited by electrons and emit atomic spectra.

ryh13@mails.tsinghua.edu.cn

W4P010 MECHANISM FOR LASER-INDUCED FLUORESCENCE SIGNAL GENERATION FROM ABLATION SEEDED, PLANAR FLAME THERMOMETRY

Dahe Gu, Zhiwei Sun, Paul Medwell, Zeyad Alwahabi, Bassam Dally, Graham Nathan, University of Adelaide, Australia

The mechanism of atomic indium generation for Laser-Induced Fluorescence (LIF) of indium from laser ablation seeding was investigated in a hydrogen flame. The morphology and particle size distribution of the ablation products was examined with Scanning Electron Microscopy (SEM) and Transmission Electron Microscopy (TEM). These investigations show that the ablation products comprise complex agglomerates of nano-sized primary particles of indium compounds and micron-sized spherical indium beads. Images of the LIF, Mie scattering of ablation products and natural fluorescence emission of indium in the flame were recorded to investigate the mechanism of fluorescence signal generation. The relative contribution of natural fluorescence towards the total fluorescence signal, the evolution of ablation products through the flame structure and the correlation between LIF signal and ablation products were assessed by comparing these images. It is revealed that the LIF signal generation is associated with conversion of indium nano-particles into the gas phase by thermal decomposition in the flame. A further way for thermal decomposition of the nano-particles is also identified, that of *in-situ* heating the ablation products by laser-ablation. This is assessed by means of a second laser, introduced prior to the excitation laser, to reveal that the LIF signal can be enhanced by laser ablation, particularly in the upstream regions of the flame.

dahe.gu@adelaide.edu.au

W4P011 LASER-BASED *IN-SITU* MEASUREMENT OF GAS-PHASE TEMPERATURE AND SiO CONCENTRATION IN A LOW-PRESSURE NANOPARTICLE SYNTHESIS REACTOR USING LASER-INDUCED FLUORESCENCE

Omid Feroughi, Andreas Langer, Thomas Dreier, Christof Schulz, University of Duisburg-Essen, Germany

Low-pressure flames represent a promising way to synthesize highly specific metal oxide nanoparticles from suitable gas-phase precursors. Examples are the production of SiO₂ particles from TEOS (Tetraethylorthosilicate) or Fe₂O₃ from Fe(CO)₅ (iron pentacarbonyl), respectively, in hydrogen/oxygen flames. The properties of the synthesized nanoparticles strongly depend on the reaction conditions, where the spatial variation of the gas-phase temperature during particle formation within the flame is a most important influencing factor and therefore of particular interest. For a more detailed understanding and validation of simulations of nanoparticle generation in combustion systems, optical, non-intrusive laser-based diagnostics can provide spatially-resolved information of gas temperature, intermediate species concentrations, and particle size.

We apply multi-line NO Laser-Induced Fluorescence (LIF) thermometry for *in situ* gas-phase temperature measurements of low-pressure H₂/O₂ flames and doped with various concentrations of Hexamethyldisiloxane (HMDSO) that is used as a precursor for the synthesis of SiO₂ nanoparticles. In order to obtain semi-quantitative SiO concentrations from the measured SiO-LIF intensities, effective SiO-LIF lifetimes were determined and used together with the measured temperature distributions. The potential of multi-line SiO-LIF thermometry is demonstrated by temperature-fitting spectral signatures to measured SiO-LIF excitation spectra.

omid.feroughi@uni-due.de

W4P012 DEVELOPMENT OF A CONTINUOUS-WAVE CAVITY RING-DOWN SPECTROMETER FOR THE STUDY OF ACETYLENE IN SOOTING FLAMES.

Gordon Humphries, Iain Burns, Michael Lengden, University of Strathclyde, United Kingdom

Cavity Ring-Down Spectroscopy (CRDS) is a sensitive technique for measuring concentrations of gases present in trace quantities. It has been used in the past for detection of radicals such as OH, CH and NCN in flames; in our own recent work we have used pulsed CRDS to measure concentrations of 1CH₂ and HCO in laminar flames of premixed ethylene and air, under sooting conditions. The great majority of previous publications on using CRDS to undertake measurements within combustion processes have utilised high power pulsed dye lasers.

Continuous-wave Cavity Ring-Down Spectroscopy (cw-CRDS) is a variant of the technique that involves the use of low-power light-sources such as diode lasers. This allows for a much less expensive instrument that is significantly more compact. Despite the widespread availability of continuous-wave diode lasers at an increasing range of wavelengths, little work has been conducted on the development of continuous-wave CRDS for use in a combustion environment. This lack of progress is largely due to perceived potential difficulties arising from optical effects, such as thermal lensing and beam-steering, due to the high temperature gradients inherent in combustion processes which can cause light to be lost from the cavity at an increased rate.

Distributed feed-back lasers (especially those at telecommunications wavelengths) are readily available in fibre coupled packages. The use of these lasers simplifies the layout of a CW CRDS system by replacement of several commonly used bulk optical components with their fibre coupled counterparts. The use of fibre coupled components means that the cavity and mode matching optics are the only bulk optical components required in the system, allowing for greater flexibility of installation and simplified alignment. A low-power (Characterisation of the spectrometer has been completed without a flame present using the weak absorption transition of ambient water at 6460cm⁻¹. It was possible to completely resolve this feature, which has a maximum absorption of 3×10⁻⁵. Analysis of the signal to noise ratio of these results has shown the spectrometer capable of measuring an absorption as low as 5×10⁻⁶. The spectrometer has been used to recover absorption spectra from the McKenna burner, showing an acetylene feature that is relatively isolated from surrounding water lines. This feature was the P17e acetylene line at 6513 cm⁻¹. The cw-CRDS method allows the measurement of substantially lower fractional absorption than is possible standard direct absorption techniques.

gordon.humphries@strath.ac.uk

W4P014 A NEW FAST TIME-RESPONSE PULSED CRDS SENSOR FOR SENSITIVE DETECTION OF ETHYLENE

Awad Alquaity, Ettouhami Essebbar, Aamir Farooq, King Abdullah University of Science and Technology, Saudi Arabia

Ethylene is a key intermediate species in combustion processes and is formed primarily during the oxidation and pyrolysis of large alkanes. Ethylene plays an important role in the formation and growth of polycyclic aromatic

hydrocarbons which are primary precursors of soot. High-fidelity kinetic models describing the high-temperature combustion of large alkanes require reliable sub-models for the oxidation and pyrolysis of alkenes, of which ethylene is most abundant due to its high-temperature stability. Measurements of ethylene time-histories in reactive environments will lead to better understanding of reactions affecting the formation and consumption of ethylene and will subsequently aid the development and validation of fuel surrogate mechanisms.

In this study, a novel fast time-response sensor based on pulsed Cavity Ringdown Spectroscopy (CRDS) has been successfully developed and used for performing sensitive absorption measurements of ethylene in the mid-IR. Using a tunable external-cavity quantum cascade laser, the sensor is able to cover a wide wavelength range from 10 to 11.1 μm (900 – 1000 cm^{-1}). Individual ringdown measurements are completed in 1 to 2 μs and repetition frequencies as high as 100 kHz are possible. The sensor operation was validated in a room-temperature static cell using absorption lines of carbon dioxide centered near 938.69 cm^{-1} and 974.62 cm^{-1} . Ethylene concentrations as low as 55 ppb were measured near 949.83 cm^{-1} in a 70 cm static cell at ambient conditions. The sensor is suitable for measuring trace ethylene concentrations in the atmosphere as was demonstrated by measuring ethylene in a sample of laboratory air and in an air sample collected from a car parking facility. The fast time response (~ 10 ms) of the sensor was demonstrated by measuring ethylene concentration time-histories in a shock tube. To the best of our knowledge, this is one of the first successful applications of the pulsed CRDS technique to perform fast-time response measurements of species time-histories in a shock tube. Cavity locking was maintained in both non-reactive and reactive shock tube experiments and the trend of ethylene decay was captured accurately in the ethylene pyrolysis experiments.

awad.alquaity@kaust.edu.sa

W4P015 SIMULTANEOUS IMAGING OF MIXTURE FRACTION, VELOCITY, AND SOOT VOLUME FRACTION IN A SOOTING JET FLAME

Okjoo Park¹, Ross Burns¹, Oliver Buxton², Noel Clemens¹

¹University of Texas at Austin, United States, ²Imperial College, London, United Kingdom

The present study seeks to experimentally quantify the mixture fraction and soot-volume fraction fields, and kinematics in the near-field soot-inception region of a low-strain jet flame using simultaneous diagnostics including Planar Laser-Induced Fluorescence (PLIF) of Krypton (Kr), in conjunction with stereoscopic Particle Image Velocimetry (sPIV) and Laser-Induced Incandescence (LII). For this case study, a turbulent, non-premixed ethylene/N₂/Kr flame is used to demonstrate these simultaneous measurement techniques. Planar laser-induced fluorescence of Krypton enables the imaging of a conserved scalar in the flow. The fluorescence of krypton is achieved by exciting the 5p[3/2]₂←4p₆ 1s₀ transition, a transition accessible via two-photon absorption at 214.7 nm. The resulting fluorescence is collected at 760.2 nm, arising from the decay of this upper state to the 5s[3/2]₂ state. The inclusion of sPIV and calibrated LII with the Kr PLIF allows for measurements of the local velocity field and soot volume fractions, respectively, crucial for understanding the formation and transport of soot within the flame. Initial results with krypton PLIF indicate minimal distortion of the measured radial concentration profiles for seeding concentration up to 4 percent krypton by mole fraction with notable distortion becoming apparent at the jet exit due to both absorption of the exciting radiation and self-quenching of the fluorescence for increasing concentration. Furthermore, contamination of the fluorescence signal due to the presence of Polycyclic Aromatic Hydrocarbons (PAHs) was found to be negligible in the soot inception region, though the intermittent soot structures affected the extinction of the incident exciting radiation to some extent. An analysis of the raw fluorescence signal indicates a strong negative correlation between the observed PLIF signal and the soot volume fraction within the stoichiometric velocity surface of the flame, indicative of the transport of fuel-lean and soot-rich fluid (or conversely, fuel-rich and soot-lean) within the shear layers of the flame, and trending to a null correlation within the potential core where the soot concentration is at a minimum. Likewise, outside of the stoichiometric velocity surface, a strong positive correlation exists between the two aforementioned quantities, consistent with the propensity of fuel-rich fluid to lead to a higher rate of soot formation and/or soot concentration. It was also found that the regions of highest soot volume fraction are present in regions of low strain. Further analysis of this data will allow for a quantitative measurement of the mixture fraction in addition to spatial correlations with temperature, strain rate, and soot volume fraction within this region.

opark@usc.edu

W4P016 SIMULTANEOUS HIGH-SPEED 2D MIXTURE FRACTION AND 3D VELOCITY FIELD IMAGING IN GAS-PHASE TURBULENT JETS

Michael Papageorge, Jeffrey A. Sutton, Ohio State University, United States

Turbulent mixing is an important process that underpins a large number of natural processes and engineering systems. A particular focus is on gas-phase mixing between fuel and oxidizer as this process plays a critical and rate-limiting role in turbulent non-premixed combustion. Over the last few decades, non-intrusive laser diagnostics have provided a wealth of

information concerning the statistical characterization of scalar mixing and detailed visualization of the topology. However, the time-dependent relationship between the turbulent flow field and the turbulent mixing process has not been investigated in gas-phase flows due to a lack of experimental capabilities.

In this poster, we will describe a new experiment designed to investigate the effect of the turbulent velocity field on scalar mixing across a broad range of spatial and temporal scales. In particular, we will describe a new high-speed (10 to 20 kHz) tracer-PLIF and Stereoscopic Particle Imaging Velocimetry (SPIV) experiment aimed at providing simultaneous time-resolved, multi-dimensional measurements of the coupled velocity and mixture fraction fields in turbulent gas-phase jets. The high-speed mixture fraction measurements will be made via acetone PLIF, in which a small amount of acetone vapor is seeded into the jet fluid to act as a tracer. The acetone will be excited by the 4th harmonic (266 nm) of the unique High-Energy Pulse Burst Laser System (HEPBLs) at Ohio State. To date, we have achieved greater than 100 mJ/pulse at 266 nm and 10 kHz. The SPIV measurement will be performed using a commercial DPSS laser capable of operating between 10 and 50 kHz. The two PIV pulses from the DPSS laser are synchronized with the HEPBLs such that they straddle the 266-nm PLIF laser pulse. The use of two independent laser systems for the SPIV and PLIF techniques allows for optimization of measurement timing and in particular, a better matching of the PIV inter-pulse separation to the local flow velocity. The resulting measurements will represent a unique data set that spans large spatial ($x/d = 10-40$ and $r/d = 0-8$), temporal and Reynolds number ($Re = 5,000 - 20,000$ based on diameter) domains. From this data the coupled space-time dynamics of the turbulent velocity field and scalar mixing will be examined through detailed visualization and spatio-temporal statistical techniques.

papageorge.3@osu.edu

W4P017 DESIGN AND DEVELOPMENT OF A MID-INFRARED CARBON MONOXIDE SENSOR FOR A HIGH-PRESSURE COMBUSTOR RIG

Alejandro Camou¹, Gabriel Cruz¹, James Anderson¹, Eric L. Petersen¹, David M. Cusano²

¹Texas A&M University, United States ²Parametric Solutions Inc., United States

A sensor for carbon monoxide measurement has been developed using a mid-infrared Quantum-Cascade (QC) laser operating in the fundamental band ($\Delta v = 1$) of CO near 4.5 μm . The fundamental band was chosen due to its stronger absorption line-strengths compared to the overtone bands near 2.3 μm and 1.55 μm . The mid-IR sensor was applied to a high-pressure combustor to determine the time-history of carbon monoxide and compare it to other measured combustor parameters to fully characterize the combustor's performance. A mixture of natural gas, oxygen, and carbon dioxide was used for combustion. An emissions probe was connected to the exhaust of the combustor that fed into an absorption cell with a known path length and two optical ports to allow mid-IR laser access for absorption. The temperature and pressure of the cell were measured, and the laser wavelength was monitored by a separate calibration process using a known CO/N₂ mixture. An air-cooled DFB-QC laser was current and temperature-tuned to access the $v=0$, R(12) transition of CO near 4.566 μm (2190.02 cm^{-1}). A series of gold mirrors was used to align the mid-IR laser through the absorption cell with a path length of about 11.8 cm. A 50/50 CaF₂ beamsplitter and a series of CaF₂ plano-convex lenses was used to split and focus the beam into two cryogenically-cooled InSb detectors (1 MHz bandwidth) for optical detection measurements. An iris and a 0.5- μm FWHM bandpass filter were placed before each InSb detector to block out an unwanted light from other wavelengths. The operating wavelength was determined by measuring the absorption coefficient using the known CO/N₂ mixture and verified using the HITRAN 2004 database. The operating wavelength was measured at the R(12) transition of 2190.01667 cm^{-1} (4.56618 μm) within $\pm 0.0008 \text{ cm}^{-1}$ ($\pm 0.01625 \mu\text{m}$) from CO absorption measurements using the known CO/N₂ mixture. This operating wavelength uncertainty was used to measure the uncertainty of the calculated CO absorption coefficient. The mid-IR sensor measured a CO concentration of 67 ppm \pm 12 ppm at a steady rig temperature and rig pressure of approximately 2300°F and 1500 psig, respectively. This measured CO concentration was comparable to equilibrium calculations with respect to the rig stable conditions.

acamou11@gmail.com

W4P018 SIMULTANEOUS MEASUREMENT OF CO AND TEMPERATURE USING TDLAS AT 2.3 μm

Majed Alrefae¹, Weichao Wang¹, Aman Satija¹, Anup Sane², Jay P. Gore

¹Purdue University, United States ²Air Products and Chemicals Inc., United States

Carbon Monoxide (CO) is one of the most important species in combustion environment. CO results from breaking of hydrocarbons fuel molecules and partial oxidation of the fragments in a fuel rich and/or vitiated environment. Carbon monoxide is a highly toxic gas and therefore the need of accurate measurement of CO concentration is crucial for human health, safety as well as for operational efficiency of a combustor. This work presents simultaneous CO concentration and temperature measurements using Tunable Diode Laser Absorption Spectroscopy (TDLAS) near 2.3 μm . Two rotational-vibrational lines were used to measure the temperature with the CO concentration simultaneously. CO concentrations and

flame temperatures were measured in an ethylene air premixed flame stabilized over a water cooled McKenna burner. The selected laser wavelength overlaps with the first overtone absorption band ($\Delta v = 2$) of CO and provides *in-situ* real-time and non-intrusive detection technique. The results are in a good agreement with results from equilibrium calculations. The spectroscopic data were obtained from HITRAN. The effects of Exhaust Gas Recirculation (EGR) on the CO concentrations will be studied using TDLAS for a low NO_x lean premixed burner.

malrefae@purdue.edu

W4P019 TEMPERATURE IMAGING IN LOW-PRESSURE FLAMES USING DIODE LASERS

Jesper Borggren¹, Iain Burns², Zongshan Li¹, Anna-Lena Sahlberg¹, Marcus Aldén¹

¹Lund Institute of Technology, Sweden ²University of Strathclyde, United Kingdom

Temperature information is of great importance in many different thermochemical processes such as combustion. For detailed chemical kinetic modelling, knowledge of the temperature is crucial for accurate modelling as the reaction rates are mainly governed by the temperature. Low pressure combustion is commonly used to develop kinetic models due to the thicker reaction zones and thus an accurate temperature measurement technique in low pressure environments is highly sought. Two-Line Atomic Fluorescence (TLAF) of indium has previously been successfully used as a temperature marker in combustion processes to acquire 2D-maps of flame temperatures. The spectral lines at 410 nm and 451 nm of indium give good sensitivity in the temperature region that is attractive in flames due to the energy splitting being in the range of kT , where k is the Boltzmann constant and T the temperature.

In the present work, a spatially resolved thermometry imaging technique has been developed using diode lasers and an intensified high-speed camera. By combining Two-Line Atomic Fluorescence (TLAF) with One-Line Atomic Fluorescence (OLAF) of seeded indium atoms, a calibration-free temperature measurement technique in low pressure flames is achieved. A novel indium seeding system is shown to give a homogenous indium distribution across the flame from reaction zone to far up in the production zone. The temperature is investigated for different equivalence ratios and compared to simulations from CHEMKIN using the GRI 3.0 mechanism.

jesper.borggren@forbrf.lth.se

W4P020 TEMPERATURE MEASUREMENTS IN COMBUSTION SYSTEM USING H₂O ABSORPTION SPECTROSCOPY

Sewon Kim, Changyeop Lee, Miyouon Yoo, Korea Institute of Industrial Technology, Korea

It is very important to measure the internal temperatures or temperature distributions precisely inside combustion systems in order to increase energy efficiency and reduce the pollutants. Especially in case of large combustion systems such as power plant boiler and reheating furnace of steel making process, it is very difficult to measure those physical properties in detail. Tunable Diode Laser Absorption Spectroscopy (TDLAS) using DFB (Distributed FeedBack) laser is very attractive method to overcome the difficulty, measuring high temperatures inside the boilers and furnaces.

In this research, experimental studies have been carried out to measure temperatures in the furnace system based on the Direct Absorption Spectroscopy (DAS), which is one of TDLAS methods. In addition, water vapor is adopted for this temperature measurement to exploit its extensive absorption wavelength and strong signal intensity.

The experiment setup is mostly consisted of electric furnace, DFB Laser, InGaAs detector, etc. The two-line technique is used to measure temperature in DAS. The gas temperature is obtained by comparing the line strength of two different transitions which have different temperature dependences. Then the water vapor temperature can be inferred from the measured ratio of integrated absorbance for two different temperature dependent transition. Also, Non-uniform temperature distribution in high temperature furnace is predicted using water vapor lasers.

The results showed that the accuracy of temperature measurement using this TDLAS techniques is within 1 percent.

swkim@kitech.re.kr

W4P021 DESIGN AND VALIDATION OF LED-BASED ABSORPTION SENSOR FOR SIMULTANEOUS DETECTION OF CO AND CO₂

Kyle Thurmond¹, Subith Vasu¹, William Partridge², Raynella Connatser²

¹University of Central Florida, United States ²Oak Ridge National Laboratory, United States

In this work we present design and validation results of an absorption sensor for simultaneous measurements of CO and CO₂ fluctuations in combustion exhaust gases. This sensor utilized four low-cost and compact LEDs that emit in the 3-5 μ m wavelength range. CO and CO₂ measurements were conducted in their fundamental bands centered at 4.7 μ m and 4.3 μ m, respectively, while a reference LED at 3.6 μ m was used as a reference for H₂O. Absorption and broadening coefficients were calculated from 2012 HITRAN database. LEDs present a solution for the development of a sensor that is

cost effective and rugged enough for practical implementation compared to laser-based methods, and at the same time provide time-resolved measurements over sampling techniques. However, LEDs have a more spectrally broad and diverging emission than the more commonly used lasers which presented many design challenges. The optical design software ZEMAX was utilized to overcome these obstacles and optimize the sensor setup. Band pass filters were used to narrow the emission spectrum; however, an integrated absorption spectrum was still necessary which required modifications of the Beer-Lambert law. Initial tests were carried out using a simple flow cell for validation and calibration of the instrument at atmospheric conditions at room temperature. Evaluation was first carried out using CO and CO₂ in separate individual tests so the sensor could be calibrated to accurately measure each gas without interference from the other. In tests where both gases were present, no interference was noticed. Experiments at high temperatures and broader pressure ranges are currently ongoing using a heated high pressure spherical chamber. As well, exhaust gas tests using internal combustion engines are planned in the near future. An affordable, fast response sensor that can measure exhaust gases has broad applications, and can be used as feedback tool for adjusting combustion strategies in highly efficient, fuel flexible engines as ignition and emission is highly dependent on fuel chemistry.

kthurmond@knights.ucf.edu

W4P022 SIMULTANEOUS MEASUREMENT OF CO AND CO₂ CONCENTRATIONS USING FIBER LASER INTRACAVITY ABSORPTION SPECTROSCOPY.

Sergey Cheskis¹, Igor Rahinov², Alexey Fomin¹, Tatiana Zavlev¹
¹Tel Aviv University, Israel ²The Open University of Israel, Israel

Simultaneous measurement of CO and CO₂ is of undisputable interest for diagnostics of combustion efficiency. In this work we demonstrate the applicability of the broadband Laser IntraCavity Absorption Spectroscopy (ICLAS) for addressing this goal. ICLAS is a very effective way to enhance the sensitivity of absorption measurements. With this technique the laser light completes many round trips through the absorber, like in a multipass cell. One of the advantages of intracavity absorption spectroscopy is its independence of broadband cavity losses and, therefore, the possibility of *in-situ* measurements of absorption spectra in contaminated samples such as combustion environment.

Fiber Laser Intracavity Absorption Spectroscopy (FLICAS) is based on homebuilt Er³⁺ doped fiber laser is worked in the spectral range from 6200 to 6550 cm⁻¹. This range includes, along with other species, the spectral lines of CO and CO₂.

The CO spectrum corresponds to the 3v and CO₂ to the 2v₁+2v₂⁰ + v₃ vibrational bands. The sensitivity of the method allows to observe spectra of CO and CO₂ with concentration better than 25 ppm. Simultaneous observation of various rotational lines allows for fast and accurate temperature measurements.

cheskis@post.tau.ac.il

W4P023 HIGH-SPEED 1D RAMAN/RAYLEIGH SCATTERING IMAGING IN TURBULENT H₂/N₂ FLAMES

Kathryn Gabet, Frederik Fuest, Jeffrey A. Sutton, Ohio State University, United States

In this poster we will describe recent work in our laboratory using a high-speed (> 10 kHz) combined 1D Raman-Rayleigh scattering imaging system. While our previous work has demonstrated the ability to acquire high-speed Raman/Rayleigh scattering images using a pulse burst laser system, this poster will show new results from experiments utilizing the High-Energy Pulse Burst Laser System (HEPBLs) at Ohio State to acquire quantitative time-resolved measurements of major species (H₂, N₂, H₂O, and O₂), temperature, and mixture fraction in turbulent nonpremixed H₂/N₂ flames. The goal of this work is to measure the time-varying radial profiles of all major combustion species and deduce temporally-resolved mixture fraction profiles in turbulent combustion environments.

This poster will include results quantifying the precision and accuracy of the kHz-rate Raman/Rayleigh scattering measurements using our CMOS-based 1D Raman/Rayleigh system in a series of near-adiabatic H₂/air flames and turbulent H₂/N₂ jet flames. A detailed analysis of the spectral response and Signal-to-Noise Ratio (SNR) of major species (H₂, N₂, H₂O, and O₂) and temperature will be presented. The ability to measure “single-shot” scalar values accurately in turbulent flames is assessed by comparing scalar results in the DLR H₃ (50% N₂/50% H₂ Re=10,000) turbulent jet flame to previous work. Using the measured time-varying profiles of the major combustion species, temperature, and mixture fraction, we will deduce the integral time-scales of the major species, mixture fraction, and temperature in the DLR H₃ flames and examine their correlation in both space and time. Our goal is to interrogate the turbulence-chemistry interaction in turbulent flames by comparing the species-specific, temperature, and mixture fraction time-scale.

gabet.1@osu.edu

W4P024 PICOSECOND PHOTODISSOCIATION OF METHANE/AIR MIXTURES AT ATMOSPHERIC PRESSURES

The possibility to measure concentrations of atmospheric trace species is of vital importance for understanding atmospheric chemistry and the evolution of global warming. Methane (CH₄) is the most abundant hydrocarbon on earth and it is an important greenhouse gas. Most natural gas today mainly contains methane. Hence, it is important to both measure and understand the methane atmospheric and combustion chemistry.

Previously, the photodissociation of methane has been studied extensively using weak nanosecond pulses in the UV regime, see e.g., but also using extremely intense femtosecond laser pulses. It has been found that the dissociation processes are completely different in these two cases; photolysis with a weak light source implies single-photon excitation to low-lying repulsive electronic states and implies that typically only one or two molecular bonds are broken, whereas photolysis using ultra-intense light sources, such as femtosecond laser pulses, results in multi-photon excitation to high-lying dissociative states, which causes breakage of multiple bonds and creation of a multitude of photofragments. Photodissociation of methane using picosecond laser pulses, i.e., photolysis with a light source of intermediate intensity, has, to the best of our knowledge, not been investigated previously.

In the work presented on this poster, we have studied the photodissociation process of methane induced by an 80-picosecond laser pulse of 266-nm wavelength. It is found that the photodissociation occur through a three-photon process and leads to the formation of several luminescent fragment species. Spectrally resolved studies of the luminescence, with a detector gate 5-ns wide, reveals emission bands corresponding to CH(A-X), CH(B-X), CH(C-X), CN(B-X) and NH(A-X). This indicates not only that several different fragments are directly formed, but also that products are formed through chemical reactions with nitrogen. This discovery might open up for two-dimensional imaging of methane, by selective imaging of the emission from one of the luminescent fragments, but also for methane/air ratio measurements in combustion-related applications by studying the ratio between emission lines originating from methane and oxygen, respectively.

malin.jonsson@forbrf.lth.se

W4P025

NON-INTRUSIVE *IN SITU* DETECTION OF METHYL CHLORIDE IN HOT GAS FLOWS USING INFRARED DEGENERATE FOUR-WAVE MIXING

Anna-Lena Sahlberg, Jianfeng Zhou, Zhongshan Li, Marcus Aldén
¹Lund University, Sweden

Biomass utilizations constitute a promising sustainable and carbon-free energy solution. However, the complicated chemical compositions in the fuels containing Cl, K and S elements require comprehensive knowledge-based understanding of the fate of the aforementioned elements in different process like combustion or gasification. Halogenated hydrocarbons such as CH₃Cl can be a major part of chlorine carrier in syngas from biomass gasification. Since CH₃Cl is an unwanted pollutant, it is important to develop a nonintrusive measurement to provide spatial resolved measurement in biomass thermochemical conversion processes for both kinetic validation and practical technique developments. The concentration of CH₃Cl generated by biomass combustion/gasification generally depends a lot on the chlorine content of the fuel. Monitoring CH₃Cl concentrations in biomass combustion *in situ* is a challenging task. We demonstrate the potential of IR-DFWM as a tool for non-intrusive *in situ* detection of CH₃Cl in biomass combustion. By probing the ro-vibrational levels around 3000 cm⁻¹, the DFWM spectrum of CH₃Cl has been measured at different temperatures, and detection limits have been estimated for the current setup.

The IR laser light is produced through a laser system that has been described in Li et al. The second harmonic of the Nd:YAG laser is used to pump a dye laser (Sirah, dye LDS798) giving tunable light of ~ 800 nm. This light is difference frequency mixed with the residual of the fundamental YAG laser at 1064 nm to generate the tunable mid-infrared pulsed laser light around 3000 cm⁻¹ with a repetition rate of 10 Hz. The DFWM setup is similar to the one used by Sun et al, which was developed for sensitive detection of trace molecular species in the mid-infrared. This article introduced a set of IR-BOXCAR plates to facilitate alignment of the forward phase-matching geometry for IR-DFWM.

The temperature dependence of the CH₃Cl spectrum is investigated to mimic the biomass thermochemical conversion processes by *in situ* DFWM measurements of CH₃Cl gas flows diluted by N₂. The flows were directed through a heating tube made of fused silica, surrounded by an electric heating wire and insulation. This arrangement insures that there are no catalyst effects in the heated gases from the inside wall surface of the heating tube. The spectrum was measured at three different temperatures and the detection limit is estimated for each temperature. These results demonstrate the potential of IR-DFWM as a promising technique for *in situ* detection of trace level products from biomass combustion. There is a list of molecular species, e.g. OCS, CS₂, H₂S, HCl, which are critical in biomass utilization. The IR-DFWM technique can potentially provide unique possibility of noninvasive spatial resolved measurement in harsh thermochemical biomass conversion environments.

anna-lena.sahlberg@forbrf.lth.se

W4P026

IR CROSS-SECTIONS, LINE STRENGTHS, AND COLLISION BROADENING COEFFICIENTS OF PROPANAL IN GAS PHASE- A MAJOR BIOFUELS COMBUSTION INTERMEDIATE

Batikan Koroglu, Zachary Loparo, Robert Peale, Subith Vasu, University of Central Florida, United States

The use of oxygenated biofuels is shown to have advantages in reducing the greenhouse gas emissions; however, they also result in toxic aldehyde by-products mainly formaldehyde, acetaldehyde, acrolein, and propanal. These aldehydes are carcinogenic and therefore it is important to understand their formation and oxidation pathways in reactive systems. Recently, there have been laser absorption schemes for the quantitative detection of the formaldehyde and acetaldehyde during shock tube oxidation. Critical to the development of such diagnostics are accurate characterization of the absorption features of these aldehydes. There exist several studies in the literature for formaldehyde and acetaldehyde - tabulated in HITRAN. However, there are very few measurements for other aldehydes which are applicable to combustion conditions. In this study, the gas phase infrared spectra of propanal ($\text{CH}_3\text{-CH}_2\text{-CHO}$), a saturated three carbon aldehyde found in the exhaust emissions of biodiesel or diesel fuels, was studied using high resolution Fourier Transform Infrared (FTIR) spectroscopy over the wavenumber range of $750\text{--}3300\text{ cm}^{-1}$ and at room temperature 293 K . The absorption cross sections of propanal were recorded at resolutions of 0.08 and 0.096 cm^{-1} and at seven different pressures ($4\text{--}33\text{ Torr}$). The calculated band-strengths were reported and the integrated band intensity results were compared with values taken from the Pacific Northwest National Laboratory (PNNL) database (showing less than 1.5% discrepancy). The peak positions of the 19 different vibrational bands of propanal were also compared with previous studies taken at a lower resolution of 1 cm^{-1} . In addition, using a DFB IC laser at 2938.24 cm^{-1} , we present results for temperature ($300\text{--}700\text{ K}$) and pressure effects ($1\text{--}10\text{ atm}$) on the absorption cross sections using a heated, high-pressure spherical chamber facility. We are in the process of developing interference-free laser absorption detection schemes for the quantitative measurement of propanal in combustion and exhaust emissions, as well its reactions using a kinetics shock tube.

bkoroglu@knights.ucf.edu

W4P027 TWO-DIMENSIONAL MULTI-ANGLE LIGHT SCATTERING (2D-MALS) OVER A WIDE ANGULAR RANGE

Stefan Will, Michael Altenhoff, Franz Huber, LTT Erlangen, Germany

To understand how soot forms in combustion processes, we need comprehensive information about local size properties of complex soot aggregates. Elastic Light Scattering (ELS) is a well-established optical technique that allows for the *in situ* determination of radii of gyration and fractal dimension of soot aggregates in flames. Laser-Induced Incandescence (LII) can be used to determine primary particle sizes and soot volume fraction. Reimann et al. used a two-dimensional combination of ELS and LII to determine various parameters of soot particles in a premixed ethylene-air flame from a porous flat-flame burner (McKenna type). Although the general approach was successful, a fixed scattering angle of 90° limited both the measuring range in terms of aggregate size and the information obtained.

Extending this approach, we performed two-dimensional ELS measurements at various scattering angles using a cw-laser, light sheet forming optics and a CCD camera. The detection angle varied equidistantly in the scattering vector q from about 15° to 165° , scattered light was acquired from 10 mm to 24 mm height above burner. For angles different from 90° , where the image plane is no longer parallel to the object plane, we used a tilted arrangement of the detection system according to the Scheimpflug condition assuring a sharp image of the measurement plane. In order to evaluate the data not only from the flame axis, we developed a camera calibration method correcting lateral magnification which becomes crucial for detection angles differing strongly from the perpendicular view. The measurement results obtained show good agreement with previous data. For a comprehensive characterization of soot particle properties the 2D-MALS technique is coupled with imaging LII.

Stefan.Will@lth.uni-erlangen.de

W4P028 MEASUREMENTS OF PR:YAG PHOSPHOR LUMINESCENCE AT ELEVATED TEMPERATURE

Dustin Witkowski, David Rothamer, University of Wisconsin, United States

The use of thermographic phosphors continues to be investigated as a diagnostic for temperature measurements in combustion applications. Their usefulness has already been demonstrated in many applications such as internal combustion engine cylinder wall surface temperature measurements and high temperature gas flows. Recently trivalent praseodymium ions doped into a yttrium aluminum garnet host (Pr:YAG) has been identified as a promising phosphor for measurements at high temperatures. Pr:YAG spectrally-resolved emission data in a tube furnace up to 1300 K was reported and temperature measurements up to 750 K in a turbulent jet were acquired utilizing $4f\text{--}4f$ emission from Pr:YAG.

The current effort builds upon previous measurements taken in a furnace by taking measurements of Pr:YAG luminescence as a function of temperature, phosphor seeding concentration, laser excitation wavelength, and laser excitation energy. The measurements are taken on a laminar premixed methane-air flame burner. The setup consists of an inner air jet of 12 mm diameter surrounded by a flat flame with an outer diameter of 72 mm. Diffusion of hot flame gases into the inner seeded laminar jet serve to heat the seeded jet to high temperatures. Temperature measurements are taken with three fine-wire type R thermocouples of different wire and junction diameters to monitor the temperature distribution in the seeded jet. Mie scattering is used to quantify the seeding concentration of the Pr:YAG phosphor in the heated jet. The laser excitation source is a 4-stage nonlinear optics system pumped with a Nd:YAG laser. The system allows us to supply tunable nanosecond duration laser pulses in the ultraviolet spectrum. The laser pulses are then formed into laser sheets using appropriate sheet-forming optics and propagated and focused in the seeded jet. Intensified CCD cameras are used to measure the signal levels of the phosphor emission.

A parametric study was conducted to study the dependence of each parameter on the luminescence intensity of Pr:YAG following excitation in the 4f5d states. The data are used to help improve and expand upon a current rate-based model. The rate based model expands upon previous modeling efforts in the literature to consider excitation into the 4f5d states and subsequent emission from the 3PJ or 4f5d states. The modeling and experimental efforts are aimed at determining the feasibility of using thermographic phosphors for measurements at flame temperatures.

dwitkowski@wisc.edu

W4P029 LASER DIAGNOSTICS ON METHANE HYDRATES

David Escofet Martin, Jeff Botimer, Derek Dunn-Rankin, Peter Taborek, Sunny Karnani, University of California, United States

This work involves the study of the formation and combustion of methane hydrates and focusses in the diagnostic methods used to study these phenomena under challenging environments. For the formation process, Raman spectroscopy is used to qualitatively describe the ratios of water-to-hydrate while the hydrate is forming. Raman spectroscopy is also used to track the methane in the water or hydrate cells. For this purpose the stretching vibration of the O-H bond of water and the C-H bond of methane gives information about the structure of the surroundings of the bond, being able to provide information about the structure of the substance. On the hydrate combustion side, gas-phase high pressure diagnostics offers many challenges. For example, high pressure Planar Laser Induced Fluorescence, suffers from line broadening, increased collisional rates, increased quenching, and transition overlap, making it very difficult to obtain high SNR at pressures over 100 atm. In this work the effects of high pressure are discussed and compared both experimentally and theoretically. The poster also examines the effect of resonant emission instead of the more widely used non-resonant emission scheme for high pressure environments.

descofet@uci.edu

W4P030 THE ROLE OF CO₂* ON CHEMILUMINESCENCE SENSORS FOR ACTIVE CONTROL

*Julia Krüger, Katharina Kohse-Hoinghaus, Andreas Brockhinke
Bielefeld University, Germany*

Because of its advantage of being inexpensive, noninvasive and reliable, there is renewed interest in using chemiluminescence as analytic tool for flame diagnostics, especially for active control. Our previous investigations focused on the most abundant chemiluminescent species in laminar, premixed low-pressure flames: OH (A-X), CH (A-X), CH (B-X) and C₂ (d-a). We acquired, interpreted and modeled spectra with high resolution and determined the absolute concentration of these electronically excited species. For other flame conditions, especially at elevated pressures, additional chemiluminescence emissions play a role as well. In the high-pressure regime (both in gas turbines and for automotive combustion) spectra are frequently dominated by broadband structures attributed to CO₂* chemiluminescence. Until now, little attention has been paid to the spectral characterization of these emissions.

We present an analysis of the spectral structure of the CO₂* chemiluminescence detected in hydrogen-oxygen flames and in methane-oxygen low-pressure flames doped with CO. Under these conditions, CO₂* emissions can be observed, with the additional benefit that the flames can readily be characterized with other techniques (both laser mass-spectrometry-based) and can be modeled with a high degree of accuracy. One challenge for the spectral characterization of the CO₂* luminescence is its broad emission spectrum which ranges between 240 and 900 nm. In this spectral region, several other chemiluminescent species emit as well, leading to a considerable spectral overlap, which has to be considered for quantitative measurements. We characterized the CO₂* emission as a function of the flame temperature and the flame stoichiometry. Additionally, the absolute number density of the chemiluminescent species has been estimated for H₂-O₂-flames and the CH₄-O₂-flames, allowing precise modelling of chemiluminescence spectra.

Julia.krueger@uni-bielefeld.de

W4P031 FLAME CHEMILUMINESCENCE MEASUREMENT FOR REAL TIME AIR/FUEL RATIO CONTROL

Jin Ki Lee, Myung Chul Shin¹, Se Won Kim, ¹Korea Institute of Industrial Technology, Cheonan, Korea

The objective of this study is to examine the change of flame chemiluminescence at various combustion conditions such as load and fuel to air ratio. Flame chemiluminescence is one of the most important factors to judge the real time flame condition like an air/fuel ratio. An optical sensor, photo diode, is used to investigate the possibility of applying it to air/fuel ratio control in domestic gas furnace. The photo diode sensor is mounted viewing the surface of metal fiber burner that produces premixed flame. The heat load and excess air ratio are considered as the key parameters. The signals of optical sensor are analyzed experimentally at various heat load and excess air ratio conditions.

In this paper, it is experimentally found that a strong relationship between the air/fuel ratio and optical element output (i.e., photo diode) exists. (Image) This is verified through the flame spectral analysis for various PD output signals. (Image) It is expected that this study will give a possibility to apply the optical sensor for air/fuel ratio control. To do that, we are intending to air/fuel control test on actual system by applying control algorithm.

jink@kitech.re.kr

W4P032 CHARACTERIZING A MINIATURE SHOCK TUBE WITH SYNCHROTRON X-RAY DENSITOMETRY

Robert Tranter¹, Alan Kastengren¹, Christopher Annesley¹, Patrick Lynch²

¹Argonne National Laboratory, United States ²University of Michigan, United States

A miniature high repetition rate shock tube has been developed for chemical kinetics and other combustion studies requiring highly averaged experiments (i.e. low S/N ratio single-shot), including synchrotron sourced experiments. The shock tube has been designed to generate reaction conditions of $T_5 > 600$ K, $P_5 < 100$ bar at a cycle rate of up to 4 Hz, with repeatability approaching 3% shot-to-shot [Tranter and Lynch, Rev. Sci. Instr. 84 (2013) 094102]. We motivate and outline the capabilities of this device and present a densitometry based characterization of this shock tube at the Advanced Photon Source at Argonne National Laboratory. X-ray absorption (8 and 10 keV) was used to measure a state property, the gas density, before and after the passage of shock waves. The initial, incident shock, and reflected shock densities were obtained for shocks in argon for thousands of experiments along with simultaneous measurements of reflected shock pressures. Excellent agreement was observed between the density measured using X-ray absorption and the density calculated from the normal shock relations in the range studied ($0.3 < P_2 < 3.5$ bar, $600 < T_2 < 900$ K, $3 < P_5 < 11.5$ bar, $600 < T_5 < 1650$ K. Similar agreement was obtained between measured and calculated post reflected shock pressures. These two measurements form a strong validation that the post shock conditions are accurately calculated in this unique miniature shock tube. Furthermore, these experiments demonstrate the ability to measure a gas property with synchrotron x-ray radiation in a single pass despite the challenges of short path length, limited observation time and rapidly changing conditions. The experiments also provide a basis for future synchrotron densitometry based studies in the shock tube, including boundary layer studies and time dependent density measurements that can be used as a target of reaction mechanism simulation.

tranter@anl.gov

W4P033 PROBING OPTICALLY DENSE GASES WITH X-RAY ABSORPTION AND FLUORESCENCE OF ARGON

Robert Tranter¹, Alan Kastengren, Christopher Annesley¹, Patrick Lynch², King Yiu Lam¹

¹Argonne National Laboratory, United States ²University of Michigan, United States

Non-invasive probing of the internal structures of optically dense flames is challenging and requires probes that can fully penetrate the flame with high spatial resolution. This is particularly important for atmospheric or higher pressure flames where large changes occur over small length scales. Synchrotron based fluorescence and absorption techniques with focused X-rays have the potential to address these problems. For example, Kastengren et al. have shown that X-ray absorption and fluorescence techniques can be used to examine mixing in non-reacting, turbulent jets that contain argon. They demonstrated that the fluorescence measurements could overcome some limitations of absorption particularly for low argon concentrations. The current work extends this simple jet experiment to the much more complex environment of a sooting flame with simultaneous X-ray fluorescence and absorption measurements at X-ray energies of 8 and 10 keV.

An ethylene/air flame was established on a McKenna burner that had been modified so that a 1/4" o.d. tube could be inserted through the center of the burner. Argon was admitted through this tube creating a jet of inert gas in the middle of the flame. Flow rates of argon were varied to examine mixing of the argon jet with the flame gases and to estimate the sensitivity of the observation technique. Experiments were also performed with the fuel gases replaced by nitrogen giving complementary measurements without the complex environment of a flame.

The X-ray configuration was based on that in Kastengren et al. with the X-ray beam focused to a $5 \times 6 \mu\text{m}$ spot at the center of the burner. The burner was translated around the X-ray beam in the X and Y directions (Z being the direction of

propagation of the X-ray beam) creating raster scanned radiographic images of argon in the jet and mixed with the burner gases. In both the cold gas and sooting flame experiments the argon jet was clearly imaged over a wide range of flow rates and heights above the burner surface up to at least 20mm. There is excellent agreement between the absorption and fluorescence measurements. For a few cold flows cases time resolved measurements were also made. These initial experiments demonstrate that gaseous structures can be resolved with X-ray fluorescence and absorption within sooting flames. Currently, the methods have only been applied to atmospheric pressure flames but the high spatial resolution and intensities achievable with focused X-rays should also make the techniques suitable for high pressure environments. Future experiments will improve spatial and temporal resolution and examine more complex e.g. turbulent structures.

tranter@anl.gov

W4P034 SYNCHROTRON VUV BEAMLINE/ENDSTATIONS DEDICATED TO COMBUSTION RESEARCH AT TAIWAN LIGHT SOURCE

Fei Qi¹, Zhouyue Zhou¹, Jiuzhong Yang¹, Yuyang Li¹, Yin-Yu Lee², Huang-Wen Fu², Di-Jing Huang²

¹University of Science and Technology of China, China ²National Synchrotron Radiation Research Center, Taiwan

Combustion provides over 80% of global energy supply and serves as the dominant emission source of air pollutants nowadays. A better understanding of combustion is crucial for the cleaner and more efficient energy utilization and requires the applications of state-of-the-art diagnostic techniques. Synchrotron-based combustion diagnostic tools are rapidly developing in recent ten years and have received great attentions of the combustion community. Here we report a newly constructed synchrotron VUV beamline/endstations dedicated to combustion research at Taiwan Light Source (TLS) in the National Synchrotron Radiation Research Center (NSRRC). The TLS is a 1.5 GeV synchrotron light source operated in the top-up mode and can produce stable synchrotron VUV light with small beam divergence and high brightness. We are now updating the BL04C (VUV CD) beamline with a two-stage differential system for the purpose of combustion research. Table 1. lists the key parameters of BL04C beamline, which indicates that this beamline is very suitable for combustion research.

Table 1. Key parameters of the BL04C beamline at Taiwan Light Source Energy range 6-17 eV Photon flux~1013 photons/s Resolving power 1000 (E/DE@10 eV) Spot size at the sample~1.2 (h)×1.0 (v) mm

Two dedicated endstations will be equipped to this VUV beamline, one for pyrolysis and oxidation studies, and the other for laminar premixed flame studies. Both endstations consist of a reactor chamber, a photoionization chamber, an ion transfer system and a homemade Reflectron Time Of Flight Mass Spectrometry (RTOF-MS). The mass resolution of the RTOF-MS is about 4000. The two endstations can be used to investigate elementary reactions initiated by laser flash photolysis, flow reactor pyrolysis, Jet-Stirred Reactor (JSR) oxidation, laminar premixed flames and thermochemical processes in energy science such as pyrolysis of biomass and coal. Pressure in the source chamber can be easily controlled to provide validation data at a variety of pressures for the pressure-dependent reactions involved in combustion. The combustion beamline/endstations at TLS will be open for users all over the world from the autumn of 2014.

fqi@ustc.edu.cn

W4P035 DIAGNOSTICS OF GLIDING ARC FOR PLASMA-ASSISTED COMBUSTION

Jiajian Zhu¹, Jinlong Gao¹, Andreas Ehn¹, Zhongshan Li¹, Marcus Aldén¹, Mirko Salewski², Frank Leipold², Yukihiro Kusano²

¹Lund University, Sweden ²Technical University of Denmark, Denmark

Plasma-assisted combustion has been regarded as a promising technology since it can provide significantly increasing amount of active species to flames and dissociate fuel molecules to more easily combusted fragments. Gliding arc is an ideal plasma source for providing low-temperature plasmas. However, its application to plasma-assisted combustion has been hindered mostly due to the lack of proper understanding of the governing mechanism. An air gliding arc at atmospheric pressure driven by a 35 kHz AC high voltage is electrically and optically diagnosed.

Simultaneous voltage, current and high-speed photography measurements are performed to obtain electrical field and power of the gliding arc. Two-dimensional gas temperature of the gliding arc is measured using laser-induced Rayleigh scattering. Rotational temperature of the gliding arc is obtained by simulate the experimental emission spectra. Excited species (NO*, N₂*, NH* and OH*) are observed from the emission of the gliding arc. It is found that the under investigated gliding arc is a powerful, low-temperature plasma source generating a large number of active species and is potential to combustion enhancement.

jiajian.zhu@forbrf.lth.se

W4P036 NON-CONTACT WALL TEMPERATURE MEASUREMENT USING MEMS WIRELESS SENSOR

Min Hyeok Lee, Yuji Suzuki, The University of Tokyo, Japan

Precise wall temperature measurement is important in various combustion studies, such as catalytic combustion, ignition, and wall thermal/chemical quenching. Thermometry using thermocouple or RTD (Resistance Temperature Detector) has been widely applied, but the thermal disturbance by mechanical contact between the detector and the target is of concern. Infrared thermometer or thermographic phosphors is often used as non-contact thermometry but they cannot be applied without optical access. In the present study, MEMS-based wireless temperature sensor is proposed for a new non-contact wall temperature measurement method. The present measurement system is based on a MEMS sensor with patterned thin-film RLC circuits fixed on the wall surface. The spiral coil on the sensor is inductively coupled with an external coil located outside of the combustion field. The phase angle of external coil impedance shows a peak at the resonant frequency, which is measured with a network analyzer. When the wall temperature changes, capacitance/resistance of the circuit is changed leading to the resonant frequency change. Because frequency shift measurement is generally very accurate, high sensitive wall temperature measurement can be expected.

An early prototype is developed with MEMS (Microelectromechanical System) technologies. On a glass wafer, a 200 nm-thick Cr/Au/Cr layer is sputtered and patterned as a bottom electrode. Then, 100 nm-thick alumina is formed as an insulator and a dielectric material. Finally, another 1 μm -thick Cr/Au/Cr layer including the spiral coil and the top electrode is patterned. The completed sensor has a size of 10 mm square, where the capacitance change of the RLC circuit is employed as the sensing principle. However, it is shown in the initial test that the resistance of the Au coil is much higher than its designed value, and the quality factor of the peak remains very low.

We also make an equivalent circuit simulation using HFSS (High Frequency Structure Simulator) to design sensor configuration with better sensitivity. Here, we employ the resistance change of the RLC circuits instead of the capacitance change. Apparent resonant frequency shifts up to several hundreds kHz per 1 Ω changes of sensor circuit resistance is observed. Considering the temperature coefficient of resistance for Au $\sim 0.4 \text{ \%}/\text{K}$, it corresponds to a sensitivity of a few kHz/K.

mlee@mesl.t.u-tokyo.ac.jp

W4P037 COMPARISON OF PHOTOPHYSICAL PROPERTIES OF SELECTED AROMATIC AND KETONE FLUORESCENCE TRACERS

Omid Feroughi, Thorsten Benzler, Thomas Dreier, Christof Schulz, University of Duisburg-Essen, Germany

Effective laser-induced fluorescence intensities and spectra of one- and two-ring aromates and ketones are frequently used as “tracers” to determine concentration or temperature in gas mixing, for example, the mixing of evaporated fuel and air. Quantitative analysis of measured signal intensities requires detailed knowledge of the dependences of the fluorescence properties on the local conditions. Besides the frequently-used tracer’s acetone, 3-pentanone and toluene, interest in other species such as anisole or 1-methylnaphthalene has grown, with the aim of expanding the range of evaporation properties and potentially increasing signal intensities.

In the present work effective fluorescence lifetimes after short-pulse UV-laser excitation were determined to provide a data base for further development. Particularly interesting are photo-physical fluorescence models for the prediction of signal intensities in practical applications. For a range of aromatics and ketones we compare the dependences of relative fluorescence quantum yields as well as signal intensities on temperature, total pressure, and oxygen partial pressure as well as fluorescence spectra and absorption cross-sections. In the experiments a frequency-quadrupled ps-Nd:YAG laser at 266 nm, a spectrometer, and a streak camera with sub-ns time resolution were used to record temporally and spectrally resolved fluorescence emission. From these, effective fluorescence lifetimes and spectra were evaluated for gaseous toluene, xylene, 1,2,4-trimethylbenzene, anisole, naphthalene, 1-methylnaphthalene, acetone, and 3 pentanone with N₂ and air mixtures as bath gases. In an optically accessible and heat able pressure vessel, a temperature and pressure range of 296 – 1075 K and 0.010 – 10 bar, respectively, was covered.

omid.feroughi@uni-due.de

W4P038 DETERMINATION OF THE WOBBE INDEX OF NATURAL GASES BY SPEED OF SOUND

Inchul Choi¹, Gwang-jung Kim²,

¹Korea Institute of Industrial Technology, Korea ²Chonnam National University, Korea

The Wobbe Index is an indicator of the specific higher heating value of natural gas. Traditionally, gas chromatography has been used to generate a composition information from samples of a gas in order to obtain the heating value of the gas. However this method is often too cost-prohibitive to be used on a wide range for energy billing because of its installation and operational costs. Especially many combustion systems such as internal combustion engine and industrial boilers require on-line measurements of heating value of gas mixtures for optimized air-fuel ratio. Recently intensified efforts have been made over the past few years to develop alternative low-cost measurement methods. We are currently developing

correlative measurement method based on speed of sound for Wobbe index measurement of natural gas with various compositions.

The objective of this study is to measure the Wobbe index of natural gas by way of speed of sound measurement, so as to correlate heating value of the gas indirectly. We used two ultrasonic transducers which have peak frequency of 200-300 kHz and configured them in the tubular test cell. The piezoelectric ultrasonic transducers has a diameter of 30 mm. One of the transducers is connected to a pulse generator with peak voltage of 600-1200 V and 5-10 Hz repetition rates. Several standard gases are supplied to the gas cell through a sample delivery system consisting of a pressure regulator, mass flow controller and needle valve. The measured heating value by acoustic method will be compared with a gas chromatographic analysis of the natural gas.

choii@kitech.re.kr

W4P039 INVESTIGATION ON MINIMUM IGNITION ENERGY OF MIXTURES OF α -PINENE-BENZENE/AIR

Bruno Coudour, University of Poitiers, France

The aim of this paper is to investigate the Minimum Ignition Energy (MIE) of α -pinene-benzene/air mixtures at a given temperature for different equivalence ratios and fuel proportions. Experiments were made in a cylindrical chamber of combustion using a nanosecond pulse at 1064 nm from a Q-switched Nd:YAG laser. Laser-induced spark ignitions were studied for several mixtures of α -pinene-benzene/air. Two molar proportions of α -pinene-benzene mixtures were selected, respectively 20%-80% and 50%-50%. The effect of the equivalence ratio (Φ) has been investigated for 0.7, 0.9, 1.1 and 1.5 and ignition of fuel/air mixtures has been experimented for two different laser energies: 25 and 33 mJ. The experiment will serve to study the interaction of benzene and α -pinene on the flammability of the mixture and to have further knowledge of the potential of Biogenic Volatile Organic Compounds (BVOCs) and smoke mixtures to cause the Accelerating Forest Fires phenomenon (AFF). Results of breakdown probability and energy absorption as well as the MIE are based on 400 laser shots for each of the two studied proportions. MIE measured values of α -pinene-benzene mixtures as functions of equivalence ratio are compared to data of pure α -pinene. We demonstrated that the presence of benzene in α -pinene-air mixture tends to increase ignition probability and reduce the energy required to obtain an ignition. These observations do not seem to depend strongly on the benzene proportion.

bruno.coudour@ensma.fr

W4P040 DUAL-GATE OPTICAL KERR EFFECT BALLISTIC IMAGING FOR DENSE SPRAY MEASUREMENTS

David Sedarsky, Said Idlahcen, Claude Roze, Chalmers University, Sweden

Ballistic Imaging (BI) is an extension of shadowgraphy for detailed quantitative measurements in optically dense systems, such as the near-nozzle region of an atomizing fuel spray. BI applications mitigate distortion from scattering interactions by aggressively limiting light collection to a subset of the overall transmitted light intensity. Individual photons traversing a turbid measurement volume are subject to a series of stochastic interactions with the medium, where each potential interaction has some probability of distorting the optical information represented by the photon. This stochastic process results in a distribution of photon classes which contribute to the final image with different degrees of fidelity. This distribution ranges from perfectly undistorted ballistic photons, to lower quality marginally interacting snake photons, to heavily distorted diffuse photons. Obtaining a high-resolution image through highly scattering materials is thus a matter of eliminating the heavily distorted, diffusely scattered signal to form an image dominated by the ballistic and snake light. This can be accomplished by a variety of photon selection methods based on optical path length, polarization, coherence, or collimation properties of the optical signal. The BI system described here is optimized for imaging Diesel fuel injection sprays and employs a compound OKE polarization scheme to realize adjustable ultrafast time-gating of the collected optical signal.

sedarsky@chalmers.se

W4P041 DEVELOPMENT OF A PHOTOACOUSTIC DETECTION SCHEME FOR SOOT MEASUREMENT

Gordon Humphries, John Black, Iain Burns, Jaclyn Dunn, Michael Lengden, University of Strathclyde, United Kingdom

Photoacoustic soot detection is based on the generation of acoustic pressure waves by an optical energy source. Soot particles in the flame are heated by absorption and produce an acoustic pressure wave by thermal release to the surrounding gas medium. Accurate modulation of the intensity of the incident light source allows for the resulting acoustic signal to be demodulated using a lock in amplifier. For this work a high power (30W), $\lambda = 808\text{nm}$, continuous wave diode laser is used to produce local heating of the soot in a premixed ethylene/air flame stabilised on a McKenna type burner. The laser

intensity can either be directly modulated or an optical chopper can be used. The resulting acoustic signal is then detected using a Wolfson MEMS microphone.

Early results acquired using this photoacoustic technique have shown close agreement to results from prompt Laser Induced Incandescence (LII) measurements performed in the same flame using a pulsed 1064nm Nd:YAG laser. An advantage of the photoacoustic detection scheme is that it allows for a relatively simple experimental setup, removing the complex detection optics inherent with purely optical techniques (such as LII) using instead only a microphone and a lock in amplifier.

gordon.humphries@strath.ac.uk

W4P042 RAYLEIGH SLIPI FOR HIGH BACKGROUND NOISE THERMOMETRY

Nathan Kempema, Marshall B. Long, Yale University, United States

Structured Laser Illumination Planar Imaging (SLIPI) was introduced in Ref. for environments such as a dense spray in order to overcome multi-scattering effects associated with conventional planar imaging. A modulated laser sheet imparts a known pattern into the collected signal such that single scattered photons retain the original pattern, while multi-scattered photons generally lose the pattern and manifest as background noise. The modulated light sheet is typically achieved by projecting the odd harmonics of an illuminated Ronchi grating onto a physical barrier that allows only the ± 1 modes to pass. Blocking all modes except the ± 1 harmonics results in a 50% loss of the energy incident on the grating in addition to the physical limitation of a Ronchi grating, which is not designed for high-energy applications. Laser energy may not be a limiting factor for scattering from particles or resonant processes but increased energy is advantageous for non-resonant scattering from small molecules such as in Rayleigh scattering.

In this work, a split-beam approach to SLIPI is demonstrated that allows for increased laser energy over use of a Ronchi grating. The second harmonic output of an Nd:YAG laser is split into two beams that are propagated 6.9 meters before interfering them in the probe volume. A long optical path length is necessary for application to macroscopic imaging since the interference pattern is proportional to the wavelength of the laser and inversely proportional to the half angle separating the two beams. Rayleigh thermometry is susceptible to error since there is no shift in wavelength between the probe laser and collected light. A simplified background correction is demonstrated through use of a structured light sheet. Temperature is then measured in a previously characterized non-sooting non-premixed methane/air flame in order to validate the application of SLIPI to Rayleigh thermometry.

A high background noise temperature measurement is made with Rayleigh SLIPI as part of the full field temperature measurement of sooting ethylene coflow diffusion flames. Two-color ratio soot pyrometry is used to measure temperature in sooting regions of the flame and intensity-ratio thin-filament pyrometry is used to measure temperature in the hot gas above 1150 K adjacent to the flame. Temperature in non-sooting regions and below 1150 K is measured with Rayleigh SLIPI. The collected Rayleigh signal is relay imaged to the detector in order to selectively image scattering from air and avoid the orders of magnitude stronger scattered signal from soot particles. However, some scattering from soot particles is collected and manifests as background noise in the measurement. Temperature was measured in cases where the magnitude of background signal to the modulated Rayleigh signal was as high as 21. Good agreement is found along the adjoining interface of Rayleigh SLIPI and intensity-ratio thin-filament pyrometry derived temperature.

nathan.kempema@yale.edu

W4P043 REAL TIME PARTICULATE MASS FLOW APPROXIMATION IN BIOMASS COOKSTOVES USING A GRAVIMETRIC SAMPLING SYSTEM

Kevin Dischino, John Mizia, Colorado State University, United States

The measurement of “real time” mass flow rate of Particulate Matter (PM) due to a combustion process is a time consuming and expensive procedure. However, especially in the realm of biomass cookstoves, determining the real time mass flow rate of PM can prove valuable in the understanding of the PM formation process. Here we present a relatively cost effective and simple to implement alternative method for measuring the real time mass flow rate of PM through a gravimetric sampling system. This method utilizes a correlation between the total mass of PM on the gravimetric system’s filter and the pressure drop across that filter. This correlation was determined through the testing of a biomass cook stove. It was found that during 45 minute simmer tests of a biomass cook stove, the pressure drop across the filter increased linearly as a function of time. Furthermore, it can be assumed that the mass production rate of PM during a simmer test is constant because all of the parameters that influence its formation are held constant. This implies that the mass of PM on the filter is a linear function of the pressure drop across that filter. Using this correlation, the mass of PM on the filter can be calculated as a function of time. In order to ensure the accuracy of this correlation, its limitations will be further explored. For example, the filter mass loading at which the relationship between the mass on the filter and the pressure drop becomes non-linear

will be explored. Additionally, the effect of the total mass flow on the pressure drop will be compared amongst varied particle size distributions. Lastly, the resulting PM mass flow rates determined by this method will be compared with mass flow rates measured with an integrating nephelometer.

kdischin@rams.colostate.edu

**W4P044 NOVEL DENSITY MEASUREMENT METHOD UNDER SUB- AND SUPERCRITICAL CONDITIONS:
VALIDATION AND APPLICATION TO RP-3**

Jianli Wang, Quan Zhu, Xiangyuan Li, Sichuan University, China

Based on the mass conservation principle and Bernoulli's equation, a novel measurement method is proposed to test the fuel density under sub- and super-critical conditions. By monitoring the mass flow at cooling condition and the differential pressure when the fluid flows through the orifice plate, the fuel density at high temperature can be estimated even with the occurrence of pyrolysis reactions, which was a huge challenge of the measurement technology in the past. According to the calibration parameters of the instrument, the conclusion can be drawn that this novel method with strict theoretical basis is valid for the density determination at high temperatures, especially applicable in the gas phase region with pyrolysis reactions.

wangjianli@scu.edu.cn

**W4P045 CHARACTERIZATION OF ORGANIC COMPOUNDS IN CIGARETTE SMOKE BY SOFT IONIZATION
MASS SPECTROMETRY**

Kenichi Tonokura, Rumiko Hayashi, The University of Tokyo, Japan

Soft ionization mass spectrometers, a Vacuum Ultraviolet Single Photon Ionization Mass Spectrometer (VUV-MS) and a Proton Transfer Reaction Mass Spectrometer (PTR-MS), were applied for the characterization of cigarette mainstream smoke and side stream smoke components from cigarettes (Mevius and VIRGINIA S. LIGHTS). Amines, pyridines, aldehydes, furans and aromatic hydrocarbons, etc. were observed as smoke components in both cigarette streams. The investigation on the difference between mainstream and side stream components was carried out. Ethylpyridine, methylbenzeneamine, and dimethylpyridine were observed in the side stream smoke, these were minor components in the mainstream smoke. In the PTR-MS measurement, ion signals, m/z 101 and 103 assigned to $C_5H_8O_2$ and $C_5H_{10}O_2$ were observed in the mainstream smoke, these were minor components in the side stream smoke. The difference between mainstream components and side stream components is caused by combustion temperature. Under active smoking condition, the combustion temperature is higher than passive smoking condition. Therefore, ethylpyridine, methylbenzeneamine, and dimethylpyridine would be decomposed in active smoking condition. In addition, oxygen containing compounds, $C_5H_8O_2$ and $C_5H_{10}O_2$ were observed in the active smoking condition in which oxygen is excessively supplied. In the PTR-MS measurement of smoke from VIRGINIA S. LIGHTS which contains menthol as additives, ion signal, m/z 157 assigned to menthol was observed, and other ion signals were almost the same as those in the case of Mevius.

tonokura@k.u-tokyo.ac.jp

W4P046 MICROSTRUCTURE AND ELECTROMAGNETIC PROPERTIES OF COAL CHARs

Haiyu Liu, Liang Xu, Yan Jin, Baoguo Fan, Yanxia Yang, Taiyuan University of Technology, China

Carbon content in fly ash is a major concern for combustion efficiency of a coal-fired boiler in the power plant. Based on much stronger microwave absorption of carbon than other oxides in fly ash, microwave technique has great application potentials for on-line determination of unburned carbon in fly ash. Since unburned carbon is produced from coal particles of incomplete combustion, coal char undergoes a complex succession of physicochemical evolution during the combustion process, which governs the degree of char burnout and carbon structure. The crystallite structure of coal chars varies during combustion and pyrolysis, and its changes may have notable effects on the electromagnetic parameters of resultant carbon, which further leads to the performance of reliability of microwave measurement. Herein, in the present work, coal chars were treated at 850-1600°C. For investigating the dielectric properties, electromagnetic parameters including the complex permittivity and the complex permeability of coal chars, were measured by the transmission/reflection method. The crystallite structure of coal chars was characterized by X-Ray Diffraction (XRD) technique. The following conclusions were drawn from the present investigation: (1) Increasing temperature made the crystallite structure of coal chars ordered, the fraction of organized carbon increased and aromatic layers periodically rearranged (2) The complex permittivity of coal chars exhibited significant dependence on treatment temperature. Both the real and imaginary part increased at higher temperature. The dielectric loss tangent behaved similar with heat treatment conditions. (3) The complex permeability and

the magnetic loss tangent of coal chars may be insignificant in this work. The dielectric properties of coal chars were mainly responsible for the attenuation properties in microwave application.

liuhaiyu@tyut.edu.cn

W4P047 FLAMMABILITY LIMITS DETERMINATION BY A SEMI-EMPIRICAL EQUILIBRIUM METHOD: PURE COMPOUNDS IN AIR AT ATMOSPHERIC PRESSURE AND MODERATE TEMPERATURES

Andres Armando¹, Mendiburu Zevallos¹, Joao Andrade de Carvalho Jr.¹, Christian Coronado²

¹Sao Paulo State University, Brazil ²Federal University of Itajubá, Brazil

The present work aims to develop a semi-empirical equilibrium method to predict the lower and upper flammability limits of combustible-air mixtures at atmospheric pressure and moderate temperatures. The method is called semi-empirical because the flame temperature at the end of the combustion process was determined by two correlations that relate the adiabatic flame temperature at the stoichiometric composition to the adiabatic flame temperatures at the lower and upper flammability limits, respectively. The correlations were determined by considering 20 flammable compounds. After this relation is known the equilibrium condition is applied and the flammability limits are determined, to this date 47 seven combustibles have been tested. The obtained model showed good accuracy for both flammability limits as they were compared with experimental data, except for the UFL of Ethylene, Dimethyl Ether, Acetaldehyde and Diethyl Ether. This divergence may be due to cold flames appearance. For these three compounds, and some others, the presence of cool flames was reported in work by Kondo et al. (2003). The presence of cool flames widens the flammability ranges. Kondo et al. (2003) also reported calculated values of 18.3%, 20.3% and 10.1%, for each of the aforementioned compounds; the UFL values obtained by using the present semi-empirical model, were 19.05%, 21.36% and 10.62%, respectively.

andresmendiburu@yahoo.es

W4P048 EXTINGUISHING PERFORMANCE OF PLANT BIOMASS FOAM EXTINGUISHING METHOD

Yuji Kudo, Kuya Yamamoto, Hachinohe Institute of Technology, Japan

We have proposed plant biomass foam extinguishing method for small packaged extinguishing systems for installation in general residential. In this study, extinguishing experiment was conducted to clarify extinguishing performance of fire by common fuel in the home. This paper describes the experimentally results of extinguishment performance change by fuel and foam gas. When using a vegetable oil or kerosene as fuel, extinguishing time is decreased as compared with the case of using as a fuel *n*-heptane. In a high boiling point fuel case, much foam was collapsed. Because the radiation intensity from high boiling fuel flame to foam is higher than *n*-heptane flame. From the foam collapse rate, we investigated the effect of heat which the inert gas takes away from flame (gas phase). Nitrogen gas and argon was almost the same value. However, the amount of heat taken away by helium was small. This shows that it is necessary that foam collapse more. After releasing the inert gas, foam gets back to liquid. The liquid evaporate at the surface of fuel and the evaporate heat take away the sensible heat of fuel. In the case of kerosene, much foam collapsed, heat of evaporation is large. However, the sensible heat of the fuel is even larger. This result shows that the cooling of condensed phase is more important for extinguishing a high boiling point fuel fire.

ykudo@hi-tech.ac.jp

W4P049 EXPERIMENTAL STUDY OF EXTINGUISHMENT OF A CONFINED PROPANE/AIR DIFFUSION FLAME BY WATER MIST

Akira Yoshida¹, Naoto Ohashi¹, Hiroyoshi Naito²

¹Tokyo Denki University, Japan, ²Fire and Disaster Management Agency, Japan

In the present study, a diffusion flame of propane was formed in a confined, co-flowing air stream, and extinguishment of the diffusion flame by water mist was investigated experimentally. Water mist was generated by three piezoelectric atomizers with the maximum droplets flow rate of 600 ml/h. When the fuel injection velocity U_f is low, an attached laminar diffusion flame with a premixed flame at the base is stabilized. At some distance from the burner rim, a transition from laminar to turbulent diffusion flame occurs, and a turbulent diffusion flame is formed in the downstream region. The stability mechanism of the attached flame can be explained by the balance of the gas velocity and the laminar burning velocity of premixed flame formed at the base. The stability of attached flame deteriorates with increase of the co-flowing air stream velocity U_a and the water mist flow rate Q_m . With increase in U_f , lift-off of the attached flame occurs and a lifted flame is stabilized at some distance from the exit of fuel jet. The lifted flame is rather stable when U_a is low, and becomes ready to blow-off with increase in U_a . When the fuel jet issues into a confined, co-flowing air stream, a recirculation zone is produced downstream of the fuel jet depending on the Craya-Curtet number C_t . The stable nature of a lifted flame appears for low U_a and high U_f and the resulting C_t is smaller than 0.8, which means that there exists a recirculation zone

downstream of the confined duct. This recirculation zone could serve to stabilize the lifted flame. The lifted flame blows off easily at low U_f when U_a is high. The corresponding C_t is large, and no recirculation zone is produced. For this regime, the lifted flame is stabilized only by the balance of turbulent burning velocity and gas flow velocity and the experimental data should suggest that the turbulent burning velocity decreases with water mist addition. The blow-off limit of U_f is rather insensitive to the water mist addition when C_t is large, whereas it decreases significantly with water mist for the case of small C_t . The dependence of the lift-off height on U_f is almost linear, which agrees well with previous studies. However, it deviates from linear relation when U_f is low. This deviation is attributed to the production of the recirculation zone due to small C_t . Thus the Craya-Curtet number C_t is significant for the stability of a confined diffusion flame.

yoshida@cck.dendai.ac.jp

W4P050 MEASUREMENT OF SUPPRESSION EFFECTIVENESS OF WATER MIST WITH VARYING DIAMETER USING COUNTERFLOW METHANE/AIR DIFFUSION FLAMES

Akira Yoshida¹, Shuhei Hashizume¹, Hiroyoshi Naito²

¹Tokyo Denki University, Japan ²Fire and Disaster Management Agency, Japan

In the present study, the effect of fine water mist on extinguishment of a methane-air counterflow diffusion flame was investigated to understand the underlying physics of fire extinguishment of highly stretched diffusion flame by water mist. The counterflow diffusion flame was stabilized in the forward stagnation region of a porous cylinder from which methane was ejected uniformly against the approaching air flow. With an increase in the non-dimensional fuel ejection parameter, the flame moves outward independently of the water mist mass loading. When the stretch rate is small, the blue flame is accompanied by a thick luminous yellow zone. With increase in the stretch rate, the luminous yellow zone disappears and then the remaining blue flame extinguishes at a critical stretch rate. When the water mist is not added, the critical stretch rate at extinguishment was 439 s^{-1} as compared to the theoretical value of 460 s^{-1} . Twin-fluid atomizers were used to generate polydisperse water mist of which Sauter mean diameters were 10, 20, 40, and 60 microns. For the case with water mist addition, when the stretch rate is small enough, almost all the water mist evaporates within the flame zone. On the other hand, for high stretch rate case, large mist droplets pass through the flame zone and can reach the stagnation plane. However, no oscillatory motion was found around the stagnation plane. Critical stretch rate at extinguishment decreases monotonously with the mass fraction of water mist independently of the mist diameter within the range from 10 microns to 60 microns. Dependences on the surface area parameter show that large droplets are more effective than small ones when the surface area parameter is constant, and are quantitatively in good agreement with theoretical predictions. The critical stretch rate at extinguishment decreases rapidly with increase in the surface area parameter and becomes less sensitive at large surface area parameter. Therefore, an appropriate combination of stretch rate and surface area parameter should be provided to suppress effectively a given fire with a small amount of water mist. When the water mist evaporates completely in the flame zone as in the present study, the mass fraction of the water mist is the dominant factor for fire extinguishment, rather than the surface area parameter.

yoshida@cck.dendai.ac.jp

W4P051 EXPERIMENTAL AND NUMERICAL STUDY OF LAMINAR FLAME SPEED RETARDATION BY WATER MIST

Akira Yoshida¹, Toichiro Okawa¹, Wataru Ebina¹, Hiroyoshi Naito²

¹Tokyo Denki University, Japan ²Fire and Disaster Management Agency, Japan

Water mist has been recognized as an alternative of halogenated hydrocarbon fire suppressants due to its high thermal, dilution and chemical effects on the flame speeds. In the present study, the effects of water mist on laminar speed of propane-air premixed flame were investigated both experimentally and numerically. In experiments, the laminar flame speeds were measured using a single jet-plate configuration for the cases with and without water mist. The numerical simulation is also performed using the OPPDIF and PREMIX codes in CHEMKIN package.

To include the phase change of evaporation, the evaporation process is assumed as a chemical reaction of which rate constant follows the Arrhenius law. The measured laminar flame speeds without water mist increase with stretch rate towards the limit of extinguishment for all the equivalence ratios tested and are in fairly good agreement with the previous data. This tendency is fairly reproducible by the numerical simulation with DLW kinetic mechanism. Both experiment and simulation show that the water mist addition reduces the flame speed significantly. In the simulation with water mist, the flame speed increases with the stretch rate similar to the case without water mist, whereas the thermal, dilution and chemical effects of water mist reduce the flame speeds. However, measured flame speed decreases with the stretch rate, in conflict with the numerical simulation. In the stagnation flow field, the flow stream line diverges with approaching the stagnation plate and water mist, even if the diameter is small, cannot follow the large radial acceleration. As a result, the mist droplet accumulation occurs around the stagnation stream line. This droplet accumulation reduces the flame speed locally as

compared to the case with uniform dispersion, leading to the negative dependence of flame speed on stretch rate. Numerical simulation reveals the thermal, dilution and chemical effects of water mist on laminar flame speed, and the chemical effect is found to be small but cannot be neglected. The sensitivity analysis of flame speed shows that the water mist reduces the rates of chemical reactions involving the radicals such as O, H and OH, which have the positive sensitivity of flame speed. Furthermore, three-body chain terminating reactions involving H₂O are enhanced. These reactions have large negative sensitivities of flame speed due to high chaperon efficiency of H₂O

yoshida@cck.dendai.ac.jp

W4P052 COMBUSTION BEHAVIOR OF FIRE WHIRL FORMED ON FUEL CONTAINER

Genichiro Kushida, Masayuki Mizuno, Aichi Institute of Technology, Japan

A fire whirl, which is generated by buoyant flow and flow gradients due to side flow, is sometimes observed in a big fire, where fire forms a tornado-like vortex of flames and the flame height becomes very high. The mechanism of fire whirl is still unclear, especially for the generating conditions and the moving direction of fire whirl. In the present study, the fire whirl formed on a fuel container is experimentally studied for the several cases of different velocity and direction of side flow, and the behavior of fire whirl is examined in detail by investigating the condition and probability of generation, the moving direction and the fuel consumption.

In the present experiments, the pool flames on a long rectangular container or a small circle pan which are filled over with ethanol fuel are investigated. A swirling flow is necessary for a fire whirl to be generated. So a uniform flow and the other directional jet flow are utilized in order to generate swirling flow components. In addition, methane gas jet diffusion flames are investigated under the swirling flow generated by four fans, and the flame heights of fire whirl are compared to the results of pool flames. Under only the uniform flow, a fire whirl hardly appears. When two perpendicular side flows are given to the flame, a fire whirl is generated by high probability, and in some cases even two or more fire whirls are formed. In the present experiments using a long rectangular fuel container, a fire whirl moves towards the downstream direction of given uniform flow, and the moving speed is proportional to the uniform flow velocity component in the direction of moving fire whirl. However, in the case of low uniform velocity, the moving speed of fire whirl is unstable. Once a fire whirl is generated, the fuel consumption rate is increased and the flame height becomes high. In the results of the similar experiments using a jet diffusion flame where the fuel supply is fixed, the flame height does not change so much. Therefore it is thought that the flame height becomes high because of the high fuel consumption rate increased by the swirling flow.

In conclusion, it is made clear in the present study that a fire whirl is generated when the swirling flow component is given to the flame, and it moves towards the direction of local wind with the speed proportional to the uniform flow velocity component of moving direction of fire whirl. Also, when the fire whirl is generated, the fuel consumption rate is increased and the flame height becomes high.

kushida@aitech.ac.jp

W4P053 FLAME SPREAD OVER THIN SOLID FUELS ON OPEN AND CLOSED CHANNELS

Bruna Comas, Toni Pujol, University of Girona, Spain

We experimentally study the flame spread over thin solid fuels that propagates in a channel with a closed cross-section, in a channel with an open cross-section (i.e., with lateral walls) and in an open environment. The tests have been done at several angles of inclination, ranging from downwards to upwards burning and at different oxygen atmospheric levels. The speed of the observed flame front and the length of the pyrolysis region are presented along with Particle Image Velocimetry (PIV) measurements of the induced gas flow velocities for atmospherical concentration cases. We find out that channels with closed cross-section reduce the flame spread velocity at low angles of inclination. We also observe a flame instability that occurs in downward combustion at low inclination angles in every configuration at low angles. This unstable behaviour leads to variations in the flame front speed values.

In horizontal burning and using a closed channel configuration we observe two flame fronts that propagate through the sample, a fast flame front with a V-shape that starts to pyrolyze the sample and a slower front that ends the pyrolyzation. In upward combustion the closed channel configuration gives the fastest flame spread rates. A sudden increase in the flame spread rate may be observed at moderate inclination angles.

bruna.comas@udg.edu

W4P054 EFFECT OF PRESSURE AND OXYGEN CONCENTRATION ON THE FLAME SPREAD LIMITS OF FIRE RESISTANT FABRICS

Danielle Kirchmeyer, University of California, United States

Space exploration vehicles may employ cabin environments that are not at standard sea level atmospheric conditions. NASA's Constellation Program proposed a human space exploration cabin environment of reduced ambient pressure and increased oxygen concentration (56 kPa and 32% O₂). There is a need to further understand the flammability of materials in these environments. In this work, normalized tests were conducted at different pressures to study the effect of oxygen concentration on the upward and downward flame spread over the Fire Resistant fabric Nomex HT90-40. The results show that for Nomex HT90-40 fabric the minimum oxygen concentration for upward and downward flame spread depends on the ambient pressure. A boundary of flame spread or not flame spread is developed in terms of ambient pressure and oxygen concentration. It is shown that at decreased pressures the oxygen concentration required for flame spread increases, and that the boundaries of upward and downward flame spread converge as the pressure is reduced. A phenomenological explanation is given in the results. It is worth noting that there are a number of situations when fires may occur at pressures and oxygen concentrations that are different than standard atmospheric conditions, such as in locations at high elevation and airplanes which extends the interest of this study to many other fields.

dani.kirchmeyer@gmail.com

W4P055 THE EXPERIMENTAL STUDY OF FLAME SPREAD RATE NEAR EXTINCTION LIMIT ON ETFE INSULATED WIRE

Ken Mizutani¹, Andres Osorio², Carlos Fernandez-Pello², Osamu Fujita¹

¹Hokkaido University, Sapporo, Japan ²University of California, Berkeley, United States

As the duration of space missions increases guaranteeing astronaut and spacecraft safety is a top priority. In spacecraft, many electric devices and particularly electrical cables represent a potential source of fires. To this date a limited number of studies have focused on flame spread over wire insulation in micro-gravity (μ g) see Takahashi et al. However, the wire insulation material has mainly been low density polyethylene, and not fire resistant materials such as Poly-Tetra-Fluoroethylene (PTFE) or Ethylene-Tetra-Fluoroethylene (ETFE). Therefore it is still not clear whether it is appropriate to apply the results from non fire resistant materials to fire resistant materials actually used inside a spacecraft. The authors carried out the experiments on ETFE insulated copper wire exposed to an external radiant flux in normal-gravity (1g) and μ g condition in 12 cm/s opposed air flow.

In the research, we mainly focused on the extinction limit of flame spread over the wire sample. In the present poster we examine the experimental data in terms of the Flame Spread Rate (FSR), oxygen concentration and external radiant flux. The results showed that FSR approaches specific value (almost zero) with oxygen concentration drop followed by extinction. Now we consider the heat balance in unit length of wire insulation in Eq.1 based on the study conducted by Takahashi et al. $V_f \rho_s \pi (r_s^2 - r_c^2) \{ c_s (T_p - T_s) + L_p \} = Q'_{net}$ Where V_f , T and Q'_{net} are FSR, temperature and net heat input to the insulation. ρ , r , c and L respectively denote density, radius, specific heat and latent heat. Subscripts s , c and p mean insulation, core and pyrolysis. According to Eq.1, FSR is controlled by material properties and net heat input. We will discuss how the controlling mechanism of FSR varies between conditions that flame keep stable and near extinction limit. This presentation will show FSR data for a varied set of conditions and discuss the controlling factors for the observed results. Understanding the flame spread behavior near the extinction limit is an important step towards estimating material flammability in different ambient conditions, including gravity. This research is supported by JAXA as a candidate experiment for the third stage use of JEM/ISS titled "Evaluation of gravity impact on combustion phenomenon of solid material towards higher fire safety".

k_mizutani@frontier.hokudai.ac.jp

W4P056 AN OBSERVATION OF PULSATING FLAME SPREAD ON COMBUSTION PROCESS OF A SOLID

Tadafumi Daitoku, Takashi Tsuruda, Akita Prefectural University, Japan

Flame spread along combustible material is governing growth and extinction of fire hazards. Understanding on the flame spread is practically important to reduce fire risk. Flame spread is controlled by heat and mass transfer, and chemical reaction. The behavior of a flame spreading along a combustible liquid is dependent on characteristics of liquid and atmosphere. The behavior of flame spread is mainly dependent on the temperature of the combustible liquid. For example, the flame spread rate along the methanol surface increases with the methanol temperature, but it becomes almost a constant value above 20 degree Celsius. The behavior of the flame spread along combustible liquids are studied by the various measurement techniques; smoke tracing, single and dual wavelength holographic, interferometer, infrared thermograph, and high-speed photography. At a combustible liquid temperature, which is higher than the flash ignition temperature, a layer of the a combustible mixture over a liquid surface exists and a premixed flame propagates in the layer. And at a combustible liquid temperature, which is lower than the flash ignition temperature, a diffusion flame spreads along the liquid surface. For flame spread, combustible liquid temperature ahead of the leading edge of the flame needs to rise, and the area evaporating of combustible liquid spreads to maintain the flame. Heat transfer in the liquid phase responds to the marangoni effect by

the temperature difference between the leading edge of the flame and surroundings. A combustible liquid at a high temperature flows ahead of the leading edge of the flame, by the marangoni effect. This causes a particular behavior of pulsating flame spread.

Several investigations of pulsating flame spread over a combustible liquid have been carried out. However, a particular behavior pulsating flame spread along a combustible solid has not been investigated. In the case of flame spread along a solid, convection is not generated in a solid combustible, and the solid combustible is gasified and burns by thermal decomposition. So, it is thought that it is not possible to fire a particular behavior of pulsating along solid. Additionally, it is difficult to observe the thermal field in the solid due to presence of thermally decomposing surface and estimated short characteristic time of heat and mass transfer in solid. In order to detect such an oscillating phenomenon, a high-speed and high-spatial resolution measurement is needed. However, in the contact type temperature measurement as a thermo couple and so on., there is a problem that it has a heat loss to a sensor and slow response. A catoptric system for infrared thermometry for microscopic and high-speed temperature measurement is employed in this study. In this paper, a particular behavior of pulsating of downward flame spread over combustible solid was examined with the catoptric system.

daitoku@akita-pu.ac.jp

W4P057 COMBUSTION CHEMISTRY AND PYROLYSIS KINETICS OF PINE NEEDLES. FIRE SPREAD ACROSS A FOREST FUEL BED

Oleg Korobeinichev¹, Alexander Tereshchenko¹, Alexander Paletsky¹, Andrey Shmakov², Munko Gonchikzhapo¹, Inna Shundrina², Lilia Kataeva³, Dmitriy Maslenniko³, Yury Naganovsk⁴, Naian Li⁵

¹Institute of Chemical Kinetics and Combustion, Russia ²Novosibirsk State University, Russia

³Nizhny Novgorod State Technical University, Russia ⁴Russian Research Institute for Fire Protection, Russia

⁵University of Science and Technology of China, China

The research addresses an experimental study of two issues, which are important for computer modeling of fire spread across of bed of pine needles – 1. Study of the flame speed and of spatial temperature distribution at various depths of the bed of pine needles of Siberian boreal forests, a study of the composition of gaseous species and distribution of their concentrations across the bed during fire spread and the study of the impact of the wind velocity on these characteristics. 2. Finding the kinetic parameters of pine needles pyrolysis in inert medium and in air. It has been found that, as the wind velocity rises in the range of 0.15 – 0.2 m/s, the burning mode changes dramatically, as well as the temperature and concentration profiles of gaseous species inside the bed. At low wind velocities, flame penetrates the bed, while at high ones it does not. At wind velocities 0.15 m/s and higher, as the wind velocity grows, together with the dramatic growth of the flame velocity the maximum temperature in the flame front inside the bed decreases from 1200 °C to 700 °C, the width of the combustion zone increases, in accordance with the temperature and O₂ and CO₂ concentration measurements. The flame front in the middle of the bed is biased relative to the flame front on the bed surface. Using the methods of differential mass-spectrometric thermal analysis and thermogravimetry, the kinetics and the composition of the pyrolysis products of the pine needles and of char oxidation have been studied. Based on the comparison of the rate constants obtained for different conditions and by different methods, the rate constants best matching the data obtained were identified. The data obtained in the study may be used in developing a ground fire spread model.

korobein@kinetics.nsc.ru

W4P058 AN EXPERIMENTAL STUDY ON FLAME SPREAD OVER SOLID SURFACE WETTED WITH COMBUSTIBLE LIQUID -EFFECTS OF GASIFICATION PROPERTIES OF COMBUSTIBLE LIQUIDS

Takeshi Suzuki, National Research Institute of Fire and Disaster, Japan

Flame spread over solid surface is a complex process. It is dependent on a lot of parameters. Gasification properties are one of them. Effects of gasification properties were studied experimentally. Stainless steel mesh screens were selected as solid materials. Seven kinds of screens ranging from 400-mesh (distance between wires=0.034 mm) to 10-mesh (distance between wires=2.1 mm) were used. Octane (flash point=13.3), decane (flash point=44), and dodecane (flash point=71.1) were selected as combustible liquids. For controlling gasification properties, mesh screens were wetted with combustible liquids of different volatilities. Horizontal flame spread over a mesh screen wetted with a combustible liquid was observed and recorded with video cameras.

Experiments were done in a still environment in normal gravity in environmental temperatures between 26 and 30. Flame spread phenomena changed with kinds of liquids and with kinds of mesh screens. Four phenomena were observed. Flame spread over upper and lower surfaces. Flames spread rate was around 3 cm/s. Flame spread phenomenon was like that over a thin filter paper sheet. A flame spread over an upper surface. Flame spread rate was around 4 mm/s. A flame did not spread over a lower surface. Flame flashed over upper and lower surfaces. Flame spread rate was more than 10 cm/s. A flame did not spread. When octane was used, phenomenon was observed irrespective of kinds of mesh screens. Since flash

point of octane was lower than environmental temperature, a flammable mixture was formed near the mesh screen and flames spread in the flammable mixture. Since flash point of decane was higher than environmental temperature, flammable mixture was not formed near the mesh screen. When screens of 400-, 200-, and 100-mesh were wetted with decane, phenomenon was observed. When screens of 60-, 40-, 20-, and 10-mesh were wetted with decane, phenomenon was observed. When a mesh screen was fine, space surrounded by wires was occupied by liquid. Thus, a mesh screen was like a thin sheet and flames spread over upper and lower surfaces. When a mesh screen was coarse, space surrounded by wires was partly occupied by liquid. Thus, a flame spread over an upper surface because of shortage of fuel supply. When screens of 400-, 200-, and 100-mesh were wetted with dodecane, phenomenon was observed. When screens of 60- and 40-mesh were wetted with dodecane, phenomenon was observed. When screens of 20- and 10-mesh were wetted with dodecane, phenomenon was observed. Dodecane is less volatile than decane. When a mesh screen was coarse, a flame did not spread because of shortage of fuel supply.

tsuzuki@fri.go.jp

W4P059 ENSEMBLE-BASED DATA ASSIMILATION FOR REGIONAL-SCALE SIMULATIONS OF WILDFIRE SPREAD

Melanie Rochoux¹, Sophie Ricci¹, Benedicte Cuenot¹, Arnaud Trounev²

¹Centre Européen de Recherche et de Formation Avancée en Calcul Scientifique, France ²University of Maryland, United States

This study presents a prototype data-driven wildfire simulator capable of forecasting the fire spread dynamics. The prototype simulator features the following main components: a level-set-based fire propagation solver called FIREFLY that treats wildfires as propagating fronts and uses a description of the local Rate Of Fire Spread (ROS) as a function of biomass fuel, terrain topography and meteorological properties based on Rothermel's semi-empirical model; a series of observations of the fire front location; and a data assimilation algorithm based on an Ensemble Kalman Filter (EnKF). This stochastic algorithm partly accounts for non-linearities in the wildfire spread model. It also features a choice between a Parameter Estimation (PE) approach in which the estimation targets are the input parameters of the Rothermel's ROS model and a State Estimation (SE) approach in which the estimation targets are the spatial coordinates of the discretized fire front. The performance of the prototype data-driven simulator is first evaluated in a series of synthetic verification tests; tests include representative cases with spatially-distributed biomass properties and temporally-varying wind conditions. In the SE-based approach, in order to properly account for uncertainties during the EnKF update step and to accurately represent error correlations along the fireline, it is shown that members of the EnKF ensemble must be generated through variations in estimates of the fire initial location and the ROS model parameters. In the PE-based approach, it is shown that a surrogate model based on a polynomial chaos expansion can be used in place of FIREFLY in order to reduce the EnKF computational cost without loss of accuracy. The prototype data-driven simulator is also evaluated by comparison with data taken from a controlled grassland fire experiment. Results indicate that data-driven simulations are capable of correcting inaccurate predictions of the fire front location and of subsequently providing an optimized forecast of the wildfire behavior at future lead-times. The complementary benefits of both PE and SE approaches in terms of analysis and forecast are also emphasized. In particular, it is found that the duration of the assimilation time window must be specified according to the persistence of the model initial condition and/or with the temporal and spatial variability of the environmental conditions. This, in order to reduce uncertainties in wildfire spread and to track sudden changes in the wildfire behavior. While wildfire spread forecast capabilities are still at an early stage of development, it is envisioned that they will be similar to current weather forecast capabilities and that they will provide real-time fire forecasts using airborne or spaceborne thermal-infrared imaging including a description of both wildfire dynamics and plume dynamics.

melanie.rochoux@graduates.centraliens.net

W4P060 COMPUTATIONAL SMOULDERING WILDFIRES: DEPTH OF BURN AND SUPER CRITICAL MOISTURE AT THE IN-DEPTH FIRE SPREAD OVER PEAT SOILS

Xinyan Huang, Guillermo Rein, Imperial College, United Kingdom

Smouldering combustion is the slow, low-temperature, flameless burning of porous fuels and the driving phenomenon of wildfires in peatlands. Smouldering fires propagate horizontally and vertically through organic layers of the ground and can reach deep into the soil. These threaten to release ancient carbon stored in the soil. Once ignited, they are particularly difficult to extinguish despite extensive rains, weather changes, or fire-fighting attempts, and can persist for long periods of time.

In this work, we establish a computational 1-D model of a reactive porous media, using the open-source code Gpyro, to investigate the in-depth spread of smouldering fires into peat samples with varying profiles of moisture content, density, inert content and porosity. The model solves the species, momentum, and energy conservation equations and a previously developed scheme of heterogeneous chemical reactions, so as to predict the transient temperature, species, and reaction

profiles during ignition, spread, and extinction. Modelling results reveal that the depth of burn and the critical moisture content to sustain in-depth spread are not uniform, but depend on fire conditions upstream of the column, the thickness of the moist layer and the thermal penetration of the drying front. The influences of thicknesses and properties of dry and moist layers are investigated. The computed depth of burn and critical moisture content are compared to the experimental results with natural organic soil samples published in the literature. This study allows to explain in heat transfer terms the previous observations of smouldering propagation in soils layers with super critical moisture.

seuhxy@gmail.com

W4P061 EFFECT OF $K_4[Fe(CN)_6]$ AEROSOL ON CH_4/AIR AND H_2/AIR FLAMES SPEED

*Andrey Shmakov, Anatoly Chernov, Tatiana Bolshova, Oleg Korobeinichev
Voevodsky Institute of Chemical Kinetics and Combustion SB RAS, Russia*

Finely dispersed water is widely used in the practice of extinguishing fires and preventing explosions. Raising the effectiveness of fire extinguishing with water may be reached both by improving water dispersity and by introducing various additives. Recently a number of studies have been conducted, the purpose of which was to determine the effectiveness of flame suppression with aerosols of the water solutions of salts. As additives, such compounds were investigated as NaCl, KCl, LiI, CH_3COOK , $CoCl_2$, $NiCl_2$, NaOH, $NaHCO_3$, $MgCl_2$, $CaCl_2$, $MnCl_2$, $FeCl_2$ and others. It has been found that some of the above compounds are more effective flame suppressors than the widely used CF_3Br . According to the literature, potassium compounds are the most effective (per mass) flame extinguishers. Therefore, the study of compounds containing the maximum number of potassium atoms is of interest because they exhibit the lowest mass extinguishing concentration. One of such compounds is potassium ferrocyanide $K_4[Fe(CN)_6]$. No studies of the impact of aerosols of the water solutions of this salt on the combustion of methane-air and hydrogen-air mixtures have been conducted.

The objective of the study is to investigate the impact of the aerosol of the water solution of $K_4[Fe(CN)_6]$ on the burning velocity of CH_4/air and $H_2/O_2/N_2$ combustible mixtures at 1 atm. For the measurement of the laminar CH_4/air and diluted $H_2/O_2/N_2$ flames propagation velocity, the Mache-Hebra burner was used. Burning velocity of hydrogen flame was measured for $H_2/O_2/N_2$ combustible mixture with dilution ratio $D=[O_2]/([O_2]+[N_2])=0.077$. The burner was a glass tube with the internal diameter of 2 cm and the length of 27 cm, tapering below to the diameter of 1 cm at the length of 3 cm. The burner temperature was maintained to be permanent and was equal to 93 °C. With this temperature, the volume flow of the stoichiometric combustible mixture of methane and air was 104 cm³/s.

The aerosol of the water solution of potassium ferrocyanide was introduced into the flow of the combustible mixture with an atomizer. The solution was introduced with a syringe, the piston of which was moved by a mechanic drive with a step-by-step motor, which allowed the additive concentration to be changed in a wide range. The mass-median diameter of the aerosol droplets was about 10-20 microns whereas after evaporation of water the size of solid particles became 2 - 4 microns. The burning velocity was measured with the PIV (Particle Image Velocity) method with an accuracy of $\pm 5\%$. The photographs taken were processed with a cross-correlation method using adaptive algorithms.

To calculate the CH_4/air flame speed, the mechanism GRI-Mech 3.0 was used. The mechanism was developed for modeling of combustion of natural gas and includes nitrogen combustion chemistry. It includes 325 reactions for 53 flame components. To consider the influence of $K_4[Fe(CN)_6]$ on the flame speed, 22 gas phase reactions [P. Glarborg, P. Marshall, Combustion and Flame 141 (2005) 22-39] of transformation of potassium-containing particles were included into the mechanism. According to experimental and modeling results, an addition of 2.2% by volume of water vapor decreased the speed of a stoichiometric CH_4/air flame for 8%. An addition of 2.2% of water vapor and 0.2 g/m³ of the salt reduces the flame speed for about 15% (modeling) and for 25% (experiments). It can be seen that small additions of $K_4[Fe(CN)_6]$ essentially influence the flame speed of a stoichiometric CH_4/air mixture both in the calculations and in the experiment. At the same time, there is some disagreement between calculation and the experiment, which may be attributed to the fact that the reactions of radicals with other active products of salt decomposition (for example, with iron and its oxides) were not taken into account, as well as the heterogeneous reactions of the loss of active centers on the surface of the salt particles and condensed products of its decomposition, and possible incorrectness of the rate constants of the reactions.

The measurements of CH_4/air flames speed demonstrated that the inhibition effectiveness of $K_4[Fe(CN)_6]$ reduces as when passing from lean to rich flames. A similar tendency is observed for N_2 -deluted ($D=0.077$) H_2/air flames doped with 1% aqueous solution of $K_4[Fe(CN)_6]$ in the equivalence ratio range 1.3-2.3.

shmakov@kinetics.nsc.ru

W4P062 EFFECT OF DISTANCE BETWEEN DOUBLE TWO-DIMENSIONAL IMPINGING OXIDIZER JETS ON BURNING RATE OF SOLID COMBUSTIBLES

Tsuneyoshi Matsuoka¹, Kyohei Kamei¹, Susumu Noda¹, Harunori Nagata²

When gaseous oxidizer issued from single nozzle is impinged on flat solid combustibles, one-dimensional diffusion flame is formed at the stagnation region above the solid surface. This geometry is widely used to investigate the fundamental characteristics of solid combustion, such as burning rate. In practical combustion systems (e.g., hybrid rocket motor), however, multiple oxidizer jets are applied and/or the shape of the solid are intricate. Hence, the flow fields in these systems usually become more complex than the single case due to the secondary impingement or roll-up flows. The flames are no longer considered as one-dimensional and the burning must be changed. In order to predict the burning rate precisely and optimize the combustion systems, the hydrodynamic effect on the burning rate due to the multiple jets and/or intricately-shaped solid must be understood. As a first step, the authors take up a simplified problem where double oxidizer jets issued from two parallel slit nozzles impinge to flat PMMA plate in this study. Experiments with two different distances between the impinging jets, $p = 4$ and 18 mm, were examined to investigate the effect of the distance on the burning rate. According to a traditional theory, the estimated half width of the free-jet indicates the flows issued from separated nozzles are merged 6.5 mm above the surface for $p = 4$. As expected, the burning rate had a broaden peak at the wide stagnation region. On the other hand, for $p = 18$ mm, the flows impinge on the surface without merging. Hence, two separated peaks of burning rate were clearly observed. It is found that the peaks are shifted outside of the stagnation region expected to be just below the each nozzle. It is considered that the outward flow caused by pressure gradient imposed on the center pushes free-jet. Although the flow fields have not been directly confirmed yet, the results suggest that the double imping jets may change the burning rate through the interaction between flows.

matsuoka@me.tut.ac.jp

W4P063 SUPPRESSION MODELING ADAPTED FOR THE EDC MODEL IN SIERRA/FLUID MECHANICS/FUEGO

Alexander Brown, Flint Pierce, John Hewson, Sandia National Laboratories, United States

Suppression of flames by diluent agents is achieved through the diluents' effect on the chemical rates, thus altering the ratio of the chemical and mixing time scales. Suppressant can act as a thermal diluent or retard rates through dilution, though the former is generally found to be significant for a larger class of suppressants. Chemical scavenging of radicals can also occur, but such suppressants are not considered here. In discretized computational models, the chemical rates of reaction are not always specifically modeled. The Eddy Dissipation Concept (EDC) model is one of the more frequently used reaction models in Sierra/Fluid Mechanics module for fires, Fuego. In the EDC model, reaction rates are generally assumed to be mixing-limited so that the addition of suppressant to create a reaction-limited state needs additional modeling. We have modified the methods of Zhang and Soteriou (2011), describing the variation of global reaction rates with suppressant addition, for predicting the suppression in the context of the EDC model in Fuego. The propensity for suppression is tied to the ratio of the reaction and diffusion timescales, and therefore is calibrated to a single parameter, the critical Damkohler number. Two experimental scenarios found in the literature are evaluated to determine the fit coefficient that best replicates existing data.

albrown@sandia.gov

W4P064 FLAME SUPPRESSION VIA OXIDIZER DILUTION IN A TURBULENT SLOT BURNER: EXPERIMENT AND LES

James White¹, Eric Link¹, Sebastien Vilfayeau¹, Andre Marshall¹, Peter B. Sunderland¹, Arnaud Trounev¹, Yi Wang², Ning Ren²

¹University of Maryland, United States ²FM Global Research, United States

This work features the suppression of a buoyant, turbulent, methane- or propane-fueled diffusion flame via added-nitrogen dilution of the oxidizer. Flames are stabilized above a 5×50 cm slot burner surrounded by a 50×75 cm air co-flow. Nitrogen gas is introduced to the co-flow to provide controlled flame suppression. Measurements include oxidizer-stream oxygen mole fraction (XO₂) via gas sampling, flame radiative (infrared) emissions via radiometer, flame luminous (visible) emissions via photodiode, and flame imaging via digital camera. A minimal flow of oxygen is supplied along the length of the burner to provide a strengthened and stabilized flame base that resists liftoff extinction. With the oxygen anchor, global flame extinguishment is the result of increasingly prevalent localized quenching throughout the flame. Flame images provide a measurement technique for mean visible flame height, which increases, then decreases with reducing XO₂. For both anchored and non-anchored conditions, radiative loss fraction decreases linearly with reducing XO₂. Flame luminosity decreases monotonically with reducing XO₂ by six orders of magnitude, where sharp bends in the trend mark transition between flame sooting regimes that manifest as visually-identifiable changes in flame color from yellow to yellow-blue to blue. Comparison of measurements between methane (minimally-sooting) and propane (appreciably-sooting) fuels reveals the dominance of soot production in determining the decay of flame radiative emissions with transition to extinction. Measurements are compared with Large Eddy Simulation (LES) results using both the Fire Dynamics Simulator (FDS) and

FireFOAM, two open-source Computational Fluid Dynamics (CFD) software packages respectively developed by the National Institute of Standards and Technology (NIST) and FM Global. Experiment/simulation comparisons provide the basis for performance evaluation of available fire modeling tools in predicting flame suppression.

jwhite21@mail.umd.edu

W4P065 SKELETAL MECHANISM FOR FLAMES INHIBITION BY TRIMETHYLPHOSPHATE

Tatiana Bolshova, Vladimir Shvartsberg, Oleg Korobeinichev, Andrey Shmakov, Institute of Chemical Kinetics and Combustion, Russia

Combustion of solids, liquids and gases is known to be the source of fires. Fires hold a special position among other disasters, which are known to be a global problem due to their ability to cause huge damage to mankind. The development of a physico-mathematical predictive model for their initiation, propagation and suppression is of great scientific and practical importance. At present, methods of computational fluid dynamics are being intensively developed. The methods make it possible to study 3D dynamics of the processes proceeding during fire propagation and suppression, including the case when the inhibitors and fire suppressants are used. The models used in these simulations involve fluid dynamics and also consider phase and chemical transformations of the substances. Successful application of these models is impossible without taking into account chemical transformations of the intermediate components. The chemical processes are usually described by detailed mechanisms that can include thousands of elementary reactions involving hundreds of chemical species. On the basis of a multi-step kinetic mechanism for flames inhibition by organophosphorus compounds including more than 200 reactions, a skeletal mechanism for flames inhibition by trimethylphosphate was developed. The skeletal mechanism consists of 22 irreversible elementary reactions, involving 9 phosphorus-containing species. The starting mechanism was developed by collecting the maximum number of elementary reactions involving phosphorus-containing species. Besides phosphorus-involving reactions, this mechanism includes submechanisms for combustion of hydrogen, methane and propane. Overall, the mechanism consists of 682 steps for 121 species, 44 of which contain P-atoms. Selection of the crucial steps was performed by analyzing P-element fluxes from species to species and by calculating net reaction rates of phosphorus-involving reactions versus the flames zone. The developed mechanism was validated by comparing the modeling results with measured and simulated (using the starting initial mechanism) speed and chemical structure of H_2/O_2 and CH_4/O_2 flames doped with trimethylphosphate. The mechanism was shown to satisfactorily predict the speed of $\text{H}_2/\text{O}_2/\text{N}_2$ flames with various dilution ratios and CH_4/air flames doped with trimethylphosphate. Besides, the skeletal mechanism satisfactorily predicts the spatial variation of H and OH radicals and final phosphorus-containing products of the inhibitor combustion. Further reduction of the skeletal mechanism without modification of the rate constants recommended in the starting mechanism was shown to result in noticeable disagreement of the flames speed and structure.

bolshova@kinetics.nsc.ru

W4P066 APPLICATION OF THE METHOD OF OPPOSED FLOW DIFFUSION FLAMES FOR THE STUDY OF THE MECHANISM OF TPP FLAME RETARDANCY FOR UHMWPE

Oleg Korobeinichev¹, Alexander Paletsky¹, Munko Gonchikzhapov¹, Andrey Shmakov¹, Alexander Tereshchenko¹, Inna Shundrina², Naian Liu³

¹*Institute of Chemical Kinetics and Combustion, Russia* ²*Novosibirsk Institute of Organic Chemistry, Russia*

³*University of Science and Technology of China, China*

The method of opposed flow diffusion flames was applied to study the combustion mechanism of polyethylene. Combustion of polymers with flame retardant additives had not been investigated with this method. The purpose of this work was to study the impact of Triphenyl Phosphate (TPP) flame retardant on combustion of Ultrahigh-Molecular Weight Polyethylene (UHMWPE) using the method of opposed flow diffusion flames. The method of mass spectrometry and the microthermocouple technique were used to study the structure of the diffusion flame of UHMWPE and UHMWPE+5%TPP in the opposed air flow. The mass burning rate of UHMWPE and UHMWPE/TPP (5%) was 18 and 8 g/(m²·s), the burning rate was 18 and 7.7 μm/s, respectively. Sampling was conducted with a quartz probe in Hiden HPR-60 mass spectrometer. The temperature was measured by a Pt-PtRh (10%) thermocouple with the diameter of 50 μm, covered with anticatalytical SiO₂ coating. To identify the products and to determine their concentration profiles, the results of GS/MS analysis of the samples taken at the distance of ~1 mm from the polymer surface were used. The main UHMWPE degradation products (propene, butadiene, benzene) were identified and the mass peak intensity profiles of the main degradation products of UHMWPE, oxygen and combustion products (H₂O, CO₂, CO) in flames with TPP additive and without it were found. In accordance with the results of temperature profile measurements, addition of TPP to UHMWPE resulted in the ~1.4-fold increase of the total width of the flame zone (from 3.7 mm to 5 mm), in the shift of the max temperature point from 1.5 mm to 2.2 mm and in the reduction of the max temperature from 1560 °C to 1280 °C. Analysis of the elution of the condensed combustion products showed the heavy organic substances with the number of carbon atoms varying from 7 to 27 and the chemical formula C₁H_{1.93} to be present in the zone of pyrolysis products of UHMWPE at the distance of ~1 mm from the

polymer surface. Oxygen in UHMWPE flame was not registered behind the glowing flame front (precision 0.3%). Adding 5% TPP resulted in the emergence of a small amount of O₂ in the max temperature point and in the emergence of new mass peaks in the flame (m/e 45, 50, 51, 65, 94), which may be related to TPP and phosphorus-containing products of its degradation. The data obtained confirm the conclusions that TPP works as flame retardant both in the gas and condensed phases. It has been shown that addition of 5% TPP leads to the increase of the width of the flame zone, reduction of the burning rate, decrease of the max temperature, and change in the composition of the products of UHMWPE degradation in flame. The method of opposed flow diffusion flames of polymers may be applied for the study of the flame retardancy mechanism.

korobein@kinetics.nsc.ru

W4P067 INVESTIGATION ON FLAMMABILITY LIMITS OF FUEL VAPORS AT ELEVATED TEMPERATURES

Marcin Grabarczyk, Rafał Porowski, Andrzej Teodorczyk, Warsaw University of Technology, Poland

To investigate the flammability limits for ethanol, methanol, 1-butanol, 2-butanol and isooctane the experimental studies were performed. The initial conditions of tested vapors were 1 atm and 40, 60 80, 100 and 1200C. Tested vapors were ignited by hot-wire which was located in the center of chamber. By means of pressure measuring system with piezoelectric PCB transducer, the pressure-time curves, which develop following the ignition, were recorded. From the pressure-time plots the maximum explosion pressure, highest rate of explosion pressure rise and flammability limits are automatically determined by dedicated software. Experimental set-up consisted of 20-litre spherical chamber resistant to high pressures (up to 25 bar) and corrosion from the combustion products, equipment for preparing a tested mixtures, an ignition system as the hot-wire method, pressure measuring system, temperature measuring system, data acquisition system and necessary safety equipment. The chamber is also equipped with heating system allowing for testing vapors up to initial temperature of 1200C. The pressure transducer is able to measure pressures up to 20 bar. Experimental data were recorded by an acquisition system with the sampling rate of 100 kHz. Temperature monitoring system included thermocouples for measuring flame temperatures in the chamber.

Tested vapors of ethanol, methanol, 1-butanol, 2-butanol and isooctane at different concentrations were introduced into the chamber and ignited. We used five values of initial temperatures for tested mixtures ranging from 40 up to 1200C. Our data acquisition system recorded a pressure profiles in time for every single shot. According to EN 1839 standard, the criterion for an explosion (self-propagating combustion) is the generation of explosion overpressure.

m.g.grabarczyk@gmail.com

W4P068 ON THE EFFECT OF HARDWOOD PALLETS ON THE FIRE GROWTH BEHAVIOR OF RACK - STORAGE FIRES - A NUMERICAL AND EXPERIMENTAL STUDY

Jaap de Vries, FM Global Research, United States

A CFD code, FireFOAM, aiming at modeling sprinkler-based fire suppression phenomena, has been developed recently based on the OpenFOAM framework. In previous model validation work, rack storage fire experiments were performed in an effort to provide validation data. To limit the amount of complexity necessary to model the experiments, these tests were “idealized” by not employing pallets. The current study advances these previous efforts by focusing on the effect of hardwood pallets on the burning behavior of industrial-sized warehouse fires. Experiments were carried out on rack storage arrays consisting of commodities made up of three nested double-wall corrugated cardboard boxes surrounding a metal liner and resting on a hardwood pallet. For comparison, tests without pallets and with “inert” (*i.e.*, steel) pallets were also performed. Calorimetry data were obtained, using a Fire Products Collector, to determine heat release rate (HRR). Modeling was also performed by proper meshing of the pallets and by implementing pyrolysis-model-effective material properties for hardwood determined in a separate study using a Fire Propagation Apparatus (FPA).

Both test video snapshots and modeled mixture fraction *iso*-contours - with and without pallets are used for comparison. Following a rapid initial vertical growth, the fire starts to spread horizontally toward the adjacent flue space and underneath the boxes. Without pallets present, the flame can ignite the bottom box surface and spread to the adjacent flue space faster. The wood pallet delays this spread process. The wood pallet has a large exposure area; once the wood pallets start to burn, the eventual fire size is larger than during the no-pallet case.

The modeled contributions from the hardwood pallets and from the corrugated cardboard boxes are compared in this study. Good agreement was observed between model and experimental results; model data indicate that the pallets account for approximately one third of the peak heat release rate.

In conclusion, both numerical simulations and experiments of freeburn fires representative of warehouse storage scenarios are presented. This study showed that the simulations, with due consideration of fuel properties and consistent

model practice, compare well with experimental data over the range of scales considered. In particular, the effect of wood pallets was successfully modeled and the results were validated by large-scale fire test data.

jaap.devries@fmglobal.com

W4P069 ASSESSING THE IGNITION OF WILDLAND FUELS EXPOSED TO TIME-VARYING HEAT FLUX PULSES

Rory Hadden¹, Claire Belcher², Guillermo Rein³

¹University of Edinburgh, Scotland ²University of Exeter, United Kingdom ³Imperial College London, United Kingdom

Ignition of forest fuels by heat fluxes pulses is a common occurrence in wildland fires. This is the scenario which occurs when fuels are subject to a heat flux from a travelling flame front. This is a significant outstanding problem in predicting wildland fire spread and transition from surface to crown fires. Furthermore, this is the real scenario that occurs in all fires during the growth phase and in travelling fires in large compartments. Despite the prevalence of these scenarios in the real world, this problem has received very little study, either experimentally or numerical, in the literature. Current ignition theory does not account for ignition under conditions of transient irradiance. Reszka et al. pioneered the ignition of common polymeric materials exposed to linearly increasing heat fluxes similar to those measured in fires in the Wildland Urban Interface and developed a model to predict ignition based on the time-integrated heat flux exposure. However there is currently no theory to account for ignition under other transient heating regimes.

The basis for the current work are the recently calculated heat flux pulses resulting from the Chicxulub asteroid impact. These are predicted to be quasi-parabolic profiles in which the heat-flux increase to a maximum before decreasing. A wide range of heat flux pulse scenarios are investigated, from short duration and high magnitude to long duration and low magnitude. The natural fuels selected for this experimental study include thin fuels (live and dead pine needles, oak leaves) and thick fuels (woody material).

Our experiments show that the heat flux required for non-piloted ignition of a material is not constant and depends, among other things, on the heating rate and the time-integrated the heat flux. We also observe that in fuels capable of smouldering, the transition from smouldering to flaming is an important mechanism leading to flaming ignition. This work challenges classical ignition theory and provides a unique set of data with application to fundamental combustion studies. It also uses established fire testing methods and techniques to answer questions in diverse research fields such as Earth Sciences.

r.hadden@ed.ac.uk

W4P070 EFFECTS OF SEASON AND HEATING MODE ON IGNITION AND BURNING BEHAVIOR OF TEN LIVE FUEL SPECIES MEASURED IN A FLAT-FLAME BURNER SYSTEM

Thomas H. Fletcher¹, Jonathan R. Gallacher¹, Victoria Lansinger¹, Sydney Hansen¹, David R. Weise²

¹Brigham Young University, United States ²USDA Forest Service, United States

The effect of season and heating mode on ignition and burning behavior of living vegetation were studied in a flat-flame burner system equipped with a radiant panel. The goal is to identify what plant characteristics have the greatest influence on burning behavior and to summarize the effects of heating mode on ignition and burning. Experiments were performed over a two-year period, with 25 runs completed for each species each month for one year. In the first year, lodgepole pine, big sagebrush and chamise were studied. Manzanita, ceanothus, douglas-fir, Gambel oak, gallberry, fetterbush, and sand pine were studied the second year. A flat flame burner (1000°C, 10 mol% O₂) and radiant panel (39-50 kW m⁻²) provide the convection and radiation sources, respectively. Moisture content (dry basis) and relative moisture content were measured for all species. Volatiles content, ash content, density and ether extractives were measured for year two species. Time-dependent mass, surface temperature and flame characteristics were measured for all species. Moisture content (dry basis) and relative moisture content were found to vary with season, species and location, with the lowest measured moisture content corresponding to the local fire season. The effect of moisture content on ignition time and temperature varied with species and location. Ignition time and temperature showed a strong dependence on heating mode for broadleaf species. Needle species (lodgepole pine, douglas-fir and sand pine) showed almost no dependence of ignition time on heating mode. Experiments with radiation as the only heat source never achieved ignition without a pilot flame. Flame characteristics were affected by heating mode and moisture content, and the dependence varied by season and species.

tom_fletcher@byu.edu

W4P071 EFFECTS OF SEASON ON IGNITION OF LIVE WILDLAND FUELS USING THE FIST APPARATUS

Sara McAllister, David Weise, USDA Forest Service, United States

The most dangerous and unpredictable wildland fires are crown fires in which the live, green foliage ignites and carries the fire. Live, green foliage also burns during prescribed fires in shrublands. Thus an understanding of what variables affect the ignition of these live fuels is crucial to predicting fire spread in living forest and shrub fuels. Of particular interest is how the flammability of these fuels changes with season. This paper presents the results of ignition tests performed over the course of an entire year for ten species known to burn as crown fires: lodgepole pine (*Pinus contorta*), big sagebrush (*Artemisia tridentata*), chamise (*Adenostoma fasciculatum*), Douglas-fir (*Pseudotsuga menziesii*), manzanita (*Arctostaphylos glandulosa*), ceanothus (*Ceanothus crassifolius*), gambel oak (*Quercus gambelii*), gallberry (*Ilex glabra*), fetterbush (*Lyonia lucida*), and sand pine (*Pinus clausa*). The ignition delay and the mass loss rate at ignition were measured using the FIST apparatus with a radiant heat flux of 50 kW/m² and flow velocity of 1 m/s. The fuel moisture content was also measured. Contrary to dead fuel results, the ignition time of the lodgepole pine, chamise, manzanita, gambel oak, fetterbush, gallberry, and sand pine were not correlated at all to the moisture content. In fact, the ignition times of the gallberry and fetterbush were slightly negatively correlated to the moisture content. The mass loss rate at ignition was somewhat positively correlated to the moisture content for some species (chamise, manzanita, gambel oak, fetterbush, and sand pine), not correlated at all for some (sagebrush, ceanothus, and gallberry), and somewhat negatively for others (lodgepole pine and Douglas-fir). The trends in the mass loss rate at ignition with ignition time were also very inconsistent between species with some negatively correlated (lodgepole pine, Douglas-fir, manzanita, ceanothus, fetterbush, gallberry) and others not at all (chamise, sagebrush, gambel oak, and sand pine). Wet wood, on the other hand, shows a positive correlation between the mass loss rate at ignition and the ignition time. Clearly, the trends in ignition are species dependent and may not follow the expected trends based on dead fuels.

smcallister@fs.fed.us

W4P072 MODELING OF SPOT-FIRE IGNITION OF NATURAL FUEL BEDS BY HOT PARTICLES

Casey Zak¹, James Urban¹, Mario Sanchez-Sanz², Carlos Fernandez-Pello¹

¹University of California, United States ²Universidad de Carlos III de Madrid, Spain

Ignition of natural fuels by hot particles is an important cause of wildland spot fires, resulting in approximately 28,000 fires annually. These hot particles include (but are not limited to): sparks produced by power line interaction, welding and grinding slag, bullet fragments, and embers produced by pre-existing fires. Despite causing numerous fires, only a small number of studies have focused on this interesting ignition phenomenon, generally from an experimental perspective.

In this work, the simplified case of a hot solid sphere partially submerged in a combustible solid is modeled to determine the particle characteristics (size, temperature, composition) necessary for flaming ignition. The non-dimensionalized governing equations are solved numerically in two dimensions for the solid fuel, the hot particle and the surrounding gas phase. A finite element method solver and implicit Euler approximation in time are used to find the spatial and temporal distribution of temperature, species and gas phase velocity. The pyrolysis of the solid phase is assumed to be ablative (i.e. no char formation) and modeled with a one-step global reaction. Similarly, the gas phase chemistry is treated with a single reaction step. The model is used to investigate the dominant physical processes for the specific case of a steel sphere landing in a cellulose fuel bed. Comparisons are made to relevant experimental results.

czak@berkeley.edu

W4P073 IGNITION BEHAVIOR OF PMMA PYROLYSIS GAS BY LASER-INDUCED BREAKDOWN SPARKS

Yoshinari Kobayashi, Rihito Takimoto, Shinji Nakaya, Mitsuhiro Tsue, The University of Tokyo, Japan

Fifteen years have passed since the operation of International Space Station (ISS) began. It is possible that manned space activities will be extended for a long period of time from now on. In that case, the important issue is the safety of all crews. The fire safety in a spacecraft is especially important, therefore the further improvement of it is required. For that purpose, combustion phenomenon and mechanism should be revealed. In present study, ignition phenomena is investigated. PolyMethyl-MethAcrylate (PMMA) is used as a test sample due to the wide use of PMMA for products for general consumers, buildings, industrial products, etc. PMMA is a flammable material, therefore it is required to understand its flammability for the damage control and the appropriate fire-extinguishing methods in the case of a fire. In order to investigate the ignition characteristics, Laser-induced Breakdown Sparks which is one of the promising methods that ensure the high ignition performance is used as an ignition method. Laser-induced Breakdown Sparks can ignite even lean mixtures certainly due to high energy density plasma at a focus through a convex lens. Also a setup of an optical system allows any ignition position to be selected and mixtures to be ignited in the center of a combustion bomb, therefore the thermal loss to the solid surface could be reduced. The objective of present study is to investigate an ignition behavior of PMMA pyrolysis gas by Laser-induced Breakdown Sparks at varied equivalence ratio and varied pressure. The mixtures are ignited in a constant volume combustion bomb. The ignition energy is measured by an energy detector and the behavior is observed by

schlieren photography using a high speed video camera. The influence of equivalence ratio and pressure on the ignition behavior of PMMA pyrolysis gas is clarified.

9353729227@mail.ecc.u-tokyo.ac.jp

W4P074 SMOULDERING COMBUSTION CHARACTERISTICS OF PHASE CHANGE MATERIALS WHEN EXPOSED TO RADIANT HEAT FLUX

Martyn McLaggan¹, Rory Hadden¹, Martin Gillie²

¹University of Edinburgh, United Kingdom ²University of Manchester, United Kingdom

Buildings in recent times increasingly include innovative construction materials. The combustion behaviour of these materials is typically poorly understood and can often be complex. One example is a group of energy saving additives known as Phase Change Materials (PCMs). These are designed to reduce the heating and cooling demand in a building by storing energy during the day and releasing it again at night. These materials have a high latent heat of fusion and a melting point which matches the intended indoor temperature within a building. This allows them to melt and absorb energy during the day, then re-solidify and release the stored energy at night. For these reasons, paraffin wax is commonly used. However, the effect on the combustion behaviour caused by its addition to a parent material has not been evaluated. This project aims to investigate the combustion characteristics of a composite paraffin wax material in a novel construction material, hempcrete, when exposed to a radiant heat flux.

Hempcrete is a porous material that has been synthesised using hemp shivs and fibres, and cement. It is typically used as an insulation material or wall lining. The porous nature of the fuel means that smouldering is the dominant mode of combustions. A microencapsulated PCM additive containing a blend of paraffin waxes can be added to the hempcrete matrix. Batches of 100mm cubes are cast with and without the PCM, and left to cure for more than 30 days. These materials are then tested under the same conditions and a comparison of the combustion behaviour between the two is made in order to ascertain the effect of adding PCMs. The materials are tested in the cone calorimeter¹ in the horizontal orientation. The sample is open to natural air flow from below, and is exposed to a constant radiant heat flux above from the cone heater. This project will discuss and characterise the smoulder scenario and the effect of PCM on ignition, spread rate and emissions. The addition of PCMs is found to cause rapid ignition and lower the critical heat flux to 3 kW.m⁻², down from 6 kW.m⁻² in the non-PCM case. PCMs are observed to increase the mass loss rate compared to non-PCM material. It is hypothesised that this is due to the higher effective heat of combustion of the PCM, as well as the additional fuel loading that it provides. This increases the amount of heat produced causing higher temperatures and increasing the rate of reactions. As a result, the CO and CO₂ fluxes and yields are also higher. By evaluating the combustion characteristics and ignition behaviour of PCMs in a real building material, a combustion framework can be developed that allows understanding of how the material would behave in a range of conditions, thereby allowing their safe usage in buildings.

mmclaggan@gmail.com

W4P076 SOOT PRODUCTION AND TEMPERATURE MEASUREMENTS IN CANDLE FLAMES

Maria Thomsen¹, Andres Fuentes¹, Pedro Reszka¹, Rodrigo Demarco¹, Jean-Louis Consalvi²

¹Universidad Tecnica Federico Santa Maria, Chile ²Aix Marseille Universite, France

An experimental study was carried out in order to analyze the influence of wick dimensions on the burning rate, flame geometry, soot production processes and temperature in candle flames. Measurements on laminar steady flames were carried out using candles with wick diameters of 2, 3 and 4 mm. Wick length was varied between 4 and 10 mm. The shape of the candle flame was obtained from CH* spontaneous emissions after the application of Ko's segmentation process. Measured flame heights showed an increase with wick dimensions, approaching an asymptotic value for increasing wick lengths. Soot volume fractions were obtained from laser extinction measurements with modulated absorption/emission.

A deconvolution technique and a regularization procedure were applied to the data. Radial profiles of soot volume fractions increase when varying the wick dimensions; this effect is produced by the greater amount of fuel released by the wick. Radially integrated soot volume fractions were also calculated, presenting a similar behaviour to the soot volume fraction radial profiles. A peak of the integrated soot volume fraction was found for each of the flames studied. The peak value was found at approximately half the flame height, independent of the wick dimensions and burning rates. Soot temperature was obtained from emission measurements at two different wavelengths considering the attenuation of the soot particles in the optical path length. An original deconvolution and regularization procedure was carried out in order to obtain temperature profiles for different heights in the flame. The increase locally observed in soot production and soot temperature profiles was directly related to the higher burning rate experimented by the candle. The results showed that peak integrated soot volume fractions are proportional to both the mass loss rates and the flame heights.

mari.thomsen@gmail.com

W4P077 BEHAVIOUR OF AERONAUTICAL COMPOSITE MATERIALS SUBMITTED TO SEVERE FIRE CONDITIONS

Sachin Dahikar, Jean-Michel Most, Institut Pprime, CNRS- France

For 20 years, the fire threat in aeronautics has been drastically reduced, but fire safety aboard aircrafts stays one of the main preoccupations of aircraft manufacturers and airlines companies. To get the flight agreement of the aeronautic authorities, the fuselage skin must be a safe barrier to protect the cabin and its occupants from an external fire up to safe landing and evacuation. In new generation of aircrafts (A350 and B787 families) the massive use of flammable composites, substituting metallic structural and fuselage elements, changes the understanding of the fire risk and can modify the fire safety approach for passenger and crew survivability. An original device was realized to characterise the flammability and burning properties of aeronautical thermoset composite (epoxy resin/Carbon fibres). It mimics, at laboratory scale, the standard burnthrough test used to qualify the fire performances of materials. The set-up consists of the stabilisation of a combustion product jet from a premixed burner impinging a composite sample of $0.05 \times 0.05 \text{ m}^2$, the total heat flux at the material surface is in the range 70 to 200 kW/m^2 and gas jet temperature around 1200°C . Before the test sets, the flow field is determined by PIV measurements and the heat fluxes at the sample front side are calibrated with a radiometer in function of the burner working conditions. During the test, the mass loss rate and the temperatures at each side of the sample are continuously measured. The data processing provides the main characteristics of the flammability and burning properties of the composites: the burnthrough time (time for the flame to penetrate the sample), the pyrolysis time (time for the composite degradation beginning), Mass Loss Rate (MLR) with the position and intensity of its maximum, the temperature evolutions at the composite front side and backsides.

The main results show that a 0.002 m thick composite is not burnthrough in 15 minutes under thermal conditions representative of engine (106 kW/m^2) and post-crash fires (182 kW/m^2) while an equivalent thickness aluminium panel (conventional aircraft) is drilled in around 80s. Consequently, composites are very efficient barrier to fire penetration in the aircraft cabin. Results provide the MLR and temperature evolution of several composites for various incident heat fluxes, ambient pressure, oxygen concentration at the surface, sample thickness and flow stretching. The composite fire behaviour is discussed. To conclude, due to their good fire performances, composites provide an efficient barrier to fire, but off gassing at the backside can potentially emit toxic and flammable composite degradation products in the cabin before the total evacuation of the aircraft during a post-crash fire without the breaking of the fuselage.

jean-michel.most@ensma.fr

W4P078 CHANGE IN THE EXTINCTION LIMIT OF ELECTROLYTE FOR LI-ION BATTERIES BY ADDITION OF PHOSPHORUS BASED FLAME RETARDANT

Masaya Inatsuk¹, Osamu Fujita¹, Katsunori Nishimura²

¹Hokkaido University, Japan ²Hitachi, Ltd, Japan

Lithium Ion Batteries (LIB) often uses Ethyl Methyl Carbonate (EMC) as a main component of electrolyte, which is flammable organic carbonate solvent. Therefore, fundamental information on EMC flammability with fire retardant would be important for improvement of fire safety of LIB. In the present study, the effect of Organophosphorus Compounds (OPC), which is known as a fire suppressant, on the flammability of EMC has been studied. Especially, relationship between the amount of OPC addition and extinction limit (=Limit of Oxygen Concentration: LOC) of EMC has been investigated experimentally.

In this study, we have been used EMC for “fuel” and Trimethyl Phosphate (TMP: $(\text{CH}_3\text{O})^3\text{P}=\text{O}$) and Triethyl Phosphate (TEP: $(\text{CH}_3\text{CH}_2\text{O})^3\text{P}=\text{O}$) for “fire retardant solvent” for the experiment. Three kinds of mixture fuel: only EMC, EMC+5wt% OPC and EMC+10wt% OPC are tested with wick combustion method to evaluate extinction phenomena of organic solvents mixture. In the experiments fuel rate is kept constant. The co-axial flow around wick flame is composed of nitrogen and oxygen. Oxygen concentration and flow velocity can be controlled by mass flow rate of nitrogen and oxygen. The diameter of wick, inner diameter of wick supporter and combustion duct are 4.0 mm , 6.0 mm and 80.0 mm , respectively. The wick height is 7.0 mm and allowed $\pm 0.5 \text{ mm}$ error. We determined the LOC according to video image and used spectrometer for flame emission intensity measurement. The view area of spectrum analyzer is a circle of 15.8 mm in diameter by spread angle fiber cable has.

LOC was determined by experiments and we found TMP's retardant effect becomes higher than TEP at the same addition amount, on the other hand the trend of LOC regarding to flow velocity doesn't change not so much. Furthermore, the difference of LOC between additive-free and 5wt% addition condition is very large but that between 5 and 10wt% addition condition is not so large. In addition, the light emission intensities of OH and CH radical's band spectrum around the flame are reduced by OPC addition (5wt% OPC condition). Furthermore, additional OPC condition (10wt% OPC condition) brings slight decrease of light emission of OH or CH radical.

In the previous experiments, we found that TMP addition increases flame temperature. Considering the results described above, there exists two opposite phenomena in terms of LOC decision on the effect of OPC: chemical retardant effect by radical trap and physical promotion effect by temperature increase. Firstly, Under 5wt% OPC condition, almost all of OPC can react with fuel radical and generate stable species like shown below circulated reactions: $\text{PO}_2 + \text{H} \rightarrow \text{HOPO}$ and $\text{HOPO} + \text{OH} \rightarrow \text{PO}_2 + \text{H}_2\text{O}$, then retardant effect prominently appear. Therefore, many OH radical captured by OPC addition then LOC much increased. Under 10wt% OPC condition, however, further added OPC (another 5wt%) is not effective to capture H or OH radical because almost all of them in flame are already reacted with first 5wt% OPC addition. Furthermore, increasing of flame temperature may decrease of LOC. Secondly, the difference of LOC between TMP and TEP are caused by chemical structure. TEP has much C than TMP so the amount of hydrocarbon species and radicals in reaction area under TEP condition increase than TMP. Therefore, LOC on TEP become lower than TMP by additional reactant. Lithium Ion Batteries (LIB) often uses Ethyl Methyl Carbonate (EMC) as a main component of electrolyte, which is flammable organic carbonate solvent. Therefore, fundamental information on EMC flammability with fire retardant would be important for improvement of fire safety of LIB. In the present study, the effect of Organophosphorus Compounds (OPC), which is known as a fire suppressant, on the flammability of EMC has been studied. Especially, relationship between the amount of OPC addition and extinction limit (=Limit of Oxygen Concentration: LOC) of EMC has been investigated experimentally.

ina-masa@mech-hm.eng.hokudai.ac.jp

W4P079 LARGE-SCALE SPACECRAFT FIRE SAFETY TESTS

David Urban¹, Gary Ruff¹, Paul Ferkul¹, Grunde Jomaas², James S. T'ien³, Carlos Fernandez-Pello⁴, Jose Torero⁵, Guillaume Legros⁶, Christian Eigenbrod⁷, Sandra Olson¹, Nikolai Smirnov⁸, Osamu Fujita⁹, Adam Cowlard¹⁰, Sebastian Rouvreau¹¹, Balazs Toth¹², . Olivier Minster¹²

¹NASA Glenn Research Center, United States ²Technical University of Denmark, Germany ³Case Western Reserve University, United States ⁴University of California, United States ⁵University of Queensland, Brisbane, Australia ⁶Université Pierre et Marie Curie France ⁷University of Bremen, Germany ⁸Moscow State University, Russia ⁹Hokkaido University, Japan ¹⁰University of Edinburgh, United Kingdom ¹¹Belisama R&D, Toulouse, France ¹²ESA ESTEC, Netherlands

An international collaborative program is underway to address open issues in spacecraft fire safety. Because of limited access to long-term low-gravity conditions and the small volume generally allotted for these experiments, there have been relatively few experiments that directly study spacecraft fire safety under low-gravity conditions. Furthermore, none of these experiments have studied sample sizes and environment conditions typical of those expected in a spacecraft fire. The major constraint has been the size of the sample, with prior experiments limited to samples of the order of 10 cm in length and width or smaller. This lack of experimental data forces spacecraft designers to base their designs and safety precautions on 1-g understanding of flame spread, fire detection, and suppression. However, low-gravity combustion research has demonstrated substantial differences in flame behavior in low-gravity. This, combined with the differences caused by the confined spacecraft environment, necessitates practical scale spacecraft fire safety research to mitigate risks for future space missions. To address this issue, a large-scale spacecraft fire experiment is under development by NASA and an international team of investigators. This poster presents the objectives, status, and concept of this collaborative international project (Saffire). The project plan is to conduct fire safety experiments on three sequential flights of an unmanned ISS re-supply spacecraft (the Orbital Cygnus vehicle) after they have completed their delivery of cargo to the ISS and have begun their return journeys to earth. On two flights (Saffire-1 and Saffire-3), the experiment will consist of a flame spread test involving a meter-scale sample ignited in the pressurized volume of the spacecraft and allowed to burn to completion while measurements are made. On one of the flights (Saffire-2), 9 smaller (5 x 30 cm) samples will be tested to evaluate NASA's material flammability screening tests. The first flight (Saffire-1) is scheduled for July 2015 with the other two following at six-month intervals. A computer modeling effort will complement the experimental effort. Although the experiment will need to meet rigorous safety requirements to ensure the carrier vehicle does not sustain damage, the absence of a crew removes the need for strict containment of combustion products. This will facilitate the first examination of fire behavior on a scale that is relevant to spacecraft fire safety and will provide unique data for fire model validation.

david.urban@nasa.gov

W4P080 A BURNING RATE EMULATOR FOR MICROGRAVITY STUDIES

James G. Quintiere
University of Maryland, United States

A gas-fueled burner with heat flux gages embedded in its porous surface is used to emulate condensed-phase fuel flames. Measurement of the heat flux, the flow rate of the fuel/inert mixture, and the burner surface temperature allows analysis of the burning characteristics of condensed fuels. The burner is named the Burning Rate Emulator (BRE). It can burn a gaseous fuel at an effective heat of gasification matching the actual heat of gasification of condensed-phase fuels. It

also can match other characteristics of the condensed-phase fuel by careful selection of certain properties of the gaseous fuel. These properties are the heat of combustion, the effective heat of gasification, the surface temperature, and the laminar smoke point. In normal gravity, the BRE is shown to reasonably emulate steady burning of methanol, heptane, polyoxymethylene and polymethylmethacrylate burning in a 50 mm diameter pool configuration. It also can be used to emulate ignition and extinction. The results can be used to predict behavior at other conditions, such as burning with external radiant heating.

The original burner has been redesigned to allow the top plate to act as a calorimeter. Two burners at 25 and 50 mm diameter have been built and are being tested. Two tiny thermopile sensors, without water cooling, are used to measure the local heat flux to each burner. Those measurements are supplemented by the average heat flux determined from the top plate calorimeter. Analyses have been made to correct the sensors for temperature and blowing effects, and tests were conducted to determine the needed emissivity and absorptivity of the plate and sensor painted surfaces.[SDP(1)] The BRE can be extended to emulate burning under diverse conditions. The utility of the BRE has been demonstrated for normal gravity conditions, but it should be able to identify which condensed-phase fuels can burn in microgravity. Therefore, the BRE experiment is in development for future conduct on the International Space Station. Preliminary test results from NASA's 2.2 and 5.18 s drop facilities suggest that quasi-steady microgravity flames may be possible with ethylene. Recent tests with methane in the 5.18 s facility have shown bubble-like flames with apparent extinction over a portion of the flame sheet. The early migration of soot to the flame sheet coincides with this extinction process.

jimq@umd.edu

W4P081 POLYMETHYLMETHACRYLATE COMBUSTION IN A SIMULATED MICROGRAVITY ENVIRONMENT
Garrett Bornand, Fletcher J. Miller, Gregory Sullivan, San Diego State University, United States

Flame spread tests were conducted with thermally thick and thermally thin Polymethylmethacrylate (PMMA) samples to study flame spread behavior in response to environmental changes. The tests were conducted using the San Diego State University Narrow Channel Apparatus (SDSU NCA). The SDSU NCA can suppress buoyant flow in horizontally spreading flames, and is currently being investigated as a possible replacement or complement to NASA's current material flammability test standard for non-metallic solids, NASA-STD-(I)-6001B Test 1. The buoyant suppression attained in the NCA allows tests to be conducted in a simulated microgravity environment-a characteristic that NASA's Test 1 lacks since flames present in Test 1 are driven by buoyant flows. The SDSU NCA allows for tests to be conducted at various opposed flow oxidizer velocities, oxygen percent by volume, and total pressure to mimic various spacecraft and habitat atmospheres. Tests were conducted at 1 atm. pressure, thin fuel thickness of 50 and 75 microns, thick fuel thickness ranging from 1 mm to 5.6 mm, opposed oxidizer velocities ranging from 10 to 25 cm/s, and oxygen concentration by volume at 21, 30, and 50 percent. The results were then compared to true microgravity experiments including; testing conducted on the International Space Station (ISS) under the Burning and Suppression of Solids (BASS) research, NASA's 5.2 second Drop Tower, and Micro-Gravity Laboratory's (MGLAB) 4.5 second Drop Tower. Data was also compared to results found by Michigan State University's NCA. Carbon dioxide, carbon monoxide, and oxygen concentrations were studied under various test conditions. Carbon monoxide levels were found to be significantly higher than expected, leading to lower carbon dioxide concentrations.

garrett.bornand@gmail.com

W4P082 SIMULATING SPRAY-PLUME INTERACTION IN A FIRE ENVIRONMENT
Karl Meredith, Xiangyang Zhou, FM Global Research, United States

Recently, fire suppression modeling has made significant progress in the areas of pyrolysis, radiation, the interaction of water with solid-fuel surfaces, and large-scale suppression modeling. The controlling mechanism for sprinkler-based fire suppression has been identified as a surface-cooling phenomenon. Thus, determination of the amount of water able to penetrate through the fire plume and reach the burning surfaces is paramount. Therefore, in-depth research is needed in the area of spray injection modeling and the interaction of spray with fire-generated plumes. The interaction of water spray and fire plume has been studied experimentally in large-scale scenarios and most recently in reduced-scale experiments. The reduced-scale experiments are able to provide detailed characterization of momentum flux for both the spray and the plume using a well-defined spray injection and a well-characterized hot plume. The current study demonstrates recent progress in numerical simulations of spray-plume interaction. Given the initial injection pattern of the spray, the momentum flux of both the spray and hot plume are simulated using FireFOAM. Simulations are performed for three regimes of spray-plume interaction, namely spray momentum flux less than, equal to, and greater than the plume momentum flux. Submodels used in the inter-phase exchange source terms for mass, momentum, and energy transfer are evaluated. Sensitivity of the results

to the model input parameters is demonstrated. Such validation provides the groundwork for larger-scale spray-plume validation and eventual improved full-scale fire suppression predictions.

karl.meredith@fmglobal.com

W4P083 EFFECTS OF CONVECTION ON COMBUSTION BEHAVIOR OF METHANE HYDRATE

Genichiro Kushida, Kento Sakata, Aichi Institute of Technology, Japan

It is necessary to elucidate the methane hydrate combustion mechanism for the fire safety during transportation and storage, in order to utilize natural methane hydrate as a new alternative energy or to put NGH transportation in practical use. Methane hydrate has different combustion characteristics from common solid fuels for the peculiar characters such as the intense thermal decomposition in room temperature or the so-called self-preservation effect. Especially in the flame spread process of methane hydrate, the thermal decomposition before ignition is an important factor, and the combustion characteristics after ignition are strongly affected by the time history of thermal decomposition before ignition. Therefore, the heat and mass transfer by convection plays an important role in combustion behavior of methane hydrate.

In the present study, the ignition of methane hydrate and the subsequent flame spread are investigated in detail by combustion experiments in a wind tunnel, and the effects of convection on combustion behavior of methane hydrate are elucidated.

The methane hydrate temperature before ignition increases by the forced convection. It is due to the high heat transfer coefficient enhanced by forced convection, since the temperature increases with the increase in wind velocity. When the thermal decomposition time before ignition becomes longer under the natural convection in the quiescent ambient air, a flammable premixed fuel gas is formed near the methane hydrate surface, and the premixed-like flame propagation occurs, where the flame speed is so much faster compared to the common flame spread rate. In the case of ignition from upstream under the forced convection, the premixed-like flame propagation in the opposite direction of flame spread is sometimes observed as well as the common flame spread. However, the premixed-like flame propagation in the direction of flame spread is not observed. It is because the oxygen concentration becomes low by the downstream flow of the combustion products, and the flammable premixed fuel gas is hardly formed since the methane gas evolved by decomposition is carried downstream away. On the other hand, the flame propagation in the opposite direction of flame spread under the forced convection is brought by the oxygen supply from upstream. Thus, it is made clear that the effects of thermal decomposition before ignition play an important role in the flame spread over methane hydrate, and the heat and mass transfer by convection is very important in the combustion behavior of methane hydrate.

kushida@aitech.ac.jp

W4P085 TRANSPORT AND CONCENTRATIONS OF EMISSIONS IN A RESIDENCE FROM A COOKSTOVE

Jennifer Jones, Daniel Murphy, Carlos Fernandez-Pello, University of California, United States

Most of the world uses cookstoves powered by the combustion of biomass fuels for residential cooking or heating, or liquid fuels such as kerosene for cooking or lighting. Emissions from residential fuels in industrializing countries create a major health concern for individual families, and in aggregate, have a significant effect on global warming and public health. Many cookstove programs exist to enable the global adoption of cleaner cookstoves. Individual programs focus on technological innovation, public policy, market economics, public health, or regional, participatory, community development programs. However there is little cross pollination between engineers, social scientists, public health researchers, and medical practitioners.

This research looks at the transport of emissions within a room from a residential stove used in industrializing countries. A smaller scale model of a room was built based on actual room dimensions and stove firepower. Room dimensions were a quarter scale of full-size. Gas temperature, carbon monoxide, particulate matter, and carbon dioxide were measured. The plume and naturally-convected flow driven by a kerosene fire in the room was visualized using Particle Image Velocimetry (PIV) for different room ventilation conditions.

In addition to the experimental work, a numerical model of the flow in the room was created using the Fire Dynamics Simulator (FDS) code. The model output was compared to experimental data to validate model results. Additionally, public health methodology for determining personal exposure by measuring indoor air pollution at a single point source is assessed using the numerical model.

jennifer.jones@berkeley.edu

W4P086 TOWARDS PREDICTIVE SCENARIO OF METHANE AND COAL DUST EXPLOSION IN A MINING ACCIDENT

V'yacheslav Akkerman¹, Ali S. Rangwala², Vitaly Bychkov³

¹West Virginia University, United States, ²Worcester Polytechnic Institute, United States, ³Umea University, Sweden

Recent fundamental computational and analytical studies of flame acceleration in combustion tubes have revealed several competitive mechanisms of a Deflagration-to-Detonation Transition (DDT) event. In particular, it has been shown that the DDT scenario incorporates several distinctive stages, with conceptually different combustion characteristics in each of the stages. Our long-term strategy is to extend this fundamental research to practical applications. Illustrative examples of such an extension are fire safety issues in subways and mine tunnels. Consequently, in this project we employ this fundamental formulation to scrutinize the evolution and key stages of methane and coal dust explosions in a mining accident. Specifically, we identify the key characteristics of these stages, aiming to predict the timing for each stage, the speed of flame spreading, as well as the expected pressure rise.

The stages of the flame evolution include:

- 1) Initial quasi-spherical expansion of a centrally-ignited, embryonic flame, with the possibility of self-similar acceleration due to the hydrodynamic (Darrieus-Landau; DL) instability;
- 2) Intermediate, so-called "finger-flame" acceleration; and
- 3) Major, large-scale-based acceleration due to wall friction and/or in-built obstacles/roughness.

The input parameters for the formulation are (i) the unstretched laminar flame speed; (ii) the thermal expansion factor (coupled to the equivalence ratio); and (iii) and transport coefficients of air/methane/dust mixture. Another set of input parameters is coupled to the size and configuration a mining passage. It is emphasized that the fundamental formulation on flame acceleration in tubes is conceptually laminar, with turbulence playing only a supplementary role. In contrast, imposed or self-generated turbulence is a key factor in the practical reality. For this reason, the formulation above is next combined with the fundamental study, theoretical and experimental, of homogenous-gaseous and particle-gas-air combustion in turbulent environment. Specifically, the analytical studies of premixed turbulent flame velocity, namely, the renormalization approach and the spectral formulation are reconciled, validated by the Hybrid-Flame Analyzer experiments on turbulent methane-air burning, and subsequently incorporated into the generalized formulation. Both the homogenous gaseous premixtures as well as the particle-gas-air systems containing coal-duct impurities are investigated. The turbulent flame velocity is tabulated as a function of various flame parameters (such as the laminar flame speed, thermal expansion coefficient, etc.) and flow parameters (such as the turbulent intensity, integral and Kolmogorov length scales, etc.), as well as a function of the sizes and concentrations of the impurity particles. Specifically, it is shown that the particles typically intensify turbulent combustion. The formulation accounts for the flame-flow feedback due to thermal expansion as well as turbulence coupling to the intrinsic combustion instabilities. It is eventually demonstrated how multi-phase impurities and turbulence-instability interaction modify the conventional turbulent combustion regimes diagram.

Vyacheslav.Akkerman@mail.wvu.edu

W4P087 COMPUTATIONAL MODELING OF POLYMETHYLMETHACRYLATE COMBUSTION IN A NARROW CHANNEL APPARATUS

Garrett Bornand, Fletcher J. Miller, San Diego State University, United States

Flame spread tests were conducted with thermally thick and thermally thin Polymethylmethacrylate (PMMA) samples to study flame spread behavior in response to environmental changes. The tests were conducted using the San Diego State University Narrow Channel Apparatus (SDSU NCA). The SDSU NCA can suppress buoyant flow in horizontally spreading flames, and is currently being investigated as a possible replacement or complement to NASA's current material flammability test standard for non-metallic solids, NASA-STD-(I)-6001B Test 1. The buoyant suppression attained in the NCA allows tests to be conducted in a simulated microgravity environment—a characteristic that NASA's Test 1 lacks since flames present in Test 1 are driven by buoyant flows. The SDSU NCA allows for tests to be conducted at various opposed flow oxidizer velocities, oxygen percent by volume, and total pressure to mimic various spacecraft and habitat atmospheres. Fire Dynamics Simulator (FDS) was used to model the combustion of PMMA within the SDSU NCA. This article presents computational modeling results for 5.588 mm (thermally thick) and 75 micron (thermally thin) PMMA at varied pressure, oxygen concentration by volume, and opposed oxidizer velocities. With gravity removed from the model a comparison can be made to show how well the SDSU NCA simulates microgravity conditions. Computational results are compared to experimental results from SDSU, Michigan State University's NCA, and true microgravity experiments including; testing conducted on the International Space Station (ISS) under the Burning and Suppression of Solids (BASS) research, NASA's 5.2 second Drop Tower, and Micro-Gravity Laboratory's (MGLAB) 4.5 second Drop Tower.

garrett.bornand@gmail.com

W4P089 COMBUSTION SYNTHESIS OF GRAPHENE FILMS

Nikolay Prikhodko, Zulkhair Mansurov, Bakhytzhany Lesbayev, Moldir Auyelkhankey, Moldir Auyelkhankey

Graphene has some unique properties: such as high carrier mobility, high electrical and thermal conductivity and mechanical strength. A promising method of producing graphene layers is the method of synthesis of graphene in flame. The studies carried out under atmospheric conditions confirm that the process of obtaining graphene in a flame can compete with other methods, as it is continuous, rapid and inexpensive. The results of the study on the formation of graphene layers in the premixed propane-oxygen or butane-oxygen flame on a nickel substrate at atmospheric and low pressure are presented. The synthesis of graphene layers was performed in premixed propane-oxygen or butane-oxygen flame on a nickel substrate, with the addition of argon at atmospheric pressure in the range of ratios $C/O = 0.75-1.05$. Argon was supplied with a flow rate of $150-500 \text{ cm}^3/\text{min}$. The residence time of the plate in the flame was $0.5-5 \text{ min}$. The temperature in the synthesis zone of graphene layers maintained in the range of $900-950 \text{ }^\circ\text{C}$. The of adding benzene to the butane/oxygen flame on the formation of graphene films was studied at a pressure of $40-100 \text{ Torr}$. The experiments were performed in the following conditions: butane flow rate of $450 \text{ cm}^3/\text{min}$, oxygen flow rate of $740 \text{ cm}^3/\text{min}$ and benzene flow rate of $70-120 \text{ cm}^3/\text{min}$ corresponding to the C/O ratio = $0.8-0.9$. The residence time of the plate in the flame was $0.5-3 \text{ min}$. Samples of carbon structures synthesized on nickel catalytic substrates was investigated on the Raman spectrometer (NTEGRA Spectra Raman, $\lambda = 473 \text{ nm}$), optical (DFC 490), atomic force (NTEGRA Force Microscope) and scanning (Quanta 3D200i) microscopes. It is established at the atmospheric pressure that formation of graphene layers occurs in propane– oxygen and butane – oxygen flames in the ratios $C/O=0.75-1.05$. In these conditions 3-10 layers of graphene are formed. The increasing C/O ratio leads to an increase of the degree of disorder of the graphene layers, which is characterized by an increase in D peak intensity. It is established, that for the formation of graphene layers at the atmospheric pressure, the optimal experimental conditions are the ratio $C/O = 0.85-0.9$ and argon flow rate of $150-250 \text{ cm}^3/\text{min}$. Graphene sheets with 1-3 layers are mainly formed in the range of $40-100 \text{ Torr}$ on a nickel substrate in butane-oxygen flame with the addition of benzene.

nik99951@mail.ru

W4P090 STUDY OF THE EVOLUTION OF SOOT PARTICLE SIZE DISTRIBUTIONS IN PREMIXED ISO-OCTANE/ETHANOL FLAMES

Isabel Frenzel¹, Steffen Salenbauch¹, Christian Hasse¹, Dimosthenis Trimis²

¹TU Bergakademie Freiberg, Germany ²Karlsruhe Institute of Technology, Germany

The legislation for soot particle emissions has become stricter by limiting not only the mass but also the total number of particles. At the same time the use of biofuels in gasoline engines is of increasing importance to reduce the CO_2 emissions from vehicles. Since the combustion of biofuels leads to different soot emissions compared to classical gasoline, the long term scope of this study is the investigation of the underlying physical and chemical phenomena leading to these differences. For spark-ignition engines renewable bio-ethanol is mainly used for blends and different blends of bio-ethanol and conventional fossil fuels having mixing ratios in the range from E_5 to E_{85} are available for commercial automotive applications. Therefore the emphasis of this work is to study the soot formation in the combustion process of various *iso*-octane/ethanol blends and to analyze the influence of ethanol addition in detail. Soot Particle Size Distributions (SPSDs) are measured at different heights above the burner in selected fuel-rich atmospheric pressure laminar premixed *iso*-octane and ethanol-flames, as well as in *iso*-octane/ethanol blends E_{20} , E_{40} and E_{85} flames. The utilized experimental setup consists of a McKenna burner with *in situ* probe sampling and a suitable gas conditioning system for online analysis with a Scanning Mobility Particle Sizer (SMPS TSI Model 3936). The equivalence ratio varied in the range from $\phi = 2.0$ to 2.5 , the cold gas velocity was fixed at 5 cm/s (at 273 K and 1 bar) and the fuel/oxidizer mixture was preheated at 363 K for all flames.

The results show that the sooting limit, in terms of the equivalence ratio, increases when the amount of ethanol in the fuel is higher and, in general, ethanol addition reduces the soot formation. When comparing the soot particle size distributions of *iso*-octane, ethanol and the investigated blends for the same flame conditions, it can be observed that especially the process of soot particle nucleation in the lower heights of the flame is influenced by the positive effect of the addition of the oxygenated fuel. This and further effects are presented and discussed in this work in progress poster based on axial temperature profiles and soot particle size distributions for different flame heights.

Isabel.Frenzel@iwtt.tu-freiberg.de

W4P091 SOOT SIZE IN ELEVATED PRESSURE DIFFUSION FLAMES

Scott Steinmetz¹, William Roberts¹, Nick Eaves², Seth Dworkin³, Murray Thomson², Tiegang Fang⁴

¹King Abdullah University of Science and Technology, Saudi Arabia ²University of Toronto, Canada

³Ryerson University, Canada ⁴North Carolina State University, United States

Many power producing devices operate at elevated pressures, which makes studying the effect of pressure on soot formation processes critical to understanding these processes. High pressure studies are often conducted in laminar diffusion flames, and while the amount of high pressure diffusion flame data is growing, there is still a significant lack of morphological information available. In this work, a combined numerical and experimental study of nitrogen-diluted ethylene-air diffusion flames from 4 to 16 atm was carried out to determine and understand the effect of pressure on soot particle size. Detailed numerical calculations were performed considering the fully coupled elliptic set of governing equations, including a sectional model tracking particle size and number density (with an assumed fractal dimension of $D_f = 1.8$). Experimental measurements were taken through a line of sight attenuation and elastic scattering technique. Simulation results were validated by comparison with measured soot volume fraction and particle size distribution moment ratio determined from Rayleigh scattering theory analysis. The simulations accurately predict the increase in soot volume fraction currently and previously observed at elevated pressures. The model predicts an increase in overall soot particle size through an increase in the number of primary particles per aggregate. This increase is due to the larger increases in growth and coagulation compared to nucleation. Rayleigh-Debye-Gans polydisperse fractal aggregate theory analysis of experimental data, using aggregate parameters from atmospheric pressure flames ($D_f = 1.8$, fractal pre-factor $k_f = 2.2$), attributes observed particle growth to an increase in primary particle diameter. While both experimental and numerical results indicate an increase in overall soot particle size, the discrepancy in reasons of observed growth demonstrates the necessity of further evaluation of soot aggregate parameters at elevated pressures.

scott.steinmetz@kaust.edu.sa

W4P092 SOOTING TENDENCIES OF $C_4 - C_7$ UNSATURATED ESTERS IN NONPREMIXED COFLOW FLAMES

Dhrubajyoti Das, Charles Stewart McEnally, Lisa D. Pfefferle, Yale University, United States

Biodiesel fuels form an important constituent of the renewable energy resources landscape, and are increasing in popularity as stand-alone fuels as well as blends in conventional petroleum-based diesel fuels. These fuels are produced through transesterification of fatty acids with methanol or ethanol to yield long-chain methyl or ethyl esters. These carbon chains are of the order of 16–18 carbon atoms long, and are frequently unsaturated, with one or more C—C bonds. The C—C double bonds are expected to play a major role in the combustion chemistry of these biodiesel fuels, especially in the area of soot emission. To better understand the effect that the presence of these double bonds has on the sooting properties of esters, we have measured the sooting tendencies of twenty isomeric C_4 to C_7 unsaturated esters. These esters have one C—C bond, with the double bond present at different locations in each CN ester group. We plan to extend this study to include compounds with $N > 7$ and with multiple C—C bonds.

We measured the maximum soot volume fraction $f_{v, \max}$ on the centerline of a coflow methane/air nonpremixed flame whose fuel was doped with 1000 ppm of the target compound, and converted these $f_{v, \max}$ into Yield Sooting Indices (YSI) as per $YSI = C \times f_{v, \max} + D$ where C and D are apparatus-specific parameters chosen so that YSI of n -hexane = 0 and YSI of benzene = 100. The $f_{v, \max}$ were measured experimentally using Laser-Induced Incandescence (LII) with a $\lambda = 1064$ nm Nd:YAG laser.

The C—C double bond was found to have a significant effect on the sooting tendency of the unsaturated esters. In all cases, the unsaturated ester was more sooting than its saturated counterpart (YSI data for the saturated esters, and other hydrocarbons, has been reported). Apart from some exceptions, the sooting tendency generally trended as methyl esters < ethyl esters < propyl esters for compounds with the same groups on the carbonyl side. The location of the C—C bond in the ester influenced its sooting tendency as well. Compounds where the C—C bond was the closest to the carbonyl group (compounds with the structure $R-C-C-C(-O)O-R'$) typically had lower sooting tendency than compounds where it was further removed from the carbonyl group.

dhrubajyoti.das@yale.edu

W4P093 OXIDATION OF SOOT: KINETIC MONTE CARLO SIMULATIONS OF GRAPHENE-EDGE GROWTH AND OXIDATION

Ravi Singh, Michael Frenklach, University of California, United States

Soot growth and oxidation must be established in order to develop predictive models of soot formation in combustion systems. The growth of soot has been extensively studied, both experimentally and theoretically, and currently understood and modeled in terms of elementary chemical reactions. The oxidation of soot received less attention and thus far has been treated empirically. Lately, new information began to appear on elementary reactions of aromatics oxidation and this, in turn, enables mechanistic exploration of soot surface oxidation. In pursuit of this goal, we augmented the recently developed Kinetic Monte-Carlo (KMC) model of graphene-edge growth with a set of newly established elementary

reactions of graphene-edge oxidation by O_2 and OH . The KMC calculations were performed at a variety of initial conditions, isolating effects of various factors in order to gain insights into mechanistic features.

One of the key findings is the influence of oxidation on the morphology of the evolving graphene edge. In the designed for this purpose KMC simulations, the graphene layer was first grown from an initial coronene substrate for 5 ms before O_2 and OH were added to the gaseous environment. A series of calculations was performed with varied concentrations of O_2 or OH to establish the level of the oxidizer at which the oxidation becomes competitive with growth. Examination of the molecular structures produced in these computer runs revealed that the addition of an oxidizer promoted the formation of five-member rings embedded in the graphene edge, and the decrease in the fraction of armchair edge sites. A detailed analysis of the edge-site distribution as a function of various factors will be presented.

ravsingh@berkeley.edu

W4P094 MECHANISM OF GRAPHENE FORMATION IN FLAMES

Z.A. Mansurov¹, M. Auyelkhankyzy¹, N.G. Prikhodko¹, R. Singh², M. Frenklach²

¹Institute of Combustion Problems, Republic of Kazakhstan ²University of California, United States

Graphene is a single layer of carbon packed in a hexagonal lattice. It offers unique properties for fundamental science and future applications. A promising method of producing graphene layers is flame synthesis, which is continuous, rapid, and, inexpensive. Experimental studies confirm that graphene production in flames can compete with a number of existing methods.

Recently, Mansurov and co-workers studied formation of layered graphene films in atmospheric, premixed propane-oxygen and propane-oxygen-argon flames at $C/O = 0.86$. The growth of graphene took place on copper or nickel substrates placed in the central part of the flame.

The present study extends the previous one by including butane-oxygen flames and expanding the range of C/O ratios. It was found that the graphene layers are formed independently of the type of fuel in the studied C/O range, with a pronounced peak of graphite, G. We observed an increase in the degree of disorder in the forming graphene layers with an increase in the C/O ratio, as indicated by an increase in the peak D intensity. For propane-oxygen flames, the degree of disorder was observed at a higher C/O ratio than for butane-oxygen flames. However, a butane-oxygen flame at a ratio of $C/O = 0.95$ produced the minimum number of graphene layers (three layers, $IG/I2D = 1.3$).

The obtained results support the general notion of graphene being an intermediate product in the process of formation of Polycyclic Aromatic Hydrocarbons (PAH) and soot. To explore this conjecture further, kinetic Monte Carlo simulations were performed by extending the graphene-edge growth model to the experimental conditions of the present study.

lesbayev@mail.ru

W4P095 MODELING FOR SOOT FORMATION PROCESSES OF LAMINAR ETHYLENE/AIR COUNTERFLOW DIFFUSION FLAME

Namsu Kim, Yongmo Kim, Tae Hoon Kim, Hanyang University, Korea

The soot formation is mostly caused by incomplete oxidation of the fuel, with the production of aromatic compound, which grow to Polycyclic Aromatic Hydrocarbons (PAH), considered important compounds in the reactions involved in the first stages of the soot formation process. The soot precursor species, i.e. PAH and C_2H_2 , are eventually contributed to form the soot particles. Especially in the non-premixed flame, the flame structure and pollutant emission characteristics are substantially influenced by soot size distribution, number density and particulate radiation. Through a sequence of the comprehensive studies for the soot formation processes, the important progress has been achieved in understanding soot formation pathway.

Among the soot formation models largely classified by empirical, semi-empirical, and detailed models, the detailed soot models have the prediction capability to realistically embrace the fundamental combustion chemistry and aerosol dynamics theory. These models are based on the detailed chemical kinetics and physical models to describe the interphase processes between gases and solid particles as well as on the surface of soot particles. These detailed models can access more precise information about the soot formation processes such as soot particle inception, condensation, surface growth, particle oxidation, and coagulation. These particle dynamics models can provide the number density and the size distribution of soot particles. Compared to previous soot models with the mono-dispersed particle distribution, these detailed soot models using advanced aerosol dynamics can address soot aggregate structure and poly-dispersed particle size distribution. The soot particle dynamics are modeled by various approaches including the Sectional Method (SM), the Method of Moment (MOM), the Direct Quadrature Method of Moments (DQMOM), the Hybrid Method of Moments and the stochastic method. These detailed soot models have the potential capability to apply to the wide-range combustion conditions.

The present study has numerically investigate the counterflow ethylene-air diffusion flames. The detailed kinetic mechanism is used to handle the chemical kinetics. The mechanism is based on the PAH formation model. In this study, the soot particle dynamics are modeled by the sectional method and the Direct Quadrature Method of Moments. Transport and thermodynamic properties for the gas-phase species are from the Chemkin data base. Radiative transfer is modeled by the discrete transfer method. The gas-phase kinetic mechanism of hydrocarbon oxidation and pyrolysis is built on the GRI mechanism for C₁ and C₂ species extended to higher hydrocarbons to account for the formation of benzene and polycyclic aromatic hydrocarbons. Numerical results indicate that SM and DQMOM realistically predict the essential features of the soot formation processes in terms of PAH distribution as well as bimodal distribution of the number density function. SM yields the precise information of soot particle distribution at a finite number of sections but it requires the excessive computational burden for the accurate results. On the other hand, DQMOM has demonstrated the inherent advantages due to computation efficiency but it provides the limited information for the soot particle distribution. Based on numerical results, the detailed discussions are made for the soot formation characteristics in the counterflow ethylene/air diffusion flame.

real_k@naver.com

W4P096 EXPERIMENTAL STUDY OF SOOT OXIDATION BY OH

Isabel Jaramillo, Hossein Ghiassi, Paulo Perez, JoAnn S. Lighty, University of Utah, United States

In this study, the reaction pathways leading to oxidation of soot by hydroxyl radicals was investigated experimentally. Soot oxidation rates of different *n*-butanol/*n*-dodecane mixtures were studied in a two-stage burner, where soot was produced in a first-stage premixed burner, while in a second stage the soot was oxidized under slightly-rich conditions. Particle Size Distributions (PSDs), were measured on the second burner to evaluate the soot oxidation rate. A detailed kinetic model was used to predict OH concentration in the secondary flame. Gas-phase compounds, O₂, CO, CO₂, H₂, were measured to validate the result of detailed kinetic model. The concentrations of O₂ and OH were used to determine the contribution of each oxidizer during the oxidation process. OH was found to be the principle oxidizer and the role of O₂ was not significant in the oxidation process. Further analysis showed that OH reacting with a radical site (oxy-radical) on the surface of the soot particle turned out to be the primary mechanism for soot oxidation. Surface chemistry analysis by X-ray Photoelectron Spectroscopy (XPS) revealed comparable surface functional groups for soot samples derived from different *n*-butanol / *n*-dodecane mixtures. This observation suggested that the fuel-bound oxygen in the *n*-butanol did not contribute in the oxidation of the particle surface.

cristyjs@hotmail.com

W4P097 SOOT OXIDATION BY OH: THEORY DEVELOPMENT, MODEL, AND EXPERIMENTAL VALIDATION

Isabel Jaramillo, Hossein Ghiassi, JoAnn S. Lighty, University of Utah, United States

The focus of this work was the theoretical development and experimental validation of a new model for soot oxidation where OH was the principle oxidizer. This model aims to improve the prediction of soot oxidation by considering aspects that had not been previously considered, principally the fraction of active area as well as the size of the soot particle, in addition to traditional parameters such as OH concentration and temperature. Validation was performed for two fuel mixtures and experimental results showed good agreement with the model. In addition, the fraction of active areas was formulated, calculated, and plotted for different soot versus particle size distributions.

Finally, a sensitivity analysis was performed to evaluate the dependency of the model results on the uncertainty of the input parameters.

cristyjs@hotmail.com

W4P098 EXPERIMENTAL AND KINETIC MODELING STUDY OF STYRENE COMBUSTION

Yuyang Li¹, Wenhao Yuan¹, Philippe Dagaut², Jiuzhong Yang¹, Fei Qi¹

¹University of Science and Technology of China, China ²Centre National de la Recherche Scientifique, France

Styrene is one of the most important intermediates in the combustion of aromatic fuels and also an important precursor of PyroAromatic Hydrocarbons (PAHs). There have been little studies on the combustion of styrene. To our knowledge, only Litzinger investigated the flow reactor oxidation of styrene at $\phi = 0.56$ and 1 atm, and Westblad investigated the batch combustion of styrene in a two-stage muffle furnace. The targets of this work are to report a new experimental study on the laminar premixed flames of styrene at 30 Torr ($\phi = 0.75, 1.00$ and 1.70) and Jet Stirred Reactor (JSR) oxidation of styrene/benzene at 1 atm ($\phi = 0.50, 1.00$ and 1.50), as well as the development and validation of a kinetic model of styrene combustion.

Synchrotron vacuum ultraviolet photoionization mass spectrometry was used to detect the flame species, and their mole fractions were evaluated as functions of distance from the burner surface. The JSR oxidation of 0.05% styrene/0.15%

benzene/O₂/N₂ mixtures was performed at a residence time of 70 ms. The oxidation species were detected with gas chromatography, and their mole fractions were evaluated as functions of temperature. A detailed kinetic model of styrene combustion with 276 species and 1721 reactions was developed to reproduce the new experimental data. The simulations of laminar premixed flames and JSR oxidation were carried out using Burner-stabilized Flame module and Perfectly Stirred Reactor module in Chemkin-pro software, respectively.

The present model can get reasonable prediction on styrene and major products in both low-pressure laminar premixed flames and JSR oxidation. The rate of production analysis at $\phi = 1.70$ shows that most of styrene is consumed by unimolecular decomposition reaction, H-atom abstraction and O-atom addition reactions. Over 25% of styrene is consumed by unimolecular decomposition reaction, producing benzene and acetylene (C₂H₂). The rest of styrene is consumed either by stepwise H-atom abstraction reactions producing phenylacetylene or by O-atom addition reactions producing phenylacetaldehyde. The subsequent decomposition of phenylacetaldehyde mainly produces benzyl radical. Further decomposition and oxidation of benzyl radical is a major formation source of smaller oxidation products. The reactions related to phenylacetylene and benzyl radical are major sources of PAHs.

yuygli@ustc.edu.cn

W4P099 STOCHASTIC SIMULATION OF POLYCYCLIC AROMATIC HYDROCARBON GROWTH IN OXYGENATED FUEL FLAMES

Tyler Dillstrom, Jason Lai, Paolo Elvati, Angela Violi, University of Michigan, United States

Carbonaceous NanoParticles (CNPs) are an inevitable exhaust product of internal combustion engines that have deleterious health effects which necessitate investigation into their formation in order to ameliorate the biological damage incurred. Because of the complex nature of CNPs and the multiscale engineering problem that it is, computational methods can provide insightful information about chemical growth that is lacking in experimental results. As such, I am using a newly developed software program called the Stochastic Nanoparticle Simulator (SNAPS) to investigate the formation and growth of CNP precursors, i.e. Polycyclic Aromatic Hydrocarbons (PAHs). This stochastic computational method characterizes the manner of chemical growth of PAHs in gas phase combustion environments. Specifically, I am characterizing how PAHs form and subsequently grow in an oxygenated fuel combustion environment because the biofuel community produces mostly oxygenated fuels and anticipates these fuels eventually replacing traditional petroleum derived hydrocarbon fuels. Though previous work has described the chemical growth of PAHs in hydrocarbon flames to some extent, this computational approach is novel for oxygenated fuel flames. Using a novel chemical growth mechanism for PAHs (presently being developed), this work applies SNAPS to simulate PAH ensembles and demonstrate how the chemical growth pathways of PAHs differs in ethanol and methyl butanoate flames as compared to hydrocarbon flames. Additionally, simulation ensembles are compared to measured data from experimental ethanol and methyl butanoate laminar flames to demonstrate the validity of the mechanism as well as the computational methodology. The insights gained from this work provide valuable information about the dominant growth pathways of PAHs; this work can inform fuel researchers as to the structure and composition of biofuels that lead to desirable PAH growth pathways, thereby helping to limit production of unwanted CNP size distributions. The results of this project are not only significant in the nanoparticle and soot community but will also benefit those developing novel fuels, those designing new combustion reactors, and those investigating the deleterious biological effects of nanoparticles.

vtillst@umich.edu

W4P100 MOLECULAR DYNAMICS SIMULATIONS ON THE FORMATION OF INCIPIENT CARBONACEOUS NANOPARTICLES AT FLAME CONDITIONS

Salvatore Iavarone¹, Andrea D'Anna², Mariano Sirignano¹

¹University Federico II of Naples, Italy, ²Università degli Studi di Napoli Federico II, Italy

Particle inception remains one of the most intriguing and obscure steps in the process of particulate matter formation in flames. Although PAH stacking/clustering has been individuated as a key step in the inception process, uncertainties remain on the size of the PAHs undergoing clustering, on the organization of the PAHs in the forming clusters and on the factors affecting the amount of order present in this texture organization. It therefore becomes important to understand the role played by factors such as PAH molecular size, shape, the presence of non-aromatic rings or heteroatom functionalities in driving the process of cluster formation. Molecular modelling and computer simulation can give further insights on these aspects. Several molecular modelling studies have been focused on non-covalent PAH interactions, but the size and complexity of the molecules involved have restricted most studies to energy calculations on simple polyaromatic clusters and simulations of large disk ensembles using molecular pseudo-potentials.

This work presents a molecular dynamics approach to systematically study the influence of the molecular structural features and molecular weight of PAHs on the coagulation process and the morphology of the formed clusters. The simulations have been conducted in a canonical NVT ensemble with cubical periodic boundary conditions, coupled with a Nosé-Hoover thermostating method. The intermolecular interactions have been modelled using a PAH anisotropic potential. Two different types of macromolecules have been analysed: PeriCondensed Aromatic Hydrocarbons -PCAH- and Aromatic Aliphatic Linked Hydrocarbons -AALH- known to be present in flame environment depending on flame temperature, equivalence ratio and fuel chemical structure. The aim is to determine the effect of molecular size and of the presence of sigma bonds between aromatic islands upon the inception and the structure of the formed aggregates. Simulations of the behaviour of four organic molecules in a range of sizes (pyrene and coronene) and shapes (single molecules and covalent bonded dimers) at two extreme temperatures, namely 500 and 1500 K, have been performed in order to investigate the morphology of the clusters generated in combustion and during the cooling process at the exhausts. Concentration of PAHs and time of integration have been chosen in order to simulate 4 ms of residence time and a concentration of $1\text{E}15\text{ PAHs/cm}^3$. Coagulation of coronene molecules at low temperature occurs through the formation of clusters consisting of not more than 8 molecules aggregated: only a maximum of 3-4 are arranged in parallel planes - columnar phase - while the remaining are arranged in a triangular pattern. The increase in the temperature induces an increase of disorder in the aggregate as it increases the number of molecules arranged in triangular structures with respect to those arranged in parallel planes. Approximately 35% of the molecules are in the form of clusters and this number remains roughly constant as the temperature increases. The remaining 65% of the molecules are constituted by isolated molecules or unstable clusters, i.e., clusters with a lifetime of less than 30 ps. Their number is much higher at high temperature. The total of the clusters, stable and unstable, turns out to be almost 53% at high temperature and only 40% at low temperature. These results show that the molecules of PAHs within particles are highly mobile at flame temperatures. The coagulation of the covalent bonded coronene dimers in the same conditions of concentration of the molecules shows that at low temperature about 70% of the molecules remain isolated. The trend is reversed at high temperature where only 38% of the molecules remain isolated. The distribution of the molecules within the cluster is not very different in the two cases except for an increase in long-distance interactions and an enhancement of the disorder of the clusters in the case of the dimer.

s.iavarone12@gmail.com

W4P101 APPLICATION OF DIRECT MONTE CARLO SIMULATION FOR MORPHOLOGY OF AGGREGATES AND PARTICLE SIZE DISTRIBUTIONS: COMPARISON OF THE CLUSTER-CLUSTER AGGREGATION MODEL WITH THE STOCHASTIC MODEL

Kiminori Ono, Tohoku Univeristy, Japan

This study presents the validity and ability of an Aggregate Mean free Path-Cluster-Cluster Aggregation (AMP-CCA) model, which is a direct Monte Carlo simulation, to predict the aggregate morphology by comparing the Particle Size Distributions (PSDs) with the results of the fixed sectional model associated with the stochastic approach. The AMP-CCA model can store the three-dimensional aggregate morphology with computational efficiency, allowing for the direct simulation model to describe the PSDs. The PSDs calculated by the AMP-CCA model with the calculated aggregate as a coalesced spherical particle are in reasonable agreement with the results of the sectional model regardless of the number concentration. The shape analysis using two methods, perimeter fractal dimension and the shape categories, has demonstrated that the aggregate structures become complex with increasing number concentration. The shape categories allow the aggregate structures to be evaluated in detail in comparison to the perimeter fractal dimension. For high structures, the AMP-CCA model with aggregate morphology enables the calculation of the actual PSD. The AMP-CCA model provides a useful tool to calculate the aggregate morphology and PSD with reasonable accuracy as a direct Monte Carlo simulation.

kiminori@tranpo.che.tohoku.ac.jp

W4P102 HOW MOLECULAR STRUCTURE AFFECTS POLYCYCLIC AROMATIC HYDROCARBON DIMERIZATION

Jeffrey Lowe, Paolo Elvati, Angela Violi, University of Michigan, United States

The widespread emission of Carbonaceous NanoParticles (CNPs) from combustion sources poses a significant health risk to humans; therefore, CNP formation has been studied in great detail. CNP formation consists of a number of steps involving both chemical and physical growth mechanisms. The particle nucleation step, or the transition from gas-phase species to solid-phase species, is not well-understood. Particle nucleation has a large impact on the structural features of final nanoclusters of molecules. Our work aims at developing a more complete picture of the particle nucleation process by modeling the atomistic growth of gas-phase molecules to the formation of the first condensed-phase nuclei. Towards this

goal, our current work invokes, as the initial step in the overall nucleation process, the dimerization of aliphatic-substituted Polycyclic Aromatic Hydrocarbons (PAHs). We have quantified the effect of particle geometry on the free energy stability of dimerized compounds of PAHs. These results will aid in the development of non-empirical correlations between molecular geometry and particle dimerization propensity. We employed molecular dynamics techniques coupled with the well-tempered Metadynamics algorithm to measure the free energy surfaces of dimerization between compounds of interest. We found that molecules with saturated chains display an increase in dimer stability with an increase in the number of substituted chains whereas molecules with unsaturated chains have dimer stabilities relatively unaffected by the number of chains. Further, we determined that the most preferential configurations of molecules within a dimer depend on the distance between each of the molecules involved in dimerization. These results form the basis for the initial step in a particle nucleation model that includes atomistic details of CNP formation. Future incorporation of the findings in the current study into an overall particle nucleation model in the gas-phase will aid researchers in minimizing the environmental impact of CNP release into the atmosphere.

jefflowe@umich.edu

W4P103 CHARACTERIZATION OF SOOT GROWTH PROCESSES AND MORPHOLOGY IN A TURBULENT NON-PREMIXED FLAME USING MONTE CARLO METHODS

Ahmed Abdelgadir, Clean Combustion Research Center, Saudia Arabia

Soot emissions in combustion devices are a combustion inefficiency as well as a health and environmental hazard. Understanding soot growth processes is a vital step for abating soot production in combustion devices. Recently, Attili et al.(2014) and Bisetti et al.(2014) performed a set of Direct Numerical Simulations (DNS) of soot formation and growth in a *n*-heptane three dimensional non-premixed jet flame using a high order method of moments to describe soot (Mueller et al(2009)). The evolution of species relevant to soot formation and growth have been sampled along a large number of Lagrangian trajectories in the DNS. In this work, the DNS results are post-processed using a Monte Carlo method and the soot evolution along selected Lagrangian trajectories is simulated. An operator splitting approach is adopted to split the deterministic processes (nucleation, surface growth and oxidation) from coagulation, which is treated stochastically. The goals of this work are twofold. Firstly, we compare the soot number density and mass fraction obtained with the method of moments to those calculated with the Monte Carlo approach. It is shown that the agreement is excellent, confirming that the simplifications and closure assumptions in the moment method are adequate under wide range of flow and soot conditions. Secondly, the Monte Carlo approach provides a complete description of the size distribution of soot everywhere in the domain. Sudden and intense nucleation events followed by rapid coagulation have the greatest effect on the particle size distribution, therefore various coagulation models are considered and compared. More calculations are done over a subset of trajectories conditioned on mixture fraction $Z = 0.3$, which is where soot mass fraction peaks. The distribution of the primary particle diameter in the soot aggregates shows a strong peak at the nucleated particle size and a broad distribution at larger sizes due to coagulation.

ahmed.abdelgadir@kaust.edu.sa

W4P104 REVISITING APPROACHES TO OBTAINING TRANSPORT PROPERTIES OF PAH AND FULLERENES

Christopher Pope, Cabrillo College, United States

Detailed elementary-step kinetic modeling of combustion processes in which diffusion velocities can be significant compared to convective velocities requires calculation of multi-component diffusion coefficients, which are functions of not only all the binary diffusion coefficients but also the local composition. The number of binary diffusion coefficients required is $K(K+1)/2$, where K is the number of chemical species. Given that K is often $O(102-103)$, there is a need for a computationally efficient way to calculate up to $O(104-106)$ binary diffusion coefficients, all of which are functions of temperature. A commonly-used method for calculating binary diffusion coefficients is via Lennard-Jones (LJ) parameters, as is done in modeling software packages like CHEMKIN.

Many existing correlations for the two LJ parameters, σ and ϵ/k , are based on the critical temperature (T_c), the cube root of the ratio of the critical temperature to the critical pressure $(T_c/P_c)^{1/3}$, and the acentric factor (ω). Few such data exist for PAH, so there is a need to resort to estimation methods. In the current work, only group-additively methods are considered, as compared to quantitative structure-property relationship (QSPR) methods. Estimation methods for T_c often require the normal boiling point (T_b), which often must also be estimated. The acentric factor can either be estimated directly (Constantinou & Gani, 1994; Nannoolal et al., 2007) or calculated from a vapor-pressure relation (e.g., Lee-Kesler, Ambrose-Walton) using T_b/T_c and P_c as inputs.

Previous analyses by Pope (1988) and Wang & Frenklach (1994) were limited by the few property estimation methods in existence then. In the meantime, many additivity methods (group, bond, atom) have been developed.

The present work compares the results from several additivity-based property estimation methods for dozens of unsubstituted PAH of three types: (1) kata-condensed benzenoid PAH with 1 to 23 fused aromatic rings; (2) peri-condensed benzenoid PAH with 1 to 37 fused aromatic rings; (3) PAH containing both five- and six-membered rings (PAH_{5/6}) ranging from acenaphthalene (C₁₂H₈) to the fullerene C₆₀.

The results show the varying abilities of the estimation methods to yield results with physically realistic behavior with respect to molecular size and structure, as well as their ability to discern structural isomers. Many methods' predictions yield reasonable values for the LJ parameters, but the range of values produced can vary considerably depending on the method chosen. In particular, predictions of the acentric factor vary widely. Differences between values for omega derived from direct group estimation methods and from vapor pressure relations are dramatic, even showing different trends with respect to molecular size and structure. The role of omega in correlations for LJ parameters is also called into question.

christopher_pope_phd@yahoo.com

W4P105 AN UPDATED KINETIC MECHANISM FOR DIMETHOXYMETHANE OXIDATION UNDER HIGH-PRESSURE CONDITIONS

Lorena Marrodán, Eduardo Royo, Ángela Millera, Rafael Bilbao, Maria Alzuet, University of Zaragoza, Spain

DiMethoxyMethane (DMM), or methylal, is a diether that is of interest because it has potential as a neat or blended diesel fuel, and also because of its similarity in structure with the potentially important, ultra-clean-burning, high-cetane, diesel fuel, DiMethyl Ether (DME). Many of the DMM properties are intermediate between those of dimethyl ether and methanol, two promising diesel fuels. Another highlight of the DMM is that, under ambient conditions, is a liquid, while DME is a gas. The used kinetic mechanism for describing the DMM oxidation is based on the C1-C2 mechanism developed by Glarborg et al., updated and extended later. Additional subsets for dimethyl ether and methyl formate have been added. For DMM, the DMM reaction sub-mechanism suggested by Dias et al. for high temperatures has been taken as a starting point. Calculations have been performed using Senkin which runs in conjunction with Chemkin library. The DMM oxidation is initiated by abstraction of either a primary hydrogen atom, to form CH₃OCH₂OCH₂, or a secondary hydrogen atom, to form CH₃OCHOCH₃. The experimental results used to validate this mechanism indicate that, working at high pressures (20, 40 and 60 bar) and under oxidation conditions ($\lambda=20$), Hydroperoxy Radicals (HO₂) and O₂ play a significant role in the DMM conversion. To account for that in the simulations, the kinetic parameters of the reactions involving these species, DMM and its main radicals, have been estimated in the present work, since no kinetic parameters are available for these interactions. These reactions have as major products CH₂O, CH₃OCHO and CH₃OCH₂O₂. The last one presents certain stability at temperatures around 573 K.

marrodan@unizar.es

W4P106 NEW IDENTIFICATIONS OF POLYCYCLIC AROMATIC HYDROCARBONS IN PRODUCTS OF SUPERCRITICAL *N*-DECANE PYROLYSIS

Nimesh Poddar, Subramanian. V. Kalpathy, Mary Julia Wornat, Louisiana State University, United States

In the pre-combustion environment of future high-speed aircraft the fuel is expected to experience temperatures and pressures up to 700°C and 130 atm; these conditions are supercritical for most hydrocarbons. Under these conditions, the fuel can undergo pyrolytic reactions that can lead to the formation of Polycyclic Aromatic Hydrocarbons (PAH), which are precursors to fuel-line deposits. To prevent clogging of fuel-delivery lines and ensure safe aircraft operation, it is important to understand the reactions that lead to the formation of PAH in the supercritical fuel pyrolysis environment. To this end, pyrolysis experiments have been performed, under supercritical conditions, with *n*-decane (critical temperature, 344.5°C; critical pressure, 20.7 atm), a model fuel representative of alkane components of jet fuels. The experiments have been conducted in an isothermal, silica-lined stainless-steel flow reactor at 570°C, 94.6 atm, and 133 sec, conditions that correspond to the onset of solids formation. At these reaction conditions, *n*-decane pyrolysis produces a mixture of unsubstituted PAH and PAH with varying degrees of alkyl substitution, which necessitates the use of a two-dimensional High-Pressure Liquid Chromatographic (HPLC) technique for the separation of the PAH products. Once separated, the products are identified by their Ultraviolet-Visible (UV) absorbance and mass spectra. In earlier work of our research group, two-dimensional HPLC analyses of the PAH products of supercritical *n*-decane pyrolysis had led to the identification of 62 unsubstituted PAH and 208 alkylated PAH of three to nine rings. However, subsequent modifications to both dimensions of the HPLC analytical techniques have led to improved component separations and the identification of 24 additional PAH—11 unsubstituted and 13 methyl-substituted PAH—of three to eight rings in the supercritical *n*-decane pyrolysis product mixture. These 24 PAH have never before been identified as products of *n*-decane pyrolysis or combustion; many have never before been identified as products of any fuel. The UV absorbance spectra and mass spectra establishing the unequivocal identities of the newly-identified PAH products of supercritical *n*-decane pyrolysis will be presented.

npodda1@lsu.edu

W4P107 POLYCYCLIC AROMATIC HYDROCARBON (PAH) AND SOOT FORMATION IN THE PYROLYSIS OF DIMETHOXYMETHANE

Fausto Viteri, Rafael Bilbao, Ángela Millera, Maria Alzueta, University of Zaragoza, Spain

The current concern for the environment protection has led to research alternative fuels and fuel additives. Some studies have shown that oxygenated compounds used as fuel additives decrease the formation of soot. A candidate is DiMethoxyMethane (DMM, $C_3H_8O_2$). There are few studies that show the formation of Polycyclic Aromatic Hydrocarbons (PAH) in the pyrolysis of oxygenated compounds. Furthermore, PAH are involved in soot formation and can be adsorbed on the soot surface. Some PAH are considered as carcinogenic, especially the 16 priority PAH, classified by the USA Environmental Protection Agency (EPA). The aim of the present work is to carry out the pyrolysis of DMM by analyzing the gas-phase, soot and PAH formed. Pyrolysis experiments are carried out under well controlled laboratory conditions, in a flow reactor, at different temperatures and DMM concentrations. The gases formed in the process are analyzed by a gas chromatograph. Soot is collected in a quartz fiber filter and its yield is determined. PAH are collected and quantified with the method developed by our research group. PAH are trapped in two phases: the first is found on the soot surface and stuck at the reactor walls. The second, here named the gas phase, is retained by XAD-2 resin which is packed in a thin-tube, placed after the filter used to collect soot. PAH stuck on the reactor walls are collected by washing the reactor with dichloromethane. PAH from the soot surface and the resin follow a Soxhlet extraction, using dichloromethane and are later concentrated by the rotary evaporator. Finally, all the samples are analyzed by Gas Chromatography-Mass Spectrometry (GC/MS). The results indicate that there is a significant influence of the temperature and DMM concentration on the formation of soot and PAH from the DMM pyrolysis. The yield to soot and PAH from this compound is low. These results indicate that DMM should be further studied in order to be considered as a suitable fuel additive.

fviteri@unizar.es

W4P108 THE EFFECTS OF TEMPERATURE ON THE YIELDS OF PRODUCTS FROM PROPYLENE PYROLYSIS

Eva Caspary, Nimesh Poddar, Mary Julia Wornat, Louisiana State University, United States

The pyrolysis reactions of C_3 hydrocarbons and their products can lead to the formation of Polycyclic Aromatic Hydrocarbons (PAH), which are known for their role in soot formation and for their carcinogenic and/or mutagenic behavior. Therefore, it is important to study the pyrolytic reactions leading to the formation and growth of PAH products from C_3 hydrocarbons. In this context, our research group has previously investigated the pyrolysis of the C_3 hydrocarbon propyne—finding that the yields of PAH products become appreciable only at the highest investigated temperature, 1000 °C, a condition at which acetylene yields are high and the breakage of the aryl C–H bond of the major product benzene can lead to the formation of phenyl radical. To further elucidate the role of C_3 species in PAH formation and growth reactions, gas-phase pyrolysis experiments have been performed with the C_3 alkene, propylene. Experiments are performed at temperatures of 700 to 1000 °C and at a residence time of 0.31 sec, the same reaction conditions as the above mentioned propyne pyrolysis study. The experiments take place, in nitrogen, in an isothermal laminar-flow reactor, and the pyrolysis products are collected and analyzed by three different techniques: gas chromatography with flame-ionization detection, for C_1 – C_6 hydrocarbon products; gas chromatography with flame-ionization detection and mass-spectrometric detection, for one- and two-ring aromatic products; and high-pressure liquid chromatography with diode-array ultraviolet-visible absorbance detection, for PAH. The temperature-dependent product-yield data from propylene pyrolysis are presented and discussed. Furthermore, product yields from propylene and propyne pyrolysis are compared, and mechanistic implications for PAH formation and growth are discussed.

ecaspal@lsu.edu

W4P109 NEW IDENTIFICATIONS OF POLYCYCLIC AROMATIC HYDROCARBONS IN PRODUCTS OF COAL SOOT EXTRACTS

Matthew Skapura, Nimesh Poddar, Mary Julia Wornat, Louisiana State University, United States

Pyrolytic reactions at high temperatures can lead to the formation of Polycyclic Aromatic Compounds (PAC), environmental pollutants that are known soot precursors. Many PAC exhibit carcinogenic and/or mutagenic activity; therefore, the composition of PAC associated with soot is not only of environmental concern but also biological concern. To investigate the composition of PAC associated with soot in coal-burning homes, soot samples have been collected from cooking woks of coal-burning homes of the Henan Province of China, a province with one of the highest rates of esophageal cancer in the world. The collected coal soot samples have been extracted with dichloromethane in a Soxhlet extractor, and the resulting PAC solutions have been concentrated in a Kuderna-Danish apparatus and analyzed on a High-Pressure Liquid

Chromatograph (HPLC) coupled to an Ultraviolet-Visible (UV) diode-array detector with Mass Spectrometer (MS). Thirty-six PAC, ranging in size from three to nine aromatic rings, have been identified by matching their UV absorbance spectra with those of our reference standards or with those published in the literature. The 36 identified product components include 28 benzenoid Polycyclic Aromatic Hydrocarbons (PAH), six fluoranthene benzologues, one alkylated PAH, and one oxygen-containing aromatic. 26 of the 36 PAC have been identified as products of these extracts in an earlier study from our research group, but advances in chromatographic techniques and the recent availability of mass spectral data have led to the identification of 10 additional PAH that have never before been reported as products in these soot extracts. Among the 10 newly-identified product components, five have never before been documented as products of any coal combustion process. The HPLC/UV/MS data establishing the unequivocal identification of the newly identified compounds will be presented.

mskapu2@tigers.lsu.edu

W4P110 EXPERIMENTAL AND MODELLING STUDY OF DIMETHYL CARBONATE OXIDATION AND ITS INTERACTION WITH NO

Maria Abian, Pablo Salinas, Ángela Miller, Rafael Bilba, Maria Alzueta, University of Zaragoza, Spain

The addition of oxygenated compounds to conventional fuels in the so-called “reformulated fuels” is a strategy to reduce the emissions of soot from combustion processes and thus to achieve a cleaner combustion. Studies on the oxidation process of ethanol and its mixtures with acetylene, as one of the main soot precursors, have already carried out in our group. In this research line, the present work aims to analyse the oxidation process of Dimethyl Carbonate (DMC), under well controlled conditions, through a combination of experimental and modelling work. Dimethyl carbonate can be considered as an interesting oxygenated fuel additive because of its high oxygen content.

Besides to the concern on soot emissions, nitrogen oxides are also important air pollutants generated in these processes. Therefore, in this work, the potential of DMC and its derives for reducing NO under combustion conditions is also analysed. To achieve these targets, experiments of DMC oxidation in the presence and absence of NO, under different operating conditions, are performed in a quartz flow reactor at atmospheric pressure. Experiments are carried out in the 300-1400 K temperature range and for fuel-rich ($\lambda = 0.3$) to fuel-lean ($\lambda = 35$) conditions. A gas chromatograph equipped with TCD and FID detectors, an FTIR (Fourier Transform Infrared) spectrometer, and continuous IR CO/CO₂ and NO analysers are used to determine the gas products.

The modelling study of this process is performed by using Senkin code which runs in conjunction with Chemkin library. The base mechanism, with minor modifications and updates, is taken from the work of Glarborg et al. to describe the combustion of small hydrocarbons and their interaction with NO, together with the ethanol reaction subset of Alzueta and Hernández. In this ongoing work, the DMC reaction subset proposed by Glaude et al. is implemented in the base mechanism.

mabian@unizar.es

W4P111 SOOTING LIMITS OF NONPREMIXED *N*-HEPTANE, *N*-BUTANOL, AND METHYL BUTANOATE FLAMES: EXPERIMENTAL DETERMINATION AND MECHANISTIC ANALYSIS

Sili Deng, Jeremy Koch, Michael Mueller, Chung King Law, Princeton University, United States

The role of oxygenated additives on soot emission reductions has not yet come to a scientific consensus. Although valuable contributions have been made, well-controlled fundamental experiments and detailed chemical kinetic analyses are still needed to understand the chemical pathways for soot formation with oxygenated fuels. Moreover, since soot formation is a kinetically controlled process, the residence times of soot precursors are also expected to influence the sooting propensities, and these effects have not yet been explored in detail for oxygenated fuels. Therefore, the present experimental and computational study focuses on the sooting limits (a residence time effect) of three neat liquid diesel/biofuel components, specifically, *n*-heptane, *n*-butanol, and methyl butanoate, in a nonpremixed stagnation-flow system. Due to the oxygen content in *n*-butanol and methyl butanoate, their flame temperatures are lower than *n*-heptane. Since soot formation is highly sensitive to temperature, this thermal effect has to be eliminated to elucidate the chemical effects. In the present study, *n*-butanol and methyl butanoate flame temperatures were kept at the same as *n*-heptane by replacing a portion of the nitrogen in the oxidizer stream with argon.

Sooting limits were determined by increasing the oxidizer flow rates until yellow luminosity appears in the flames. The local strain rate at which this yellow luminosity first appears was determined as the axial velocity gradient upstream of the flame utilizing standard single-component Laser Doppler Velocimetry. In parallel, computations were conducted for the same configuration using detailed Polycyclic Aromatic Hydrocarbon (PAH) chemistry and a detailed soot model based on the Hybrid Method of Moments (HMOM). Both experimental and computational results showed the critical strain rates of the three fuels, based on the absolute soot volume fraction, increase with increasing oxygen mole fraction in the oxidizer,

due to the increase of flame temperature. In addition, although *n*-heptane and *n*-butanol show similar sooting propensities, methyl butanoate produces significantly less soot and a lower critical strain rate. Sensitivity and reaction path analysis was performed for naphthalene, the first PAH species from which soot is thought to form. This analysis revealed that, despite different sooting tendencies, the three fuels shared similar PAH chemical pathways. C₅, C₆, C₇, C₉ rings, and naphthalene are formed sequentially through the combination of C₃ and smaller chain radicals resulting from fuel cracking processes. Due to the fuel bound oxygen in methyl butanoate, less and shorter chain radicals are available for soot formation, compared with the other fuels, such that methyl butanoate forms the least soot and has the lowest critical strain rates. Furthermore, despite different sooting propensities, for all three fuels, C₅ and C₆ ring formation reactions are the same rate limiting steps with concentrations of these species dropping as the residence time is decreased, such that the subsequent PAH chemistry is consequently inhibited.

silideng@princeton.edu

W4P112 STRAIN RATE EFFECT ON SOOTING CHARACTERISTICS IN LAMINAR COUNTERFLOW DIFFUSION FLAMES

Yu Wang, Suk-Ho Chung, University of King Abdullah Science & Technology, Saudi Arabia

The effect of strain rate on the sooting characteristics of Counterflow Diffusion Flames (CDF) of various gaseous hydrocarbon fuels was investigated in this study. The counterflow burner featured two opposing nozzles of 10 mm I.D. with a separation distance of 8 mm and the fuels tested included ethylene, ethane, propene and propane. The sooting structures of ethylene CDF was first studied with nozzle exit velocity ranging from 10 to 30 cm/s using laser light extinction and scattering techniques. The results show that increase in strain rates reduces Soot Volume Fraction (SVF), average size and peak number density, which are reasonable considering the reduced residence time and temperature as strain rate increases. The SVF were also measured for different fuels with varying oxygen mole fraction (XO) in the oxidizer side using laser induced incandescence. It was observed that for a fixed fuel, SVF increases with increase in XO while for a fixed XO, SVF was dependent on fuel type with propene the most sooting fuel and ethane the least. Moreover, it was found that SVF were less sensitive to strain rate for more sooting flames.

Further experiments were conducted at conditions where the SVF for different fuels were matched at a reference strain rate, which can be achieved through using different XO for different fuels. Then, as shown in Fig. 1, the dependence of SVF on strain rate became comparable among the tested fuels. This may indicate soot loading itself (instead of fuel type or XO) is the controlling factor that dictates the sensitivity to strain rates, at least for the fuels tested here. Relative PAH concentrations were measured using laser induced fluorescence techniques. For all the cases tested, PAH concentrations were shown to decrease with increase in strain rate and the dependence on strain rate is more pronounced for larger PAHs. Kinetic simulations for species up to coronene were also performed to study strain rate effect on PAH concentrations. A qualitative agreement was obtained between experimental and simulation results, while the simulation result was more sensitive to strain, especially for large PAHs, which may be improved when incorporating soot modeling.

yu.wang@kaust.edu.sa

W4P113 SUPERCRITICAL PYROLYSIS OF 1-OCTENE

Elizabeth Hurst, Subramanian V. Kalpathy, Mary Julia Wornat, Louisiana State University, United States

Fuels in future hypersonic aircrafts will not only act as the propellant but will also play a role as the coolant in order to remove excess heat from the engine components. These fuels will be subjected to temperatures and pressures up to 700°C and 130 atm, which is in the supercritical regime for jet fuels as well as most hydrocarbons. These extreme conditions can cause decomposition of the fuel, which can lead to the formation of Polycyclic Aromatic Hydrocarbons (PAH), precursors to solid deposits. These solid deposits can clog the fuel delivery line, rendering the aircraft's operation unsafe. In order to prevent the formation of these solid deposits, it is important to understand the reaction mechanisms of these PAH under supercritical conditions. Previous work in our research group showed that alkane components of jet fuels are the most problematic with regards to solids and that 1-alkenes are major products of supercritical alkane pyrolysis. Since 1-alkenes are abundant in the supercritical alkane fuel pyrolysis environment, it is of interest to examine the role that 1-alkenes have in PAH formation and growth reactions. To this end, experiments have been conducted with the model fuel, 1-octene (critical temperature, 294 °C; critical pressure 26.4 atm), a representative product of the pyrolysis of *n*-decane and *n*-octane. By comparing the products of 1-octene to the products of *n*-octane, it is possible to examine how the presence of the double bond in 1-octene affects PAH formation. The supercritical experiments with 1-octene are carried out in an isothermal silica-lined stainless steel tubular reactor immersed in a fluidized alumina bath. The product is a highly complex mixture of unsubstituted and alkylated PAH; therefore, a two-dimensional chromatographic technique is used to separate the PAH products. The PAH products are identified and quantified using ultraviolet-visible diode-array detection and mass

spectrometry. The detailed quantification of the 1-octene products in its comparison to that of the *n*-octane products will be presented, and the mechanistic implications for PAH formation will be discussed.

ehurst4@tigers.lsu.edu

W4P114 DQMOM APPROACH FOR POLY-DISPERSED SOOT FORMATION PROCESSES IN TURBULENT NON-PREMIXED ETHYLENE/AIR FLAME

Taehoon Kim, Yongmo Kim, Hanyang University, Korea

Modeling and simulation of soot formation process in turbulent flames is one of the most complex and challenging task in the combustion science. According to Kennedy, the soot formation models are largely classified by empirical, semi-empirical, and detailed models. Empirical soot models were developed by the experimentally phenomenological correlations of soot formation rates for combustion conditions. But this model has the dependency of flame condition. To overcome this dependency, the semi-empirical concept is proposed, which is typically called two-equation soot model. Even if this semi-empirical soot model realistically describes the basic information for the soot formation mechanism, it has the limitation of providing the detailed soot properties due to the mono-dispersed assumption. The detailed soot models embrace the fundamental combustion chemistry and particles dynamics theory. In addition, various approaches for soot particle dynamics under nucleation, coagulation, surface growth and oxidation processes have also been implemented. Representative approaches are the sectional method, Method of Moment, Direct Quadrature Method of Moment (DQMOM), Hybrid Method of Moments and stochastic method. These particle dynamics models can provide the number density and the size distribution of soot particles. Compared to previous soot models with the mono-dispersed particle distribution, these detailed soot models using advanced aerosol dynamics can address soot aggregate structure and poly-dispersed particle size distribution. But the detailed soot models are usually difficult to implement as well as to couple with the gaseous chemistry.

Recently, Marchisio et al. developed the DQMOM procedure for the pseudo-bivariate population balance model to simulate the soot formation characteristics in the turbulent non-premixed flame. However, this DQMOM approach is based on the steady flamelet model which is unable to realistically predict the slow processes including soot formation and radiation. Moreover, this model neglects the soot/gas chemistry coupling which substantially influences the soot formation characteristics. In this aspect, in the framework of the transient flamelet model, the population balance model via DQMOM together with the soot/gas chemistry coupling has been developed in the present study. In present work, the transient flamelet model is adopted to treat the turbulence-chemistry interactions and the two-equation soot model is used to account for the interaction between soot and gas chemistry. Because the two-equation soot model is straightforward to couple the soot formation with gas chemistry and it also has the prediction capability to address the flame structure interacted with the soot formation without the excessive computational cost. Moreover, the DQMOM has been also employed to simulate the poly-dispersed soot particle dynamics. To validate the present approach for analyzing the soot formation processes of the turbulent non-premixed flame, the turbulent non-premixed C_2H_4 /Air flame has been chosen as the benchmark problem. The population balance equation of soot particle distribution is approximated using the multi-environment probability density function which consists of multiple weights and abscissas on physical space. The transient flamelet model is employed to treat the turbulence-chemistry interactions and the two-equation soot model is used to account for the soot/gas chemistry coupling allowing mass and energy exchange. In the framework of the transient flamelet model, the physical soot source terms such as nucleation, surface growth and oxidation for the population balance equation of soot particle distribution have been closed. In terms of the mean temperature, soot volume fraction, primary soot particle number density, primary soot aggregate number density, mean number of primary particle per aggregate, mean radius of soot aggregate, and mean primary soot particle diameter, the predicted profiles are reasonably well agreed with experimental data.

susyboy@hanyang.ac.kr

W4P115 SOOTING BEHAVIOR OF HYDROCARBONS IN A MICRO FLOW REACTOR WITH A CONTROLLED TEMPERATURE PROFILE

Ajit Kumar Dubey, Kaoru Maruta, Hisashi Nakamura, Takuya Tezuka, Susumu Hasegawa, Tohoku University, Japan

In this work sooting tendencies of normal and branched alkanes namely *n*-heptane, *iso*-octane, *n*-octane and *n*-decane are studied using a micro flow reactor with a controlled temperature profile to understand effects of carbon number and structure. Two different temperature profiles with same maximum temperature of 1300 K were used in order to investigate the effects of temperature gradient on sooting behavior of concerned hydrocarbons. In the first setup a flat-flame premixed hydrogen/air burner was used and the reactor was horizontal which is similar to the setup used for methane and acetylene sooting studies. In the second setup, the external heater is co-axial hydrogen-air-oxygen diffusion flame burner and reactor (a 2 mm inner diameter quartz tube) is vertical. The reactor was fitted concentrically to the hydrogen tube and flow in

reactor was in reverse direction to hydrogen flow. The temperature gradient for second setup is smaller than that of the first setup. The second setup generates symmetrical temperature profile compared to the first setup.

Equivalence ratio (1.5-4.5) and mean inlet flow velocity (10-100 cm/s) were varied and effects on sooting and flame's tendencies were observed for both setups. Four kinds of flame and soot responses were obtained for all the fuels used: only flame, soot + flame, only soot and none. Due to symmetrical temperature profile the soot images obtained from second setup were one dimensional, whereas the images from first setup are not so. The sooting lengths for normal alkanes are larger than that for branched alkanes for same flow conditions in the first setup.

The results were plotted on an equivalence ratio-flow velocity plane. The sooting limits in second setup were extended to lower equivalence ratios. The equivalence ratio-flow velocity region where both soot and flame were observed diminished with increasing carbon number in the second setup. Thus second setup can differentiate better between concerned hydrocarbon fuels. The first setup could differentiate well only between normal and branched hydrocarbons but not among normal hydrocarbons. The luminosity of flame reduces with increasing equivalence ratio and decreasing velocity for both soot and flame region. Soot was observed at wall temperatures above 1200 K in both setups. One dimensional computation done with CHEMKIN-PRO using CRECK mechanism for PRF+PAH showed very high mole fractions of large PAHs like anthracene and pyrene for *n*-heptane compared to *iso*-octane. The computation was done for equivalence ratio of 3 and inlet velocity of 2cm/s. In this condition no flame is observed so wall temperature is very close to gas temperature which permits us to use given gas temperature profile assumption without solving energy equation.

ajit@edyn.ifs.tohoku.ac.jp

W4P116 EFFECT OF TEMPERATURE AND RESIDENCE TIME ON SOOT FORMATION DURING PYROLYSIS OF ASPHALTENE

Vinoj Kurian¹, Nirlipt Mahapatra¹, Ben Wang¹, Frans Martens², Rajender Gupta¹

¹University of Alberta, Canada ²Nexen Energy ULC, Canada

The effects of temperature and residence time were investigated on the formation of soot particles during the pyrolysis of asphaltene in a Drop Tube Furnace (DTF). Asphaltenes are highly aromatic and contain substantial quantities of coke precursors, metals (V, Ni), sulfur, and nitrogen. The feedstock for this study is asphaltene obtained by de-asphalting bitumen resourced from the Athabasca basin. The cold crushed and sieved asphaltene used for the pyrolysis was between 150-212µm. The pyrolysis is carried out in an atmospheric entrained flow DTF that is electrically heated to a set temperature between 800 and 1400°C. The pyrolysis products are air cooled in the collection probe after DTF and passed through a cyclone for the separation of the particles larger than 10µm. The particles smaller than 10µm subsequently pass through a cascade impactor for collection of the soot and ash. Soot is usually formed when the process conditions are sufficiently fuel rich to allow condensation or polymerization reactions of the fuel. Polycyclic Aromatic Hydrocarbons (PAH) are products of primary pyrolysis and the pre cursors of the soot particles in a secondary pyrolysis process. Soot exists in the form of both individual particles and agglomerate comprised of several primary particles. In addition to contributing to pollution, the trace metals in feed asphaltene being concentrated in these soot particles causing erosion/corrosion in the equipments. It is observed that the size of the soot particles decreases with an increase in temperature. The Sulfur and Hydrogen content in the soot decrease with temperature due to the liberation of Sulfur as hydrogen sulfide during the pyrolysis reactions. The association of trace metals in soot is analyzed using ICP-MS. It is observed that main metals present in the soot are Vanadium, Nickel and Iron. With increase in residence time the size of the soot particles collected in the cascade impactor increases. Understanding the decomposition of asphaltene, subsequent formation of soot and the interaction of trace metals with soot enables optimization of processes like asphaltene gasification.

vinoj@ualberta.ca

W4P117 MODELING SOOT FORMATION IN PREMIXED FLAMES USING A CONDITIONAL QUADRATURE METHOD OF MOMENTS (CQMOM) APPROACH

Steffen Salenbauch¹, Alberto Cuoci², Isabel Frenzel¹, Dimosthenis Trimis³, Tiziano Faravelli², Christian Hasse¹

¹TU Bergakademie Freiberg, Germany ²Politecnico di Milano, Italy ³Karlsruhe Institute of Technology, Germany

As the legal requirements for particle emissions from vehicles are more and more tightened, a detailed understanding of the processes leading to formation, growth and oxidation of soot in combustion systems is required. Therefore, the application of detailed, kinetic soot models in multidimensional CFD simulations is needed. Such computations can be conducted using Eulerian approaches like moment methods, where the high-dimensional populance balance equation is tranformed to moment equations, which can be closed using the Quadrature Method Of Moments(QMOM) approach. QMOM provides an accurate description of the moments of the particledistribution for a univariate model description, where the particles are considered to be spherical. However, since soot particles are known to build aggregates, a univariate description is not sufficient to describe the shape of the particles accurately. Recently, a numerically robust, multivariate

QMOM method called ‘Conditional Quadrature Method of Moments (CQMOM)’ was developed and applied to model TiO_2 particle formation in flames. It is within the scope of this study to transfer and apply this framework to modeling the soot particle evolution in flames using a detailed, kinetic soot model. The emphasis of this work is twofold. First, it is shown, that the widely-used phenomenological soot model, which considers the processes of nucleation, coagulation, condensation and HACA surface growth, is able to predict the particle population in fuel-rich premixed flames with different equivalence ratios accurately. Therefore, three fuel-rich, burner-stabilized laminar premixed $\text{C}_2\text{H}_4/\text{O}_2/\text{Ar}$ flames with $\Phi=2.07\text{--}2.31$ are investigated both numerically and experimentally. The simulations are carried out using a 1D-Monte Carlo tool, which enables both a pure spherical as well as an aggregation view of the particles. The measurements are conducted using a flat flame burner with *in situ* probe sampling and a gas conditioning system for online measurement of soot particle size distributions with an Scanning Mobility Particle Sizer (SMPS). The results show, that the process of aggregation is a determining effect, especially at high equivalence ratios. Therefore, aggregation needs to be considered in the soot model and bivariate approaches like CQMOM are needed. The second aim of the study is the application and validation of the bivariate soot model within a CQMOM framework. In order to validate the CQMOM approach, the results are compared to the Monte Carlo predictions for the simulation of the three above mentioned flames. A 1D version of the inhouse CQMOM soot solver is used to enable a comparison with the Monte Carlo tool. The results show, that CQMOM is able to predict the soot volume fraction as well as the total surface of the soot particles with the same accuracy as the Monte Carlo tool, small differences are found for the total number density. Therefore, the numerically stable, multivariate Eulerian CQMOM method is found to be a feasible approach to model soot ensembles in CFD combustion simulations in an efficient and accurate way.

steffen.salenbauch@iec.tu-freiberg.de

W4P118 SOOT INTERNAL NANO-STRUCTURE AND ITS EFFECTS ON SOOT SURFACE REACTIVITY AND TRANSITION FROM COALESCENCE COLLISIONS TO AGGLOMERATION

Mohammad Reza Kholghy, Murray Thomson, University of Toronto, Canada

Soot is usually an undesirable product of combustion which has adverse environmental and health effects and it is produced from the combustion of hydrocarbon fuels. Soot formation starts with inception, which is the appearance of the first nano-scale soot particles. The newly incipient soot particles grow through surface growth via surface chemistry and Polycyclic Aromatic Hydrocarbons (PAH) condensation, and through particle coagulation and coalescence. Finally, the soot particles lose mass and size during oxidation and fragmentation processes. Surface reactivity of soot particles and transition from coalescent collision to agglomeration for the primary particles are two important factors in the process of soot formation that significantly affect the soot particle size distribution. The reactivity of surface sites reduces with increasing particle growth or age and is called soot surface aging. Many researches have tried to relate surface aging to temperature, curvature radii of the soot graphene layer, or soot lifetime and have proposed empirical relations but no fundamental physical relation has been proposed yet. Also, transition from coalescent collision to agglomeration for the primary particles is the second least understood step in the soot formation process. Coalescent or non-coalescent collisions and their interplay with soot surface growth also affect the size distribution and the nanostructure of soot primary particles. In this study, both soot aging and transition from coalescence collision to agglomeration are described based on the internal nanostructure of soot primary particles. It is assumed that incipient soot particles are composed of randomly oriented PAH stacks with up to four PAH layers. The equilibrium configuration of the stacks in the soot primary particle is a strong function of the temperature. At low temperatures surface PAH stacks are oriented in an edge-on-surface configuration which causes abundant hydrogen atoms on the soot surface resulting in high surface reactivity. It is proposed that this configuration also enhances the strength of adsorptive bonds formed by the adsorption of PAHs on the surface of incipient soot primary particles. As the temperature increases and soot particles age, PAH stacks on the surface move to realign in the face-on-surface configuration which results in the formation of outer graphene layers or outer shell in the soot primary particle. The face-on-surface configuration significantly reduces the number of hydrogen atoms on the surface of mature soot particles which results in lower surface reactivity for mature soot primary particles. It is proposed that the transition from coalescence collisions to agglomeration can also be explained by the formation of the outer shell in soot primary particles. The formation of the outer graphene layer shell in soot primary particles can be interpreted as the point of transition from coalescence collision to agglomeration as it gives structural stability to the primary particles and increases coalescence time constant.

mrk6785@gmail.com

W4P119 A STUDY OF SOOT PROPERTIES AT DIFFERENT STAGES IN THE SOOT FORMATION PROCESS IN PREMIXED ONE-DIMENSIONAL FLAT FLAMES BY LASER HEATING AND LIGHT SCATTERING

Nils-Erik Olofsson, Johan Simonsson, Sandra Török, Henrik Bladh, Per-Erik Bengtsson, Lund University, Sweden

Laser-Induced Incandescence (LII) is a laser-based diagnostic technique for measurements of soot particles. It enables evaluation of soot particle sizes, soot volume fractions and soot optical properties. The basic principle of the technique is rapid heating of soot particles up to about 4000 K using pulsed laser light, leading to an increased incandescence due to the increased temperature. By detecting this incandescence increase and the subsequent decline, when the particles cool down, it is possible to evaluate the aforementioned soot properties. When performing LII measurements and evaluations there are several different factors affecting the results and thus it is important to try to take these factors into account. In this work the heating and sublimation effects of the LII laser pulse on soot at different heights in the soot growth region of premixed ethylene/air flames ($F=2.1$ and $F=2.3$) have been studied by combination of LII and Elastic Light Scattering (ELS). By using an Nd:YAG laser at 1064 nm for LII and another Nd:YAG laser at 532 nm for ELS, and intersecting the laser beams in the probe volume, the ELS could be utilized to probe heating and sublimation effects of soot as a result of being exposed to the 1064 nm laser light. To generate the sooting flames a McKenna burner was used, producing premixed flat flames where the soot growth could be followed from nascent soot particles close to the burner surface to more mature soot higher up in the flame.

Results show significant differences as function of Height Above Burner (HAB), where the newly formed soot particles low in the flame require a higher laser energy to get vaporized than the more mature soot higher up in the flame. A possible explanation for this behavior is varying absorption properties of the particles as function of height. These properties are given by the soot absorption function, $E(m)=-\text{Im}[(m^2-1)/(m^2+2)]$, where m is the complex refractive index of the soot matter. Evaluating the $E(m)$ from the experimental data results in an increasing value of $E(m)$ with height in the studied flames. A clear difference is seen between the flames studied, where the leanest flame produces soot with lower $E(m)$, suggesting that $E(m)$ could be used as a measure of soot maturity. The magnitude of soot sublimation is estimated from the ELS measurements and the attained experimental results are compared to our LII model predictions. Additionally, 2-color pyrometry of the laser heated soot provides peak temperatures obtained during laser heating and analyzing these shows that the sublimation temperature of the soot is reasonably stable as function of height.

nils-erik.olofsson@forbrf.lth.se

W4P121 SOOTING TENDENCY OF SURROGATES FOR THE AROMATIC FRACTIONS OF DIESEL AND GASOLINE IN A WICK-FED DIFFUSION FLAME

Maria Botero, Markus Kraft, Sebastian Mosbach, Jethro Akroyd, University of Cambridge, United Kingdom

Aromatic species in commercial fuels are present in significant amounts, and this content can vary between 15-45% by weight depending on each country regulations. Being hydrocarbons that contain benzenoid rings, aromatics soot much more heavily than other types of hydrocarbons, particularly in non-premixed combustion. They are known to be important contributors to the formation of Polycyclic Aromatic Hydrocarbons (PAHs) which are well-known soot precursors. The sooting characteristics of pure substituted-aromatic fuels are studied in order to investigate the influence of their structure on the Particle Size Distribution (PSD). The aromatics were selected to be representative of those present in commercial fuels. The PSDs of soot formed using a non-premixed wick-fed burner were measured at the tip of flames of different heights, using a Differential Mobility Spectrometer (DMS). Temperature was measured using an ultrathin r-type thermocouple and a fast insertion technique. At the smallest flame height the PSD is bimodal with a slightly larger coagulation mode, except for TriMethylBenze (TMB) which exhibits a large nucleation mode. For larger flame heights the PSD is multimodal, as the coagulation mode enlarges and shifts to larger particle diameters. After the smoke point the PSD presents a single mode of particles with sizes of about 100 nm. Close to the smoke point, all fuels show a slight decrease in the rate of particle growth while the flame changes from having a closed tip to an opened soot trail. The two main modes in the PSDs were studied as a function of flame height. The mean particle diameter of the first mode increases rapidly to an approximately constant value of 20 nm for all fuels. The mean particle diameter of the accumulation follows the trend of the overall mean particle diameter. Tetralin produced the largest soot particles followed by toluene and TMB, ButylBenzene (BB) produced smallest. This evidence suggests that aromatics substituted with larger aliphatics tend to produce smaller soot particles.

mlb42@cam.ac.uk

W4P122 SOOT CHARACTERISATION OF *N*-HEPTANE/TOLUENE MIXTURES IN A WICK-FED DIFFUSION FLAME

Maria Botero, Sebastian Mosbach, Jethro Akroyd, Markus Kraft, University of Cambridge, United Kingdom

Commercial fuels are mixtures of hundreds of hydrocarbons. The high complexity of petroleum-based fuels encouraged the search for mixtures of limited components to ease the development of new combustion technologies through computational tools, and to generate insight and understanding of underlying fundamental processes. One of the simplest and most studied surrogate for both gasoline and diesel engines is the binary mixture of *n*-heptane and toluene. The sooting

characteristics of three mixtures of *n*-heptane/toluene (90/10, 70/30, 50/50 % v/v) are being studied in order to investigate the influence of the molecular structure on the Particle Size Distribution (PSD). Soot was sampled at the tip of laminar wick-fed diffusion flames of different heights. The flame height was adjusted by increasing the wick exposure, hence the fuel flow rate. The PSDs of soot were measured using a Differential Mobility Spectrometer (DMS). This is a fast particle analyser that enables the PSD to be measured in realtime. The particles are therefore sized based on their mobility diameter. From the PSD important quantities are calculated such as the total number of particles (N) and the mean particle diameter (\bar{d}). Centerline temperature measurements were performed with an uncoated 75 μm type R thermocouple (Pt/Pt-13%R), using a rapid insertion procedure to minimise soot deposition. The Smoke Point (SP), Threshold Sooting Index (TSI) are also measured.

mlb42@cam.ac.uk

W4P123 SOLID-LIQUID TRANSITIONS IN HOMOGENOUS OVALENE, HEXABENZOCORONENE AND CIRCUMCORONENE CLUSTERS: A MOLECULAR DYNAMICS STUDY.

Dongping Chen, Jethro Akroyd, Sebastian Mosbach, Markus Kraft, University of Cambridge, United Kingdom

In the present work the melting behaviour of ovalene ($\text{C}_{32}\text{H}_{14}$), hexabenzocoronene ($\text{C}_{42}\text{H}_{18}$) and circumcoronene ($\text{C}_{54}\text{H}_{18}$) clusters is analyzed using molecular dynamics simulations. It is found that the melting mechanism of these molecules obeys a liquid nucleation and growth model. The bulk melting point is estimated by linear extrapolation of cluster data. The value obtained from ovalene clusters is in good agreement with the phase-transition temperature determined by experiment. Combined with the bulk melting point of other Polycyclic Aromatic Hydrocarbons (PAH), we find that the bulk melting point of peri-condensed PAHs is linearly related to their size. A phase diagram is constructed which classifies the phase of a cluster into three regions, a liquid region, a size-dependent region and a solid region according to the size of the PAHs which build up the cluster. The size-dependent region highlights a range where the phase of a cluster also depends on the cluster size. A detailed investigation of the phase diagram reveals that the critical size for nascent and mature soot particles in the solid state is $\text{C}_{78}\text{H}_{22}$ and $\text{C}_{54}\text{H}_{18}$ at 1500K respectively.

dongping.chen516@gmail.com

W4P124 ADHESIVE AND ATTRACTIVE FORCES OF FLAME-FORMED CARBON NANOPARTICLES BY ATOMIC FORCE MICROSCOPY

Gianluigi De Falco¹, Mario Commiato², Patrizia Minutolo², Andrea D'Anna

¹Università degli Studi di Napoli Federico II, Italy ²Istituto di Ricerche sulla Combustione, Italy

Atomic Force Microscopy (AFM) is a well-known scanning probe technique, mainly used for its capability to achieve topographic images with subnanometer resolution. In addition to surface topographies characterization, AFM is also a powerful tool for sensitive force spectroscopy measurements. The forces acting between the AFM tip and the surface under investigation can be recorded during approach and retract of cantilever to and from the sample, and plotted as force-distance curves. From these measurements, short-range attractive and adhesive forces can be quantitatively evaluated. The purpose of this work is to study surface properties, i.e. van der Waals interactions and Hamaker constants, of different flame-formed nanoparticles as derived from AFM force-distance measurements. These properties are of fundamental relevance for a deeper understanding of the coagulation and coalescence phenomena between carbon particles occurring during soot growth process. To this aim, carbon nanoparticles were produced in fuel-rich ethylene/air laminar premixed flames with different equivalent ratios Φ , and analysed at fixed Height Above the Burner (HAB), namely 15 mm. Particles were collected on mica substrates by means of a thermophoretic sampling system and analyzed by AFM operating in contact and force spectroscopy modes. Attractive and adhesive forces between titanium nitride probe and collected particles were found to increase with flame equivalence ratio, moving from flame conditions, in which unimodal particles diameter distribution, with average size of 2-5 nm, are produced ($\Phi=1.85$), up to fully-sooting conditions ($\Phi=2.58$), in which 50-100 nm soot aggregates are mainly produced. Adhesive forces are 5-7 times greater than attractive forces in the same conditions. This is evidenced by the fact that particle deformation and bonding with AFM tip occurring during contact results in a curve-distance hysteresis contribution. The measurement of the attractive force by the AFM force-distance curve allowed the evaluation of the Hamaker constant for the different carbon particles, assuming that van der Waals forces are the main contribution to the attractive forces. By means of the van der Waals theory for sphere-flat surface and sphere-sphere interaction, the Hamaker constants were derived as a function of both the particle equivalent diameter as evaluated from AFM images and flame equivalence ratio. Highly-Ordered Pyrolytic Graphite (HOPG) was used as reference material.

gianluigi.defalco@unina.it

W4P125 OPTICAL PROPERTIES OF MATURE SOOT

Elizabeth Rieken¹, Hope Michelsen², Ronald Hanson¹

¹Stanford University, United States ²Sandia National Laboratories, United States

In order to make accurate optical measurements of soot for combustion and atmospheric applications, we require knowledge of soot optical properties such as absorption cross-section. Soot has a non-spherical morphology as well as a changing composition and fractal dimension over time that make it complicated to determine accurate optical property values. We are interested in understanding how absorption and scattering cross-sections vary with wavelength and temperature. We made Laser Induced Incandescence (LII) and transmittance measurements of mature soot in a laminar diffusion flame. Mature, combustion-generated soot particles are made up of small primary carbon spheres, 10-50nm in size that are held together by covalent bonds forming branched-chain aggregates. We measured the absorption and scattering of the particles at 532nm and 1064nm excitation wavelength at a range of laser fluencies. The experiment was repeated, first using a Santoro burner, and then using a Gulder burner to generate the flame. We are interested in comparing the relative absorption cross-section and single-scattering albedo values obtained from analyzing the absorption and scattering data from each burner.

bethrieken@stanford.edu

W4P126 LARGE-EDDY SIMULATION OF PARTIAL OXIDATION REFORMING OF TAR IN SYNGAS FROM WOODY BIOMASS USING FLAMELET MODEL

Noriaki Nakatsuka¹, Hiroaki Watanabe², Ryoichi Kurose³

¹Osaka University, Japan ²Central Research Institute of Electric Power Industry, Japan ³Kyoto University, Japan

In terms of achieving propagation of distributed electric power generation systems, small gas engines are needed as the energy conversion system. Tar reforming technology in gas reformers is essential for the gas engines. Partial oxidation gas reforming system is regarded as one of attractive gas reforming systems. In a gas reformer by using partial oxidation method, tar in a syngas from woody biomass gasification is reformed by oxidative and thermal cracking by partial combustion of the syngas in the gas reformer, an apparatus stage subsequent to the biomass gasifier. Inverse diffusion flame is formed when the oxidizer is supplied to the syngas, during partial oxidation process of the syngas. Cracking and polymerization of the tar occur simultaneously at proximity of the inverse diffusion flame. The numerical study have been performed to clarify the spatial distribution of tar reforming region, tar polymerization region and soot formation region by applied large-eddy simulation and flamelet model. In the present work, toluene, a single-ring aromatic hydrocarbon is supplied as a model tar. Tar reforming process is defined as cracking of toluene and benzene into aliphatic hydrocarbons. On the other hand, tar polymerization process is defined as chemical reactions of single-ring aromatics into 2-ring aromatics and 2-ring aromatics into 3-ring aromatics. The gas phase reaction mechanism by Narayanaswamy et al. [Combustion and Flame, 157, 2010] are introduced in the elementary reaction analysis in the flamelet library namely lookup table for the flamelet model in the present work. The main results are as follows. Flame length was determined by spatial distribution of CH radical mass fraction. Reaction rates per unit flame length of dominant cracking and polymerization of tar were calculated, respectively. Though reaction rates per unit flame length of dominant cracking of tar were dramatically small in the post flame region compared to the flame region, reaction rates per unit flame length of dominant polymerization of tar in the post flame region were comparative to that in the flame region. In addition, reaction rates per unit flame length of dominant cracking of tar were at least 10 times larger than that of dominant polymerization of tar.

nakatsuka@combu.mech.eng.osaka-u.ac.jp

W4P127 COMBUSTION AND SECTIONAL SOOT MODELING FOR SPRAY SIMULATIONS

Damien Aubagnac-Karkar, Olivier Colin, IFPEN, France

Soot particles are formed during the combustion of hydrocarbon/air mixtures in most combustion devices related to transportation. Even if Diesel engines are today equipped with particle filters, being able to predict soot particles number and size is still important to car manufacturers. Indeed, some emitted particles are small enough to get through particle filters and these particles are now taken into account by norms on the number of particles emitted. In this context, experimental and numerical tools to predict Soot Volume Fraction (SVF) and Soot Number Density Function (SNDF) in Diesel engine conditions are required. The closest academical set-up to these conditions is high-pressure sprays which can be measured with more accuracy than engine cases in order to compare experiments with simulations. The Engine Combustion Network (ECN) proposes a set of sprays whose conditions have been chosen in order to reproduce Diesel ones. The Spray A is the reference spray so far obtained in terms of fuel (*n*-Dodecane) and thermodynamic conditions. A set of parametric variations have been ran with state-of-the-art instrumentation, including soot volume fraction measurement, on this single hole injector spray. They offer a large enough panel of cases to validate combustion and soot models in an academical set-up close to the real conditions of Diesel engines.

Therefore, Spray A simulations have been ran testing the ability of combustion and soot models to predict the spray behavior. Two combustion models have been used, ADF-PCM and ECFM3Z-VPTHC. They are both based on the same homogeneous constant pressure reactors tabulation method but the ADF-PCM approach includes effect of stretch not taken into account in the ECFM3Z-VPTHC approach and it also considers a continuous mixture fraction distribution while this distribution is only represented by 3 Dirac delta functions in the ECFM3Z-VPTHC approach. These difference's allow an evaluation of the two more phenomena modeled in ADF-PCM effects compared to the higher cost in memory required by ADF-PCM tables. These combustion models have been coupled to a sectional soot model specifically developed for 3D-Diesel simulations. It accounts for inception, condensation, surface growth, coagulation and oxidation processes and directly predicts the SVF and SNDF at each time and location. By comparing them to the experimental data provided by the ECN, the simulations ran with these models will give information on the ability to predict diffusion flame structure in a Diesel spray as well as soot mass or volume fraction location. They will also offer a first numerical prediction on the SNDF in this type of spray which might be compared with some sample taken during the experiments.

Damien.aubagnac@gmail.com

W4P128 THE EFFECT OF ETHANOL ADDITION ON POLYAROMATIC HYDROCARBON FORMATION INVESTIGATED THROUGH DETECTION OF NATURALLY OCCURRING IONS IN FLAMES

Tina Kasper¹, Thomas Bierkandt¹, Denis Knyazkov², Oleg Korobeinichev², Erdal Akyildiz¹

¹University of Duisburg-Essen, Germany ²Institute of Chemical Kinetics and Combustion, Russia

Charged species exist in many gaseous reactive systems and are also formed in combustion systems. Measurement of flame ions is used in analytical applications, e.g. flame-ionization detectors or as a means to monitor motor operation. Especially, laminar premixed low-pressure flames are suited to investigate chemical processes of ion formation in flames. PAHs are considered soot precursors and hazardous emissions of combustion devices. The presence of positive ions of Polyaromatic Hydrocarbons (PAHs) in flames, formed mostly through chemi-ionization reactions, provides the opportunity to perform quantitative measurements of concentrations of ionized PAHs in flames under well-controlled conditions using time-of-flight mass spectrometry without preceding ionization step. Since the concentrations of ions are closely related to the concentration of the corresponding neutral species, the ion profiles can be used as vehicles to investigate the formation of neutral PAHs in flames. For example, the influence of the additive on PAH ion concentration provides a very sensitive way to measure changes on species composition when ethanol is added to hydrocarbon fuels. Ethylene/O₂/Ar and ethylene/ethanol/O₂/Ar were investigated. The stoichiometry of 1.8, pressure of 130 torr, and the total flow rate (4slm) were kept constant in order to be able to reveal the effect of ethanol addition to the ethylene flame adequately. The flames were stabilized on a home-built McKenna-type burner. Ions from the flames were sampled by a Hastelloy skimmer and were transferred through three differentially pumped consecutive chambers (Fasmatech ion transfer system) into an orthogonal reflectron Time-Of-Flight (TOF) mass analyzer (Kaesdorf). A +300 V potential was applied to the skimmer and burner to sample ions and avoid an electrical potential gradient in the flame. The ion transfer system was used to measure positively charged species as a function of distance from the burner in a neat ethylene flame and a mixed flame with ethanol. The presence of many naturally occurring ions up to 520 atomic mass units was observed. Among the detected and identified species are typical flame ions such as propargyl and allyl ions, H₃O⁺ ions, hydrated clusters, polyyne, and PAH ions. The experimental results show a strong dependency of ion signals on the distance from the burner. These height profiles have the expected form for most positive ions, including PAHs. It is seen that the replacement of half of the ethylene fuel with ethanol reduces the PAH signal intensities significantly in agreement with earlier findings. The relative concentrations of the predominately observed species are in good agreement with the abundances of ions reported for the exhaust gas of fuel-rich hydrocarbon flames in the literature. This observation hints that C₁₃H₉⁺, C₁₉H₁₁⁺ and C₂₇H₁₃⁺ ions are particularly stable at high temperatures and survive collisions in the ion transfer system intact. To convert integrated mass peak intensities to absolute ion concentrations, the total ion current in the molecular beam just beyond the skimmer was measured using a Faraday cup. In addition, the main species profiles in the flame were determined by sampling the neutral gases through the ion transfer system and ionizing with a filament at the entrance to the TOF. The profiles of fuel, O₂, Ar, H₂, H₂O, CO, CO₂, C₂H₂ and C₄H₂ were quantified using literature cross sections and show good agreement with chemical kinetic simulations of the flames. The data obtained within this work can aid the development and validation of chemical kinetic mechanisms for PAH formation in hydrocarbon flames because of their sub-ppb sensitivity towards PAH ions that provides access to species which are difficult to measure in other experiments.

tina.kasper@uni-due.de

W4P129 EFFECT OF WATER MIST ADDITION ON AGGREGATION OF PM FROM A DIFFUSION FLAME

Yoshihiro Kobayashi, Tokyo Denki University, Japan

Nanometer size Particulate Matter (PM) emission exhausted from combustion equipment is concerned about human health, and its reduction from burned gas stream is strongly required. In order to remove nano-PM from burned gas stream, after-treatment technologies of PM size and number control should be established. In this study, PM aggregation technology in high humidity field was attempted by means of water mist addition. PM exhaust from a laminar diffusion flame formed on a small pool of benzene (C_6H_6) was used for test sample. Size distribution and mass of PM were measured by a Scanning Mobility Particle Sizer (SMPS3936, TSI Inc.), a Low Pressure Impactor (LP-20, Tokyo Dylec Corp.) and filter method. Water mist of which peak diameter was around 10 micro-meters was co-flowed and mixed with burned gas stream containing PM. As for the PM from benzene flame, PM diameter corresponding to a peak number concentration existed within a range of 200nm – 300nm and its number was around $4 \times 10^7 \text{ \#/cm}^3$. Number of PM mixing with water mist decreased to around $1 \times 10^6 \text{ \#/cm}^3$, however its diameter range shifted from nano-meter range to micro-meter range over 5 micro-meters. This diameter shift was confirmed by the LP-20 that had wide measurable range of particle diameter. Moreover, PM captured on glass-fiber filter showed that moisture of water-mist-treated PM was extremely higher than non-treated PM. From this result, it was considered that PM aggregation with water mist was the main reason of peak diameter shift mentioned above.

ykoba@mail.dendai.ac.jp

W4P130 SEMI-VOLATILE NANOPARTICLE NUCLEATION AND GROWTH IN LOW TEMPERATURE COMBUSTION EXHAUST

Will Northrop, Glenn Lucachick, University of Minnesota, United States

Low Temperature Combustion (LTC) is a category of engine operational strategy that uses a primarily premixed charge with high levels of dilution to avoid in-cylinder formation of NO_x and soot. A key disadvantage of LTC is increased HydroCarbon (HC) emissions compared to more Conventional Combustion (CC) in diesel engines due to over-lean mixtures and low temperature regions in the combustion chamber. HCs found in LTC exhaust consist of partially reacted volatile organics, unburned fuel and lubricating oil, and combustion-derived semi-volatile species like polycyclic aromatic compounds that have higher molecular weight than the original fuel. In practice, low engine exhaust temperature and high CO concentrations resulting from LTC may potentially inhibit conversion of the aforementioned compounds within an oxidation catalyst meant to eliminate them. This poster presents our work investigating the nucleation and growth of semi-volatile HCs from LTC into nanoparticles upon primary dilution with air. Semi-volatile species of interest for nucleation cover a wide range of volatilities, with a significant portion having volatility sufficiently low to form particles. We have shown in previous work that while the mass concentration of nanoparticles from LTC has a significant dependence on dilution temperatures, LTC particle number concentrations show extreme sensitivity to dilution conditions. This manifests as high concentration of nucleation mode ($D_p < 50 \text{ nm}$) particles forming under cool dilution conditions, and are absent under warm dilution conditions. In CC exhaust, accumulation-mode particles comprised of soot agglomerates serve as absorption sites for semi-volatile material as it converts from gas to the particle phase. Because solid agglomerates are mostly absent from LTC, formation of large quantities of nucleation-mode particles is further enhanced. Our recent results have shown that particles from LTC are sensitive to dilution conditions due to their volatility, but that their volatility is highly dependent on particle size. This suggests that different mechanisms are influencing particle formation and opens the door for new hypotheses to explain measured nanoparticle concentrations. One such hypothesis is that low concentrations of extremely low volatility material form the nucleus for growth and thus a site for heterogeneous nucleation of lower volatility species. Our research activities include the implementation of techniques such as Tandem Differential Mobility Analysis (TDMA) to investigate particle volatility as a function of particle size. Preliminary work has shown that TDMA in combination with an evaporation model is effective for estimating composition as a function of radial position within the particle. Further development of these techniques is necessary to further the understanding of LTC particle formation, and to improve regulatory particle measurement practices.

wnorthro@umn.edu

W4P131 A NUMERICAL STUDY ON THE SENSITIVITY OF LARGER POLY-AROMATIC HYDROCARBONS IN NUCLEATION PROCESSES OF SOOTING FLAMES

Prabhu Selvaraj¹, Paul Arias¹, Yang Gao², Sungwoo Park¹, Hong Im¹, Mani Sarathy¹, Tianfeng Lu²

¹King Abdullah University of Science and Technology, Saudi Arabia ²University of Connecticut, United States

Soot particles are considered to be a major pollutant that constitutes a health hazard and serious global environmental effects. In an effort to mitigate pollutant formation, it is important to develop computational models that capture the soot formation behavior. An improved chemical mechanism, which includes detailed Polycyclic Aromatic Hydrocarbon (PAH) species growth up to coronene ($C_{12}H_{24}$), is used to study soot formation characteristics for a range of flame condition. As a first step in the validation of a sophisticated model for use in direct numerical simulation the chemical mechanism is

reduced using Directed Relation Graph (DRG) from 397 to 97 species. Our study seeks to understand the sensitivity on soot formation characteristics by the choice of nucleation model. Preliminary results show that the higher PAH concentrations result in higher soot nucleation rate in the counter flow diffusion flames. The numerical simulation predicted that the average size of the particles in both pure fuel and the mixing cases were similar, which is in agreement with experimental results. Consequently, the mass fraction and number density of soot also shows to be consistent with numerical results with the full chemical mechanism.

prabhu.selvaraj@kaust.edu.sa

W4P132 SOOT FORMATION IN A LAMINAR ETHYLENE DIFFUSION FLAME

Edward Yapp¹, Markus Kraft¹, Jethro Akroyd¹, Sebastian Mosbach¹, Anthony Knobel¹, Alastair Smith¹, Dongping Chen¹, Erin Adkins², Houston Miller²

¹University of Cambridge, United Kingdom, ²George Washington University, United States

A detailed population balance model is used to investigate soot formation in a laminar ethylene co-flow diffusion flame. The model incorporates the aggregate structure of particles and includes detailed compositional knowledge of the individual primary particles that constitute an aggregate. It thereby extends the range of comparisons that can be made with experimental measurements. A parametric sensitivity study on the computed soot volume fraction was performed and was found to be most sensitive to the growth factor, the reduced rate at which PAHs within particles grow. It had a more pronounced effect on soot formed in the wings than on the centerline. A small growth factor in the range of 3 to 10 % resulted in qualitative agreement in the soot volume fraction. Soot formation on the centreline and in the wings of the flame was also studied using transmission electron microscope-like projections of aggregates. Two different growth mechanisms were identified where soot particles formed on the centreline were made up of a larger number but smaller primaries than in the wings, consistent with experimental observations. Computed C_xH_y (x = 6 to 42 and y = 6 to 16) structures within particles were compared to the most thermodynamically stable aromatics (stabilomers) and a good correspondence was found. While some of the comparisons between numerical simulations and experimental data were satisfactory, the results of this study shows that further work is required to improve the soot chemistry model, particularly the oxidation rates on different surface site types.

ekyy2@cam.ac.uk

W4P133 PRODUCTION AND OXIDATION OF CARBON PARTICLES USED FOR A SOLAR ABSORPTION MEDIUM

Lee Frederickson¹, Fletcher J. Miller¹, Mario Leoni²

¹San Diego State University, United States ²ETH Zurich, Switzerland

Current research at San Diego State University is underway to develop a high temperature solar receiver which will utilize small (sub-micron) carbon particles mixed with air as a solar absorption medium. The receiver is designed to be installed in a Brayton cycle and situated in a concentrating solar power field. Compressed air from the compressor is mixed with the carbon particles and sent to the windowed receiver where the particles absorb incident radiation, heating the air, and eventually oxidize prior to leaving the receiver. The gas stream is sent to a high-temperature combustor for additional heating (if needed), and then enters a conventional gas turbine to produce power. Although the process is predominantly driven by solar energy, combustion enters into three important areas: carbon particle production before the receiver, particle oxidation in the receiver, and high temperature air combustion in the combustor. This poster will discuss the first two of these processes. To produce the absorbing medium for the solar receiver, a lab-scale Carbon Particle Generator (CPG) has been designed, built, and tested. The CPG is a heated ceramic tube reactor with a constant wall temperature above 1100°C at 6 bar pressure. A mixture of natural gas and nitrogen is fed to the CPG where the natural gas undergoes pyrolysis resulting in carbon particles. This gas-particle mixture is met downstream with dilution air and an extinction tube is used to measure the opacity of the mixture. The particles in the mixture are also analyzed by Scanning Electron Microscopy (SEM) and a Diesel Particulate Scatterometer (DPS) to measure particle size distribution. To predict carbon particle yield and general trends such as mean particle size, a model has been setup in Reaction Design CHEMKIN-PRO software to which our experimental data are compared.

For determining particle oxidation rates, a separate oxidation experiment has been set up. This consists of a tube furnace with extinction tubes upstream and downstream of the furnace. During testing, the CPG outlet mixture is fed to the tube furnace where the tube wall temperature is controlled and monitored. The extinction tube measurements combined with Mie Theory are used to determine inlet and outlet mass loading, which can be used to calculate the oxidation rate based on wall temperature and residence time in the furnace.

The goals of this research are to accurately measure the particles being produced by pyrolysis, model the performance of the CPG, determine oxidation rates with various particle sizes, and adjust operational parameters to obtain the optimum particles for the solar receiver.

lfrederi@rohan.sdsu.edu

W4P134 AN EXPERIMENTAL AND MODELING STUDY OF SOOT FORMATION IN PROPENE FLAMES

Chiara Saggese¹, Joaquin Camacho², Tiziano Faravelli¹, Hai Wang²

¹Politecnico di Milano, Italy ²Stanford University, United States

Nascent soot formation in premixed ethylene flames have been examined extensively over the past two decades. In contrast, very few studies have been performed for propene flames. Because of the subtle differences in the fuel structures between ethylene and propene, different pathways to aromatics and hence different rates to aromatic growth are expected. The fuel structure difference can impact the nucleation rate of soot and its subsequent mass and size growth, and such effect remains un-explored for premixed flames. The aim of this work is to investigate experimentally the time evolution of the Particle Size Distribution Function (PSDF) in a Burner-Stabilized Stagnation (BSS) propene flame at the ambient pressure. The well-defined boundary conditions allow the flame to be simulated with minimal probe effect. Experiments are carried out under conditions similar to the previous studies on ethylene BSS flames. The flame structure and soot formation is simulated using the recently advanced model developed by the group of Politecnico di Milano. Gas-phase kinetics involves the formation of Polycyclic Aromatic Hydrocarbons (PAHs) from the first aromatic ring to large PAHs (C₂₀H₁₆ and C₂₀H₁₀).

The lumping approach, extensively used in kinetic modeling of large hydrocarbon species, is used here to describe the gas-surface reactions and is a necessity in modeling heterogeneous reaction kinetics of soot surface growth. Analogy and similarity rules are employed to describe the surface reaction kinetics using known kinetic rates of gas-phase species. A discrete sectional method is employed to solve the time evolution of the particle size distribution function. Comparisons between the experimental data and model predictions permit us to investigate and understand the PSDF data more in detail and help to refine and validate the soot model.

chiara.saggese@polimi.it

W4P135 SIZE EVOLUTION OF SOOT FORMED IN PREMIXED C₆ HYDROCARBON FLAMES

Joaquin Camacho¹, Hai Wang¹, Sydnie Lieb¹

¹Stanford University, United States ²University of Southern California, United States

Nascent soot was examined in premixed Burner Stabilized Stagnation (BSS) flames of *n*-hexane, *n*-hexene, 2-methylpentane, cyclohexane, and benzene-oxygen-argon mixtures at a fixed carbon-to-oxygen ratio of 0.69 and maximum flame temperature of 1800 K. The evolution of the Particle Size Distribution Function (PSDF) was measured from the onset of nucleation to a later stage of growth by mobility sizing. Comparison of the PSDFs shows that qualitatively, the overall sooting processes of these flames are similar. However, the time to nucleation and the persistence of nucleation was strongly dependent on the structure of the parent fuel. For the given conditions, the fastest onset of soot nucleation was observed in flames of cyclic hydrocarbon fuels, including cyclohexane and benzene. This observation is consistent with the faster aromatics formation expected for these parent fuels. At the same time and as evidenced by the disappearance of nucleation-size particles, soot nucleation in cyclohexane and benzene flames ended sooner than in flames of non-cyclic hydrocarbon fuels. Fuel specific chemistry in cyclic hydrocarbon-fuel flames may contribute to the later depletion of soot nuclei by causing earlier particle formation and growth which subsequently allows for greater scavenging of soot precursors by the particle surface. The morphology of nascent soot was also examined by Atomic Force Microscopy (AFM) and the assumption of spherical nanoparticles which is typically taken in soot mobility studies was found to be invalid for nascent soot with effective D_p > 5nm. The morphology of soot aggregates from later stages of the *n*-hexane and benzene flames was also observed by AFM and the disappearance of nucleation size particles has no significant impact on the overall soot aggregate nanostructure.

jocamach@stanford.edu

W4P136 EXTINCTION MEASUREMENTS FOR DETERMINATION OF OPTICAL BAND GAPS FOR SOOT IN NITROGEN-DILUTED, ETHYLENE/AIR NON-PREMIXED FLAMES

Erin Adkins, Houston Miller, George Washington University, United States

Visible light extinction was measured in a series of nitrogen-diluted, ethylene/air, non-premixed flames and this data was used to determine the optical band gap, E_g, as a function of flame position. This work builds on recent Raman and Optical Band Gap (OBG) studies in our lab, which provided experimental support to the model of soot formation where the transition from chemical to physical growth starts with species with molecular masses of only several hundred Daltons. In the current study, light from a SuperContinuum light source is collimated, expanded, and directed into a monochromator. The dispersed light is split into a power metering channel and a channel that is periscoped and focused into the flame. The transmitted light is then recollimated before the detector. After tomographic reconstruction of the radial extinction field, the

OBG was derived from the near edge absorption feature using Tauc analysis. This approach was repeated through the full range of heights for four flames of varying dilution levels, from 32%Ethylene/68%Nitrogen to 80%-Ethylene/20%-Nitrogen.

An evolution in OBG was observed throughout all flame systems with a consistent range of OBG observed between approximately 1.9eV and 2.3eV. Averaging over all positions the average OBG was approximately 2.09eV for all flame systems. Comparing these results to previously published computational results from our lab relating calculated HOMO-LUMO gaps for a variety of D_{2h} PAH molecules to the number of aromatic rings in the structure, showed that observed optical band gap is consistent with a PAH of about 14 rings or a conjugation length of 0.96nm. This result agrees with the lower edge of the PAH sizes reported in our recent Raman work that suggest 1.0 – 1.2nm conjugation lengths. These results are consistent with PAH condensation beginning with species about the size of circumpyrene.

webster@gwmail.gwu.edu

W4P137 SOOT FORMATION IN NONPREMIXED BIODIESEL FLAMES

J.F. Correa-Pugliese, S. McCollam, W. Merchan-Merchan, University of Oklahoma, United States

We are reporting measured soot volume fraction profiles in coflow diffusion flames of vaporized Canola Methyl Ester (CME) and Soy Methyl Ester (SME) fuels. The soot volume fraction profiles are determined using the laser extinction technique. The effect of fuel blending on the formation of soot particulates was studied in flames formed using CME blended with No.2 diesel. The blends with diesel consist of 80% (B 80) and 50% biodiesel (B 50). The effect of oxygen content in the oxidizer stream on soot formation was also studied in the neat/blended fuels formed flames by varying the oxygen content from 21%, 35%, 50% and 80%. For the CME/air flame the maximum measured soot volume fraction peak (fv) was 4.07 ppm and was measured at the symmetry axis at a height above the burner Z=17.5 mm. For SME/air, the fv was measured to be 3.95 ppm at approximately the same flame height as the CME/air flame. For the B 100 (CME) oxygen enriched-air flames the peak values at 35%, 50% and 80% are 6.50, 5.82 and 3.22 ppm, respectively. It is observed that by increasing the oxygen content in the B100CME flame from 21% to 35% oxygen the fv peak increases by approximately 64 percent. However, a further increase in oxygen content in the oxidizer stream suppressed soot formation.

A similar trend in the fv is observed for B100SME oxygen-enhanced combustion flames. For the B80 (CME)/air and B50 (CME)/air flames the soot volume fractions were measured to be 4.32 ppm and 4.63 ppm, respectively. The addition of oxygen content in the oxidizer stream in these blended fuels flames (from air to 35% O₂) resulted in an increase in the fv peak of approximately 47 and 70 percent, respectively. Temperature measurements were also conducted along the symmetry axis of selected flames at different heights.

wmerchan-merchan@ou.edu

W4P138 ANALYSIS OF SOOT MORPHOLOGY IN A CO-FLOW NONPREMIXED METHANE OXY-FLAME

J.F. Correa Pugliese, A.D. Ngo, D. Orr, W. Merchan-Merchan, University of Oklahoma, United States

The experimental study of soot morphology is performed in a co-flow flame formed using methane as the fuel and 100% oxygen as the oxidizer. High oxygen content (100%) in the oxidizer significantly altered the flame structures, compressing the flame volume. Soot samples were collected directly from inside of the compressed flame volume using thermophoretic sampling. The evolution of soot formation (particle diameter, degree of agglomeration, and soot microstructure) was observed in the narrow range of the flame volume through the application of special transmission electron microscope grids. Scanning electron microscope imaging analysis collected from samples extracted at various locations on the axial flame height show that the particles are approximately spherical with a nearly monodisperse distribution in the upper zone of the flame. HR-TEM was employed to study the internal structure of the soot. Although previous experiments have been conducted for studying the soot morphology (degree of particle agglomeration, nanostructure and diameter size) in co-flow oxygen-enhanced flames, this is the first work to study the soot formation in a methane co-flow oxy-flame.

wmerchan-merchan@ou.edu

W4P139 THE ROLE OF ALKYL AROMATICS ON PARTICLE FORMATION IN DIFFUSION FLAMES

Marielena Contorso, Mariano Sirignano, Andrea D' Anna, Università degli Studi di Napoli Federico II, Italy

Aromatic hydrocarbons are important constituents of engine fuels: they are used as anti-knock additives to enhance the octane number, to suppress auto-ignition and to increase the energy density of transportation fuels. However, they play an important role also in soot formation being possible precursors of PAHs. In this poster we present an experimental study on the formation of particulate matter from the combustion of blends containing four C₈H₁₀ isomers (ethyl benzene, orto-,

meta- and para-xylene) and three C₉H₁₂ isomers (cumene, *n*-propyl benzene and mesitylene) which are characterized by the presence of one aromatic ring with different positions and lengths of the alkyl chain. Counter-flow diffusion flames with ethylene/alkyl-aromatic blend as fuel stream have been studied by *in-situ* spectroscopic techniques (laser induced emissions) and then compared to the ethylene/toluene flame to understand the effect of alkyl chain position and length on the particulate formation. The analysis of spectral emission from the flames allows distinguishing between laser induced fluorescence, associated to PAHs and nanoparticles, and laser induced incandescence, associated to large soot aggregates.

The flame configuration chosen for this study better allows the investigation of the nanoparticles and soot profiles along the flame with respect to co-flow flames employed in the earlier studies about the sooting tendency of aromatic hydrocarbons. Also the percentage of aromatic used in this study reaches values of molar fraction as high as 3%, similar to those found in real fuels.

The experimental results show that the presence of a long side alkyl chain, such as in ethyl benzene, cumene and *n*-propyl benzene, promotes a larger formation of PAHs and nanoparticles probably because radical attack is facilitated with respect to the presence of single methyl groups; also the presence of three single methyl groups promotes a larger formation of PAHs and nanoparticles with respect to alkyl aromatics with two methyl groups. Among the xylenes, the orto- position allows the largest nanoparticles production by a faster ring closure with respect to meta- and para- configurations. This behaviour is similar in both pyrolytic and oxidative conditions encountered in the counter-flow flame configuration.

Looking at the sooting tendency of the investigated hydrocarbons, in the pyrolytic and oxidative region of the flame there are not evident changes in soot production for the xylenes, while mesitylene gives a contribution similar to that of xylenes. When ethylbenzene, cumene and *n*-propylbenzene are used a stronger effect is found. Also for soot, the presence of a single side chain is more effective with respect to the presence of single methyl groups.

marielena.conturso@unina.it

W4P140 CARBON PARTICLE BEHAVIOR IN FLAMES EXPOSED TO AN ELECTRIC FIELD

Jesse Tinajero, Derek Dunn-Rankin, University of California, United States

When placed within an electric field, a flame acts as an ion source, where charged particles are forced to traverse away from the reaction zone and towards the electrode of opposite polarity. These charged particles consist of positively charged chemi-ions and electrons, and the flux of charged particles generates an ion-driven wind as they collide with neutral molecules in the electrode space region. Carbon particles have been seen to acquire a positive charge even in the absence of an electric field. Thermionic emission is thought to be the best explanation of this. Some interesting effects occur when a flux of charged particles is present in the pyrolysis zone where soot production occurs. These effects include a reduction in particle size and a reduction in rates of formation and deposition. The effects vary based on the polarity of the flux and electric field strength. The transient response of flame properties related to carbon particle formation is the focus of this study. High speed videos capture the disappearance of the luminous, sooty region of the flame after a sudden exposure to a flux of positively charged ions. The timescale of this disappearance is approximately 300ms for the small flames studied. This disappearance time is significantly slower than the timescales related to the generation of an ion flux and an ion-driven wind (10ms and 100ms, respectively). This difference suggests that the positive ion-driven wind is producing a change in the overall combustion environment to reduce soot. When the pyrolysis zone is suddenly exposed to a flux of negative charges (electrons), however, the disappearance of the sooty region occurs in half the time it takes to generate an ion-driven wind, suggesting that the charged particles may have some direct effect. This poster helps describe the possible mechanisms behind these flame carbon related timescales.

jatinaje@uci.edu

W5P001

DNS OF A LEAN PREMIXED CH₄-H₂/AIR SLOT FLAME

Donato Cecere, Eugenio Giaomazzi, Franca Rita Picchia, Nunzio Maria Salvatore Arcidiacono
Italian National Agency for New Technology Energy and Sustainable Economic Development, Italy

Direct Numerical Simulation of a three-dimensional spatially developing turbulent slot CH₄-H₂/Air premixed flame has been performed with a detailed kinetic mechanism. The compressible code solves the 3D Navier-Stokes equations, species and energy conservation with a compact sixth order staggered finite difference scheme in space and an explicit third order Runge-Kutta in time. The mean and fluctuating velocity profiles of the reactant jet, assigned by means of Klein procedure, are 100 m/s, and 12 m/s respectively, leading to a turbulent Reynolds number of 95. The central reactant jet was chosen to be a premixed CH₄-H₂/Air flow at equivalence ratio of 0.7 with molar fractional distribution of 20% H₂ and 80% CH₄ surrounded on both slot sides by a heated coflow, whose composition and temperature are those of the complete combustion products. The effects of flow straining and flame front curvature on the mean flame morphology are quantified through conditional mean flame thickness and data are analyzed to study the influences of turbulence on reaction and preheat zone.

donato.cecere@enea.it

W5P002

DIRECT NUMERICAL SIMULATION AND REACTION RATE MODELLING OF PREMIXED TURBULENT FLAMES

Haioi Wang, Kun Luo, Jianren Fan, Zhejiang University, Hangzhou, China

Direct Numerical Simulation (DNS) is employed to investigate the flame characteristics and the mean chemical source term of hydrogen/air premixed turbulent combustion in the thin reaction zones regime. Three flames with different initial radius and equivalence ratio are considered. The Probability Density Functions (PDFs) of the flame curvature, shape factor and turbulent flame velocity are plotted and compared for different flames. The distributions of the flame curvature and shape factor indicate that the local geometries for both of the flame kernel and planar flame are similar, irrespective of their difference in the global geometry. The Modified Laminar Flamelet PDF (MLF-PDF) shows improvements over the widely used β -PDF for the progress variable distribution. Several closures for the conditional mean reaction rate are integrated with the presumed PDFs and compared with the DNS data. It is demonstrated that the predictions of the first-order reaction rate integrated with the MLF-PDF are satisfactory for H₂ but not for the intermediate species OH. The second-order closure integrated with the MLF-PDF is proved to be promising in predicting both of the major and intermediate species.

ballack@zju.edu.cn

W5P003

A STUDY OF CONDITIONAL SCALAR DISSIPATION RATE IN A PREMIXED HYDROGEN FLAME USING CHEMICAL EXPLOSIVE MODE ANALYSIS

Michael Kuron¹, Zhuyin Ren², Jacqueline H. Chen³, Tianfeng Lu¹

¹University of Connecticut, United States ²Tsinghua University, China ³Sandia National Laboratories, United States

Scalar dissipation rate is a quantity of fundamental importance in turbulent combustion as it appears either directly or indirectly in many modelling approaches. In premixed combustion, the scalar dissipation rate represents the rate at which hot products mix with cold reactants and is defined as $\chi = \Gamma \nabla c \cdot \nabla c$, where c is the progress variable and Γ is the appropriate diffusivity. In the context of Conditional Moment Closure (CMC) and PDF modelling methods, the conditional mean of scalar dissipation rate, rather than the Favre-mean of scalar dissipation rate $\langle \chi | c \rangle$, is the quantity of significance for modelling purposes.

In the present work, Chemical Explosive Mode Analysis (CEMA) is used to analyze the scattering of the instantaneous scalar dissipation rate in a turbulent premixed flame of lean H₂-air simulated with Direct Numerical Simulation (DNS) using Sandia's S3D code and a detailed chemical kinetic model. The flame is in a configuration of a temporally evolving slot jet at different Damköhler numbers and fixed Reynolds number. As the first step of the flame analysis, CEMA is applied to a 3-D subvolume of the DNS dataset to calculate a local chemical timescale, $\tau_{chem} = 1/\lambda_e$ where λ_e is the largest eigenvalue associated with non-conservative modes in the chemical Jacobian. A local Damköhler number ($Da_e = \lambda_e/\chi$) is then defined based on λ_e and the local instantaneous scalar dissipation rate computed from the DNS data. The Damköhler number is then used to divide the flow field into four distinct flame zones involving fresh mixture ($|\lambda_e| < 1$), autoigniting ($Da_e > 100$), reaction front ($-100 \leq Da_e \leq 100$), and post-ignition near-equilibrium mixtures ($Da_e < -100$), respectively.

The temperature field and flame zones in a representative cross section are shown in the (Image) for the case of $Da < 1$ at time $t/t_j = 15$, where t_j is the jet time. The scatter plot in the right panel shows the instantaneous scalar dissipation rate in different flame zones, using the same color scheme as that in the middle panel. The overlaid black line represents the global conditional mean of scalar dissipation rate, which is calculated based on all of the points in the DNS data subvolume. The CEMA results demonstrate that the scalar dissipation rate in the reaction front zone ranges within an order of magnitude above or below the global conditional mean for this case. The scalar dissipation rate in the autoignition zone, however, is an order of magnitude or more smaller than the global conditional mean. Zone-dependent modelling of the scalar dissipation rate is therefore needed and performed to improve the modeling accuracy.

kuron@caeai.com

W5P004 TURBULENCE-CHEMISTRY INTERACTIONS ON STATISTICALLY PLANAR H₂-AIR PREMIXED FLAMES USING DIRECT NUMERICAL SIMULATION

Paul Arias¹, Hong Im², Swetaprovo Chaudhuri³, Chung King Law³

¹University of Michigan, United States ²King Abdullah University of Science and Technology, Saudi Arabia

³Princeton University, United States

The effects of Damköhler number and Karlovitz number on the flame dynamics of three-dimensional statistically planar turbulent premixed flames are investigated by Direct Numerical Simulation incorporating detailed chemistry and transport for the hydrogen-air system. The mixture equivalence ratio was chosen at 0.7, which exhibits diffusive-thermally neutral behavior. The mean inlet velocity was dynamically adjusted to ensure a stable flame within the computational domain, allowing the investigation of time-averaged quantities of interest. A particular interest was on understanding the effects of turbulence on the displacement speed of the flame relative to the local fluid flow.

The results show that the displacement speed dynamics in response to turbulent eddies depends strongly on the specific choice of the *iso*-surfaces in the progress variable. As such, the statistical distribution of the flame speed versus the strain/curvature relations shows a significant sensitivity on the definition of the flame speed. PDFs of flame thickness and scalar dissipation rate conditioned upon these *iso*-surfaces are also examined to understand the role of turbulence in flame thickening or thinning as suggested in classical regime diagrams. These are further clarified by analysis examining the behavior of the alignment between the flame surface and the strain rate eigenvectors. The results for the reference conditions are compared against different parametric conditions in order to assess their effects on flame-flow interaction characteristics.

paul.g.arias@gmail.com

W5P005 TRANSFORMATION OF TURBULENCE IN PREMIXED TURBULENT COMBUSTION

Brock Bobbitt, Guillaume Blanquart, California Institute of Technology, United States

The study of premixed turbulent combustion involves turbulence and chemistry independently and, more importantly, their effects upon one another. The transformation of the turbulence across the flame is not yet well understood and, currently, it is common to assume homogeneous, isotropic turbulence before and after the flame. As the qualitative behavior of premixed turbulent combustion is expected to vary with the Karlovitz number (Ka), this study investigates the transformation of turbulence based on this parameter. Towards this end, a Direct Numerical Simulation (DNS) of a high Ka flame is performed of incoming homogeneous isotropic turbulence interacting with a statistically-stationary, statistically-planar premixed flame. The chemistry of this *n*-heptane/air flame is modeled by a reduced chemical mechanism. The integral length scale is nearly equal to the laminar flame thickness, while the smallest turbulent scales are 50 times smaller.

The transformation of these turbulent scales, which are initially mainly smaller and faster than the flame length and velocity scales, is investigated throughout and behind the flame. These results are compared previous work at both low and high Karlovitz numbers, showing different evolution of the fluctuating velocities and vorticity based on the Karlovitz number. The results emphasize the varying importance of physical mechanisms based on the Karlovitz number and furthers a cohesive understand on the transformation or turbulence across the flame.

bbobbitt@caltech.edu

W5P006 MODELLING TURBULENCE-CHEMISTRY INTERACTION IN PREMIXED FLAMES WITH A STRAINED FLAMELET MODEL

Konstantin Kleinheinz¹, Philipp Trisjono¹, Evatt Hawkes², Heinz Pitsch¹

¹RWTH Aachen University, Germany, ²The University of New South Wales, Australia

Interaction between turbulence and combustion in premixed flames is an area of ongoing research. A recently proposed strained flamelet model of Knudsen et al. uses strain as additional parameter to represent this interaction and its influence on key quantities of premixed combustion models. In this work, an analysis of high quality DNS data of a lean hydrogen--air flame in intense turbulence is carried out, which evaluates capabilities and limitations of this strained flamelet model with respect to two important quantities: the flame displacement speed and the reaction source term. It is assessed both, how these quantities respond to strain and whether the strained flamelet model captures this response. One challenge to incorporate strain effects into the combustion model, is its parameterization. Different mass fractions of reaction radicals are considered and analyzed using flamelet data of a back-to-back configuration with varying strain. The OH radical is identified as suitable parameter, which is unambiguous and sensitive to modeled quantities in regions of high interest, where the chemical reaction features high dynamics, and the space spanned by the strained flamelets is suitable to cover the combinations found in the DNS data set. The flame displacement speed describes the propagation of an isosurface and stems of contributions from curvature, normal diffusion, and reaction. Interestingly, the mean displacement speed of the flame surface in the DNS is lower than the laminar burning velocity, which is shown to be a consequence of locally high strain rates. On the contrary, negative strain does not influence the flame displacement speed. This indicates that negative strain does not have to be accounted for in the strained flamelet model, which supports the modeling strategy of Knudsen et al. To understand the response of the flame displacement speed to high strain rates,

the effect of strain on the individual contributions of displacement speed is analyzed and it is shown that the decrease of the flame displacement speed at high strain rates is caused by a reduction of the contribution due to reaction. The OH radical is sensitive to strain and its concentration decreases with increasing strain. The strained flamelet model describes this decrease very well at conditions that correspond to the burning branch of the back-to-back flamelet configuration, while flamelets of the unstable branch over predict the flame speed. Next, the reaction rate of the progress variable is analyzed. In the DNS, this quantity shows a strong correlation with the strain rate and also the OH radical that parametrizes the strain. The optimal estimator concept is used in order to understand modeling errors showing that the so called irreducible error of the progress variable source at a given progress variable is significantly reduced by the inclusion of the OH radical in comparison with the standard unstretched premixed flamelet model. It is further shown that the progress variable source term is parametrized by the strained flamelet model at a much smaller error compared to the unstretched model. In conclusion it is found that the extension of the flamelet model is a significant improvement over an unstretched flamelet parametrization, as the description of the chemistry processes benefit considerably from the extension to strained flame conditions. The modeling error of the progress variable source term is strongly reduced and flamelets of the burning branch of the back-to-back-configuration describe the flame speed very well. Further, modeling of the flame speed is needed for conditions associated with flamelets of the unstable branch. Overall, findings from this study confirm the modeling idea of Knudsen et al. and highlight the potential of the strained flamelet model for simulations of highly turbulent premixed flames.

konstantin.kleinheinz@itv.rwth-aachen.de

W5P007 PROPAGATION OF THE ENSEMBLE AVERAGED FLAME FRONT IN TURBULENT FLOW

Dong-Hyuk Shin¹, Edward Richardson¹, Tim Charles Lieuwen²

¹University of Southampton, United States ²Georgia Institute of Technology, United States

This paper describes numerical and theoretical analyses of the nonlinear dynamics of harmonically forced, turbulent premixed flames. The objective of this work is to analyze the role of the nonlinear flame propagation and the turbulent fluctuations on the turbulent flame displacement speed and the flame phase speed, which are key parameters in modelling flame transfer functions. In the previous study, it was shown that the turbulent displacement flame speed varies with the ensemble averaged flame curvature in the Landau limit, and it has conjectured that the flame phase speed differs from the mean tangential velocity ($=u_t, 0$). This study extended the previous study by analytically showing the flame curvature effect and the flame phase speed change by the G-equation.

ds1m13@soton.ac.uk

W5P008 STRUCTURE AND PROPAGATION OF TURBULENT METHANE/AIR PARTIALLY PREMIXED FLAME: A DNS STUDY

Vivianne Holmén, Henning Carlsson, Bai Xuesong, Rixin Yu, Lund Institute of Technology, Sweden

A methane/air partially premixed flame propagating in a turbulent flow is studied using three-dimensional Direct Numerical Simulation (3D DNS), taking into account detailed transport and chemical kinetic mechanism. The structure and the propagation velocity of the flame are analysed to determine the interaction between the premixed and non-premixed parts of the flame. The case studied presents stratified premixed combustion in the thin reaction zone regime. Initial conditions for the study are set using the steady solution of a 2D rectangular geometry homogeneously extended in the lateral direction (z). The equivalence ratio at the inflow boundary is varied as a Gaussian function ranging from 0 to 1.5. Turbulence is introduced by synthesizing Fourier waves satisfying a prescribed turbulence energy spectrum in a cubic box with periodic boundary conditions. The Karlovitz number varies between 40-880 for different equivalence ratios in the initial state and 30-500 after 1.5 integral times. The unburned methane/air mixture has a temperature of 298K. The ambient pressure is 1 atm. The computations are run for two integral times.

The flame is featured by a leading premixed flame front with equivalence ratio 0.5 and above, a trailing diffusion flame around stoichiometric mixture, and a long trailing lean premixed flame at equivalence ratio 0.39-0.5. Intense chemical reactions with high heat release rate occur in the leading premixed flame in the vicinity of the stoichiometric mixture. There are weak reaction zones distributed behind the premixed front owing to the interaction between the leading premixed flame front and the trailing diffusion flame. The adequacy of using a progress variable based on fuel mass fraction in partially premixed combustion is addressed by noting that it fails to identify the diffusion flame trailing behind the premixed front. A progress variable based on the products of combustion is therefore introduced. This variable can identify the diffusion flame and parts of the premixed flame simultaneously. Using this new progress variable and equivalence ratio as modelling parameters is considered and tested by mapping heat release rate to this parameter space. The mapping is non-unique, suggesting these parameters are not sufficient to model a partially premixed flame. The displacement speed of the premixed flame front is shown to correlate closely with local flame curvature and equivalence ratio. At zero local flame curvature the displacement speed of the flame is shown to be lower than that of the corresponding planar laminar premixed flame. At large curvatures convex to the burnt gases the displacement speed of the partially premixed flame is however several times higher than that of the laminar premixed flame. It is concluded that the non-premixed flame helps sustain the premixed flame allowing it to burn at very lean conditions. This is further helped due to the progressive increase of the temperature of the unburnt gases downstream.

W5P009

A DNS STUDY OF IGNITION OF LEAN PRF/AIR MIXTURES WITH TEMPERATURE INHOMOGENEITIES UNDER HIGH PRESSURE AND INTERMEDIATE TEMPERATURE

Chun Sang Yoo¹, Minh Bau Luong¹, Seung Oook Kim¹, Jacqueline H. Chen²

¹Ulsan National Institute of Science and Technology, Korea, ²Sandia National Laboratories, United States

Two-dimensional Direct Numerical Simulations (DNSs) of ignition of lean Primary Reference Fuel (PRF)/air mixtures at high pressure and at intermediate temperature near the Negative Temperature Coefficient (NTC) regime were performed with a 116 species-reduced mechanism to elucidate the effects of fuel composition, thermal stratification, and turbulence on PRF Homogeneous Charge Compression-Ignition (HCCI) combustion. In the DNSs, temperature and velocity fluctuations are superimposed on the initial scalar fields with different PRF compositions. In general, it was found that the mean heat release rate increases slowly and the overall combustion occurs rapidly with increasing thermal stratification regardless of the fuel composition. In addition, the effect of the fuel composition on the ignition characteristics of PRF/air mixtures was found to be significantly reduced with increasing thermal stratification. Chemical Explosive Mode (CEM) and displacement speed analyses revealed that the high degree of thermal stratification induces deflagration rather than spontaneous ignition at the reaction fronts, rendering the mean heat release rate more distributed over time subsequent to thermal runaway occurring at the highest temperature regions in the domain. These analyses also revealed that the reduction of the fuel composition effect under a high degree of thermal stratification is caused by the nearly identical propagation characteristics of deflagrations of different PRF/air mixtures. Ignition Damköhler number is proposed to quantify the successful development of deflagrations from nascent ignition kernels. It was verified that for cases with large ignition Damköhler number, turbulence with high intensity and short timescale can advance the overall combustion by increasing the overall turbulent flame area instead of homogenizing initial mixture inhomogeneities.

csyoo@unist.ac.kr

W5P010

A CONDITIONALLY-AVERAGED DYNAMIC SUB-GRID MODEL FOR TURBULENT NON-PREMIXED COMBUSTION

Graham Hendra, W. Kendal Bushe, University of British Columbia, Canada

The Germano Dynamic model for the sub-grid stresses in Large Eddy Simulation relies on averaging across ensembles of statistical homogeneity to generate a stable solution. Within a circular non-premixed jet flame, symmetry is expected in the azimuthal direction, meaning ensembles could reasonably be chosen as annuli of constant downstream distance and radius. Alternatively, in light of the significant variation in conditions across the mixing layer and the layer's expected turbulent oscillations, mixture fraction is proposed as a more reliable indicator of local conditions than radius. The new averaging scheme is similar to the Germano Model in that planes of constant downstream distance as taken as ensembles, but different in that a conditional average of Smagorinsky Coefficient given mixture fraction is calculated in place of an arithmetic mean. Due to sub-grid variation in mixture fraction, calculating such a conditional average requires inverting an integral expression; the method therefore has a natural synergy with the Conditional Source-Term Estimation (CSE) closure for the chemical source term, in which conditional averages of progress variables given mixture fraction are also calculated by integral inversion. Previous CSE simulations of Sandia Flame D gave unsatisfactory results due to a poor turbulence model which under-predicted mixing. This work-in-progress builds upon the existing code by adding a conditionally-averaged dynamic sub-grid model. It is expected that the new model will more faithfully represent the sub-grid stresses, generating to a more developed mixing layer and improving overall result accuracy.

grrhendra@gmail.com

W5P011

APPLICATION OF COHERENT STRUCTURE METHOD FOR SIMULATION OF TURBULENT PREMIXED LABORATORY-SCALED FLAMES IN CFMLES FRAMEWORK

Luka Perkovic¹, Neven Duic¹, Priesching Peter²

¹University of Zagreb, Croatia, ²AVL List GmbH, Germany

In this work Coherent Structure Method (CSM), introduced by Kobayashi in 2005, will be used as a Sub-Grid Scale model (SGS) for simulation of turbulent premixed combustion. CSM smoothly modifies Smagorinsky coefficient C_s as a function of local coherence in the flow. The aim of this work is to show that the CSM SGS model in LES framework can be used as a general framework for modelling the turbulent transport in all varieties of laboratory-scale turbulent premixed flames, especially when compared with two standard Smagorinsky approaches, where Smagorinsky coefficient is kept constant, one having $C_s = 0.1$ and another having $C_s = 0.2$. All three approaches are showing good agreement when comparing mean flame velocity and progress variable, but LES-CSM gives better representation of their variances. This conclusion is derived based on comparison of radial profiles of velocity, temperature and main species between simulation and experimental data for two significantly different flames: the highly stretched and the swirl flame.

luka.perkovic@fsb.hr

W5P012

THE UNIFORM CONDITIONAL MOMENT CLOSURE MODEL FOR PREMIXED COMBUSTION OF A TURBULENT ENCLOSED METHANE JET

Carlos Velez¹, Subith Vasu¹, Scott Martin²

The Uniform Premixed Conditional Moment Closure (UCMC) method has demonstrated the capability to model turbulent, premixed methane flames with detailed chemistry and reasonable runtimes in a RANS environment. The advantage of the premixed UCMC method is that it incorporates detailed chemical kinetics while accounting for the effects of small scale turbulence on the reaction rates with reasonable runtimes. Here the premixed CMC method is extended to Unsteady RANS and LES for the transient prediction of a reacting methane jet. The new model is validated with the PIV and Raman data for a turbulent, enclosed reacting methane jet data from DLR. The experimental data has a rectangular test section at atmospheric pressure and 573 K with a single, offset inlet jet. A jet velocity of 90 m/s is used with an adiabatic flame temperature of 2049 K. Contours of major species, temperature and equivalence ratio along with their RMS values are provided. The UCMC model falls into the class of table lookup turbulent combustion models where the combustion model is solved offline over a range of conditions and stored in a table that is accessed by the CFD code. The scalar dissipation is used to account for the effects of the small scale mixing on the reaction rates. A presumed shape beta function Probability Density Function (PDF) is used to account for the effects of large scale turbulence on the reactions. The unsteady RANS version of the open source CFD code OpenFOAM is used with the PISO algorithm and solved with the finite volume method. Temperature, major species, mean and RMS velocities are compared to the experimental data. Once validated, this tool will be useful for designing lean premixed combustors for gas turbines. The URANS and LES results match the experimental data better than the steady RANS of and are able to resolve the transient features of the flame.

velezcar@yahoo.com

W5P013 PREDICTION OF A TURBULENT ENCLOSED PREMIXED HYDROGEN FLAME WITH THE UNIFORM CONDITIONAL MOMENT CLOSURE MODEL

Carlos Velez¹, Subith Vasu¹, Scott Martin², Aleks Jemcov³

¹University of Central Florida, United States ²Embry-Riddle Aeronautical University, United States

³University of Notre Dame, United States

The use of alternative fuels, such as Hydrogen, under premixed conditions require robust and well developed CFD and chemical kinetics solvers to accurately predict flame behavior. The resulting combustion models are to be used for the design of the next generation of air transportation propulsion systems as well as ground based gas turbines. An alteration to the Conditional Moment Closure (CMC) method is presented here which is capable of accurately predicting highly turbulent ($Re \sim 100000$) premixed flames at a pressure of 1 atm. The proposed model named the Uniform Premixed Conditional Moment Closure (UCMC) method has been shown to successfully model premixed methane flames with detailed chemistry in a RANS environment. The model offers short run times, in comparison to the traditional CMC method, with the inclusion of transient effects, detailed kinematics, effects of small scale turbulence on reaction rates and the effects of differential diffusion from non-unity Lewis number fuels such as Hydrogen. The proposed formulation allows the CMC equations to be solved offline and stored in table for a range of progress variable, variance and scalar dissipation. The inclusion of scalar dissipation in the CMC table allows for the effect of small scale mixing on the reaction rates to be accounted for. In order to include the effects of large scale turbulence on the reactions, a Beta function Probability Density Function (PDF) is used. The PDF transforms the conditioned scalars, in the CMC tables, to an unconditional state, in the flow field. The unconditioned scalars are then coupled with the CFD through the governing equations for the velocity-pressure coupling, energy, progress variable, variance and scalar dissipation. These governing equations are solved in an unsteady fashion by means of the PISO algorithm with the Finite Volume Method (FVM) implemented in the open source CFD software OpenFOAM. The resulting flow field is used to index the chemical kinetic information from the table providing the temperature, density and source terms for the flow field and above mentioned governing equations. The UCMC model is validated with the PIV and Raman data for a turbulent, enclosed reacting Hydrogen jet data from DLR. The experimental data measures a single Hydrogen jet at atmospheric pressure and 573 K. A jet velocity of 90 m/s is used with an adiabatic flame temperature of 2,224 K with a premixed equivalence ratio of 0.7. The effects of turbulence modelling in a URANS and LES environment are studied to determine the effect of turbulence in the prediction of the Hydrogen flames. In order to validate the model contours of the major species, velocity and temperature of the Hydrogen flame, along with their rms values, are provided for validation of the CFD results relative to the experimental measurements.

velezcar@yahoo.com

W5P014 FOLDS AND POCKETS IN THE PROPAGATION OF PREMIXED TURBULENT FLAMES

Navin Fogla¹, Francesco Creta², Moshe Matalon¹

¹University of Illinois at Urbana-Champaign, United States ²University of Rome La Sapienza, Italy

This work extends our earlier reports on the propagation of premixed turbulent flames, examined within the context of a hydrodynamic model in which the flame is treated as a surface of density discontinuity separating the burned gases from the fresh unburned mixture. Primary focus of the present work is to extend the discussion from wrinkled, to highly corrugated multi-valued flame surfaces and provide a systematic characterization of the effects of flame folding and detachment of flame pockets on the flame topology and its propagation. To this end the hybrid Navier-Stokes/interface

tracking methodology that we have employed to numerically address the problem was generalized to tackle multivalued and disjointed interfaces. Results obtained are limited to “two-dimensional turbulence” and to mixtures with positive values of Markstein length that are not contaminated by thermo-diffusive instabilities, such as lean hydrocarbon- or rich hydrogen-air mixtures.

Three regimes of distinct turbulent flame behavior are identified, depending on the mixture composition, thermal expansion coefficient and turbulence intensity: (i) a subcritical regime where, on the average, the flame brush remains planar and unaffected by the ever-present Darrieus-Landau (DL) instability, (ii) a supercritical regime where the DL effects, responsible for frequent intrusions of the flame front into the burned gas region, have a marked influence on the flame brush whose dynamics remains resilient to turbulence, and (iii) a highly turbulent regime where the influences of the DL instability progressively decrease and play limited to no role in flame propagation. These regimes are further delineated by statistical properties of various flame characteristics, including the thickness of the flame brush, flame curvature and hydrodynamic strain. Of practical interest is the dependence of the turbulent flame speed on the turbulence intensity, which was found to vary from a quadratic law arising from an increase in the flame surface area, to a sub-critical exponential law that results from flame folding and frequent detachment of unburned gas pockets.

fogla1@illinois.edu

W5P015

THE DAMKÖHLER-SHELKIN PARADOX IN THE THEORY OF TURBULENT FLAME PROPAGATION

Vladimir Zimont, CRS4 Reserch Centre, Italy

We call known qualitative estimation of the turbulent premixed flame speed at strong turbulence, which means that the turbulent flame speed does not depend on physico-chemical properties of the mixture, the “Damköhler-Shelkin paradox”, as this result contradicts numerous experimental observations. Our solution to this paradox has two sides:

- (i) An theoretical analysis of the flame speed of the steady state flame using an original hyperbolic combustion equation confirms and refines the Damköhler and Shelkin estimation.
- (ii) The disagreement with experiments is explained by a transient structure of actual flames and out theoretical analysis shows strong dependence of their on the laminar flame speed.

1. A theoretical analysis of the speed of the steady state flame is based on the known Zel'dovich concept of “leading points” (the tips of the instantaneous flame surface) The locus of these leading points is the front edge of the turbulent flame, which controls the speed of the turbulent flame. This front is described by an original hyperbolic combustion equation: established in. Analysis of its characteristics gives an expression for the flame speed, which becomes in the case of strong turbulence. We notice that often used formula differs from the Shelkin's expression (is an empirical coefficient) and our result.

2. We analyze the transient flame in the flame-surface regime in the context of Kolmogorov's method modified to the case of turbulent combustion. We assume that the small-scale wrinkles of the instantaneous flame, which control its area and hence, are statistically equilibrium, while the large-scale wrinkles, which controls the flame brush width, are not equilibrium. A theoretical analysis similar to presented in for the case of the thickened flamelet regime results in constant speed and increasing width (is the turbulent diffusion coefficient). Experimental Bunsen and V- flames show constant and increasing along the flames.

zimont@crs4.it

W5P016

GENERAL CORRELATION OF TURBULENT BURNING VELOCITY OF VARIOUS MIXTURES AT HIGH PRESSURE UP TO 3.0 MPa

Jinhua Wang¹, Wu Jin¹, Meng Zhang¹, Zuohua Huang¹, Hideaki Kobayashi²
¹Xi'an Jiaotong University, China ²Tohoku University, Japan

Turbulent burning velocity reveals the turbulence-flame interaction which is the main problem for turbulent combustion and it is still far from well understood. From the practical point of view, turbulent burning velocity is a very important parameter for combustor design and turbulent combustion modeling. A general correlation between turbulent burning velocity and experimental condition is essential. However, due to the experimental difficulties, reports on the turbulent burning velocities at high pressures are very limited.

Experiments were performed using the High-Pressure Combustion Test Facility at the Institute of Fluid Science, Tohoku University. The main objective of this study is to obtain a generation correlation of turbulent burning velocities of various mixtures at high pressure and understand the effect of flame properties and pressure on turbulence-flame interaction. Turbulent premixed flame was generated using a stainless steel nozzle-type burner at high pressure up to 3.0 MPa with perforated plate as turbulence generator. OH-PLIF measurements were performed to visualize the instantaneous flame front. Turbulent burning velocity was derived from the OH-PLIF image processing with conventional angle method. Various mixtures were conducted to investigate the effect of mixtures on turbulent burning velocity, such as CH₄/air, C₂H₄/air, C₃H₈/air, CO/H₂/CO₂/air and CO/H₂/CO₂/O₂ mixtures. The instantaneous flame front images were obtained as shown in (Image) and indicated that the flame front structure changed for various mixtures at the same turbulence condition, which indicated that the flame intrinsic properties had significant influence on turbulence-flame interaction. The general correlation of ST/SL with (P/P₀)(u'/SL) was derived and shown in (Image) which indicated the similar trend for various mixtures, however, the intercept and slope is different for various mixtures. The different flame

intrinsic instability for various mixtures was ascribed to the different flame-turbulence interaction, thus leads to the different instantaneous flame front structure and turbulent burning velocity.

jinhuawang@mail.xjtu.edu.cn

W5P017 **TURBULENT DISPLACEMENT SPEEDS OF A NATURAL GAS SURROGATE WITH HYDROGEN ADDITION**

Anibal Morones Ruelas¹, Sankaranarayanan Ravi¹, Eric L. Petersen¹, Felix Guethe²

¹Texas A&M University, United States ²Alstom Switzerland, Switzerland

Natural gas is the prevailing fuel for stationary, power-generation gas turbines; however co-firing of natural gas with hydrogen is gaining popularity in the industry due to the increased power-density delivered by the fuel, the extended flammability limit and the possibility to operate at leaner combustion regimes that in turn enable reduction of emissions. All of these benefits provide the motivation to study the effects of hydrogen addition on the combustion of natural gas at engine-relevant (turbulent) conditions. The composition of natural gas varies depending on the fuel source, therefore a surrogate (NG₂: 81.25% CH₄ + 10% C₂H₆ + 5% C₃H₈ + 2.5% C₄H₁₀ + 1.25% *n*-C₅H₁₂) has been utilized recently by the authors to aid chemical kinetics modeling using ignition delay times and laminar flame speed experiments. This study focused on measuring turbulent flame speeds (displacement speeds) of NG₂ and hydrogen blends over a wide range of equivalence ratios and at two different blending ratios. The turbulent displacement speeds were measured using a fan-stirred flame bomb. The apparatus is a closed, cylindrical chamber fitted with four radial impellers that generate a central spherical volume of homogeneous and isotropic turbulence with negligible mean flow. Schlieren imaging was used to visually track the growth of the spherically expanding turbulent kernels during the constant-pressure period. The turbulence levels were fixed at an average RMS intensity level of 1.5 m/s and at an integral length scale of 27 mm. Additionally, the progress on the design of a new double-chamber, fan-stirred, flame bomb is presented. The new facility is intended to operate at pressures substantially above one atmosphere to obtain turbulent flame speed measurements that closely mimic the conditions in gas turbines.

anibal.morones@tamu.edu

W5P018 **DISTRIBUTED REACTIONS IMAGED IN HIGH REYNOLDS NUMBER PREMIXED TURBULENT COMBUSTION**

Aaron Skiba, Timothy Wabel, Jacob Temme, James Driscoll

University of Michigan, United States

Distributed reactions zones are imaged within premixed turbulent flames that are operated at high turbulence Reynolds numbers (Ret) up to 70,000 and low Damköhler numbers (Dat). A new piloted burner, called the Hi-Pilot, was developed to achieve these conditions. Velocity data was measured with PIV and hotwire anemometers to characterize turbulent flow properties. Most previous experiments were operated at Ret less than 5,500 (and at larger Dat). Present results show that primary reaction zones can be successfully identified by the overlap of formaldehyde (CH₂O) and OH PLIF signals. Additionally, CH₂O PLIF successfully identifies preheat zones where secondary (low-temperature) reactions occur. Thickened flamelet behavior is observed at moderate to low Ret times thicker than those in a laminar flamelet. As Ret increases to 28,000 the primary reaction layers become “shredded” (short and disconnected). Shredding allows products to mix with reactants and the formaldehyde preheat zones/secondary reaction zones are found to be very broad. Surprisingly, at higher Ret the thickness of reaction layers only increases slowly, but the total area of reaction regions increases dramatically. Flame surface density was calculated from the PLIF of the primary reaction zone.

skiba@umich.edu

W5P019 **ZIMONT SCALE VORTEX INTERACTIONS WITH PREMIXED FLAMES**

Runhua Zhao, Nicole Aeina, Vyaas Gururajan, Fokion N. Egolfopoulos

University of Southern California, United States

The vortex-flame interaction has been studied extensively in the past in order to provide insight into turbulent combustion phenomena. However, most of the studies have been conducted in the wrinkled flamelet or corrugated flamelet regime using small molecular weight hydrocarbons.

In the current work, the interaction of Zimont scale vortex/vortices and flame is investigated numerically in a confined 2-D domain to characterize the broadening of the flame front at Re numbers relevant to high-speed air-breathing propulsion. The derived temperature-time history is then used to assess the attendant effects on the fuel decomposition for methane and *n*-dodecane.

rzhao@usc.edu

W5P020 **ON THE ROLE OF INTERMEDIATE SPECIES IN TURBULENT PREMIXED COMBUSTION OF PROPANE AND PROPANOL ISOMERS AT HIGH PRESSURE**

Tomohiro Uchida¹, Shungo Souyoshi¹, Shun Nakajima¹, Thwe Thwe Aung², Taku Kudo¹, Akihiro Hayakawa¹, Satoshi Kadowaki², Hideaki Kobayashi¹

¹Tohoku University, Japan ²Nagaoka University of Technology, Japan

Observations of flame structure of Bunsen-type turbulent premixed flames for 1-propanol/air, 2-propanol/air and propane/air mixture at a high pressure of 0.5 MPa were performed using OH Planner Laser-Induced Fluorescence (OH-PLIF), and local flame surface density was measured to explore the effects of isomers on flame structure from the viewpoint of intrinsic flame instability in turbulent premixed flames. Numerical analysis of flame instability, considering variable density, a two-step reaction model which deals fuel dissociation reaction, and heat release reaction from intermediate species in the diffusive-convective region, were also performed. Further numerical analysis of 1-D flame using detail chemistry was made to estimate which intermediate species enhances or restrains the flame instability in turbulent premixed flames.

The distribution of local flame surface density, Σ_{local} , for each mixtures which were analyzed from OH-PLIF images. It is shown that flame surface density for 2-propanol/air flames was the greatest among these mixtures, indicating that the intrinsic flame instability for high pressure turbulent premixed flames depends on isomers although thermal properties of the isomers are almost the same. The order of magnitude of the local flame surface density, which indicates the strength order of intrinsic flame instability at high pressure, was 2-propanol/air, 1-propanol/air, and propane/air flames. Lewis numbers of propanol isomers mixture are the same and that of propane is smaller than these, indicating that the Lewis number of the initial reactant is not suitable for understanding the strength of flame instability predominant for flame surface density for relatively low u'/S_L turbulent premixed flames.

In addition, numerical calculations of 1-D laminar premixed flame using detail chemistry at high pressure were carried out. These results proved that the intermediate species predominant for flame instability and which correspond to the two-step reaction analysis are presumed to be C_2H_2 and C_2H_4 which release the heat of combustion. Thus, we calculated the distribution of the summation of nominal heat of combustion in the flame. It appeared that these peaks clearly differ each other and the order of peak value of heat release from these species being consistent with the opposite strength order of flame surface density.

uchida@flame.ifs.tohoku.ac.jp

W5P021

INVESTIGATIONS OF THE INFLUENCE OF TURBULENT LENGTH SCALES ON PREMIXED FLAMES BY AN ACTIVE GRID BURNER

Markus Höltermann, Christoph Hennecke, Friedrich Dinkelacker, Leibniz University, Hannover, Germany

The specific heat release of turbulent flames is higher than the one of laminar flames, because the chemical reaction is supported by the turbulent flow. The different resulting flame types can be displayed for instance in the Borghi-Peters diagram. However, the interactions between turbulence and chemistry are so far mostly investigated for either rather small flames with low turbulent Reynolds number or flames with quite anisotropic turbulence (jet flames or bluff body stabilized flames). Aim of the ongoing work is to reach higher turbulent Reynolds numbers in nearly isotropic turbulence conditions. Therefore, an active grid burner is currently investigated with the potential to reach up to 200 kW thermal powers. The turbulence is generated by rotating shafts with vanes instead of a static grid. Thus, the fluctuation speed is variable, as it is dependent on the rotation speed of the vanes, while the integral length scale remains constant for a given active grid size. In order to approach isotropic turbulence, the burner is fitted with two layers of rotating vanes. The flame is stabilized between diverging adjustable glass plates, to reach a kinematic equilibrium of the flame stabilization for variable operating points. This stabilization method has been carried out by Savarianandam and Lawn. This configuration provides great optical accessibility and thus allows various optical measurements of both the flow and the flame. These essentially include recording the flow velocity fields by stereoscopic Particle Image Velocimetry (Stereo PIV) and a detailed flame front and flame zone characterization by means of Laser Induced Fluorescence (LIF) or laser Rayleigh scattering. Besides providing the velocity fields, the raw images of the PIV can be used to determine the length scales of the vortices in the flow. First results of the cold flow show that the sense of rotation of the vanes has a non-negligible influence on the flow. To achieve isotropic turbulence, the configuration and construction design of the vanes has to be improved.

hoeltermann@itv.uni-hannover.de

W5P022

AN EXPERIMENTAL STUDY OF TURBULENT PREMIXED C_1 - C_8 HYDROCARBON FLAMES IN A STAGNATION FLOW CONFIGURATION

Jennifer Smolke, Francesco Carbone, Fokion N. Egolfopoulos, University of Southern California, United States

A systematic study was carried out for the first time for turbulent premixed flames of fuels with wide ranges of molecular weight and chemical classifications such as C_1 - C_8 normal and branched alkanes and alkenes, cyclo-alkanes, and aromatics. The flames were stabilized in a jet-plate stagnation flow configuration and detailed mapping of the flow field was achieved using Particle Image Velocimetry. Results showed that nearly ideal homogeneous and isotropic turbulence was achieved for all cases, with turbulence intensities varying between 8.6% and 12.5%. Among the main advantages of the jet-plate configuration are the statistically static position of the flame, the orthogonality between the mean flow and the flame brush, and the preservation of the turbulence properties throughout the flow field except at the vicinity of the stagnation plane. The experiments were performed at atmospheric pressure, unburned temperature of 310 K, and a maximum turbulent Reynolds number to about 160 due to the presence of the cooled plate. The extinction results were found to be consistent with what is expected based on the fuel chemical classification and molecular size, providing thus confidence in the vaporization system and the burner configuration to handle complex heavy fuels at high flow rates.

Furthermore, it was determined that for the thin flamelet regime considered in the present investigation, the extinction results scale closely with the laminar flame speed and that the turbulent to laminar flame speed ratio varies nearly linearly with the turbulent Reynolds number.

smolke@usc.edu

W5P023 SYSTEMATIC INVESTIGATION OF PREMIXED METHANE IMPINGING FLAMES

Jin Fu, The Hong Kong Polytechnic University, Hong Kong

Various impinging flame information of premixed methane/air mixtures has been systematically collected: A high speed camera was used to capture flame images. The OH-PLIF system was applied to obtain the flame OH distribution of flames. Also, flame noise was captured by a microphone and impinging plate temperature was monitored by a thermal image camera. Experimental conditions covered a wide range of burner to plate distance (impinging distance) from 30mm to 70mm. Results show that with the increase of impinging distance, impinging plate temperature changed significantly. In order to investigate the influence of impinging distance to the impinged plate, flame structure was captured by OH-PLIF system and high speed camera, by which flame OH radical distributions and flame fronts could be observed. Results show that, with the increase of impinging distance, flame turbulence were getting more intense and combusting noise were getting louder. In order to figure out the relationship between combusting noise and flame turbulence. A Fast Fourier Transform (FFT) method was employed to transform the flame image and combusting noise signals into frequency signals. The turbulent area which was fixed to make a FFT transform can be seen in the picture, and the results of FFT from both acoustic and image signals is shown in a plot. The same peak of acoustic and image signals can be found at 45 Hz.

colin8741@163.com

W5P024 HEAT RELEASE RATE MEASUREMENTS ON METHANE, SIMULATED BIOGAS AND SYNGAS TURBULENT FLAMES

Irfan Mulla¹, Aadil Dowlut², Satyanaryanan Chakravarthy¹, Ramanarayanan Balachandran², N. Swaminathan³

¹Indian Institute of Technology Madras, India ²University College London, United Kingdom

³University of Cambridge, United Kingdom

Limited fuel resources and ever more stringent environmental regulations will continue to motivate researchers to invent new techniques to reduce the pollutants from combustion along with efficient energy utilization. Additives such as hydrogen, carbon dioxide to natural gas can provide control over the flammability limits and in turn may over the combustion stability. The ability of combustion systems to operate on alternative sustainable fuels is highly desirable for the development of fuel-flexible combustion systems. It is known that the fuel properties have a strong influence on the dynamic response of flames and one of the key parameters required to enable detailed understanding of flame response is heat release rate. The commonly used approaches to deduce heat release rate are i) natural chemiluminescence, ii) flame surface density using tomography/Planar Laser Induced Florescence (PLIF) of OH, & iii) product of OH and H₂CO PLIF. Among the three methods only simultaneous OH/H₂CO PLIF can provide planar local heat release rate, and it has been shown to work on premixed hydrocarbon flames (methane, propane and ethylene air flames) and ethanol. The present work estimates the heat release rate by using simultaneous OH/H₂CO PLIF. Although few previous works reported this technique, there is still a limited understanding of its applicability on multi-component fuels in highly turbulent premixed flames. The objective of this work is to apply this diagnostic technique to the flames with different compositions, and investigate systematically the response of these flames to strong acoustic oscillations. In this work, three classes of mixtures are selected to simulate methane flames (CH₄), biogas flames (CH₄/CO₂) and syngas flames (CH₄/CO/H₂). Turbulent flames are stabilised with a bluff body in a model gas turbine combustor. The flames are subjected to acoustic forcing (velocity fluctuations) generated by loudspeakers. The oscillations with different amplitude and frequencies are employed. The response of the flames to these oscillations is recorded with a phase locked simultaneous H₂CO and OH PLIF. Additionally, the line of sight measurement of heat release (OH*) rate is acquired with a photomultiplier tube setup. Simultaneously to this, acoustic pressure is recorded. The product of H₂CO and OH PLIF signals provide an estimate of the heat release rate. Apart from this, the OH PLIF signal is used to deduce the local flame curvature and Flame Surface Area (FSA) which is obtained by revolving a traced planar flame front. The FSA and OH* chemiluminescence is observed to vary linearly with the bulk velocity. The turbulence level increases with velocity, which wrinkles the flame front thus increasing the FSA and OH*. This suggests both of these quantities are strongly correlated. The heat release rate varies linearly with the forced amplitude at low frequency (30 Hz) whereas it shows a non-linear variation at higher forcing at higher frequencies (255 Hz and 330 Hz). The combined analysis offers an insight into the response of the flame to the acoustic oscillations.

irfan071084@gmail.com

W5P025 TURBULENT FLAME EXTINCTION PREDICTION IN PARTIALLY PREMIXED COUNTER FLOW FLAMES

William Calhoon, Jr., Combustion Research & Flow Technology, Inc., United States

The accurate characterization of extinction phenomena in turbulent reacting flows is of significant importance to

both ground based gas turbine power generation systems and high performance aircraft propulsion systems. In both of these applications flame stability and extinction are controlled by the interaction of the flame with flow strain induced by turbulence at both large and small scales. The prediction of local and global flame extinction is a very challenging problem that requires a detailed accounting of the interaction of a wide range of turbulent scales with the flame structure. To address this difficult challenge a modeling formulation based on the Linear-Eddy Model (LEM) has recently been developed for application to the counter flow configuration. The LEM is a comprehensive stochastic mixing model formulation that directly accounts for the interaction of microscale flow turbulence with flame structure. Applying the LEM within the counter flow configuration allows for large scale strain to be applied to the flame as well. As a consequence, the LEM/counter flow (LEM-CF) model may be used to directly investigate turbulent flame extinction effects resulting from both large and small scale strain. This 1-D formulation has been shown to capture the experimentally observed trend that flame extinction limits are reduced as the turbulence level is increased. The LEM-CF model may also be used to develop efficient database driven subgrid models for Large-Eddy Simulation (LES). Subgrid modeling formulation for both nonpremixed/partially premixed and premixed flows have been developed. Turbulent counter flow flame experiments offer an opportunity to evaluate the LEM-CF's ability to capture turbulent flame extinction. Geyer, et al. Investigated turbulent flame extinction in counter flow flames of partially premixed methane/air – air. Experimental data for both velocity and scalars were collected just below the extinction limit. The global blow-out limit was also measured by increasing the counter flow bulk strain rate. This experiment has been investigated using Large-Eddy Simulation (LES) and a 1-D turbulent counter flow model based on the Monte Carlo PDF transport formulation. Results from the application of the LEM-CF formulation to these cases will be presented for velocity and scalar statistics prior to blow-out, and for the prediction of the blow-out limit.

calhoon@craft-tech.com

W5P026 NUMERICAL SIMULATIONS OF HIGHLY TURBULENT COUNTERFLOW FLAMES (TCFS) IN NON-PREMIXED AND PREMIXED MODES

Ranjith Tirumagari, Stephen B. Pope, Cornell University, United States

Results are reported from a computational study of Turbulent Counterflow Flames (TCFs). The TCF configuration consists of two opposed nozzles emitting fuel, oxidant or a pre-mixture, depending on the case considered. A turbulent flame then exists close to the mean stagnation plane. A series of experiments on TCFs, operating in both non-premixed and premixed modes, have been performed at Yale University and at Sandia National Labs; and the same flames are being studied computationally at Cornell University. The principal components of our computational methodology are (a) a finite-difference code (NGA) to solve the LES transport equations (b) a PDF code (HPDF) implementing a particle/mesh method for the PDF transport equations and, (c) a tabulation procedure (ISAT) for combustion chemistry. In this computational approach, LES is used to represent flow and turbulence, and the PDF method is used to represent turbulence-chemistry interactions. In LES simulations, the flame is intentionally not fully resolved thereby underlining the importance of a good combustion model like the PDF method. A new treatment is developed for the inflow velocity boundary conditions at the nozzle exits to match the mean & r.m.s. velocities and the turbulent length scales in the simulations to those in the experiments. This capability is validated by performing non-reactive counterflow simulations. The statistics of the mean and the r.m.s. quantities on the jets centerline obtained from the simulations match well with the experimental data. Subsequently, reactive simulations of counterflow flames, with diluted CH₄ as fuel, are performed in both non-premixed and premixed modes. This study is conducted using high-fidelity simulations and increasingly detailed modes of comparison with the experimental data. Both the unconditional and conditional centerline statistics show a good agreement with the experimental data. In the present ongoing study, the classical form and a modified version of the Interaction-by-Exchange with the Mean (IEM) mixing models are tested in order to assess their accuracy in modeling molecular transport and mixing in the PDF method. In this Work-in-Progress poster, we will describe the experimental details, working of the coupled code, effects of critical experimental and simulation parameters on the turbulent flame behavior, validation of the simulation results and computational accomplishments associated with the highly-turbulent counterflow simulations in non-reactive, non-premixed and premixed modes.

rtr38@cornell.edu

W5P028 AN EFFICIENT TRANSPORTED FDF AND FLAMELET HYBRID APPROACH FOR LARGE EDDY SIMULATION

Martin Rieth¹, Jyh-Yuan Chen², Fabian Proch¹, Andreas Kempf¹

¹IVG, University of Duisburg, Germany ²University of California, United States

A hybrid flamelet and finite rate chemistry transported Filtered Density Function (FDF) method has been developed and used to simulate the Darmstadt Turbulent Opposed Jet (TOJ) flame in a combined Large Eddy Simulation (LES)/Lagrangian Monte Carlo (LMC) framework. The LMC particles describe the chemical composition whereas the LES is used to solve for the flow field. The PsiPhi LES code solves the filtered Navier-Stokes equations in low-Mach number formulation and with an eddy-viscosity closure. The Lagrangian and Eulerian fields are consistent through coupling by a density feedback from the particles to the Eulerian field and by the interpolation of the LES velocity onto the particle positions by the Parabolic Edge Reconstruction Method (PERM). A formulation as reported in previous studies is used for the FDF transport while the Modified Curl's mixing model provides closure for the fluxes in

composition space.

The proposed hybrid method efficiently combines flamelet and finite rate chemistry, using cost effective flamelet solutions where possible, reverting to a direct chemistry solver only where needed. The switch-over from flamelet to finite rate chemistry and vice versa is done by checking if the LMC particle is close to the flamelet solution after the mixing step. The flamelet model is then used only if the particle is close to the flamelet solution for its given mixture fraction. Quantities used for checking the proximity to the flamelet solution are temperature and product species mass fractions. This method reduces the need for the finite rate chemistry solver to regions where a flamelet solution does not sufficiently describe the chemical composition, as for example in regions of high strain. To further reduce computational cost, Lagrangian flamelets are replaced by Eulerian flamelets away from the reaction zone, reducing the number of Lagrangian particles dramatically. With this method, the evolution of the composition of a part of the flow field is solved using the LES Eulerian fields and the evolution of the composition inside the flame zone is solved using the LMC particles. By applying this approach, the whole TOJ burner was simulated while only around 14% of the computational domain is occupied by LMC particles. Resulting load balancing issues are addressed in the poster. The aim of the present work is to demonstrate the feasibility, effectiveness and efficiency of the hybrid approach and to evaluate possible numerical issues. In summary, no instabilities or other major numerical issues have occurred. A significant speed-up compared to using a direct chemistry solver only is demonstrated. Additionally, a comprehensive analysis of the results is provided with a comparison to Raman/Rayleigh data by Geyer et al., showing the good agreement between simulation and experiment for the fine simulation conducted.

martin.rieth@uni-due.de

W5P029

IMPROVED POLLUTANT AND EXTINCTION PREDICTION IN LARGE EDDY SIMULATION OF TURBULENT PILOTED JET DIFFUSION FLAMES

Seung Hyun Kim, The Ohio State University, United States

A second-order Conditional Moment Closure (CMC) model for Large Eddy Simulation (LES) is presented and shown to improve pollutant and extinction prediction in turbulent non-premixed flames. The second-order CMC formulation is based on the work of Kim and Huh (2004). Second-order closure of conditionally filtered reaction rates is applied only to the rate limiting steps, while first-order closure is used for all the other reaction steps in a detailed chemical mechanism for a hydrocarbon fuel. The plane-averaged form of the conditionally filtered equations is solved with the effects of scalar dissipation fluctuations considered primarily through conditionally filtered variances and covariances. The effects of intermittent mixing fluctuations are incorporated into the model formulation through the Filtered Density Function of scalar dissipation rates. The information on the resolved mixing field is used to estimate the level of scalar dissipation fluctuations that drive the conditional fluctuations of reactive scalars. This allows for the correct incorporation of finite Reynolds number effects regarding transitional scalar structures. The second-order CMC-LES is applied to turbulent methane/air piloted jet diffusion flames (Sandia Flames D, E, and F). The filtered equations for the flow and mixing fields are solved using a structured-grid LES code. The computational domain is $[-d, 56d] \times [0, 16d] \times [0, 2\pi]$ in the axial, radial, and azimuthal directions, respectively, where d is the fuel jet diameter, and is discretized into $288 \times 160 \times 64$ control volumes. The first-order CMC equations are solved by the stiff-ODE solver, DVODE. The GRI 2.11 mechanism is used. Results show that the second-order CMC-LES leads to substantial improvement in the prediction of pollutants. Local extinction in Flame F is also captured by the second-order CMC-LES. At $x/d=7.5$, temperature and species, including OH, CO, and NO, for all the flames are well predicted by second-order CMC-LES. The second-order CMC-LES performs well at all axial locations for Flame D. The prediction errors at downstream locations of Flame F will be analyzed and further study regarding the improvement of submodels will be presented.

kim.5061@osu.edu

W5P030

FULLY CONSERVATIVE KINETIC ENERGY PRESERVING SCHEMES FOR HIGH REYNOLDS NUMBER TURBULENT COMBUSTION

Ayaboe Edoh, University of California, United States

The emergence of Large Eddy Simulations (LES) as a complement to other CFD approaches (i.e., DNS and RANS) in the study of turbulent combustion and unsteady flow dynamics calls for deeper understanding of its two comprising elements: the numerical schemes and Subgrid Scale (SGS) modeling. While a lot of work has addressed the latter, the design of optimal numerical schemes for LES remains an area of some speculation; different schemes have been shown to produce vastly different turbulent reactive results, even with the same SGS model. The current research study is focused on exploring the merits of Kinetic Energy Preserving schemes for compressible flow and assessing their associated stability and low-dissipation properties. Inherent numerical dampening and phase error of a scheme is of high importance, and associated errors need to be tempered with respect to the subgrid. Central differencing schemes are often preferred to upwinding techniques due to low damping and preservation of high wavenumbers. Unfortunately these schemes suffer from numerical instability and are often applied in conjunction with artificial viscosity. The concept of a Kinetic Energy Preserving property, which is considered important to LES calculations, is presented and explored as a potential technique of enforcing non-linear stability while eliminating (or, at least, minimizing) the need for numerical dissipation.

Generalization of the Kinetic Energy Preserving concept includes secondary conservation of all the solution scalars, i.e., the species equations. This is formulated and cast as a candidate for compressible high Reynolds Number

computations for turbulent reacting flows. The resulting scheme is of Crank-Nicolson type, resembling Roe-averaging in time, and is discretely Fully Kinetic Energy Preserving (F-KEP) in both a local and global sense. Implementation may be supported on both Collocated and Staggered grid arrangements and shows potential to be extended to higher order ($p > 2$) in space and time using Richardson extrapolation and energy-stable Runge Kutta methods, respectively. This study serves as a preliminary survey of numerical algorithms to be further investigated in the context of practical LES computations of non-reacting and reacting flows with appropriate sub-grid closure models. Additional insights on the scheme characteristics will be discussed in detail in the poster.

acedoh@gmail.com

W5P031 MULTI-ENVIRONMENT PROBABILITY DENSITY FUNCTION APPROACH FOR TURBULENT STRATIFIED BLUFF-BODY FLAMES

Sangtae Jeon, Yongmo Kim, Hanyang University, Korea

The transported PDF model has an essentially capability to directly treat the non-linear chemical source terms without any assumptions. However, the solution of the PDF transport equation together with a detailed chemistry requires the computationally excessive cpu time to simulate the turbulent flames encountered in the practical combustors. To relax this computational burden, the multi-environment PDF approach has been developed as an alternative approach to solve the transported PDF.

In the present study, the multi-environment Probability Density Function method has been applied to simulate the turbulent stratified premixed flames. The Direct Quadrature Method Of Moments (DQMOM) has been adopted to solve the transport PDF equation due to its computational efficiency and robustness. The multi-environment PDF method has the form of conventional Eulerian scheme and contains all one-point statistical properties of the particle-based method. In present study, the joint composition PDF is estimated using the two-environment PDF expressed by the combination of weights and abscissas on composition and physical space. Compared to the Lagrangian PDF transport model, this DQMOM procedure is computationally efficient and can be easily implemented into the existing routines of the scalar transport equation in context with RANS and LES. The IEM mixing model is employed to represent the mixing process and the chemical mechanism is based on the detailed chemistry. In terms of numerical singularities, the correction and micro-mixing terms yield two kinds of singularity related to recover abscissas from weighted and the difference of abscissas on composition space. To avoid these numerical singularities, the present study employs the methods suggested by Wang and Koo. Moreover, the multi-environment PDF model with the multiple reactive scalars maintains the inherent capability of the joint PDF transport method to treat the highly nonlinear chemical reaction source terms exactly. However, in terms of the solution procedure, unlike the computationally excessive particle-tracking Monte-Carlo solution schemes in the PDF transport model, the DQMOM based formulations in the multi-environment PDF approach are efficiently solved by conventional Eulerian grid-based techniques.

In present study, the governing equations are solved in unstructured based grid system, and the chemical mechanism is adopted the GRI 2.11 mechanism. Computations are made for the non-swirling turbulent stratified premixed flames including SWB₅ and SWB₉. SWB₅ flame is moderately stratified while SWB₉ flame is highly stratified. Numerical results obtained in this study are precisely compared with experimental data in terms of unconditional and conditional means for scalar fields including temperature and species mass fraction.

jist1004@hanyang.ac.kr

W5P032 TEMPERATURE AND OH FIELD MEASUREMENTS IN TURBULENT PREMIXED AND STRATIFIED METHANE/AIR FLAMES

M. Mustafa Kamal, University of Cambridge, United Kingdom

Practical combustion applications typically feature stratified flow fields, and often utilize swirl in order to achieve increased turbulent mixing, lean flammability limits and the flame stability over a wider range of global stoichiometry. The interaction between a flame and the turbulence in which it propagates is of fundamental importance in combustion theory. The characteristic properties of flame and turbulence are strongly dependent on the relative strength of chemical and turbulent processes and the coupling between them. Combustion process result in heat release which then influence the flow field by altering the fluid properties such as density and viscosity, whereas turbulence not only affect the macro and micro structure of the flame but also transports the reactants and products. It is, therefore, important to understand the effects of turbulence characteristics on a local flame structure in highly turbulent flows by investigating the statistical characteristics of the thermal and compositional structure of a flame.

Recent experiments by Sweeney et al. and Ruigang et al. investigated the effects of stratification and swirl on highly turbulent methane/air flames under globally lean conditions using spatially resolved multi-scalar and flow field datasets respectively. Sweeney et al. provided a comprehensive assessment of the various methods for measurement of flame surface density from crossed planar OH and line measurements, though such measurements offer only a partial view of the mixing and reaction field, limiting the interpretation of the flow physics. Planar scalar measurements can help us gain a more detailed understanding of the turbulent mixing and scalar dissipation of the flow. In this study, simultaneous 2D measurements of OH and temperature is considered, and the statistical properties of the measured scalars and their

gradients, conditioned on the local temperature to understand how turbulence affects the pre-flame and the flame region of turbulent premixed and stratified flames with and without swirl.

The Cambridge/Sandia Stratified Swirl Burner, designed to generate reacting flow conditions representative of turbulent flows in practical systems, including sufficiently high turbulence levels, swirl and operation under premixed and stratified conditions, was used for the experiments. Simultaneous Rayleigh scattering and OH-PLIF imaging measurements were performed in the Advanced Imaging Laboratory at Sandia National Laboratories. The experimental arrangement consisted of the high-resolution Rayleigh imaging apparatus described in previous papers, combined with an additional laser/camera system for simultaneous Oh-PLIF imaging.

The preliminary analysis of the acquired data shows that the pre-flame zone can be significantly disrupted by swirl and turbulence, whilst the high temperature reaction zone as marked by OH remains relatively intact. Swirl effects arise from enhanced turbulence as well as entrainment. The maximum temperature gradients are enhanced by stratification and lowered by swirl and turbulence. In all cases, temperature gradients are shown to be significantly lower than corresponding unstrained laminar flames, whilst OH gradient are less affected, which is consistent with previous line measurements of 3D gradients.

mmk44@cam.ac.uk

W5P033

STABILITY CHARACTERISTICS OF PARTIALLY PREMIXED FLAMES

Mohamed Senosy¹, Mohy Mansour¹, Assaad Masri², Mohamed Zayed¹, Mrinal Juddoo²

¹Cairo University, Egypt ²University of Sydney, Australia

Partially premixed flames are used in many combustion systems. The level of partial premixing affects the flame stability and structure. Characterization of this level and proper description of partially premixed flames are not yet fully resolved. This requires measurements of the stability characteristics for different mixture fraction field distribution at the nozzle exit of the burner. The present burner is similar to the concentric tubes burner by Mansour. The burner consists of two stainless steel tubes where the inner tube supplies air and the fuel is supplied between the inner and outer tubes. The level of partial premixing is controlled by the recess of the inner tube a distance L below the exit of the outer tube. This creates variable mixing length inside the outer tube. In addition a conical nozzle is added at the nozzle exit in order to enhance the flame stability. In the present investigation, the burner diameter D (defined as the inner diameter of the outer tube) is 9.7 mm and an outer diameter is 12.7 mm, while the inner tube has an inner diameter of 4 mm and an outer diameter of 6 mm. The aim of this work is to discuss the stability characteristics of jet and conically stabilized partially premixed flames based on different levels of Reynolds number, equivalence ratio, degree of partial premixing and co-flow velocity.

Two sets are investigated for natural gas and liquid petroleum gas as the selected fuels with and without cone at the nozzle exit. In addition, the effect of the velocity of the air co-flow is also investigated. This provides a complete set of stability curves for open jet flames for non-premixed, fully-premixed and partially premixed. The stabilization mechanisms are then investigated and discussed in this work. Mansour investigated the stability characteristics of partially premixed turbulent lifted methane flames at a certain level of partial premixing and provided similar stability curves of Wohl et al. This work extended beyond the limits investigated in. Understanding the stability characteristics of partially premixed flames for a wide range between non-premixed and fully premixed flames is essential for the design of many combustion systems where the range of partial premixing is broad.

The flame structure is affected by the recess distance L , the cone, the co-flow and the jet Reynolds number. The full set of flames with and without cone is investigated and the data are discussed in this work. Higher stability can be achieved in partially premixed jet as compared to fully- and non- premixed cases. Higher stability can also be achieved by increasing the co-flow velocity of the air where the flame structure is more distributed and highly intense. The flames are presented and discussed in this work for different levels of partially premixed, with and without cone, and different co-flow velocity. The data show that the flame structure varies significantly for the different cases from long flame to distributed highly intense flames with distributed reaction zone. The exit mixture fraction field at the nozzle exit is one of the main parameters that affect the flame stability. Accordingly further analyses of the current data are required base on mixture fraction measurements at the nozzle exit using advanced measurements technique.

m.samy@niles.edu.eg

W5P034

LINE RAMAN/RAYLEIGH MEASUREMENTS IN PARTIALLY PREMIXED SLOT BURNER FLAMES FOR CONSERVED AND REACTION SCALAR GRADIENT MEASUREMENTS

Stephan Kruse¹, David Broll¹, Emilien Varea¹, Mohy Mansour², Ayman Elbaz³, Gerd Gruenefeld¹, Heinz Pitsch¹

¹RWTH Aachen University, Germany, ²Cairo University, Egypt ³King Abdullah University of Science and Technology, Saudi Arabia

In many prevalent combustion systems, fuel and air are neither homogenously mixed nor fully separated before reactions occur. Besides premixed and diffusion flames, partially premixed combustion is essential for practical combustion systems and it is imperative to understand its governing processes. Therefore, data of important flame quantities have to be provided for this combustion mode. In this study, a combined line Raman/Rayleigh technique is applied to turbulent partially premixed flames in a slot burner for simultaneous measurements of temperature, species concentration, and mixture fraction. The technique provides profiles within the flame; hence one-dimensional gradients can be obtained.

The investigated burner features three slots. The turbulent flame is generated in the main slot with a 12 mm x 100 mm orifice. Laminar premixed pilot flames are located on the two sides of the main slot with a cross section of 24.5 mm x 100 mm to stabilize the turbulent flame. The burner has a height of 96 mm. Fuel and air enter the main slot through three slits separated by removable plates. The degree of premixing can be adjusted by varying the height of the plates. In this work, two configurations are investigated, a 48 mm high plate for partially premixed flames and no plates for premixed flames. Simultaneous radial profile measurements of temperature and species concentrations are conducted to determine their gradients using the line Raman/Rayleigh techniques. Earlier line Raman/Rayleigh/LIF techniques for temperature and concentration measurements have been presented by Mansour and Chen and by Barlow et al. A KrF excimer laser (Lambda Physics) produces a laser beam of 248 nm wavelength and 230 mJ pulse energy. The beam is focused by a 300 mm focal length lens. The focal point is centered to the probe volume which has a length of 10 mm. Unlike the previous studies, one detection system is used for simultaneous Raman and Rayleigh signal detection. The detection system consists of two convex lenses for collecting the scattered light and focusing it on the slit of the spectrograph. For signal detection along the focused laser beam, the slit of the spectrograph is aligned parallel to the beam. The spectrograph is a Chromex 250 ($f/\# = 4$) equipped with a holographic grating with 1800 grooves/mm and a blaze wavelength of 250 nm. For imaging, an intensified CCD camera (LaVision DynaMight, 512 x 512 p²) is used. The resulting resolutions are 18 pixel/nm in wavelength direction and 50 pixel/mm in slit direction. A liquid filter of butylacetate is positioned in front of the spectrograph as proposed by Cheng et al. The filter decreases the Rayleigh signal roughly by a factor of a thousand so that it is in the same range as the Raman signal and can be imaged with the same detector. For signal calibration, a nozzle with a heating system and a flat flame burner (McKenna-Burner) are used. For detecting the Raman line crosstalk, the Raman signals of the pure gas species CO₂, O₂, N₂ and diluted CH₄ mixtures are measured at various temperatures ranging from 293 – 623 K at 2,5 mm above the nozzle exit. To calibrate the H₂O line and to detect the broadening of the Raman lines, Raman and Rayleigh measurements are performed for different boundary conditions 4 and 15 mm above the exit of a McKenna-burner. Measurements are conducted at several positions downstream of the burner exit for various equivalence ratios of 0.8, 1.0, and 1.2 and different Reynolds numbers Re of 3500, 5250, and 7000. The results indicate very good signal to noise ratio resulting in sufficient spatial resolution of 0.25 mm along the beam axis. The measurements provide profiles across the flames of temperature, species concentrations, and mixture fraction. One-dimensional gradients are also presented and analyzed. The structure of the current partially premixed flames and the stability characteristics are discussed for better understanding of highly turbulent flames. The data are presented in this poster for further discussions of the level of partial premixing based on the local gradients.

s.kruse@itv.rwth-aachen.de

W5P035 EFFECT OF THERMAL BOUNDARY CONDITIONS ONTO THE FLAME STABILIZATION OF A TURBULENT PREMIXED STRATIFIED FLAME

Anja Ketelheun, Guido Kuenne, Amer Avdic, Matthias Euler, Andreas Dreizler, Johannes Janicka, Technische Universitat Darmstadt, Germany

Stratification is found in many practical applications. Besides being just the unintended result of incomplete mixing it can specifically be used to achieve certain stability and/or pollutant requirements. In this regard, particularly lean premixed flames that face inhomogeneously mixed reactants are of increasing importance. Within this work a Large Eddy Simulation (LES) study is performed in order to investigate the influence of thermal boundary conditions onto the flame stabilization.

The burner investigated here is the turbulent stratified piloted flame. A comprehensive set of validation data for this annular flame burning in a premixed mode is available from experiments in Darmstadt and Sandia national labs. The configuration has already been subject of several numerical investigations carried out by different groups. The issue investigated within this study arose from those simulations as well as experimental observations. The thermal boundary conditions of the central tube in which the pilot flame is positioned seemed to play a vital role in the stratified flame's leading edge position. As observed from flame luminescence, a suppression of heat release was obvious and subsequently performed gas phase temperature measurements revealed a drop by several hundred Kelvin here. Hence, a significant amount of heat gets removed from the flame causing a lift-off whose height is still not quantified and surely not captured in the initial adiabatic simulations.

The purpose of this work is both to provide insight into the underlying physics as well as to study the sensitivity of the simulation related to the heat transfer treatment. The study is supplemented by very accurate wall temperature measurements using phosphor thermometry to remove the large uncertainty revealed in the past for this configuration. Three Simulations are compared. First, the initial adiabatic, second an estimated wall temperature treatment used by various groups of the last TNF workshop and third, the usage of the phosphor measurements.

The results obtained from the three LES for the TSF-A-r flame are evaluated by means of an illustration of the different flame stabilizations and comparisons with experimental data. A very important finding is that not only the inclusion of enthalpy losses is important but also their thermodynamic consistent treatment only met in the third case. In this regard it became clear that the heat removed at the pilot flame causes a preheating of the fresh reactants. It turned out that this effect initially thought to be negligible has a strong influence locally onto the dynamics at the flame's leading edge but also globally as visible within the mean profiles.

ketelheun@ekt.tu-darmstadt.de

W5P036 THE ROLE OF TEMPERATURE, MIXTURE FRACTION, AND SCALAR DISSIPATION RATE ON AUTO-IGNITION OF A TRANSIENT METHANE JET IN A HOT COFLOW
Christoph Arndt¹, Michael Papageorge², Frederik Fuest², Jeffrey A. Sutton², Wolfgang Meier¹
¹German Aerospace Centre, Germany, ²Ohio State University, United States

Auto-ignition of (cold) fuel in a hot oxidizer is of great importance in several technical systems such as internal combustion engines and gas turbine combustors employing reheat, flameless, or MILD combustion. Particularly, the study of fuel jets issuing into hot, vitiated air (Jet-in-Hot-Coflow, JHC) and the subsequent flame stabilization has gained significant research interest in recent years. Due to the fast and transient nature of auto-ignition, its experimental investigation requires high-repetition-rate imaging techniques. High-speed planar imaging has become a wide-spread tool in combustion research, primarily relying on commercial lasers with relatively low pulse energies, for OH Planar Laser-Induced Fluorescence and Particle Image Velocimetry. However, measurement techniques such as planar Rayleigh scattering or Raman scattering cannot be utilized using commercial high-speed lasers due to the limited pulse energies available. For these applications, pulse-burst laser systems are a promising tool to generate a limited number of high-energy laser pulses at high repetition rates. In this work, the High Energy Pulse Burst Laser System (HEPBLS) at Ohio State University has been used for high-speed (10 kHz) planar Rayleigh scattering imaging. The goal was to study the roles of the mixture fraction, temperature, and scalar dissipation rate fields during fuel injection and the subsequent auto-ignition of a transient, turbulent methane jet issuing into a coaxial laminar coflow of hot exhaust gas from a lean premixed hydrogen/air flat flame. The experiments are conducted in the well-characterized DLR Jet-in-Hot-Coflow Burner with highly repeatable boundary conditions and excellent optical access for non-intrusive laser diagnostics. The burst length of more than 20 ms, corresponding to more than 200 consecutive laser pulses at a repetition rate of 10 kHz, was sufficient to capture the complete temporal development of the mixing field between the transient fuel jet and the surrounding coflow prior to and through the occurrence of auto-ignition. Simultaneous high-speed OH* chemiluminescence imaging was applied to gain 3D-information of the ignition kernel location. This information allowed the selection of ignition events in which the initial flame kernel formed inside the laser-sheet.

The Rayleigh scattering signal depends on the density and scattering cross section of the probed gas. With the assumption of adiabatic mixing between fuel and oxidizer, the mixture fraction and temperature during the fuel injection and prior to the onset of auto-ignition can be measured simultaneously. Great care was taken to assess potential error sources in the data processing in order to gain quantitative data that can be used for model validation. For example, effects of thermal decomposition during mixing of fuel and hot exhaust gas were considered for the residence times of interest in the experiment and were found to have no significant influence on the data reduction accuracy and the deduction of the mixture fraction and temperature fields. The evaluation of the transient jet tip position for a large number of fuel injection events revealed extremely reproducible fuel injection and system behavior, with a precision of less than 10 microseconds. The transient high-velocity jet was found to reach a quasi-stationary state a few milliseconds after the start of the fuel injection and before the occurrence of the initial auto-ignition event. Thus, the auto-ignition can be considered to occur in a stationary state, which is an important finding for numerical modelling of this experiment. The time series of Rayleigh scattering images revealed a highly turbulent mixing field prior to the onset of auto-ignition. Flow conditions which favored auto-ignition consisted of low mixture gradients, lean fuel mixtures and high temperatures at the periphery of the jet, above axial locations of $z/D = 17$. The analysis of selected ignition events revealed that auto-ignition occurred at the windward side of bulges of the inflowing jet, where the measured scalar dissipation rate was low. This result has been proposed by Direct Numerical Simulation of igniting mixing layers, but, to the author's knowledge, the current work presents the first experimental results displaying these phenomena.

christoph.arndt@dlr.de

W5P037 STRUCTURE AND STABILIZATION OF A HYDROGEN-RICH TRANSVERSE JETS IN A VITIATED TURBULENT FLOW

Sgouria Lyra¹, Benjamin Wilde², Hemanth Kolla¹, Tim Charles Lieuwen², Jacqueline H. Chen¹
¹Sandia National Laboratories, United States ²Georgia Institute of Technology, United States

Fuel rich hydrogen transverse jets in high temperature vitiated fully developed turbulent channel flow under inert and chemically reacting conditions is studied in a joint experimental and numerical approach. Simultaneous stereoscopic PIV, OH-PLIF, three-dimensional dynamic pressure measurements and results from direct numerical simulations with detailed H₂/CO-air chemistry are reported. The paper investigates the effects of the elevated temperature, composition and broadband turbulence of the vitiated cross-flow on the transverse jet, the mixing and flow field, flame stabilization, structure and combustion mode. The three dimensional DNS results of the inert and reacting JICFs show good agreement with the measured mean velocity fields. The mean flame location demarcated by the OH concentration is well captured.

Instantaneously, the inert and reacting shear layers are unstable, characterized by the formation of Kelvin-Helmholtz vortical structures responsible for the fuel-oxidant mixing. In the inert JICF the vortex roll-up has a pronounced preferred shedding frequency, whereas the shedding is more broadband when reactions are initiated. Dilatational effects induced by the density drop in the presence of the flame are important contributors to the increased jet width. Frequency spectra of the span-wise vorticity at distinct locations suggest that the shear layer instability corresponds to a Strouhal number of 0.69 and that the presence of significant near-field heat release and a fully-developed turbulent cross-flow does not alter

the jet's stability properties. The propensity of the mixture to ignite prior to ignition and the global structure of the resultant burner attached diffusion flame is investigated using both CEMA and the Takeno flame index. The mixture is highly explosive prior to ignition and after reactions is activated, a diffusion flame establishes anchored at the stagnation point in the wind-ward side and at the low velocity region in the lee-ward side.

snlyra@sandia.gov

W5P038

PREMIXED FLAME KERNEL PROPAGATION IN HIGH SPEED CHANNEL FLOWS WITH MODERATE TURBULENCE AND COMPRESSIBILITY

Nathan Grady¹, Robert Pitz¹, Bradley Ochs², Suresh Menon², David Scarborough², Tom Slais²

¹Vanderbilt University, United States ²Georgia Institute of Technology, United States

Premixed flame propagation has been studied extensively over a range of turbulence intensities and length scales. However, most of these measurements have used burners, which impose "memory effects" on flame propagation due to their particular geometry thus obscuring a fundamental, phenomenological understanding of premixed flame propagation without these large-scale effects. Additionally, some new types combustors may have compressible and/or supersonic mean flows and intense turbulence intensities. Therefore, there is a need to study turbulent flame propagation: 1) without the use of any burner and/or stabilization device, and 2) with compressible mean flows. One such way of eliminating geometric dependence is to use freely propagating kernels that are propagating in a uniform mean flow and significant small-scale turbulence. While experiments studying kernels exist, previous works are at low turbulence and low mean flow conditions. Therefore, to study the impact of higher turbulence intensity on freely propagating flame kernels and to investigate the effect of mean flow compressibility, a new premixed CH₄-air facility has been developed and used for these studies.

Although this facility is capable of creating mean flow up to a flow Mach number of 0.7 the current studies are limited for flows with $M < 0.5$. The turbulence is generated via an active blown-grid design upstream of 9.3:1 contraction nozzle to accelerate the flow to compressible conditions inside a constant area square channel. Turbulence intensity up to 4 m/s has been generated under current operating conditions. A premixed flame kernel is ignited in the channel using a 5 mJ laser pulse from a doubled Nd: YAG laser at 532 nm. An OH PLIF system is used to determine kernel radius, flame thickness, flame surface density, and flame speed at multiple downstream positions (i.e., propagation times) for a range of inlet turbulence intensities ($u' = 0.4$ -4 m/s, or $u'/SL = 1$ -10) and mean flow Mach numbers ($M = 0.1$ -0.5) all at stoichiometric conditions. The interaction between the flame kernel and the mean flow Mach number is analyzed and the effect of increased turbulence levels on flame propagation is accessed.

nathan.r.grady@vanderbilt.edu

W5P039

TURBULENT FLAMMABILITY AND EXTINCTION STUDIES APPLIED TO PREMIXED CONFINED MIXTURES BETWEEN BIOADDITIVES AND PRF GASOLINE FUELS

Ricardo Hartmann¹, Robert A. Schiessl¹, Amir A.M. Oliveira¹, U. Maas²

¹Federal University of Santa Catarina, Brazil ²Karlsruhe Institute of Technology, Germany

Experiments are carried out to investigate the lean extinction limit of alkane/ethanol mixtures after spark-ignition. The fuels studied were *n*-heptane, *iso*-octane and ethanol (pure and in binary alkane/ethanol mixtures). In the studies, a large cylindrical constant-volume (55 liters) bomb equipped with fans for turbulence generation and electrodes for spark generation was filled with a fuel/air mixture at atmospheric pressure and room temperature. Then, a spark was issued into the mixture, and an ICCD-camera was used to capture luminescence from the spark region. Initial experiments with pure air showed that luminosity from the spark ceased after a certain time span after spark initiation. Luminescence that was still visible in fuel/air mixtures after a significantly larger time span relative to spark initiation was attributed to a developing flame kernel. It was investigated whether such a flame kernel lead to a globally self-propagating flame; absence of a self-propagating flame was interpreted as flame kernel extinction. The extinction limit was determined for each fuel as a function of the fuel/air equivalence ratio and the turbulence intensity. The latter was adjusted by varying the fan speed. Measurements with Phase Doppler Anemometry (PDA) were previously performed in the cell, providing a calibration of turbulence intensity vs. fan speed. The spark timing, spark voltage/current measurements were synchronized with the acquisition of pressure traces and luminescence images. One individual experiment delivers a binary outcome (flame propagation or not).

Results from multiple experiments with varied values of equivalence ratio and turbulence intensity were analyzed using a statistical approach using a maximum likelihood-method. This treatment is in accordance with the interpretation of the extinction in a turbulent flow as a statistical phenomenon, instead of a purely deterministic one. Using this concept, estimates of the extinction limit together with confidence intervals (or uncertainty limits) can be obtained. Results will allow to assess the influence of bio-components on the extinction limits.

ricardo@labcet.ufsc.br

W5P040

DYNAMICS OF AN OSCILLATING MIXTURE OF REACTING FLUIDS

Martin Jurisch, William Jones, Andrew Marquis, Imperial College, United Kingdom

The dynamic behaviour of mixtures of reacting fluids places challenges on the design of combustion engines in that

it may adversely affect the efficiency or even lead to failure of the engine. Self-induced oscillation which is perceived by the observer as sound appears particularly significant and is to date a subject of intensive research. The thermodynamic fields describing the mixture vary periodically with amplitudes which are usually an order of magnitude larger than those in a generic turbulent flow. This can prove particularly destructive to components of the combustor. It is the consequence of a complex interaction between the zone in which chemical reactions proceed (reaction zone) and the hydrodynamic fields. To design a combustor such that an undesired self-induced oscillation of the mixture be avoided requires models that describe accurately the motion of the mixture. In this regard the constitutive modelling, in particular the phenomenological description of reacting materials through reaction mechanisms, plays an important part. Papers by Zambon and Chelliah have demonstrated that one-step reaction mechanisms are unable to predict accurately the dynamic response of the pressure field in an oscillating methane-air mixture. A detailed reaction mechanism (17 chemical species and 39 elementary reactions) was taken as a reference to describe the chemical reaction. The results revealed the shortcomings of the one-step mechanism, which failed to reproduce the temporal growth rate and the value of the pressure amplitude in the stabilised dynamic response of the oscillating mixture. It appears that this finding has not been sufficiently accounted for in the modelling of self-induced oscillation of reacting mixtures in combustion engines, such as gas turbine combustors. The aim of this presentation is to improve the understanding of the dynamic behaviour of an oscillating mixture in a turbulent flow. For this reason, the self-induced oscillation of a lean premixed ethylene-air mixture in a bluff-body stabilised combustion chamber is analysed. The flow around a bluff body is highly relevant as it allows for passive control of the position of the reaction zone in a combustion chamber. In view of the above the detailed reaction mechanism of LUO ET AL., which consists of 22 chemical species and 18 global reactions, has been selected to model the ethylene oxidation. The field equations of fluid dynamics are solved numerically using the sgs-pdf Large Eddy Simulation (LES) framework. The results show that the mixture undergoes a sudden transition after the onset of oscillation in which the initially smooth reaction zone appears highly wrinkled. Consequently, the stabilised dynamic response of the hydrodynamic fields is greatly affected by turbulent fluctuations. Such is not the case before the sudden transition. In the stabilised dynamic response the total thermal power generated by the chemical reaction varies with an amplitude of up to 30% of the mean value. Two characteristic frequencies, interpreted as the resonant frequencies of the combustor, are identified in the frequency domain representation of the time signals for the pressure and thermal power generated by reaction. The strong interaction between the reaction zone and the hydrodynamical fields is evident only at the harmonic resonant frequency but not the fundamental resonant frequency.

martin-jurisch@gmx.de

W5P042

OH-ZONE STRUCTURE OF SWIRLED, STRONGLY-PULSED TURBULENT JET DIFFUSION FLAMES

Ying-Hao Liao, Jim Hermanson, University of Washington, United States

Planar Laser-Induced Fluorescence (PLIF) imaging of the OH radical was used to study the reaction-zone structure of strongly-pulsed, turbulent, jet diffusion flames in the presence of a swirling co-flow. The pulsed flames were investigated over a wide range of fuel injection conditions and different swirl levels. The fuel injection was controlled by strongly-pulsing the fuel flow (ethylene) by a fast-response solenoid valve such that the fuel flow was completely shut off between pulses. This control strategy allowed the fuel injection to be controlled over a wide range of operating conditions, allowing the flame structure to range from isolated fully-modulated puffs to interacting puffs to steady flames. The swirl level was controlled by varying the ratio of the volumetric flow rate of the tangential air to that of the axial air.

OH PLIF imaging was successfully employed in these highly-sooting flames by careful selection of the laser fluence and camera gate width to minimize soot-related signal interference. The excitation wavelength, generated by a dye laser and frequency doubler pumped by an Nd: YAG laser, for OH PLIF imaging was approximately at 283 nm. The reaction-zone structure, as indicated by OH PLIF, is broadly consistent with the observations of luminous flame structure for these types of unsteady flames. The OH PLIF imaging confirms the existence of compact, puff-like structures for short injection times, while elongated flames, similar in behaviors to steady flames, occur for long injection times. The flames with swirl are found to be shorter for the same fuel injection conditions. The decreased flame length is consistent with an increased rate of air entrainment due to swirl.

The overall area of the OH zones, as indicated by statistics generated from the OH PLIF signals, is generally higher for strongly-pulsed flames compared to steady flames. In addition, the OH-zone area generally increases with increased swirl level, consistent with a broader and more convoluted OH-zone structure for flames with swirl. The Root-Mean-Square (RMS) of the OH-zone area, which is broadly indicative of the degree to which the OH zones are impacted by the local flow fluctuations, is generally higher for flames with swirl than for those without swirl, suggesting a relatively stronger impact of flow turbulence on the flame structure of swirled flames. In many cases, the OH zones were observed to exhibit discontinuities at the instantaneous flame tip in the early period of fuel injection. The discontinuities were less evident for the case of flames with swirl.

liao@uw.edu

W5P043

STRAIN RATES AND REACTION ZONE STRUCTURES IN SYNGAS TURBULENT NON-PREMIXED JET FLAMES NEAR EXTINCTION

Jeongjae Hwang, Taesung Kim, Jisu Yoon, Youngbin Yoon, Seoul National University, Korea

Turbulent non-premixed jet flames with coaxial air are widely used in practical combustors due to their increased mixing rate and simple configuration. If the coaxial air velocity increases with the fixed fuel flow rate, the detachment (blowoff or liftoff) by local extinction occurs at a certain air velocity. Then the detached flame can be lifted at the stabilization point, if the conditions (e.g., turbulent properties, flow velocity and chemical kinetics) at the point are favorable. Otherwise, the flame is blown off. The detachment of coaxial jet flames with moderate lip thickness appears in two types. In the relatively low fuel jet velocity region (regime I), the detachment of the flame is governed by local extinction due to the lean flammability on the nozzle lip. However, in the relatively high fuel jet velocity region (regime II), the detachment is controlled by local extinction near the nozzle exit due to high strain or high scalar dissipation.

Recently, with increasing concern regarding the Integrated Gasification Combined Cycle (IGCC), a great deal of research on Hydrogen (H_2) and Carbon Monoxide (CO) syngas combustion has been conducted for fundamental studies and for practical gas turbine combustors. In this study, we investigated H_2 /CO syngas turbulent jet flames. We examined their stability characteristics and particularly focused on the detachment of the flame in regime II, which is controlled by high strain or high scalar dissipation. Simultaneous measurements of Planar Laser-Induced Fluorescence (PLIF) of OH radicals and Particle Image Velocimetry (PIV) were used to investigate the effect of strain rates and OH thicknesses on the detachment of turbulent syngas non-premixed jet flames. We focused on the extreme near field region ($0.25 < x/df < 5.0$) where local extinctions cause the flames to detach. Mean values of the extensive principal strain rate on OH layer decrease with the axial distance and the maximum value appears near the nozzle. For pure hydrogen flames, the maximum values of mean strain rate are the almost same in the flames near detachment. However, for higher CO contents H_2 /CO flames, the maximum mean strain rate is higher in the stable flames than in the flames near detachment. Flames with various fuel jet Reynolds number near detachment have almost identical minimum mean OH thicknesses. The scattered plot of OH thickness and principal strain rate shows that they have inverse relationships although OH thickness is widely distributed within a small principal strain rate range. Probability Density Functions (PDFs) of OH thickness show that the distribution is skewed toward a lower value within a higher principal strain rate range while it is broaden around larger value within a lower principal strain rate range.

astro706@snu.ac.kr

W5P044

STATISTICS OF UNSTEADY EXTINCTION USING A SIMPLE STOCHASTIC MODEL

John Hewson, Sandia National Laboratories, United States

While the existence of a critical dissipation rate, above which steady flames are unstable and extinguish, has been known for a long time, quantitative predictions of extinction under unsteady conditions have been limited to fully resolve unsteady simulations. In recent work, we identified a quantitative extinction criterion for flames subject to unsteady dissipation rates (Hewson, *Combust. Flame*, 2013). This extinction criterion is expressed in terms of a critical dissipation impulse magnitude that is related to the characteristics of the steady-state S-curve for the given fuel mixture. In the present work, we extend this analysis to better understand the frequency this extinction criterion suggests extinction will occur in turbulent flows by studying dissipation rate evolution in a model system. The model system employs an Ornstein-Uhlenbeck process to evolve the dissipation rate. We find that the frequency with which the critical dissipation impulse is exceeded follows a power law scaling as a function of the impulse magnitude. The frequency also depends on relative values of the extinction dissipation rate, the average dissipation rate and its variance. This work was conducted at Sandia National Laboratories, a multiprogram laboratory operated by Sandia Corporation, a Lockheed Martin Company, for the United States Department of Energy's National Nuclear Security Administration under Contract DE-AC04-94AL85000 and supported in part by Sandia National Laboratories' Advanced Simulation and Computing program and in part by Sandia National Laboratories' Laboratory Directed Research and Development program.

jchewso@sandia.gov

W5P045

TURBULENT COMBUSTION SUBGRID CLOSURE OF RANS USING LEM3D

Alan Kerstein¹, Sigurd Sannan²

¹*Stochastic Sciences, United States* ²*SINTEF Energy Research, Norway*

Major limitations of Reynolds Averaged Navier Stokes (RANS) modeling of turbulent combustion include the lack of small-scale resolution and unsteadiness. A natural complement to RANS to improve its performance while keeping computational cost low relative to Large-Eddy Simulation (LES) would be a subgrid closure that is multiscale in nature and captures unsteadiness at flame scales. For this purpose, we have developed a 3D subgrid closure approach, LEM3D, which is based on the Linear Eddy Model (LEM). Previous work has demonstrated the performance of LEM3D through comparison to measurements in a challenging passive-scalar mixing configuration. In this poster, the current status of efforts directed toward the coupling of LEM3D to RANS and the incorporation of combustion phenomenology (chemical kinetics, thermal expansion, etc.) in LEM3D is reported. LEM is a turbulent mixing model that is formulated on a one-dimensional (1D) spatial domain in order to keep computational cost low while resolving small length and time scales in an unsteady simulation. This is accomplished by introducing a representation of turbulent advection that involves instantaneous spatial rearrangements (maps) of the flow, formulated to obey the applicable conservation laws. Structurally, LEM3D involves a 3D lattice-work of orthogonal arrays of LEM domains. The spacing of the LEM domains within this structure is coarse and is intended to capture large-scale 3D effects through domain coupling. As in

LEM, this coupling involves spatial rearrangement of fluid elements (control volumes in a finite-volume interpretation), but extended to include transfer of fluid elements between, as well as within, LEM domains. During LEM3D time advancement, the domain-coupling operations are implemented on a slow time scale corresponding to the coarse 3D length scale. The remainder of the LEM3D time-advancement cycle consists of time advancement of the individual LEM domains.

When LEM3D is coupled to a RANS solver, RANS provides LEM3D with the inputs needed to specify the LEM3D turbulence parameterization, namely local values of the turbulent diffusivity, turbulence integral scale, and the quantities needed to determine the dissipative cutoff (Kolmogorov scale). For constant-density mixing, there is no feedback from LEM3D to RANS. For variable-density applications such as combustion, work is in progress to implement two-way coupling between LEM3D and RANS in which LEM3D output specifies a mean density field that is used to obtain a new RANS solution. This new solution provides updated input for a new LEM3D simulation, and so forth. This RANS-LEM3D advancement cycle is iterated to convergence, subject to the statistical precision of the stochastic LEM3D simulation. Key development steps that are underway are as follows: Development of a combustion-capable LEM code suitable for use in RANS-LEM3D. Formulation of the control algorithm for the RANS-LEM3D iteration. Transfer of information between the Cartesian LEM3D mesh structure and RANS meshes, including possible implementation of LEM3D within a sub-region of the flow domain. Parallelization to allow sub-cycling of LEM domain advancement on different processors, followed by processor communication to couple the domains. The poster describes details of these model features and shows preliminary results illustrating current capabilities.

alan.kerstein@gmail.com

W5P046

A STUDY ON COMBINED DIMENSION REDUCTION AND TABULATION FOR TURBULENT PREMIXED FLAME SIMULATIONS

Jeonglae Kim¹, Stephen B. Pope²

¹Stanford University, United States, ²Cornell University, United States

A turbulent lean-premixed flame is simulated using the Lagrangian Large-Eddy Simulation/Probability Density Function (LES/PDF) formulation to assess the accuracy and computational efficiency of a novel combined dimension reduction and tabulation of chemistry. The flame is stabilized by a bluff-body flame-holder and matches the experiments conducted in the Volvo validation rig. The fuel-air ratio is close to the lean blow-off limit and the confined flame configuration substantially increases unsteadiness, for which LES prediction is suitable. A two-way coupling between LES and PDF is applied to obtain resolved density with reduced statistical fluctuations. Composition mixing is evaluated by the modified Interaction-by-Exchange with the Mean (IEM) model, which avoids the spurious production of scalar variance. A baseline case with a full 30-species detailed propane-air mechanism uses In Situ Adaptive Tabulation (ISAT) to efficiently calculate chemical reaction. The baseline simulation shows reasonably good agreement with the Volvo measurement data in turbulence statistics, temperature, and species mass fractions. In contrast to non-premixed flame simulations using LES/PDF, chemical reaction takes only a minor portion of the overall computational cost, presumably due to the restricted manifold of purely premixed combustion. For dimension reduction, a variant of Rate Controlled Constrained Equilibrium (RCCE) is applied in conjunction with ISAT. Represented species (11 and 16 species) are chosen based upon a one-dimensional laminar flame profile and the Greedy algorithm, respectively. The combined use of dimension reduction and tabulation results in nearly indistinguishable predictions compared with the baseline case using ISAT alone. Using RCCE/ISAT, the overall computational cost is reduced by more than 15%. More than 50% reduction in the computational time is achieved for chemical reaction, demonstrating the efficiency of RCCE/ISAT. The composition mixing achieves most of the cost reduction since the mean-drift term, which is computationally expensive, is computed for the reduced representation.

jeokim@stanford.edu

W5P047

JET FLAME SIZE AND FLAME SURFACE DENSITY CORRELATIONS FOR AN EXTENSIVE RANGE OF FUELS AND FLOW RATES

Adriana Palacios¹, Derek Bradley¹, Philip Gaskell², Xiao Gu²

¹University of Leeds, United Kingdom ²Daresbury Laboratory, Germany

The Poster will show results compiled from a vast experimental data base, covering 880 turbulent jet flame heights, including measurements made by the authors. This encompasses pool fires and flares, as well as choked and un-choked jet flames of a range of gases which includes CH₄, C₂H₂, C₂H₄, C₃H₈, C₄H₁₀ and H₂, over a wide range of conditions. This ranges from buoyant laminar flames to supersonic turbulent jet flames. Pressures range from 0.06 to 90 MPa, discharge diameters from 0.4 mm to 1.32 m, and flame heights from 0.08 to 110 m. Some results of the authors on computational modelling of such jet flames, which allow for stretch rate effects, are presented, including spatial distributions of the volumetric heat release rates. The computations suggested a modified form of the Karlovitz stretch factor as a rational basis for correlating flame heights normalised by the pipe flow exit diameter. The new dimensionless parameter is of the form u/\bar{u} , where u is the mean fuel jet mean velocity, SL the maximum laminar burning velocity of the fuel/air mixture, and the bracketed term the pressure ratio. The normalised flame heights are shown diagrammatically to correlate amazingly well with the new U^* parameter over the full range. For comparison, normalised flame heights from the new vast data bank are also plotted against various other dimensionless flow parameters that have been proposed.

The computational studies enabled reaction zone volumes to be derived, as a proportion of the overall fire plume volumes, as revealed by both flame photographs and computations. From these it was possible to derive mean flame surface densities. It will be shown that these values remain fairly constant at the higher values of U^* and are close to those for initially premixed turbulent flames. This and the fact that they do not change with U^* in the regime where the plume volumes were measured, suggests the existence of a “saturation” value of flame surface density at high turbulence.

menapa@leeds.ac.uk

W5P048 PARTICLE TIME-TEMPERATURE HISTORIES IN TURBULENT FLAMES STUDIED THROUGH STOCHASTIC MODELING

John Hewson¹, David Lignell², Guangyuan Sun²

¹Sandia National Laboratories, United States ²Brigham Young University, United States

This work addresses the interaction of particles with turbulent non-premixed flames with a focus on the degree to which particles are heated by flame-particle interaction. Since chemical reactions and vaporization typically follow Arrhenius form, varying degrees of heating can significantly affect the conversion of particles from one form to another. We employ a computationally affordable stochastic model, the One-Dimensional Turbulence (ODT) model with a recently developed method of particle-flow coupling that captures the full spectrum of turbulent scales and their interaction with particles.

The ODT model is applied to canonical piloted non-premixed jet flames with particles added at various locations. We present the time scales of particle-flame interactions and compare the rate of particle-observed gas temperature to lognormal distributions that are characteristic of turbulent time scales. The time-temperature statistics of particles are examined in terms of moments and distributions of maximum particle temperatures. Of particular interest is the low-temperature particle tail of the distribution that indicates the fraction of particles that are not sufficiently heated. We relate these tails to characteristics of the turbulent flow. Both small and large Stokes number particles are investigated. This work was supported by supported by the Defense Threat Reduction Agency under Award Number HDTRA-11-45031. This work was conducted in part at Sandia National Laboratories, a multiprogram laboratory operated by Sandia Corporation, a Lockheed Martin Company, for the United States Department of Energy's National Nuclear Security Administration under Contract DE-AC04-94AL85000

jchewso@sandia.gov

W5P049 TURBULENT COMBUSTION MODELLING FOR SPLIT FUEL INJECTION

Edward Richardson, Dong-Hyuk Shin, Nabil Meah, Roderick Johnston, University of Southampton, United Kingdom

Engineers have demonstrated the potential of split fuel injection for controlling combustion timing and reducing emissions in compression ignition engines. This Direct Numerical Simulation (DNS)-based study addresses the need for fundamental understanding and for computational design tools that can account for the turbulence-chemistry interactions occurring in engines with complex split-injection schedules.

First, the dependence of entrainment transients and local scalar dissipation rate statistics in gaseous fuel jets are examined for a selection of injection schedules. The mixture fraction is used in combination with an aging scalar variable to characterise the rate of mixing between fluids injected at different times. The age, a , is defined by its boundary conditions and transport equation (Enjalbert et al. 2012).

Second, the effect that mixing between fluid injected at different times has on ignition and flame propagation is examined in a decaying turbulence simulation configuration, similar to (Doran et al. 2013), with up to three separate injection events. Double-Conditional Moment Closure for the mean reaction source term is evaluated against the DNS data, considering alternative conditioning variables: injection-based mixture fractions (Hasse and Peters, 2005); progress variable – mixture fraction; and a novel approach conditioning on mixture fraction and age.

e.s.richardson@soton.ac.uk

W5P050 THE INFLUENCE OF OXYGEN-ENHANCED COMBUSTION METHODS ON NO_x EMISSIONS, IN-FLAME TEMPERATURES AND HEAT FLUX DISTRIBUTION

Petr Belohradsky, Pavel Skryja, Igor Hudak, Brno University of Technology, Czech

The present work is aimed at experimental investigation and comparison of characteristics of three various Oxygen-Enhanced Combustion(OEC) methods, namely Premix Enrichment(PE), Air-Oxy/fuel combustion (AO) and Oxygen Lancing (OL). The combustion tests are carried out with an experimental two-staged gas burner at a large-scale burners testing facility. As for the PE method, the high-purity oxygen is injected into the incoming combustion air stream through the diffuser inserted in the air supply duct before entering the burner, while in the AO and OL methods the oxygen is injected directly into the flame through oxygen nozzle heads inserted in the center burner pipe and near secondary gas nozzles, respectively. The total oxygen concentration is varied from 21% to 38% which corresponds to the flow rate of oxygen in the range from 0 Nm³/h to 100 Nm³/h (“N” denotes the normal conditions, i.e. 0 °C, 101.325 kPa). All tests are carried out at the burner thermal input of 750 kW for two combustion regimes – one-staged and two-staged fuel combustion. The target oxygen concentration in dry flue gas is kept around 3% by volume.

The characteristics of OEC methods such as the concentration of nitrogen oxides in flue gas, flue gas temperature,

heat flux to the combustion chamber wall, in-flame temperatures distribution in the horizontal symmetry plane of the combustion chamber, and the stability of flame are investigated. The progress results can be summarized as follows: NO_x emissions increased more than 40 times and 20 times for the PE method if one-staged and two-staged combustion regime was used, respectively. Significantly better results were obtained during the tests of both AO and OL methods, especially when the fuel was staged. Then the NO_x emissions were below 120 mg/Nm³ and 150 mg/Nm³ at all oxygen flow rates, respectively.

The radiative heat transfer was enhanced as the oxygen concentration was increased for all OEC methods. The heat flux to the walls was higher by 20% at 38% O_2 compared with that at 21% O_2 . Flue gas temperature decreased with increasing oxygen concentration due to both the decrease of N_2 concentration in the oxidant and enhanced heat transfer to the chamber walls. The increase of oxygen concentration also resulted in higher temperature gradient near the burner tile in the horizontal symmetry plane of the combustion chamber. The OEC flames produced by PE and AO methods were observed stable at all oxygen flow rates. As for OL method, the flame began to be unstable when the O_2 flow rate was about 70 Nm³/h. The presented work will be further focused on the investigation of OL method in terms of flame stability, and on the assessment of fuel consumption when oxygen concentration is increased and furnace temperature is maintained around certain value at the same time.

belohradsky@fme.vutbr.cz

W5P051 INVESTIGATION OF PREFERENTIAL DIFFUSION EFFECTS IN TURBULENT LIFTED CH_4/H_2 FLAMES USING LES WITH A NOVEL FGM-PDF MODEL

Ebrahim Abtahizadeh, Jeroen van Oijen, Philip de Goey, Eindhoven Univ. of Technology, The Netherlands

Realization of Mild combustion in large scale flows is a challenging field due to the stabilization of reaction zone by autoignition. This requires sophisticated models which are able to predict complex autoignition events. In the laboratory scale Mild burners (JHC burners), these autoignition events are typically initiated at very small mixture fractions due to an intense dilution of oxidizer stream. In this region, turbulent structures in the fuel stream can hardly intrude the ignition events. This induces that influence of molecular diffusion on autoignition is comparable to that of turbulence transport (eddy viscosity). Addition of H_2 to fuel makes molecular diffusion and preferential diffusion effects increasingly important. This paper reports on the numerical investigation of preferential diffusion effects in the lift-off height and stabilization mechanism of turbulent lifted CH_4/H_2 flames in a hot and diluted environment. The Delft Jet-in-Hot coflow (DJHC) burner is chosen as a test case in which methane base fuel has been enriched with 0%, 5%, 10% and 25% of H_2 .

First, a novel numerical model is developed based on the FGM technique to account for preferential diffusion effects in autoignition. Such development is inevitable since investigations with detailed chemistry indicate that preferential diffusion affects strongly autoignition of the hydrogen enriched mixtures. Igniting Mixing Layer (IML) flamelets are introduced and analyzed to accommodate preferential diffusion effects in a flamelet database. Furthermore, transport equations for the controlling variables are derived with additional terms to account for preferential diffusion effects. Comparison of predictions using this extended FGM model with those of detailed chemistry reveals that the model is able to predict autoignition time scales accurately for all considered cases. In the next stage, the developed FGM approach is implemented in LES of the H_2 enriched turbulent lifted jet flames. A presumed beta-PDF approximation together with a gradient based model has been used to account for turbulence-chemistry interaction. Predictions of the velocity field are compared with measurements of velocity indicating a very good agreement. Computations of the combined LES and FGM-PDF model reveal that the enrichment of fuel with hydrogen leads to a significant change in the lift-off height and stabilization mechanism of the lifted flames. Main features of these turbulent lifted flames such as the formation of ignition kernels and stabilization mechanisms are thoroughly analyzed and compared with the measurements of OH chemiluminescence.

e.abtahizadeh@tue.nl

W5P052 MODELLING LIFTED JET FLAMES IN A HEATED COFLOW USING AN OPTIMISED EDDY DISSIPATION CONCEPT MODEL

Paul Medwell, Michael Evans, Zhao Feng Tian, The University of Adelaide, Australia

Moderate or Intense Low oxygen Dilution (MILD) combustion has been established as a combustion regime with improved thermal efficiency and decreased pollutant emissions, including NO_x and soot. MILD combustion has been the subject of numerous experimental studies, and presents a challenge for computational modelling due to the strong turbulence-chemistry coupling within the homogeneous reaction zone. Models of flames in the Jet in Hot Coflow (JHC) burner have typically had limited success using the Eddy Dissipation Concept (EDC) combustion model, which incorporates finite-rate kinetics at relatively low computational expense.

A systematic study has been conducted to identify the possibility of improving EDC modelling capabilities under MILD combustion conditions. Previous studies have demonstrated that modifications to the C_τ and C_ξ parameters in the EDC model can improve the accuracy of the simulations. However, these studies have looked at each parameter independently. Through a combined parametric study it has been shown that “new” values of $C_\tau=3.0$ and $C_\xi=1.0$ give significantly improved performance of the EDC model under MILD and transition to MILD conditions.

The optimised EDC model gives better agreement with experimental measurements of temperature, Hydroxyl (OH) and formaldehyde (CH_2O) profiles. The visual boundary of a chosen flame is subsequently defined using a kinetic

mechanism for OH* and CH*, showing good agreement with experimental observations and less sensitivity to variations in the fuel jet inlet temperature and turbulence intensity than the standard EDC model trialled in previous studies. The sensitivity of the newly modified model to the chemical composition of the heated coflow boundary also demonstrates robustness and qualitative agreement with previous work. The modified EDC offers results comparable to the more sophisticated, and computationally expensive, transport Probability Density Function (PDF) approach, and offers a viable alternative to significantly more computationally expensive modelling methods for lifted flames in a heated and vitiated coflow. Importantly, the visually lifted flame behaviour observed experimentally in this configuration is replicated, a phenomenon which has not been successfully reproduced using the EDC model in the past.

Using the optimised EDC model, a comprehensive modelling campaign has been conducted to investigate the role of coflow temperature and oxygen level on the establishment of MILD combustion. Additionally, the influence of major and minor species concentrations has been considered. These results show that the stabilisation of these flames is a direct result of a build-up of precursors ahead of the reaction zone, and that this effect is most prominent under MILD combustion conditions.

paul.medwell@adelaide.edu.au

W5P053

TOWARDS MILD COMBUSTION UNDER HIGH PRESSURE CONDITIONS

Paul Medwell¹, Michael Evans¹, Zhao Feng Tian¹, Qing Nian (Shaun) Chan², Alessio Frassoldati³, Alberto Cuoci³, David Blunck⁴, William Roquemore⁵

¹The University of Adelaide, Australia ²The University of New South Wales, Australia ³Politecnico di Milano, Italy

⁴Oregon State University, United States ⁵Air Force Research Laboratory, United States

The efficiency and emissions benefits of MILD (moderate or intense low oxygen dilution) combustion are well established. This combustion regime proceeds in an environment of low oxygen concentration and high reactant temperatures to create a uniform and distributed reaction zone. MILD combustion, also known as flameless oxidation (FLOX[®]), has been successfully implemented into a range of practical combustion devices. However, progress on integrating MILD combustion into high-pressure combustors is currently limited by fundamental understanding of this regime under pressurised conditions.

To develop understanding of the unique MILD combustion regime, a Jet in Hot Coflow (JHC) burner was developed by Dally. This burner replicates the exhaust gas recirculation encountered in practical MILD combustion systems with the use of a secondary burner mounted upstream of a central fuel jet. This creates a hot and vitiated coflow that can be controlled independently from the main combustion zone. The JHC burner is similar to the Vitiated Coflow Burner (VCB) developed by Cabra. Both burners have been widely used for a range of autoignition and flame stabilisation studies. The experimental flames have also been extensively modelled.

Through the fundamental studies made possible with well-controlled experimental burners, significant insight into the behaviour and structure of MILD combustion has been made. However, the role of pressure on the reaction zone remains poorly understood. To address this gap, a confined jet in hot coflow burner has been designed and built. The burner follows the same operating principle as the JHC and VCB, but is confined to enable pressurisation. The secondary burner has also been redesigned to prevent flashback at elevated pressure. The low-cost prototype combustor has been successfully operated over a range of conditions, including MILD combustion. Whilst significant in their own right, the preliminary results obtained will also be used for a revised combustor featuring more than one window and enabling operation at higher pressures.

In addition to providing new understanding of flames in a hot and vitiated coflow, the operation at high pressure also has potential application to sequential combustion gas turbines. Also known as reheat or inter-turbine burners, these feature combustion occurring in the exhaust stream from a conventional combustor. The confined Jet in Hot Coflow burner will facilitate future studies spanning conditions of interest to such gas turbine combustors.

paul.medwell@adelaide.edu.au

W5P054

AERODYNAMIC BEHAVIOR OF DIFFUSION FLAMES IN LOW AND HIGH SWIRL COMBUSTOR

Teresa Parra, Ruben Perez, Francisco Castro, University of Valladolid, Spain

The present work focuses on the numerical simulation of diffusion flames in a confined high-swirl burner. Navier-Stokes equations, expressed for a time - dependent, compressible and three-dimensional flow were solved using a structured mesh and lean methane/air mixtures. The setup corresponds with the physical domain of the Roback and Johnson₁ benchmark. Swirler has 8 flat blades 50 mm chord. The mesh was carefully designed for the enhanced wall treatment and therefore, y+ shows values lower than four. The RNG k-ε swirl dominated model provided the best results for validation in the isothermal case.

Different combustion approaches are used: Eddy Dissipation Concept, PDF and detailed chemical kinetics. Local properties of the mixture and reaction rates are calculated with ChemKin library of subroutines. Reactive cases are contrasted for swirl number 0.0, 0.6 and 1.0. In high swirling flows, the Inner Recirculation Zone (IRZ) is mainly composed by reaction products that help the ignition of incoming fuel. Besides, its forward stagnation point plays an important role while azimuthally deflecting the flame front.

The higher the Swirl number is, the bigger the IRZ is and the smaller the Outer Recirculation Zone (ORZ) due to the

sudden expansion. Swirl number equals to 1.0 provides a reaction rate with V shape. Whereas the model with swirl equals to 0.6 with smaller IRZ and larger shear layer, provides a reaction rate with M shape, two flame fronts and therefore less stable. Bearing in mind the criterion to locate the flame front as the maximum temperature gradient, it is clear the thin reaction zone for swirl numbers of 0.6 and 1.0 are located ahead of the lead stagnation point of the IRZ. In the case of 0.0 swirl, the lack of IRZ produces a thick reaction zone associated to the small gradient. The authors thankfully acknowledge the project reference ENE2011-25468 from the Spanish Ministry of Science and Innovation.

terpar@eii.uva.es

W5P055 **TURBULENT COMBUSTION MODELING OF COMPLEX FUELS USING TABULATED CHEMISTRY FOR LARGE-EDDY SIMULATION**

Daniel Mira¹, Simon Gover², Mariano Vazquez¹, Guillaume Houzeaux¹, Jim Kok²

¹Barcelona Supercomputing Center, Spain ²University of Twente, The Netherlands

The development of new combustion technologies to increase thermal efficiency and reduce pollutant emissions is leading to the use of alternative fuels for engineering applications such as gas turbines, combustion engines, furnaces or rotary kilns. The use of biomass is becoming a common practice to reduce fuel dependency when keeping the thermal power. The investigation of such fuels can be addressed numerically provided the combustion chemistry can be correctly represented without compromising the pollutants predictions.

The present work addresses the coupling of a flamelet database that can accurately represent the flame structure in composition space with a compressible code. The CFI combustion model was used for the chemistry tabulation and the coupling is implemented by extracting the transport coefficients and source term of the energy equation from the CFI table. This model can be applied to different combustion regimes from premixed to non-premixed combustion and requires to solve a transport equation for a reaction progress, mixture fraction along with their second moments when turbulent combustion is intended. This methodology is applied to a DLR confined burner in a premixed regime and some preliminary results are shown in (Image). The aim of the work is to apply the aforementioned model in a partially premixed regime burning biomass.

daniel.mira@bsc.es

W5P056 **VALIDATION OF THE TURBULENT BURNING SPEED MODEL ON NUMERICAL SIMULATION OF A GAS-TURBINE COMBUSTOR**

Kagenobu Murase¹, Nobuyuki Oshima¹, Yuta Hamada¹, Kohshi Hirano², Yoshiharu Nonaka²

¹Hokkaido University, Japan ²Kawasaki Heavy Industry, Ltd, Japan

This paper focused on the numerical simulation of an 18-MW-class industrial Gas-turbine Combustor manufactured by Kawasaki Heavy Industries, Ltd. A turbulence model with Large Eddy Simulation (LES) is applied for an unsteady turbulent field. A combustion model of the 2-scalar flamelet approach is applied for combustion field. The model uses the scalar G used for tracking a flame surface and the mixture fraction of a fuel and an oxidizer. The aim of this study is to validate the 2-scalar flamelet approach by comparing analysis results with experimental results. The experimental condition use methane as a fuel and air as an oxidizer. The turbulent premixed combustion flame is placed in the chamber. The turbulent burning speed has a great influence on the performance of flame holding. In the LES, the effect of resolved grid scale fluctuation is calculated directly, while two models applied to the Sub-Grid Scale (SGS) turbulent burning speed by the effect of SGS fluctuation. One is Yakhot's model based on the experimental data under 1_atm. The other model is Daniele's model based on the experimental data under 1_atm to 20_atm. The instantaneous temperature distribution along the X-Y cross-section under 18_atm for the case_1 (Yakhot' model) and the case_2 (Daniele's model) are shown in (Image). Yakhot's model predicts that exhaust gas is still unburnt and its temperature is predicted lower than Daniele's. In Yakhot's model there is high temperature region only behind the pilot burner, but lower in the other regions. On the other hand, Daniele' model predicts high temperature in the whole combustor and the exhaust gas becomes close to the adiabatic flame temperature observed in the experiment. The instantaneous SGS turbulent burning speed distributions along the same section for the two models are shown in (Image). In Yakhot's model, we get lower SGS turbulent burning speed in the dashed circle at the primary and the supplemental burners so that combustion delays and flameout occurs in the downstream. In Daniele's model, higher SGS turbulent burning speed predicted in the same region, where SGS turbulent burning acceleration is higher and additionally the turbulent intensity is larger. Therefore the inlet gases turn to be burnt immediately. In conclusion, Daniele's model is better in this type of the Gas-turbine Combustor.

km3086@ec.hokudai.ac.jp

W5P057 **LARGE EDDY SIMULATION OF PREMIXED FLAME FLASHBACK IN A TURBULENT CHANNEL**

Malik Hassanaly¹, Christopher Lietz¹, Venkat Raman¹, Hemanth Kolla², Jacqueline H. Chen², Gruber Andrea³

¹The University of Texas at Austin, United States ²Sandia National Laboratory, United States ³SINTEF Energy Research, Norway

In the design of high-hydrogen content gas turbines for power generation, flashback of the turbulent flame by propagation through the low velocity boundary layers in the premixing region poses an operational hazard. Predictive models that could capture the onset and the propagation of a flashback event would be indispensable for burner design in these combustors. In this work, the use of Large Eddy Simulation (LES) for describing boundary layer flashback is

studied. LES resolves large scale features of the flow, but both near-wall turbulent flow and combustion occur at scales that are unresolved. Consequently, models for these physical processes become important. Here, a progress variable based description of the flame front is used to determine if existing models for turbulent flux and flame propagation are accurate in the context of flashback. The flow configuration studied is based on Direct Numerical Simulation (DNS) of Gruber et al. A flat flame front is initialized in a turbulent channel flow and allowed to propagate upstream. The LES computations are performed using different closures for the progress variable source term as well as filter sizes. In the DNS computation, the Kolmogorov length scale is larger than the flame thickness as well as the inner layer of the premixed flame. The LES, in order to maintain reasonable number of grid points, uses filter sizes that are comparable to the Kolmogorov length scale. Hence, these LES computations represent a unique regime where the gas phase flow is almost completely resolved but the flame processes remain unresolved. The computations found certain intriguing features. The baseline case at filterwidth of 8 times DNS grid-size produced a flame front that is comparable in statistics to that in the DNS. Using quantities such as the depth parameter and the Probability Density Function (PDF) of front fluctuations, it was found that the LES computations are very accurate in predicting the structure of the turbulent flame front. However, there was a large discrepancy in the propagation velocity of the flame front. In other words, a slowly moving LES flame front was able to produce the structures of a faster moving DNS front. The flamelet-based source term closure models produced lesser variability to simulation conditions, including the choice of other subfilter models. This is expected, given that the chemical source term is the predominant quantity in the progress variable transport equation. On the other hand, the Algebraic Flame Surface Density (AFSD) model produced unexpected results, with lower reaction rates reproducing the DNS depth and the higher velocities reproducing the DNS propagation velocity. Further, the flame depth decreases with increasing filterwidth, and the flashback velocity increases with filterwidth.

malik.hassanally@gmail.com

W5P058 DNS ANALYSIS OF THERMOCHEMICAL EFFECTS ON TURBULENT PREMIXED FLAMES NEARBY A WALL SURFACE

Kazuya Tsuboi¹, Eiji Tomita¹, Tatsuya Hasegawa²

¹Okayama University, United States ²Nagoya University, Japan

Since the middle of the 20th century, it has been required to be the enhancement of energy efficiency and the reduction of emission with environmental load for actual combustors for automobiles, ships, airplanes, power generation, and industrial furnaces. For the design of actual combustors, it is necessary to understand the conditions of flow and combustion in the combustors in detail and to predict them precisely. In the combustors, turbulent flames mainly occurs, hence to investigate their detailed structure quantitatively, it is effective to utilise high accuracy database constructed by DNS. Numerical simulations such as RANS and LES are often used for the development and design of combustors recently. Many turbulent combustion models used in their simulations have been developed, however chemical processes on the wall surfaces of combustors are not considered in any current models. For example, in the engine cylinder for automobiles, very narrow space is surrounded by metal walls such as a cylinder liner, a cylinder head, a piston, etc. around the top dead centre on the compression stroke, hence it is easy to imagine that the influence of metal walls on the combustion occurred in the vicinity of the walls is not negligible. Therefore chemical processes on the wall surface should be considered to investigate the condition of combustion in the engine cylinder exactly. Any numerical works considered surface reactions on the wall surface are implemented in one dimension or in two dimensions with turbulent model, there are no studies in two or three dimensional DNS. Under no consideration of surface reactions, recently, the behaviours of turbulent premixed flames near walls were discussed in detail by using three dimensional DNS. In our previous study, it was found that for laminar flames without surface chemistry a flame is attached on the wall and spreads along the wall without quenching, while with surface chemistry a flame quenches without attaching on the wall and does not spread. Subsequently, the DNS of turbulent premixed flames with surface chemistry was performed under the adiabatic wall condition, and it was found that the results were similar to the laminar flame case. In the present study, two dimensional DNS of turbulent premixed flames was conducted with chemical processes on the *iso*-thermal wall surface, and the influence of chemical and thermal conditions and adsorbates on the walls on turbulent premixed flames were discussed.

tsuboi@mech.okayama-u.ac.jp

W5P059 EXPERIMENTAL INVESTIGATION OF BOUNDARY LAYER FLASHBACK IN H₂/CH₄-AIR SWIRL FLAMES

Dominik Ebi, Noel Clemens, University of Texas at Austin, United States

Boundary layer flashback of lean-premixed, confined swirling flames is investigated in a model swirl combustor. The combustor consists of a circular combustion chamber and a mixing tube with axial swirler and center body. A hydrogen-methane-air (H₂/CH₄-air) flame with 97% H₂ and 3% CH₄ by volume is compared to a CH₄-air flame. Flashback is induced by first establishing a stable lean-premixed swirl flame in the combustion section and then increasing the equivalence ratio. The upstream flame propagation occurs along the center body wall. Simultaneous chemiluminescence imaging and three-component Particle Image Velocimetry are applied to study the flame-flow interaction inside the mixing tube. Regions of negative axial velocity upstream of the flame tip are observed in agreement with previous studies; however, no reverse flow occurs in the streamwise (swirling) direction and thus the flow is not separated. Instead, the negative axial velocity is caused by the deflection of the streamlines in the negative axial direction due to the presence of the flame. The flow deflection is believed to be a result, rather than a cause, of the upstream flame propagation,

although it likely contributes to an enhancement of the propagation speed. The shape of the flame tip associated with upstream propagation is concave towards the reactants side. Vortical structures interacting with the flame front are found to promote or halt the upstream flame propagation. Flashback of the high hydrogen content H_2/CH_4 -air flame is found to also be associated with regions of negative axial velocity upstream of the flame tip. An increase in flame speed is observed, which is consistent with models of thermo-diffusive effects on flame propagation.

dominik.ebi@utexas.edu

W5P060

LOW LEWIS NUMBER FLAME PROPAGATION IN NARROW CHANNELS

Jonathan Gross¹, Daniel Fernandez-Galisteo², Xiaojun Pan¹, Paul D. Ronney¹

¹University of Southern California, United States, ²CIEMAT, Spain

The potential benefits of hydrogen as a fuel for mainstream use are well known. These benefits include the ability to burn at flame temperatures lower than those possible for hydrocarbons in order to mitigate NO_x formation, and the fact that hydrogen does not contain any carbon and thus does not contribute any carbon dioxide to the atmosphere when burning. Despite the long history of scientific investigation into hydrogen combustion, its properties in confined volumes corresponding to those in internal combustion engines, gas turbines, etc., have not been studied systematically. With this motivation the propagation of flames in hydrogen-oxygen-inert mixtures was studied in a quasi-2D volume, i.e., a chamber much smaller in one dimension than in the other two. This chamber was made using an aluminum frame sandwiched between acrylic panels with interior dimensions 40 cm x 60 cm x 1.27 cm. A computer-controlled partial pressure mixing system, vacuum pump and mixing chamber were used to prepare the test gases and transfer them into the test volume. A spark generator with 3 sets of electrodes was used to ignite the mixtures. A low-restriction relief valve system ensured that the combustion occurred at nearly constant (atmospheric) pressure. The flames propagated from the open (relief) end of the chamber towards the closed end, so that the observed propagation speeds of the flames in the laboratory frame of reference correspond to the propagation rates relative to the (stationary) unburned gases ahead of the front. A Vision Research Miro eX2 high speed camera was used to image near-IR emissions from water vapor in the flames produced. Videos were processed with MATLAB to extract quantitative data on propagation rate and flame shape. With this apparatus the relative importance of various types of flame instabilities on propagation rates and flame shapes could be determined. These instabilities include the effects of thermal expansion of the burned gas (Darrieus-Landau, DL), buoyant forces (Rayleigh-Taylor, RT), the contrast in viscosity between the burned and unburned gas (Saffman-Taylor, ST), and the difference between the rate of diffusion of chemical enthalpy in the form of reactants to the front vs. thermal enthalpy away from the front (diffusive-thermal, DT, or Lewis number [Le] effects). The relative influence of these instabilities could be modified through the selection of fuel, oxidizer, and diluent concentrations, as well as by changing the orientation of the chamber relative to the gravity vector. A wide range of flame instabilities were observed. For most cases, small-scale low-Le DT instabilities were observed, an interesting exception being very weak, upward propagating flames subject to large-scale RT deformation but that were very smooth on the small scale. For sufficiently strong (fast-burning) mixtures, behavior was similar for all propagation directions, consisting of small-scale DT instabilities superimposed with larger-scale DL instabilities. For weaker (slower burning) mixtures propagating horizontally, heat losses suppressed the thermal expansion induced DL instabilities; the flames were very smooth on the large scale but still exhibited DT instability at small scale. For downward propagation of weaker mixtures, a very robust jagged sawtooth-like flame shape at moderate scale was superimposed on the small-scale DT instability. As expected, propagation rates were significantly lower for weaker (more diluted) mixtures but surprisingly were nearly independent of the fuel-to-oxidizer ratio (or equivalence ratio) for a given flame temperature. These results show that the behavior of flames in narrow quasi-2D channels is significantly different from those in unconfined geometries, and, low-Le DT instabilities couple to the hydrodynamic (DL) instabilities in ways that are sometimes consistent with a simple superposition concept but are in other ways drastically different and unintuitive ways.

grossjr@usc.edu

W5P061

EXPERIMENTAL AND NUMERICAL INVESTIGATION OF THE PREMIXED FLAME

PROPAGATION ACROSS THE VARIED COMPOSITION FIELD IN A STRAIGHT RECTANGULAR CHANNEL

Zakaria Movahedi, Andrzej Sobiesiak, Indika Gallage, Univeristy of Windsor, Canada

Investigations on the flame propagation and its appearance in a channel have been reported in combustion literature quite frequently. The majority of those studies are concerned with the flame classic tulip shape formation, fast moving flames, transition to detonation and detonations itself. However, the flame evolution after the formation of classic tulip flame has not generated much interest and deserves to be inspected in more detail. Moreover, the composition field and the channel exit end open area have major impacts on the flame evolution and its propagation speed along the duct. The objective of this study is to investigate experimentally and numerically the influence of local air/propane mixture composition field (lean, stoichiometric and rich) on the flame shape evolution and its propagation speed along the straight channel with closed and fully opened exit end. Experiments are carried in the channel that is 1600 mm long with a rectangular cross-section of 25mm x 50mm. The duct is fitted with a spark plug at one (closed) end and an injecting nozzle located at 300mm from the spark plug end. This allows for the local injection of either fuel (local enrichment) or air (local leaning) of the air/fuel mixture in the channel. The exit end of the channel can be fully or partially open at

different experiments. Initially, in each experiment, the channel was filled with the air/fuel mixtures of equivalence ratio of 0.8, 1 and 1.1 (in separate runs). A varied injection timing (of fuel and air in separate trials) with respect to the spark timing is also an additional variable. The flame propagation process was captured with a high speed camera. A Turbulent Flame speed Closure model (TFC) available in Star CCM+ 9.02.005 was employed in the numerical simulation part to gain an insight into the premixed and partially premixed flame propagation. The TFC combustion model assumes that in a premixed combustion system, the reaction takes place in a thin layer which separates the whole domain into unburnt and fully burnt mixtures. The reaction rate is closed by the Zimont correlation for the turbulent flame speed. Numerical simulation results from 2-D geometry are compared with the experimental trials results.

movahedz@uwindsor.ca

W5P062

MODEL-BASED IMAGING OF INFRARED RADIATION INTENSITY FROM A TURBULENT NONPREMIXED JET FLAME AND PLUME

Brent Rankin¹, Matthias Ihme², Jay P. Gore³

¹Innovative Scientific Solutions, Inc., United States ²Stanford University, United States ³Purdue University, United States

Existing and emerging reacting flow simulations can benefit from the development of highly scalable quantitative visualization methods for volume rendering and displaying three-dimensional time-dependent results in the form of planar images. In this work, a new method is developed for quantitatively comparing measured and simulated images of the infrared radiation intensity from turbulent reacting flows. This method is demonstrated by considering a turbulent nonpremixed jet flame (at Reynolds number 15,200 and CH₄/H₂/N₂ fuel composition), which has been identified as a benchmark flame configuration at the International Workshop on Measurement and Computation of Turbulent Nonpremixed Flames (TNF Workshop). Quantitative images of the radiation intensity from the flame are acquired using a calibrated high speed infrared camera and band-pass filter. The camera and filter enable measurements of radiation from water vapor and carbon dioxide over the entire flame length and beyond. Results of the solution to the radiative transfer equation are rendered in the form of images using scalar values from (LES) and a narrowband radiation model. The measured and simulated images of the radiation intensity display qualitative features which are remarkably similar, including localized regions of high and low intensity characteristic of turbulent flames. The quantitative comparison of the measured and computed temperature profiles and radiation intensities, particularly in the plume region downstream of the stoichiometric flame length, indicate that simulating radiation heat loss effects is important even for weakly radiating flames. The results demonstrate the promise and potential of utilizing quantitative model-based imaging of radiation intensity for interpreting distributions of gas temperatures and species concentrations and validating radiation and combustion models.

brent.a.rankin@gmail.com

W5P063

CONDITIONAL ANALYSIS OF A HIGH SPEED LIFTED JET FLAME

Tai Jin, Kun Luo, Jianren Fan, Zhejiang University, China

Conditional statistics of a turbulent Mach 1.2 lifted flame have been investigated within the framework of Conditional Moment Closure models based on DNS data. The lifted flame (Image) is auto-ignited and stabilized with a flame base. Further downstream, the reacting flow develops to be turbulent and the flame surface presents to be quite corrugated due to interactions with turbulence. The mean reaction heat release rate conditioned on mean curvature of the flame surface presents to be larger for positive curvature than negative. The supersonic jet spreads slower than subsonic case. The mean center line velocity increases slightly far field due to heat release, which is definitely different from the non-reacting flows where the velocity decays monotonously. Sub-models for the unclosed terms in the CMC approach are assessed with DNS results. The large fluctuations of the species mass fraction and temperature in the mixture fraction space result in large discrepancy when using the first order CMC closure neglecting the fluctuations around the conditional mean. Correction of the chemical reaction source terms using the conditional PDF approach based on the doubly condition moment closure has been proved to be effective.

jintai@zju.edu.cn

W5P064

PREMIXED FLAME KERNEL PROPAGATION AND INTERACTION WITH A SHOCK WAVE IN A SUPERSONIC TURBULENT CHANNEL FLOW

Bradley Ochs¹, John Berlette¹, David Scarborough¹, Suresh Menon¹, Nathan Grady², Robert Pitz²

¹Georgia Institute of Technology, United States ²Vanderbilt University, United States

The behavior of premixed flames at high Mach numbers remains largely unexplored in the experimental setting. For example, flame interaction with turbulent eddy shocklets is primarily studied via numerical simulations. This is in part due to the difficulty of producing high-speed flows with simultaneously high turbulent fluctuations in a laboratory setting. In addition, flame kernel generation and measurements under these conditions present unique challenges that are not present in low speed mean flows. A new premixed test facility has been developed to study flame kernel growth and propagation in supersonic (Mach 1.5) mean flow. This facility is also designed to study shock-flame kernel interactions (e.g., when a kernel propagates through an oblique shock). The supersonic flame kernel investigation facility includes a stagnation chamber, turbulence generator, converging-diverging nozzle, and expanding test section. Turbulence is

generated via an active, blown grid upstream of a 9.3:1 contraction nozzle. The blown grid has been shown to generate turbulent fluctuations on the order of 4 m/s. The throat is sized for a mean flow Mach number of 1.5 in a 5cm x 5cm channel test section. Downstream of the nozzle a set of hinges are used to expand the test section to account for Fanno and Rayleigh flow deceleration, while maintaining a shock-free tunnel. Quartz side and top windows provide inline and orthogonal viewing access. Natural gas-air kernels are initiated via laser ignition. To this end, a frequency doubled Nd:YAG laser at 532 nm is focused at the center of the test section channel through the side windows. Time-locked camera measurements provide multi-kernel statistics at a single location while high speed video provides single kernel propagation statistics. OH* chemiluminescence, OH PLIF, and Schlieren are used for time-locked measurements while CH* and OH* chemiluminescence, and Schlieren are used for high-speed measurements. These measurements will be used to generate statistics such as mean kernel growth rates and to evaluate turbulent flame speed models under these operating conditions. Velocity measurements via Laser Doppler Velocimetry will characterize the mean and turbulent flow field. Analysis will focus on the characteristics of: 1) a freely propagating flame kernel, and 2) a kernel propagating through an oblique shock in the test section.

brad_ochs@gatech.edu

W5P065

NUMERICAL ANALYSIS OF IGNITION AND FLAME STABILIZATION IN AN *N*-HEPTANE SPRAY FLAME

Zhuyin Ren¹, Zhen Lu¹, Lei Zhou¹, Tianfeng Lu², Kai Hong Luo¹

¹Tsinghua University, China ²University of Connecticut, United States

Understanding and accurate modeling of spray combustion processes are essential for efficiency improvement and emissions reduction in diesel engines. The present numerical study targets at the well-documented experimental data for a constant volume combustion chamber, often denoted as the “Spray H”, from the Sandia National Laboratories. The transient, convection, diffusion and chemical reaction terms in the species transport equations are analyzed to gain insight into flame stabilization mechanisms, showing the dominant effects from the auto-ignition process. The influence of the Turbulence-Chemistry Interaction (TCI) on the ignition and flame stabilization is studied for two cases with different initial ambient temperatures by reconstructing the Probability Density Function (PDF) of mixture fraction.

Comparisons among the magnitudes of terms in the species transport equations are denoted as the transport budgets. For the flame being stabilized by the auto-ignition process, it is expected that the diffusion term is small compared to the other terms at the flame base. The transport budgets of CO₂ for 850 K and 1000 K are computed, and it is observed that diffusion terms are negligible at the flame base, indicating that the flame stabilization is strongly governed by the auto-ignition process. Similar observations are made for other species such as OH.

The effect of TCI on auto-ignition is investigated by reconstructing the PDF of mixture fraction. Assuming that the PDF of mixture fraction is a beta distribution, the mean ignition delay considering TCI can be obtained. In this study, local ignition delay variation with respect to the mixture fraction is analyzed in the radial direction, at some upstream locations of the flame base. The upstream locations are chosen such that reactions have not started to significantly influence the local temperatures yet. Ignition delay times with and without taking the turbulence fluctuation into consideration is compared to investigate the significance of TCI. The difference in ignition delay time with and without TCI is 0.95ms for 850K, compared to that of 0.27ms for 1000K. This indicates that TCI becomes more significant at low initial temperature, which is consistent with the previous work by transported PDF.

zhuyinren@tsinghua.edu.cn

W5P066

TRANSIENT SIMULATIONS OF AN *N*-HEPTANE SPRAY FLAME WITH DYNAMIC ADAPTIVE CHEMISTRY

Zhuyin Ren¹, Zhen Lu¹, Lei Zhou¹, Tianfeng Lu², Kai Hong Luo¹

¹Tsinghua University, China ²University of Connecticut, United States

Detailed chemical kinetics is essential though challenging for accurate prediction of combustion as well as emissions in practical combustion engines. In this work, Dynamic Adaptive Chemistry (DAC) is employed in both Unsteady Reynolds-Averaged Navier-Stokes (URANS) simulations and Large Eddy Simulations (LES) of an *n*-heptane spray flame in a constant volume chamber with realistic application conditions. DAC accelerates the time integration of the governing ordinary differential equations for chemical kinetics through the use of locally (spatially and temporally) valid skeletal mechanisms. Instantaneous flame structures and global combustion characteristics such as ignition delay time, flame Lift-Off Length (LOL) and emissions are investigated to assess the effect of DAC on URANS-DAC and LES-DAC results.

For URANS, good agreements are observed on instantaneous flame structures and global characteristics between simulations with and without DAC. For LES, it is shown that the errors in scatter distribution in the composition space and global combustion characteristics incurred by DAC are small even though the instantaneous flame structures in the physical space from the simulations with and without DAC are significantly different. The different DAC convergence characteristics between URANS and LES are due to the strong coupling between chemical reactions and the flow field. The errors in species evolution and heat release, induced by the elimination of species and reactions in DAC during the reaction substeps, may alter the local small flow structures through the coupling of density. In LES, these stochastic local small disturbances may grow in time and finally alter the instantaneous fuel vapor distribution and consequently the flame

structure. In contrast, in URANS, these stochastic local small disturbances are mostly averaged out at all length scales. The study reveals that in LES-DAC simulations, manifolds in the composition space, conditional quantities and global combustion characteristics need to be used to assess the solution accuracy.

The study shows that a speed-up factor of more than two can be achieved by DAC with an 88-species skeletal mechanism with less than 0.2% and 3.0% discrepancy in ignition delay and LOL, respectively. The evolutions of retained species and reactions during the simulations imply that the 88-species skeletal mechanism cannot be further globally reduced for the *n*-heptane spray flame considered.

zhuyinren@tsinghua.edu.cn

W5P067

ADOPTION OF ANALYTICAL DESIGN METHODS FOR THE DESIGN OF HIGH-PRESSURE COMBUSTION CHAMBERS IN LOW-POWER EVAPORATING BURNERS

Volodymyr Ilchenko, Vitali Dell, Webasto Thermo, Germany

Aiming at the reduction of CO₂-emissions, the efficiency of combustion engines is continuously being increased. Due to the high efficiency of new engines there is an insufficient residual heat for heating up the passenger cabin at low outside temperatures. Additionally for hybrid vehicles, the insufficient residual heat has to be compensated. Thus, auxiliary heating systems become more important to ensure general comfort levels in passenger cabins. In the field of independent vehicle heaters, burners with evaporating units of low heating capacity are commonly applied. During the operation of a burner the liquid fuel is pumped into the burner's evaporating unit consisting of porous materials. The fuel is distributed in the porous medium and is evaporated due to the heat flux from the combustion zone. The generated fuel vapour is mixed with the combustion air entering through the holes on the side wall of the burning chamber and is ignited in the next step. The stabilization of the flame occurs in the shear layers produced by the swirl flow and/or by the cross-flows as well as in the upstream aligned zones of the combustion chamber. Actual burners reach their limits regarding the reduction of exhaust emissions as well as the extension of power modulation range, when taking into account the future requirements in the automotive sector. Because of the lack of analytical approaches, an empirical approach is commonly applied to the design of such kind of burners. For this reason there exists a demand for the transfer of combustion technologies and analytical design approaches established in other industry sectors, for the optimisation of the given combustion systems. The aim of this project is to apply analytical methods used in the field of gas turbine development to the geometric design of combustion chambers with boundary conditions existent in low-power evaporating burners. Thus, an analytical design tool for dimensioning the geometry of a swirl burner with an evaporating unit was developed, addressing the criteria of flame stability and combustion quality. Both of the criteria are affected by the total pressure drop over the combustion chamber as well as the distribution of the combustion air through the swirler and the holes in the burner chamber. The design tool enables the calculation of the burner geometry on the basis of input data such as the total pressure drop, the desired burner power, total and local air-fuel ratio values, swirl number, penetration depth of the air jets, as well as the length of the primary zone. While designing the analytical tool, empirical values known from the field of gas turbines were applied for certain parameters, such as recirculation rate and swirl number. In order to estimate the empirical parameters at the boundary conditions given in the evaporation burners, and for the verification of the analytical tool, flow measurements were conducted in a water channel by means of a Stereo-PIV system. For this reason scaled combustion chambers of different geometries were designed and built from PMMA (e.g. Plexiglas) after consideration of the Reynolds similitude. Hereby parameters such as swirl number, combustion air distribution between primary and secondary zone, as well as mass flow were varied. The pressure loss was held constant for all burners. Measurements in the water flow, seeded with hollow glass spheres with a diameter of 15µm, provided information on the distribution of the mass flows through the axial swirler and the holes in the side wall of the combustion chamber, the velocity fields, recirculation ratio, and penetration depth of the inlet jets. In addition to the water channel measurements, a parameter study was conducted on burners of different geometries for the estimation of optimal burner parameters on the basis of the exhaust gas emissions, burning noise, as well as flame-out limits. Hereby parameters such as swirl number, combustion air distribution between primary and secondary zone, length of the primary zone, as well as load level were varied. Finally, both types of measurements were shown to correlate with each other, and thus the analytical design tool could be successfully verified for the whole range of the varied parameters.

ilchenko@gmx.net

W5P068

FLOW STRUCTURE MEASUREMENT DOWNSTREAM OF AXIAL GUIDE VANE SWIRLER

Jiri Vondal, Jiri Hajek, Brno University of Technology, Czech Republic

An axial guide vane swirl generator is widely used in process furnaces as a flame holder for non-premixed gas and oil combustion. It generates swirling flow with recirculation zones which provide reactants with sufficient mixing intensity. Tangential momentum is often introduced to the stream with higher momentum – typically the air stream. Swirler (swirl generator, flame holder) is a key burner design element that significantly influences the flow pattern in combustion chambers. Specific design of swirl generator might be used in process burner, it combines an axial guide vane design with a bluff body flame holder since swirler has smaller diameter than a pipe. This type of swirl generation is utilized at a low-NO_x burner – subject of current research. The aim of this work is to understand complex flow produced by a specific axial guide vane swirl generator and provide validation data for CFD predictions. It adopts experimental approach to characterize flow structures under cold flow conditions. Experimental setup is designed according to the

existing low-NO_x staged gas burner – it respects its inner diameter of air supply duct and adopts full-scale swirler with diameter 280 mm, 8 vanes and 45° vane angle. The air flow rate was chosen to respect amount of combustion air delivered for 745 kW firing rate of natural gas burner with excess air ratio 1.1. A sudden expansion was not included in the setup to allow for straightforward comparison of different swirlers with each other and their effect on the flow without any influencing parameters. The Reynolds number is 73660 based on the inner diameter D=300 mm and the mean flow velocity 3.85 m/s. Flow field properties are measured downstream of the swirler by a hot wire anemometer probe Dantec 55R04 and 55R54 connected to a constant temperature MiniCTA system. Calibration and temperature correction is employed for each measurement. The velocity components, turbulence properties and power spectrum are evaluated on multiple downstream positions from 0.2D up to 2D.

vondal@fme.vutbr.cz

W5P069

SOOT PARTICLE SIZE DISTRIBUTION MEASUREMENTS ALONG THE CENTERLINE OF A PILOTED TURBULENT NON-PREMIXED FLAME AT ATMOSPHERIC PRESSURE

Wesley Boyette, Snehaunshu Chowdhury, William Roberts, Abdullah University of Science and Technology, Saudi Arabia

Validation of various numerical models of turbulent non-premixed flames has been very challenging due to the lack of experimental data. In this study, we designed and built a burner based on the experiments performed by Zhang, Shaddix, and Schefer at Sandia National Laboratories. The burner includes a central fuel tube delivering ethylene with 65% nitrogen as diluent to keep the soot loading within measurable range. An annular fuel tube delivers premixed ethylene and air for the pilot flame. The pilot mixture accounts for 6% of the total heat release of the main jet. An air co-flow jet is formed by a concentric tube with an outer diameter of 245 mm including an aluminum foam flow-straightener at its exit section. The co-flow velocity is maintained at 0.6 m/s. To build on the work of Zhang and others, we conduct soot Particle Size Distribution (PSD) measurements in the range of 6 to 228 nm at different centerline locations using a Scanning Mobility Particle Sizer (SMPS). The measurements are made for two different Reynolds number of the jet, Re=10000 and 20000. A soot-sampling probe is built with a tube having a 500-micron orifice diameter to pull in a small amount of gas sample from the flame. This incoming gas is then immediately diluted by nitrogen at a flow rate of 30 slpm. The ends of the sample probe are cooled by passing chilled water (T = 6.5 C) through water jackets at both ends. A fraction of the diluted sample gas is passed into the SMPS thus providing the PSD. This may be converted to the PSD in the flame by knowing the dilution factor which is the ratio of the nitrogen flow rate through the tube to that of the volume of sample flowing into the probe. We find that the PSD is skewed heavily toward small particle diameters close to the nozzle while further away; the PSD shows relative invariance with particle sizes up to 40 nm. The dilution factor is not known a priori. As a first estimate, the dilution factor is calculated by Line-Of-Sight Attenuation measurements (LOSA). In this technique, a 632.8 nm Helium-Neon laser beam is passed along the beam with and without the flame and the intensities are recorded. Since soot absorbs and/or scatters the laser beam, the intensity with the flame will be lower than that without the flame. Future work will focus on using gas analyzers and laser-induced incandescence (LII) to properly evaluate the dilution factor.

wesley.boyette@kaust.edu.sa

W5P070

SIMULATION OF INSTANTANEOUS COAL GASIFICATION FLAMES WITH ONE DIMENSIONAL TURBULENCE MODEL

Yuxin Wu¹, Philip Smith², Hai Zhang¹, Alan Kerstein³

¹Tsinghua University, China ²The University of Utah, United States ³Stochastic Sciences, United States

In near nozzle region in a coal gasifier, strong interactions exist between coal gasification and turbulent fluctuations. These interactions have essential effects on the coal gasification process and shall be considered. Based on a proposed particle-eddy interaction model and the spatially developing One Dimensional Turbulence (ODT) method, instantaneous coal gasification flames are simulated with mesh resolution down to Kolmogorov scales. Turbulent fluctuations of gas temperature, species, and velocities are directly used in a Lagrangian particle tracking procedure. Characteristics of coal gasification flames are studied based on instantaneous realizations and average results. It is observed that a central fuel rich region is formed firstly due to rapid devolatilization and slower particle dispersion in the near-nozzle region. Then stronger heterogeneous coal-char reactions occur at the edge of the gasification flame. Oxygen entrainment causes the high temperature region to converge toward the center line in the developed region. Particle-size-dependent coal gasification processes and particle-eddy interactions are also studied. Dependence on particle response time is shown in a straightforward way by comparing instantaneous configurations of coal particles and the local gas phase.

wuyx02@gmail.com

W5P071

NUMERICAL INVESTIGATION ON DEVOLATILIZED SUBSTANCES IN A COAL COMBUSTION FLAME USING LES

Hiroaki Watanabe, Seongyool Ahn, Tetsuya Shoji, Nozomu Hashimoto, Kenji Tanno

Central Research Institute of Electric Power Industry, Japan

Large-eddy simulation of a coal jet flame was performed to investigate the detailed behavior of devolatilized substances in the flame. The chemical mechanism used in this study consists of 67 species and 152 reactions were

generated from the detailed chemistry of 257 species and 1107 reactions with DRGEPSA and CSP methods. The simulated result was compared with the experimental data obtained by means of LIF and LII methods. It was confirmed that the results showed good agreement with the experiment and the LES could precisely capture the detailed structure of the coal jet flame.

whiroaki@cripi.denken.or.jp

W5P072 OBSERVATION AND QUANTIFICATION OF COMBUSTION BEHAVIOR OF A SINGLE COAL PARTICLE ENTRAINED INTO HOT GAS FLOW

Hookyung Lee, Sangmin Choi, Korea Advanced Institute of Science and Technology, Korea

This experimental investigation focuses on the heat-up, volatile release and apparent flame formation till extinction, and initiation of char reaction of a single coal particle which is injected into hot flow field. Pulverized coal particles transported by cold air as carrier gas are injected perpendicularly into hot gas environment of 1240K temperature and 16-40% O₂. Individual coal particle in a nearly single particle condition in the controlled environment is traced; starting from the point of introduction and sequential progress of burning particle is recorded and presented. Characteristic regions in the overall coal combustion process are identified based on the visual appearance of particle and its associated flame. Visual observation was quantified in terms of time and space (location and size). Unambiguous definition of counting time by clearly defining the starting point enabled critical assessment on the particle heat-up, ignition point, and ignition delay, distinction of volatile flame from luminous particle surface. Quantification of size and intensity of images further allowed discussions on the dynamic formation and extinction of volatile flame, progress of heterogeneous oxidation of char which was produced 'in-situ' from a pulverized coal.

hookyung@kaist.ac.kr

W5P073 SOOT PARTICLE GROWTH IN A COMBUSTION FIELD FORMED BY SMALL PULVERIZED COAL JET BURNER

Nozomu Hashimoto¹, Jun Hayashi², Noriaki Nakatsuka², Hirofumi Tsuji¹, Satoshi Umemoto¹, Kazuki Tainaka¹, Fumiteru Akamatsu², Hiroaki Watanabe¹, Hisao Makino¹

¹Central Research Institute of Electric Power Industry, Japan ²Osaka University - Suita

Pulverized coal combustion is utilized in the majority of coal-fired thermal plants. Although the basic pulverized coal combustion technology was established many decades ago, the soot formation characteristics in a pulverized coal flame have not been investigated completely. In this study, the soot formation characteristics in a coal flame were investigated by using Time-Resolved Laser Induced Incandescence (TIRE-LII) and thermophoretic sampling. The schematic of TIRE-LII measurement system is shown in (Image). The second harmonic wave (532 nm) from the Nd:YAG laser was employed as a light source to incandesce soot particles. Two high speed CMOS camera with the image intensifier were used to detect the LII signal. The time interval between the first acquisition and the second acquisition of LII signals for the two cameras was set to 450 ns. (Image) shows the PDF of the LII signal decay ratio between the two cameras at different heights from the burner exit. It is found that the ratio of large soot particles increases with the height, i.e., the size of primary soot particles is increased at the downstream region. This particle growth was also confirmed from the results of thermophoretic sampling. (Image) shows TEM images of soot particles sampled by the thermophoretic sampling. It is found that the primary particle size for h = 65 mm is larger than that for h = 25 mm. The increase in primary soot particle size in a coal flame was clearly captured by this study.

nozomu@cripi.denken.or.jp

W5P074 CHARACTERISTICS OF NO REDUCTION BY CHAR LAYER IN FIXED-BED COAL COMBUSTION

Hailiang Du, Shanghai Jiao Tong University, China

Traveling grate boilers are widely used in China with high pollutant emissions. However, they are often reported to have relatively low combustion efficiency and high pollutant emissions. The main objective of this study is to investigate the characteristics of NO reduction by char layer. Experiments were carried out on a fixed-bed furnace with two different coal bed heights (6cm and 12cm) under the same air supply. The concentrations of NO, O₂, CO₂, CO and H₂ were measured and compared to reveal the effect of char layer. Results show that the trend of NO emission presents a double-peak distribution on the coal bed surface for different stoichiometries. And the first peak is higher than the second one. The nitrogen in volatiles is almost completely oxidized at early stage of combustion process. The yield of NO forms the first peak at about 5 minutes after the ignition of coal bed. The maximum yields of NO emission are 493.30mg/m₃ (6cm) and 384.09 mg/m₃ (12cm) for Huainan Coal and 560.19 mg/m³ (6cm), 468.29 mg/m₃ (12cm) for Neimeng Coal. The thicker bed height condition forms more char. The NO generated from the flame front is reduced by the char layer. The NO-char reaction is strongly enhanced by the presence of CO.

whdul@sjtu.edu.cn

W5P075 INFLUENCE OF ASH COMPOSITION Fe₂O₃ ON COAL PYROLYSIS IN A TUBULAR REACTOR

Qinhui Wang, Yukun Yang, Mengxiang Fang, Jinsong Zhou, Zhongyang Luo, Zhejiang University, China

Hot coal ash is usually used as the solid heat carrier to supply the heat needed for coal pyrolysis in the coal pyrolysis/gasification-combustion cascade conversion process, and to some degree coal ash itself can also affect coal pyrolysis. As the first step to explore the impact of external ash on coal pyrolysis, we conduct research work on the influence of Fe_2O_3 , which is one of the most important minerals in coal ash, on coal pyrolysis in a tubular reactor from 500°C to 1000°C in terms of the change of yields of pyrolysates including gas, tar, pyrolysis water and char, and of gas composition. $[\text{Fe}_2\text{O}_3]/[\text{coal}]$ is 5%, 10% and 20% by weight, respectively, in the coal- Fe_2O_3 mixtures which are pyrolyzed in a series of experiments. As is founded in the experiments, when coal is pyrolyzed with the addition of Fe_2O_3 , gas yields increase at the relatively higher temperature. Tar yields and CO production decrease in the whole temperature range from 500°C to 1000°C, while pyrolysis water yields and CO_2 production show an opposite tendency in the same temperature range. Char yields and H_2 production increase at low temperature but decrease at high temperature, while CH_4 production decreases at 500°C but increases at higher temperature. All these are attributed to the following: the catalytic effect of Fe_2O_3 and its reaction with some of the coal pyrolysates, such as H_2 and CO. More addition of Fe_2O_3 can often enhance the tendency to some degree, especially at elevated temperatures.

qhawang@zju.edu.cn

W5P076 THE TRANSITION OF HETEROGENEOUS-HOMOGENEOUS IGNITIONS OF DISPERSED COAL PARTICLE STREAMS

Ye Yuan, Shuiqing Li, Tsinghua University, China

This work is assessing a study of the collective ignition behaviors of dispersed coal particle streams, with ambience temperature from 1200K to 1800K and oxygen mole fractions in the range of 10%-30%. The dispersed coal particles of 65-74 μm are injected into an optical Hencken flat-flame burner by a novel de-agglomeration feeder. Three kinds of pulverized coals from different ranks, Hulunbel lignite, high-ash-fusion bituminous and low-ash-fusion bituminous, are considered. The normalized visible light signal intensity with deleting the background noise is established to characterize the ignition delay of coal particle streams. Firstly, the prevalent transition from heterogeneous ignition to heterogeneous ignition due to ambience temperature is often observed. The pure homogeneous ignition rarely occurs, with an exception under high temperature and low oxygen for high-volatile coal. By comparing time scales between pyrolysis and heating processes, the competition of the volatile evolution and heterogeneous surface reaction are discussed. Then, the effects of ambience temperature, oxygen concentration and coal rank on the characteristic ignition delay are examined. Finally, the transient mode is developed, and it not only well interprets the observed ignition transition phenomena, but also approximately predicts a variation of heterogeneous ignition time as a function of oxygen concentration.

yuanye0427@gmail.com

W5P077 ENHANCEMENT OF GASIFICATION REACTIVITY OF LOW-RANK COAL THROUGH HIGH TEMPERATURE TREATMENT

Xian Li¹, Ryuichi Ashida², Kouichi Miura², Hong Yao¹

¹Huazhong State Key Laboratory of Coal Combustion, China ²Kyoto University, Japan

We have recently proposed a degradative solvent extraction method to upgrade and fractionate various types of low-rank coals by non-polar solvent at temperature below 350°C. The main products obtained are solvent-soluble fractions (extracts) and insoluble fraction which we call "Upgraded Coal (UC)". The UC samples were prepared from eight low-rank coals and one bituminous coal in this work. It was found that the gasification reactivities of the UC chars prepared from seven coals of the eight low-rank coals were larger than those of the raw coal chars. The CO_2 gasification rates of the UC chars prepared from an Australian brown coal, Loy Yang, (LY/UC) and an Australian bituminous coal, Gregory, (GR/UC) were surprisingly larger than the gasification rates of the corresponding raw coal chars by 2.4 to 1.9 times. The mechanism of gasification reactivity enhancement was examined from the viewpoints of catalytic effect of coal inherent minerals, pore surface area, and carbon structure of the chars. The reactivity enhancement of GR/UC was well explained by the increase of pore surface area through the degradative solvent extraction. On the other hand, neither the catalytic effect of minerals nor the pore surface area was responsible for the gasification reactivity enhancement for LY/UC. XRD measurement and elemental analysis showed that LY/UC had more disordered carbon structure than raw coal char. The reactive surface area estimated by the transient gasification method was judged to be a good index to explain the significant gasification enhancement for LY/UC. Although more detailed examination is required to elucidate the mechanism of the gasification enhancement, the proposed degradative solvent extraction method of low-rank coal can be one of the ways to enhance the gasification reactivity of coal char without using catalyst.

lxlixian@hotmail.com

W5P078 DETERMINING THE OPTIMUM COAL CONCENTRATION IN A GENERAL TANGENTIAL-FIRED FURNACE WITH RICH-LEAN BURNERS: FROM A BENCH-SCALE TO A PILOT-SCALE STUDY

Xuebin Wang, Houzhang Tan, Shien Hui, Tongmo Xu, Xi'an Jiaotong University, China

The mass ratio of pulverized coal and air (coal concentration, kg/kg) in fuel-rich streams is important in the design and operation of rich-lean burners, in which the optimum coal concentration (Copt) that corresponds to the best

combustion situation should be achieved. This study aims to establish a practical identification method to evaluate the Copt of the different ranks of coal in rich-lean burners. A wide range of tests were conducted in a bench-scale down-fired furnace and a pilot-scale tangential-fired furnace with rich-lean burners. Temperature distribution, unburned carbon in ash, and NO_x emissions were measured, and the effects of coal quality aside from burner type and burner layout method were considered. Results show that the optimum coal concentration corresponds to the highest furnace temperature for each group of tests both in the bench-scale and pilot-scale furnaces. Copt is significantly affected by coal quality even if a change from the use of a corner-tangential to a wall-tangential furnace lowers Copt; however, the effect of a vertical rich-lean burner or a horizontal rich-lean burner on Copt is negligible. The value of Copt mainly decreases from 1.14 to 0.67 with a decrease in the volatile content from anthracite scale (< 0.1) to lignite scale (> 0.35). The empirical formula of $C_{opt}=1.19-0.15V_{daf}Q_{net,0.7}/100M_{ad,0.1}$ is obtained to evaluate the optimum coal concentration of a general pulverized coal flame, and another formula, $C_{opt}=1.18-0.17V_{daf}Q_{net,0.7}/100M_{ad,0.1}$, is especially derived for a tangential-fired furnace with a rich-lean burner. The optimum value obtained is also critical to NO_x emissions because when the coal concentration surpasses the value of Copt, NO_x emissions can be much more efficiently controlled through reduction of air. The findings of this study can provide practical guidance for the design and operation of rich-lean burners to achieve high combustion efficiency and low NO_x emissions.

wxb005@mail.xjtu.edu.cn

W5P079 SIMULTANEOUS MEASUREMENTS OF MIE SCATTERING, PAHS LASER INDUCED FLUORESCENCE AND SOOT LASER INDUCED INCANDESCENCE TO LAB-SCALE PULVERIZED COAL JET FLAMES

Jun Hayashi¹, Noriaki Nakatsuka¹, Nozomu Hashimoto², Kazuki Tainaka², Hirofumi Tsuji², Hiroaki Watanabe², Hisao Makino², Fumiteru Akamatsu²

¹Osaka University, Japan ²Central Research Institute of Electric Power Industry, Japan

The formation processes of soot from coal particles through Polycyclic Aromatic Hydrocarbons (PAHs) in a lab-scale pulverized coal jet flame were investigated by performing two-dimensional laser diagnostics. Two-dimensional distributions of pulverized coal particles, formation areas of PAHs and soot primary particles were measured instantaneously by Mie scattering imaging, Laser Induced Fluorescence (LIF) and Laser Induced Incandescence (LII), respectively. Two of these laser diagnostics, i.e. a pair of Mie scattering from pulverized coal particles and of PAHs-LIF and a pair of PAHs-LIF and Soot-LII, were conducted simultaneously by using the Nd:YAG laser of 355 nm. In addition, the radial distributions of the pulverized coal particles, PAHs and soot volume fraction were compared with each simultaneous measurement result. The results indicated that the simultaneous measurements of Mie scattering, PAHs and LII were successfully achieved. The spatial distribution of pulverized coal particles, PAHs and soot were correlated but not covered each other at the same time. The peak of signals located in order of pulverized coal particles, PAHs-LIF, soot-LII in a radial direction. Although the order of each signal in the radial direction was not changed in all of the height of coal jet flame, trends of the intensity of Mie scattering, PAHs-LIF and soot-LII in height direction were different depending on the overall progress of combustion reaction. Meanwhile, the peak intensity of Mie scattering has the maximum value at the bottom of the jet flame, the peak intensity of PAHs-LIF has the maximum value at the middle height of the jet flame and the value of peak intensity of soot-LII increases with the increase of height from the burner.

j.hayashi@mech.eng.osaka-u.ac.jp

W5P080 EFFECT OF COAL RANK ON PCI COMBUSTION ZONE IN BLAST FURNACE

JinHo Kim, Pusan National University, Korea

Pulverized Coal Injection (PCI) is one of the most effective technologies to reduce coke consumption in blast furnace. The main role of PCI coal is heating source and generation of CO gas. Generally, PCI coal is high rank coal. But the steel mill company attempts to use low rank coal as an energy source on PCI combustion in blast furnace since high rank coal price is increasing and reserves is decreasing over time. The purpose of this investigation is to know the pulverized coal particle temperature and CO emission according to the effect of coal ranks. This study was performed by using a Laminar Flow Reactor (LFR) which can represent combustion environment of pulverized coal inside blast furnace. Since PCI system was developed for iron making, combustion characteristics of pulverized coal is important in the iron and steel industry. According to different type of coal, the coal flame structure, coal particle temperature and exhaust gas (CO, CO₂) were investigated. The study demonstrated that combustion characteristic of coal was influenced by several properties of individual coals. Especially, coal particle temperature and CO emission as well as the content of volatile matter of individual coals were found to have a strong influence on the combustion characteristics of coals. So, this study considered coal properties significantly and focused on the burning coal particle temperature and CO/CO₂ emissions.

jinolfc@gmail.com

W5P081 EFFECT OF NEW AUXILIARY AIR INJECTION ON WATER-WALL WASTAGE IN PULVERIZED COAL BOILER

Ho Lim, Pusan National University, Korea

The interest of fired power generation is increased opposite to nuclear power generation ever before in the world since the Fukushima Daiichi nuclear disaster. In this situation, the important thing is efficient operation of the pulverized coal boiler (pc boiler) in fired power generation industry. To increase efficient, most design parameters of pc boiler are focused on achieving the maximum life of the boiler and boiler tubes, maximum thermal efficiency, low NO_x emissions and maximum power generation. In pc boilers, entrained fly ash particles in the flue gas may cause erosive wear on metal surfaces along the flow field. This can have a significant effect on the operational life of various sections of the boiler. Especially, the boiler life time is related to water-wall, which is corroded and/or eroded by various factors. Water-wall wastage in coal-fired boilers has increased significantly since the introduction of staged combustion systems to reduce NO_x emissions. Further reduction in NO_x emissions are scheduled for the near future, which may require deeper staging, thus increasing the severity and extent of water-wall wastage further. Latest, it has been revealed that water-wall wastage is caused by ash particle impaction including unburned coal particles. The purpose of this paper is to investigate the way for reduction of water-wall wastage by particle impaction during combustion process in pc boiler as introducing air curtain that restricts particles flown to water-wall. For this, the numerical analysis based on finite volume method has been used. New auxiliary air injection nozzles are added beside coal burners of A level to E level. It has been studied the effect of added nozzle and air flow rate. Firstly, it has been to understand the flow field and identify the area where are erosion and corrosion. And then the results are compared to real phenomenon obtained from pc boiler. As a result, new air affects impaction of particles, impaction rate is decreased with air flow rate.

holim@pusan.ac.kr

W5P082

THE SEPARATE PHYSICO-CHEMICAL EFFECTS OF CARBON DIOXIDE ON COAL CHAR COMBUSTION IN O_2/CO_2 ENVIRONMENTS

Yuegui Zhou, *Shanghai Jiao Tong University, China*

The thermo-physical and chemical effects of CO_2 on char particle temperature and char reaction rate in O_2/CO_2 environments are intercoupled in the complicated char combustion process. CO_2 exerts three main effects when high concentration of CO_2 is introduced into char combustion process. These three effects are: (a) dilution effect, because of the variation of oxygen concentration in the main stream of the oxidizer; (b) thermal effect, due to the increase in heat capacity of the oxidizer and the reduction in flame temperature; (c) chemical effect, because CO_2 is an active species and it participates chemically in the combustion process. A method of adjusting char particle temperature in O_2/CO_2 environments was firstly presented by replacing an appropriate portion of CO_2 in the oxidizer with Argon (Ar) to match the same temperature in O_2/N_2 environment at the same oxygen mole fraction due to the mole heat capacity of $\text{Ar} < \text{N}_2 < \text{CO}_2$. In this way, the concentrations of the reactive species are not affected by the temperature adjustment technique and the transport properties of Ar and N_2 are similar enough. Then the method was used to investigate the separate physico-chemical effects of CO_2 on coal char combustion in O_2/CO_2 environment by a more accurate continuous-film model with specially designed combustion environments (O_2/CO_2 , $\text{O}_2/\text{CO}_2/\text{Ar}$ and O_2/N_2). One set of credible experimental data of Pittsburgh bituminous coal particle combustion temperatures in O_2/CO_2 environments with various oxygen mole fractions (12-36%) at a gas temperature of 1700 K in the literature was adopted to validate the accuracy of continuous-film model in O_2/CO_2 environments. The results indicate that char particle combustion temperature increases with the increasing oxygen mole fraction after char particle ignites, and the maximum relative error between the simulated and experimental results is 2.3%. The results also show that the char particle temperature in O_2/CO_2 environment is much lower than that in O_2/N_2 environment at the same oxygen mole fraction due to the combined effects of lower gas temperature due to higher mole heat capacity of CO_2 , lower diffusivity of O_2 in the mixture and endothermic char- CO_2 gasification reaction. Coal char particle temperature increases with the increase of oxygen mole fraction and char particle temperature in 52.5% $\text{O}_2/47.5\%$ CO_2 environment are equivalent to that in 21% $\text{O}_2/79\%$ N_2 environment. The ignition time and ignition temperature of single char particle in O_2/CO_2 environments are a little higher than those in O_2/N_2 environment at the same oxygen mole fraction, and they decrease with the increase of oxygen mole fraction. Most importantly, the effects of CO_2 on the char combustion rate in O_2/CO_2 environments were quantitatively isolated to account for the relative contribution on the char combustion rate with specially designed combustion environments. The results show that the relative contributions of the dilution, thermal and chemical effect on the char combustion rate are 82%, 11% and 7%, respectively, for Pittsburgh bituminous coal. The dilution effect of CO_2 is predominant because the increase of oxygen mole fractions directly improves the char consumption rate and sequent $\text{CO}-\text{O}_2$ reaction rate. The thermal effect of CO_2 is minor due to the increase of the char particle temperature. And the contribution of char- CO_2 chemical effect on the char combustion rate is only 7%, which agrees with the previous results.

ygzhou@sjtu.edu.cn

W5P083

EVALUATION OF ASH FREE COAL COMBUSTION CHARACTERISTICS IN A DROP TUBE FURNACE

Sang-in Kim, *Pusan National University, Korea*

Korean thermal power plants are currently using a large amount of low-rank coal, and many studies have focused on how to increase the efficiency of the low-rank coals. This study experimentally investigated the effect of ash free coal which is one of the up-grading coal almost has no-ash content and its residue on combustibility and NO_x emission. The ash free coals made from two coal sources that are utilized by Korean thermal power plants and were evaluated each

reaction rate of devolatilization and char oxidation in a Drop Tube Furnace (DTF). Combustion experiments were carried out by using several temperatures to show its kinetics parameters. The result of this study shows that comparisons of various combustion factors between two different ash free coals based on low rank coals and confirmed whether the combustibility has increased.

kim_sangin@naver.com

W5P084

COMBUSTION BEHAVIOR OF PULVERIZED PETROLEUM COKE IN BOILER SYSTEM

Chun Loon Cha, Ho Yeon Lee, Pil Hyong Lee, Sang Soon Hwang, Incheon National University, Korea

Petroleum coke has high heating value and low price. Moreover, owing to the steadily increasing demand for heavy oil processing, the production of petroleum coke tends to be increased. The high availability and low price of petroleum coke make its combustion for power generation increasingly attractive. However the high carbon content, high sulfur content and nitrogen content are known to give relatively large quantity of CO₂, high NO_x and SO₂ emission. In this work, a series of numerical simulations using Ansys Fluent 14.5 have been carried out in order to investigate the effects of Particle Size Distribution on reaction of petroleum coke particle and the effects of the flow field in furnace on petroleum coke particle behavior. Also, the effect of composition change of the particle was analyzed by the comparison between coal and petroleum coke particle combustion. Results show that as the particle diameter was increased from 10 μ m to 100 μ m, the time required for ignition was increased from 0.04s to 1s. When the reaction phase of petroleum coke is divided into two parts, the time required for devolatilization was maintained almost 0.02s for all of particle diameters. But the char reaction needed longer time by the increase of particle diameters. In terms of oxidation, the required time difference between petroleum coke and coal became larger because of petroleum coke has much more fixed carbon content. Analyzing the effect of swirl flow intensity on combustion furnace, it was found that the temperature distribution was spatially uniform about 1600K but the position of high temperature region had quite different position for each case of swirl numbers. In addition, numerical temperature data was compared with experimental temperature data and its temperature difference was less than 10%, indicating that the numerical results could be used for combustion design of petroleum coke boiler system.

clcha@incheon.ac.kr

W5P085

CFD SIMULATION OF CO-COMBUSTION OF SOLID RECOVERED FUEL AND COAL IN A CEMENT CALCINER

Hrvoje Mikulcic¹, Eberhard von Berg², Milan Vujanovic¹, Priesching Peter², Reinhard Tatschl², Neven Duic¹

¹University of Zagreb, Croatia ²AVL-AST, Graz, Austria

Disposal of large quantities of waste has a negative effect on human health, quality of life and particularly on the environment. Due to the named negative effects the European Landfill directive (1999/31/EC), prohibits the disposal of untreated waste in landfills. Consequently, a variety of waste-to-energy technologies are the focus of many research and development activities. One of these waste-to-energy technologies is the thermal utilization of Solid Recovered Fuels – SRF. SRF is defined as solid fuels prepared from non-hazardous waste materials intended for firing in industrial furnaces. The thermal utilization of SRF, especially the co-combustion of SRF with coal is increasingly gaining on importance in cement industry. One possibility for the control and investigation of the co-combustion process are CFD simulations. Early comprehensive information, parametric studies and initial conclusions that can be gained from CFD simulations are very important in handling modern combustion units. The purpose of this paper is to present a CFD simulation of the co-combustion process in a cement calciner. Numerical models of pulverized coal and SRF combustion were developed and implemented into the commercial CFD code AVL FIRE®, which was then used for the investigation. This code was used to simulate turbulent flow field, interaction of particles with the gas phase, temperature field, and concentrations of the gaseous species and the reaction products, by solving the set of conservation equations for mass, momentum and enthalpy that govern these processes. A three dimensional geometry of a real industrial cement calciner was used for the CFD simulation. The results gained by this simulation can be used for the optimization of cement calciner's operating conditions, and for the reducing of its pollutant emissions depending on coal-SRF ratio and composition of both fuels.

hrvoje.mikulcic@fsb.hr

W5P086

EXPERIMENTAL DETERMINATION OF THE KINETICS OF PRESSURIZED OXY-FUEL CHAR COMBUSTION

Ethan Hecht, Manfred Geier, Christopher R. Shaddix, Sandia National Laboratories, United States

Oxy-fuel combustion of coal has received much attention recently as a promising way to continue to generate electrical power from coal while implementing Carbon Capture and Storage (CCS). Utilization of oxy-fuel combustion of coal with CCS could significantly reduce CO₂ emissions and thereby mitigate the climate change due to this greenhouse gas. The efficiency penalty associated with the implementation of oxy-fuel combustion with carbon capture as compared to air-fired combustion without capture (roughly 10 percentage points when using boilers operating at 1 atm) can be reduced by around 3 percentage points through better heat integration, which can be enabled by combusting the fuel in a pressurized environment. Oxy-fuel combustion of coal under pressure also prevents air leakage into the system and may produce lower NO_x emissions than oxy-combustion under atmospheric pressure. Kinetic models and rates of pressurized

oxy-fuel coal combustion are valuable for the system design and process optimization, facilitating rapid implementation of this promising technology. In this work, we utilize an electrically heated, pressure-capable entrained flow reactor to generate experimental conditions to investigate oxy-combustion of pulverized coal in a pressurized environment. In controlled experiments we conduct *in-situ* optical measurements of particle temperatures and collect partially reacted chars for analysis of the extent of burnout, using a well-established ash tracer technique. For the optical temperature measurement, we developed a system that includes a horizontal optical probe to collect the thermal radiation from individual particles falling in the vertical reaction tube. The optical probe consists of a water-cooled sheath, collection optics coupled to a fiber-optic bundle that conducts the collected light to a two-color pyrometer. In order to minimize the influence of thermal radiation from the reactor tube wall, a water-cooled background surface is mounted in the wall opposite of the optical probe. In the work presented here we discuss the details of the system design, experimental methods, and present some initial results on the kinetics of pressurized oxy-fuel char combustion.

ehecht@sandia.gov

W5P087 EFFECT OF DEVOLATILIZATION PROCESS ON PM₁₀ FORMATION DURING OXY-FUEL COMBUSTION OF A BITUMINOUS COAL

Jingying Xu¹, Chang Wen², Dunxi Yu¹

¹Huazhong University of Science and Technology, China ²Huazhong State Key Laboratory of Coal Combustion, China

The devolatilization process has important influence on particle formation in pulverized coal combustion, but has little been explored. Its effect on the formation of PM₁₀ (particulate matters with an aerodynamic diameter less than or equal to 10.0 μm) was investigated under oxy-fuel combustion conditions. A bituminous coal sample (45-100 μm) was devolatilized in either CO₂ or N₂ at 1573 K on a Drop Tube Furnace (DTF) to produce two char samples (CO₂-char and N₂-char). Coal and char samples were burned at 1573 K and in 29 vol% O₂/71 vol% CO₂. PM₁₀ was collected and segregated into 13 size fractions, which were subjected to composition analyses. The results show that the particle mass size distributions of PM₁₀ from coal and its chars have similar peak sizes, suggesting that the devolatilization process has insignificant influence on the major pathways of PM₁₀ formation. Based on the mass fraction size distribution of the elements Al+Si in PM₁₀, three particle modes can be clearly identified, i.e. ultrafine mode (0.5), central mode (0.5-2.5 μm, PM_{0.5-2.5}) and coarse mode (2.5-10 μm, PM_{2.5-10}). Coal combustion produces more PM_{0.5} than char combustion, which is mainly due to the contribution of the vaporized species generated in the devolatilization process that is absent in char combustion. The burning volatile matter poses higher particle burning temperature of coal combustion, and dominantly enhances the char fragmentation to form more PM_{0.5-2.5} than char combustion (Image). The char-CO₂ gasification reaction occurred during devolatilization in CO₂ affects the properties of CO₂-char and leads to its higher particle burning temperature compared to N₂-char. Consequently, both the vaporization of inorganic materials and the fragmentation of char during CO₂-char combustion are promoted to generate more PM_{0.5} and PM_{0.5-2.5} compared to N₂-char. Under the investigated conditions, devolatilization process shows no significant effects on the production of PM_{2.5-10} from coal and chars combustion, implying the little influence of char combustion behavior. The particle burning temperature of samples appears to be a major factor to control the yields of PM_{0.5} and PM_{0.5-2.5}, accordingly, new experiments in our future work will be conducted to quantify the effect of char burning temperature on particle formation.

272920896@qq.com

W5P088 SELF-IGNITION OF H₂/O₂/CO₂ IN THE FIXED-BED CATALYTIC REACTOR

Chih-Yung Wu¹, Ian Shou-Yin Yang², Qin Hui Zeng¹, Yu Shun Hong¹

¹Kao Yuan University, Taiwan, ²National Formosa University, Taiwan

The purpose of this paper is to present the experimentally study of self-ignition of H₂ in different oxidation conditions and the assistance of H₂ on CO oxidation in CO₂-diluted stoichiometric stream via the catalytic reactor that filled with lab-made catalyst. The light-off process in terms of time traces of temperature and radial temperature distribution at reactor exit, axial temperature distribution in the reactor, and the averaged reaction temperature with various energy input in different oxidation conditions are measured and characterized. The results show that the self-ignition of hydrogen is found in the stream of excess air, N₂-, and CO₂-diluted stoichiometric O₂ without reactant preheating. However, the self-ignition cannot be initiated if the fuel contains CO. Hence, a light off process is also proposed in this paper. The hydrogen mixed with CO₂-diluted stoichiometric O₂ can be used as the preheating process of the catalytic reactor. As the temperature reaches a stable value, CO can be added and oxidized in the CO₂-diluted stoichiometric O₂ stream. As the volume fraction of CO is larger than that of H₂ in the reactant stream, the oxidation still cannot be sustained without reactant preheating.

chihyungwu@gmail.com

W5P089 NUMERICAL STUDY AND APPLICATION TO THE ACTUAL BOILER OF A NEW LOW-NO_x COAL-FIRED BURNER BASED ON THE LOW-NO_x PRINCIPLE

Keigo Matsumoto¹, Koutaro Fujimura¹, Kazuhiro Domoto², Ryuichiro Tanaka², Tomonori Saeki², Munehiro Kakimi²

¹Mitsubishi Heavy Industries Ltd., Japan, ²Mitsubishi Hitachi Power Systems, Ltd., Japan

We developed a new coal-fired burner following the low-NO_x concept based on the numerical study and adopted it

to an actual plant. Recent progresses in combustion analysis make it possible to simulate the combustion behavior, NO_x generation and reduction inside the flame. This new simulation capability allowed us to observe the location of NO_x generation in the flame. Based on the simulation results, we created new concepts for reducing not only NO_x but also unburned carbon significantly. The principle of our low NO_x concept is to realize "Premixed combustion" of the volatile matter from coal and combustion air. Generally, strong diffusion combustion occurs at the outer flame sheet between the primary air mixed with coal volatile matter and the secondary air, which causes high NO_x generation. To realize premixed combustion and to weaken diffusion combustion of the outer flame relatively, below items are effective.

- To install a well-designed flame holder inside the pulverized coal flow. On the other hand, outer flame holder is not installed. Not only NO_x reduction but char-burning are accelerated simultaneously.
- To design the proper distance between the neighboring auxiliary air nozzles and the coal burner. Secondary air is provided gradually according to progress of combustion. NO_x can be reduced without unburned carbon increase by combining their configuration with inner ignition.
- To keep or reduce the AA ratio with above mentioned concept. AA increasing causes the unburned carbon increasing.

The combustion characteristics of the new burner was also computationally evaluated and it was found that NO_x concentration at the furnace outlet becomes smaller than that of the original burner with a flame holder installed around the burner by about 40%. Moreover, almost the same NO_x concentration was obtained for this new burner even with the smaller AA ratio. In the actual plant with 700 MW output, NO_x concentration and unburned carbon in ash both decreased, and the operation result agreed well with the simulation results. It shows that our new concepts were realized in the practical situation and that a flame holder installed inside the burner and the suitable air nozzle arrangement suppressed the formation of high-temperature, high-oxygen zones on the outer circumference of the flame which coincide with the locations of NO_x generation source.

francegermanspain@yahoo.co.jp

W5P090 TOWARDS UNDERSTANDING THE IMPACT ON CHAR SURFACE AREA WHEN COAL AND BIOMASS ARE CO-FIRED IN GASIFICATION ENVIRONMENTS

Matthew Tilghman, Reginald E. Mitchell, Stanford University, United States

Co-firing coal and biomass has the potential to reduce the carbon footprint of power generation, while requiring little retrofitting. This work focuses on implications of co-firing into gasification environments, specifically on changes in the specific surface areas and reactivities of the char particles formed during devolatilization when co-firing. Wyodak coal, a sub-bituminous coal from Wyoming, was the coal used in the study and corn stover was the primary biomass additive. Torrefied corn stover was also used in selected tests. Chars were produced by injecting size-classified fuel particles into a laboratory-scale laminar entrained flow reactor, in which a reducing environment was established at a temperature representative of a real entrained flow gasifier. The injected fuel was either a pure coal or biomass or a pre-mixed blend of the two, containing up to 50% biomass by weight. Char particles were extracted from the reactor just subsequent to devolatilization (at about 30 ms after injection) using a solids sampling quench probe, and subsequently analyzed for specific surface area (BET) and reactivity to CO₂ and H₂O, via thermogravimetry. Results indicate a significant change in the char specific surface area resulting from co-firing with biomass, a consequence of biomass particle devolatilization altering the condition in which the coal particles devolatilize. When the coal is co-fired with biomass, the resulting char specific surface area is lower than that of either pure fuel. This effect depends on the mixture fraction of biomass in the blend, but not linearly. We hypothesize that this effect stems from the fact that the biomass particles devolatilize before the coal particles, and thus alter the conditions in which the coal particles devolatilize. A model is proposed to predict these observed trends, based on the fraction of coal particles which are likely to experience altered conditions due to nearby biomass particles. The change in specific surface area of the char also impacts its char reactivity. This impact can explain the observed decrease in reactivities of the mixed chars compared to the reactivities of the pure coal and biomass chars in CO₂ environments but in environments containing H₂O, the observed differences seems to be due to other factors as well.

mtilghma@stanford.edu

W5P091 EFFECT OF TORREFACTION ON PHYSICAL PROPERTIES AND CONVERSION BEHAVIOR OF HIGH HEATING RATE CHAR OF FOREST RESIDUE

Tian Li¹, Manfred Geier², Liang Wang³, Xiaoke Ku¹, Berta Matas-Guell³, Terese Løvås¹, Christopher R. Shaddix²

¹Norwegian University of Science and Technology, Norway ²Sandia National Laboratories, United States

³SINTEF Energy Research, Norway

Torrefaction is an effective way to upgrade lignocellulosic biomass into higher quality fuel. However, the thermochemical conversion of torrefied biomass has not been well studied. In the work reported here, Forest Residue (FR) was first torrefied at 584 K for 30 minutes. Then devolatilization of both FR and Torrefied Forest Residue (TFR) were carried out in a drop tube reactor at 1473 K with a heating rate around 1×10⁴ K/s. Using a scanning electron microscope and a granulometer, the physical properties of parent fuel particles and their corresponding char particles were examined. It was observed that the TFR particles have a smaller size and smaller aspect ratio than FR particles. The char particles

produced from both FR and TFR consist two types of particles with different sizes and morphologies. One kind of particles has typical sizes on the order of tens of micrometers, presumably representing fragments produced during devolatilization. The TFR produced fewer char particle fragments than the FR. Both types of char show distinctive structural porosity. Char gasification and char oxidation experiments were carried out in the same drop tube reactor at 1573 K and 1473 K, respectively. The ash tracer technique was thoroughly evaluated. Metal elements calcium, manganese, barium, and magnesium were chosen as the tracers and used to determine organic elements release of fuel particles during thermochemical conversion. The results revealed that regardless of the torrefaction or not, and the types of reactive environment, hydrogen is released much faster than is the total mass while oxygen is released slower than is the total mass. The release of oxygen for the FR char is slightly faster than it for the TFR char on mass loss basis. In addition, the TFR char shows slower carbon conversion rate than the FR char. Char size, O/C ratio, and alkali metals content may explain the negative effect of torrefaction on char reactivity.

tian.li@ntnu.no

W5P092

COAL AND BIOMASS HYBRID FUEL FOR IMPLEMENTATION OF RPS IN COAL POWER PLANT

Se-Joon Park, Dong-Wook Lee, Jong-Soo Bae Young-Joo Lee, Ju-Hyoung Park, Jai-Chang Hong, Jeong-Geun Kim, Young-Chan Choi
Korea Institute of Energy Research, Korea

Coal and biomass hybrid fuel (Hybrid Coal by Korea Institute of Energy Research; HCK) is a novel technology to cope with a renewable energy regulation or policy by promoting biomass consumption in a coal power plant. HCK is defined as a two-in-one fuel combining low rank coal with a sugar cane derived bioliquid, such as molasses and sugar cane juice, by bioliquid diffusion into coal intrapores and precarbonization of the bioliquid. Unlike the simple blend of biomass and coal showing dual combustion behavior due to their different reactivity, HCK provides a single coal combustion pattern. If HCK (biomass/coal ratio = 28 wt %) is used as a fuel for 500 MW power generation, the net CO₂ emission is 21.2–33.1% and 12.5–25.7% lower than those for low rank coal and designed coal, and the required coal supply can be reduced by 33% compared with low rank coal. In addition, HCK has a low water readsorption rate along with strong hydrophobicity leading to lower transportation costs, suppressed moisture adsorption during transportation and storage, and self-ignition suppression after drying. We are currently investigating the diversification of bioliquid to promote economic feasibility for HCK demonstration plant.

ssejoo@kier.re.kr

W5P093

AN EXPERIMENTAL STUDY OF THE PYROLYSIS AND COMBUSTION CHARACTERISTICS OF COAL AND PINE SAWDUST BLENDS

Zhezi Zhang¹, Guangjun Lu², Mingming Zhu¹, Pengfei Liu¹, Setyawati Yani¹, Fangqin Cheng², Dongke Zhang¹
¹The University of Western Australia, Australia, ²Shanxi University, China

The pyrolysis and combustion characteristics of Jincheng Anthracite (JCA), Pine Sawdust (PS) and their blends were investigated in order to understand the interaction between JCA and PS during pyrolysis and combustion. The experiments were conducted using a Thermogravimetric Analyser (TGA) and the PS to JCA blending ratios (P/J) ranged from 0/10, through 2/8 and 3/7, to 4/6 and 10/0 were used. The TGA experiments were carried out at a linear heating rate of 20K min⁻¹ from 373K to the final temperature of 1123K in both air and nitrogen atmospheres. The ignition temperature was determined by using the TG ignition method. Three generic characteristic thermal events, namely, pyrolysis (in N₂)/devolatilisation (in air) of the raw material (stage A), oxidation of the high reactivity char (stage B) and oxidation of the low reactivity char (stage C) were identified during the pyrolysis and/or combustion process. The results showed that the ignition temperature decreased and the oxidation rate of char increased with increasing P/J ratio in the fuel blends. Synergistic interaction between the pine sawdust and the anthracite during pyrolysis and combustion in TGA were also observed, with the latter being more profound.

zhezi.zhang@uwa.edu.au

W5P094

DEVELOPMENT OF A TIER 4 SEMI-GASIFIER BIOMASS COOKSTOVE THROUGH THE APPLICATION OF FUNDAMENTAL COMBUSTION SCIENCE

Jessica Tryner, Torben Grumstrup, Azer Yalin, Morgan DeFoort, Anthony John Marchese
Colorado State University, United States

Approximately 3 billion people worldwide use solid biomass fuel for cooking. As a result, they are exposed to indoor air pollution that leads to adverse health effects such as chronic Obstructive Pulmonary Disease (COPD) and Acute Lower Respiratory Infections (ALRI). One avenue that is currently being pursued to help eliminate the adverse health effects that result from cooking with solid biomass fuel is the development of improved biomass cookstoves that exhibit very low emissions of carbon monoxide and particulate matter. Some popular existing cookstove designs, such as the rocket-elbow, have been demonstrated to reduce emissions substantially in the laboratory in comparison to an open three-stone fire. However, emissions reductions observed in the field are not as great as those observed in the laboratory, and cookstove designs that achieve even greater reductions in emissions are being sought.

Improved household biomass cookstoves that utilize a "semi-gasifier" design are appealing because they have been

shown to exhibit lower carbon monoxide and particulate matter emissions than any other cookstove design during some laboratory tests. However, the performance of semi-gasifier cookstoves can be quite variable and performance under transient operating conditions (e.g. start up, refueling, transition to char combustion mode, and shut-down) has been demonstrated to be especially poor. The goal of this research study is to design semi-gasifier cookstoves that consistently exhibit very low emissions under a range of steady and transient operating conditions. To help achieve this goal, two devices have been developed to study the combustion process that occurs inside a semi-gasifier cookstove in more detail. The first device is a test bed in which many of the parameters that affect the combustion process can be controlled and varied. The second device is a two-dimensional semi-gasifier that has been designed with optical access. The semi-gasifier test bed has been developed so that a series of tests can be conducted to produce a more complete picture of semi-gasifier cookstove performance and identify how various operational parameters affect the combustion process. The parameters that can be controlled in the semi-gasifier test bed include the fuel type, bulk density, and moisture content; primary and secondary air flow rates; secondary air temperatures; and the geometry of the inlets where the air mixes with the solid and gaseous fuels. These parameters can be varied, one at a time, while the performance of the test bed is monitored across a range of operating conditions to determine the effect that each of these parameters has on emissions and the relative magnitude of that effect. Experiments have been conducted in which three different primary air flow rates (20, 25, and 32 L/min) and three ratios of secondary to primary air flow were tested. Based on the measured fuel consumption rate, the equivalence ratio inside the fuel bed was determined to be approximately four. The rate at which the fuel bed was consumed and the power output of the test bed increased as the primary air flow rate increased. The power output of the test bed decreased as the ratio of secondary to primary air flow increased.

The two-dimensional optical semi-gasifier has been developed for the purpose of using Planar Laser-Induced Fluorescence to study the flame that heats the cooking surface in a semi-gasifier cookstove. In the two-dimensional optical semi-gasifier, the secondary combustion zone in a semi-gasifier cookstove has been replicated using an approximation that is amenable to two-dimensional imaging (and future simulation). The manner in which this flame is affected by various operational parameters and different operational modes will be studied. Overall, experiments with these two devices will contribute to a greater understanding of the combustion process that occurs inside a semi-gasifier cookstove and will allow semi-gasifier cookstoves that exhibit reliably low emissions to be developed in the future.

jessica.tryner@gmail.com

W5P095 FINE ASH PARTICLE EMISSIONS FROM COMBUSTION OF COALS AND BIOMASS PROCESS RESIDUES

Feyza Kazanc¹, Yiannis Levendis², Amanda Ruscio²

¹Middle East Technical University, Turkey ²Northeastern University, United States

This work compared the particulate emissions generated from combustion of three pulverized biomass process residues (olive residue, corn residue, and torrefied pine sawdust) and three pulverized coals (bituminous, sub-bituminous, and lignite) in air. The fuels were burned in a Drop Tube Furnace heated to $T_{wall}=1400$ K. The mass fractions of collected sub-micron to super-micron particulate matter (PM_1/PM_{18}) from biomass were higher than those from coal. PM_1 particles constituted approximately 50 wt% and 20% of the collected ash particles (PM_{18}) from coal and biomass combustion, respectively. PM_1 collected from coal combustion contained large amounts of silicon and aluminum whereas PM_1 from biomass contained large amounts of alkalis (potassium and sodium) and chlorine. Additionally, phosphorous and sulfur existed prominently in the PM_1 of corn residue. If fired in boilers, the higher alkali content is projected to increase the tendency of the biomass ash to deposit on combustion surfaces while the high sulfur and chlorine contents are expected to enhance the corrosion of boiler surfaces and, thus, reduce plant outputs. The slagging and fouling indices of olive and corn process residues were much higher than those for coals. The torrefied pine sawdust has a lower slagging index than coal but a much higher fouling index.

feyzakazanc@gmail.com

W5P096 AN EXPERIMENTAL AND KINETIC INVESTIGATION INTO THE PYROLYSIS OF PINE SAWDUST HEATED AT VARIOUS HEATING RATES

Zhezi Zhang, Dongke Zhang, Mingming Zhu, Wenchao Wan, Pengfei Liu, Yii Leng Chan

The University of Western Australia, Australia

Pyrolysis of pine sawdust heated in nitrogen at various heating rates was investigated to study the effect of heating rate on the yield, oxidation reactivity, morphology and surface function groups of biochar produced. The pyrolysis experiments were carried out using Thermogravimetric Analysers (TGA) and a CDS Pyroprobe at heating rates ranging from 0.6 to 6000 K min⁻¹. A kinetic model was also developed to reveal the pyrolysis mechanism. The pyrolysis process was modelled as a single step reaction, in which the activation energy and pre-exponential factor were obtained using a combined model-free and model-fitting method, considering the compensation effect based on the experimental data. The results revealed that the heating rate played an insignificant role in controlling the four aforementioned parameters under conditions studied. The activation energy was almost constant at 175.9 kJ mol⁻¹ in the pyrolysis conversion range of 0.03 to 0.72, validating the single-step model in the major pyrolysis region of the pine sawdust. The kinetic modelling results using the method in the present study showed better agreement with the experimental results than the other selected methods from the literature, suggesting that the present method can serve as an accurate yet simple tool to perform the kinetic analysis and to predict the pyrolysis behaviour of the pine sawdust.

W5P097 **PARAMETRIC STUDY OF BIOMASS GASIFICATION IN A PILOT-SCALE GASIFIER**

Yunye Shi, Tejasvi Sharma, Guiyan Zang, Albert Ratner, University of Iowa, United States

A parametric study of the gasification of corn kernels has been performed on an experimental, pilot-scale (250 lbs/hour) gasification unit. A comparison was made of the performance of the gasifier as a function of operational parameter, in terms of producer gas production and composition. In these experiments, corn kernels were used, so that the shapes and sizes of the materials did not influence the results. Experiments were conducted with varying temperature of fuel bed, fuel-to-air ratio and fuel bed level. For each experimental condition, the permanent gas composition was measured continuously by Gas Chromatography (GC). Tars were collected according to CEN Standard. Bio-char was weighted for mass balance. The results from the study indicate that there were significant differences between various operational parameters in terms of producer gas concentration, tar production and char percentage.

yunye-shi@uiowa.edu

W5P098 **BIO-OILS PRODUCED BY STEAM ASSISTED PYROLYSIS OF ARUNDO DONAX AND AXILAN, CELLULOSE AND LIGNIN MIXTURE: A PRELIMINARY STUDY ON SALT EFFECT**

V. Gargiulo¹, P. Giudicianni², M. Alfe¹, R. Ragucci¹

¹Istituto di Ricerche sulla Combustione, Italy, ²Università degli studi di Napoli "Federico II", Italy

Slow steam pyrolysis of Arundo donax is proposed as a possible process for the recovery of a solid material suitable to be used as biochar. In view of the evaluation of the feasibility of such a process, products yields, char properties and energetic content of gaseous and liquid products (bio-oils), needed to assist energetically the process, are relevant data to be evaluated in dependence on process operating conditions and biomass characteristics. Biomass main components (hemicellulose, cellulose and lignin) contribute to a different extent to the determination of products yield and characteristics both for their own intrinsic chemical nature and for the onset of possible interactions due to their simultaneous presence in a real biomass. Moreover, it is known that inorganic elements present in the biomass can affect pyrolysis mechanisms and consequently products yields and characteristics. The investigation of combustion behavior of bio-oils cannot disregard the analysis of their chemical composition responsible of their peculiar chemical and physical properties: chemical instability, high density, viscosity and surface tension, low pH and calorific value, a wide evaporation range represent critical aspects for their utilization in the traditional combustion systems. Definitely, the chemical characterization of pyrolysis derived bio-oils is fundamental to investigate their reactivity in view of the exploitation of their energetic content.

In the present paper the influence of inorganic species and of possible interactions between biomass main components on bio-oil derived from pyrolysis of Arundo donax has been studied. To this aim steam assisted pyrolysis tests have been carried out on untreated and demineralized samples of Arundo donax canes in a proper experimental apparatus, up to 973 K, at pressure 5×10^5 Pa and heating rate 5 K/min. As reference test, a mixture of xylan (one of the major hemicellulose component in hardwoods), cellulose and lignin resembling the composition of Arundo donax canes has been processed in the same experimental apparatus at the same operating conditions. Bio-oils composition has been compared to the data computed by the superimposition of the results obtained from pyrolysis tests on the single biomass components. Given the high chemical complexity typical of these liquids, the application of different experimental approaches and analytical techniques has been required for an overall characterization and for tailoring specific analytical procedures to face the high dilution of pyrolysis liquid in process water.

vale.gargiulo@gmail.com

W5P099 **EULERIAN-LAGRANGIAN SIMULATION OF BIOMASS GASIFICATION IN A HIGH-TEMPERATURE ENTRAINMENT FLOW REACTOR: EFFECTS OF BIOMASS TYPE AND PARTICLE SIZE**

Xiao Ku, Tian Li, Terese Løvås, Norwegian University of Science and Technology, Norway

A multi-scale CFD model based on OpenFOAM has been constructed, which takes into account heat transfer, pyrolysis, homogeneous and heterogeneous reactions, radiation, as well as the interactions between the continuous gas phase and discrete particles. The proposed model is validated and applied to a lab-scale biomass entrainment flow reactor. Very little research has been conducted on such reactors for biomass fuels.

xiaokuke@gmail.com

W5P100 **UNDERSTANDING THE REDUCTION OF PARTICULATE EMISSIONS IN BIOMASS COOKSTOVES**

Kathleen Lask¹, Cristian Birzer², Paul Medwell², Ashok Gadgil³

¹University of California, United States, ²University of Adelaide, Australia, ³Lawrence Berkeley National Laboratory, United States

Three billion people worldwide cook on open fires or rudimentary stoves, burning fuels such as wood and charcoal. These traditional cookstoves tend to be highly inefficient and polluting; approximately 20% of global organic and black carbon emissions result from residential biomass combustion, contributing to environmental concerns, such as global warming, as well as the 4 million premature deaths each year from exposure to cooking smoke. In order to address these negative effects, continuing research needs to be conducted to improve heat transfer and combustion in cookstoves to

reduce the production of harmful emissions, such as particulate matter.

Manipulation of air in cookstove combustion chambers has been shown to drastically reduce the total mass of particulates emitted. However, the mechanisms responsible for these reductions are not well understood, partly because current stove investigations are based on emission samples collected away from the actual combustion environment, sampling emissions from a hood instead of viewing the combustion zone directly. Also, it is unknown if such modifications reduce the total number of emitted particulates or if they primarily reduce the number of large, coarse particles without affecting, or possibly increasing, the number of small, ultrafine particles. Particulate emission reductions are typically reported on a mass basis, and since the mass of ultrafine particles is almost insignificant compared to that of larger, micron-size particles, it is very possible to observe drastic reductions in the mass of particulates while actually increasing the number concentration of ultrafine particles. As ultrafine particles are considered more dangerous to human health than larger particles, it is important to understand and separate the distinction between a reduction in mass versus number concentration and size distribution for achieving the overarching goal of bettering human health.

The current work focuses on identifying the mechanisms responsible for particulate reductions due to air flow modifications in cookstoves and deducing the effect of these mechanisms on the size distribution of emitted particles. Preliminary investigations were conducted using several promising airflow modifications in a simplified cookstove manufactured to have optical access for future laser-based measurements. Each modification has been tested using a modified Water Boiling Test to assess the effect on particulate mass, number concentration, and size distribution emitted from the stove. Emitted particulates were measured in real time (1 Hz) with high spatial resolution over a wide range of particle sizes (5 nm – 20 µm). From these measurements, modifications that best identified differences in the size distribution of emitted particles were selected for further exploration (e.g., reduction of primarily coarse particles versus total reduction in number concentration of particles). Future work will utilize laser diagnostic techniques, such as Particle Image Velocimetry and laser-induced incandescence, to evaluate the effects of the modifications within the combustion chamber and better understand the mechanisms behind the particulate reductions. The results from different modifications will be compared to identify which mechanisms are responsible for reducing the total number of particulates versus primarily reducing the number of large particles while increasing the number of ultrafine.

klask@berkeley.edu

W5P101

UNDERSTANDING THE PRIMARY AND SECONDARY PYROLYSIS MECHANISMS OF CELLULOSE, LIGNIN AND WOOD WITH LASER-INDUCED FLUORESCENCE

Alba Dieguez-Alonso¹, Andres Anca-Couce², Nico Zobel³, Frank Behrendt⁴

¹Berlin Institute of Technology, Germany, ²Graz University of Technology, Austria

³Fraunhofer Institute for Factory Operation and Automation IFF, Germany ⁴Technische Universität Berlin, Germany

This study has the objective of contributing to the understanding of the complex reaction mechanism in pyrolysis of biomass. Volatile pyrolysis products of biomass are characterized on-line by Laser-Induced Fluorescence (LIF) together with on-line measurements of permanent gases by GC-TCD (Gas Chromatograph- Thermal Conductivity Detector) and of temperature. The focus is to determine the source of fluorescence from wood with respect to cellulose and lignin as its two main macromolecular components and their reactions leading to species emitting fluorescence. A technical-scale fixed-bed reactor is used to identify primary and secondary reactions involved in pyrolysis. The excitation wavelength used for the LIF measurements is 266 nm and the detected species are aromatic compounds (including one-ring phenolics and two-, three- or four- ring PAHs) and species containing carbonyl groups. It is observed that cellulose volatiles show fluorescence most probably due to the formation of two-ring PAHs and carbonyl compounds (Image) during heterogeneous secondary char forming reactions, which also enhance the production of CO₂. Volatiles from lignin show first fluorescence typical of one-ring phenolics and small (two - three rings) PAHs. Then, due to the enhancement of secondary reactions, fluorescence is detected from bigger PAHs (three - four rings), which are produced in parallel to gas species as CH₄ (Image) right). The fluorescence in wood comes mainly from the lignin fraction, undergoing also heterogeneous secondary reactions resulting in the formation of bigger PAHs, although a contribution from cellulose should be also present. (Image): The graphic on the left shows a typical fluorescence spectrum obtained during cellulose decomposition and fitted with spectra typical of two-ring aromatic compounds (naphthalene) and carbonyl groups. The graphic on the right shows the temporal evolution during lignin decomposition of species representative of one-ring phenolics and two-, three- and four-rings PAHs (guaiacol, naphthalene, phenanthrene and pyrene respectively).

alba.dieguez@mailbox.tu-berlin.de

W5P102

THE OIL COMBUSTION AT THE SURFACE OF WATER

Zulkhair Mansurov, Nikolay Prikhodko, Gauhar Smagulov, Bakhytzhon Lesbayev, Kazakh University, Kazakhstan

The emergency oil spills during transportation of them by water way, from offshore oil drill rigs and other sources causes a significant harm to the ecosystem and leads to negative and social impacts. Over the time, it's very difficult to control and hold, extract or processing the oil which was spilled. As a consequence the quick mobilization and deployment of the equipment on oil spill clean-up is essential, and method of oil combustion, as compared to other methods, remains the most effective and fastest.

In this paper the researches on oil combustion from the Tengiz oilfield on the surface of the water were conducted. The researches were carried out at the facility in which the actual conditions were simulated: the heaving of water surface

with wave height from 10 to 20 cm, variation of water temperature from 0° C to 25° C, variation of water salinity state from 0‰ to 18‰. The oil from Tengiz oilfield is characterized by: a density of about 726 kg/m³ and a kinematic viscosity of about 1.6 mm² / s at 20° C, the wax concentration of about 6.35% as well as fraction yield at the temperature up to 200° in C 51.4%. The oil, when falling on the surface of the water, is forming trolly oil. The experimental researches which were conducted by us, have shown that the surface heating of trolly oil leads to its separation into oil and water and combustion process is supported by surface evaporation of divided oil. In work a simple balance of energy distribution at combustion of oil blanket at the water surface is offered: Useful energy = 0.02Q_{comb} - Q_{Lo} - c_{po}(T_{ov} - T_a), where Q_{comb} - is energy formed in oil combustion process, Q_{Lo} - is energy, expendable for oil evaporation, c_{po} – is oil specific heat, T_{ov} – is oil evaporation temperature, T_a – is atmospheric temperature. The calculation which was performed in accordance with formula, for our researches shows that the useful energy is required for sustaining of combustion process of trolly oil at average must be at least 3500 kJ / kg. This process is very important at the very beginning of ignition process of trolly oil. The research results have shown that time changing for mixing in the range of from 1 to 4 hours (at a wave height of 10-20 cm) is not affected on volume of burnt oil. Time of mixing during wave disturbance affects only on the process of initial ignition. Thus, during mixing time up to 2 hours, for ignition of oil film the energy and temperature generated by the torch at a temperature up to 900°C is sufficient. For ignition of oil film at the time of mixing more than 2 hours the application of special igniters with combustion temperature of 1500°C is necessary. In consequence of undertaken studies was determined that the oil spill clean-up in the real conditions by burning, is necessary to perform taking into account the effects of temperature and water salinity on the process of stable flame propagation. We have found that in the case of Tengiz oil spill the efficiency of oil combustion decreases when the water temperature in the range from 5°C to 20°C and degree of water salinity is increased.

lesbayev@mail.ru

W5P103 SYNTHESIS OF HYBRID COAL CONTAINING GLYCEROL AND ITS COMBUSTION CHARACTERIZATION

Jong-Soo Bae, Young-Joo Lee, Dong-Wook Lee, Se-Joon Park, Ju-Hyoung Park, Jai-Chang Hong, Joeng-Geun Kim, Young-Chan Choi
Korea Institute of Energy Research, Korea

For the environment-friendly aspects, many countries are encouraging the use of biomass blended with coal. However, it is difficult to use existing boilers due to the individual combustion characterizations of biomass and coal. Glycerol-impregnated hybrid coal is a new fuel technology in which glycerol is converted into an artificial volatile matter by replacing moisture in the coal pores with glycerol. Even though glycerol is a biomass whose production volume is increasing every year along with biodiesel, it is difficult to mix it with coal for combustion because it exists in the liquid phase. In addition, even if glycerol is blended with coal, the combustion behaviors of glycerol and coal are independent because glycerol evaporates at 443.15 K. However, if the coal pores are filled with glycerol as in this study, glycerol takes on a combustion behavior like that of a volatile matter, so it becomes a two-in-one fuel having a single combustion behavior. With this technique, glycerol is saturated into the hydrophilic coal pores, and the excessive quantity maintains the existing glycerol combustion behavior. The glycerol-impregnated hybrid coal makes it possible to use glycerol as a fuel for coal-fired power plants while using existing, conventional facilities and reducing carbon dioxide emissions.

jongsoo@kier.re.kr

W5P104 INFLUENCE OF COMBUSTION PARAMETERS ON FOULING AND BOTTOM ASH AFTER COMBUSTION OF WOOD PELLET IN AN EXPERIMENTAL LOW-POWER BOILER

Enrique Granada, Lara Febrero, Raquel Perez, Araceli Regueiro, University of Vigo, Spain

The growing awareness of environmental issues causes an increase in energy applications based on renewable sources such as biomass. Specially, the combustion of biomass for heat and electricity generation is widespread worldwide. However, biomass combustion leads to operational problems in boilers such as fouling, slagging and corrosion, mainly due to the ash generated. The present study aims to evaluate the effect of different operating conditions in certain aspects of fouling and ash generation. The available facility is an experimental low-power fixed-bed boiler built specifically for research purposes where areas susceptible to fouling are easily removable and combustion parameters can be controlled, modified and registered. Particularly, the influences of temperature, airflow and airflow distribution have been studied on the organic and inorganic matter comprising fouling and bottom ash. Combustion of wood pellets was performed with a total airflow of 20 m³/h and three different primary and secondary airflow distributions were set in 15%-85%, 20%-80% and 30%-70%. Moreover, it was also accomplished the combustion of wood pellets remaining water temperature between 17°C and 25°C and airflow distribution in 25%-75% and varying only the total airflow. Then, samples of three different areas were collected; bottom ash, fouling deposited on the tube and fouling adhered on the tube. ThermoGravimetry and Differential Scanning Calorimetry were performed to the samples collected heating them up with air from 20°C to 550°C until mass stabilization in order to determine the content of organic and inorganic matter. Moreover, certain physical and chemical properties of samples were measured, such as mass loss or heat flow attempting to find out a relationship between results and the combustion parameters used. In general, results of thermal analysis of samples showed a first mass loss associated with an endothermic heat flow representative of the content on moisture at temperatures below 110°C, and a second mass loss associated with an exothermic heat flow representative of oxidation of organic matter in the temperature range of 350°C and 550°C depending on the type of sample. Furthermore, heat flow

curves from fouling adhered to the tube presented an endothermic peak at the range of 200°C and 250°C associated also with a mass loss particularly in the samples with an airflow distribution of 20%-80%. This peak could correspond to the volatilization of a volatile organic compound that did not appear in the other samples, surely combined with Cl which was the most abundant element found in the inner layers of fouling detected using SEM-EDS. Bottom ash contained the least amount of organic matter and SEM-EDS showed that Ca and Ti were the main elements comprising this type of sample. However, fouling of the superficial layers had more organic matter than fouling of the inner layers, mainly because the latter was composed mostly of inorganic condensable salts composed of C, O, Cl, K and Ca, the major elements found using SEM-EDS. Otherwise, results showed that as primary air percentage is increased, the organic matter content decreased, indicating a better yield of combustion when airflow distributions are close to 1/3 in the primary air and 2/3 in the secondary air. Furthermore, by keeping the temperature and the air distribution constant and increasing the total airflow, it has been observed a tendency to increase the inorganic material, thereby diminishing the amount of unburned carbon in the fouling.

egranada@uvigo.es

W5P105 **A COMPARATIVE STUDY OF BOTTOM ASH AND FOULING FROM WOODY BIOMASS COMBUSTION IN AN EXPERIMENTAL PILOT BOILER**

Enrique Granada, Lara Febrero, David Patino, Pablo Eguia, Araceli Regueiro, University of Vigo, Spain

Bottom ash and fouling collected from an experimental fixed-bed low-power boiler after wood pellet combustion were studied using different analytical techniques in order to characterize the samples and compare results obtained. Fouling on the tube was separated into superficial fouling, deposited on the surface, and interior fouling, adhered to the tube. Ash content of wood pellet was less than 0.5% and pH of the ash was 9.77 what indicated its basic character, which was dominated by alkali and alkaline earth metals. Moreover, this wood pellet presented a base-to-acid ratio of 2.76, which indicated a low fouling tendency. This low fouling tendency and an acceptable heating value of 16.17 MJ/kg make wood pellets as one of the best options for power generation through biomass combustion. Then, elemental chemical analysis of the samples was carried out using Organic Elemental Analysis, X-Ray Fluorescence Spectroscopy (XRF) and Scanning Electron Microscopy with Energy Dispersive X-Ray Spectroscopy (SEM-EDS). Furthermore, compositional chemical analysis was implemented using X-Ray Diffraction Spectroscopy (XRD). Results of XRF and SEM-EDS revealed Ca and K as the main inorganic elements in woody biomass, followed by Si, Mg and Fe, as well as a significant tendency in the content of Cl that appeared negligible in bottom ash and increased in concentration as it penetrated into the inner layers of fouling. Remarkably, bottom ash and superficial fouling presented greater similarity between them in terms of concentration of inorganic elements, hence interior fouling was the most different. Otherwise, the appearance of chlorine in much higher concentrations in interior fouling samples, confirmed the volatile nature of this element and its role of transport in the early stages of combustion. Concerning compounds, calcite (CaCO_3), magnesia (MgO) and silica (SiO_2) appeared as major crystalline phases of all samples; however, bottom ash was mainly comprised of calcium silicates due to the high temperatures reached in the combustion. According to the tendency of Cl, potassium chloride (KCl) behaved identically, preferably appearing in the samples of interior fouling. This salt, with a low melting point, condensed when it reached the heat exchange surface of the tube with lower temperatures; and therefore it played a crucial role in the early stages of fouling formation. Regarding techniques applied, XRD was the most useful technique for a semiquantitative determination of crystalline phases. And, in relation to the elemental analysis, XRF and SEM-EDS, even being entirely different techniques, concluded to comparable results.

egranada@uvigo.es

W5P106 **EFFECTS OF AIRFLOW ENTRANCE CONDITIONS ON GASIFICATION PROCESS**

Ching-Po Lin¹, Hsiao-Kang Ma¹, Chun-Hao Peng¹, Hsin-Luen Tsai Tsai²

¹National Taiwan University, Taiwan, ²Kao Yuan University, Taiwan

A small-sized gasifier, which can provide thermal energy and power output, can be considered as a good solution to switch bioresource to available fuel gas, such as hydrogen, methane and carbon monoxide. In this study, the downdraft gasifier system mainly includes feeder, downdraft gasifier, catalyst reactor, and scrubber. However, the important parameter of the gasification performance including syngas High Heating Value (HHV_{syn}) and Cold Gas Efficiency (CGE). This study aims to alter the different airflow entrance angles and increase the airflow entrance type to improve the gasification performance for waste biomass. The Japanese cedar and rice husk with the High Heating Value (HHV) at 21.1 MJ/kg and 17.2 MJ/kg respectively are adopted as feedstocks. Results of this study showed at one-side airflow entrance angle with 90° the Cold Gas Efficiency (CGE) of the Japanese cedar and rice husk were 76.62% and 53.05%, respectively. The syngas composition produced from Japanese cedar and rice husk gasification are shown in (Image). 1 respectively. Experimental results by varying airflow entrance angles and type shown in Table 1 will find the optimal operating condition.

gene50532@gmail.com

W5P107 **EFFECTS OF COAL-CHAR HEATING RATES AND SIZES ON KINETICS OF STEAM AND CO₂ GASIFICATION**

Jaya Raman, I. Gökalp, ICARE-CNRS, France

Char particles of high ash Indian coal with different sizes are produced using thermo-gravimetric system using the heating rates of 100 K/min, 500 K/min, 800 K/min and 1000 K/min in argon ambience. Particle diameter and porosity changes during pyrolysis significantly affect char gasification rates. The measurements of the steam and CO₂ gasification rate for the produced chars are performed by an isothermal thermo-gravimetric analysis at temperatures of 900, 950, and 1,000 °C until the complete char conversion at ambient pressure conditions. The effect of coal particle size on char production under various heating rates is evaluated. The mass loss curves show that the devolatilisation (or coal pyrolysis) mainly depends on the heating rate. As the heating rate increases, the pyrolysis process is independent of particle sizes and the rate of volatilization is almost constant. The coal undergoes structural modifications throughout the pyrolysis process due to phenomena such as pore enlargement, coalescence or blocking. Char gasification is affected by operating conditions such as reaction temperature, char production method, and particle size in addition to chemical composition and physical structure of char. The thermo gravimetric results indicate that the char produced from high heating rates show improved gasification rates in steam and CO₂ ambiances over the tested temperatures. This is due to the variation in external surface area of the chars and also heating rate influences the pore structure of the generated char particles. This leads to variations in the number of carbon-active sites available for the gasification. The smaller particles exhibited higher gasification rates. The decrease in coal particle size leads to shift the TG and the DTG curves to lower temperature zone, hence the burning rate of coal increases. The smaller sized coal particles have more specific area than the larger ones and are propitious to the gas evolution and ignition to the reaction surface. Three kinetic models are applied to describe the varying conversion rate: Volumetric Model (VM), Grain Model (GM), and Random Pore Model (RPM). The activation energy of the gasification is varied based on the char generation method and particle sizes. The activation energy for steam gasification is varying from 129 to 177 kJmol⁻¹ and the reaction rate constants from 2*10⁴ to 3*10⁶. The activation energies estimated by the GM are in the range from 138 to 193 kJ mol⁻¹ and the RPM model presented in the range from 129 to 187 kJ mol⁻¹ in CO₂ gasification. It can be seen that the variation in activation energy over the char heating rate is almost consistent for the smaller sized particles.

jayaraman_mit@yahoo.com

W5P108 PYROLYSIS AND GASIFICATION CHARACTERISTICS OF SEWAGE SLUDGE AND BIOMASS

Jaya Raman, I. Gökalp, ICARE-CNRS, France

The energetic conversion of biomass into syngas is considered as reliable energy source. In this context, biomass (Miscanthus) and sewage sludge have been studied. A simultaneous thermal analyzer and mass spectrometer was used for the characterization of samples and identified the volatiles evolved during the heating of the sample up to 1000°C under combustion cum gasification related conditions. The TG and DTA results were discussed under argon, oxygen, steam and steam blended gas atmospheres. The effect of the ambiances during pyrolysis, combustion and gasification of the samples are examined. Different stages of pyrolysis, combustion and gasification of the samples have been discussed. The TA-MS profile of the sample gives information on combustion and gasification process of the samples (ignition, peak combustion and burnout temperatures) and gases released (H₂, O, CO and CO₂). The results showed that the different processes were highly dependent on temperature. In the primary devolatilisation process of miscanthus, CO, CO₂, H₂O, O₂, H₂ and CH₄ gases are major products. The burn out temperature of sample is around 560°C in combustion. The gasification process of miscanthus char starts above 800°C at steam ambience whereas under steam and air/oxygen blended gases, it starts above 750°C. The evolution of H₂ commences at 350°C with the continuation of the pyrolysis process, reached its peak at 950°C in gasification process and then decreased rapidly, similar trend observed for CO also. The release of the CO₂ is reached the peak at 950°C in the steam blended ambience during gasification process.

During devolatilization process of sewage sludge, the major mass loss starts at 280°C and completed at 380°C. The secondary pyrolysis occurred between the temperature range of 380 and 600°C. The oxidation of the sewage sludge starts at 380°C and continued until 550°C. There is continuous release of CO, CO₂ and H₂ gases during the burning process. During gasification, the maximum mass loss is occurred at the temperature of 940°C under the steam and steam blended atmospheres. The complete burn out of both the miscanthus and sludge char occurs at 950°C while isothermal conditions maintained for specified time. These results show that the gasification of these samples can be carried out at around 950 °C using the blended gaseous steam, oxygen and air with efficient carbon conversion. The kinetic parameters of the biomass and waste materials are estimated for TGA using a model based on first-order reactions with a distribution of the activation energies. Two methods, the differential isoconversional technique (Friedman method) and integral method (Coats and Redfern integral method) are used to study the activation energy of the non-isothermal degradation of hydrocarbon samples. Activation energy during the combustion of the miscanthus is 116 kJ/mol using Friedman method, and 88 kJ/mol using CR method. The activation energy of the sewage sludge combustion process using Friedman method is 38.9 kJ/mol and CR method is 60.4 kJ/mol. The activation energy of the miscanthus during gasification is almost twice when compared to sewage sludge using Friedman method. The sewage sludge gasification is dominated by mass-loss at lower temperature whereas miscanthus loses more mass by mid- to high temperature char gasification.

jayaraman_mit@yahoo.com

W5P109 GASIFICATION OF MIXING FUELS ON DOWNDRAFT GASIFIER

Howping Wu, National Taiwan University, Taiwan

Energy problem has become an important issue need to be solved nowadays. In past few decades, fossil fuel was the

main resource that has been used to generate power run vehicles, etc. Although several aspects of using it has been developed, fossil fuel also has negative effect on environment. Therefore, searching for alternatives has gradually turned into an inevitable trend that more and more studies are involved in. Gasification, a technology to transform fuel into high heating value syngas, has been widely applied to industrial processes. Comparing to direct combustion, it provide a way to deal with fuel with less carbon dioxide emission; furthermore, the technology is suitable to treat biomass waste such as rice husk, making better use of resources. Previous study has shown that there are great potential in gasifying rice husk and Japanese cedar. The aim of the study is to extend previous work, combining advantages of both rice husk and Japanese cedar, to discover gasification properties by gasifying in fixed bed downdraft gasifier. The result has shown that though syngas composition in mixing case has less hydrogen, but carbon dioxide concentration also decrease, respectively. The maximum hydrogen concentration in mixing case is measured 12.14vol%, while carbon dioxide is less than 1vol% in this case. The future work is to gasify different ratio of biomass fuel to find out gasification properties.

b97502164@ntu.edu.tw

W5P110

NUMERICAL ANALYSIS OF HYDROGEN INHIBITION DURING COAL GASIFICATION

Jonas Krueger, Norwegian University of Science and Technology, Norway

In this work, hydrogen inhibition during the gasification of coal, an effect that has also been observed in recent experimental studies, is investigated. Simulations with different initial conditions are performed and the connection between the overall conversion rate and hydrogen content of the gas phase is studied. The heterogeneous adsorption-desorption reaction mechanism includes char reactions with oxygen and steam. Values for the pre-exponential Arrhenius factors and activation energies are obtained via thermogravimetric analysis. The main result is that the conversion rate of the char particle is decreased with increased hydrogen content. This is due to the hydrogen adsorption on free carbon sites on the char particle surface. Adsorbed hydrogen is relatively stable and does not easily desorb into the gas phase, which means that it clogs the char surface, leading to less free carbon sites available. Another effect is the de-oxygenation of char, where hydrogen reacts with oxygen already adsorbed to a carbon site, preventing the desorption of this molecule into the gas phase. The de-oxygenation of char is important because the release of CO from carbon with an adsorbed oxygen is the dominant char conversion path. A stand-alone model for particle-gas reactions is used to simulate char conversion. The code describes the gas phase reactions with the GRI-3.0 mechanism and a simplified heterogeneous adsorption-desorption mechanism for particle-gas interactions. The influence of species diffusion into the particle on internal conversion processes is taken into account by introducing internal gradients, following the ideas of Thiele, into the equation for the reaction rate. This code, and the simulations conducted with it, is part of a wider effort to supply an extended sub-model for particle conversion processes in CFD.

jonas.krueger@ntnu.no

W5P111

FILTRATION COMBUSTION OF CARBON AND INERT MATERIAL CHARGED IN INTERMITTENT LAYERS

Eugene Salgansky, Institute of problems of chemical physics, Russia

Filtration Combustion (FC) of solid fuels often encounters instabilities of the combustion front. To cope with the instabilities, e.g., with a front distortion, intermittent charging of fuel with an inert solid material was considered. In this study we consider the influence of stratified charging on thermal characteristics of FC. Considered was air gasification of a mixture of carbon particles with an inert material in a non-adiabatic counterflow reactor. The carbon and inert solid material are fed into reactor from above in intermittent layers: a carbon layer with the thickness h_c — an inert layer of inert material. An oxidant gas (air) is continuously fed into the reactor from the bottom.

The mathematical model considers the FC in the one-temperature unidimensional approximation; the level of heat loss being proportional to local temperature, pressure drop is small and atmospheric pressure is assumed throughout the reactor; chemical reaction with the formation of a single product $C + O_2 = 2 CO$, the reaction rate takes the Arrhenius form. With the above assumptions, the process is described by the balance equations of energy and mass of the reactants. The gas velocity is determined by the constancy of gas flow. Similarly to the case of premixed fuel and inert, the ratio of the average consumptions of carbon and inert in the charge is an important control parameter for the layered system. The thermal structure of the combustion wave is determined by the ratio of heat capacities of the flows (product of linear velocity, specific heat, and density) of the solid and gas. For a constant gas composition, this ratio changes with a varied content of carbon in the charge; for the layered charge, with the ratio of thickness of the carbon and the inert layers. For a low content of inert, the wave has the reaction trailing structure. The heat released in the oxidation of carbon is carried with the gas stream and a zone of preheated solid phase is formed ahead of the reaction front. Stratified organization (fuel/inert) of the solid charge leads to a temporary temperature rise in the combustion zone, when the reaction front moves from one carbon layer to another one ("skips" through a heated inert layer). Immediately after the skip, the combustion temperature becomes significantly higher than the steady-state combustion temperature for pure carbon. This is due to the combustion of a consecutive carbon layer starting with the carbon preheated with the heat wave, the air supplied to the reaction front being also preheated as it filters through the preheated inert layer. Once the heat accumulated in the layer of inert is consumed, the combustion temperature drops and further the FC of the carbon layer proceeds as a steady combustion typical of pure carbon. For a low carbon content in the charge, the FC of a stratified charge becomes dramatically different from that of a premixed system with the same average carbon content (reaction leading structure of

FC wave). The FC becomes intermittent: burning phases (high temperature propagation of the combustion front in a carbon layer) alternate with depression phases, when the layer of solid inert heated during combustion of a previous carbon layer does not reach the next layer of the fuel. In this phase, the gas flows through the fuel at a low temperature without reacting. Further, owing to the convective propagation of the heated zone over the inert layer, the hot zone reaches the carbon layer and ignites it. And then, high temperature carbon combustion phase is repeated, the air being supplied from inert layer at high temperature. An increase in the relative thickness of inert layers (for low level of lateral heat loss) results mainly in a longer duration of the depression phase, while the temperature reached during the combustion phase decreases but slightly, due to the spreading of the heat pulse during its propagation in the inert layer. For a premixed carbon–inert system with low carbon content and relatively low combustion temperature, oxidation of carbon primarily yields CO₂. The combustion of carbon layers in the stratified charge occurs periodically with alternating high-temperature and depression phases. During each combustion phase, the main combustion product is CO. For thicker inert layers, the spread of the heat pulse during propagation in the inert layer and temperature drop due to heat losses ultimately result in a heat pulse reaching a fresh layer of carbon, being no longer able to ignite it. For an inert layer thicker than the critical value (hi^*) the wave propagation through a stratified charge becomes impossible.

salgansky@mail.ru

W5P112 A THEORETICAL ANALYSIS OF TRANSIENT OXIDATION OF MAGNETITE TO HEMATITE IN CHEMICAL LOOPING COMBUSTION

Tianxiang Li, Yunqing Han, Kunlei Liu, Kozo Saito, University of Kentucky, United States

The transient oxidation of magnetite to hematite has been theoretically analyzed, with emphasis on the influences of particle size, particle temperature, and environmental conditions on the oxidation rates and burnout times of magnetite particles, with the view of using magnetite as Oxygen Carriers (OCs) in Chemical Looping Combustion (CLC). Two-step solid-state reaction/transition was applied for quasi-steady gas-phase heat and mass transfers along with transient particle heating and radiative heat transfer. The results show that solid phase radiation is significant in affecting surface oxidation reaction, particularly for particles initially at low temperature. High environmental temperature and large particles exhibit high oxidation rates, while high initial particle temperature shortens the burnout time of particles. High pressure operational conditions increase the oxidation rates, and reduce particle burnout times, mainly due to increased surface Damköhler number through increased bulk density of gas, while the non-Lewis number at high pressure weakly affected the reaction rates. A lowest final particle temperature existed at the completion of oxidation and occurs for the initial particle sizes around 100 μm at 1 atm; this lowest final temperature shifted to the smaller sizes under elevated pressures.

txli1@engr.uky.edu

W5P113 NUMERICAL STUDY OF SUGARCANE BAGASSE GASIFICATION IN A FLUIDIZED BED REACTOR

Albino Leiroz, Gabriel Verissimo, Jean de Pinho, Manuel Cruz, Federal University of Rio de Janeiro, Brazil

Gasification is a process that converts carbonaceous liquid and solid materials into a useful gas that can be used as fuel or feedstock for the chemical industry. Despite its increasing importance as a renewable energy source, literature on biomass gasification is scarce when compared to coal studies. A numerical study of the sugarcane bagasse gasification process in a pilot-scale fluidized bed reactor is discussed in the present work. The multiphase flow field within the reactor is described using an Euler-Euler approach with a smooth-transition model to describe the solid stress tensor. The chemical reaction mechanisms and associated kinetics used in the present work are adapted from well established models available in the literature. Simulations are performed using the open code MFIx (Multiphase Flow with Interphase eXchange). The obtained results are initially used to address numerical issues of the simulations such as the evaluation the influence of considering less computation intensive two-dimensional domains in an intrinsically three-dimensional fluidized bed gasification process. Results indicate little influence on the syngas composition when two-dimensional domains are used despite observable changes in flow field. Different procedures to control computational costs associated with the simulation are also discussed. These procedures involve the usage of simpler non-reactive solutions as initial condition for more computationally demanding reactive calculations. Speed-ups of 75% were achieved when parallel computing techniques were also applied. Physical results were obtained for two different reactor wall temperatures. The results are analyzed in terms of the relative contribution of each chemical model reaction to the concentrations of different syngas components and the reaction rates profiles along the reactor. Results show that hydrogen (H₂) syngas content is more dependent on the methane-steam reforming, Water-Gas Shift (WGS) and hydrogen oxidation reactions. Results also show that Carbon Monoxide (CO) and Carbon Dioxide (CO₂) contents are mainly dependent on the char oxidation mechanism, carbon monoxide oxidation and WGS. In the absence of experimental data, the results were compared with the data obtained with the CeSFaMB code, which uses a fluidization model. The comparison shows a good agreement between the results of both models.

leiroz@mecanica.ufrj.br

W5P114 COMBUSTION BEHAVIOR OF AQUEOUS HAN SOLUTIONS CONTAINING METHANOL AND NANOPARTICLE ADDITIVES

Kenneth McCown, Gabriel Homan-Cruz, Eric L. Petersen, Texas A&M University, United States

The past two decades have seen an elevated interest in the replacement of hydrazine-based propellants in the aerospace industry to reduce the growing costs associated with their toxic nature. Monopropellants based on aqueous solutions of hydroxylammonium nitrate (HAN) have received considerable attention due to their low vapor pressures, high thermal stabilities, and reduced toxicities that increase their viability for long-term storage and handling. The addition of liquid reducing agents and nano-scale additives allow the burning rates and specific impulses of aqueous HAN solutions to be altered to better match the requirements of specific propulsion applications. The authors' current work examines the effects of methanol and various nanoparticle additives on the combustion behavior of aqueous HAN, using a pressure-based method previously demonstrated by the authors to measure the linear burning rates of nitromethane-based heterogeneous mixtures with high precision. The linear burning rates of numerous HAN-based mixtures were measured in a constant-volume strand burner at chamber pressures ranging from 3 to 22 MPa. For each test, this system recorded the instantaneous pressure, light intensity, and electromagnetic emission spectrum of a small sample of liquid propellant throughout the entire combustion process. The baseline aqueous mixture contained 82.4% HAN by weight, and various quantities of anhydrous methanol were added to this solution to create entirely novel formulations and compare with previous studies completed by other groups. Aluminum nanoparticles with a mean diameter of 100 nm, fumed silica powder consisting of 200- to 300-nm aggregate particles, and titania nanoparticles with a mean diameter of 20 nm were chosen as additives based on previous studies that showed marked increases in the burning rates of nitromethane-based propellants. The current study expands the range of tested pressures for propellant mixtures containing aqueous HAN and methanol, and it characterizes the effects of various weight percentages of particle additives on the same group of monopropellants. Examples of the burning rate trends measured in the current study are shown in (Image) for the aqueous HAN baseline and two propellant mixtures containing nanoparticle additives. (Image) included in the uploaded file version)

kenneth.mccown@gmail.com

W5P115 TURBULENT FLAME PROPAGATION IN DUST CLOUDS

Trygve Skjold, University of Bergen, Norway

Accidental explosions cause severe material damage, injuries, and loss of life in the process and mining industries. Dust explosions pose a hazard whenever combustible solid material is present in the form of fine powder, there is a possibility of dispersing a sufficient mass of the material in air to form an explosive dust cloud within a relatively confined and/or congested volume, and there is an ignition source present. Dust explosions are inherently complex phenomena. A dust cloud is a mechanical suspension, i.e. a system of fine particles dispersed by agitation. Most dust samples have a relatively wide particle size distribution, and particles of different size react differently to variations in the flow field. This implies that the particle-laden flows in dust explosions are inherently turbulent, the overall process is inherently transient, and the dynamics of the turbulent structures creates local concentration gradients. The purpose of the present study is to review the state-of-the-art in numerical modelling of flame propagation in dust clouds, with particular emphasis on empirical and theoretical correlations for turbulent flame propagation. Selected correlations for the turbulent burning velocity as function of turbulence intensity, turbulent length scale, dust concentration and other relevant variables will be implemented in the Computational Fluid Dynamics (CFD) code DESC. Model predictions will be compared with results from large-scale dust explosion experiments.

trygve@gexcon.com

W5P116 CATALYTIC BEHAVIOR OF FLAME-MADE PD/TIO₂ NANOPARTICLES IN METHANE OXIDATION AT LOW TEMPERATURES

Fang Niu, Shuiqing Li, Yichen Zong, Qiang Yao, Tsinghua University, China

The titania-supported palladium nanoparticles (Pd/TiO₂) are synthesized in one-step using a unique premixed Stagnation Swirl Flame (SSF) with ultra-fine spray feeding system. The self-assembly, arising from the difference between chemical time scales of palladium acetate decomposition and TTIP hydrolysis in gas phase, results in palladium clusters (2 particles (7-8 nm)). Methane oxidation over this kind of flame-made Pd/TiO₂ at low temperatures is performed, achieving much higher catalytic activity in contrast to the impregnated catalysts under same Pd loading. A distinct loop hysteresis loop is discovered, which implies the transient behavior of the catalysts in cycles. In the case of flame-made nanoparticles, as the interaction between palladium and titania is enhanced, the reduction of oxides is found once the temperature starts to drop. The further characterizations by using BET, TEM, XPS and XRD reveal that the low-temperature reaction rate is limited by the metallic Pd content on surface, and partially reducing the surface will increase the reactivity. The deactivation of the catalysts is mainly caused by Pd dispersion decrease. The competition between Pd dispersion decrement and surface PdO reduction dominates the catalytic behavior upon heating and cooling, and then they together drive the methane conversion varies in loop curve.

nf37@163.com

W5P117 LAMINAR FLAME SPEEDS OF AN AEROSOL MIXTURE CONTAINING NANO-ALUMINUM IN CH₄/O₂/N₂

Travis Sikes, Eric L. Petersen, M. S. Mannan, Texas A&M University, United States

An existing flame speed bomb which uses optical techniques to measure laminar flame speed was employed to study the fundamental phenomena of flame propagation through a uniformly dispersed aerosol. These experiments used the low-pressure laminar flame facility at Texas A&M University which is a 28.1-L, 35.6-cm long cylindrical vessel designed to be filled with gas-phase components up to a maximum of 5 atm. The vessel is filled using the partial pressure method using two pressure transducers with precisions of 0.1 torr and 0.1 psi. Fuel-air mixtures are ignited using a central ignition system, and the resulting propagating flame is captured using a high-speed camera in a Z-type schlieren setup. The facility was upgraded to disperse dust into the test chamber through a strong blast of gas; this aerosol was then allowed to settle for a minimum of 45 seconds to assure that the conditions inside the test chamber were quiescent and that the dust was uniformly distributed.

Extinction of laser light through the resulting aerosol was measured through the large optical access with a 632.8-nm, 5-mW HeNe laser so that the mass of suspended nano-particles could be determined as a function of time up until combustion has occurred. The particles used were aluminum nano-particles with an average diameter of 100 nm. A hybrid mixture of Al/CH₄/O₂/N₂ was chosen as it would provide a well-characterized parent fuel to measure the contribution of nano-aluminum on combustion. The results thus far show that there is an overall decrease in flame speed when the nano-aluminum is introduced. There is some contribution to combustion because qualitative analysis of the raw images reveals the onset of instability occurs more rapidly with an increasing suspended mass.

ace2187@tamu.edu

W5P118

PERFORMANCE OF A MECHANICALLY ALLOYED AL-CUO THERMITE FOR APPLICATIONS IN DRUG DELIVERY AND CELLULAR TRANSFECTION

Geoffrey Maines¹, Matei Radulescu¹, Kadeem Dennis¹, Julian Lee²

¹University of Ottawa, Canada ²DRDC, Suffield Research Centre, Canada

In recent years, pressure pulses generated by piezoelectric generators, gas-driven shock tubes and lasers have shown the capability of transferring genetic material into biological cells. More recently, the use of thermite-based pressure waves for applications in cellular transfection and drug delivery have shown significant improvements over previous technologies, attaining transfection rates as high as 99%. This comes as a result of a relatively new finding that certain nano-scale thermites produce pressures much lower than those predicted by Chapman-Jouguet (CJ) theory for conventional explosives. In the present study, a new technique for producing thermite-generated pressure pulses using fully-dense nano-scale thermite mixtures was evaluated. This was accomplished by evaluation of a stoichiometric mixture of Aluminium (Al) and Copper (II)-Oxide (CuO) prepared via mechanical alloying. Flame propagation speeds, constant-volume pressure characteristics and underwater pressure characteristics of both a micron-scale and mechanically alloyed mixture were measured experimentally and compared with conventional nano-scale thermites. It was determined that mechanically alloyed mixtures are capable of attaining flame propagation speeds on the same order as nano-scale mixtures, with flame speeds reaching as high as approximately 100 m/s. Constant-volume pressure experiments indicated that mechanically alloyed mixtures result in lower pressurization rates compared with conventional nano-scale mixtures, however, an improvement by as much as an order of magnitude was achieved compared with micron-scale mixtures. Results from underwater experiments indicated that the mechanically alloyed samples produced peak shock pressures and waveforms similar to those for a nano-scale Al-Bi₂O₃ mixture.

While this work provides a novel technique for producing pressure profiles conducive to applications in cellular transfection, future work aims to determine the relationship between the characteristics of the pressure profile and the permeabilization of individual cells.

gcmaines@gmail.com

W5P119

ASSEMBLY OF NANOTHERMITE VIA ELECTROPHORETIC DEPOSITION OF ALUMINUM NANOPARTICLES ON COPPER OXIDE NANOWIRES

Ming-Hsun Wu, Hendrik Hartono, National Cheng Kung University, Taiwan

Nanothermites are energetic materials that contain nano-size metal (e.g. aluminum) and metal oxides (e.g. CuO, Fe₂O₃, MoO₃, Bi₂O₃) particles mixed at nanometer scale. These materials find their applications in propellants, weldings, explosives and pyrotechnics. Nanothermites generally feature higher reaction rates comparing to conventional thermite due to the increased interfacial contact and the reduced diffusion distance between fuel and oxidizer. Several methods have been developed for assembling nanothermite, including physical mixing, arrested reactive milling, sol-gel, self-assembly, chemical vapor deposition, and Electrophoretic Deposition (EPD). A novel approach for assembling nanothermites using EPD is proposed and validated in this study. Unlike the EPD method demonstrated by Sullivan, in which both aluminium and copper oxides nanoparticles were first dispersed in ethanol/water solution to form a nanothermite layer on the platinum electrode surface via EPD of the particles, only aluminum nanoparticles were dispersed in the solution in our approach, and Al particles were then directly embedded into copper oxide nanowires fabricated on the surface of a copper wire through electrophoresis. The copper wire was also the electrode in the EPD process. The copper oxide nanowires were grown on the copper wire through thermal oxidation. Better control of mass density and homogeneity of the nanothermite can potentially be achieved through the approach. Reaction rate may also be customized through manipulating the number density and geometry of the CuO nanowires as well as EPD parameters.

Effects of key oxidation parameters including temperature and duration on CuO nanowire growth were first carried out. Thermal oxidations of copper wires were performed both in a high temperature furnace purged with air and in a thermogravimetric analyzer (Q600, TA Instruments). For the study of temperature effects, copper wires of 30 μm in diameter were individually heated in furnace from room temperature to 450, 550, and 650°C for 3 hours. The heating rate was 20°C/min, and the flow rate of the purging air was 100 ml/min. Using the same heating and flow rate, another set of experiment was performed at 550°C for durations of 2, 3, and 5 hours to reveal the effects of oxidation duration. Thermogravimetric analyses showed that nanowire growth was relatively slow at temperatures below 450°C, and the oxidation rate increased linearly with temperature above this threshold value. Scanning microscopic images of the wires oxidized in the high temperature furnace showed that the length of nanowires increased with temperatures; however, the density of the nanowires was the highest at 550°C comparing to 450°C and 650°C. Oxidation duration, on the other hand, did not significantly affect the length of nanowire, but the number density of the nanowire, which first became denser then sparser as the oxidation duration became longer. Copper wires oxidized at 550°C for 3 hours were chosen for nanothermite assembly because of the longer and denser nanowires on the copper wire surface.

Preliminary tests have shown that aluminum particles (50 nm mean diameter) dispersed in a 3:1 vol.% EtOH:H₂O solution can be directly deposited onto the copper wire covered with copper oxide nanowires via electrophoresis. The total solids loading of the solution was 0.2 vol.%, and the solution was ultrasonicated for 5 minutes before EPD. The electric field strength used was 40 V/cm and applied for 10 seconds. After the EPD process, the Al/CuO composite wire was dried in the air. Differential scanning calorimetry measurement performed on the EPD assembled nanothermite wire showed that exothermic nanothermite reaction did occur at approximately 550°C, further validating the feasibility of the concept. More detailed characterizations of the reaction performance as well as optimization of the assembly process are underway.

minghwu@mail.ncku.edu.tw

W5P120 SYNTHESIS OF SRSiO₃-SiO₂ AND ZrO₂-SiO₂ CORE-SHELL PARTICLES BY FLAME SPRAY PYROLYSIS

Takuro Kusunoki, Hiroshi Hasegawa, Toshihisa Ueda, Takeshi Yokomori, Keio University, Japan

The motivation of this research is to (Image) out the possibility to synthesize core-shell particles by flame spray pyrolysis and to clarify the influence of immiscibility of components on the core-shell structure. The Sr-Si-O or Zr-Si-O system oxide particles were synthesized with the spray of precursor solution dissolving Sr(NO₃)₂ or ZrO(NO₃)₂ · 2H₂O and dispersing colloidal SiO₂. In this technique, the formation of the core-shell structure was caused by the separation of each component at the liquid phase in the synthesis route. Synthesized particles were characterized by Transmission Electron Microscopy (TEM), Energy Dispersive X-Ray spectroscopy (EDX), and X-Ray Diffraction (XRD). The structure of synthesized particles varied depending on the flame temperature and the precursor molar ratio. In the case of Sr-Si-O system oxide, the desirable well-structured core-shell particles could be prepared at the high flame temperature and the low SiO₂ precursor concentration. Furthermore, the perfectly homogeneous particles were synthesized at the high SiO₂ precursor concentration, and the heterogeneous particles were also synthesized at the low flame temperature. According to the EDX and XRD analyses of the core shell particle, the core and the shell could be recognized as SrSiO₃ and SiO₂, respectively. In the case of Zr-Si-O system oxide, the well-structured core-shell particles could not be prepared by the present flame spray pyrolysis, but partially-shelled particles could be obtained. According to the EDX and XRD analyses of the partially shelled particle, the core and the shell could be considered as ZrO₂ and SiO₂, respectively. In the Sr-Si system, the immiscibility of Sr and Si was low, resulting in the SrSiO₃ core. In the Zr-Si system, on the other hand, the immiscibility was so high that those components could be separated each other, resulting in the pure ZrO₂ core. The surface tension at the liquid phase of components was dominant on the formation of the core-shell structure. In the case of Sr-Si-O system, the difference between surface tensions of components was large, so that the well-structured core-shell particles were synthesized.

takuro.kusunoki@z3.keio.jp

W5P121 ROLE OF FLAME STOICHIOMETRY ON PHASE STABILITY OF NANOCRYSTALLINE TiO₂ SYNTHESIZED IN PREMIXED FLAME STABILIZED ON A ROTATING SURFACE

Ruxiao An, Hai Wang, Stanford University, United States

Rutile and anatase are two major phases of titanium dioxide. In general, anatase has a range of electric and surface properties more attractive than rutile in its applications. For example, as a photoelectrode anatase performs superior to rutile in a dye-sensitized solar cell. Obviously, a good understanding of the phase stability of nanocrystalline TiO₂ is fundamental to its applications. As a standard working knowledge, bulk-phase rutile is known to be more stable thermodynamically than anatase under standard pressure and room temperature; yet, anatase TiO₂ is the preferred phase at very fine size (less than 14 nm diameter) due to contribution of surface free energy. Previously, we synthesized TiO₂ nanoparticles over a range of sizes using the method of Flame Stabilized on a Rotating Surface (FSRS). Results show that flame stoichiometry has a significant impact on the phase even for particles smaller than 14 nm. It was found that anatase is the dominant phase under fuel-lean condition. What was surprising is that under fuel rich condition, rutile was found to dominant. The experimental data thus points out to a deficiency in theory with which we predict the phase of oxide materials using flame synthesis. The purpose of the study is to analyze the role of flame stoichiometry on the phase

stability of nanocrystalline TiO₂. The goal is to explain the inconsistency observed between theory and experiment. The result of the study suggests that surface oxygen vacancies resulting from gas-phase oxygen deficiency in the flame weakens or eliminated the effect of surface free energy contribution to the phase preference of TiO₂. That is, under fuel rich condition, rutile is preferred over anatase for any crystalline size.

ruxiaoyf@stanford.edu

W5P122 FUNDAMENTAL STUDY OF FLAME SYNTHESIS OF TiO₂ NANOPARTICLES BY MOLECULAR DYNAMICS SIMULATION

Kai Luo¹, Qian Mao²

¹University College London, United Kingdom ²Tsinghua University, China

In flame synthesis of nanoparticles, polydisperse rather than monodisperse particles are more often encountered and off-center as well as head-on collisions occur. Such realistic phenomena have not been studied systematically before and fundamental understanding of the detailed dynamic processes and mechanisms behind is still lacking. The main objective of the present study is to fill the knowledge gap about flame synthesis of nanoparticles, focusing on the sintering process. In this paper, we use Molecular Dynamics to study the influence of an impact parameter (off-center distance D) and the nanoparticle diameter ratio on the sintering process of nanoparticles. Moreover, we study and employ a variety of parameters to quantify the sintering process. A full spectrum of dynamic processes have been observed by varying D, with the collision and sintering processes being very different from the head-on collision cases. There is a critical value of D that is larger than the initial nanoparticle diameter. Within this critical D, particles always collide due to intermolecular attractive force. Beyond the critical D, two nanoparticles would rotate around each other and finally separate without collision. This is attributed to the increased repulsive intermolecular force at certain angles (e.g. 180 degrees) between the lattice orientations of the two nanoparticles when they rotate around each other. Shrinkage and local lattice orientation are calculated, which offer additional insight into the sintering rate and corresponding structural changes. The sintering processes of unequal-sized particles are found to be fundamentally different from those of equal-sized nanoparticles. While the smaller particle experiences dramatic changes in morphology and crystalline structures, the larger particle remains quite stable. The necking growth seems to be mainly due to ions from the smaller particle migrating to the surface of the larger particle. The smaller particle finally infuses into the core of the larger particle. The mean square displacement also confirms the different diffusion rates of ions from the smaller particle to the larger particle. Finally, the relative gyration radius shows that the larger the nanoparticle diameter ratio, the faster the coalescence rate at the initial stage when the surface diffusion of ions dominates.

K.Luo@ucl.ac.uk

W5P123 MULTI-VARIABLE MEASUREMENT BASED ON DUAL THERMOPHORETIC SAMPLING WITH DIFFERENT TIME INTERVALS DURING FLAME SYNTHESIS NANOPARTICLES

Zuwei Xu, Haibo Zhao, Huazhong University of Science and Technology, China

Understanding the underlying fundamental processes is essential to the synthesis of specific materials with specially tailored properties. Multiple key internal and external variables of nanoparticles in flame (such as temperature, flow velocity, Particle Volume Fraction (PVF) and size distribution(PSD), Aggregate Fractal Dimension(AFD) were measured and characterized simultaneously in this study by a simple and novel dual time-interval thermophoretic sampling at single point (DTSP) method. A co-flow diffusion CH₄ flame for TiO₂ nanoparticles synthesis by feeding TiCl₄ vapor was measured via the DTSP method. The flame temperature and nanoparticles were measured by a fine-wire thermocouple, and thermophoresis probes (TEM grids) respectively, then PVF, PSD and AFD were obtained by analyzing these Scanning Electron Microscope (SEM) images. Differently, two TEM grids were used for nanoparticles sampling at a position, and they were exposed in flame with two different time intervals. Since the amount of particles deposited on TEM grids surface by thermophoretic force is a function of gas temperature, flow velocity, PVF and the probe exposure time in flame, we proposed a comprehensive solution for these desired multiple parameters using the two samples by accounting for the effects of unsteady probe temperature gradient. The effects of flow velocity on convection heat transfer of flame and TEM grids were considered by analyzing the visible microscopic state of thermophoretic-deposited particles. The experimental measurements of PVF, flow velocity and temperature at the different heights of flame showed a close agreement with the simulation results by a coupled Computational Fluid Dynamics-Population Balance Model (CFD-PBM) ((Image).₁). It was found that thermophoretic deposition rate and heat flux exhibits the same regular pattern ((Image).₃), namely the synergetic effect of particle thermophoretic deposition and heat transfer.

xu_zuwei@163.com

W5P124 SINTERING AND GROWTH OF ALUMINA NANOPARTICLES USING MOLECULAR DYNAMICS SIMULATIONS

Alauddin Ahmed, Paolo Elvati, Nathan Taylor, Richard Laine, Angela Violi, University of Michigan, United States

Solid state sintering is an integral component of many combustion techniques, e.g., flame spray pyrolysis and liquid-feed flame spray pyrolysis. Growth, morphology, and structural phase of a coalesced nanoparticle are determined by the phases, temperatures, and size of nanoparticles involved. However, the detailed atomistic mechanism(s) of sintering and

growth of alumina nanoparticles are not known. In this work, we present Molecular Dynamics (MD) simulations of the sintering of alumina nanoparticles of different sizes at various temperatures. It is found that solid-state diffusion plays significant role in the formation of final coalesced nanoparticle. During sintering, surface diffusion in the neck region is significantly higher than bulk diffusion in the cores of participating nanoparticles. The oxygen diffusion coefficient is significantly larger than that of Al^{3+} . The diffusion process in the neck region is vacancy mediated because of the distorted structure. Sintering-induced structural phase transformations are evaluated using X-Ray Diffraction (XRD) data computed from MD trajectories and are compared with experimental XRD data. We found that one of the phases of sintering nanoparticles always dominates the phase transformation and eventually transformed to that phase after coalescence. The results of this study will be useful in understanding how specific nanoparticle structures form and may also guide efforts to synthesize customized nanostructures using alumina nanoparticles.

alauddin@umich.edu

W5P125 HYBRID ROCKET BURNING RATE ENHANCEMENT BY NANO-SCALE ADDITIVES IN HTPB FUEL GRAINS

James Thomas¹, Eric L. Petersen¹, John Desain², Brian Brady²

¹Texas A&M University, United States ²The Aerospace Corporation, United States

Traditional hybrid rockets are composed of solid fuel grains and a flowing oxidizer and have distinct advantages over their pure solid or liquid counterparts. Hybrid rocket propellants are more controllable, safer to store and transport and can allow for higher specific impulses than solid propellants. Additionally, hybrids are mechanically simpler and allow for denser fuels than liquid propellant systems. However, a major drawback of hybrid chemical propulsion is low solid fuel regression rates during combustion that ultimately cause low engine thrust. Typical solutions to the observed lower fuel burning rates include varying the oxidizer-to-fuel ratio; modifying the geometric dimensions of the solid grain; adding additional oxidizer ports to the grain; using unconventional, non-polymeric fuels; and including catalysts or burning rate modifiers in the solid grain. Energetic nano-scale Aluminum has proven to be an effective catalyst in composite solid propellants containing Hydroxyl-Terminated-Polybutadiene (HTPB) and in hybrid propellants with a solid HTPB grain. To support this hypothesis, the authors were motivated to manufacture and test several hybrid motors, including some with nano-Al additives, for their combustion rates. HTPB fuel grains were cast into hollow cylinders with embedded Miniature Resistive Regression and Ablation Sensors (MIRRAS) capable of producing instantaneous or averaged burning rate data. Hybrid motors were burned with gaseous oxygen at various oxidizer mass fluxes. The burning rate of each individual motor was calculated by the typical diameter change measurement and by analyzing the MIRRAS data. MIRRAS burning rate data were examined using a time step interval method, capable of producing averaged or instantaneous values, and various Fourier transform analyses. Combustion rate results are plotted against oxidizer mass flux measurements for plain HTPB and aluminized motors and compared to literature correlations. These burning rate experiments were performed to confirm burning rate enhancement in HTPB hybrid motors by the addition of nano-scale Aluminum and to establish baseline burning rate values at the authors' laboratories for future hybrid motor testing.

christforeal@neo.tamu.edu

W5P126 COMBUSTION OF MECHANICALLY ALLOYED AL/MG POWDER WITH WATER

Evgeny Shafirovich¹, Daniel Rodriguez¹, Aly Yasmine², Mirko Schoenitz², Edward L. Dreizin²

¹The University of Texas at El Paso, United States ²New Jersey Institute of Technology, United States

Combustible mixtures of water with aluminum powders have been investigated by several research teams for hydrogen generation and space propulsion applications. It was determined that nanoscale Al powders must be used in such mixtures. In nanoscale powders, however, the content of free metallic Al is reduced and, in addition, they are quite expensive. Recently, mechanically alloyed Al/Mg powders have been fabricated. These powders are micron-sized, but, at the same time, they have a high reactivity and excellent storage characteristics. The objective of the present paper is to explore the feasibility of using mechanically alloyed Al/Mg (1:1 mass ratio) powder in combustible mixtures with water. The Al/Mg powder was mixed at different mixture ratios with deionized water, gelified by adding 1–3 wt% polyacrylamide. Combustion of the obtained mixtures was investigated in a windowed chamber, equipped with a laser ignition system, a video camera, a pressure transducer, and a mass-spectrometer. A quartz tube with the mixture was installed vertically on a brass pedestal and the chamber was filled with argon at 1 atm. An infrared beam of a CO₂ laser was introduced into the chamber vertically through the ZnSe window, located at the chamber lid, and directed to the top of the pellet. The experiments have shown that mixtures of the tested powder with 10–60 wt% water (gelified with 3 wt% polyacrylamide) are combustible. The measured front velocities exceed the values obtained for the mixtures of water with nanoscale Al. The measurements of hydrogen yield based on the pressure increase have led to experimental values exceeding the theoretical maximum for Al–H₂O reaction, which indicates that decomposition of polyacrylamide produces significant amounts of gases. This was confirmed by the experiments with 1 wt% polyacrylamide and by mass-spectrometry. The kinetic studies of the reaction between the mechanically alloyed Al/Mg powder and deionized water at 80°C show that the reaction is extremely slow, which indicates that combustible mixtures of this powder with water are storable.

eshafirovich2@utep.edu

W5P127 TEMPERATURE DEPENDENCE OF FLAME PROPAGATION OVER METHANE HYDRATE SURFACE UNDER A NATURAL CONVECTION

Tomoki Yoshioka, Takeshi Yokomori, Ryo Ohmura, Toshihisa Ueda, Masanori Suemitsu, Keio University, Japan

Experimental study was conducted to investigate the axisymmetric flame spreading over the methane hydrate surface under a natural convection. The methane hydrate particles with the diameter less than 0.5 mm were filled with cylindrical insulating vessel with the diameter 100 mm. The flame was ignited at the center of methane hydrate, and propagated outward over the methane hydrate surface. The behavior of flame ignition and propagation were recorded by a high speed camera up to 250 frames per second. The flame ignition took place as a function of ignition temperature of methane hydrate ($T_{s,ig}$) which was measured by a thermocouple located 1mm beneath from the hydrate surface at the center of hydrate. The methane hydrate used in the experiment was made in our laboratory under the condition of high pressure more than 3 MPa. The test section was surrounded by the enclosure in order to prevent the effect of convection from the external. We observed the behavior of flame propagation under the condition of $T_{s,ig} = -100^{\circ}\text{C}$, -80°C , -60°C , -40°C , and -20°C . When $T_{s,ig} = -100^{\circ}\text{C}$, which was lower than nominal equilibrium temperature (-80°C), the flame propagated axisymmetrically with low speed around 10 mm/s. This is referred to "low speed flame propagation." In this case, the flame propagates slowly with melting the methane hydrate in front of the flame front by the heat transfer from the flame. When $T_{s,ig} = -80^{\circ}\text{C}$, -60°C and -40°C , which were higher than the nominal equilibrium temperature of methane hydrate and lower than the temperature range of self-preservation effect, the dissociation rate was extremely suppressed, and as a result, the flame propagated with high speed around 1000 mm/s. This is referred to "high speed flame propagation." In this case, the methane hydrate dissociated well and a lot of methane gas was ejected from the surface, and the methane-air premixed gas was accumulated over the surface of methane hydrate. As a result, the flame propagated fast in the methane-air premixed gas. In addition, when $T_{s,ig} = -40^{\circ}\text{C}$, the flame propagation changed from "high speed flame propagation" to "low speed flame propagation" during the flame propagation. This is referred to "transition flame propagation." In this case, there were two regions; 1) the region in the self-preservation where methane gas ejection was suppressed, 2) the region with high-dissociation where enough gas was ejected. When $T_{s,ig} = -20^{\circ}\text{C}$, the flame propagated slowly because the temperature range was in the self-preservation effect ($-31^{\circ}\text{C} \sim -2^{\circ}\text{C}$). This shows the "low speed flame propagation" occurs again.

t.yoshioka@z2.keio.jp

W5P128 POOL FIRE EXTINCTION BY A CARBON DIOXIDE HYDRATE

Hirotaka Nakano, Kosuke Sasakura, Ryo Ohmura, Takeshi Yokomori, Toshihisa Ueda, Keio University, Japan

The CO_2 hydrate is a solid crystal in which CO_2 is trapped in "cages" of hydrogen bonded water molecules. When the CO_2 hydrate is dissociated in the combustion area, we can expect two effects of fire extinguishing, that is, the intercept of the oxygen supply to a flame with CO_2 and the fuel cooling by the dissociation heat and the evaporation heat. In addition, it can reach the flame base against the strong buoyancy because it is the solid crystal. In the present study, we investigated a scale effect of a pool flame on the extinction using the CO_2 hydrate by experiment. Two sizes of fuel container, S ($\Phi=50$) and L ($\Phi=100$), and two types of fuel, methanol (boiling point: 64.7°C) and 1-propanol (boiling point: 97.4°C) were used. The experiments were carried out to extinguish the pool flame by dropping a dry ice or the CO_2 hydrate from the top. In the case of methanol, much more mass of the CO_2 hydrate is necessary to extinguish the flame compared to that of the dry ice without regard to the size of fuel container. In fact, the ratio of the mass of the CO_2 hydrate and that of the dry ice of extinction, α , is more than 2. In the case of 1-propanol, the value of α for container S is about 0.7 and 1.5 for container L. These results show that α for 1-propanol is less than that of methanol. The boiling point of 1-propanol is almost the same as that of water while that of methanol is less. It suggests that the evaporation heat is used to cool down the fuel temperature in the case of 1-propanol, which results in the extinction of 1-propanol flame. The effect of the evaporation heat seems to be weakened when the fuel container becomes bigger. This is supposed to be attributed to the difference of the dependence of the effect of CO_2 and the cooling effect with the size of the fuel container. The effect of CO_2 is supposed to be proportional to the diameter of the fuel container while the cooling effect is supposed to be proportional to the square of the diameter of the fuel container, in other words, the surface area of the fuel.

kanoto_fill@yahoo.co.jp

W5P129 MECHANISMS OF THERMITE REACTIONS IN THE MIXTURES OF MAGNESIUM WITH LUNAR AND MARTIAN REGOLITH SIMULANTS

Evgeny Shafirovich, Armando Delgado, The University of Texas at El Paso, United States

The use of lunar and Martian regolith for *in-situ* production of construction materials is of interest for future space exploration missions. Metals such as Al and Mg exhibit thermite reactions with lunar and Martian regolith simulants, the mineral compositions of which include oxides of Si, Fe, Al, Mg, Ca, Ti, and Na. It would be attractive to use these reactions for the production of ceramic materials that could be used as construction materials on the Moon and Mars. The required Al or Mg could be obtained by recycling the lander parts as well as from the regolith. Previous research has revealed, however, that combustion of JSC-1A lunar regolith simulant with aluminum requires significant preheating. The mixtures of this material with magnesium ignite much easier, leading to a steady or spinning propagation of the combustion wave over the pellet at relatively low concentrations of Mg. Because of complex composition of lunar

regolith, however, the combustion mechanisms of these mixtures are not fully understood.

In the present work, two Martian regolith simulants (JSC-Mars-1A and Mars Mojave) have been studied in addition to JSC-1A. The combustion characteristics of the three simulants mixed with magnesium were determined and their correlation with the simulant compositions was analyzed. To understand the reaction mechanisms, thermogravimetric and differential thermal analyses were conducted for these mixtures as well as for binary mixtures of magnesium with silica and iron oxide. X-Ray Diffraction analysis was used to examine the products obtained in the combustion experiments and in thermal analysis after interrupting the heating process at different temperatures. Based on the results of both combustion experiments and thermal analysis, it has been concluded that iron oxide, despite the lower concentration in the regolith simulants, may play a more important role than silica in the combustion of lunar and Martian regolith with magnesium.

eshafirovich2@utep.edu

W5P130

ON SOME FEATURES OF HETEROGENEOUS COMBUSTION IN POROUS MEDIA UNDER FREE CONVECTION

Nickolay Lutsenko, Far Eastern Federal University, Russia

The work is devoted to the numerical investigation of one-dimensional unsteady processes of heterogeneous combustion in porous object under free convection. Combustion is due to the exothermic reaction between the fuel in the porous solid medium and oxidizer contained in the gas flowing through the porous object. In considered porous objects the gas pressure at object boundaries is known but the flow rate and velocity of the gas at the inlet to the porous objects are unknown, so the flow rate of oxidant, which enters into the reaction zone in porous object, regulates itself. The mathematical model is based on the assumption of interacting interpenetrating continua using the classical approaches of the theory of filtration combustion; it includes equations of state, continuity, momentum conservation, energy for each phase (solid and gas) and oxidizer concentration. The proposed mathematical model is similar to the one used in and allows to describe the processes for both free convection and forced filtration. The cocurrent wave, when the gas moves in the same direction as the combustion wave, and countercurrent wave, when the gas and the combustion wave move in opposite directions, have been numerically investigated for different parameters in the present work. It has been revealed that reaction-trailing type of wave structure, when the reaction occurs at the trailing edge of the heated region of the porous object, may not occur when the analytical criterion for reaction-trailing combustion wave takes place. The analytical criterion, which determines the reaction-leading or reaction-trailing regime of combustion wave for simple model, cannot determine types of wave structure for more complicated model. Using some different expressions of the dependence of permeability on porosity, the effect of the changing of permeability due to the changing of porosity has been numerically investigated. It has been revealed that taking into account the dependence of permeability on porosity can significantly change the solution quantitatively in one-dimensional case; it can also increase the temperature in the countercurrent combustion wave.

NickL@inbox.ru